ENGINEERING-TRANSPORTATION
LIBRARY

THE UNIVERSITY
OF MICHIGAN
MAR 15 1966
ENGINEERING
LIBRARY

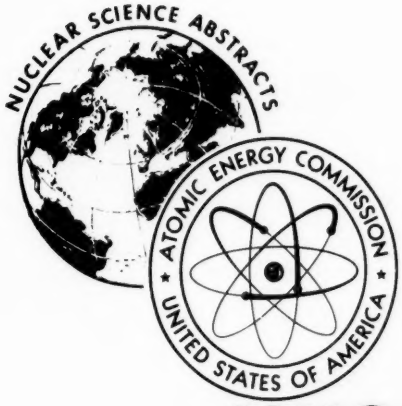

NUCLEAR SCIENCE ABSTRACTS

Volume 20 Number 3

Abstracts 3649–5227

February 15, 1966

UNITED STATES ATOMIC ENERGY COMMISSION
Division of Technical Information

DEPOSITED BY THE
UNITED STATES OF AMERICA

USAEC DEPOSITORY LIBRARIES

Collections of USAEC reports are maintained in the libraries of the organizations listed below for reference use by the general public. Facilities for making photocopies are available. The USAEC also makes available through these libraries atomic energy reports of countries other than the U. S. that are abstracted in *Nuclear Science Abstracts*.

ALABAMA
Auburn, Auburn University

ARIZONA
Tucson, University of Arizona

ARKANSAS
Fayetteville, University of Arkansas

CALIFORNIA
Berkeley, University of California
Davis, University of California
Los Angeles, University of California
San Diego, Public Library
Stanford, Stanford University

COLORADO
Boulder, University of Colorado
Denver, Public Library

CONNECTICUT
New Haven, Yale University

DELAWARE
Newark, University of Delaware

DISTRICT OF COLUMBIA
Washington, Library of Congress

FLORIDA
Coral Gables, University of Miami
Gainesville, University of Florida
Tallahassee, The Florida State University

GEORGIA
Atlanta, Georgia Institute of Technology

HAWAII
Honolulu, University of Hawaii

ILLINOIS
Chicago, John Crerar Library
Chicago, University of Chicago
Evanston, Northwestern University
Urbana, University of Illinois

INDIANA
Bloomington, Indiana University
Lafayette, Purdue University

IOWA
Ames, Iowa State University

KANSAS
Manhattan, Kansas State University

KENTUCKY
Lexington, University of Kentucky
Louisville, University of Louisville

LOUISIANA
Baton Rouge, Louisiana State University
New Orleans, Tulane University

MARYLAND
Baltimore, Johns Hopkins University
College Park, University of Maryland

MASSACHUSETTS
Cambridge, Harvard University
Cambridge, Massachusetts Institute of Technology

MICHIGAN
Ann Arbor, University of Michigan
Detroit, Public Library
East Lansing, Michigan State University

MINNESOTA
Minneapolis, University of Minnesota

MISSISSIPPI
State College, Mississippi State University

MISSOURI
Kansas City, Linda Hall Library
Rolla, University of Missouri School of Mines and Metallurgy
St. Louis, Washington University

MONTANA
Bozeman, Montana State College

NEVADA
Las Vegas, Nevada Southern University
Reno, University of Nevada

NEW JERSEY
Princeton, Princeton University
Teaneck, Fairleigh Dickinson University

NEW MEXICO
Albuquerque, University of New Mexico

NEW YORK
Albany, The University of the State of New York
Buffalo, State University of New York at Buffalo
Ithaca, Cornell University
New York, Atomic Industrial Forum, Inc.
New York, Columbia University
New York, New York University
Rochester, University of Rochester
Schenectady, Union College
Syracuse, Syracuse University
Troy, Rensselaer Polytechnic Institute

NORTH CAROLINA
Charlotte, Public Library of Charlotte and Mecklenburg County
Durham, Duke University
Raleigh, North Carolina State College

NORTH DAKOTA
Grand Forks, University of North Dakota

OHIO
Cincinnati, University of Cincinnati
Cleveland, Public Library

OHIO (CONT.)
Columbus, Ohio State University
Toledo, University of Toledo
Youngstown, Youngstown University

OKLAHOMA
Norman, University of Oklahoma
Stillwater, Oklahoma State University

OREGON
Corvallis, Oregon State University
Portland, Reed College

PENNSYLVANIA
Philadelphia, University of Pennsylvania
Pittsburgh, Carnegie Library
University Park, Pennsylvania State University

PUERTO RICO
Rio Piedras, University of Puerto Rico

RHODE ISLAND
Providence, Brown University

SOUTH CAROLINA
Columbia, University of South Carolina

TENNESSEE
Knoxville, University of Tennessee
Memphis, Public Library
Nashville, Joint University Libraries
Oak Ridge, Oak Ridge Associated Universities

TEXAS
Austin, University of Texas
College Station, Texas A & M University
Dallas, Southern Methodist University
Houston, Rice University
Lubbock, Texas Technological College
San Antonio, Public Library

UTAH
Salt Lake City, University of Utah

VIRGINIA
Blacksburg, Virginia Polytechnic Institute
Charlottesville, University of Virginia
Norfolk, Old Dominion College

WASHINGTON
Pullman, Washington State University
Seattle, University of Washington

WEST VIRGINIA
Morgantown, West Virginia University

WISCONSIN
Madison, University of Wisconsin
Milwaukee, Public Library

WYOMING
Laramie, University of Wyoming

DEPOSITED BY THE
UNITED STATES OF AMERICA

Volume 20, Number 3, February 15, 1966

NUCLEAR SCIENCE ABSTRACTS

A semimonthly publication of the USAEC Division of Technical Information, Edward J. Brunenkant, Director.
Published by the USAEC Division of Technical Information Extension, Robert L. Shannon, Extension Manager.

Nuclear Science Abstracts covers the international literature on nuclear science and technology and provides the only comprehensive abstracting and indexing of this body of information. Published twice each month since 1947, *NSA* covers technical reports of the U. S. Atomic Energy Commission and its contractors, technical reports of U. S. Government agencies and other governments, universities, industrial and research organizations, as well as patents, books, and journal literature on a world-wide basis. Nearly 350,000 abstracts have appeared in *NSA* through Volume 19. The subject matter covered in *NSA* is described in issue Number 1 and in TID-4552, *Subject Scope of Nuclear Science Abstracts*, available free from the U. S. Atomic Energy Commission, Division of Technical Information Extension, P. O. Box 62, Oak Ridge, Tennessee 37830.

Abstracts are arranged according to a number of subject categories and subcategories. Definitions of categories appear in issues Number 1 and 13. If the language of the original item is not English, the language will be indicated. Translations are not abstracted where an abstract of the original item has appeared in *NSA*.

INDEXES TO NSA

Corporate author, personal author, subject, and report number indexes appear in each issue and are cumulated quarterly, semiannually, and annually. Multi-volume cumulations have been issued as indicated on the following page. Report number indexes for all volumes (1–18) were issued at the end of Vol. 18. At the end of Vol. 19, the indexes for Vols. 1–15 were reissued to include additional public availability information. This cumulation will be a permanent shelf item and will not be reissued. Report number indexes for Vol. 19 are included as a cumulation beginning with Vol. 16.

AVAILABILITY OF PUBLICATIONS ABSTRACTED

The public availability of all U. S. Atomic Energy Commission reports is indicated in the report number indexes. The availability of other reports, when known, is also indicated. The availability of some unnumbered reports is given in the abstract.

Dissertations abstracted in *Dissertation Abstracts* and included in *NSA* are available from University Microfilms, Inc., 315 N. First Street, Ann Arbor, Michigan 48103.

Most of the published literature abstracted in *NSA* is on deposit at the Library, Oak Ridge Associated Universities, Oak Ridge, Tennessee, (a USAEC depository library) and is available through interlibrary loan. When requesting papers from this source, it is important that *NSA* volume and abstract number be cited.

HOW TO OBTAIN NUCLEAR SCIENCE ABSTRACTS

NSA is available on an exchange basis to universities, research institutions, industrial firms, and publishers of scientific information. Inquiries should be directed to the U. S. Atomic Energy Commission, Division of Technical Information Extension, P. O. Box 62, Oak Ridge, Tennessee 37830.

Government agencies may obtain *NSA* free of charge.

NSA is available to the general public on a subscription basis from the Superintendent of Documents, U. S. Government Printing Office, Washington, D. C. 20402, as follows:

For the 24 regular issues, $30.00 domestic, $37.00 foreign. A single issue costs $1.75, plus 25 per cent for foreign mailing. Domestic rates apply to the United States, Canada, Mexico, and Central and South American countries except Argentina, Brazil, British and French Guiana, Surinam, and British Honduras. Foreign rates apply to the countries excepted above and to all other countries throughout the world.

For the quarterly, semiannual, and annual indexes, $22.00 domestic, $25.00 foreign.

Multivolume subject and author indexes are available as follows:

Vols. 1–4 (1948–1950) Johnson Reprint Corporation, 111 Fifth Avenue, New York, N. Y. 10003, $30.00.

Vols. 5–10 (1951–1956) Superintendent of Documents, U. S. Government Printing Office, Washington, D. C. 20402, $5.25.

Vols. 11–15, Subjects, Superintendent of Documents, U. S. Government Printing Office, Washington, D. C. 20402, $19.00.

Vols. 11–15, Personal Authors, Superintendent of Documents, U. S. Government Printing Office, Washington, D. C. 20402, $14.25.

Vols. 11–15, Corporate Authors, Superintendent of Documents, U. S. Government Printing Office, Washington, D. C. 20402, $2.50.

Cumulative Report Number Index, Vols. 1–15, Revised, is available from the Superintendent of Documents, U. S. Government Printing Office, Washington, D. C. 20402, $4.00.

Cumulative Report Number Index, Vols. 16–19, is available from the Superintendent of Documents, U. S. Government Printing Office, Washington, D. C. 20402, $2.50.

Annual Indexes are available separately from the U. S. Government Printing Office as follows:

Vol. 16, Subject and Authors, $9.75.
Vol. 17, Subject and Authors, $12.25.
Vol. 18, Subject and Authors, $12.50.
Vol. 19, Subject and Authors, $12.50.

ACKNOWLEDGMENTS

Agreements between the United States Atomic Energy Commission and the following organizations with regard to providing continuing services and specific literature coverage for *Nuclear Science Abstracts* are gratefully acknowledged:

American Institute of Physics; Atomic Energy of Canada Limited; Atomic Energy Research Establishment, United Kingdom; European Atomic Energy Community (EURATOM); Gmelin Institute; International Atomic Energy Agency; Japan Atomic Energy Bureau—Japan Atomic Energy Research Institute; Netherlands Patent Office; Reactor Centrum Nederland.

TABLE OF CONTENTS

Volume 20, Number 3, February 15, 1966

Category	Page
BIOLOGY AND MEDICINE	437
General	437
Ecology	437
Metabolism, Tissue Distribution, and Toxicology	438
Radiation Effects on Biochemicals	443
Radiation Effects on Tissues	446
Radiation Effects Therapy and Countermeasures	461
Radiation Hazards and Protection	463
Radiotherapy and Radiodiagnosis	464
CHEMISTRY	475
General	475
Analytical Procedures	475
Inorganic and Physical Chemistry	481
Organic Chemistry	488
Radiation Chemistry	490
Radiochemistry	498
Separation Processes and Procedures	498
ENGINEERING	503
General	503
Applications of Nuclear Explosions	503
Facilities and Equipment	504
Heat Transfer and Fluid Flow	505
Materials Testing	507
Protective Structures	510
Space Propulsion	510
Vacuum Engineering	511
GEOLOGY, METEOROLOGY, AND MINERALOGY	512
General	512
Meteorology	512
Natural Radioactivity and Fallout	513
Techniques and Equipment	515
Thorium and Uranium Minerals	516
HEALTH AND SAFETY	517
INSTRUMENTATION	523
General	523
Radiation Detection	525
Radiation Effects	528
ISOTOPE TECHNOLOGY	529
General	529
Industrial Applications	529
Power Application	529
Separation and Production	530
MATHEMATICS AND COMPUTERS	531
METALS, CERAMICS, AND OTHER MATERIALS	532
General	532
Corrosion	534
Fabrication	537
Properties and Structure	539
Radiation Effects	552
PHYSICS	555
General	555
Accelerators	556
Astrophysics and Cosmology	560
Atomic Physics	561
Cosmic Radiation	564
Direct Energy Conversion	566
Elementary Particles and Radiations	567
Field Theory, Scattering Theory, and Symmetries	574
Fluid Physics and Thermodynamics	581
Geophysics	584
Gravitation, Quantum Mechanics, and Relativity Theory	589
Low Temperature Physics	590
Neutron Physics	594
Nuclear Properties and Reactions	597
Plasma Physics and Thermonuclear Processes	610
Shielding	618
Solid State Physics	619
REACTOR TECHNOLOGY	623
General	623
Auxiliaries and Components	623
Criticality Studies	626
Design and Feasibility	629
Fuels	630
Power and Power-Breeder Reactors	632
Process Heat Reactors	640
Production Reactors	640
Propulsion and Space	641
Research and Test Reactors	642
WASTE DISPOSAL AND PROCESSING	645
GENERAL AND MISCELLANEOUS	646
CORPORATE AUTHOR INDEX	INDEX-1
PERSONAL AUTHOR INDEX	INDEX-10
SUBJECT INDEX	INDEX-41
REPORT NUMBER INDEX	INDEX-119

STAFF OF NUCLEAR SCIENCE ABSTRACTS

MANAGING EDITOR

John W. Norris

ASSISTANT MANAGING EDITOR

Donald D. Davis

ASSOCIATE EDITORS

Lawrence T. Whitehead
David E. Bost
Robert C. Kelly
Lee M. Thompson

SUBJECT INDEX EDITOR

Everett J. Hoffman

EVALUATORS

William D. Matheny
John H. Mitchell
Mary H. Newman

ABSTRACTORS

F. S. Armstrong (AECL)
Jane G. Buchanan
D. Lamar Cason
Helen G. Donald
James R. Dulaney
Wells L. Green
Mary Catherine Grissom
Fernando J. Hamilton
Phyllis C. Hansen
Thomas F. Heagerty
Carolyn D. Houston
Rose V. Jermain
Betty L. McDowell
Jean F. Peckham
Mona H. Raridon
Julia Redford
Lila B. Smith
Charles E. Stuber
Martha J. Thomas
Anne G. Ward
David C. West
Milton O. Whitson

SUBJECT HEADING SPECIALIST

Robert E. Upchurch

CORPORATE AUTHOR SPECIALIST

Clara L. Fox

DESCRIPTIVE CATALOGING SPECIALIST

J. Paul Meredith

SCHEDULING AND PUBLISHING COORDINATOR

Brainard L. Patton

Communication concerning the editorial policy and content of *NSA* should be addressed to the Managing Editor, *Nuclear Science Abstracts*, AEC Division of Technical Information Extension, P. O. Box 62, Oak Ridge, Tennessee 37830.

Use of funds for printing this publication approved by the Director of the Bureau of the Budget, May 20, 1963

Volume 20, Number 3 February 15, 1966

NUCLEAR SCIENCE ABSTRACTS

BIOLOGY AND MEDICINE

General

3649 (UCRL-11475) NUCLEIC ACID CONTENT OF CHLOROPLASTS OF SPINACH ISOLATED BY A NON-AQUEOUS TECHNIQUE. Biggins, J.; Park, R. B. (Lawrence Radiation Lab., Univ. of California, Berkeley). May 1964. Contract W-7405-eng-48. 6p. Dep. mn; CFSTI $1.00 cy, $0.50 mn.

The DNA content of spinach chloroplasts prepared in non-aqueous media is similar to that of chloroplasts prepared in aqueous buffers. However, the RNA content of non-aqueous chloroplasts is higher than that of aqueously prepared chloroplasts by a factor of two. The RNA is localized in the stroma phase of the chloroplast and is not bound to the quantum conversion apparatus. It is suggested that the low RNA content of aqueous chloroplasts is due to leaching of the polynucleotide during chloroplast isolation. (auth)

3650 PROGNOSTIC VALUE OF MARROW CHROMOSOME STUDIES IN HUMAN PRELEUKEMIA. Nowell, Peter C. (Univ. of Pennsylvania, Philadelphia). Arch. Pathol., 80: 205-8(Sept. 1965).

Chromosome studies were made on bone marrow cells in 23 patients, some of which had received radiation, who were believed to be developing leukemia. In ten individuals a stemline of cells with a chromosome abnormality was demonstrable in the marrow. Three of these patients had previously received therapeutic irradiation (^{32}P) for polycythemia vera. Among the seven patients with chromosome aberrations who had not been treated with ^{32}P, five died within three months; four with subacute granulocytic leukemia and one with an aleukemia proliferation of neoplastic megakaryocytes throughout the hematopoietic tissues. Only 2 of 13 patients without marrow chromosome changes developed leukemia when followed up to 26 months. A positive marrow chromosome study in an unirradiated patient with preleukemia suggests that a leukemic phase is imminent; a negative study may indicate a protracted nonleukemic course. However, some limitations are apparent. If the patient has previously received therapeutic irradiation chromosome aberrations may not indicate that a leukemic phase is imminent. This observation does not rule out a possible leukemogenic effect of ^{32}P therapy in polycythemia vera. It merely indicates that ^{32}P may increase the incidence of marrow chromosome abnormalities even more than it increases the incidence of leukemia. Even in the absence of a history of irradiation, two of seven patients with chromosome abnormalities in the present study have not yet developed leukemia, although one has been followed for only five months. Furthermore, the particular type of chromosome change does not appear to be of prognostic value, since a variety of changes were represented in both those who did and those who did not develop leukemia. (BBB)

3651 DEUTERIUM ISOTOPE EFFECTS IN CYTOLOGY. Flaumenhaft, E. (Univ. of Akron, Ohio); Bose, S.; Crespi, H. L.; Katz, J. J. Int. Rev. Cytol., 18: 313-61 (1965).

Data on the growth of microörganisms (viruses, bacteria, fungi, algae, protozoa) cultured cells, and higher plants in D_2O, cytologic effects of D_2O, and effects of D_2O on cell division and genetics are reviewed. Some applications of deuterium to biology are discussed. (TCO)

3652 FUNCTIONAL CAPACITY OF CANINE BONE MARROW IMPLANTS IN THE SPLEEN. Terz, Jose J.; Melamed, Myron; Lawrence, Walter Jr. (Memorial Sloan-Kettering Cancer Center, New York). J. Surg. Res., 5: 448-52(Oct. 1965).

Previous attempts to produce chimerism by whole-organ spleen transplants in dogs, either with or without total-body radiation or immunosuppressive drugs, failed to produce more than slight prolongation of graft survival. Recovery from the effects of total-body radiation of the recipient prior to the transplant has not heretofore been assisted by the presence of a technically successful splenic allograft. Although bone marrow chimeras can be produced in other species by marrow infusion after total-body radiation, marrow chimeras have been more difficult to produce in dogs. The efficiency of transplanting hematopoietic tissue, as an immediately vascularized organ, might yield more satisfactory marrow transplants in the dog. This report describes tests of the functional capability of ectopic marrow following the insertion of autologous rib fragments in the canine spleen. Systemic administration of nitrogen mustard was used instead of radiation as a means of suppression of the other hematopoietic tissues since the ectopic marrow depot to be tested for functional capacity could easily be protected from the toxicity of the drug by a 10 to 15 min period of occlusion of the splenic vascular pedicle. Results showed that normal-appearing marrow can be cultivated in the canine spleen by implantation of multiple autologous rib fragments, but the functional capacity of this quantity of marrow appears to be insufficient to consider utilizing this modified organ for marrow transplantation. (BBB)

Ecology

3653 (BNL-8466) WATER BUDGET OF A FOREST DAMAGED BY IONIZING RADIATION. Reiners, W. A.; Woodwell, G. M. (Minnesota Univ., Minneapolis. Dept. of Botany. Brookhaven National Lab., Upton, N. Y.). [1964]. Contract AT(30-2)-Gen-16. 18p. Dep. mn; CFSTI $1.00 cy, $0.50 mn.

Changes in soil moisture were measured in an irradiated oak-pine forest at Brookhaven National Laboratory, Long Island, New York, along a gradient of radiation effects. Soil moisture contents were lowest during the grow-

ing season where the ecosystem was intact and increased with increasing radiation damage. Moisture contents were essentially identical at all depths along the gradient during the recharge period. Rates of evapotranspiration increased with decreasing vegetation damage during the first half of the growing season, but losses were roughly equal during the latter half. Cumulative evapotranspiration was only slightly greater from intact zones of the forest at the end of the growing season than from damaged zones. Differences in moisture content and evapotranspiration rates were detectable during the first half of the growing season at chronic exposures as low as 11.5 R/day where the dominants retained about 50% of their foliage. These observations are of particular significance to consideration of potential nuclear catastrophes, since it is clear that exposures below lethal exposures for the dominants would alter rates of evapotranspiration, potentially increasing surface runoff. (auth)

3654 THE RADIOACTIVITY OF SOME FORMS OF VEGETATION STUDIED IN THE NEIGHBORHOOD OF THE CITY OF CLUJ. Szabo, A.; Piciu, Doina (Inst. of Atomic Physics, Cluj). Acad. Repub. Pop. Rom. Stud. Cercet. Fiz., 17: 9-12(1965). (In Rumanian).

Studies were carried out to determine the atmospheric contamination caused by nuclear weapons testing prior to the 1963 test ban and to examine the selective accumulation of radionuclides by plants. The method employed included measurement of the β activity of various grains and grass as a function of time. The activity of the incinerated plants was expressed as equivalent of pC(^{90}Sr + ^{90}Y). The results indicated that carrots had the highest ability to concentrate radioactive elements. In the case of grains, a smaller amount was found in the roots. Marked differences were noted in the activity of plants collected at various times of the year; this was probably due to the changes in radioactivity of the air and to the different rates of metabolism of fallout by the plants. By means of chromatographic and spectroscopic techniques, it was established that the same nuclides were incorporated by all the plant species, indicating that the contamination found is due to fallout products and to aerosols. (TTT)

Metabolism, Tissue Distribution, and Toxicology

Refer also to abstract 4162.

3655 (BNWL-SA-224) PULMONARY CLEARANCE OF $^{59}Fe_2O_3$ AND $^{51}Cr_2O_3$ IN RATS AND DOGS EXPOSED TO CIGARETTE SMOKE. Bair, W. J.; Dilley, J. V. (Battelle-Northwest, Richland, Wash. Pacific Northwest Lab.). June 18, 1965. Contract AT(45-1)-1830. 12p. (CONF-650906-2). Dep. mn; CFSTI, $1.00 cy, $0.50 mn.

From 2nd International Symposium on Inhaled Particles and Vapours, Cambridge, Eng.

The inhibitory effects of cigarette smoke on tracheal ciliary activity have been reported by several authors. Because of the possible consequence of this effect on the toxicity of inhaled particles, preliminary studies were undertaken to determine whether cigarette smoke altered the clearance of particles from the lung. Acute exposures of rats to cigarette smoke did not influence the clearance of $^{59}Fe_2O_3$ or $^{51}Cr_2O_3$ particles from the lung. The possible effects of chronic cigarette smoking were examined in beagle dogs smoking 20 cigarettes per day. Deposition of inhaled insoluble particles was tested periodically by exposing the dogs to aerosols of $^{59}Fe_2O_3$ or $^{51}Cr_2O_3$. Subsequent pulmonary clearance was measured by whole-body counting and body-scanning techniques. No effects were seen in dogs after smoking cigarettes five days per week for over a year. (auth)

3656 (BNWL-SA-225) FATTY ACID SYNTHESIS BY SUBCELLULAR FRACTIONS OF LUNG TISSUE. Tombropoulos, E. G. (Battelle-Northwest, Richland, Wash. Pacific Northwest Lab.). June 18, 1965. Contract AT (45-1)-1830. 5p. (CONF-650906-1). Dep. mn; CFSTI, $1.00 cy, $0.50 mn.

From 2nd International Symposium on Inhaled Particles and Vapours, Cambridge, Eng.

The incorporation of acetate-1-^{14}C into long-chain fatty acids was studied in dog, rabbit, and rat lungs. Disrupted (by freezing and thawing) lung mitochondria preparations are avidin insensitive and do not require biotin or HCO_3^- for the incorporation of ^{14}C-labeled acetate into long-chain fatty acids. Degradation studies showed that the above incorporation proceeds mostly by elongation of pre-existing fatty acids rather than through the malonyl-CoA pathway. Although the relative subcellular contribution of the mitochondrial fraction in the incorporation of acetate-1-^{14}C is more important in the lung than in liver tissue, the mechanisms of incorporation appear to be similar. The importance of these findings in relation to lung surfactants is discussed. (auth)

3657 (CEA-R-2818) CONTAMINATION EXPERIMENTALE DE CREVETTES ROSES PAR LE ^{137}Cs. (Experimental Contamination of Pink Shrimps by ^{137}Cs). Ancellin, Jacques; Michon, Georges; Vilquin, Alain (Commissariat a l'Energie Atomique, Fontenay-aux-Roses (France). Centre d'Etudes Nucleaires). Aug. 1965. 16p. Dep. mn.

The technique used to determine ^{137}Cs concentration factors in the pink shrimp (Leander Serratus Pennant) is described. Experiments over three months showed that the specific activity of the shrimps became stable between the 30th and the 40th day. The concentration factors then have values between 30 and 40. (tr-auth)

3658 (EUR-2414.f,i) RESEARCH INTO NEW MEANS OF DIAGNOSIS AND TREATMENT BY METHODS DERIVED FROM NUCLEAR TECHNIQUES. Annual Report, 1963. (Brussels Univ. (Belgium). Pisa Univ. (Italy)). 1965. 48p. Dep. mn.

Text appears in French and Italian.

Results of research and planning are described for: analog models of the metabolism of phospholipides and proteins; a clinical absorption test on ^{125}I and ^{131}I labeled fats; a routine method for the external measuring of renal excretion with ^{125}I hippurane; two methods for the measurement of the coronary flow using external and internal counting (^{85}Rb,^{87}Kr); a method for measuring the cerebral circulation (^{85}Kr); a method for the detection of cancers and cancerous metastases by external counting (^{131}I Fibrinogen); a method for measuring in vitro glucosated catabolism (^{14}C glucose); methods for dosing erythropoietin, insulin, and thyreotropic hormone; the use of double labeling with ^{125}I and ^{131}I and isotopic equilibrium in the diagnosis of thyroid disorders; and neutron activation dosing of urinary, plasmatic, and thyroidal iodine and tissue ions in muscular biopsies. The projects commenced include: development of a high-sensitivity whole-body radioactivity counter for high-speed measurements; and studies on the origin of anemia in radiation sickness. (P.C.H.)

3659 (NP-15156) AN EXPERIMENTAL STUDY OF ^{90}Sr CONTAINED IN MARINE ANIMALS FOLLOWING POSSIBLE RELEASE OF RADIOACTIVE WASTE IN SEA WATER. Final Report, 1963-1964. Gohar, H. A. F. (Institute of Oceanography (Egypt)); Hashish, S. E. E.; Hassan, A.; Moulokhia, K. (Atomic Energy Establishment, Inshas (Egypt)). Contract 58/RI/RB. 65p. Dep. mn.

The radioactive contamination of marine environment has been one of the most serious subjects of world concern. The ^{90}Sr cycle in marine life seems to be of great interest from the biological point of view. Results are reported from a study of the nature and kinetics of ^{90}Sr uptake and release by and from a gastropod Nerita forskali Recluz abundant in the Red Sea area. (29 references.) (C.H.)

3660 (NP-15528) NORMALIZACION DE LA CAPTACION TIROIDEA DE ^{131}I DE ACUERDO A LAS RECOMENDACIONES DEL O.I.E.A. INFORME NO. 148 (Standardization of the Capture of ^{131}I by Thyroid in Ac-

cordance with the Recommendations of O.I.E.A. Report No. 1148). Degrossi, O.; Forcher, H.; Watanabe, T. (Comision Nacional de Energia Atomica, Buenos Aires (Argentina)). 1965. 12p. Dep. mn.

The values of thyroid up-take of ^{131}I for normal thyroids and for patients with pathological thyroid conditions are reported. These data were obtained with the standardization of the up-take technique by means of collimator and shielding according to the recommendations of the O.I.E.A. The values were compared with the international standards and there was a difference of 1%. (J.S.R.)

3661 (NP-15594) PREPARACION BIOSINTETICA DE SELENIOMETIONINA Y SELENIOCISTINA MARCADAS CON ^{75}Se. SU INCORPORACION Y DISTRIBUCION EN RATONES. INFORME NO. 154. (Biosynthetic Preparation of ^{75}Se-Methionine and ^{75}Se-Cystine. Its Incorporation and Distribution in Mice. Report No. 154). Anghileri, L. J.; Marques, R. O. (Comision Nacional de Energia Atomica, Buenos Aires (Argentina)). 1965. 12p. Dep. mn.

^{75}Se-methionine and ^{75}Se-cystine were prepared by adding sodium selenite (^{75}Se) to Saccharomyces cerevisiae culture free of sulphur compounds. The proteins obtained were hydrolized and the selenium aminoacids separated by exchange resin. The radiochemical purity was tested by paper ascendent chromatography using tertiary butyl alcohol, methyl-ethyl-ketone, amonium hydroxide, or water as solvent. The ^{75}Se-methionine and ^{75}Se-cystine distribution and elimination in mice were studied. The results indicate higher localization of ^{75}Se-cystine in pancreas compared with that of ^{75}Se-methionine. Information about biological half-life of both amino acids is given as well as the influence of methionine and cystine on the elimination and distribution of ^{75}Se cystine. (tr-auth)

3662 (PG-Report-650) THE BIOLOGY OF THE SOLWAY FIRTH IN RELATION TO THE MOVEMENT AND ACCUMULATION OF RADIOACTIVE MATERIALS. IV. ALGAE. Williams, B. R. H.; Perkins, E. J.; Gorman, J. (Production Group, United Kingdom Atomic Energy Authority, Annon (Scotland)). 1965. 18p. Dep.; BIS $0.60; HMSO 2s, 2d.

The relationship of certain insoluble radio-active nuclides, viz., ^{106}Ru and $^{95}Zr/^{95}Nb$, with the brown algae inhabiting the fucoid belt of the Solway Firth was examined. It was shown that the quantity of insoluble ^{106}Ru associated with each species of brown alga can vary according to position in an estuary. Of the four species investigated, Fucus spiralis was generally associated with the largest amounts of ^{106}Ru. (auth)

3663 (TID-22318) DISTRIBUTION AND EXCRETION OF TECHNETIUM IN HUMANS. Beasley, T. M.; Palmer, H. E.; Nelp, W. B. (Battelle-Northwest, Richland, Wash. Pacific Northwest Lab.). [1965]. Contract AT(45-1)-1830. 25p. (BNWL-SA-319). Dep. mn; CFSTI $1.00 cy, $0.50 mn.

Widespread use of ^{99m}Tc as a tracer in medicine and large scale separation of ^{99}Tc from fission product waste require that adequate knowledge of the metabolic properties of technetium be known so that realistic exposure limits can be imposed for the isotopes of interest. Results are reported from a metabolic experiment using ^{95m}Tc (60 day T $\frac{1}{2}$) and ^{96}Tc (4.3 T $\frac{1}{2}$) in which long term excretion, retention, and localization of these isotopes were measured using whole body counting techniques. Following intravenous and oral administration, both urinary and fecal excretion rates were measured and mathematical models were derived for technetium elimination. The latter should be helpful in estimating body burdens of the weak beta emitting ^{99}Tc following inadvertent exposure. (auth)

3664 (TID-22324) DYNAMIC ASPECTS OF SKELETAL METABOLISM IN MAN. Final Report. Terepka, A. Raymond (Rochester Univ., N. Y.). [nd]. Contract AT(30-1)-1981. 42p. Dep. mn; CFSTI $2.00 cy, $0.50 mn.

Results are reported from studies of metabolism of the human skeleton in normal individuals and patients with various metabolic disturbances in which about 30 μg of non-enriched U was used as a tracer. A simple method was developed for the quantitative colorimetric or fluorimetric determination of μg quantities of μ in ashed urine. After intravenous administration, U was rapidly cleared from the body in the urine or deposited in bone by a stable linkage of the uranyl ion, probably with phosphate groups, on the surface of hydroxy-apatite crystals. Marked differences in U retention were found in normal individuals and in patients with Paget's disease, hyperparathyroidism, hypoparathyroidism, osteomalacia, in patients with senile osteoporosis before and after estrogen treatment, and in patients before and after the administration of parathyroid extract. Results indicated that U urinary excretion provides a rapid clinical screening procedure for metabolic bone diseases in man. Results are reported from a kinetic analysis of ^{45}Ca blood content in patients with and without bone disease and simultaneous ^{45}Ca and ^{22}Na blood content studies in several patients for whom the urinary UO_2 excretion pattern had been determined. An IBM 7074 FORTRAN computer program was developed which carried out the mathematical analysis of the experimental data automatically and provided both a print-out of the calculations and a direct plot of the derived curves of ^{45}Ca blood disappearance. (C.H.)

3665 (CEA-tr-X-619) ENRICHISSEMENT DE LA VEGETATION FOURRAGERE EN STRONTIUM ET EN CESIUM. (Enrichment of Forage Vegetation in Strontium and Cesium). Fredriksson, Lars. Translated into French from Kgl. Lantbrukshogskol. Statens Lantbruksforsok, Statens Lantbruksforsok Medd., No. 137, 1-16(1962). 57p. Dep. mn; JCL $5.60 fs, $1.91 mf.

Studies have been made since 1956 at the National Center of Agronomy Research to determine under specific Swedish conditions the quantitative transport of radioactive fission products into forage. The enrichment of vegetation in ^{90}Sr and ^{137}Cs in two pastures of different types were studied by watering the pastures with solutions of the two nuclides. One of the pastures was of natural sandy soil whereas the other was a pasture cultivated on clay containing humus. The results showed that ^{90}Sr deposited on the soil is absorbed by the vegetation in significant quantities and can be transferred to animals by forage. The enrichment of the plants in ^{90}Sr was higher on arid soils poor in lime and in nutritive materials than on soils rich in lime and containing much clay. Approximately 3 to 4% of the Sr deposited on natural heather pastures of sand, poor in lime, was transported by forage to the animals during the first year. On cultivated pastures composed of clay soil with a satisfactory concentration in lime the quantity of Sr transported by forage decreased by half. The yield of pastures of the humus-clay type was five times higher per hectare and per year than that of sandy soil. The milk from animals pastured on the sandy soil contains less ^{90}Sr. The concentration of ^{137}Cs administered to the soil in the same manner as ^{90}Sr increased in the vegetation to a much less degree. This was especially the case for soils rich in clay. The Cs concentration deposited in the surface layers decreased with time and especially during the first two months after the deposition. A systematic utilization during a period of 10 years of calcium nitrate instead of nitrogen fertilizers containing ammonia resulted in a decrease in the Sr by a factor of 2 because of the action of the soil characteristics. (137 references.) (tr-auth)

3666 METABOLIC STUDIES ON EXPERIMENTAL NEPHROSIS. I. STUDIES ON RENAL METABOLISM OF AMINONUCLEOSIDE NEPHROSIS IN RATS. Kinoshita, Yasutami; Hirasawa, Yoshihei; Watabe, Yoshikazu; (and others) (Niigata Univ. School of Medicine, Japan). Acta Med. Biol. (Niigata), 11: 297-308(Mar. 1964).

A comparison was made of enzymatic and metabolic changes in rats made nephrotic by uranium nitrate, mercuric chloride, and aminonucleoside. The kidneys were examined 24 hr after a single subcutaneous injection of 0.2 ml of 0.1% uranium nitrate solution, 0.15 ml of 0.2%

mercuric chloride solution, and after 7 to 8 injections of 1.5 mg/100 g body weight aminonucleoside. Uranium, $HgCl_2$, and aminonucleoside (6-dimethyl-amino-9-(3′-amino-3′-deoxy-β-D-ribofuranosyl) purine), a derivative of puromycin, produce in rats a nephrotic syndrome similar to that observed in human lipoid nephrosis. In aminonucleoside-treated rats, succinic dehydrogenase and malic dehydrogenase activities showed no changes in nephrotic animals as compared with controls. Cytochrome oxidase activity was slightly elevated in the nephrotic group. Acid phosphatase activity decreased significantly in the nephrotic group, but adenosine triphosphatase activity showed no difference between nephrotic groups. Oxidative rates for several substrates, namely, glucose, fructose, succinate, glutamate, lactate, and alanine, did not change in nephrotic renal cortical slices. The rate of oxidative phosphorylation in the isolated renal mitochondria showed insignificant indifference between nephrotic and normal groups. The oxidation rate of the normal renal cortical slice for several substrates was unchanged by the addition of aminonucleoside in vitro, nor was the rate of the mitochondrial oxidative phosphorylation influenced in normal and nephrotic kidneys by adding of aminonucleoside in vitro. In the kidneys subjected to uranium nitrate and mercuric chloride poisoning, the decrease in succinic dehydrogenase activity was marked, while in the kidneys of rat which had developed proteinuria by the injection of egg white and the kidneys of aminonucleoside-induced nephrotic rat, its activity was normal. Uranium poisoning produced only slight, insignificant increases in malic dehydrogenase and cathepsin, and decreases in acid phosphatase and adenosine triphosphatase. (BBB)

3667 RAPID MICROBIOLOGICAL DETERMINATIONS WITH RADIOISOTOPES. **Levin, Gilbert V. (Resources Research, Inc., Washington, D. C.). Advance. Appl. Microbiol., 5: 95-133(1963).**

Use of various radioisotope technics to detect and identify microörganisms is reviewed. A practical bacteriological test using isotopes requires that the radioisotope be easily introduced and easily recovered from the bacteria or metabolic products. If the bacteria or the metabolic products retained in the medium are to be sought as evidence, the problem becomes difficult. This is because a physical separation of the unused, labeled substrate from the bacteria or metabolic products must be accomplished. The first goal of the radioisotope technique was a rapid test for the coliform group of organisms. One-third of the gas produced by coliform organisms is carbon dioxide, thus appropriate labeling of the lactose with ^{14}C results in the production of $^{14}CO_2$, which can be captured readily with barium hydroxide. The radioactivity collected can then be measured and is an index of the metabolic activity in the sample. Hazards associated with handling radioisotopes in the test are described. Other than normal, sensible care, no special precautions are required with the method. The β particles emitted by ^{14}C are of relatively low energy and are completely attenuated by the flask and planchets containing the radioactive medium. Even in open flasks or planchets, the ^{14}C cannot project β particles beyond several cm in air. The gas produced by the test has a ^{14}C content of several μμC. Small amounts of gas which may escape collection are vastly diluted with air, but use of a hood to carry off the minute traces of $^{14}CO_2$ is recommended. Upon completion of the test, a drop of disinfectant is added to each planchet to prevent further generation of $^{14}CO_2$. Although the planchet contents could readily be washed down the sink, the practice that should be followed is to store all spent radioactive materials and containers for shipment to a commercial isotope disposal center. Use of ^{3}H, ^{32}P, and ^{35}S labeling of metabolites in various bacterial tests is also described. Labeled tritium in appropriate compounds assimilated by cells is conveniently recovered in gaseous form as $^{3}H_2$, $^{3}H_2S$, $C^{3}H_4$, or $N^{3}H_3$. Various applications of radioisotope microbiologic tests are considered. Radioisotope techniques which, through their extreme sensitivity, render extended incubation of organisms unnecessary, and meet the important requirement for speed and accuracy. (BBB)

3668 ^{90}Sr, ^{95}Zr, AND ^{137}Cs ACCUMULATION IN CORN PLANTS AS INFLUENCED BY SOIL TEMPERATURE. **Haghiri, F. (Ohio Agricultural Experiment Station, Wooster). Agron. J., 54: 278-9(1962).**

The accumulation of ^{90}Sr, ^{95}Zr, and ^{137}Cs by young corn plants as influenced by soil temperature was studied in the greenhouse. Ohio hybrid W-64 seeds were planted in 2-gallon pots of Canfield silt loam. Carrier-free ^{90}Sr, ^{95}Zr, and ^{137}Cs (as chlorides) were applied to the surface soil at the rate of 40 μC per pot. Two days later, the corn tops were harvested for yield determination and radioassay. There were no significant differences in dry matter production due to temperature, probably because of the short exposure (4 days) to temperature differences. However, temperature did have a significant influence upon the accumulation of ^{90}Sr and ^{137}Cs by the 3-week-old corn plants. The multiple-range test on the mean values of the activity of ^{90}Sr in corn plants grown at four different soil temperature levels indicated that ^{90}Sr activity at 70°F was significantly higher than at 80° and 50°F, but not significantly different from those at 60°F. The highest ^{137}Cs activity in the corn plants was obtained at the 70°F. The decreasing order of ^{137}Cs activity in 3-week-old corn plants grown at four different soil temperature levels was 70, 80, 60, 50°F. It is known that ^{95}Zr is taken up by plants in a small quantity, but no measurable activity of ^{95}Zr in the corn tops was detected at any of the temperatures used. (TCO)

3669 COMPARISON OF INTESTINAL DISCRIMINATION BETWEEN ^{47}Ca, ^{85}Sr, AND ^{133}Ba. **Marcus, C. Silber; Wasserman, R. H. (Cornell Univ., Ithaca, N. Y.). Amer. J. Physiol., 209: 973-7(Nov. 1965).**

A mathematical treatment of data is described for comparing the fractional rates of Sr and Ca movement in gastrointestinal absorption. This is done by assuming that the ratio of various rate constants of absorption for the two elements is a constant which we have called the instantaneous intestinal strontium-calcium discrimination factor and designated as K. It was observed that this K value averaged 0.72 in studies on strontium and calcium absorption by the entire gastrointestinal tract of rats under in vivo conditions. This was in good agreement with a similar value for the reabsorption of these alkaline earths by mammalian kidney, reported by others as 0.7. The comparative absorption of barium could not be characterized by this mathematical model. Any treatment that alters the over-all comparative absorption of strontium and calcium can do so in two ways: by changing the absorption of both alkaline earths proportionally, and by changing the comparative rate constants of strontium and calcium transport. These two effects can be experimentally delineated. In the present study both lactose and lysine, which are known to alter Sr–Ca discrimination, were found to do so by increasing absorption and not by changing the rate constants. Results are included from a study of gastrointestinal absorption from 1 to 8 hr after the administration of ^{47}Ca, ^{85}Sr, and/or ^{133}Ba, plus glucose lactose, or lysine, by stomach tube to fasted rats. The entire alimentary tract from each rat was removed and samples were counted in a well-type scintillation counter. (C.H.)

3670 CHOLINESTERASE ACTIVITIES IN MOUSE LIVER AND KIDNEY DURING EXPERIMENTAL INTOXICATION WITH URANYL NITRATE (BIOCHEMICAL AND HISTOCHEMICAL STUDY). **Alibert, A.; Rigal, M.-Th.; Malet, P.; Bastide, P.; Turchini, J.-P.; Dastugue, G. (Faculte Mixte de Medecine et de Pharmacie, Clermont-Ferrand, France). Ann. Biol. Clin. (Paris), 22: 1075-81 (Oct.-Dec. 1964). (In French).**

Mice were given intraperitoneal injections of uranyl nitrate solution (400 mg/1 H_2O) in doses of one ml per 20 g body weight. The mice were sacrificed 24, 48, 72, or 96 hr after injection. In the liver, 24 hr after injection, there was slight degree of hepatitis. Lesions were maximal 72 hr after injection. Lesions of the kidney were more pronounced than those of the liver and similar at all four times of observation. There were parenchymous lesions, alterations of the inner wall of the convoluted tubules, massive exudation in the tubules, and vascular congestion. In a

histoenzymological study, a diffuse granular reaction was observed in the hepatic cells of the controls. The reaction was not as intense in the U-injected animals. In the kidneys of the controls the reaction was positive in the cortical zone, in the arterial lining, and on the fibrillary structures. After injection, the reaction was the same in the cortical zone, but more pronounced on the tubule linings of the intermediate medullary zone. The percentages of acetylcholine metabolized by a liver and kidney homogenate after intoxication with uranyl nitrate was determined. It was concluded that uranium poisoning markedly lowers hepatic cholinesterase activity within 48 to 72 hr while increasing renal cholinesterase activity. (BBB)

3671 STUDIES OF INHIBITION OF INTESTINAL ABSORPTION OF RADIOACTIVE STRONTIUM. IV. ESTIMATION OF THE SUPPRESSANT EFFECT OF SODIUM ALGINATE. Skoryna, Stanley C.; Paul, T. M.; Waldron-Edward, Deirdre (McGill Univ., Montreal). Can. Med. Ass. J., 93: 404-7(Aug. 28, 1965).

Studies on the inhibitory effects of the administration of sodium alginate on bone uptake of radiostrontium were conducted to establish whether the activity of extracts of brown algae (the source of alginate) extends to a wide range of strontium dosage corresponding to accidentally ingested amounts. The effects of continuous administration of small quantities of sodium alginate to rats on ^{89}Sr and ^{45}Ca bone uptake was also studied. The results indicated that sodium alginate reduces ^{89}Sr uptake in constant proportions. This effect was observed at all three levels of administration, 1.4%, 12%, and 24% of sodium alginate. The lowest dose of ^{89}Sr administered was 0.2 μC/day/100 g body weight, which is higher than the doses used in the estimation of the amounts accidentally ingested, but the linear relation between the dose of radioisotope and bone uptake in the presence of sodium alginate suggests that the same proportion would be maintained at the lower level of intake of radiostrontium. Small constant doses of sodium alginate (1.4% addition to drinking water) reduced appreciably bone uptake of Sr over a long period (administration to rats corresponded to ~ three yr of the human life span). Calcium uptake by bone was not affected significantly. This is of interest because the experiments were conducted on growing rats (weight increase 10 g per week) at a period when their skeletal demands for Ca were high. It is concluded that small, repeated doses of alginate are effective in reducing radiostrontium deposition without depressing bone formation. (BBB)

3672 THE RADIOISOTOPE OSTEOGRAM IN RICKETS. Harris, F.; Hoffenberg, R.; Black, Elizabeth G. (Univ. of Cape Town, Africa). Clin. Sci., 28: 75-82(Feb. 1965).

The use of ^{47}Ca to investigate rickets in children is described. Calcium-47 (15 to 20 μC) was administered intravenously to patients in a postabsorptive state. External counting was performed over selected sites twice daily for the first 3 days and daily thereafter for up to 10 days. In some patients the accumulation of ^{47}Ca was studied in detail in the early postinjection phase. The counting unit consisted of a lead-shielded plastic phosphor fitted to a photomultiplier tube and pre-amplifier, the output of which was fed into an automatic scaling unit. Design of the plastic phosphor is described. Under standard conditions it was shown to be twice as efficient for ^{47}Ca as a 2.54-cm NaI crystal. Contributions from ^{47}Sc were eliminated by appropriate voltage discrimination. A lead brick wall was constructed to reduce the background contribution made by the overall body radioactivity. The patient's leg was introduced through an aperture in the lead wall, and the marked sites were aligned over the counting face of the plastic phosphor. The upper fibula-tibial metaphysis was shown to accumulate ^{47}Ca most avidly in normal and rachitic subjects. In controls and healing rickets the lower fibula-tibial metaphysis was more active than the midshaft. In active rickets, accumulation over all three sites was depressed and the lower metaphysis was less active than the midshaft; these changes could be reversed by therapy with vitamin D. In a case of healing rickets a fracture-site showed striking avidity for ^{47}Ca. It is suggested that superficial exchange processes are largely responsible for bone turnover of Ca in rickets and that vitamin D acts by increasing this exchange. The failure to find consistent significant differences in the rate of removal of radioactivity from the selected bone sites between untreated, treated, and nonrachitic patients suggests that increased bone resorption is not a feature of untreated rickets. (TCO)

3673 EFFICIENCY OF MOLECULAR IODINE REMOVAL FROM AIR. Dworkin, Howard J.; Simeck, Charles M. (Univ. Hospital, Ann Arbor, Mich.). J. Clin. Endrocrinol. Metab., 25: 1505-10(Nov. 1965).

Unexplained persistent negative iodine balance studies have stimulated interest in the possibility that ingestion of atmospheric iodine may be of importance. Quantitative measurement of airborne iodine has suffered from lack of evaluation of the extraction efficiency of the trapping systems used. The efficiency of molecular iodine removal from air is evaluated for a liquid scrubbing system using sodium thiosulfate as the trapping solution and for a newly proposed dry system of glass boiling beads coated with sodium thiosulfate. The latter system was found to have a trapping efficiency of greater than 90% with better precision than the former system. Using these systems no atmospheric iodine could be detected on a ward where iodine balance studies were in progress. (auth)

3674 FACTORS AFFECTING IODINE CONCENTRATION IN BOVINE MILK. Lengemann, F. W. (New York State Veterinary Coll., Ithaca). J. Dairy Sci., 48: 197-202(Feb. 1965).

In view of the fact that radioiodine from fallout enters the food chain of man through milk, experiments were done on the transfer of iodide from plasma to milk in the cow. Also investigated was the effect upon the secretion of iodine into cows' milk of various compounds demonstrated to alter thyroid function. Nine cows were given 100 μC radioiodine orally twice daily to achieve a steady state condition. After a control sampling period the cows were given $KClO_4$, NaI, NaCl, and L-thyroxine, D-thyroxine, or 2,4-dinitrophenol. $KClO_4$, NaI, NaCl, and L-throxine reduced the accumulation of radioiodine in milk and reduced the milk-^{131}I/plasma-^{131}I ratio, whereas D-thyroxine and 2,4-dinitrophenol did not. L-thyroxine, although probably acting directly upon the mammary gland, was limited in its ability to reduce ^{131}I accumulation in milk. It was concluded that transfer of iodide into milk was in part an active process and that thyroxine could affect the transfer of iodide from plasma to milk and from milk to plasma. That the thyroxine took about two days to produce its effect upon milk radioiodine is evidence that its mechanism of action may differ from that of the inorganic anions. This action of thyroxine is unexplained at this time, but preliminary experiments on three cows indicate that it may not be mediated through thyroid-stimulating hormone (TSH). Daily injection of up to ten units of TSH had no consistent effect upon the milk/plasma ^{131}I ratio in these cows. The lack of effect of 2,4-dinitrophenol means that more than a phenolic group is necessary to elicit the thyroxine response. That D-thyroxine increased the milk/plasma ratio, in contrast to the action of L-thyroxine, suggests a specificity for L-thyroxine. There was a definite max response that could be elicited by the max response that could be elicited by the exogenous thyroxine. The percent of ^{131}I per liter of milk and the milk/plasma ^{131}I ratio could be decreased to only about 50% of the control value. (BBB)

3675 THE RETENTION BY THE BODY OF ^{131}I-POLYVINYLPYRROLIDONE AND ITS EFFECT ON RADIATION DOSE. Tothill, P. (Royal Infirmary, Edinburgh). J. Nucl. Med., 6: 582-7(Aug. 1965).

The metabolism of ^{131}I-labeled polyvinylpyrrolidone (PVP-^{131}I) following intravenous injection was studied in seven persons. For the course of the experiment, thyroidal uptake of any free iodide-^{131}I was blocked by administration of potassium iodide. Concentrations of PVP-^{131}I were

determined in plasma, urine, and feces samples collected for varying periods after injection. Whole-body counting was done with a single crystal scintillation counter. It was shown that approximately half of the PVP-^{131}I is excreted in the urine during the 1st 24 hr post-injection, while the remaining half is retained for long periods primarily in the liver. Radiation doses were determined to be quite high when amounts required for brain scanning were given. (H.G.D.)

3676 BONE SCANNING WITH ^{68}Ga: A CARRIER EFFECT. Hayes, R. L.; Carlton, J. E.; Byrd, B. L. (Oak Ridge Inst. of Nuclear Studies, Tenn.). J. Nucl. Med., 6: 605-10(Aug. 1965).

Animal studies are reported that indicate the use of ^{68}Ga as a rapid localizing agent for bone scanning when stable carrier Ga is administered simultaneously. Experiments were performed in 3-month-old rats in which the carrier level of Ga and the ratio of citrate to Ga were varied. Gallium-68 localized rapidly in bone when rats were given carrier gallium citrate, but ^{68}Ga citrate administered in the carrier-free form tended to distribute diffusely. (H.G.D.)

3677 EFFECTS OF CHLORPROMAZINE ON RADIOIODINE UPTAKE AND METABOLISM IN C-57 BROWN MICE. Ksycki, Joecile; Lockett, Clodovia (Notre Dame Coll., St. Louis). Life Sci., 4: 1877-86(Oct. 1965).

Previous reports indicated that acute and chronic administration of chlorpromazine (CPZ) to rats decreased the 6-hour thyroidal ^{131}I uptake. On the other hand, an increase in thyroidal iodine uptake due to one dose of CPZ has been reported. Because of these conflicting reports on the antithyroidal activities of CPZ, further experimental studies were conducted. The results indicated that a single 0.25 mg dose of CPZ, given 30 min previous to ^{131}I injection in C57 mice causes an inhibition of ^{131}I uptake by thyroid, of organic binding of ^{131}I, and of biosynthesis of thyroxine. By the end of 1 hr, the results showed a 38% decrease in ^{131}I, uptake and a 16% decrease in organic binding of ^{131}I; by the end of 4 hrs, a 56% decrease in ^{131}I uptake and a 38% decrease in thyroxine synthesis; and by the end of 24 hr, a 35% decrease in thyroxine synthesis. In salivary glands, a significant increase was noted in ^{131}I uptake during the 24-hr interval, as well as a significant decrease in organic binding of ^{131}I during the 12-hr interval. In serum, an increase in ^{131}I concentration, persisting for 24 hr was observed. In urine, a decrease occurred in ^{131}I concentration and in the rate of ^{131}I excretion during the first 4 hr, followed by a marked increase. The inhibitory effects of CPZ were less pronounced in mice which were not under the influence of the drug during ^{131}I injection, although pretreated with CPZ. These data indicate that CPZ, in addition to interfering with the ^{131}I trapping mechanism in the thyroid, interferes with organic binding of iodine and with the coupling of diiodothyronine to form thyroxine. The inhibitory effect of CPZ on the biosynthesis of thyroxine could be due to an inactivation of the enzyme system required for this synthesis; although other mechanisms, such as the inhibition of the hypothalmus by CPZ causing a decrease in thyrotropin secretion, and interference with iodide transport may be contributing factors. The reduced renal clearance might be due to a decreased glomerular filtration rate caused by CPZ. (BBB)

3678 THE INFLUENCE OF IONIZING RADIATION AND METHIONINE SULPHOXIMINE ON THE INCORPORATION AND EXCRETION OF ISOTOPICALLY LABELLED GLUCOSE AND THIOGLUCOSE IN THE RAT. Kolousek, J.; Gyoergyi, S.; Jiracek, V. (Charles Univ., Prague. Budapest Univ.). Neoplasma, 12: 385-90(1965).

The influence of x irradiation and administration of L-methionine sulfoximine on the excretion of uniformly U-^{14}C-labeled D-glucose and 1-^{35}S-thio-β-D-glucose in the urine and their distribution in blood cells and serum was studied in rats. Whereas neither irradiation nor methionine sulfoximine caused any significant change in the ^{14}C-labeled substances content in the blood, the excretion of ^{14}C-labeled compounds in the urine was increased by the action of methionine sulfoximine. After application of 1-^{35}S-thio-D-glucose the content of ^{35}S-labeled compounds in the blood cells and serum was not influenced by irradiation, but decreased after administration of L-methionine sulfoximine. The ^{35}S-activity in the urine was influenced only by irradiation, which caused a decrease of this activity. On the contrary L-methionine sulfoximine caused an increased excretion of ^{35}S-labeled methionine in the urine. (auth)

3679 REDUCING THE UPTAKE OF ^{90}Sr BY PLANTS ON CONTAMINATED OHIO SOILS. Jones, J. Benton Jr.; Haghiri, F. (Ohio Agricultural Experiment Station, Wooster). Ohio J. Sci., 62: 97-100(Mar. 1962).

The effect of crop species, liming, and soil type on the uptake of ^{90}Sr from Ohio soils by various plants was determined. Thirteen soil samples were limed at various rates to establish a pH range of 5 to 7 for each soil type. Ten μC of carrier-free ^{90}Sr was mixed into each soil sample, and used to grow corn, soybeans, wheat, and alfalfa. The aerial portions of the plant were used for counting. The amount of ^{90}Sr found in the plant tissues varied considerably depending upon the crop species, liming rate, and soil type. The ^{90}Sr content of various plant species was in the order: soybean > corn = alfalfa > wheat. As the soil pH increased (as a result of liming), less ^{90}Sr was accumulated in all crop species. An increase in soil pH from 5.0 to 7.0 reduced the ^{90}Sr content of all the plants by about one-half. However, the ^{90}Sr content of the plants was not similar in the case of all soils used. A highly significant correlation was found between the percent clay content of soil and the level of ^{90}Sr in the plant. As the clay content increased, the ^{90}Sr content of the plant decreased. It appeared that soil texture and soil pH are equally important. The use of low clay content soils may result in plants with a sufficiently high ^{90}Sr level to make them undesirable for animal or human consumption. The colloidal clay fraction largely accounts for the cation exchange capacity of mineral soils. As the clay content increases for a particular mineral soil, the cation exchange capacity usually increases. Although soil texture would be expected to have an influence upon the uptake of ^{90}Sr, the extent of its influence was unexpected. The colloidal organic matter in soils also exhibits a cation exchange capacity. As the percent organic matter increased, the ^{90}Sr content in the plant generally decreased. However, there were exceptions and in some cases the decreases in ^{90}Sr uptake were very small compared to magnitude of the organic matter content differences. The effect of organic matter upon the uptake of ^{90}Sr for the soils used in this study was considered of slight significance. The results indicate that the amount of ^{90}Sr entering the plant from a contaminated acid soil can be significantly reduced by liming, selection of a high clay content soil, and selection of plant species which is a low accumulator of Sr. (BBB)

3680 EXPERIMENTAL STUDY OF THE CLEARANCE OF COLLOIDAL ^{198}Au. TECHNICAL DATA AND RESULTS IN THE NORMAL DOG. Francois, B.; Maillet, P.; Aimard, G.; Brunerie, D. (Hopital de l'Antiquaille, Lyon). Pathol. Biol. Semaine Hop., 12: 854-6(Aug.-Sept. 1964). (In French).

The disappearance of colloidal ^{198}Au from the blood stream after a single injection depends on its uptake by the reticuloendothelial system, especially in the liver. The resulting blood disappearance curve is essentially an hepatic phenomenon. The process of fixation by liver depends on two distinct factors. These are the function of the reticuloendothelial system and the circulating status of the liver. Radiocolloidal ^{198}Au particles in gelatin suspension with a size range of 200 to 400 Å were injected intravenously into 25 dogs. Blood samples were taken starting at 4 min after injection and for each minute thereafter until 15 min after injection. Measurements of the radioactivity in the blood samples gave extremely variable results when plotted against time. The quality of the curves seemed to depend on the method of sampling. The smoothest curves were obtained when samples were obtained from the femoral vein. Values obtained from 15 of the normal dogs gave an average clearance time of

17.60 ± 3.51 min, with a range of 11.51 to 24.62 min. The values obtained were not related statistically to the wt of the animal, the amount of the gelatin injected, or the amount of the ^{198}Au mixture that was administered. The values obtained were closely comparable to values obtained previously in humans. These amounted to 14.75 ± 2.3 min, with an experimental range of 10.3 to 19.3 min. (BBB)

3681 THE CLEARANCE OF RADIOACTIVE COLLOIDAL GOLD IN THE DOG WITH A PORTO-CAVAL ANASTOMOSIS. PHYSIOPATHOLOGICAL CONCLUSIONS. Aimard, G.; Francois, B.; Maillet, P.; Metais, B.; Chabal, J. (Hopital de l'Antiquaille, Lyon). Pathol. Biol. Semaine, Hop., 12: 857-8(Aug.-Sept. 1964). (In French).

In normal dogs the value of the fractional clearance of radiocolloidal ^{198}Au by the liver was measured as 17.60%. In 11 dogs with a portocaval anastomosis the average clearance value was 14.69%. This small difference suggested that hepatic flow was not greatly altered by the operation. This would depend on how much the efficiency of removal of ^{198}Au by the liver or the blood flow itself had been altered. Probably the amount of blood was the most important factor. Two factors may have influenced the results obtained in these studies. One was that a secondary portal circulation may have developed after the anastomosis, and the other was that the filtration efficiency of the liver may have increased because of increased blood flow velocity. Comparison of the values obtained in this study with some results reported elsewhere indicated that it is not possible to measure variations in liver blood flow by comparison of clearance values before and after carrying out a portocaval anastomosis. (BBB)

3682 STUDIES OF ^{144}Ce METABOLISM IN LIVER CELLS OF RATS [Thesis]. Hansmann, M. Heidelberg, Univ., 1964. 31p. $2.00 Gmelin, AED-DISS. 64-739.

The distribution of carrier free ^{144}Ce in rat liver cells after intravenous injection was studied. Results are explained by a model with a compartment system. Cytoplasmic nucleoproteins function as the central compartment. (Gmelin Inst.)

3683 BIOPHYSICAL STUDIES OF PERSONS WITH DEPOSITS OF RADIONUCLIDES OF THE NATURAL Th SERIES [Thesis]. Grillmaier, R. E. Saarlandes, Ger., Univ., 1964. 115p. $2.00 Gmelin, AED-DISS. 64-484.

Excretion of ^{232}Th decay products in breath, urine, and feces of 44 Thorotrast patients was investigated. Results were compared with whole-body counting data. Four to eight percent of the total Th was excreted by respiration. On the average, the blood contains 8% of total ^{212}Pb and 0.5% of ^{224}Ra. Daily excretion with urine is 0.6% for ^{212}Pb, 0.022% for ^{224}Ra, and 0.0014% for ^{228}Ra. Data on elimination of decay products from deposits are presented. (Gmelin Inst.)

3684 ISOTOPE STUDIES OF THE BIOCHEMISTRY OF FRUCTOSE METABOLISM AND GLUCONEOGENESIS IN THE LIVER [Thesis]. Rauschenbach, P. Munich, Tech. Univ., 1964. 107p. $2.00 Gmelin, AED-DISS. 64-578.

Transmutation of ^{14}C-labeled fructose in liver after in vivo infusion is studied using a liquid scintillation counter. Methods for the determination of ^{14}C distributions in glucose are described. (Gmelin Inst.)

3685 L'EMPLOI DES RADIOISOTOPES EN SCIENCES NUTRITIONNELLES ET DES RAYONNEMENTS IONISANTS EN TECHNOLOGIE ALIMENTAIRE, STRASBOURG, 1–6 OCTOBRE 1962. (Uses of Radioisotopes in Nutritional Sciences and of Ionizing Radiation in Food Technology, Strasbourg, October 1–6, 1962). Les Journees Scientifiques du Centre National de Coordination des Etudes et Recherches sur la Nutrition et l'Alimentation. XII. Paris, Centre National de la Recherche Scientifique, 1963. 497p. (CONF-621005).

The 28 papers presented at the conference on the use of radioisotopes in nutritional sciences and in food technology are presented. The discussions that followed each paper are included. (J.S.R.)

Radiation Effects on Biochemicals

3686 (TID-22352) INHIBITION OF THE SYNTHESIS OF MACROMOLECULES BY ULTRAVIOLET RADIATIONS. Progress Report. Swenson, Paul A. (Massachusetts Univ., Amherst). [1965]. Contract AT(30-1)-3511. 5p. Dep. mn; CFSTI $1.00 cy, $0.50 mn.

It is proposed that the inhibition of β-galactosidase formation in cells irradiated prior to induction is the result of gene inactivation, by dimers acting as blocks to the synthesis of messenger RNA. The results of experiments on the effects of UV irradiation on bacterial cells showed this to be the case. (P.C.H.)

3687 THE EFFECT OF γ RAYS ON SERUM ALBUMIN. Colson, C. (Univ., Liege). Arch. Int. Physiol. Biochim., 73: 558-9(June 1965). (In French).

Serum albumin in aqueous solution (1 g/100 ml, pH 7) was irradiated with ^{60}Co γ rays in the presence of air. The sensitivity of the protein to trypsin and chymotrypsin was modified by irradiation. With weak doses, it increased due to an effect of denaturation revealed by measurement of viscosity. With strong doses, it decreased sharply due to aggregation and partial destruction of the protein by radiolysis. During irradiation a nonprotein material appeared (dialyzable, not precipitated by trichloracetic acid), formed at the expense of the serum albumin. The amino acids of the protein were, therefore, partially destroyed by γ rays. All were affected, but to various degrees. The most affected, in order of increasing sensitivity, were: threonine, serine, proline, cystine-cysteine, phenylalanine, tryosine, histidine, and methionine. This modification of the substrate entailed a decrease in sensitivity with regard to the enzymes. This effect became important only with strong doses; with weak doses, denaturation predominated. The uv absorption spectrum (3200 to 2500 Å) was greatly modified. Absorption increased, but the max at 2800 Å became less and less prominent, and finally disappeared completely. This spectral effect appeared to have no relation to the variation of enzymatic sensitivity. (BBB)

3688 ULTRAVIOLET LIGHT INHIBITION OF GALACTOSIDE PERMEASE INDUCTION. Brownell, Arnold S.; Witt, Dorothy M. (Army Medical Research Lab., Fort Knox, Ky.). Biochem. Biophys. Res. Commun., 21: 113-19 (Oct. 26, 1965).

Experiments are reported that fail to support the contention of Pardee and Prestidge that the inactivation of galactoside permease by uv is an all-or-none phenomenon. When E. coli was exposed to uv immediately before induction with thiomethyl-β-D-galactopyranoside (TMG), the reduction in the overall rate of synthesis of both galactoside permease and β-galactosidase by the cell population was basically of the same order at both inducer concentrations used and at all doses of irradiation tested. Therefore, if uv results in an all-or-none effect on induction, it must simultaneously affect the induction of both permease and β-galactosidase. However, results indicated that with the high concentration of inducer, the permease system was essentially superfluous for β-galactosidase induction. (H.G.D.)

3689 STUDY OF FORMATION OF HEMOLYTIC ANTIBODIES IN THE RABBIT. EFFECTS OF TOTAL IRRADIATION OR INJECTION OF LIPOPOLYSACCHARIDES. Flatt, J. P. (Univ., Lausanne, Switzerland). Helv. Physiol. Pharm. Acta, 64: C117-19(Oct. 1964). (In French).

Rabbits were irradiated with 500-R doses of x rays 24 hr after the injection of an antigen to study the effect of radiation on differences between the formation of 7S and 19S (γ-globulin) hemolytic antibodies. The formation of 19S antibodies provoked by an intravenous injection of 10^8 sheep erythrocytes/kg body weight was considerably diminished and retarded by irradiation. It was found, however, that the inhibitory effect of the irradiation could be suppressed to a great degree by the administration of 50 to 400 μg/kg of lipoid A, a lipid fraction obtained from lipopolysaccharide of Escherichia coli which acts as a powerful stimulant on the reticuloendothelial system, in-

volved in the production of antibodies. In comparison, when rabbits, immunized 10 to 13 weeks earlier with 1.6×10^8 sheep cells/kg, were injected with 50 to 100 μg/kg of lipopolysaccharide, the total amount of γ-globulin was significantly increased, to 2 to 30 times its amount before the injection. From these experiments, a relation between the stimulation of the reticuloendothelial system and the synthesis of 19S hemolytic antibodies was suggested. Under certain conditions, it is possible to compensate for the diminution of immunological response due to x rays by the administration of substances stimulating the reticulo-endothelial system. (BBB)

3690 CALCIFEROL ESTIMATION IN IRRADIATED YEAST AND MYCELIA. Knobloch, E.; Jelinek, V.; Auskova, R.; Bacik, Z. (Inst. for Pharmacy and Biochemistry, Prague). Int. Z. Vitaminforsch., 35: 1-9(1965). (In German).

The method developed for estimation of calciferol (vitamin D_2) in mixtures of irradiated yeast and mycelia in fodders consist of extraction, saponification, condensation with maleic anhydride, and adsorption chromatography on a MgO-Kieselguhr mixture with mineral oil as the stationary phase and 85% methanol as the mobile phase. The concentration of calciferol was measured by uv spectrophotometry. Use of MgO permitted the calciferol to be separated from the ergosterol most efficiently. The extraction was performed with ether in a soxhlet apparatus, followed by saponification of the extract in an inert atmosphere in the presence of a small amount of ascorbic acid. The unsaponified material was removed and condensed with maleic anhydride. This removed any tachysterol that had been produced during the irradiation, and resulted in products whose absorption maxima did not interfere with that of the calciferol. The solution was subjected to adsorption chromatography on a MgO-Kieselguhr mixture with hexane or heptane as the solvent. The course of elution was followed by measurement of the samples at a wavelength of 265 mμ. The fractions that contained vitamin D were combined, the hexane was evaporated off, and the residue was subjected to partition chromatography on a hydropholized Kieselguhr column with mineral oil as the stationary phase and 85% methanol as the mobile phase. The fractions that contained vitamin D, as shown by absorption at 265 mμ, were combined and evaluated. The sample should contain between 10000 and 20000 units. A colorimetric method leased on reaction with $SbCl_3$ can also be used to evaluate the vitamin D. (BBB)

3691 THE EFFECT OF CULTURE DENSITY ON THE FREQUENCY OF CHROMOSOME ABERRATIONS IN MOUSE FIBROBLASTS UNDER NORMAL CONDITIONS AND UNDER X IRRADIATION OF 35 r. Mitrofanov, Yu. A. (Inst. of Biological Physics, Moscow). Izv. Akad. Nauk SSSR, Ser. Biol., No. 5, 783-7(Sept.-Oct. 1965). (In Russian).

The increase in cell density from 6 to 20 cells per 750 μ^2 diminished the amount chromosome rearrangements in unirradiated cultures of mouse fibroblasts. The increase of cell density above 20 cells per 750 μ^2 had no practical effect on the number of abnormal cells in the culture. In dense cultures fewer cells were affected by x rays than in the sparse ones. The beginning of mitosis in cells cultivated in the dense cultures is accelerated as compared to the cells of sparse cultures, which puts them close to cells of embryonic tissues (in vivo). Fibroblasts of mouse embryos are in worse condition in vitro than in the organism of the animal (in vivo). Hence mutability is increased. (TCO)

3692 THE EFFECT OF MASSIVE DOSES OF 32 Mev PROTONS AND ^{60}Co GAMMA RADIATION ON SERUM ENZYME LEVELS OF WHOLE BODY IRRADIATED PRIMATES. Dalrymple, Glenn V.; Lindsay, Ian R.; Ghidoni, John J.; Kundel, Harold L.; Still, Edwin T. (School of Aviation Medicine, Brooks AFB, Tex.). J. Nucl. Med., 6: 588-93(Aug. 1965).

The effects of protons on serum levels of lactic dehydrogenase (LDH) and glutamic oxaloacetic transaminase (SGOT) were compared with the effects of γ- and x radiations on LDH and SGOT in Macaca mulatta. Animals were irradiated with 32-Mev protons (6500 or 6700 rad doses), ^{60}Co γ-rays (6500 rad doses), or 2-Mev x rays (802 rad doses). Enzymes were assayed in preparations from blood samples taken at 4 hr intervals up to 48 hrs post-irradiation. Increases in both LDH and SGOT levels were found in all groups, but more marked increases were observed at the higher doses of the proton- and γ-irradiated monkeys. The mechanism of elevation appeared to be a consequence of cell injury with subsequent leakage of enzyme into the blood stream. (H.G.D.)

3693 AGREEMENT BETWEEN CARCINOMA EXPERIMENTS IN VIVO AND LOW-ENERGY X-RAY IRRADIATION OF THE METALLOPROTEIN CARBONIC ANHYDRASE. Addink, N. W. H. (Philip's Gloeilampenfabrieken, Eindhoven, Netherlands). Nature, 207: 1271-2(Sept. 18, 1965).

The effects of x radiation on the metalloprotein carbonic anhydrase were examined in vitro and in vivo. Irradiation of aqueous solutions of the enzyme showed that: x radiation initiates the effect of bringing firmly bound Zn into the soluble ionogenic form and the activity of carbonic anhydrase is correlated with its content of firmly bound Zn. Clinical observations indicated that during prolonged radiotherapeutic treatment, the Zn content of the urine could increase from 0.5 ppm to 1.5 ppm. However, in carcinoma patients where the Zn content of whole blood was extremely low, radiotherapy did not increase the Zn content in urine. (H.G.D.)

3694 DEMONSTRATION OF IMMUNOLOGICAL DIFFERENCES BETWEEN GRAFFI AND GROSS LEUKEMIAS. Pasternak, G.; Hoelzer, B. (Institut fuer Kernforschung der Deutschen Akademie der Wissenschaften, Berlin). Neoplasma, 12: 339-55(1965). (In German).

Results of previous experiments according to which mouse leukemias induced by Graffi virus possess specific antigens were confirmed. Suspensions of irradiated leukemic tissue induced resistance to isologous cells of leukemias of the same viral origin in mice with different genotype. On the other hand, in AKR mice which were implanted with x irradiated tissues of spontaneous leukemia induced by Gross virus it was not possible to demonstrate resistance against isologous cells of this viral leukemia. Two leukemias induced in AKR mice by Graffi virus possessed the antigenic characteristics of Graffi leukemias; immunized AKR mice reacted specifically to isologous cells of Graffi leukemia. No cross reactions were noted between Graffi and Gross leukemias. After inoculation of isologous cells of Gross leukemia in AKR mice, in which resistance against Graffi leukemia could be demonstrated, generalized leukemias developed. In spite of the fact that generalized gross leukemia developed, the serum of these animals contained antibodies against cells of Graffi leukemias. Serological examinations supported these in vivo findings. By the test cytotoxicity and the indirect method of fluorescent antibodies it was possible to show that animals resistant to Graffi leukemia possess humoral antibodies which only react with cells of Graffi leukemia. Sera did not react with cells of spontaneous Gross leukemia of AKR mice. Results of several experiments in vitro suggest that spontaneous Gross leukemia possesses the characteristic antigens of experimentally induced Gross lymphoma of the C3H strain. The hypothesis is discussed according to which the inability of AKR mice to react to Gross leukemia may be caused by the development of immunological tolerance to specific antigens of these leukemias. (auth)

3695 THE EFFECT OF X-IRRADIATION ON THE TAKE AND GROWTH OF THE GUERIN-TUMOUR. I. BIOLOGICAL EXPERIMENTS. Unger, E. (National Research Inst. for Radiobiology and Radiohygiene, Budapest). Neoplasma, 12: 417-23(1965).

Results are reported from a study in rats of the take and growth of florid and necrotic parts from the Guerin-tumor, both after transplantation of a previously irradiated tumor and after local x irradiation of a normally transplanted tumor in the recipient. Tumors seldom took in the first case, while tumor-take occurred almost always in the sec-

ond, despite local irradiation. Take was delayed in both groups as compared to the control. Consequently, the survival of animals was also prolonged. In addition to this, an appreciable slackening in the growth of the tumor was observed in a part of the cases in both experiments. (auth)

3696 STUDIES ON THE LEUKEMOGENESIS OF MOUSE LEUKEMIA BY X IRRADIATION. PART I. CHANGES IN THE PRELEUKEMIC STAGE. Sota, Susumu (Okayama Univ. Medical School, Japan). Okayama Igakkai Zasshi, 77: 1-23(Jan. 1965). (In Japanese).

To clarify the process of leukemogenesis by x rays, observations were carried out on peripheral blood cells and on the histological changes of hematopoietic organs from time of x irradiation to the onset of leukemia in mice. After one whole-body irradiation of 350 R in mice of the RF strain, leukemia developed in 77.3%; 75.4% had lymphocytic leukemia and 1.8% myelogenous leukemia. After the x irradiation, these mice showed hypoplasia of hematopoietic organs, followed by a compensatory proliferation. In the preleukemic stage, a decrease in total leukocyte counts and an increase in eosinophil counts were observed. In addition, the spleen, lymph nodes, and thymus showed findings that could be histologically considered as leukemia, but tissue culture findings suggested a transient stage of hypoplasia. From these findings it is concluded that leukemia induced by x irradiation originates in the thymus in the case of lymphocytic leukemia of the thymoma type, while in lymphocytic leukemia of the nonthymoma type, leukemia makes its appearance first in the spleen or in lymph nodes after passing through a hypoplastic stage. (TCO)

3697 BINDING OF RADIOCALCIUM (^{47}Ca) AND RADIOSTRONTIUM (^{85}Sr) WITH SERUM PROTEINS. Guerin, M.-Th.; Guerin, R. A. (Institut National de Sante et de Recherche Medical, Paris). Pathol. Biol. Semaine Hop., 13: 297-301(Mar. 1965). (In French).

Binding of ^{47}Ca and ^{85}Sr was studied by precipitation of serum proteins labeled in vivo, and by electrophoresis after labeling in vitro. After electrophoresis in Veronal buffer, samples of serum labeled with ^{47}Ca from two human subjects showed the following distribution between proteins: the γ-globulin radioactivity was 19.8 and 13.6%, the β-globulin fraction contained 72.2 and 81.9%, the α_2-globulin fraction contained 3.3 and 1.7%, the α_1-globulin fraction contained 1.3 and 1.1%, and the albumin fraction contained 3.2 and 1.6% of the total ^{47}Ca bound by the proteins. Only 41% of the ^{47}Ca in serum was bound by the proteins. In Tris-EDTA buffer the pattern of distribution after electrophoresis was different. The amounts of ^{47}Ca bound by the globulin fractions from the sera of the two human subjects were as follows: γ-globulin, 2.0 and 3.0%; β_1-globulin, 18.1 and 8.8%; β_2-globulin, 57.8 and 70.5%; β_3-globulin, 5.1 and 2.9%; α_1-globulin, 1.8 and 1.3%; α_{2A}-globulin, 1.8 and 1.2%; and α_{2B}-globulin, 1.4 and 1.8%. The albumin was associated with 10.5 and 11.5% of the ^{47}Ca bound by protein. When ^{85}Sr was studied, almost all of it was found to be totally dissociated from serum proteins. Only a trace was bound by the serum proteins. The differences found in protein binding of ^{47}Ca and ^{85}Sr may be related to differences observed in their deposition and excretion. (BBB)

3698 RESTORATION OF CYTOPLASMIC STREAMING AS SOON AS POSSIBLE AFTER IRRADIATION. Gillet, C. (Univ., Liege). Protoplasma, 60: 24-30(1965). (In French).

Thirty isolated internodal cells of Nitella flexilis were irradiated in the presence of air by 50-kv x rays at doses of 100, 250, 500, or 750 kR. After 100 and 250 kR, cyclosis was only $1/15$ to $1/19$ as fast as normal, but within 20 min, had returned almost to normal. After 500 to 750 kR, cyclosis was only $1/22$ to $1/27$ normal speed. Recovery was slow, cyclosis being below normal an hr later. Superimposed on the general recovery of cyclosis was a variation in speed, accentuated by increasing irradiation doses. During the first minutes of recovery, cyclosis was slowed for a short period after 100 and 250 kR, but slowed for a longer time after 500 to 750 kR. The rapid phase of recovery was due to restoration of the protoplasmic viscosity. The slower recovery phase was due to restoration of the motive force. The periods of the two recovery processes increased exponentially with the increase in radiation dose. When represented in graphical form (periods, in sec, vs doses, in kR), the two curves of restoration were almost parallel. Processes superimposed on cyclosis temporarily altered it. Cytoplasmic zones of varying viscosity were induced by irradiation and caused variations in the protoplasmic streaming. The marked slowing of cyclosis after 500 and 750 kR remains unexplained. (BBB)

3699 THE EFFECT OF ^{60}Co γ RADIATION ON RESPIRATION OF AEROBIC BACTERIA [Thesis]. Winterhoff, D. H. Muenster, Ger., Univ., 1965. 59p. $2.00 Gmelin, AED-DISS. 65-26.

The influence of ^{60}Co γ radiation on the oxygen consumption of various bacteria was studied. Bact. pyoc. had the highest radiosensitivity of the species studied. Growth was inhibited after irradiation with 70 kR. (Gmelin Inst.)

3700 EXPERIMENTAL STUDIES OF LUNG CHANGES AFTER IRRADIATION WITH 180 kv X RAYS, FAST ELECTRONS, AND ^{60}Co γ RAYS [Thesis]. Graf, G. Marburg, Ger., Univ., 1964. 44p. $2.00 Gmelin, AED-DISS. 64-735.

Albino rats were irradiated with 180 kv x rays, 17 Mev electrons, and ^{60}Co γ rays in three groups with 3000 rad total dose. The first group was irradiated with fractionated doses of 6×500 rad, the second group with single doses, and the third fractionated with 3×1000 rad. Histological lung changes were equivalent in all groups. However, they occurred more rapidly in the third group than in the first. (Gmelin Inst.)

3701 DNA SYNTHESIS AND RADIATION EFFECTS. EXPERIMENTAL STUDIES WITH TRITIATED THYMIDINE IN NORMAL TISSUE AND IN TUMORS [Thesis]. Feine, U. Tuebingen, Ger., Univ., 1964. 167p. $2.00 Gmelin, AED-DISS. 64-582.

Incorporation of tritiated thymidine in normal tissue and in Yoshida sarcomas of rats was studied. For DNA synthesis inhibition in tumors and normal tissue, a linear dose relation was found between 100 and 800 R. It is concluded that the radiosensitivity of mitosis is not caused by DNA synthesis but by some other process, which takes place at about the same time. (Gmelin Inst.)

3702 AUTORADIOGRAPHIC STUDIES OF THE RADIATION SENSITIVITY OF DNA SYNTHESIS WITH YOSHIDA ASCITES SARCOMA CELLS [Thesis]. Knodel, W. Tuebingen, Ger., Univ., 1964. 33p. $2.00 Gmelin, AED-DISS. 64-483.

Incorporation of ^{3}H-thymidine in ascites sarcoma cells was studied. Abdominal irradiation with 1000 R inhibited ^{3}H-thymidine incorporation after 3 hrs. It is concluded that synthesis inhibition is independent of thymidine concentration. (Gmelin Inst.)

3703 THE INFLUENCE OF WHOLE BODY IRRADIATION ON THE SYSTEM HYPOTHALAMUS—POSTERIOR PITUITARY LOBE OF THE LOIR (GLIS GLIS). STUDIES DURING HIBERNATION AND APPLICATION OF CYSTEINE AFTER IRRADIATION [Thesis]. Nyire Nya, E. U. Hamburg, Univ., 1964. 40p. $2.00 Gmelin, AED-DISS. 64-486.

Neurosecretion was studied in the hypothalamus pituitary system after whole body irradiation with 1000 R normally and during hibernation. For normal animals neurosecretion was decreased in the central region after 4 days. In animals irradiated during hibernation a decrease of neurosecretion on the frontal section of the posterior lobe was observed. No protective action of cysteine was detected. (Gmelin Inst.)

3704 I. IN VITRO STUDIES ON THE EFFECTS OF X-IRRADIATION ON THE PHYSICO-CHEMICAL PROPERTIES OF SERUM LIPOPROTEINS. II. IN VIVO EFFECTS OF X-IRRADIATION ON MOUSE PLASMA LIPIDS. III. IN VITRO EFFECTS OF INCUBATION AND ETHYL ETHER ON THE PHYSICO-CHEMICAL PROPERTIES OF SERUM

LIPOPROTEINS [Thesis]. Rehnborg, Carl Samuel. Berkeley, Calif., Univ. of California, 1964. 133p.

In part I, the possible role of membranes in radiobiological phenomena is reviewed. In order to ascertain what effects low doses of ionizing radiation have on lipid-protein interactions, the following systems were studied: (1) the binding of fatty acids to albumin, (2) the physicochemical properties of serum lipoproteins, and (3) the ethyl ether degradation of high density lipoproteins (HDL). In all three cases and in all parameters studied, no significant differences between control and irradiated samples were observed. The significance of these findings is discussed and suggestions for further work are offered. In part II, the blood lipid changes in mice subjected to whole-body x irradiation were investigated and compared with the lipid response observed in the fasted mouse. When the fasting mouse was subjected to either whole-body x irradiation or to an intraperitoneal (IP) injection of methyl oleate, the normal elevation of albumin-bound unesterified fatty acids (UFA) did not occur. It is postulated that the protective effect of an IP injection of methyl oleate in the midlethally irradiated mouse is due to RES stimulation by methyl oleate. In part III are presented the results of experiments in which the lipid chemistries of the three major lipoprotein species (S_f20-10^5, S_f0-20, HDL) were determined after the incubation of human serum at 38°C for 36 hours. The extraction of lipids from HDL and S_f0-20 lipoproteins by ethyl ether at room temperature was also investigated. (A.G.W.)

Radiation Effects on Tissues

Refer also to abstract 4188.

3705 (AD-617601) CHROMOSOMAL DAMAGE IN HUMANS PRODUCED BY X-IRRADIATION. Annual Progress Report. Louro, Jose M. (Brooke General Hospital, Fort Sam Houston, Tex.). 1964. 44p. CFSTI $2.00 cy, $0.50 mn.

Results from the first year of a three year study of the effects of x irradiation on the chromosomes of human subjects are reported. The purpose of the study is to determine if chromosomal damage can be used as a means of estimating the amount of irradiation a person has received. The three year study is divided into three periods: analysis of spontaneous chromosomal damage and aberrations occurring in normal, non-irradiated human subjects; analysis of chromosomal aberrations in human subjects receiving large amounts of x irradiation; and evaluation of chromosomal aberrations as a dosimeter in human subjects receiving serial x irradiation. (TAB)

3706 (AD-623365) EVIDENCE FOR HUMORAL MEDIATION OF RADIATION-INDUCED MOTIVATION OBTAINED FROM PARABIONT RATS. Hunt, E. L.; Carroll, H. W.; Kimeldorf, D. J. (Naval Radiological Defense Lab., San Francisco, Calif.). Aug. 25, 1965. 22p. (USNRDL-TR-891).

Parabiotic rat pairs with a skin-vascular anastomosis were used to test for a radiation-induced transferrable humoral factor which would motivate aversive conditioning in a non-irradiated (shielded) recipient. The shielded partner, by tasting saccharin-flavored fluid shortly after its partner was x irradiated (360 R), was aversively conditioned to saccharin. This was interpreted as evidence for a humoral factor. (auth)

3707 (AD-623641) AN ANALYSIS OF LOCAL AND SYSTEMIC EFFECTS OF IONIZING RADIATION ON BONE GROWTH. Phillips, R. D.; Kimeldorf, D. J. (Naval Radiological Defense Lab., San Francisco, Calif.). Sept. 3, 1965. 23p. (USNRDL-TR-898). CFSTI $1.00 cy, $0.50 mn.

Radiation-induced retardation of femur and tibia growth was determined in young male rats at 60 days after total- or partial-body exposure to 450 R of x rays. Approximately 52% of the growth reduction could be attributed to local irradiation effects on the limb, and the remaining 48% of the retardation was ascribed to systemic irradiation effects. The systemic response did not appear to be dependent upon the mass of tissue irradiated, nor upon the induction of postirradiation partial inanition. However, the region of the animal exposed did appear to be important. By exposing various regions of the body, the systemic response was subdivided into abscopal components. Head, abdomen, and thorax irradiation yielded 42%, 40%, and 18%, respectively, of the total systemic effect. The local and abscopal responses appeared to be additive rather than synergistic, with the total radiation effect the resultant sum of the abscopal and local components. (auth)

3708 (CEA-R-2833) ETUDE CRITIQUE DE QUELQUES MATERIAUX EQUIVALENTS AUX TISSUS MOUS. SENSIBILITE AUX NEUTRONS DE 1 kev A 14 Mev. (Critical Study of Some Soft-Tissue Equivalent Material. Sensitivity to Neutrons of 1 kev to 14 Mev). de Kerviler, Herve; Pages, Lucien; Tardy-Joubert, Philippe (Commissariat a l'Energie Atomique, Saclay (France). Centre d'Etudes Nucleaires). July 1965. 14p. Dep. mn.

The elastic and inelastic reactions of various elements contributing to kerma in standard soft tissue of mice were studied and as a function of neutron energy from 1 Kev to 14 Mev. The ratio of kerma in tissue equivalent material to kerma in soft tissue was also measured. The results of calculations are presented for materials without hydrogen in order to state exactly their neutron sensitivity and for the following hydrogeneous materials: Rossi and Failla plastic, MixD, pure polyethylene, and a new CEA tissue equivalent material, a magnesium fluoride and polyethylene compound. Results for γ rays are included. (tr-auth)

3709 (CEA-R-2865) ACTION DU FRACTIONNEMENT DE 100 R DE RAYONS X SUR L'HEMOGRAMME ET LE PROTEINOGRAMME DU LAPIN. (The Effect of Fractionating 100 R Hard X-ray Doses on the Hemogram and Proteinogram of the Rabbit). Alix, Denise (Commissariat a l'Energie Atomique, Grenoble (France). Centre d'Etudes Nucleaires). Sept. 1965. 22p. Dep. mn.

Eighty-one rabbits received total exposure of 50 to 200 R x rays, by fractional doses of 5, 10, 25, 50 and 100 R per irradiation. Blood count and blood protein content were determined before, during, and after the irradiation time. Seventeen controls were subjected to the same investigations with the same periodicity. Statistical analysis of experimental data indicated that irradiation induces drop in the leukocyte count, resulting from a drop in mononuclear cells. It is more difficult to determine its action on the protein profiles because the observed changes were likewise observed on the controls, although at a lesser degree. Results indicated an increase of albumin concentration and some instability of the γ-globulins concentration. The possible mechanisms of x rays effects including perturbations of protein metabolism following loss of mitotic activity and histolysis are discussed. (tr-auth)

3710 (EUR-2493.e) APPLICATION OF ATOMIC ENERGY IN AGRICULTURE. Annual Report, 1964. (Instituut voor Toepassing van Atoomenergie in de Landbouw, Wageningen (Netherlands)). 1965. 68p. Dep. mn.

The EURATOM-ITAL Association research activities during 1964 are reviewed. Emphasis was placed on studies concerned with problems of radiation induced changes in plants, food preservation by means of ionizing radiations, the behavior of specific chemical elements in soils and plants, and the improvement of nuclear techniques for agricultural research. (auth)

3711 (NYO-3314-2) GENETIC CONTROL OF AGING AND RADIATION-INDUCED LIFE SHORTENING IN MICE. Progress Report, January 1–September 30, 1965. Storer, John B. (Roscoe B. Jackson Memorial Lab., Bar Harbor, Maine). Contract AT(30-1)-3314. 9p. Dep. mn; CFSTI $1.00 cy, $0.50 mn.

Progress is reported in studies of the natural rate of aging of mice, the effects of various doses of x radiation on the life span of mice, the rate of accumulation of mutations with age, and the effects of mouse strains on sensi-

tivity to radioinduced mutations. Results are included from studies of the incidence of chromosome aberrations in regenerating liver of several mouse strains with increasing age, strain differences in the incidence of lethal mutations in spermatozoa with increasing age, the effects of 200 R x radiation on the incidence of chromosome aberrations in regenerating liver of mice of different strains, and the effects of exposure of male mice to 600 R x radiation on the viability of embryos produced following mating to females of similar or different strains. (C.H.)

3712 (JPRS–31514) STUDIES IN GENETICS. Lobashev, M. E. Translated from Issled. Genet., No. 2, 3-20; 46-85; 125-39(1964). 115p. (TT–65-32010). CFSTI $4.00 cy, $0.75 mn.

A translation of 9 articles from the Russian-language publication "Research on Genetics" is presented. Separate abstracts were prepared for 5 articles. Other articles discuss the genetics of behavior in animals and results of studies on plant genetics. (C.H.)

For abstracts of individual sections see: 3713–3717.

3713 (JPRS–31514, pp 29-43) INDUCED MUTATION PROCESS—THE EFFECT OF HIGH TEMPERATURE AFTER IRRADIATION ON THE FREQUENCY OF OCCURRENCE OF LETHAL MUTATIONS AND CHROMOSOMAL BREAKS. Vatti, K. V.; Yanoosh, I. M. Translated from Issled. Genet., No. 2, 46-55(1964).

The consecutive action of high temperature (+37°) within one hour after irradiation of Drosophila larvae with x rays in a dosage of 100 R causes potential chromosomal injuries and sharply increases the frequency of lethal mutations (2.3 times) in comparison with their sum under the action of temperature and x rays separately. The relative amount of potential damage exceeds by 1.53 times the number of actual lethal mutations. Under the conditions of a high spontaneous level of chromosomal breaks x rays in the same dosage of 100 R do not cause actual breaks, producing only potential chromosomal breaks caused by high temperature. Their relative amount is equal to 0.73. The facts which have been derived emphasize that the state of the after-effect of low radiation dosages is characteristic both for lethal mutations and for chromosomal aberrations. The after-effect is hypothetically explained by the presence of both potential chromosomal injuries as well as their high capacity for closing the initial breaks. (37 references.) (tr-auth)

3714 (JPRS–31514, pp 44-58) NON-DIVERGENCE OF CHROMOSOMES UNDER THE INFLUENCE OF X-RAYS OF VARIED HARDNESS AND INTENSITY. Tikhomirova, M. M. Translated from Issled. Genet., No. 2, 56-64(1964).

During the irradiation of female imagoes of Drosophila the predominance of XO males is observed in the progeny in comparison with XXY females (3.44 ± 0.147% and 0.20 ± 0.034%). The hard x rays applied in the experiment (200 kv) cause not only actual but also potential and long-duration breaks (no less than one hour), which is confirmed by the great frequency of the appearance of males (2.81 ± 0.163%) in this group in comparison with the frequency of their appearance in a group where the irradiation was effected with soft rays (1.84 ± 0.124% and 0.97 ± 0.128%). In addition to this, the males appear with great frequency (4.45 ± 0.379%) in a group where there is additional high temperature (37°) within one hour after the irradiation with hard rays. The effect of the hard-ray after-effect is detected for a period of one hour, and not detected within two hours after irradiation. Soft rays (voltage of 50 kv) cause the appearance of rapidly repairable chromosome breaks which are maintained for less than 30 minutes, a fact which is corroborated by the absence of after-effect (1.84 ± 0.124% and 1.76 ± 0.145%; 0.97 ± 0.128% and 1.29 ± 0.161%) and by the effect of the intensity. Soft rays of high intensity (1932 r/min) are more effective (1.84 ± 0.124%) than those same rays of lesser intensity. Possible mechanisms involved in the primary non-divergence of X-chromosomes during irradiation of Drosophila females are discussed. (54 references.) (tr-auth)

3715 (JPRS–31514, pp 59-64) A COMPARATIVE STUDY OF THE RESULT OF RADIATION AFTER-EFFECTS ON CHROMOSOMAL NON-DIVERGENCE. Tikhomirova, M. M.; Dubrova, S. E.; Yanoosh, I. M. Translated from Issled. Genet., No. 2, 65-8(1964).

X rays caused an after-effect on the non-divergence of X-chromosomes in two comparable lines of Drosophila. The after-effect result proved to be higher in the radioresistant w^a line in comparison with the Canton-S line. (tr-auth)

3716 (JPRS–31514, pp 65-76) A COMPARATIVE STUDY OF THE MUTAGENIC ACTION OF DIFFERENT TYPES OF RADIATION AND ETHYLENEIMINE ON THE ALGA CHLORELLA. Khropova, V. I.; Kvitko, K. V.; Zakharov, I. A. Translated from Issled. Genet., No. 2, 69-76(1964).

The dependency of the frequency of induced pigment mutations in Chlorella upon the survival capacity of cells proves to be linear under irradiation with varied dosages of x rays. During the action of ethylenimine the dependency of the frequency of the mutation upon the survival capacity coincides with that for x rays. The dependency curve for ultra-violet rays is S-shaped. Under dosages which produced a high mortality rate of the cells, ultra-violet rays prove to be the most effective mutagen; under doses which induce less than a 90% mortality rate x rays and ethylenimine are more effective in inducing pigment mutations. A relative specificity is observed in the action of mutagens. For comparable mutagens the ratio of the number of apple-green mutants to the number of yellow is highest under the action of ultra-violet rays (especially during photoreactivation) and lowest under the action of ethylenimine. (26 references.) (tr-auth)

3717 (JPRS–31514, pp 77-91) COMPARISON OF THE SPECIFICITY OF THE ACTION OF ULTRA-VIOLET RAYS AND X-RAYS ON THE MUTABILITY OF YEAST. Ingevechtomov, S. G.; Kozhin, S. A. Translated from Issled. Genet., No. 2, 77-85(1964).

Mutations requiring adenine with a simultaneous accumulation of red pigment in the yeasts Saccharomyces cerevisiae take place in two loci which have been conditionally designated ad_1 and ad_2. Under the action of x rays and ultraviolet rays locus ad_2 mutates two to three times more frequently than locus ad_1. In comparing the action of x rays and ultraviolet rays on loci ad_1 and ad_2 the differences in the specificity of the action of these agents was not detected either at the gene or intragene levels. (20 references.) (tr-auth)

3718 IRRADIATION OF LYMPH NODES AND VESSELS: EXPERIMENTS IN RATS, WITH REFERENCE TO CANCER THERAPY. Engeset, Arnfinn (Norsk Hydro's Inst. for Cancer Research, Oslo). Acta Radiol. Diagn., Suppl. 229: 125p.(1964).

Radiation damage to the lymphatic system in 3-month-old rats was followed after x irradiation of the right knee node or of the renal nodes on the right side. The standard dose measured in the lymph node was 3000 R. Animals were examined at various intervals from 12 hours to 88 weeks after irradiation. Whole-body irradiation and fractionated local irradiation were compared. The weight of the irradiated knee node decreased as compared to the controls. The difference was demonstrable 2 weeks after irradiation and increased with time. Microscopy of the nodes the first day after irradiation revealed a severe degeneration of lymphocytes and disappearance of the follicles. At 24 hr the nodes were almost completely restored, but contained few mitoses, fewer mast cells than the controls, and no germinal centers. The germinal centers reappeared a few days after the irradiation, and after 8 weeks the granulated mast cells were again abundant. Secondary atrophy was observed after about 2 weeks. It progressed slowly and was manifested by gradual disappearance of lymphocytes, germinal centers, and follicles. There was a simultaneous increase in connective tissue which led to almost complete eradication of the structure of the node after 9 to 12 months. Three days after whole-body irradiation with 600 R there was considerable accumulation of intravascular granulocytes in the node, but this reaction did not occur in nodes irradiated locally, 4,

18, 30, or 56 weeks previous to whole-body irradiation. A reduction in the number of blood vessels was related to the late disappearance of lymphocytes from the nodes. The barrier function of the lymph nodes was reduced after irradiation for both human erythrocytes (smallest diameter about 7 μ) but not for charcoal particles (smallest diameter about 60 μ). The failure of the barrier function was demonstrable 2 weeks after irradiation. Intralymphatic injection of Walker carcinoma cells distal to the irradiated node led to more pulmonary metastases in the irradiated animals than in the controls and equal numbers of tumor takes in the nodes in both groups. An inflammatory reaction induced with diphtheria-tetanus-pertussis vaccine spread more readily through the irradiated than through the unirradiated nodes at 2, 16, and 30 weeks after irradiation. The clinical implications of the findings are that irradiation of a lymph node area should be performed only for lymph node metastases, and that surgery after pre-operative irradiation of lymph nodes should be performed before the barrier function is seriously impaired. (BBB)

3719 STUDIES OF CORNEAL GRAFT REACTION: EFFECT OF X-IRRADIATION OF THE DONOR TISSUE. **Narain, L.; Baker, D. G.; Basu, P. K. (Univ. of Toronto). Amer. J. Ophthalmol., 59: 799-802(May 1965).**

This study was designed to determine whether x irradiation of the donor cornea prior to grafting would modify the corneal graft reaction. To elicit a standard and reproducible graft reaction in rabbits, bovine corneal tissues were used. Following sterilization by the usual eye-bank procedure, one eye out of the pair was irradiated and the other was not. The nonirradiated eye served as the control donor material. One whole eyeball was exposed to 250-kv x rays at a dose rate of 160 R/min to doses of 62.5 to 2000 R. Each rabbit received one irradiated corneal disc in the right (experimental) eye and one nonirradiated disc in the left (control) eye. Histologically, no grossly identifiable difference was found between the irradiated and nonirradiated corneal tissue. In tissue culture, all irradiated corneas were viable. Corneas which received a 2000 R dose had long latent period (10 to 12 days) before any cellular growth was observed. Thereafter, within two to four days, mitosis stopped and the cells gradually died. Cytologic preparation from the out-growths showed pleomorphic cells with multiple nuclei and chromosomal abnormalities. In tissue culture, corneas irradiated at 1000 R behaved in the same manner but suitable chromosome preparations could not be made. Corneas irradiated with 500- and 250-R doses showed abnormal cells in vitro, but those irradiated with 125 and 62.5-R doses showed no cellular change and normal chromosomes. In the control eye, the graft rejection reaction started about the 10th to 12th day after operation and was fully established by the 18th to 21st day. In the experimental eyes receiving grafts irradiated with 250 to 2000 R, the time of onset of the reaction was shorter and the intensity of graft reaction was more severe as compared to the control eyes. The results indicate an increase of the antigenicity of heterologous corneal grafts following irradiation of the donor material, possibly on account of denaturation of the corneal proteins. Cytologic preparations from the donor corneal tissues irradiated at and above 250 R showed large numbers of abnormal cells. The enhanced graft reaction could possibly be attributed to changes in the antigenicity of the irradiated tissue as a result of altered cytology. Another possible explanation for the early and severe graft reaction to irradiated cornea would be their enhanced permeability, leading to escape of increased quantities of antigenic tissue constituents, as it is known that irradiation causes increased permeability of the cell membrane. (BBB)

3720 RADIATION INJURY TO THE INTESTINAL TRACT. **Rosenblum, Earl. Amer. J. Proctol., 16: 280-5(Aug. 1965).**

Injury to the intestinal tract following irradiation for pelvic malignancy is reviewed and a new case is presented. Incidence of such damage is reported in 2.1% to 17.7% of cases treated or gynecologic malignancies. The factors responsible for radiation injury are discussed. (BBB)

3721 SIZE CONSTANCY AS A FUNCTION OF AGEING AND X-RAY IRRADIATION IN RHESUS MONKEYS. **Davis, Roger T.; Lovelace, William E.; McKenna, Virgil V. (Univ. of South Dakota, Vermillion). Anim. Behav., 12: 16-24 (Jan. 1964).**

Size constancy was studied in three groups of rhesus monkeys: young nonirradiated monkeys, old nonirradiated monkeys, and old chronic survivors of whole-body irradiation with large doses (1100 R, in three fractions). The animals were given a discrimination problem involving 6-in. and 9-in. squares placed at various distances from the subjects in a homogeneous background. The performance of subjects reached a level comparable to that of nonconstancy trials between the 32nd and 42nd constancy trials. The old nonirradiated monkeys required an average of 36.2 days, the young ones 46.2, and the old irradiated ones 61.0 days to meet all five criteria of preliminary training. The performance of the old nonirradiated monkeys was significantly better than that of either the young nonirradiated or old irradiated ones. Both the old nonirradiated and young monkeys were significantly less likely than the old irradiated ones to have errors attributable to a response based on confusion of size because of visual angle. Several error-producing factors were considered as alternative to the size of the visual angle. Of these the distance between subject and the large square had nearly as much error-producing potential as visual angle. The results were interpreted as supporting the position that a perception represents one problem of many on a continuum of a learning set. (TCO)

3722 CANCERS OF THE BILE DUCT IN THOROTRASTOSIS OF THE LIVER. **Batzenschlager, A.; Keiling, R.; Kuntzman, F. (Institut d'Anatomie Pathologique, Strasbourg). Ann. Anat. Pathol., 6: 457-78(Oct.-Dec. 1961). (In French).**

Two complete clinical and pathological reports of epithelial cancers with thorotrastosis are presented. Sixteen yr after arteriography, a 64-yr-old man developed an epithelioma of the intrahepatic biliary ducts as a result of Thorotrast deposition in the liver, with cirrhosis. In the second case, 17 yr after arteriography, a 29-yr-old man developed an epithelioma of the biliary ducts of the liver, associated with a large Thorotrast-induced granuloma. The carcinogenic role of the Thorotrast is discussed. Morphological relations between Thorotrast-induced and other hepatic and hepato-biliary cancers, based on the nature of the cancers and the topography of the thorotrastic deposits, are reviewed. Since the range of α particles emitted by Th in tissue deposits of ThO_2 is 2.62 cm, topographical factors are of great importance. Causal relations between ThO_2 deposits, Thorotrast-induced sclerosis, and cancer are discussed. Statistical comparison is made between the incidence of cirrhosis of the liver, primary cancer of the liver, and cancer of the extrahepatic biliary ducts, with and without generalized thorotrastosis. From these data, the carcinogenic role of Thorotrast seems proven, whether by a direct ionizing action of Th or indirectly by an irritative action in the intermediary stage, thorotrastic sclerosis. (BBB)

3723 STUDIES ON INDUCED MUTANTS OF CORYNEBACTERIUM FASCIANS AND ON THEIR PATHOGENICITY IN COMPARISON WITH THAT OF NATURAL STRAINS. **Jacobs, S. E.; Habish, H. A.; Dadd, A. H. (Imperial Coll. of Science and Tech., London). Ann. Appl. Biol., 56: 161-70(Aug. 1965).**

After uv irradiation, colon-type, non-pigmented and nutritional (auxotrophic) mutants of C. fascians were isolated from a highly virulent s rain. Irradiation was carried out by exposing a bacte al suspension to uv light for 10-11 min at a distance of 30 in. from a Hanovia bactericidal lamp. The dose selected killed 99 to 99.9% of the cells. Following irradiation the suspensions were incubated for 2-3 hr in a dark chamber to prevent photoreactivation. The irradiated suspensions were spread on the surface of nutrient agar plates and incubated for 4 to 5 days at 25°C. Colonial type mutants were selected from colonies which differed in shape or color from that of the

parent strain. Biochemical mutants which were auxotrophic were obtained by the random isolation method in which colonies growing on the complete medium were tested for their ability to grow on the minimal medium. The auxotrophs selected had single requirements for glycine, aspartic acid, arginine, methionine, creatine, or adenine and the amount of their growth in a minimal medium adequate for the parent strain was controlled by the amount of the respective nutrients added. Results indicated that the pathways by which C. fascians synthesizes the substances (with the exception of methionine) required by the mutants were those already known for other microörganisms. The induced auxotrophic mutants were examined, in comparison with natural or wild strains, for ability to infect sweet pea seedlings and to grow in the environment provided by the host. The mutants were avirulent or weakly virulent unless the specific nutrient was added, and this was correlated with the amount of growth made by the mutants in an aqueous extract of the host tissue. Addition of the specific nutrient improved the growth of the mutant, suggesting that avirulence was due, at least in part, to the inability of the pathogen to grow sufficiently in the host environment. (BBB)

3724 HIGH-ENERGY ELECTRON INJURY FROM ACCELERATOR MACHINES (CATHODE RAYS): RADIATION BURNS OF CHEST WALL AND NECK: 17-YEAR FOLLOW UP OF ATOMIC BURNS. **Brown, James Barrett; Fryer, Minot P. (Washington Univ., St. Louis). Ann. Surg., 162: 426-36(Sept. 1965).**

A description, with numerous illustrations, is given of the development and treatment of burns in persons using cathode rays and in patients undergoing β-ray therapy, and the present status of research workers receiving radiation burns at Eniwetok is described. One cathode-ray burned patient showed breakdown in irradiated areas within 4 years. He required replacement of the skin of the nose, upper and lower lips, left forehead, neck, chin, right abdomen, and fingers. Two other patients have had resection and grafting, required because of chronic radiation burn. Pathologic studies of the skin show chronic radiation dermatitis, with telangiectasis, atrophy or focal homogenization of the dermis, and loss of skin appendages. Vessel walls show hyalinization and arteritis and marked endophlebitis. Some vessels are completely thrombosed and nearby arteries have hyalinization of the media; surrounding these vessels the derma is fibrosed as subepidermal hyaline fibrosis. Keratosis, atrophy of the epithelium and dermis, loss of skin appendages, telangiectasia or thrombosed vessels just below the epithelium are also seen. Radiation injury of the chest wall and neck following radiation treatment of carcinoma of the breast is also considered. Loss of the skin and necrosis of cartilage and bone with open lesions have resulted. Secondary breakdown sometimes required widespread removal of skin, muscle, bone, and cartilage of the chest wall. A 17-year follow up of the progress of the surgical repair in atomic radiation injuries that were reported in 1956 is given. The research workers that suffered these burns at Eniwetok were cared for at Los Alamos and later at the Barnes Hospital in St. Louis. They have returned to full-time investigative work, and none of the 40 fingers that were involved were lost, but have been saved with resection and repaired with thick, split skin grafts. This record of repair of these hands is better than that of the high energy electron injuries where they were losses of parts of the fingers because there was no circulation left in them. (BBB)

3725 RADIATION AND RADIOMIMETIC CHLORAMBUCIL AND THE FETAL RETINA. **Rugh, Roberts; Skaredoff, Ludmila (Columbia Univ., New York). Arch. Ophthalmol., 74: 382-93(sept. 1965).**

Retinal development was followed in mice, rats, and monkeys exposed to x rays at various stages of gestation. An instance is also reported of exposure of a human embryo to chlorambucil at three to four week of gestation. Exposure time for the three animal species varied: mice from 10.5 to 16.5 days gestation; rats at 15.5 days gestation; monkeys at 72 and 90 days gestation (midpregnancy). The radiation exposures ranged from 195 to 400 R, and the chlorambucil was 25 mg single exposure. The developing retina of all of these mammals was shown to be highly radiosensitive, more so than other parts of the eye (lens or pigmented layer) and yet there was an attempt in all cases at restitution, following a clean-up by phagocytes of necrotized neuroblasts. Attempts at organization of the residual neural elements, following injury, invariably resulted in rosette formation which is a manifestation of unlimited or unrestricted movement of constituent cells, as in vitro. Extensive loss of neuroblasts resulted in linear arrangement of these rosettes, which can hardly have efficient visual function. There was evidence that the embryonic retina develops in waves from the posterior to the anterior, and that the position of the wave of neuroblasts (transforming from neurectoderm to neurons) in the retina will be the wave of gross destruction in the retina. Thus, the time of injury will determine that region of the neural retina which suffers most from exposure to ionizing radiations or to the radiomimetic agent. The pre- and postneuroblast stages appear to be quite radioresistant in the retina. Like most other organs, when the retina is finally differentiated, it becomes resistant to damage by ionizing radiations. This stage is apparently reached at or shortly after birth in the mammals studied. (BBB)

3726 THE EFFECTS OF ULTRAVIOLET AND VISIBLE RADIATIONS ON MICROORGANISMS. **Philippot, Jean (Faculte de Medecine, Montpellier, France). Biol. Med. (Paris), 53: 476-500(Sept.-Oct. 1964). (In French).**

Experiments done with Escherichia coli B and E. coli 15_T showed that after uv irradiation at about 2600 Å (with less than 150 erg/mm^2), the quantity of protein synthesized increased exponentially as a function of time. After larger doses, the speed of synthesis remained constant. The synthesis of RNA was less sensitive to uv irradiation. The presence or absence of thymine had no influence on the speed of synthesis of protein or RNA. Weak irradiation (20 erg/mm^2) slowed the synthesis of DNA. Doses of 150 erg or more completely inhibited DNA synthesis. After irradiation at 2600 Å, there was an increase in acid-soluble cell constituents and an accumulation of deoxyguanosine and thymidylic acid, immediate precursors of DNA. There was also an accumulation of soluble organic phosphorus, orthophosphate, ribose, and deoxyribose. Apparently, the last stages of DNA synthesis were blocked. E. coli irradiated in the resting phase and maintained in aerobic cultures had a higher percentage content of adenosine triphosphate (ATP) than the controls. Bacteria irradiated in the growth phase maintained a high percentage of ATP until DNA synthesis was resumed, 40 min after exposure. In irradiated bacteria placed in an anaerobic culture, the percentage of ATP remained about that of the controls. The ATP content did not drop until DNA was synthesized again, about an hr after exposure. In an experiment utilizing chloramphenicol, an inhibitor of protein synthesis, it was demonstrated that DNA synthesis could not take place without the presence of protein and RNA synthesis. Lesions induced by uv were sometimes restored by exposure to visible light (photoreactivation), depending on the microorganism and the radiation wavelength. Maximum restoration came after exposure at 3800 or 4358 Å. The efficacy of photoreactivation depended on the temperature, the presence of a chemical equilibrium, and the induction of a photochemical reaction. (BBB)

3727 ENHANCEMENT OF RADIOSENSITIVITY OF SKIN OF PATIENTS BY HIGH PRESSURE OXYGEN. **van den Brenk, H. A. S.; Kerr, R. C.; Richter, Wendy; Papworth, M. P. (Cancer Inst. Board, Melbourne). Brit. J. Radiol., 38: 857-64(Nov. 1965).**

The results are reported of a clinical experiment designed to evaluate the radiosensitivity of skin of anesthetised patients exposed to four atmospheres absolute of oxygen, relative to that of skin in the same patients breathing air under ambient conditions. Single radiation doses over the range 250 to 1,250 rads of ^{90}Sr β radiation were delivered to eight 1.2 cm diameter circular areas of anterior thigh skin. Skin damage produced in HPO was in-

creased at all dose levels. A quantitative analysis of the skin damage in air and HPO respectively resulted in an estimate that x rads administered in air produced the same damage to skin as 0.75 x rads administered in HPO for single doses in the range 250 to 750 rads. At doses > 750 rads human skin irradiated in HPO showed further progressive increase in radiosensitivity relative to that in air. These results are discussed in terms of previously reported experimental work. (auth)

3728 THE EFFECT OF FRACTIONATION ON FOUR DAY SURVIVAL OF MICE AFTER WHOLE-BODY NEUTRON IRRADIATION. Hornsey, Shirley; Vatistas, S.; Bewley, D. K.; Parnell, C. J. (Hammersmith Hospital, London). Brit. J. Radiol., 38: 878-80(Nov. 1965).

The proportion of animals surviving four days after whole body neutron irradiation was not altered by giving the radiation in two fractions separated by four to six hours. This result is compared with previously reported data after 250 kv x irradiation when it was found that a dose higher by 400 to 600 rads was necessary to produce the same killing effect if the radiation was given in two fractions rather than a single dose. This results in a larger RBE (250 kv/neutron) for the fractioned radiation than for single-dose irradiation and any increase in the number of fractions would increase the RBE further. These results may be relevant to the use of neutrons for therapy. (auth)

3729 SELECTIVE LYMPHOPENIA BY USE OF INTRALYMPHATIC ^{198}Au AND SPLENECTOMY: IMMUNOSUPPRESSIVE ACTION ON REJECTION OF CANINE RENAL HOMOGRAFTS. Wheeler, J. R.; White, W. F.; Calne, R. Y. (Westminster Hospital, London). Brit. Med. J., 2: 339-42(Aug. 7, 1965).

Experiments in dogs are described in which intralymphatic injection of colloidal ^{198}Au was used to deplete peripheral lymphocytes and cause severe damage or destruction to the lymph nodes, with little effect on the myeloid cells, and delay the rejection of renal homografts. Equal volumes of a sterile suspension of colloidal ^{198}Au stabilized with gelatin and 2.8% w/v sodium citrate at pH 6-7 with a particle size of 200-300 Å were injected into the four extremities. An identical fifth aliquot of colloidal ^{198}Au was injected directly into the mesenteric lymph nodes at the time of splenectomy and renal transplantation. The dose of colloidal ^{198}Au varied from 25 to 100 mC; splenectomy, renal transplantation, and mesenteric node injections were performed seven days after the intralymphatic injections. In all ^{198}Au-treated animals there was a selective lymphopenia which began on the second post-operative day and became progressively more severe until the seventh or eighth day and continued until the third to fourth week. The lymphopenia was much more pronounced than in control dogs given Imuran alone. The total white cell count was maintained, while there was a marked decrease in total lymphocyte count. Histological examination showed marked early depletion of the lymph node cell population; by two weeks there was greater than 50% destruction of lymph nodes. The dogs receiving 100 mC did not show proportionately larger changes in lymphocyte count or lymphonode destruction than those receiving 37.5 mC. However, lymphopenia was less severe in those given 25 mC. The early changes in the axillary, iliac, aortic, and mesenteric nodes showed a decreased cell population followed in about one week by nearly complete replacement of the node with hemorrhage and disappearance of the normal lymphocyte population. After about 30 days the nodes were surrounded by fibrous tissue with only a shell of amorphous material representing the lymph node. The cervical and mediastinal nodes showed some depletion with no fibrosis. The dogs receiving Imuran alone had only minor changes in the lymph nodes, in marked contrast to the ^{198}Au-treated animals. Injection of 37 mC or more of intralymphatic radiogold prolonged renal homograft survival twice that of normal. The results of ^{198}Au in combination with Imuran suggested added immunosuppression, but the numbers in each experimental group were insufficient for statistical analysis. (BBB)

3730 CHROMOSOMES AND LEUKEMIA. Bernard, Jean; Tanzer, J. (Centre de Recherches de l'Association Claude Bernard, Paris). Bull. Ass. Franc. Etude Cancer, 51: 7-24(Jan.-Mar. 1964).

Chromosome aberrations, induced by ionizing radiation, based on in vitro and in vivo observations are discussed in relation to leukemogenesis. In vitro observations have been made on various cell cultures, and on human leucocytes in the presence of phytohemagglutinin. In vivo studies involve mainly examinations of peripheral blood cells and hematopoietic cells. In vitro, achromatic lesions and breaks involving one or two S chromatids can be provoked by the irradiation. Quantitative studies of the relation between irradiation and the anomalies it produces reveal a possible difference in radiosensitivity of various chromosome sites. After irradiation of hamster cells, lesions were observed in preferential sites. Studies in vivo emphasize the importance of lesions caused by even weak doses from diagnostic radiographic examination, as well as by strong doses, for example, in the therapeutic use of ^{131}I, or in vertebral irradiation for spondylarthritis. Above all, it was noted that chromosome anomalies may persist long after irradiation, as in subjects irradiated in accidents in atomic centers, or subjects irradiated for spondylarthritic ankylosis of the spine. Chromosome aberrations induced by viral and chemical agents are also reviewed. (BBB)

3731 IS THE SKIN A SCREEN FOR COSMIC RADIATION? Bory, Louis; Bory, Philippe (Bull. Soc. France Dermatol. Syphilol., 70: 291-5(Apr.-May 1963). (In French).

The concept that the hazards due to cosmic radiation are negligible is refuted. It is emphasized that, although cosmic radiation accounts for only 25% (25 mrem out of a total of 100) of the yearly dose of natural radiation, its emission is continuous and its energy great. The surface of the human body (about 0.1 m^2) receives about 30 photons per sec of cosmic radiation. The fact that matter exposed to cosmic radiation is subjected to changes in its chemical and isotopic composition is emphasized, so it is evident that continuous cosmic radiation must affect living matter, as well as inert matter. The analogy of the structure of skin and an electronic system is cited, and the possible function of skin as a radiation screen is hypothesized. It is suggested that cosmic radiation is linked to various skin diseases, such as eczema. The formation of skin lesions in these diseases is visualized as resembling small explosions, disrupting of the electromagnetic system of the skin. Organic halogeno-magnesium derivatives, specifically bromides or iodides, are cited as capable in abnormal form of developing an electromotive force which produces electrolysis. It is suggested that high-energy photons or particles in cosmic radiation may be capable of activating such highly reactive compounds in skin. (BBB)

3732 LATE SMALL BOWEL OBSTRUCTION SECONDARY TO POST-RADIATION ENTERITIS. Rabwin, Marcus H.; Karlan, Mitchell S. (Cedars of Lebanon Hospital, Los Angeles). Calif. Med., 102: 449-52(June 1965).

A brief review of the literature on the incidence of radioinduced gastrointestinal stricture or enteritis is given, and a case is reported wherein operation was required for an obstruction of the small bowel secondary to radiotherapy carried out nine years previously. (TCO)

3733 MUTANTS OF THE PARASITIC WASP DAHLBOMINUS FUSCIPENNIS (ZETT.) (HYMENOPTERA: EULOPHIDAE). Baldwin, W. F.; Shaver, E.; Wilkes, A. (Atomic Energy of Canada Ltd., Chalk River, Ontario). Can. J. Genet. Cytol., 6: 453-66(Dec. 1964).

Some radiation induced-mutants are described for this wasp, which produces haploid males from unfertilized eggs and diploid females from fertilized eggs. An account is given of the life history of the species and a description of the adult and immature stages of the wild stock as a basis for comparison with the mutant lines. A simple method is given for rearing large numbers in the laboratory. The main phenotypic effects of 12 visible mutants are reported.

All but two of the mutations occurred among haploid males, following irradiation of wild females, the others during pedigree breeding of irradiated stock. Eight of the mutations affected pigmentation of the eyes or body, three produced morphological abnormalities in the wings and antennae and one reversed the sex ratio. All but the last one were controlled by recessive factors, each of which has been assigned a name and symbol. The sex-reversing (SR) factor was dominant and sex-limited, being transmitted by females to their sons. Although tests for linkages between the mutations were not completed, in initial crosses between four of the bright eye-colors and the wing mutations, segregation was independent indicating that these arose as separate mutations. Although the mode of action of the male-producing SR mutation is unknown, its effects are not due to selective mortality, nor is it transmitted by the egg alone. Its presence appears to hinder successful fertilization of the egg, either through failure of a much greater proportion of SR sperm to enter the egg or through the inability of the SR sperm nucleus to unite with the female pronucleus after it has entered the egg. The action of the mutation in D. fuscipennis is clearly independent of the factors considered to be responsible for causing variations in the sex ratio of most arrhenotokous animals. It is suggested that this mutation, if it occurs in nature, may account for the variability of the sex ratio of this species in natural populations. (BBB)

3734 THE EFFECTS OF RADIATION OF THE NORMAL RECTUM. **Deeley, T. J. (Hammersmith Hospital, London). Cancer Progr., 157-63(1963).**

The present attitude of radiotherapists to rectal injuries is described and illustrated with a series of 107 cases of cervical carcinoma in which there was evidence of damage to the rectal mucosa, and with a series of cases treated by supervoltage x rays for carcinoma of the bladder. Out of 327 patients who were treated for a carcinoma of the bladder, 110 (35%) developed some diarrhea during treatment. Examination of the rectal mucosa at this time showed it to be edematous and reddened with patchy mucous membrane reaction. It appears that doses of 5500 rad to the bladder of 4500 rad to the whole pelvis in four weeks can be given without causing severe rectal complications. (BBB)

3735 THERAPEUTIC POSSIBILITIES OF HIGH-ENERGY CHARGED PARTICLES. **Morgan, Rowland L. Cancer Progr., 176-84(1963).**

Use of various types of charged particles for radiotherapy are reviewed and some radiobiological problems encountered in their use are examined. Experiments are described on the effect of x and neutron radiations on pig skin were carried out with an 8-Mev linear accelerator and the fast neutron beam from the 45-in. cyclotron. The average RBE of the fast neutron beam for a single dose of irradiation was 2.5, while that for a fractionated dose was 3.3. Over a period of 2 years following the irradiation, no evidence was observed of any differential increase in damage in the areas irradiated with fast neutrons compared with those given doses of x rays. On the other hand the observation that the RBE of fast neutrons is increased in the ratio of about 1.3 to 1 by dividing the dose into 6 fractions spread over 3 weeks has important implications. The increase of RBE with fractionation provides an explanation of the serious long-term skin damage observed, which therefore can be avoided in a future trial of neutron therapy. The feasibility of using negative π mesons in radiotherapy is considered. (TCO)

3736 THE EFFECTS OF NITROGEN MUSTARD AND DIMETHYL MYLERAN ON MURINE LEUKEMIA CELL LINES OF DIFFERENT RADIOSENSITIVITY IN VITRO. **Goldenberg, Gerald J.; Alexander, Peter (Royal Cancer Hospital, London). Cancer Res., 25: 1401-9(Oct. 1965).**

The effects of nitrogen mustard and dimethyl myleran on 3 mutants of murine leukemia L5178Y, radioresistant and radiosensitive diploid cell lines and a tetraploid line, were studied. A close parallelism was found in the response of radioresistant and radiosensitive cells to treatment with nitrogen mustard, dimethyl myleran, and x radiation; in each case the D_0 for the radioresistant line was twice that of the radiosensitive cell line. The tetraploid cell line showed marked differences in response to the 3 agents: it showed increased resistance to nitrogen mustard, increased sensitivity to dimethyl myleran, and no change in response to x radiation, all relative to the response of the radioresistant diploid cell line to these same agents. The effect of dimethyl myleran more closely resembled that of x radiation in that cell division continued for some time after treatment and storage at suboptimal temperature facilitated post-treatment recovery processes. The monofunctional mustard, dimethyl chloroethylamine, was approximately 35 times less potent in its cytocidal effect than nitrogen mustard. The cyclic ethyleneimmonium ion of nitrogen mustard appeared to retain the full cytocidal action of nitrogen mustard in this system. Attempts to induce mutants of L5178Y more resistant to nitrogen mustard and dimethyl myleran by repeated treatment of surviving cells were unsuccessful. (auth)

3737 RADIOSENSITIVITY OF NORMAL AND 5-BROMODEOXYURIDINE TREATED MAMMALIAN CELLS DURING DIFFERENT PHASES OF THE CELL CYCLE. **Humphrey, R. M.; Dewey, W. C. (Univ. of Texas, Houston). Exp. Cell Res., 39: 483-95(Sept. 1965).**

Changes in sensitivity to γ radiation during various phases of the division cycle of both asynchronous and synchronized populations of Chinese hamster cells have been investigated following the incorporation of BUdR into the DNA. Radiosensitivity was measured in terms of chromosomal damage. Following one replication (single-strand label) in BUdR, cells irradiated during S phase were found to be maximally sensitized and cells irradiated during the G_1 phase were not sensitized by single-strand BUdR incorporation. Subsequent replication in the presence of BUdR to obtain double-strand label resulted in the sensitization of the G_1-phase cells. Therefore, the position of the cell in the cell cycle may be an important factor in determining a radiosensitizing effect. Furthermore, the results on exchange formation were consistent with an impairment in the restitution process for cells which have BUdR in the DNA. The work further substantiated the hypothesis that the chromosome consists of two subunits which separate either slightly before or as the cell enters S phase. (auth)

3738 STUDIES ON IMMUNE UNRESPONSIVENESS INDUCED BY RADIATION. **Nachtigal, D.; Feldman, M. (Weizmann Inst. of Science, Rehovoth, Israel). Israel J. Exp. Med., 11: Suppl., 239(Oct. 1964).**

Specific immune unresponsiveness to purified protein antigens can be induced in adult rabbits exposed to 550 R total-body irradiation and subsequently treated with immunogenic doses of the test antigen. To compare the specificity of radiation-induced tolerance to heterologous proteins with that of natural tolerance to homologous proteins, experiments were performed with rabbits which had been made tolerant to human serum albumin (HSA) after x irradiation and given an immunizing course of sulfanil-azo-HSA injections. Similarly, a group of untreated rabbits was immunized with sulfanil-azo-rabbit serum albumin (sulfanil-azo-RSA). Both groups of animals produced two types of antibodies: one type was specific to sulfanil-azo conjugates of proteins in general, while the other was specific to each respective conjugated carrier protein, although the animals did not respond to the native carriers as such. Since this observation applied to the group of rabbits that were made unresponsive to the carrier by x-ray treatment as well as to the rabbits that were tolerant to the respective carrier naturally, it appears that both systems of tolerance exhibit a similar specificity. At the end of the experiment the induced tolerance to HSA broke down as a result of immunization with conjugated HSA. This difference, however, between induced and natural tolerance was only apparent: tolerance was not broken when rabbits were immunized with a mixture of native and conjugated HSA, an analogous situation to that of normal rabbits immunized with conjugated RSA. These

findings may reflect a similarity of mechanism in both systems of tolerance. (BBB)

3739 CARCINOMA OF THE THYROID GLAND IN CHILDREN AND ADOLESCENTS. Nishiyama, Ronald H.; Schmidt, Robert W.; Batsakis, John G. (Univ. of Michigan, Ann Arbor). J. Amer. Med. Ass., 181: 1034-8(Sept. 22, 1962).

Thirty-six children and adolescents were treated for carcinoma of the thyroid gland over a 30-year period. The average age at the time of histological diagnosis was 11.8 years. A histologic diagnosis of carcinoma was made from 5 to 12 years (average of 8.8 years) after exposure to x rays or other radioactive materials. The most frequently encountered histologic type of carcinoma (72%) was a mixed papillary and follicular form. Treatment varied from simple biopsy of a cervical lymph node to total thyroidectomy with unilateral radical neck dissection. Some patients were given therapeutic doses of radioiodine postoperatively; 8 of these also received external x radiation. The geographic distribution, possible association with ionizing radiation, and the apparently increased incidence of carcinoma of the thyroid gland in children are discussed. The incidence of a history of irradiation is higher than expected in the cases reported here. (TCO)

3740 THE EFFECT OF RELATIVE HUMIDITY AND LIGHT ON AIR-DRIED ORGANISMS. Webb, S. J. (Univ. of Saskatchewan, Saskatoon, Can.). J. Appl. Bacteriol., 26: 307-13(Dec. 1963).

The effect of relative humidity (RH) on the lethal action of uv and visible light of various wavelengths was studied. Serratia marcescens was irradiated in aerosols at various RH levels, and the action of inositol in modifying radiation damage examined. The lethality of these radiations is shown to be strongly dependent on RH provided the intensity of the light was not too great. A critical region between 55 and 65% RH exists in which there was an abrupt change in the sensitivity of airborne cells to all wavelengths tested. Not only did the death rate change suddenly in this RH region but so also did the rate of mutant production. This critical RH region corresponded to the RH level at which bound water is removed from the nucleic acid bases and it is suggested that these water molecules are able to prevent lethal excitations or migration of excitation energy. Inositol was shown to prevent radiation damage and, because of its structure, it is assumed to replace water in the dried cells. About 5 water molecules/nucleotide are removed from these DNA groups as the RH is lowered from 75 to 55% RH. The water molecules are responsible for maintaining the normal stereochemistry of DNA, and when they are removed the DNA molecule takes on a different helical form. Water molecules or inositol will prevent radiation damage to the cell. Presumably bound water molecules are able to prevent the production in these macromolecules of excitation states, or energy migrations, which would otherwise prove lethal. Since they are bound directly to the nucleic acid bases, they affect the available energy levels. The abrupt change in the sensitivity of cells in aerosols between 55 and 65% RH is probably associated with the presence or absence of the five water molecules/nucleotide. (BBB)

3741 THE LASER AS A POTENTIAL TOOL FOR CELL RESEARCH. Rounds, Donald E.; Olson, Robert S.; Johnson, Fred M. (Pasadena Foundation for Medical Research and Electro-Optical Systems, Inc., Calif.). J. Cell Biol., 27: No. 1, 191-7(Oct. 1965).

Freshly prepared hemoglobin solutions were successively irradiated up to five times with 1 MW (monochromatic wavelength) of green (530 mμ) laser power. Oxygenated hemoglobin showed no detectable change, but the spectral absorption of reduced hemoglobin showed a shift toward the characteristic curve for the oxygenated form. Intact human erythrocytes exposed to a power density of 110 MW/cm^2 of green laser radiation showed no appreciable change in diameter or mass, but they became transparent to a wavelength range from 400 to 600 mμ. A similar power density from a ruby laser failed to produce this bleaching effect. The response in the erythrocyte demonstrates a principle that suggests the laser as a tool for cell research; specific molecular components within a cell may be selectively altered by laser irradiation when an appropriate wavelength and a suitable power density are applied. (auth)

3742 EXPERIMENTAL RADIO-OSTEONECROSIS OF THE JAWS. Gowgiel, Joseph M. (Zoller Memorial Dental Clinic, Univ.of Chicago). J. Dent. Res., 39: 176-97 (Jan.-Feb. 1960).

Experiments in monkeys were undertaken to elucidate: the relation between the quantity of fractionated irradiation and the deleterious bone changes (radio-osteonecrosis); possible differences in sensitivity of different bones regarding development of radio-osteonecrosis; and pathogenesis of the disease, particularly of the jaw. The maxilla and mandible of 18 Macacus rhesus monkeys (15 to 18 months old) were subjected to external fractionated irradiation, ranging from 4500 to 11,000-R of 250-kvp x rays. The time of onset of necrosis and the dose of irradiation were in direct relation to each other. The severity and extent of the necrosis were in direct relation to the time of onset. Microscopically, the interdental papilla was the first area that demonstrated inflammation, followed by ulceration of the epithelial attachment and necrosis of the underlying corium. The necrosis spread by two routes: the periodontal ligament and the gingival tissue. Radio-osteonecrosis appears to result primarily from the direct effect of irradiation on the osteocyte, but changes in the blood vessels played a role in the aggravation and prolongation of the irradiation effects. Radiation produced marked thickening of the walls of arteries and arterioles. The veins and capillaries were not affected, and there was no evidence of ischemic necrosis. Radio-osteonecrosis can occur under an intact gingiva. After a sufficiently long time, restoration of the radio-osteonecrotic damage is possible. Application of these experimental results to clinical problems is discussed. Most of the lesions in these experiments occurred earlier and ran a much faster course than do human lesions, but some lesions in the middle dose-range group (7500 R) followed a course that was comparable to clinical reports in man. Irradiation doses of 11,000 and 9500 R produced a massive destruction of all tissues at the site of irradiation that was already evident at the time of completion of irradiation or shortly thereafter. (TCO)

3743 ERUPTION OF IRRADIATION-PRODUCED ROOTLESS TEETH IN MONKEYS. Gowgiel, Joseph M. (Chicago Coll. of Dental Surgery). J. Dent. Res., 40: 538-47(May-June 1961).

Eighteen Macacus rhesus monkeys were subjected to fractionated external 250-kv x irradiation to the mandible and maxilla. The animals were irradiated with doses of 4500, 5500, and 7500 R and lived up to 3¼ yr postirradiation. They were irradiated 5 days a week to alternating sides of the face. The length of irradiation treatment varied from 5½ to 12½ weeks, depending on the dose administered. The animals varied in age from 14 to 28 months and therefore had complete deciduous dentition. At all dose levels, irradiation completely inhibited further crown and root development and destroyed the anlage of the third molar tooth, but calcification of the crown matrix was not inhibited. The size and shape of the permanent teeth were dependent on their state of development at the time of irradiation. The maxillary permanent teeth always had some root formation, usually short and thin, while the mandibular teeth were completely rootless. This was in striking contrast to the dentition of a normal, nonirradiated monkey. The pulp chamber of the irradiated teeth closed at a more rapid rate than in the normal teeth and was completely closed before they erupted a short distance. Layers of dense bone were usually formed under erupting crowns. The roots of the deciduous molars resorbed in the normal manner. The aberrant size of the permanent bicuspids did not alter this process. The eruption rate of the partially formed permanent teeth was retarded, but the degree of retardation was not precisely

determined. The partially formed teeth eventually erupted into full occlusion. Irradiation produced profound histologic changes, which are described. (BBB)

3744 RADIATION-INDUCED CHANGES IN THE EPITHELIUM OF THE BUCCAL MUCOSA. Chase, Lawrence P.; Toto, Patrick D.; Magalotti, Marion F. (Loyola Univ. School of Denistry, Chicago). J. Dent. Res., 40: 929-35(Sept.-Oct. 1961).

In 13 patients undergoing radiotherapy for oral cancer a study was made of exfoliated oral epithelial cells by the Papanicolaou method. Changes in keratinization, particularly any change in the distribution of nonkeratinized, keratinizing, and keratinized cells were observed. The x-ray doses varied from 1187 to 4650 R. A shift in the distribution of cells from nonkeratinized to keratinized occurred as a result of radiation therapy. There was a decrease in the number of exfoliated cells per microscopic field as therapy progressed. Also, the size of the keratinizing cell widened to twice the dia late in therapy, as compared with similar cells taken earlier in therapy. The mitosis-inhibiting effect of ionizing radiation on the normal oral epithelium of the buccal mucosa caused a reduction in the number of cells. A reduced number of cells called upon to function as the lining of the oral mucosa remain in situ longer, permitting the normally nonkeratinized cells to keratinize and increasing the number of keratinized exfoliated cells. The widening of keratinizing cells is a functional adaptation of subnormal epithelium to carry on the function of lining the oral mucosa and is an indirect effect of ionizing radiation. The increase in keratinization of normally nonkeratinized cells is a function of oxidative effects within the cytoplasm of the epithelial cells. It is suggested that sulfhydryl groups are converted to disulfides as in cystine, as a result of oxidation, thereby accelerating the keratinization process. The rate at which nonkeratinized cells decrease during radiation therapy varied in individuals, indicating variation in the cellucidal effect of ionizing radiation. (BBB)

3745 EFFECT OF GAMMA RADIATION ON THE REPRODUCTIVE POTENTIAL OF THE MEXICAN FRUIT FLY. Rhode, R. H.; Lopez D., F.; Eguisa, F. (Sociedad de Beneficencia Espanola, Mexico City); Telich C., J. J. Econ. Entomol., 54: 202-3(1961).

Two ^{60}Co sources rated at 800 and 1300 C each were used to irradiate puparia of the Mexican fruit fly in preliminary experiments. There was no further development when 4-day-old puparia were exposed to doses above 2000 R. Within the 7000 to 12,000 R exposure range, emergence from puparia treated when they were 8 days old was 20% to 60% lower than from untreated pupae. Emergence from puparia treated when 12 days old, or about 4 days before they would emerge at 77°F, appeared to be normal at all radiation levels from 1000 to 12,000 R. The rate of exposure was less than 100 R/min in these tests. Adults of both sexes were rendered sterile when 12-day-old pupae were exposed to 5000 R. The irradiated females did not develop eggs. Longevity appeared to be normal, and neither mating behavior nor aggressiveness of young treated males were adversely affected by this dose. A latent effect on mating behavior was apparent, however, 30- to 39-day-old males being able to mate first only 59 times compared with 141 times for normal flies in competition trials. Effect of the dose rate was also investigated. In 1000-R increments, doses of 1000 to 5000 R were applied to 12-day-old puparia at rates of 90, 70, 50, 30, and 10 R/min at each level. At the critical 2000-R dose, as the dose rate increased irradiated females deposited fewer eggs and irradiated males became less fertile. Females receiving more than 2000 R developed no eggs and the number of viable eggs deposited by untreated females mated with irradiated males gradually diminished until complete sterility was obtained at 5000 R. In overflooding tests with caged fly populations there were marked reductions in the fertility of eggs, despite the frequent mating habits of the females when sterile flies dominated normal individuals at ratios of 5, 10, 25, and 50 to 1. An almost total effect at the 50 to 1 overflooding ratio was seen. (TCO)

3746 ROLES OF THE LIVER AND APPENDIX IN THE SERUM HEMOLYSIN RESPONSE IN RABBITS. Draper, Laurence R.; Sussdorf, Dieter H. (National Cancer Inst., Bethesda, Md.). J. Immunol., 95: 306-13(Aug. 1965).

Participation of nonsplenic sites in antibody production after antigenic stimulation was studied in splenectomized, appendectomized, and partially hepatectomized rabbits which received multiple as well as single injections of antigen. Particular attention was paid to the role of the liver in the hemolysin response, not only because of that organ's possible antibody-forming ability but also because the liver is a major depository for intravenously injected antigen and is a site for γ-globulin catabolism. These experiments included x irradiation of the liver, immunization via the portal vein, and passive transfer of hemolysin into hepatectomized or liver-irradiated rabbits. Surgically exteriorized liver, positioned in the cup of a body shield, was irradiated with 1400 R at a rate of about 170 R/min using a 250-kv machine. The ability of the rabbit's liver to remove circulating particulate antigen was evident from the shortened rise of titer to peak following partial hepatectomy and a single injection of antigen. While intact rabbits displayed a longer antibody rise than did hepatectomized rabbits after one antigen injection, this difference was not observed after multiple injections. The latter dosage apparently was in sufficient excess to override any significant effect of the diversion of antigen by the liver. When antigen passed first through the liver before entering the general circulation, the response was delayed about one day when compared with that in animals injected via the ear vein. Thus immunization via the portal vein permits a greater retention of antigen by the liver and significantly restricts the early production of antibody by the spleen. Irradiation of the liver prior to immunization via the ear vein resulted in a shortened time of antibody rise to peak titer. If irradiation of the liver reduces this organ's capacity to remove antigen from the circulation, it should prevent the delay of the response found after intraportal immunization. As was anticipated, the latent period was not lengthened following intraportal antigen injection when the liver had been irradiated before immunization (i.e., it was the same as that of the irradiated rabbits immunized via the ear vein). In fact, the mean latent period was significantly shorter in these animals than in the nonirradiated rabbits immunized by the same route. Increased disappearance rates of passively transferred hemolytic antiserum in partially hepatectomized and liver-irradiated rabbits suggest that the regenerating or recovering liver catabolizes antibody faster than normal liver. (BBB)

3747 ENVIRONMENTAL TERATOGENS AND BIRTH DEFECTS. Fish, Stewart A. (Univ. of Arkansas Medical Center, Little Rock). J. Lancet, 85: 208-12(May 1965).

Hereditary, genetic, and environmental causes of developmental defects are reviewed, and teratogenic effects on the human embryo, of trauma, temperature changes, ionizing radiation, oxygen deficiency, drugs, and viruses are considered. The second major teratologic mechanism considered is the problem of chromosomal aberrations, and the third major cause of developmental defects include factors that affect the maternal-fetal environment and may interfere with orderly organogenesis, thereby producing developmental abnormalities. Ionizing irradiation can produce many types of developmental defects in the human embryo when administered during the period of organogenesis. The least amount of radiation needed to produce damage to the human fetus in utero has not been accurately determined. However, fetal malformations and abortion have been recorded following exposure to radiation of the degree required for barium enema, intravenous pyelography, gastrointestinal diagnostic studies, and fluoroscopy. (TCO)

3748 THE PROCESS OF INFECTION WITH BACTERIOPHAGE ϕX174. V. INACTIVATION OF THE PHAGE-BACTERIUM COMPLEX BY DECAY OF ^{32}P INCORPORATED IN THE INFECTING PARTICLE. Den-

hardt, David T.; Sinsheimer, Robert L. (California Inst. of Tech., Pasadena). J. Mol. Biol., 12: 663-73(July 1965).

The ^{32}P-inactivation experiments described were undertaken to learn more about both the nature of the ϕX infection process and the nature of the mechanism of ^{32}P decay inactivation. Because of the single-stranded structure of ϕX DNA, it is possible to label the double-stranded replicative form specifically in one strand; the kinetics of inactivation of a double-stranded DNA labeled in only one strand is relevant to proposed mechanisms for the lethal action of disintegrating ^{32}P. ϕX bacteriophage containing 2 to 4 ^{32}P atoms per particle were used to infect cells in nonradioactive medium. The phage and early complexes were killed by ^{32}P decay with an efficiency of 1; mature complexes were inactivated with an efficiency of about 0.2, even though unlabeled, infective replicative form ϕX DNA had been synthesized in them. At about the same time as progeny single-strand DNA was synthesized, the complexes became completely refractory to inactivation by ^{32}P decay. In chloramphenicol the efficiency of ^{32}P decay inactivation in the complexes also decreased to about 0.2; thereafter complexes formed (in chloramphenicol) from cells that had not been starved became fully resistant to inactivation, whereas complexes formed from starved cells did not. The behavior of ϕX complexes in ^{32}P-decay inactivation experiments is very different from that of the other virus-cell systems (except possibly for poliovirus) studied so far. The sensitivity to ^{32}P decay of ϕX complexes begins to decrease immediately after infection, even in the presence of chloramphenicol, where the sensitivity to ^{32}P decay of T phage complexes begins to decrease significantly only after a lag of three to six minutes, and no decrease is observed in the presence of chloramphenicol. Furthermore, the degree of stabilization observed in the T phage system is much larger than that observed in the ϕX system. These differences are probably intimately connected with the single, as opposed to double-stranded, nature of the DNA of these viruses. (BBB)

3749 THE PROCESS OF INFECTION WITH BACTERIOPHAGE $\phi X174$. VI. INACTIVATION OF INFECTED COMPLEXES BY ULTRAVIOLET IRRADIATION. Denhardt, David T.; Sinsheimer, Robert L. (California Inst. of Tech., Pasadena). J. Mol. Biol., 12: 674-94(July 1965).

The sensitivities to uv irradiation of complexes formed by infection with bacteriophage $\phi X174$ in Escherichia coli strains C, C_s (a strain lacking the capacity to perform host cell reactivation), and CR (a strain requiring thymine) were determined at various wavelengths, stages of development, and growth conditions. Action spectra for the infected complexes and for cell capacity are presented. The uv sensitivities of bacteriophages $\phi X174$ (normal and bromouracil-labeled), lambda (normal and bromouracil-labeled), and Ms2 are compared. (BBB)

3750 STUDIES OF THE LSA ASCITES LYMPHOMA OF C57BL MICE. I. TRANSPLANTATION CHARACTERISTICS AND RADIOSENSITIVITY OF CELLS DURING SERIAL PASSAGES. Silini, Giovanni; Maruyama, Yosh (Stanford Univ., Palo Alto, Calif.). J. Nat. Cancer Inst., 35: 841-9(Nov. 1965).

A new transplantable tumor, the LSA ascites lymphoma of the C57BL/Ka mouse, was used in radiobiological experiments. A progressive increase in the transplantability of the tumor was observed with serial passage. The sensitivity of the cells to x rays was studied in early and late passage. The increased radioresistance of late passage cells can be accounted for on the basis of hypoxia after an increase in ascites volume. (auth)

3751 CHROMOSOMAL NUMBER AND THE RADIOSENSITIVITY OF EXPERIMENTAL TUMORS. Malaise, E. P.; Tubiana, M.; Barski, G. (Institut Gustave-Roussy, Villejuif, France). J. Radiol. Electrol. Med. Nucl., 45: 101-5(Jan.-Feb. 1964). (In French).

Adult female mice of the C3H strain were injected with 8×10^5 tumor cells of the N1 (NCTC, clone 2472) or M strain in the right side. N1, a sarcomatous strain of mouse fibroblasts, is hyperdiploidal (55 chromosomes) and M is hypertetraploidal (116). The mice were immobilized and the injection area subjected to four 500 R irradiations with 200-kv x rays over a 17-day period. The irradiations were made during the period of exponential tumor growth in the controls. Results were measured 30 days after initial irradiation. In the N1 tumor group, average survival was 31.6 ± 5.6 days for the controls and 55.5 ± 5.7 days for the irradiated animals; thus, irradiation prolonged survival 44%. The N1 tumors measured 23.4 ± 3.3 mm in the controls, but only 9.8 ± 2.5 mm in the irradiated mice, a decrease of 58%. In the M tumor group, average survival was 48 ± 3.4 days for the controls and 61 ± 7.5 days for the irradiated group. This was a survival increase of 27%. The M tumors measured 21.5 ± 2.5 mm in the controls and 12.5 ± 3.3 mm in the irradiated mice, a decrease of 40%. The growth curves of N1 and M tumor cells were not significantly different over a 30-day period. It is concluded that in the aneuploid cells there was no apparent correlation between the number of chromosomes and radiosensitivity. (BBB)

3752 EFFECTS OF PHYSICAL TREATMENTS ON THE INFECTIVITY OF MYC. LEPRAEMURIUM. Nakamura, Masahiro; Muraoka, Shinya; Kinoshita, Tusneo (Kurume Univ. School of Medicine, Japan). Kurume Med. J., 11: 144-7(1964).

The effects of heat, uv irradiation, and shaking on the infectivity of Mycobaterium lepraemurium were investigated. The results showed that the infectious activity of the bacillus was completely inactivated by heating at 55°C for 30 min or by exposure to a germicidal lamp. To investigate the effect of uv irradiation on infectivity, bacterial suspensions were prepared in 2 ml of sterile distilled water and placed in open Petri dishes and exposed at a distance of 15 cm to a 10-w Shimazu germicidal lamp. After specified times of irradiation, the suspensions were tested for infectivity. The results obtained indicated that the infectivity of the bacillus was maintained after irradiation for 60 min, but was largely inactivated by irradiation for 90 min. A complete loss of infectivity of the bacillus by irradiation for 120 min was observed. When the effect of uv irradiation on the infectivity of M. lepraemurium was studied earlier, infectious activity of the bacillus was lost by exposure of uv at a distance of 30 cm for 10 min. This differs from the results of present experiment in which the activity of the bacillus was inactivated by irradiation at a distance of 15 cm after 120 min. This discordance may be due to the differences of the materials tested and of the kind of germicidal lamps used. Infectivity of the bacillus was lost after shaking (90/min) for 5 days at 37°C in a water bath, whereas it was maintained for 10 days under stationary conditions. There were no morphological changes observed by light microscopy in the bacilli that were shaken. (BBB)

3753 MALIGNANCY AND OTHER LATE EFFECTS FOLLOWING ADMINISTRATION OF THOROTRAST. da Silva Horta, J.; Abbatt, John D.; Cayolla da Motta, L. (Univ. of Lisbon). Lancet, 2: 201-5(July 31, 1965).

A systematic investigation was made of the late effects of Thorotrast as used in 2377 individuals in Portugal as an intravascular contrast agent. Among the 1107 cases which could be traced, 699 had died and up to Dec. 31, 1963. Of those who had died many had more than one pathological condition probably attributable to Thorotrast. In the absence of a matched control series these factors are difficult or impossible to evaluate, and this preliminary report presents only the most important results. None of the late effects except local granulomata has been observed in patients who had received Thorotrast nonsystemically, presumably because the dose was small and little of the Thorotrast was retained in the body. The most striking findings were the large numbers of granulomas, hemangioendotheliomas (sarcomas), and, particularly, of fatal blood dyscrasias. The incidence of leukemias (8) is statistically significant when compared with the figures available for Portugal since 1955. Of 8166 autopsies and 52,945 biopsies made between 1936 and 1964 in the Institute of Pathology of

the Lisbon University Hospital, hemangioendotheliomas were found only in those patients who had received Thorotrast. (TCO)

3754 FAT ABSORPTION TESTS PERFORMED WITH ^{131}I-LABELED TRIOLEIN COMBINED WITH WHOLE-BODY IRRADIATION. Nagy, Eva J.; Elekes, Istvan; Nyiro, Lasz'lo (MTA Orvosradiologiai Kutatocsoportja, Budapest). Magy. Radiol., 17: 200-8(Aug. 1965). (In Hungarian).

Experiments were performed on rats to determine the effects of various doses of whole-body irradiation on fat absorption and to what extent these effects can be influenced by sulfhydryl compounds given prior to irradiation. After 550- to 600-R whole-body x irradiation (at 200 kv, 41.5 R/min) significant changes in fat absorption were noted at 72 hr postirradiation. After 700 R, absorption was markedly reduced and after 800 R the ^{131}I-labeled triolein was not absorbed by the radioinjured stomach. It was found that 650 R whole-body irradiation was most suitable for these experiments, in which 0.035 ml triolein (4 to 5 μC) was given in 0.965 ml milk with Tween 80 added. Both blood and plasma were analyzed. In the second series of tests 280 mg/kg AET was given intraperitoneally 5 min prior to irradiation and plasma values were found to be less than those of controls. In further experiments lead shielding was used to cover the abdomen and doses of 650 R and 1500 R were given. In these groups the absorption values varied within normal limits with the maximum changes at the 6th hr. Attempts were also made to determine the inorganic iodine released from the triolein in the intestine; for this, 6 hr after ingestion the jejunum was washed with 0.01N $Na_2S_2O_3$. The lumen of the jejunum contained no released iodine, and it was found that in normal animals only 0.001% of the ingested activity remained in the intestinal walls after 6 hr. It was also found that 650-R irradiation slowed the speed with which the stomach emptied and also the rate of fat absorption. Histologic examination revealed that the small intestine was acutely inflamed, the epithelium had been sloughed off, and no gastric secretion was noted. The experiments dealing with irradiation and lead shielding in this connection are not considered finished and further work is planned. (BBB)

3755 SOME PHYSIOLOGICAL PECULIARITIES OF ULTRAVIOLET-INDUCED MUTANTS OF ASPERGILLUS. Grebeshova, R. N. (All-Union Research Inst. for the Fermentation and Spirit Industry, Moscow). Microbiol. (USSR) (Engl. Transl.), 33: 702-5(Sept.-Oct. 1964).

Translated from Mikrobiologiya, 33: 787-91(Sept.-Oct. 1964).

Metabolic characteristics were investigated for three uv-induced mutants that produce large amounts of amylolytic enzymes. The three mutants used were obtained by uv irradiation of original strains Aspergillus niger S-4, A. batatae 3324, and A. oryzae 153. Maximum accumulation of amylolytic enzymes both in the original and mutant variants was on the 3rd to 4th day of fermentation when the growth processes were completed. As regards carbohydrate and phosphorus consumption, intake by the variant of A. niger was lower than the original strain by 5% and 60%, respectively, while variants of A. oryzae and A. batatae exceeded the original strains by 8 and 25, and 15 and 16%, respectively. There was no significant difference in the growth of biomass between the mutant and original strain. On the other hand, the strains differed from each other in the pH values of the culture fluids. It is concluded that significant changes in metabolic reactions were produced in uv-induced mutants. (TCO)

3756 BIOCHEMICAL CHARACTERISTICS OF ASPERGILLUS UV MUTANTS. Grebeshova, R. N. (All-Union Scientific Research Inst. of the Fermenting and Alcohol Industries, Moscow). Microbiol. (USSR) (Engl. Transl.), 33: 858-61(Nov.-Dec. 1964).

Translated from Mikrobiologiya, 33: 971-4(Nov.-Dec. 1964).

Biochemical characteristics of the uv-induced mutants A. niger S-$4_{10=10=III}$, A. oryzae 3-9-15, and A. batatae 3859 are described. Carbohydrate, nitrogen, phosphorus, and nucleic acid levels were followed in the mycelium of these variants which produce amylolytic enzymes in greater amounts than the parent strains. In the experimentally obtained strains changes were found in phosphorus metabolism as manifested in a decrease of total phosphorus in the mycelium and its fractions in A. niger S-$4_{10=10=III}$ by 50% and an increase in A. oryzae 3-9-15 by 25% and in A. batatae 3859 by 15% as compared with the original strains. Appreciable changes were also noted in nucleic acid metabolism as manifested by a change in the RNA level in the mycelium of the variants, while the DNA level remained similar in all strains, i.e., about 0.15 to 0.20 mg%. A. niger S-$4_{10=10=III}$ contains 13% less nucleic acid (DNA + RNA) in the mycelium, and A. oryzae 3-9-15 and A. batatae 3859 contain 23 and 16% more, respectively, compared to the original strains. Analyses of the nucleic acid content both in the original and variant strains occurs at 24 hr, i.e., at the period of active synthesis of protein components in the cytoplasm. These data indicate essential alterations in the metabolism of the mutants compared with the original strains. The most marked difference was observed in the phosphorus content of the mutant mycelia. Evidently the system regulating phosphorus metabolism is particularly sensitive to uv light. (BBB)

3757 LOCUS FOR RADIATION SENSITIVITY IN ESCHERICHIA COLI B_{III}. Greenberg, Joseph (Palo Alto Medical Research Foundation, Calif.). Mutat. Res., 2: 297-303(Aug. 1965).

The locus of the gene for radiation sensitivity in Escherichia coli B_{III} was found in crosses with several K_{12} Hfr's to be closely linked to the his marker. Despite the fact that B_{III}, a derivative of strain B, differs from the K_{12} donor in two radiation-sensitivity genes, only one type of radiation-resistant recombinant was observed, that resembling the donor parent. (auth)

3758 RADIATION SENSITIVITY IN ESCHERICHIA COLI. SOME PROPERTIES OF THE RADIATION-SENSITIVE Hfr K12 MUTANT, PAM 401. Greenberg, Joseph (Palo Alto Medical Research Foundation, Calif.). Mutat. Res., 2: 304-11(Aug. 1965).

A radiation-sensitive mutant of Escherichia coli, PAM 401, was obtained from among survivors of treatment with 1-methyl-3-nitro-1-nitrosoguanidine of a K_{12} Hfr strain. PAM 401 is Hfr; its UV survival curve resembles that of strain B; it reactivates UV-treated T_1 phage; it forms filaments after UV irradiation; it is not significantly sensitive to radiomimetic chemicals; and it is non-mucoid. The gene responsible for radiation sensitivity of this mutant was found to be closely linked to the T_6 locus, but in crosses with strain B and AB1899, whose radiation-sensitivity genes are also closely linked to T_6 radiation-resistant recombinants were obtained. This is interpreted to mean that there are at least two, possibly three, genes closely linked to T_6, a mutation of any one of which will produce phenotypically similar but not identical radiation-sensitive mutants. (auth)

3759 EFFECT OF NITRIC OXIDE ON X-RAY SENSITIVITY OF CROTALARIA INTERMEDIA SEEDS. Bhatia, C. R.; Sybenga, J. (Univ. of Agriculture, Wageningen, Netherlands). Mutat. Res., 2: 332-8(Aug. 1965).

Nitric oxide and oxygen effect were studied in dry seeds of Crotalaria intermedia equilibrated to relative humidities of 5, 32, and 80%. The frequency of mutated sectors appearing in the first leaf was used as the measure of x-ray sensitivity. The results indicate that nitric oxide enhances the effect of x rays at all moisture levels studied, and that the nitric oxide effect increases with increase in seed moisture content. Pretreatment with nitric oxide eight days before irradiation was also found to enhance the sensitivity under anoxia. The observed oxygen effect shows an inverse relationship with seed moisture content. It is suggested that the moisture effect observed under aerobic conditions may be complex with components due

to moisture, oxygen and the interaction of the two. Possibly, oxygen dissolved in the seed moisture also modifies the effect and for isolating the truly oxygen-independent effect it would be important to eliminate these last traces of dissolved oxygen. (auth)

3760 SURVEY ON DEATH RATE AND CAUSES OF DEATH IN X-RAY TECHNICIANS. Kitabatake, Takashi; (Nagoya Univ., Japan); Komiyama, Kihachiro (and others). Nippon Acta Radiol., 25: 213-23(June 1965). (In Japanese).

Death of 52 x-ray technicians was certified in Aichi, Gifu, and Aomori prefectures from 1933 to 1963. The corrected death rate in x-ray technicians through this period was 8.33, which was significantly higher than that in the general population with professional and technological occupation over age 15 in 1955. The corrected death rate tended to increase with an increase of x-ray service period. The age at commencement of x-ray work was not related to the death rate. Causes of death in x-ray technicians was similar to the general population with technological occupation, except for skin cancer which was significantly higher incident in x-ray technicians. The life expectancy in each year class was shorter than in the general male population over 15 years of age that was technologically employed in 1951 to 1952. Life spans were shortened an estimated 6.63 years in x-ray technicians, a rate corresponding to 0.92 days per R. (TCO)

3761 STUDIES ON THE CHANGES OF THE ULTRASTRUCTURE OF EPITHELIAL CELLS OF THE LENS AND CILIARY BODY IN EXPERIMENTAL BETA IRRADIATION CATARACT. Okamoto, Takao (Tottori Univ., Yonago, Japan). Nippon Ganka Gakkai Zasshi, 65: 1021-35(July 10, 1961). (In Japanese).

Rabbit eyes were exposed to a ^{90}Sr applicator with an active surface of 2.2 mm to give 30-, 60-, or 90-min exposures corresponding to 3240, 6480, or 9720 rep of β radiation. To study the genesis of cataracts the changes of the epithelial cells of the lens and ciliary body of the cataractous eye, caused by β irradiation, were investigated in the electron microscope. The main change of the epithelial cells of the cataractous lens was the formation of vacuoles in the cytoplasm. These vacuoles apparently originated partly from mitochondria and partly from endoplasmic reticulum. There was, however, no change in the unpigmented cells of cilliary body in the specimens exposed to equivalent doses of β rays. (BBB)

3762 EFFECTS OF 14-Mev NEUTRONS IN HETEROZYGOTIC EINKORN WHEAT. Fujii, Taro (National Inst. of Genetics, Misima, Japan). Nippon Idengaku Zasshi, 40: 209-18(June 1965).

The effect of neutrons on somatic mutation and fertility in X_1 plants and the relation between dose and the number of mutated tillers in diploid wheat, Triticum monococcum var. flavescens were studied. Heterozygotic F_1 seeds from the cross between normal and a chlorina mutant were subjected to γ rays and 14-Mev neutrons from the T(d,n) reaction neutron generator. Total neutron intensity was 9×10^9 neutrons/sec. For comparison, 8600 rad of γ ray exposure was given at 10 kR/hr intensity using ^{137}Cs. Up to 900-rad neutron doses had no apparent effect on germination rate. Survival rates slowly decreased with increasing dose. A similar tendency was observed in the average number of tillers, but it was not marked. Somatic mutation rate calculated on a spike basis showed an almost linear relation with neutron dose. A very high mutation rate (high RBE) with 14-Mev neutrons was obtained; for instance, the somatic mutation rate in the γ-ray 8600-rad series was 0.18 and that of neutron 324-rad series was 0.39. The decrease of fertility was marked with increasing dose. When the fertility was compared between mutated and nonmutated tillers (including the main stalk) within each individual, average fertility in the former was lower than in the latter, supporting the view that most of somatic mutation arises from chromosome aberrations. The average number of mutated tillers per individual increased with increasing dose, as the result of repeated occurrence of the same kind of mutation within the same individual. (BBB)

3763 RESULTS OF CLINICAL RADIATION ENZYMOLOGY. Kato, H. T.; Kaercher, K. H. (Univ., Heidelberg). Nippon Igaku Hoshasen Gakkai Zasshi, 24: 404-17(July 25, 1964). (In German).

Measurements of enzymatic activities during irradiation therapy are useful as indicators of tumor radiosensitivity. The concentrations of aldolase, malic dehydrogenase, and phosphoglucose isomerase in blood sera of 207 patients with tumors of various types were measured before and after the first irradiation treatment, and after the final irradiation treatment. The results of the measurements were somewhat similar to results previously obtained with lactic dehydrogenase. However, the aldolase concentrations changed more markedly than lactic dehydrogenase did in response to irradiation. The results suggested that estimation of malic dehydrogenase, lactic dehydrogluase, or aldolase during irradiation, or supplemental treatment with cytostatic agents or hormones, is adequate to indicate the status of the tumor during the course of the treatment, or the appearance of recurrences. In many cases the pattern of enzyme concentrations observed gave a quicker and better indication of the progress of the disease than the x irradiation pattern, which was always obtained after the clinical findings. Furthermore, the enzyme studies, because of the pattern found, often showed that the tumor had been affected by the irradiation treatment, while the x-ray picture often remained unchanged. The rational use of enzymological studies in the field of irradiation therapy of malignant tumors can lead to a number of useful conclusions as to the status of the tumor under treatment, as well as to better prognostic indications. In this study it was evident that malic dehydrogenase served as a valuable indicator of the radiosensitivity of several tumor types observed, while the aldolase and phosphoglucose isomerase patterns provided considerable information as to the clinical and developmental status of the malignancies. (BBB)

3764 THE EFFECT OF X-RAY RADIATION ON THE MITOKINETIC APPARATUS OF THE CELL. Srb, Vladimir (Charles Univ., Hradec Kralove, Czechoslovakia). Nucleus (Calcutta), 7: 105-8(1964).

Radiation-induced changes of the mitokinetic apparatus in apical cells of the roots of Allium cepa were examined. The bulbs of the Vsetaty variety of the onion were irradiated by x rays to doses of 1000 R. Immediately after irradiation, the onions were put into tap water to germinate for 3 days; then their root tips were excised for squash preparations in acetocarmine. The effect of radiation on the nuclear apparatus was evaluated by observing aberrant metaphases, anaphases (mainly bridges), and multipolar mitoses. After irradiation, the number of aberrant mitoses markedly increased, mainly from the occurrence of anaphase bridges and multipolar (predominantly tripolar) mitoses. Lobular nuclei, breakage of chromosomes, micronuclei, and other morphological changes were also seen. In the development of radiation-induced aberrations of the mitokinetic apparatus, the importance of damage of the fibers of the achromatic dividing spindle have been emphasized. Anaphase or telophase bridges, and also multipolar mitoses, may develop in this way. On the basis of studies of HeLa cell tissue cultures after irradiation, abnormal development is probably due to radiation damage of the centrosome (by dividing the centrioles into more parts). Because of the absence of the centrosome, other factors are involved in plant cells; the position of the polar centrioles (and their function) is taken by the so-called polar caps from the gelated protoplasma. The dividing spindle is, however, formed and affected by radiation in the same way as animal cells. The aberrant mitoses observed here are interpreted as showing the final phase of tripolar mitosis, with numerous micronuclei. No multipolar mitoses were found in nonirradiated roots; after irradiation, however, their occurrence markedly increased. It is concluded that in the mitokinetic apparatus of plant and animal cells, ionizing radiation induces similar changes, although certain structural and functional differences between the two kinds of cells occur. (BBB)

3765 EXPERIMENTAL STUDIES ON X RAYS AND LEUKEMIA. PART IA. COMPARATIVE STUDY OF THE EFFECT OF X IRRADIATION ON THE PERIPHERAL BLOOD PICTURE IN VARIOUS STRAINS OF MICE. **Ikejiri, Joji (Okayama Univ., Japan). Okayama Igakkai Zasshi, 77: 59-69(Jan. 1965). (In Japanese).**

As the first of a series of studies on radiation leukemogenesis, changes in the peripheral blood picture with time were followed in Cb, D103, StA, and Zb strains of mice (30 to 50 days old) after a single whole-body x irradiation of 350 R. Both the erythrocyte counts and hemoglobin content of blood showed minimum values two weeks after irradiation, and after recovering transiently they tended to decrease again. Results suggest from these findings that there are no marked differences in the peripheral blood picture immediately after a single whole-body x irradiation of 350 R between the RF strain of mice that develop leukemia from x rays and the Cb, D103, StA, and Zb strains that do not develop leukemia from x irradiation, but after a lapse of time there are several distinct differences in the changes of the leukocyte series observable between them. (TCO)

3766 A POSSIBLE ARTIFACT IN CYCLIC VARIATIONS IN RADIOSENSITIVITY. **McDowell, A. A.; White, R. K.; Gallo, K. M.; Brown, W. Lynn (Univ. of Texas, Austin). Percept. Mot. Skills, 20: 46(Feb. 1965).**

Earlier data have suggested cyclic variations in radiosensitivity in the rat, but subsequently presented data argue against cyclic variations in the radiosensitivity of mice. The present study was conducted in an attempt to elucidate one of the many possible artifacts that may inadvertently lead to a conclusion of cyclic sensitivity to radiation. The specific aim of the study was to determine whether ingestion of food prior to radiation exposure influences mortality rate regardless of time of day at which exposure occurs. The experimental subjects were individually caged female Sprague-Dawley rats weighing on the average 229 g. Twenty were exposed to x radiation at 8 a.m. and 20 at 8 p.m. Food was removed from each cage 24 hr prior to exposure. For 10 rats exposed at 8 a.m. and for 10 exposed at 8 p.m., food was replaced for the 3 hr prior to radiation exposure. Irradiations were accomplished using a 250-kv x-ray machine to give a total air dose of 900 R at a dose rate of 93.5 R/min. The dose rates were checked with a meter and the animals were restrained on a rotating table (12 rev/min) in the beam to assure homogeneity of dose. Analysis of the data on days survived during the first 30 postexposure days, using the Kruskal-Wallis one-way analysis of variance, yielded a significant difference between groups. The orthogonal comparison between fed and fasted rats yielded a significant difference, with fasted rats surviving longer. The other two orthogonal comparisons, that between fed rats exposed in the a.m. and p.m. and that between fasted rats exposed in the a.m. and p.m. showed no significant differences. The results show that ingestion of food just prior to radiation exposure decreases survival time for rats during the first 30 days after exposure. Thus, the possibility exists that decreased survival time of rats exposed coincidentally during or shortly after maximal feeding time could easily be attributed to time of day of exposure as contrasted with exposure at some other time of day. (BBB)

3767 RECENT ADVANCES IN ULTRAVIOLET IRRADIATION: PHOTOSENSITIVITY TESTS. **English, J. (London Hospital School of Physiotherapy). Physiotherap., 51: 156-8(May 1965).**

Photosensitivity tests are useful in determining the degree of sensitivity in relation to the uv and visible spectra. Patients who show photosensitivity usually present a dermatitis or similar light-sensitivity reaction. The test is described in detail. (C.H.)

3768 EFFECTS OF GAMMA IRRADIATION ON SYMPTOM EXPRESSION OF BARLEY STRIPE MOSAIC VIRUS DISEASE AND ON TWO VIRUSES IN VIVO. **Halliwell, Robert S.; Langston, Ruble (Texas A and M Univ., College Station). Phytopathology, 55: 1039-40(Sept. 1965).**

The influence of γ radiation on symptoms induced on barley leaves by seed-borne barley stripe mosaic virus (BSMV), potato virus X (PVX) in potato tubers, and on tobacco plants infected with tobacco mosaic virus (TMV) was investigated. Barley seeds (Hordeum vulgare) infected with BSMV, were exposed to γ rays from ^{60}Co source. Dry seed and seed soaked in water for 18 hr, received radiation in 10 steps from 0 R to a lethal dose. Potato (Solanum tuberosum) tubers harboring PVX were treated in a similar manner. As radiation dose increased, the ratio of healthy to diseased barley plants increased. Data taken from plants exposed to 32,000 R and above were not reliable because the radiation damage was often indistinguishable from disease symptoms. The increase in the ratio of healthy to diseased plants could be explained as a result of a lethal effect on infected seed or on the virus in some infected seed or an effect on symptom expression in the seedlings. Experiments with tobacco inoculated with TMV were done to determine the effect of irradiation on infection and virus multiplication. Plants of Nicotiana tabacum infected with TMV were placed in a γ flux of 0, 10, 50, and 100 R/hr. There were no significant differences in virus titer between nonirradiated and irradiated plants. Hypersensitive N. glutinosa was inoculated with TMV and immediately placed in the same γ flux for 0, 24, and 48 hr. Lesions on irradiated plants were counted and compared to the nonirradiated control plants after 72 hr. The appearance of new lesions after 72 hr was negligible and older lesions tended to coalesce. The 50- and 100-R doses for 24 and 48 hr significantly reduced the number of local lesions. After 48 hr irradiation, at all doses, there was a lower reduction in the number of lesions than after 24 hr. Plants irradiated 24 to 48 hr prior to inoculation with TMV had an average increase of 56 and 54% more lesions, respectively, than the nonirradiated leaves. (BBB)

3769 EFFECTS OF NEAR ULTRAVIOLET AND GREEN RADIATIONS ON PLANT GROWTH. **Klein, Richard M.; Edsall, Pamela C.; Gentile, Arthur C. (New York Botanical Garden, Bronx, N. Y.). Plant Physiol., 40: 903-6(Sept. 1965).**

Removal of all of the near-uv (355 to 385 mμ) or half of the green (530 to 585 mμ) radiation from white light increased the fresh and dry weight, height of the plants, and the lengths of the peduncle of marigold plants. Peduncle weight and length were reduced when either near-uv or green wavelengths were filtered but were increased above control levels when both wavelengths were filtered. Tomato plants showed a similar response as did corn and bean plants. Since marigold, tomato, and corn are semi-tropical, high-light-requiring species, identical experiments were performed with Impatiens, a temperate zone, semi-shade plant. Selective removal of near-uv and/or green wavelengths from white light caused growth responses similar to those observed in marigold. Thus, monocot and dicot species from widely separated families are responsive to selective removal of these wavelengths. Selective removal of near-uv and green wavelengths from white light also permitted enhanced growth of Chlamydomonas cells and the mycelium of Sordaria. The oxidation rate of marigold leaf tissues from plants grown under white light supplemented with near-uv or green radiations for 21 days did not differ from that from plants grown under white light. Neither filtration or the near-uv or green wavelengths from white lights nor supplementary near-uv or green radiations to white light had any effect on the endogenous O_2 uptake of stationary or growing cultures of Euglena. No changes were observed in the cytochrome oxidase activity of cauliflower mitochondria measured spectrophotometrically at 550 mμ. Light did not cause any diminution in succinoxidase activity of washed mitochondria. It is concluded that the observed growth changes caused by near-uv and green light are unlikely to be due to alterations in energy metabolism as determined by O_2 uptake. There was no repression in the rates of synthesis of chlorophylls or carotenoids by Euglena cells when the near-uv or green components of the white light were filtered or when the white light was supplemented with these radiations. (BBB)

3770 BIOLOGICAL EFFECT OF SMALL DOSES OF IONIZING RADIATION ON THE HUMAN ORGANISM. Klener, Vladislav. Prac. Lek., 17: 260-4(Aug. 1965). (In Czech.).

An account of the effect of small doses of ionizing radiation on the human organism is presented in order to demonstrate the possibilities of medical control of the health status of occupational groups exposed to radiation. Seeking sensitive indicators of ionizing radiation is based on certain theoretical considerations and is elaborated in particular in the sphere of cytogenetics. Epidemiological investigations based on the statistical evaluation of certain somatic and genetic signs in exposed populations are also discussed. Groups of exposed subjects can also be examined by epidemiological methods. However, methodological and organizational conditions for more extensive long-term investigations have not yet been created. (auth)

3771 RADIATION-INDUCED MYELITIS. Vaeth, Jerome (Univ. of California, San Francisco). Progr. Radiat. Therapy, 3: 16-26(1965).

Reports of radioinduced myelitis are reviewed, and its incidence in one series of patients is reported. The method by which myelitis is radioinduced is postulated. Myelitis was detected in 3 patients out of 323 in the series, and was transient in two and progressive or irreversible in one. The treatment records of these patients are reviewed, particularly in regard to tissue reactions during radiation therapy, dose administered, and volume of spinal cord included. Most of the patients were treated over an extended period at weekly dose rates of 800 R or less delivered by either 1-Mev x rays or ^{60}Co teletherapy to the spinal cord. In all patients, large segments of the spinal cord were irradiated throughout the course of treatment. The relation of treatment time to spinal cord dose for individual cases in this series was plotted. The time-dose relation of radiation administered to most of these patients was well over the usual limits of safe tolerance. The results show that damage may be of three levels, the most severe of which is seldom seen in clinical practice: early transient myelitis, which is reversible, characterized only by symptoms; progressive myelitis with initial symptoms and signs; an interval without symptoms followed months later by progressive signs indicative of damage to nerve tissue secondary to injury to the vasculoconnective tissue; and severe reaction characterized by massive neurologic deficits, the result of radiation doses large enough to destroy nerve and glial cells almost immediately after irradiation. A single factor, extension of treatment time, appeared to contribute the most towards preservation of normal tissues undergoing irradiation. (TCO)

3772 FACTORIAL COMPARISON OF THE EFFECTS OF PENTOBARBITAL SODIUM AND WHOLE-BODY X-IRRADIATION ON VR-3 FOOD REINFORCED BAR-PRESSING. Smith, Richard K. (Tulane Medical School, New Orleans); Elder, S. Thomas; Stokes, Stuard K.; Rye, Merrill M.; Meckstroth, George R. Psychol. Rep., 16: 1245-8(June 1965).

A study was made of the extent to which a VR-3 reinforced bar-pressing response in rats is affected by whole-body x-irradiation doses in conjunction with standard amounts of pentobarbital sodium (Nembutal). The experiment was carried out in two replications. In each replication one subject was rejected for failure to learn the bar-pressing response and another for reasons of health. On the day immediately following the 13th VR-3 session (experimental day 15), 10 male rats were assigned to each of three treatment groups: (1) no x irradiation, (2) 4.75-rad, and (3) 475-rad whole-body x irradiation. Each of the three groups of 10 were subdivided into two equal groups of 5 each; one subgroup received an intraperitoneal injection of 9.0-mg pentobarbital while the other subgroup (control) received isotonic saline. All injections were administered 10 min prior to the x irradiation treatments. Analysis over the first three days following experimental treatments yielded a significantly reduced response due to 475-rad x irradiation; the main effect for anesthesia failed to reach a significant value. Data from the second replication which continued through the 12th day after treatment (experimental day 28) suggested complete bar-pressing recovery from the effects of anesthesia is achieved by about the fourth day. These data and subsequent work show that response recovery from a large dose of whole-body irradiation takes place sometime later depending upon the magnitude of the dose. Some rats which received the 475-rad radiation treatment failed to eat the 10 g of chow placed in the cage after the posttreatment training. This decrease in food intake tends to support the earlier suggestion that performance decrements which follow exposure to whole-body x irradiation are due, in part, to a motivational deficiency rather than a memory loss. (BBB)

3773 EFFECTS OF IONIZING RADIATION ON THE DEVELOPMENT OF AMPHIBIANS. Brunst, V. V. (Roswell Park Memorial Inst., Buffalo). Quart. Rev. Biol., 40: 1-67(Mar. 1965).

A review, citing 299 references, is given concerning the effects of radiation on living organisms, the effect of irradiation on cells, tissues, and organs, and especially the effects of total and local irradiation on the development of amphibians. The effects of irradiation on amphibians are compared with those on higher forms (mammals, including man) and lower forms (invertebrates, microorganisms, and plants), especially by considering general problems such as formation of giant cells, phagocytosis and regression, sensitivity of cells, tissues, and organisms, and the problem of radiostimulation. The influence of irradiation on germinal cells, fertilization, embryonic development, larval development, and adult amphibians is also considered. (BBB)

3774 EXAMINATIONS OF RADIATION REACTIONS OF THE LIVER BY MEANS OF ^{131}I BENGAL ROSE TESTS. Loebe, J.; Neumeister, K.; Gursky, S. (Karl-Marx-Univ., Leipzig). Radiobiol. Radiotherap., 6: 609-13(1965). (In German).

The determination of radiation-induced changes of the hepatic function is important for the medical control of occupationally exposed persons and for the control of tumor irradiations. Systematic examinations of parenchymal and mesenchymal functions of the liver showed an impairment of activity (bromsulphalein test) after abdominal irradiations as well as an unequivocal disturbance and impairment of several hepatic functions in persons with injured liver following therapeutic x irradiations. Tests with ^{131}I-bengal rose performed with these examinations yielded no significant changes of the initial values. From the result of examination, it is concluded that single hepatic functions may be disturbed by a radiation-effect but that the injury cannot be determined certainly by the hitherto existing function tests. (tr-auth)

3775 HUMORAL FACTORS RESPONSIBLE FOR RADIOLOGICAL EFFECTS AT A DISTANCE AFTER SELECTIVE IRRADIATION OF LYMPHATIC ORGANS. Maurice, P. A.; Jeanrenaud, A. (Hopital Cantonal, Geneva). Radiol. Clin. Biol., 34: 113(1965). (In French).

Some clinical observations suggest that irradiation of the spleen frees a factor capable of depressing mitotic activity in organs situated at a distance from the irradiation zone. With the intention of throwing light on the mechanism of this radiobiological effect, the spleen and small intestine of rabbits and rats were exposed to 300 R of x rays after surgical exteriorization of these organs. The bodies of the animals were protected from irradiation. A temporary inhibition of erythropoiesis following treatment was manifested by a drop in the number of circulating reticulocytes and the mitotic index of the erythroblastic marrow. The same effects were obtained in nonirradiated animals after injection of serum from donors whose lymphatic organs had undergone selective irradiation. Serum taken from animals operated on, but not irradiated, remained inactive. The antimitotic factor appeared in the circulation 30 min after irradiation in the rat and two hr after in the rabbit. Its activity was not limited to one animal species, and

active serum obtained by irradiation of the lymphatic organs of a rabbit induced the antimitotic effect in the rat equally well. Fractions of active serum, isolated by chromatography and electrophoresis, showed that the antimitotic activity was present exclusively in a fraction having physiochemical properties similar to those of the γ-globulins. (BBB)

3776 SOME RECENT ADVANCES IN THE RADIATION BIOLOGY OF BACTERIA. Powers, E. L. (Argonne National Lab., Ill.). Radiol. Clin. N. Amer., 3: 197-208 (Aug. 1965).

Recent advances in understanding the mechanisms by which high- and low-energy radiations bring about their effects in bacterial cells are reviewed, and some interpretations of recent results are offered. (TCO)

3777 COMPARISON OF REACTIVITY AGAINST THE HOST OF THYMOCYTES AND SEMI-ALLOGENIC LYMPH NODE CELLS. Mathe, G.; Amiel, J.-L.; Brezin, Colette; Choquet, Claudine (Institut de Cancerologie et d'Immunogenetique, Villejuif, France). Rev. Franc. Etud. Clin. Biol., 9: 988-90(Nov. 1964). (In French).

F_1 hybrid mice (DBA/2 × C57B1/6) were irradiated in toto with a dose of 500 rad of 200-kv x rays to compare the immunological activity of thymocytes and lymph node cells. The test depends on development of fatal immune disease by cells of the parental line in the F_1 irradiated hybrids. The mice each received 10^7 bone marrow cells (C57B1/6) from donors of the same age and sex. They were then separated at random into four groups, series A, B, C, and D. Series A received 4×10^7, 10^7, 10^6, and 10^5 thymocytes from C57B1/6 mice three months old. Series B received 4×10^7, 10^7, 10^6, and 10^5 lymph node cells from the same donors. Series C received 4×10^7, 10^7, and 10^6 thymocytes from adult C57B1/6 donors kept for 2 hr at 37°C in Tyrode's solution. All these injections were administered intravenously on the day of irradiation. One hundred times as many thymocytes as lymph node cells were required to achieve an equivalent immunological reaction. This result could be interpreted in two ways. Either thymocytes are 100 times less active for immunological purposes than lymph node cells, or lymph node cells have the same activity, but are 100 times as numerous. The fact that storage in the Tyrode's solution seemed to have no effect on the sensitivity of lymphocytes and immunologically competent thymus cells confirms their cellular identity. (BBB)

3778 SURVIVAL TIME IN GERMFREE MICE AFTER LETHAL WHOLE BODY X-IRRADIATION. Matsuzawa, Taiju (Tohoku Univ. School of Medicine, Sendai). Tohoku J. Exp. Med., 85: 257-63(Apr. 25, 1965).

Mortality rate and survival time of germfree Swiss-Webster mice subjected to whole-body x irradiation in the dose range of 500 to 35,000 R were compared to that of conventional Swiss-Webster mice. The log-log plot of survival time vs x-ray dose in both germfree and conventional mice showed three different straight line segments and one curved segment, each with distinctive dose response characteristics. No essential difference was noted in the dose-response relations between germfree and conventional mice. However, the mean survival time of germfree mice in the dose range which causes so-called hemopoietic death was 12.5 days as compared to 11.2 days for conventional mice, a difference of 1.3 days. The mean survival time of germfree mice in the so-called gut death range was 7.2 days as compared to 3.4 days of conventional mice, more than twice the difference. In general, the survival time of germfree mice in the zone of death caused by damage to the cell renewal system was much longer than that of conventional mice. However, the survival time of germfree mice in the so-called brain death x-ray dose range (over 17,500 R) was reversed and was shorter than that of conventional mice. It is suggested that these differences of dose range in each curve segment between germfree and conventional mice is based on the difference in susceptibility of their respective radiosensitive systems to damage. The prolonged survival time of germfree mice in the gut-death dose range is probably due to the prolonged life span of the intestinal epithelial cells, and this may be due to the absence of microbial flora. The prolonged survival time of germfree mice in the hemopoietic death zone is probably the result of the prolonged life span of some blood cell line. No data are available at present to explain the difference of the survival time between germfree and conventional mice in the highest dose range where neural injury predominates. (BBB)

3779 ENVIRONMENTAL AGENTS IN CANCER. Miller, Robert W. (National Cancer Inst., Bethesda, Md.). Yale J. Biol. Med., 37: 487-507(June 1965).

The possible roles of various environmental factors in inducing cancer or leukemia are discussed, with a consideration of ionizing radiation as an etiologic factor in several situations. The effects of radiation are being evaluated among 6500 men trained during 1941-45 as radiology technicians as compared with an equal number of men trained as hematology or pharmacy technicians. To date no influence on total mortality or causes of death has been detected. These results are reassuring since the radiology technicians in general were subjected to substantially greater radiation exposures than patients who undergo diagnostic x-ray procedures. As a measure of the genetic effect of radiation, questionnaire data are being evaluated to determine if there has been a shift in the sex ratio of live-born children of the radiology technicians. Disturbance of the sex ratio is thought to be the best available epidemiologic indicator of radiation-induced genetic damage. When males are exposed to radiation, lethal mutants that occur on the X chromosome can be transmitted only to their daughters. The Y chromosome, which the sons receive, is thought to be relatively inert with respect to lethal mutants. On the basis of this reasoning, daughters of irradiated males would experience an increased fetal mortality, and consequently the sex ratio (M/F) of live-born infants would rise. The most convincing evidence that ionizing radiation can induce leukemia in man comes from the studies of the atomic bomb survivors in Hiroshima and Nagasaki. The response was proportionate to the dose and, unlike studies involving x ray exposures for medical purposes, there were no variables known that could could confound the interpretation. As yet there has been little evidence that the exposure induced cancers of other sites, the chief exception being the thyroid, in which microscopic foci of neoplastic cells have been reported. It is concluded that through the use of a variety of existing data resources, specific ideas about the environmental origins of cancer can be tested through epidemiologic research. The observations so made are helpful in determining the applicability to human carcinogenesis of concepts developed in the experimental lab. Conversely, epidemiologic research can provide new ideas concerning carcinogenesis that may be further explored by lab study. (BBB)

3780 THE INFLUENCE OF WATER CONTENT ON THE INACTIVATION AND MUTATION RATE OF X- AND γ-IRRADIATED NEUROSPORA CRASSA CONIDIA. Klingmueller, Walter (Max-Planck-Institut fuer Vergleichende Erbbiologie und Erbpathologie, Berlin). Z. Vererbungsl., 96: 116-27(1965). (In German).

Experiments were conducted on a wild strain of N. crassa as well as on seven macroconidia-forming and one microconidia-forming mutant strains (induced by nitrous acid). The conidia, suspended in water or with water contents of 32.2, 11, or 2%, were irradiated with x rays (250-kv, 5 kR/min, up to 150-kR total doses) or ^{60}Co γ rays (210 kR/hr, up to 210-kR total doses). The inactivation- and reversion-rates for conidia of HNO_2-induced mutants were measured. With constant radiation dose, inactivation rate was lowest for conidia of medium moisture content. It increased for higher and also for very low moisture content. The semilogarithmic plot of inactivation data for conidia irradiated in suspension or at medium moisture content resulted in a shouldered curve. A formal analysis using the number of nuclei of multinucleated conidia as numerical reference indicated that about 0.5 hits per nucleus are needed to in-

activate such a conidium. The data for extremely dry conidia plotted from 0 to 210 kR likewise closely approximated a single-hit curve with a steeper slope than that of the corresponding curve for conidia of medium moisture content. Reversion rates of 5 among the 7 macroconidia-forming mutants tested ran parallel with inactivation, with low figures for conidia of medium water content and increasing figures for high as well as for very low moisture contents (class I). The reversion rate of conidia of very low moisture content of the other 2 mutants was equal or nearly equal to that of conidia of medium moisture content (class II). (BBB)

3781 DEVELOPMENTAL HISTORY OF MUTANTS OF FUNARIA HYGROMETRICA L. INDUCED BY X IRRADIATION. Oehlkers, Friederich (Univ., Freiburg i. B.). Z. Vererbungsl., 96: 234-49(1965). (In German).

Funaria hygrometrica samples were exposed to from 10 to 60 R of x irradiation. The germination of the irradiated spores was much slower than that of unexposed spores and frequently when a germinal tube was formed, and fission was about to take place, growth ceased. This indicated that the cell nucleus was damaged by the irradiation more than was the cytoplasm. The protonema (chloronema and caulonema) may remain completely unchanged during irradiation, but newly formed genes may become active later. Vegetative propagation is rare. Buds appear on the caulonema and on the basal cells of the side branches. If two edged or single edged vertex cells are formed on the buds instead of three edged vertex cells they have a leaf like or infrequently a filamentous appearance. Some buds with normal three-sided vertex cells appear normal but do not continue to grow. Their external cells become chloronema filaments. This abnormal formation of chloronema represents a mutation effect. The polarity of the entire structure remains unchanged. An additional mutational effect is that the rhizoids at the base of a stem fall away. For this reason, and because a large number of substances must circulate through the basal cells, the water balance must eventually become insufficient. Other reports also have indicated that the rhizoids are the source of water uptake. The hybridization of the antheridia by the presence of one or less archegonia indicates that untreated spores produce plants with very few hybrid stands, but if the spores are irradiated with a dose of 20 kR, a maximum are produced. Plants of this type without hybrid stands amounted to 37.5%. At a dose of 40 kR, 62.6% of the plants lacked hybrid stands. (BBB)

3782 THE FREQUENCY OF CHLOROPHYLL MUTATIONS AFTER X IRRADIATION OF A HETEROZYGOUS M_2-SEED STOCK OF BARLEY. Keppler, E.; Siegert, W. (Univ., Jena, Ger.). Zuechter, 35: 98-102(1965). (In German).

Polykernelled stocks harvested from M1 ears of two types of barley were x irradiated with 14 kR. The varieties used were Certina and DFG, type 460_{47}. The chlorophyll mutation rate was measured in unthreshed ears. In comparison to the more resistant crossed populations, the polykernelled stocks, which included simple heterozygotic genotypes, were no less radiosensitive than corresponding pure lines. In the $M_{\frac{1}{2}}$ generation significantly more chlorophyll mutations appeared than in the M_2 generation. The mutation rate induced by a second irradiation given to the M_2 and $M_{\frac{1}{2}}$ generations was equivalent to the effect of the first irradiation. The irradiation effects of both were additive. The possibility that the mutation frequency in heterozygotic stocks was increased by additional factors was suggested by the data, but it could not be confirmed statistically. (TCO)

3783 THE GENETICS OF SORDARIA BREVICOLLIS [Thesis]. Chen, Kuo-chun. New York, Columbia Univ., 1964. 40p.

Sordaria brevicollis is the first described heterothallic species of the genus Sordaria. Heterothallism is controlled by a single pair of compatibility factors symbolized by A and a. The hyaline microconidia from either of the 2 mating types of S. brevicollis are highly effective in fertilization and are ideal for mutagenic treatment with ultraviolet irradiation. Irradiated microconidia are placed on mycelium of opposite mating types. By means of uv-induced mutation, a total of 25 mutants were obtained of which 20 are ascospore mutants and 5 are mycelial mutants. All these mutants are found to be single-gene mutation with respect to genetic segregation analysis. A significantly greater frequency of asymmetrical over symmetrical second division asci was observed in most crosses in S. brevicollis. Crosses between ascospore color mutants of seven different linkage groups and their wild types of opposite compatibility were made. Calculations of the degree of inequality between the frequency of symmetrical and asymmetrical patterns of second-division segregation were made on the basis of the percentage of invalid asymmetrical MII asci in the various crosses. The values vary greatly in the different crosses studied, ranging from 0.4% in one cross up to 77.8% in others. The extent of biased segregation is probably controlled by a number of unidentified genetic factors. This feature was further demonstrated in crosses involving the g_2 mutant and others. The centromere distances in S. brevicollis are calculated from the number of symmetrical MII asci. According to the data for the relationships of mutant loci thus far studied, seven different linkage groups were established. (A.G.W.)

3784 GENETIC ANALYSIS OF BEHAVIOR TRAITS IN SWINE [Thesis]. Beilharz, Rolf George. Ames, Iowa, Iowa State Univ. of Science and Tech., 1965. 79p.

Data on open field scores of 1853 pigs and social dominance value of 1629 pigs were obtained from Iowa State University's swine irradiation project. The pigs were Durocs and Hampshires. Open field score (OF) is the number of squares, marked on the floor of a strange pen, into which a pig stepped in the first two minutes when put into the pen alone. Dominance value (DV) is the average social dominance position of a pig in its group. OF data were analyzed in a hierarchical analysis of variance with subclasses, sires, dams, and individuals as the levels of hierarchy. Factors distinguishing subclasses were sex, breed, x irradiation of sires, and season of the year. DV was estimated relative to a pig's litter. The major analysis of DV was done within subclasses differentiated by irradiation treatment of sires and breeds. Sexes were balanced within each litter by random elimination of some DV records. Components of variance due to sex and its interactions were studied. Heritability of DV could not be found. Heritability of OF was 16%. OF had a significant phenotypic correlation of –0.23 with weight at 154 days. It was uncorrelated with other weights or with backfat thickness on the live animal. Raw DV and least squares DV were highly correlated within sex, within litters. Ranking of pigs was practically identical by the two methods. Barrows were more dominant than gilts. The sex difference was larger in Hampshires than in Durocs. Sire irradiation increased the variance component for interaction of sire by sex in DV, and increased variance within litters. DV had highly significant positive correlations, within sex, within litter, with weight at all ages. (Dissertation Abstr.)

3785 THE MORPHOLOGIC CHANGES INDUCED IN THE LUNGS OF HAMSTERS AND RATS BY EXTERNAL RADIATION (X-RAYS). A STUDY IN EXPERIMENTAL CARCINOGENESIS [Thesis]. De Villiers, Arnoldus Jakobus. Pittsburgh, Univ. of Pittsburgh, 1964. 117p.

Eight-week old Syrian hamsters (99 irradiated and 70 controls) and Wistar rats (112 irradiated and 69 controls) were used in six experiments. Hamsters were exposed at 99 R/min to a total dose of 3958 R delivered through a 2-cm lead-shielded collimator to the chest region, spread over five equal daily portions further fractionated into four equal doses by varying the portal of entry through 90°. Rats were similarly exposed to a total dose of 3540 R. Mortality for both species was low during the first six post-irradiation weeks (one hamster, two rats) but high in the case of hamsters (75 per cent) during the eighth to twentieth post-irradiation weeks. In hamsters that survived this period, considerable life shortening occurred. The most extensive changes were observed in the lungs of

hamsters that died during the tenth to sixteenth post-irradiation weeks. Increasing nuclear atypism, perivascular cuffing by plasma-cytoblast-like cells and an increase in mast cells in the alveolar interstitium occurred during this period. Areas of unphysiological hyperplasia, focal proliferations, metaplasia including adenomatoid lesions, pre-invasive cancer and invasive squamous cell carcinomata (12 per cent of deaths in first twenty weeks) were seen. Evidence of vasculo-connective tissue damage, intrapulmonary hemorrhages, pulmonary edema, and intra-alveolar collections of eosinophilic (proteinaceous) material were noted. Large areas appeared to become necrotic. Dissolution of alveolar septa and the development of true (noncompensatory) radiation-induced emphysema was clearly shown by reticulin studies. A delayed autosensitivity state was suggested as the fundamental cause of death during the eighth to twentieth week. By contrast, the rat studies did not reveal severe delayed changes and life shortening. Interest was centered chiefly on radiation-induced alveolar cell adenomata (mouse type) and four malignant lung neoplasms. (Dissertation Abstr.)

3786 EFFECTS OF IRRADIATION ON BIOLOGY AND IMMUNOLOGY OF INFECTIVE LARVAE OF NIPPOSTRONGYLUS BRASILIENSIS (TRAVASSOS, 1914) LANE, 1923, IN RATS [Thesis]. Shaikh, Hefazuddin. College Station, Tex., Agricultural and Mechanical Univ., 1965. 74p.

An investigation was undertaken to study the effects of gamma irradiation on immunologic responses produced in white rats by infective larvae of Nippostrongylus brasiliensis subjected to graded total dose levels of gamma irradiation. The dose levels to which different batches of infective larvae were subjected were 25,000, 30,000, 35,000, 40,000, 45,000, and 50,000 R. White rats infected with Nippostrongylus brasiliensis were received and cultures of infective larvae were made from their fecal samples with animal charcoal or with sphagnum moss. The strain of the parasite was maintained by infecting white rats throughout the experiment. Infective larvae were recovered and either the normal infective larvae or the irradiated larvae were inoculated into apparently parasite-free young rats. The biological behaviors of the normal and irradiated larvae in the hosts were observed by necropsy at different intervals of infection. Individual rats initially infected with normal or irradiated larvae were subsequently challenged with normal infective larvae. The percentage of development and recovery of worms at different periods after inoculations was observed at postmortem. In challenge infections few worms were recovered from rats initially infected with larvae irradiated with 30,000 and 35,000 R, than from rats initially infected with irradiated larvae subjected to 25,000, 40,000, 45,000, and 50,000 R. The prepatent period of the parasite in rats from infections with normal infective larvae was six days, but this period was longer in infections with irradiated larvae with the production of fewer eggs. Larvae subjected to total irradiation doses of 45,000 R and 50,000 R when inoculated in rats did not produce any eggs. Some effects of irradiation on the biology of the parasite were delayed migration from the site of inoculation, stunting in growth, wrinkling and thickening of the cuticle as a result of possible failure to undergo complete ecdysis in different molts, lack of development or improper development of different organ systems, and considerable deposition of brownish granular materials beneath the cuticle. Pathological changes produced in the hosts by irradiated larvae were severe in contrast to the changes produced by the normal infective larvae. Irradiation of the infective larvae at dosage levels of 30,000 and 35,000 R of gamma irradiation had antigenic value in the production of immunologic responses in the hosts. (Dissertation Abstr.)

3787 STUDIES OF THE RADIATION BIOLOGY OF THE T5 RECEPTOR [Thesis]. Bohne, F. Karlsruhe, Ger., Tech. Univ., 1965. 59p. $2.00 Gmelin, AED-DISS. 65-6.

Inactivation of the T5 receptor by soft x rays and γ rays and the dependence on type of suspension medium, O_2 concentration, and S containing substances were studied. Results indicate that inactivation is caused directly by radiolysis products of the water. It is probable that the primary radicals are the inactivating agents. Target theory gives a target volume of 25.10^{-19} cm^3. Presence of cystamine increases inactivation doses by a factor of 10. Protective action of cysteamine is less than that of cystamine. (auth)

3788 THE DEVELOPMENT OF AN ATYPICAL SECONDARY DISEASE IN X-IRRADIATED GERMFREE MICE TREATED WITH ALLOGENIC AND SYNGENIC BONE MARROW. Wilson, Raphael. 9p. (CONF-650560-7). ORINS. Gmelin, AED-CONF-65-157-10.

From 13th Annual Meeting of the Radiation Research Society, Philadelphia.

Germfree and conventional C3H and CFW mice were used to establish a dose-response curve after x irradiation and syngenic and allogenic marrow transplants. The LD_{50} of untreated conventional mice was 660 R; for germfree, it was 705 R. Treatment with allogenic and syngenic bone marrow raised these values to 770 to 890 R for conventional mice and to 1280 to 1650 R for germfree mice. Mice that survived after marrow treatment were maintained for 150 days post-irradiation and examined regularly for the lesions associated with secondary disease, including diarrhea, weight loss, ataxia, kyphosis, depilation, skin lesions, and lymphoid aplasia. With the exception of skin lesions and depilation, conventional mice developed typical symptoms between 20 and 60 days post-irradiation. In general, symptoms were not as severe in germfree mice and appeared at later times. No mice which had been irradiated with doses of 800 to 1100 R showed extreme depilation. Doses of 1200 R or more to germfree mice were followed by hair loss between 30 and 60 days post-irradiation. This was equally manifest in allogenic and syngenic chimeras. Mice which had received 1200 and 1300 R showed some new growth of hair, but C3H mice which had been treated with CFW marrow became greyer than those treated with C3H marrow. Observations made over a 150-day period failed to indicate a clear-cut secondary disease in germ-free mice comparable to that observed in conventional mice. (C.H.)

Radiation Effects Therapy and Countermeasures

3789 REGENERATION OF BONE MARROW: A CLINICAL AND EXPERIMENTAL STUDY FOLLOWING REMOVAL OF BONE MARROW BY CURETTAGE. Branemark, P. I. (Univ. of Gothenburg, Sweden); Breine, U.; Johansson, B.; Roylance, P. J.; Roeckert, H.; Yoffey, J. M. Acta Anat., 59: 1-46(1964).

The increasing use of radioelements in industry and research has increased the risk of radiation injury and hence stimulated greater interest in the study of the effects of ionizing radiation on bone marrow. Many workers have studied its regeneration after damage by radiation, and the possible influence of transplanted bone marrow, mainly in the form of intravenous cell suspensions, on the process of regeneration. In studying regeneration in normal bone marrow, marrow damaged by radiation or toxins is not appropriate because of the accompanying effects of irradiation on adjacent tissues and the whole body. Hence, mechanically removed marrow is preferable for regeneration studies, and information on the basic biological phenomena which can be obtained will lead to better understanding the regeneration of marrow damaged by radiation. Thus, bone marrow regeneration after mechanical ablation was studied in rabbits by histologic, microradiographic, and vital microscopic techniques and in humans by histologic techniques. The various stages in regeneration are described and analyzed, considering periosteum, diaphysial compacta, endosteum, cancellous bone, vessels, and hemopoietic tissue. It was demonstrated that the processes of regeneration in the rabbit as well as in man follow a characteristic schedule. The findings indicate a correlation in

time between the appearance of hemopoietic cells and the disappearance of a regularly formed trabecular network in the medullary cavity. This indicates a transformation of osteoblasts into reticulum cells in the process of marrow regeneration. Marrow regeneration in man resembles that in rabbit, except that the marrow regenerates to the cellularity of marrow normally found at the site at the same age. Microradiographic studies enabled a thorough analysis of changes in structure and mineralization occurring in the bone after marrow ablation. Vascular architecture and flow characteristics in the regenerating tissue, studied in the living tissue by a vital microscopic chamber technique, demonstrated a close connection between newly formed sinusoids and osteoblasts. (BBB)

3790 POTENTIAL RADIATION PROTECTIVE AGENTS. III. MERCAPTO ANALOGS RELATED TO EPHEDRINE. Venkatramana Bhat, K.; McCarthy, Walter C. (Univ. of Washington, Seattle). J. Pharm. Sci., 54: 225-8(Feb. 1965).

Since certain sympathomimetic amines possess radiation protective activity, the mercapto analogs related to ephedrine were selected for investigation. Previously it was shown that chlorodeoxypseudoephedrine-HCl reacted with thiourea to give, instead of the expected isothiouronium salt, a cyclization product, 3,4-dimethyl-5-phenyl-2-iminothiazol-idine-HCl. Because of the difficulty in isolating a crystalline mercapto amine from the hydrolysis of this compound, other routes were investigated for the synthesis of these mercapto analogs. Reaction of (+)-chlorodeoxypseudoephedrine-HCl with sodium thiosulfate gave a Bunte salt. This compound required 12 to 20 recrystallizations to bring it to constant mp and optical rotation. Because of the tedious recrystallization required, other methods for the introduction of the sulfur function were investigated. It was shown that reaction of chlorodeoxypseudoephedrine-HCl with sodium thioacetate gives 1-phenyl-1-mercapto-2-(N-methylacetamido)propane. This product was resistant to hydrolysis by aqueous acid or base, but the corresponding disulfide was reduced by lithium aluminum hydride to 1-phenyl-1-mercapto-2-(N-methyl-N-ethylamino)propane. Condensation of chlorodeoxypseudoephedrine-HCl with potassium ethyl xanthate gave 3,4-dimethyl-5-phenylthiazolidine-2-thione, which was also resistant to hydrolysis, but was reduced to 1-phenyl-1-mercapto-2-(N,N-dimethylamino)propane. The Bunte salt, when administered to mice in the dose range of 51 to 150 mg/kg showed no protective activity against an LD_{100} dose of radiation. Another ephedrine derivative, 3,4-dimethyl-5-phenyl-2-iminothiazolidine-HCl, administered to mice in the dose range of 50 mg/kg or less, also showed no protective activity. (BBB)

3791 ON RECOVERY-PROMOTING CHEMICALS AFTER GAMMA-RAY IRRADIATION TO MOUSE STRAIN L CELLS CULTURED IN VITRO. Aoyama, Takashi; Sawayama, Toshiko; Fujiwara, Yoshisada; Kondo, Teruo (Kobe Medical Coll., Japan). Kobe J. Med. Sci., 11: 31-7(Mar. 1965).

The effect of inosine on the radiation injury of mouse strain L cells cultured in vitro was investigated, using per cent survival as an indicator. L cells were grown in YLH medium and inosine was added at a concentration of 100 μg/ml immediately before irradiation, with 100 to 900 R of ^{60}Co γ rays. After irradiation, 0.5 ml of YLH medium containing RISA (radioiodine-labeled human serum albumin) was added to 1.5 ml of cell suspension on the 0, 2nd, 4th, and 7th day of incubation at 37°C. Inosine had a slight effect in decreasing the radiosensitivity as well as a strong recovery-promoting action on cells cultured in vitro although it had no effect on cell proliferation when given alone. The slope of the dose-percent survival curve was slightly less steep than that of the control curve only when it was given before irradiation; when it was added simultaneously with or after irradiation, no change of the slope of survival curves was observed. The recovery-promoting effect was such that radiation-induced growth depression by about 300 R was almost cancelled and this effect was demonstrated irrespective of the time of administration. (BBB)

3792 RADIOPROTECTIVE ACTION OF RNA IN MICE. Roberts, Merritt E.; Jones, Carolyn; Gerving, Martha A. (Pasadena Foundation for Medical Research, Calif.). Life Sci., 4: 1913-22(Oct. 1965).

Three strains of mice were γ irradiated with ^{60}Co to doses of 800, 750, and 700 R and observed for 30 days. At 800 R the Swiss mice showed an average survival time of 11.2 ± 0.5 days. A corresponding death time for C3H mice occurred between 700 and 750 R. Injections of various RNA preparations were given both pre- and post-irradiation at intervals from 30 min to 16 hr. None of the RNA preparations protected the C3H mice from radiation effects. Control DBF1 mice were radioresistant at 800 R. Of the four commercial yeast RNA products tested, only one indicated a significant degree of protection. A high polymer RNA preparation at 20 mg per mouse gave better protection than the commercial material at the 20 mg dose. It likewise protected at the 6-mg level but was ineffective at the 3-mg level. Treatment with various yeast preparations was also tested. An alcohol fraction of both Baker's yeast and Brewer's yeast extract, which should contain high polymer RNA, gave protection. Good results were also obtained by recognized protective agents (MEA and AET). Histamine was effective, but benadryl was not. Two DNA preparations were tested, but neither was effective. The white cell count of the unprotected mice dropped rapidly and leukopenia became severe before death. Many of the protected mice showed a similar blood picture, but the mice which eventually showed prolongation of life had a less severe initial leukopenia, with the count usually staying above 1000 cells/cm^3. Radiation protection from purines, pyrimidines, their nucleosides, nucleotides, and their analogs was also tested. About 80 of these compounds were tested, all at a screening concentration of 20.0 mg/mouse, injected intraperitoneally 30 min before irradiation with 800 R. The average survival times in days for the best of these were as follows: hypoxanthine, 18.0; uric acid, 14.7; calcium ureate, 14.0; thiouracil, 14.0; guanine, 13.2; cytidine, 13.0; and 8-azaxanthine, 13.0 (untreated mice survived an average of 10.7 days). (BBB)

3793 THE TREATMENT OF BONE MARROW FAILURE WITH MASSIVE ANDROGEN THERAPY. West, Wilk O. (Lexington Clinic, Ky.). Ohio State Med. J., 61: 347-55(Apr. 1965).

Massive-dose androgen therapy was administered to 68 patients with bone marrow failure associated with chronic lymphocytic leukemia (21 cases), hypoplastic anemia (33 cases), primary myelofibrosis (nine cases), and achrestic anemia (five cases). Fifty-one patients received testosterone enanthate, 12 received methandostenolone, and five had fluoxymesterone therapy. Forty-five of the 68 patients completed a 3-month course of massive androgen therapy. Treatment was interrupted by death in 15 cases and by drug intolerance in eight others (local irritation in four, jaundice in four) before adequate trials were completed. Favorable results were obtained in patients with bone marrow failure complicating chronic lymphocytic leukemia. Thus 11 of the 20 patients with favorable responses to androgen therapy in the present series had lymphocytic leukemia, while only seven patients with the same condition showed no improvement. The complication of bone marrow failure was foreshadowed by the appearance in these patients of refractoriness to conventional suppressive agents such as ^{32}P, x irradiation, and alkylating agents, the continued use of which merely hastened hematopoietic decompensation. This refractory state was rapidly complicated by heavy lymphocytic infiltration of the marrow and consequent failure of hematopoiesis. Massive androgen therapy appears to stimulate erythropoiesis predominantly, but in some instances granulopoiesis and thrombopoiesis as well. In chronic lymphocytic leukemia, there may be concomitant lymphopoietic activity. The mechanism of the hematopoietic action of pharmacologic doses of androgens is not known, nor is there any available explanation for the success of therapy in some instances and failure in others. (BBB)

3794 CHANGES OF THE PERMEABILITY OF THE ISOLATED FROG HEART IRRADIATED WITH X RAYS.

PROTECTIVE ACTION OF GLUCOSE, OF CYSTEAMINE, AND OF SODIUM THIOSULPHATE. Millo, Aldo; Debenedetti, Alessandro (Istituto di Fisiologia della Facolta di Medicina Veterinaria, Perugia, Italy). Riv. Biol., 57: Suppl. 2, 151-67(1964). (In Italian).

Isolated, perfused frog (Rana esculenta) hearts were x irradiated (70 kv) at various dose rates and total doses to investigate changes in permeability of the heart, measured by exchange of ^{86}Rb between the heart and perfusion fluid. Strong irradiation (55 kR/min for 15 min, 10.7 kR/min for 15 min, and 5.3 kR/min for 15 min) caused a marked increase in the rate with which ^{86}Rb penetrated the heart from the perfusing liquid. A similar effect was observed in the movement of ^{86}Rb in the opposite direction, that is, from the heart, which had accumulated ^{86}Rb by injection in vivo, into the perfusing liquid. Cysteamine at a concentration of 0.013M, and sodium thiosulfate at a concentration of 0.0033M protected the heart against permeability modifications provoked by irradiations at 10.7 kR/min for 15 min. Thiosulfate is more effective than cysteamine. Glucose in concentration 0.1% did not protect against permeability changes. The isolated frog heart was shown in these experiments to be exceptionally resistant to radiation. The doses of radiation used, although relatively big, did not modify the functioning of the heart and its survival time. However, prolonged periods of radiations sometimes caused an increase in the height of contraction, followed later by a diminution, and a premature lowering of the electrocardiographic tracing. Modifications in the permeability of the cellular membrane, and subsequently in the polarization, might explain these observations. By using ^{86}Rb, which presumably behaves like potassium, it was possible to show that radiation facilitates the movement of ^{86}Rb both from the perfusing liquid to the cardiac muscle and, in a more marked fashion, inversely. The increase in permeability takes place mainly during the period of radiation and is directly proportional to the dose. A given dose is more effective when concentrated than when prolonged in time. (BBB)

3795 SOME OBSERVATIONS IN EXPERIMENTAL TRANSPLANTATION OF BONE MARROW. Mraz, Josef; Smid, Antonin; Takadlecek, Ludvik (Charles Univ., Hradec Kralove, Czechoslovakia). Sb. Ved. Praci Lekar. Fak. Karlovy Univ. Hradci Kralove, 6: Suppl., 373-80 (1963). (In Czech).

The protective effect of transplantation of homologous bone marrow was studied in whole-body x-irradiated rats, and by means of a ^{32}P-labeled compound incorporated into the marrow cells, their distribution in the recipients was traced. The rats were given 600- to 800-R doses of x rays and injected with 4×10^7 bone marrow cells previously incubated with ^{32}P-diisopropylfluorophosphate. Radioactivity of $DF^{32}P$ bound to transplanted marrow cells in peripheral blood, lungs, and livers decreased rapidly with an exponential dependence on the time. Excretion of $DF^{32}P$ in urine and stools showed an analogous course; 73% of the activity of the isotope administered was eliminated within 7 days of injection. The activity of $DF^{32}P$ was relatively stable in the bone marrow; in the spleen it was constant and very low. Administration of bone marrow increased the regeneration of the blood cell formation in the marrow; the number of cells of the bone marrow was significantly higher in the experimental animals as compared with the controls. In the white cell component of peripheral blood, no marked improvement was observed up to the 7th day after the administration of the marrow. Therapeutic effects of homologous bone marrow in rats after irradiation began to be manifested after LD_{60} dose (600 R) and ceased after irradiation with a supralethal dose (800 R). The highest effect was observed after irradiation with LD_{95-100} (700 R); at decreasing and increasing doses of irradiation the favorable effect of bone marrow diminished gradually. (BBB)

3796 PROTECTION MECHANISMS OF NON-MALIGNANT AND MALIGNANT CELL AGAINST IONIZING RADIATION. II. THE CYTOLOGICAL EFFECT OF 2-MERCAPTOETHYLAMINE AND SOME CHEMICALS ON THE HELA CELLS. Kobayashi, Jindo; Yoshizaki, Tsutae; Kawamura, Fumio (Univ. of Tokushima, Japan). Tokushima J. Exp. Med., 11: 34-9(May 1964).

The morphologic effects of radioprotective agents were studied in tissue cultures to obtain basic information which might contribute to an understanding of radioprotection mechanisms. Effects of 2-mercaptoethylamine and antitumor agents were examined on HeLa cells. Before treatment the nucleus of HeLa cells had a homogeneous appearance under phase microscopy. Addition of this agent at a dose of 6 mg/ml induced an active movement of internuclear structures, leading then to the formation of chromonemata in the nucleus. Later, the nucleus appeared as the prophasic state. The nucleolus became hazier in outline than before treatment. It is concluded that 2-mercaptoethylamine exerted a promoting effect on nucleus to divide from the resting state. Some antimitotic agents were also tested. After addition of tespamine at a dose of 2.5 mg/ml, the nuclear membrane disappeared, leaving a structure with a coarse network. Nuclear membrane disappearance was rapid and the network structure appeared 10 min later. The nucleoli showed a gradual decrease in size and became rounded. The cells showed a slight shrinkage, with irregular indentations on their surface. Thus, tespamine damages the cell as a whole as a result of nuclear membrane disappearance and cellular shrinkage. In cells treated with azan at a dose of 5 mg/ml, the first response was a transient irregularity of nuclear membrane. Nitromin at a dose of 1 mg/ml caused a partial alteration of the nuclear membrane soon after the treatment. Cytologically, 2-mercaptoethylamine seemed to affect cells in a quite different manner from the three anti-tumor agents. 2-Mercaptoethylamine apparently accelerates division of tumor cells. (BBB)

Radiation Hazards and Protection

See also HEALTH AND SAFETY

Refer also to abstract 4505.

3797 PROTECTION AGAINST NUCLEAR WEAPON FALLOUT IN EMERGENCY HEALTH SERVICES UNITS. Pace, F. C. (Dept. of National Health and Welfare, Ottawa). Med. Serv. J. (Can.), 21: 95-112(Feb. 1965).

An outline is presented of methods developed by Federal Emergency Health Services to reduce the effects of early nuclear weapon fallout on patients and attending personnel within activated health units. The emphasis is on protection against the fallout γ radiation and its attenuation by shielding. The radiation detection instruments required are described and an example of the equipment issued to one type of Emergency Health Services unit, the 200-bed emergency hospital, is provided. Methods of calculating radiation intensities at various times after detonation are examined, and a new method of estimating shelter habitation times is presented, involving the use of mathematical tables of which the basic model and an example of the derived tables are given. Staff requirements for radiation control are discussed, and the qualification and duties of the responsible officer are explained. Priority demands of patients for shelter are defined, based on considerations of clinical conditions and physiological states. The potential hazards arising from direct contamination of persons, articles, and the interiors of buildings, as well as water and food, are discussed and an attempt is made to evaluate these contact and internal hazards in relation to the more serious external hazard within the framework of the early fallout situation. A discussion of protection of hospital diagnostic x-ray film against fogging by the fallout radiation is also presented. (TCO)

3798 WORKING HAZARD IN RADON SPAS. Halik, Jaroslav. Prac. Lek., 17: 249-53(Aug. 1965). (In Czech.).

The hazard involved in work in a balneological institute using natural thermal springs containing radon was surveyed. In the spaces of the bathrooms a radon concentra-

tion of $3.6.10^{-10}$ c/l of air was found, the activity of the aerosol reached concentrations of 7.10^{-11} c/l air. It is assumed that in non-ventilated spaces the weekly radiation dose affecting pulmonary tissue is 5.5 times greater than the permissible standard. Recommendations are made how to reduce the working hazard. (auth)

3799 RADIATION PROTECTION IN EMERGENCY HEALTH SERVICES UNITS PLANNING AND OPERATIONAL PROCEDURES. Ottawa, Canada, Emergency Health Services, Dept. of National Health and Welfare, 1965. 92p.

Protection of hospital services, mainly from fallout radiation, in event of a thermonuclear war is examined in detail. A scale of tissue of radiation detection instruments is recommended. The recommended types and numbers of such instruments are explained. Possible methods of reducing exposures of patients and staff to the external γ hazard are discussed. Of these means, shielding by the building-structure itself is emphasized as the best developed method at the present time, and the most practical. The examination of buildings for their shielding value (shielding analysis), and calculations to determine radiation intensities and integrated radiation exposures at various times after arrival of fallout and in various shielding situations are discussed. Measures recommended for the protection of undeveloped x-ray films against fogging by the fallout radiations are presented. Extensive tabulated data are presented for calculating the hazards to hospital patients under various fallout conditions, shielding factors of various building types, duration of stay in shelters, and decay times of mixed fission products. Guides for distribution of monitoring instruments and protective clothing to various categories of hospital personnel are also considered. (TCO)

Radiotherapy and Radiodiagnosis

Refer also to abstracts 3658, 3739, 4111, 4115, and 4517.

3800 (NP–15150) PERFECCIONAMIENTO DE LA TECNICA DEL RADIORENOGRAMA Y COMPARACION CON OTROS TESTS DE FUNCION RENAL. (Improvement of Renogram Techniques and Comparison with Other Tests of Renal Functions). Final Report. Chwojnik, A.; Garcia del Rio, H.; Gotta, H.; Olivaria, A.; Pecorini, V.; Varela, J. E. (Comision Nacional de Energia Atomica, Buenos Aires (Argentina)). [1963]. IAEA Contract 146/OB. 67p. Dep. mn.

The ^{131}I-RISA or ^{131}I-Hippuran radiorenogram and urography are the most suitable methods for obtaining data on urinary tract morphology and renal function separately. Renal insufficiency and the obstructive state is reflected earlier on the radiorenogram than by urography. The results show that the radiorenogram and urography are complementary procedures and cannot be substituted one for the other. (tr-auth)

3801 (ORNL-IIC–5, pp 222-38) INDUSTRIAL ANALYSIS OF ^{147}Pm X RAYS FOR RADIOGRAPHY AND IMAGING READOUT. Coleman, E. W.; Furnas, T. C.; Ball, J.; Rosumny, M. R.; Beard, D. W. (Picker X-Ray Corp., Cleveland, Ohio).

In experiments with a 100-C ^{147}Pm source on radiography and fluoroscopy of medical phantoms and of various metal step wedges with standard penetrameters, exposure times required generally were excessively long. Studies of the spectral output and use of the source to excite secondary spectra, which were evaluated with a scintillation detector and 400-channel pulse-height analyzer, demonstrated interesting capabilities on sorting materials. A third series of experiments was on determination of the effective focal spot size and relating this to theoretical excitation conditions in the source. (auth)

3802 (ORNL-IIC–5, pp 239-42) MEDICAL APPLICATIONS OF LOW-ENERGY X-RAY AND GAMMA RADIATION SOURCES. Wagner, Henry N. Jr. (Johns Hopkins Univ., Baltimore, Md.).

Experiments using a nuclear image amplifier with ^{133}Xe and ^{99m}Tc for measuring blood flow and respiration are described briefly. Initial results were found to be promising. (P.C.H.)

3803 (ORNL-IIC–5, pp 257-76) RADIOISOTOPIC DEVICE FOR MEASURING BONE MINERAL. Lanzl, Lawrence H. (Chicago Univ., Ill. Dept. of Radiology, Argonne Cancer Research Hospital, Chicago, Ill.); Strandjord, Nels (Chicago Univ., Ill. Dept. of Radiology).

An instrument using radioactive ^{125}I was devised for nondestructive determination of mineral changes in the skeleton by measuring the transmission of a small beam of radiation emanating from ^{125}I through a single human finger bone. For small animals, the rear leg is used. Radiographs must be used for accurately positioning the anatomical part under consideration. Built into the unit are an automatic repositioning feature and an automatic print-out device. The absorption coefficients of bone in vivo can be determined to an accuracy of ±1%. The apparatus is being used to study osteoporosis in post-menopausal females, including the effect of stilbesterol in decreasing osteoporosis, and demineralization in experimental animals. (auth)

3804 (ORNL-IIC–5, pp 309-28) PORTABLE DEVICES FOR ISOTOPE CHEST RADIOGRAPHY AND OTHER APPLICATIONS. Green, Farno L. (Viso Corp., Detroit, Mich.).

Ytterbium-169 was found to be the best isotope source now available for medical diagnostic radiography. Ytterbium sources were used for general diagnosis in a lightweight system with a tripod-mounted radiographic exposure unit and x-ray film cassettes. The Viso chest radiography system is easily transported into essentially any populated area, assembled in minutes, and operated without electrical power. Only minor maintenance is required. Such systems also allow very low dose to the patient and to the operator. (auth)

3805 CLINICAL APPLICATION OF WHOLE-BODY COUNTING OF ^{85}Sr AND ^{47}Ca IN PATIENTS WITH AND WITHOUT WIDESPREAD MALIGNANT SKELETAL DISEASE. Cederquist, Ebbe (Univ. Hospital, Lund, Sweden). Acta Radiol., Suppl. 232, 118p.(1964).

Whole-body counting techniques, including instrumentation, scanning geometry, use of various isotopes, evaluation of counting data, and previous clinical applications and results, are reviewed preliminary to a detailed report on the detection of bone tumors with bone-seeking radioisotopes. Studies were conducted in 32 patients and 9 healthy volunteers by whole-body counting in a low background room after a single intravenous injection of usually less than 1 μC of ^{85}Sr and less than 1.5 μC of ^{47}Ca. In 21 studies the retention determined by whole-body counting was compared with that calculated from excreta measurements. In 28 patients, 14 with and 14 without skeletal involvement, short-term retention and distribution of the isotope were studied with whole-body counting, scanning geometry, with measurement of each patient prone and supine. Long-term retention and distribution were studied in most of these patients, in some of them with measurements throughout a six-month period. Results indicated that the whole-body counting technique described, can replace conventional calculation from excreta analysis in routine clinical estimation of the total body retention of radioisotopes, such as ^{85}Sr and ^{47}Ca. This measuring technique does not require hospitalization of the patient and the measuring method with the patient lying on a couch causes no inconvenience to him. The high sensitivity of the method using large scintillation crystal in a low background room allows use of very low activities of the tracer, corresponding to only about $1/100$ of that necessary for conventional methods, an advantage allowing studies with repeated injections of the tracers. This high sensitivity makes it possible to carry out long-term studies over months after a single intravenous injection of less than 1 μC of ^{85}Sr, for example, which is practically impossible by conventional excreta analysis. The high energy resolution of the NaI(Tl) crystal

used with multichannel analysers makes the method particularly useful for double tracer studies, e.g. with ^{85}Sr and ^{47}Ca. The geometry used with measurement of the patient in the prone and supine positions allow short-term studies not only of the retention but also of the distribution of ^{85}Sr and ^{47}Ca, the ratio between the counting rates in the prone and the supine positions, apparently reflecting the transfer of these isotopes from the body fluid and soft tissue in the anterior portion of the body to the cancellous bone in the posterior portion. It was possible to distinguish between patients with and without widespread skeletal disease, often within 1 hr of the injection of the isotope. (BBB)

3806 RADIATION CANCER OF THE PHARYNX. CASE REPORTS. Goolden, A. W. G.; Morgan, R. L. (Hammersmith Hospital, London. Medical School of London). Acta Radiol. Therapy, Phys., Biol. (N.S.), 3: 353-60(Oct. 1965).

Cancer of the pharynx in four female patients, who had received x ray therapy of the neck for thyrotoxicosis, is described. In two of them, tumors in the pyriform fossa and in the oesophagus, respectively, developed 45 years after the irradiation, while in the two other patients tumors in the hypopharynx developed at 28 and 42 years, respectively, after the irradiation. The main features of radiation cancer of the pharynx are briefly reviewed. The latent interval for this type of tumor ranges between 10 and 45 years, with a peak at about 30 years. (auth)

3807 SQUAMOUS CELL CARCINOMA OF THE CERVIX. Amer. J. Obstet. Gynecol., 92: 436-40(June 1, 1965).

Treatment planning in a case of stage III squamous cell carcinoma of the cervix is described in detail to illustrate the dose and distribution of radiation required in such cases and the nature of the resulting complications. (TCO)

3808 THE EFFECT OF IONIZING IRRADIATION ON THE DEVELOPING MAXILLA AND MANDIBLE. Byrne, John J. Amer. J. Orthodont., 47: 646-60(Sept. 1961).

The pertinent literature is reviewed and a case is reported wherein radiotherapy of the mandible in childhood impaired its later development. At the age of 5, the patient received 3500 R of 200-kv x rays to the right malar area for hemangioma. At the age of 21, he exhibited a flattened right zygomatic area. The skin from the tragus to the inferior border of the orbit was pale in color, with patchy pigmentation. The right malar bone was about 2 cm distal to the left one. There was moderate scarring of the right ala, with the nasal septum deviating to the right. On frontal examination, the left side of the face was seen to be longer and larger than the right. The mechanism of the medium-voltage x-ray effect on bone is discussed. The precise quantity of irradiation which stops tooth development or alters growth of the maxilla or mandible is still unknown. However, it appears to lie somewhere between 800 and 1500 R, depending upon the age and physical characteristics of the individual patient. (BBB)

3809 BIOLOGIC AND HORMONAL RESULTS OF THE DESTRUCTION OF THE PITUITARY BY ^{90}Y. Paillaud, A.; Abbes, M. Anaesth. Analg., 22: 293-7(Apr.-June 1965). (In French).

Twenty-two cases of breast cancer, treated by hypophysiolysis induced by implantation of ^{90}Y in the pituitary area, were observed for physio-pathological effects of destruction of the pituitary gland as well as therapeutic effects. Since the method of implanting ^{90}Y used does not effect destruction of the pituitary until about the tenth day, immediate complications were not anticipated. However, each patient received 50 mg of cortisone intramuscularly twice a day beginning the night before surgery, the dose decreasing to 35 to 40 mg/day administered orally. Later 15 to 25 mg/day prednisone was substituted. Hormonal side-effects observed included ovarian hypofunction, adrenocortical hypofunction, disturbances in electrolyte balance as demonstrated by sodium retention and increased potassium loss in ten cases after the 10th day, polyuria and polydypsia in several cases, decreased uptake of radioiodine by the thyroid in several cases, and retention of calcium and phosphorus, with a reduction of Ca in urine, in 11 cases. It was concluded that the endocrine and metabolic changes observed did not reflect total destruction of the pituitary gland by ^{90}Y. (BBB)

3810 KIESELGEL AS A SUPPORT IN TRITIUM LABELING OF CARDIAC GLYCOSIDES. Rabitzsch, Georg; Herzmann, Hermann (Deutsche Akademie der Wissenschaften, Berlin). Ann. Chem., 685: 261-6(1965). (In German).

Use of Kieselgel as a support for cardiac glycosides allows higher labeling ratios in ^{3}H labelings by the method of Wilzbach (J. Am. Chem. Soc., 79: 1013(1957)) in good yield. Methods are described for the preparation of labeled digitoxin; carriers studied were Kieselgel at various concentrations of digitoxin, and active charcoal. Complete separation of labile ^{3}H was affected with methanol washings, followed by column chromatography. At long incubation times under ^{3}H, Kieselgel gives considerably relatively higher yields of labeled product than charcoal. Autoradiolysis destroys nearly 50% of the labeled product after 60 days at 0°C. A procedure for labeling the digitoxin is given: absorption from chloroform onto 20 times its weight of Kieselgel is followed by drying 75° at 10^{-2} Torr 10 hours and maintained under ^{3}H (4 C) at 0°C and 350 Torr for 21 days. It is eluted with 9:1 chloroform-methanol, which is evaporated; the residue is treated with methanol four times with evaporation each time. It is chromatographed twice over 10 g Al_2O_3 in a capillary column with H_2O-saturated ethyl acetate +1% methanol, and is maintained at 0°C as 0.5% solution in abs ethanol. (BBB)

3811 SQUAMOUS CELL EPITHELIOMA. Traub, Eugene F. Arch. Dermatol., 91: 409-10(Apr. 1965).

A case representing possible radiation-induced squamous cell carcinoma is presented and discussed. Repair of radiation-injured skin by surgery was another feature of this case. The patient, a 70-year-old man, was first seen nine yr ago. For the past 30 yr he had been having numerous keratoses and epitheliomas removed from his face with x-ray and radium treatments. At least three basal cell epitheliomas and one prickle cell epithelioma on the back of the neck were removed during the period of observation. A family history of skin epitheliomas was noted. Palliative therapy was replaced by more radical surgery because of the previous damage to the skin and underlying structures from radiation. He had received at least eight extensive treatments with either x ray or radium. The areas on the left cheek showed extensive damage, and there was a question of bone involvement. Three successive operations were required to remove the skin and involved underlying tissue of both cheeks, extending well down on the neck, as well as the nose. Seven yr later a tumor in the right parotid gland was removed, and reported as a squamous cell carcinoma; it was thought to be a metastatic lesion. In a discussion by several participants, the likelihood of radioinduced carcinoma in this case is commented on and several previously unreported cases of radioinduced cancer are mentioned. One discussant has recently seen four cases of carcinoma of the thyroid in patients who received radiation for acne vulgaris, and suggests that the radiation given for the skin tumor in the present case induced the squamous cell carcinoma in the gland. Another discussant refers to several patients who developed anaplastic carcinoma of the parotid gland after having been chronically exposed to x rays. One patient who had been working with radiation, in the preparation of radon tubes, developed carcinoma of the parotid. (BBB)

3812 DERMATOLOGIC RADIOTHERAPY 1965. Epstein, Ervin (Univ. of California, San Francisco). Arch. Dermatol., 92: 307-14(Sept. 1965).

The use of x rays in benign dermatologic conditions is discussed from the point of view of carcinogenic, leukemogenic, and genetic hazards, with the conclusion that these hazards are greatly overemphasized. With careful measurement of dose, it is suggested that the hazards are minimal and controllable. Most dermatologists who have used x-ray therapy in the past have decreased its use and

some have discontinued it completely. A questionnaire sent to the members of the American Dermatological Association in 1960 reflected changes that have occurred in the utilization of this modality. There were 132 replies to the query, an 88% response. Comparing their activities in this regard in 1960 in contrast to 1950, one decade earlier, 1.6% gave more x-ray therapy, 79.1% less, and 19.1% an equal amount. Thus, four out of five dermatologists were administering less ionizing radiations. As the use of radiation has decreased, it has been necessary to find substitutes for it. Ultraviolet light and other physical modalities are ineffective in this regard, and the use of grenz rays has increased. The results obtained in the management of superficial dermatoses with grenz rays are equal to those secured with conventional x rays. Another substitute for x radiation is local drug treatment, including intralesional injections, such as with 1% hydrocortisone. Many physicians use internal medications, corticosteroids, antibiotics, estrogens, griseofulvin, etc. instead of x rays, but it is suggested that the potential hazards of these agents are greater than those of superficial x-ray therapy. When the risk of unpredictable idiosyncrasies, is examined, x rays must be considered as much safer to use than are these approaches. There is no question about the fact that x radiation is carcinogenic and that chronic radiodermatitis is precancerous. However, among 19,384 consecutive patients in the author's practice of dermatology, including 55 patients with chronic radiodermatitis, there were only two examples of malignant degeneration. One woman who had received postmastectomy irradiation 55 years previously, developed multiple superficial basal-cell epitheliomas within the area of radiodermatitis. Another developed a sarcoma following radiotherapy for an epithelioma. These two cases constituted an incidence of 3.62% for carcinomatous degeneration in this series. In a control series of about 20,000 unirradiated patients, there were 676 patients with epitheliomas, an incidence of 3.49%. Thus, there was no significant difference between the two groups in regard to the development of malignancy (3.62% vs 3.49%). (BBB)

3813 THE TREATMENT OF MALIGNANT DISEASE OF THE FACE AND JAWS BY RADIATION. Wood, Constance A. P. (Hammersmith Hospital, London). Brit. Dent. J., 110: 234-5(Apr. 4, 1961).

The use of various types of radiation to treat oral cancer, with emphasis on prevention of complications, is considered. Precautions before and after radiation treatment are enumerated. The most serious complication of radiation treatment in buccal cancer is that of bone necrosis. This hazard has been greatly reduced by the use of supervoltage therapy, and in no case treated by the linear accelerator has there been evidence of bone necrosis. (TCO)

3814 THE CONSTRUCTION OF INDIVIDUALISED INTENSITY MODIFYING FILTERS IN ^{60}Co TELETHERAPY. van de Geijn, J. (H. Joannes de Deo Hospital, The Hague). Brit. J. Radiol., 38: 865-70(Nov. 1965).

The theory and construction of individualised intensity modifying filters for use with irregular surfaces in ^{60}Co teletherapy are described. The theory results in a conversion function which is independent of the source-surface distance and which can be derived from standard depth dose tables. The practical application is greatly simplified by the special surface copying device which is described. (auth)

3815 IMAGE CONTRAST AND RADIATION PROTECTION: A FIGURE OF MERIT. PART II. WIDE BEAMS. Speigler, G.; Keane, B. E. (Royal Sussex County Hospital, Brighton, Eng.). Brit. J. Radiol., 38: 871-4(Nov. 1965).

The beneficial and adverse effects of hardening the x ray beam on protection and contrast during diagnostic radiography are discussed and merit figures established inside and outside the beam for parts of various thickness. By the merit figure of a technique, the beneficial effect on exit dose related to critical-organ dose is balanced against the adverse effect on perceptible thickness difference. Merit inside the beam, high for thin parts, decreases with hardening of the beam and increases for thick parts. The importance of the interpretation of merit is emphasised. The effect of added filters on merit on account of prolongation of exposure is considered and some suggestions on the desirable filtration are made. Outside-beam merit depends little on added filtration but decreases markedly with increasing the tension at greater depths. Direct and scatter dose to the critical organ referred to contrast and primary exit dose, i.e. merit, decreases rapidly with the proximity of the organ to the exit side. The connection of the authors' findings with previous work of other authors is discussed. (auth)

3816 THE ABSORPTION OF X RAYS IN A BODY EQUIVALENT PHANTOM. Pychlau, P.; Bunde, E. (Physikalisch-Technische Werkstatten Dr. Pychlau KG, Freiburg i. B.). Brit. J. Radiol., 38: 875-7(Nov. 1965).

A man-shaped phantom, built of natural bones molded in wax, was used to measure the absorption of x rays by the body. Measurements are described that were made to show if the unit R × cm^2, or ergs or milli-Joule are in the best relationship to the energy absorbed in a patient during diagnostic radiography. The measurements show that the unit R × cm^2 in the region from 2 to 4.5 mm Al HVT seems useful. (C.H.)

3817 ANNULAR COUNTING OF RADIOISOTOPES IN LARGE LIQUID VOLUMES ON A WELL TYPE SCINTILLATION CRYSTAL OF SODIUM IODIDE. Bell, T. K. (Royal Victoria Hospital, Belfast). Brit. J. Radiol., 38: 886-7 (Nov. 1965).

A scintillation detector fitted with a Tl-activated NaI crystal 2 in. high and 1.75 in. diameter containing a well 1.5 in. deep and 0.75 in. diameter was coupled to a scaler incorporating a stabilized high voltage supply, a pulse height analyzer, and an automatic timer. The crystal was surrounded by a 1 in. thick lead shield with a hole in the lid which allowed insertion of a tube accommodating up to 400 ml of solution for annular type counting. Good counting results were obtained using 400 ml liquid volumes containing small concentrations of ^{125}I, ^{57}Co, ^{51}Cr, ^{131}I, ^{58}Co, ^{59}Fe, and a mixture of ^{57}Co and ^{58}Co. It is suggested that the annular cell will allow a reduction in the quantity of radioactivity administered in clinical investigations. (C.H.)

3818 ISOTOPE TECHNICS IN CLINICAL CARDIOLOGY. Love, William D. (Univ. of Mississippi, Jackson). Circulation, 32: 309-15(Aug. 1965).

A critical review of isotope technics is given to ascertain which ones are actually of value in caring for patients. Some present trends in instrumentation and selection of isotopes that aid in reducing patient exposure while providing more diagnostic information are also considered. The most useful isotope technic at present is the heart scan. The circulating blood can be effectively labeled by a single intravenous injection of ^{131}I albumin, and the intracardiac blood pool then outlined with a commercial scanning apparatus designed for thyroid studies. This helps determine whether a large heart shadow is caused by dilatation of the heart or by pericardial effusion. Scans of the lung can be used to improve the diagnosis of pulmonary embolism. The lung is outlined by injecting fine particles of labeled albumin that form microemboli which lodge in the pulmonary capillaries and therefore outline the pattern of blood flow to the lung. In pulmonary embolism, there is a nonradioactive zone corresponding to the unperfused area of the lung. The rate of coronary blood flow in man has been estimated by measuring how fast an isotope which is injected into the blood is taken up by the myocardium, by following a bolus of tagged blood as it flows through the coronary vessels, and by measuring the rate at which a freely diffusible inert gas is washed out of the heart muscle by the blood. Uptake of ^{86}Rb from the blood as an index of coronary flow is discussed. Recently this procedure has been modernized by substituting ^{84}Rb for ^{86}Rb; ^{84}Rb is a positron-emitting isotope, therefore, it is possible to eliminate heavy shielding, and to limit the zone monitored to the tissue that lies between a pair of scintillation crystals. None of the methods of measuring

coronary flow has been shown to be useful in the care of patients. Techniques and instrumentation are discussed. (BBB)

3819 TREATMENT OF CARCINOMA OF THE BLADDER WITH RADIUM. van der Werf-Messing, B. (Radiotherapy Inst., Rotterdam). Clin. Radiol., 16: 16-26(Jan. 1965).

Radium therapy for bladder cancer in 148 patients is described, with data on dose distribution and incidence of complications. (BBB)

3820 LIPOMATOSIS INTERNA OF THE DESCENDING COLON WITH THE APPEARANCE OF RADIATION INJURY. Schulze, E. (Strahleninstitut des Knappschafts-Krankenhauses, Recklinghausen, Ger.). Fortschr. Geb. Roentgenstr. Nuklearmed., 100: 411-12(Mar. 1964). (In German).

A patient was x irradiated with three series of treatments ¼ yr apart. The field size of the left lumbar field was 20 × 24 cm, the lateral field was 10 × 15 cm, and the abdominal field was 15 × 20 cm. Two fields were irradiated daily with 200 R each. The total focal dose was 3576 R. Six months later the patient developed symptoms of intestinal stenosis. The affected portion of the colon was resected. Generally, irradiation reactions of the intestine appear only after maximum radiation doses. The smaller the single doses and the longer the treatment interval the less are the irradiation effects. The scattered irradiation from focal dose of 3576 R administered over a period of 9 months should not have led to any severe manifestation of irradiation injury. The irradiation tolerance of the large intestine is between 6000 and 8000 R, depending on the fractionation and total dose used. Pathogenetically, it should be taken into consideration that a minor, unnoticed residual reaction of the mucosa to irradiation could have caused the development of a submucosal lipomatosis. However, there was no definite histological evidence of the usual symptoms of irradiation injury, such as thickening of the serosa, telangiectases and defects of the mucosa, or fibrosis and hyalinization of the supporting tissue. (BBB)

3821 MALIGNANT ZOLLINGER-ELLISON SYNDROME IN A BANTU WOMAN WITH A PROLONGED REMISSION AFTER GASTRIC RADIOTHERAPY. Bank, S.; Marks, I. N.; Sealy, R.; Louw, J. H.; Silber, W. (Groote Schuur Hospital, Cape Town). Gut, 6: 279-85(June 1965).

Gastric radiotherapy is effective in inducing a prolonged remission in patients with the Zollinger-Ellison syndrome. This disease is characterized by the presence of a tumor of the pancreas associated with gross acid hypersecretion, intractable peptic ulceration, and, often, severe diarrhea. The acid hypersecretion is due to gastrin or a gastrin-like substance elaborated by the tumor tissue. The mortality of the disease remains high. A review of 138 cases of the syndrome reported to date reveals an overall mortality of 58%, with postoperative deaths accounting for more than half of this figure. The hazard of surgery is particularly great in patients subjected to repeated operations for recurrent jejunal ulceration. An examination was made of the effect of gastric radiotherapy in reducing acid hypersecretion in such patients. The published results of radiotherapy have not been encouraging. In the case described, gastric radiotherapy first was given in the left upper quadrant, through 15 × 15 cm anterior and posterior fields, over 21 days. The total dose of x ray was 2640 R skin dose to 2244 R central dose at 250 kv. Symptomatic remission persisted throughout the 21 months of follow-up period. Body weight increased during the first months after radiotherapy. No medical treatment was necessary. The results of serial histamine tests carried out before, during, and after gastric radiotherapy showed a reduction in acid secretion during the course of radiotherapy, and secretion diminished progressively over the next few months. Virtual achlorhydria became established four months after the conclusion of the course of radiotherapy, and the gastric secretory status thereafter remained more or less unchanged. The failure of other radiotherapists to induce achlorhydria or a satisfactory remission in this disease may have been due, in part at least, to the smaller dose of radiotherapy employed by them. Although an individual susceptibility of the mucosa to irradiation exists, 1600 to 2500 R has been recommended as the most effective dose in the treatment of uncomplicated duodenal ulceration. Available data suggest that a higher dose level may be required in the treatment of the Zollinger-Ellison syndrome and that radiotherapy in such patients should not be abandoned before a minimum dose of 2500 R has been administered. (BBB)

3822 ON THE METABOLIC EFFECTS OF THE THERAPEUTIC USE OF RADIOCOLLOIDS ON THE RETICULOENDOTHELIAL SYSTEM. Mueller, J. H. (Univ., Frauenklinik, Zurich). Gynaecologia, 159: 322-8(1965). (In German).

When a colloid such as Au colloid is introduced into the tissues, part is carried in the lymphatic system where it becomes fixed by the microphages of the lymph nodes. Another part is phagocytized by the widely distributed histiocytes of the reticuloendothelial system. These reactions produce the final, paraselective distribution observed after administration of a radiocolloid. If the colloid is injected intraperitoneally or intrapleurally in a large volume of fluid, it is deposited directly onto portions of the serosa where cancerous infiltration has evoked histiocytic phagocytosis, and a substantial amount is deposited in the regional lymph nodes. If a cancerous region is grossly infiltrated interstitially with radiocolloid, the deposition of radiocolloid may be equivalent to that in indirect lymphography, resulting in a therapeutic effect. The irradiation dose amounts to as much as 200000 R in some areas of the reticuloendothelial system when 125 mC of colloidal ^{198}Au is administered intraperitoneally for ovarian carcinoma with peritoneal metastases. Doses as high as 100000 R of β irradiation can be delivered to the lymph nodes by infiltration with radiocolloidal Au. Radiocolloids injected directly into the blood stream are deposited in liver, spleen, and bone marrow. However, the phagocytic reaction of the reticuloendothelial system is not the only effect of radiocolloid injection. When the reticuloendothelial elements are irradiated by radiocolloids that have been incorporated, an antimitotic factor appears to be released. This becomes bound by the γ-globulin fraction of serum. This has been demonstrated in dogs by irradiation of the exteriorized spleen or ileocecal region. It is reasonable to believe that a factor of this type could have value for treatment of metastases. (BBB)

3823 STUDY OF MEASUREMENT OF RADIATION DOSE, RECEIVED BY MOTHER AND FETUS AT X-RAY EXAMINATION AND DEVICES TO LOWER THE DOSE. Tabuchi, Akira (Hiroshima Univ. School of Medicine, Japan); Nakagawa, Shigeru; Yoshinaga, Haruma; Antoku, Shigetoshi. Hiroshima J. Med. Sci., 13: 117-24(June 1964).

Phantom studies were conducted to measure radiation doses received by maternal pelvis and the fetus, especially the gonads and whole-body of fetus, at x-ray examinations during pregnancy. Means to lower the dose were investigated. In a preliminary investigation, data on radiation factors, employed in x-ray examinations at 20 hospitals in Hiroshima prefecture and adjacent prefectures, were collected. In the experiments with phantoms, a boneless Mix-D phantom, equivalent to the size of woman in terminal pregnancy and a cuboidal phantom (17 × 28 × 60 cm) were used. Radiation dose inside the phantom was determined with fluorescent glass dosimeters on the surface and at 3, 6, 9, 12, and 15 cm depths. The average site maternal ovaries were estimated by x-ray films at hysterosalpingography, radiography, and direct measurement on operative patients, and the posture and presentation of fetus in terminal pregnancy was obtained from x-ray films. Dose distribution in the maternal pelvis, measured in a boneless Mix-D phantom with a fluorescent glass dosimeter, for 80-kvp x rays is illustrated. Radiation dose at various sites, such as maternal ovaries, and fetal gonads and spine, were calculated in relation to tube voltage. Radiation dose of the examined pelvis and fetus is lowered by higher voltage radiography and use of sensitive materials of high quality. Tables indicate the lower radiation

dose possible by use of high voltage x rays. Lower radiation doses obtained by use of more sensitive films are also shown. The results show that fluoroscopy of the gastrointestinal tract, pelvimetry, or x-ray examination of the pelvis during early pregnancy gives a fetal dose of more more than 1 R. By use of higher voltage, radiation dose of fetus and maternal gonads may be lowered to ~¼. By using the most sensitive materials and higher voltage at hysterosalpingography, it may be lowered to about ⅕, when compared with routine radiography. (BBB)

3824 ANALYSIS OF 96 ABNORMAL BRAIN SCANS USING ^{99m}Tc (PERTECHNETATE FORM). Quinn III, James L.; Ciric, Ivan; Hauser, William N. (Northwestern Univ. School of Medicine, Chicago). J. Amer. Ass., 194: 157-60(Oct. 11, 1965).

The use of ^{99m}Tc in brain scanning is described, and its advantages over other radioisotopes, such as ^{197}Hg and ^{203}Hg (as chlormerodrin), is described. Because ^{99m}Tc is an almost pure γ-ray emitter and has a short physical half-life (six hr), large amounts of radioisotope (10 to 15 mC) can be administered without excessive radiation exposure to the patient. Using these doses and a standard commercial scanner, counting rates of 15,000 to 30,000 cpm over the head are obtained, compared to 800 to 1500 cpm with chlormerodrin-^{203}Hg or chlormerodrin-^{197}Hg. Because of the increased counting rates the scanning speed can be increased and a view of the brain can be completed in as little as five min. Pertechnetate is cleared from the blood more slowly than chlormerodrin. The result is a display of normal intracranial vascular structures on the pertechnetate brain scan which are not seen on the chlormerodrin scan. This may mask the visualization of abnormal radioisotope concentrations in the base of the brain and posterior fossa. Pertechnetate concentrates in the thyroid, salivary glands, and gastric mucosa, and has also been shown to concentrate in primary and metastatic intracranial neoplasia as well as in cerebral infarcts and arteriovenous malformations. After about 15 min pertechnetate equilibrates with the extracellular space and is then removed from the blood with a half-time of about three hr. Thyroid and gastric concentration can be reduced by administering 1.0 g of potassium perchlorate one hour before the brain scan. Technetium-99m is the daughter decay product of ^{99}Mo. Molybdenum-99 generators with 250 mC of ^{99}Mo adsorbed on aluminum oxide and packed into a small plastic tube can be obtained weekly from the Brookhaven National Lab. Since the physical half-life of ^{99}Mo is 67 hr, satisfactory yields of ^{99m}Tc are possible for seven to ten days. The ^{99m}Tc in the pertechnetate form can be obtained by pouring 20 ml of either 0.1N HCl or 0.9% NaCl through the generator. The brain scan is started 30 min after the intravenous administration of ^{99m}Tc in the pertechnetate form. Of 625 patients scanned by this technique, 96 (15%) with proved or probable intracranial disease had positive results from brain scan. The diseases associated with positive brain scans in intracranial neoplasia are listed. Eleven patients with proved intracranial neoplasia had negative results from brain scans after administration of ^{99m}Tc. Pertechnetate brain scans differ from chlormerodrin brain scans in that they display the normal vascular structures within the cranial vault to a much greater extent, and this may be a serious limitation to the use of pertechnetate as a brain scanning radioactive pharmaceutical. More specific localization in abnormal intracranial tissue is desirable, and another radioactive pharmaceutical which shows promise, ^{99m}Tc in the Tc-Fe complex form, is now under investigation. (BBB)

3825 ROENTGEN STUDY OF THE SOFT TISSUES OF PREGNANCY. Boudette, W. V. J. Amer. Osteopath. Ass., 64: 596-601(Feb. 1965).

The use of x-ray pelvimetry has declined because the present concern of over radiation exposure of the fetus and maternal ovaries so that other x-ray examinations, especially of the soft tissues, have assumed a greater importance in pregnancy. Localization of the placenta is usually the primary consideration in such studies. Other indications for the procedure include vaginal bleeding during the last trimester, abnormal enlargement of the maternal abdomen, hydramnios, suspicion of fetal death, or a history suggesting erythroblastosis fetalis. There are two x-ray methods for localizing the placenta: (1) direct lateral soft tissue study of the abdomen, and (2) the indirect method, in which air is injected into the urinary bladder just before examination, the films being exposed with the patient erect. In the lateral soft tissue study of the maternal abdomen a wedge filter should be employed, as it compensates for the relative thinness of the anterior aspect of the maternal abdomen as compared with the pelvis and the posterior limits of the abdomen. A high-quality picture must be obtained if the examination is to be of diagnostic significance. High-kilovoltage techniques, using 125 to 130 kv, are not successful, as satisfactory contrast is not obtained with these levels. Lower kilovoltage ranges, about 30 kv less than used in normal lateral pelvimetry done at table top level with a 36- or 40-in. distance, consistently yield better results. However, some success was achieved with 8-ft film studies done with the patient erect and employing the wedge filter, combining this with regular pelvimetry. The chief advantage of such a procedure is a reduction in the amount of radiation to the fetus yet the diagnostic objectives are obtained. (BBB)

3826 THE TREATMENT OF MIKULICZ'S DISEASE WITH RADIATION THERAPY. Hazel, J.; Bouchard, J. (Royal Victoria Hospital, Montreal). J. Can. Ass. Radiol., 15: 70-3(June 1964).

The effectiveness of x-ray therapy is 10 patients with this condition is reported. Mikulicz's disease is characterized by the painless swelling of one or more of the salivary or lacrimal glands, usually chronic and of long standing, and shows a typical pathologic picture. Generally the treatment of Mikulicz's disease has involved surgical excision or, more recently, cortisone, but the best treatment of this disease from the point of view of symptomatic improvement and reduction in glandular swelling is radiation therapy localized to the involved regions. In the ten cases reported here, the symptoms had been present from 6 to 36 months, with an average of 15 months. All showed marked improvement by the time radiation treatment was completed, except for one case which did not receive an adequate course. In all the others the involved glands had regressed at the completion of treatment or shortly thereafter, and there were no cases of recurrent swelling. A tissue dose of 800 to 1200 R to each involved gland area in 2 to 3 weeks is all that is necessary to reduce the swelling and relieve the symptoms. Radiation treatment offers symptomatic relief but does not effect the underlying process in this condition. (BBB)

3827 ^{60}Co SIMULATOR FOR TREATMENT PLANNING. Horsley, R. J.; Price, R. H. (Ontario Cancer Treatment and Research Foundation Hamilton Clinic). J. Can. Ass. Radiol., 16: 25-9(Mar. 1965).

A treatment planning unit is described which simulates a ^{60}Co therapy device. When a tumor situated below the surface is to be treated, checking the path of the treatment beam is useful, particularly when using small treatment fields. Such verification may be done by taking x-ray radiographs with therapy equipment under actual treatment conditions. The head of the simulator contains an x-ray tube in place of a cobalt source. The simulator has proved useful in checking the paths of treatment fields when using the pin and arc attachment for treating bladder, esophagus, and lung lesions. In such cases, the position and depth of the lesion has been estimated previously from tube-shift pictures or pairs of radiographs taken at right angles. One problem in using conventional x-ray film is the delay in processing the film. Even with fast development technique, there is an appreciable delay from time of exposure to viewing of the wet films. If a series of check films have to be taken, the whole procedure becomes time consuming. Polaroid x-ray film with 10-sec development was tried but has proven to be unsuitable for interpretation when taking oblique and lateral fields. Xeroradiography requiring only

12-sec processing has been considered, but pictures taken in the pelvic region require relatively long exposures of from 15 to 30 sec and are not of diagnostic quality. One system which would give instantaneous verification would be an image amplifier in which the image is viewed by a television camera and displayed on a monitor in the same room. (BBB)

3828 GROWTH HORMONE IN ACROMEGALY: EFFECT OF HEAVY PARTICLE PITUITARY IRRADIATION. Linfoot, J. A.; Greenwood, F. C. (Univ. of California, Berkeley; Imperial Cancer Research Fund, London). J. Clin. Endrocrinol. Metab., 25: 1515-18(Nov. 1965).

Heavy-particle pituitary irradiation was found superior to x or γ teletherapy for producing the cessation of acral growth with soft tissue and bony regression, as well as symptomatic improvement and other biological changes in patients with acromegaly. A marked fall in the circulating level of growth hormone was found in patients with acromegaly after heavy-particle irradiation of the pituitary with doses between 4000 and 9000 rads delivered over an 11 day period, the fall in growth hormone was gradual, and only one of 16 patients examined 2 yr after treatment had an elevated growth hormone level in the blood plasma. (C.H.)

3829 RADIOIMMUNOASSAY OF HUMAN PLASMA THYROTROPIN. Utiger, Robert D. (Washington Univ., St. Louis). J. Clin. Invest., 44: 1277-86(Aug. 1965).

A sensitive radioisotope method, employing ^{131}I-labeling of the hormone, was developed for measuring plasma levels of human thyroid-stimulating hormone (HTSH). Highly purified HTSH (10 IU/mg) was used for immunization, radioiodination, and immunoassay standard. The assay depended on the binding of HTSH-^{131}I by rabbit anti-HTSH serum. This binding was competitively inhibited by unlabeled HTSH. The method was sensitive to as little as 0.075 mμg unlabeled HTSH, permitting detection of plasma HTSH concentrations as low as 1.5 mμg/ml (0.015 mU/ml) under the conditions employed. Separation of free and antibody bound HTSH-^{131}I was effected by chromatoelectrophoresis. Plasma from hypothyroid patients and human pituitary extracts produced dose responses identical to that of the purified HTSH preparation. No HTSH was detectable in plasma from various animals, in plasma from hypopituitary patients, in most patients receiving exogenous thyroid therapy, or in bovine or ovine pituitary TSH preparations. HTSH added to plasma could be recovered quantitatively. Plasma HTSH levels ranged from undetectable to 15 mμg/ml (0.15 mU/ml) in euthyroid subjects, measurable activity being found in 55%. Most values were lower than 10 mμg/ml (0.1 mU/ml). In 32 patients with primary hypothyroidism, plasma HTSH concentrations ranged from 18 to 180 mμg/ml (0.18 to 1.8 mU/ml). In 34 hyperthyroid patients, plasma HTSH was undetectable in 25. No change in plasma HTSH followed insulin hypoglycemia or hyperglycemia, and no diurnal variation was found. In all hypothyroid patients studied, the initially elevated plasma HTSH concentrations fell to within the normal range during the course of replacement therapy. In patients in whom assays were performed at frequent intervals, plasma HTSH was reduced to normal after 7 to 10 days of maintenance L-triiodothyronine or desiccated thyroid therapy. The response to L-thyroxine was slower. Oral administration of 500 μg L-triiodothyronine to a hypothyroid patient produced a 50% fall in plasma HTSH concentration in 4 hr and a maximum reduction in 24 hr. (BBB)

3830 THE ISOTOPE ENCEPHALOGRAM IN BRAIN TUMOR DIAGNOSIS. Goodrich, Jack K.; Tutor, Forrest T. (Univ. of Mississippi, Jackson). J. Nucl. Med., 6: 541-8 (Aug. 1965).

Use of radioactive tracers in diagnosing intracranial disease is reviewed, and the procedures for brain scanning used at the University of Mississippi Medical Center are discussed. Of 558 consecutive isotope encephalograms, 160 positive scan results were obtained. Sixty-one had subsequent nontumor diagnoses made, and 118 brain tumor diagnoses were recorded. Of these, 99 had positive scan results. Tabulated results are compared with those from 9 other medical centers. (H.G.D.)

3831 THE USE OF ^{99m}Tc PERTECHNETATE IN CARDIAC SCANNING. Witcofski, Richard L.; Bolliger, Theodore T. (Bowman Gray School of Medicine, Winston-Salem, N. C.). J. Nucl. Med., 6: 555-9(Aug. 1965).

Technetium-99m pertechnetate was utilized for scanning the cardiac blood pool. The delineation of the heart pool and surrounding vasculature was comparable to that obtained with the standard ^{131}I compounds now in use. Advantages of ^{99m}Tc are discussed. (H.G.D.)

3832 ALBUMIN MACROAGGREGATES FOR BRAIN SCANNING: EXPERIMENTAL BASIS AND SAFETY IN PRIMATES. Kennady, J. C.; Taplin, G. V. (Univ. of California, Los Angeles). J. Nucl. Med., 6: 566-81(Aug. 1965).

Ten monkeys were given repeated internal carotid artery injections of radioalbumin aggregates (10 to 100 μ) in doses of 0.8 to 11.0 mg. Doses below 2.0 mg produced no detectable central nervous system abnormalities. Studies indicated that if the entire carrier dose (0.2 to 0.6 mg) of radioalbumin macroaggregates injected for lung scanning in man were shunted into the general circulation, the likelihood of cerebral microembolization is extremely remote. The cerebral toxicity of macroaggregates must be reevaluated after prior injection of 50 percent sodium diatrizoate in the monkey, inasmuch as the brain hemisphere scan may be performed in conjunction with angiography in man. Initial arteriolar entrapment of macroaggregated albumin appeared to be a purely physical mechanism. However, further study is needed to elucidate the mechanisms by which these friable particles are removed. Before brain hemisphere scans are performed in man, long term studies in primates are needed to evaluate changes in behavior, intelligence, and motor performance as well as detailed histological examination of brain sections. (auth)

3833 AN INTRAORAL STENT FOR THE DIRECTION OF RADIATION BEAM THERAPY. Santiago, Arturo (Univ. of Puerto Rico, San Juan). J. Prosth. Dent., 15: 938-44(Sept.-Oct. 1965).

Use of an intraoral cone and stent to prevent radioinjury during irradiation of oral tumors is described. The intraoral stent, an acrylic resin device designed and made for the individual patient, aids in simplifying and improving the technique of intraoral therapy. Procedures in the construction of an intraoral radiation stent are described. The patient described was treated with a 6-Mev electron beam. The daily exposure dose was 300 rad, and the total tumor dose delivered was 5500 rad in 24 days. The beam was directed by using the intraoral stent to provide a rigid and reproducible connection between the gingival lesion and the betatron. The case provided an example of the type of malignant lesion of the oral cavity particularly well suited to treatment with radiation delivered by an intraoral cone. (TCO)

3834 DEMONSTRATION OF VESICOURETERAL REFLUX WITHOUT RADIATION EXPOSURE. Amar, Arjan D. (Presbyterian Medical Center, San Francisco). J. Urol., 92: 286-8(Oct. 1964).

Reduction of radiation exposure in the management of patients with vesicoureteral reflux is both especially desired and unusually difficult. Urinary tract infection, acute or chronic, may be associated with reflux. Chronic urinary infection often necessitates repeated x-ray examination to establish diagnosis, to observe the course of disease, and to detect recurrence after treatment. In such cases radiation exposure mounts, perhaps throughout life. The diagnosis of vesicoureteral reflux is usually made by means of voiding cystography, with or without cinefluoroscopic control. Voiding cineradiography may reduce radiation exposure but requires costly equipment available only in a few centers. During cystographic examination, with or without cine control, the female gonads cannot be shielded, and vesicoureteral reflux is more common in young female patients and cumulative x-ray exposure may reach high levels in them. A new, simple, inexpensive technique which does not entail the use of x rays or

radioisotopes to demonstrate vesicoureteral reflux is described. The test involves introduction of an indigo carmine solution into the bladder, voiding to produce reflux if the anatomic situation permits, and immediate cystoscopic examination of the ureteral orifices. Results of the test in 40 cases are presented. Of the 40 patients, 18 showed unilateral or bilateral vesicoureteral reflux, and in 17 of the 18 cases, the indigo carmine test indicated the presence of reflux. Evidence of reflux appeared on one x-ray film in the case in which the indigo carmine technique did not demonstrate it. (BBB)

3835 MANAGEMENT OF POLYCYTHAEMIA VERA. Lancet, 1: 849-50(Apr. 17, 1965).

The advantages and possible hazards, especially leukemogenic, of use of ^{32}P to treat patients with this disease are discussed. The first report of possible neoplastic action of ^{32}P was made in 1955 of six cases of acute leukemia and five of subacute leukemia among 73 patients treated with ^{32}P; this raised the possibility that the radiation administered therapeutically might be the cause of the leukemia. The changes induced in blood cell chromosomes in patients with polycythemia vera treated with radiophosphorus are discussed. In cells from 14 patients examined, three types of damage to chromosomes were detected: some cells had more or less than the diploid number of chromosomes; some had chromatid gaps or breaks; and a third group had a variety of abnormalities. There seemed to be no specific abnormality, and no sign of the Philadelphia (Ph^1) chromosome seen in chronic myeloid leukemia. These chromosome abnormalities were most apparent soon after the administration of ^{32}P, but some were still present several months after the dose, and repeated doses caused increased damage. Since ^{32}P has been widely used, the average survival time is about 13 years. This is compared with another group of polycythemic patients, followed for over 13 years, who were treated with cytotoxic drugs and not given any form of radiation. The outcome of this study shows that the results are at least as good as those achieved with radiophosphorus. The median survival of these patients was 13.6 years, about the same as with ^{32}P treatment, but, in contrast to the irradiated groups of patients, leukemia developed in none of the 127 patients. (BBB)

3836 RADIOTHERAPY IN HERPES ZOSTER. Rhys-Lewis, R. D. S. (Essex County Hospital, Colchester, Eng.). Lancet, 2: 102-4(July 17, 1965).

Results of a controlled study are presented which showed that use of x rays in this benign disease is not therapeutically beneficial, and the hazards associated with the use of x rays in herpes zoster (shingles) are emphasized. The rationale of radiotherapy in benign dermatologic problems is discussed. Small doses of radiation are known to exert a beneficial effect on inflammatory processes. The mechanism may be by causing capillary dilatation and increasing the blood-flow (thereby speeding the arrival of leucocytes at the site of inflammation), and by breaking down lymphocytes, which possibly releases certain essential enzymes and antibodies. Further, radiation dilates the efferent pathways, which favors the removal of debris and toxic substances. Radiation is also believed to affect the cells that anchor the lymphatic channels, and, by causing them to swell, to become shorter, thus dilating the lymphatic channels with a consequent more rapid flow of lymph. Radiation acting on fibroblasts and glioblasts will also probably reduce fibrosis outside the ganglion and gliosis within it. In this way, if post therapeutic neuralgia is a kind of causalgia, radiation could be supposed to reduce its incidence. In the cases treated here, conventional x-ray treatment to a dose of 1000 R was given over ten days on the overlying skin, calculated to give a dose of ~600 R over the same period to the affected root ganglia. Of the 409 patients with herpes zoster investigated to determine the value of x-ray therapy, 342 patients were submitted to a random clinical trial. Radiation had no apparent clinical value in the treatment of the sensory root ganglia. As a basis for assessment, the symptoms were graded as slight, moderate, and severe, and the objective assessment of relief as none, some, or complete. There was no difference whether the patients actually had received any radiation or were sham-irradiated. A series of patients with ophthalmic zoster was studied separately, because clinically they require special attention. Here again, there was no clear evidence that treatment with radiation was of any value. Moreover, the late complications of corneal ulceration in patients with an insensitive cornea (as evidenced by an absent corneal reflex) was as frequent in the patients who had received radiation as in the controls. Thus, radiation revealed no apparent benefit in ophthalmic zoster, either. It is likely that the herpes zoster virus lies dormant in the body and that a clinical attack is precipitated only when the resistance of the affected dermatome has in some way been lowered. This probably explains why attacks of shingles are common in patients who have had radiotherapy to the same part of the body. (BBB)

3837 PROBLEMS AND RESULTS OF RADIOPHOSPHORUS THERAPY (^{32}P) OF POLYCYTHEMIA VERA IN 50 PATIENTS ON THE BASIS OF 5-YR OBSERVATION TIME. Nagy, Gyorgy; Petranyi, Gyula (Debreceni Orvostudomanyi Egyetem II. sz Belklinikaja, Debrecen, Hung.). Magy. Radiol., 17: 208-13(Aug. 1965). (In Hungarian).

Observations made from 1959 to 1964 on 50 patients receiving ^{32}P therapy for polycythemia vera are described. The average age of the patients was 48 yr, 50% of the patients was in the 40- to 50-yr group. The effects of ^{32}P were latent for 2 to 3 months. It was found that 25 to 50% of the ^{32}P was eliminated by the body within 3 or 4 days. The remainder was retained in bone marrow and was eliminated slowly. Remission was achieved in 85 to 92% in the various groups; no patients were found to be radiophosphorus resistant. It was noted that the white blood cell count and the thrombocyte count decreased 4 to 6 weeks after radiophosphorus treatment before there was any change in the red blood cell count. This change occurred only at the end of the second month and reached normal levels after 2 or 3 weeks. Of the 98 treatments administered, none required medical attention because of complications due to the treatment. To date, no cases of leukemia have been noted among the patients. (TCO)

3838 THE QUESTION OF THE DOSE USING THE CHAOUL IRRADIATION TUBE. Hrabovszky, Zoltan; Nikl, Istvan (Joliot-Curie Sugarbiologiai Kutato Intezet, Budapest). Magy. Radiol., 17: 226-33(Aug. 1965). (In Hungarian).

Dose measurements were made on Chaoul-type x-ray tubes with the aid of a phantom to verify the data provided by the manufacturer. Measurements were made with a Siemens Universal dosimeter (SUD) which was used in conjunction with a phantom chamber specially constructed for the measurement of Chaoul-type tubes. The manufacturer provided the chamber with a plastic shield (window) which was to be used when making dose measurements on Chaoul tubes. It was found that the window absorbed the equivalent of 0.07 mm Al. Since the window is not normally used when the tubes are in actual operation, control measurements were made with and without this shield and showed considerable variation between the two measurements. A table shows in detail the measurements made on 18 different tubes; the min variation was 49.5 R/min, the max variation 1822.5 R/min. If the measurements were taken as 100% with the window, the variation was spread between 134.0 to 274.0%. There was considerable difference found in the dose delivered on the surface and in depth by the various tube sizes, and in some instances the window increased the depth dose. This, of course, would lead to an inadequate dose in treating a tumor and an unnecessarily large dose on the surface. It is pointed out that a rubber glove type covering was used frequently in these tubes by the author both in phantom measurements and in actual treatment use to give a more accurate dose and the results were satisfactory. Some of the gynecological tubes are covered with an aluminum cap which emits a considerable amount of soft radiation that should be taken into consideration. It is stressed that the conditions under which tubes are checked should be the same as those in actual use. (BBB)

3839 A RULER TO DETERMINE RELATIVE DEEP DOSES AND SELECTION OF PROPER CONDITIONS FOR IRRADIATION BY TELEGAMMA-UNITS. Krongaus, A. N.; Shagimardanov, N. Sh. Med. Radiol., 10: No. 7, 83-6 (July 1965). (In Russian).

Modern radioactive cobalt irradiators are provided with regulating diaphragms so that a wide variety of radiation fields at various source-to-skin distances can be created. In order to simplify the dose calculations of the cobalt irradiator, a slide rule was designed to give the relative (percent) depth dose with respect to the surface dose as a function of the dimensions S of the irradiation field and of the source-to-skin distance F for a depth d varying from 0.5 to 30 cm. The irradiation field can be varied from 16 to 150 cm^2, and the source-to-skin distance can be varied from 35 to 75 cm. The slide-rule is easy to use. For example, on moving the ruler so that the radiation field S = 80 cm^2 intersects with the curve of the source-to-skin distance F = 35, it is possible to read off relative depth doses of 95% at 1 cm, 91% at 2 cm, 85% at 3 cm, 79% at 4 cm, and 74% at 5 cm. The relative dose is 10% at a depth of 25 cm. With a radiation field of 60 cm^2 at a depth of 10 cm it is necessary to obtain a 50% relative depth dose. The slide-rule quickly gives a value of about 43.5 cm for the source-to-skin distance under these conditions of irradiation. A comparison with tabulated value shows that the average relative error is about 2%. The slide rule should simplify depth dose calculations on ^{60}Co irradiators. (TTT)

3840 ON THE TREATMENT OF THE IRRADIATION REACTION OF THE MUCOSA. Harms, I.; Kaercher, K. H.; Kleinert, H. (Univ., Heidelberg). Med. Welt, 20: 1125-9(May 16, 1964). (In German).

Supervoltage therapy of malignant tumors is becoming increasingly widespread because it permits the depth dose to be increased more readily as compared to conventional x irradiation. However, the mucosa in the region of the focal dose also receives increased irradiation. The reaction of the mucosa to irradiation often requires medical treatment. The irradiation effect in the organism probably depends about 20% on physical factors and about 80% on chemical factors so that probably the best way to alleviate these effects is by means of a chemical agent of some sort. Up to now the radioprotective substances used have been sulfhydryl compounds, biogenic amines, or substances that affect the central nervous system. A newer material has been obtained from rutin. This is the derivative, trihydroxyethylritosidum. This substance is related to the vitamin P-factors originally obtained from citrus fruits. Experimental animal studies have shown that this substance reduces the capillary permeability and hemorrhagic diathesis produced by irradiation. This substance has other effects that include improvement of heart activity and circulation, increased diuresis, and reduction of the serum lactic acid concentration. Trihydroxyethylrutosidum is water soluble and can be administered orally, intravenously, subcutaneously, or intraperitoneally. It was tested clinically in 62 patients who had been treated with telecobalt or telecesium, or with fast electrons from a betatron. The patients had been irradiated in the head region where irradiation reactions are frequently observed. The γ irradiation doses received by the mucosa ranged from 1360 to 6800 R, and the fast-electron doses ranged from 1150 to 4950 R. When the test compound was administered at the beginning of irradiation, the symptoms of the reaction were markedly decreased. In a few cases pantothenyl alcohol or prednisone was used to alleviate radiodermatitis. Using trihydroxyethylrutosidum it was possible to carry out all but one of the irradiation series without interruption because of mucosal reactions to the irradiation. (BBB)

3841 ON THE PROBLEM OF MALIGNANT DEGENERATION LONG AFTER PREVIOUS X IRRADIATION. Full-Scharrer, G. (Univ., Muenchen, Ger.). Monatsschr. Ohrenheilk. Laryngol-Rhinol., 98: 62-6(Feb. 1964). (In German).

A 68-yr-old female patient who had been treated 40 yr previously with α irradiation developed a hypopharyngeal tumor and an unrelated squamous cell epithelioma of the left lower jaw. There was a three-yr interval between appearance of the two tumors. Skin carcinomas sometimes result from previous x irradiation, but it is rare that carcinomas of internal organs result from excessive irradiation. The depth effects of x irradiation are related, in general, to absorption in the tissue, the divergence of the beam, and the scattering of the radiation. In the earlier period when x radiation was beginning to be used for therapy it would have been difficult without the proper filters and high voltages to produce really high-energy irradiation. Considering the energy loss and the irradiation scatter, it might have been possible to produce a hypopharyngeal tumor, but this would not explain the tumor free area between this and the skin tumor. Probably these differences might be explained by individual responses to the interaction between physical and biological characteristics. The usual neoplastic response to x irradiation is squamous cell carcinomas, but spindle cell tumors also have been observed, suggesting that the individual response to irradiation may be a deciding factor. However, considering the wide-spread and almost uncontrolled use of irradiation in the past, it is surprising that relatively few carcinomas have been observed even after such long periods of latency. (BBB)

3842 TRACKING COBALT PROJECT. Green, Anthony (Royal Northern Hospital, London). Nature, 207: 1311(Sept. 18, 1965).

An adaptation of moving-beam therapy is described that proves to be a new and accurate method for treating malignant disease by radiation. The cobalt tracking project permits accurate irradiation of the spread of malignant disease from the primary growth along the lymph node chain. The uniform dose zone of moving-beam therapy irradiates the sinus track of the lymph node spread that is fed through it by moving the patient on a treatment couch guided along a track in up-and-down and side-to-side movements controlled by electric motors. The shape of the dose pattern is changed from a circle to an oval in cross-section at any point by slowing the speed of the arc movement. Preliminary computer calculations and measurements showed that a field of approximately 8 cm × 3 cm with reasonable definition is attainable. Hence the feasibility of irradiating diseased tissues while sparing normal tissue is enhanced. (H.G.D.)

3843 A CASE OF ASEPTIC MENINGITIS SECONDARY TO INTRATHECAL INJECTION OF ^{131}I HUMAN SERUM ALBUMIN. Detmer, Don E.; Blacker, H. Martin (Johns Hopkins Hospital, Baltimore). Neurology, 15: 642-3 (July 1965).

Radioisotope-tagged human serum albumin can be used to detect the site of occult leakage in cerebrospinal rhinorrhea. Untoward reactions to intrathecal injections of ^{131}I-human serum albumin have been noted previously but they are not common. No documented case of meningitis secondary to subarachnoid instillation of radioiodinated serum albumin could be found in the literature, but such an occurrence is reported here. In an attempt to locate the source of rhinorrhea in a 43-yr-old woman, radioisotope cisternography was performed by lumbar puncture followed by injection of 0.45 ml of 6 g% ^{125}I-human serum albumin (100 μC) into the subarachinoid space. Scans made one, three, and 24 hr later revealed no rhinorrhea, and nasal secretions were negative. At six hours after the injection, the patient was completely disoriented, and remained in this state for the next six hours. For the next three days, the patient had severe frontal and occasional occipital headaches, but no vomiting. Symptoms and signs disappeared four days after onset of meningitis. The reaction described points to aseptic meningitis and suggests that infection is unlikely to have been a contributory cause. Other possibilities are nonspecific reactions to protein, to carriers in the injectant, and to substances entering the subarachnoid space secondary to the skin preparation. The protein concentration in this case was 6% in solution, and

the total amount of protein injected was 27 mg. Carriers in the Albumotype solution used are 0.25% guanidine hydrochloride, 1.6% dibasic sodium phosphate, and 0.16% monobasic sodium phosphate. The possibility that these agents were responsible for the reaction cannot be excluded. It is suggested that further evaluation of the intrathecal use of radioiodinated serum is necessary. The reaction seen here confirms that introduction of any agent into the subarachnoid space is hazardous. (BBB)

3844 ^{125}I IN THE CLINICAL EVALUATION OF THYROID DISEASE. Riccabona, G. (Chirurgische Univ., Innsbruck). New Engl. J. Med., 273: 126-30(July 15, 1965).

In view of the possible hazards of ^{131}I scanning, especially in children, and other shortcomings of the use of ^{131}I in thyroid diagnosis, the use of ^{125}I as a replacement for ^{131}I was investigated. Iodine-125, obtained by cyclotron irradiation of tellurium or by neutron activation of ^{124}Xe, decays into xenon, emitting soft γ radiation. The effective energy emitted per disintegration is 62 kev; the photopeak is at 35.5 kev. Owing to the low energy there is no Compton scatter. The half-life is 56 days. The photon emission per μC is considerably higher than with ^{131}I. Thus, one μC of ^{131}I measured 400,000 cpm in a well-type scintillation counter with pulse-height analyzer, whereas one μC of ^{125}I gave 750,000 cpm. For satisfactory in vivo counting rates in clinical samples the dose of ^{125}I was therefore roughly half the dose of an adequate ^{131}I tracer. The soft γ radiation of ^{125}I has the disadvantage of high absorption by tissue, so an evaluation of this factor was made. An absorption rate of 14.1% per cm of water was found, and absorption coefficients for different depths were calculated. A variation of only ±4 per cent of the counting rate was found in volumes from 25 to 100 ml with 25 μC of ^{125}I. The problem of dosimetry with ^{125}I was also investigated. The total dose delivered with 50 μC of ^{125}I to a thyroid gland of 20 g, a 20% uptake, and an effective half-life of ^{125}I of 36.5 days is 40.0 rad. A 50-μC dose of ^{131}I under the same conditions but with an effective half-life of 7.5 days (same biologic half-life) would deliver 56.3 rad. But in a thyrotoxic patient with a 70-g gland, a 70% uptake of only 13.2 rad would result with 50 μC whereas ^{131}I would deliver 42.9 rad. In hypothyroidism, with slow turnover, the dose advantage of an ^{125}I tracer is lower. To investigate the clinical value of ^{125}I and ^{131}I, phantom scans were done, and 210 patients were examined. It was possible to identify lesions with a diameter of 0.5 cm underneath 2 cm of water with 7 μC of ^{125}I in a phantom and 1-cm lesions underneath 3 cm of water. Less accurate resolution in deeper layers was obtained with ^{131}I when compared with ^{125}I. Results in patients examined with ^{131}I and ^{125}I are shown. Scans with ^{125}I showed a good resolution even in doses of 20 μC. When ^{131}I scans were compared to ^{125}I scans, the better resolution in the ^{125}I scintiscans was obvious. Therefore, ^{125}I tests of thyroid function and scans are recommended in special studies in which ^{125}I seems preferable for other reasons such as long half-life and elimination of radiation artifacts, and for thyroid scans in children and other patients when a reduction of the radiation dose seems advisable. (BBB)

3845 THE APPEARANCE OF THE ISOENZYMES OF VARIOUS ENZYMES DURING IRRADIATION THERAPY. Kaercher, K. H.; Kato, H. T. (Univ., Heidelberg). Nippon Igaku Hoshasen Gakkai Zasshi, 24: 418-25(July 25, 1964). (In German).

The heterogeneity of the enzymes lactic dehydrogenase, alkaline phosphatase, and acid phosphatase was studied by agar gel electrophoresis for isolation of their isoenzymes. The enzyme mixtures were obtained from tumor tissues of patients who had clinically demonstrable hemangioendotheliomas, bone metastases from mammary tumors, liver metastases from melanomas, and gastric adenocarcinoma. Estimation of the isoenzymes did not have specifically diagnostic value. However, detection of the isoenzymes of lactic dehydrogenase appeared to have supplemental diagnostic value if it accompanied other clinical symtomology of the tumor. The phosphatases had some diagnostic value for differentiation between liver and skeletal tumors, and between benign and malignant changes in the prostate. The particular value of estimation of the isoenzymes of lactic dehydrogenase was that it directly indicated the destruction of tumor cells by irradiation and release of the isoenzymes into the serum. Thus, this analytical method offers a very specific procedure for following the progress of irradiation therapy. In a similar way, an estimation of the isoenzymes of alkaline phosphatase in serum, after they have been released after irradiation of mammary or prostatic cancers, can offer clues as to the effects of treatment. (BBB)

3846 RADIATION DOSES IN ORAL RADIOGRAPHY. IV. A RE-INVESTIGATION OF DENTAL X-RAY UNITS. Hollender, Lars (Royal Dental School, Malmo, Sweden). Odontol. Revy (Lund), 13: 34-8(1962).

X-ray units in Malmo surveyed in 1960 were reinvestigated to ascertain whether any improvements had occurred. Dental x-ray units and procedures used in 42 of the 62 units formerly investigated were available for reinvestigation. Added filtration, field diameter, exposure dose rate at the tip of the cone, exposure time for full-mouth roentgenography (14 films), and development time were recorded. Comparable data collected in the 1960 and in 1961 surveys are tabulated. It was evident that only few reductions of radiation hazards were made during the interval between the investigations. Thus, a reduction in radiation hazards was not accomplished since very few alterations in the equipment of the units and of the x-ray procedures were found. (BBB)

3847 DERMATOMYOSITIS FOLLOWING TREATMENT OF CANCER. Calvert, H. T. (Reading Group of Hospital, Eng.). Neale, E. J. E. Postgrad. Med. J., 41: 371-3(June 1965).

A 45-year-old woman was first examined for a lump in her right breast which had been present about six weeks. There was no evidence of lymph node involvement or secondary deposits. After a right radical mastectomy and bilateral cophorectomy was performed, histologic studies showed a scirrhous carcinoma and deposits within lymphatics. Her post-operative recovery was uneventful, and she received x-ray therapy (250 kv) to chest wall to give a tumor dose of 3500 R and telecobalt to lymph node areas, 4900 R. She was noted to have a small patch of erythema and scaling over the right scapula and right anterior chest wall when examined three weeks later. After another three weeks the rash had spread to her back, upper chest, arms, neck and face, and she had developed swelling and edema of these areas, with complete closure of her left eye. She also complained of pruritus and weakness of her upper limbs; and later of some difficulty in swallowing. On examination at this time she presented the typical appearance of a patient with dermatomyositis. She was treated with 80 mg prednisolone daily and testosterone propionate, 200 mg twice weekly, replaced later by Nilevar. On this regime her skin lesions regressed and her muscle strength improved. Seven months later there was a recurrence of edema and erythema of face, chest, and arms, which required an increased dose of steroids. At present the patient is clinically healthy. Dermatomyositis is an inflammatory and degenerative parenchymatous myositis. The skin changes when present are nonspecific and may be followed by atrophy. It is usually considered as a disease of autoimmunity, which would account for its rare haphazard occurrence in patients suffering from a wide variety of cancer. Some have postulated that sensitivity plays a role in the genesis of dermatomyositis, but it could also represent a failure of immunity. The sequence of dermatomyositis following radiotherapy points to products of tumor destruction as the primary cause, but does not help decide whether they act as allergens or carcinotoxins. (BBB)

3848 RADIOTHERAPEUTIC MANAGEMENT OF MALIGNANT TUMORS OF THE VAGINA. Chau, Paul M.; Green, Allan E. (M.D. Anderson Hospital, Houston, Tex.). Progr. Clin. Cancer, 1: 728-50(1965).

Methods and doses for various types of radiation to treat

tumors at different sites in or near the vagina are described. Means for preventing injury to normal tissues and reducing the postradiotherapeutic complication rate are also included. Examples of cancer at various subsites with treatment by radium implants, cone therapy, or external irradiation are shown. (TCO)

3849 PROGRESS IN RADIATION THERAPY: INTRODUCTION. **Buschke, Franz (Univ. of California, San Francisco). Progr. Radiat. Therapy, 3: 1-15(1965).**

Advances in radiotherapy are reviewed. It is concluded that the most important progress made during the last decade is in the reduction of damage to normal structures with the consequence of less morbidity and greater safety. Late sequelae of major clinical consequence, which 20 years ago might have been accepted as unavoidable and calculated risks, are now considered traceable to some error in technique or judgment. Within the dose range necessary for the treatment of most radiocurable neoplasms, the damage to the normal cellular components of parenchymatous organs in the treatment volume appears to be of less importance than the damage to the vasculoconnective tissue (including bone and cartilage). Within the dose range considered, such cellular damage can be repaired by regeneration, whereas injury to the vasculoconnective tissue, once it has reached a certain degree, continues to progress, and its late direct and indirect effects are responsible for the late complications. Thus, the limit of radiation tolerance is determined in general by the tolerance of the vasculo-connective tissue. Some recent clinical studies related to late radiation injuries following the treatment of neoplasms in different anatomic sites are reviewed. Among 93 patients who received spinal cord doses above 5000 rad (68 of whom received more than 5500 rad) with a weekly dose of not more than 800 rad and who survived at least $1\frac{1}{2}$ years, no progressive myelitis (presumably secondary to injury to the vasculo-glial tissue) and only one case of transient myelitis occurred. Based on other clinical investigations cited, it is concluded that, regardless of the anatomic site, serious radiation injury can consistently be avoided by prolongation of overall treatment time to a weekly dose of about 800 rad for a total dose of 6000 rad. Even doses up to 8000 and 9000 R are well tolerated with fractionation, and permit safe treatment of neoplasms which require very high doses, such as certain parotid gland carcinomas, adenocarcinomas of the nasopharynx, and neurogenic and fibrosarcomas. Radical surgery following doses of this level is possible without any major surgical complications. It is concluded that prolongation of treatment time has accomplished the main purpose expected of progress in radiation therapy, namely, to increase the differential between tumor vulnerability and tolerance of the normal structures. The vulnerability of specific tissues, pediatric radiotherapy, chemotherapy-radiotherapy combinations, and training of radiotherapists are also discussed. (BBB)

3850 RADIATION THERAPY IN CHILDHOOD. **Darte, John M. (Univ. of Toronto). Progr. Radiat. Therapy, 3: 141-71(1965).**

Special problems encountered in radiation treatment in children are considered, especially: differences in the radiation response of children compared with adults; possibilities of carcinogenesis; use of radiation in benign conditions; and specific uses of radiation in pediatric malignancies. It is suggested that with present techniques the incidence of radioinduced malignancy is low and is comparable with other acceptable risks of anesthetic and operative mortality. Because of the possible deleterious effects of irradiation in children, the indications for its use should be definite and not based on considerations of ease, availability, or simplicity. The treatment of benign conditions with radiation should be limited to certain conditions in which it is the best treatment, including hemangioma of the larynx, hemangioendothelioma of liver and certain lesions of histiocytosis X. The major contribution of pediatric radiotherapy lies in the control of certain malignant conditions, such as Wilm's tumor, neuroblastoma, retinoblastoma, central nervous system tumors, and other less frequent malignancies in childhood. (TCO)

3851 THE MALABSORPTION SYNDROME FOLLOWING RADIOTHERAPY. **Duncan, W.; Leonard, J. C. (Christie Hospital and Holt Radium Inst., Manchester, Eng.). Quart. J. Med., 34: 319-29(July 1965).**

Six patients are described who developed evidence of intestinal malabsorption after radiotherapy. These patients were among 3000 other patients who received radiotherapy to the abdomen and pelvis. A review of the literature revealed only five similar examples of an established malabsorption syndrome following radiotherapy. Megaloblastic anemia occurred in three patients and another patient had impaired absorption of vitamin B_{12}. Vitamin B_{12} is wholly absorbed in the ileum and folic acid mainly in the jejunum. Since the ileum is close to the uterus, ovary, and bladder, it is frequently included in the field of high-dose pelvic irradiation for malignant tumors of these organs. Thus megaloblastic anemia secondary to radiation changes in the intestine is much more likely to be due to deficiency of vitamin B_{12} than of folic acid. In the six patients described, diarrhea, wasting, intestinal obstruction, steatorrhea, and megaloblastic anemia were the main clinical features; one patient also had subacute combined degeneration of the spinal cord. The pathological changes included widespread ulceration of the small intestine, with diffuse inflammatory change, endarteritis, fibrosis, and the development of strictures. The ileum is especially likely to be damaged by high-dose pelvic irradiation. Two of these patients had strictures, and the remainder probably had diffuse inflammatory and fibrotic changes in the ileum. It is emphasized that manifestations of the malabsorption syndrome may be often ascribed to a recurrence of the original neoplasm, and that correct diagnosis of this condition is essential so that effective medical and surgical treatment can be instituted. In acute and subacute radiation enteritis, experimental evidence indicates that oral succinylsulfathiazole or an antibiotic should be given to eliminate secondary infection in the intestinal wall. Diarrhea should be treated with an opiate and if an established malabsorption syndrome develops, a high-calorie, low-fat diet should be given and, if necessary, cyanocobalamin. Prompt attention to fluid and electrolyte balance is essential in ill patients, and sometimes blood transfusion and adrenocortical steroids may be helpful. If a stricture is found or suspected, laparotomy is necessary after the patient has been rendered fit by medical measures. If resection of the stricture is impossible or hazardous because of damage to the adjacent small intestine, a bypass operation should be performed. (BBB)

3852 MODIFICATIONS OF ILIAC AND LUMBO-AORTIC LYMPHOGRAPHIC FINDINGS, FOLLOWING IRRADIATION. **Miceli, Roberto; Corinaldesi, Alberto; Rimondi, Carlo (Univ., Bologna). Radiol. Med., 51: 629-50(June 1965). (In Italian).**

The changes in the inguino-iliac and lumbo-aortic lymphographic findings consequent on x irradiation for therapeutic purposes were studied. Correct evaluation of these modifications, especially those intervening at a certain distance of time from the irradiation, requires knowledge of the modes of spontaneous dismissal of the contrast medium out of the normal and neoplastic lymph nodes. Data are presented on modifications of the normal lymphadenographic findings at various intervals from the time of introduction of the contrast medium, post-irradiation alterations of the normal lymphadenographic images, and semeiological alterations of the lymphadenographic neoplastic findings, at various intervals after irradiation. (tr-auth)

3853 DOSAGE PROBLEMS OF RADIOIODIDE TREATMENT OF THYROID GLAND DISORDERS. **Pfeifer, W.; Wuerdinger, H. (Oldenburgischen Landeskrankenhauses, Sanderbusch, Ger.). Radiologe, 5: 70-3(Feb. 1965). (In German).**

Treatment of thyroid disorders with radioiodine has been extended to most cases of diffuse thyroid hyperfunc-

tion, to about 67% of toxic adenomas, 33% of nontoxic goiters, 20% of malignant tumors, and to cardiac insufficiency refractory to glycoside therapy. The possibility of exacerbation of thyrotoxic symptoms, psychotic reactions, rheumatoid symptoms, hypothyroidism, carcinogenesis, induction of leukemia, or gonadal genetic mutations is always present when radioiodide treatment is used. The authors report results of treatment of 108 patients who were studied for periods of from 6 months to 8 yr after treatment. The patients consisted of 53 with hyperthyroid goiter, 35 cases of hyperthyroidism without goiter, and 20 euthyroid goiters. Permanent myxedema resulted in only three cases after ^{131}I treatment. This amounted to only 2.8%, a value which contrasted markedly with values of from 5.8 to 28% reported elsewhere. Probably the main reason for the excessive amounts of ^{131}I administered elsewhere is the calculation of the treatment dose in curie units without regard to the I turnover and also without regard to the energy dose absorbed in terms of rep or R. Other sources of error may be errors in evaluation of the effective half-value time and of the thyroid weight. (BBB)

3854 THE GONADAL X-RAY DOSE TO CHILDREN FROM DIAGNOSTIC RADIOGRAPHIC TECHNICS. Aspin, N. (Hospital for Sick Children, Toronto). Radiology, 85: 944-51(Nov. 1965).

Measurements were determined of the x ray dose to the gonads of children from some of the basic diagnostic radiographic technics. Ionization chamber measurements were made on wax phantoms representing children of six months, four years, and twelve years of age. Comparisons were made between the doses received from the various technics. It was concluded that examinations in which the gonads are within the primary x ray beam contribute by far the greatest gonadal dose per film; the difference between the male and female gonadal dose for a given radiographic examination is not large, except for the type of study where the gonads of a child of one sex would be inside the primary beam and those of the other sex outside; under conditions of good collimation the variation of gonadal dose with age is small; limiting the x ray beam to the area under examination by means of an adjustable rectangular collimator always reduces the gonadal dose, often to a large degree. This practice also improves the quality of the resulting radiograph by reducing the amount of scattered radiation reaching the film. (auth)

3855 TUMOR/AIR RATIO CALCULATORS. Scott, Walter P. Radiology, 85: 962-4(Nov. 1965).

The designs for two tumor/air ratio calculators for ^{60}Co γ radiation are described: Model 1 is more applicable to the average thickness method and Model 2, to the average tumor/air ratio method. Although the former, based on Jacobson's system, is by far the simpler, its accuracy does decrease as the tumor moves from a central to a peripheral site. The difference between the dose calculated from twelve 30-degree sectors and that calculated from the average thickness is less than 4 per cent. The latter method of Johns is preferred in dealing with tumors that are not symmetrically placed so that determining the dose from each sector is found necessary. (auth)

3856 SIMULTANEOUS BILATERAL INTRACAPSULAR FRACTURES OF THE HIPS: ONE CASE DUE TO TRAUMA, ONE OF FATIGUE FRACTURE, AND ONE FOLLOWING PELVIC IRRADIATION. May, Virgil R. Jr. (Medical Coll. of Virginia, Richmond). S. Med. J., 57: 306-11(Mar. 1964).

Three rare instances of simultaneous bilateral fractures of the hip, are described; the causes are discussed and the treatment outlined. A detailed case history is given for one patient who suffered bilateral intracapsular fractures following x and radium irradiation for cervical cancer and the literature relating to this condition is reviewed. (BBB)

3857 DOUBLE DOSE CONTRAST MEDIUM IN EXCRETORY UROGRAPHY. Amar, Arjan D. (Presbyterian Medical Center, San Francisco). Surg. Gynecol. Obstet., 118: 1083-7(May 1964).

A method is described for avoiding repeated x rays in urography and thus reducing the exposure of the patient to ionizing radiation. Disadvantages of excretory urography are indicated. It is shown that 30 ml of 50% Hypaque injected intravenously yields satisfactory delineation on the excretory urogram if the patient is of average size with adequate renal function, is well dehydrated, and is prepared in the routine manner. Sixty ml of 50% Hypaque may be required under certain conditions. The double-dose technique may improve visualization if renal function is poor, reduce examination time, and decrease the number of follow-up x rays required. In hypertension with suspected renal ischemia the double-dose injection technique has improved the changes of diagnosis. No increase in the incidence or severity of untoward reactions was noted after use of the double-dose technique. (TCO)

3858 PRECAUTIONS IN THE RADIOGRAPHY OF FEMALE PATIENTS. Whitehouse, Walter M. (Univ. of Michigan Medical Center, Ann Arbor). Univ. Mich. Med. Center J., 30: 178-9(July-Aug. 1964).

Means for lowering the gonadal dose in women (and the fetal dose in pregnant subjects) are enumerated. Because of the internal location of the female gonads, and because of the possibility of pregnancy during the childbearing period, precautionary measures are more of a problem in female patients, and vary with the age of these patients. The use of shaped Pb-rubber shields for gonadal protection of women during child-bearing age is recommended. Radiation precautions for any patient group are reviewed. (BBB)

3859 APPLICATIONS OF RADIOACTIVE ISOTOPES IN VETERINARY MEDICINE. Holmes, J. R. (Univ. of Bristol, Eng.). Vet. Bull. (Commonwealth Bur. Anim. Health), 32: 65-72(Feb. 1962).

A review (with ~100 references) is presented of diagnostic and therapeutic uses of radioisotopes in domestic animals. Diagnostic applications are discussed in terms of five categories: uptake tests in which the isotope is selectively collected by a specific organ or tissue; function studies; flow or diffusion measurements; dilution techniques, involving particularly measurements of volume; and delineation of certain areas of the body. (TCO)

3860 NUCLEAR MEDICINE. Blahd, William H. (ed.). New York, McGraw-Hill Book Co., 1965. 831p. $17.95.

The fundamentals of nuclear medicine, the principles of measurement of radioactivity, and instrumentation are reviewed. Applications of radioisotopes in diagnosis and therapy, and the use of external and implanted radioactive sources and high-energy nuclear particles in the treatment of cancer are discussed by 48 authorities. The field of nuclear medicine is treated as an integrated medical discipline. While the approach is primarily clinical, subjects are considered in sufficient depth to be of value and interest to both the medical investigator and instructor. Most of the 30 chapters contain complete bibliographies so the book will serve as a useful reference source. (C.H.)

3861 RESULTS OF BREAST TUMOR TREATMENT BY RADICAL OPERATION INCLUDING PREOPERATIVE X IRRADIATION AND STUDIES OF RADIATION DAMAGE IN THE OPERATED TISSUE, WHICH CAN BE DETECTED BY HISTOLOGICAL METHODS [Thesis]. Durczok, H. Marburg, Ger., Univ., 1964. 55p. $2.00 Gmelin, AED-DISS. 64-736.

One-hundred-fifty-one breast tumor cases treated by radical operation with and without preirradiation in the years 1950 to 60 are analysed. Percentage of cured patients is 50% with preirradiation and 47% without. The difference is not significant. (Gmelin Inst.)

3862 FILM DOSIMETRIC STUDIES OF CONVERGENCE IRRADIATION OF CEREBRAL TUMORS [Thesis]. Stoltze, D. Erfurt, Ger., Med. Akademie, 1963. 74p. $2.00 Gmelin, AED-DISS. 63-788.

Isodose distributions in a head phantom were measured by film dosimetry. Results are compared with data from the literature. (Gmelin Inst.)

CHEMISTRY

General

Refer also to abstracts 4086, 4146, 4184, 4185, and 4345.

3863 (IS–1200(Sect. C)) CHEMISTRY DIVISION. (Ames Lab., Iowa State Univ. of Science and Tech.). 105p.

Research and development summaries are presented on physical and inorganic chemistry, analytical chemistry, spectrochemistry, and radiochemistry. (J.R.D.)

Analytical Procedures

See also Separation Processes and Procedures

Refer also to abstract 3984.

3864 (AERE-L–166) THE USES OF REACTORS IN: (1) NEUTRON ACTIVATION ANALYSIS; (2) THE DETERMINATION OF CROSS-SECTIONS BY ACTIVATION AND MASS SPECTROMETRIC METHODS. Cabell, M. J. (Atomic Energy Research Establishment, Harwell (England)). Oct. 1965. 36p. Dep.; BIS $1.10; HMSO 5s. 6d.

Basic information that is required in order to understand what is involved in experiments using reactors in neutron activation analysis is discussed, and the application of this information in designing experiments and in interpreting results is reported. The determination of integral cross sections by chemical methods is also described. (P.C.H.)

3865 (ANL–7064) CONSOLIDATION OF LANTHANON FISSION PRODUCTS IN ALLOYS. Knighton, J. B.; Mancini, R. A.; Steunenberg, R. K. (Argonne National Lab., Ill.). Aug. 1965. Contract W-31-109-eng-38. 22p. Dep. mn; CFSTI $1.00 cy, $0.50 mn.

The feasibility of extracting the lanthanon elements from a molten chloride salt into binary magnesium alloys which could serve as a medium for both interim and permanent disposal, and possibly as a useful source of heat and activity, was investigated. The salt composition selected was the ternary system 50 mole % $MgCl_2$-30 mole % NaCl-20 mole % KCl (mp 396°C). Distribution coefficients of praseodymium, a representative lanthanon fission product, were determined between the molten salt and liquid binary alloys of magnesium with aluminum, copper, lead, antimony, and nickel. The most favorable distribution coefficients were obtained with the magnesium–aluminum system. Distribution coefficients of yttrium, lanthanum, cerium, and praseodymium between the salt and magnesium–aluminum alloys were determined, and their solubilities in the liquid-metal phase were measured at various temperatures and magnesium concentrations. The results indicated that an aluminum–20 wt % magnesium alloy provides excellent removal of lanthanons from the salt in a single-stage extraction. The technique also appears to be applicable to fission product oxide and fluoride wastes, and to the consolidation of noble and refractory metal fission products, as well as lanthanons, in metallic alloys. (auth)

3866 (CEA-R–2630) CONTRIBUTION A L'ETUDE MICROCALORIMETRIQUE DES CARACTERISTIQUES DES RADIOELEMENTS ET A LEURS ANALYSES QUALITATIVE ET QUANTITATIVE [Theses]. (Contribution to the Microcalorimetric Study of the Characteristics of Radioelements and to their Qualitative and Quantitative Analysis [Thesis]). Ozias, Yves (Commissariat a l'Energie Atomique, Chusclan (France). Centre de Production de Plutonium de Marcoule). 1965. 104p. Dep. mn.

Submitted to Aix-Marseilles Univ. (France). Faculte des Sciences.

Studies were made on use of the E. CALVET microcalorimeter for recording the energy flux emitted by radioelements as a function of time, and in determining from this curve either their characteristics (half life and radiation energy), or the composition of a mixture of radioelements. Theoretical relationships describing radioactivity were adapted to the microcalorimetric study. An experimental determination was made using the E. CALVET microcalorimeter of the characteristics of various radioelements, yttrium-90, phosphorus-32, sulphur-35, iodine-131, etc., and of their mixtures. In particular a study was made of the isotopic analysis of a $^{239}Pu-^{240}Pu$ mixture, sometimes in the presence of ^{241}Pu. The calorimetric method makes it possible to attain an accuracy equal to that obtained by mass spectrography (destruction of the sample) 1 to 3%, and higher than that obtained by counting techniques (greater than 5%). Other advantages and limitations of the calorimetric method are discussed. (P.C.H.)

3867 (CEA-R–2844) DOSAGE RADIOCHEMIQUE DU ^{90}Sr SUR DES VOLUMES IMPORTANTS D'EAUX POTABLES. (Radiochemical Determination of ^{90}Sr in Large Volumes of Drinking Water). Jeanmaire, Lucien; Patti, Francois; Bullier, Denise (Commissariat a l'Energie Atomique, Fontenay-aux-Roses (France). Centre d'Etudes Nucleaires). Aug. 1965. 22p. Dep. mn.

The method consists of fixing all the cations present in the water on a resin, elution using 5N nitric acid and precipitation of strontium as the carbonate, concentration of the strontium using the fuming nitric acid method, and purification of the strontium on a resin by selective elution with ammonium citrate. The strontium-90 is measured by separation of the ^{90}Y equilibrium in the form of the oxalate which is then counted. The concentration of the radioactivity starting from large volumes (100 l) is generally tedious but this method makes use of fixation on a cationic resin. The rest of the method consists of a series of simple chemical operations using ion-exchange on resins and coprecipitation. Finally, it is possible to dose stable strontium. (auth)

3868 (CEA-R–2860) METHODES ANALYTIQUES UTILISEES DANS LES CYCLES DE PURIFICATION DU PLUTONIUM PAR LA TRILAURYLAMINE. (Analytical Methods Used in Cycles for Plutonium Purification by Trilaurylamine). Perez, Jean-Jacques (Commissariat a l'Energie Atomique, Fontenay-aux-Roses (France). Centre d'Etudes Nucleaires). Aug. 1965. 86p. Dep. mn.

The use of trilaurylamine as a solvent extractant for the purification of plutonium was studied. The organic impurities of the solvent can be titrated by gas-liquid chromatography. Also the titration of the main degradation product, the dilaurylamine, can be accomplished by spectrocolorimetry. Potentiometry is used for the analysis of the different salts of amine-nitrate-sulfate-bisulfate and also for the extracted nitric acid. The determination of the nitrate in aqueous phase is carried out by constant current potentiometry. The range of application, accuracy, and procedure are discussed. (auth)

3869 (CEA-R–2869) COMPARISON DES METHODES SPECTROGRAPHIQUES D'ANALYSE DU PLUTONIUM ET DE SES COMPOSES. (Comparison of Spectrographic Methods of Analysis of Plutonium and its Compounds). Chaput, Michel; Robichet, Jacques (Commissariat a l'Energie Atomique, Fontenay-aux-Roses (France). Centre d'Etudes Nucleaires). Sept. 1965. 36p. Dep. mn.

Two spectrographic analysis methods are described for dosing impurities in compounds containing plutonium or its salts. These are: distillation method with a carrying-over agent; and spark method in graphite electrodes. Test results concerning factors which may be considered responsible for the discrepancies observed are appended. All the comparisons were carried out on samples taken in such a way as to ensure a perfect homogeneity and to make it possible to study separately the parameter in question, such as, influence of the internal standard, influ-

ence of the carrying-over agent, and influence of the conditions used for separating the plutonium and of the purity of the reagents. (auth)

3870 (EUR–2459.f) MESURE DE LA RADIOACTIVITE PAR SCINTILLATION EN MILIEU LIQUIDE: APPLICATIONS BIOLOGIQUES. (Measurement of Radioactivity by Scintillation in a Liquid Medium: Biological Uses). Apelgot, S. (Paris Univ. (France). Laboratoire Curie). 1965. 18p. Dep. mn.

For quantitative dosing of low-energy β^- particle emitters by the scintillation method in a liquid medium, close contact must be effected between radioactive atoms and scintillating molecules. It is difficult to fulfil this condition in the special case of aqueous solutions or suspensions (customary in biology) which are not miscible with conventional scintillating media. The use of a membrane support eliminates both this difficulty and in general the associated quenching phenomena also. (auth)

3871 (EUR–2497.e) STUDIES ON THE SEPARATION OF ^{137}Cs AND ^{90}Sr FROM FISSION PRODUCTS IN AN ACID MEDIUM ON MINERAL ION EXCHANGERS. Baetsle, L. H.; Van Deyck, D.; Huys, D.; Guery, A. (Centre d'Etude de l'Energie Nucleaire, Mol (Belgium)). 1965. 70p. Dep. mn.

Studies were made on the recovery of ^{137}Cs and ^{90}Sr by means of new inorganic ion exchangers such as molybdenum ferrocyanide, tungsten ferrocyanide, polyantimonic acid, and the preparation and use conditions of these exchangers. Work was also performed on zirconium phosphate, the deacidification of solutions, and the construction of a ^{137}Cs and ^{90}Sr separation cell. (auth)

3872 (EUR–2507.d) LITERATURSTUDIE UEBER MOEGLICHKEITEN UND UEBER VERFAHREN ZUR DEKONTAMINIERUNG RADIOAKTIV KONTAMINIERTER MILCH. (Bibliographical Survey on Facilities and Processes for Radioactive Milk Decontamination). Knoop, E.; Buchheim, W. (Versuchs- und Forschungsanstalt fuer Milchwirtschaft, Kiel (West Germany)). 1965. 66p. Dep. mn.

A survey was made and data compiled for the purpose of ascertaining the progress achieved in processes for milk decontamination. The main point at issue concerned the practicability and economics of the various techniques. Consequences are drawn as to the methods holding out most promise from the technical and economic standpoints. It was found that 3 processes are used for milk decontamination: ion exchange; electrodialysis; and dairy processes. 80 references covering the period 1954 through mid-1964 are cited. (P.C.H.)

3873 (EUR–2523.i) DETERMINAZIONE DI ZOLFO IN TERFENILI MEDIANTE ANALISI PER ATTIVAZIONE NEUTRONICA. (Determination of Sulfur in Terphenyl by Neutron Activation). Pietra, R.; Sabbioni, E. (European Atomic Energy Community, Ispra (Italy). Joint Nuclear Research Center). 1965. 20p. Dep. mn.

A method for the determination of sulphur in terphenyl by neutron activation is described. The results obtained, evaluation of errors, and sensitivity are reported. (auth)

3874 (EUR–2535.f) DECONTAMINATION EN ^{137}Cs DES SOLUTIONS CONCENTREES DE PRODUITS DE FISSION. (^{137}Cs Decontamination of Concentrated Fission Product Solutions). Aubertin, Ch.; Lefevre, I.; Raggenbass, A. (Commissariat a l'Energie Atomique, Saclay (France). Centre d'Etudes Nucleaires). 1965. 52p. Dep. mn.

In order to obtain a ^{137}Cs decontamination factor of at least 10^4 for concentrated fission product solutions, two separation techniques were examined in detail. These are: phosphotungstate precipitation by addition of phosphotungstic acid; and Cs fixation by exchange on a preformed insoluble ammonium phosphotungstate. For the conditions studied, the most promising solution was found to be double precipitation by phosphotungstic acid using as carrier the ammonium already present in the concentrated fission product solutions. (auth)

3875 (IS-T–37) SIMULTANEOUS EQUILIBRIA OF D2EHPA AND TBP WITH $Pr(NO_3)_3$ AND $Nd(NO_3)_3$ SOLUTIONS [Thesis]. Owens, Thomas Charles (Ames Lab., Iowa State Univ. of Science and Tech.). Aug. 1965. Contract W-7405-eng-82. 32p. Dep. mn; CFSTI $2.00 cy, $0.50 mn.

The method of successive equilibrations was used in comparing tributyl phosphate (TBP) and di-(2-ethylhexyl) phosphoric acid (D2EHPA) as solvents for the separation of $Nd(NO_3)_3$ from $Pr(NO_3)_3$ in an aqueous solution containing a small amount of nitric acid. A mathematical analysis indicated that if the effect of the organic activity coefficients were negligible, the ratio of the separation factors of TBP and D2EHPA would be constant. Experimentally it was found that at low lanthanide concentrations, the separation factors were nearly equal, but at high concentration the ratio of the separation factor of D2EHPA to that of TBP was 0.780. The method of successive equilibrations was successful in obtaining equilibrium between both solvents and a common aqueous solution. Both acidity and lanthanide concentration of the aqueous phase were constant before and after equilibration when eight equilibrations using equal volumes of aqueous and organic liquids were used. With undiluted D2EHPA as the solvent a gelatinous third phase formed and the rate of phase separation was slow. Except at very low total lanthanide concentrations the distribution coefficients and separation factor for TBP were higher than those of D2EHPA. Based on these considerations, TBP was found to be the better of the two solvents for separating $Nd(NO_3)_3$ from $Pr(NO_3)_3$. (auth)

3876 (ISS–65/8) IL DOSAGGIO DEL TRITIO (RASSEGNA). PARTE I. (Determination of Tritium Content in Samples (A Review). Part I). Corti, F. (Istituto Superiore di Sanita', Rome (Italy). Laboratori di Fisica). Mar. 24, 1965. 68p. Dep. mn.

After a brief description of the physical properties of tritium, of its use in scientific research, and of its maximum permissible doses, some methods used in preparing tritiated samples to be directly measured are reviewed. Different processes in the handling of samples are described according to the materials and measurement technique. After a brief explanation of the sensitivity limits of instruments now on the market, some methods are described for enriching tritiated samples that are not sufficiently active. 110 references are cited. (auth)

3877 (LA-DC–7483) THE DETERMINATION OF LOW LEVEL PLUTONIUM ACTIVITY; AUTORADIOGRAPHIC TECHNIQUES VS. SCINTILLATION COUNTING. Moss, William D.; Campbell, Evan E. (Los Alamos Scientific Lab., Univ. of California, N. Mex.). [1965]. Contract W-7405-eng-36. 7p. (CONF-651008–4). Dep. mn; CFSTI $1.00 cy, $0.50 mn.

From Annual Bio-Assay Meeting, Albuquerque, N. Mex.

A comparison was made between autoradiographic techniques and scintillation counting for determination of low level plutonium activity. The human error was considered. As a result the decision was made to return to electronic counting. Reasons for this are: 7 days less time to complete an analysis; less human error; release of a technician from tedious track counting and dark room work; and complete control of contamination to the counters. (P.C.H.)

3878 (LYCEN–6524) MICRODOSAGE DE L'OXYGENE DANS LES METAUX PAR REACTIF RADIOACTIF ET PAR ACTIVATION AUX NEUTRONS RAPIDES DE 14 Mev [THESES]. (Microdetermination of Oxygen in Metals by Radioactive Reagents and by Activation with Fast Neutrons at 14 Mev [Thesis]). Lepetit, Henri (Lyon Univ. (France). Institut de Physique Nucleaire). July 21, 1965. 115p. Dep. mn.

An original method was developed for the determination of oxygen traces in the metals Be, Mg, and Al by radioactive reagent. It was found that the action of phosphorous tribromide labeled with ^{32}P and of bromine on the metallic oxides of these metals leads under certain conditions to labeled phosphates; the separation of these phosphates with an excess of reagent was realized by passage of a slow cur-

rent of bromine at high temperatures (700 to 900°). A study was also made to improve the precision and the reproducibility in the determination of oxygen by activation with 14-Mev neutrons. Two methods were utilized. The secondary standard method made it possible to obtain convenient results (0.6% slope between two standards) by making a series of tests for the sample and one for the standard and by taking the mean of the activities found even at the dispersion, which is relatively significant. The internal standard method makes it possible to eliminate all cases of error due to flux variations in time and space. Agreement of the two results is good and the precision in the most unfavorable case can be estimated at 2% for oxygen contents between 0.1 to 10% and from 2 to 5% for oxygen concentrations between 100 and 1000 ppM. (P.C.H.)

3879 (MLM–1266) MOUND LABORATORY PROGRESS REPORT FOR MAY 1965. Eichelberger, J. F.; Grove, G. R.; Jones, L. V. (Mound Lab., Miamisburg, Ohio). May 21, 1965. Contract AT(33-1)-Gen-53. 32p. Dep. mn; CFSTI $2.00 cy, $0.50 mn.

Basic and applied research is being conducted on a number of radioelements to determine their physical properties, develop analytical techniques, and study the basic radiochemistry involved. Of particular interest are alpha emitters, their decay chains, their isotopes, and their chemical homologs. Results on ^{223}Fr and ^{209}Po decay, determination of ^{210}Po in process solutions, ^{227}Ac recovery from process wastes, and preparation of sources for alpha spectrometry are reported. Studies on methods of separation and purification of purified ^{3}He and the isotopes of other noble gases and ^{13}C and on thermal diffusion are included. Methods for the determination of impurities in boron and determination of U and Fe in solutions containing Ni are described. (P.C.H.)

3880 (MSAR–65-150) DEVELOPMENT OF TECHNIQUES FOR MEASUREMENT OF IMPURITIES IN SODIUM. Quarterly Progress Report, July–September 1965. (MSA Research Corp., Callery, Pa.). Oct. 25, 1965. Contract AT(11-1)-765. 29p. Dep. mn; CFSTI $2.00 cy, $0.50 mn.

The feasibility of selected approaches that might lead to the development of techniques for the measurement of impurities in sodium was evaluated. The studies included laboratory techniques, such as magnetic effects, surface tension, organic solvent extraction, and mass spectrometry during high temperature refluxing and instream techniques, such as physical property change of metals due to carburization, electrical sensing of particles in liquid metals, sodium oxide determination by electrical potential concentration, and continuous hydrogen monitoring. (P.C.H.)

3881 (NBL–228) SPECTROPHOTOMETRIC DETERMINATION OF GALLIUM IN PLUTONIUM–GALLIUM ALLOY. Pietri, C. E.; Wenzel, A. W. (New Brunswick Lab. (AEC), N. J.). Nov. 1965. 8p. Dep. mn; CFSTI $1.00 cy, $0.50 mn.

Macro amounts of gallium in plutonium-gallium alloys were determined by an improved rhodamine B chlorogallate-benzene extraction-spectrophotometric method. The alloy is dissolved in hydrochloric acid, converted to the nitrate, and separated from the gallium and impurities by adsorption on Dowex-1 anion resin in 8N HNO_3. After dilution to the optimum concentration range the effluent is used for the gallium determination and an emission spectrographic impurity analysis. The plutonium is assayed after its elution from the resin bed. The relative standard deviation was within 2.2% for samples in the 3–15 μg gallium range with no apparent bias. Analyses of alloy samples for gallium, plutonium, and impurities gave material balances of 100.1 ± 0.2%. (auth)

3882 (ORNL–IIC–5, pp 51-71) X-RAY ABSORPTIOMETRY WITH BETA-STIMULATED X-RAY SOURCES AND PROGRESS REPORT ON COMPILATION OF BETA-EXCITED SPECTRA. Preuss, Luther E.; Collins, H.; Kann, J. (Edsel B. Ford Inst. for Medical Research, Detroit, Mich.).

Characteristic x radiation and bremsstrahlung photons, produced by ^{147}Pm betas in copper, iron, and molybdenum targets, were studied for their application in absorptiometry. A device designed specifically for absorptiometry with beta-excited sources was used. Spectral hardening proved to be a prevalent phenomenon with some of these sources. Properly designed beta-stimulated sources showed promise. Progress in the compilation of a comprehensive series of beta-excited spectra is also reported. (auth)

3883 (ORNL–IIC–5, pp 154-81) DEVELOPMENTS IN A PORTABLE X-RAY FLUORESCENCE INSTRUMENT USING RADIOISOTOPE EXCITATION SOURCES. Karttunen, John O.; Henderson, Dale J. (Argonne National Lab., Ill.).

The radioisotope ^{147}Pm in an aluminum matrix and emitting bremsstrahlung was found to be a more universal excitation source for fluorescence x rays of elements in the Z range 19 through 92 than titrated Zr. The quantitative analysis of binary, ternary, and quaternary mixtures is illustrated. The apparatus is miniaturized, has a total weight of 11 lb, and can be contained in a volume of less than 1 ft^3. This project was originally undertaken to develop a portable x-ray fluorescence instrument for various uses. Because of its relatively low cost, compactness, versatility, and simplicity, the apparatus developed has merit as a possible lunar probe and as a geological field instrument, as well as in other applications. (P.C.H.)

3884 (ORNL–IIC–5, pp 206-21) ORE AND COAL ANALYSIS USING RADIOISOTOPE TECHNIQUES. Rhodes, J. R. (Research Group, United Kingdom Atomic Energy Authority, Wantage (England)).

X-ray excitation by radioisotope sources and energy selection with filters are briefly reviewed and discussed. A new arrangement of source and secondary target for efficient production of spectrally pure K x rays is described and its use in x-ray fluorescence analysis to obtain detection limits of 10 to 40 ppm of tin in tin ores is reported. Three methods of reducing inaccuracy due to matrix absorption effects are described with special reference to analysis of zinc, copper, and tin ores and to coal-ash monitoring. Errors of this nature, which can exceed 30%, have thus been reduced to ~1%. The results are being applied to development of apparatus for laboratory and on-stream analysis of coal and ores. An "Isotope Portable Analyzer" is being made commercially available for geological applications in prospecting and field assay and for industrial use in measurements of coating thickness and alloy composition. (auth)

3885 (ORNL–IIC–5, pp 277-89) BODY COMPOSITION BY DIFFERENTIAL ABSORPTION OF MONOCHROMATIC X RAYS. Sorenson, James A.; Cameron, J. R. (Wisconsin Univ., Madison).

The technique of determining the fractional composition of a two-component system by x-ray beam-attenuation measurements was studied. The method was tested on sodium acetate–polyethylene mixtures of known compositions and was applied to samples of animal muscle and fat. The results were within 3% of other independent determinations. Statistical errors and the problems of nonmonochromatic x-ray sources and scattered radiation were also examined. It was concluded that the technique is an accurate method for quantitative determination of the composition of the mixtures studied. (auth)

3886 (ORNL–IIC–5, pp 290-4) IN VIVO MEASUREMENT OF BONE MINERAL CONTENT BY A TRANSMISSION TECHNIQUE. Goodman, Leonard S. (Argonne National Lab., Ill.); Levin, Bertram (Michel Reese Hospital, Chicago, Ill.).

A preliminary investigation of a method for in vivo determination of bone mineral content is presented. Linear transverse scans of transmission are made across a bone for two different monoenergetic x rays. The information so obtained can be reduced to give the $Ca_3(PO_4)_2$ equivalent per centimeter of bone. The transmission scan also yields an effective diameter of the bone. Division of

the equivalent amount of tricalcium phosphate by the diameter yields an index of mineral content which has less scatter from individual to individual than the amount alone. (auth)

3887 (PG-Report-677) ANALYTICAL METHOD FOR THE DETERMINATION OF RADIO-RUTHENIUM IN REACTOR FUEL PROCESSING PLANT SOLUTIONS (RUTHENIUM TETROXIDE DISTILLATION). (Production Group, United Kingdom Atomic Energy Authority, Sellafield (England)). 1965. 10p. Dep.; BIS $0.30; HMSO 1s. 9d.

Radioruthenium, with added carrier, was separated from other fission products by distillation from an oxidizing medium. The volatile tetroxide is absorbed in sodium hydroxide solution and ruthenium precipitated as dioxide. The dioxide is dissolved in acid, a portion of the solution evaporated on a counting tray, and the activity measured. (auth)

3888 (TID-22402) ION EXCHANGE SEPARATION OF URANIUM AND THORIUM IN MIXED AND NON-AQUEOUS SOLVENTS. Final Technical Report. Korkisch, J. (Vienna Univ. (Austria). Analytisches Institut). Oct. 1965. Contract 67/US. 150p. Dep. mn; CFSTI $4.00 cy, $1.00 mn.

Data on the cation and anion exchange behavior of uranium, thorium, lanthanides, and other metal ions in mixed and non-aqueous solvents containing mineral or organic acids as complexing agents for these elements are summarized. Based on equilibrium studies carried out in mixtures consisting of organic solvents such as the aliphatic alcohols, ketones, ethers, organic acids, and of acids such as hydrochloric, hydrobromic, nitric, sulfuric, and organic acids, the most suitable conditions for analytical separations of uranium, thorium, etc. were worked out. The methods thus developed are applicable for the isolation of microgram and milligram quantities of these elements in a variety of materials such as minerals, rocks, sediments, steel, high purity materials, etc. Furthermore the application of a number of azo dyes of the Solochrome class for the spectrophotometric determination of uranium, thorium, rare earth elements, and other metal ions in hydrochloric or nitric acid-methanol media is described. The methods make possible the accurate and rapid quantitative determination of microgram amounts of these elements. 205 references are cited. (auth)

3889 (UNC-5113) ELECTROCHEMICAL OXYGEN METER OPERATING MANUAL. Minushkin, B. (United Nuclear Corp., White Plains, N. Y. Development Div.). Aug. 31, 1965. Contract AT(30-1)-2877. 51p. Dep. mn; CFSTI $3.00 cy, $0.50 mn.

The Electrochemical Oxygen Meter is an on-line device for measuring oxygen activity in sodium. It is installed directly in an operating sodium system and provides continuous indication of changes in oxygen activity without necessity for sampling and chemical analysis. Information is given on the design, construction, installation, operation, and maintenance of the meter. Instructions for unpacking and storing the meter are also included. (P.C.H.)

3890 (AEC-tr-6617) DETERMINATION OF URANIUM IN ITS ALLOYS. Gerard, J.; Van Hove, L. Translated from IAEA preprint SM-63/34, a paper presented at the Symposium on Non-Destructive Testing in Nuclear Technology, Bucharest, May 17-21, 1965. 58p. Dep. mn; JCL $5.60 fs, $1.94 mf.

Includes original.

Various methods for the determination of uranium in its alloys are discussed and evaluated. Criteria are given for choosing between the determination by gamma counting and by measurement of the density. Advantages of certain methods are also given. (P.C.H.)

3891 (CEA-tr-A-1838) METHODE DE DOSAGE DES ISOTOPES RADIOACTIFS ^{55}Fe ET ^{59}Fe DANS L'EAU DE MER. (Method of Determination of Radioactive Isotopes ^{55}Fe and ^{59}Fe in Sea Water). Kautsky, H.; Schmitt, D. E. Translated into French from Deut. Hydrograph. Z., 15: No. 5, 199-204(1962). 16p. Dep. mn; JCL $1.60 fs, $0.80 mf.

A method of analysis is given that makes it possible to separate ^{55}Fe and ^{59}Fe from seawater. The separation is made by precipitation in series. The discrimination between ^{55}Fe and ^{59}Fe is obtained by the same measurement method. A concentration of 0.45 pC/l of ^{55}Fe can be obtained by treating 100 l of seawater. (tr-auth)

3892 DIFFERENTIAL SPECTROPHOTOMETRIC DETERMINATION OF BORON WITH DIAMINOCHRYSAZIN. Eberle, A. R.; Lerner, M. W. (U. S. Atomic Energy Commission, New Brunswick, N. J.). Anal. Chem., 37: 1568-72(Nov. 1965).

Differential spectrophotometry with diaminochrysazin was found to be a useful technique for the accurate and precise determination of 1- to 20-mg single samples of boron. High concentrations of impurities can be tolerated and multiple aliquot results can be obtained. Larger samples of commercial elemental boron can be assayed by the same technique without the necessity of the usual separation step. The assay values agree with those obtained by other procedures involving the mannitol titration. (auth)

3893 THE INFLUENCE OF POLYNUCLEAR ZIRCONIUM SPECIES ON DIRECT TITRATION OF ZIRCONIUM WITH EDTA. Pilkington, E. S.; Wilson, W. (Commonwealth Scientific and Industrial Research Organization, Melbourne). Anal. Chim. Acta, 33: 577-85(Dec. 1965).

Accurate results in EDTA titration of zirconium at all concentration levels could be obtained if zirconium ions were converted to a depolymerized form. Treatment with strong sulfuric acid was more generally applicable for this conversion than treatment with other mineral acids. To avoid the zirconium species becoming repolymerized under the conditions required for a direct titration, EDTA was added at high acidity (1 to 2 N sulfuric acid, depending on zirconium concentration). At an appropriate stage of the titration, easily determined by a color change obtained with xylenol orange indicator, a single addition of a fixed quantity of ammonia solution established the correct pH for a sharp end-point. Results were quantitative and amounts of zirconium from 10 μg to 500 mg could be determined with appropriate standard EDTA solutions. (auth)

3894 THE USE OF A LITHIUM-DRIFTED GERMANIUM-DIODE TO DETERMINE CARBON IN STEELS BY MEASUREMENT OF PROMPT γ-RADIATION. Pierce, T. B.; Peck, P. F.; Henry, W. M.; Hooton, B. W. (Atomic Energy Research Establishment, Harwell, Eng.). Anal. Chim. Acta, 33: 586-92(Dec. 1965).

A lithium-drifted germanium p-i-n diode was used as detector to measure the prompt radiation emitted by the reaction $^{12}C(d,p)^{13}C$ during irradiation of steels with low-energy deuterons. Typical spectra obtained using a diode and a thallium-activated sodium iodide crystal are compared, and results given for a number of standard steel samples. (auth)

3895 THE SPECTROPHOTOMETRIC DETERMINATION OF ZIRCONIUM WITH 8-HYDROXYQUINOLINE. van Santen, R. T.; Schlewitz, J. H.; Toy, C. H. (Wah Chang Corp., Albany, Oreg.). Anal. Chim. Acta, 33: 593-6(Dec. 1965).

A spectrophotometric method is proposed for determining small amounts of zirconium as the 8-hydroxyquinolinate in chloroform, measured at 386 mμ. The molar absorptivity is 14,700. In contrast to other available methods, anions such as chloride, sulfate, perchlorate, tartrate, oxalate, and fluoride do not interfere. (auth)

3896 DETERMINATION OF TITANIUM AND ZIRCONIUM IN MOLYBDENUM BASE ALLOYS BY ION EXCHANGE. Shakashiro, Mouffac; Freund, Harry (Oregon State Univ., Corvallis). Anal. Chim. Acta, 33: 597-601 (Dec. 1965).

The anion-exchange behavior of titanium, zirconium, and molybdenum in the sulfuric-oxalic acid system was studied. The systematic use of distribution coefficients

defined conditions for determination of zirconium and titanium in molybdenum-base alloys. Less than 0.1% zirconium and 0.1% titanium can be determined. Molybdenum was found to form the most stable anionic species with oxalic acid. (auth)

3897 DETERMINATION OF MICRO QUANTITIES OF NIOBIUM IN URANIUM. Shrimal, S. K.; Varde, M. S. (Atomic Energy Establishment, Trombay, India). Anal. Chim. Acta, 33: 683-5(Dec. 1965).

A method was developed for determination of niobium in uranium metal and alloys in the presence of comparatively large amounts of the interfering elements. It is shown that as little as 5 ppM of niobium in uranium can be separated by fuming with perchloric acid using tantalum as carrier. Spectrophotometric methods were used after separation. (M.C.G.)

3898 ELEMENTAL SURVEY ANALYSIS BY NEUTRON ACTIVATION: SIMPLIFIED ESTIMATION OF UPPER LIMITS. Lukens, H. R. Jr. (General Atomic Div., General Dynamics Corp., San Diego, Calif.). Anal. Chim. Acta, 34: 9-16(Jan. 1966).

A procedure is described for the rapid estimation of concentration upper limits of elements not observed in a sample by routine neutron activation analysis. Experimental and theoretical justifications of time-saving steps are given, and necessary precautions in the use of the procedure are discussed. Tables for use with the procedure are included. (auth)

3899 DETECTION OF VOLATILE ^{14}C LABELED COMPOUNDS BY A MODIFIED GAS CHROMATOGRAPHY-IONIZATION CHAMBER TECHNIQUE. White, Roderick E.; Davis, Hubert G. (Union Carbide Corp., South Charleston, W. Va.). Anal. Chim. Acta, 34: 105-7(Jan. 1966).

Improvements in the gas chromatography-ionization chamber technique for radio-assay of volatile ^{14}C-labeled compounds are described. The radioactive compounds are separated by preparative gas chromatography, but instead of simultaneously counting with a flow ionization chamber, the compounds are trapped out as they elute from the chromatographic column, and then are transferred to a static ionization chamber where entire separated fractions are counted. Specific activities of the oxidation products of ^{14}C-labeled propylene are reported. Advantages of the method are discussed. (M.C.G.)

3900 PROBLEMS OF INTERFERENCE IN NEUTRON ACTIVATION ANALYSIS. Rakovic, Miloslav (Charles Univ., Prague). Chem. Listy, 59: 1038-46(Sept. 1965). (In Czech).

The possibility of the occurrence of interference in neutron activation analysis depends first of all on the composition of the sample, on the nuclear characteristics of the elements contained in the sample, and on the energy spectrum of the neutrons used in the activation. Six types of interference are considered. Fast neutrons most often bring about interference in which the same radionuclide is produced from more than one element-F, for example, $^{23}Na(n,\gamma)^{24}Na$; $^{24}Mg(n,p)^{24}Na$; and $^{27}Al(n,\alpha)^{24}Na$. Slow neutrons cause chiefly another type of interference, namely, that where the same radionuclide results from a second-order reaction on another element. This occurs especially when it is necessary to determine traces of one element in the presence of a large quantity of one giving the same radionuclide by second-order reaction. (TTT)

3901 SOME ASPECTS OF THE DETERMINATION OF METALS IN VEGETABLE PRODUCTS USING NEUTRON ACTIVATION ANALYSIS. Fourcy, Andre (Centre d'Etudes Nucleaires, Grenoble, France). Compt. Rend., 261: 830-3(July 19, 1965). (In French).

Activation analysis was applied to the determination of Mn, Cu, Co, Fe, Zn, and K in vegetable matter. Mn was determined by a nondestructive method. The other elements were determined by a destructive method followed by a radiochemical separation using ion exchange or electrolysis in the case of copper. The details of each method are given. (J.S.R.)

3902 DETERMINATION OF CALCIUM IN SEA WATER: ANALYTICAL EXPERIMENT USING THE RADIONUCLIDE ^{45}Ca. Corless, James T. (Univ. of Rhode Island, Kingston). J. Chem. Educ., 42: 421-3(Aug. 1965).

An experiment is described, which employs radiotracer, ion exchange, complexometric titration, and spectrophotometric technics for determination of Ca in sea water. The Ca in an aliquot of sea water is separated from the Mg and Sr using a column of Dowex 50W-X8 ion exchange resin, and ^{45}Ca is used as a tracer for monitoring the elution of the Ca from the column. The Ca fraction is then titrated with EDTA using a weight buret and murexide as the indicator. The endpoint is determined spectrophotometrically. As a demonstration of the separation of Ca from Mg by the cation column, two μC each of ^{89}Sr and ^{54}Mn, a tracer whose cation exchange properties are very similar to Mg, may be added to the samples in addition to ^{45}Ca. The Mn^{2+} has a distribution coefficient almost identical to that of Mg^{2+} under those conditions. In the absence of sea water, the experiment may be performed using a solution of the chlorides of Mg, Ca, and Sr in the mole ratio 540:110:1. Distribution coefficients and tracer characteristics of ^{54}Mn, ^{45}Ca, and ^{89}Sr are tabulated. (BBB)

3903 DETERMINATION OF SMALL AMOUNTS OF U(VI) IN THE PRESENCE OF LARGE AMOUNTS OF U(IV). Nemodruk, A. A.; Palei, P. N.; Glukhova, L. P. Radiokhimiya, 7: 372-3(1965). (In Russian).

On the basis of data obtained by studying the extractive separation of U(VI) from U(IV), an extraction method for determining small amounts of U(VI) in the presence of large amounts of U(IV) is described. It permits the determination of U(VI) in hydrochloric and nitric acid solutions containing 0.2 to 500 μg U(VI) per ml in the presence of up to 150 times this amount of U(VI). Tributyl phosphate is used to extract U(VI). If it is necessary to determine U(VI) when its content is higher than 50 μg ml, such solutions are first diluted. The procedure takes 30 to 35 min. Amounts of SO_4^{2-} greater than 2500 times the U(VI) content lower the results. The influence of other elements interfering with the determination of U(VI) is either negligible or completely absent, except in the case of rare earth metals, which do not interfere if their ratio to U(VI) does not exceed 100. For determining U(IV) in the solution being analyzed, the most suitable method is one involving the titration of U(IV) with a solution of ammonium vanadate in the presence of N-phenylanthranilic acid. (CFSTI)

3904 SIMULTANEOUS ULTRAVIOLET SPECTROPHOTOMETRIC DETERMINATION OF NIOBIUM AND TANTALUM BY THE HYDROGEN PEROXIDE METHOD. Kokubu, Nobuhide; Matsuda, Kiyoshi (Inst. of Physical and Chemical Research, Tokyo). Rika Gaku Kenkyusho Hokoku, 38: 21-7(1962). (In Japanese).

Optimal conditions for simultaneous determination of niobium and tantalum by the uv spectrophotometric method using hydrogen peroxide were investigated in detail. Effects of the niobium–tantalum ratio, addition of sulfates of other metals and phosphates, temperature, and time of standing of the reactants were examined. Conformity to Beer's law, application of a method of adding standard solution, and a method of decomposition of tantalum by hydrogen ammonium fluoride were also studied. The analytical procedure was found to be suitable for determinations in the range of 0.55 to 5.7 mg Nb/50 ml and 0.55 to 8.4 mg Ta/50 ml when 1-cm quartz cells are used. For the determination of Nb and Ta mixtures, the method was precise in the range from 1:10 to 10:1 of the niobium–tantalum ratio. The method of adding standard solution was successfully applied to the determination of samples having niobium–tantalum ratios ranging from 60:1 to 1:120. The sensitivity of the method was not as high as in some colorimetric methods. (BBB)

3905 THE ANALYTICAL APPLICATION OF FLUORIC ION. V. METHOD OF SEPARATING THORIUM FROM RARE EARTH ELEMENTS. Seki, Jisuke (Inst. of Physical and Chemical Research, Tokyo). Rika Gaku Kenkyusho Hokoku, 38: 348-53(1962). (In Japanese).

In the separation of thorium from rare earth elements, thorium can be precipitated as oxalate after chelating these elements with EDTA. The precipitate obtained by this method is filtered, washed, and dissolved in hydrochloric acid. The amount of thorium obtained is determined by direct titration with fluoric ion, keeping the solution at pH 2.4. Good results were obtained by applying this method to the analysis of monazite for its thorium content. (BBB)

3906 DETERMINATION OF URANIUM IN BOMB WASTE BY THE EMISSION SPECTROCHEMICAL METHOD. Nishihara, Kiyokado; Matsumura, Yoshitaka (Kyoto Univ.). Suiyokaishi, 15: 145-50(Dec. 1963). (In Japanese).

The determination of uranium in the bomb waste from UF_4 reduction with magnesium by the emission spectrochemical method was studied. The recommended procedure for determination of uranium in bomb waste containing 0.01 to 10.0% was as follows: thirty mg of sample was loaded into an anode electrode, the sample was excited by forming a d-c arc of 12 amp between the electrodes spaced 4 mm apart and a pre-burn of 15 sec and an exposure time of 20 sec was used. The coefficients of variation for each concentration of uranium were calculated and found to be lower than by other procedures, 3 to 5%. (auth)

3907 A 14-Mev NEUTRON-ACTIVATION ANALYSIS UNIT FOR OXYGEN DETERMINATION. Miyoshi, Katsuhiko (Tokyo Shibaura Electric Co., Ltd.). Toshiba Rebyu, 20: 671-6(July 1965). (In Japanese).

The determination of oxygen by 14-Mev neutron-activation is discussed. The analyzer unit for this method consists of a 14-Mev neutron generator (10^{10}n/s), a pneumatic sample transfer system, and an automatic measuring unit with a C-R monitor (an automatic normalizing unit). The results of its application to the analyses of coal, pure compounds, oxides, and metals, such as iron, titanium, zircaloy, and copper are presented. These results showed good agreement with the results obtained by the vacuum fusion technique. (auth)

3908 THE ANALYSIS OF XENON AND KRYPTON USING AN OMEGATRON. Fox, P. G. (Univ. of Melbourne). Vacuum, 19: 17-28(Jan. 1965).

In a study of the adsorption of mixtures of xenon and krypton on evaporated nickel films, an omegatron was used to analyze the gas phase in equilibrium with the film. Operating characteristics of the instrument and the method of analyzing the mixture of Xe and Kr are described. In the omegatron the electron beam current was automatically regulated and the electron energy set at 78 ev. The magnetic field strength was 3000 G. Partial pressure measurements of both xenon and krypton were made down to 10^{-8} torr. The relation between positive ion current and pressure for ionized species of both gases is shown. For the quantitative analysis of gas mixtures, the omegatron should be operated at r-f voltages for which the ion current is independent of r-f voltage for each species analyzed. Since this condition is not obtained for Xe^+ and Kr^+ but is satisfied for the doubly ionized species, it was necessary to make analyses of mixtures using the Xe^{2+} and Kr^{2+} peaks. In addition, while the resolution was inadequate to separate Xe^+ and Kr^+ in these experiments, it was good enough to completely resolve Xe^{2+} and Kr^{2+}, 4.7 for Xe^{2+} and 7.5 for Kr^{2+}. With careful processing of the omegatron tube before each experiment (to ensure cleanliness of the electrode assembly), reproducible sensitivity for both gases was obtained. (BBB)

3909 DETERMINATION OF THE RADIOACTIVITY OF REACTOR COOLING WATER FOR THE DESIGN OF A FISSION PRODUCT MONITOR [Thesis]. Hauser, H. Hamburg, Univ., 1964. 159p. $2.00 Gmelin, AED-DISS. 64-764.

Qualitative radiochemical analysis of coolant water samples of the FRG swimming pool after a fuel element rupture is described. Seventeen fission products were identified. ^{95}Zr was determined quantitatively 1.5 years after the rupture. Design of a fission product monitor using ^{95}Zr determination is discussed. (Gmelin Inst.)

3910 X-RAY DIFFRACTOMETER—MODIFIED (Engineering Materials). (Phillips Petroleum Co., Idaho Falls, Idaho. Atomic Energy Div.). (CAPE-1260).

8 drawings.

The diffractometer described, was modified to be used in the examination of medium-level, radioactive samples. It was used with samples emitting nearly 1,000 r/hr of γ radiation. The modification uses direct rather than reverse optics. A curved crystal monochromator is used between the sample and the detector. A moving concentric shield arrangement provides 2 in. of biological and 5 in. of detector shielding from the sample radiation. This arrangement provides the required shielding with a minimum of cost. The instrument can be converted in about 1 hr for conventional use. (For details, see TID-4100.) (M.C.G.)

3911 X-RAY SPECTROSCOPY AS AN ANALYTICAL TOOL. Loomis, T. C. (Bell Telephone Labs., Inc., Murray Hill, N. J.). 30p. (CONF-650521-3). ORINS. Gmelin, AED-CONF-65-113-2.

From Conference on Purification of Materials, New York.

The potential and development of x-ray spectroscopy for chemical analysis are discussed. Techniques for handling special analytical problems of chemical and metallurgical research including materials purification are described. The x-ray tubes for spectrometers have maximum power ratings of from 2 to 4 kw and are available with a wide range of targets, including platinum, tungsten, silver, rhodium, molybdium, chromium, and titanium. The analyzing crystals are lithium fluoride, sodium chloride, quartz, ethylenediamine tartrates, pentoerythritol, ammonium dihydrogen phosphate, gypsum, potassium acid phthalate, Langmuir-Blodgett soap films, and topaz. The emergent x rays are detected by means of scintillation counters or various types of gas-filled proportional counters, all of which convert x-ray quanta to electrical pulses that are registered on electronic consoles usually containing both ratemeters and scalers. (F.J.H.)

3912 A NEW ELECTRON PROBE X-RAY MICROANALYZER. Merrill, H. E. Jr. (Acton Labs., Inc., Mass.). 9p. (CONF-650320-2). ORINS. Gmelin, AED-CONF-65-114-1.

From IEEE International Convention, New York.

A brief history of electron probe x-ray microanalyzers is given. The probe and its principle of operation, conversion of European electronic circuits to United States standards, and the problems involved in repackaging are discussed. Applications of the microprobe to various qualitative and quantitative problems are discussed and diagrams of specimen current and x-ray scanned surfaces are shown. The readout circuit must have good sensitivity and stability since the probe is gathering information from a submicron spot and the energies involved are low. Methods of using crystal materials in the spectrometers, proportional detectors, different gas mixtures for these detectors, and solid-state electronics all added to the improvement in higher resolution, better quantitative results and the extension of the useful range of this instrument. (F.J.H.)

3913 METHOD AND APPARATUS FOR MEASURING HYDROGENOUS MATERIAL. Burley, Harvey, A.; Diamond, Milton, J.; Danforth, John P.; Block, Arthur D. (to General Motors Corp.). U. S. Patent 3,213,280. Oct. 19, 1965. Filed Aug. 24, 1960.

The thermalizing effect of hydrogen nuclei on fast neutrons is used as the basis of a method for the accurate determination of small amounts (5% or less) of hydrogenous material present in a nonhydrogenous material, such as sand. A thermal neutron detector positioned adjacent to a fast neutron source is inserted into and adjacent to the center of a sand mass of predetermined limited size. The count from the thermal neutron detector is translated into a reading of the amount of moisture in the sand and preferably also into a reading of the amount of water that must be added in order to attain the desired moisture content. (B.L.M.)

Inorganic and Physical Chemistry

3914 (AERE-M-1654) THE DRYING OF OXIDE POWDER SAMPLES FOR NEUTRON TRANSMISSION MEASUREMENTS. Elliott, R. A.; Pattenden, N. J. (Atomic Energy Research Establishment, Harwell (England)). Sept. 1965. 8p. Dep.; BIS $0.30; HMSO 1s. 9d.

Oxides of Ba, Cd, Mo, and Y were heated to temperatures up to 600°C to determine the amount of water vapor removed. The minimum temperature required to remove all water vapor was different for different oxides. The oxides were assessed for their value as sample material for neutron transmission measurements. It was concluded that, when accurate determinations of total cross sections are required from measurements of the transmission of oxide powders, it is necessary to perform a detailed investigation of the water retention properties of the powder. (auth)

3915 (CEA-Bib-61) LES COMPOSES DES GAS RARES. (Noble Gas Compounds). Contamin, Ghislaine (Commissariat a l'Energie Atomique, Saclay (France). Centre d'Etudes Nucleaires). Aug. 1965. 50p. Dep. mn.

Preparations and properties of noble gas fluorides, their oxygenated compounds, and other derivatives are described. The various theories which have been put forth up to now in order to explain the structure of these compounds are briefly reviewed. 107 references are cited. (P.C.H.)

3916 (CONF-650902-20) THE APPLICATION OF NUCLEAR HEAT TO THE PRODUCTION OF AMMONIA. Slansky, Cyril M. (Phillips Petroleum Co. Idaho Falls, Idaho. Atomic Energy Div.). Aug. 25, 1965. Contract AT(10-1)-205. 6p. Dep. mn; CFSTI $1.00 cy, $0.50 mn.

From American Chemical Society, 150th National Meeting, Atlantic City.

It is suggested that ammonia might be produced efficiently and economically with nuclear heat. The high temperature gas cooled reactor and multipurpose operation of the reactor offer the technology for cheap ammonia production. Advantages and economics of the method are discussed. (P.C.H.)

3917 (LA-3405) THERMODYNAMIC-TRANSPORT AND RELATED PROPERTIES OF PARA-HYDROGEN FROM 36 TO 5000 deg R AT PRESSURES TO 5000 psia. Farmer, Otis A. (Los Alamos Scientific Lab., Univ. of California, N. Mex.). Oct. 1, 1965. Contract W-7405-eng-36. 34p. Dep. mn; CFSTI $2.00 cy, $0.50 mn.

Tables and graphs of thermodynamic-transport and related properties of para-hydrogen are provided from the best available source data for the temperature range from 36 to 5000°R. (auth)

3918 (LA-DC-7276) STRUCTURE, CHEMISTRY, AND INSTABILITY OF DETONATION IN HOMOGENEOUS, LOW DENSITY FLUIDS-GASES. Schott, Garry L. (Los Alamos Scientific Lab., Univ. of California, N. Mex.). [1965]. Contract W-7405-eng-36. 31p. (CONF-651003-7). Dep. mn; CFSTI $2.00 cy, $0.50 mn.

From 4th Symposium on Detonation, Silver Spring, Md.

A brief history of the state of understanding of detonations in gases that existed 25 years ago is given. Attempts are made to outline current thinking about the detonation process, and its development from observations and considerations of gaseous detonations. 66 references are cited. (P.C.H.)

3919 (ORNL-3870, pp 3-6) CRYSTAL PHYSICS. Clark, G. W. (Oak Ridge National Lab., Tenn.).

A geometry favorable for the growth of large high-quality UO_2 crystals was obtained by the centrifugal distribution of an inductively melted central zone that is caused to traverse the rod. The crystal chemistry investigation of the lanthanide germanomolybdates was extended to germanotungstates. The rate of hydrothermal growth of non-nucleated ferrite crystals was related to temperature, pressure, time, solvent normality, and metallic additives. An arc-modified Verneuil system was improved. A superconducting magnet design for magnetic susceptibility measurements by the Faraday method was analyzed with the conclusion that a properly dimensioned solenoid is very promising. The temperature dependence of magnetic susceptibilities, lattice constants, and optical absorption spectra of the lanthanide germanomolybdates is being measured and will be related by a theoretical analysis of crystal field parameters. (W.L.G.)

3920 (ORNL-3870, pp 27-37) ELECTRONIC PROPERTIES OF METALS AND ALLOYS. Betterton, J. O. (Oak Ridge National Lab., Tenn.).

The effects of Nb on the low-temperature specific heat of hexagonal Zr were studied. In the quenched hexagonal solid solution, the sharp increase in superconducting transition temperature is a result of an increase in density of electronic states and a decrease in the Debye temperature, in agreement with theory. In the heat-treated form, the precipitation of other superconductors with high critical field and temperature depended upon alloy purity. In these dilute Zr–Nb alloys, the specific heats and the resistivity both changed with 2-hr anneals at 120°C. Nb affected the superconductivity transition temperature, the density of electronic states, and the Debye temperature of Zr more than did Sc and B-subgroup elements. In cubic Zr alloys containing Mo, Re, and Ru these low-temperature properties were very nearly the same as for the hexagonal Zr–Nb alloys with the same additive content, so the low-temperature specific heat coefficients of cubic Zr must not be very different from those of hexagonal Zr. An ion-pumped zone refining system was built and used to produce Zr crystals with resistance ratios 450 to 850 and new higher purity zone-leveled Zr alloys for specific-heat study. The resistivity of the Zr crystals was not a function of impurity content alone but depended on redistribution of impurities. Galvanomagnetic properties of Zr were studied with additional orientations of current. The closed and compensated Fermi surface was fairly well established. Each crystal has nearly isotropic magnetoresistance with quadratic field dependence. The Hall field shows no large anisotropy but alternates in sign. The Mössbauer effect was observed in ^{61}Ni and ^{73}Ge following Coulomb excitation. (auth)

3921 (ORNL-3870, pp 56-60) SPECTROSCOPY OF IONIC MEDIA. Smith, G. P. (Oak Ridge National Lab., Tenn.).

Optical spectroscopy was employed to investigate the structure of molten salts. The coordination geometry of Ni^{2+} ions in these media and the behavior of bismuth ions in unusual oxidation states was emphasized. (auth)

3922 (ORNL-TM-1281) PREPARATION OF THORIA AND MIXED-OXIDE MICROSPHERES. Haas, Paul A.; Clinton, S. D. (Oak Ridge National Lab., Tenn.). Nov. 1965. Contract W-7405-eng-26. 29p. Dep. mn; CFSTI $2.00 cy, $0.50 mn.

A process was developed for preparing thoria, thoria-urania, or other oxide spheres of 50–1000 micron diameter, high strength, and nearly theoretical density. The starting materials were colloidal oxide sols. The sols were dispersed as uniform droplets in an organic liquid by use of two-fluid nozzles or rotary feeders. The drops of sol were suspended and converted to gel spheres in the organic solvent which extracted water at slow, controlled rates. In order to fluidize the sol drops and to avoid coalescence, clustering, and deposition on the wall, the use of surfactants in the solvent and of special vessel configurations were necessary. The gel spheres were separated from the solvent, dried, and calcined to 1150°C. Microspheres were prepared using 2-ethylhexanol as the drying solvent in a continuous column system including solvent recovery. Demonstrated capacities of the system were 5 kg of 240 micron thoria spheres in one day or 700 g/hour for short periods. Thoria-8% urania spheres of 250 to 300 micron diameter had the following properties: particle density, 99.4% of theoretical;

krypton BET surface area, 0.003 m^2/g; particle crushing strength, greater than 5.7 kg/particle for 25 particles tested. (auth)

3923 (ORNL-TM-1299) SALINE: A FORTRAN COMPUTER PROGRAM FOR THE PROCESS DESIGN OF SALINE WATER CONVERSION PLANTS USING THE MULTI-STAGE, FLASH-EVAPORATION PROCESS. Griffith, W. L.; Keller, R. M. (Union Carbide Corp., Oak Ridge, Tenn. Y-12 Plant). Nov. 1965. Contract W-7405-eng-26. 81p. Dep. mn; CFSTI $3.00 cy, $0.75 mn.

For Oak Ridge National Lab., Tenn.

A Fortran IV computer program that performs heat balance, material balance, and cost calculations on saline water conversion plants using the multi-stage, flash-evaporation process is described. The code is a modified revision of a program written by the Bechtel Corporation for OSW. Under the simplifying assumptions inherent in the mathematical model, a complete heat and material balance is calculated by a stage-to-stage numerical technique from the design parameters supplied. Costs are calculated from these results and the economic data supplied. Optimum design parameters which minimize total cost over a 30-year period can be determined either by a series of computer runs or by an optimization procedure supplied. Details of the numerical procedure, program options, and usage are presented. Results obtained with an IBM-7090 from typical design data and a complete listing of the Fortran program are included. (auth)

3924 (TID-22366) THE THERMODYNAMIC PROPERTIES OF IONS IN AQUEOUS AND NON-AQUEOUS SOLUTIONS AT VARIOUS TEMPERATURES. Final Report. Criss, Cecil M. (Vermont Univ., Burlington. Dept. of Chemistry). Oct. 1965. Contract AT(30-1)-3019. 55p. Dep. mn; CFSTI $3.00 cy, $0.50 mn.

Heats-of-solution were measured for several alkali metal, magnesium, and gadolinium halides in the anhydrous solvents, N-methylformamide and N, N-dimethylformamide at 25°C. Whenever possible these data were extrapolated to infinite dilution both by the simple and an extended Debye-Huckel equation to obtain the standard heats-of-solution. Standard potentials were determined for cells of the type, M/MX(NMF)/AgCl; Ag, where M is Li, Na, K, or Cs and X is either Cl^- or Br^-. These potentials were used in evaluating activity coefficients and obtaining standard free energies of formation for LiCl, NaCl, KCl, CsCl, and NaBr in anhydrous N-methylformamide. Solubility measurements on numerous alkali metal, magnesium and gadolinium halides have been used to obtain free energies of solution of the corresponding salts in N,N-dimethylformamide. These heat and free energy data, and corresponding data for formamide solutions taken from the literature were used to calculate the partial molal entropies for numerous simple electrolytes in these three solvents. These were used in correspondence plots and to elucidate the structure of these solutions. Unexpected heats-of-dilution for some electrolytes were observed in these solvents. (auth)

3925 (TID-22366, App. B) THERMODYNAMIC PROPERTIES OF NON-AQUEOUS SOLUTIONS. II. FREE ENERGIES, ENTROPIES AND ACTIVITY COEFFICIENTS OF SELECTED ALKALI METAL HALIDES IN ANHYDROUS N-METHYLFORMAMIDE. Luksha, Eugene; Criss, Cecil M. (Vermont Univ., Burlington. Dept. of Chemistry). 22p.

Electrode potentials were measured for cells of the type, M_y (Hg)/MX(NMF)/AgX;Ag where M is Li, Na, K, or Cs and X is either Cl^- or Br^-. These potentials were combined with data in the literature to evaluate standard potentials for cells of the type, M/MX(NMF)/AgX;Ag, from which standard free energies of formation and activity coefficients of LiCl, NaCl, KCl, CsCl, and NaBr in anhydrous N-methylformamide were obtained. The activity coefficients were determined from 0.01 to approximately 0.1 m. Activity coefficients for KCl solutions were extended to saturation by means of the cell, Ag;AgCl/KCl(m_1)/K_y (Hg)/KCl(m_2)/AgCl; Ag. The free energies were used in conjunction with heat data to obtain the standard partial molal entropies of the corresponding electrolytes. (auth)

3926 (TID-22374) THE THERMODYNAMICS OF NON-AQUEOUS ELECTROLYTIC SOLUTIONS [Thesis]. Held, Robert Paul (Vermont Univ., Burlington). Aug. 1965. Contract AT(30-1)-3019. 158p. Dep. mn; CFSTI $5.00 cy, $1.00 mn.

A precision submarine solution calorimeter was constructed and used to measure the heats of solution of LiCl, LiBr, NaCl, KCl, CsCl, NaBr, NaI, $MgCl_2$, and $GdCl_3$ in anhydrous N-methylformamide and LiCl, LiBr, NaBr, NaI, KBr, CsI, $MgCl_2$, and $GdCl_3$ in anhydrous N,N-dimethylformamide at 25°C in the concentration range of 7×10^{-5} to 10^{-2} molal. Data for the alkali metal halides in both solvents were extrapolated to infinite dilution to obtain the standard heats of solution of the corresponding salts. The slopes for $MgCl_2$ and $GdCl_3$ in both solvents were too steep for extrapolation purposes. With the exception of CsCl and KCl, the limiting slopes of the heat data in N-methylformamide vary from the value predicted by the Debye-Hückel theory. The limiting slopes of the heat data in N,N-dimethylformamide as well as conductance data in the literature indicate that with the exception of NaBr, KBr, and CsI there are significant ionic interactions to cause large deviations. The standard heats of solution were combined with standard free energies of solution to calculate the standard partial molal entropies. 113 references are cited. (P.C.H.)

3927 (AERE-Trans-1026) STUDY OF COMPLEX AND COVALENT IRON COMPOUNDS USING THE ^{57}Fe MOESSBAUER EFFECT. Kerler, Werner; Neuwirth, Wolfgang; Fluck, Ekkehard; Kuhn, Peter; Zimmermann, Bodo. Translated by A. Crozy (U.K.A.E.A. Atomic Energy Research Establishment, Harwell, Eng.), from Z. Phys., 173: 321-46(1963). 31p. Dep.

A number of complex and covalent iron compounds in the oxidation states 0, 2+, 3+, 6+, and with coordination numbers 4, 5, and 6 was investigated at different temperatures. A source of ^{57}Co in Pd was found to be well suited for such measurements. The influence of the crystalline environment was studied by putting iron complexes in different lattices. Ligands of iron complexes were exchanged to look for influences of different bonds. It was found that measurements are also possible in frozen solutions and applications of this method are discussed. It was found that in Prussian blue and Turnbull's blue there is no so-called electron exchange between the different Fe. The Curie point of $KFeS_2$ was determined to be −28°C and it was possible to study the fields and line-shifts in its neighborhood. For some compounds indications of their structure and the sign of the electric field gradient could be derived from the data. The data are compiled in tables to allow further discussions from different points of view. (auth)

3928 (UCRL-Trans-1254(L)) INVESTIGATIONS ON THE SALT-LIKE NATURE OF LITHIUM HYDRIDE. Moers, Kurt. Translated for Univ. of California Lawrence Radiation Lab., Livermore, from Z. Anorg. Allg. Chem., 113: 179-228(1920). 91p. Dep. mn; JCL $8.60 fs, $2.93 mf.

A convenient method for the preparation of pure lithium hydride and its analysis was developed and some general properties of the substance were investigated. Special consideration was given to the question of whether lithium hydride has the nature of a salt. For a direct proof, the electrical conductivity of the substance was investigated by means of both d-c and a-c. The a-c experiments showed a rise in the conductivity with temperature as far as the order of magnitude of sulfuric acid of maximum conductivity was found. An empirical formula was calculated and the temperature coefficient determined. The presence of galvanic polarization was established and followed by measurement. The results showed that lithium hydride is a salt consisting of lithium as cation and hydrogen as anion and that hydrogen itself represents an acid, even if an extremely weak one. The amphoteric nature of hydrogen is illustrated by some

theoretical discussions. The results of thermal measurements were evaluated by using Lindemann's melting point formula and the reaction isochore equation modified by the Nernst heat theorem. (P.C.H.)

3929 REACTION OF LIQUID TITANIUM WITH SOME REFRACTORY COMPOUNDS. Garfinkle, M.; Davis, H. M. (Pennsylvania State Univ., University Park). Amer. Soc. Metals, Trans. Quart., 58: 520-9(Dec. 1965).

The reaction of liquid titanium with various nonmetallic refractory substances was investigated by observation of the melting behavior of titanium blocks in contact with polished plaques of the ceramic materials. After the reaction, the metal-ceramic interface was investigated by metallographic techniques, with the aid of hardness measurements, and with an electron-probe microanalyzer. The principal mechanisms of attack were simple dissolution of the plaque, melting of an intermediate phase formed by solid-state reaction, and eutectic reactions between the titanium block and intermediate phases. The materials tested were carbides, borides, a silicide, and a sulfide. (auth)

3930 MAGNETIC SUSCEPTIBILITY OF SOME SAMARIUM SALTS BETWEEN 1.2 AND 4 deg K. Quadros, Carlos; Ramos, J. G. P.; Azevedo, A. E. G. (Universidade de Sao Paulo, Brazil). Anais Acad. Brasil. Cienc., 34: 407-11(1964).

The magnetic susceptibilities of $Sm(ClO_4)_3 \cdot 8H_2O$, $Sm(ClO_4)_3 \cdot 9H_2O \cdot 4C_4O_2H_8$, and $Sm_2(C_2O_4)_3 \cdot 10H_2O$ were measured in the temperature range from 4 to 1.2°K. The results agree qualitatively with those of Van Vleck's theory for the free ion, showing a susceptibility χ_0 independent of T and a variable part proportional to 1/T. From the slope of χ versus 1/T the effective magnetic moment at K, μ_{eff}, in Bohr magnetons was computed. Both μ_{eff} and χ_0 differ from those computed from Van Vleck's formula for the free ion. (auth)

3931 STUDY OF EQUILIBRIUM DIAGRAM OF La_2O_3–PbO. Cassedanne, Jeannine (Universidade de Recife, Brazil). Anais Acad. Brasil. Cienc., 34: 413-16(1964). (In French).

The equilibrium diagram for La_2O_3–PbO is studied. The samples were prepared and annealed for the determination of the curves and levels of the liquids. The specimens were examined by x rays in order to identify the phases present in the solid state and to give evidence of the compound $La_2O_3 \cdot 6PbO$. The equilibrium diagram is shown; it was established as far as 1,500°C. The presence of two levels was determined, one at 770 and the other at 1320°C. The binary compound $La_2O_3 \cdot 6PbO$ was identified. Its system and parameters are given. (J.F.P.)

3932 THE CRYSTAL STRUCTURE OF TECHNETIUM(IV) CHLORIDE. Elder, Michael; Penfold, Bruce R. (Univ. Canterbury, Christchurch, N. Z.). Chem. Commun., No. 14, 308-9(July 21, 1965).

Technetium(IV) chloride crystals were found to be orthorhombic with the centro-symmetric space group Pbca. There are 8 $TcCl_4$ units in a unit cell of dimensions a = 11.58, b = 13.97, and c = 5.98 Å. All atoms were located by means of projections of the Patterson function down each of the three crystallographic axes. The structure consists of octahedral groups of composition $TcCl_6$ linked into endless linear chains extended parallel to the c-axis by the sharing of 4 chlorine atoms. (M.C.G.)

3933 REACTIONS OF THORIUM TETRACHLORIDE WITH o-PHENANTHROLINE AND TRIPHENYLPHOSPHINE. Fitzsimmons, B. W.; Gans, P.; Smith, B. C.; Wassef, Marguerite A. (Birkbeck Coll., London). Chem. Ind. (London), No. 40, 1698-9(Oct. 2, 1965).

The reaction of an excess of o-phenanthroline with thorium tetrachloride in ethanol gives o-phenanthroline hydrochloride and a precipitate of ethoxytrichlorothorium(IV)-bis(o-phenanthroline). Reaction in ethanol saturated with hydrogen chloride gives quantitative yields of bis(o-phenanthrolinium)hexachlorothorate(IV). Reaction in ethyl acetate gives thorium tetrachloride-bis(o-phenanthroline). Triphenylphosphine does not form an addition compound with thorium tetrachloride, but reaction with hydrogen chloride in ethanol gives a precipitate of bis(triphenylphosphonium)hexachlorothorate(IV). This is oxidized by air in boiling nitromethane to thorium tetrachloride-bis (triphenylphosphine oxide), identical to the compound prepared from thorium tetrachloride and triphenylphosphine oxide in ethyl acetate. Triphenylphosphine sulfide does not form an addition compound of this type. The reaction between triphenylphosphine, methyl iodide, thorium tetrachloride, and hydrogen chloride in ethanol gives bis(methyltriphenylphosphonium)hexachlorothorate-(IV), mp 256°. The thorium compounds are colorless crystalline solids which (except the last one) do not melt below 360°C. Their spectra resemble those of the corresponding compounds of uranium(IV). Satisfactory analytical data were obtained. (BBB)

3934 STUDY OF THE RESISTIVITY OF SOLID PHASES OF THE LUTETIUM–HYDROGEN SYSTEM. Daou, Joseph N.; Bonnet, Jacques (Univ., Paris). Compt. Rend., 261: 1675-7(Aug. 18, 1965). (In French).

Measurements of the electric resistance make it possible to characterize both at 25°C and at higher temperatures a primary solution of hydrogen atoms (or α phase), a dihydride, and a solution of hydrogen atoms in the dihydride. The α phase and the dihydride coexist between 0.34 and 1.8 atoms H/atom Lu at 500°C and between 0.22 and 1.8 atoms H/atom Lu at 25°C. The resistivity of each of the solid solutions increases almost linearly with the concentration in dissolved hydrogen. The particularly low resistivity of the dihydride (9.2 $\mu\Omega$/cm at 25°C) places it among the good metallic conductors. The significance of these results is discussed. (tr-auth)

3935 CHEMICAL AND KINETIC STUDY OF THE REACTION BETWEEN SULFUR DIOXIDE AND URANIUM HEXAFLUORIDE. Moncelon, Bernard; Lucas, Jacques; Kikindai, Tivadar (Ecole Centrale des Arts et Manufactures, Paris; CEN, Saclay, France). Compt. Rend., 261: 1855-8(Aug. 18, 1965). (In French).

SO_2 reduced gaseous UF_6; the fluorides αUF_5, βUF_5, U_2F_9, and UF_4 were obtained under various conditions of pressure and temperature. The reaction was followed by continuous reading of the pressure from 60 to 380°C for different ratios SO_2/UF_6. Study of the kinetics showed that for SO_2/UF_6 #2 the reductions obeyed a second order law. For the value of 1 or 5 for the ratio the secondary reactions interfered with the principal reaction. (tr-auth)

3936 A METASTABLE EQUILIBRIUM OF THE LANTHANUM–HYDROGEN SYSTEM. Daou, Joseph N.; Viallard, Rodolphe (Univ., Paris). Compt. Rend., 261: 1845-7(Aug. 23, 1965). (In French).

The nature of the face-centered-cubic phase with the parameter $\underline{a} = 5.292 \pm 0.022$ Å, detected under certain experimental conditions by the radiocrystallographic study of the solid constituents of the La–H system, is discussed on the basis of some recent observations. (tr-auth)

3937 THE HYDROLYSIS OF THORIUM DICARBIDE. Besson, Jean; Blum, Pierre; Del Litto, Bernard (Centre d'Etudes Nucleaires, Grenoble, France). Compt. Rend., 261: 1859-61(Aug. 23, 1965). (In French).

The action of water at 100°C on thorium dicarbide led to the formation of gaseous and condensed carbon hydrides. Analysis of the gaseous phase made it possible to propose a reaction mechanism analogous to that of the hydrolysis of uranium carbides. (tr-auth)

3938 REGIONS OF HOMOGENEITY OF THE NaCl TYPE FORMED BY THE MONOSULFATES OF THE RARE EARTHS. Guittard, Micheline (Univ., Paris). Compt. Rend., 261: 2109-12(Sept. 6, 1965). (In French).

Regions of homogeneity of the NaCl type between the compounds LS and $LS_{0.75}$ (where L = trivalent La, Ce, Pr, Nd, Gd, Tb, Dy, Ho, Er, Tm, Lu, and Y) were determined. In the particular case of lutetium, the region of homogeneity was extended from below LuS up to $LuS_{1.25}$. The variation of the parameter in these regions was largest with Lu. It was insignificant from Nd to Ce. The densities were also studied. (tr-auth)

3939 HIGH-TEMPERATURE STUDY OF THE ALLOTROPIC TRANSFORMATIONS OF THE SESQUIOXIDES OF YTTRIUM, ERBIUM, AND THULIUM. Foex, Marc; Traverse, Jean-Pierre (Centre National de la Recherche Scientifique, Montlouis, France). Compt. Rend., 261: 2490-3(Sept. 27, 1965). (In French).

The sesquioxides of Y, Er, and Tm were studied by thermal analysis and by high-temperature x-ray diffraction. Each oxide had a hexagonal form above 2300°C. (tr-auth)

3940 INFRARED SPECTRUM AND VIBRATIONAL ANALYSIS OF DIBROMOBORANE AND DIBROMOBORANE-d. Lynds, L.; Wolfram, T.; Bass, C. D. (North American Aviation Science Center, Thousand Oaks, Calif.). J. Chem. Phys., 43: 3775-9(Dec. 1, 1965).

The vibrational spectrum of the perturbed molecules $H^{11}BBr_2$, $H^{10}BBr_2$, $D^{11}BBr_2$, and $D^{10}BBr_2$ were generated from the Green's function of the unperturbed boron tribromides $^{11}BBr_3$ and $^{10}BBr_3$. The effect of geometry changes imposed by replacing a halogen by hydrogen on the B_1 modes was calculated and the results indicated a strong dependence on the BH or BD bond length. Using information provided by the calculations, five of the six $HBBr_2$ and $DBBr_2$ fundamentals were observed and identified. The calculated in-plane frequencies were brought into alignment with the observed frequencies by considering mass and geometry changes without altering the force field. (auth)

3941 LIGHT SCATTERING OF WATER, DEUTERIUM OXIDE, AND OTHER PURE LIQUIDS. Cohen, Gerald; Eisenberg, Henryk (Weizmann Inst. of Science, Rehovoth, Israel). J. Chem. Phys., 43: 3881-7(Dec. 1, 1965).

The Rayleigh ratio and the Cabannes factor for water, deuterium oxide, and a number of other pure liquids were determined at 25°C, at angles of observation ranging from 30 to 150°, at 546 and 436 mμ. It was found that the Rayleigh ratio of water is substantially lower than the values reported in the literature; the values found $R_u^{516}(90) = 0.865\ 10^{-6}\ cm^{-1}$, $R_u^{436}(90) = 2.32\ 10^{-6}\ cm^{-1}$ for H_2O, and $R_u^{436}(90) = 0.843 \times 10^{-6}\ cm^{-1}$, $R_u^{436}(90) = 2.30\ 10^{-6}\ cm^{-1}$ for D_2O, were in excellent agreement with the predictions of the Einstein density-fluctuation theory, modified by the Cabannes anisotropy factor. The temperature dependence of the Rayleigh ratios for H_2O and D_2O was also satisfactorily predicted by the variation of the bulk parameters appearing in the Einstein–Cabannes equations. In contradistinction to such liquids as benzene, the Rayleigh ratios of H_2O and D_2O had a minimum at about 22 and 28°C, respectively. No significant new information on the structure of water as a function of temperature could be derived from light-scattering experiments. (auth)

3942 VIBRATIONAL SPECTRA AND POTENTIAL FUNCTION FOR SnH_4 AND SnD_4. Levin, Ira W.; Ziffer, Herman (National Institutes of Health, Bethesda, Md.). J. Chem. Phys., 43: 4023-9(Dec. 1, 1965).

The Coriolis zeta constants of the triply degenerate modes of normal and heavy stannane were obtained from rotational analyses and from band-contour considerations. These coupling data were then applied toward characterizing unique force constants for the F_2 species. (auth)

3943 HEAT PULSE MEASUREMENTS OF URANIUM COMPOUNDS. Moser, J. B.; Kruger, O. L. (Argonne National Lab., Ill.). J. Nucl. Mater., 17: 153-8(Oct. 1965).

Thermal diffusivities and heat capacities of uranium monocarbide, uranium monosulfide, and uranium monophosphide were measured at room temperature by a heat pulse method. The front surface of a thin small plate was heated with a pulse of thermal energy and the resultant rear surface temperature rise was detected by a thermocouple. From an analysis of the rate and extent of this rise, the thermal diffusion coefficient and heat capacity were obtained. The thermal conductivity was then calculated from the product of the density, thermal diffusivity, and specific heat. The thermal conductivities of uranium monocarbide and uranium monophosphide corrected to theoretical density were 0.055 and 0.025 cal/cm·sec·°C, respectively. Uranium monosulfide with a density of 96.4% of theoretical had a thermal conductivity of 0.019 cal/cm·sec·°C. Effects of porosity on this type of measurement are considered. The data are compared with heat capacity and thermal conductivity values obtained by other investigators. (auth)

3944 A STUDY OF INERT-GAS DIFFUSION IN IONIC CRYSTALS AND SINTERS WITH EMPHASIS ON THE ION-BOMBARDMENT TECHNIQUE. Kelly, Roger (Solid State Physics Section, Euratom, Ispra, Italy); Matzke, Hansjoachim. J. Nucl. Mater., 17: 179-91(Oct. 1965).

The diffusion of inert gases in a series of ionic crystals and sinters was studied. The main emphasis was put on the ion-bombardment technique, though data are also presented for α-recoil radon and fission-recoil xenon. A basic principle in interpreting the results was to assign the pre-exponential factor an idealized range of values ($k_0 = 10^{15\pm1}$/sec or $D_0 \approx 3 \times 10^{-1\pm1}\ cm^2$/sec). In addition, the system of stages was used: stage I = "damage diffusion," stage II = "normal diffusion," and stage III = "bubble diffusion." CaF_2 was found to exhibit stages I and II, with ΔH_{normal} lying between 60 and 70 kcal/mole for four different techniques. BaF_2 was examined only by ion bombardment: stage II dominated, with ΔH_{normal} equal to about 58 kcal/mole. The two techniques for UO_2 and ThO_2 used require that ΔH_{normal} be greater than about 90 kcal/mole for both materials. KCl was difficult to interpret because of the low vaporization temperature and the lack of agreement among different techniques. A possible interpretation was that it shows stages I and II, with ΔH_{normal} lying between 38 and 46 kcal/mole. $\alpha-Al_2O_3$ showed a prominent release process at 550 to 1000°C, which was believed not to be stage II. The true stage II seemed, rather, to occur above 1000°C and to correspond to a ΔH_{normal} of 89 to 95 kcal/mole. (auth)

3945 INTERNAL FRICTION IN ZrO_2 CONTAINING CaO. Wachtman, J. B. Jr. (Iowa State Univ., Ames); Corwin, W. C. J. Res. Nat. Bur. Stand., A, 69A: 457-60 (Sept.-Oct. 1965).

Internal friction was measured on polycrystalline ZrO_2 containing 4, 7, 10, 13, 16, and 20 mole % CaO. In the range from 10 to 20% a symmetrical internal friction peak occurred with its maximum at about 300°C at 1 kHz; below 10% a nonsymmetrical peak occurred at somewhat higher temperature, which may be associated with the presence of two phases. The symmetrical peak in as-sintered specimens had the same dependence on CaO content as that reported for electrical resistivity at 1000°C and was probably caused by motion of oxygen vacancies. Annealing at 1000°C for 1000 hours caused reduction of the peak height but with a different composition dependence from that reported for annealing of electrical resistivity. The results suggest that oxygen vacancies in calcia-stabilized zirconia exist in several states of binding. (auth)

3946 THE SOLUBILITY OF HELIUM IN URANIUM DIOXIDE. Rufeh, Firooz; Olander, Donald R.; Pigford, Thomas H. (Univ. of California, Berkeley). Nucl. Sci. Eng., 23: 335-8(Dec. 1965).

A high-pressure furnace that operates up to 2000°C in the pressure range of 100 atm to 10^{-5} torr was designed and constructed to saturate UO_2 powder of 4-μm average particle size with ^4He. The powder was then dissolved in a fused salt in an induction chamber. The released ^4He was mixed with a known quantity of ^3He, and the mixture was analyzed with a mass spectrometer to determine the ^4He:^3He ratio, hence the original mass of ^4He in the sample. The solubility of He in UO_2 at 1200 and 1300°C was found to be 6.71×10^{-4} and $3.23 \times 10^{-4}\ cm^3$ (STP)/(g atm), respectively. It was also found that the He–UO_2 system obeys Henry's law. From a plot of He concentration as a function of time, the diffusion coefficient at 1200°C was estimated to be $1.5 \times 10^{-13}\ cm^2$/sec. (auth)

3947 THE MICROWAVE ROTATIONAL SPECTRA OF THALLIUM MONO-CHLORIDE. De Wijn, H. W. (Univ., Amsterdam). Physica, 31: 1193-1214(Aug. 1965).

With a Stark-spectrometer the pure rotational spectra of the four natural isotopic species of thallium monochloride, $^{205}Tl^{35}Cl$, $^{203}Tl^{35}Cl$, $^{205}Tl^{37}Cl$, $^{203}Tl^{37}Cl$, were observed in the wavelength region from 15 mm down to 4.8 mm. Rotational lines were measured for molecules in vibrational states up to v = 12; quadrupole hyperfine structure due to the quadrupole moment of the Cl nuclei was observed for v up to 4. A description is presented of the Stark-absorption cell, which can be operated at high temperatures, and therefore is suitable for observing spectra of substances being in the solid state at room temperature. The spectra are described in terms of six theoretical constants, viz., the four Dunham coefficients Y_{01}, $Y_{11}(\approx -\alpha_e)$, $Y_{21}(\approx \gamma_e)$, $Y_{02}(\approx -D_e)$, the quadrupole coupling constant $eq_{v=0}Q$, and its variation e(dq/dv) Q with increasing molecular vibration. For each isotopic species these constants were determined by an adjustment to the measured line frequencies by use of the method of the least squares. From the spectrum constants a number of molecular constants were calculated: the rotational constants B_e; the internuclear distance r_e; the vibrational frequencies ω_e; the coefficients a_0, a_1, a_2 belonging to the quadratic, the cubic, the quartic part, respectively, of the internuclear potential; the electric field gradient q along the internuclear axis and its variation dq/dv with vibration, both at the site of the Cl nucleus. The results are compared with values from literature. Mass ratios of Tl and Cl nuclides, calculated from the rotational spectra, compare satisfactorily with mass ratios from nuclear reactions. Finally, the collision broadening constant was measured. The results are tabulated. (auth)

3948 ON THE FLUORESCENCE SPECTRUM OF URANYL ION CONTAINED IN SOME RARE-EARTH CHLORIDES. Dixit, R. M. (Atomic Energy Establishment, Trombay, Bombay). Proc. Indian Acad. Sci., Sect. A, 62: 104-11(Aug. 1965).

The mutual effect of the rare-earth ion and the uranyl ion on each other is studied by the fluorescence spectra of 10% UO_2Cl_2 contained in the rare-earth chlorides (La, Sm, Eu, Dy, and Tb). While the spectra of rare-earth ions remain unchanged in the presence of 10% UO_2Cl_2 the spectrum of the uranyl ion is very much influenced. The spectrum now consists of, instead of discrete bands, groups of diffuse bands. Analysis shows that in the case of Y, La and Eu, which all show a similar effect, the resonance band is shifted towards the longer wavelength side to 20319 cm^{-1} and the symmetric frequency is reduced to ~877. In the case of Sm, Dy, and Tb the resonance band is further shifted to 19255 cm^{-1} and the symmetric frequency is reduced to 841. In the case of UO_2Cl_2 the resonance band is at 20537 cm^{-1} and the symmetric frequency is 883. (auth)

3949 INFRA-RED ASSIGNMENTS AND FORCE CONSTANTS IN METAL-NITRATO COMPLEXES. Topping, G. (Atomic Energy Research Establishment, Harwell, Eng.). Spectrochim. Acta, 21: 1743-51(Oct. 1965).

A normal co-ordinate treatment of the NO_3 ion is given and used to explore the effects of nitrato complex formation on infrared spectra. By considering the unidentate complex $Cs_2U(NO_3)_6$ and the bidentate complex $RbUO_2(NO_3)_3$ it is shown that while the splitting of a band at about 1400 cm^{-1} is a good criterion of complex formation, its magnitude is not suitable for deciding between unidentate and bidentate complexes. A better criterion, based on far infrared spectra of the metal–oxygen stretching frequencies is suggested and experimental work in support of this suggestion is presented. (auth)

3950 THERMODYNAMIC PROPERTIES OF DEUTERIUM AND TRITIUM SUBSTITUTED NON-LINEAR TRIATOMIC HYDRIDES. Morozov, V. P.; Kovalenko, N. F.; Khlebnekova, V. N.; Fedorov, Yu. K. (Dnepropetrovsk Inst. of Chemistry and Tech., USSR). Teor. Eksp. Khim., 1: 462-7(July-Aug. 1965). (In Russian).

The reduced isobar-isothermal potentials and entropies of isotopic modifications of hydrogen sulfide and hydrogen selenide were calculated for ideal gas conditions. (tr-auth)

3951 SOLUBILITY OF METAL OXIDES IN FUSED BORAX. Delimarskii, Yu. K.; Nazarenko, G. D. (Inst. of General and Inorganic Chemistry, Academy of Sciences, Ukrainian SSR). Ukr. Khim. Zh., 31: 813-17(1965). (In Russian).

The solubility of 10 oxides (PbO, Bi_2O_3, NiO, ZrO_2, CuO, WO_3, Fe_2O_3, CdO, TiO_2, and MoO_3) in borax was determined at 760 and 900°C by the method of isothermal saturation. It is shown that the solubility of the metal oxides in borax do not follow quantitatively the Shreder equations and the Semenchenko rule. The character of the solubility of the metal oxides in borax is connected with the chemical interactions between the components of the melt. (tr-auth)

3952 STUDIES OF URANIUM DIOXIDE OXIDATION BY MEANS OF HIGH-TEMPERATURE ELECTROCONDUCTIVITY, X-RAY PHASE STUDIES, AND CONTINUOUS WEIGHING. Bessonov, A. F.; Strekalovskii, V. N.; Neuimin, A. D.; Ust'yantsev, V. M. Zh. Fiz. Khim., 39: 1708-11(July 1965). (In Russian).

High temperature x-ray phase analysis confirms the earlier suggested scheme of the phase transformation of UO_2 proposed on the basis of the measurement of the electroconductivity of the oxidation products and the kinetic investigation of the oxidation process of uranium dioxide by continuous weighing methods. In particular, the tetragonal forms of the dioxide (γ-UO_2 with the composition $UO_{2.33-2.37}$) and the α-$U_3O_8 \rightarrow \beta$-U_3O_8 near 340°C were observed. A good correlation was observed between the character of the change of the curve of the electroconductivity–composition of oxidation products and the change of the phase composition of the sample under the experimental conditions, determined by the method of high temperature x ray analysis. (tr-auth)

3953 INVESTIGATION OF CERTAIN OXIDE SYSTEMS IN A HIGH-TEMPERATURE INSTALLATION USED FOR MEASURING SIMULTANEOUSLY ELECTRIC RESISTANCE AND X-RAY ANALYSIS OF SPECIMENS. Bessonov, A. F.; Ustyantsev, V. M. (Eastern Research and Design Inst. of Refractory Industry, USSR). Zh. Fiz. Khim., 39: 1932-7(Aug. 1965). (In Russian).

A method was developed and an installation constructed for the simultaneous-high temperature plotting of the electrical resistance curve and the x-ray analysis of solid crystalline materials. The behavior during annealing and subsequent chilling of zirconium oxide with additions of magnesium and yttrium oxides was studied. The temperature of the polymorphic transformation of ZrO_2 in the presence of supplements of MgO and Y_2O_3 was established. The data of the electrical resistance investigation and the x-ray analysis supplemented each other. (tr-auth)

3954 THERMOCHEMISTRY OF CERIUM(IV) NITRATES. Afanas'ev, Yu. A.; Ryabinin, A. I.; Koroleva, I. I. (Inst. of Inorganic Chemistry, Academy of Sciences, Siberian SSR). Zh. Fiz. Khim., 39: 2296-8(Sept. 1965). (In Russian).

The heats of solution of basic and neutral cerium(IV) nitrates were determined in water and tributyl phosphate. The heats of extraction of cerium(IV) nitrates with TBP were calculated and measured. The standard enthalpy for the formation of basic and neutral cerium(IV) nitrates was calculated. (tr-auth)

3955 SOLUBILITY OF TRIBUTYLPHOSPHATE IN AQUEOUS SOLUTION $UO_2(NO_3)_2$. Mikhailov, V. A.; Nozin, A. G. (Inst. of Inorganic Chemistry, Academy of Sciences, Siberian SSR). Zh. Fiz. Khim., 39: 2312-14(Sept. 1965). (In Russian).

The solubility and molar activity coefficients of TBP in an aqueous solution of $UO_2(NO_3)_2$ were determined at different concentrations. In contrast to poorly extractable electrolytes, uranyl nitrate absorbs TBP in the gaseous phase, which indicates an intense reaction between TBP and $UO_2(NO_3)_2$ in the aqueous solution. (tr-auth)

3956 HEATS OF DILUTION OF SOME AQUEOUS RARE-EARTH CHLORIDE SOLUTIONS AT 25 deg C [Thesis]. De Kock, Carroll Wayne. Ames, Iowa, Iowa State Univ. of Science and Tech., 1965. 166p.

The heats of dilution of aqueous $PrCl_3$, $TbCl_3$, and $YbCl_3$ solutions were determined from zero molal to saturation

and aqueous $LaCl_3$ and $HoCl_3$ solutions from 0.25 molal to saturation at 25°C. Aqueous heats of solution of $TbCl_3 \cdot 6H_2O$ and $HoCl_3 \cdot 6H_2O$ were determined at 25°C. From these data empirical least square equations for the relative apparent molal heat contents, ϕ_L, were determined as a function of $m^{\frac{1}{2}}$ using an IBM 7074 computer. Expressions for the relative partial molal heat content of the water, $\bar{L}_1$, and of the salt, $\bar{L}_2$, were determined from these empirical equations. The relative partial molal excess entropies of the water $(\bar{S}_1 - \bar{S}_1^0)$ and of the salt $(\bar{S}_2 - \bar{S}_2^0)$ were determined from the $\bar{L}_1$ and $\bar{L}_2$ data and from the activity coefficient data of these electrolytes. Values for $\bar{L}_1$, $\bar{L}_2$, $T(\bar{S}_1 - \bar{S}_1^0)$ and $T(\bar{S}_2 - \bar{S}_2^0)$ were calculated at rounded concentrations. The data show that aqueous $PrCl_3$ and $TbCl_3$ solutions obey the Debye-Hückel limiting law, and there is strong indication that aqueous $YbCl_3$ solutions also obey the limiting law. It is postulated that the heat of dilution data below 0.15 molal for all the aqueous rare-earth chloride solutions studied can be understood in terms of two series within the rare earths. These two series have different water coordination numbers with a gradual shift in the equilibrium between these two coordination numbers occurring from beyond Nd to around Tb or Dy. The lighter rare earths, from La to Nd, favor the higher coordination number, while the heavier rare earths, from around Tb or Dy to Yb, favor the lower water coordination number. The data for $PrCl_3$ indicate that for this salt the equilibrium between two water coordination numbers shifts toward the lower coordination number with increasing concentration above 2.0 molal. (Dissertation Abstr.)

3957 MASS SPECTROMETRIC STUDIES OF THE VAPORIZATION OF STRONTIUM SULFIDE, LANTHANUM MONOSULFIDE, AND SOME LANTHANUM–SILVER ALLOYS [Thesis]. Johnson, Ernest Walter. Iowa City, Iowa, State Univ., 1965. 81p.

The sublimation of strontium sulfide and lanthanum monosulfide and the vaporization of Ag from some La–Ag alloys were studied using mass spectrometric techniques. Gaseous species in equilibrium with solid strontium sulfide over the temperature range of 1700 to 2000°K were strontium, strontium sulfide, monatomic sulfur, and diatomic sulfur. The variation of effusion rates of these four components with temperature was measured and expressions relating partial pressures to temperature were calculated. These expressions were used to calculate thermodynamic properties for the sublimation reactions by the second law method, and the dissociation of strontium sulfide was also treated by two different third law approaches. In the study of the sublimation of lanthanum monosulfide, the species observed in the gas phase over solid lanthanum sulfide were lanthanum monosulfide and lanthanum monoxide. The variation of effusion rates of lanthanum monosulfide with temperature yielded a second law enthalpy of sublimation of 107.7 ± 2.5 kcal/mole at 2000°K. The presence of lanthanum monoxide in the effusate beam was due to a gas-phase reaction between lanthanum monosulfide and oxygen. Enthalpies were calculated from studies of effusion rate of Ag over three alloy compositions of Ag and La. (A.G.W.)

3958 STARK EFFECT STUDIES OF CH_3F, CD_3F, CH_3CN, AND CD_3CN [Thesis]. Steiner III, Pinckney Alston. Durham, N. C., Duke Univ., 1965. 104p.

The small changes expected in the dipole moment when deuterium is substituted for hydrogen in a symmetric-top molecule were investigated. The dipole moment measurements were extended to molecules in higher rotational states than had previously been determined. The equipment and techniques that have become standard at Duke University were used. The $J = 1 \rightarrow 2$ transition was used in the measurement of the dipole moment of CD_3F. The measurements used both σ and π transitions with both first-order and second-order Stark effect over a wide range of field strengths. The average dipole moments obtained from the measurements are 1.8682 ± 0.0010 Debye for CD_3F and 1.8572 ± 0.0010 Debye for CH_3F. There is thus a change of 0.6 per cent in the value of the dipole moment of CH_3F from this isotopic substitution. The measurement of dipole moments of molecules in high rotational states was investigated with the $J = 4 \rightarrow 5$ transition of CH_3CN and the $J = 5 \rightarrow 6$ transition of CD_3CN. The results were found to fit completely the equations for Stark effect obtained from perturbation theory. The spectra for these molecules were considerably complicated by nuclear quadrupole coupling of the ^{14}N nucleus as well as by the large number of Stark components because of the high J transitions. The average dipole moments found for these two isotopic species are 3.913 ± 0.0020 Debye for CH_3CN and 3.919 ± 0.0025 Debye for CD_3CN. The change in dipole moment from this isotopic substitution in CH_3CN is therefore 0.2 per cent. No shift in dipole moment was observed for different rotational states even though measurements were made on the K = 1, 2, and 3 lines. (Dissertation Abstr.)

3959 THE DETERMINATION OF Cl AND Fe COMPLEXING IN MOLTEN SALTS (ESPECIALLY FOR FISSION PRODUCTS AND ACTINIDES) BY DISTRIBUTION METHODS USING γ ALUMINA [Thesis]. Wirries, H. Brunswick, Univ., 1964. 87p. $2.00 Gmelin, AED-DISS. 64-760.

Distribution equilibria of Co^{II}, Cd^{II}, Zn^{II}, U^{IV}, Ce^{III}, and Np^{V} between a molten K-Li eutectic and γ-alumina were investigated for various chloride concentrations. Chloride complexion constants were calculated using the IBM-7090 computer. (Gmelin Inst.)

3960 ISOTOPE EXCHANGE STUDIES WITH METAL-ORGANIC COMPOUNDS OF Tl USING ^{204}Tl [Thesis]. Tennstedt, K. Brunswick, Ger., Tech. Univ., 1964. 81p. $2.00 Gmelin, AED-DISS. 64-576.

Isotope exchange between monophenyl-Tl^{III} ions and radioactive Tl^{III} ions in perchloric acid was relatively slow. Exchange was more rapid in sulfuric acid. Activation energies are given. (Gmelin Inst.)

3961 CONTRIBUTIONS TO THE CHEMISTRY OF 4 AND 6 VALENT U [Thesis]. Andrae, K. Halle-Wittenberg, Ger., Univ., 1964. 110p. $2.00 Gmelin, AED-DISS. 64-753.

Possibilities for the preparation of water-free uranyl chloride are discussed. Methods for the preparation of various organic uranium compounds are given. (Gmelin Inst.)

3962 ACCELERATION OF THE ELECTRON-EXCHANGE REACTION BETWEEN $SbCl_3$ AND $SbCl_5$ IN CARBON TETRACHLORIDE BY ADDITION OF ANHYDROUS HCl. Price, K. R.; Brubaker, C. H. Jr. (Michigan State Univ., East Lansing). Vienna, International Atomic Energy Agency, 1965, Preprint No. SM-64/14, 10p. (CONF-650549–9). ORINS.

From IAEA Symposium on Exchange Reactions, Upton, N. Y.

The effect of added anhydrous hydrochoric acid on the exchange between antimony trichloride and pentachloride in anhydrous carbon tetrachloride was investigated as a function of concentration of added HCl. Barker and Kahn found the exchange, in the absence of HCl, proceeded by two paths, one of which depended only on the concentration of $SbCl_5$ and the other depended on the concentration of $SbCl_3$ and the concentration of $SbCl_5$ squared. In the presence of added HCl the exchange proceeded at a much faster rate and depended on the concentration of added HCl. A complex rate law was found, which indicated a contribution by the Barker and Kahn paths plus a new route involving the HCl. This third path appeared to involve $SbCl_3$ and $HSbCl_6$ or $SbCl_6^-$ and had the form $k_3(HSbCl_6)(SbCl_3)$. A mechanism was proposed, which involves the formation of a triply chlorobridged diantimonate species, consisting of two octahedra face to face and which was formed by the interaction of the $SbCl_6^-$ ion and an $SbCl_3$ molecule. This path is much faster than the two Barker and Kahn paths and after the HCl concentration is approximately equal to the $SbCl_5$ concentration, it is the only path contributing to the exchange. The possibilities of direct transfer of the electrons between the two bridged antimony species are discussed. (auth)

3963 INTERMEDIATES IN ISOTOPIC EXCHANGE REACTIONS INVOLVING DIBORANE. Koski, W. S. (Johns Hopkins Univ., Baltimore). Vienna, International Atomic Energy Agency, 1965, Preprint No. SM-64/16, 11p. (CONF-650549-11). ORINS.

From IAEA Symposium on Exchange Reactions, Upton, N. Y.

Using conventional mass spectrometric analysis, the self-exchange reaction of diborane was studied by using boron and hydrogen isotopes as tracers. The ratio of deuterium to boron exchange was found to be 2.8. This suggests that the reaction does not completely proceed by exchange of BH_3's as an entity, and that the mechanism is more complicated than simply a stripping reaction between diborane and a borane. Using a specially constructed mass spectrometer of high sensitivity coupled with a flow reactor, it was possible to make a direct detection of the intermediates involved in diborane equilibria. The intermediates BH_3 and BH_2 were found to be present and their ionization potentials were measured. In addition, a small amount of B_3H_n was observed but the value of n could not be determined because of the weak peaks obtained. An attempt was made to interpret the self-exchange reaction of diborane in terms of these intermediates. The results suggested that diborane is in rapid equilibrium with borane (BH_3). In addition, apparently diborane can also dissociate into BH_2, which was about twice as abundant as BH_3. The B_3H_n intermediate that was observed is believed to arise from the reaction $BH_2 + B_2H_6 \rightarrow B_3H_9$. In applying this information to the isotopic self exchange in diborane, it appeared that the exchange cannot proceed by a stripping mechanism such as $BD_3 + BH_3 - BH_3 \rightarrow BD_3 - BH_3 + BH_3$ since the deuterium-to-boron isotopic ratio then should be three. Another possible mechanism of exchange is $BD_3 + B_2H_6 \rightleftharpoons B_3D_3H_6$. The B_3 complex can be pictured as a symmetrical one. If the bonds were all exactly equivalent the D/B^{10} ratio would statistically become 3; however, some isotope effect may be present in the fragmentation of the complex and the ratio could deviate from three. Another possible way in which the ratio could be reduced below three is if a small amount of the exchange proceeded through the intermediate BH_2. A second exchange reaction in which these intermediates appear to play a significant role is the exchange between molecular hydrogen and diborane. It is shown that by assuming the reaction $B_3H_9 \rightleftharpoons B_3H_7 + H_2$, it is possible to account for the $^3/_2$ order dependence on diborane in the $B_2H_6 - D_2$ exchange, as well as the first order dependence on H_2 at low pressures and the zero order dependence on H_2 for high pressures. (auth)

3964 EXCHANGE REACTIONS INVOLVING URANIUM AND NEPTUNIUM IONS SOLVENT, SALT AND ION EFFECTS TEMPERATURE COEFFICIENTS. Amis, E. S. (Univ. of Arkansas, Fayetteville). Vienna, International Atomic Energy Agency, 1965, Preprint No. SM-64/26, 40p. (CONF-650549-17). ORINS.

From IAEA Symposium on Exchange Reactions, Upton, N. Y.

The rates, orders, and temperature coefficients of certain exchange reactions involving neptunium and uranium ions of different valences were studied in pure and mixed solvents and in the presence of inert salts and of certain specific ions. Counting and spectrophotometric techniques were used. The rates and the orders were found in some cases to depend on solvent composition. Salt effects and specific ion effects were demonstrated. In one case the exchange reaction was found to be independent of the solvent and of the physical properties of the solvent. Theories and mechanism were advanced to explain these phenomena. In some cases the change of rate of reactions with solvent composition was observed to depend on the change of energy of activation with solvent composition. Selective solvation by the more polar component of the solvent was the governing factor in the cases of certain reactions in solvents of different compositions. Solvolysis, in certain instances, governed the rates and orders found. Stepwise processes were used to explain certain specific ion effects. In one instance an irreversible, chain-breaking step in which a cation was removed as the metal was offered to explain the effect of a specific ion on an exchange rate. For a possible mechanistic picture of one reaction an ion was found to accelerate only one step in the reaction and that only above a critical concentration of the ion. Specific solvation of ions and other solvent effects were demonstrated in other than chemical kinetic processes to lend support to these proposed effects in electron exchange reactions. (auth)

3965 ISOTOPIC EXCHANGE REACTIONS IN THIONYL CHLORIDE AND SULFURYL CHLORIDE. Bain, R. L.; Norris, T. H. (Oregon State Univ., Corvallis). Vienna, International Atomic Energy Agency, 1965, Preprint No. SM-64/29, 17p. (CONF-650549-19). ORINS.

From IAEA Symposium on Exchange Reactions, Upton, N. Y.

Isotopic exchange studies were carried out with the solvents thionyl chloride and sulfuryl chloride. ^{36}Cl exchange rates between the two mixed solvents over a full range of concentrations revealed that in all cases only an exceedingly slow reaction occurred with half times at 25°C between about 80 and 1200 days, depending on concentrations. The results appeared to suggest a lesser importance for ready ionic dissociation equilibria in these media than was previously proposed. ^{35}S exchange rates between the two solvents were also studied. This exchange was found to be, at best, a great deal slower than the chlorine exchange. Minimum half times at 25°C of about 5000 days or more were indicated. The data implied that the chlorine exchange must, at least in large part, go via a pathway independent of any sulfur exchange mechanism. In further experiments, ^{36}Cl exchange between the acid solute antimony pentachloride and each of the two solvents was examined. While rapid exchange occurred with thionyl chloride, only a negligible rate was found with sulfuryl chloride. In other experiments (in acetonitrile), the addition of an ionic chloride was shown to effectively block the antimony pentachloride-thionyl chloride exchange, presumably through hexachloro-antimonate formation. Supplementing the implications of the slow chlorine exchange between the two mixed solvents, these results suggest that, at least in the presence of a strong chloride acceptor, the solvent thionyl chloride may well undergo ionic dissociation, but that, even under such circumstances, sulfuryl chloride fails to do so. (auth)

3966 SOME EXCHANGE AND SUBSTITUTION REACTIONS OF HEXACHLORORHODIUM(III) AND PENTACHLORAQUORHODIUM(III) IONS IN AQUEOUS ACID SOLUTIONS. Robb, W.; Harris, G. M. (State Univ. of New York, Buffalo). Vienna, International Atomic Energy Agency, 1965, Preprint No. SM-64/25, 20p. (CONF-650549-16). ORINS.

From IAEA Symposium on Exchange Reactions, Upton, N. Y.

An extension of previous studies on the chemistry of rhodium(III) complexes is reported. An investigation was made of the kinetics of the equilibration, $RhCl_6^{-3} + H_2O \rightleftharpoons RhCl_5H_2O^{-2} + Cl^-$, utilizing spectrophotometric and tracer techniques. The reaction was studied in perchloric–hydrochloric acid media of constant ionic strength. The aquation of $RhCl_6^{-3}$ and the anation of $RhCl_5H_2O^{-2}$ were examined independently by spectrophotometry. It was shown that either process is described by the rate law: $-d(RhCl_6^{-3})/dt = k_f(RhCl_6^{-3}) - k_r(RhCl_5(H_2O)^{-2})(Cl^-)$. Values of k_f and k_r were obtained at several temperatures by both aquation and anation procedures, and excellent agreement was obtained between the two sets of data. At 25°C, $k_f = 1.7 \times 10^{-3}$ sec^{-1} and $k_r = 2.5 \times 10^{-4}$ M^{-1} sec^{-1} and the Arrhenius energies of activation were 25 and 19 kcal/mole, respectively. The reaction was essentially independent of acid concentration up to 4M. In order to test whether the aquation path is the only one available for exchange of chloride by chloride, a direct study was made of the reaction $RhCl_6^{-3} + {}^{36}Cl^- \rightleftharpoons RhCl_5{}^{36}Cl^{-2} + Cl^-$. The kinetics of the isotopic exchange could be accounted for almost entirely by an aquation mechanism as follows:

$RhCl_6^{-3} + H_2O \rightarrow RhCl_5H_2O^{-2} + Cl^-$ and $RhCl_5H_2O^{-2} + {}^{36}Cl^- \rightarrow RhCl_5{}^{36}Cl^{-2} + H_2O$. The rate constant for exchange evaluated on this basis was practically identical with k_f and had the same energy of activation. The aquation reaction may involve a unimolecular dissociation of chloride ion as the rate-determining step, or bimolecular substitution of water for chloride. (auth)

3967 ELECTRON EXCHANGE REACTIONS MEDIATED BY OXYANIONS. Miller, R. G.; Peters, D. E.; Fraser, R. T. M. (Univ. of Kansas, Lawrence). Vienna, International Atomic Energy Agency, 1965, Preprint No. SM-64/22, 21p. (CONF-650549-14). ORINS.

From IAEA Symposium on Exchange Reactions, Upton, N. Y.

The electron exchange rates were measured between Co(III) and Cr(II), V(II), and Eu(II) using oxyanions as bridging groups. The measurements were carried out spectrophotometrically, using pentaamminecobalt(III) complexes in perchlorate and sulfate media. Bridging groups included metaborate, carbonate, nitrate, nitrite (both as the nitro and the nitrito ligands), sulfite, sulfate, thiosulfate, selenite, selenate, and tellurate. Specific rates increased along a series such as $-OBO$, $-OCO_2^-$, $-ONO_2$, and down a series such as $-OSO_3^-$, $-OSeO_3^-$ ($k = 23 m^{-1} sec^{-1}$ for the Cr(II) reduction of the sulfato complex, $360 m^{-1} sec^{-1}$ for that of the selenato). In general, rates were more rapid with Cr(II) as the reducing agent. Some experiments with Ti(III) showed it to be the slowest. It appeared possible to correlate changes in specific rate with the central atom of the ligand and the number of oxygen atoms present in the ligand but not bound to the cobalt center (that is, with the number of attack sites available to the reductant). For example, at 25°C, the specific rate for the Cr(II) reduction of the sulfito complex was $18 m^{-1} sec^{-1}$ and that for the sulfato was $20 \pm 2 m^{-1} sec^{-1}$; both ligands possess three oxygens not bound to the cobalt; for the bonding in the sulfito complex is Co–S, while that in the sulfato is Co–O–S. The activation parameters for the two reactions are almost identical. Another example was found in the tetraammine series: the specific rate for the reaction of the chelated sulfate was $35 m^{-1} sec^{-1}$, while that for the chelated sulfite was $17 m^{-1} sec^{-1}$. The sulfato complex possesses two oxygens free, the sulfito only one. (auth)

3968 IMPROVEMENTS IN OR RELATING TO ZIRCONIUM PHOSPHATE PREPARATION. Lefevre, Jean; Ollivier, Jean; Prospect, Jacques; Staroz, Claude (to Commissariat a l'Energie Atomique). British Patent 1,007,871. Oct. 22, 1965. Priority date Dec. 29, 1961, France.

A process for the preparation of zirconium phosphate in granular form, particularly for use as a cation exchanger, consists of the addition of H_2O_2 to an aqueous solution of a suitable Zr salt; precipitating the phosphate by the addition of phosphoric acid to the solution; and recovering the precipitate in the form of granules by decanting, washing, filtering, drying, and comminution steps. The granules obtained have an average diameter of 0.2 to 0.4 mm and a molar ratio of PO_4/Zr of about 1.8. (B.L.M.)

3969 FINE SIZED POWDERS OF THORIA, URANIA AND MIXTURES THEREOF AND METHODS FOR THEIR PREPARATION. Acker, Ellsworth G.; Sanchez, Moises G.; Burnie, Glen; Vanik, Milton C. (to W. R. Grace and Co.). U. S. Patent 3,211,518. Oct. 12, 1965. Apr. 23, 1963.

A process is patented for the preparation of colloidal sized hydrophilic or organophilic powders of thoria, urania, or thoria–urania that are useful in the preparation of fuel for liquid homogeneous reactors. A suitable aqueous sol of the desired actinide is prepared by dissolving a suitable salt in de-ionized water, placing the solution in a suitable vessel, and withdrawing part of the solution through a cathode compartment of an electrodialysis cell divided by a membrane of ion exchange material. This portion is returned to the larger body of solution maintained at an elevated temperature, and this withdrawal, dialysis, and addition back is continued until the solution is essentially electrolyte free. The sol is densified and passed through an ion exchange resin. At this point in the process, sol may be clad with silica or some other material. The deionized sol is treated with an agent capable of neutralizing the charge on the particle that acts as a flushing agent, and the water is removed from the resulting sol or suspension by azeotrope distillation from a suitable organic medium such as an alcohol. After the sol is completely converted to the alcohol form, it is dehydrated using conventional vacuum or air-drying techniques. (B.L.M.)

3970 APPARATUS FOR DETERMINING THE QUANTITY OF CONTAMINANT IN A SUBSTANCE. Bayly, John G.; Stevens, William H. (to Atomic Energy of Canada Ltd.). U. S. Patent 3,211,961. Oct. 12, 1965. Filed May 12, 1961.

A method is described for the determination of a contaminant in a pure substance, e.g., light water in heavy water, in which the pure substance has a transmission in the visible, ultraviolet, or infrared region of the spectrum and the contaminant has a characteristic absorption in the same region of the spectrum. The apparatus includes a radiation source and at least two filters mounted to be presented in sequence to intercept radiation from the source transmitted by the contaminated substance. One of the filters is adapted to pass radiation transmitted by the uncontaminated substance but at least partially absorbed by the contaminant, and the other filter(s) is adapted to pass radiation transmitted by the uncontaminated substance in a wavelength band other than that absorbed by the contaminant. A detector is illuminated by the radiation from the source passing through the sample and transmitted by each filter, respectively, and furnishes an output signal directly related to the intercepted radiation. The outputs occasioned by the respective filters are fed to integrating means to obtain the integral of the opposite phase outputs, and means sensitive to the integrating means varies the amplitude of at least one of the outputs in a sense to balance the outputs. (B.L.M.)

3971 METHOD OF PREPARING URANIC OXIDE IN GRANULATED FORM. Burko, Jakub; Pigeot, Alain; Jouannaud, Claude; Nollet, Patrick (to Commissariat a l'Energie Atomique). U. S. Patent 3,212,846. Oct. 19, 1965. Priority date June 5, 1961, France.

A method of preparing UO_3 in granulated form consists of feeding a starting material of a concentrated aqueous solution of uranyl nitrate or ammonium uranate paste and of fine particles of uranium oxide into a container heated at 170–250°C to form an intimate mixture. The mixture is caused to travel through the container so as to form a mass of juxaposed grains consisting of particles coated with the starting material. The grains are roasted at 290–350°C. (B.L.M.)

Organic Chemistry

3972 (EUR–2528.f) SYNTHESE DE PRODUITS APPARENTES AUX POLYPHENYLES. (Synthesis of Products Akin to the Polyphenyls). Baudet, C.; Marcq, A. (Societe d'Etudes, de Recherches et d'Applications pour l'Industrie, Brussels (Belgium)). 1965. 72p. Dep. mn.

The synthesis and properties of six hexahydroterphenyls isomers, some alkylpolyphenyls, and 9-phenylphenanthrene are described. (P.C.H.)

3973 (IS–1222) CATALOG OF NUCLEAR QUADRUPOLE INTERACTIONS AND RESONANCE FREQUENCIES IN SOLIDS. PART II. HALOGEN RESONANCES IN ORGANIC COMPOUNDS. Segel, S. L.; Barnes, R. G. (Ames Lab., Iowa State Univ. of Science and Tech.). Sept. 1965. Contract W-7405-eng-82. 109p. Dep. mn; CFSTI $4.00 cy, $0.75 mn.

Where available in literature, the halogen quadrupole resonance frequencies and the coupling constants in or-

ganic compounds are listed. The sources of the information are the more commonly available journals through August, 1965. Literature references to the original sources are given as well as references to articles immediately concerned with the quadrupolar coupling. A brief introduction to the theory of quadrupole resonance is also given. 467 references are cited. (auth)

3974 (ORNL-TM-1314) SYNTHESIS OF 3,9-DIETHYLTRIDECYL-6-AMINE. Holsopple, H. L.; Seeley, F. G. (Oak Ridge National Lab., Tenn.). Nov. 5, 1965. Contract W-7405-eng-26. 12p. Dep. mn; CFSTI $1.00 cy, $0.50 mn.

The preparation of 3,9-diethyltridecyl-6-amine is described. The basic starting material, 3,9-diethyltridecanol-6, was oxidized to the ketone, converted to the oxime, then catalytically hydrogenated to the amine. Purification was by fractional vacuum distillation and ion-exchange sorption of the amine. A description is given of the equipment used in the hydrogenation procedure. The preparation of Raney nickel catalyst is also described. (auth)

3975 SYNTHESIS OF [CARBOXYL-^{14}C]3,4-DEHYDRO-DL-PROLINE. Hudson, C. B.; Robertson, A. V. (Univ. of Sydney). Austral. J. Chem., 18: 1677-80 (Oct. 1965).

The series of steps employed in the preparation of [carboxyl-^{14}C] 3,4-dehydro-DL-proline are presented. The 3,4-dehydro-DL-proline was synthesized by reduction of pyrrole-2-carboxamide with phosphonium iodide in fuming hydriodic acid. Carbonation of a pyrrole Grignard reagent was chosen as the method for incorporating ^{14}C. (F.J.H.)

3976 THIOPHENE-^{35}S. Zel'venskii, Ya. D.; Shalygin, V. A.; Andreeva, N. I. Zh. Obshch. Khim., 35: 1039-73 (Aug. 1965). (In Russian).

The isotopic exchange of sulfur between thiophene and elementary sulfur and between couples of thiophene and metallic sulfides was investigated. For production of thiophene-^{35}S it was found advisable to use isotopic exchange between couples of thiophene and Ni^{35}S at 600°C. The optimum conditions for exchange were determined. (tr-auth)

3977 A STUDY OF ISOTOPE EFFECTS ON MOLECULAR DIPOLE MOMENTS [Thesis]. Muenter, John Stuart. Stanford, Calif., Stanford Univ., 1965. 115p.

The Stark effect in pure rotational spectra in the microwave region is used to measure molecular dipole moments. A parallel plate microwave absorption cell is described, which may be used to determine moments to an accuracy of 0.1%. This cell is used to study the effect of deuterium substitution on the dipole moments of small organic molecules. The observed isotope shifts are of the order of 0.003 to 0.01 D, and are qualitatively explained in terms of the shortening of the C-D bond. The existence of such isotope shifts indicate that nonpolar molecules will acquire a permanent dipole moment if the molecule's symmetry is removed by deuteration. To demonstrate the existence of such a moment, the J = 0, M = 0 to J = 1, M = 0 rotational transition was investigated in HC ≡ CD. Stark modulation was utilized, and the observed Stark coefficient is -0.917×10^{-10} mC/(v/cm)^2. The transition probability depends only on the permanent moment, while the Stark coefficient depends on both the induced moment and the permanent moment. From measured isotope shifts of polar molecules, a permanent moment of 0.012 D is assumed for HC ≡ CD and with this and the Stark coefficient, a polarizability anisotropy of 1.85×10^{-24} cm^3 is calculated. The observed rotational constant Bo is 29,725.3 ± 0.1 mC. The microwave spectrum, structure, and dipole moment of $H_3SiC \equiv CH$ is also reported. The rotational constants for the isotopic species, $H_3{}^{28}Si^{12}C \equiv {}^{12}CH$, $H_3{}^{29}Si^{12}C \equiv {}^{12}CH$, $H_3{}^{30}Si^{12}C \equiv {}^{12}CH$, $H_3{}^{28}Si^{13}C \equiv {}^{12}CH$, $H_3{}^{28}Si^{12}C \equiv {}^{13}CH$ were determined to be 4,828.66, 4,775.65, 4,725.65, 4,803.98, 4,662.34 mC/sec, respectively. From these data the structural parameters r_{SiC} = 1.862 Å and r_{CC} = 1.208 Å are determined. If r_{CH} is assumed to be 1.056 Å then r_{SiH} = 1.455 Å, <HSiH = 110.3°. Measurement of the Stark effect leads to a dipole moment of 0.316 D. (Dissertation Abstr.)

3978 PREPARATION OF ^{3}H LABELLED AMINO ACIDS WITH HIGH SPECIFIC ACTIVITY AND STUDIES OF THE STORAGE TIME [Thesis]. Nouvertne, W. Cologne, Univ., 1964. 77p. $2.00 Gmelin, AED-DISS. 64-482.

^{3}H labeling of amino acids by decarboxylation and chain lengthening was studied. Methods of preparation and maximum possible storage times for various compounds are given. (Gmelin Inst.)

3979 POLIMERNYE POKRYTIYA V ATOMNOI TEKHNIKE. (Polymer Coatings in Nuclear Techniques). Tikhomirov, V. B. Moscow, Atomizdat, 1965. 274p.

A brief review is given of the properties, technology and uses of polymer coatings in laboratories using radioactive materials and in atomic industry. Basic data are presented on varnish-type coatings and vaporized coating from suspensions or free masses. Descriptions are given of various types of polymer coatings including epoxides, polyesters, perchlorovinyls, fluoroplastic, silico-organic etc. Special attention was given to the life of polymer coatings in liquid aggressive media. (R.V.J.)

3980 MASS SPECTROMETRIC INVESTIGATIONS OF ISOTOPIC EXCHANGE REACTIONS OF GASEOUS HYDROCARBON IONS. Wexler, S. (Argonne National Lab., Ill.). Vienna, International Atomic Energy Agency, 1965, Preprint No. SM-64/17, 32p. (CONF-650549-12). ORINS.

From IAEA Symposium on Exchange Reactions, Upton, N. Y.

Techniques of high-pressure mass spectrometry were employed to study the exchange of hydrogen isotopes in carbon-containing products of ion-molecule reactions. Comparison of the positively charged mass spectra of $H_2 + CH_4$, $D_2 + CH_4$ and $T_2 + CH_4$ mixtures with those of the individual components, observed for source pressures of approximately 0.1 torr, demonstrated that the CH_3^+ and molecular hydrogen primary ions react rapidly with the other component of the gas mixture to create secondary and tertiary ionic species in which the hydrogen isotopes are extensively exchanged. When methane was added to D_2, the principal species of deuterium, D_2^+ and D_3^+, were almost completely quenched; and $C_2H_4D^+$, $C_2H_3D_2^+$ and $C_2H_2D_3^+$ were formed in high yield. The CH_3^+ ion also reacted readily with D_2 molecules to produce the same deuterated ethyl species. Analogous findings came from a study of $T_2 - CH_4$ systems. The deuterated and tritiated products in $H_2 + CH_4$ mixtures were $C_2H_5^+$-type ions with one, two, or three hydrogen atoms replaced by the heavier isotope. Correspondence of appearance potentials and ionization efficiency curves gave further evidence that D_2^+ and CH_3^+ are the primary precursors of the deuterated ethyl ions. The linear enhancements of the $C_2H_4D^+/C_2H_5^+$, $C_2H_3D_2^+/C_2H_5^+$ and $C_2H_2D_3^+/C_2H_5^+$ intensity ratios observed with increasing deuterium concentration (at constant CH_4 pressure) suggested that the isotopically-exchanged species are produced by a mechanism involving consecutive ion-molecule reactions one kinetic order higher in D_2 concentration than those for formation of $C_2H_5^+$. This was consistent with the analysis of the possible reaction paths, which led to the conclusion that the deuterated species are the products of reactions both first and second order in D_2, and that $C_2H_5^+$ is formed by ionic reactions with both first and zero order dependences on deuterium concentration. The kinetic rates of the isotopic exchange reactions responsible for the rapid diminution of primary species with added opposite component must be within an order of magnitude of the rates of the respective competing reactions for which cross sections of 27×10^{-16} and 41×10^{-16} cm^2/molecule were measured. These cross sections corresponded to the rate constants of 9.9×10^{-10} and 2.9×10^{-9} cc molecule/sec. The isotopically enriched methyl ions must also react very rapidly with D_2 and/or CH_4 to form labeled $C_2H_5^+$ species. (auth)

Radiation Chemistry

See also BIOLOGY AND MEDICINE — Radiation Effects on Biochemicals Radiation Effects on Tissues

Refer also to abstracts 3879 and 4364.

3981 (AERE-R-5051) IRRADIATION OF THE CARBON DIOXIDE-METHANE SYSTEM: THE FORMATION OF FORMALDEHYDE. Hearne, J. A. (Research Group, United Kingdom Atomic Energy Authority, Wantage (England)). Sept. 1965. 14p. Dep.; BIS $0.50; HMSO 2s. 6d.

Carbon dioxide containing 1000 ppM of methane-^{14}C was irradiated with 4 Mev electrons and the yield of formaldehyde-^{14}C determined by liquid scintillation counting of the dimedone derivative. Temperatures were varied from 25 to 400°C, and some experiments were performed with unlabeled methane and the products analyzed for methanol. Initial G values for formaldehyde were in the range 1-6 molecules/100 ev. Addition of 1% CO reduced $G(CH_2O)$. Equilibrium CH_2O concentrations at high doses were about 2 ppM. No methanol was detected. Consideration of mechanisms involving CH_3 and CH_2 radicals indicate that reactions of the latter are largely responsible for CH_2O formation. (auth)

3982 (AGN-8156) FISSIOCHEMICAL DEVELOPMENT PROGRAM. Semiannual Progress Report, January 1–June 30, 1965. Elliott, D. M.; Hamling, B. H.; Kahn, S.; Meisels, G. G.; Miller, R. I.; Osterholtz, F. D. (Aerojet-General Nucleonics, San Ramon, Calif.). Aug. 1965. Contract AT(04-3)-596. 171p. Dep. mn; CFSTI $5.00 cy, $1.00 mn.

The program is concerned with use of fission fragment energy to bring about chemical reactions of interest. The number of fuel atoms per fission ejected from a given fuel source was determined to be 67 to 6200 ejected atoms per escaping fragment for UO_2 plates of varying thickness (in vacuua). The calculated range of U-235 fragments in a U-Pd alloy is 5.77μ based on Cf 252 fragment energy degradation measurements. A study of reaction variables arranged as a Factorial Block Experiment was performed on the N_2-CH_4 system. Effects on product yield were established for various combinations of temperature (250-410°C), pressure (200-395 psig), flow (200-800 cc/min), and CH_4 concentration (5.6-20.2%). Maximum G values (molecules formed per 100 ev of energy deposited) for HCN and CH_3CN were 1.0 and 0.5, respectively. Addition of water vapor, He, or mixed CH_4 radiolysis products had little effect on yield structure. Nitrogen atom formation owing to 1-Mev electron energy absorption in N_2 was found to be about 4.3 atom/100 ev when NO was present. The radiolysis of pure CH_4 led to measured yields (number of species per 100 ev) of CH_4, methyl, and methylene ions and of methyl and methylene radicals of 1.5, 1.5, 0.24, 1.4, and 0.24, respectively. Fissiochemical irradiations of CO-N_2-H_2 mixture generally result in a solid polymeric product with total G_N as high as 2.5. Irradiations of C_6H_6-NH_3 mixtures led to $G_N \sim 1.8$, with less than a third of the fixed N as aniline. Preliminary conceptual design of a plant for the fissiochemical production of HCN indicated that, under the most optimistic conditions, a gross annual return of 32% of capital would be realized. (auth)

3983 (BNL-9589) THERMOLUMINESCENCE INDUCED BY LOW ENERGY ALPHA PARTICLES. Woodley, Robert G.; Johnson, Noye M. (Brookhaven National Lab., Upton, N. Y. Dartmouth Coll., Hanover, N. H. Dept. of Geology). [1965]. Contract AT(30-2)-Gen-16. 13p. (CONF-650637-5). Dep. mn; CFSTI $1.00 cy, $0.50 mn.

From International Conference on Luminescent Dosimetry, Palo Alto, Calif.

Low energy alpha particles are approximately 10–20% as effective as gamma radiation in producing thermoluminescence. Experimental determination was made by irradiating powdered samples of CaF_2 and $CaCO_3$ with polonium-210 alpha particles and by irradiating powdered samples of LiF with thermal neutrons. The thermal neutron irradiation results in the $^6Li(n,\alpha)^3H$ reaction. The geometry of the phosphor crystals was arranged to ensure homogeneous irradiation of the samples. Comparisons were made with equivalent samples which were irradiated with cobalt-60 gamma radiation. The mode of ionization of alpha particles in the materials of this experiment evidently is less efficient than beta or gamma radiation for filling electron traps. (auth)

3984 (ORO-633) INVESTIGATION OF THE PYROLYTIC PRODUCTS OF IRRADIATED CIGARETTES. Boenig, Herman V. (Spindletop Research, Lexington, Ky.). Oct. 1965. Contract AT(40-1)-3268. 36p. Dep. mn; CFSTI $2.00 cy, $0.50 mn.

The smoke of gamma-irradiated and nonirradiated cigarettes was compared. The smoke of the irradiated cigarettes was found to contain less tar and tar-like compounds and fewer free radicals. The actual irradiated cigarettes were found to contain different types of acids and phenols than the nonirradiated cigarettes. Irradiation also was found to reduce the amount of toluene in the smoke. (auth)

3985 (RFP-624) FORTRAN II DATA REDUCTION PROGRAM FOR GAS PHASE RADIOLYSIS STUDIES. Werkema, G. J. (Rocky Flats Div., Dow Chemical Co., Golden, Colo.). Nov. 3, 1965. Contract AT(29-1)-1106. 25p. Dep. mn; CFSTI $2.00 cy, $0.50 mn.

A computer program (RADF) is described whose purpose is to convert analytical data obtained at several times during a gas phase radiolysis experiment into the molar and molecular quantities more useful to the chemist. These quantities are presented in tabular form for each gas, along with the computed radiation dose, as a function of time. (auth)

3986 RADIATION CHEMISTRY. Schwarz, Harold A. (Brookhaven National Lab., Upton, N. Y.). Ann. Rev. Phys. Chem., 16: 347-74(1965). (BNL-8820).

The radiation chemistry of aqueous solutions is discussed according to the types of processes involved (ionic, free radical, etc.). Research in the radiation chemistry, consisting of studies of electron energy loss spectra, ions and ionic reactions, free radical processes, and energy transfer and excited state effects, is discussed. (150 references). (F.J.H.)

3987 THE CHANGES OF POLYMER CRYSTALS DUE TO IRRADIATION WITH ELECTRONS ACCELERATED AT VARIOUS VOLTAGES. Kobayashi, Keinosuke; Sakaoku, Kiichiro (Kyoto Univ.). Bull. Inst. Chem. Res., Kyoto Univ., 42: 473-93(Nov. 1964).

Damages to organic polymer crystals by electron bombardment were studied with a 300-kv microscope. All of the measurements were carried out with the specimen thicknesses permitting only single inelastic collisions of the incident electron. The dose necessary to change the diffraction spots of polymer single crystals into halo rings was constant when the velocity of incident electrons was fixed, and was independent of the dose rate applied. The necessary dose decreased with an increase of the accelerating voltage of the incident electrons in the range from 75 to 300 kv. It was proved that the damage to the specimen is inversely proportional to the energy (ev) of the incident electron. This result suggested that the rate of the secondary reactions was not linearly proportional to the primary events. Cooling of the specimen did not prevent radio-induced defects in it. The decay process of polymer crystals irradiated with electrons is discussed. (auth)

3988 STUDY OF THE NO_3 RADICAL IN SODIUM NITRATE IRRADIATED AT 77 deg K. Adde, Robert (Univ. Paris, Orsay, France). Compt. Rend., 261: 685-8 (July 19, 1965). (In French).

An unstable paramagnetic center in sodium nitrate irradiated with 1.5-Mev electrons at 77°K was studied. The center was attributed to the NO_3 radical. The EPR spectrum was discussed as a function of the electron configuration of NO_3. (tr-auth)

3989 DIELECTRIC PROPERTIES OF IRRADIATED PARAFFIN WAX. Akimune, Hideo; Suita, Tokuo (Osaka Univ.). Denki Gakki Zasshi, 85: 714-21(Apr. 1965). (In Japanese).

Paraffin wax with a melting point of 70°C was irradiated by γ rays at 2×10^5 r/hr in air at room temperature for periods up to 720 hrs. A paraffin sample admixed with palmitostearone $C_{17}H_{35}COC_{15}H_{31}$ was also irradiated. The ketone was expected to play a role as a model compound of the oxidation product produced in the paraffin by the action of high-energy radiation, as indicated by the absorption band at 1720 cm^{-1} in the infrared spectrum of the irradiated paraffin, which corresponds to a carbonyl structure. The dielectric loss tangent and the dielectric relaxation time of the irradiated samples at 3 to 10 Mc were determined in the temperature range from 0 to 52°C. The tan δ of the paraffin was increased considerably by the irradiation and the curve of tan δ vs. temperature has a maximum at 32°C. However, for the sample admixed with ketone, there appeared to be a maximum at 38.5°C before the irradiation, and an additional peak at 32°C after the irradiation. The tan δ of the ketone-containing sample at 38.5°C decreased as the radiation dose increased. The activation energies for the orientation of the ketone molecules are 14.0 and 29.0 kcal/mole for the irradiated paraffin and the unirradiated palmitostearone-containing sample, respectively. This difference may be due to the fact that the ketone molecules produced by the oxidative action of the radiation are surrounded by the amorphous region, while the molecules of the admixed ketone are embedded in the crystalline region. The crosslinking/degradation ratios, calculated from the tan δ data, are $<0.54 \times 10^{-10}$/rad and 3.3×10^{-10}/rad for the crystalline region and the amorphous region, respectively. (NSA of Japan)

3990 LUMINESCENCE PHENOMENA IN GAMMA-IRRADIATED PURE ALKANE GLASSES: RELAXATION MECHANISMS. Funabashi, Koichi; Herley, Patrick J.; Bueton, Milton (Univ. of Notre Dame, Ind.). J. Chem. Phys., 43: 3939-47(Dec. 1, 1965).

It was shown previously that gamma irradiated pure 3-methylpentane glass at 77°K emits a characteristic luminescence according to a law, which can be expressed as the sum of three first-order decays. In this work on both 2-methylpentane and 3-methylpentane, it is shown: that the two pentanes emit at 77°K, as nearly as can be established, in precisely the same fashion; that the intensity of luminescence is decreased and the decay curve is flattened by permitting the glassy sample to relax at 77°K between vitrification and gamma irradiation; that the decay law at both 77 and 90°K is the sum of three first-order decay laws; that the activation energies, as established by fixed-temperature measurements at those two temperatures, are all near 0.04 (±0.01) ev, but that the characteristic frequencies of the three laws vary by a factor of $\sim 10^2$; that, in addition, to light, which appears isothermally at 77°K and, is stimulated also by infrared irradiation, there is a glow portion which appears only at temperatures near 100°K; that while the long-wavelength portion of the luminescence spectrum is unaffected by the treatment to which the sample is subjected, there are significant changes in the shorter wavelength region on prolonged irradiation; that at least two different kinds of electron traps are involved; that chemical products are involved in the luminescence; and that in gamma-sensitized luminescence as well as in radiation chemistry, radiolytic products play an important role in determination of the elementary processes responsible for the effects observed. (auth)

3991 RELATIVE RADIATION STABILITY OF SOME PARA-POLYPHENYLS. Amemiya, Ayao; Matsuzawa, Michio (Tokyo Univ.). J. Nucl. Sci. Technol. (Tokyo), 2: 363-8(Sept. 1965).

The cross sections for excitation of π electrons in para-polyphenyls by electron impact are calculated by means of the Born approximation, using the free electron model and Davydov's exciton theory. The results indicate that the relative radiation stability of para-polyphenyls tends toward a certain value as the number of benzene rings involved in para-polyphenyl increases. Qualitative agreement with experiment is obtained in a satisfactory manner. (auth)

3992 RADIATION-INDUCED POLYMERIZATION OF 1,2-CYCLOHEXENE OXIDE. Cordischi, D.; Lenzi, M.; Mele, A. (Univ., Rome). J. Polymer Sci. Pt. A, 3: 3421-6(Oct. 1965).

Radioinduced polymerization of 1,2-cyclohexene oxide was investigated in the liquid and in the solid state. Addition of water drastically reduced the rate of polymerization and the molecular weight of the obtained polymer. The results were interpreted according to an ionic mechanism. (auth)

3993 PROBLEMS OF TECHNOLOGICAL PARAMETERS OF RADIOCHEMICAL APPARATUS. Seliga, Mojmir (Lab. of Polymers, Slovak Academy of Sciences, Bratislava). Jaderna Energie, 11: 263-7(July 1965). (In Czech).

A theoretically sound method of calculating the basis parameters of the characteristics of the interaction of gamma radiation with a reaction system is given. From these quantities the radiation-chemical yield was calculated. The method derived was applied to the calculation of the basic parameters for the radiation-chemical synthesis of γ-chloropropylsilane. The calculations were carried out by an approximate method which; however, was proved to give results not very different from the more exact and more complicated one. (TTT)

3994 OXYGEN EFFECT AND TEMPERATURE DEPENDENCE OF FLUORESCENCE INTENSITY IN NAPHTHALENE SCINTILLATORS. Kobayashi, Shigeo; Hayakawa, Sohachiro (Tokyo Inst. of Tech.). Jap. J. Appl. Phys., 4: 881-5(Nov. 1965).

In solution scintillators with molten naphthalene as a solvent, fluorescence quenching by dissolved oxygen and the temperature dependence of light output were studied with excitation by gamma rays and uv radiation. The fluorescent solutes are PPO, BBO, POPOP, QP, DPH, and DPS. Dissolved oxygen can be removed rapidly by bubbling nitrogen. Quenching by oxygen is shown to be in competition with energy transfer from solvent to solute. It was estimated that the lifetime of excited molecules in molten pure naphthalene is almost doubled by removal of oxygen. The bubbling of nitrogen increased the fluorescence intensities of solutions by 20 to 40%. The negative temperature coefficients of light output of naphthalene solutions were $2-7 \times 10^{-3}$/°C, independent of excitation modes. The fluorescence intensities of the solutions equilibrated with air remained almost constant over the temperature range from 80 to 130°C. (auth)

3995 GRADUAL INCREASE OF COERCIVE FIELD OF X-IRRADIATED ROCHELLE SALT. Abe, Ryuji (Nagoya Univ., Japan). Jap. J. Appl. Phys., 4: 906-10 (Nov. 1965).

The aging of x-irradiated rochelle salt was studied through the change of coercive field at very low frequencies. The increase of coercive field just after x-irradiation was almost independent of frequency. This result can be explained if it is assumed that the radioinduced defects decrease the domain wall velocity through a certain interaction between the wall and the defects. The coercive field gradually increased at room temperature for 3 or more weeks after x-irradiation. This phenomenon should be closely related to Okada's observation in which two dimensional thin cavities were seen on crystallographic basic planes when the x-irradiated crystal was annealed at 40°C for about 3 hours. (auth)

3996 RADIATION-INDUCED GRAFT COPOLYMERIZATION OF METHYLMETHACRYLATE ON POLYETHYLENE IN AN EMULSION SYSTEM. Watanabe, Tsutomu; Ito, Isamu (Sumitomo Bakelite Co., Ltd., Yokohama, Japan). Kogyo Kagaku Zasshi, 68: 552-7(Mar. 1965). (In Japanese).

The ^{60}Co γ-induced graft copolymerization of low-

molecular weight polyethylene latex and methylmethacrylate monomer was conducted. The reactants formed an emulsion. The influence of the addition of ferrous ion on polymerization and grafting rates was studied. The initial rate was considerably reduced by the addition of ferrous ion, probably because of the diminution of the amount of hydroxyl radicals available through a redox process. Total polymerization and grafting rates increased with increasing monomer concentration and radiation intensity. Dose rates of 2×10^3 to 1×10^5 were used. These results could not be explained by the reaction mechanism proposed for typical chemically catalyzed emulsion polymerization. The marked reduction of the degree of grafting during prolonged irradiation must be attributed to degradation of the grafted poly(methylmethacrylate) branch. To explain shifting of optimum dose, which gives a maximum degree of grafting, with the radiation intensity, competition of propagation with degradation of the poly(methylmethacrylate) branch is assumed to occur. (BBB)

3997 RADIATION-INDUCED COPOLYMERIZATION OF CARBON MONOXIDE WITH α-OLEFINES; SUCH AS PROPYLENE, BUTENE-I, AND ISOBUTYLENE. Hamanoue, Kumao (Kyoto Univ.); Tabata, Yoneho. Kogyo Kagaku Zasshi, 68: 700-2(Apr. 1965). (In Japanese).

Radioinduced polymerization of carbon monoxide with α-olefines (propylene, butene-1, and isobutylene) was carried out both at room temperature and –78°C in single liquid phase or vapor-liquid mixed phase. Resulting polymers were grease-like materials, and the structure of the polymer was that of a typical polyketone. In the carbon monoxide-propylene system, the polymerization was not preceded by an induction period and the yields increased linearly with the radiation dose. The rate of polymerization was increased by increasing the concentration of carbon monoxide, and decreased by decreasing the temperature. On the other hand, the molecular weight of polymer decreased with the concentration of carbon monoxide. From elementary analysis, the ratio of propylene to carbon monoxide in the polymer was determined to be 1.3 to 1.4. The propylene-carbon monoxide polymer was soluble in methyl ethyl ketone, acetone, and a large amount of benzene. (auth)

3998 ELECTRON-MICROSCOPIC STUDIES ON FORMATION OF CROSSLINKING IN POLYETHYLENE SINGLE CRYSTALS BY ^{60}Co γ-RAY IRRADIATION. Urabe, Masayoshi; Fukuda, Takashi (Kyushu Univ., Japan). Kuyushu Daigoku Kogakuba Kogaku Shuho, 37: 367-72(Jan. 1965). (In Japanese).

Crystallographic and morphological studies were carried out on the radiation-crosslinked polyethylene single crystals by electron-diffraction and electron-microscopic techniques. The single crystals were irradiated with ^{60}Co γ rays at a dose rate of 5×10^5 r/hr at room temperature, suspended in the mother solution in which the single crystals had a hollow, pyramidal structure, or after drying on a collodion film where the pyramidal structure became flattened. The total doses given were up to 455 Mr. As the radiation dose increased, the interference spots in the electron diffraction disappeared, successively, beginning with spots of higher order. A plot of the logarithm of radiation dose vs the highest order recognizable at the given radiation dose gave a straight line, which crossed the axis of abscissa at about 1000 Mr; the crystallinity disappeared completely at this point. A slight deviation of a lattice constant (an axis) was observed. The relative difficulty of the movement of the chain segments in the irradiated single crystals was demonstrated by the absence of the thickening effect, observed in the heat treatment of unirradiated polyethylene single crystals above 110°C, and also by the infusibility of the irradiated single crystals at 133°C. The fiber structure observed in the single crystals cleaved by ultrasonic irradiation could not be recognized in single crystals irradiated with γ rays to 20 Mr. It is shown by the appearance of lines parallel to (110) on the corrugation parallel to (310) in the single crystals irradiated as pyramidal structure and then flattened that the crosslinkings are formed predominantly at first in (110) lattices. (NSA of Japan)

3999 DEGRADATION OF POLYTETRAMETHYLENE OXIDE. II. IONIZING RADIATION. Golden, J. H. (Explosives Research and Development Establishment, Waltham Abbey, Eng.). Makromol. Chem., 81: 51-6 (1965).

The solubility and viscosity characteristics of the polymer after electron irradiation were examined. Polytetramethylene oxide polymerization was carried out in the presence of air; the final polymer film had an intrinsic viscosity of 3.97 and molecular weight of 570,000. Samples were exposed to a linear accelerator electron beam (4 Mev) at a dose rate of 1.04 Mrad/min. Doses varied from 6.4 to 800 Mrad. After an initial reduction in viscosity, the polymer crosslinked to form a tough translucent film which, on further irradiation, became brittle and slightly yellow. Infrared analysis (2 to 15 μ) revealed no significant changes. Mass spectrographic analysis of the gases evolved after a dose of 500 Mrad showed the presence of hydrogen (98%) together with traces of carbon monoxide, ethylene, and higher hydrocarbons. The swelling of the irradiated polymer specimens in benzene at 20°C and the corresponding gel fractions are tabulated. The ratio of chain scission to crosslinking was found to be 0.37. An approximate value of G(X), the number of crosslinks formed per 100 ev of energy absorbed, is 0.93. The behavior of polytetramethylene oxide on irradiation is similar to that of polyethylene oxide, which also undergoes chain scission and crosslinking (ratio 0.6). Since polymethylene oxide undergoes exclusive chain scission and polyethylene crosslinks, scission must take place primarily at the weaker C–O bond, and the lower ratio of scission to crosslinking, which occurs in polytetramethylene oxide, can be attributed to the fact that the C–O/C–C ratio is lower in this case than in polyethylene oxide. The gases evolved during irradiation consist almost entirely of hydrogen and, assuming the rate of evolution to be linear with dose, a value of $G(H_2) = 0.8$ was calculated from the volume evolved after a radiation dose of 500 Mrad. This hydrogen probably arises from the formation of crosslinks, since no unsaturation, as found in irradiated polyethylene, was detected in irradiated polytetramethylene oxide. (BBB)

4000 THERMAL-NEUTRON-INDUCED RECOIL DEFECTS IN CADMIUM SULFIDE. Oswald, Robert B. Jr.; Kikuchi, Chihiro (Univ. of Michigan, Ann Arbor). Nucl. Sci. Eng., 23: 354-60(Dec. 1965).

The production of defects by thermal neutrons in CdS results from the recoil of an energetic ^{114}Cd nucleus. The recoil results from prompt emission of 9 Mev of gamma energy following thermal-neutron capture by ^{113}Cd through the nuclear reaction: $^{113}Cd + n_{th} \rightarrow (^{114}Cd)^* \rightarrow {}^{114}Cd + \gamma$. The changes in the optical and electrical properties of CdS were measured to determine the effect of such recoils. A recombination center for the 7200A emission is produced and both the 4880A emission and edge emission are reduced. In addition, the conductivity of initially conducting CdS crystals is decreased by many orders of magnitude. The temperature dependence of the conductivity of thermal-neutron irradiated crystals indicates the production of a state about 0.5 ev below the conduction band. (auth)

4001 RADIOLUMINESCENCE OF STYRENEMETHYLMETHACRYLATE COPOLYMERS. Polacki, Zenon; Grodel, Mar'yan. Nukleonika, 10: 469-76(1965). (In Russian).

The concentration dependence of the radioluminescence efficiency of solutions of styrene in methylmethacrylate were studied before and after polymerization. Conclusions were drawn indirectly from the measurements of the relative light emission intensity of 2-(1-naphthyl)-5-phenyloxazole, which was added to the solutions as an admixture with unchanged concentration. With dilution of styrene by methylmethacrylate the radioluminescence intensity decreased, thus methylmethacrylate can be considered as absorbing substance causing the quenching of radioluminescence. It was established that the radioluminescence efficiency of solutions of 80% styrene and 20% methylmethacrylate was equal to that of polystyrene solutions. (auth)

4002 THE EFFECT OF CRYSTALLIZATION CONDITIONS ON RADIATION-INDUCED CROSSLINK FORMATION IN POLYETHYLENE. PART I. THE BASIC RADIATION-SOLUBILITY RELATIONSHIP. Kawai, T. (Univ. of Bristol, Eng.); Keller, A.; Charlesby, A.; Ormerod, M. G. Phil. Mag. (8), 12: 657-71(Oct. 1965).

The decrease in solubility with radiation dose was measured in bulk Marlex 50 polyethylene and in a series of solution-crystallized polyethylene prepared under different conditions. It was found that the solubility-dose curves were all of a similar shape and could be superimposed by multiplying the radiation doses given to each sample by a constant factor which is a measure of the effectiveness of the radiation. The bulk material needed the lowest gelation dose while the gelation dose for the solution-crystallized specimens depended on the method of preparation. Measurements of hydrogen gas evolution and free radical formation indicated that these results could not be explained by differences in the overall number of crosslinks formed. They can be explained by assuming that there are effective and ineffective crosslinks and the relative numbers of these are a function of crystallization conditions. The results are in accord with the hypothesis that crosslinks are formed preferentially at the chain folds at lamellar surfaces and that the effective and ineffective crosslinks are inter- and intra-lamellar crosslinks respectively. The amount of inter-lamellar contact is reflected by the degree of effectiveness of the radiation. (auth)

4003 THE EFFECT OF CRYSTALLIZATION CONDITIONS ON RADIATION-INDUCED CROSSLINK FORMATION IN POLYETHYLENE. PART II. THE EFFECT OF LAMELLAR PACKING AND INTER-LAMELLAR TIES. Kawai, T.; Keller, A. (Univ. of Bristol, Eng.). Phil. Mag. (8), 12: 673-9(Oct. 1965).

The effect of lamellar packing in polyethylene single crystals on radiation-induced crosslinking was examined. The stacks of crystal layers were systematically loosened and dispersed by ultrasonic treatment. This led to large reductions in the radiation-induced insolubility with only slight change of molecular weight. It could be shown that even these small changes had no effect on the gelation which accordingly was entirely due to the state of aggregation of the lamellae. This is in agreement with the proposition that the links which lead to networks are the ones between lamellae. It was concluded that initially molecular links between layers are scarce even in the compact unirradiated crystals and attention is drawn to the fold surface as a possible source of cohesion. Some new observations on the morphology of compact crystals and results on their irradiation while in suspension are reported relevant to the problem of lamellar packing. (auth)

4004 THE EFFECT OF CRYSTALLIZATION CONDITIONS ON RADIATION-INDUCED CROSSLINK FORMATION IN POLYETHYLENE. PART III. FREE RADICAL FORMATION AND REACTIONS. Ormero, M. G. (Royal Military Coll. of Sciences, Swindon, Eng.). Phil. Mag. (8), 12: 681-6(Oct. 1965).

It was previously found that the decrease in solubility of single crystal polyethylene with high energy radiation dose was different from that in the bulk material. The radiation dose needed to obtain gelation also depended on preparation conditions. As part of a series of experiments investigating these effects electron spin resonance spectroscopy was used to study free radical formation in irradiated single crystal and bulk polyethylene. It was found that the radical yields were the same in all the polyethylene preparations studied. It was also found that the rate of alkyl radical decay at room temperature depended on the crystallization conditions and the pre-irradiation annealing. The longer the crystal long spacing, the more stable were the radicals. (auth)

4005 THE EFFECT OF CRYSTALLIZATION CONDITIONS ON RADIATION-INDUCED CROSSLINK FORMATION IN POLYETHYLENE. PART IV. ANNEALING AND CROSSLINK FORMATION IN SINGLE CRYSTALS. Kawai, T.; Keller, A. (Univ. of Bristol, Eng.). Phil. Mag. (8), 12: 687-92(Oct. 1965).

Annealing treatment before irradiation was observed to change the radiation-induced gelation behavior of single crystals. After a decrease on short annealing times the gel content increases on prolonged annealing and approaches the behavior of the bulk. Variations in lamellar contact are invoked to account for this behavior. In other experiments single crystal samples were first irradiated and subsequently annealed. It was found that even a high degree of crosslinking which might be expected to immobilize the chains did not prevent re-folding. The conclusion is reached that the folds are preferential sites where the crosslinks form, the ineffective ones giving rise to small rings which can thread through the lattice on re-folding. Lattice distortions are expected to occur during this process and are in fact indicated by the x-ray diffraction pattern. (auth)

4006 THE EFFECT OF CRYSTALLIZATION ON THE RADIATION-INDUCED CROSSLINKING IN POLYETHYLENE. PART V. THE SOLUBLE CROSSLINKED MOLECULE. Kawai, T.; Keller, A. (Univ. of Bristol, Eng.). Phil. Mag. (8), 12: 699-18(Oct. 1965).

Polyethylene irradiated by doses below the gelation level, hence where the sample is still fully soluble by our tests, was examined in regard to viscosity, light scattering and recrystallization behavior. In the course of this the molecular dispersion of the material previously designated as soluble was verified. The intrinsic viscosities pass through a minimum followed by a maximum with increasing dose while light scattering indicates steadily increasing molecular weight, this increase being in the expected relation to the appropriate gel points. On irradiation the molecular weight distribution widens and the molecules become more compact, increasingly so with the larger molecules. It is concluded in conjunction that there can be only very little if any crosslinking between molecules in a given layer and that the crosslinks which lead to an increase of the molecular weight even below the gel point must be those which link the different layers together. Most of the ineffective links should be in the fold and some could be multiple ones between molecules in consecutive layers. Accordingly crosslinking must be highly selective and the type of selectivity inferred here demands regularity at the fold surface. (auth)

4007 GAMMA IRRADIATION POLYMERIZATION OF ACRYLONITRILE IN THE PRESENCE OF SOLID ADDITIVES. Provoost, F. (Studiecentrum voor Kernenergie, Mol-Donk, Belg.). Polymer, 6: 515-21(Oct. 1964).

An attempt was made to polymerize acrylonitrile under gamma radiation at 26 and −78°C in the presence of additives having various electric properties, chemical compositions, and specific surface areas. In the liquid phase the rate of polymerization was greatly increased by the presence of additives having a large specific surface area. The factors responsible for this are discussed and the probable mechanism considered. (auth)

4008 RADIATSIONNAYA FIZIKA. III. IONNYE KRISTALLY. (Radiation Physics. III. Ionic Crystals). Kristapson, Ya. Zh. (ed.). Riga, Izdatel'stvo Zinatne, 1965. 157p.

A survey is given of the composition of radiation defects and the process of energy transfer from the basis material to the luminescence centers during excitation by u-v light and ionizing radiation. The electric properties of irradiated crystals (ion conduction and electron emission) are treated. Studies made of the microstructure of impurity centers using EPR, the energy structure of luminescence centers, and the kinetics of internal-center luminescence are presented. The process of radiolysis of alkali–halide crystals under the action of large doses of reactor and gamma radiation is considered. Work on the determination of the purity of crystals using the neutron-activation method is discussed. Sixteen articles are included. (tr-auth)

4009 RADIATION-INDUCED OXIDATION OF Sb(III) IN AQUEOUS SOLUTION. [PART] III. Matsuura, Niro;

Kurimura, Yoshimi; Takizawa, Masao (Inst. of Physical and Chemical Research, Tokyo). Rika Gaku Kenkyusho Hokoku, 38: 41-4(1962). (In Japanese).

In a study of the γ-induced oxidation of Sb(III) in aerated 0.8N H_2SO_4 solution the dilution effect of solute Sb(III) on yield of the reaction was examined. The samples were irradiated at a dose rate of 2.60×10^4 r/hr at about 20°C. The yield, G(−Sb(III)), of the radiolytic oxidation product Sb(V) was found to decrease with decreasing concentration. It was 2.10 at 0.52×10^{-4}M Sb(III), 3.30 at 9.15×10^{-4}M, 2.90 at 1.77×10^{-4}M, and 2.65 at 1.05×10^{-4}M. These G(−Sb(III)) values could be expressed by the empirical equation: $G(-Sb(III)) = 1.5 + 1.9/\{1 + (8 \times 10^{-5})/[Sb(III)]\}$. Reactions for the oxidation in this system are: $Sb(III) + OH + H^+ \rightarrow Sb(IV) + H_2O$; $Sb + HO_2 + H^+ \rightarrow Sb(IV) + H_2O_2$ (reaction 3); and $Sb(IV) + Sb(IV) \rightarrow Sb(III) + Sb(V)$. The decrease in G(−Sb(III)), especially at solute concentration of lower than 2×10^{-4}M, represents the onset of the bimolecular recombination of HO_2: $HO_2 + HO_2 \rightarrow H_2O_2 + O_2$ (reaction 5), which then competes with reaction (3). If all the HO_2 disappears by either (3) or (5), the probability for (3) is $1/\{1 + k_5[HO_2]/k_3[Sb(III)]\}$, where k_3 and k_5 are the rate constants for (3) and (5) respectively, and $[HO_2]$ is the concentration of HO_2. Then the following relations hold: $G(-Sb(III)) = 1/2G_{OH} + 1/2G_H/\{1 + k_5[HO_2]/k_3[Sb(III)]\}$; $1/2G_{OH} + 1/G_{HO_2}$ (or G_H) = 3.4; and $1/2G_{OH} = 1.5$. Values of G_{OH} and G_H calculated from the last two relations are 3.0 and 3.8, respectively, and $k_5[HO_2]/k_3 = 8 \times 10^{-5}$ mole/l. (BBB)

4010 A NOTE ON THE CROSSLINKING OF POLYETHYLENE BY HIGH ENERGY RADIATION. Shinohara, Kenichi (Inst. Phys. and Chem. Res. (Tokyo). Sci. Pap. Inst. Phys. Chem. Res. (Tokyo), 59: 101-5(Sept. 1965).

The temperature dependence of the G value of crosslinking of polyethylene is discussed. It is shown that, if the cage effect is taken into account, the temperature-independent behavior of G value below the glass transition temperature and the exponential rise above the same temperature can be explained. An explanation is also given on the increase of the G value of crosslinking by irradiation in an atmosphere of N_2O. (auth)

4011 γ-RAY-INDUCED OXIDATION OF LIQUID METHANOL. Imamura, Masashi; Seki, Hiroshi (Inst. Phys. and Chem. Res. (Tokyo)). Sci. Pap. Inst. Phys. Chem. Res. (Tokyo), 59: 146-51(Sept. 1965).

Gamma-induced oxidation with oxygen of liquid methanol and of aqueous methanol solutions was investigated. The high radiolytic yield of formaldehyde at a comparatively small dose for aerated or oxygenated methanol was found to decrease with increasing dose and increasing oxygen concentration. General reaction mechanisms are discussed. (auth)

4012 FREE RADICALS OF γ IRRADIATED OLEFINOORGANIC SILICATES. Burushina, T. N.; Chuiko, A. A. (Pisarzhevskii Inst. of Physical Chemistry, Kiev). Teor. Eksp. Khim., 1: 394-9(May-June 1965). (In Russian).

The effects of γ radiation on the olefinoorganic silicates

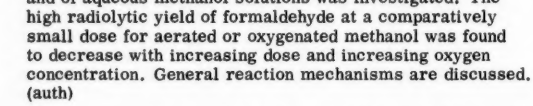

and 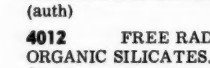 were investigated. Each of the irradiated silicates revealed a characteristic EPR spectrum with a hyperfine structure. The splitting between components of the hyperfine structure in the EPR spectrum, after exclusion of the spectrum of phenyl silicates, was 23 to 25 Oe, which is characteristic of the alkyl radicals. The change of the temperature of the sample during recording of the spectra from −196 to 20°C improved the resolution of the spectral lines. The high thermal stability of the radicals indicated their surface bonds. Contact of the irradiated samples with air at 20°C led to the conversion of the alkyl radicals to peroxides. In all spectra, except the spectrum of allyl silicate, 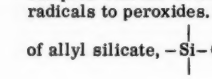 , hyperfine splitting on the hydrogen atom ($\Delta Hp \cong 500$ Oe) was observed. (tr-auth)

4013 EVIDENCE FOR DISSOCIATIVE ELECTRON ATTACHMENT IN γ-IRRADIATED HYDROCARBON GLASSES. Gallivan, J. B.; Hamill, W. H. (Univ. of Notre Dame, Ind.). Trans. Faraday Soc., 61: 1960-7(Sept. 1965).

The γ-radiolysis of toluene and homologous compounds in dilute solution in 3-methyl pentane at 77°K was investigated. For substituents X the evidence indicates that $RX + e \rightarrow R + X^-$ is an efficient process for electrons of thermal energy when the electron affinity of X exceeds the bond dissociation energy of R−X. Other modes of producing R were much less efficient under the conditions used. (auth)

4014 ENERGY TRANSFER EFFECTS IN THE IRRADIATION OF BENZENE + BUTENE-2 MIXTURES. Cundall, R. B.; Griffiths, P. A. (Nottingham Univ., Eng.). Trans. Faraday Soc., 61: 1968-80(Sept. 1965).

The geometrical isomerization of cis- and trans-butene-2 solutions in benzene brought about by γ-rays and fast electrons is due to a triplet-triplet energy interchange from an excited state of the benzene. Comparison with the corresponding photochemical reaction supports this mechanism and suggests that the $^3B_{1u}$ state of benzene is involved. A number of additives were examined and relative quenching efficiencies measured for oxygen, galvinoxyl, naphthalene, anthracene, iodine, butadiene, cyclohexene, tetracyanoethylene, butene-1, isobutene, cis- and trans-butene-2. A study of the effect of temperature suggests that the excitation is delocalized in domains and that the benzene triplet is deactivated by perturbations in the liquid. A very short lifetime for the benzene triplet, less than 10^{-7} sec, is required by marked dependency of the isomerization upon additive concentration. (auth)

4015 EFFECTS OF HIGH ENERGY IONIZING RADIATION ON COLLOIDAL SYSTEMS AND SUSPENSIONS. Grune, Werner N. (Merrimack Coll., North Andover, Mass.). Water Sewage Works, 112: 262-7(July 1965).

In a study of the effect of high-energy ionizing radiation on solid-liquid systems, i.e., lyophilic and lyophobic sols and suspensions, significant parameters were evaluated before and after exposure of these systems to radiation. To evaluate the influence of radiation on the stability of the colloidal system, experiments were carried out with carefully controlled lab dispersions. Initial studies were conducted with x rays using an aluminum oxide sol, prepared by spontaneous peptization methods and characterized by determination of pH, conductivity, turbidity, concentration, and electrophoretic mobility. Radiation doses up to 30,000 R had little or no perceptible effect on the aluminum oxide sol. A threshold value of radiation dose was found to exist at which a Fe_2O_3 sol coagulates sufficiently to permit settling. When 1.04×10^5 R was delivered, the turbidity, expressed as percent transmittance, of the control sol was 2.9 as compared to 1.5 for the irradiated sample. Though the sol did not coagulate sufficiently to induce settling, comparison with the turbidity of the control revealed that some coagulation did occur. Aerosols of solid particles of such substances as polymethacrylate, sodium chloride, and silica, prepared by atomization of dilute solutions and suspensions, after exposure to x radiation showed significantly reduced electrostatic charges. The carrier gas had a pronounced effect on the discharging of silica aerosols exposed to ionizing radiation. When air and helium were used as carrier gases the total positive electrostatic charge on the particles was reduced by ~75 and 80%, respectively. However, with argon as the carrier gas the total positive electrostatic charge on the aerosol was reduced by only about 25% upon exposure to x radiation. Radiation doses up to 30,000 R appeared to exert no measurable effect on aluminum oxide sols prepared by spontaneous peptization methods. With ferric oxide sols, radiation doses up to 120,000 R appeared to induce some coagulation as exhibited by doubling the transmittance from 2.9 to 1.5% for the control and the irradiated sample, respectively. The smaller aerosol particles were discharged preferentially by ionizing radiation. This is so despite the fact that all the particles in the size range studies are believed to carry only single charges. (BBB)

4016 AMINO ACID CHANGES IN CATTLE INSULIN BY UV-IRRADIATION. Siebert, W.; Fiore, C.; Dose, K. (Max-Planck-Institut fuer Biophysik, Frankfurt am Main). Z. Naturforsch., 20b: 957-9(Oct. 1965). (In German).

In the uv-irradiation (2537 Å) of Zn insulin, a direct correlation between the inactivation and the photoreduction of one of the three disulfide breaks was observed for small doses (up to 10 Einstein/mol). With increasing dose the quantum yield for the reduction of the disulfide rates (formation of SH groups) was very small, and other processes lead to increased photochemical perturbation of the disulfide break. For large radiation doses (over 100 Einstein/mol) extrapolation showed that for the complete inactivation of the insulin three cysteine radicals must be destroyed. Of the usual amino acids, only the trysine fraction was significantly reduced by doses of about 100 Einstein/mol. With increasing radiation dose the photosensitivity of the acids changed, probably as a result of the conformation changes of the polypeptide chains. (tr-auth)

4017 ON THE γ RADIOLYSIS OF HYDROGEN SULFIDES IN ALL AGGREGATE STATES. Meissner, G.; Henglein, A. (Hahn-Meitner-Institut fuer Kernforschung, Berlin). Z. Naturforsch., 20b: 1005-6(Oct. 1965). (In German).

The radiolysis yield of H_2, S, and H_2S_2 from H_2S in the gaseous, liquid, and solid states was determined. The effects of dissolved benzene, N_2O, methylmethacrylate, carbon tetrachloride, and carbon disulfide on the H_2 yield were investigated. The possible occurrence of various processes to explain the variation in the hydrogen yield was considered. (J.S.R.)

4018 EFFECTS OF ^{60}Co γ-RAY ON PHARMACEUTICAL POWDERS. I. ON THIAMINE HYDROCHLORIDE MIXED WITH CALCIUM CARBONATE AND DIBASIC CALCIUM PHOSPHATE. Takahashi, Tomoo. Yakugaku Zasshi, 85: 804-8(Sept. 1965). (In Japanese).

The effects of γ rays from ^{60}Co on thiamine hydrochloride powder, mixed with calcium carbonate and dibasic calcium phosphate, were about the same as when the powder was warmed. The decomposition of thiamine hydrochloride was accelerated. This effect of acceleration was in proportion to the dilution of the powder and the radiation dose. By calculating the specific inactivation dose from the residual rate curve obtained from the powder of low concentration, the decomposition rate of thiamine hydrochloride in powders of high concentration by optional dose of γ rays can be predicted. The effects of sodium chloride added as a stabilizer to the powder of thiamine hydrochloride, mixed with dibasic calcium phosphate, appeared to counteract the effects of γ irradiation or warming. These results seemed to indicate the possibility that γ rays could be used effectively for stability test of powdered drugs. (auth)

4019 EFFECTS OF ^{60}Co γ-RAY ON PHARMACEUTICAL POWDERS. II. ON METHYL LINOLEATE MIXED WITH LACTOSE. Takahashi, Tomoo; Ishihara, Shinichi. Yakugaku Zasshi, 85: 808-11(Sept. 1965). (In Japanese).

Effect of γ rays from ^{60}Co on methyl linoleate mixed with lactose was the same as the effect from warming it in the presence of air. The oxidative decomposition of the methyl linolate was accelerated. This effect was proportional to the dilution of the powder and dose of irradiation. By calculating the specific inactivation dose from the residual rate curve obtained from the powders of low concentration, the decomposition rate of the linoleate in powders of high concentration by optional doses of γ ray can probably be predicted. These results indicated that γ rays could be used effectively for stability tests even in the case of powdered drugs of a lipoid nature. (auth)

4020 MODIFICATIONS OF CRYSTALLINE SUGARS BY ROENTGEN RADIATION. Geissler, G. (Universitaet, Bonn). Z. Lebensm. Untersuch. Forsch., 125: 452-7 (1964). (In German).

Samples of D-glucose, D-fructose, D-galactose, and sucrose were irradiated with 55-kv x rays, and examined after doses of 6×10^6, 12×10^6, 24×10^6, 48×10^6, and 96×10^6 R. Changes in the color of samples were tabulated. The melting points of irradiated samples and pH of 1% aqueous solutions uniformly decreased from the values for unirradiated samples. The values for unirradiated samples and those irradiated with 96×10^6 are, respectively: glucose, 148 and 127°C, pH 6.01 and 3.23; fructose, 103 and 78°C, pH 5.83 and 3.41; galactose, 161 and 135°C, pH 5.92 and 3.68; sucrose, 185 and 104°C, pH 6.08 and 3.22. The decrease in glucose concentration was determined by oxidation of glucose to yield H_2O_2, which oxidizes o-dianisidine hydrochloride to a dye estimated at 436 μ. The decrease in glucose concentration in crystalline glucose is reported as % for the following doses: 6 Mr, 5.3%; 12 Mr, 9.2%; 24 Mr, 10.7%; 48 Mr, 14.6%; and 96 Mr, 16.5%. (BBB)

4021 KINETICS AND SENSITIZATION OF AMMONIA RADIOLYSIS IN GASEOUS PHASE UNDER FAST ELECTRON IRRADIATION. Sorokin, Yu. S.; Pshezhetskii, S. Ya. (Karpov Inst. of Physics and Chemistry, Academy of Sciences, USSR). Zh. Fiz. Khim., 39: 1955-9(Aug. 1965). (In Russian).

The kinetics of the radiolysis of ammonia and the formation of hydrazine in the gaseous phase were investigated under the effects of fast electron irradiation. With an increasing pressure, the order changed from first to zero. The activation energy of the reaction approached 1 kcal/mol. The reaction kinetics were interpreted on the basis of elementary processes with the participation of the NH_2 radical. The sensitization of ammonia radiolysis with inert gases and propylene was investigated. The transfer of the energy from the inert gas to ammonia occurred with an efficiency of approximately 80%. Propylene in the quantity of several per cent increased the formation of hydrazine and suppressed the radiolysis reaction of ammonia, leading to the formation of molecular nitrogen and hydrogen. The effect of propylene was connected with the capture of atomic hydrogen and radicals. (tr-auth)

4022 METHOD AND EQUIPMENT FOR INVESTIGATIONS OF THE ELECTRIC FIELD EFFECT ON RADIOLYLIS OF GASES. Larin, I. K.; Tal'roze, V. L. (Inst. of Chemical Physics, Academy of Sciences, USSR). Zh. Fiz. Khim., 39: 2071-2(Aug. 1965). (In Russian).

A method making it possible to investigate separately the products of volumetric and heterogeneous recombination of ions formed during the radiolysis of gases was constructed and tested. There was superposition of an electric field on the reacting volume and spatial separation of the products of the volumetric and heterogeneous recombinations. (tr-auth)

4023 RECOIL TRITIUM REACTIONS WITH CHLOROCARBONS [Thesis]. Tang, Yi-noo. Lawrence, Kan., Univ. of Kansas, 1964. 256p.

Recoil tritium reactions with CH_3Cl, C_2H_5Cl, iso-C_3H_7Cl, and CH_2Cl_2 were carried out with pressure and phase as the variables. Three of the main hot products observed from each system are HT, tritium-labeled parent molecule, and T-for-Cl substitution products. Olefins and radicals are also detected as hot products. Variation of the gas pressure during irradiation shows that most of the yields are pressure dependent in a manner consistent with the assumption that excited species produced from hot tritium reactions decompose by molecular elimination or bond-breakage to give olefins or radicals. Measurements in the liquid phase indicate that approximately half of the original molecules formed by substitution of T-for-H decompose at 1 atm gas pressure before de-excitation can occur. The pressure-dependent reactions demonstrate the presence of a long-lived excited molecule and indicate that the double-substitution reaction is an event of two steps instead of one. A hypothetical model of a reaction mechanism for hot tritium interactions bearing the name "dynamic collision-complex model" is proposed. The model treats electron density, bond strength, and steric hindrance as the possible controlling factors of hot reactions. It is tested by experimental results and it implies that the electron density effect is more pronounced than the steric effect in every case. (Dissertation Abstr.)

4024 RECOIL TRITIUM REACTIONS WITH ALKANES [Thesis]. Root, John Walter. Lawrence, Kan., Univ. of Kansas, 1964. 887p.

Results are reported from experimental and theoretical investigations of the major reactions of recoil tritium with gaseous alkanes. The theoretical calculations are also applied to experimental data obtained by other workers in studies of recoil tritium reactions with simple alkane derivatives. Major emphasis is given to the mechanisms for recoil tritium substitution and abstraction reactions and to the deuterium isotope effects for these processes. Evidence was found for the approximate equivalence of carbon–hydrogen bonds in alkanes with respect to the recoil tritium substitution reaction. Conclusive evidence was found for a probability integral dependence of recoil tritium abstraction reactions upon carbon–hydrogen bond strengths. This correlation was found to be quantitatively applicable to simple alkane derivatives as well as to the alkanes. The deuterium abstraction isotope effect is also quantitatively included in this bond strength correlation. Possible microscopic theoretical models are discussed for abstraction reactions, and an analytic form for the bond strength probability integral factor was obtained. The evidence supports an inverse exponential bond dissociation energy dependence for this factor. Related evidence pertaining to the moderating efficiencies of alkanes and to energy range differences for recoil tritium reactions is also discussed. In connection with the absolute yield calculations carried out in all the experiments, a molecular orbital approach was developed, which allows the calculation of stopping cross sections and recoil ranges for hydrogen ions in a wide variety of organic compounds. Other supplementary considerations include the calculation of molecular sizes and carbon–hydrogen bond dissociation energies for a wide variety of substances including deuterated species. (Dissertation Abstr.)

4025 EFFECTS OF IONIZING RADIATION ON AQUEOUS SOLUTIONS OF THE DETERGENT ALKYLBENZENESULFONATE AND SEVERAL LOWER HOMOLOGS [Thesis]. Cohen, Jules Bernard. Pasadena, Calif., California Inst. of Tech., 1965. 143p.

A study was conducted of the degradation of benzene-, p-toluene-, and alkylbenzenesulfonates under the action of ionizing radiation from a 3400-curie, cobalt-60 irradiator. Effects of varying solute concentrations, pH, and dissolved oxygen concentrations were observed as functions of the energy absorbed by the solutions. The rates of oxygen depletion and the rates of hydrogen peroxide, enol, and sulfate production were followed by irradiating the solutions for varying periods of time. Results of the irradiations indicate that, in aerated solutions, the major mode of degradation is by desulfonation of the molecule. Degradation was accompanied by significant losses in oxygen, possibly a result of direct oxidation of the solute by radiation, rather than by free radical reactions. Enols were also found to occur, but at very low concentrations. The product formed as a result of desulfonation of benzenesulfonic acid appeared to be quinonoid rather than phenolic in nature. In deaerated solutions, enol yields were found to decrease, while sulfates were not observed. A more rapid decrease in the ultraviolet absorption peaks of these homologs in deaerated solutions was attributed to the formation of dimers. The study indicates that the use of radiation, as a water or wastewater treatment process for degrading organic compounds, would necessarily be limited to aerated solutions in situations where the large losses of oxygen would not be detrimental. (Dissertation Abstr.)

4026 THE REACTIONS OF RECOIL CARBON ATOMS IN THE ACETAMIDE SYSTEM [Thesis]. Diehn, Bodo. Lawrence, Kan., Univ. of Kansas, 1964. 135p.

The reactions of energetic carbon atoms activated by nuclear recoil were investigated in the acetamide system. In order to study the influence of extraneous radiation dose on the radiochemical product yields, the $^{14}N(n,p)^{14}C$ nuclear reaction was used at irradiation times from 1 to 8000 minutes in the Brookhaven Graphite Research Reactor, as well as the $^{12}C(n,2n)^{11}C$ reaction. A dose range of approximately 10^{-4} to 10 ev/molecule was covered. It is shown that significant radiation damage effects persist down to 10^{-3} ev/molecule and less. Acetamide, N-methylacetamide, propionamide, acetone, and perhaps acetonitrile are the only non-gaseous products formed by hot-atom reactions, while a large number of other compounds is produced as a result of radiolytic reactions. By extrapolation, the following estimates are given for the hot yields in the absence of radiation damage effects: Acetamide = 0.5%, N-methylacetamide = less than 5%, propionamide = less than 5%, acetone = 2%, acetonitrile = 2%. Annealing and phase effects are discussed, as well as degradation studies that support the above conclusions. Evidence for a related origin of acetamide, acetonitrile, and acetic acid activities is given by the results of the degradations. These results also seem to indicate that in the acetamide molecule the relative replacement probabilities of the carbonyl and methyl carbon atoms are about 65 and 35%, respectively. For a 14-hour pile irradiation, the % activity found in sixteen compounds was determined, and the results are critically compared with widely different values reported for similar conditions by another research group. New analytical techniques and the relative merits of the ^{14}C and ^{11}C methods are discussed. (Dissertation Abstr.)

4027 THERMAL NEUTRON INDUCED RECOIL DEFECTS IN CADMIUM SULFIDE [Thesis]. Oswald, Robert Bernard Jr. Ann Arbor, Mich., Univ. of Michigan, 1964. 99p.

Experimentally, the effects produced by thermal neutron-induced (n, γ) recoil on the physical properties of cadmium sulfide were determined by monitoring the changes produced in the luminescence and conductive properties of CdS. Neutron irradiation was accomplished by placing the samples in the Ford Nuclear Reactor operating at various power levels. The effect of the thermal neutron damage was separated from the effect of fast neutron damage by irradiating samples having the same physical properties with and without a 40-mil cadmium sheath around them. The difference in the effects produced by these two techniques is interpreted as the effects produced by thermal neutrons and thus are the properties related to the nuclear recoil of the ^{114}Cd nucleus. The experimental results show that thermal neutron-induced defects completely alter the optical and electrical properties of the CdS crystals. ^{114}Cd recoil produces a recombination center corresponding to the 7200 Å red emission and the reduction of the other emission lines at liquid nitrogen temperature. In addition, the conductivity of initially conducting CdS crystals is reduced by many orders of magnitude due to the introduction of an acceptor. The energy level of the acceptor was determined to be 1.1 ev above the valence band. The predictions based on radiation damage theory were found to be in good agreement with the experimental results. From the knowledge of the nature of the dominant defects created by ^{114}Cd recoil, it is concluded that these defects are native lattice imperfections. This is given additional support by the 500°C annealing of the defects introduced by the ^{114}Cd recoil. (Dissertation Abstr.)

4028 RADIOLYSIS OF CS_2 [Thesis]. Janssen, O. Berlin, Tech. Univ., 1964. 123p. $2.00 Gmelin, AED-DISS. 64-744.

Radiolysis of liquid or gaseous CS_2 yields only two reaction products, elementary S and a polymer substance. G-values are independent on dose rate but dependent on total dose. For gas radiolysis by electrons or protons a G-value of 15.4 was observed, for γ radiation, 17.2. It was concluded that excited molecules play an important role in CS_2 radiolysis. The energy for the production of 1 ion pair in CS_2 is 26.5 ev. (Gmelin Inst.)

4029 THE AMELIORATION OF THE ADHESIVE PROPERTIES OF POLYETHYLENE FOILS INCLUDING RADIATION CHEMICAL MIXED POLARIZATION [Thesis]. Friese, K. Leipzig, Univ., 1964. 113p. $2.00 Gmelin, AED-DISS. 64-837.

Amelioration of the adhesive properties of polyethylene by treatment with various methacrylic acid esters as a function of polarity and quantity was studied. Homopoly-

merization of methacrylates by ^{60}Co γ rays was investigated. (Gmelin Inst.)

4030 THE EFFECT OF REACTOR IRRADIATION ON THE ELECTRICAL POLARIZATION AND CONDUCTIVITY OF HIGH POLYMERS [Thesis]. Heyne, L. Leipzig, Univ., 1964. 62p. $2.00 Gmelin, AED-DISS. 64-758.

Measurements of electrical conductivities of various high polymers during irradiation by mixed reactor radiation (120 rad/min) indicated that the changes of the electrical polarization are nearly the same for all materials. An apparatus for the measurement of extremely low currents during irradiation is described. Polarization increased immediately after the beginning of the irradiation. Various mechanisms of the polarization effects are discussed. (Gmelin Inst.)

4031 BASIC RADIATION CHEMISTRY WITH REFERENCE TO THE APPLICATION OF RADIATION IN THE TEXTILE INDUSTRY. Swallow, A. J. (Christie Hospital and Holt Radium Inst., Manchester, Eng.). pp 71-84 of Anwendung Radioaktiver Isotope in der Textilforschung und -Technik. Munich, Verlag Karl Thiemig KG, 1964.

Uses of high doses of ionizing radiation in the textile industry are discussed. Gamma radiation and fast electrons are the principal types of radiation employed, and bring about essentially the same effect. The extent of the reaction caused by the radiation depends on the dose. The excited and ionized primary particles formed by the radiation frequently react to form free radicals, whereby chemical reactions can be initiated. One of the most important reactions is the polymerization of vinyl monomers. The irradiation of polymers can produce crosslinking reactions, as in the case of nylon, or degradation, as in the case of cellulose. Radiation can also be used to graft new side chains onto polymers to improve the properties of fibers. Various ways of carrying out graft polymerization are discussed. (auth)

4032 PROCESSES OF RADIATION CHEMISTRY MODIFYING NATURAL AND SYNTHETIC TEXTILE FIBRES. Schwarz, Eberhard (Firma Zschimmer and Schwarz, Oberlahnstein, Ger.); Roudeix, Henri. pp 85-103 of Anwendung Radioaktiver Isotope in der Textilforschung und -Technik. Munich, Verlag Karl Thiemig KG, 1964). (In German).

Possibilities for the treatment of textile materials by ionizing radiation are discussed. The choice of radiation sources and the relevant technological problems are considered along with the changes in the textile fibers and the effects of such changes on the merits of the products. The results of extensive experimental work aimed at achieving radiation grafting of 4-vinylpyridine on PVC fibers, to improve the dye absorption, are reported. (auth)

4033 RECENT DEVELOPMENTS IN IRRADIATION TREATMENT OF POLYMERS. Morris, J.; Charlesby, A. (Royal Military Coll. of Science, Shrivenham, Eng.). pp 104-20 of Anwendung Radioaktiver Isotope in der Textilforschung und -Technik. Munich, Verlag Karl Thiemig KG, 1964.

It is shown that a better understanding of the effects of radiation on polymers is obtained by considering irradiation in aqueous solutions. Advances in polymerization techniques (solid state) showed that highly crystalline fibrillar polyoxymethylene can be formed directly by low radiation doses. Permanent flameproofing of cellulose-type materials is a modification, which may possibly be achieved by radio-induced halogenation. Waterproofing of cotton and other fibers, may be obtained by utilizing a semi-stable radical formed when vinyl silicone fluid is irradiated in vacuo, although true grafting may not be involved. (auth)

4034 IRRADIATION OF CELLULOSE AND ITS DERIVATIVES. Muenzel, F.; Schenkel, J. (INRESCOR, Schwerzenback, Switzerland). pp 141-64 of Anwendung Radioaktiver Isotope in der Textilforschung und -Technik. Munich, Verlag Karl Thiemig KG, 1964. (In German).

Fundamental theoretical facts of radiation chemistry, are reviewed, and the different effects of gamma and electron irradiations are illustrated by the example of cellulose derivatives. It appeared that under the effect of ionizing radiation crosslinking of cellulose derivatives, particularly methyl cellulose, is practicable even with low doses, without interference from degradation reactions. This applies not only in aqueous solutions, but also in the case of films. The significance of the water and the reasons why only electrons of high energy give good results are discussed. The choice of suitable sources for the production of ionizing radiation, and the prospects for their practical use in textile research and industry, are discussed. (auth)

4035 RADIATION-INDUCED ELECTRONIC PHENOMENA IN POLYETHYLENE. Zack, J. F. Jr.; Berg, S. (Atomics International, Canoga Park, Calif.). pp 3-19 of Radiation Effects in Electronics. ASTM Special Technical Publication No. 384. Philadelphia, American Society for Testing and Materials, 1965.

Several electronic phenomena are produced in polyethylene subsequent to exposure to ionizing radiation at cryogenic temperatures. Electric conductivity is very much increased and luminescence of specific wavelengths occurs at certain threshold temperatures. Spontaneous current generation may occur under certain conditions. These phenomena are used to investigate the mechanisms by which the electrical conductivity of polyethylene, normally an electrical insulator, is altered by ionizing radiation to the range of semiconducting materials. Several variations of a simple hypothesis are offered to describe the observed phenomena and the relative merits of the hypothesis are discussed. An analogy is inferred between the model presented and the band model of conduction for semiconductors. (auth)

4036 EPR MEASUREMENTS OF RADIATION IMMUNIZATION IN POLY (METHYL METHACRYLATE) BY ORGANIC ADDITIVES. Atwater, H. A. (Pennsylvania State Univ., University Park). pp 32-41 of Radiation Effects in Electronics. ASTM Special Technical Publication No. 384. Philadelphia, American Society for Testing and Materials, 1965.

Electron paramagnetic resonance techniques were used to compare the relative radiation immunity against free-radical formation given to poly(methyl methacrylate) by the addition of various protective agents at low concentration (5%). Under irradiation by x rays and pile gamma rays, it was found that the degree of protection afforded varied rapidly with the total radiation dose. (auth)

4037 DYNAMIC POLARIZATION OF PROTONS AND NUCLEI OF FLUORINE IN IRRADIATED POLYMERS. Burget, J.; Petricek, V.; Sacha, J. (Inst. of Nuclear Research, Czechoslovak Academy of Sciences, Rez). pp 246-7 of Physics and Techniques of Low Temperatures. Prague, Publishing House of the Czechoslovak Academy of Sciences, 1964.

The "effet solide" method was used for the polarization of protons and nuclei of fluorine in irradiated polymers. The samples were polytetrafluorethylene irradiated with a dose of 10^{16} neutrons, low-pressure polyethylene irradiated with a dose of 10^{17} neutrons, and polypropylene irradiated with a dose of 10^{19} neutrons. The measurements were made at temperatures of 4.2 and 2.1°K the increase observed in the signal was eight to ten times, which corresponds to an absolute polarization of approximately 1%. It is expected that higher polarization will be obtained with a larger microwave power in the cavity. (J.F.P.)

4038 IMPROVEMENTS IN GRAFTED COPOLYMERS AND METHODS OF OBTAINING THEM. Chapiro, Adolphe; Bonamour, Anna-Maria (to Centre National de la Recherche Scientifique). British Patent 1,007,884. Oct. 22, 1965. Priority date June 29, 1963, France.

A method of producing a graft copolymer consists of irradiating solid polyvinyl chloride swollen with a monomeric mixture of acrylonitrile and styrene containing from 50 to 99% by volume of acrylonitrile with a sufficient dose of high energy ionizing radiation to cause the monomer to polymerize as a graft chain polymer. (B.L.M.)

Radiochemistry

See also Separation Processes and Procedures

Refer also to abstracts 4279 and 4916.

4039 HOT ATOM CHEMISTRY. Wolfgang, Richard (Yale Univ., New Haven). Ann. Rev. Phys. Chem., 16: 15-42(1965).

The techniques used in the study of hot atom chemistry, consist of beam techniques to study the dynamics of single collisions and the exploration of chemical reactions occurring at high energies in the electron-volt or bond-energy region. Nuclear recoil technique, the kinetics of recoil-produced hot atoms, and the hot atom chemistry of hydrogen and halogens are discussed. (78 references). (F.J.H.)

4040 INTERNATIONAL SYMPOSIUM ON WORKING METHODS IN HIGH ACTIVITY HOT LABORATORIES, GRENOBLE, 15–18 JUNE 1965. VOLUMES I AND II. Papers/Communications Discussions. Sessions I, II, III, IV, V, and VI. Paris, Organization for Economic Cooperation and Development, 1965. 1030p. F 96; FS 96; DM 80; £6 12s. 6d.; $24.00. (CONF-650601).

Proceedings of the International Symposium on Working Methods in High Activity Hot Laboratories are presented. Separate abstracts were prepared for 40 of the 54 papers. The remaining 14 papers were previously abstracted for NSA and appeared as 19: 22507, 24588, 27765, 28478, 30435, 34292, 38792, 38795, 39793, 40270, 46558, 46559, and 48002 and 20: 236. (M.C.G.)

For abstracts of individual papers see: 4041–4045, 4062–4066, 4092, 4093, 4117–4130, 4208–4214, 4351, 4452, 5093, 5153, and 5203–5205.

4041 GENERAL DESIGN PRINCIPLES AND EXPERIENCE OF THE FLOW, TRANSFER AND STORAGE OF RADIOACTIVE MATERIAL IN THE STUDSVIK HOT LABORATORY. Djurle, S.; Nanberg, R. (Aktiebolaget Atomenergi, Studsvik, Sweden). pp 501-10 of International Symposium on Working Methods in High Activity Hot Laboratories. Vol. II. Paris, Organization for Economic Cooperation and Development, 1965.

The active laboratory for fuel elements at Studsvik, Sweden, includes seven concrete cells and a lead cell. The design of the laboratory with special regard to the flow, transfer, and storage of materials is discussed. Operating experience indicated that the design principles were correct in general, although some modifications of the laboratory proved beneficial. (auth)

4042 TRANSFER OF MATERIALS, EQUIPMENT AND PERSONNEL THROUGH ALPHA-GAMMA BARRIERS IN THE RISOE HOT CELLS. Bundgaard Larsen, F. (Danish Atomic Energy Commission, Roskilde, Denmark). pp 511-22 of International Symposium on Working Methods in High Activity Hot Laboratories. Vol. II. Paris, Organization for Economic Cooperation and Development, 1965.

The hot-cell facility at the Research Establishment, Risö, Denmark, was designed as an alpha-gamma facility. The way in which the gamma shield and/or the alpha seal of the concrete-shielded cell bank are maintained during transfer of materials, equipment, and personnel by the use of shutters, mechanical alpha seals, air barriers, and air locks is discussed. (auth)

4043 METHODS USED IN THE UNITED STATES FOR TRANSFERRING MATERIALS THROUGH RADIATION BARRIERS. Schulte, J. W. (Los Alamos Scientific Lab., N. Mex.); Peterson, P. J.; Wilson, M. T.; Deily, G. J.; Fleischer, E. S. pp 523-44 of International Symposium on Working Methods in High Activity Hot Laboratories. Vol. II. Paris, Organization for Economic Cooperation and Development, 1965.

Various methods in use throughout the United States by which materials are passed through the shielding of high-activity hot cells are described. Distinctions are made between operations involving the transfer of cold materials into cells, the introduction and removal of hot materials through gamma barriers, and the introduction and removal of hot materials through alpha-gamma barriers. (auth)

4044 TRANSFER IN A HIGH ACTIVITY CHEMISTRY CELL. Lefort, G. (CEN, Fontenay-aux-Roses, France). pp 571-82 of International Symposium on Working Methods in High Activity Hot Laboratories. Vol. II. Paris, Organization for Economic Cooperation and Development, 1965. (In French).

The Cyrano cell was designed to study the reprocessing of very intense alpha-emitting highly irradiated fuel elements. The transfer and maintenance processes chosen, are described. The fixed and exchangeable fluid tubing, ejectable air-tight sleeves, air-tight communication procedures between two rigid alpha-gamma cells, and transfer of hot samples to the analytical cell are discussed. (auth)

4045 DIRECTORY OF HIGH ACTIVITY HOT LABORATORIES HANDLING RADIOACTIVE MATERIALS WITH AN ACTIVITY OF MORE THAN 1,000 CURIES FOR RESEARCH PURPOSES. pp 927-1013 of International Symposium on Working Methods in High Activity Hot Laboratories. Vol. II. Paris, Organization for Economic Cooperation and Development, 1965.

Separation Processes and Procedures

See also Analytical Procedures
ISOTOPE TECHNOLOGY — Separation and Production

Refer also to abstract 4077.

4046 (EURAEC–1340) REPROCESSING OF IRRADIATED FUELS. Quarterly Report No. 18, July 1–September 30, 1964. (Centre d'Etude de l'Energie Nucleaire, Mol (Belgium)). Contract 004-64-4 RCIB(RB). 30p. Dep. mn; CFSTI $2.00 cy, $0.50 mn.

Work Performed under United States–Euratom Joint Research and Development Program.

Hydrofluorination and fluorination of PuO_2-UO_2 mixtures using ClF_3 established a relation between the rate and PuO_2 content. Results of experiments on PuO_2 conversion to PuF_4 by hydrofluorination indicate that efficiency is difficult to obtain in large processing units. In studies of UF_4 pyrohydrolysis in the presence of steam and oxygen, the value of O/U ratio and reaction rates were established. In molten alkaline chlorides the $^4U/^6U$ ratio of absorbed U is not dependent on both dryness. Investigations revealed that UF_6 attaches to alkaline chlorides at 325 to 400°C. (J.R.D.)

4047 (LFEN–32) ALGUNS ASPECTOS IMPORTANTES DA VALORIZACAO E UTILIZACAO DOS COMBUSTIVEIS NUCLEARES. CONTRIBUICAO DO LABORATORIO DE FISICA E ENGENHARIA NUCLEARES NA RESOLUCAO DOS PROBLEMAS NACIONAIS. (Certain Important Aspects on Improvement and Utilization of Nuclear Fuels. The Contribution of the Laboratory of Nuclear Physics and Engineering to the Solution of National Problems). Marques Videira, F. H.; Peixoto Cabral, J. M.; Ramalho, A. J. (Laboratorio de Fisica e Engenharia Nucleares, Junta de Energia Nuclear, Sacavem (Portugal)). 1964. 12p. (CONF-611102–1). Dep. mn.

For Presentation at World Conference on Energy, Lisbon.

An overall view of the contribution of the Laboratory of Nuclear Physics and Engineering to the study of the evaluation of some Portuguese uranium ores is given. The basic operation of the uranium cycle is described and some important aspects of the use of U as nuclear fuel are discussed. The results already obtained in the evaluation of the ores are presented. Several courses worthy of further investigation are also indicated. (tr-auth)

4048 (NP–15406) EUROCHEMIC SECOND ACTIVITY REPORT, 1962–1964. (European Nuclear Energy Agency, Paris (France)). 313p. Dep. mn.

Development of the Eurochemic Company plant to process spent fuels for U and Pu recovery is summarized. The information is presented in parts concerning administrative and legal matters, safety programs, research and development, and plant location and equipment. (J.R.D.)

4049 (RL-SA-52) A CRITICALLY SAFE FLAT BED CONTACTOR FOR PROCESSING SOLID FISSILE MATERIALS. Fullam, H. T. (General Electric Co., Richland, Wash. Hanford Atomic Products Operation). [nd]. Contract AT(45-1)-1350. 12p. (CONF-651010-2). Dep. mn; CFSTI $1.00 cy, $0.50 mn.

From Electrochemical Society 6th Regional AIChE Meeting, Union, Wash.

A flat-bed reactor for processing solid fissile materials was developed. The body of the contactor consists of a hollow cylindrical slab which is divided by a porous plate into an upper and lower section. The contactor design as it finally evolved is felt to possess a number of advantages over the other gas-solids contactors for processing fissile materials. Based on experimental work, it is felt that the flat bed contactor meets all the original design criteria and is a practical unit for carrying out gas solid reactions involving fissile material. (P.C.H.)

4050 ECONOMIC PROBLEMS IN THE PROCESSING OF IRRADIATED FUEL MATERIALS. Barendregt, T. J. Atoomenergie Haar Toepassingen, 7: 160-6(Aug. 1965). (In Dutch).

A review is given of the cost connected with the reprocessing of irradiated fuel materials. An insight into this economic problem is necessary for the selection of one of the two possibilities— storage or reprocessing of nuclear fuels. (tr-auth)

4051 EXTRACTION OF CERIUM AND YTTRIUM BY NAPHTHENATES. Alekperov, R. A.; Makov, N. N.; Efendiev, G. Kh.; Paskhalov, V. V. (Inst. of Chemistry, Academy of Sciences, USSR). Azerbaidzh. Khim. Zh., No. 1, 114-19(1965). (In Russian).

The dependence of the distribution coefficients of cerium and yttrium on the concentration of naphthenates in the organic phase and the pH of the aqueous phase in equilibrium was inyestigated. It was established that the distribution coefficients of Ce and Y during extraction with naphthenates are directly proportional to the third power of the concentration of the naphthenates in the organic phase and inversely proportional to the third power of the concentration of the hydrogen ions in the aqueous phase. The apparent reaction constants for the extraction of cerium and Y with naphthenates were determined to be $K_{Ce} = 5.94 \times 10^{-12}$ and $K_Y = 6.79 \times 10^{-12}$ and equations characterizing the extraction process for these two elements are suggested. (tr-auth)

4052 STUDIES ON URANIUM REFINERY. Kinoshita, Hideo; Nishikawa, Kazuyuki (Furukawa Electric Co., Ltd., Japan). Furukawa Denko Jiho, No. 36, 23-7(Dec. 1964). (In Japanese).

A method for producing well-sintered uranium oxide is described; uranium was first extracted as $(NH_4)_4UO_2(CO_3)_3$ from 5 g U/l 0.2M amberlite-LA-2-kerosene solution with $(NH_4)_2CO_3$. Well-sintered uranium oxide was obtained by calcination and reduction at high temperature. Many repeated extractions are possible when the impurity concentration is not large. The extracted uranium is in the form of $(NH_4)_4UO_2(CO_3)_3$ (AUT). The thermal decomposition of AUT proceeds as $(NH_4)_4UO_2(CO_3)_3 \rightarrow 4NH_3 + UO_3 + 3CO_2 + 2H_2O$. The DTA curve of AUT showed two endothermic points (elimination of the adsorbed water at 110°C and transformation to the oxide at 175°C) and one exothermic point (oxidation of the undecomposed ammonia above 200°C). At above 230°C, the conversion of AUT to uranium oxide was completed. In order to obtain well-sintered uranium oxide, temperatures between 500 and 600°C are desirable for both the calcination and reduction. (NSA of Japan)

4053 ION-EXCHANGE RESIN SEPARATION AND FLAME PHOTOMETRIC DETERMINATION OF SODIUM, POTASSIUM, MAGNESIUM, CALCIUM, AND STRONTIUM. Breault, Eugene A. (Food and Drug Administration, San Francisco). J. Assoc. Offic. Agr. Chemists, 48: 719-22(Aug. 1965).

A method is presented for the cation exchange separation of metallic chlorides by HCl on an Amberlite CG-120 resin (200 to 400 mesh) column. The fines were removed from the resin by several water washings. A resin column 24 cm × 12 mm gave excellent separation of sodium and potassium, with a total volume of 500 ml of 0.5N HCl at a flow rate of 0.55 ml/min. Sharp separation of each element was obtained and no cross contamination occurred. Recovery of Na and K from their eluates was 100%. Elution of Mg, Ca, and Sr from the resin column required an additional volume (1100 ml) of 1N HCl eluting agent. Recoveries from eluate fractions were 97% for Mg, 50% for Ca, and 59% for Sr. All of the metals were determined by flame photometry. All flame photometry curves were linear except the Na curve, which tended toward the parabolic. It was recommended that the techniques for resin grading be investigated, that fritted glass disks of different porosity be tried, and that other metal chlorides be incorporated into this separation scheme. (BBB)

4054 ION-EXCHANGE PROCEDURES. VIII. SEPARATION OF SILVER FROM A NUMBER OF ELEMENTS BY PARTITION CHROMATOGRAPHY. Nelson, Frederick (Oak Ridge National Lab., Tenn.). J. Chromatog., 20: 378-83(Nov. 1965). (ORNL-P-1197).

The procedure for separating silver from other elements in HNO_3 solution by partition chromatography using tri-iso-octyl thiophosphate (TOTP) and tri-n-butyl thiophosphate (TBTP) as extracting agents is described. A small column of finely divided polyfluorocarbon impregnated with a TOTP-CCl_4 solution is used to effect separation. The procedure permits separation of macro or tracer amounts of Ag(I) from other elements. (F.J.H.)

4055 ROTATING DISK STUDY OF THE DISSOLUTION OF ZIRCONIUM IN HF-H_2SO_4. Meyer, R. E.; Zettl, Sandra Massey (Oak Ridge National Lab., Tenn.). J. Electrochem. Soc., 112: 1092-6(Nov. 1965). (ORNL-P-1196).

The dissolution of crystal-bar zirconium in mixtures of hydrofluoric acid and sulfuric acid was investigated by use of a rotating disk electrode system. The presence of the sulfuric acid in relatively large amounts reduced the rates as compared to solutions of hydrofluoric acid and nitric acid. In addition, the reaction, normally first order, changed to second order in the presence of large amounts of sulfuric acid. A kinetic equation, which accounts for these results, could be derived if it was assumed that both the hydrofluoric acid and the sulfate ion are adsorbed. (auth)

4056 PURIFICATION OF RUBIDIUM COMPOUNDS FROM TRACES OF CAESIUM. Smit, J. Van R. (National Chemical Research Lab., Pretoria). J. S. African Chem. Inst., 17: 138-41(1964).

A method is described for removing Cs activity from ^{86}Rb, especially for purification of substantial amounts of rubidium chloride target material. An aqueous solution of RbCl, containing 0.45 mg of Cs per g, was tagged with carrier-free ^{137}Cs, and passed through a column containing molybdophosphoric acid and ammonium nitrate at a linear flow rate of 0.9 cm/min. Fractions of 5 ml were collected and counted in a well-type scintillation counter. For a 0.2N RbCl solution, more than 85 column volumes of solution were collected before the Cs concentration in the eluate rose to 0.001 of that in the feed solution. For the elimination of ammonium chloride and purification from traces of molybdate and phosphate, the RbCl solution was passed through a column of anion exchanger in the hydroxide or carbonate cycle. In another typical experiment, 7.74 g RbCl reagent was purified by passing as a 0.2N aqueous solution, tagged with about 12,000 cpm/ml of ^{137}Cs, through a 100 to 200 mesh molybdophosphoric acid column (0.27 cm^2 × 14.8 cm) at a linear flow rate of 0.76 cm/min. No ^{137}Cs activity could be detected in the eluate, which was passed through a column of 100 to 200 mesh AG 1X8 anion exchange resin in the hydroxide cycle (0.9 cm^2 × 15 cm, representing 18.9

meq) at a flow rate of 1.1 cm/min. Interstitial liquid was finally displaced with 2 column volumes of 1:100 ammonia. Molybdate, as well as phosphate, was quantitatively retained in the top 2 cm of the column. The eluate was evaporated to dryness, dissolved in water, filtered, HCl added to pH 6, and crystallized. The yield was over 90%. (BBB)

4057 TRIBUTYL PHOSPHATE EXTRACTION OF PROTACTINIUM. PART I. NONEXTRACTABLE FORMS OF PROTACTINIUM. Spitsyn, Vikt. I.; D'yachkova, R. A.; Khlebnikov, V. P. Radiokhimiya, 7: 257-61(1965). (In Russian).

The kinetics of extraction of protactinium from nitric acid solutions as a function of the "age" and concentration of the Pa solutions are reported. The results of a determination of Pa present in a nonextractable form in HNO_3 solutions are given. In order to determine the conditions under which polymeric forms of Pa exist, the distribution ratio was studied as a function of the Pa concentration. It was found that when fresh Pa solutions were used, the equilibrium was established in a few minutes, and the distribution ratios for the extraction and reextraction were the same. In the case of aged solutions, the extraction equilibrium was not reached after 100 hr of stirring because of the presence of nonextractable forms of Pa; up to 45% Pa can be present in such forms even in 6M HNO_3. In extraction from fresh solutions, the distribution ratio was independent of the Pa concentration in the 10^{-7} to 10^{-12}M range; this indicated the absence of polymerization of Pa both in the aqueous and in the organic phase. It was concluded that in studying the state of Pa by the extraction method, it is desirable to use the distribution ratio obtained from data on the reverse extraction from the organic phase into the aqueous phase. (CFSTI)

4058 TRIBUTYL PHOSPHATE EXTRACTION OF PROTACTINIUM. PART II. DETERMINATION OF THE SOLVATION NUMBER OF THE EXTRACTED PROTACTINIUM COMPLEX. D'yachkova, R. A.; Spitsyn, Vikt. I.; Khlebnikov, V. P. Radiokhimiya, 7: 262-5(1965). (In Russian).

The distribution ratio of protactinium was studied as a function of the tributyl phosphate (TBP) concentration in extraction from nitric and perchloric acids. The ionic strength of the aqueous phase was kept constant. The initial and equilibrium concentrations of HNO_3 and TBP were calculated by taking into account their interaction, which causes the formation of the complexes $HNO_3 \cdot$ TBP and $(HNO_3)_2 \cdot$ TBP in the organic phase. The slope of the straight line representing the log of the distribution ratio versus the log of the concentration of free TBP for extraction from 1 to 5M HNO_3 was found to be 2.13. It was concluded that in the concentration range under consideration, protactinium is extracted with the formation of a dissolvate in the organic phase. In the case of extraction from perchloric acid, a whole series of complexes of the type $mHClO_4 \cdot n$TBP were formed whose equilibrium constants (except that of $HClO_4 \cdot$ 4TBP) were not known, so that the interaction of $HClO_4$ and TBP could not be accurately determined. It was found that the number of TBP molecules attached to protactinium in extraction from 1 to 5M $HClO_4$ is close to 3. (CFSTI)

4059 THE ANALYTICAL APPLICATION OF FLUORIC ION. III. SOLVENT EXTRACTION OF THORIUM. Seki, Jisuke (Inst. of Physical and Chemical Research, Tokyo). Rika Gaku Kenkyusho Hokoku, 38: 334-41(1962). (In Japanese).

Thorium in ore can usually be extracted into mesityl oxide by means of solvent extraction. In this study, tributyl phosphate (TBP) was used instead of mesityl oxide. Experiments were conducted to determine the optimal conditions of the solvent extraction of thorium and the effects of TBP diluents. A method of separating thorium from cerium was also examined. (BBB)

4060 THE ANALYTICAL APPLICATION OF FLUORIC ION. IV. SOLVENT EXTRACTION OF THORIUM IN FLUORIDE. Seki, Jisuke (Inst. of Physical and Chemical Research, Tokyo). Rika Gaku Kenkyusho Hokoku, 38: 342-7(1962). (In Japanese).

Thorium fluoride was dissolved in a mixture of 50% aluminum nitrate and nitric acid, and from this solution thorium was extracted with tributyl phosphate (TBP)–n-hexane. The ions extracted with 20% TBP–n-hexane were mainly thorium and a small amount of cerium. A few rare earth elements beside cerium were also extracted. It was concluded that with the method described, extraction of thorium from thorium ore can be satisfactorily done with 50% TBP–n-hexane. (BBB)

4061 EXTRACTION OF TITANIUM AND ZIRCONIUM FROM SULFURIC ACID SOLUTIONS. Zharovskii, F. G.; Vyazovskaya, L. M. (Kiev State Univ.). Ukr. Khim. Zh., 31: 839-44(1965). (In Russian).

The distributions of titanium and zirconium in aqueous sulfuric acid-organic solvent systems were investigated in relation to the original concentration of the sulfuric acid and the metal and to the nature of the organic solvent. Tests were made with 13 organic solvents. It was established that with increasing concentration of sulfuric acid the distribution coefficients of titanium and zirconium increased. Under comparable conditions titanium was extracted better than zirconium. The extractions decreased in going from alcohol to ether. For normal alcohols the extraction capacity increased with increasing dielectric permeability. It was found that in extraction with 50% solutions of tributyl phosphate in carbon tetrachloride, titanium and zirconium are almost completely extracted from 12.2M solutions of sulfuric acid. (tr-auth)

4062 DECANNING PROBLEMS IN HOT LABORATORIES AND ATTEMPTED SOLUTIONS. Peray, R.; Humbert, J. (CEN, Cadarache, France). pp 355-63 of International Symposium on Working Methods in High Activity Hot Laboratories. Vol. I. Paris, Organization for Economic Cooperation and Development, 1965. (In French).

The decanning of irradiated fuel in hot cells causes several problems, such as the recovery either of the fuel or of the can with the minimum of distortion. The three methods used at L.E.C.A. (Hot Laboratory of Cadarache) are described. (auth)

4063 TRANSFER METHODS FOR IRRADIATION RIGS AND FUEL ELEMENTS FOR POSTIRRADIATION EXAMINATION IN THE HOT CELLS OF THE EIR, WUERENLINGEN (SWITZERLAND). Graf, P.; Stauffer, M. (Eidgenoessisches Institut fuer Reaktorforschung, Wuerenlingen, Switzerland). pp 485-500 of International Symposium on Working Methods in High Activity Hot Laboratories. Vol. II. Paris, Organization for Economic Cooperation and Development, 1965.

Transfer methods for highly active materials in the five interconnected hot cells with adequate shielding up to 10^5 Mev-C of the high-level laboratory of the Swiss Reactor Research Center are described. All transfer systems of the cells are β-γ shielded and tight, but they are not α-sealed. Work with irradiated fuel with high plutonium concentration is accomplished in in-cell boxes under pressure. The transfer methods used between the shielded cell and the sealed box with the help of the power manipulator are by the adapted glove box technique through airlocks. (auth)

4064 DISMANTLING WORKSHOP FOR ORGEL FUEL ELEMENTS. Biteau, J.; Garric, C.; Wilhelem, A. (Communaute Europeenne de l'Energie Atomique, Ispra, Italy). pp 759-78 of International Symposium on Working Methods in High Activity Hot Laboratories. Vol. II. Paris, Organization for Economic Cooperation and Development, 1965. (In French).

The dismantling workshop for ORGEL fuel elements (ADECO) is connected to the ESSOR reactor by a swimming pool. This workshop will be used for: cleaning, visual observations and radiography of the ORGEL fuel cluster; dismantling of the cluster; sectioning and evacuation of the different parts; and for feed element treatment. The different concept and intervention principles, as well as the equipment, are described. (auth)

4065 WORKING METHODS—EQUIPMENT IN USE AT THE 1000 CURIE-1 Mev TRANSPLUTONIUM COMPLEX AT THE MEDIUM ACTIVITY LABORATORY. Gandolfo, J.M. (CEN, Mol, Belg.). pp 791-804 of International Symposium on Working Methods in High Activity Hot Laboratories. Vol. II. Paris, Organization for Economic Cooperation and Development, 1965. (In French).

The chemical separation of transplutonium elements obtained by irradiation of targets containing ^{241}Am, ^{242}Pu, ^{243}Am, and ^{244}Cm in the BR-2 reactor made necessary a group of 1000-Curie, 1-Mev $\alpha^-\beta^-\gamma^-n$ cells. This group includes an $\alpha^-\beta^-\gamma^-n$ working cell, a $\beta^-\gamma^-n$ working cell, and an $\alpha^-\beta^-\gamma$ cellar. The equipment used for the chemical processing of a slug containing 2.5 g of ^{241}Am irradiated for four years in the MTR is described. For this processing, special equipment adaptable to the existing facilities had to be designed. This included an α-glove box of small volume suitable for the cells originally designed for β-γ work only, and specially adaptable transfer locks allowing isolation of the α-working-box from the normal transfer mechanism. (auth)

4066 A PILOT PLANT FACILITY FOR THE REPROCESSING OF IRRADIATED MTR TYPE FUELS AT THE SPANISH J.E.N. Perez, B. Lopez; Nogueira, E. D.; Uriarte, A.; Salvador, L. Ramos (Junta de Energia Nuclear, Madrid). pp 869-81 of International Symposium on Working Methods in High Activity Hot Laboratories. Vol. II. Paris, Organization for Economic Cooperation and Development, 1965.

The general layout and main features of a pilot plant facility for the reprocessing of irradiated MTR-type fuels under construction at the Centro Nacional de Energía Juan Vigón, Madrid, are discussed. The plant will be used for reprocessing the JEN-1 reactor elements, to obtain direct information on the subject, and to train personnel with a view to the future needs of the Spanish nuclear power programs. (auth)

4067 ANION EXCHANGE SEPARATIONS OF THE RARE EARTHS IN NONAQUEOUS SOLVENTS [Thesis]. Greene, Richard George. Ames, Iowa, Iowa State Univ. of Science and Tech., 1965. 92p.

Many metal ions were separated from the rare earth elements using a nitrate-form anion-exchange column. This was accomplished by eluting the various metals from the more highly sorbable rare earths with 1.5M nitric acid in 85% isopropyl alcohol. The higher rare earths can be eluted from the column using lower percentages of isopropyl alcohol and separated from bismuth(III), lead(II), and thorium(IV), which remain on the column. A study was made of the conditions necessary to separate various rare earths from each other using anion-exchange techniques. This was accomplished by determining the distribution coefficients of various rare earths as a function of concentration of organic solvent, nitric acid, and lithium nitrate. Various organic solvents were studied. Separation factors were determined in a solvent mixture of 92.5% methanol –3.00M lithium nitrate –0.95M nitric acid and were found to compare favorably with separation factors obtained by investigators using different systems. Invation (the sorption of significant amounts of electrolyte by an ion exchanger) of anion-exchange resin by lithium nitrate and nitric acid from organic-water solvent mixtures was studied. It was concluded that the solubility of an electrolyte in the solution being equilibrated with the resin is an important factor in determining the extent of invasion. The Donnan potential concept was used in explaining some of the results. Mean ligand numbers for various metal ions with the nitrate ligand were determined in water-organic solvent mixtures using ion-exchange techniques. The ligand numbers were found to increase in going from the solution to the resin phase. The metal ions studied did not appear to reach their saturated coordination number in the resin phase. (Dissertation Abstr.)

4068 STUDIES OF VARIOUS METHODS FOR THE DECONTAMINATION OF RADIOACTIVE RESERVOIR WATERS WITH HIGH POWER FAST FILTER EQUIPMENT [Thesis]. Baumgaertel, F. Brunswick, Ger., Tech. Univ., 1964. 76p. $2.00 Gmelin, AED-DISS. 64-574.

Decontamination factors for Al and Fe coagulation were 0.46 for ^{90}Sr and 0.99 for ^{144}Ce. An increase of the decontamination factor for ^{89}Sr by phosphate precipitation was possible, but this method was not applicable for fast filtration. It was concluded that a combination of a fast filter with an ion exchanger is suitable for large scale water decontamination. Decontamination factors can be higher than 0.998. Economic aspects of water purification are discussed. (Gmelin Inst.)

4069 RECOVERY OF SPENT NUCLEAR FUELS: PROCESSING. Cairns, R. C. (Australian Atomic Energy Commission). pp 57-77 of Atomic Power: A Review. Kensington, N. S. W., Univ. of New South Wales [1964].

Some of the available spent fuel processes are discussed with emphasis on power fuels. The new plants under construction or being commissioned, and the development of the newer processes are reported. The aqueous methods are discussed primarily. These topics include the Purex Process, the United Kingdom Civil Reactor Fuel Processing Plant, aqueous plant developments in Europe, in the United States, and in Japan. Pyrometallurgical and halide volatility methods are also considered. Schematic diagrams are shown of some of these processes. The costs of reprocessing are considered and the development of processing technology in Australia is discussed. A strong competition by the newer halide process for treating power reactor fuels already established is expected. (J.F.P.)

4070 A PROCESS FOR THE TREATMENT OF SOLUTIONS OF PRODUCTS FORMED BY THE FISSION OF URANIUM–MOLYBDENUM ALLOYS. Lefevre, Jean; Raggenbass, Andre (to Commissariat a l'Energie Atomique). British Patent 1,008,066. Oct. 27, 1965. Priority date Mar. 30, 1962, France.

A process is described for the treatment by phosphoric acid of a nitric acid solution containing Mo and fission products. The process is particularly applicable to the recovery of Mo, Cs, and Zr from the nitric acid solution. The process consists of the following steps: concentration of the solution by evaporation, progressive addition, during the concentration, of phosphoric acid in quantities at least equal to the stoichiometric quantity corresponding to the transformation of the Mo into phosphomolybdic acid, of the Zr into zirconium phosphate, and Cs into cesium phosphomolybdate, separation of the mixture of the precipitated cesium phosphomolybdate and zirconium phosphate from the solution containing the phosphomolybdic acid; treatment of the mixture of precipitates with an alkali metal hydroxide to dissolve the Cs leaving the Zr in the form of the insoluble $Zr(OH)_4$; separation of the solution containing the Cs from the $Zr(OH)_4$ precipitate; and reacidification of the solution causing the reprecipitation of the cesium phosphomolybdate. (B.L.M.)

4071 REMOVAL OF VANADIUM FROM AQUEOUS SOLUTIONS. Hart, James L.; Reusser, Robert E. (to Phillips Petroleum Co.). U. S. Patent 3,212,845. Oct. 19, 1965. Filed Dec. 12, 1960.

A method of removing soluble V values from aqueous solutions consists of passing the V-containing solution over a bed of or through a column of lead shot that have been contacted with an aqueous H_2SO_4 solution of H_2O_2 and eluting the V values from the resulting lead vanadate-loaded substrate by passing a dilute solution of H_2SO_4 solution through the loaded substrate. The method is particularly applicable to the pregnant U-containing liquor obtained by carbonate leaching of uranium ores or to the solution obtained by leaching roasted yellow cake. (B.L.M.)

4072 REDUCTIVE CHLORINATION OF ACTIVATED ORES CONTAINING HIGH MELTING METALS. Lerner, Bernard J. (to Dominion Gulf Co.). U. S. Patent 3,212,847. Oct. 19, 1965. Filed Feb. 26, 1962.

A metallurgical process is described for extracting in chloride form a high melting metal selected from the group consisting of Nb, Ta, Ti, V, Cr, Zr, Mo, W, and Sb from

an ore that contains the metal in a complex oxyfluoride form. The ore must be nonrefractory to reductive chlorination and contain a predominant proportion of gangue material. The ore is activated for the reductive chlorination by contacting the finely divided ore with oxygen at 200 to 500°C. The reductive chlorination is carried out with a vapor phase chlorinating agent, such as CCl_4, that forms a nonhydrogenous reducing agent at the conditions of the reaction. The chlorination is carried out at a temperature of 240 to 450°C that is sufficient to form the vaporous metal chloride but insufficient to chlorinate a substantial portion of the gangue material. (B.L.M.)

4073 REGENERATION OF NUCLEAR FUEL. **Knighton, James B.; Feder, Harold M.; Steunenberg, Robert K. (to U. S. Atomic Energy Commission). U. S. Patent 3,218,160. [Nov. 1965].**

A process is described for regenerating uranium fuel including the steps of introducing the fuel into a fused-salt mixture containing a molten cadmium–magnesium–zinc alloy, separating an alloy phase containing uranium and plutonium from a salt phase containing fission products and heating the alloy phase to volatilize the cadmium, zinc and magnesium. (AEC)

4074 CHEMICAL DISINTEGRATION AND RECOVERY OF URANIUM FROM SINTERED GRAPHITE–URANIUM COMPACTS. **Bradley, M. J.; Ferris, L. M. (to U. S. Atomic Energy Commission). U. S. Patent 3,219,408. Nov. 23, 1965.**

A process is described for dissolving uranium from a graphite-uranium compact having a minimum dimension of 1000 microns, which comprises contacting the compact with at least a 20 M aqueous solution of nitric acid in order to disintegrate the graphite and form a solution of uranyl nitrate. (AEC)

ENGINEERING

General

4075 (GA-6267) ON THE STRESS ANALYSIS OF AN AXISYMMETRIC DISK WITH VARIABLE THICKNESS. Cavallaro, Leonardo (General Atomic, San Diego, Calif. John Jay Hopkins Lab. for Pure and Applied Science). Sept. 20, 1965. Contract AT(04-3)-167. 170p. Dep. mn; CFSTI $5.00 cy, $1.00 mn.

The equilibrium of disks with variable thickness, symmetrical with respect to their axes, is analyzed under three types of loadings: centrifugal, lateral, and thermal. In establishing the equilibrium conditions, the stresses acting in the direction of the axis of symmetry, as well as the influence of shear stresses, are neglected, and the lengthwise distribution of stresses is considered as uniform in the case of centrifugal or thermal load, and linear in the case of lateral load. Also symmetry with respect to the midplane is assumed in the case of centrifugal load. The differential equilibrium equation is written, and integration procedures, as well as stress analysis methods, are suggested for various thickness distributions, load patterns, and boundary conditions. (J.F.P.)

4076 (HIC-1-1564-3(Vol.2)) PLANE THERMAL STRESS ANALYSIS OF THICK-WALL CYLINDERS. VOLUME II. TEMPERATURE DISTRIBUTION OF FORM (T = R cos n θ). Stanek, Floyd J. (Hayes International Corp., Huntsville, Ala.). Jan. 15, 1964. 36p.

Formulas are presented for plane thermal stress analysis of the thick-wall cylinder when the temperature function is of the form T = R cos nθ where R is a function of the radial coordinate only and n is an integer. The cylinder may be in a condition of plane strain or a condition of plane stress. The external stresses at each of the two cylindrical surfaces are zero. The procedure for application of these formulas is then explained and illustrated with several examples. The derivation of the formulas is presented by two methods: by the classical theory of elasticity; and by complex theory. The derivation by complex theory illustrates the application of the complex representation of the general equations of plane elasticity. (P.C.H.)

4077 (IS-1200(Sect. E)) ENGINEERING DIVISION. (Ames Lab., Iowa State Univ. of Science and Tech.). 35p.

Research and development in chemical, ceramic, and mechanical engineering are summarized. (J.R.D.)

4078 (SWRI-1228-67) FUNDAMENTAL INVESTIGATION OF LIQUID-METAL LUBRICATED JOURNAL BEARINGS. Quarterly Technical Report No. 4, April 1–July 31, 1965. Burton, R. A.; Carper, H. J.; Hsu, Y. C. (Southwest Research Inst., San Antonio, Tex.). Aug. 1, 1965. Contract AT(11-1)-1228. 92p. Dep. mn; CFSTI $3.00 cy, $0.75 mn.

The momentum and continuity equations for a turbulent fluid are integrated across a thin film with arbitrary thickness variation. Velocity profile and friction parameters required for the solution of these equations are calculated for the power-law approximation. The results are applied to calculation of pressures in a short-full journal bearing and a tilted pad without end leakage, showing good agreement with experimental measurements. Experimental velocity profile data are reported which should help in future improvement of the computations. (auth)

4079 (UCRL-13187) DEFORMATION, VIBRATION, AND STABILITY OF SHELLS. A PARTIALLY ANNOTATED BIBLIOGRAPHY. McGhie, R. D. (California Univ., Davis. Coll. of Engineering). June 1965. Contract W-7405-eng-48. 72p. Dep. mn; CFSTI $3.00 cy, $0.75 mn.

For Lawrence Radiation Lab., Livermore, Calif.

The citations are listed in three major subject sections; rings and cylindrical shells, spherical shells, and conical shells. Within each section, the citations are listed by the year of publication. An author index is also included. The bibliography covers the period 1957 to 1965. (M.O.W.)

4080 (WAPD-TM-535) AN EXTENSION OF HOT-1 TO TREAT NEUMANN BOUNDARY CONDITIONS—WITH APPLICATIONS TO CERTAIN VIBRATION PROBLEMS. Kellogg, R. B.; Peterson, W. D.; Spanier, J. (Bettis Atomic Power Lab., West Mifflin, Pa.). June 1965. Contract AT(11-1)-Gen-14. 13p. Dep. mn; CFSTI $1.00 cy, $0.50 mn.

An extension of the HOT-1 program to treat problems in (x,y) geometry in which the normal derivative of the solution function is specified at every point on the boundary is described. The program is also applicable to more general problems with Neumann boundary conditions. The treatment of the effects of water on the natural frequency of a beam, theoretical analysis needed for the extension of HOT-1 to the Neumann problem, and the input changes required and the output produced for such problems are described. (P.C.H.)

4081 PROBLEMS OF THE SUPPLY OF ELECTRICAL ENERGY IN SPAIN. Cervera, J.; Hernandez-Varela, J. L.; Zubeldia, J. M. Paper No. 5 of Anglo-Spanish Nuclear Power Symposium. Vol. 1. [Risley, Eng., United Kingdom Atomic Energy Authority, 1965]. 18p.

Various aspects of the following technical-economical problems concerned with electrical energy are discussed: production and operation; transmission; and distribution. A brief exposition is given on the present status of the electrical industry in Spain. Future prospects are examined, with particular reference to the factors that are influencing the introduction of nuclear power. (L.B.S.)

Applications of Nuclear Explosions

Refer also to abstracts 4847 and 4848.

4082 (BM-RI-6684) A STUDY OF RADIOACTIVE CONTAMINATION RESULTING FROM THE USE OF NUCLEAR EXPLOSIVES FOR STIMULATING PETROLEUM PRODUCTION. Arthur, C. E.; Armstrong, F. E. (Bureau of Mines, Washington, D. C.). Mar. 1965. 13p. Dep. mn; CFSTI $1.00 cy, $0.50 mn.

The problem of radioactive contamination when using nuclear explosives to fracture petroleum reservoirs in an attempt to stimulate production was investigated. It was concluded that some contamination of petroleum products will almost certainly occur. However, the degree of contamination cannot be predicted except by a full-scale experiment, since simulating the problem in the laboratory is economically impossible because of the extremely high temperatures and pressures that must be reached in extremely short time intervals if a reasonable analog is to result. (auth)

4083 (SC-RR-65-478) CRATERS FROM A SINGLE ROW OF CHARGES BURIED BENEATH THE CRATERS FROM PARALLEL ROWS OF CHARGES. Vortman, L. J. (Sandia Corp., Albuquerque, N. Mex.). Oct. 1965. Contract AT(29-1)-789. 33p. Dep. mn; CFSTI $2.00 cy, $0.50 mn.

Two-step experiments are described in which excavations were accomplished by a single row buried in the craters of an earlier detonation of two and three parallel rows of explosive charges. Firing of a single row in the crater of a double or triple row is less efficient than a single row of larger charges. It requires 35 and 50% more explosives to provide the same crater with double and triple rows, respectively, each followed by a single row. The double row, however, permits about 10% less charge to be fired at one time, providing only a slight advantage.

There is no comparable advantage for the triple row configuration. Ground-shock-induced airblast should reflect the 10% smaller charge weight for the double row as contrasted to the single larger-charge row because each of the double rows is at the same scaled burial depth as the larger single row. However, coalescence may increase pressures from venting gases and tend to offset the advantage of the smaller charge weight required by the double row. (auth)

4084 (VUF–3017) FEASIBILITY OF CAVITY PRESSURE AND TEMPERATURE MEASUREMENTS FOR A DECOUPLED NUCLEAR EXPLOSION. Final Technical Report. Project DRIBBLE. Swift, L. M.; Rubin, S.; Passell, T. O. (Stanford Research Inst., Menlo Park, Calif.). Sept. 1965. Contract AT(04-3)-115. 53p. Dep. mn; CFSTI $3.00 cy, $0.50 mn.

A study was made of the feasibility of measuring the pressure produced at the wall of a 14.5-meter spherical cavity by a 0.1-kton nuclear explosion. It was concluded that it will be feasible to make the desired measurements, and an experiment plan is recommended that appears to promise the most useful results. Gages and gage systems were examined with regard to time resolution, susceptibility to damage by ionizing radiation, and mechanical ruggedness. It was found that several systems, applied at the same time, give maximum probability of useful results. Studies also showed that it is feasible to measure the temperature of hot air near the edge of an underground cavity in which a 0.1-kton nuclear explosion has occurred. Measurement of the relative brightness of the radiating air in bands 100 Å wide centered at 2500 and 3500 Å will give the temperature to ±8 percent if the brightness ratio is determined to ±20 percent. With existing sensors, temperature can be followed to 20 msec after detonation, using a 100-meter long × 0.1-meter diameter nitrogen-filled light pipe with a reflecting aluminum liner. (P.C.H.)

4085 DIE FRIEDLICHE ANWENDUNG VON NUKLEAREN EXPLOSIONEN. EIN BERICHT UEBER DAS FORSCHUNGSPROGRAMM PLOWSHARE. (The Peaceful Applications of Nuclear Explosions. A Report on the Plowshare Program). Ginsburg, Theo. Munich, Verlag Karl Thiemig KG, 1965. 239p.

The peaceful applications of nuclear explosions are summarized. After a report on the Plowshare Program, the construction of nuclear bombs, the effect of nuclear explosions, and explosion research already carried out is reviewed. A number of applications, such as the production of electric energy from underground explosions, harbor dredging, the creation of cavities for subterranean storage, desalting of sea water, and the exploitation of presently unusable oil deposits are discussed. Applications of nuclear explosions in the study of the earth's crust, the atmosphere, and weather modification are also considered. (J.S.R.)

Facilities and Equipment

Refer also to abstracts 4049, 4284, 4570, and 5136.

4086 (ORNL–3843, pp 137-67) FILTRATION AND ADSORPTION UNDER ACCIDENT CONDITIONS. (Oak Ridge National Lab., Tenn.).

A study of the behavior of known nonradioactive methyl iodide in activated-charcoal adsorbers was undertaken. Gas chromatography (with electron-capture detection) is being utilized as the analytical technique for methyl iodide detection. Humidity, gas velocity, duration of flow, and charcoal depth are being varied in this study. A laboratory investigation of the filtration of particulate aerosols is in progress. Work is continuing on the development of a device with which to generate in the laboratory an aerosol that is similar to those expected in reactor accidents. Characterization of simulant aerosols generated by the device showed the presence of two particulate species (or size groups) with different tendencies to penetrate high-efficiency filters. The larger size particle is trapped by a fibrous filter with an efficiency of greater than 99.99%, while the smaller size is trapped somewhat less efficiently (> 99.9%). When fission products are released into the reactor containment system, the charcoal adsorbers used for removal of I_2 are heated by decay of I_2. An experiment was designed to measure and compare the ignition temperature of the charcoal with and without fission-product adsorption. The in-pile apparatus was assembled and the experiment is in progress. (J.R.D.)

4087 (ORNL-TM–1293) THERMALLY COMPENSATED CLOSURE FOR LIQUID DENSITY AUTOCLAVE. Rom, A. M. (Oak Ridge National Lab., Tenn.). Oct. 14, 1965. Contract W-7405-eng-26. 10p. Dep. mn; CFSTI $1.00 cy, $0.50 mn.

An improved mechanical closure was designed for the Liquid Density Autoclave, one that employs the thermal expansion properties of titanium 100-A, type 316 stainless steel, and Monel K to keep the autoclave tightly closed while going from room temperature and pressure to an operating temperature of 400°C and an operating pressure of 5000 psi. The closure consists of a titanium 100-A spacer washer, a titanium 100-A sealing cap, followed by a type 316 stainless steel backup plate fastened to the titanium 55-A body with Monel K socket head cap screws. The actual liquid seal depends on a gold-plated Inconel, static face seal. (auth)

4088 (TIM–949) USERS REPORT FOR PUMP IMPELLER CODES. Bourque, J. M. (Pratt and Whitney Aircraft, Middletown, Conn. Connecticut Advanced Nuclear Engineering Lab.). July 30, 1965. Contract AT(30-1)-2789. 67p. Dep. mn; CFSTI $3.00 cy, $0.75 mn.

Pump impeller codes written in FORTRAN-53 for the CDC-1604B computer using the standard control system with the FORTRAN-63 library, standard input and output units, and 32K storage are reported. The codes include: Impeller Redesign; Meridional Plane Velocity; Coordinates; Milling Coordinates; Minimum Channel Width; Machining; and Inspection Coordinates. (P.C.H.)

4089 (TLW–1055A) A SURVEY AND RECOMMENDATIONS FOR RADIOISOTOPE APPLICATIONS PERTINENT TO THE U. S. NAVAL CIVIL ENGINEERING LABORATORY OPERATIONS. Supplementary Report. Beaufait, L. J. Jr.; Kohl, J. (Tracerlab/West, Richmond, Calif.). Aug. 10, 1959. 16p.

Based on the large number of possible radioisotope applications, it is recommended that NCEL establish the means of effectively utilizing radioisotopes in their operations on a permanent basis. A modest laboratory and instrumentation for handling up to at least 10 mC of β- and γ-emitting radioisotopes is proposed. Economics are also considered. (P.C.H.)

4090 (JPRS–32842) GAMMA RADIATION SOURCES AT THE RUDJER BOSKOVIC INSTITUTE. I. THE 340-CURIE ^{60}Co SOURCE. Dvornik, Igor; Zec, Ursula. Translated from Tehnika (Belgrade), 20: 1656-60(Sept. 1965). 11p. (TT–65-33420). CFSTI $1.00 cy, $0.50 mn.

The purpose, design, and properties of a closed type gamma source are described. The source is used in experimentation in the fields of radiation chemistry, physics, and radiobiology. Radioactive cobalt is placed solidly in a container, and the samples are put into the space designed for irradiation by means of a manual mechanism. Depending on the position of the samples in relation to the source, the rate of dosage can be between 50 and 50,000 R per hr. (P.C.H.)

4091 HIGH-VOLTAGE WAVEFORMS AND ABNORMAL VOLTAGES IN SINGLE-PHASE TYPE X-RAY UNITS. Kanamori, Hitoshi (Schimadzu Seisakusho Ltd., Kyoto). J. Inst. Elec. Engrs. Japan, 85: 118-27(1965). (In Japanese).

The voltage waveforms applied to x-ray tubes greatly affect quality and quantity of the x rays produced. A theoretical treatment was applied, and voltage and current waveforms were analyzed in detail with a single-phase unit. Theoretical waveforms of the following cases coincided with experimental results: (1) normal case under resistive load, (2) tube-voltage waveforms are smoothed

by the condenser effect of high-voltage cables under resistive load, and (3) voltage-current characteristic curves of an x-ray tube are represented by two segments. (TCO)

4092 TECHNIQUES FOR DISMANTLING IRRADIATED RIGS. Cesarano, C.; Ghezzi, E.; Lauro, M. (CNEN, Casaccia, Italy). pp 441-51 of International Symposium on Working Methods in High Activity Hot Laboratories. Vol. I. Paris, Organization for Economic Cooperation and Development, 1965.

Post-irradiation dismantling is first started in the reactor hall, above the gamma pool. The rig is sectioned with a hydraulically operated cutting machine in two sections. The lower one drops in a basket and is subsequently transported via water in the gamma cell. This section, containing the capsule trains, is then dismantled and the capsules are recovered. The dismantling of the capsules is carried out at the Casaccia hot laboratory and the specimens are then recovered. (auth)

4093 IMPROVING ECONOMY WITH THE USE OF STANDARDIZED, MOVABLE, IN-CELL BOXES, AND THE DECONTAMINATION OF THEIR EQUIPMENT AT THE CENTRAL DECONTAMINATION FACILITY. Brinkmann, G.; Schenk, W.; Schulz, W.; Stockschlaeder, F. (Kernforschungsanlage, Juelich, Ger.). pp 653-66 of International Symposium on Working Methods in High Activity Hot Laboratories. Vol. II. Paris, Organization for Economic Cooperation and Development, 1965.

When a nuclear research center has several hot laboratories, all of which use in-cell boxes, it is desirable to standardize the cells and boxes as far as possible in order to achieve maximum economy, efficiency, and convenience. The principles of planning laid down at KFA-Jülich, in connection with the construction of several plants, are discussed. The advantages are enumerated and the conditions, which must be observed during planning, are described. The decontamination facility is also described. A manipulator exchange technique is discussed. (auth)

4094 SHUTTER CONTROLLED RADIOGRAPHIC EXPOSURE UNIT. (to General Motors Corp.). British Patent 1,008,590. Oct. 27, 1965. Filed Aug. 22, 1962.

A radiographic exposure unit suitable for either medical or industrial radiography is made up of a housing, a body of shield material secured to the housing and having an aperture in it, a shutter of shielding material rotatably mounted in the housing and having an exposure aperture in it, a rotor of shielding material rotatably mounted in the housing, and a radiation source mounted on the rotor. Two spring means are provided; one for biasing the rotor in one direction to a source-shielded position, and another for biasing the shutter in the same direction. Means are provided also for moving the shutter and rotor together in the other direction to align the source with the aperture and to align the aperture in the shutter with the aperture in the body. (B.L.M.)

4095 IMPROVEMENTS IN OR RELATING TO METHODS OF AND APPARATUS FOR TRANSFERRING LIQUIDS UNDER REMOTE CONTROL. Amaury, Paul; Labroche, Claude (to Commissariat a l'Energie Atomique). British Patent 1,008,865. Nov. 3, 1965. Priority date July 8, 1961, France.

A method and apparatus are described for transferring, by remote control, from a first hermetic enclosure through an outlet pipe, controlled amounts of a noxious liquid, particularly radioactive liquids, contained in the enclosure. A gas cushion is caused to act on the liquid to be transferred with the gas being under pressure and occupying a volume that is divided into two partial volumes. The first partial volume is limited by the walls of the first hermetic enclosure and the surface of the noxious liquid, and the second partial volume is limited by the walls of a second hermetic enclosure separated from the first enclosure but in communication with it. A driving liquid is introduced into the second enclosure at a controlled rate of flow so as to cause the second partial volume to decrease and correspondingly to increase the first partial volume. The pressure of the gas is at such a value that each time the driving liquid is introduced into the second enclosure, the amount of noxious liquid transferred out of the first enclosure is the same as the amount of driving liquid introduced. The pressure of the gas is maintained between transfers. (B.L.M.)

4096 IMPROVEMENTS IN OR RELATING TO ENTRANCE ARRANGEMENTS FOR AN IRRADIATION CELL. Jefferson, Sidney; Shepherd, George Henry (to United Kingdom Atomic Energy Authority). British Patent 1,009,000. Nov. 3, 1965. Filed Apr. 2, 1963.

An entrance or exit to a cell containing radioactive material includes a door in the form of a right vertical cylinder of shielding material rotatable about its vertical axis. A vertical recess is provided in the door with means for moving a material container into the recess. The door is rotated to bring the recess into register with the interior or exterior of the cell. (B.L.M.)

4097 DIFFUSION BOARD FOR FILTERING HIGH PRESSURE GASES. Silverman, L. (to U. S. Atomic Energy Commission). U. S. Patent 3,217,471. Nov. 16, 1965.

A diffusion board is designed for filtering high pressure gases which may emanate from an explosion releasing nuclear products. The diffusion board is a construction type material suitable for use in constructing a building to house nuclear apparatus. The board will filter particulate out of the released gases and at the same time adsorb radioactive halogens to prevent the latter from being released to the surroundings. (AEC)

Heat Transfer and Fluid Flow

See also PHYSICS — Fluid Physics and Thermodynamics

Refer also to abstracts 5031 and 5122.

4098 (AD-614633) STEADY DISTURBANCES TO VISCOUS, HIGHLY CONDUCTING LAMINAR BOUNDARY LAYER FLOW OVER A NONCONDUCTING WALL WITH PARALLEL MAGNETIC FIELD. Jarvis, Stephen Jr. (Frankford Arsenal, Philadelphia, Pa.). Dec. 1962. 47p. (M63-20-1). CFSTI $2.00 cy, $0.50 mn.

Steady disturbances to laminar boundary layer flow over a flat wall bounding a nonconducting rigid medium in the presence of a parallel magnetic field were examined. Disturbances were assumed due to both small wall irregularities and to weak incident waves when these may exist in the uniform stream outside of the boundary layer. The viscosity and electrical resistivity were assumed to be small, and heat conduction was assumed to be absent. It is shown that, adjacent to the wall, there is a critical layer in which the flow behavior depends on the relative smallness of the viscosity and the resistivity. Outside this layer, the flow is adequately given by a solution of the degenerate equation obtained by taking the viscosity and the resistivity zero. The resulting emitted waves, current sheet, wall pressure, and upstream behavior depend critically on the relative smallness of the viscosity and resistivity. (auth)

4099 (AECL-2333) FURTHER GEOMETRICAL FACTORS AFFECTING THE DRYOUT HEAT FLUX IN VERTICAL, INTERNALLY HEATED ANNULI COOLED BY STEAM/WATER MIXTURES AT 1000 PSI. Collier, J. G.; Wikhammer, G. A.; Moeck, E. O.; Macdonald, I. P. L. (Atomic Energy of Canada Ltd., Chalk River (Ontario)). Aug. 1965. 70p. Dep.; AECL $1.50.

Experiments designed to investigate the geometrical factors affecting the dryout heat flux in steam/water cooled annuli at 1000 psi were carried out in the FLARE facility at the Chalk River Nuclear Laboratories. In all cases power was applied to one or two round rods, 0.598 inches dia., held concentrically in an unheated round tube of 0.825 inches inside diameter. Unheated rods or dummies, also 0.598 in dia., were attached upstream or between the heated rods. Uniformly heated lengths of 9.92, 19.2, and 38.4 in. were employed, together with unheated dummies ranging in length from 0 to 42 in. Steam and water were

sprayed into the test section to give inlet qualities between 17 and 80% by weight steam, and mass flow rates from 2.8×10^5 to 1.2×10^6 1 bm/sq ft-hr. An analytical film flow model previously proposed was applied to the new data and modified to take into account the greater variety of test section arrangements. Dryout heat fluxes for about 300 experimental flow and geometry conditions were predicted with root-mean-square deviations less than 20%. (auth)

4100 (BW-67-2(a)) SODIUM-HEATED STEAM GENERATOR DEVELOPMENT. Addendum to PRELIMINARY DESIGN REPORT, FULL-SIZE GENERATOR. (Babcock and Wilcox., Barberton, Ohio. Boiler Div.). Sept. 15, 1965. Contract AT(11-1)-1280. 160p. Dep. mn; CFSTI $5.00 cy, $1.50 mn.

Sodium-water reactions in the sodium heated steam generator are discussed. The discussions include the prediction of the maximum credible sodium-water reaction pressures and volumes, the dynamic strength of the steam generator shell, localized bulge failure analysis, corrosion of material of construction in products of a sodium-water reaction, strain hardening data, structural analysis of the center pipe assembly under external pressure loading, structural analysis of the boiler coil supports under sodium-water reaction conditions, analysis of the tube vibration supports and baffles during a sodium-water reaction condition, and credibility of overheating the shell and liner during a sodium-water reaction. (M.O.W.)

4101 (EURAEC-1354) RESEARCH INTO THE CRITICAL HEAT FLUX (BURNOUT) IN BOILING WATER. Quarterly Progress Report No. 14, January 1, 1965–March 31, 1965. Mayinger, F.; Weiss, E.; Schad, O. (Maschinenfabrik Augsburg-Nuernberg A. G., Nuremberg (West Germany)). Apr. 13, 1965. Contract 057-61-RDD. 75p. Dep. mn; CFSTI $3.00 cy, $0.50 mn.

Work Performed under United States–Euratom Joint Research and Development Program.

Investigations were carried out in round channels with internal flow on the influence of the hydrodynamic form of flow at the start of the heated length of the test channel on the critical heat flux during boiling. The channels had an inside diameter of 7 π, and the tests were carried out with length/diameter ratios of 10, 40 and 80 at pressures of 70 and 100 atm with flows between 200 and 400 g/cm^2 sec. and qualities at the outlet of the test channel of $-0.2 < x_4 < +0.25$. As opposed to the investigations described in the previous quarterly report, in which the hydrodynamic flow profile was able to form fully in a long inlet and stabilizing section connected ahead of the heated length of the test channel, the present test channel has a sudden cross section change with sharp-edged inlet at the start of the heated length, so that the formation of the flow profile can only begin at this point. The results indicate the definite influence of the inlet conditions on the critical heat flux for short heated lengths of the test channels. Omission of the inlet and stabilizing section causes an increase of the critical heat flux by approximately 10% with channels having an L/D ratio of 10 and about 5% for channels with L/D = 40. With an increasing L/D ratio, this influence decreases and disappears completely at L/D = 80. Tests were also carried out on channels with an L/D ratio of the heated lengths of 5 and 140 which had a long inlet and stabilizing section. Two types of boiling crisis were observed. With the first type, as indicated by the light-beam oscillograph traces, hydraulic instability occurred a few seconds before the start of film boiling, the effect being noticeable due to the occurrence of variation in pressure and flow. In the second type, the boiling forms overlapped in a completely stable manner. The change from one type of the boiling crisis to the other took place suddenly in a range of the inlet quality of about –0.04 to –0.15. The attainable critical heat fluxes alter suddenly at this point whereby the boiling crisis with the hydraulic instability is on the side of greater sub-cooling and provides values of lower heat flux. (auth)

4102 (HW-SA-3640) MAXIMUM TEMPERATURES IN FLAT-PLATE FUEL ELEMENTS WITH FUEL-CLAD BONDING DEFECTS. Rowe, D. S. (General Electric Co., Richland, Wash. Hanford Atomic Products Operation). Nov. 17, 1964. Contract AT(45-1)-1350. 20p. (CONF-654-98). Dep. mn; CFSTI $1.00 cy, $0.50 mn.

From American Nuclear Society Meeting, San Francisco, Nov.–Dec. 1964.

A mathematical model that describes the heat transfer in a defectively bonded flat-plate fuel element is presented for a single circular spot or infinite strip defect on one side of the fuel plate. The general solution to the heat conduction equation for the mathematical model is shown for the strip defect. For a particular defect, the temperature distribution is dependent upon three dimensionless parameters which are functions of the defect size and the heat transfer properties of the defect. Data are provided in terms of the three dimensionless parameters which permit rapid estimates of maximum fuel temperatures in fuel plates with strip and spot defects. These defects are assumed to be step reductions in the normal fuel boundary conductance. Under certain conditions, defect sizes on the order of a couple of fuel thicknesses cause significant increases in the maximum central fuel temperature. (auth)

4103 (NAA-SR-Memo-11099) CAT—CONCENTRATION AND TEMPERATURE. A CODE DESCRIBING SIMULTANEOUS HEAT AND MASS TRANSFER FOR AN INFINITE CYLINDER. Berland, R. F. (Atomics International, Canoga Park, Calif.). Apr. 30, 1965. Contract AT-11-1-GEN-8. 45p. Dep. mn; CFSTI $2.00 cy, $0.50 mn.

CAT solves the simultaneous heat and mass transfer partial differential equations with respect to time and radial position, assuming a concentration diffusion coefficient of the form: $D = D_0 e^{-(E/RT)}$ where T is the temperature, D_0 and E are experimentally determined constants, and R is the universal gas constant. The density is assumed constant, but the heat capacity, thermal conductivity, heat of transport, and thermal diffusion ratio may be expressed as functions of concentration and temperature. The heat generation rate may be a function of time and radial position. (auth)

4104 (NP-15622) THE EFFECT OF NONUNIFORM AXIAL HEAT FLUX DISTRIBUTION. Report No. 9843-37. Todreas, Neil E.; Rohsenow, Warren M. (Massachusetts Inst. of Tech., Cambridge. Dept. of Mechanical Engineering). Sept. 20, 1965. Contract NsG-496. 245p.

A systematic experimental and analytic investigation of the effect of nonuniform axial heat flux distribution on critical heat flux was performed with water in the quality condition. Utilizing a model which ascribes the critical condition, to either a nucleation-induced disruption of the annular liquid film or annular film dryout, the experimental results taken at low pressures (50-200 psia) were confirmed. Application of this model to higher pressure conditions (500–2000 psia) indicated qualitative agreement with available data. Experimental data were obtained for flux distributions representing cosine, linear increasing and decreasing, inlet and exit peaked, spike, and uniform shapes. These flux distributions were achieved by electrical resistance heating of test sections. In each case the critical location as well as the total critical power was obtained. The analytic prediction of the results for all flux shapes was achieved by development of a model which considers the effect of nucleation within the annular film. It is shown that the occurrence of the critical condition is related to the local degree of nucleation and the local film flow rate. Both the experimental total critical power and the critical location were confirmed by this model. The results indicate that the total critical power for the outlet peaked flux distributions tested (ratios of maximum to minimum flux of 2, 4, and 5.75 to 1) can be 15 to 30% lower than for uniform flux distributions at comparable hydrodynamic operating conditions. In addition, from this model for given operating conditions, a locus of critical conditions can be constructed from uniform flux distribu-

tion data which will enable prediction of the performance of nonuniform flux distributions at similar conditions of mass velocity, pressure, and diameter. (auth)

4105 (TID–22321) CRITICAL HEAT FLUX FOR LARGE DIAMETER, INTERNALLY HEATED ANNULI IN FORCED CONVECTION BOILING AT 1000 PSIA. Topical Report No. 6. Matzner, Bruce (Columbia Univ., New York. Engineering Research Labs.). Sept. 1965. Contract AT(30-3)-187. 46p. Dep. mn; CFSTI $2.00 cy, $0.50 mn.

Critical heat flux data are obtained for an outlet pressure of 1000 psia. Several test-section geometries are tested, and an annular heater with stripping rings is found to give the highest thermal-power/pumping-power ratio of the geometries tested, while an eccentric heater with the same dimensions gives the lowest ratio. (T.F.H.)

4106 (BNL-tr–43) MEASUREMENT OF PARTICLE RESIDENCE TIMES IN A FLUIDIZED BED WITH ISOTOPES. Borlai, Oszkar; Hazi, Endre; Badacsonyi, Tivadar. Translated for Brookhaven National Lab., Upton, N. Y., from Veszpremi Vegyipari Egyet. Kozlem., 7: 55-60 (1963). 10p. Dep. mn; JCL $1.10 fs, $0.80 mf.

Studies showed that the relationship between mixing coefficient and residence-time distribution is valid for particle mixing. The particle residence-time curve was obtained by using grains tagged with a radioactive isotope. Chromium-51, a gamma isotope of slight toxicity, was used for the tagging. An insoluble, homogeneous, and satisfactorily bound layer of chromium oxide was formed on the surface of the tagged grains, so that a specific activity of 150 μC/g was readily obtainable. The residence-time distribution curve (i.e., the change in the activity of the grains leaving the fluid bed, expressed as a function of time) was measured by means of an NaI(Tl) crystal scintillation counter and recorded by means of a compensograph connected to a fast rate meter. The method is equally applicable to liquid and gas fluidization. (auth)

4107 (NASA-TT-F-262) THE FLOW OF GAS IN CHANNELS IN THE PRESENCE OF HEAT TRANSFER. Nazarchuk, M. M. Translation of Techeniya Gaza v Kanalakh pri Nalichii Teploobmena, Publishing House of Academy of Sciences, Ukranian SSR, Kiev, 1963. 188p. CFSTI $5.00 cy, $1.00 mn.

Information is included on the one-dimensional theory of the flow of gas in channels in the presence of heat transfer between walls and gas. New methods of calculation based on the theory of the boundary layer are given for the flow of gas in tubes; the conditions of crisis in such flows were examined, and the limits of applicability of Reynolds analogies are indicated. Tables of gas-dynamic functions for air are appended. 59 references are cited. (P.C.H.)

4108 ABLATION MECHANISM FOR IMPREGNATED TUNGSTEN. Ungar, E. W. (Battelle Memorial Inst., Columbus, Ohio); Touryan, K. J. AIAA (Amer. Inst. Aeron. Astronaut.) J., 3: 1949-51(Oct. 1965).

Some comments and observations relative to the ablation mechanism for impregnated tungsten materials are presented. Experimental observations of surface temperature and current output from copper-impregnated tungsten emitters in 83% N_2–20% O_2 are shown. Similar tests were conducted in argon. It is found, in both cases, that the formation and retention of a relatively stable liquid layer strongly influences the time to specimen failure and the internal temperature history. It is pointed out that the formation of a liquid layer through the process of phase change expansion appears to be a critical phenomena which must be included in heat-transfer calculations. (L.B.S.)

4109 HEAT EXCHANGE UNIT SPACER GRIDS. Shaw, Trevor; Taylor, Derek (to United Kingdom Atomic Energy Authority). British Patent 1,007,997. Oct. 22, 1965. Filed Oct. 14, 1963.

A spacer grid for locating a number of elongate heat exchange elements is made up of an array of corrugated strips. The troughs of each strip engage the crests of adjacent strip. The strips are so arranged that each trough provides with its flank two points of location for an element and the crest of an adjacent strip provides the third point. Such a grid may be used to locate the elements in staggered rows so close that visual inspection along the rows makes the lateral dimensions of the elements in adjacent rows appear to overlap. Preferably, the troughs and crest of each strip are truncated to give an area of engagement between adjacent strips, and a welded joint may be made in this area. (B.L.M.)

Materials Testing

Refer also to abstract 5033.

4110 (ORNL–3870, pp 146-54) NONDESTRUCTIVE TEST DEVELOPMENT. McClung, R. W. (Oak Ridge National Lab., Tenn.).

In continuing development of computer calculation of parameters of an induced electromagnetic field, the phase and amplitude of the vector potential, field shaping, flow of current in the specimen, and force on the specimen were studied. A phase-sensitive eddy-current instrument was improved and applied to test problems for the HFIR, GCR, Fermi, HTM, and Desalination Projects. Work on nonbond detection was directed toward dispersion-core fuel elements, such as used for HFIR and ATR. A device was prepared for hot-cell examination of fuel tubes such as used for PM-1 and proposed for HWOCR. Electrodischarge machining techniques were studied for fabricating reproducible reference notches in small-diameter tubing. The sensitivity of x-ray attenuation techniques were studied and extended to the determination of total fuel content in fuel plates used for HFIR, ATR, and ORR. A scanner was designed and built to develop techniques for measuring homogeneity of fuel rods. A photomultiplier calibration system was assembled and used to optimize radiation detector operation. The sensitivity of a x-ray television was improved and a projection x-ray microscope for evaluating finely divided materials was assembled. Inspection techniques for refractory alloys based on Ti, Mo, Ta, and Tw, which are useful in space-power and other high-temperature systems, were studied. An ultrasonic scanner tank for use in a hot-cell facility was modified. (W.L.G.)

4111 (ORNL–IIC–5) PROCEEDINGS OF SYMPOSIUM ON LOW-ENERGY X- AND GAMMA SOURCES AND APPLICATIONS HELD AT ILLINOIS INSTITUTE OF TECHNOLOGY RESEARCH INSTITUTE, CHICAGO, ILLINOIS, OCTOBER 20-21, 1964. Baker, Philip S.; Gerrard, Martha (eds.) (Oak Ridge National Lab., Tenn.). Oct. 1965. Contract W-7405-eng-26. 380p. (CONF-641017). Dep. mn; CFSTI $4.00 cy, $1.75 mn.

Twenty-three articles are included; separate abstracts were prepared for 12. The remaining 11 were previously abstracted in NSA as: 19: 15849, 18340, 22152, 22154, 23326, 23950, 24477, 24690, 24901, 42377, and 42775. (P.C.H.)

For abstracts of individual papers see: 3801–3804, 3882–3886, 4219, 4268, and 5000.

4112 (SC-TM–65-443) SHOCK SPRINGS AND PULSE SHAPING ON IMPACT SHOCK MACHINES. Brooks, R. O. (Sandia Corp., Albuquerque, N. Mex.). Sept. 1965. Contract AT(29-1)-789. 48p. Dep. mn; CFSTI $2.00 cy, $0.50 mn.

An investigation was conducted to find materials and practical shock spring designs that can be used to generate different shock pulses on impact shock machines. Four classical pulse shapes considered are half-sine, triangle, haversine, and parabolic cusp. The theoretical dynamic stress-strain behavior of shock springs to generate these shapes and the differences between them are reviewed, and in one case, compared to actual test results. Dynamic mechanical properties, such as stress-specific energy relationships, modulus of elasticity in dynamic compression, and coefficient of restitution, were determined experimentally for several types of polymers and plastics. In addition, for rubber the effect of unrestrained and

semirestrained boundary conditions upon pulse shape and mechanical properties is shown. Also discussed are three different designs of variable rate liquid springs and the pulse shapes they generated. (auth)

4113 (TID–22358) THE RELATIONSHIP BETWEEN QUALITY CONTROL AND QUALITY ASSURANCE. Speech at the Production Review Meeting, August 25, 1965. Meyer, H. N. Jr. (Albuquerque Operations Office (AEC), N. Mex.). 11p. Dep. mn; CFSTI $1.00 cy, $0.50 mn.

Objectives of the AEC Weapons Quality Assurance Program are stated and discussed. Contractor responsibility is stressed. (P.C.H.)

4114 (AD–621784) DEVELOPMENT OF METHODS OF DEFECTOSCOPY OF METALS WITH APPLICATION OF GAMMA RADIATION. Luppov, G. M. Translated from Tr. Moskov. Inst. Inzh. Zheleznodarozhnogo Transporta, No. 165, 82-91(1963). 13p. (FTD-MT-65-33). CFSTI $1.00 cy, $0.50 mn.

The photographic, ionization, xerographic, and television methods of gamma defectoscopy of metals are discussed and evaluated. The advantages of each method are also considered. (P.C.H.)

4115 NEUTRON RADIOGRAPHY. METHODS, CAPABILITIES, AND APPLICATIONS. Berger, Harold. New York, Elsevier Publishing Company, 1965. 154p. $9.00.

Topics covered include neutron sources, neutron image detection methods, application of neutron radiographic techniques, radioactive, accelerator, and nuclear reactor neutron sources. Photographic techniques are emphasized, but other detection methods, including neutron image intensification techniques are also considered. Nuclear applications are discussed, and also applications in the metallurgical, solid-state, and biological fields are considered. (J.F.P.)

4116 APPLICATION OF ADVANCED AND NUCLEAR PHYSICS TO TESTING MATERIALS. A Symposium, Philadelphia, Pa., Feb. 3, 1964. ASTM Special Technical Publication No. 373. Philadelphia, Pa., American Society for Testing and Materials, 1965. 140p. $6.25. (CONF-640207).

Building materials are considered as well as some insights into advanced physical processes and measurements and their applications to the investigation of materials. Included are extremely short electromagnetic waves and their absorption by moisture, spectrochemical analysis of materials by x rays, and an examination of neutron diffraction, its similarities to and differences from x-ray diffraction, the relative limitations of the methods, and a discussion of the types of measurements possible with neutron diffraction compared with x-ray diffraction, and irradiation by nuclear fission products including the use of radioisotopes. These physical and nuclear processes are used to determine moisture contents, thicknesses, densities, and other properties of materials in situ, and to make a variety of difficult measurements, to study effects of irradiation on organic and inorganic materials, to follow manufacturing processes, and to make other determinations, some hitherto unavailable, slow or uncertain. Ten papers are included in the conference. (J.F.P.)

4117 RADIOSCOPY AND RADIOGRAPHY EQUIPMENT FOR IRRADIATED FUEL ELEMENTS ASSOCIATED WITH THE EL 3 AND PEGASE RESEARCH REACTORS. Briffaud, G. (CEN, Saclay, France). pp 25-39 of International Symposium on Working Methods in High Activity Hot Laboratories. Vol. I. Paris, Organization for Economic Cooperation and Development, 1965. (In French).

The problems in radioscopy and radiography of highly irradiated materials are discussed. The various processes developed to solve these problems, in particular to eliminate the parasitic effects of gamma rays, are discussed. (auth)

4118 INSTALLATION FOR NON-DESTRUCTIVE X-RAY TESTS OF IRRADIATED FUEL ELEMENTS. Spalthoff, W. (Schiffbau und Schiffahrt mbH, Geesthacht, Ger.). pp 57-64 of International Symposium on Working Methods in High Activity Hot Laboratories. Vol. I. Paris, Organization for Economic Cooperation and Development, 1965.

The installation consists of a 300-kv apparatus and a working unit, which holds the fuel rod on a sled in a shielded tunnel and the x-ray film on a rotatable drum. This method of x-raying yields a vertical projection of the fuel rod on the film. Darkening of the film by the gamma radiation of the fuel rod is kept at a minimum. (auth)

4119 THE DEVELOPMENT OF ACTIVE RADIOGRAPHIC INSPECTION TECHNIQUES AT HARWELL. Sharpe, R. S.; Derbyshire, R. T. P.; Parish, R. W. (Atomic Energy Research Establishment, Harwell, Eng.). pp 75-88 of International Symposium on Working Methods in High Activity Hot Laboratories. Vol. I. Paris, Organization for Economic Cooperation and Development, 1965.

Radiography of highly radioactive components and samples is made difficult by the superimposed ambient radiation level and the special techniques are required. Developments at Harwell led to a better understanding of the problems involved and, as a result, a number of techniques were satisfactorily introduced for in-cell inspection. Programs based on image projection, high-speed techniques, color films, and energy discrimination are discussed and typical applications described. Using an x-ray source with a 1-μ dia focal spot it was possible to extend active sample inspection into the fields of microradiography and crystal analysis. (auth)

4120 NON-DESTRUCTIVE TESTING OF FUEL IN THE DOUNREAY ALPHA-GAMMA HOT CELLS. Swanson, K. M. (United Kingdom Atomic Energy Authority, Caithness, Scotland). pp 155-65 of International Symposium on Working Methods in High Activity Hot Laboratories. Vol. I. Paris, Organization for Economic Cooperation and Development, 1965.

Nondestructive testing methods allow repeated irradiations of the same specimens with the advantage of accuracy of measurement of changes with burnup. Savings in cost and time are also realized. Experimental methods used on specimens repeatedly irradiated are described, particularly x-radiography and gamma densitometry. (auth)

4121 NON-DESTRUCTIVE TESTING OF FUEL ELEMENTS IN THE HOT CELLS AT BERKELEY NUCLEAR LABORATORIES OF THE CENTRAL ELECTRICITY GENERATING BOARD. Sharpe, B. F.; Greenwood, G. W. (Central Electricity Generating Board, Berkeley, Eng.). pp 167-78 of International Symposium on Working Methods in High Activity Hot Laboratories. Vol. I. Paris, Organization for Economic Cooperation and Development, 1965.

The cells described are equipped for examination of approximately 500 fuel elements per year. Emphasis is placed on nondestructive examination because radioactive contamination and waste disposal problems are minimized. Optical equipment for detailed inspection and photography of fuel elements through the cell windows, a radiographic technique for accurate measurement of uranium bar distortion, and a bubble leak testing method whereby leaks as small as 10^{-3} lusecs can be precisely located and their size and shape assessed are described. (auth)

4122 EQUIPMENT FOR NON-DESTRUCTIVE EXAMINATION. Walrave, W. K. A. (Reactor Centrum Nederland, Petten, Netherlands). pp 221-8 of International Symposium on Working Methods in High Activity Hot Laboratories. Vol. I. Paris, Organization for Economic Cooperation and Development, 1965.

Nondestructive observation techniques for highly radioactive objects, such as televiewing and photography through a lead glass window, in-cell television, autoradiography, fluoroscopy, pictures taken with a pinhole camera, and gamma spectroscopy are described. (auth)

4123 PROCEDURES FOR THE NON-DESTRUCTIVE TESTING OF FUEL RODS. Djurle, S. (Aktiebolaget Atomenergi, Studsvik, Sweden). pp 229-43 of Interna-

tional Symposium on Working Methods in High Activity Hot Laboratories. Vol. I. Paris, Organization for Economic Cooperation and Development, 1965.

The nondestructive testing methods for fuel rods, used in the Active Laboratory for Fuel Elements at Studsvik, Sweden, are described. Procedures are discussed for visual examination, photography, metrology of both short rods and large bundles of rods, gamma scanning for relative and absolute determination of burnup, and fission gas sampling. (auth)

4124 REMOTE METROLOGY AND EXAMINATION TECHNIQUES ON IRRADIATED FUEL MATERIALS AS PRACTISED IN THE UNITED STATES. Brown, F. L. (Argonne National Lab., Ill.); Murphy, W. F.; Stearns, E. H. pp 245-65 of International Symposium on Working Methods in High Activity Hot Laboratories. Vol. I. Paris, Organization for Economic Cooperation and Development, 1965.

Nondestructive tests performed on irradiated materials as they are received from the reactor provide useful data without physically altering or damaging the specimen. Tests that relate to visual observation, metrology, and self-emitted radiation are discussed. Commonly accepted test methods and various operating techniques, primarily for the examination of small samples irradiated in capsules, are described. Details are included on viewing and photography, metrology, density determination, gamma scanning, thermal diffusivity, electrical resistivity, and replication. (auth)

4125 MACHINING AND DISMANTLING METHODS IN HIGH ACTIVITY CELLS AT THE ISPRA ESTABLISHMENT OF THE EUROPEAN ATOMIC ENERGY COMMUNITY. Cauwe, J.; Bonnet, G.; Junger, J. M. (Communaute Europeenne de l'Energie Atomique, Ispra, Italy). pp 315-28 of International Symposium on Working Methods in High Activity Hot Laboratories. Vol. I. Paris, Organization for Economic Cooperation and Development, 1965. (In French).

The processes used in hot cells for dismantling or machining irradiation capsules, fuel elements, and various materials, including ceramic fuels, are described. Operations carried out in the metallurgy cells and the processes used in pilot cells for dismantling vertical fuel elements by unscrewing are considered. (auth)

4126 DISMANTLING AND MACHINING OPERATIONS ON HIGH ACTIVITY RIGS AT HARWELL. Ritchie, A. B.; Serrels, G. A. (Atomic Energy Research Establishment, Harwell, Eng.). pp 329-46 of International Symposium on Working Methods in High Activity Hot Laboratories. Vol. I. Paris, Organization for Economic Cooperation and Development, 1965.

The work of the high-activity handling facilities at A.E.R.E. Harwell is reviewed. The dismantling of large irradiated assemblies, fuel element examination, and other operations involving the precision machining of irradiated material are described. The use of a transportable cell to permit rig unloading at the reactor is described. (auth)

4127 DISMANTLING AND MACHINING METHODS USED IN HOT CELLS AND WORKSHOPS. Stauffer, M.; Graf, P. (Institut Federal de Recherches en Matiere de Reacteurs, Wuerenlingen, Switzerland). pp 395-414 of International Symposium on Working Methods in High Activity Hot Laboratories. Vol. I. Paris, Organization for Economic Cooperation and Development, 1965. (In French).

The hot laboratory of Würenlingen, designed for post-irradiation examinations of all types of irradiated materials, proved to be extremely flexible in operation. Thus it was necessary to develop dismantling and machining methods that depend on the type of experiments to be made, on prescribed machining tolerances, and on the basic training level of the operatives. One method relates to operations required for complicated inpile rigs, hot loops, and repairs to reactor components. Currently available standard equipment, tools, and measuring instruments are used. The majority of operations are carried out using master-slave manipulators. In other methods, used mainly with simpler irradiation rigs intended for intensive testing programs, small semi-automatic machining complexes are used. The manipulator provided with an additional remote control system for difficult operations only. The last method concerns mainly the machining and preparation of specimens. Since in this case a large number of parts are handled, processes are automatic so that a semi-skilled operator may be used. Master-slave manipulators are only used as standby equipment in breakdown. Comparison of the methods resulted in a division of the operations into two sequences. The first one consists of isolating the hot loops from their metal or ceramic jackets and mechanical supports, the second one is used for isolating and machining the irradiated objects. Different machining processes, which are possible in a conventional workshop, were tried with varying degrees of success. Some methods are described in detail, especially those including dry-cutting techniques developed to avoid water consumption and time-consuming decontamination in the hot cells. (auth)

4128 DEMOUNTING AND MACHINING TECHNIQUES IN THE HOT CELLS AT BERKELEY NUCLEAR LABORATORIES OF THE CENTRAL ELECTRICITY GENERATING BOARD. Sharpe, B. F.; Morter, W. F. (Central Electricity Generating Board, Berkeley, Eng.). pp 415-27 of International Symposium on Working Methods in High Activity Hot Laboratories. Vol. I. Paris, Organization for Economic Cooperation and Development, 1965.

Approximately 500 fuel elements per year are examined in the hot cells at Berkeley Nuclear Laboratories and all are dismantled and machined to some extent. The reasons for selecting or rejecting the possible machining techniques finally selected are examined in the light of operating experience. Development of these techniques is described and consideration is given to the most likely future techniques. (auth)

4129 REMOTELY CONTROLLED UNIVERSAL MILLING MACHINE CONSTRUCTION AND OPERATIONAL EXPERIENCE. Wervers, H. J. (Reactor Centrum Nederland, Petten, Netherlands). pp 453-65 of International Symposium on Working Methods in High Activity Hot Laboratories. Vol. I. Paris, Organization for Economic Cooperation and Development, 1965.

A description is presented of a modified, commercially available milling machine, which is being used in the high-activity cells of the Reactor Centrum Nederland. The machine is intended for the longitudinal slitting of capsules of approximately 600 mm length, for cross-sectional cutting of irradiated rigs and for the incidental production of tensile specimens. The machine will also be used in conjunction with a radiation detector/collimator assembly for the recording of burnup profiles of fuel elements. (auth)

4130 TECHNIQUES AND WORKING METHODS FOR THE EXAMINATION OF IRRADIATED CERAMIC FUEL ELEMENTS AT WINDSCALE. Skinner, J.; Vaughan, G. A.; Vallely, J. (Reactor Development Labs., Windscale, Eng.). pp 825-41 of International Symposium on Working Methods in High Activity Hot Laboratories. Vol. II. Paris, Organization for Economic Cooperation and Development, 1965.

The remote handling facilities used for examination of irradiated ceramic fuel stringers discharged from the Windscale AGR are briefly described. These facilities are of two types, concrete-shielded caves and separate lines of lead-shielded cells, and are capable of use for examining some 3000 fuel pins per year. The techniques used in dismantling fuel stringers and for cutting samples of can and fuel from irradiated fuel pins are described, with emphasis on the working methods employed. Four cutting techniques were developed for ceramic fuel pins, simple pipe cutting, underwater high-speed diamond cutting, spark machining, and ultrasonic drilling. Decontamination and maintenance problems in the facilities are discussed. The nondestructive examination of fuel pins by various methods such as radiography, metrology, leak testing, or gamma scanning is described together with

specialized equipment used for carrying out mechanical tests on fuel pins. Administrative control of the work done in the facilities is discussed. (auth)

Protective Structures

4131 (AD-622552) SHALLOW-BURIED MODEL ARCHES SUBJECTED TO A TRAVELING-WAVE LOAD. Type C, Final Report. Allgood, J. R.; Seabold, R. H. (Naval Civil Engineering Lab., Port Hueneme, Calif.). Oct. 1965. 135p. (R-375). CFSTI $4.00 cy, $1.00 mn.

Operation Snowball Project 3.4 consisted of tests performed on twelve model arches to determine their behavior under a traveling-wave blast loading. The prime objective was to define the body motions for a comparison with a previously developed theory. On recovery of the structures after test it was found that the four 30-inch span arches were in relatively good condition; however, most of the eight 12-inch span arches were badly damaged. The damage was inflicted by ejecta of large, densely-compacted, hard lumps of clay. Fortunately, the ejecta did not obscure the results from the large arches on which all of the electronic instrumentation was located. All electronic instrumentation operated and records were obtained for all transducers. Actual body motions were larger than those determined from the theory. Test results indicate that the foundation modulus varies and that arching shear should be expressed as a function of deflection. Considerable data were obtained on shell response. Thrust distribution around the arch was fairly uniform, even though moments on the lee side were 30 percent greater than those at the same distance from the spring line on the blastward side. Among other information, it was found that: the floor displaced about the same as the free field at the corresponding elevation; and large forces developed in the footing tie bars. (auth)

4132 (AWRE-O-93/65) BLAST LOADING ON A RIGHT CIRCULAR CYLINDER. Martin, Valerie C.; Mead, K. F.; Uppard, J. E. (Atomic Weapons Research Establishment, Aldermaston (England)). Nov. 1965. 34p. Dep. mn; BIS $1.00; HMSO 5s. 0d.

Aspects of blast loading on circular cylinders are discussed and experimental details presented. (P.C.H.)

Space Propulsion

See also ISOTOPE TECHNOLOGY — Power Application
REACTOR TECHNOLOGY — Propulsion and Space

4133 (N64-25007) CHARGED COLLOID GENERATING SYSTEM FOR ELECTRIC PROPULSION. Final Report. Report No. 68. Gignoux, D.; Anton, H. F.; Shea, J. J. (Cosmic, Inc., Washington, D. C.). Oct. 12, 1963. Contract NAS3-2509. 79p. (NASA-CR-54049). CFSTI.

An induction-charged colloid generating system was operated satisfactorily. The rotating speed was varied between 1,000 and 18,000 rpm, the mass flow between 1.5×10^{-6} and 120×10^{-6} kilograms/second, and the voltage between 0 and 50,000 volts. Mass flow, beam current, voltage, and thrust were measured with a sufficient accuracy to make possible direct measurements of the efficiency. An efficiency of 80% was obtained in repeated experiments. The system has interesting potential application to electrostatic thrustors with low specific impulse. (auth)

4134 (SEL-63-120) A SEMITOROIDAL REFLEX DISCHARGE AS A PROPULSION DEVICE. Technical Report No. 0253-4. Pigache, D. R. (Stanford Univ., Calif. Stanford Electronics Labs.). Nov. 1963. Contract AT (04-3)-326. 13p. Dep. mn; CFSTI $1.00 cy, $0.50 mn.

The PIG reflex discharge is one of the plasma devices that may be used for the electrical propulsion of space vehicles. The efficiency of the linear reflex discharges used thus far seems to be seriously limited by the loss of energy due to ions falling on the emitting cathode. A reflex discharge having a semitoroidal shape and using two cylindrical emitting cathodes avoids this limitation and therefore an efficiency greater than 50 percent may be obtained. (auth)

4135 CHARACTERISTICS OF POROUS TUNGSTEN IONIZERS. Husmann, O. K.; Turk, R. (Hughes Aircraft Co., Malibu, Calif.). AIAA (Am. Inst. Aeron. Astronaut.) J., 3: 1653-8(Sept. 1965).

An important characteristic of the electric propulsion system is its total efficiency: the product of power and ionization efficiency. A total efficiency of over 90% is desirable. High pore densities improve the ionization efficiency and reduce electrode erosion. Neutral efflux of 2.7% at 10 ma/cm^2 cesium ion current density is reported here for porous tungsten pellets as surface ionizers, coated with a thin layer of fine tungsten powder. Both coat and substrate pore density influence the neutral efflux, and pore densities exceeding 5×10^6 pores/cm^2 (line intercept method) are desirable. Neutral efflux measurements up to 25 ma/cm^2 ion current density are reported. Extrapolated measurements of the sintering rate of spherical tungsten powder as fine as 3.9 μ show it to be sufficiently stable for use at 1373°K for one year at densities of 80% or above. Change of direct pore count over one year is about 2%. (auth)

4136 PROPELLANT TRIGGERED GAS DISCHARGES IN PULSED PLASMA ENGINES. Levy, M. E. (Vitro Labs., West Orange, N. J.); Schwalb, A. J. AIAA (Am. Inst. Aeron. Astronaut.) J., 3: 1743-6(Sept. 1965).

A study is made of the events occurring within the accelerator between the time the injection valve is pulsed and the time appreciable current starts flowing in the discharge. This involves the development of analytical expressions for the space time distribution of neutral gas-propellant density in the interelectrode space and the establishment of the sequence of events leading to electric breakdown. In the experiments the accelerator electrodes are replaced by two flat, circular, parallel plates in a linear pinch configuration. The propellant is injected from the propellant reservoir tank by a pulsed valve, through a duct leading to a single orifice in the center of one of the electrodes. An analytical model is introduced that reflects the physical aspects of the neutral gas injection mechanism. The results of the study of the time delay between initial penetration of the gas propellant into the interelectrode space and the electric breakdown are given as a function of reservoir pressure and interelectrode potential. (J.F.P.)

4137 FEASIBILITY STUDY OF THE USE OF ANTIMATTER AS A ROCKET PROPELLANT. Miller, Gordon H. (Texaco Experiment Inc., Richmond, Va.). AIAA (Am. Inst. Aeron. Astronaut.) J., 3: 1758-60(Sept. 1965).

In the annihilation process of matter with antimatter extremely high energy release occurs. Thus antimatter is considered for possible use as a rocket propellant. But the problems of production, storage, and use of such material are extremely difficult. These considerations are discussed from a feasibility standpoint to see what may be the limiting factors on the production rates, storage concentrations, and containment times possible in magnetic and electric fields, and the propulsion efficiency and weight problems inherent in use. It is concluded that although antimatter would be a desirable propellant, its preparation in useful quantities is not currently possible, and no way can be visualized at present for the storage of antiparticles. The high energies necessary to reduce Coulomb scattering cause unbearable energy losses due to electron radiation. Thus no further feasibility work is justified for the present. (J.F.P.)

4138 EJECTION OF A PINCHED PLASMA FROM AN AXIAL ORIFICE. Jahn, Robert G.; von Jaskowsky, Woldemar; Burton, Rodney L. (Princeton Univ., N. J.). AIAA (Amer. Inst. Aeron. Astronaut.) J., 3: 1862-6(Oct. 1965).

The ejection of an argon plasma produced in a large-radius pinch discharge chamber from an axial orifice in one electrode is studied photographically, and with magnetic probes. The development of the discharge within the chamber is found to be disturbed very little by the presence of the large aperture, but a luminous front and current sheet are observed to diffract radially and axially outward through the orifice, establishing an exhaust plume that embodies large current densities and magnetic fields. The intense plasma column created by the radial pinch within the chamber also expands axially out through the orifice, eventually overtaking and piercing through the previously ejected diffracted front. In some cases the velocity of this axial expansion exceeds that of the prior interior radial motion, indicating significant recovery of the thermal energy resident in the pinch column. (auth)

4139 HIGH CURRENT STEADY STATE COAXIAL PLASMA ACCELERATORS. Stratton, T. F. (Univ. of California, Los Alamos, N. Mex.). AIAA (Amer. Inst. Aeron. Astronaut.)J., 3: 1961-3(Oct. 1965). (LA-DC-7021).

A theory is presented for the mechanisms that dominate the behavior of coaxial arc plasma. A schematic diagram is presented of the appearance of the arc and the features of the model, which predicts the scaling properties of the arcs with respect to arc current, arc voltage, arc power, mass flow rate and mass number, and charge of the emergent ions. Comparisons are made of the predictions with previous measurements of exhaust velocity and thrust of hydrogen plasma, and acceleration of lithium plasma. (L.B.S.)

4140 ELECTROSTATIC PROPULSION SYSTEM WITH A DIRECT NUCLEAR ELECTRO GENERATOR. Low, Charles A. Jr.; Mickelson, William R. (to U. S. Atomic Energy Commission). U. S. Patent 3,184,915. May 25, 1965.

A propulsion system is designed wherein an electrostatic rocket thruster is embodied with a direct nuclear electro-generator. The electro-generator consists of a decaying radioisotope which emits charged particles as it decays and serves as a nuclear energy source in the electro-generator. The emitted particles impinge on, into, or through a collector, thereby creating an electric potential difference between the emitting surface and the collector. The kinetic energy of the emitted charged particles is directly converted into electrical energy as the emitted charged particles do work against an electric field which has been created between the emitting surface and the collector. The potential difference thus created is used to accelerate charged propellant particles or molecules in an electrostatic thruster whereby thrust is produced. (AEC)

Vacuum Engineering

Refer also to abstract 4144.

GEOLOGY, METEOROLOGY, AND MINERALOGY

General

4141 (AD–618733) THE PHYSICS OF THE BASE SURGE. Young, George A. (Naval Ordnance Lab., White Oak, Md.). June 17, 1965. 294p. CFSTI $6.00 cy, $1.50 mn.

The column and base surges formed by the underwater nuclear explosion were measured in detail. The primary surge originated as a spillout of sea-water jets which broke into spray and formed a dense toroidal shaped cloud. Computations were made for the coalescence and rainout of drops and a theory was developed for mixing of the surge with the air. The late behavior was strongly influenced by the convectively unstable atmosphere and the high relative humidity. (TAB)

4142 (AD–619053) FEASIBILITY OF MODELING RUN-UP EFFECTS OF DISPERSIVE WATER WAVES. Jordaan, Jan M. Jr. (Naval Civil Engineering Lab., Port Hueneme, Calif.). May 1965. 57p. (TN-N-691). CFSTI $3.00 cy, $0.75 mn.

Studies were made in a laboratory test basin to determine the feasibility of modeling run-up effects of explosively generated water waves on beach and waterfront structures. Results were compared with analytically derived predictions, and wave measurements (but not run-up) made in the ocean with high-energy (HE) explosives as the generating source. The test basin is 92 by 94 feet in size with 1:5, 1:13.6 and 1:5 sand beaches on three sides and on the fourth a 14-foot-diameter semiparaboloidal plunger which by sudden plunge or retraction generates dispersive waves with dominant period of 2 seconds, height of 0.2 feet, and length of 20 feet in water 2½ feet deep. It was found that wave motions are: predicted well by Green's Law, as modified for dispersive waves; and related to waves generated in the ocean by HE by the Froude scaling law. (auth)

4143 (AD–619969) CLOSE-IN EFFECTS FROM A SURFACE BURST. Final Report. Fugelso, L. E. (MRD Div., General American Transportation Corp., Niles, Ill.). Aug. 1965. Contract AF29(601)-5009. 153p. (WL-TR-64-113). CFSTI $5.00 cy, $1.00 mn.

A computer program for the solution of stress wave propagation into a real rock material near the center region from a surface burst of a large yield nuclear device was prepared. Preliminary numerical results are shown. The computer program was prepared from a set of finite difference equations representing the differential equations of motion. The differential equations of motion are taken in a form that includes large displacements, large strains, large rotations, large velocities, and accelerations. A constitutive equation relating stresses to displacements, strains, and temperature was derived. This equation accounts for plasticity, finite strains, and temperature. The equation was developed in two stages. The form of the reversible component was derived in accordance with classical thermodynamics and finite elasticity theory. The irreversible component of the macroscopic deformation was derived from the microscopic theory of the motion of crystalline imperfections and their relationship and response to stresses and temperature. (auth)

4144 (PNE–810F) GEOLOGY AND SURFACE EFFECTS, HANDCAR EVENT. Davis, R. E.; Carr, W. J.; D'Agostino, J. P. (Geological Survey, Denver, Colo.). Aug. 1965. Contract 1105-4227-61. 29p. Dep. mn; CFSTI $2.00 cy, $0.50 mn.

Continuous monitoring and geologic supervision was performed during the drilling of Handcar instrument holes U10b #4, U10b #5, and U10b #6. The interpretation of the geology along a north-south line from hole U10b #1 to hole U10b #6, as derived from the studies of cuttings, core, and geophysical logs, revealed variations in the thickness of the alluvium, tuff, shale, and dolomite encountered in the drill holes. In addition, several faults were penetrated and several others were postulated in places appropriate to provide the interpretative geologic situation most consistent with the regional geologic setting. Following the Handcar event, surface fractures were mapped in the alluvium in the vicinity of the site as part of the Geological Survey's continuing program of postshot mapping in Yucca Flat. The pattern of induced surface fractures was almost unique in Yucca Flat in that it was more nearly rectilinear and appeared to be more closely related to a major known structure (the Yucca fault) and to possible fracture patterns in the bedrock than do most other surface fracture patterns in Yucca Flat. (auth)

4145 POTASSIUM, RUBIDIUM, STRONTIUM, THORIUM, URANIUM, AND THE RATIO OF ^{87}Sr TO ^{86}Sr IN OCEANIC THOLEIITIC BASALT. Tatsumoto, M. (U. S. Geological Survey, Denver); Hedge, C. E.; Engel, A. E. J. Science, 150: 886-89(Nov. 12, 1965).

The average concentrations of potassium, rubidium, strontium, thorium, and uranium in oceanic tholeiitic basalt are (in parts per million) K, 1400; Rb, 1.2; Sr, 120; Th, 0.2; and U, 0.1. The ratio ^{87}Sr to ^{86}Sr is about 0.702, that of K to U is 1.4×10^4, and of Th to U is 1.8. These amounts of K, Th, U, and radiogenic ^{87}Sr are less than in other common igneous rocks. The ratios of Th to U and ^{87}Sr to ^{86}Sr suggest that the source region of the oceanic tholeiites was differentiated from the original mantle material some time in the geologic past. (auth)

4146 GEOKHIMIYA I ANALITICHESKAYA KHIMIYA REDKOZEMEL'NYKH ELEMENTOV. Y. I. AKTSESSORNYE REDKOZEMEL'NYE MINERALY I ELEMENTY TSERIEVOI PODGRUPPY UKRAINSKOGO KRISTALLICHESKOGO SHCHITA. (Geochemistry and Analytical Chemistry of Rare Earth Elements. I. Accessory Rare Earth Minerals and Elements of Cerium Subgroup in the Ukrainian Crystalline Belt). Ivantishin, M. N.; Kul'skaya, O. A.; Gornyi, G. Ya.; Eliseeva, G. D. Kiev, Naukova Dumka, 1964. 168p.

The statigraphy, mineralogy, and petrochemistry of the granitoids of the Ukrainian crystalline belt and the chemical characteristics of the accessory rare-earth minerals associated with them are considered. The methods of chemical, spectrochemical, and chromatographic-separation analyses used and data on the quantitative investigations of the rare-earth elements of the cerium subgroup are presented. On the basis of the data obtained, the regularities of the spreading of the individual rare-earth elements of the cerium subgroup and of the rare-earth minerals in the Precambrian stratigraphic sequence of the Ukrainian crystalline belt are clarified. (tr-auth)

4147 ^{14}C AND THE UNWARY ARCHAEOLOGIST. Stuckenrath, Robert Jr. (Univ. of Pennsylvania, Philadelphia). 13p. (CONF-650652-9). ORINS. Gmelin, AED-CONF-65-158-14.

From International ^{14}C and ^{3}H Dating Conference, Pullman, Wash.

Applications of ^{14}C in dating archeological specimens are discussed. Emphasis is placed on problems that arise when the sample has been contaminated in situ or when the site from which the sample was taken contains overlapping stratigraphic sequences. (C.H.)

Meteorology

See also Site Survey and Selection

4148 (AD–623515) THE INFLUENCE OF WEATHER ON SALT DISTRIBUTIONS AND AEROSOLS ON BEACHES.

Devine, R. T.; Tomnovec, F. M.; Da Gragnano, V. L.; Jones, E. W.; Buser, W. H. (Naval Radiological Defense Lab., San Francisco, Calif.). Sept. 14, 1965. 50p. (USNRDL-TR-902).

A method is described which will allow samplings of the mass loading of the atmosphere of an hour's duration while twelve hours was previously necessary. The method is applied in measuring the salt content above seashores as a function of sea, wind, and microseismic action. It was observed that sea and wind are indicators but that microseismic action gives the best indication of the sodium content. The distribution of exchangeable sodium on various California beaches was studied as well as the time variations of this quantity. An average profile of exchangeable sodium is reported and a means of determining the profile within an order of magnitude from weather data is described. (P.C.H.)

4149 (AD-623639) SIZE ANALYSIS OF MINUS 44 MICRON DUST PARTICLES. Nuckolls, M. J.; Fuller, R. K. (Naval Radiological Defense Lab., San Francisco, Calif.). Aug. 19, 1965. 8p. (USNRDL-TR-907). CFSTI $1.00 cy, $0.50 mn.

A method of particle size analysis utilizing ultrasonic energy and Micro Mesh sieves was developed for dust particles with diameters less than 44 microns. The particle size distributions of volcanic dust and dust from ground surface explosions were determined. The new method yields discrete particle size fractions, rather than fractions that contain all particle sizes less than a stated size, as produced by liquid sedimentation methods. Particulate samples were wet sieved through a 44-micron Tyler sieve onto a 40-micron Micro Mesh sieve. The surface of the screen and the particles were immersed in water in an ultrasonorator tank for a few minutes. Particles with diameters less than 40 microns passed through and were collected and transferred to a 30 micron screen. The process was repeated for 30-, 20-, and 10-micron Micro Mesh sieves. Each sieve and the material retained by it were dried in an oven at 110°C. The dried particles were recovered, weighed, and later used for photomicrographic studies, density measurements, etc. (auth)

4150 (MIT-2241-7) EDDY FLUXES AND THE BIENNIAL OSCILLATION IN THE STRATOSPHERE. Report No. 14. Wallace, John M.; Newell, Reginald E. (Massachusetts Inst. of Tech., Cambridge. Dept. of Meteorology). July 19, 1965. Contract AT(30-1)-2241. 54p. Dep. mn; CFSTI $3.00 cy, $0.50 mn.

The zonal wind and the heat and momentum transports in the lower stratosphere of the northern hemisphere are examined for a two year periodicity. The winds at midlatitudes are found to display a periodicity, but the amplitude and phase are different from those observed in the southern hemisphere. An oscillation in the heat transports in the subtropics is found to be of the proper size and phase to account for the temperature oscillation at low latitudes. It is found that the poleward momentum transports at middle latitudes exhibit a strong two year periodicity which is seen to be due to an alternating sequence of weak and strong winters in the stratosphere. Time records of total ozone over middle latitude stations indicate that both hemispheres have shown this tendency throughout the past decade. It is proposed that the zonal wind oscillation in the tropical stratosphere is a simple response to this forcing from the two hemispheres. The apparent 26 month period is seen to be an accidental feature of the time record. There are indications that the wind oscillation is not a permanent feature of the tropical stratosphere, though it may be a persistent one. It is suggested that the tendency for alternating strong and weak winters in the stratosphere is related to the biennial pulse in the troposphere. (auth)

4151 (MIT-2241-14) STRATOSPHERIC WIND TEMPERATURE AND ISOBARIC HEIGHT CONDITIONS DURING THE IGY PERIOD. PART III. Report No. 15. Peng, Li (Massachusetts Inst. of Tech., Cambridge. Dept. of Meteorology). Sept. 1, 1965. Contract AT(30-1)-2241. 204p. Dep. mn; CFSTI $6.00 cy, $1.25 mn.

The stratospheric wind, temperature, and isobaric height conditions of the Northern Hemisphere during the period from July to December 1958 were statistically studied. Three-month seasonal averages of these quantities and of the covariances between them were computed and are presented in the form of hemispheric maps. Zonal averages of various important quantities are also given in tables. General discussions of the results are given briefly. (auth)

4152 (TID-22266) EARLY-TIME CLOUD RISE FROM CHEMICAL HIGH EXPLOSIVE DETONATIONS. Armstrong, Robert H. (Weather Bureau, Las Vegas, Nev.). Aug. 1965. Contract SF-54-351. 29p. Dep. mn; CFSTI $2.00 cy, $0.50 mn.

A photographic method of scaling the dimensions of dust clouds produced by explosive detonations is described. Rates of cloud rise were compared with meteorological parameters and the relative independence of rise rate upon atmospheric stability through the surface boundary layer was demonstrated. An empirical model relating cloud rise rates to explosive yield was developed. (auth)

4153 (UCRL-14360, pp 73-85) FLUID AND HYDRODYNAMICS. (Lawrence Radiation Lab., Univ. of California, Livermore).

A model for the convection of heat and water vapor in the atmosphere was developed, and the two-dimensional weather code ZAM was improved. The spectral and grid methods of hemispheric numerical weather prediction were evaluated, and a computer program was developed for the expansion of hemispheric meteorological data in antisymmetric surface spherical harmonic (Laplace) series. A three-dimensional, time-dependent model of the oceans in the Northern Hemisphere was coded in FORTRAN. Wave production by travelling pressure in shallow water was analyzed, and high-altitude shock structure was studied. An approximate solution to the hypersonic blunt body problem was obtained, and moving point singularities were studied. The propagation of disturbances was also investigated. (D.C.W.)

Natural Radioactivity and Fallout

See also HEALTH AND SAFETY

Refer also to abstracts 3665, 3745, 3797, and 3799.

4154 (AD-620003) THE INFLUENCE OF LOCAL WINDS ON FALLOUT. Semiannual Progress Report No. 1, October 15, 1964-April 15, 1965. Kangos, James D.; Gerrity, Joseph P. Jr. (Travelers Research Center, Inc., Hartford, Conn.). Aug. 1965. Contract DA28043-AMC00392E. 75p. (ECOM-00392-1). CFSTI $3.00 cy, $0.75 mn.

Information on the structure of the sea breeze obtained by previous observational and theoretical studies was employed to formulate a kinematic model of the wind field associated with the sea breeze. Existing information on the structure of the stabilized fallout cloud was compiled for use in the numerical computation of the deposition of the cloud particles through specified local wind fields. A program was constructed for the numerical computation of fallout transport through an analytically prescribed two-dimensional local wind circulation and for the computation of its ground deposition pattern. A computer program was used to evaluate the fallout deposition pattern from simple models of the stabilized cloud through alternative models of the sea-breeze wind fields. The planned development of a three-dimensional kinematic model of the sea-breeze wind field and of a computer program for the computation of fallout transport through it, is discussed. (auth)

4155 (EUR-2516.d,f,i,n) RESULTS OF ENVIRONMENTAL RADIOACTIVITY MEASUREMENTS IN THE COMMUNITY COUNTRIES IN 1964. AIR — FALLOUT — WATER. (European Atomic Energy Community). 1965. 56p. Dep. mn.

Text appears in German, French, Italian, and Dutch.

Results are reported of the measurements carried out

in 1964 by the Euratom member states at the environmental radioactivity monitoring posts, together with certain data obtained at Euratom's Joint Research Centre, Ispra. Data are included from measurements of radioactivity in the air at ground level, in fallout, and in surface waters. The majority of the measurements related to total beta radioactivity. The measurement results for certain specific radionuclides are also indicated, as well as the amount of precipitation observed at fallout sampling posts. Graphs are given to show the pattern followed throughout the year, a comparison being drawn with the development over the years 1962 and 1963, as well as with the situation in 1964 in the United States and Canada. (tr-auth)

4156 (USNRDL-TR-899) PHYSICAL AND RADIOCHEMICAL PROPERTIES OF FALLOUT PARTICLES. Crocker, G. R.; O'Connor, J. D.; Freiling, E. C. (Naval Radiological Defense Lab., San Francisco, Calif.). June 15, 1965. Contract AT(49)-2505 (4). 20p. Dep. mn; $1.00 cy, $0.50 mn.

A survey was made of the very large body of literature now existing on the characteristics of fallout particles. An attempt was made to summarize in concise form the ranges of physical and radiochemical properties of particles of the debris produced by devices detonated under various conditions. The results of studies of the leaching action of various solvents on fallout particles are also summarized. (auth)

4157 (ORNL-tr-702) RADIOACTIVITY OF A FEW SWISS ROCKS. PART I. PETROGRAPHIC-MICROSCOPIC INVESTIGATIONS. Hirschi, Hans. Translated for Oak Ridge National Lab., Tenn., from Vierteljahresschr. Naturforsh. Ges. Zuerich, 65: 209-47(1920). 44p. Dep. mn; JCL $4.60 fs, $1.52 mf.

Petrographic-microscopic investigations on the radioactivity of syenites of Piz Giuf and surroundings, granites in the Val Placi near Disentis, both rock zones in the eastern Aar massif, and tertiary granites in Bergell are reported. (P.C.H.)

4158 ON THE METHOD FOR DETERMINING THE EFFECTS OF METEOROLOGICAL CONDITIONS ON AIR CONTAMINATION AT EARTH SURFACE BY STRATOSPHERIC RADIOACTIVE SUBSTANCES. Kopcewicz, T. (Univ. of Warsaw). Acta Geophys. Polon., 13: 75-84 (1965). (In Polish).

Effects of meteorological conditions on air contamination by radioactive substances from the stratosphere were analyzed, and a new method for classifying and grouping daily contamination data is suggested. Tables are given of measurements carried out at the Uccle and Warsaw stations during 1959, 1962, and 1963. (R.V.J.)

4159 SEPARATION AND MEASUREMENT OF ^{137}Cs IN PRECIPITATION. Johnson, J. E.; Wilson, D. W.; Ward, G. M.; Thompson, R. D. (Colorado State Univ., Fort Collins). Anal. Chim. Acta, 34: 59-63(Jan. 1966).

In rainwater samples containing fallout debris of recent origin, the ^{137}Cs absorption peak in a γ scintillation spectrum contained, and was often completely obscured by, contributions from other γ-emitting radionuclides, so that the ^{137}Cs activity could not be determined directly. Precipitation samples were collected with rain funnels and passed through Dowex 50W-X12 cation-exchange columns. The ^{137}Cs was selectively eluted with 0.5M ammonium nitrate. The absolute recovery of ^{137}Cs was complicated by the presence of airborne sediments that were invariably collected with the sample and could irreversibly fix ^{137}Cs from the rainwater. (auth)

4160 DECIDUOUS TEETH USED AS RADIOACTIVITY GUIDE. Bull. Akron Dent. Soc., 23: 15(Nov. 1963).

A Public Health Service-sponsored program making use of the baby teeth of thousands of U. S. children as indirect means of monitoring fallout radioactivity in human bones is discussed. A five-year study of the ^{90}Sr content of children's deciduous teeth is being made on 6000 teeth collected annually from youngsters in the Gulf Coast area of the United States and Puerto Rico. Strontium-90 behaves in the body very much as calcium and enters bony structures along with calcium, and because bones of children born during periods of fallout contain greater quantities of ^{90}Sr than those of adults, children are an important group for studies on the absorption and deposition of radionuclides such as ^{90}Sr. Monitoring ^{90}Sr absorption by children has been made difficult by the scarcity of adequate bone samples, which must be obtained at autopsy. Teeth are a suitable substitute because they have chemical composition similar to bone and they absorb ^{90}Sr. It is believed that the ^{90}Sr content of baby teeth, which is readily available for study, is an accurate indicator of the fallout level of this radionuclide that has entered the life cycle during the prenatal period. More than 125,000 baby teeth have been collected in a similar PHS-sponsored project conducted since 1959 in the St. Louis area. To determine the usefulness of concentrations in teeth as an indicator of the body burden of ^{90}Sr, an attempt is being made to correlate ^{90}Sr content of the deciduous teeth with levels in the diet during the period of tooth formation. The Division of Radiological Health also is conducting a study of long-term population exposure from radium-bearing deep-well waters in certain areas of Illinois, Iowa, Missouri, Minnesota, and Wisconsin. Collection and analysis of teeth is one important phase of the study since Ra is also deposited in bones and teeth. (BBB)

4161 THE OCCURRENCE OF ^{22}Na IN SOME SPECIES OF CANADIAN BIOTA. Guthrie, J. E. (Whiteshell Nuclear Research Establishment, Pinawa, Manitoba, Can.). Can. J. Zool., 43: 889-90(Sept. 1965).

Cosmic-ray spallation of argon and fallout from testing of high-yield nuclear weapons has increased the amount of ^{22}Na present in the environment. Consequently, it has been possible to measure ^{22}Na in Alaskan natives, caribou, elk, and some foods. Samples of flora and fauna were routinely collected in the vicinity of Pinawa, Manitoba, as a part of the Whiteshell Nuclear Research Establishment's radiation survey program. Gamma spectrometric analysis methods revealed the presence of ^{22}Na in samples taken during 1964, in addition to other long-lived fission products such as ^{144}Ce, ^{125}Sb, ^{106}Ru, ^{137}Cs, and ^{54}Mn. Sodium-22 was measured in samples of muscle tissue taken from the red squirrel (Tamiasciurus sp.) and hare (Lepus americanus), but was not detected in the flesh of the short-tailed weasel (Mustela erminea). Sodium-22 was detected neither in the sweet (white) clover which grew profusely in the area where the mammals were trapped nor in composite samples of Winnipeg River water in any of the species of fish taken from the river during this period: rock bass (Ambloplites rupestris), sucker (Castostomus sp.), pike (Esox lucius), pickerel (Stizostedion vitreum), and sauger (Stizostedion canadense). However, ^{22}Na has been reported in bass caught in the Columbia River, Washington. Potassium-40 and ^{137}Cs means in the samples examined indicate an apparent increase in the amounts of ^{137}Cs. The amount of ^{22}Na measured in rabbits is much less than the maximum permissible body burden for the nuclide (10 μC). (TCO)

4162 TRANSFER OF RADIOSTRONTIUM FROM COWS' FEED TO MILK. Kahn, B. (Robert A. Taft Sanitary Engineering Center, Cincinnati); Jones, I. R.; Porter, C. R.; Straub, C. P. J. Dairy Sci., 48: 1023-30 (Aug. 1965).

The fraction of radiostrontium transferred from forage to cows' milk and the effect of a change in feed on this transfer were studied to obtain information useful in predicting and controlling the intake by humans of this component of fallout. This information was obtained for three herds of cows given feed contaminated with ^{89}Sr and ^{90}Sr from fallout under normal environmental conditions. One herd was maintained on pasture for 19 days, then placed in dry lot and fed stored feed containing relatively little radiostrontium. A second herd was kept on pasture throughout the 8 weeks of the experiment, whereas a third was in dry lot, first eating stored feed containing relatively little radiostrontium, then recently harvested grass silage with a larger radiostrontium concentration. Transfer of Sr from feed to milk was described by the observed ratio (OR), defined as the fractional Sr transfer from feed to

milk, divided by the fractional Ca transfer. The stored feed was low and the pasture grass high in radiostrontium content. Change from the high- to the low-radiostrontium diet decreased radiostrontium concentration in milk with combined half-times of 0.77 and 4.6 days. The OR from feed to milk for stable Sr to Ca was 0.12. For radiostrontium, a higher OR occurred with a low-radiostrontium diet and a lower one with a high-radiostrontium diet. This was due to a change in sp act. between feed and milk and was attributed to the appearance in milk of Sr from the cow's body pool. Of the stable Sr in milk, about 40% was estimated to derive from the skeleton. Since 40% of the stable strontium and 60% of the calcium in the milk are derived from the skeleton under normal feeding conditions, predictions of radiostrontium content in milk must be based on the radiostrontium content of both sources. As shown by OR values for the herds on high-radiostrontium diets in this experiment, predictions based on a value of 0.1 are correct under normal feeding practices. However, for cows that ingest no radiostrontium at the period of measurement, all of this radionuclide in the milk would come from the body pool, and its concentration could not be predicted from the OR. In this case, the magnitude of the exchangeable radiostrontium body pool could be computed from radiostrontium measurements in milk if the fractional contribution by the body pool were known. (BBB)

4163 RADIOACTIVITY IN THE ATMOSPHERE. Murgatroyd, R. J. World Meteorol. Organ. Bull., 13: 73-7(Apr. 1964).

Some recent reports on distribution of radionuclides at various levels of the atmosphere are reviewed, and the general trends of research in this field are discussed. (TCO)

4164 UMWELTRADIOAKTIVITAT UND STRAHLENBELASTUNG. Bericht II/65. (Environmental Radioactivity and Radiation Burden. Second Quarterly Report, 1965). Bad Godesberg, Bundesminister fuer Wissenschaftliche Forschung, 1965. 168p. DM 8.--.

The content of radioactive materials in air, water, soil, and food materials and the radiation burden of the population in the German Federal Republic measured during the second quarter in 1965 were reported in graphic and tabular form. (J.S.R.)

4165 RADIATION MEASUREMENTS OF PORPHYRIES IN THE REGION OF THE SAAR-NAHE BASIN [Thesis]. Mathes, H. Berlin, Tech. Univ., 1963. 71p. $2.00 Gmelin, AED-DISS. 63-790.

Uranium and thorium contents of various porphyries from the Saar-Nahe region are given. Results indicated that increased U contents are correlated to tectonic disturbances. (Gmelin Inst.)

Techniques and Equipment

4166 (AERE-R-4980) SILT MOVEMENT INVESTIGATION IN THE OXCARS SPOIL GROUND, FIRTH OF FORTH, USING RADIOACTIVE TRACERS, 1961 AND 1964. Smith, D. B.; Parson, T. V. (Research Group, United Kingdom Atomic Energy Authority, Wantage (England)). 1965. 52p. Dep.; BIS $0.90; HMSO 4s. 6d.

Radioactively labeled ground glass (scandium-46) was used to investigate the movement of spoil deposited in the Oxcars Deep, Firth of Forth. In 1961, the glass was deposited directly on the bed of the estuary and in 1964 it was used to label a hopper load of spoil. Depositions were at slack high water. Extensive upstream movement of the spoil was observed. Measurement of the depth distribution of tracer in the dockyard enabled a quantitative estimation to be made. Between 3 and 7% of the deposited material was transported directly to Rosyth dockyard. Additional sources of siltation in the dock and the contribution of the deposited spoil to these are also considered. (auth)

4167 (RM-3727(RAND)) NUCLEAR EXPLOSIONS IN CAVITIES. Brode, H. L. (RAND Corp., Santa Monica, Calif.). Nov. 1965. 70p.

Underground cavities have been suggested as an effective means of reducing the seismic signals from nuclear detonations. The wall pressures, temperatures, and densities are reported for five specific examples, for which average cavity pressures range between 44 and 420 bars, with peak pressures between 0.2 and 8.2 kbars. One nuclear yield, 1.7 kilotrons, was exploded (theoretically) in two cavities of 20 and 40 meters radius, each with normal and one-tenth normal air density in it. The larger cavity was also used with a density of one-hundredth normal. In addition to the wall pressures, temperatures, and densities as functions of time for each case, some typical pressure, temperature, and density profiles in the cavity interiors at various times are also reported. (auth)

4168 ON THE FAST CONVERGENCE IN MONTE CARLO METHOD OF RESOLVING PROBLEMS OF RADIOACTIVE LOGGING. Dyad'kin, I. G.; Lisenenkov, A. T.; Ponyatov, G. I. Zh. Vychisl. Mat. Mat. Fiz., 5: 763-8 (July-Aug. 1965). (In Russian).

The fast convergence of the Monte Carlo method was used for resolving two geophysical problems: on determining configurations of neutron logging curves according to epithermal neutrons at the boundary of adjacent rocks with varying hydrogen content (due to oil or water) and on the configurations of gamma-gamma logging on the boundary of rocks of various density (due to variable porosity) considering the drilled holes eccentric distribution of the gamma source, and the presence of lead screening reducing the γ background in the hole. (R.V.J.)

4169 URANIUM–THORIUM–LEAD AGES OF ZIRCONS AND MODEL LEAD AGES OF FELDSPARS FROM THE SAGANAGA, SNOWBANK AND GIANTS RANGE GRANITES OF NORTHEASTERN MINNESOTA [Thesis]. Anderson, Daniel Harvie. Minneapolis, Univ. of Minnesota, 1965. 140p.

Uranium-lead and thorium-lead ages of thirteen suites of zircons from the northeastern Minnesota Giants Range and Snowbank Granites of Algoman age and the Saganaga Granite of Laurentian age were determined by the method of isotope dilution after a preliminary x-ray fluorescence survey. The Snowbank and Giants Range Granites were intruded 1.1×10^9 years ago by the 820-meter-thick Duluth Gabbro sill, and the heat evolved by this event had some effect upon the zircon ages. The U/Pb and Th/Pb ages for all zircon samples are discordant; however, the degree of discordance shows little relationship to the distance from the sill contact. At distances greater than 400 meters, volume diffusion of lead is apparently the predominant factor causing discordance. Zircons from one sample of the Snowbank Granite less than five meters from the sill contact have acquired the 1.1 b.y. age of the gabbro. Except for this closest sample, the zircon ages from all three granites indicate an age of 2.70 ± 0.05 b.y. The temperature history of the region adjacent to the gabbro intrusion was calculated, and from this the activation energy associated with the diffusion of ^{206}Pb and ^{207}Pb from zircons was computed to be about 11.4 kilocalories/mole when assuming particular values for the diffusion rate at 300°K. The Pb isotope composition and uranium content of nine feldspars and one whole rock sample from the Algoman granites were determined. The initial lead-isotope compositions inferred from the thermally undisturbed feldspars from both granites is the same and gives a model age of 2.75 ± 0.05 b.y. for a 4.55 b.y. closed system lead evolution model. (Dissertation Abstr.)

4170 HYDROGEN INDEX AND GAMMA RAY WELL LOGGING. Owen, Joe D. (to Phillips Petroleum Co.). U. S. Patent 3,211,909. Oct. 12, 1965. Filed Jan. 9, 1961.

An apparatus and method is provided for downhole well logging for indication of the presence of liquid hydrocarbons in siliceous and carbonate formations. The apparatus includes a source of neutrons, a thermal neutron detector, a gamma ray detector, and a shield between the source and the detectors to eliminate direct passage of radiation to the detectors. The thermal neutron detector is adapted to emit a first signal related to the neutron flux detected, and the gamma detector detects rays emitted by atoms bombarded from the source and emits signals related to gamma

rays characteristic of neutron bombardment of Si, O, and Ca atoms. First, second, and third pulse height analyzers are in separate operative communication with the detectors, and the analyzers are adjusted to a 1.78-Mev Si peak, a 6-Mev O peak, and a 3.35-Mev Ca peak, respectively. The analyzers are adapted to emit signals related to the respective peaks. Analyzer means are provided for indicating the ratio of Si to O and Ca to O, and separate means communicate with the neutron detector for indicating the porosity of the formation logged. (B.L.M.)

4171 CALIBRATION OF RADIOACTIVE WELL LOGGING SYSTEM. Caldwell, Richard L. (to Socony Mobil Oil Co., Inc.). U. S. Patent 3,213,279. Oct. 19, 1965. Filed June 7, 1961.

A method for calibrating a radioactive well logging system including an energy discriminator is described for particular application to apparatus for detecting the presence of chlorine in subsurface formations. The method includes the following steps: positioning the source of neutrons and the gamma ray detector within an environment containing substantial amounts of H_2 and Fe, detecting the resulting hydrogen-capture and iron-capture gamma rays, producing from the hydrogen-capture and iron-capture gamma rays pulses having magnitudes proportional to the energies of the selected energy band (4.6 to 6.3 Mev); converting the pulses into an observable energy spectrum including energy peaks occurring at energy levels representative of the hydrogen-capture and iron-capture gamma rays; and adjusting the discriminator with the spectral peaks at known energy levels for response to neutron-capture gamma rays only within the selected energy band. (B.L.M.)

Thorium and Uranium Minerals

4172 HALLIMONDITE, A NEW URANIUM MINERAL FROM THE MICHAEL MINE NEAR REICHENBACH (BLACK FOREST, GERMANY). Walenta, Kurt (Technische Hochschule, Stuttgart). Amer. Mineral., 50: 1143-57 (Sept. 1965).

Hallimondite is a lead uranyl arsenate mineral found at the Michael Mine near Reichenbach in the Black Forest. It forms small yellow crystals and coatings in cavities and fractures of quartz and is associated with hiigelite and mimetite. The crystals of hallimondite have triclinic symmetry. They are tabular and more or less elongated along the c-axis. Unit cell dimensions were determined from calibrated Weissenberg photographs. The formula $Pb_2(UO_2)(AsO_4)_2$ was derived from synthetic material. For natural material the results of microchemical and spectrochemical analyses are given. The DTA curve of synthetic hallimondite showed a distinct endothermic effect at 940°C. (auth)

4173 MOCTEZUMITE, A NEW LEAD URANYL TELLURITE. Gaines, Richard V. Amer. Mineral, 50: 1158-63(Sept. 1965).

A new mineral whose composition is lead uranyl tellurite was found at the La Moctezuma mine, Moctezuma, Sonora, Mexico. The mineral occurs as minute blades and rosettes in cracks and vugs in the oxidized zone of a tellurium–gold deposit. Dimensions of the largest crystal observed are 3 × 1 × 0.2 mm, but most crystals are much smaller. Associated minerals are barite, pyrite, limonite, emmonsite, zinc tellurite, a dark-red lead tellurite or tellurate, and a uranium tellurite or tellurate occurring as straw colored micaceous aggregates. The color is bright to dark orange. Cleavage (100) is perfect, hardness is about 3, and specific gravity, measured using a pycnometer, is 5.73. Most crystal faces are curved and give unsatisfactory reflections on the goniometer, but x-ray studies proved the mineral to be monoclinic, with elongation parallel to b. Crystals tend to be multiple, with nearly parallel growth and other structural imperfections, resulting in spots on the level photographs being smeared out as long lines rather than sharp dots. Best results were obtained with the Buerger precession camera. Cell dimensions are: a = 7.82, b = 7.07, and c = 13.84 Å and β = 93°37.5′. Principal powder lines are 3.156, 3.492, 2.997, 3.088, and 3.385 Å, in decreasing order of intensity. Composition by wet chemical analysis is $PbO \cdot UO_3 \cdot 2TeO_2$. Proportions of Pb : U : Te were confirmed by x-ray fluorescence analysis comparing the natural mineral with an artificial mixture. Optically the mineral is biaxial (−), with all indices above 2.11. The name moctezumite was proposed. (auth)

4174 CRYSTAL MORPHOLOGY OF THORIUM-BEARING SYNTHETIC MONAZITE. Anthony, John W. (Univ. of Arizona, Tucson). Amer. Mineral., 50: 1421-31(Sept. 1965).

Crystals of $CePO_4$ containing thorium and calcium and having the monazite structure were synthesized by a fusion method in order to examine physical property changes related to variation in content of these cations. Goniometrical studies showed that the principal habit-controlling forms in synthetic $CePO_4$ are x{$\bar{1}$01}, m{110}, and e{011}; also present are b{010}, n{120}, l{210}, u{021}, and r{111}. The presence of thorium and calcium diadochically substituting for cerium in the structure induces marked changes in crystal habit. Twinning on c{001} appears and is common. The previously unreported forms j{313} and Y{$\bar{4}$12} are recognized, as are the rare λ{212} and γ{041}. The proportions of three distinct habit types recognized in the thorium- and calcium-bearing crystals vary with the amount of thorium present. Twins on c{001} are plentiful among crystals of low thorium content but are rare in samples containing the maximum amount of thorium (13.8 wt % ThO_2); plate crystals, tabular on x{$\bar{1}$01}, predominate among crystals of high thorium content. From consideration of the effects on axial ratio of other rare earth cations in the monazite structure, it was concluded that systematic morphological changes in natural monazite, which might be expected as a consequence of differing thorium content could easily be masked by variations in proportions of rare earths. (auth)

HEALTH AND SAFETY

See also BIOLOGY AND MEDICINE — Radiation Hazards and Protection
GEOLOGY, METEOROLOGY, AND MINERALOGY — Natural Radioactivity and Fallout

Refer also to abstracts 3662, 3674, 3679, 3877, 4068, 4082, 4156, and 4160.

4175 (BNL–9650) HEALTH PHYSICS PROGRAM FOR THE BROOKHAVEN NATIONAL LABORATORY SYNCHROTRONS. Cowan, Frederick P. (Brookhaven National Lab., Upton, N. Y.). [1965]. Contract AT(30-2)-Gen-16. 13p. (CONF-651109–5). Dep. mn; CFSTI $1.00 cy, $0.50 mn.

From 1st Symposium on Accelerator Radiation Dosimetry and Experience, Upton, N. Y.

The basic approach to synchrotron dosimetry has been to measure absorbed dose with ionization chambers and to convert to Rem using conservative values of quality factor based on available knowledge of the composition of the radiation. Initially, experience at the Cosmotron was with a partially shielded machine. Later, an intense external primary proton beam was provided and a massive earthen dike was constructed as a beam catcher. More recently, complete shielding has been provided and exposure control problems have been minor. Exposure control at the Alternating-Gradient Synchrotron (AGS) has become increasingly difficult as a result of increased intensity and multiplication of facilities. Locations of Health Physics interest are the experimental halls including an area where μ meson dosage predominates, the accelerator ring where dosages during shutdown are presently a major problem, the linac injector, the 80″ bubble chamber, and the neutrino experiment area, as well as nearby areas and buildings. Extensive measurements of dosage levels, studies of skyshine and investigations of shielding effectiveness have been made and will be used in designing the shielding for the rebuilt AGS converted machine. In addition to ionization chambers, Bonner spheres, and the C(n,2n) reaction have been used extensively for surveys of experimental areas, beams, and outside locations. A wide diversity in radiation composition is encountered, depending on location. The depth dose patterns for typical locations at the Cosmotron and AGS were studied and are reported. A study of the response of personnel monitoring equipment at typical AGS locations has continued. A Rossi LET counter was assembled. (auth)

4176 (BNL–9684) LINEAR ENERGY TRANSFER SPECTRA AND EFFECTIVE QUALITY FACTORS IN STRAY RADIATION AREAS AT THE BROOKHAVEN NATIONAL LABORATORY PROTON SYNCHROTRONS. Phillips, Leigh F.; Champagne, Robert J.; Scalsky, Edward D. (Brookhaven National Lab., Upton, N. Y.). [1965]. Contract AT(30-2)-Gen-16. 15p. (CONF-651109–12). Dep. mn; CFSTI $1.00 cy, $0.50 mn.

From 1st Symposium on Accelerator Radiation Dosimetry and Experience, Upton, N. Y.

The radiation hazard to personnel working in stray radiation fields around the Brookhaven 3 and 33 Bev proton synchrotrons was evaluated. Special emphasis was placed on obtaining information concerning the effective quality factors (QF) and the distribution of dose as a function of linear energy transfer (LET) for the high energy, mixed radiation fields. The Rossi-type tissue equivalent (TE) ionization chamber and spherical proportional counter were used to measure the total absorbed dose and to derive the absorbed dose and dose equivalent as a function of LET. With this method the effective QF and the dose equivalent were obtained without complete knowledge of the nature and energy of the stray radiation. Effective QF's of from one to five were observed for various shielding geometries. The sensitivity of the system to small changes in LET distribution is indicated. (auth)

4177 (JAERI–1083) DETERMINATION OF RADIOACTIVE FALLOUT FROM NUCLEAR WEAPON TESTS. DETECTION AND DETERMINATION OF RADIOACTIVE NUCLIDES IN RAIN WATER. Yamaoka, Y.; Ueno, K.; Kaido, J.; Kaziyama, H. (Japan Atomic Energy Research Inst., Tokyo). June 1965. 10p. Dep. mn.

Rain water samples were collected in Japan from Oct. 1961 to Nov. 1962. The radioactivity detected was increased after the series of nuclear detonations by Soviet Russia. The determination of radioactive nuclides were carried out both by the ion exchange method using Dowex 1 or 50 resin and γ ray spectrometry. By the former method, group activities of rare-earth and alkali-earth elements were determined, and by the latter, nuclides of $^{95}Zr-^{95}Nb$, $^{99}Mo-^{99m}Tc$, $^{103,106}Ru-^{103,106}Rh$, $^{132}Te-^{132}I$, ^{133}I, and $^{140}Ba-^{140}La$ were determined. Methods for the determination of small amounts of ^{238}U and ^{237}U in rain water were investigated, using fluorometry and isotope dilution method, respectively. (tr-auth)

4178 (JUL–284-ST) UMWELTRADIOAKTIVITAET DER KERNFORSCHUNGSANLAGE JUELICH. (Environmental Radioactivity of the Nuclear Research Center, Juelich). Vogt, K. J.; Jacobs, H.; Polster, G. (Kernforschungsanlage, Juelich (West Germany). Zentralabteilung Strahlenschutz). Apr. 1965. 79p. Dep. mn.

The measurement program, the monitoring system, and the results obtained during the environmental monitoring of the Juelich Research Center in 1964 are reported. Tabulations are made for the results obtained for air, water, soil, and agricultural products. (J.S.R.)

4179 (LA–3363) ^{131}I SAMPLING WITH ACTIVATED CHARCOAL AND CHARCOAL-IMPREGNATED FILTER PAPER. Ettinger, H. J.; Dummer, J. E. Jr. (Los Alamos Scientific Lab., Univ. of California, N. Mex.). Aug. 1965. Contract W-7405-eng-36. 18p. Dep. mn; CFSTI $1.00 cy, $0.50 mn.

Samples of stack effluent from an operating reactor, and from a hot cell complex in which spent reactor fuel elements are examined, showed activated charcoal efficiencies ranging from 70–99%, with a median efficiency of 90%. Three different charcoal-impregnated filter papers were unsatisfactory for monitoring radioiodine because their collection efficiencies varied widely. Both impregnated filter papers and activated charcoal cartridges were tested at various sampling velocities. The effects of methyl chloroform on the iodine collection efficiency of activated charcoal were evaluated. The collection efficiencies of charcoal cartridges soaked in methyl chloroform ranged from 72–90%, with a median of 81%. Concurrent sampling with charcoal cartridges not treated with methyl chloroform showed an efficiency range of 71–95%, with a median of 86%. Field tests indicate the need for carefully considering the iodine collection efficiency of activated charcoal for air cleaning systems and respirators. (auth)

4180 (NP–15571) DANISH LAWS AND REGULATIONS RELATING TO RADIATION HYGIENE. (National Health Service, Copenhagen (Denmark)). 1965. 42p. Dep. mn.

Laws and regulations relating to the installation and operation of x-ray equipment and the use of radioactive materials in Denmark are summarized. Emphasis is placed on the radiation protection of personnel using the materials. (C.H.)

4181 (NP–15620) LA REGLEMENTATION INTERNATIONALE DU TRANSPORT DES MATIERES RADIO-

ACTIVES. Tendances Actuelles. (International Regulation of Transport of Radioactive Materials. Present Trends). Salleron, Claude (Paris Univ. (France). Institut de Droit Compare). 1964. 45p. Dep. mn.

The modifications and alterations made in 1963 by the International Agency for Atomic Energy in the regulations for the transport of radioactive materials are summarized. The definitions or terms are first given and the materials exempt from international regulation are described. The conditions for packaging and permission for transportation are outlined. The regulations concerning storage and transportation are then indicated. (J.S.R.)

4182 (ORNL–3843) NUCLEAR SAFETY PROGRAM SEMIANNUAL PROGRESS REPORT FOR PERIOD ENDING JUNE 30, 1965. (Oak Ridge National Lab., Tenn.). Sept. 1965. Contract W-7405-eng-26. 266p. Dep. mn; CFSTI $6.00 cy, $1.00 mn.

The progress report is divided into five parts. Abstracts were prepared for each. (J.R.D.)

For abstracts of individual sections see: 4086, and 4183–4186.

4183 (ORNL–3843, pp 2-70) RELEASE AND TRANSPORT OF FISSION PRODUCTS UPON IN-PILE DESTRUCTION OF REACTOR FUELS. (Oak Ridge National Lab., Tenn.).

Types of experiments being carried out by in-pile destruction of reactor fuels include a simulated loss-of-coolant accident experiment in which fuel is melted by fission and gamma heat during several-minute time periods in the Oak Ridge Research Reactor, and a simulated transient-type accident in which the fuel is melted rapidly as a result of a transient in the TREAT reactor. The conditions under which fission-product behavior is being studied in the loss-of-coolant experiments include variations in atmospheric composition, cladding material, fuel burnup, temperature, and fission-product aging. The conditions being investigated in the transient experiments include variations in atmospheric composition, cladding material, fuel burnup, fuel type, and transient characteristics. The atmospheres investigated in the loss-of-coolant experiments are He, moist He, steam-He–H_2 mixtures, dry air, moist air, and steam-air mixtures. Atmospheric conditions that have been investigated in the transient experiments have included Ar, steam-air, and high-pressure steam. Stainless steel and Zircaloy have been used as cladding materials in both the loss-of-coolant and transient experiments. Both experimental programs have shown that chemical reactions between the cladding and the atmosphere, or between the cladding and the fuel, or between the cladding and fission products can have a significant effect on fission-product behavior. (J.R.D.)

4184 (ORNL–3843, pp 71-135) RELEASE AND TRANSPORT BEHAVIOR OF FISSION PRODUCTS IN CONTAINMENT SYSTEMS. (Oak Ridge National Lab., Tenn.).

Transport phenomena, such as agglomeration, absorption, adsorption, deposition, and steam condensation within the containment vessel, serve to reduce the amounts of fission products available for release. The forms of fission products and the transport phenomena are being investigated in ORNL facilities such as the Containment Mockup Facility and the Nuclear Safety Pilot Plant. The Containment Research Installation is being constructed to provide an additional capability. Simulated high-burnup fuel (i.e., fuel to which inactive fission-product elements corresponding to the desired burnup have been added, together with just enough radiotracer to facilitate analysis) was used in three experiments performed in the Containment Mockup Facility. Two runs were made in the Nuclear Safety Pilot Plant in which fission products were released into the containment system by melting stainless steel-clad UO_2 fuel specimens in steam atmospheres. The behavior of fission products was observed by the analysis of time-dependent data from exposure of deposition coupons, collection of fallout and condensate, and filtration of air samples by May packs and paper tape. The removal of particulate materials from gases under simulated reactor accident conditions is being investigated with an arc source with a UO_2-stainless steel electrode system and a fibrous-filter particle size analyzer. Under these conditions, two distinct particle size distributions were observed. The effectiveness of activated-charcoal adsorbers in removing the various forms of I is being investigated under a variety of conditions so that their applicability as an engineered safeguard can be evaluated. By designing for methyl iodide retention, the elemental I retention is assured. (J.R.D.)

4185 (ORNL–3843, pp 169-234) CHARACTERIZATION AND BEHAVIOR OF ACCIDENT-RELEASED FISSION PRODUCTS. (Oak Ridge National Lab., Tenn.).

It is agreed that radioiodine occurs in gases in a number of vapor forms that differ in their properties and that in order to predict the behavior of radioiodine in reactor accidents, these forms must be characterized. Equipment is being assembled that will permit selective detection of radioactive I compounds in gas samples from experiments that realistically simulate reactor accidents. Studies were continued for determining the extent of the reaction at various temperatures between I_2 and organic vapor sources and to observe the behavior of any I compounds in activated-charcoal adsorbers. One of the organic sources was dioctylphthalate (DOP) and the second source was a mixture of lubricating oil, plastic and rubber insulation, and paint scrapings, materials commonly found in reactor containment zones. Organic vapors from both sources were observed to react with elemental iodine to the extent of 5 to 15 or 20%. Methyl iodide is retained by activated charcoal in an efficient manner only if moisture is excluded from the system. Retention of methyl iodide by coconut charcoal was studied as a function of stay time and bed depth in the presence of saturated water vapor at 75°C. It was found that the distribution of methyl iodide deposited in beds from saturated air was strongly dependent on the flow velocity, the loading time, and the water content of the charcoal during loading. The behavior of radioiodine vapor in a composite diffusion tube of a design for use in in-pile fuel meltdown experiments was compared (in the laboratory) with the behavior in the more usual type of composite diffusion tube. (J.R.D.)

4186 (ORNL–3843, pp 235-44) NUCLEAR SAFETY INFORMATION. (Oak Ridge National Lab., Tenn.).

The Nuclear Safety Information Center has now completed its second year of operation. Its experience was summarized in a report entitled "Operating Experience of the Nuclear Safety Information Center, March 1963–March 1965" that was issued in May. A report on "Behavior of Iodine in Reactor Containment Systems" was issued in February, and a report on "Secondary Shutdown Systems of Nuclear Power Plants" was prepared and distributed in edited draft form for review. Other "state-of-the-art" studies are in various stages of development. Two indexed bibliographies of the Center's accessions were processed by the computer and issued. A reactor containment handbook draft was reviewed and revised in light of comments submitted by the reviewers. (J.R.D.)

4187 (SC-RR–65-333) LAUNCH HAZARDS ASSESSMENT PROGRAM. REPORT ON ATLAS/CENTAUR ABORT. Kite, F. D.; Webb, D. M.; Bader, B. E. (Sandia Corp., Albuquerque, N. Mex.); Golub, C. N. (Pan American World Airways, Inc., Patrick AFB, Fla. Guided Missiles Range). Oct. 1965. Contract AT(29-1)-789. 53p. Dep. mn; CFSTI $3.00 cy, $0.50 mn.

Information and analysis concerning the aborted launch of the Surveyor-Mission Atlas-Centaur, March 2, 1965, is summarized. The data reported are the first contribution of field measurements to the over-all data which are required to complete the explosion model. Discussion is included on the system with which the measurements were taken, characteristics of the measurements, and reduction of these data. The launch vehicle is described and all the relevant data (meteorological, time, etc.) at launch are presented. The instrumentation configuration and system performance during the accident are also described. Con-

clusions and recommendations based on the results of this accident and on the experience gained in PAMS operation are given. A description of the Pad Abort Measuring System is appended. (P.C.H.)

4188 (TID–22268) OPERATIONAL ACCIDENTS AND RADIATION EXPOSURE EXPERIENCE WITHIN THE UNITED STATES ATOMIC ENERGY COMMISSION, 1943–1964. (Division of Operational Safety (AEC), Washington, D. C.). Apr. 1965. 55p. Dep. mn; GPO $0.40.

The occupational injury and fatality experience, through 22 years of the development of the atomic energy industry under the guidance and direction of the Atomic Energy Commission and its predecessor, the Manhattan Engineer District, demonstrates that when management vigorously promotes accident prevention programs, aimed at a specific type of injury, the occurrence of the injury can be practically eliminated. The early unknown qualities and effects of nuclear energy provided the incentive to develop the most effective specialized injury prevention program ever devised, with the result that, during 22 years, there were only six deaths attributable to nuclear causes. Three of these occurred at Los Alamos (8-21-45, 5-21-46, 12-30-58) and were a direct result of exposure to a massive dose of nuclear radiation. The immediate causes of death of the three additional fatalities were the physical effects (i.e., blast, flying missiles, etc.) associated with the SL-1 nuclear accident of January 3, 1961; however, the radiation levels associated with that accident were extremely high and probably would have been fatal. It is also significant that during this 22 years there were 33 workers involved in lost-time radiation nonfatal accidents. Most of these accidents, producing ionizing radiation exposures, were caused by human error, faulty manipulation of controls, deviation from standard operating procedures, faulty mechanical equipment, and other causes, such as may be encountered in any other industry. The total number of fatalities from all causes was 251 during the 22-year period. Of this number, 152 occurred in construction, 88 in production, research and services, and 11 in Government operations. Brief descriptions of all fatalities, criticality accidents, summaries of radiation exposures over 15 REM, and data on property damage are presented for the AEC and AEC Operations' contractors from 1943 through 1964. (C.H.)

4189 (VUF–1030) STRUCTURAL RESPONSE OF RESIDENTIAL-TYPE TEST STRUCTURES IN CLOSE PROXIMITY TO AN UNDERGROUND NUCLEAR DETONATION. SALMON EVENT—PROJECT DRIBBLE. Final Report. (Blume (John A.) and Associates Research Div., San Francisco, Calif.). Aug. 1965. 30p. Dep. mn; CFSTI $2.00 cy, $0.50 mn.

Response was measured in three one-story simulated residential structures at distances of 2,000, 3,000 and 4,000 meters from Surface Zero for the Salmon event. Statham accelerometers were mounted at roof and floor levels in concrete block and wood frame structures. Peak measured accelerations ranged from about 1.5g (gravity units) at the near structure (concrete block) to about 0.7g at the middle structure (wood frame) to about 0.4g at the most distant structure (wood frame). No damage was observed in any of the instrumented structures; a companion block structure to the wood frame structure at the 4,000-meter distance suffered extension of pre-existing cracks. (auth)

4190 (VUF–1031) STRUCTURAL RESPONSE OF TALL INDUSTRIAL AND RESIDENTIAL STRUCTURES TO AN UNDERGROUND NUCLEAR DETONATION. SALMON EVENT—PROJECT DRIBBLE. Final Report. (Blume (John A.) and Associates Research Div., San Francisco). Aug. 1965. 31p. Dep. mn; CFSTI $2.00 cy, $0.50 mn.

Two tall refinery structures and an eight-story University women's dormitory structure were instrumented for measurement of response to ground motion generated by the Salmon event. The refinery was about 18 kilometers from Surface Zero and the dormitory about 30.8 kilometers. NGS 19L velocity meters were deployed at several levels on the refinery structures, and Sprengnether portable displacement meters were used on the top and bottom floors of the dormitory. Measured peak top level velocities in the two refinery structures were 7.31 centimeters per second in the taller TCC structure and 5.6 centimeters per second in the DIB tower, at periods of 0.19 seconds and 0.20 seconds, respectively. Peak top floor displacement in the dormitory was 0.15 centimeters with a period of about 0.43 seconds. Blume observers reported a clearly perceptible motion in the dormitory, felt by uninformed persons on bottom and top floors. No official observers were present at the refinery but personnel working there also reported clearly perceptible motion. (auth)

4191 (JPRS–31014) ENGINEERING AND RESCUE OPERATIONS AT THE SITE OF AN ATOMIC STRIKE. Volkov, I. D.; Ulanovskii, B. Ya.; Usov, N. A.; Tsivilev, M. P. Translated from pp 1-151 of Inzhenero-Spasatel'nye Raboti v Ochage Yadernogo Porazheniya, Publishing House for Literature on Construction, Moscow, 1965. 191p. (TT–65–31512). CFSTI $5.00 cy, $1.00 mn.

Information is included on: characteristics of the site of an atomic strike and the kinds of operations which are performed; the composition of the forces; principles of their organization and training; means of mechanization and methods of conducting and organizing engineer-rescue operations; and fundamentals of the utilization of civil defense units and of control and material-technical support when performing rescue operations at the site of a nuclear strike. (P.C.H.)

4192 (JPRS–32686) SAFEGUARDING FOOD PRODUCTS AND WATER FROM AGENTS OF MASS DESTRUCTION. Kovalenko, V. Translated from pp 1-30 of Zashchita Pishchevykh Produktov i Vody ot Sredstv Massovogo Porazheniya, Moscow, 1964. 19p. (TT–65–33165). CFSTI $1.00 cy, $0.50 mn.

One of the most dangerous features of bacteriological, chemical, or radiological warfare is the ability to contaminate foods, water supplies, crops, and forage and thus make them unfit for consumption. A nuclear explosion may contaminate them with radioactive fallout or make them radioactive as a result of neutron or γ exposure; bacterial or chemical agents can cause contamination by poisonous substances or bacterial preparations. The use of these agents can contaminate a vast territory and all its warehouses and industries and render them useless for a fairly long period of time. Methods for safeguarding food and water supplies, precautions in using food and water in contaminated regions, and methods of decontaminating food products, water supplies, and forage are discussed. (C.H.)

4193 CANCER AND GEOGRAPHY. Guelfi, J.; Pincet, J. (Faculte Mixte de Medecine et de Pharmacie, Rennes, France). Acta Univ. Int. Contra Cancr., 20: 612 (1964). (In French).

The content of uranium, radium, and radon in rocks and water of Cotes-du-Nord (France) was measured to determine a possible link between this content and the frequency and age level of deaths from cancer. The β activity of the dry residue from water evaporated without boiling was measured with a G-M counter. Uranium, as the fluoride, was determined by ascending chromatography and fluorometry. The measurement of radium was effected by a scintillation counter. It was necessary to measure the content of the radon directly to evaluate not only the radon emanating from radium in solution, but also from the radium in the river bed. Thus, the measurement was effected under conditions corresponding to those under which the population consumed the water. In one community Rn was present in water at a level of 35 mμC/l. Though the number of subjects was small, it was possible to establish tentatively a correlation between the increased ratio of deaths from cancer of the digestive tract in nonalcoholics and the increased quantity of radon ingested by the population. In areas underlain with uraniferous rock, the percentage of deaths from cancer was increased to as much as 35% above expected values with, however, no reduction in the average age of the subjects dying of cancer. (BBB)

4194 CRITICALITY SAFETY IN THE PREPARATION AND HANDLING OF NUCLEAR FUEL ELEMENTS. At. Strom, 11: 65-6(July 1965). (In German).

The precautions that should be observed in the planning of installations for the production, machining, and processing of irradiated and non-irradiated fuel elements, in the performance of individual technological methods, and in the storage of nuclear fuel elements in order to prevent a criticality incident are summarized. (J.S.R.)

4195 THE GENETICALLY SIGNIFICANT RADIATION DOSE FROM DENTAL X-RAY DIAGNOSIS IN JAPAN. I. Murai, Takeo (Tokyo Medical and Dental Univ.); Kikughi, Atsushi; Nakamura, Tadashi; Ishikawa, Mamoru; Aoki, Hatsue; Ueda, Masao. Bull. Tokyo Med. Dent. Univ., 6: 121-5(1959).

This report outlines a means of estimating the annual genetically significant dose received by the population of Japan in dental x-ray examinations on the basis of the number of dental radiograms made each year and the distribution of the types of examination in terms of age and sex, also on the knowledge of how the average projection technique for the intra-oral radiography affects the dose delivered to the gonads. Estimation of the total number of dental radiograms taken in 1958 in Japan was based on the fact that in 1958, 3272 m^2 of x-ray film was used to make dental film packs (1,300,000 standard size dental film packs with two films each). Bite-wing, occlusal, and extra-oral radiograms were neglected because they are used infrequently compared with the standard type intra-oral radiograms used in dental clinics. To determine the distribution of the projection types of intra-oral radiograms in terms of age and sex, considering the gonad dose, projection types were divided in 6 types: three types each in maxilla and mandible (incisor, canine-premolar, and molar region). The probability of conception of male and female infants was assessed from vital statistics for 1956 by using figures for live births. The future number of the children expected for an average exposed individual of 5-yr age class is given. It is assumed that all patients in dental clinics are normally fertile and the risk of subsequent parenthood the same at any age-class as for the population at large. The average gonad dose for each projection technique is to be obtained and then the annual genetically significant dose will be calculated. These data are given in a later report. (BBB)

4196 THE GENETICALLY SIGNIFICANT RADIATION DOSE FROM DENTAL X-RAY DIAGNOSIS IN JAPAN. II. Murai, Takeo; Kikuchi, Atsushi; Nakamura, Tadashi; Yamamoto, Akira (Tokyo Medical and Dental Univ.). Bull. Tokyo Med. Dent. Univ., 8: 319-24(1961).

For the estimation of genetically significant radiation dose from dental x-ray diagnosis, some dosimetric data were obtained during the intra-oral radiography. Data from other types of radiography were neglected because they are less frequently used in Japan. Gonad doses from dental x-ray exposure were measured in 242 male outpatients. Gonad doses for the female were estimated from previous reports. The genetically significant radiation dose from dental x-ray diagnosis in Japan in 1958 was estimated to be 1.2×10^{-3} mrem. This value is considered very small, in comparing it to that from medical diagnostic x-ray procedures in Japan. (TCO)

4197 STOMACH CANCER AND SOIL. Wynne Griffith, G. (World Health Organization, Washington, D. C.). Cancer Progr., 94-102(1963).

The possible role of factors in soil, including radioelements and other trace elements, in causing stomach cancer is reviewed. For gastric cancer, more so than for any other form of malignancy, there are causal influences which the sexes share whether considered geographically or by occupational group. It is suggested that one such common influence might be exposure to natural radioactivity. In England and Wales the gradient of mortality seems unmistakably related to geology, being high where acid igneous rocks and shales predominate and low where there is underlying chalk and limestone. This mortality gradient runs parallel to the gradient of natural radioactivity of geological formations. The intake of radioisotopes by man as indicated by storage in the skeleton is related to locality, and is presumably dependent on material inhaled or ingested in food or water. Foodstuffs show a wide range in their radioactive content, and water supplies are also very variable. It has been suggested that, in areas of high rainfall, radioactive materials might be leached from the soil, and in North Wales the type of garden soil associated with gastric cancer is one with a fluctuating water table where, if the underlying rock contained radioactive material, the soil would also show higher than average levels of radiation. There are some striking differences in the mortality from gastric cancer among mine workers according to various coalfields. Underground workers in the South Wales coalfields have a standardized mortality ratio which is nearly twice as high as that of men in similar occupations in the coal mines of Derby, Leicester, and Warwick. North eastern coalfields and the north Midland area occupy an intermediate position. It is not known whether the levels of background radiation show similar differences, though a priori this is possible. (BBB)

4198 ON THE INDIVIDUAL DOSIMETRIC CONTROL TECHNIQUE. Korenkov, I. P.; Golikov, V. Ya.; Sobolevskii, M. A. (Medical Inst., Dept. of Radiation Protection, Moscow). Gig. Sanit., No. 8, 67-71(Aug. 1965). (In Russian).

The health protection laws concerning operations with radioactive materials and other sources of ionizing radiation require that the institutions in which such work is carried take steps for the effective dosimetric control of the operations. This requires individual monitoring of the personnel. Data obtained by means of the usual fixed and portable instruments placed in work areas are not sufficient for this purpose; personal meters must be used to determine the integral dose to the critical organs and the type of radiation involved. Ionization chambers, photographic films, and thermoluminescent alumino-phosphate glasses are used mostly for this purpose; the actual method depends primarily on the type of radiation expected and its range. For emergency use, dosimeters with direct reading are most suitable. Correct positioning of the meters on the body of the workers is important; errors are mostly due to poor placement and to improperly chosen reading period of the instrument. The self-discharge characteristics of the instruments used must be known and a calibration program must be instituted. Upon advice of the medical department, the management of the institution must decide on the basis of the dose data obtained whether to authorize continued work of an individual in a radiation zone. (TTT)

4199 MEDICAL EXAMINATION OF RADIATION WORKERS. Holman, W. P. (Cancer Inst. Board, Melbourne). J. Coll. Radiol. Austral., 8: 289-90(Oct. 1964).

Medical examination of occupationally exposed persons is discussed with regard to: the pre-employment stage, routine examination during employment, and after an accident. In pre-employment examination the abnormality sought would be either a gross degree of anemia or a specifically low white count. An adequate standard type of general medical examination before employment should also include an inquiry about previous occupational exposures to marrow poisons and to radiation in previous employment or in the form of extensive or repeated diagnostic x-ray examinations, or to previous radiotherapy. Routine precautionary procedures, including monitoring and medical examinations as used by the Cancer Institute Board are outlined. Dose meters are supplied to all people handling radon or large radioactive sources and to others who may be occupationally exposed. From the group subject to the highest exposure, an immediate check on dose levels is obtained. No correlation has ever been found between exposure received and health. Blood counts are done at the beginning and end of employment. The most important post-accident information is an accurate physical record of the exposure. The typical clinical syndromes

associated with various levels of whole-body irradiation can then be predicted. (TCO)

4200 BEHAVIORAL FACTORS IN DISASTER SITUATIONS. Palmer, George J. Jr.; Sells, S. B. (Texas Christian Univ., Fort Worth). J. Soc. Psychol., 66: 65-71(June 1965).

Psychologic factors which would condition the response of the population to a thermonuclear attack are discussed. Data from other disaster situations are projected to situations to be expected in a thermonuclear war. Attempts are made to analyze some of the problems of civil defense planning for possible nuclear attack on the United States. The focus is principally on postnuclear attack phenomena, but emphasis is placed on the critical importance of preattack warning and preparation in conditioning the adequacy and extent of postattack performance. The approach is to extrapolate from a survey of the literature on natural and man-made disasters to the new situations implied by nuclear weapons. Such studies indicate that cataclysmic events are determined by natural law and demonstrate predictable, causal relations that offer opportunities for human intervention to reduce loss of life and property. One of the principal conclusions drawn from the disaster literature is that preparation is both possible and effective. The destructiveness of any disastrous event depends on the impact force and on the state of readiness of the target personnel with respect to defensive construction (shelters), special equipment (fire fighting, protective personal equipment), organization (for rescue, evacuation, medical care, welfare, police, traffic control, and communication), warning, and postimpact restoration of people and property for some degree of normal living. The special conditions that nuclear warfare imposes, from the viewpoint of preparation, are short warning time of attack, expectation of more widespread destruction than ever before experienced, including radiation fallout at remote points, and the need for special equipment and information for survivors. The importance of warning and preparation lies largely in their conditioning influence on expectations when situations develop. Data from various sources confirm the relation between warning and advance information of threatening events and the nature of response at the time of impact and after. Warning initiates fear-motivated problem solving and vicarious rehearsal of alternative solutions. While fear is normally experienced in some relation to the extent of danger, warning can reduce irrational fear to a moderate level when associated with information about danger and risks. There is evidence that high preimpact fear is followed by high postimpact anxiety, preoccupation with the threat, and alarm at the person's own psychophysiological reactions; moderate preimpact fear is accompanied by the lowest level of postimpact disturbance and the best chance for constructive self-preparation of all levels of preimpact fear; low preimpact fear in relation to the realistic dangers faced is followed by hostility and resentment against authority figures; and preimpact denial, as well as ignorance of the danger, is followed by postimpact neurotic collapse. Psychological readiness implies both sufficient fear to activate worry and coping activities and to surmount the resistances expected as a result of financial and other sacrifices that preparation entails. Analysis of disaster studies emphasizes the importance of effective warning and preparation for civil defense. (BBB)

4201 THE CONTROL OF THE RADIOACTIVITY IN FOOD PRODUCTS IN AMERICA. Ramuz, A. (Laboratoire Cantonal, Lausanne, Switzerland). Mitt. Gebiete Lebensm. Hyg., 54: 549-53(1963). (In French).

A brief review is given of the monitoring systems in the United States for the control of radioactivity in food products. The general surveillance covering most of the country, the special monitoring systems instituted for a particular purpose, the local monitoring systems set up around nuclear installations, and the emergency monitoring systems to be set in operation in case of a nuclear incident are described. (J.S.R.)

4202 AN APPARATUS FOR STUDYING THE RETENTION OF INHALED RADIOACTIVE VAPOURS BY HUMAN SUBJECTS. Morgan, D. J. (Atomic Energy Research Establishment, Harwell, Eng.). Nature, 207: 1310-11 (Sept. 18, 1965).

An apparatus is described for use in accurately determining the percentage retention of radioactive vapors inhaled by human subjects. Design features emphasized are: the evaporator, analysis, the inhalation-exhalation unit, and air supply. Methyl iodide labeled with ^{132}I was used to test the apparatus. Preliminary results on four volunteer subjects indicate retention values varying between 55 and 80 per cent. (H.G.D.)

4203 THE DANGERS OF X RAYS TO THE PHYSIOTHERAPIST. Simon, George (St. Bartholomew's Hospital, London). Physiotherapy, 51: 84(Mar. 1964).

Radiation hazards to physiotherapists assisting during patient radiography are considered. The responsibility of radiologists in protecting staff and patient is pointed out. It is concluded that the risk to physiotherapists is small provided normal precautions are taken. (TCO/H.G.D.)

4204 THE DOSE DISTRIBUTION FOR IRRADIATIONS WITH VAN DE GRAAFF ELECTRON ACCELERATORS [Thesis]. Gruenewald, T. Karlsruhe, Ger., Tech. Univ., 1965. 57p. $2.00 Gmelin, AED-DISS. 65-5.

The inhomogeneity of dose distributions from electron accelerators was studied. It is shown that for a linear sample transport system inhomogeneities can be minimized by proper choice of the transport speed. Methods for dose distribution measurements are discussed. Dose distributions for electrons and bremsstrahlung for spherical samples and for liquids are given. (Gmelin Inst.)

4205 DOSE MEASUREMENTS FROM Ra NEEDLES [Thesis]. Holtzhauer, R. Jena, Ger., Univ., 1964. 44p. $2.00 Gmelin, AED-DISS. 64-734.

Isodose distributions from Ra needles in the jaw of a phantom head were measured with photographic films. Calibration methods are discussed. (Gmelin Inst.)

4206 IRRADIATION OF PATIENTS DURING EXTRAORAL RADIOGRAPHY OF THE TEETH AND THE JAW [Thesis]. Kruse, D. Goettingen, Ger., Univ., 1964. 73p. $2.00 Gmelin, AED-DISS. 64-590.

The dose to various body parts including gonads during dental radiography was determined. Results indicate that gonad doses are negligible if appropriate protection methods are used. (Gmelin Inst.)

4207 COMPARING STUDIES OF THE ABSORPTION OF 200 kv X RAYS AND ^{60}Co γ RAYS IN THE HUMAN BODY AND IN A PHANTOM [Thesis]. Boon-Long, P. Goettingen, Ger., Univ., 1964. 75p. $2.00 Gmelin, AED-DISS. 64-589.

Depth dose distributions as a function of the angle of incidence were determined with an ion chamber in a tissue equivalent phantom and in female patients. It is concluded that tabulated irradiation parameters should serve as a guide only and should be supplemented by individual depth dose measurements. (Gmelin Inst.)

4208 THE TRANSFER OF RADIOACTIVE SOURCES. Ritchie, A. B.; Webb, C. G. (Atomic Energy Research Establishment, Harwell, Eng.). pp 551-70 of International Symposium on Working Methods in High Activity Hot Laboratories. Vol. II. Paris, Organization for Economic Cooperation and Development, 1965.

Methods in use at a number of handling facilities in the UKAEA for the transfer of kilocurie sources of radioactive material between shielded flasks and beta-gamma, alpha-beta-gamma, and controlled-atmosphere cells are reviewed. (auth)

4209 TRANSFER PROCEDURES USED IN THE ALPHA-GAMMA HOT LABORATORY AT KARLSRUHE. Boehme, G.; Gottlob, P.; Nowak, A. (Karlsruhe Nuclear Research Center, Ger.). pp 583-94 of International Symposium on Working Methods in High Activity Hot Laboratories. Vol. II. Paris, Organization for Economic Cooperation and Development, 1965.

Several systems are used for gas-tight inter-cell transfer and loading and unloading of radioactive materials

and parts of cell equipment under gas-tight and alpha-tight conditions without personnel having to enter the cells. Tests were carried out to show the reliability of the transfer operations. (auth)

4210 SPECIAL PROCEDURE FOR ALPHA-BETA-GAMMA TRANSFERS OF LARGE PIECES OF EQUIPMENT. Pesenti, P.; Cazalis, J. P. (Communaute Europeenne de l'Energie Atomique, Pays-Bas, Netherlands). pp 611-26 of International Symposium on Working Methods in High Activity Hot Laboratories. Vol. II. Paris, Organization for Economic Cooperation and Development, 1965. (In French).

Equipment was designed to provide a multipurpose transfer system consistent with the largest useful size and the most dangerous products (α-β-γ). Its utilization requires a gamma-shielded transfer zone communicating with the hot cells by an opening in their ceiling. A remote-controlled travelling bell equipped with a winch is used for hoisting. Double remote welding was carried out on the junction sleeve to separate the bell from the cell. Prototype equipment was tested at Mol (Belgium). (auth)

4211 DECONTAMINATION EXPERIENCE AT THE HOT LABORATORY OF CASACCIA. Cesarano, C.; Ghezzi, E.; Lauro, M. (CNEN, Casaccia, Italy). pp 705-18 of International Symposium on Working Methods in High Activity Hot Laboratories. Vol. II. Paris, Organization for Economic Cooperation and Development, 1965.

The experience gained in three years of operation is described. The key factors for efficient and fast decontamination are summarized. The in-cell equipment should be as small as possible and easy to disassemble and remove. The decontamination process should be planned in detail in advance. A suitable transfer technique should be adopted in order to keep the contamination as confined as possible in the loading area. Since the laboratory considered was not equipped with isolation rooms, plastic tents were built in the back of the cell door. The contaminated equipment was transferred out of the hot cell by personnel wearing frog suits or preferably tunnel suits. (auth)

4212 DECONTAMINATION PROCEDURES FOR HIGH ACTIVITY CELLS AT A.E.R.E. HARWELL. Wells, H. (Atomic Energy Research Establishment, Harwell, Eng.). pp 719-34 of International Symposium on Working Methods in High Activity Hot Laboratories. Vol. II. Paris, Organization for Economic Cooperation and Development, 1965.

Efforts aimed at preventing contamination taken at Harwell are illustrated. Procedures that ensure that the decontamination of cells and equipment, whenever necessary, is carried out efficiently and safely are described. (auth)

4213 DECONTAMINATION PROCEDURES AND FREQUENCIES IN α-β-γ METALLURGICAL HOT CELLS. Valentin, A.; Hayet, L. (CEN, Fontenay-aux-Roses, France). pp 735-47 of International Symposium on Working Methods in High Activity Hot Laboratories. Vol. II. Paris, Organization for Economic Cooperation and Development, 1965. (In French).

An α-β-γ laboratory at Saclay, used for metallurgical research on irradiated plutonium since 1961, consists of α-sealed removable boxes contained in a β-γ-shielded enclosure. On the completion of an operation, the box is taken by a special crane to the decontamination room. Decontamination is accomplished manually. The process was improved with use and the time necessary for a decontamination cycle was decreased. Pre-equipped boxes were used to replace those being decontaminated; thus the operating speeds were increased. The experience gained on this installation is now being used in the construction of a α-β-γ laboratory, named "Laboratoire de Radiométallurgie" at the Fontenay-aux-Roses Nuclear Center. (auth)

4214 UNITED STATES PRACTICES IN THE CONTROL AND CONTAINMENT OF RADIOACTIVE CONTAMINATION. Ferguson, K. R. (Argonne National Lab., Ill.). pp 889-917 of International Symposium on Working Methods in High Activity Hot Laboratories. Vol. II. Paris, Organization for Economic Cooperation and Development, 1965.

The types of radiological containment systems and operating practices used in research operations requiring thick biological shielding are surveyed. Some containment enclosures are an integral part of the shielding and others are separate and removable. The parts of the complete containment system are chosen on the basis of numerous safety and economic factors, such as site location, aerosol handling hazard, type and size of the operations, manipulators used, and long-range objectives of the facility. Initial operating experience was obtained with several large containment complexes. Developments in ventilation, fire control, and master-slave manipulation are reviewed. (auth)

INSTRUMENTATION

General

Refer also to abstract 4084.

4215 (ANL–7081, pp 134-49) MASS-SPECTROMETRIC INVESTIGATIONS. (Argonne National Lab., Ill.).

Several aspects of mass-spectrometric research are briefly discussed. These include ionization and fragmentation of gas molecules, high-temperature studies of equilibria and chemical kinetics, atomic impact phenomena on metal surfaces, ionic impact phenomena on metals, and the installation of a 2-Mev Van de Graaff and an associated beam handling system. (M.O.W.)

4216 (AWRE-O–70/65) A NEW LONG-PERIOD VERTICAL-COMPONENT SEISMOMETER. Beach, A. D. (Atomic Weapons Research Establishment, Aldermaston (England)). Nov. 1965. 41p. Dep. mn; BIS $1.60; HMSO 8s. 0d.

A seismometer is described whose performance is intended to be comparable with the best existing vault instruments and yet which should be suitable for field work at remote sites. It incorporates a new type of leaf-spring suspension, which allows long periods to be attained, yet permits severe handling of the fully assembled instrument. The leaf-spring suspension was found to be superior to the usual helical spring system, in that transverse and other modes of vibration of the spring itself are of higher frequency than most noise sources, thereby avoiding resonances which can lead to spurious long-period response. (auth)

4217 (MATT–378) AC RESPONSE OF SPIRALLY WOUND CAPACITORS. Tenney, F. H. (Princeton Univ., N. J. Plasma Physics Lab.). Sept. 1965. Contract AT (30-1)-1238. 20p. Dep. mn; CFSTI $1.00 cy, $0.50 mn.

The impedance of a spirally wound capacitor is calculated. The current distribution is also determined. The capacitor is treated as a nested set of coaxial cylinders. It is found that at high enough frequencies the capacitor displays many characteristics of a transmission line. (auth)

4218 (NYO–3421-4) PHOTOMULTIPLIER INVESTIGATION. Quarterly Report No. 3, May 15–August 14, 1965. Smith, H. M. Jr.; Wasserman, R. (David Sarnoff Research Center, Princeton, N. J.). Aug. 16, 1965. Contract AT(30-1)-3421. 24p. Dep. mn; CFSTI $1.00 cy, $0.50 mn.

Two problems often encountered by users of photomultiplier tubes are those of dark pulses and gain shift with count rate or short term stability. Recent investigations carried out on the causes of these problems are summarized. With regard to the dark current problem, it has now been found that the larger dark pulses (type B) may be eliminated by an oxidation process and/or elimination of insulating supports. These results suggest that some mechanism taking place in the alkali metal films on insulators may be causing the type B pulses. Further study of the stability problem indicates that much of the observed pulse-height shift may be due to insulator charging in the front end of the tubes. (auth)

4219 (ORNL-IIC–5, pp 182-205) RADIOISOTOPE SOURCES OF LOW-ENERGY ELECTROMAGNETIC RADIATION AND THEIR USE IN ANALYSIS AND MEASUREMENT OF COATING THICKNESS. Cameron, J. F.; Florkowski, T. (International Atomic Energy Agency, Vienna (Austria)).

Recent developments in the application of radioisotope sources of low-energy electromagnetic radiation outside the USA are reviewed. Such sources have advantages over electrical x-ray generators, viz., their small physical size, comparatively low cost, stability of output in terms of energy and time, and independence of power supplies. They are being increasingly applied in industry, particularly for analysis, the techniques of which are discussed in some detail. The use in measuring coating thickness is discussed only briefly. (auth)

4220 (SC-TM–65-424) THIN-FILM, FIELD-EFFECT DEVICES. Williams, J. D.; Terry, L. E.; Komarek, E. E. (Sandia Corp., Albuquerque, N. Mex.). Oct. 1965. Contract AT(29-1)-789. 36p. Dep. mn; CFSTI $2.00 cy, $0.50 mn.

An investigation was conducted to determine the feasibility of depositing active devices by vacuum deposition techniques which are compatible with the techniques used to form some types of thin-film passive elements. The insulated gate, thin-film, field effect device was the particular active device investigated in both the coplanar and staggered configuration. Although active devices were made with transconductances that ranged from 2 to 800 micromhos there are still many unsolved problems. The main problems are those associated with the insulating film and its interfacial properties. The unpredictability of the interfacial regions is believed to be the major contributing factor to the general lack of reproducibility and stability of these devices. A detailed account of the present progress, a survey of the pertinent literature, and an outline of future efforts in this area are included. (auth)

4221 (UCRL–12394-T) A LOGARITHMIC CURRENT-TO-VOLTAGE AMPLIFIER WITH HIGH SENSITIVITY, STABILITY, AND DYNAMIC RANGE, SUITABLE FOR FIELD APPLICATION. Bishop, Stanley R. (Lawrence Radiation Lab., Univ. of California, Livermore). Oct. 12, 1965. Contract W-7405-eng-48. 30p. (CONF-651001–9). Dep. mn; CFSTI $2.00 cy, $0.50 mn.

From IEEE Nuclear Science Symposium, San Francisco.

A logarithmic amplifier is described which has a dynamic range of 6 decades of input current (from 10^{-13} to 10^{-7} A) while maintaining very good logarithmic response (output voltage deviates less than ±1% from a logarithmic function). A high degree of temperature stability is also achieved (total offset less than ±2% of full scale voltage over ambient temperature range from –10°C to +70°C). It has a useable range (by nonlogarithmic response extensions) to 9 decades. The circuit covers its exceptionally wide dynamic range without range switching. Power requirement is less than 1 W, and the circuit fits on two 4 × 4 inch printed circuit boards. It is readily portable and performs well under rugged field conditions, as demonstrated by its successful use in Plowshare nuclear cratering experiments. (auth)

4222 (UCRL–13186) MALFUNCTION DETECTION AND DIAGNOSIS. Alcone, J. M.; Osborne, R. L.; Ramanujam, H. R.; Rao, D.; Costanza, J. L. (California Univ., Berkeley. Inst. of Engineering Research). Aug. 1965. Contract W-7405-eng-48. 108p. (MD–65-7). Dep. mn; CFSTI $4.00 cy, $0.75 mn.

Techniques are sought and analyzed for detecting and diagnosing the causes of malfunctions in arbitrary systems. A computational approach is used. The particular areas of study include the nature, extent, and distribution of malfunction sensors on the system to be monitored; the requisite data processing operations; and feasibility of the malfunction-detection system. (T.F.H.)

4223 (UCRL–14345) THE EFFECT OF HIGH VELOCITY TRANSLATION ON PHOTON CORRELATIONS IN LASER INTERFEROMETERS. Burgess, Thomas J. (Lawrence Radiation Lab., Univ. of California, Livermore). Aug. 17, 1965. Contract W-7405-eng-48. 12p. Dep. mn; CFSTI $1.00 cy, $0.50 mn.

It is shown that high velocity translation of one of the mirrors of a laser Michelson interferometer diminishes the correlation of the photons in the wave field. This diminution is manifested by deterioration of the visibility of interference effects. An expression is obtained for

fringe visibility as a function of the Doppler frequency-shift upon reflection from the moving mirror, the line width of the laser Lorentzian spectral distribution, and the optical path difference. The implications for pulsed displacement measurements are discussed. (auth)

4224 (UCRL–14448) QUARTZ PRESSURE TRANSDUCER PACKAGE. O'Brien, Joseph F.; Wasley, Richard J. (Lawrence Radiation Lab., Univ. of California, Livermore). Sept. 27, 1965. Contract W-7405-eng-48. 10p. Dep. mn; CFSTI $1.00 cy, $0.50 mn.

A useful method to package quartz crystal pressure transducers is described. The assembly consists of the transducer crystal (or crystals) with appropriate resistors and conveniently accessible terminals, all potted with epoxy resin in a brass cylinder. These assemblies are particularly valuable for use in experiments assembled in the field, when self-contained units must be maintained in inventory and be available for quick usage, or when the propagation of disturbances in reactive materials are investigated and special handling procedures are required. (auth)

4225 REQUIREMENTS ON NUCLEAR ELECTRONICS. Zander, K. (Hahn-Meitner-Institut fuer Kernforschung, Berlin). Atomwirtschaft, 10: 502-6(Oct. 1965). (In German).

The concern in the development of nuclear electronics and auxiliary components in Germany is discussed from the viewpoint of the user. The requirements for research and industry in the development of adequate nuclear electronics are summarized. (J.S.R.)

4226 FLEXIBLE SYSTEM FOR COLLECTING AND RECORDING OF INFORMATION. Liebendoerfer, Helmut (Borer and Co., Soleure, Switzerland). Ind. At., 9: No. 7-8, 87-8(1965). (In French).

The system described understands numbers varying between 1 and 98, from instruments furnishing diverse information. In most cases it is a question of levels of counting. But often measuring instruments such as digital voltmeters, angular position detectors, and electric time clocks are a part of the system. Even values of different parameters are transformed into the same electronic form of information as those arising from other instruments with the help of a parameter unit furnished with four multiple digital selectors. All the information is collected from time to time by a center for automatic reading and registering, which is composed of a readout logic and a drive unit. It controls the punching of tape or cards, the printing, etc. The counting levels, the automatic reading, preselection, posting, testing, information given in series, and the registering of information are described. (J.F.P.)

4227 RADIOISOTOPE FLOWMETER. Oppelt, Jiri (Inst. of Investigation, Production and Utilization of Isotopes, Prague). Jaderna Energie, 11: 382-4(1965). (In Czech).

A brief review is given of a number of possible methods of measuring the velocity of flow of a fluid by means of radioisotopes. These methods include: injection of a radioisotope sample and measurement of time lapse until radiation is detected at a second point; measurement of the revolutions of a turbine wheel with a radioactive source on one side; measurement of position of the bob in a rotameter; measurement of position of a small radioactive source on a flap or spring in the flowing stream; measurement of the movement of activated zones from a pulsed neutron source; and measurement of movement of ionized zones (in a gas) using a radioactive source pulsed with a shutter. Two variations of the technique of flow measurement with a rotameter are described. The first uses a radioactive source on the bob of a rotameter and a pair of ionization chambers located at the ends of the rotameter tube and connected in opposition. The second uses a collimated radiation source on one side of the rotameter tube and a detector on the other. The position of the bob is indicated by its attenuation of the radiation. (TTT)

4228 X-RAY GENERATORS. Mester, H. (C.H.F. Mueller, GmbH, Hamburg). Medicamundi, 10: 73-5(1965).

An explanation is given of the new system of terminology for x-ray generators according to DIN 6814 "Terms and nomenclature in X-ray engineering." The significance of the different types of generators for the practical use of x-ray tubes, as well as the correlation between the circuitry of the generator and the ripple factor of the tube voltage is pointed out. On the basis of previously published data it is shown that the importance of the ripple factor in a six- and twelve-pulse generator is, for practical purposes, by no means as high as is generally assumed. (auth)

4229 AN INDUCTION COUPLED SUPERCONDUCTING BOLOMETER [Thesis]. Gerig, John Sebastian. Stanford, Calif., Stanford Univ., 1965. 103p.

An induction-coupled, superconducting bolometer, developed for use in an infrared ultramicrospectrometer is described. The sensitivity obtained corresponds to an NEP of 5.5×10^{-12} watts using a one-second correlation interval and a 6-cps chopping rate. The sensitive element is a ring of high-purity lead foil, which is the primary of an air core r-f transformer. The secondary winding, also superconducting, is tuned to 600 kc with a shunt capacitor and is made part of a low-noise, negative-resistance oscillator whose level of oscillation reflects changes in ring resistance. Bolometer thermostating at the transition temperature is achieved by means of a heat input controlled by the level of oscillation. An analysis of the dynamics and noise theory of the bolometer is given. The analysis appears to account satisfactorily for the observed sensitivity and points to conventional amplifier noise as the limiting factor in the experimental equipment. Relatively simple modifications are suggested, which should yield substantial improvements in sensitivity. (Dissertation Abstr.)

4230 IMPROVEMENTS IN OR RELATING TO APPARATUS FOR CONTROLLING SMALL RATES OF FLOW OF GASES. Hart, Ralph James; Williams, John Llewellyn (to United Kingdom Atomic Energy Authority). British Patent 1,008,517. Oct. 27, 1965. Filed May 18, 1961.

An apparatus, which is sensitively operated by remote means, is provided for controlling small rates of gas flow. The apparatus includes a chamber for containing a sample of the gas and valved ducting means for introducing the gas to the chamber and for discharging the gas from the chamber. One or more thermoelectric cooling couples are associated with the chamber for varying the temperature and therefore the pressure of the gas within the chamber. The apparatus is applicable to a source leak valve for mass spectrometric equipment. (B.L.M.)

4231 HOMOPOLAR GENERATOR. Musset, Edmond E. (to U. S. Atomic Energy Commission). U. S. Patent 3,217,199. Nov. 9, 1965.

A means for increasing the power capacity and efficiency of homopolar generators is described. A plurality of axially spaced rings of nonmagnetic material are embedded in the cylindrical periphery of the rotor of a homopolar machine so as to be in electrical contact therewith along the active portion thereof. (AEC)

4232 ANGLED PLATE SCANNING INTERFEROMETER. Gardner, Andrew S.; Barr, William L. (to U. S. Atomic Energy Commission). U. S. Patent 3,217,591. Nov. 16, 1965.

An interferometer is designed for producing interference patterns from the light emitted by a source for diagnostic purposes, e.g., temperature measurement of a plasma and the like. The interferometer comprises two interferometer plates mounted at a small angle with respect to one another. A beam displacer is disposed to receive and cyclically sweep a selected spectral line of the source light across the face of the first interferometer plate. The light beam is divided into an array of parallel phase-shifted light beams by reflection and transmission between the interferometer plates. The phase-shifted light beams emerging from the interferometer plates are focused onto a photomultiplier tube by means of a condensing lens. The intensity change of the interfering focused light beams is indicative of the Doppler frequency shift which is coupled to the photomultiplier tube. (AEC)

Radiation Detection

Refer also to abstracts 4089, 4111, 4523, 4548, 4583, 4797, 4997, 5066, 5109, 5181, and 5187.

4233 (AD-618676) APPLICATION OF AN ANTI-COINCIDENCE-SHIELDED SCINTILLATION SPECTROMETER TO THE STUDY OF THE $^{14}N(p, GAMMA)^{15}O$ REACTION. Evans, Albert E. Jr. (Naval Ordnance Lab., White Oak, Md.). May 11, 1965. 82p. (NOL-TR-65-72). CFSTI $3.00 cy, $0.75 mn.

A gamma spectrometer was built using a liquid-scintillator anticoincidence shield for a 5 in. dia × 10 in. long NaI(Tl) crystal. The spectrometer was used to study radiation from the $^{14}N(p,gamma)^{15}O$ reaction for proton energies of from 0.97 to 1.96 Mev. Decay schemes for the 8.29, 8.75, 8.92, and 8.98 Mev levels in ^{15}O were derived. (auth)

4234 (AD-619177) MODIFICATION OF THE TECH/OPS PHOTOMETRIC MEASUREMENT ASSEMBLIES. Final Report, January 4–May 3, 1965. Kofsky, I. L.; Miller, C. S.; Theriault, A. J.; Johnson, R. H. (Technical Operations Research, Burlington, Mass.). June 1965. Contract AF19(628)-4962. 39p. CFSTI $2.00 cy, $0.50 mn.

Four Tech/OPs photometric assemblies, consisting of photometers, radiometers, and radiometrically calibrated cameras, were modified. The twelve-channel photometer was improved by the addition of two filters for measuring the irradiance in ultraviolet N_2 Second Positive bands. The near-infrared photometer was fitted with a six-position interference filter wheel to permit observation of some of the N_2 First Positive bands and OI permitted lines; in addition, its S-1 surface photomultiplier was enclosed in a thermoelectric refrigerator. The infrared radiometer now has a four-position filter wheel, and the temperature of its PbS photoconductive cell is monitored by a thermistor thermometer. De Havilland Mark 7A 35-mm data-recording cameras (with 100-ft magazines and flexible shutter programming) fitted with lenses having 108 degree circular fields replace the Nikon cameras and 77 degree lenses formerly used. All equipment was made compatible with the mechanical mounts, windows, electrical power, and data-recording arrangements of the two Air Force KC-135 aircraft in which it will eventually be used. (auth)

4235 (AECL-2283) A PORTABLE TRITIUM-IN-AIR MONITOR. Sannes, F.; Banville, B. (Atomic Energy of Canada Ltd., Chalk River (Ontario)). July 1965. 19p. Dep.; AECL $0.20.

A plastic scintillator detector was developed for the measurement of tritiated water vapor in air. The scintillations produced by the beta rays from tritium are detected by two photomultiplier tubes mounted on each end of the scintillator detector. A tunnel diode coincidence circuit and a three channel pulse height selector are employed to analyze the photomultiplier pulses. With this system, detection efficiencies of 20% were observed. Concentrations as low as 1 $\mu\mu$Ci/ml or 0.2 MPC can be measured. An electronic circuit was incorporated into the instrument to make it less sensitive to external gamma radiation. The response time of the system to a sudden increase in tritium concentration in the sampled air is one minute, and approximately five minutes for a corresponding sudden decrease. (auth)

4236 (BNL-9605) A THERMOLUMINESCENT NEUTRON DOSIMETRY SYSTEM. Distenfeld, C.; Bishop, W.; Colvett, D. (Brookhaven National Lab., Upton, N. Y.). [nd]. Contract AT(30-2)-Gen-16. 18p. Dep. mn; CFSTI $1.00 cy, $0.50 mn.

A neutron dosimetric system was developed by using lithium fluoride phosphors within a Bonner Sphere. Use is made of the large difference in neutron absorption characteristics between ^6Li and ^7Li fluoride to permit evaluation of the neutron and gamma dosages for mixed fields. This depends upon a detailed knowledge of the neutron and gamma response characteristics of the two isotopic phosphors. The gamma responses are very similar, except for a minor mass correction, allowing precise gamma subtraction and thereby unmasking the neutron contribution. Neutron response was evaluated by using a positive ion Van de Graaff generator to produce mono-energetic neutrons. Protons on lithium, protons on tritium, deutrons on deutrons and deutrons on tritium allowed coverage of the range between 150 kev and 18 Mev. Sensitivity of the sphere to 1.5 Mev neutrons is about 10 ^{60}Co roentgen equivalents per neutron Rad. (M.O.W.)

4237 (BNL-9665) CALIBRATION AND RESPONSE OF PERSONNEL MONITORING FILM DOSIMETERS TO SYNCHROTRON STRAY RADIATIONS. Phillips, Leigh F.; Champagne, Robert J. (Brookhaven National Lab., Upton, N. Y.). [1965]. Contract AT-30-2-GEN-16. 10p. (CONF-651109-7). Dep. mn; CFSTI $1.00 cy, $0.50 mn.

From 1st Symposium on Accelerator Radiation Dosimetry and Experience, Upton, N. Y.

In order to determine effectiveness of personnel monitoring techniques at high energy proton synchrotrons, a careful evaluation of the film badge performance was made. These evaluation studies were performed in various work areas and under a variety of experimental conditions because the synchrotron parameters, such as shielding and experimental arrangements, vary greatly, thus radically changing the quality and quantity of the stray radiation fields. Among the dosimeters employed for this study were the BNL film badge and specially designed tissue-equivalent (TE) ionization chambers. The film badge contains an aluminum and a cadmium filter and an open window. The DuPont sensitive 555 and insensitive 1290 beta/gamma films are used along with the Kodak NTA film packet. Test assemblies containing the film badges and the dosimeters were placed in experimental areas around the two BNL proton synchrotrons. Machine parameters that may influence the data are recorded. Film badge data are analyzed and the assigned dose, as indicated by standard method of film badge interpretation, was compared with the absorbed dose as determined by the ionization chambers. Quality factors implied by the standard personnel monitoring procedure was found to vary from one to 30. These implied quality factors were also compared with measured quality factors, where such information is available. Various factors complicate the interpretation of film badges exposed at the synchrotrons. For example, maintenance work in tunnels during accelerator shutdown results in relatively high gamma exposures which are a result of the induced activity of the machine components. Due to the lack of electronic equilibrium in the area and the occasional occurrence of thermal neutrons, the use of the open window and cadmium portions of the film badge is restricted, leaving only the aluminum filter for proper gamma evaluation at the synchrotrons. Also, the economical procedure of not reading the NTA film in personnel film badges, when no exposure is indicated by the beta/gamma film, is not valid at high energy synchrotrons. Neutron exposures, up to several hundred mRem, have been measured by film badges worn by radiation workers, without any positive exposure indicated on the beta/gamma film. (auth)

4238 (EUR-2487.e) EFFICIENCY OF A SEMICONDUCTOR SANDWICH DETECTOR IN A FLUX OF FISSION NEUTRONS FROM A DISK SOURCE. Rydin, R. A. (European Atomic Energy Community, Ispra (Italy). Joint Nuclear Research Center). 1965. 20p. Dep. mn.

The detection efficiency of a semiconductor sandwich spectrometer is calculated as a function of energy and distance from a disk type fission neutron source. The efficiency is found to vary with the angular distribution of incident neutrons as well as with the incident neutron energy. The difference between the actual differential cross sections for the ^6Li reaction and the isotropic cross sections is not large. (auth)

4239 (IAE-900) DIFFERENTSIAL'NYI GAZOVYI CHERENKOVSKII SCHETCHIK. (A Differential Gaseous Cherenkov Counter). Klebanov, Yu. D.; Kruchinin, S. P.; Lozina, L. A. (Institut Atomnoi Energii, Gosudarstvennyi

Komitet po Ispol'zovaniyu Atomnoi Energii SSSR, Moscow). 1965. 11p. Dep. mn.

The construction and testing results of a differential gas Cherenkov counter, intended for work with a hodoscope device for a bubble chamber, are described. A resolution of $\Delta\beta/\beta = 2 \times 10^{-3}$ and an efficiency of 0.96 ± 0.02 were obtained. (tr-auth)

4240 (JINR-P-2277) IZMERENIE ENERGETICHESKIKH I UGLOVYKH KHARAKTERISTIK ELEKTRONOV I γ-KVANTOV V PROPANOVOI PUZYR'KOVOI KAMERE. (A Measurement of Energy and Angular Characteristics of Electrons and γ-Quanta in a Propane Bubble Chamber). Grishin, V. G.; Kistenev, E. P.; Lepilova, L. I.; Moroz, V. I.; Mu Tzung (Joint Inst. for Nuclear Research, Dubna (USSR). Lab. of High Energy). 1965. 32p. Dep. mn.

The introduction of the correction for the radiation and ionization losses is considered in detail. It is necessary to make this correction to obtain an unbiased estimate of the electron momentum. The π^0 meson mass determined experimentally by the measurements of electron-positron pairs was found to be 136 ± 2 Mev against 122 ± 3 Mev obtained without introduction of the above-mentioned corrections. The calculation of the error is considered in measuring the momentum. The ways of its possible reduction are indicated. The smallness of the corrections to the angles α and β is shown experimentally. These angles determine the direction of electron motion at the first point. Effects are considered which give a contribution to the errors in the measured angles. A comparison of the obtained formulas with experiment was made and showed a good agreement. (auth)

4241 (JINR-P-2364) ELEKTROSTATICHESKOE POLE PROVOLOCHNYKH ELEKTRODOV ISKROVOI KAMERY. (Electrostatic Field of Wire Electrodes for a Spark Chamber). Matyushin, A. T.; Matyushin, V. T. (Joint Inst. for Nuclear Research, Dubna (USSR). Lab. of High Energy). 1965. 10p. Dep. mn.

Using the complex potential the electrostatic field of different systems of wire electrodes for a spark chamber is found. According to the analysis of the results some considerations are given concerning the choice of electrodes providing a performance of the chamber. (auth)

4242 (JINR-P-2376) UPLOTNENIE ILLYUMINATOROV BOL'SHIKH VODORODNYKH PUZYR'KOVYKH KAMER JINR. (Inflatable Gaskets for JINR Large-Volume Hydrogen Bubble Chambers). Lebedev, R. M.; Saitov, I. S.; Ustenko, E. P.; Shishov, Yu. A. (Joint Inst. for Nuclear Research, Dubna (USSR). Lab. of High Energy). 1965. 10p. Dep. mn.

Inflatable gaskets designed for one- and two-meter hydrogen bubble chambers are described. The design has some advantages owing to using an inflatable gasket with indium along the flexible metallic surface of a free inflatable element. Gasket characteristics were obtained on the stand at a liquid nitrogen temperature. In the course of the first hydrogen runs of the one-meter chamber the main conclusions of the stand tests were confirmed. (auth)

4243 (LAL-1102) UTILISATION DES DETECTEURS A SEMICONDUCTEUR AUPRES D'UN ACCELERATEUR A HAUTE ENERGIE. I. ETUDE EXPERIMENTALE D'UN DETECTEUR A SEMICONDUCTEUR AUPRES DE L'ACCELERATEUR LINEAIRE. II. AMPLIFICATEUR A FORT DEBIT D'IMPULSIONS POUR DETECTEUR A SEMICONDUCTEUR. (Utilization of Semiconductor Detectors With a High-Energy Accelerator. I. Experimental Study of a Semiconductor Detector With the [Orsay] Linear Accelerator). Amsel, G.; Benaksas, D.; Zajde, C. (II. High-Pulse-Rate Amplifier for a Semiconductor Detector). Boshard, R. (Laboratoire de l'Accelerateur Lineaire, Univ. de Paris, Orsay (France)). Mar. 1965. 87p. Dep. mn.

The special techniques required for the use of semiconductor detectors near a beam of high energy electrons are studied and their advantages discussed. An amplifier is described with capabilities of handling very high counting rates without pile up. The amplifier has a 6 ns risetime; pulses can be clipped down to 10 ns. Gain is 300 and noise levels in the range of 30 Kev (F.W.H.M. for silicon) are achieved. α particle pulses in presence of 10^8 counts per second due to protons from an electrostatic accelerator were correctly measured. Operation with pulsed accelerators yields satisfactory background reduction. The structure of the amplifier is given in detail. Pile up problems are discussed both in pulsed and continuous operation. The noise characteristics are studied, taking into account the effect of amplifier and detector risetimes and clipping time. (M.O.W.)

4244 (NP-15416) LES CHAMBRES A BULLES A LIQUIDES LOURDS [Theses]. (The Heavy Liquid Bubble Chamber [Thesis]). Roullet, Robert (Cleremont-Ferrand Univ. (France). Faculte des Sciences). 1963. 44p. Dep. mn.

After a short historic review of the development and utilization of bubble chambers, the superheated state and the scheme of operation of a bubble chamber are outlined. The different theories for the germination under radiation and the bubble growth are developed in detail and illustrated by results that confirm or deny these theories. The characteristics of different heavy liquids are studied. The development and construction of a propane–freon chamber is then described. (tr-auth)

4245 (ORNL-P-1723) THE USE OF A DIGITAL COMPUTER IN TIME-OF-FLIGHT EXPERIMENTS. Gwin, R.; Weston, L. W.; Ingle, R. (Oak Ridge National Lab., Tenn.). [1965]. Contract W-7405-eng-26. 8p. (CONF-651001-8). Dep. mn; CFSTI $1.00 cy, $0.50 mn.

From IEEE Nuclear Science Symposium, San Francisco.

A general purpose PDP-4C digital computer was incorporated as an integral part of a data acquisition and processing system for neutron time-of-flight experiments. The performance of the computer for these calculations is discussed. (M.O.W.)

4246 (RPI-328-40, pp 49-55) NEW INSTRUMENTATION PROGRAMS (PRIMARILY FOR NEUTRON CROSS SECTION MEASUREMENTS). (Rensselaer Polytechnic Inst., Troy, N. Y.).

Brief discussions of 2 papers on instrumentation for neutron cross section measurement are presented. The papers are the stored program data recorder and the multiplate Moxon–Rae detector development. (M.O.W.)

4247 (TID-21362) COMPACT PHOTOMULTIPLIER-TUBE BASE. Barna, Arpad; Boyarski, Adam (Stanford Linear Accelerator Center, Stanford Univ., Calif.). [Nov. 1964]. Contract AT(04-3)-400. 7p. Dep. mn; CFSTI $1.00 cy, $0.50 mn.

A small-size photomultiplier-tube base for the 6810A and 56AVP photomultiplier tubes was constructed. A schematic diagram is shown. The base operates on a negative high voltage of 0 to –3 kv. The dynode divider chain has a resistance of approximately 2.7 MΩ. Dynodes 10 to 14 are accessible via a multicontact connector for the connection of additional capacitors and/or voltage stabilization. (M.O.W.)

4248 (TID-22333) EXTENSION OF THE INTERNAL-EXTERNAL CONVERSION METHOD TO A LENS BETA-RAY SPECTROMETER BY MEASUREMENT OF THE 662 Kev CONVERSION LINE OF ^{137}Ba [Thesis]. Feuerbacher, John Larry (Vanderbilt Univ., Nashville, Tenn.). May 1965. Contract AT(40-1)-1087. 42p. Dep. mn; CFSTI $2.00 cy, $0.50 mn.

An experiment was performed in order to test the theoretical calculation of the correction factor f (conversion coefficient measurement) for the lens type of β-ray spectrometer for a different energy. The 662-kev transition in ^{137}Ba was used. The source used was ^{137}Cs. The magnetic lens spectrometer was used for the experiment. The results are included. (M.O.W.)

4249 (UCRL-16311) THREE TYPES OF 4π NEUTRON SPECTROMETERS. Wallace, Roger (Lawrence Radiation Lab., Univ. of California, Berkeley). Oct. 18, 1965. Contract W-7405-eng-48. 15p. (CONF-651109-8). Dep. mn; CFSTI $1.00 cy, $0.50 mn.

From 1st Symposium on Accelerator Radiation Dosimetry and Experience, Upton, N. Y.

Emulsion, liquid scintillator, and ^{3}He types of 4π neutron spectrometers are described. (J.F.P.)

4250 (UCRL-16446) SOME USES AND CHARACTERISTICS OF MOS TRANSISTORS FOR HEALTH PHYSICS APPLICATIONS. McCaslin, Joseph B. (Lawrence Radiation Lab., Univ. of California, Berkeley). July 1965. Contract W-7405-eng-48. 31p. (CONF-651109-6). Dep. mn; CFSTI $2.00 cy, $0.50 mn.

From 1st Symposium on Accelerator Radiation Dosimetry and Experience, Upton, N. Y.

Some of the characteristics of metal-oxide-semiconductor field-effect transistors (MOS), which may be useful in problems of radiation detection, are studied. It was found that these transistors are particularly suitable for electrometer applications. Input leakage currents of $\approx 10^{-16}$ A and transconductances of 750 μmhos are typical. Semi-guarded MOS's exhibit leakage currents near 10^{-18} A, but the transconductance is down to about 70 μmhos. The MOS, unlike its vacuum-tube counterpart, is a high-frequency device which is capable of operation in the nanosecond region. A fast BF_3 detector, pulse shaper, and line driver were constructed which produce pulses of 30 to 80 ns duration at half-maximum pulse height. This moderated BF_3 system was useful for fast-neutron monitoring at the Bevatron during rapid beam extraction. The sensitivity is 2 counts/n-cm^2. A 4π anticoincidence G-M foil counter was constructed with MOS's in digital circuitry. The saturated zero-time sensitivity for 2-in.-dia. 2-g indium foils is 21 counts/min per n/cm^2-sec. Background with 2 in. of lead is 21 counts/min. Static radiation damage tests were made in order to determine the suitability of MOS's in areas of high-level radiation such as target areas. Tests were performed with 7.5-Mev electrons in the range of absorbed dose from 10^4 through 10^8 rads, 7.5-Mev bremsstrahlung gammas at 10^6 rads, and an integrated thermal neutron exposure of 4×10^{14} n/cm^2. Data are presented that show postirradiation shifts in gate threshold voltage V_{GST}, d-c transconductance g_m, drain-source leakage current I_{DSS}, and gate leakage current I_G. Effects of radiation on the drain-source and gate-source breakdown voltages are also given. The predominant effect of ionizing radiation on these devices is a gradual upward shifting of the gate threshold voltage such that at 10^8 rads the required bias is ≈ -15 v instead of the preirradiated value of -4.5 to -5 v. Gate input leakage current is considerably increased to 10^7 rads and is unpredictable at 10^8 rads. These tests indicate that MOS transistors, although superior in most respects to conventional vacuum-tube electrometers, are more easily damaged by large doses of ionizing radiation. They must be shielded when used in areas of sustained high radiation intensity. (auth)

4251 (USNRDL-TR-917) CHARGED PARTICLE TRACKS IN POLYMERS. NUMBER 1. DELINEATION AND MEASUREMENT OF SUB-SURFACE TRACKS. Collver, M. M.; Benton, E. V.; Henke, R. P. (Naval Radiological Defense Lab., San Francisco, Calif.). Oct. 4, 1965. 20p.

A technique for the delineation of sub-surface charged particle tracks by a successive chemical removal of surface material is presented. A method of measuring the approximate range of heavily ionizing charged particles in polymers is given. The techniques are applied to the observation and measurement of low-energy ^{4}He-ion tracks in cellulose nitrate. (auth)

4252 (FTD-TT-64-1228) SOVIET INSTRUMENTS FOR STUDYING COSMIC RADIATION INTENSITY. Translated from Wojskowy Przegl. Latniczy, No. 4; 91(1964). 4p. CFSTI.

Special devices for studying the intensity of cosmic radiation such as Cherenkov counters for describing the number of lithium, beryllium, and boron nuclei encountered in cosmic space are described. Such devices are installed in Soviet satellites and cosmic ships. The results obtained in flight can be immediately transmitted to earth by radio and analyzed. (J.F.P.)

4253 PHOTOGRAPHIC STORAGE OF PULSE-HEIGHT INFORMATION IN SCINTILLATION EXPERIMENTS. Work, Richard N. (Pennsylvania State Univ., University Park). Amer. J. Phys., 33: 888-94(Nov. 1965).

A simplified arrangement is described for making gray wedge and two-dimensional coincidence pulse-height analyses. Examples of different types of spectra are given and application is made to an experiment on the Compton effect. (auth)

4254 ON THE REASONS OF WORK INSTABILITY OF G-M COUNTERS EXCITATION PULSES. Lesinski, J. Arch. Elektrotech., 14: 403-18(1965). (In Polish).

The reasons involving the appearence of excitation pulses in G-M counters are discussed. The mechanism of formation of excitation pulses as a result of exoemission from the cathode, chemical emission, and Malter effect are considered. (auth)

4255 STUDY OF A SPECTROMETER SENSITIVE TO WEAK TRANSVERSE STATIC FIELDS. Ribotta, Roland; Ottavi, Henri (Univ. Paris, Orsay, France). Compt. Rend., 261: 1670-3(Aug. 18, 1965). (In French).

An alternating field with some amplitude parallel to the static field on a liquid sample in flow was used. The resonance is caused by the introduction of a weak transverse static field. The intensity of the resonance signal was studied experimentally as a function of the amplitude of the alternating field for a given intensity of the transverse static field. The results obtained confirm satisfactorily the theoretical predictions. (tr-auth)

4256 CALCULATION OF DIFFERENTIAL FAST-NEUTRON SPECTRA FROM THRESHOLD-FOIL ACTIVATION DATA BY LEAST-SQUARES SERIES EXPANSION METHODS. Di Cola, G.; Rota, A. (C.C.R., Euratom, Ispra, Italy). Nucl. Sci. Eng., 23: 344-53(Dec. 1965).

The use of series expansion methods in treating threshold-detector activation data were analyzed. Normally the indiscriminate use of detectors having similar responses leads to unstable and ill-conditioned systems. The reasons for these deficiencies are determined and a new method for overcoming them is proposed. To make optimum use of the experimental data in obtaining a solution for the incident neutron spectrum, the series expansions coefficients are obtained through the Gauss method by solving a least-squares problem. A procedure, based on the Monte Carlo method, was set up to statistically study the effect of experimental input errors on the solution obtained. The most important results indicate that: any set of threshold detectors can be used independent of their cross-section shapes, the reliability increases as the number of detectors increases, and the reliability decreases when the number of series expansion terms increases. (auth)

4257 EXPANSION MECHANISM OF A 40 cm HYDROGEN BUBBLE CHAMBER OF JINR. Belonogov, A. V.; Dyachkov, E. I.; Zeldovich, A. G. (Joint Inst. of Nuclear Research, Dubna, USSR). pp 226-8 of Physics and Techniques of Low Temperatures. Prague, Publishing House of the Czechoslovak Academy of Sciences, 1964.

The design of the expansion mechanism is described. There are 55 liters of liquid hydrogen in the chamber. The purpose of this mechanism is to drive a periodic change of the hydrogen in the chamber into a metastable state. The mechanism must be capable of causing the expansion of liquid hydrogen in the chamber from 6 to 3 atmospheres in 8 to 15 milliseconds. Also at 3 atmospheres it must be able to hold a pressure plate and to compress liquid hydrogen to initial pressure. This expansion mechanism is of the bellows type and is shown at the moment when the chamber is in the compressed state. The operation of the mechanism is described. The differences in properties of the expansion mechanism from those of other such mechanism are also noted. (J.F.P.)

4258 IMPROVEMENTS IN OR RELATING TO RADIATION DETECTORS. Just, Richard; Waly, Adnan (to Specialty Electronics Development Corp.). British Patent 1,007,371. Oct. 13, 1965. Filed July 2, 1962.

A sensitive element for a dosimeter is composed of a

radio-photoluminescent phosphate glass square adapted to luminesce under ultra-violet radiation after exposure to x-ray or gamma radiation and a fritted coating formed of an opaque, non-reflecting, non-fluorescent material on one face of and three edges of the square. The phosphate glass is composed of a mixture of Ag, Ba, K, and Al metaphosphates, and the frit is composed of powdered glass mixed with metallic oxides. (B.L.M.)

4259 RADIATION MONITOR. Moncaster, Michael Edward; Northrop, David Covell; Raines, John Arthur (Services Electronics Research Lab.); Pretty, William Edward (to Admiralty Research and Development Services). British Patent 1,008,945. Nov. 3, 1965. Filed May 2, 1962.

A solid state radiation detector comprises a slice of a single crystal high resistivity Si having one of its opposite faces converted into a P-N junction and the other face into an ohmic contact by the diffusion into them of appropriate impurities. The slice is mounted and sealed in a metal capsule by attachment of one of the faces to the metal of the capsule constituting an external connection to the detector. If the slice is to serve as a gamma ray detector, the capsule is hermetically sealed around the slice by enclosing it with its ohmic contact face attached to the capsule and an insulated spring contact to the junction face as the other external contact. If the detector is to be used for charged particles, the slice is sealed at its junction face across an aperture in the capsule with the insulating spring contact bearing on the ohmic contact face. (B.L.M.)

4260 IMPROVEMENTS IN OR RELATING TO NEUTRON DETECTORS. Linguet, Roger; Rodier, Georges; Roger, Joel; Sagot, Marcel (to Commissariat a l'Energie Atomique). British Patent 1,008,966. Nov. 3, 1965. Priority date Dec. 15, 1961, France.

A process is described for the manufacture of a neutron detector composed of a sensitive layer of dysprosium oxide deposited on a metal or metal oxide upon a metal or metal oxide support. A mixture composed of dysprosium oxide, an adhesive, and a metal or metal oxide is sprayed at elevated temperatures on to a metal or metal oxide support. The surface of the support is sandblasted to roughen it before the mixture is projected onto it. (B.L.M.)

Radiation Effects

4261 (AD-623078) THE INFLUENCE OF TEMPERATURE ON RADIATION-INDUCED SURFACE EFFECTS IN TRANSISTORS. Ramstedt, C. F.; Zagorites, H. A.; Lee, D. Y. (Naval Radiological Defense Lab., San Francisco, Calif.). Aug. 5, 1965. 190p. (USNRDL-TR-885).

Tests were performed to determine the influence of junction temperature on radiation-induced surface effects in transistors. Sets of the germanium transistor types 2N526, 2N501A, 2N43A, and 2N599 and the silicon transistor type 2N329A were irradiated to an exposure of 13,100 R in controlled ambient temperatures of 0, 25, and 50°C while individual collector leakage current, common emitter current gain, and common emitter input impedance levels were measured. The responses were shown to be significantly dependent on junction temperature. Thermal annealing of radiation effects was observed. Post-irradiation recovery rates increased with temperature. (auth)

4262 (NP-15610) FLASHING LIGHT SATELLITE SYSTEM FOR SNAP RADIATION ENVIRONMENTS. Burnett, J. R.; Azary, Z.; Sandifer, C. W. (Edgerton, Germeshausen and Grier, Inc., Santa Barbara, Calif.). Jan. 1963. Contract AF19(628)-495. 45p. (S-227-R). CFSTI $2.00 cy, $0.50 mn.

A study of design modifications was performed on the EG&G Flashing Light Satellite System for reliable operation in a Space Nuclear Auxiliary Power (SNAP) nuclear radiation environment. Components found to be sufficiently radiation tolerant to the proposed SNAP environment are resistors, capacitors, and computer and rectifier diodes. Other components tested fell into an area of marginal radiation tolerance or were considered to have excessive degradation in the proposed radiation environment. Data are tabulated. (P.C.H.)

4263 (ORNL-TM-1320) EXPERIENCE WITH STAINLESS STEEL SHEATHED CHROMEL-ALUMEL THERMOCOUPLES IN IRRADIATED EXPERIMENTS. Trauger, D. B. (Oak Ridge National Lab., Tenn.). Nov. 12, 1965. Contract W-7405-eng-26. 5p. Dep. mn; CFSTI $1.00 cy, $0.50 mn.

Experience with type-304 stainless steel-clad Chromel-Alumel thermocouples in the conduction of the EGCR fuel irradiation program, other gas-cooled experiments, and some other programs having similar thermocouple applications are reviewed. All thermocouples included were insulated by packed MgO. Data are tabulated. (P.C.H.)

4264 EQUIVALENCE OF STRESS- AND RADIATION-INDUCED DEFECTS IN DEGENERATE p-n JUNCTIONS. Rindner, W.; Roth, H.; Bernard, W. (Raytheon Research Div., Waltham, Mass.). J. Appl. Phys., 36: 3625-7(Nov. 1965).

Excess current, irreversibly introduced by inhomogeneous stress in germanium tunnel diodes, has been found to be annealable by the application of suitable forward bias in a manner analogous to that in the case of electron-irradiated tunnel diodes. Thermal and voltage-anneal characteristics of radiation- and stress-induced excess currents were studied over a temperature range from 4.2° to 300°K. Strong similarities in the voltage-anneal characteristics, as well as certain common features of the thermal anneals, suggest that the electrically active defects introduced by electron-irradiation and by inhomogeneous stress may be of a similar nature. (auth)

4265 THE INFLUENCE OF NUCLEAR RADIATION ON THE ELECTRICAL PROPERTIES OF SEMICONDUCTOR PARTS [Thesis]. Zander, K. Berlin, Tech. Univ., 1964. 149p. $2.00 Gmelin, AED-DISS. 64-745.

The properties of diodes and transistors are influenced more by radiation with fast particles if the original doping is small. In most cases decay times of semiconductor circuits are smaller after irradiation. (Gmelin Inst.)

4266 RADIATION EFFECTS IN ELECTRONICS. ASTM Special Technical Publication No. 384. Presented at a Joint Meeting of ASTM Committee E-10 on Radioisotopes and Radiation Effects and the Niagara-Finger Lakes Section of the American Nuclear Society Syracuse, N. Y., Oct. 5-7, 1964. Philadelphia, American Society for Testing and Materials, 1965. 236p. $5.00. (CONF-641009).

Twelve papers are included; separate abstracts were prepared for 3. Nine papers were previously abstracted for NSA; see 19: 13816, 13818, 13819, 15941, 16833, 18554, 22815, 25754, and 28814. (L.B.S.)

For abstracts of individual papers see: 4035, 4036, and 4267.

4267 INFLUENCE OF OPERATING CONDITIONS ON RADIATION DAMAGE TO TRANSISTOR GAIN. Frank, Max; Taulbee, C. D.; Chambers, H. L. (Bendix Research Labs. Div., Southfield, Mich.). pp 172-97 of Radiation Effects in Electronics. ASTM Special Technical Publication No. 384. Philadelphia, American Society for Testing and Materials, 1965.

Gain degradation rates were obtained for various transistor operating conditions of current and voltage during ^{60}Co irradiation and compared with the degradation rate for a radiation exposure in the passive state. The effects of emitter current alone, collector voltage alone, and normal transistor operating modes were studied. The results showed that increasing levels of carrier injection from the emitter caused decreasing rates of damage. For a 2N1613 type silicon transistor, the maximum reduction observed was approximately a factor of 2. This behavior is believed to be due to an alteration of the charge state of the radiation induced defect at the time the defect is formed. A lesser dependency with collector voltage was also observed. The effects of temperature in the range 105°F to 140°F, during gamma irradiation, were found to be small in comparison with the effects of active-passive current variations. Tests conducted in a neutron environment, where normal transistor operating modes were compared with the passive irradiation state, indicated very little influence upon damage rate. (auth)

ISOTOPE TECHNOLOGY

General

Refer also to abstract 5152.

4268 (ORNL-IIC-5, pp 353-73) GENERATION AND PRACTICAL USE OF MONOENERGETIC X RAYS FROM ALPHA-EMITTING ISOTOPES. Sellers, Bach; Ziegler, C. A. (Parametrics, Inc., Waltham, Mass.).

The various methods of generating x radiation by ejection of orbital electrons through the interaction of radioactive particles and gamma rays with materials are summarized. Excitation by beta particles produces, in addition to monoenergetic characteristic radiation, a large quantity of continuous bremsstrahlung. In many situations this bremsstrahlung is an undesirable background and must be removed. The use of alpha particles to excite characteristic radiation alleviates this problem, since the bremsstrahlung produced by such massive particles is not of practical concern. Therefore, with alpha-emitting isotopes, it is possible to make essentially monoenergetic x-ray sources that would have important application in areas such as composition analysis, density and thickness measurement, and absorption-edge microradiography. Theoretical and experimental results on the x-ray yield of such sources are presented, and these yields are shown to be consistent with those observed by others using proton excitation. (auth)

4269 [BULK CALIBRATION OF ^{99m}Tc ELUATE FROM BNL ^{99}Mo COW]. Murano, Robert; Nelp, Wil B. (Univ. of Washington, Seattle). J. Nucl. Med., 6: 610-12 (Aug. 1965).

A method for bulk calibration of the ^{99m}Tc eluate from the BNL ^{99}Mo cow is presented, which does not require the preparation of aliquots, employs simple electronics, and uses a low-energy ^{57}Co source as a comparator for calibration. (H.G.D.)

4270 INDUSTRIAL APPLICATIONS OF RADIATION. Clouston, J. G. (Australian Atomic Energy Commission). pp 93-110 of Atomic Power: A Review. Kensington, N. S. W., Univ. of New South Wales [1964].

Radiation sources are discussed from the standpoints of production, economics, and safety. Applications in such things as polymer modification, chemical synthesis, radiosterilization, food preservation, and power sources are reviewed, and future trends are considered. (J.F.P.)

Industrial Applications

Refer also to abstracts 3685, 3710, 4114, and 4219.

4271 (WASH-1063) WORLD OUTLOOK FOR FOOD IRRADIATION. Weiss, F. J. (Library of Congress, Washington, D. C. Science and Technology Div.). [1964]. 9p. (CONF-639-4). Dep. mn; CFSTI $1.00 cy, $0.50 mn.

From 24th Annual Meeting of the Institute of Food Technologists, Washington, D. C., May 1964.

Developments in radiosterilization of food and their impact on the world food situation are discussed. (P.C.H.)

4272 (JPRS-32813) IRRADIATION POSSIBILITIES IN THE 2 KILOCURIE ^{60}Co RADIATION UNIT AT THE BORIS KIDRIC INSTITUTE AT VINCA. Draganic, Zorica; Kosanic, Miroslav. Translated from Tehnika (Belgrade), 20: 1852-7(Oct. 1965). 13p. (TT-65-33391). CFSTI $1.00 cy, $0.50 mn.

The design and possible uses of the 2 kC ^{60}Co radiation unit are discussed. Efforts toward industrial application of strong sources of radiation in various areas, including radiation chemical synthesis, polymerization and improvement of the properties of polymers, vulcanization of natural and synthetic rubbers, food conservation, and sterilization of drugs and medical equipment are mentioned. (P.C.H.)

4273 SOME NEW IDEAS IN APPLICATION OF RADIOISOTOPES FOR MEASURING THICKNESS AND DENSITY. Faudrowicz, Adam; Gierdalski, Jerzy. Nukleonika, 10: 513-16(1965).

A self-compensation system for stabilizing measurements of thickness or density using radioisotopes. Detector gain variation with temperature and voltage is compensated. (M.C.G.)

4274 ANWENDUNG RADIOAKTIVER ISOTOPE IN DER TEXTILFORSCHUNG UND -TECHNIK. Symposium des Bundesministers fuer Wissenschaftliche Forschung in Lindau im Bodensee, 8. bis 10. Juli 1964. (Uses of Radioactive Isotopes in Textile Research and Industry. Symposium of Federal Ministers for Scientific Research, Lindau/Bodensee, July 8-10, 1964). Schmidt-Kuester, W. J.; Weisner, L. Thiemig-Taschenbuecher. Band 9. Munich, Verlag Karl Thiemig KG, 1964. 310p. (CONF-640707).

Seventeen papers presented at the Symposium of Federal Ministers for Scientific Research on Uses of Radioactive Isotopes in Textile Research and Industry are given. Separate abstracts were prepared for four papers. Two papers were previously abstracted in NSA and appeared as abstracts 20: 238 and 358. (M.C.G.)

For abstracts of individual papers see: 4031–4034.

4275 RADIOAKTIVNYE PRIBORY, IKH PRIMENENIE V PROMYSHLENNOSTI. (Radioactive Instruments—Their Application in Industry). Fedorko, Yu. P.; Stepanovich, A. S. Kishinev, Gosizdat "Kartya Moldovenyaske," 1964. 166p.

The principal properties of nuclear radiation are reviewed. Uses of radioisotopes in instruments and radiation sources for industrial applications are discussed. The characteristics of some industrial instruments are described. Methods of determining the economic efficiency of using instruments with radioactive elements are presented and recommendations for their use are given. (M.C.G.)

Power Application

***See also* ENGINEERING — Space Propulsion**

4276 (AGN-8128) RISE. RADIOISOTOPE SUBMERSIBLE ENGINE. Buck, K. E. (Aerojet-General Nucleonics, San Ramon, Calif.). Jan. 7, 1965. Contract AT(04-3)-368. 98p. Dep. mn; CFSTI $3.00 cy, $0.50 mn.

The investigation and evaluation of potential radioisotope applications was broken down into five separate phases: an application survey; design analysis of radioisotope equipment for the potential applications; a comparison of parameters of radioisotope and other types of power systems capable of accomplishing the same objective; a compilation of attractive radioisotope applications; and a projection of future radioisotope use in hydrospace. At the completion of the survey phase it was apparent that there was significant interest in the use of radioisotopes as power sources to propel small submersible vehicles and as power sources for stationary underwater platforms. As a result, a considerable amount of the total effort on the design analysis and parameter comparison phases was spent in this area. (auth)

4277 (DP-1012) RADIOACTIVE COBALT FOR HEAT SOURCES. Joseph, J. Walter Jr.; Allen, Harvey F.; Angerman, Carl L.; Dexter, Arthur H. (Du Pont de Nemours (E. I.) and Co., Aiken, S. C. Savannah River Lab.). Oct. 1965. Contract AT(07-2)-1. 36p. Dep. mn; CFSTI $2.00 cy, $0.50 mn.

A program is in progress to develop the required data for the application of ^{60}Co with a high specific activity (curies of ^{60}Co per gram of product) for use in multikilo-

watt heat sources. The penetrating radiation of cobalt-60 is converted to usable heat with good efficiency in compact, high-strength sources, and in such sources the ratio of shielding weight to contained activity is kept small. Pertinent data on natural and radioactive cobalt are presented as background information. (P.C.H.)

4278 (MND-P-2229) CONCEPTUAL DESIGN [OF A] 100-WATT THERMOELECTRIC GENERATOR. ADVANCED SNAP TECHNOLOGY SUB-TASK 5.7. Preliminary Heat Transfer Analysis. Jicha, J.; Peiffer, M. (Martin Co., Baltimore, Md. Nuclear Div.). Nov. 1959. Contract AT(30-3)-2217. 42p. Dep. mn; CFSTI $2.00 cy, $0.50 mn.

A conceptual design of a radiative type thermoelectric generator powered by Curium-242 for the following SNAP VII design criteria; 100 electrical watts flat output, 225 days life, and 28 volts is discussed. Shielding requirements for the fast neutrons encountered with Cm_2O_3 form the basis of design since the biological shield is wholly contained for the unit studied. The shielding calculations were carried out by both the Albert-Welton kernel method and the moments method for neutron attenuation in water. A dose of one rem is received at the unit's surface when 8¾ inches of shielding is employed. Thermoelectric calculations were carried out by optimizing the segmentation temperature for both the N and P elements at hot and cold junction temperatures of 1000°F and 305°F, respectively. The resulting unit has a thermoelectric efficiency of 6.59% and an overall efficiency of 5.16% as given by 3M's data for PbTe elements. The hot junction temperature of 1000°F is maintained constant by means of a thermal shutter. The overall size and weight (130 lbs) of the unit indicates that weight loss will be realized if all or part of the biological shield is mounted outside the unit. This can be readily accomplished since the shield is light and the resultant unit relatively compact. (auth)

4279 (ORNL-TM-1177) ^{147}Pm—RADIATION MEASUREMENTS OF A ONE-WATT, PROTOTYPE HEAT SOURCE. O'Brien, H. A. Jr.; Box, W. D. (Oak Ridge National Lab., Tenn.). Nov. 1965. Contract W-7405-eng-26. 18p. Dep. mn; CFSTI $1.00 cy, $0.50 mn.

Measurements of dose rates and bremsstrahlung spectrum of a 2763-curie, aged, $^{147}Pm_2O_3$ heat source were made under varying conditions. The ratio of ^{146}Pm to ^{147}Pm was measured and found to be 3.7×10^{-7}. (auth)

4280 (SC-DC-65-1601) AERO HEATING RESULTS FROM THE RFD-2 FLIGHT TEST. Clark, A. J. Jr. (Sandia Corp., Albuquerque, N. Mex.). Oct. 8, 1965. Contract AT(29-1)-789. 16p. (CONF-651101-37). Dep. mn; CFSTI $1.00 cy, $0.50 mn.

From 13th Conference on Remote Systems Technology, Washington, D. C.

The Re-entry Flight Demonstration No. 2 test was conducted to study the response of the isotopic generator during the re-entry portion of the flight. The primary objective of this flight test was to study generator disassembly and fuel capsule burnup as a result of re-entry heating. Data obtained by thermocouple measurements are presented. (M.O.W.)

Separation and Production

See also CHEMISTRY — Separation Processes and Procedures

Refer also to abstract 4277.

4281 (IAE-926) STATICHESKIE KHARAKTERISTIKI STABILIZATORA NAPRYAZHENIYA ELEKTROMAGNITNOGO SEPARATORA IZOTOPOV. (Static Characteristics of the Voltage Stabilizer in an Electromagnetic Isotope Separator). Naftulin, S. M. (Institut Atomnoi Energii, Gosudarstvennyi Komitet po Ispol'zovaniyu Atomnoi Energii SSSR, Moscow). 1965. 12p. Dep. mn.

The circuit for a high-voltage stabilizer in an electromagnetic separator for isotope separation with voltage 40 kv and load current about 1 amp is presented. An accuracy of stabilization on the order of 2×10^{-4} was obtained. An analysis of static characteristics was carried out to determine the effect of various perturbing influences on the stabilized voltage and to determine the parameters of the elements of the system. A stabilization coefficient $K_{st} = 3700$ was obtained. The time for control of the transition process of the stabilizer voltage for a spark probe in the ion source is 6×10^{-4} sec. (tr-auth)

4282 (ORNL-3861) REVIEW OF ORNL ELECTROMAGNETIC SEPARATIONS PROGRAM. Love, L. O.; Bell, W. A. (Oak Ridge National Lab., Tenn.). Nov. 1965. Contract W-7405-eng-26. 47p. Dep. mn; CFSTI $3.00 cy, $0.50 mn.

A review is presented on ion source and receiver development, 180° sector studies, vacuum and contamination studies, isotope recovery, ion implantation, and new equipment for radioisotope applications. (P.C.H.)

4283 (SGAE-PH-27/1965) OPERATING EXPERIENCE WITH THE SEIBERSDORF INHOMOGENEOUS SECTOR FIELD ISOTOPE SEPARATOR. Formann, E.; Hechtl, E.; Lugmair, G.; Ruedenauer, F.; Viehboeck, F. P.; Wotke, H. (Oesterreichische Studiengesellschaft fuer Atomenergie G.m.b.H., Seibersdorf). [1965]. 13p. Dep. mn.

The Seibersdorf Electromagnetic Isotope Separator was used during the last 3 years for focused ion currents between 10^{-14} and 5.10^{-3} amp. The work in the low current region concerned investigations on high temperature reactor fuel particles for nuclear spectroscopy. Targets of radioactive isotopes were produced using total ion currents in the order of 100 μamp. For neutron cross section measurements in the rare earth region stable isotopes were separated at ion currents up to 5 mamp. (auth)

4284 (CEA-tr-X-617) ISOTOPES NATURELS. III. CASCADE DE SEPARATION. QUELQUES PROBLEMES D'ECONOMIE ET DE GENIE. (Natural Isotopes. III. Cascade Separation. Some Problems of Economy and of Engineering). Selecki, A. Translated into French from Przemysl Chem., 40: 626-31(1961). 20p. Dep. mn; JCL $1.60 fs, $0.80 mf.

In the design of an industrial separation cascade, numerous and diverse cost elements must be taken into consideration, some of which depend on technical conditions of the design and others depend on the parameters of the cascade and the process. The cost per unit of enrichment in the product, expressed as a sum of the amortization cost and the exploitation cost of the installation, are considered. (J.S.R.)

4285 ISOTOPE SEPARATION BY CONCURRENT GAS CENTRIFUGE. Kanagawa, Akira; Takashima, Yoichi (Tokyo Inst. of Tech.). Bull. Tokyo Inst. Tech., No. 61, 43-50(Dec. 1964).

The development of the gas centrifuge in Japan is described. Experiences suggested that the simplification of the centrifuge by using the concurrent type instead of the countercurrent type may be essential, as some mechanical and material problems still exist unsolved. The separation performance of the concurrent type consisting of more than two streams was calculated and the results showed that three streams can give a little better performance than two streams. (auth)

MATHEMATICS AND COMPUTERS

4286 (ANL–7054) COLLECTED ALGORITHMS 1960–1963 FROM THE COMMUNICATIONS OF THE ASSOCIATION FOR COMPUTING MACHINERY. Grench, R. E.; Thacher, H. C. Jr. (comps. and eds.) (Argonne National Lab., Ill.). July 1965. Contract W-31-109-eng-38. 165p. Dep. mn; CFSTI $5.00 cy, $1.00 mn.

The first 220 algorithms previously published in the Communications of the Association for Computing Machinery are included with remarks and certifications pertaining to them. A tutorial description of the ALGOL language was also reprinted. (M.O.W.)

4287 . (EUR–2519.e) SAHYB (SIMULATION OF ANALOGUE AND HYBRID COMPUTER): A GENERAL PURPOSE PROGRAMME FOR THE SOLUTION OF INITIAL AND BOUNDARY VALUE PROBLEMS. D'Hoop, H.; Monterosso, R. (European Atomic Energy Community, Ispra (Italy). Joint Nuclear Research Center. European Atomic Energy Community, Ispra (Italy). European Scientific Data Processing Center). 1965. 54p. Dep. mn.

The purpose of the SAHYB (Simulation of Analog and Hybrid computer) program is to concentrate in one subroutine an initial value problem, and in two subroutines a boundary value problem. The other subroutines handle the following operations: output; modification of integration and/or print-out; interpolation of tabulated functions; fixed or variable delays; and plot of curves on CALCOMP plotter. SAHYB is designed to be used by physicists or engineers who are not specialists in programming. Moreover, since it is written in FORTRAN and FAP, it can be modified and adapted to special cases. SAHYB is an easy way to obtain digital solutions to be compared with analog results. (auth)

4288 (SC-DR-65-312) A DIGITAL COMPUTER PROGRAM FOR THE SIMULATION OF SAMPLED DATA SYSTEMS. Phaklides, G. D. (Sandia Corp., Albuquerque, N. Mex.). Sept. 1965. Contract AT(29-1)-789. 41p. Dep. mn; CFSTI $2.00 cy, $0.50 mn.

The Sampled Data Simulator is a program written for the Control Data Corporation 3600 computer. The program simulates a fixed-frequency sampling and reconstruction system. Program options, system specifications, and a digitized input waveform are supplied by the user. Simulation results are presented in both printed and plotted forms. No computer experience is required to use the program. (auth)

4289 (SC-DR-65-318) DIGITAL COMPUTER SIMULATION AS AN EXPERIMENTAL TOOL IN THE EVALUATION OF SAMPLED-DATA SYSTEMS. Andreas, R. D. (Sandia Corp., Albuquerque, N. Mex.). Nov. 1965. Contract AT(29-1)-789. 21p. Dep. mn; CFSTI $1.00 cy, $0.50 mn.

The problem of determining the accuracy of an instrumentation system which acquires a periodically sampled representation of an analog time function is an important but difficult step in the evaluation of alternative systems during system design. The basic aspects of the problem are described, a lack of available theoretical tools to attack the problem is pointed out, and thus digital computer simulation is offered as an experimental tool. (auth)

4290 (UCRL–14360, pp 94-7) MATHEMATICAL AND COMPUTATIONAL METHODS. (Lawrence Radiation Lab., Univ. of California, Livermore).

A program was written which will calculate, from a given metric tensor, Christoffel symbols of the first and second kind; and a program was developed for performing algebraic manipulations. The treatment of field theory on a computer was considered, and a FORTRAN code optimizer was developed for the CDC-6600. (D.C.W.)

4291 (UCRL–14425) PLOT3D: A FORTRAN SUBROUTINE FOR THREE-DIMENSIONAL PLOTTING. McCall, John R.; Gumm, Barbara (Lawrence Radiation Lab., Univ. of California, Livermore). Sept. 10, 1965. Contract W-7405-eng-48. 27p. Dep. mn; CFSTI $2.00 cy, $0.50 mn.

A FORTRAN II subroutine for computer-controlled plotting of three-dimensional surfaces on peripheral cathode ray tube equipment is presented. The technique, required subroutines, and method of use are discussed. (auth)

4292 (UCRL–14427-T) CRT PLOTTING ROUTINES IN USE AT LRL-LIVERMORE. Ford, Judith D.; Welsh, Marilyn J. (Lawrence Radiation Lab., Univ. of California, Livermore). Aug. 1965. Contract W-7405-eng-48. 112p. CFSTI $4.00 cy, $0.75 mn.

A system of cathode ray tube plotting routines is described. These FORTRAN routines provide a flexible package for point, line, and character plotting via a data display model dd80C. (auth)

4293 THE LAPLACE TRANSFORM OF A PRODUCT OF TWO WHITTAKER FUNCTIONS. Olsson, Per O. M. (Royal Inst. of Tech., Stockholm). Arkiv Fys., 28: 113-20(1965).

The Laplace transform of the product of two Whittaker functions is expressed in various functions connected with Appell's hypergeometric function F_2. Results are obtained for very rapid oscillation of one or both of the Whittaker functions. (auth)

4294 A METHOD FOR COMPUTING $\int_{-1}^{1} dx P_k^l(x) P_n^m(x)$. Pomraning, G. C. (General Atomic Div., General Dynamics Corp., San Diego, Calif.). Nucl. Sci. Eng., 23: 395-7(Dec. 1965).

A set of recurrence relations is derived for calculating $Q_{nm}^{kl} \equiv \int_{-1}^{1} dx P_k^l(x) P_n^m(x)$ for all values of the indices. (L.B.S.)

4295 THE HIGHER ORDER VIRIAL EQUATIONS AND THEIR APPLICATIONS TO THE EQUILIBRIUM AND STABILITY OF ROTATING CONFIGURATIONS. Chandrasekhar, S. (Univ. of Chicago). pp 1-72 of Lectures in Theoretical Physics. Vol. VI. Boulder, Colo., The University of Colorado Press, 1964.

In describing and developing the method of the virial the emphasis is on illustrating the usefulness of the method by applying it to the solution of certain concrete problems rather than on presenting the method in its most general framework. Topics considered are virial equations of the various orders, for uniformly rotating systems, potentials and superpotentials of homogeneous ellipsoids, and the Maclaurin and Jacobian sequences for equilibrium of rotating homogeneous masses. Other topics are the points of bifurcation along the Maclaurin and the Jacobian sequences, and the stability of the Maclaurin spheroids. (J.F.P.)

4296 PROCEEDINGS OF THE FOURTH NATIONAL CONFERENCE, UNIVERSITY OF OTTAWA, MAY 11, 12, 1964. THEME—COMPUTERS: THE CHALLENGE OF THE FUTURE. The Computing and Data Processing Society of Canada, 4th Conference, 1964. Toronto, University of Toronto, 1964. 68p. $5.00. (CONF-640510).

The general aspects of computer science are considered. These include automation and information retrieval advantages, some of the techniques used in the implementation of the Algol 6000 computer language, a description of a fully automatic film reading system which is capable of scanning medical roentgenograms, detecting the presence of important patterns and radiological masses, and providing the outputs. Other topics are the information content of various biological phenomena, and a duel digital computer system description for high-control reliability for a nuclear reactor. (J.F.P.)

METALS, CERAMICS, AND OTHER MATERIALS

General

Refer also to abstracts 4077, 4999, and 5181.

4297 (IS–1200(Sect. M)) METALLURGY DIVISION. (Ames Lab., Iowa State Univ. of Science and Tech.). 108p.

Research and development are reported in sections on metal preparation and purification, phase equilibria and thermodynamic properties, plastic deformation of alloys, solid state metallography, and separation methods. (J.R.D.)

4298 (LA-DC–7275) AN ARC SPRAY POWDER FEEDER FOR ULTRA-FINE PARTICLES WITH A WIDE RANGE OF DENSITIES. Bradley, Edward L.; Stoddard, Stephen D. (Los Alamos Scientific Lab., Univ. of California, N. Mex.). [1964]. Contract W-7405-eng-36. 15p. (CONF-651018–3). Dep. mn; CFSTI $1.00 cy, $0.50 mn.

From Joint Electronics Fall and 8th Pacific Coast Regional Meeting, Los Angeles.

The results of efforts directed toward designing and building a powder feeder capable of effectively feeding submicron particles of a wide range of densities into a plasma arc spray gun are described. A number of powder feeder designs were tried unsuccessfully. However, the rotating brush powder feeder was found to allow effective feeding and arc spraying of ultrafine particles of widely varying densities, such as 3.9 to 19.3 g per cc. Other advantages of this feeder are also discussed. (P.C.H.)

4299 (ORNL–2711) AIRCRAFT NUCLEAR PROPULSION PROJECT SEMIANNUAL PROGRESS REPORT FOR PERIOD ENDING MARCH 31, 1959. (Oak Ridge National Lab., Tenn.). May 5, 1959. Contract W-7405-eng-26. 162p. Dep. mn; CFSTI $5.00 cy, $1.00 mn.

Developmental studies on a pilot plant scale of methods for the production of high-purity yttrium metal were continued. Numerous alloys of niobium with small amounts of Zr, Be, and rare earth metals were prepared to test the effects of these additions in stabilizing dissolved oxygen in the niobium. The reaction rates of oxygen with niobium at low pressures and at temperatures of 850 and 1000°C were investigated. Extrusion billets of niobium clad with type 446 stainless steel and Nb and Mo clad with aluminum bronze were prepared. Corrosion studies on Nb, 316 stainless steel, and TiC base cermets in lithium are reported. The solubility of lithium oxide in lithium was determined for the temperature range 250 to 400°C. Welding of Nb sheet and plate was studied. Techniques were developed for tensile tests of Nb in the temperature range 1800 to 2000°F in an inert atmosphere. A method for obtaining pure BeO by calcining beryllium oxalate was tested. A phase diagram for the $LiF-YF_3$ system was constructed. Studies were made of the process for obtaining oxygen-free $LiF-MgF_2-YF_3$ mixtures for reduction to Y–Mg alloys. An apparatus was set up for lithium metal purification. Methods of analysis were developed for samples from the steps in the production of yttrium. The I_0 of a grown-junction, single-crystal silicon diode was measured as a function of reciprocal temperature before and after irradiation. Tube burst tests of Inconel in air in the MTR and the ORR at a temperature of 1500°F indicate that irradiation reduced the time to rupture. The oil-lubricated pump rotary element that was operated in the MTR canal was disassembled and inspected. Another test was completed in the investigation of the thermal stability of thin metal shells. Studies of the effect of thermal-stress cycling on structural materials were continued with the pulse-pump system. An experimental system for determination of the local heat transfer coefficients for molten lithium was completed. Several thermocouple metals and insulating materials were tested for compatibility in He. Studies were carried out on the elastic behavior of cylindrical shells and of tapered circular plates. Advanced power plant design studies are summarized. Various codes for shielding theory use are described. Predictions of the thermal fluxes to be expected near the BSR were made on the basis of LTST data transformed to the BSR geometry. Dose rates from ^{8}Li in some of the Pratt and Whitney Aircraft systems were computed. An investigation is under way at the LTSF to determine the thermal flux depression in a medium caused by the presence of a gold-foil detector. Fabrication of the grid plate and the fuel elements for the BSF stainless steel clad UO_2-fueled reactor BSR-II is nearing completion. The cross section for the reaction $^{6}Li(n,\alpha)^{3}H$ was measured at 1.2 to 8.0 Mev. Data from the prompt gamma spectrum of ^{235}U thermal fission were analyzed. The 2π experiments performed by GE at the TSF two years ago were checked and extended by ORNL. The subcriticality of the TSR-II is discussed. (W.D.M.)

4300 (ORNL–3870) METALS AND CERAMICS DIVISION ANNUAL PROGRESS REPORT FOR PERIOD ENDING JUNE 30, 1965. Peterson, Sigfred (comp. and ed.) (Oak Ridge National Lab., Tenn.). Nov. 1965. Contract W-7405-eng-26. 345p. Dep. mn; CFSTI $7.00 cy, $1.75 mn.

Separate abstracts were prepared for the 34 sections of the report. (W.L.G.)

For abstracts of individual sections see: 3919–3921, 4110, 4301–4309, 4320–4223, 4342, 4343, 4384–4391, 4460, 5006, 5024, 5126, and 5173–5175.

4301 (ORNL–3870, pp 102-35) HIGH-TEMPERATURE MATERIALS. Thurber, W. C.; Harms, W. O. (Oak Ridge National Lab., Tenn.).

Progress in the fabrication of refractory metals and alloys included experiments on the extrusion of W and W–26% Re tube shells, use of flow turning to fabricate tubing, simplification of the fabrication of electrodynamic pump cells, development of welding techniques, improvement of welds, development of brazed joints stable well above the brazing temperatures, and fabrication of loops and other hardware for testing compatibility with alkali metals. Properties of high-temperature metals studied include the equilibrium and kinetics of nitrogen sorption by Nb–1% Zr, aging and recrystallization of the alloy D-43, vacuum evaporation of constituents of refractory alloys, annealing behavior of the alloy T-111, effect of cold working and annealing on creep of Nb–1% Zr, prediction of creep and rupture under variable stress, creep of refractory alloys and strengthening of these alloys by carburization, the state of oxygen in Ta-base alloys, the resistance of refractory alloys to molten K and Li, some physical properties of W, including thermal conductivity from 50 to 1000°C, emittance of Nb–1% Zr and its improvement by surface treatment, and thermal conductivity of D-43 and T-111. (auth)

4302 (ORNL–3870, pp 155-63) TUNGSTEN METALLURGY. Thurber, W. C.; Harms, W. O. (Oak Ridge National Lab., Tenn.).

High-purity tungsten sheet was thermochemically deposited on a partially sintered molybdenum mandrel. Deposition conditions were investigated to enable successful deposition of new shapes without extensive empirical adjustment of the deposition parameters. After annealing at 1000°C, thermochemical tungsten was as strong as and more ductile than recrystallized wrought powder-metallurgy tungsten. The causes of low-temperature brittleness in tungsten were investigated and it was found that a hydrostatic prestrain improves ductility. Promising joining methods for tungsten include brazing with alloys that contain a fugitive melting-point depressant, fusion with stress relief, and thermochemical deposition of weld metal at temperatures too low to em-

brittle the base metal. Creep of thermochemical tungsten was similar to that of wrought material. (auth)

4303 (ORNL–3870, pp 164-70) URANIUM NITRIDE. Harms, W. O.; Thurber, W. C. (Oak Ridge National Lab., Tenn.).

Research and development on uranium nitride as a nuclear fuel for high-temperature reactors with high power densities included studies of sintering kinetics and pellet fabrication, nitrogen solubility, the effect of carbon on the solubility of oxygen, relation of microstructure to the properties of sintered material, and fission-gas release by neutron activation. Pertinent data and interpretations are presented. (auth)

4304 (ORNL–3870, pp 171-83) ZIRCONIUM METALLURGY. Picklesimer, M. L. (Oak Ridge National Lab., Tenn.).

The texture of the matrix had little effect on the orientation of hydride precipitated during cooling in unstressed fully annealed Zircaloy-2. Plastic deformation caused the hydride plates to form parallel to the tensile strain component. Hydride precipitated under elastic stress redistributed only when the tensile stress axis was parallel to a high concentration of basal poles. The redistribution of hydride increased as the stress increased. A technique was developed for rapidly determining, by quantitative metallography, the pole figure of hydride plates in Zircaloy-2 and the crystallographic basal pole figure in close-packed hexagonal metals. Sheet tensile specimens could not be used to characterize the three-dimensional anisotropy of Zircaloy-2. The location of the neck could be determined immediately after yielding, and the position of the neck shifted during its formation and growth. An extrapolation of the octahedral shear stress theory predicted that the shapes of the yield loci for Zircaloy-2 in biaxial stress are elongated ellipses. This indicates that for certain conditions of biaxial stress encountered in service, the maximum permissible design stress can be increased by at least 50% by controlling the orientation of the texture relative to the applied stress geometry. Blistering encountered in fuel element cladding can probably be lessened by use of cladding material having a certain texture. An apparatus was built for studying the strain anisotropy of Zircaloy-2 tubing in biaxial stress which allows simultaneous application of axial stress, torsional stress, and internal pressure. The indices of refraction of anodized oxide films on zirconium decreased when they were stripped from the metal, indicating that the film in situ is strained. Similar measurements made on irradiated films showed that neutron doses up to 10^{19} neutrons/cm^2 did not produce defects that could be detected by such techniques, nor would they appreciably affect the rate of dissolution of the oxide in the base metal at 600°C. Such dissolution caused a strong absorption of light and caused the base metal to be strongly attacked through the oxide film by a stripping solution. Zone refining and single crystal production was demonstrated in ¾-in.-dia as-deposited iodide zirconium bar. Recrystallization of cold-worked zone-refined zirconium was detected at 150°C and was almost complete in 100 hr at 175°C. The recrystallization behavior of material at the head differed from that at the center of a zone-refined bar, although the impurity contents did not differ more than 50 ppM total. The interference color pattern developed by an oxide film on a single-crystal sphere of zirconium showed very graphically the variation of oxidation rate with crystallographic direction. The rate at 350°C in dry air was the highest on the basal plane, the $(10\bar{1}0)$ plane, and in a band near the $(20\bar{2}1)$, $(11\bar{2}1)$, and $(11\bar{2}2)$ planes. (auth)

4305 (ORNL–3870, pp 187-90) ARMY REACTORS PROGRAM. Adamson, G. M. Jr. (Oak Ridge National Lab., Tenn.).

Europium molybdate, a promising control or poison material, exists in two forms depending on cooling rate. Both have good corrosion resistance and are compatible with stainless steel. Fuel elements fabricated for PM-1 and PM-3A reactors were examined visually, radiographically, dimensionally, and metallographically to determine realistic tolerances. (auth)

4306 (ORNL–3870, pp 194-213) GAS-COOLED REACTOR PROGRAM. Harms, W. O.; Coobs, J. H. (Oak Ridge National Lab., Tenn.).

In-reactor testing of moderator graphite at temperatures of 150 to 350°C showed that irradiation-induced creep is consistent with a theoretical model and enables graphite to accommodate much greater strains without fracturing. The effects of specific methane flow rate and deposition temperatures from 1300 to 2000°C on the anisotropy, density, and crystallite size of pyrolytic-carbon coatings on fuel particles were determined. These three properties along with diamagnetic susceptibility were used to characterize bulk pyrolytic carbon deposited on static substrates. The effects of these structural properties on the diffusion of thorium in pyrolytic graphite were investigated. The thermal stability of pyrolytic-carbon-coated oxide fuel particles was demonstrated, and specimens were prepared that showed excellent behavior under irradiation. Irradiation experiments to test mathematic simulation of coated-particle behavior were initiated. Factors affecting the impact resistance of fueled-graphite spheres were studied and the results of irradiation experiments on such spheres analyzed. The thermal conductivity of fueled graphite is unaffected by irradiation, but differential neutron-induced shrinkage of fueled inserts and machined shells may complicate the removal of heat from the fuel. A proposed phase diagram for the UC_2-ThC_2 system was modified using further results of dilatometry, thermal analysis, and other techniques. The weldability of new high-strength nickel alloys was investigated. Stress-rupture properties of a British stainless steel showed that heat treatment at 800°C yields a structure that is more ductile and relatively unaffected by irradiation, although somewhat weaker. An evaluation of UO_2 specimens irradiated at high temperatures was completed and measurements of thermal conductivity of AGOT graphite refined. (W.L.G.)

4307 (ORNL–3870, pp 238-42) MEDIUM POWER REACTOR EXPERIMENT. Thurber, W. C.; Adamson, G. M. Jr. (Oak Ridge National Lab., Tenn.).

Nine turbine pumps were fabricated in which tungsten carbide bearings were brazed to refractory metals with nickel–silicon–boron alloys. Techniques were perfected for brazing relatively thick stainless-steel-clad copper fins to tapered radiator tubes. Small stainless steel angles were first spot welded to both the tubes and the fins, holding both in a proper position while they were brazed. Natural-circulation loop test results on the compatibility of conventional nickel-, iron-, and cobalt-base high-temperature alloys in boiling potassium are reported. Haynes alloy No. 25 was superior at 980°C, and both it and type 316 stainless steel were acceptable at 870°C. A commercial coating improved the emittance of stainless steel at temperatures to 800°C. (auth)

4308 (ORNL–3870, pp 243-60) MOLTEN-SALT REACTOR PROGRAM. Taboada, A. (Oak Ridge National Lab., Tenn.).

Grade CGB graphite was evaluated to determine the acceptability of this material as a moderator. INOR-8 specimens resisted O_2-N_2 mixtures ranging from 0.03 to 5.6% O_2 for periods up to 700 hr, and reaction rates of these materials were measured. The investigation of mechanical properties of welds of INOR-8 was concluded. In some specimens, as-welded creep-rupture properties were comparable to wrought metal properties. Microstructures of INOR-8 weldments were analyzed and the composition of several phases is reported. Techniques were studied for making transition joints of graphite-to-INOR-8 and INOR-8-to-dissimilar metals using brazing with various fluoride-resistant brazing alloys, including a new palladium–nickel alloy. The dose dependency of the ductility and rupture of reactor heats of INOR-8 in postirradiation creep was studied. Boron content affected the behavior. Results of in-reactor creep tests in progress are given. Vacuum melting improved the ductility of INOR-8, and the influence

of various minor elements on its properties was investigated. Thermal convection loops were operated to study the compatibility of several coolants and structural materials. Lead was found to mass transfer in steel loops at 1200°F, forming dendritic crystals of iron and chromium. (auth)

4309 (ORNL–3870, pp 300-4) METALLOGRAPHY. Gray, R. J. (Oak Ridge National Lab., Tenn.).

A new electron microprobe analyzer was placed in operation and used to analyze microstructural constituents in nuclear fuel and structural materials. The instrument was particularly efficient in diffusion studies connected with tests of materials compatibility. Since being pressed into service a year ago, a new microhardness tester has performed satisfactorily at temperatures up to 2200°C. The design of the unit was based on experience accumulated during operation of a prototype model for the past several years. New and useful metallographic techniques developed during the past year include (1) a procedure for speeding up the epoxy mounting of metallographic specimens, (2) a technique for the metallographic preparation of thorium carbide specimens in a desiccated glove box, (3) identification of carbides, oxides, and nitrides in niobium by color staining, and (4) complete technology for making routine color transparencies and prints. (auth)

4310 (ORNL-P–1699) PROGRESS REPORT FOR THE PHYSICAL PROPERTIES GROUP OF THE REACTOR DIVISION AT THE OAK RIDGE NATIONAL LABORATORY. Cooke, J. W. (Oak Ridge National Lab., Tenn.). [1965]. Contract W-7405-eng-26. 9p. (CONF-651020–5). Dep. mn; CFSTI $1.00 cy, $0.50 mn.

From 5th Thermal Conductivity Conference, Denver.

The variable-gap apparatus developed for studies of the thermal conductivity of molten fluoride salts was completed, and its precision and accuracy were checked using mercury and water. For measurements of the thermal diffusivity of solids, a parametric study was made of several of the factors that affect the precision and accuracy of the flash-diffusivity technique. (D.C.W.)

4311 (AEC-tr–6486/2) BULLETIN OF THE BORIS KIDRIC INSTITUTE OF NUCLEAR SCIENCES. Translation of Bilten Instituta za Nuklearne Nauke "Boris Kidric," 16: No. 2, 65-122(1965). 61p. Dep.; CFSTI $3.00 cy, $0.75 mn.

4312 SPACE MATERIALS HANDBOOK. Goetzel, Claus G.; Rittenhouse, John B.; Singletary, John B. (eds.). Contract AF 33(657)-10107. Reading, Mass., Addison-Wesley Publishing Co., Inc., 1965. 633p. $15.00.

Information on space environment and the effects of space environments on materials are discussed. Topics covered include: ascent aerodynamic environment; the ascent vibration environment; structure of the upper atmosphere; solar radiation; albedo and earth radiation; penetrating radiation; physical impact phenomena; minor environment; thermal control materials; optical materials; materials for lubricated systems; adhesives; materials for sealing applications; organic materials for structural and related applications; electronic components and materials; metallic and ceramic materials for structural applications; spacecraft materials experience; selection of materials for optimum performance; and an introduction to biological interaction with spacecraft materials. (F.J.H.)

4313 PRODUCTION OF NUCLEAR FUELS. Myers, Rupert H. (Univ. of New South Wales, Kensington). pp 25-38 of Atomic Power: A Review. Kensington, N. S. W., Univ. of New South Wales [1964].

In the discussion of nuclear fuel production, reactor types, suitable atomic species for reactors including fuels, moderators, coolants, cladding, and tube materials are considered. The development of fuel elements to the present time is also considered. This includes early metallic fuels, the use of carbon dioxide as a coolant, and the development of the magnox alloys, uranium alloys, ceramic and cermet fuels, and cladding materials. Thermal and fast reactors are considered. Interesting research developments are mentioned. (J.F.P.)

4314 PROCESS FOR THE PRODUCTION OF TANTALUM OR NIOBIUM IN A HYDROGEN PLASMA JET. Scheller, Walter; Beguin, Claude; Schuett, Klaus (to Ciba Ltd.). U. S. Patent 3,211,548. Oct. 12, 1965. Priority date Nov. 23, 1961, Switzerland.

A process for the reduction of tantalum or niobium pentachloride in a hydrogen jet in the presence of a condensed substance having a vapor pressure that enables it to remain substantially in the condensed state at reaction conditions is described. The condensed substance has a particle size smaller than 500 μ, and the contact of the substance with the hydrogen jet ranges from 10^{-2} to 10^{-4} sec at a reaction temperature of between 2000 and 5000°C. If the dispersed material is particles or Ta or Nb powder, these particles grow as the metal deposits progressively on them from the reaction mixture; but if the particles are of another substance, the Ta or Nb form a coating on them. The process is applicable also to the reduction of the compounds only to a lower valence state. (B.L.M.)

4315 OXIDATION RESISTANT COATINGS ON NIOBIUM. Sama, L.; Kling, H. P.; Bender, H. (to U. S. Atomic Energy Commission). U. S. Patent 3,216,806. Nov. 9, 1965.

A fabricable high temperature oxidation resistant aluminum alloy is described for protectively coating a titanium–niobium alloy consisting of 20-75 at. % titanium and the balance niobium. (AEC)

4316 PROCESS OF PREPARING THORIUM METAL FROM THE OXIDE. Knighton, James B.; Hariharan, Alleppey V. (to U. S. Atomic Energy Commission). U. S. Patent 3,219,441. Nov. 23, 1965.

A process is given for reducing thorium dioxide to thorium metal comprising mixing the thorium dioxide with a flux consisting of at least 11 mole % magnesium chloride, up to 15 mole % calcium fluoride, and up to 89 mole % calcium chloride at 650 to 900°C., adding a magnesium–zinc alloy containing from 1 to 50% by weight of magnesium, agitating the mixture in an inert dry atmosphere, and separating a thorium–magnesium–zinc alloy from the flux. (AEC)

Corrosion

Refer also to abstract 4370.

4317 (BAW–1280-30) THE CORROSION OF CROLOY 2 1/4 STEEL IN THE PRODUCTS OF A SODIUM-WATER REACTION; SYSTEMS OF SODIUM HYDROXIDE IN WATER AND IN MOLTEN SODIUM. Research Report No. 7657. Rubright, M. M. (Babcock and Wilcox Co., Alliance, Ohio. Research Center). Nov. 15, 1965. Contract AT(11-1)-1280. 44p. Dep. mn; CFSTI $2.00 cy, $0.50 mn.

Tubular specimens of Croloy 2¼ were immersed in aqueous sodium hydroxide solutions ranging in concentrations from 24.2 to 98.6 weight percent at temperatures from 140 to 700°F at atmospheric pressure, and in 98.6 weight percent sodium hydroxide solution at 900°F under a water vapor pressure of 40 psig. Similar specimens were immersed in molten sodium containing varying amounts of sodium hydroxide at temperatures from 900 to 1400°F under an inert atmosphere, and in sodium containing sodium hydroxide and sodium hydride at 900°F under a mixed nitrogen-hydrogen atmosphere. Corrosion rates were calculated from the weight losses occurring during the immersion. Metallographic examinations of selected specimens were conducted to determine the type of corrosion occurring during the exposure periods. The corrosion rate of Croloy 2¼ steel in aqueous sodium hydroxide solutions was found to be a function of temperature and concentration. In general, the corrosion rate in aqueous sodium hydroxide solutions was very high at temperatures above 200°F, reaching a maximum of 2.67 ipy at 900°F. The corrosion rate in sodium (containing ≈90 ppm Na_2O) was comparatively low at temperatures up to 1250°F. Corrosion in a sodium hydroxide-sodium system increased as the concentration of sodium hydroxide increased, but was not as great as that for aqueous sodium hydroxide solutions at the same temperature. The corrosion

rate in a sodium hydroxide-sodium hydride-sodium system was lower than the rate in a sodium hydroxide-sodium system having the same starting concentration of sodium hydroxide. The mechanisms of corrosion are discussed. (P.C.H.)

4318 (CNLM–5359) ALKALI METAL CORROSION. I. MAXIMUM TEMPERATURE APPLICATION OF SODIUM–NaK/STAINLESS STEEL. Schenck, G. F.; Cleary, R. E. (Pratt and Whitney Aircraft, Middletown, Conn. Connecticut Advanced Nuclear Engineering Lab.). [1964]. Contract AT(30-1)-2789. 17p. Dep. mn; CFSTI $1.00 cy, $0.50 mn.

A review is presented on the corrosion of structural metals by sodium and sodium–potassium alloys with particular reference to stainless steel. Solubility, impurity effects, and mechanisms are discussed. As a result of the gross differences that exist between individual tests, it was concluded that to properly evaluate stainless steel, sodium, or sodium–potassium alloys for 1400°F application, the testing must be performed where cleanliness control is the major factor in the program. (P.C.H.)

4319 (EURAEC–1457) IMPERFECTIONS IN METALS. II. CORROSION AND OXIDATION. Quarterly Report No. 11, April 1–June 30, 1965. (Centre d'Etude de l'Energie Nucleaire, Mol (Belgium)). Contract 054-64-4 TEE B. 24p. (EUR–2386; R–2355). Dep. mn; CFSTI $1.00 cy, $0.50 mn.

Work Performed under United States–Euratom Joint Research and Development Program.

Transmission electron microscopy of corrosion-oxidation films formed on both Van Arkel zirconium and Zircaloy-2 in air from 250 to 450°C and in water from 225 to 325°C showed that gross differences existed in the film morphology depending on the environment and surface preparation. Annealed Zr, oxidized in air, formed monoclinic zirconia films which replicated the metal grain structure but which also contained fine-grain regions, pseudo-amorphous areas, pustules, and preferentially oxidized grain boundaries. Etched Zr, oxidized under the same conditions, formed uniform films having only one heterogeneity, viz. preferentially oxidized twins. Oxidation of annealed Zr in water produced a high density of oxide nuclei (monoclinic oxide) on a single crystal monoclinic matrix. Longer oxidation produced pustules which were much more numerous than those formed by air oxidation. Zircaloy-2 generally formed more uniform films than Zr in both air and water and did not exhibit the preferential grain boundary oxidation so prevalent in Zr oxidation films. Annealed Zircaloy-2 formed mottled films, whereas etched Zircaloy-2 oxidized similarly, showed unmottled grains which were sharply delineated and which clearly showed local areas corresponding to the intermetallics. (P.C.H.)

4320 (ORNL–3870, pp 70-4) SURFACE REACTIONS OF METALS. Cathcart, J. V. (Oak Ridge National Lab., Tenn.).

Alloying with small quantities of Ni, Al, and Ag caused large variations in the oxidation rate of Cu single crystals; changes in the extent of lattice disregistry in the oxide films on these crystals were correlated with changes in the rate of oxidation. Small Y additions improved the aqueous corrosion resistance of Al at 200°C significantly. Studies of stress generation due to oxygen solution in the surface layers of refractory metals were continued. Measurements of diffusion in Ta and Nb, using the very sensitive anodic film technique, were extended in temperature and agreed well with values obtained using mechanical sectioning. Use of the anodic film method extended the range of measurable diffusion coefficients to as low as 2×10^{-19} cm^2/sec. The contribution of magnetic order to the specific heats of Ni and several Ni–Cu alloys was evaluated. (auth)

4321 (ORNL–3870, pp 136-9) MATERIALS COMPATIBILITY. DeVan, J. H. (Oak Ridge National Lab., Tenn.).

Time, temperature, and the level of oxygen contamination enhanced corrosion and mass transfer in couples of niobium with liquid potassium. The presence of ternary compounds of the form $K_xNb_yO_z$ helps explain the complex corrosion phenomena observed. Oxygen in potassium was determined accurately by a gettering–vacuum-fusion technique despite variations in the thermal and environmental history of the potassium. From oxygen depletion of niobium in contact with potassium, diffusion coefficients of 7.9×10^{-10} and 6.4×10^{-9} cm^2/sec were measured for oxygen in polycrystalline niobium at 600 and 815°C respectively. (auth)

4322 (ORNL–3870, pp 305-7) SNAP-8 CORROSION STUDIES. Taboada, A. (Oak Ridge National Lab., Tenn.).

Materials compatibility problems associated with the primary circuit of the SNAP-8 electrical generating system were studied in forced-flow loop tests. Hydrogen contamination in the NaK coolant had no deleterious effect on corrosion. Increasing oxygen content increased the corrosion rate of iron-base alloys but not Hastelloy N. Corrosion was approximately linear with time. Carbon migrated from the hot portions of the loop to the rest of the system, severely decarburizing Croloy 9M. (auth)

4323 (ORNL–3870, pp 308-11) SNAP-50 CORROSION STUDIES. Taboada, A. (Oak Ridge National Lab., Tenn.).

The nature and extent of corrosion in a NaK heat-rejection circuit made of type 316 stainless steel and Nb–1% Zr alloy was studied. A test loop with removable specimens was built and operated for approximately 3000 hr. Examination of specimens removed from the loop after 2000 hr indicated only a minor transfer of carbon and nitrogen from the stainless steel to the niobium alloy. (auth)

4324 (PWAC–460) THE LOW PRESSURE OXIDATION OF PURE COLUMBIUM. Delgrosso, E. J.; Carta, J. S.; Ricard, A. (Pratt and Whitney Aircraft, Middletown, Conn. Connecticut Advanced Nuclear Engineering Lab.). Sept. 1965. Contract AT(30-1)-2789. 34p. Dep. mn; CFSTI $2.00 cy, $0.50 mn.

The reactions of niobium with oxygen were investigated at various temperatures and pressures. Continuous weight gain measurements were made using a vacuum thermobalance capable of detecting a 0.15 ± 0.05 mg weight change at temperatures up to 3500°F from atmospheric pressure to 10^{-6} mm Hg. These data are presented for oxidation at 870 to 1205°C from 1×10^{-3} to 1×10^{-5} mm Hg for 1 to 25 hour test periods. Corresponding quantitative internal oxidation measurements were performed to correlate hardness, penetration depth, and oxygen content. Oxidation parameters are indicated for protective and non-protective scale formation and corresponding internal oxidation. The structural changes, subscale, and scale formation caused by oxidizing niobium are illustrated. All data were subjected to rate analysis. The reaction rates were correlated with oxidation parameters and oxide structures to permit the formulation of pertinent mechanisms. Both recrystallized and annealed but unrecrystallized niobium were tested to determine the effect of metallurgical structure on oxidation kinetics. (auth)

4325 (TB–58) THE EFFECT OF URANIUM ADDITIONS ON THE CORROSION BEHAVIOUR OF AISI TYPE 430 STAINLESS STEEL. Biefer, G. J. (Department of Mines and Technical Surveys (Canada). Mines Branch). Nov. 1964. 18p. Dept. of Mines and Technical Surveys, Ottawa, $0.50.

AISI Type 430 stainless steels, and similar steels with 0.017-3.11% uranium, were subjected to laboratory corrosion tests in several aqueous solutions. The results indicated that uranium additions in the range 0.1-0.5% brought about improvements in corrosion resistance. To determine whether the laboratory results are correlated with improved corrosion resistance under service conditions, AISI Type 430 steels with 0%, 0.25% and 0.5% uranium are undergoing long-term field tests. (auth)

4326 (TRW-ER–6561) THE CORROSION OF SUPERALLOYS BY LITHIUM FLUORIDE IN A CYCLIC HIGH TEMPERATURE ENVIRONMENT. Engineering Report. Sch-

ulze, R. C. (TRW Equipment Labs., Thompson Ramo Wooldridge Inc., Cleveland, Ohio). June 21, 1965. Contract NAS 3-2779. 147p. (NASA-CR-54781).

Eleven superalloys were evaluated to determine their resistance to corrosion by lithium fluoride in a cyclic temperature environment. The tests were operated under simulated NASA Brayton Cycle system conditions (maximum lithium fluoride temperature–1850°F, minimum lithium fluoride temperature–1500°F) to determine the best material for fabrication of the heat receiver. The results of the program indicated Haynes alloy No. 25 to be the best alloy. (auth)

4327 (UNC–5138) STUDY OF URANIUM–PLUTONIUM MONOXIDES. Quarterly Progress Report, July 1–September 30, 1965. Forbes, R. L.; Fuhrman, N. (United Nuclear Corp., White Plains, N. Y. Development Div.); Andersen, J.; Taylor, K. (Carborundum Co., Niagara Falls, N. Y.). Oct. 30, 1965. Contract AT(30-1)-3305. 45p. (EURAEC–1494). Dep. mn; CFSTI $2.00 cy, $0.50 mn.

Work Performed under United States–Euratom Joint Research and Development Program.

Uranium–plutonium monoxide-type compositions stabilized with carbon, (UPu)(OC), were synthesized by carbon reduction of mixed UO_2 and PuO_2 in helium and vacuum. Materials containing as high as 85 wt % of a (UPu)(OC) composition were produced with oxygen atom fractions as high as 0.56. Carbon-stabilized and nitrogen-stabilized uranium–plutonium monoxides, (UPu)(OCN), were synthesized by the uranium metal and carbon reduction routes in helium and vacuum. Essentially single-phase compositions were obtained having oxygen atom fractions as high as 0.36. Specimens containing (UPu)(OCN) compositions were subjected to water corrosion tests. A material containing 91 wt % of $(U_{0.9}Pu_{0.1})(O_{0.21}C_{0.37}N_{0.42})$ was intact after exposure to boiling water for 137 hr, but it disintegrated in 550°F water. (auth)

4328 (WCAP–3269-50) STRESS CORROSION IN ALLOYS FOR FUEL ELEMENT CLADDING—STAINLESS STEEL AND ZIRCALOY. Thomas, K. C.; Allio, R. J. (Westinghouse Electric Corp., Pittsburgh, Pa. Atomic Power Div.). Sept. 1965. Contract AT(30-1)-3269. 136p. Dep. mn; CFSTI $4.00 cy, $1.00 mn.

Studies were made to determine the factors responsible for the stress-corrosion failure of stainless steel and Zircaloy-4 fuel element cladding so that they can be controlled and the susceptibility to failure minimized. At room temperature, Zircaloy-4 and crystal bar zirconium were found to be susceptible to brittle failure when stressed at 30,000–50,000 psi (2,109–3,515 kg/cm^2) in aqueous solutions of up to 20 wt % ferric chloride, having a pH of 0.6. The time to failure decreased with increases in stress, increase in chloride solution concentration, and increase in hydrogen content of the metal. The failures observed in zirconium alloys containing hydrogen are explained by a mechanism that involves the initiation of cracks in the hydride phase by piled-up groups of dislocations. Increase in strain at a given temperature, and increase in temperature at a given strain increased the dislocation density of 304 stainless steel and Incoloy 800. The time to failure of 304 stainless steel, in boiling magnesium chloride solution, at 40,000 psi was less than 1 hr, whereas failure did not occur in Incoloy 800 in less than 350 hr under similar conditions. (P.C.H.)

4329 (CEA-tr-R-1868) CLINETIQUE D'OXYDATION DE L'AIR L'OXYGENE ET LE GAZ CARBONIQUE. (Kinetics of Oxidation of Uranium by Air, Oxygen, and Carbon Dioxide). Bessonov, A. F.; Vlasov, V. G. Translated into French from Izv. Vysshikh Uchebn. Zavedenii, Tsvetn. Met., 5: No. 4, 137-42(1962). 14p. Dep. mn: JCL $1.60 fs, $0.80 mf.

The oxidation kinetics of metallic U was studied in atmospheres of air, oxygen, and carbon dioxide. It was established that the oxidation process in all aggressive media obeys the linear time law; the process velocity is proportional to the square root of the pressure of the air and the oxygen. The apparent activation energy of the oxidation process is equal to approximately 18 kcal/mole in all stages. The probable mechanism for U oxidation was examined. The determining stage is the diffusion of oxygen atoms across the dense layer of U dioxide. (tr-auth)

4330 (ORNL-tr-854) TECHNOLOGY OF LIQUID METALS. Savage, H. Wesley (Comitato Nazionale per l'Energia Nucleare, Rome (Italy)). Translated for Oak Ridge National Lab., Tenn., from report RTI/ING(65)-1. 96p. Dep. mn; JCL $8.60 fs, $3.08 mf.

Information is included on: liquid metal technology at ORNL; American sources of data on sodium technology; sodium technology research program and development at CNEN; handling of sodium; and components of sodium loops. (P.C.H.)

4331 PREDICTION BY COMPUTER OF CORROSION AND HYDRIDING OF ZIRCALOY-4 UNDER HEAT TRANSFER CONDITIONS. Thomas, K. C.; Allio, R. J. (Westinghouse Electric Corp., Pittsburgh). Amer. Soc. Metals, Trans. Quart., 58: 658-64(1965).

A general set of equations was developed from heat transfer theory and isothermal corrosion data, describing the corrosion of Zircaloy-4 as a function of heat flux, time, and average bulk coolant temperature. These equations were programmed for solution on an IBM 7094 digital computer. The program enables the computer to determine the change point from forced convection to nucleate boiling conditions and consequently carry out the calculations under such conditions. The output from the program are corrosion weight gain, hydrogen pickup, interface temperature between the oxide and metal, and clad surface temperature. Predicted curves illustrating the corrosion and hydriding as a function of time and heat transfer for the Saxton pressurized water reactor are given and compared to actual values obtained from this reactor. (auth)

4332 INITIAL OXIDATION OF TANTALUM OBSERVED IN A FIELD ION MICROSCOPE. Nakamura, Shogo; Mueller, Erwin W. (Pennsylvania State Univ., University Park). J. Appl. Phys., 36: 3634-41(Nov. 1965).

The distribution of oxygen atoms diffused into a tantalum crystal as a function of temperature, oxygen pressure, and time was observed in a field ion microscope. Light oxidation below 450°K causes corrosion of the first atomic layer only, while there is no diffusion into the matrix. The distribution of oxygen interstitials occurring at higher temperature with an activation energy of 1.1 ev is measured by direct counting of surface concentration of interstitials using the field evaporation sectioning technique. Heavy oxidation causes a breakup of the lattice and homogeneously dispersed nuclei of oxide. Tantalum with 1% oxygen content only shows the statistically expected number of interstitial pairs when quenched from 1100°K. In situ annealing between 395 and 360°K causes up to 14.5% of the interstitials to associate in pairs or clusters. (auth)

4333 THE EFFECT OF NITROGEN ON THE OXIDATION OF TANTALUM AT HIGH TEMPERATURES. Stringer, John (Battelle Memorial Inst., Columbus, Ohio). J. Electrochem. Soc., 112: 1083-91(Nov. 1965).

The effect of nitrogen on the oxidation of tantalum was studied at 600, 820, and 925°C. In all cases, the oxygen partial pressure was close to 360 torr; nitrogen partial pressures in the range 0 to 250 torr were investigated. At all three temperatures, nitrogen reduced the rate of oxidation. This effect increased with increasing temperature. Although the oxidation in pure oxygen followed a linear rate law, with nitrogen present the reaction ceased to be linear. The interpretation of the results in terms of the existing kinetic models is discussed. It is suggested that the pressure drop associated with the flow of the gas through the porous outer scale cannot be neglected. (auth)

4334 SCALING OF YTTRIUM IN AIR. Evans, E. B. (Thompson Ramo Wooldridge, Ltd., Cleveland). J. Less-Common Metals, 9: 465(Dec. 1965).

Yttrium (99.6% pure) was scaled in air at 1100°C for 1 hr. A tight covering of white scale formed on yttrium and spalled free on cooling, revealing a black scale. The spalled white scale was identified as yttrium oxide (Y_2O_3) by x-ray diffraction. The black scale surface showed all the diffraction lines of the oxide (Y_2O_3) and the nitride (YN). When the scale surface was lightly ground away the oxide x-ray diffraction lines decreased in intensity while the nitride and metal lines became stronger. These features demonstrated that a triple scale was formed on scaling yttrium in air at 1100°C: an outer white oxide; a middle black oxide, and an underlying layer of nitride. (F.J.H.)

4335 HIGH TEMPERATURE, SHORT-TERM, COMPATIBILITY OF SOME REFRACTORY METALS WITH THE THERMIONIC CONVERTER FUEL UC–ZrC. Allinson, J. D.; Riviere, J. C. (Atomic Energy Research Establishment, Harwell, Eng.). J. Nucl. Mater., 17: 97-110(Oct. 1965).

Short-term compatibility tests of the thermionic cathode material UC · ZrC (equimolar) with the refractory metals tungsten, tantalum, molybdenum, niobium, and rhenium were carried out, in which the temperature of the carbide-metal couple was raised by short steps until reaction was observed. Tungsten, tantalum, and rhenium appeared to be compatible for periods of up to 35 min at temperatures near 2100°C, but molybdenum and niobium both reacted vigorously at temperatures well below 2000°C. These results are shown to be fairly consistent with thermodynamic properties and with U–C-refractory metal phase diagram considerations for all the metals except tantalum, whose behavior in the tests is considered anomalous. The preferred materials for canning the cathode of a thermionic converter for operation in the region of 2000°C are therefore tungsten and rhenium. (auth)

4336 MORPHOLOGY AND MECHANISM OF ATMOSPHERIC CORROSION OF URANIUM MONOCARBIDE. Rousset, P.; Accary, A. (Section de Metallurgie des Combustibles Refractaires, Saclay, France). J. Nucl. Mater., 17: 149-52(Oct. 1965). (In French).

Observations on the corrosion of uranium–carbon systems in moist air, using the technique of optical fractography are described. It was concluded that when the C/U ratio slightly exceeds unity, "moist corrosion" produces intergranular fissures, which is accompanied by cleavage of the monocarbide grains caused by a corner effect due to corrosion products. Cleavage was propagated by successive leaps. (auth)

4337 CORROSIVITY OF CESIUM. Winslow, P. M. (Hughes Aircraft Co., Culver City, Calif.). 36p. (CONF-650325–1). ORINS. Gmelin, AED-CONF-65-037-2.

From National Assn. of Corrosion Engineers, 21st Annual Meeting, St. Louis.

Cesium used as a propellant for ion engines was evaluated for compatibility with container materials. These studies were directed toward the corrosive effects on the materials of containment as well as the extent of propellant contamination by the corrosion reactions. Exposures were made in both liquid and vapor environments at a temperature of 400°C for 500 hr. From this investigation a number of alloys were selected that possessed adequate corrosion resistance. A preponderance of evidence indicated that the chief reaction was oxidation-reduction between the cesium oxide contained in the cesium and the metal under test. (auth)

Fabrication

Refer also to abstract 5029.

4338 (AD–620055) SILICA FIBER/CORE-SHEATH FIBER. Final Technical Report, February 1, 1964–June 1, 1965. Plaskon, D.; Bradford, D.; Otto, W. H. (Narmco Research and Development Div., Whittaker Corp., San Diego, Calif.). June 15, 1965. Contracts N600-19-61810; N600-19-59607. 63p. CFSTI $3.00 cy, $0.75 mn.

A study was made of fused quartz fiber formed from a fluid melt contained in a bushing of tungsten and other materials in an argon atmosphere and of the development of a composite ceramic-glass fiber of core-sheath configuration. Continuous fused quartz fiber forming was achieved from silica melts contained in both tungsten and yttria-stabilized zirconia bushings operated in an argon atmosphere. Fiber forming temperatures ranged from approximately 1900 to 2300°C. Fiber tensile strengths approaching 600,000 psi were obtained. Bushings were indirectly heated, which permitted flexibility of design and materials. A systematic study of the crystalline core vitreous sheath concept was conducted using a double-compartmented platinum alloy bushing in which the inner compartment contained a core material and the outer compartment the sheath material. Fourteen candidate core materials and four sheath glasses were evaluated. It was found that fibers with a core volume as high as 80% could be successfully formed with this bushing design. The fibers so formed were vitreous and the core was crystallized by subsequent heat treatments. After core crystallization, modulus increases up to 75% were obtained, with values approaching 0.00002 psi. Tensile strengths over 100,000 psi were measured. (auth)

4339 (BNWL–131D) FABRICATION COSTS FOR PLUTONIUM FUEL ELEMENTS. PART D. VARIABLE COST OF FABRICATING UO_2–PuO_2 FUEL ELEMENTS FOR THE PLUTONIUM RECYCLE TEST REACTOR. Bloomster, C. H. (Battelle-Northwest, Richland, Wash. Pacific Northwest Lab.). Oct. 1965. Contract AT(45-1)-1830. 21p. Dep. mn; CFSTI $1.00 cy, $0.50 mn.

The variable (shop) cost of fabricating the HPD fuel element for the PRTR is $113/kg of fuel (as oxide) or a unit cost of $3900 per fuel element. The costs are based on the fabrication of the first 24 fuel elements by the pneumatic impaction-vibrational compaction processes. The shop labor requirements for each fuel element are 113 man-hours direct labor and 44 man-hours indirect labor. The variable costs include direct materials, some processing costs for nuclear materials, shop labor, direct overhead, and consumable supplies. Each fuel element contains 19 fuel rods and 34.6 kg of natural UO_2–2 wt % PuO_2 fuel. The fuel rods are 170 cm long and 1.4 cm OD with 0.76 mm Zircaloy-2 cladding. The fuel length is 149 cm, and an 18 cm plenum extends above the fuel. (P.C.H.)

4340 (COO–1518-1) FABRICATION OF TUNGSTEN ALLOY TUBING. Progress Report, July 1–October 22, 1965. Sowman, H. G.; Milner, A.; Rowenhorst, D. D. (Minnesota Mining and Mfg. Co., St. Paul). Nov. 10, 1965. Contract AT(11-1)-1518. 12p. Dep. mn; CFSTI $1.00 cy, $0.50 mn.

Small diameter tungsten–26% rhenium tubing was fabricated by the plastic extrusion of tungsten and rhenium powders combined with organic binders followed by sintering. Electron microprobe and metallographic analyses indicated a uniform alloy structure. Density exceeded 95% of theoretical. Bend tests were performed to determine ductility. (auth)

4341 (NAA-SR-Memo–10927) THE METALLOGRAPHY OF ZIRCONIUM-BASE ALLOY HYDRIDES. Raymond, J. W.; Shoop, D. T. (Atomics International, Canoga Park, Calif.). Feb. 5, 1965. Contract AT-11-1-GEN-8. 9p. Dep. mn; CFSTI $1.00 cy, $0.50 mn.

Techniques currently employed in the metallographic preparation of hydrides of zirconium and zirconium-base alloys are presented. A complete tabulation of metallographic procedures applicable to these materials is included. (auth)

4342 (ORNL–3870, pp 85-101) FUEL ELEMENT DEVELOPMENT. Adamson, G. M. Jr. (Oak Ridge National Lab., Tenn.).

In a one-step thermochemical process from UF_6, H_2, and O_2 gases at low pressures, UO_2 was synthesized as a stoichiometric solid approaching theoretical density, a dendritic needle-like deposit, or a submicron-size powder. A variety of refractory metals were fabricated by thermochemical techniques. With W–Re alloys, problems were encountered in obtaining homogeneous and uniformly thick deposits. Alloying was accomplished at relatively low de-

position temperatures and short lengths of tubing with only moderate composition variation. The products exhibited columnar grain structures, low impurity contents, and no sigma phase. A β-tungsten-type phase was observed for the first time in this system. Mo and Re were deposited as smooth coatings of high density and uniform thickness, but difficulty was encountered with uniformity and metal recovery in thick deposits. The physical characteristics of U_3O_8 affected the quality of Al dispersion fuel elements made from it. The optimum oxide was dense, spherical, and low in surface area. Both arc-cast and powder-metallurgy-produced U–Al intermetallics were fabricated into acceptable Al-dispersion fuel plates. The powder process contains more operations but provides closer control of stoichiometry and composition. Sintering UC with U_3Si_2 circumvented problems previously encountered in sintering with UAl_2 or UBe_{13} and attained densities over 96% from impure commercial UC sintered at 1575°C. The mechanisms of the improved sintering were determined, and preliminary testing indicates the techniques may also be useful with UN. (auth)

4343 (ORNL–3870, pp 266-89) THORIUM UTILIZATION. Douglas, D. A. Jr. (Oak Ridge National Lab., Tenn.).

Development of equipment for fabricating graphite elements fueled with coated particles was continued. A pilot line consisting of a sol-gel sphere-forming column, a dryer, a calciner, and a coater was designed, fabricated, and placed in operation to provide experience needed to establish process control requirements and bases for automated equipment for remote fabrication. The deposition of pyrolytic carbon on the fuel microspheres is the most expensive step in the process, primarily because of the small batch sizes that can be treated and the time required to complete each cycle. Processes for coating particles in a rotating drum and in an entrained bed were developed, and each offers potential for substantial cost reduction. Fully dense carbide fuels were prepared by treating calcined sol-gel oxide microspheres in a carbon bed. A scaled-down model of a production bed was designed and fabricated. Fuel pellets were pressed and fired from oxides in the gel state to densities over 90% of theoretical with good dimensional control. Differential thermal analysis of dried thoria gel showed that crystallite growth during heating begins at about 700°C. A high radial acceleration of the tube wall is a major factor in the vibratory compaction of sol-gel oxide. Irradiation testing of bulk oxide vibratorily compacted into metal tubes continued to demonstrate the excellent characteristics of thoria-base fuels. Relatively low fission-gas release and moderate structural changes were observed in three capsules irradiated at heat fluxes around 100 w/cm. Fission-gas release from ceramic fuels was related simply to the surface area. Platinum-rhodium thermocouples high in rhodium were satisfactory in vacuum near carbon at 1400°C. (auth)

4344 (ORNL-P-1725) PREPARATION, COATING, EVALUATION, AND IRRADIATION TESTING OF SOL-GEL OXIDE MICROSPHERES. Wymer, R. G.; Coobs, J. H. (Oak Ridge National Lab., Tenn.). Sept. 27, 1965. Contract W-7405-eng-26. 43p. (CONF-651041-2). Dep. mn; CFSTI $2.00 cy, $0.50 mn.

From Nuclear and Engineering Ceramics Conference, Harwell, Eng.

Microspheres of ThO_2, PuO_2, $ThO_2–UO_2$, $ThO_2–PuO_2$, rare earth oxides, and americium and curium oxides were prepared at ORNL by sol-gel techniques. Thoria, $ThO_2–UO_2$, and UO_2 microspheres were coated with pyrolytic carbon in fluidized beds and evaluation has begun. Sphere forming was accomplished by dispersing sols in 2-ethyl-1-hexanol containing appropriate surfactants or adulterants. Engineering feasibility of microsphere forming was demonstrated using a variety of sol dispersing techniques. Sol-gel microspheres, because of their sphericity and uniform size, are well suited to coating in fluidized beds and have been used extensively in coating studies at ORNL. The thermal and chemical stabilities of pyrolytic-carbon-coated ThO_2, $ThO_2–UO_2$, and UO_2 microspheres were demonstrated by their ability to withstand severe heat treatments (100 hr at 1900°C in vacuum, or 15 min at temperatures as high as 2600°C) without failure, provided the coating thickness is over about 65 μ. Irradiation results indicate that carbon-coated oxide microspheres will be satisfactory fuels for high-temperature, gas-cooled reactors. (auth)

4345 CHEMICAL CONSIDERATIONS IN THE SELECTION OF REACTOR FUELS. Verkerk, B. Atoomenergie Haar Toepassingen, 7: 153-9(Aug. 1965). (In Dutch).

The present article is an introduction to a series on the chemical aspects of fuel element fabrication. A review is given on the available fission and breeder materials and on the requirements placed on the fuel material by various reactor types. (tr-auth)

4346 THE PREPARATION OF HIGH PURITY URANIUM METAL BY THE ELECTROLYSIS OF FUSED URANIUM TETRACHLORIDE. Kuroda, Tadashi (Tokyo Inst. Technol.). Denki Kagaku, 33: 116-21(Feb. 1965). (In Japanese).

The process for obtaining high-purity uranium from UCl_4 by electrolysis is described. Uranium oxide is prepared from the uranyl nitrate, UCl_4 prepared from the uranium oxide, and uranium obtained by fused-salt electrolysis of UCl_4. U_3O_8 or UO_2 was obtained by heating (in a flow of O_2 at 300 to 800°C depending on the species of oxides) the precipitate from an aqueous solution of purified uranyl nitrate. UCl_4 was then prepared by heating, in an electric furnace, the oxide mixed with carbon in flowing Cl_2. The products of the reaction of UO_2 and C with Cl_2 are UCl_4, CO, and CO_2. Large crystals of UCl_4 are desirable for the electrolysis and they must be free from impurities. To depress the vapor pressure of UCl_4, the electrolysis was carried out in the presence of alkaline or alkaline earth salts. A variety of examples of the electrolysis is given. The electrodes, the deposition condition, the amount of vaporization, the amount of impurities, and the optimum concentration of UCl_4, etc, are discussed. (NSA of Japan)

4347 PRODUCTION OF HIGH PURITY URANIUM BY FUSED SALT ELECTROLYSIS. Nakajima, Kentaro; Kuroda, Tadashi. Denki Kagaku, 33: 122-6(Feb. 1965). (In Japanese).

A method is described for producing uranium with a 99.99% purity uranium by fused salt electrolysis in $UF_4–KCl–LiCl$, followed by purification of the obtained crystal uranium by electron impact techniques. The composition of the mixture was KCl (44 wt %)–LiCl (36 wt %)–UF_4 (20 wt %). The electrolytic cell, made of translucent quartz, was kept in argon atmosphere, and electrolysis was carried out at 400 to 500°C. The voltage applied was 1.0 to 1.5 v. The uranium obtained was washed by an ultrasonic wave of 28 kc/sec. The washed uranium crystal was melted and purified, either in an arc-furnace or an electron-impact fusion furnace. The electrolysis was carried out with W–W or U–U electrodes. In general, the size of the crystals increased with decreasing applied voltage; the amount of impurities decreased but the amount of salt, KCl, LiCl, and others increased. To remove the contaminating salts by ultrasonic waves, small sizes of the uranium crystals were desirable. The purification by an arc furnace was better than by the conventional methods, but the removal of volatile impurities was not sufficient. The electron impact fusion gave a good removal of these impurities and Al and no contamination from the electrodes. The uranium crystal, after washing, had to be free from moisture; it had to be dried after washing with alcohol or water. The electron impact fusion furnace was also used for zone refining. (NSA of Japan)

4348 MECHANISM OF THE PYROLYTIC GRAPHITE FORMATION. Yajima, S.; Satow, T.; Hirai, T. (Tohoku Univ., Sendai). J. Nucl. Mater., 17: 116-26(Oct. 1965).

Pyrolytic graphites were prepared by pyrolysis of commercial propane gas on a directly heated substrate. The formation rates of the pyrolytic graphites were measured from the density and thickness of deposits obtained at 1440 to 2215°C, flow rates of 280 to 1050 cm^3/min, and pressures of 5 to 200 torr. The reaction order of formation was

estimated from the time dependence of reciprocal resistance of the deposit. The formation rate obeyed a linear law. The effects of pressure and temperature on the formation rate were appreciable, but the formation rate was almost independent of the flow rate. The activation energy of pyrolytic graphite formation was divided into three types: ~3, ~10, and ~60 kcal/mole. The various mechanisms of formation are closely related to the microstructures of the pyrolytic graphite produced and they are named the fine regenerative structure, the string structure, and the coarse structure. (auth)

4349 THE SINTERING OF URANIUM MONONITRIDE. McLaren, J. R.; Atkinson, P. W. M. (Atomic Energy Establishment, Harwell, Eng.). J. Nucl. Mater., 17: 142-8(Oct. 1965). (AERE-R-4662).

Uranium nitride powder was found to sinter to 95% of theoretical density when suitably milled, compacted, and sintered at 1700°C in pure argon. The sintered pellets did not contain free uranium. The fine sinterable powder gained weight slowly when exposed to the pure argon atmospheres in which all the experimental work was carried out. It appeared that small amounts of oxidation reduce the sinterability of the powder. (auth)

4350 PRODUCTION OF URANIUM SINGLE CRYSTALS. Kutka, J. (Zentralinstitut fuer Kernforschung, Rossendorf, Ger.). Kernenergie, 8: 436(July 1965). (In German).

The Cahn method was used for the preparation of well-developed U single crystals. Zone-purified U was used as the starting material. Samples of the selected form were drawn from rods with a deformation degree of 60% and were transferred by recrystallization into the upper α range in the initial state. The samples were deformed by stretching and fused in the high vacuum. The samples were then stretched and annealed at a temperature of 650°C. The samples were drawn with a velocity of 0.5 mm/hr at this temperature. (J.S.R.)

4351 RIG DEMOUNTING AND MACHINING PROCESSES FOR IN-CELL USE. Jansson, L. (Aktiebolaget Atomenergi, Studsvik, Sweden). pp 385-94 of International Symposium on Working Methods in High Activity Hot Laboratories. Vol. I. Paris, Organization for Economic Cooperation and Development, 1965.

A description is given of demounting and machining processes used for irradiated rigs and loop specimens in the dismantling cells of AB Atomenergi's Active Laboratory for Fuel Elements at Studsvik, Sweden. After a brief description of the cells themselves, various dismantling operations and equipment used are described and illustrated. In-cell handling and transport of material, demounting operations without the use of cutting tools, demounting processes involving the use of cutting tools, and collection of active waste are discussed. (auth)

4352 ENCAPSULATED ELEMENTS. (to Air Reduction Co. Inc.). British Patent 1,007,173. Oct. 13, 1965. Priority date June 30, 1961, United States.

A method of producing an encapsulated element containing carbonaceous material, a particulate loading of metal or nuclear fuel material, and a carbonaceous binder is described. The method comprises the following steps: mixing the powdered carbonaceous material and the binder to form an encapsulating mix; forming a shell open only at the top of the encapsulating mix; forming a core mix of the carbonaceous material, the binder, and the particles of the loading; charging a predetermined quantity of the core mix into the shell; shaping the core mix in the shell; closing the top of the shell with a quantity of the encapsulating mix; and compressing the material of the shell and core. During the compression the core and shell become a compact unitary element in which the materials of the shell intimately contacts the core. The element is then heated at a high temperature of at least 900°C. (B.L.M.)

4353 IMPROVEMENTS IN THE CASING OF NUCLEAR FUEL ELEMENTS. (to Commissariat a l'Energie Atomique). British Patent 1,008,804. Nov. 3, 1965. Priority date July 24, 1961, France.

A process of encasing fuel elements for reactors in which the casing has a higher coefficient of thermal expansion than the element is carried out by hydrostatic pressure in two stages, the first in the cold state and the second at a temperature within the range of 300-400°C. The process is particularly applicable to the encasing of U elements in a Mg casing. (B.L.M.)

4354 CERAMIC TO METAL BONDING PROCESS. Erickson, George F. (to U. S. Atomic Energy Commission). U. S. Patent 3,214,833. Nov. 2, 1965.

A method of bonding beryllia to tantalum or niobium is described wherein an interface foil of titanium is inserted between the ceramic and metal, and the stack is heated to a temperature about 50-75°C below the melting point of the foil. (AEC)

4355 COATING FOR NIOBIUM. Baranow, S.; Lever, R. C. (to U. S. Atomic Energy Commission). U. S. Patent 3,216,851. Nov. 9, 1965.

A method is given for protectively coating niobium against oxidation at elevated temperatures that consists in dipping the niobium in a molten solution of aluminum and tin, with or without chromium and titanium, maintained at a temperature between about 1900 to 2300°F for a period of 1 to 30 minutes. The coated niobium may subsequently be given a diffusion treatment at about 1900°F in an inert atmosphere for a period of one hour. (AEC)

4356 PROTECTIVE COATINGS FOR NIOBIUM AND ITS ALLOYS. Priceman, S.; Sama, L. (to U. S. Atomic Energy Commission). U. S. Patent 3,219,474. Nov. 23, 1965.

A method is given for protecting niobium and niobium-base alloys against oxidation in air at temperatures in the range of 1100 to 2300°F. The method consists of establishing a titanium-rich zone on the surface of the niobium and thereafter depositing a protective aluminum alloy coating on the titanized surface by pack calorizing. (AEC)

4357 OXIDATION RESISTANT COATINGS FOR Nb AND Nb ALLOYS. Grubessich, J.; Sama, L. (to U. S. Atomic Energy Commission). U. S. Patent 3,219,477. Nov. 23, 1965.

This patent discloses a method of protectively coating niobium and its alloys against oxidation in air at high temperature. The metal to be coated is first cleaned, then dipped into a molten bath consisting of approximately 85% tin, 10% aluminum, the balance being selected from zinc, iron, chromium and tin. (AEC)

Properties and Structure

Refer also to abstracts 3880 and 5089.

4358 (AD-438516) GROWTH AND CHARACTERIZATION OF SINGLE CRYSTALS OF RARE EARTH COMPOUNDS. Quarterly Technical Report No. 3. (Westinghouse Electric Corp., Pittsburgh, Pa.). [nd]. Contract AF49(638)-1245. 14p. CFSTI $1.60 cy, $0.50 mn.

Single crystalline films of EuS, having either (100) or (111) orientation, were prepared by vapor-deposition techniques. Three alkali halides, NaCl, NaBr, and CaF_2, were found satisfactory as substrate materials for the epitaxial growth of EuS. A simple mode of epitaxy was observed for both the (100) and (111) cleavage surfaces. Conditions for the deposition and quality of the films were critically examined. Some striking effects were noted from doping on the electrical conduction of EuS. In addition to a marked decrease in resistivity at all temperatures between 4.2 and 300°K, La substitution also caused a slight increase of the Curie temperature. Ferromagnetic EuS with La as little as 1% exhibited metallic behavior in the electrical conduction below the Curie temperature. In all doped compounds, the resistivities dropped by several orders of magnitude accompanying the paramagnetic approached ferromagnetic transition. A study was made on the magnetic structures in CrTe-CrSb solid solutions. Theoretical consideration of the Th_3P_4 structure from both electrostatic and valence bond viewpoints was completed. (auth)

4359 (AD–618923) RESEARCH STUDIES ON THERMIONIC CONVERTERS, EMITTER SHELL PHASE. Report No. 5 (Final), July 1, 1963–February 28, 1965. Eastman, G. Y. (Radio Corp. of America, Lancaster, Pa. Direct Energy Conversion Dept.). Mar. 1965. Contract DA36-039AMC03197E. 134p. CFSTI $4.00 cy, $1.00 mn.

Studies were made on a barrier shell to protect thermionic energy converters from the combustion products of a fossil fuel flame. Two material properties are of prime importance; impermeability, and corrosion resistance. Three types of materials were selected for extensive testing; alumina, beryllia, and silicon carbide. Equipment of very high sensitivity was developed which permitted the determination of gas permeation rates. The identification of individual gases was made possible by the latest mass spectrometer equipment. It was determined that high purity alumina has the lowest permeation rate, the highest material strength, good thermal shock resistance, and is resistant to corrosion. Beryllium oxide had a poor corrosion resistance and a high permeation rate for carbon monoxide. The pyrolytic silicon carbide samples obtained evidenced high permeation rates for carbon monoxide and showed a tendency toward unpredictable fracture after extended periods at elevated temperatures. (auth)

4360 (AD–619399) DEVELOPMENT OF A STABLE-BETA TITANIUM ALLOY. Quarterly Report No. 9, July 1–September 30, 1964. Hunter, D. B. (Titanium Metals Corp. of America, New York). Contract DA30069ORD-3743. 41p. (WAL-TR–405/2-8). CFSTI $2.00 cy, $0.50 mn.

An x-ray examination of Ti-17V-10Cr-3Al-1Si revealed the presence of alpha and Ti_5Si_3 lines in a sample quenched from 2050°F and aged at 1250°F. No hardening response on aging at 1250°F was found in Ti-17V-10Cr-3Al-2Ge. Room temperature tensile tests on the agable beta alloy Ti-17V-2Fe-2Co-3Al indicated that a yield strength of 180,000 psi was reached after aging for 8 hours at 900°F. Aging for 24 hours at 800 to 900°F produced yield strengths exceeding 200,000 psi. Creep tests on Ti-8Mo-8V-2Fe-3Al showed that, when aged at 900°F for 8 hours, after 500 hours exposure at 600°F, under a load of 128,000 psi, deformations did not exceed 0.43%. Ti-17V-4Fe-3Al, exposed under similar conditions, showed creep deformations of 2%. Oxidation and stress corrosion tests on these alloys indicated that Ti-8Mo-8V-2Fe-3Al was the superior alloy. Weldability tests on agable beta alloys suggested their performance was similar to the commercial alloy Ti-13V-11Cr-3Al, whereas the two stable beta alloys Ti-17V-10Mn-3Al and Ti-8Mo-8V-6Fe-3Al had poor weldability relative to Ti-13V-11Cr-3Al. Tests on the overaging agable beta alloy Ti-17V-7.5Co-3Al showed that little increase in hardness over that of the solution-treated condition occurred on aging at 1100°F for up to 16 hr. (auth)

4361 (AD–619719) THERMAL AND ELECTRICAL CONDUCTIVITIES OF Mo–Re ALLOYS IN THE SUPERCONDUCTING AND NORMAL STATES. Lerner, E.; Daunt, J. G. (Ohio State Univ. Research Foundation, Columbus). July 1965. Contract Nonr49520. 37p. (TR-16). CFSTI $2.00 cy, $0.50 mn.

Research was carried out on the low-temperature properties of Mo–Re alloys in the superconducting and normal states. Measurements were made on a variety of Mo–Re alloys in various states of anneal. The alloys were in the form of fine wires, as suitable for the winding of high-field superconducting solenoids. Micrograph studies were made to determine the percentage of the various phases present in each specimen. The low-temperature measurements covered observations on the various specimens of the electrical resistivity as a function of temperature and of magnetic field and the thermal conductivity also as a function of temperature and magnetic field. The measurements yielded evaluations of two of the three critical magnetic fields H as a function of temperature and alloy constitution, the transition temperatures and the Landau–Ginsburg parameter. The results were compared with theoretical predictions and with results by previous authors on similar high-field superconducting alloys. (auth)

4362 (AD–620033) RARE EARTH TUNGSTEN BRONZES. Summary Report, August 1964–January 1965. Ostertag, Werner (Air Force Materials Lab., Wright-Patterson AFB, Ohio). July 1965. 26p. (ML-TR–65-120). CFSTI $2.00 cy, $0.50 mn.

Rare earth tungsten bronzes such as cerium tungsten bronze (Ce_xWO_3), europium tungsten bronze (Eu_xWO_3), and gadolinium tungsten bronze (Gd_xWO_3) were prepared. All compounds were cooled rapidly from 1000°C to room temperature and exhibited a cubic perovskite type structure. The rare earth bronzes have a wide homogeneity range. For the europium tungsten bronze, the range of x-values was $0.08 < x < 0.15$. The lattice parameter a_0 depends on the rare earth concentration. The electrical conductivity was measured as a function of temperature. The data indicate that the conductivity of the rare earth tungsten bronzes is nearly metallic. Magnetic susceptibility measurements were carried out by using a Faraday balance. The measurements proved that the rare earth ions are trivalent in the rare earth tungsten bronzes. The results of the magnetic data are discussed on the basis of the electron gas model. (auth)

4363 (AEET/CD/31) DIFFUSION OF COPPER IN NICKEL. Murarka, S. P.; Anand, M. S.; Agarwala, R. P. (Atomic Energy Establishment, Trombay (India). Chemistry Div.). 1964. 8p. Dep. mn.

Diffusion of copper in nickel was studied using radioactive tracer and residual activity method, in the temperature range of 800–1050°C. The diffusion coefficient (in cm^2/sec.) is given by: $D_{Cu/Ni} = 0.724 \exp(-61{,}000/RT)$. A vacancy mechanism of diffusion is suggested. Good agreement was observed with different theoretical calculations for the impurity diffusion in metal. (auth)

4364 (AERE–M–1644) GAS EVOLUTION FROM SOLID PLUTONIUM-BEARING RESIDUES DURING STORAGE. Hodkin, D. J.; Pitman, R. S.; Mardon, P. G. (Atomic Energy Research Establishment, Harwell (England)). Sept. 1965. 15p. Dep.; BIS $0.70; HMSO 3s. 6d.

Hermetically sealed cans containing solid plutonium-bearing residues have on occasions pressurized during storage. This was found to be due to radiolysis of moisture chemisorbed during the experimental life of the samples and in particular during long periods of storage in non-airtight containers sealed in PVC bags. Pressurizing of the cans can be prevented by vacuum drying of the samples immediately before canning. (auth)

4365 (AES–3) STUDIUM AV STRAECKGRAENSEN I MJUKT STAL. (Study of the Tensile Strength in Soft Steel). Oestberg, G.; Attermo, R. (Aktiebolaget Atomenergi, Stockholm (Sweden)). Aug. 1963. 17p. Dep. mn.

The tensile strength of a soft steel was studied by analysis of patterns in the stress-expansion curves. Details in the curve patterns were interpreted, using direct observations of test deformations on the broadening of the Luder band. (tr-auth)

4366 (AWRE-O–90/65) THE PERMEATION AND DIFFUSION OF HYDROGEN ISOTOPES THROUGH STAINLESS STEELS. PART 2. EN58B LOW CARBON STEEL. Jones, P. M. S.; Gibson, R.; Evans, J. A. (Atomic Weapons Research Establishment, Aldermaston (England)). Nov. 1965. 20p. Dep.; BIS $0.60; HMSO 3s.

The permeability and diffusion of hydrogen and deuterium through EN58B steel were investigated. No significant isotope effect on the diffusion coefficient was found, but hydrogen permeates 1.4 times more rapidly than deuterium. This difference is due in part to membrane deactivation and not true permeation differences. Temperature dependence data were obtained early when the rate of permeation through the membrane at 400°C was 2.35×10^{-4} std ml s^{-1}. Immediately prior to the deuterium runs hydrogen at 400°C gave 1.38×10^{-4} std ml s^{-1} and immediately after 1.25×10^{-4} std ml s^{-1}, compared with

0.94×10^{-4} std ml s^{-1} for deuterium. The true isotope effect on permeation would therefore be 1.38, with a 1.8 fold drop in membrane efficiency during the course of the experiments. (P.C.H.)

4367 (BNWL–162) A STUDY OF TUNGSTEN–TECHNETIUM ALLOYS. Quarterly Progress Report, July 1, 1965–October 1, 1965. (Battelle-Northwest, Richland, Wash. Pacific Northwest Lab.). Oct. 1965. Contract AT(45-1)-1830. 8p. Dep. mn; CFSTI $1.00 cy, $0.50 mn.

Arc melted W alloys containing 50 at. % (35 wt %) and 60 at. % (45 wt %) Tc were examined with an electron beam microprobe in attempts to determine compositions within the second phase regions. The composition of the dendritic second phase was determined to be 38 wt % Tc, which is in good agreement with the maximum solubility of Tc in W determined from lattice parameter measurements of the as-cast alloys. The average matrix composition was determined to be 49 to 50 wt % Tc which is less than sigma composition (58 to 60 wt % Tc). The results indicate that the nonequilibrium structure of both alloys is alpha solid solution plus a region of alpha and sigma. (P.C.H.)

4368 (CEA-R–2845) ETUDE DU DIAGRAMME TERNAIRE URANIUM–CARBONE–NICKEL. (Survey of Uranium–Carbon–Nickel Ternary Diagram). Anselin, Francois; Calais, Daniel; Passefort, Jean-Claude (Commissariat a l'Energie Atomique, Fontenay-aux-Roses (France). Centre d'Etudes Nucleaires). Aug. 1965. 32p. Dep. mn.

The U–C–Ni ternary diagram presents, in addition to the intermetallic compounds of U–Ni and uranium carbides, two mixed carbides UC_2Ni and U_2C_3Ni. The first carbide is decomposed from 1400°C; the second is stable up to 1800°C. (auth)

4369 (CEA-R–2871) MESURE DE LA TENSION DE VAPEUR DU BIOXYDE D'URANIUM UO_2 PAR LA METHODE D'EFFUSION. (Vapor Pressure Studies of Uranium Dioxide (UO_2) by the Effusion Method). Ohse, Roland W. (Commissariat a l'Energie Atomique, Fontenay-aux-Roses (France). Centre d'Etudes Nucleaires). Sept. 1965. 64p. Dep. mn.

A high temperature apparatus for vapor pressure measurements by the Knudsen effusion method is described. The sample is heated in a tungsten cell in an electronic bombardment furnace. Several critical factors affecting the accuracy of measurements such as: temperature distribution and measurement in the effusion cell; Clausing factor and molecular flow; and compatibility between cell material and sample heated, are discussed. The vapor pressure of UO_2 was studied between 2200 and 2800°K. (auth)

4370 (CEND–3256-250) CORRELATIONS BETWEEN SENSITIZATION AND STRESS CORROSION CRACKING OF 300 SERIES STAINLESS STEELS. Progress Report, July 1–September 30, 1965. Koziol, J. J.; Christopher, S. S. (Combustion Engineering, Inc., Windsor, Conn. Nuclear Div.). Oct. 1965. Contract AT(30-1)-3256. 37p. (EURAEC–1508). Dep. mn; CFSTI $2.00 cy, $0.50 mn.

Work Performed under United States–Euratom Joint Research and Development Program.

Efforts were concentrated on procurement and installation of the test equipment, procurement of specimen materials, and design and fabrication of the test specimens. Checkout of the test system and chemical sampling procedures are currently underway. Arrangements for drawing, swaging, and application of a nickel surface layer to the tubing are being made. (auth)

4371 (EUR–2514.e) COMPUTER ANALYSES OF TENSILE TESTS. Boerman, D. J.; Bonnet, P.; Grin, M.; Hubaux, A. (European Atomic Energy Community, Ispra (Italy). Joint Nuclear Research Center). 1965. 48p. Dep. mn.

Several graphical representations of the tensile test are described and two well-known laws are verified; the law of Hooke in the elastic region, and the law of Ludwig in the strain-hardening region. Tensile tests of SAP, pure aluminum, and aluminum alloys were executed on an Instron machine, at different temperatures. In order to obtain a higher accuracy, several strain-measuring methods were applied and compared. Only with the aid of an IBM-7090 computer and a data-plotter was it possible to obtain 36 parameters and 7 curves from each test in a very short time. The advantages of time saving, decrease of human errors, plus an increase of quantity and quality of information are discussed. (auth)

4372 (GA–6724) A RESEARCH PROGRAM ON THE EFFECT OF SUBSTRUCTURE ON THE IRRADIATION STABILITY OF ASTM A302 GRADE B STEEL. Quarterly Progress Report No. 2. Trozera, T. A.; Flynn, P. W. (General Atomic, San Diego, Calif. John Jay Hopkins Lab. for Pure and Applied Science). Oct. 8, 1965. Contract AT(04-3)-167. 14p. (EURAEC–1513). Dep. mn; CFSTI $1.00 cy, $0.50 mn.

Work Performed under United States–Euratom Joint Research and Development Program.

A new section of ASTM A302-B steel was cut to provide samples for testing. Tensile specimens in the three principal directions were cut at four points in the section and tested to characterize the section. The lower yield point and stress at maximum uniform strain were ±2% in the worst case, while the maximum uniform strain ranged from 0.10 to 0.14. Prestrains of 0.03, 0.06, and 0.09 combined with 1-hr heat treatments at temperatures of 375, 425, and 475°C caused the lower yield stress to increase from 16% to 41%, with decreases in maximum uniform strain of from ~0.13 (as-received) to within the range 0.06 to 0.11. Material from the section of A302-B previously tested was prestrained 0.03 and 0.06 and heat-treated 1 hr at 475°C. Charpy impact tests showed a 4 and 36°C NDT temperature increase for the 0.03 and 0.06 prestrains, respectively. (auth)

4373 (GEAP–4794) HIGH-TEMPERATURE TENSILE PROPERTIES OF SELECTED ALLOYS AFTER PROLONGED THERMAL EXPOSURE. Comprelli, F. A. (General Electric Co., San Jose, Calif. Atomic Power Equipment Dept.). Feb. 1965. Contract AT(04-3)-189. 43p. Dep. mn; CFSTI $2.00 cy, $0.50 mn.

Data are presented in which are documented the tensile properties of selected superheat alloys at 75, 1100, and 1300°F. The alloys include Incoloy-825, Inconel-718, Hastelloy-X, Hastelloy-F, Inconel-625, René-62, Incoloy-801, and Incoloy-800. The properties of each alloy were evaluated after exposure for periods up to 5000 hours at temperatures of 1000, 1100, 1200, and 1300°F. (auth)

4374 (IITRI–578-P27-12) YIELD POINT OCCURRENCE IN POLYCRYSTALLINE ALPHA-ZIRCONIUM. Summary Report, September 1, 1964–August 31, 1965. Weinstein, D. (IIT Research Inst., Chicago, Ill.). Sept. 30, 1965. Contract AT(11-1)-578. 35p. (IITRI–B6035-12; EURAEC–1507). Dep. mn; CFSTI $2.00 cy, $0.50 mn.

Work Performed under United States–Euratom Joint Research and Development Program.

An abrupt yield point was found to exist during the tensile deformation of high-purity zirconium having grain diameters smaller than 0.0065 mm. Yield point occurrence was favored by air cooling from the recrystallization temperature as compared to water quenching. Specimens cut transverse to the rolling direction showed greater yield drops, and the discontinuity persisted to larger grain sizes. Existence of a yield point was favored at temperatures above –22°C, and disappearance of abrupt yield was noted at lower temperatures. Discussion is presented showing that a Cottrell pinning/subsequent-unpinning mechanism does not account for the results; other mechanisms proposed for yield point occurrence in zirconium were examined in the light of these data. On the basis of supplementary microstraining experiments and in consideration of other known deformation characteristics of zirconium, the occurrence of a yield point is best explained by the

dynamic dislocation model for yielding in body-centered cubic materials developed by others. (auth)

4375 (IS–1241) APPLICATION OF GIBBS-DUHEM EQUATION TO BINARY VAPOR-LIQUID EQUILIBRIUM DATA OF METAL SYSTEMS USING NEWTON'S INTERPOLATION FORMULAE. Sater, V. E.; Stevenson, F. D. (Ames Lab., Iowa State Univ. of Science and Tech.). Aug. 1965. Contract W-7405-eng-82. 33p. Dep. mn; CFSTI $2.00 cy, $0.50 mn.

Integration of the Gibbs-Duhem equation using Newton's interpolation formulas was programmed in Fortran for both smoothed and unsmoothed activity coefficient data of binary systems, giving values of the second activity coefficient as a function of concentration. The conventional area test was also programmed to test the thermodynamic consistency when both activity coefficients have been independently determined. The Gibbs-Duhem equation is additionally used with numerically differentiated values of the log activity coefficient-concentration curves to indicate local consistency of the data. The programs and examples of their application are included. (auth)

4376 (JUL–268-RG) PHYSIKALISCHE STOFFWERTE VON FLUORIDSALZSCHMELZEN, SPEZIELLE ANWENDUNG AUF DAS MOSEL-REAKTORKONZEPT. (Physical Properties of Fused Fluoride Salts, Special Application to the MOSEL Reactor Concept). Vornhusen, H. W. (Kernforschungsanlage, Juelich (West Germany). Institut fuer Reaktorentwicklung). May 1965. 25p. Dep. mn.

A compilation of the available physical properties of melts of fluoride salt melts that were developed as fuel salts, blanket salts, or coolants for reactors is presented. The specific physical properties which were experimentally determined include densities for the solid and fused state, specific heat, viscosity, heat conductivity, melting point, and boiling point. The special application of fused salts to the molten salt epithermal reactor (MOSEL) is discussed. (P.C.H.)

4377 (NAA-SR-Memo–10741) LEAST SQUARE DETERMINATION OF THE DIFFUSION COEFFICIENTS OF GASES IN SPHERICAL SOLIDS. Young, W. A. (Atomics International, Canoga Park, Calif.). July 8, 1965. Contract AT-11-1-GEN-8. 81p. Dep. mn; CFSTI $3.00 cy, $0.75 mn.

A general least square method is presented for the treatment of data to give the best fit to any well behaved function. The method is specifically applied to the determination of the diffusion coefficient of a gas in a homogeneous spherical solid. A FORTRAN IV computer program for use with IBM-7090/7094 is described which effects this determination and graphically displays the calculated sorption curve by means of SC-4020 automatic display equipment. A second program is also described which yields a graphic display of sorption curves for given diffusion coefficients. (auth)

4378 (NAA-SR-Memo–11542) X-RAY DIFFRACTION DATA FOR $ZrC.ZrH_2$. Korst, William L. (Atomics International, Canoga Park, Calif.). July 10, 1965. Contract AT(11-1)-Gen-8. 5p. Dep. mn; CFSTI $1.00 cy, $0.50 mn.

The ternary compound $ZrC \cdot ZrH_2$ was prepared by heating powdered ZrC and ZrH_2 in a hydrogen atmosphere, confirming earlier reports of its existence. The hexagonal lattice constants were determined to be: $a_0 = 3.3467 \pm 0.0001$ Å, $c_0 = 5.4898 \pm 0.0001$ Å, $c/a = 1.640$. A listing of the x-ray diffraction powder pattern is given. (auth)

4379 (NASA-CR–54091) RESEARCH AND DEVELOPMENT PROGRAM ON MAGNETIC, ELECTRICAL CONDUCTOR, ELECTRICAL INSULATION, AND BORE SEAL MATERIALS. Magnetic Materials Topical Report. Kueser, P. E. (and others) (Westinghouse Electric Corp., Lima, Ohio. Aerospace Electrical Div.). Sept. 1964. Contract NAS 3-4162. 585p.

Thermophysical, magnetic, and mechanical property data on magnetic materials of interest to advanced space electric power systems are reported. Only a meager amount of reliable design data was found in the literature in the 500–1600°F temperature range. Therefore, tests were run under consistent guidelines to provide the data. Over 500 specimens were prepared and tested and 7300 test points evaluated at elevated temperature. Typical applications for magnetic materials are discussed and various materials are suggested for these applications. The maximum operating temperature is presented along with the mechanical and magnetic properties which may limit the application. In general, the magnetic materials can be grouped into three temperature ranges together with their fields of application. These are 600–800, 800–1100, and 1100–1400°F. Approximately 150 references are cited. (P.C.H.)

4380 (NASA-CR–54761) MATERIAL SPECIFICATIONS FOR ADVANCED REFRACTORY ALLOYS. Potassium Corrosion Test Loop Development. Topical Report No. 3. Miketta, D. N.; Frank, R. G. (General Electric Co., Cincinnati, Ohio. Space Power and Propulsion Section). Oct. 1, 1965. Contract NAS 3-2547. 311p.

Comprehensive material specifications for the procurement of advanced refractory alloys for evaluation in boiling and condensing potassium environments which simulate projected space electric power systems are presented. Candidate containment alloys selected include FS-85 and D-43 niobium alloys and T-111 and T-222 tantalum alloys. The candidate turbine alloys are Nb-132M niobium alloy and Mo-TZC molybdenum alloy. (P.C.H.)

4381 (NMI–8001.4) STUDY OF METHODS TO CONTROL GRAIN SIZE, PURITY AND TEXTURE IN BERYLLIUM AND BERYLLIUM ALLOYS. Bi-Monthly Letter Report, April–May 1965. (Nuclear Metals, Inc., West Concord, Mass.). June 15, 1965. Contract NOw-65-0084-f. 14p.

Studies are being made to determine the effects of grain size, texture, and alloying on the mechanical properties of wrought Be produced by splatcooling. Work continued on the processing of high purity SSR-grade flake to produce fine-grained Be and Be binary alloys containing Cu, Ni, and Fe. All of the materials were splatcooled and the splats broken up into many smaller particles, the latter being the final step prior to producing isotropic hot-pressings of these materials. Negligible contamination in all processing steps was verified by chemical analysis. Experiments showed that 700°C is a suitable hot-pressing temperature for the unalloyed SSR material. A compaction temperature for the alloys is to be investigated next. (P.C.H.)

4382 (NUMEC–3505-8) UO_2–PuO_2–ZrO_2 FUEL DEVELOPMENT PROGRAM. [Quarterly] Progress Report, July 1, 1965–September 30, 1965. (Nuclear Materials and Equipment Corp., Apollo, Pa.). Oct. 21, 1965. Contract AT(30-1)-3505. 34p. (EURAEC–1509). Dep. mn; CFSTI $2.00 cy, $0.50 mn.

Work Performed under United States–Euratom Joint Research and Development Program.

Studies on the development of the $UO_2-PuO_2-ZrO_2$ fuel system were continued. The enriched uranium ceramic powders from which pellets will be fabricated for in-reactor testing were prepared by coprecipitation. Other experimental compositions were prepared by mechanical blending. Test pellets of these were sintered to densities in excess of 90% of theoretical. Thermophysical studies of the $UO_2-PuO_2-ZrO_2$ system were made and x-ray crystallographic data were obtained as part of the phase diagram studies. Preliminary data were also obtained for melting points, thermal expansion, thermal cycling stabilities, and air oxidation stabilities. Apparatus for thermal analysis studies is being built. Design of the irradiation test pins and the irradiation test capsule was completed and major components for fabrication of the assembled capsule were procured. (P.C.H.)

4383 (ORNL–3795(Pt.2)) A BIBLIOGRAPHY ON TRACER DIFFUSION IN METALS. PART II. IMPURITY DIFFUSION IN PURE METALS. Askill, John (comp.) (Oak Ridge National Lab., Tenn.). Nov. 1965. Contract

W-7405-eng-26. 23p. Dep. mn; CFSTI $2.00 cy, $0.50 mn.

Data on frequency factors and activation energies for tracer solute diffusion in pure metals are compiled from the literature reported between 1938 and December 1964. 116 references are cited, and an author index is included. (auth)

4384 (ORNL–3870, pp 7-14) DEFORMATION OF CRYSTALLINE SOLIDS. Williams, R. O. (Oak Ridge National Lab., Tenn.).

Flow parameters for tantalum and tantalum alloys were explained in terms of the effect of alloying on the shear modulus, which enters into the calculation of the energy of double-kink formation, the proposed rate-controlling mechanism. The temperature dependence of stage II work hardening of single crystals was tentatively explained in terms of the difference in mobility of edge and screw dislocations, which gives rise to cell formation. The flow parameters in irradiated copper showed that the deformation is controlled by a single process, which probably results from the tetragonal distortions associated with small vacancy loops. An analytical method for inverting conventional pole figures into inverse pole figures was devised. Using it, the texture of rolled copper was redetermined and showed to consist of ridges rather than one or more isolated orientations. A calorimeter is being constructed to measure the increase in internal energy resulting from deformation over a wide temperature range, the partial release of this energy immediately following the deformation, and the subsequent isothermal release at higher temperatures. (auth)

4385 (ORNL–3870, pp 15-19) DIFFUSION IN SOLIDS. Lundy, T. S. (Oak Ridge National Lab., Tenn.).

The volume diffusion coefficients were determined for ^{95}Nb and ^{182}Ta in both pure Ta and pure Nb, ^{181}Hf in the β-phase of reactor-grade Hf, and ^{44}Ti in the alloy V–20% Ti. The diffusion of ^{51}Cr in Cr was measured from about 1500°C to the vicinity of the melting point and the atmosphere effects on diffusion rates of ^{182}Ta in β-Ti was investigated. A combined theoretical and experimental study of the effect of alpha bombardment on the diffusion of Pb in Ag was completed. (W.L.G.)

4386 (ORNL–3870, pp 20-6) ELECTRON MICROSCOPY. Stiegler, J. O. (Oak Ridge National Lab., Tenn.).

Using transmission electron microscopy the dislocation configuration in deformed Nb foils was shown to be determined primarily by the level of the applied stress and not by the temperature of deformation. It is suggested that the structure of a slip band depends on the stress at which the band is formed and proposed that fracture and twinning are initiated by narrow densely packed bands of dislocations generated at high stress levels. Recrystallization and grain growth, temperature and grain-size dependencies of the lower yield stress, ductile-brittle transition temperature, and brittle fracture characteristics of W sheet having a grain size range exceeding three orders of magnitude were studied. The results are consistent with a picture of grain growth and embrittlement controlled by impurities segregated at grain boundaries. An extensive study was made by electron microscopy of various as-deposited and annealed pyrolytic carbons. Graphitization was accelerated by the presence of actinide impurities. A procedure for preparation of specimens for electron microscopy from small highly radioactive samples is briefly outlined. (auth)

4387 (ORNL–3870, pp 38-43) PHYSICAL CERAMIC STUDIES. Yust, C. S.; Morgan, C. S. (Oak Ridge National Lab., Tenn.).

The creep rate of thoria in the temperature range 1400 to 1800°C and at stresses of 4000, 7500, and 11,000 psi was measured. Formation of intergranular voids and grain-boundary sliding are associated with the deformation process. Addition of calcium oxide accelerated creep of thoria, whereas addition of aluminum oxide inhibited creep. The compressive strength of thoria is greater than indicated by current literature. The mode of failure varied from completely brittle fracture at low temperatures to essentially ductile deformation at high temperatures, although intergranular void formation was still observed during the high-temperature deformation. Rectilinear inert-gas bubbles were observed in irradiated magnesium oxide crystals. (auth)

4388 (ORNL–3870, pp 44-9) PHYSICAL PROPERTIES. McElroy, D. L. (Oak Ridge National Lab., Tenn.).

Measurements on iron specimens of different purity showed the thermal conductivity of any relatively pure iron to be calculable to ±1.5% to 900°C from simple electrical resistivity measurements, the Wiedemann-Franz-Lorenz relation, and values of the lattice portion of the thermal conductivity. Measurements to 1000°C of the temperature dependence of the thermal conductivity of tungsten were made and the results analyzed in terms of electronic and lattice contributions to yield a Debye temperature of 284 to 318°K. A rapid method of measuring specific heat was developed and results on iron show the Curie phenomenon to be a second-order transition. (auth)

4389 (ORNL–3870, pp 61-4) STRUCTURE OF METALS. McHargue, C. J. (Oak Ridge National Lab., Tenn.).

Copper impurity atoms interact strongly (interaction energy of 2500 to 5200 cal/mole) with a moving grain boundary in aluminum. The effective interaction distance is two atom diameters and is large relative to the width of the grain boundary. The twinning tendency was correlated with dislocation substructure for niobium–vanadium alloys. This correlation suggests a model for dislocation behavior in body-centered cubic metals, which explains the effects of composition, temperature, and strain rate on flow. The major portion of the ⟨001⟩ texture in aluminum rods fabricated at low temperatures results from deformation band formation. The effects of initial orientation, temperature, and fabrication technique on preferred orientation can be explained in terms of this inhomogeneous deformation. (auth)

4390 (ORNL–3870, pp 65-9) SUPERCONDUCTING MATERIALS. Picklesimer, M. L. (Oak Ridge National Lab., Tenn.).

The transformation kinetics of Nb–Zr alloys with 25 to 60% Zr to a pearlitic structure was sluggish, only slightly sensitive to Zr content, relatively insensitive to atmospheric contamination, and sensitive primarily to grain size. A second mode of transformation was observed in the centers of large grains. Superconducting measurements at low fields on Nb–33% Zr alloys that had been partially or completely transformed to a pearlitic structure with interlamellar spacings of about 900 μ showed remarkably high critical currents. These specimens did not exhibit a large change in critical current caused by small changes in the applied field, as occurs in conventionally heat-treated material. Use of the Bean technique permitted evaluation of the effects of some metallurgical variables on the critical current properties of massive Nb–Zr alloy samples without the attachment of current leads. In Nb–Zr superconducting samples a surface layer was detected that had critical current densities and thicknesses near those of the London layer observed in ideal soft superconductors. The apparent thickness of the surface layer is not a function of the applied dc field (in the range of 6 to 40 kilogauss) and was greater in the cold-worked (735 Å) than in the annealed specimens (355 Å). The delta phase of the Zr–U alloy system was not superconducting at 4.2°K in zero magnetic field. (auth)

4391 (ORNL–3870, pp 75-82) X-RAY DIFFRACTION. Yakel, H. L. (Oak Ridge National Lab., Tenn.).

The complete crystal structure of calcium beryllate ($Ca_{12}Be_{17}O_{29}$) was derived from x-ray diffraction data. This unusual structure contains large isolated voids over 5 Å in maximum diameter, in which guest atoms could be trapped. Studies of single crystals of BeO irradiated to fast-neutron doses in the range 0.4 to 7.1×10^{20} neutrons/cm^2 have revealed marked changes that occur in x-ray scattering patterns as this range is traversed. The significance of these changes, which were not observed

previously, is discussed in relation to the theory of the damaged structure, which was developed from data at higher doses. By a new method, diffuse x-ray scattering from disordered alloys for contributions due to thermal motion and static atomic displacements are corrected. Unlike other techniques, it requires measurements at only one temperature and needs no models describing the character of the displacements. Its use yields the true short range order diffuse scattering, unobscured by intensity contributions due to other causes. (auth)

4392 (PWAC–461) PHASE DIAGRAM OF THE Cb–Zr–C SYSTEM AT 1538C AND 1092C. Cornie, James A.; Delgrosso, Eugene J.; Granger, Roger (Pratt and Whitney Aircraft, Middletown, Conn. Connecticut Advanced Nuclear Engineering Lab.). Oct. 1965. Contract AT(30-1)-2789. 59p. Dep. mn; CFSTI $3.00 cy, $0.50 mn.

The 1538°C isotherm of the niobium corner of the Nb–Zr–C system was determined. Two methods were used to identify the phases present in alloys representative of this section of the ternary diagram: x-ray diffraction of extracted phases; and chemical analysis of electrolytically extracted phases. The outstanding feature of this corner of the ternary diagram was the three-phase triangular region consisting of: a Nb–Zr body centered cubic solid solution containing 1.3 wt % (1.3 at. %) Zr and less than 200 ppM C, designated as beta, β; a (Nb, Zr) C_{1-x} face centered cubic phase containing 44.7 wt % (29.5 at. %) Zr and 7.64 wt % (39 at. %) C, designated as gamma, γ; and a $(Nb, Zr)_2C$ hexagonal phase containing 5.15 wt % (3.7 at. %) Zr and 6.15 wt % (33.62 at. %) C, designated as delta, δ. The γ phase represents a continuous series of solid solutions between NbC_{1-x} and ZrC_{1-x}, respectively. The lattice parameters of the δ phase varied between: $C_0 = 4.965$ Å, $a_0 = 3.133$ Å at the 0 wt % Zr level and $C_0 = 4.985$ Å, $a_0 = 3.132$ Å at the 4.91 wt % Zr level. A similar but much less extensive determination of the 1092°C isotherm was made in order to delineate phase field boundaries at this temperature. An additional, anomalous face centered cubic phase, designated as γ_2, was observed in some of the ternary alloys, but only when the Zr/C atomic ratio was greater than one. It is postulated that this phase was stabilized by oxygen and/or nitrogen, the common interstitial contaminants in niobium. A tentative quaternary phase model is advanced to support the proposition that the γ_2 phase owes its existence to the presence of interstitial contaminants. (auth)

4393 (PWAC–472) HIGH TEMPERATURE TITANIUM ALLOY DEVELOPMENT. Delgrosso, E. J.; Kaminsky, J. J.; Raring, L. M. (Pratt and Whitney Aircraft, Middletown, Conn. Connecticut Advanced Nuclear Engineering Lab.). Oct. 1965. Contract AT(30-1)-2789. 30p. Dep. mn; CFSTI $2.00 cy, $0.50 mn.

Studies were made on the development of a titanium base structural alloy with useful properties to 1200°F. A number of solid solution-dispersion strengthening combinations were investigated. Most of these were alpha alloys but a few beta-isomorphous types were also evaluated. The most promising results in the alpha compositions were shown by alloys in the range Ti–(5–7)Al–(1.5–4.0)Zr–(0.2–0.4)C. The best combination of strength and ductility was achieved when material was worked entirely below the beta transus and then heat treated to produce a fine carbide dispersion. Rupture life at 1200°F and 30,000 psi was comparable to austenitic stainless steel. Consumably melted ingots, up to four inches in diameter, were extruded to rod or forged and rolled to sheet. Alpha alloys in the Ti–Al–W–B and variations thereof were also investigated but to a lesser extent. Preliminary data were encouraging. The best beta composition was an alloy of Ti–(25–35)V–(6–10)W–(4–6)Al–(2–4)Zr–(0.1–0.4)C. However, more exhaustive fabrication and test evaluation is needed to assess the engineering merits of these alloys. (auth)

4394 (PWAC–477) SELF DIFFUSION OF NITROGEN IN URANIUM MONONITRIDE. Sturiale, T. J.; DeCrescente, M. A. (Pratt and Whitney Aircraft, Middletown, Conn. Connecticut Advanced Nuclear Engineering Lab.). Sept. 1965. Contract AT(30-1)-2789. 25p. Dep. mn; CFSTI $1.00 cy, $0.50 mn.

The self-diffusion rate and activation energy for diffusion of nitrogen in uranium mononitride was studied by a gas-solid exchange technique. The results indicated that the exchange is not surface reaction controlled. Diffusion coefficients were calculated from the slopes of these plots and the square of the particle radius. The diffusion coefficients for both the large (125 μ) and small (25 μ) size material follow a straight line relation above 1500°C. However, the low temperature data for the small grain size material deviates significantly from the extrapolated high temperature data. This suggests that grain boundary diffusion becomes a dominant factor in mass transport at the lower temperatures. A least squares fit of the low temperature data, indicates an apparent activation energy for grain boundary diffusion of 29 kc/mole. (P.C.H.)

4395 (PWAC–478) THERMODYNAMIC PROPERTIES OF URANIUM MONOCARBIDE. Vozzella, P. A.; DeCrescente, M. A. (Pratt and Whitney Aircraft, Middletown, Conn. Connecticut Advanced Nuclear Engineering Lab.). Sept. 1965. Contract AT(30-1)-2789. 21p. Dep. mn; CFSTI $1.00 cy, $0.50 mn.

Uranium monocarbide was found to lose uranium preferentially in the temperature range 2250 to 2525°K until a constant vaporizing, non-stoichiometric composition approaching $UC_{1.1}$ was formed. Rates of evaporation of this composition, measured from 2190 to 2525°K by the Langmuir method, are described by $\log_{10}m(UC_{1.1(s)}) = 9.148 - 3.574 \times 10^4T^{-1}(g\text{-}cm^{-2}\text{-}sec^{-1})$. Based on the decomposition process $UC_{1.1(s)} \rightarrow U_{(g)} + n_1C_{1(g)} + n_2C_{2(g)} + n_3C_{3(g)}$ the partial pressure of uranium is given by $\log_{10}PU_{(g)}(atm) = 8.191 - 3.624 \times 10^4T^{-1}$. The rate of evaporation and consequently the vapor pressure of carbon was found to be equivalent to that over graphite. A third law analysis yields a heat of vaporization at 298°K of 235.1 ± 2.7 kcal/mole for the above vaporization process. The resultant standard heat of formation of $UC_{1.1(s)}$ at 298°K is –21.2 ± 4.1 kcal/mole if 125 ± 3 kcal/mole is taken as the heat of sublimation of uranium. (auth)

4396 (PWAC–482(Pt.1)) COMPRESSIVE CREEP OF UC AND UN. PART I. Fassler, M. H.; Huegel, F. J.; DeCrescente, M. A. (Pratt and Whitney Aircraft, Middletown, Conn. Connecticut Advanced Nuclear Engineering Lab.). Oct. 1965. Contract AT(30-1)-2789. 17p. Dep. mn; CFSTI $1.00 cy, $0.50 mn.

Out-of-pile compressive creep tests were performed on uranium carbide and uranium nitride. Preliminary values were determined for the creep parameters n and K in the quasi-viscous creep law relating creep rate to stress $\dot{\epsilon} = (\sigma^n/K)$. These values were used to correlate out of pile creep with observed in pile fuel density decreases according to an analysis developed by Foreman (AERE-T/M-134, March 1956). (auth)

4397 (TIM–955) STABILITY OF CARBON STRENGTHENED COLUMBIUM–ZIRCONIUM ALLOYS AT ELEVATED TEMPERATURE IN ULTRA-HIGH VACUUM. Hogan, J. F.; Limoncelli, E. A.; Slotnick, H. (Pratt and Whitney Aircraft, Middletown, Conn. Connecticut Advanced Nuclear Engineering Lab.). Oct. 1965. Contract AT(30-1)-2789. 17p. Dep. mn; CFSTI $1.00 cy, $0.50 mn.

A test program at pressures below 1×10^{-8} torr was initiated to investigate the stability of carbon strengthened niobium–zirconium alloys at high temperatures. Data at 2000°F with PWC-11 alloy (Nb-1 Zr-0.08 C) and PWC-33 alloy (Nb-3 Zr-0.3 C) showed no effect due to low pressure or to oxygen added to the specimen, or to the test environment. Preliminary oxidation studies at 3×10^{-8} torr oxygen pressure and 2000°F indicated PWC-11 alloy reaction rate was one-half that of Nb-1 Zr alloy. (auth)

4398 (TRG-Report-1021) AGEING OF CHROMEL–ALUMEL THERMOCOUPLES. Callcut, V. A. (Reactor Group, United Kingdom Atomic Energy Authority, Risley

(England)). July 2, 1965. 8p. Dep.; BIS $0.60; HMSO 3s, 0d.

Calibration changes in Chromel-Alumel thermo-couples arising from aging drift, thermal cycling, and depth of immersion are associated with a reversible change in the thermo-electric power of the Chromel leg which occurs on heating. Metallographic examination by optical, electron microscopic, and thin-film transmission techniques were used, but no evidence of chemical attack or precipitation was found. It was concluded that the change in thermo-electric power is produced by ordering effects which occur in a range of nickel–chromium alloys, and hence cannot be eliminated by special preparation or by small changes in the alloy composition. (auth)

4399 (UCRL-16301) STRUCTURE AND HIGH STRENGTH METALS. Thomas, G.; Zackay, V. F.; Parker, E. R. (Lawrence Radiation Lab., Univ. of California, Berkeley). Aug. 1965. Contract W-7405-eng-48. 64p. (CONF-650830-1). Dep. mn; CFSTI $3.00 cy, $0.75 mn.

From Sagamore Conference, New York.

Knowledge concerning the plastic behavior of simple solids in terms of atomistic processes are summarized briefly. Emphasis is on the relatively uncomplicated but important properties of strength and ductility. The limitations of the principal strengthening mechanisms are delineated and optimum procedures for achieving very high strength in complex solids are suggested. Some of the progress made to date in achieving these goals is reviewed. 47 references are cited. (P.C.H.)

4400 (WCAP-3269-41) PHYSICAL AND MECHANICAL PROPERTIES OF ZIRCALOY 2 AND 4. Scott, D. B. (Westinghouse Electric Corp., Pittsburgh, Pa. Atomic Power Div.). May 1965. Contract AT(30-1)-3269. 68p. Dep. mn; CFSTI $3.00 cy, $0.75 mn.

Various mechanical and physical properties of Zircaloy-2 and Zircaloy-4 are presented suitable for engineering design. Where published information was not available, tests were initiated to determine the necessary properties. The data are assembled and as much as possible expressed graphically. Temperature was found to have a pronounced effect on metal properties. (P.C.H.)

4401 (ANL-Trans-218) EXAMINATION BY ELECTRON MICROSCOPE OF NIOBIUM CONTAMINATED AT HIGH TEMPERATURE BY INTERSTITIAL ELEMENTS. Bibring, Herve; Jouffrey, Bernard; Girard, Francois. Translated by D. G. Westlake (Argonne National Lab., Ill.), from a communication presented to the Journees d'Automne de la Societe Francaise de Metallurgie, Paris (October 1964). 24p. Dep. mn; JCL $2.60 fs, $0.92 mf.

Specimens of niobium heated to 1625°C under reduced pressures of air or nitrogen were examined by transmission electron microscopy. Direct observation showed a fine precipitate, more or less coherent with the solid solution and some large precipitates (1000 to 20,000 Å), micro-twins, these last being due especially to the reaction with nitrogen. The electron diffraction patterns showed some superstructure spots that permit the conclusion that nitrogen is concentrated in the bcc solid solution deforming it until it provokes a transformation of the lattice into hcp by crystallographic shear. Certain precipitates act as sources of dislocation loops but they can also block dislocations and be the origin of the formation of tangles. Some dipoles created in the beginning from screw dislocations, some dissociated dislocations, and rather rarely a dislocation pileup were also observed. (auth)

4402 (ANL-Trans-230) FERRIMAGNETISM OF Mn_4N AND OF SOME MIXED CRYSTALS OF Mn_4N. Juza, Robert. Translated by Elmar K. Wilip (Argonne National Lab., Ill.), from Z. Elektrochem., 61: 810-19(1957). 24p. Dep. mn; JCL $2.60 fs, $0.92 mf.

Investigations on the low magnetic moment of Mn_4N(1.2 Bohr magnetons), the saturation magnetic behavior in a reduced diagram, and the behavior of the paramagnetic susceptibility above the Curie point suggest that Mn_4N exhibits ferrimagnetism (uncompensated antiferromagnetism). Four series of samples were made starting from Mn_4N: samples with vacancies in the N-partial lattice $Mn_4N_{1-x}\square_x$; carbonitrides $Mn_4N_{1-x}C_x$; and mixed crystals with Cu, $Mn_{4-x}Cu_xN_{1-x/4}\square_{x/4}$ and with Zn, $Mn_{4-x}Zn_xN_{1-x/4}\square_{x/4}$. The lattice constants of the samples with vacancies decrease with the number of vacancies, the lattice constants of the others agree essentially among one another. Cu and Zn occur only in 000 sites. The Curie points of the vacancy samples and of the carbonitrides rise, those of the Cu and Zn-containing samples fall with increasing concentration. The saturation magnetization and the magnetic moments decrease sharply for the vacancy samples, less so for carbonitrides. For Cu and Zn-containing samples they fall first and rise thereafter at higher concentrations. The magnitude and the concentration dependence of the magnetic moments are explained by the ferrimagnetic coupling of atom moments. One sublattice contains a Mn atom at 000 and a face-centered Mn atom; the other sublattice contains the two other face-centered Mn atoms. (auth)

4403 (JPRS-32317) EFFECT OF HOT PLASTIC DEFORMATION ON THE STRUCTURE AND PROPERTIES OF MOLYBDENUM, NIOBIUM, AND TITANIUM. Gurevich, Ya. B.; Orzhekhovskii, V. L. Translated from Izv. Akad. Nauk SSSR, Metal., No. 4, 137-43(July-Aug. 1965). 11p. (TT-65-32807). CFSTI $1.00 cy, $0.50 mn.

Studies were made on the mechanical properties (in particular under conditions of tensile testing) of Mo, Nb, and Ti, which were rolled in a vacuum and in air correspondingly. The results indicated that the strength and ductility characteristics of Nb and Ti depend substantially on the atmospheric conditions of their hot rolling. Deformed in a vacuum of $\sim 10^{-5}$ mm Hg, the metals possessed lower tensile strength and yield point values and higher relative elongation and reduction of area values than metal rolled under the usual conditions in air. Rolling of Mo in a vacuum and in air did not result in substantial differences in mechanical properties. (P.C.H.)

4404 (JPRS-32773) THE ELECTROLYTIC DEPOSITION OF THICK AND REGULINE RHENIUM LAYERS. Kvokova, I. M.; Layner, V. I. Translated from Zashita Metal., 1: 515-20(1965). 8p. (TT-65-33351). CFSTI $1.00 cy, $0.50 mn.

Studies were made on the absence of bonding between thick films of rhenium and copper and molybdenum bases, the effects of heat treatment on the bonding of succeeding rhenium films, and the role of co-deposited Cr in the formation of thick (up to 50 μ) regulines of a Cr–Re alloy. The absence of bonding was found to be explained by the development of cracks in the coating. When relatively thick deposits of Re were obtained by a layer building up intermediate heat treatment at temperatures above 800°C in a reducing atmosphere, a good bonding was assured owing to the formation of a Re-base diffusion alloy. The effects of Cr are explained by the formation of a solid substitution solution with the Re, rise in the average dislocations density, crystallization in the form of large and regularly shaped crystals which grow satisfactorily and fasten along the thickness. (P.C.H.)

4405 (K-Trans-9) THERMAL ELECTRONIC PROPERTIES OF THE TUNGSTEN–HAFNIUM SYSTEM. Bondarenko, D. V.; Tsukrov, F. G. Translated for Oak Ridge Gaseous Diffusion Plant, Tenn., from Radiotekhn. Elektron., 10: 971-2(1965). 5p. Dep. mn; CFSTI $1.00 cy, $0.50 mn; JCL $1.10 fs, $0.80 mf.

In order to determine the emission properties of the W–Hf alloys, studies were made on deposits of hafnium powder baked on W, and of Hf precipitated from the gaseous phase. During initial rise of the temperature (the measurements were started at 1100°K at 10^{-8} amp), a monotonic increase of the work function was observed from 3.20 ev at 1100°K to 3.93 ev at 2000°K, which apparently is related to the sintering of the powder and to the decrease of the real emitting surface up to a temperature of 2000°K. After exposure to 2000°K, the work function decreased from 3.93 to 3.70 ev. Emission of the alloy precipitated from the gaseous phase corresponded to an effective work function of 3.98–4.01 ev. (P.C.H.)

4406 (ORNL-tr-873) SOME IDEAS ON THE CONSTRUCTION OF CONCRETE CONTAINERS. Koenne, W. Translated for Oak Ridge National Lab., Tenn., from Nucl. Struct. Eng., 2: 126-33(1965). 17p. Dep. mn; JCL $1.60 fs, $0.80 mf.

Problems in the use of concrete in containment structures are discussed. Consideration is given to the relations between wall temperatures and leak rates and the contained temperatures and pressures. (P.C.H.)

4407 PREFERRED ORIENTATION IN A SHEET OF ALPHA-ROLLED PLUTONIUM. Berndt, Alan F.; Lloyd, Lowell T. (Argonne National Lab., Ill.). Amer. Soc. Metals, Trans. Quart., 58: 470-5(Dec. 1965).

The preferred orientation in a sheet of alpha-plutonium rolled to 98.8% reduction in thickness at room temperature was determined by x-ray measurements. Pole figures were drawn for the (013), (004), (20$\bar{3}$), and (21$\bar{3}$) poles and are discussed in terms of ideal orientation diagrams. The results indicated a two-component texture; one with the two-fold axis of the monoclinic structure, [010], aligned approximately parallel to the rolling direction, and the second with the [010] nearly parallel to the cross direction. Comparison of the x-ray results with those of resistivity measurements suggested that the former texture is the predominant one. (auth)

4408 STRENGTHENING OF TUNGSTEN AT INTERMEDIATE TEST TEMPERATURES FROM 300 TO 1600 C. Schnitzel, R. H. (Westinghouse Electric Corp., Bloomfield, N. J.). Amer. Soc. Metals, Trans. Quart., 58: 687-90(1965).

The strengthening effect of interstitials on the tensile properties of tungsten was observed in measurements on carburized and quenched crystals. The strengthening effects of carbide precipitation during strain aging was clearly demonstrated. Carburizing followed by a high-temperature quench produced a most significant strengthening contribution. Even greater strengthening was realized at these temperatures if these specimens were deformed after carburizing and quenching. (M.C.G.)

4409 COMPARISON OF THE EFFECTS OF CARBON AND TUNGSTEN ON THE FLOW STRESS RECOVERY OF MOLYBDENUM. Potter, L. C.; Lytton, J. L. (Lockheed Missiles and Space Co., Palo Alto, Calif.). Amer. Soc. Metals, Trans. Quart., 58: 695-9(1965).

Studies were made to determine the effects of recovery on the tensile flow behavior of sintered molybdenum sheet with low carbon content and to determine the effect of a 1% substitutional solid-solution addition of tungsten on the recovery behavior of sintered low-carbon molybdenum. The sheet materials employed were Mo and Mo-1 wt % W. Results are presented in graphs. The initial yield stress for the recrystallized condition, as well as the flow stress at 10% true strain, was increased by only about 2000 psi as a result of the solid-solution tungsten addition. It was concluded that there is little interaction between the tungsten atoms and moving dislocations. (M.C.G.)

4410 THE SURFACE POTENTIAL OF OXYGEN ON THORIUM. Riviere, J. C. (Atomic Energy Research Establishment, Harwell, Eng.). Brit. J. Appl. Phys., 16: 1507-11(Oct. 1965). (AERE-R-4951).

The contact potential difference between ultrahigh vacuum-deposited films of gold and of thorium was followed during the admission of oxygen at room temperature. With the knowledge that the work function of gold remains invariant in pressures of oxygen up to 10^{-3} torr and varies in a known fashion thereafter, the work function of the thorium film could be deduced under all conditions of coverage. Initial adsorption of oxygen produced a positive surface potential rising to a maximum of 0.47 ev, but continued adsorption under a constant rate of admittance caused a reversal to a negative surface potential after a long time. After reaching a minimum of -0.48 ev, the direction of change of the surface potential reversed abruptly and then rose steadily to a constant value of 0.48 ev, corresponding to a work function of 2.98 ev. The latter figure is within the range of values observed for ThO_2. The results have been interpreted in terms of penetration of the surface layers of the thorium by oxygen, followed by transformation of the saturated layers to ThO_2. It is suggested that the initial steps in the reaction between any electronegative element and a metal are penetration of the element into the metal followed by transformation of the surface layers into a new phase, the reaction product. (auth)

4411 CRYSTALLINE AND MAGNETIC PROPERTIES OF MIXED GARNETS OF DYSPROSIUM AND CERIC EARTHS. Villers, Gerard; Lombard, Paul; Loriers, Jean (CNRS, Bellevue, France). Compt. Rend., 260: 5723-6 (May 31, 1965). (In French).

The effect of the substitution of dysprosium by the ceric earths (La, Pr, Nd, Sm, and Eu) was studied in the compound $5Fe_2O_3 \cdot 3Dy_2O_3$. An expansion of the crystalline cell, a decrease in absolute saturation, compensation temperature, and a slight increase of the Curie temperatures were observed. (tr-auth)

4412 APPLICATION OF α SPECTROMETRY TO THE MEASUREMENT OF LOW DIFFUSION COEFFICIENTS; CASE OF URANIUM DIOXIDE. Marin, Jean-Francois; Michaud, Henri (Centre d'Etudes Nucleaires, Grenoble, France). Compt. Rend., 261: 693-6(July 19, 1965). (In French).

The spectrometric analysis of α radiation emitted by a thin radioactive layer makes it possible under certain conditions to study the evolution of concentration profiles during diffusion. It was shown by this method that the self-diffusion coefficient of uranium is very weak in the stoichiometric dioxide (5×10^{-16} cm^2 sec^{-1} at 1700°C) and is much more important in the super-stoichiometric UO_2. The diffusion in this case is accompanied by considerable volatilization. (tr-auth)

4413 THE RECRYSTALLIZATION, GRAIN GROWTH, AND PREFERRED ORIENTATIONS OF ZIRCONIUM PURIFIED BY ZONE FUSION. Billion, Marc; Langeron, Jean-Paul (Centre d'Etude de Chimie Metallurgique, Vitry-sur-Seine, France). Compt. Rend., 261: 2351-4(Sept. 20, 1965). (In French).

A study was made on a bar of zirconium purified by zone fusion. For the major part of this bar, the metal had a ratio of resistivity (R_{H_2}/R_{Am}), after annealing to 715°C, $\leq 38 \times 10^{-4}$ and recrystallized at approximately 170°C. During the recrystallization there was no change in texture and the evolution of the texture for anneals at increasing temperatures was much slower up to 600°C than that of a zirconium relatively less pure. The effect of the annealing temperature on the grain growth was at first weak, then accentuated, reached a maximum, and then decreased. This phenomenon was much more marked for the fused-zone metal than for the initial metal. (tr-auth)

4414 INVESTIGATION OF CERIUM DISTRIBUTION IN CAST IRON BY MEANS OF ELECTRON PROBE. Lev, I. E.; Belai, G. E.; Taran, Yu. N.; Yatsenko, A. I. (Dnepropetrovsk Inst. of Metallurgy, USSR; Dnepropetrovsk Inst. of Ferrous Metals, USSR). Fiz. Metal. Metalloved., 20: 236-42(Aug. 1965). (In Russian).

By the means of local x-ray spectral analysis, the distribution of Ce between phases and structural components of modified cast iron was investigated. The Ce enrichment in spherical graphite inclusions, growing in contact with the liquid phase, and in colonies of austenite-graphite eutectic with finally differentiated graphite was established. In the carbide phase and in the spherical graphite of eutectic origin, the presence of Ce was not detected. (tr-auth)

4415 TEMPERATURE AND COMPOSITION EFFECTS ON THE ELECTRIC CONDUCTIVITY OF THE β AND γ PHASE IN THE TANTALUM-CARBON SYSTEM. Dubrovskaya, L. B.; Matveenko, I. I.; Gel'd, P. V. (Inst. of Chemistry, Academy of Sciences, USSR). Fiz. Metal. Metalloved., 20: 243-50(Aug. 1965). (In Russian).

The temperature and concentration effects on the electric conductivity of tantalum carbide were measured in the concentration range from $TaC_{0.21}$ to $TaC_{1.22}$ and the temperature range from 80 to 1500°K. The electric conductivity of

the carbides of all compositions studied, with the exception of the carbon-saturated monocarbide $TaC_{0.98}$, had a linear temperature dependence, which indicated the small sensitivity of the electron spectra in the carbide to temperature. (tr-auth)

4416 EFFECT OF OXYGEN ON MECHANICAL PROPERTIES OF HIGH PURITY ZIRCONIUM. Nagasaki, Ryukichi; Endo, Kuminori. Fuji Jiho, 38: 559-64(Aug. 1965). (In Japanese).

The mechanical properties of zirconium were found to be affected by oxygen concentration. By increasing the oxygen content of zirconium from 770 to 1,300 ppM, the 0.2% yield strength at 250°C increased about 55%, but an increase in oxygen content to more than 1,300 ppM had little effect on the 0.2% yield strength at higher temperatures than 250°C. It seemed that the effect of oxygen was lost at temperatures higher than 350°C. (auth)

4417 THE BEHAVIOR OF MATERIALS AT CRYOGENIC TEMPERATURES. Heltemes, E. C.; Packard, J. R. Ind. Res., 7: No. 12, 53-4; 56-8(Nov. 1965).

The development and study of suitable materials for use at ultralow temperatures in aerospace, in the life sciences, in industry, and in research are discussed. The electron motion in the lattice and its dependence on temperature and the effects of impurities are discussed. Some fundamental properties of materials include: specific heat, electric and thermal conductivity, thermal expansion, and mechanical properties. The resistivity of pure materials at room temperature and low temperature and impure metal effect on resistivity over the same range of temperature are discussed. Impurity effects on the electric properties of semiconductors at low temperatures are considered. The attraction and repulsion of atoms near absolute zero are nearly the same. These effects are discussed in terms of the expansion of different metals from 0°K to room temperature. Generally the properties of greatest concern for structural applications at cryogenic temperatures are tensile and yield strengths and ductility. Crystal structure, grain size, dislocations, and alloying effects were all found to play intricate roles in determining mechanical properties. The tendency toward brittleness in materials at cryogenic temperatures is undesirable but tensile and yield strengths usually increase as the temperature is lowered. The magnitude of strength increase depends on the material in question. (F.J.H.)

4418 THE BEHAVIOR OF MATERIALS AT HIGH TEMPERATURES. Probst, Hubert B. (Lewis Research Center, Cleveland). Ind. Res., 7: No. 12, 60-6(Nov. 1965).

The effects of recrystallization on the strengthening effects of work hardening of refractory metals are discussed, molybdenum and tungsten are considered. Hafnium, titanium, and zirconium addition to molybdenum proved to be effective in raising the recrystallization temperature. Addition of 0.1% weight of zirconium to arc-melted molybdenum increased the recrystallization temperature to 2800°F from 2150°F for unalloyed molybdenum. The strength of tungsten at 3500°F was increased by adding small amounts of alloying elements in solid solutions. Hafnium was an effective strengthener. The technique of dispersion strengthening is discussed for thoria-dispersed (TD) nickel. The stronger nickel at 2200°F could withstand ~4500 psi for 1000 hr. Unalloyed nickel would have to be restricted to a temperature no higher than ~1200°F. TD nickel displayed a strength of 4,100 psi at 2500°F, only 150°F below its melting point. The problem of thermal shock may arise, if the rate of reaching high temperature or returning is rapid. The environmental effects on materials at high temperature are discussed. Improving the oxidation resistance of metals by alloying the base with elements that resist oxidation (Cr, Al) is considered. Separation of the oxidation-prone material from its environment by covering it with a protective coating is discussed. Typical processes include flame, plasma, and slurry coating; cladding; and vapor and electrodeposition. Silicides and aluminides are effective protective coatings for refractory metals. Application of both precipitation and dispersion strengthening techniques to refractory metals for further high-temperature strength improvements is discussed. (F.J.H.)

4419 ANOMALOUS THERMAL CONDUCTIVITY OF THE RARE EARTH METALS—GADOLINIUM, TERBIUM, AND DYSPROSIUM. Gallo, C. F. (Xerox Research and Engineering, Webster, N. Y.). J. Appl. Phys., 36: 3410-13(Nov. 1965).

Recent measurements of the thermal (K) and electric (σ) conductivities of the rare earth metals (gadolinium, terbium, and dysprosium), indicate that the ratio $K\sigma^{-1}T^{-1}$ T^{-1} is considerably larger than the value predicted by the Wiedemann–Franz law. At low temperatures, a significant lattice contribution to the thermal conductivity (and possibly some magnon contribution) seems to account for the experimental results. At higher temperatures, the bipolar mechanism of heat transport is probably responsible for the observed behavior. If this interpretation is correct, other transport properties should exhibit anomalous behavior. In particular, the Nernst and Ettingshausen effects should be anomalously large and therefore these rare earth metals may be useful in devices for refrigeration or electric power generation. (auth)

4420 MAGNETOCALORIC EFFECT IN DYSPROSIUM. Hudgins, A. C. Jr.; Pavlovic, A. S. (West Virginia Univ., Morgantown). J. Appl. Phys., 36: 3628-31(Nov. 1965). (TID–21911).

The magnetocaloric effect and magnetization of a polycrystalline ellipsoid of dysprosium were measured in magnetic fields up to 20 kOe from the temperature of liquid nitrogen to room temperature. Dysprosium exhibits both heating and cooling upon adiabatic magnetization depending on its magnetic state (ferromagnetic, paramagnetic, or antiferromagnetic) and a change in state is reflected by its magnetocaloric behavior. The magnetocaloric effect was correlated with temperature, magnetization, and magnetic field intensity. These various behaviors are discussed in terms of some of the existing ideas concerning dysprosium. (auth)

4421 SHORT-RANGE ORDER IN SOME NICKEL-BASE ALLOYS. McManus, G. M. (Westinghouse Electric Corp., Pittsburgh). J. Appl. Phys., 36: 3631-3(Nov. 1965).

The first-nearest-neighbor short-range-order and size-effect coefficients were determined for the solid-solution alloys Ni + 12% Ta, Ni + 15% W, and Ni + 20% Mo by the method of x-ray diffuse scattering. In these alloys a strong preference for unlike nearest neighbors was found, with the Ni + 12% Ta, Ni + 15% W, and Ni + 20% Mo alloys having $\alpha_1 = -0.10, -0.12$, and -0.13, respectively. The corresponding size-effect coefficients for these alloys were found to be $\beta_1 = 0.017$, 0.015, and 0.000, respectively. (auth)

4422 ELASTIC CONSTANTS OF NIOBIUM FROM 4.2 deg TO 300 deg K. Carroll, Keith J. (Rice Univ., Houston, Tex.). J. Appl. Phys., 36: 3689-90(Nov. 1965).

An unrectified r-f pulse-echo method was used to find elastic constants of niobium from 4.2 to 300°K. Two cylindrical specimens were used with diameters and lengths of about 1.5 and 3 cm, respectively, and their ends polished flat and perpendicular to the [100] and [110] crystalline directions. The results are tabulated. (L.B.S.)

4423 MAGNETIC CHARACTERISTICS OF LANTHANIDE ELEMENTS COMBINED WITH TIN, LEAD, AND INDIUM. Tsuchida, T.; Wallace, W. E. (Univ. of Pittsburgh). J. Chem. Phys., 43: 3811-14(Dec. 1, 1965).

The magnetic behavior of $CeIn_3$, $CePb_3$, and the series of compounds represented by the formula $LnSn_3$ with Ln = Ce, Pr, Nd, Sm, and Gd was investigated over the temperature range from 2° to 300°K. Curie–Weiss behavior was observed in the upper portion of the temperature range for all compounds except $SmSn_3$, and effective moments were in close agreement with those expected for the free tripositive ions. The behavior for $SmSn_3$ was attributed to the contribution of the first excited multiplet ($J = 1/2$). Néel points were observed for $CeIn_3$, $PrSn_3$, $NdSn_3$, and $SmSn_3$.

Deviations from Curie–Weiss behavior at low temperatures were observed in all cases and were ascribed to antiferromagnetic ordering, crystal-field effects, and ionization of Ce in the Ce compounds into the quadripositive state. $GdSn_3$ was complex in that it showed deviation from Curie–Weiss below 40°K but had no susceptibility peak. (auth)

4424 THE EFFECT OF YTTRIUM ON THE RECRYSTALLIZATION AND GRAIN GROWTH OF TANTALUM. Kirkbride, L. D.; Basmajian, J. A.; Stoller, D. R.; Ferguson, W. E.; Perkins, R. H.; Dunning, D. N. (Los Alamos Scientific Lab., N. Mex.). J. Less-Common Metals, 9: 393-408(Dec. 1965). (LA-DC-7123).

The recrystallization and grain growth behavior of tantalum–yttrium alloys containing 14 to 72 ppm yttrium was studied. The recrystallization temperature for highly cold-worked alloys was found to be between 1500 and 1750°C for 1-hr anneals compared to 1050°C for high-purity tantalum. Little grain growth was observed in the alloys after 1-hr anneals up to 2250°C. An anneal at 1900°C for 1000 hr showed essentially no grain growth over that found for a 1-hr anneal at the same temperature. Although loss of yttrium was not observed during heat treatment, yttrium was lost during welding operations. Calculations indicated a critical concentration of ~5 ppm yttrium is required to obtain the effects observed. The elevation of the recrystallization temperature and the retardation of grain growth is shown to be due to segregation of yttrium to grain boundaries. Yttrium in the alloys in excess of the critical content is shown to segregate to dislocations and to be present as particulate matter, which has little effect on recrystallization and grain growth behavior. (auth)

4425 EFFECT OF PURITY ON THE MECHANICAL PROPERTIES OF NIOBIUM. Votava, E. (Union Carbide European Research Associates, Brussels). J. Less-Common Metals, 9: 409-15(Dec. 1965).

The change in the mechanical properties of cold-swaged niobium reduced 90% in cross section was investigated on isochronal annealing before and after electron-beam zone melting. It was found that zone-melted niobium had greater ductility, greater uniform elongation, increased work hardening, but lower strength. Furthermore, zone-melted niobium showed, after swaging and in the temperature range from 20 to 700°C, a yield point. For both kinds of niobium increased strength was found between 400 and 600°C and attributed to the influence of carbon in the samples. (auth)

4426 THE VANADIUM–GALLIUM SYSTEM IN THE REGION OF V_3Ga. Fischer, John J.; Probst, Hubert B. (Lewis Research Center, Cleveland). J. Less-Common Metals, 9: 416-22(Dec. 1965).

Melted samples were studied by x-ray diffraction and metallographic techniques after slow cooling from 1100°C. The superconducting V_3Ga phase was found to exist over a very limited compositional range. V_3Ga exists in equilibrium with either V_6Ga_5 or a vanadium solid solution depending on composition. The microstructures of samples near 75 at. % vanadium (V_3Ga) were essentially identical whether compositions were slightly gallium rich or slightly vanadium rich. Both V_6Ga and the vanadium solid solution are nonsuperconducting at 4.2°K. (auth)

4427 PHASE RELATIONS AND INTERMETALLIC COMPOUNDS IN THE SYSTEMS NEODYMIUM–ALUMINIUM AND GADOLINIUM–ALUMINIUM. Buschow, K. H. J. (Philips' Gloeilampenfabrieken, Eindhoven, Netherlands). J. Less-Common Metals, 9: 452-6(Dec. 1965).

The binary systems neodymium–aluminum and gadolinium–aluminum were investigated by thermoanalytical and metallographic methods and by x-ray diffraction. For both systems the equilibrium diagrams were constructed. The neodymium–aluminum system contained the compounds Nd_3Al, Nd_2Al, $NdAl_2$, $NdAl_3$, and $NdAl_4$. For $NdAl_4$ a transformation point was observed. The gadolinium–aluminum system contained the compounds Gd_3Al, Gd_3Al_2, GdAl, $GdAl_2$, and $GdAl_3$. For the compounds found in both systems the lattice constants are given. (auth)

4428 SOME INTERMEDIATE PHASES IN THE THORIUM–TECHNETIUM AND URANIUM–TECHNETIUM SYSTEMS. Darby, J. B. Jr.; Berndt, A. F.; Downey, J. W. (Argonne National Lab., Ill.). J. Less-Common Metals, 9: 466-8(Dec. 1965).

The intermediate phases, $ThTc_2$, U_2Tc, and UTc_2, in thorium–technetium and uranium–technetium systems, were studied. The alloys were prepared from the elements (99.9+% pure Th and U, 98+% pure Tc) by an arc-melting technique. The buttons were homogenized for one week at 900°C for U_2Tc and UTc_2 or 1100°C for $ThTc_2$ in evacuated quartz capsules and air cooled. X-ray-diffraction photographs were taken with CuK_α or CrK_α radiation. The crystal structures of $ThTc_2$, U_2Tc, and UTc_2, and the procedures used in determining the structures are discussed. (F.J.H.)

4429 ON PHASE TRANSFORMATIONS OF U_3O_8. Ermischer, W.; Hauser, O.; Schenk, M. (Zentralinstitut fuer Kernforschung, Deutsche Akademie der Wissenschaften, Rossendorf, Ger.). J. Nucl. Mater., 16: 341-3(July 1965). (In German).

The phase transformation of orthorhombic U_3O_8 was investigated at temperatures between 50 and 600°C in intervals of 50°C. It was established that between 150 and 200°C a complete transformation to a hexagonal structure occurred; this structure was stable up to 600°C. The rhombic structure reoccurred on cooling to room temperature. The retransformation of the hexagonal to the orthorhombic modification was studied as a function of the annealing temperature. The results showed that the retransformation of the hexagonal to the orthorhombic phase was not complete but that with increasing annealing temperature an increasing fraction of the hexagonal phase remained. With increased annealing time the hexagonal constituent in the U_3O_8 increased, i.e., the transformation had a significant time dependence. In annealing in argon a much smaller hexagonal constituent was obtained than during annealing in air. Studies of the effects of the cooling conditions on the residual constituents of the hexagonal modification showed that the residual constituent depended both on the annealing temperature and the annealing time as well as on the annealing conditions. (J.S.R.)

4430 GRAIN SIZE DEPENDENCE OF FRACTURE IN α-URANIUM. St. John, C. F.; Teghtsoonian, E. (Univ. of British Columbia, Vancouver). J. Nucl. Mater., 17: 111-15(Oct. 1965).

Fracture stresses of α-uranium were determined over a grain size at temperatures from −196 to 270°C. The Hall-Petch relation was found to be valid at the extremes of temperature, but inapplicable in the brittle to ductile transition region near 100°C. The results were interpreted in terms of the deformation and fracture modes and their variation over the temperature range studied. (auth)

4431 MICROSTRUCTURE AND DENSITY OF PYROLYTIC GRAPHITE. Yajima, S.; Satow, T.; Hirai, T. (Tohoku Univ., Sendai). J. Nucl. Mater., 17: 127-35(Oct. 1965).

Effects of different conditions during pyrolytic graphite preparation on the microstructure and density of the pyrolytic graphite were examined. Pyrolytic graphite was obtained by pyrolysis of commercial propane gas in the deposition temperature range of 1345 to 2215°C at pressures of 5 to 200 torr and flow rates of 280 to 1050 cm^3/min. The microstructure can be divided into fine regenerative, string, coarse, and pebble structures, which depend on the temperature and pressure, but are independent of the flow rate. These structures are closely related to the density. The density depends sensitively on the temperature and pressure and shows a minimum value in a certain condition. Three different heteromorphic phases are observed in the microstructure. (auth)

4432 SIMPLE THEORY FOR THE RELEASE OF FISSION GAS FROM POWDERS. Shaked, H. (Atomic Energy Commission, Tel-Aviv, Israel). J. Nucl. Mater., 17: 136-41(Oct. 1965).

When the fraction of gas released from a powder is so

large that the smallest particles are largely depleted, the commonly used equivalent sphere model for calculating diffusion coefficients from the experimentally measured release is not valid. An approximate model was formulated that takes into account the continuous depletion of small grains. On the basis of this model, a correction function M was derived. Diffusion coefficients obtained by using the equivalent sphere model have to be multiplied by M in order to yield the correct diffusion coefficients. (auth)

4433 THERMAL CONDUCTIVITY OF BERYLLIUM OXIDE AT 1.5 TO 300 deg K. De Goer, A. M.; Doulat, J.; Dreyfus, B. (Centre d'Etudes Nucleaires, Grenoble, France). J. Nucl. Mater., 17: 159-66(Oct. 1965). (In French).

Thermal conductivity measurements were made in the temperature range from 1.5 to 300°K on samples of sintered beryllium oxide to some of which calcium oxide was added. A quantitative analysis of the curves $\varkappa(T)$ showed that a relaxation time of the type, $\tau^{-1} = \alpha + \beta\omega + A\omega^4 + \delta\omega^2T^3$, gives a good fit to the experimental data. It proved possible to relate the coefficients of this formula to several features of the samples. For instance, it is shown that the pores of such a sintered material have an important effect on the thermal conductivity and that the solubility of CaO in these samples is very low. (auth)

4434 THE EFFECT OF UNIAXIAL COMPRESSION UPON THE TRANSFORMATION OF METASTABLE DELTA-PHASE PLUTONIUM. Hambling, P. G.; Spicer, B. R.; White, J. S. (Atomic Weapons Research Establishment, Aldermaston, Eng.). J. Nucl. Mater., 17: 172-8(Oct. 1965).

The transformation behavior of metastable δ-phase Pu-0.85 at. % Al, Pu-2.2 at. % Ce, and Pu-0.85 at. % Ga alloys, as a result of uniaxial compression, was investigated in the temperature range from 20 to 180°C. The decomposition was followed by measuring the change in the density of the specimens as a function of strain. The mode of transformation was determined by making an x-ray examination of selected specimens. (auth)

4435 THE BEHAVIOUR OF FISSION PRODUCT GASES IN URANIUM DIOXIDE. Cornell, R. M.; Williamson, G. K. (Berkeley Nuclear Labs., Eng.). J. Nucl. Mater., 17: 200(Oct. 1965).

Data previously obtained for krypton diffusion in UO_2 were analyzed and the results are shown. It was previously suggested that krypton bubbles in UO_2 migrated by a surface diffusion process. The range of observed movement x was plotted as a function of 1/r where r is the radius. The UO_2 was clearly nonstoichiometric. This would affect the diffusion coefficient. (F.J.H.)

4436 THE THERMAL EXPANSION OF UAl_3 IN THE TEMPERATURE RANGE 20 deg TO 750 deg C. Pearce, R. J. (Berkeley Nuclear Labs., Eng.). J. Nucl. Mater., 17: 201-2(Oct. 1965).

UAl_3 was prepared by a vapor-phase reaction between uranium and aluminum monochloride. The thermal expansion was measured using a high-temperature camera previously calibrated by accurate measurement of the angular positions of the knife edges. The lattice parameters were determined at temperatures up to 750°C. In a series of determinations on different specimens carried out at room temperature (20-23°C), the extrapolated parameters agreed to within ±0.0003 to 0.0005 Å. Runs were carried out with the camera evacuated to $<10^{-2}$ torr. In the first series of lattice parameter determinations the temperature could only be determined with an accuracy of ±10, this was improved to ±3°C. The lattice parameter of UAl_3 at room temperature (20°C) was measured before and after high temperature determination. Before heating, a value of 4.2651 ± 0.0003 Å was obtained but after heating the value was 4.2666 Å. (F.J.H.)

4437 THE EFFECT OF GRAIN SIZE ON THE TENSILE PROPERTIES OF MAGNOX AL80. Nagasaki, Ryukichi; Shiraishi, Kensuke (Japan Atomic Energy Research Inst., Tokyo). J. Nucl. Sci. Technol. (Tokyo), 2: 369-74(Sept. 1965).

Tensile tests were made on wires of Magnox AL80, Mg-Al alloy, and unalloyed magnesium at room and liquid nitrogen temperatures. The grain size dependence of the yield and ultimate tensile stresses were investigated. It was found that the Petch relation, $\sigma_y = \sigma_0 + kd^{-\frac{1}{2}}$, was satisfied even for specimens as slender as 1 or 2 mm diameter, though definite values of σ_0 and k were not obtained. It is thought that the preferred orientation in the wire has an influence on both σ_0 and k. Similar results were also obtained for ultimate tensile stress. The strain rate dependence of the yield and ultimate tensile stresses were also investigated. (auth)

4438 VAPOR PRESSURE AND HEAT OF SUBLIMATION OF TUNGSTEN. Szwarc, R. (Univ. of Cincinnati); Plante, E. R.; Diamond, J. J. J. Res. Nat. Bur. Stand. A, 69A: 417-21(Sept.-Oct. 1965).

The vapor pressure of tungsten was measured by the Langmuir method in the temperature range from 2574 to 3183°K using a vacuum microbalance. The least-squares line through the data, log P (atm) = 7.790 - 44680/T, yielded a second law $\Delta H_s^0(2850°K) = 204.4 \pm 2.7$ kcal/mole and $\Delta S_s^0(2850°K) = 35.64 \pm 0.97$ cal/mole deg. The equation recommended for the vapor pressure is log P (atm) = 7.933 - 45087/T based on the experimentally determined mean third law $\Delta H_s^0(298°K) = 203.5$ kcal/mole and tabulated values for the entropies and enthalpies. (auth)

4439 ELECTRICAL PROPERTIES OF NON-STOICHIOMETRIC URANIUM DIOXIDE. Iida, Shoji (Mitsubishi Atomic Power Industries, Inc., Ohmiya, Japan). Jap. J. Appl. Phys., 4: 833-8(Nov. 1965).

The electrical conductivity, drift mobility, and Seebeck voltage of uranium dioxides, UO_{2-x}, were measured over the temperature range between 77 and 1200°K and the conduction was found to be n-type. In the temperature region below about 700°K, the conductivity and drift mobility were found to increase with temperature but Seebeck voltage did not increase. The activation energies in this temperature region were smaller than the specimen having the ratio O/U > 2. The values of effective mass, m*, and coupling constant, α, were estimated to be $m^* = 1.05$ m and $\alpha = 2.81$, respectively, at room temperature, which indicates the specimen is an ionic crystal and that the hopping conduction mechanism predominates in this temperature region. In the temperature region higher than about 700°K the Seebeck voltage did not increase with rising temperature but the conductivity increased rapidly. (auth)

4440 A MECHANICAL PROPERTY EVALUATION OF Be-38 percent Al ALLOY FROM -320 TO 800F. Fenn, R. W. Jr.; Crooks, D. D.; Watts, G. H.; Neiman, A. S. (Lockheed Missiles and Space Co., Palo Alto, Calif.). Met. Eng. Quart., 5: 37-47(Nov. 1965).

Detailed studies were made on six heats of commercially produced Be-38 wt % Al alloy in the annealed temper to determine the level and reproducibility of the mechanical properties, microstructural features, and general metallurgical quality of the material. Young's modulus, tensile, compressive, shear, bearing, and bend properties were determined at temperatures between -320 and 800°F. Tensile properties at 75°F were found to be unaffected by exposure at temperatures up to 800°F for times up to 1000 hr. Sheet properties were consistently isotropic, while the extrusion properties displayed some anisotropy. Reproducibility of properties from heat to heat was investigated by statistical analysis; variations were found to be equal to or less than those reported for several commercial alloys in current use. The substantial decrease in strength in the 400°F temperature region, normally associated with aluminum alloys, was not observed for the Be-38% Al alloy. Over 50% of the room-temperature tensile properties was retained at 800°F. (auth)

4441 CONTRIBUTION TO THE SYSTEM MERCURY-THORIUM. Ettmayer, P. (Technische Hochschule, Vienna). Monatsh. Chem., 96: 443-9(1965). (In German).

Measurements of the pressure of Hg over alloys of Hg with Th of various compositions indicated the existence of three intermetallic compounds, $ThHg_3$, $ThHg_2$, and ThHg.

The vapor pressure isotherms showed definite inconsistencies at the compositions 25 at. % Th, 33 at. % Th, and 50 at. % Th. It was possible to obtain a pure compound by interrupting the pressure-controlled distillation from a Hg-rich alloy at the moment of a sharp drop in the Hg vapor pressure. At the point of sudden transition of the vapor pressure isotherms a pure and homogeneous phase were obtained. Thus, it was possible to determine the composition of this phase with a precision that could not be obtained with other methods. In addition, the system remained in a state of equilibrium. Following this technique, $ThHg_3$, $ThHg_2$, and ThHg could be prepared. The structures of $ThHg_3$ and $ThHg_2$ were determined and some indications as to the correct structure of ThHg were obtained. Unit cell dimensions are given from x-ray diffraction data for $ThHg_2$. Its structure is of the AlB_2 type. (BBB)

4442 ON THE ALLOYS OF NICKEL WITH LITHIUM, BARIUM, AND STRONTIUM. Takeuchi, Yo; Mochizuki, Ken; Watanabe, Masaharu; Obinata, Ichiji (Tohoku Univ., Sendai). Nippon Kinzoku Gakkaishi, 29: 801-6(1965). (In Japanese).

The nickel–lithium, nickel–barium, and nickel–strontium systems were investigated using structure observation, x-ray studies, and thermal and chemical analyses. In the nickel–lithium and nickel–barium systems no intermetallic phase was found. Both constituents of these alloys were only partially miscible in the liquid state and formed a miscibility gap in a broad concentration range. Nickel, for example, could dissolve at 1200°C only 0.4% lithium and only 0.08% barium. Nickel was dissolved in barium melts at 1200°C to 20.97% and in lithium melts at the same temperature up to 3.47%. In the nickel–strontium system a previously unknown intermetallic compound occurred, which was formed at 860°C through the peritectic reaction between the primary nickel crystals and the residual melt. This intermetallic phase, whose composition is probably NiSr (59.89% Sr and 40.11% Ni), crystallized in a hexagonal structure with the lattice constants a = 3.332 and c = 7.009 Å and c/a = 2.112. The NiSr phase and strontium formed a eutectic system. The eutectic point was at 92% strontium and at 660°C. (tr-auth)

4443 ON THE EFFECT OF THE CRYSTALLINE STRUCTURE ON FATIGUE: COMPARISON BETWEEN BODY-CENTERED METALS (Ta, Nb, Mo AND W) AND FACE-CENTERED AND HEXAGONAL METALS. Ferro, A. (Univ., Torino, Italy); Mazzetti, P.; Montalenti, G. Phil. Mag. (8), 12: 867-75(Oct. 1965).

The fatigue resistance for several body-centered pure metals (Nb, Ta, Mo and W) was determined. The form of the fatigue curves are similar to those of iron and, as in this case, the fatigue limit is reached before 10^7 cycles. It is also more generally confirmed that, when compared to some suitable static property, such as the ultimate tensile strength of the hardness, the fatigue of body-centered structures is much higher (FL/UTS 0.5–0.8) than that of face-centered or hexagonal structures such as nickel or cobalt, (FL/UTS 0.3–0.4). The difference has to be related to the different behavior of dislocations in the former structures because of the very high friction stress and easy cross slip characteristic of bcc metals. (auth)

4444 INTERACTION OF CARBON MONOXIDE WITH TANTALUM. Gasser, R. P. H.; Thwaites, R. (Oxford Univ.). Trans. Faraday Soc., 61: 2036-43(Sept. 1965).

The sticking probability of carbon monoxide on a clean tantalum filament was found to be 0.14 between −70 and 20°C. The pumping action of the filament above 2400°K had first-order kinetics. The reversible absorption of carbon monoxide by a tantalum filament was established at pressures between 2×10^{-8} and 1×10^{-6} torr and temperatures between 790 and 1960°K. First-order kinetics for the initial absorptive uptake were found. (auth)

4445 TEMPERATURE DEPENDENCE OF THE CRITICAL SHEAR STRESS OF MOLYBDENUM SINGLE CRYSTAL. Lung, Chi-wei; Ho, Tsing; Chou, Chin. Wu Li Hsueh Pao, 21: 1264-75(June 1965). (In Chinese).

The temperature dependence of the critical resolved shear stress (CRSS) of molybdenum single crystal was investigated. It was found that the logarithm value of CRSS varies linearly with the absolute temperature which is not in agreement with Cottrell-Bilby's relation based on atmosphere locking. Assuming that a chemical exchange bond between the impurity and dangling atoms would be weakened with rise in temperature and using the Morse function, the experimental linear $\ln \sigma$-T relation could then be accounted for and a slope of the right order of magnitude established. (auth)

4446 A STUDY ON RUPTURE PROPERTIES OF LARGE WELDED SPECIMENS OF HT 70 STEEL FOR NUCLEAR PRESSURE VESSELS (REPORT 2). SOME ASPECTS OF ITS CREEP RUPTURE AND HIGH TEMPERATURE PROPERTIES AS SYNTHETIC HAZ SPECIMENS. Okane, Isao (National Res. Inst. Metals (Tokyo)). Yosetsu Gakkaishi, 34: 903-10(Sept. 1965). (In Japanese).

The creep rupture configuration of large welded specimens, having the shape as welded, was different from that of conventional small welded specimens cut off from the weld joint. The initiation of cracks in rupture occurred at the toe of the weld metal and at the intersection of the bonds in both sides of the welded metal. The crack propagated along the grain boundary of austenite in the bond in the heat-affected zone of the base metal. The mechanism of creep rupture for large welded specimens was investigated in high-temperature tensile tests and creep rupture tests at 500°C for synthetic HAZ specimens. The specimens were synthesized with a coarse-grain part near the bond (maximum heating temperature 1,350°C), a fine-grain part (maximum heating temperature 900°C), and an intermediate part (maximum heating temperature 1,100°C) in the heat-affected zone of the base metal. High-temperature tensile and creep rupture properties of the coarse-grain part near the bond were inferior to the other parts and rupture occurred in austenite boundary. The energy required for rupture of the coarse-grain part near the bond was smaller than that of the other parts above 400°C. Consequently, the creep rupture of large welded specimens may occur along the grain boundary of austenite of the bond in the heat-affected zone of base metal. (auth)

4447 ON THE CRYSTAL STRUCTURE OF THE PHASES AgSm, Ag_3Sm. Steeb, Siegfried, Godel, Dieter (Max-Planck-Institut fuer Metallforschung, Stuttgart). Z. Metallk., 56: 612-15(Sept. 1965). (In German).

The existence of two intermetallic phases, Ag_3Sm and AgSm, was derived from Guinier patterns at room temperature and x-ray patterns obtained at various temperatures up to 730°C in a high-temperature camera. Ag_3Sm extends from 6 to 49 at. % Sm and has a primitive orthorhombic unit cell with a = 7.995, b = 7.843, and c = 7.204 kX at room temperature. The coefficient of linear thermal expansion between 20 and 680°C amounts to $1.3 \cdot 10^{-5}$ kX/°C. The unit cell contains approximately 20 atoms. AgSm exhibits CsCl-type crystal structure with a = 3.662 kX in accordance with a previous investigation. It extends from 37 to 88 at. % Sm. A phase diagram previously derived is presented in accordance with the x-ray results. (auth)

4448 STRUCTURAL AND MAGNETIC PROPERTIES OF SOME 1:1 INTERMETALLIC COMPOUNDS OF LANTHANIDE METALS WITH NICKEL, COPPER, AND SILVER [Thesis]. Walline, Robert Elm. Pittsburgh, Univ. of Pittsburgh, 1964. 123p.

The structural and magnetic properties of intermetallic compounds characterized by the formula LnA are reported. Here Ln represents Y or any of the trivalent lanthanide metals except La, Pm, or Lu and A represents either Ni, Cu or Ag. The LnNi series is ferromagnetic with the exception of YNi and CeNi, which are Pauli paramagnetic. The Ni appears to have no magnetic moment and the Ce is in the +4 state. The LnNi series is orthorhombic with a structure transition between TbNi and DyNi from the CrB structure to the FeB structure. The saturation moments obtained at liquid helium temperature are lower than the free tripositive ion values. The effective moments determined from the paramagnetic region are in good agreement

with the free tripositive ion values. Curie temperatures for the ferromagnetic compounds range from 8°K for TmNi to 71°K for GdNi. The LnCu series from CeCu to SmCu crystallizes in the FeB structure. The other members of the series crystallize in the CsCl structure. The LnCu series is antiferromagnetic with the exception of YCu which is a Pauli paramagnet and PrCu and NdCu whose behavior cannot be unambiguously interpreted from the magnetic measurements. The nature of the transitions in the LnCu compounds cannot be fully elucidated on the basis of the bulk magnetic measurements alone. Neel temperatures range from 2.7°K for CeCu and 115°K for TbCu. Effective moments determined from the paramagnetic region are in good agreement with the free tripositive ion values. The LnAg series crystallizes in the CsCl structure. YAg has a very slight temperature dependent paramagnetism while CeAg and PrAg are ferromagnetic. The other members of the series appear to be antiferromagnetic with Neel temperatures ranging from 138°K for GdAg to 10°K for TmAg. Effective moments determined from the paramagnetic region are in good agreement with the free tri-positive ion values. (Dissertation Abstr.)

4449 THE CLUSTERING OF OXYGEN IN SOLID SOLUTION IN NIOBIUM [Thesis]. Gibala, Ronald. Urbana, Ill., Univ. of Illinois, 1965. 129p.

Over the oxygen concentration range 0.1 to 1.5 at. %, the anelastic behavior of niobium–oxygen solid solutions is found to be best described as the sum of either three or four discrete relaxation processes, depending upon the oxygen concentration in this range. The relaxations are identified as stress-induced ordering processes involving single, unassociated oxygen atoms (the Snoek effect), clusters of two oxygen atoms (pairs), clusters of three oxygen atoms (triplets), and clusters of four oxygen atoms (quadruplets). The identifications are made by noting the constancy of the relaxation times of these processes over the composition range studied and by observing that the law of mass action apparently holds when the component relaxation strengths are used as measures of the cluster concentrations. The binding energies for the pairs, triplets, and quadruplets of oxygen in niobium are determined from the temperature dependence of the relaxation strengths, to be 1.6, 4.2, and 6.1 kcal/mole, respectively. (Dissertation Abstr.)

4450 DIFFUSION OF ^{133}Xe IN UC NUCLEAR FUEL AS A FUNCTION OF COMPOSITION AND RADIATION DOSE [Thesis]. Papathanassopulos, K. Brunswick, Ger., Tech. Univ., 1964. 67p. $2.00 Gmelin, AED-DISS. 64-573.

Diffusion of ^{133}Xe in UC in the temperature range between 950 and 1830°C was studied by two methods. Continuous measurements were made in a high vacuum and discontinuous measurements with a gas stream. Results from both methods were in agreement. The activation energy of Xe diffusion was 54 to 82 kcal/mole. (Gmelin Inst.)

4451 REDKIE I REAKOZEMEL'NYE ELEMENTY V TEKHNIKE. (Rare Elements and Rare Earths in Technology). Samsonov, G. V. (ed.). Kiev, Naukova Dumka, 1964. 132p.

Fourteen articles are included on: the content of Ce in cast iron; reactions of rare earths with elements dissolved in C–Fe alloys; the use of rare earths during the smelting of open-hearth steel and for alloying electrode wires; the effect of dyes containing rare metals and their oxides on castings; the use of rare metals in ceramics and glass; the production and properties of carbides of La, Sc, and Y, and of nitrides, sulfides, and phosphides of rare earths and rare metals; the transformation of the magnetic properties of the spinel structure. (M.J.T.)

4452 GAS RELEASE METHODS USED IN THE HARWELL METALLURGICAL POST-IRRADIATION LABORATORY. Venables, J. H. (Atomic Energy Research Establishment, Harwell, Eng.). pp 267-78 of International Symposium on Working Methods in High Activity Hot Laboratories. Vol. I. Paris, Organization for Economic Cooperation and Development, 1965.

Several methods used in the post-irradiation laboratories of the Metallurgy Division at Harwell to obtain samples of gas from encapsulated or unclad irradiated specimens are described. The remote piercing of capsules under high vacuum and the extraction of gas at temperatures up to 2500°C from a wide range of materials and capsules is regularly carried out. The methods of piercing the capsules, measuring the volume and pressure of the extracted gas, and collecting the gas for subsequent analysis are described and the precautions necessary in gas release experiments at pre- and post-irradiation stages are discussed. (auth)

4453 ELECTRICAL RESISTIVITY OF ELECTRON-BEAM ZONE-REFINED TUNGSTEN SINGLE CRYSTALS BETWEEN 1.4 AND 27 deg K. Berthel, K. H. (Inst. of Applied Physics of Pure Substances, Dresden). pp 116-26 of Physics and Techniques of Low Temperatures. Prague, Publishing House of the Czechoslovak Academy of Sciences, 1964.

The electric resistivity of tungsten is studied between 1.4 and 27°K. Samples of 1 to 3 times electron-beam zone-refined tungsten single crystals were used. The resistance was measured according to a direct-current method. The resistance ratio is plotted as a function of current. The effect of surface on electric resistivity, from the additional scattering of the charge carriers on the surface of the sample, is considered. The residual resistance and the ideal resistance ratio are each plotted as a function of temperature. Magnetoresistance in a transverse magnetic field is also discussed. (J.F.P.)

4454 AN EXAMINATION OF HENRY'S LAW IN LIQUID METAL SYSTEMS WITH INFINITELY DILUTE SOLUTIONS OF OXYGEN. Tankins, Edwin S. (Naval Air Engineering Center, Philadelphia). 34p. (CONF-650502-6). Gmelin, AED-CONF-65-169-7.

From Electrochemical Society, San Francisco.

Thermodynamic properties of dilute solutions of oxygen in various liquid systems were investigated and evidence is presented that Henry's Law is obeyed by oxygen within experimental error over a substantial composition range. An intensive investigation showed that oxygen obeys Henry's Law up to 0.50 at. % in the pure metals, Fe, Co, Ni, and Cu at 1550°C. Further experiments were made over a wide range of oxygen for binary alloys at 1550°C and Henry's Law was found to be obeyed. In light of these results, the thermodynamic studies utilizing the equilibrium constant are meaningful. The data of other investigators were analyzed and their probable error was of the order of the deviation from Henry's Law that they claimed. Various reasons that can account for their deviations are postulated and discussed. Some of the alloy systems such as Fe–Co and Fe–Ni showed a minimum in the composition range of 0.70 to 0.80 mole fraction Co and Ni. This nonideal behavior in the oxygen is discussed in light of reported physical properties in the literature. (auth)

4455 IMPROVEMENTS IN TANTALUM-BASE ALLOYS. (to General Electric Co.). British Patent 1,007,091. Oct. 13, 1965. Priority date Oct. 14, 1963, United States.

A Ta-base alloy consisting of 1 to 5 wt % Re, 8 to 16 wt % W and Re combined, and the balance Ta is reported to have a tensile strength at 3500°F in excess of 10,000 psi. (B.L.M.)

4456 IMPROVEMENTS RELATING TO HEAT TREATMENT PROCESSES FOR MAGNESIUM ALLOYS. Greenfield, Peter; Smith, Colin Charles; Taylor, Albert Major (to English Electric Co.). British Patent 1,007,139. Oct. 13, 1965. Filed Mar. 22, 1961.

A heat-treatment process for a Mg-base alloy containing between 0.05 and 1 wt % Zr includes heating the alloy in a furnace at a temperature of between 550 and 640°C for a period of between 70 and 100 hours in an atmosphere of CO_2 and cooling in the furnace. The creep rate of such a heat treated alloy is about 2×10^{-7} in./in./hr at 400°C under a load of 200 lb/in.^{2} as compared to 8×10^{-4} in./in./hr for an untreated alloy. (B.L.M.)

Radiation Effects

See also CHEMISTRY — Radiation Chemistry

Refer also to abstract 4344.

4457 (EURAEC–1474) THE DEVELOPMENT OF A NEW METHOD TO DETERMINE THE BRITTLE-DUCTILE TRANSITION IN STEEL USING SMALL SPECIMENS, IN PARTICULAR WITH RESPECT TO EMBRITTLEMENT BY IRRADIATION. Special Technical Progress Report M-65-876-30010, April 1, 1964–September 30, 1965. van Elst, H. C. (Nijverheidsorganisatie (TNO), The Hague (Netherlands)). Contract 060-64-11-TEEN. 28p. (EUR–2395). Dep. mn; CFSTI $2.00 cy, $0.50 mn.

Work Performed under United States–Euratom Joint Research and Development Program.

The nil ductility temperature, according to the drop weight test was determined for 5 reactor pressure vessel steels. No clear relation with the earlier determined crack arrest temperature in the isothermal Robertson test was found to exist. However, this was not expected, as is discussed. The dependence of the arrest temperature on the thickness of the test plate was investigated for the HSB 55 C steel. As the Charpy-V and stress wave attenuation test data had been determined for these steels already, the relation between arrest temperature for a certain thickness and the corresponding energy absorption level or percentage crystallinity of the fracture appearance (or deformation level) in the notch impact and (or) stress wave attenuation at that arrest temperature was established. A method for predicting the shift in arrest temperature by irradiation is also described. The instrumentation of the notch impact test was improved and stress-time, strain-time and stress-strain diagrams of this test can now be satisfactorily recorded. (P.C.H.)

4458 (GA–6485) DESCRIPTION AND RESULTS OF THE P9 COATED PARTICLE IRRADIATION EXPERIMENT. Luby, C. S. (General Atomic, San Diego, Calif. John Jay Hopkins Lab. for Pure and Applied Science). Sept. 15, 1965. Contract AT(04-3)-167. 44p. Dep. mn; CFSTI $2.00 cy, $0.50 mn.

Twelve types of coated fuel particles were irradiated to burnups of 10 to 13% fissions per initial heavy metal atom at temperatures of 1350 to 1700°C. Postirradiation examination indicated that coating failure for these particles decreased with increasing coating thickness (with constant fuel particle diameter) and that a minimum coating-thickness to fuel-particle-diameter (T/D) ratio of 0.5 may be required for stability under these high temperature and high burnup rate irradiation conditions. Thick buffer coatings appeared to impart greater radiation stability than thin buffer coatings (with the same total coating thickness). Isotropic-isotropic coatings appeared roughly equivalent in radiation stability to buffer-isotropic coatings. (auth)

4459 (GEAP–4850) IRRADIATION PERFORMANCE OF UO_2 PRODUCED BY ALTERNATE FABRICATING PROCESSES. Baroch, C. J.; Megerth, F. H. (General Electric Co., San Jose, Calif. Atomic Power Equipment Dept.). Apr. 1965. Contract AT(04-3)-189. 112p. Dep. mn; CFSTI $3.00 cy, $0.75 mn.

Sixteen fuel rods fabricated by coextrusion of UO_2 and stainless steel, three fuel rods containing low-temperature sintered pellets, and twelve fuel rods containing UO_2 extrusions were irradiated in the Vallecitos Boiling Water Reactor (VBWR). Both destructive and nondestructive examinations of the irradiated and unirradiated fuel rods were used to evaluate the performance of these fuel rods prepared by alternate fabricating processes. Although the target burnups of 2.75×10^{20} fissions per cc (10,000 Mwd/T) were not achieved, some significant data were obtained regarding the performance of these rods. The over-all performance of the coextruded fuel rods, the fuel rods containing low-temperature sintered pellets, and the fuel rods containing the UO_2 extrusions to exposures of 1.92×10^{20}, 0.72×10^{20}, and 0.63×10^{20} fissions per cc respectively, compared favorably with pellet fuel operated in identical modes. From the results of the experiments, the justification for the use of coextruded rods, UO_2 extrusions, and/or low-temperature sintered pellets (LTSP) must be based on factors other than initial irradiation performance. Because of the low power levels at which all of the rods operated, no grain growth of the UO_2 was expected nor observed. The amounts of fission gases released from the coextruded rods, UO_2 extrusions, and LTSP were comparable to amounts released from conventional UO_2 pellets. The fracturing of the LTSP was somewhat more severe than conventional pellets; however, this fracturing did not impair the operation of the rods. (auth)

4460 (ORNL–3870, pp 140-5) MECHANICAL PROPERTIES. Weir, J. R. Jr. (Oak Ridge National Lab., Tenn.).

The embrittlement of stainless steels at elevated temperatures by irradiation was traced to He from not only the thermal neutron reaction with ^{10}B but also fast neutron reactions with the major components. Consistent with this observation, the postirradiation ductility was improved by several methods: decreasing the grain size, increasing the amount of carbide precipitate, decreasing the B content, and alloying with 0.2% Ti. No significant effect on the mechanical properties of aluminum alloy 6061 irradiated to doses greater than 10^{20} neutrons/cm^2 was found. (auth)

4461 (REIC-Memo–28) RADIATION EFFECTS ON PROPELLANTS AND EXPLOSIVES: AN ANNOTATED BIBLIOGRAPHY. Gilmour, B. A. (comp.) (Radiation Effects Information Center, Battelle Memorial Inst., Columbus, Ohio). Oct. 29, 1965. Contract W-7405-eng-92. 31p. Dep. mn; CFSTI $2.00 cy, $0.50 mn.

References (153) are given to reports published since 1962. The references are listed alphabetically according to corporate author. (P.C.H.)

4462 EFFECT OF NEUTRON BOMBARDMENT ON THE KINETICS OF SOME RECONSTRUCTIVE PHASE TRANSFORMATIONS. Roy, Rustum; Bushmer, Charles P. (Pennsylvania State Univ., University Park). Amer. Mineral., 50: 1473-7(Sept. 1965).

Quartz, cristobalite, PbO, γ-Ca_2SiO_4, and SiO_2 glass were irradiated with neutrons. Radioinduced transformations with positive volume change were observed in quartz and transformations with negative volume change were observed for the other materials. No marked change was observed in the rate of the quartz → cristobalite transition after neutron irradiation to a total flux of 2.4×10^{19} n/cm^2. Radioinduced defects had a marked effect on the reconstructive quartz → coesite transition in that conversion proceeded twice as fast after exposure of the quartz to a total flux of 2×10^{19} n/cm^2. The data indicated a marked influence of neutron irradiation on the rate of devitrification of SiO_2 glass under the pressure-temperature conditions of the coesite stability field. (M.C.G.)

4463 STUDY OF THE EFFECT OF ELECTRON IRRADIATION ON PIEZOELECTRIC QUARTZ FILMS. Felden, Marceau; Comets, Jean-Claude; Haug, Robert (Laboratoire de Physique Theorique et Nucleaire, Nancy). Compt. Rend., 261: 1841-4(Aug. 23, 1965). (In French).

The variations of the resonance frequency of two different cuts of quartz film exposed to electron irradiation were studied. A theoretical interpretation that can be generalized is given for the kinetics of the creation of faults. (tr-auth)

4464 THE BEHAVIOR OF MATERIALS EXPOSED TO RADIATION. Feng, Paul Y. (Illinois Inst. of Tech., Chicago). Ind. Res., 7: No. 12, 84-9(Nov. 1965).

Bombarding a material with radiation causes chemical interactions or atomic rearrangement. Radiation is used to sterilize food and medical supplies, improve the properties of existing materials, and create new products. Radioinduced polymerization of organic compounds is discussed. Radiation sources and their uses are discussed. Radioinduced inactivation of cells and decomposition of organic systems are considered. Radiation effects on inorganic compounds are also discussed. Bombardment of

materials with heavy particles can also result in the particles becoming entrapped to act as impurities. In the case of neutron irradiations, impurities are created through nuclear transmutations caused by neutron capture. (F.J.H.)

4465 THE INFLUENCE OF X RADIATION ON THE ELECTROPHYSICAL PROPERTIES OF GERMANIUM AND GERMANIUM p-n TRANSITIONS. I. EFFECTS OF SOFT IRRADIATION ON THE ELECTRIC CONDUCTIVITY OF GERMANIUM. Krivov, M. A.; Malyanov, S. V. (Kuznetsov Inst. of Physics and Tech., Academy of Sciences, Siberian SSR). Izv. Vyssh. Ucheb. Zavendenii, Fiz., No. 4, 156-65 (1965). (In Russian).

The effects of soft x radiation on the electrophysical properties of germanium were investigated. Equations describing the relaxation of excess concentrations of carrier currents during collision recombination were derived. The gradients of excess concentration of carrier currents throughout the sample volume during irradiation were calculated. Experimental proof of collision recombination in germanium under x irradiation is presented. (J.S.R.)

4466 DETERMINATION OF THE MEAN SIZE OF DISORDERED REGIONS INDUCED IN GERMANIUM BY FAST-NEUTRON BOMBARDMENT AT LOW TEMPERATURE. Nguyen Van Dong (Centre d'Etudes Nucleaires de Saclay, Gif-sur-Yvette, France). J. Appl. Phys., 36: 3450-2(Nov. 1965).

Thermal conductivity measurements were performed on germanium at 80°K during fast-neutron bombardment. By using Callaway's formula it is established that the change in thermal conductivity can be related to the size of disordered regions by a simple expression. From experimental data, it is found that the mean radius of disordered regions is about 70 Å. (auth)

4467 ELECTRON MICROSCOPE OBSERVATION OF HIGH-ENERGY-NEUTRON-IRRADIATED GERMANIUM. Bertolotti, M.; Papa, T.; Sette, D.; Vitali, G. (Univ., Rome). J. Appl. Phys., 36: 3506-12(Nov. 1965).

The damage regions predicted by Gossick in n-type germanium irradiated with fast neutrons were directly observed with an electron microscope. The technique employed and the characteristics of these regions are described. (auth)

4468 INFRARED PROPERTIES OF 40-60 Mev ELECTRON-IRRADIATED GERMANIUM. Becker, J. F.; Corelli, J. C. (Rensselaer Polytechnic Inst., Troy, N. Y.). J. Appl. Phys., 36: 3606-9(Nov. 1965).

The infrared properties of germanium containing low oxygen concerntration ($<10^{16}$ cm^{-3}) and high oxygen concentration ($>10^{17}$ cm^{-3}) were studied after irradiation at $T \leq 25$°C by 40- to 60-Mev electrons. One cold-temperature irradiation at 125°K was also performed on a high oxygen concentration germanium sample. The germanium samples that were n type initially exhibit p-type infrared properties in the 2- to 8-μ wavelength range after being converted to p type by the irradiation. Germanium containing high oxygen concentration exhibits new vibrational bands in the 9- to 16-μ wavelength range which are associated with oxygen-defect complexes. No radiation-induced bands from 9 to 16 μ are observed in oxygen-free germanium. Detailed isochronal annealing experiments (up to ~700°K) were performed on all samples. Strong evidence is given which shows that one of the oxygen vibrational bands induced in germanium (at 618 cm^{-1}) appears to be a single oxygen atom plus a vacancy defect which corresponds to the comparable defect found in silicon, namely the silicon A center. (auth)

4469 AN X-RAY STUDY OF FISSION FRAGMENT DAMAGE IN STEELS. Smith, B. E. (Atomic Energy Research Establishment, Harwell, Eng.). J. Nucl. Mater., 17: 167-71(Oct. 1965). (AERE-R-4546).

Lattice parameter measurements were made on steels bombarded with fission fragments at ~60°C. The results for one austenitic steel (Cr, 20, Ni, 20, and Nb, 0.44 wt %) are discussed in conjunction with published results obtained by electron microscopy and are considered consistent with the hypothesis that the proportion of small defects present in this steel is greatest when irradiation dose rates are high. In two other austenitic steels (Cr, 18 and Ni, 37 wt %) and (Cr, 18 and Ni, 12 wt %) and a ferritic steel (Cr, 15 and Ni, 5 wt %) a measurable proportion of small defects was present after irradiation at a dose rate intermediate between the two rates used for the 20/20 austenite. (auth)

4470 RELATIVE EFFICACY OF VARIOUS TYPES OF TEXTURE MEASUREMENTS AS MEANS OF PREDICTING IRRADIATION-GROWTH IN URANIUM. Slattery, G. F.; McLeish, J. A. (United Kingdom Atomic Energy Authority, Preston, Eng.). J. Nucl. Mater., 17: 192-9 (Oct. 1965).

Indices for predicting anisotropic irradiation growth in uranium based on the pre-irradiation measurements of thermal expansion, electrical resistivity, and x-ray diffraction were correlated with the dimensional changes encountered in uranium irradiated in the burnup range 0.04 to 0.12% heavy atoms at a temperature of 260 ± 5°C. The specimens were taken from the rim and core of uranium rods and comprised core electropolished, rim electropolished, and rim machined groups. The correlation coefficients between actual irradiation growth and that predicted from the indices of expansivity and resistivity were highly significant but that from the x-ray index was rather less so. Regression equations for predicting radio-induced length change were derived from analyzing the experimental data and these were found to be superior for prediction purposes to the growth indices in this range of burnup. In view of the different textures and irradiation behaviors of the three group classifications, it was recommended that prediction equations derived separately for each group of specimens, be used. (auth)

4471 FISSION GAS RELEASE FROM NUCLEAR FUELS. II. RELEASE DURING LOW TEMPERATURE, LOW DOSE IRRADIATION. Osawa, Yasutaka (Mitsubishi Atomic Power Industries Inc., Omiya-shi, Japan). J. Nucl. Sci. Technol. (Tokyo), 2: 296-303(Aug. 1965).

The release behavior of fission gases in U-metal, UO_2, and uranium carbides, irradiated at a relatively low temperature (below 100°C) to low dosage, was studied by out-of-pile experiments. It was found that fission gas (^{133}Xe) released from a specimen by fission fragment recoil is mostly captured in the wall of the irradiating capsule or in the capsule support material. The amount of fission gas released into the void space of the capsule is proportional to the surface area and to the fuel burnup, and is controlled by a knock-out release mechanism. The number of U atoms considered to take part in the knock-out mechanism by evaporation or displacement due to the intrusion of a recoil fission fragment, is estimated to be $1.4 \times 10^5 \sim 2.7 \times 10^5$ atoms for U-metal and $5 \times 10^4 \sim 10 \times 10^4$ atoms for UO_2 and uranium carbides. (auth)

4472 A PRELIMINARY EXPERIMENT ON RADIAL DISTRIBUTION OF ^{137}Cs, ^{89,90}Sr AND ^{95}Zr IN SINTERED URANIUM DIOXIDE PELLET. Murata, Toshifumi; Wolschrijn, R. A. (Hitachi Research Lab., Tokyo). J. Nucl. Sci. Technol. (Tokyo), 2: 315-24(Aug. 1965).

The determination of the radial distribution of fission products (Cs, Sr, and Zr) in neutron irradiated UO_2 pellets. The results obtained by gradual dissolution of a pellet are given. The fission products distribution was also determined by micro-sampling along the cross-sectional surface of a UO_2 pellet. (auth)

4473 THE INFLUENCE OF THE SCATTERING LAW ON THE RADIATION DAMAGE DISPLACEMENT CASCADE. Robinson, Mark T. (Atomic Energy Research Establishment, Harwell, Eng.). Phil. Mag. (8), 12: 741-65(Oct. 1965). (AERE-R-4908).

The Laplace transform technique was used to develop asymptotic solutions to the integral equations describing the radiation damage displacement cascade, for scattering laws whose symmetrical parts are functions of the relative transferred energy alone. The solutions are presented explicitly for the truncated Coulomb approximation and for

a scattering law varying as an inverse power of the transferred energy. The results indicate that the scattering law is rather more significant in determining the number of defects produced during the irradiation of solids than has been previously suggested. The influence of channeling on the cascade is discussed, but appears to be less important than indicated by hard-core scattering models. The asymptotic calculation agrees very well with the experiments of Coltman et al., as well as with the machine calculations of Beeler and Besco. (auth)

PHYSICS

General

Refer also to abstracts 4037, 4141, and 4311.

4474 (ANL–7081) PHYSICS DIVISION SUMMARY REPORT. Annual Review, April 1, 1964–March 31, 1965. (Argonne National Lab., Ill.). Contract W-31-109-eng-38. 195p. Dep. mn; CFSTI $6.00 cy, $1.00 mn.

Separate abstracts were prepared for the 11 included sections. (M.O.W.)

For abstracts of individual sections see: 4215, 4475, 4491, 4535, 4821–4826, and 4936.

4475 (ANL–7081, pp 95–119) THEORETICAL PHYSICS. (Argonne National Lab., Ill.).

A review of theoretical work is presented for nuclear spectroscopy, computer programming, statistical properties of nuclear states, transitions, and cross sections, density of levels with high angular momentum in excited nuclei, the influence of experimental limitations on the accuracy of the theory of fluctuations in nuclear cross sections, Monte Carlo tests of techniques for the determination of parameters from fluctuations of measured nuclear cross sections, analytic criteria for selecting an optimum set of measurements, the effect of long-range perturbations in scattering, inclusion of Mott–Schwinger scattering in optical model calculations, general theory of scattering, relativistic theory of multiparticle scattering, consistency of relativistic particle theories, internal symmetry and Lorentz invariance, rigorous symmetries of elementary particles, quantum theory of measurement, studies of hypernuclei and the interactions of Λ particles, and the origin of the geomagnetism. (M.O.W.)

4476 (IS–1200(Sect. P)) PHYSICS DIVISION. (Ames Lab., Iowa State Univ. of Science and Tech.). 78p.

Research and development progress is summarized on high energy physics, low energy nuclear physics, solid state physics, thermal and thermodynamic properties of solids, and semiconductors and compounds with variable stoichiometry. (J.R.D.)

4477 (LA-DC–7289) A CYLINDRICAL EXPLOSIVE FLUX-COMPRESSION SYSTEM. Caird, R. S.; Garn, W. B.; Thomson, D. B.; Fowler, C. M. (Los Alamos Scientific Lab., Univ. of California, N. Mex.). [1965]. Contract W-7405-eng-36. 10p. (CONF-650937–2). Dep. mn; CFSTI $1.00 cy, $0.50 mn.

From Conference on Megagauss Magnetic Field Generation by Explosives and Related Experiments, Frascati, Italy.

A simple device for producing megagauss magnetic fields consists of a hollow resistive metal cylinder with a ring of explosive around it. An initial axial field is produced within the cylinder by a pair of coils situated on either side of the explosive. The basic techniques and some results were described in earlier publications. Further developments of these techniques and more recent results are presented. An extensive series of shots using stainless steel cylinders with a 1.6 mm wall shows that field compression ratios in the range of 120–150 are attainable reliably within a 2.5 mm diameter. Fields as high as 5.4 MG were measured starting with initial fields of 28 kG. A 300 kJ capacitor bank allows still higher initial fields with correspondingly greater final fields. Fields in excess of 6 MG were measured with stainless steel liners. Coil construction problems are discussed. (auth)

4478 (TID–22179) QUARTERLY PROGRESS REPORT NO. 78. Zimmermann, H. J.; Harvey, G. G. (Massachusetts Inst. of Tech., Cambridge. Research Lab. of Electronics). July 15, 1965. Contract AT(30-1)-1842. 298p. Dep. mn; CFSTI $6.00 cy, $1.50 mn.

Separate abstracts were prepared for sections on general physics and plasma dynamics. No abstract was prepared for the third of three sections. This section is concerned with communications sciences and engineering. (J.R.D.)

For abstracts of individual sections see: 4479 and 4948.

4479 (TID–22179, pp 1–83) GENERAL PHYSICS. (Massachusetts Inst. of Tech., Cambridge. Research Lab. of Electronics).

Research and development are reported on molecular beams, microwave spectroscopy, radio astronomy, optical and infrared spectroscopy, geophysics, noise in electron devices, physical electronics and surface physics, and physical acoustics. (J.R.D.)

4480 (UCRL–11802) ANALYSIS OF ELLIPTICALLY POLARIZED LIGHT. Muller, Rolf H.; Mowat, J. Richard (Lawrence Radiation Lab., Univ. of California, Berkeley). Oct. 1965. Contract W-7405-eng-48. 115p. Dep. mn; CFSTI $4.00 cy, $0.75 mn.

The measurement of elliptically polarized light results in quantities from which the characteristics of the polarization must be computed. Equations are derived that furnish the geometrical properties of the ellipse (orientation and ellipticity) and the physical parameters of two orthogonal component waves (phase difference and amplitude ratio) from data obtained using compensator and intensity techniques. (auth)

4481 (UCRL–14170) AN ELECTRONIC SCHEME FOR MEASUREMENT OF EXPLODING WIRE ENERGY. Thomas, R. J.; Hearst, J. R. (Lawrence Radiation Lab., Univ. of California, Livermore). July 17, 1965. Contract W-7405-eng-48. 43p. Dep. mn; CFSTI $2.00 cy, $0.50 mn.

With the exception of a nuclear explosion, the highest energy density that can be obtained at a given point for a short time results from a wire explosion induced by a sudden large pulse of electrical current. The energy (of the order of 8.5 kJ) in an exploding wire is measured as a function of time by means of a scheme which, except for oscilloscope sweep circuits, uses only passive circuit elements and requires no calculated corrections for inductive effects. The energy values thus obtained compare favorably with those obtained from measurements of the shock wave in air caused by the wire explosion. Slow expansion of the wire as energy entered it, followed by rapid explosion, can be seen. (auth)

4482 (UCRL–14360) PHYSICS DEPARTMENT PROGRESS REPORT, FEBRUARY–MAY 1965. Lorenz, A. (ed.) (Lawrence Radiation Lab., Univ. of California, Livermore). Contract W-7405-eng-48. 108p. Dep. mn; CFSTI $4.00 cy, $0.75 mn.

Separate abstracts were prepared for the five sections of the report. (D.C.W.)

For abstracts of individual sections see: 4153, 4290, 4708, 4849, and 4949.

4483 AN EXPERIMENT ON THE DETERMINATION OF THE RELATIVE INTENSITY OF THE SCATTERING OF X RAYS IN AQUEOUS SOLUTIONS OF SODIUM CAPRYLATE. Danielsson, Ingvar; Witting, Thorolf (Inst. for Physical Chemistry, Abo Akademi, Abo, Finland). Finska Kemistsamfundets Medd., 74: 6-19(1964). (In German).

An apparatus and technique are described for obtaining diffraction patterns of x ray scattering by soap solutions. A teflon cell and 40-kv x rays were used to study solutions of Na caprylate. The relation between the intensity of the scattered radiation and the optical density of the scattered radiation and the optical density of the developed photographic film is checked by means of a series of reference films. In order that the reference films and the experi-

mental films would be comparable, both films are exposed simultaneously to the radiation from a tube for the same length of time and are developed side by side in the same bath. The intensity of the radiation impinging on the reference film is reduced to a suitable level by inserting an aluminum filter with a known absorbancy between the film and the course of radiation. The maximum intensity of the radiation scattered by Na caprylate solutions which lies at an angle 2θ equal to 3°20′ varied almost linearly as the soap concentration when the latter increases from 15 to 40.5% by weight. A weak scattering is observed when the caprylate is less than 10%, but the lowest concentration at which the scattering of x rays begins cannot be accurately determined with the methods employed. (BBB)

4484 REFRACTIVE INDICES AND PIEZO-OPTIC COEFFICIENTS OF DEUTERIUM OXIDE, METHANOL, AND OTHER PURE LIQUIDS. Reisler, Emil; Eisenberg, Henryk (Weizmann Inst. of Science, Rehovoth, Israel). J. Chem. Phys., 43: 3875-80(Dec. 1, 1965).

The piezo-optic coefficients of deuterium oxide and of methanol and the refractive index of methanol were determined over a range of temperatures up to 35°C. These results, and data available in the literature for benzene and a number of other pure liquids, were examined in terms of an equation recently proposed for the dependence of refractive index of pure liquids on temperature and volume. (auth)

4485 MULTIPLE SCATTERING OF MEDIUM FAST ELECTRONS IN FILMS. Hilgner, Wilfried; Kessler, Joachim (Technische Hochschule, Karlsruhe, Ger.). Z. Physik, 187: 119-39(1965). (In German).

Electrons with an initial energy of 100 kev were shot through thin films of Ni, Ge, Ag, and Au. The angular distribution of the plurally scattered electrons was measured between 0 and 0.3 radian. The experiments show that the plural scattering theories give no correct results when the scattering cross sections of Lenz or Ibers-Weinstein are used. The reasons for these discrepancies are discussed. Empirical cross sections are communicated by means of which a good description of the plural scattering distributions is possible. (auth)

4486 FIZKIA I TEKHNIKA SIL'NYKH MAGNITNYKH POLEI. (Strong Magnetic Field Physics and Techniques). Krasik, V. P. Moscow, Publishing House Nauka, 1964. 348p.

Powerful constant-current solenoids are discussed; methods are presented of calculating the magnetic-field intensity, the electromotive forces, and the cooling systems, and very large solenoids are described. Methods of obtaining pulsed magnetic fields are set forth; detailed descriptions are given of the apparatus and separate subassemblies — the discharge rods and the pulse-formation circuits. Methods for calculations of electromagnets and pole pieces of various configurations are presented. Magnets with superconducting windings are discussed. (M.J.T.)

4487 LECTURES IN THEORETICAL PHYSICS. VOLUME VI. Lectures Delivered at the Summer Institute for Theoretical Physics, University of Colorado, Boulder, 1963. Brittin, Wesley E.; Chappell, Willard R. (eds.). Boulder, Colo., The University of Colorado Press, 1964. 521p. $7.00.

Eleven lectures were included, one of which appeared previously in NSA as 18: 24436. Separate abstracts were prepared for 10 papers. (J.F.P.)

For abstracts of individual papers see: 4295, 4488, 4533, 4534, 4635, 4636, 4700, 4701, 4772, and 4789.

4488 RIGOROUS RESULTS IN STATISTICAL MECHANICS. Ruelle, D. (Inst. for Advanced Study, Princeton, N. J.). pp 73-111 of Lectures in Theoretical Physics. Vol. VI. Boulder, Colo., The University of Colorado Press, 1964.

Recent rigorous results in equilibrium statistical mechanics are described. Classical systems of particles interacting by two-body central forces are considered, and the formalism of the grand canonical ensemble is used. The method of proving general theorems, using as little as possible the detailed nature of the system, is employed with the restriction that only systems with two-body forces are considered. The questions considered are a particular aspect of the general problem of explaining the macroscopic properties of systems with a great number of degrees of freedom in terms of their microscopic properties. The cluster property is discussed and placed in its natural algebraic form, the conditions on the potential are investigated, and the correlation functions in the limit of infinite volume, with analyticity properties derived including the convergence of the virial expansion, is studied. (J.F.P.)

4489 SOLENOIDS FOR STRONG MAGNETIC FIELDS. Litomiskii, Miroslav (Inst. of Nuclear Research, Czechoslovak Academy of Sciences, Rez). pp 222-5 of Physics and Techniques of Low Temperatures. Prague, Publishing House of the Czechoslovak Academy of Sciences, 1964.

A description is given of the Bitter-type solenoid which was recently put into operation. A field of 48 kG was obtained for an output of 649 kw. It is assumed that after performing the heating tests of the motor-generator a field of at least 52 kG for permanent operation and 57 kG for short-term operation will be possible. The feed circuit and the cooling circuit are each shown schematically and described. Both this solenoid and another one, which was also mentioned, are intended primarily for obtaining very low temperatures by adiabatic demagnetization of paramagnetic salts, for experiments with polarized nuclei and for investigation of the properties of superconductors. (J.F.P.)

4490 HUNDRED-AND-FIFTY CENTIMETRE HYDROGEN TARGET. Golovanov, L. B. (Joint Inst. of Nuclear Research, Dubna, USSR). pp 229-31 of Physics and Techniques of Low Temperatures. Prague, Publishing House of the Czechoslovak Academy of Sciences, 1964.

A 159 cm liquid hydrogen target constructed for experimental work on the proton synchrotron is described, and a diagram is shown. The inner vessel of the target consists of a cylinder 200 mm in diameter and 1500 mm in length. The space for the liquid hydrogen is widened at the center of the target. The first pumping of the vacuum envelope is accomplished by a pre-vacuum pump. Under working conditions, the vacuum is maintained by adsorption on coal which is at liquid hydrogen temperature. Pressure in the vacuum chamber is measured by means of three different gages. Tests were performed showing that if the target is filled with liquid hydrogen then the vacuum stays at 2×10^{-5} to 4×10^{-6} mm Hg for a duration of one week. (J.F.P.)

Accelerators

Refer also to abstracts 4243, and 4822–4824.

4491 (ANL–7081, pp 78-80) DEVELOPMENT OF THE VARIABLE-ENERGY CYCLOTRON HIVEC. Benaroya, R.; Johnson, K. W.; Khoe, T. K.; Livingood, J. J.; Mogensen, H. P.; Ramler, W. J. (Argonne National Lab., Ill.).

The development of the Variable-Energy Cyclotron is briefly discussed. The major design parameters of the cyclotron are listed. (M.O.W.)

4492 (BNL–9640) COMMENTS ON DEFLECTORS WITH ECCENTRIC BEAM HOLE. Hahn, H. (Brookhaven National Lab., Upton, N. Y.). Oct. 1, 1965. Contract AT(30-2)-Gen-16. 12p. Dep. mn; CFSTI $1.00 cy, $0.50 mn.

A theoretical treatment of a deflector with eccentric beam hole is presented. The theory is applied to deflecting structures and the ensuing conclusions are presented. It was shown that the R/Q of the rotational symmetric HEM_{11} deflector can be increased by reducing the diameter of the coupling hole. (M.O.W.)

4493 (BNL–9642) THE BROOKHAVEN RADIO FREQUENCY BEAM SEPARATOR. Hahn, H.; Halama, H. J.;

Foelsche, H. W. J. (Brookhaven National Lab., Upton, N. Y.). Sept. 17, 1965. Contract AT(30-2)-Gen-16. 36p. Dep. mn; CFSTI $2.00 cy, $0.50 mn.

The Brookhaven r-f beam separator is described. The systems design and the performance of the microwave components are considered. Relevant studies on the beam optics, the operating momenta, and targeting considerations are discussed. The important deflector parameters are given, and the microwave system and the microwave components are described in some detail. The objective of this system is to generate r-f pulses of correct frequency, amplitude, phase, and duration in each deflector so that exact cancellation of unwanted particles is possible, and wanted particles will pass the beam stopper. (J.F.P.)

4494 (CEA-R-2843) ETUDES DES MOUVEMENTS TRANSVERSAUX DU FAISCEAU D'ELECTRONS DANS UN ACCELERATEUR LINEAIRE. (Study of Some Transversal Motions of the Electron Beam in a Linear Accelerator). Bergere, Roland; Beil, Hans; Veyssiere, Andre (Commissariat a l'Energie Atomique, Saclay (France). Centre d'Etudes Nucleaires). July 1965. 45p. Dep. mn.

It is well known that when the magnetic focusing field along the axis of an electron linac increases the output accelerated current does not increase regularly. Such a behavior is shown to be connected with rotations, in the output plane of the linac, of the center of charges of the beam. These rotations were displayed experimentally by means of a beam position monitoring system and related to the transverse momentum transferred to the beam by the spurious TM_{11} mode existing in the input coupler changing the TE_{01} mode from the input rectangular waveguide into a circular TM_{01} mode on the accelerator structure. (auth)

4495 (CONF-650923-16) IMPROVEMENT OF THE CALTECH 1.5 Gev ELECTRON SYNCHROTRON. Maloy, J. O. (California Inst. of Tech., Pasadena). [nd]. Contract AT(11-1)-63. 16p. Dep. mn; CFSTI $1.00 cy, $0.50 mn.

From 5th International Conference on High Energy Accelerators, Frascati, Italy.

The CalTech Synchrotron now operates at energies up to 1.5 Bev as a result of the completion of a 200 kw 40 MHz r-f system. Repetition rate varies from 1.6 to 1.0 pulses per second. Length of beam spill is typically 100 to 200 milliseconds. Effects of beam loading are substantially reduced by operating the cavity with a double-tuned coupling to lower the impedance presented to the beam. With the new 10-Mev linac injector and the new r-f configuration, a typical intensity of 4×10^{10} electrons per pulse is attained. Maximum intensity observed is about 10^{11} electrons per pulse. This intensity is still primarily limited by beam loading, and cavity interactions are observed at high intensity. Nearly all machine controls, including the low level r-f amplifiers and oscillator, were transistorized. Control of the magnet is effected by a solid-state digital control whose 60 and 360 Hz signals are derived from the magnet power supply. (auth)

4496 (JINR-P-2375) SISTEMA KRATNOGO USKORENIYA ELEKTRODINAMICHESKOGO SEPARATORA CHASTITS VYSOKIKH ENERGII. (A Multiple Acceleration System for High Energy Particle Electrodynamic Separator). Borisov, N. G.; Vagin, V. A.; Volodin, V. D.; Zaitsev, V. I.; Plyashkevich, N. N.; Saenko, A. P.; Semenyushkin, I. N.; Stepanyuk, V. L. (Joint Inst. for Nuclear Research, Dubna (USSR). Lab. of High Energy). 1965. 14p. Dep. mn.

The characteristics of the multiple acceleration system for the JINR electrodynamic antiproton separator are given. The results of tests of this system are reported. At a frequency of 150 MH, the proton capture coefficient was found to be 70% at a beam energy of 10 Bev, resonator voltage being 70 kv. (auth)

4497 (KFK-310) THE USE OF AVF-CYCLOTRONS FOR NUCLEAR PHYSICS. Schopper, H. (Kernforschungszentrum, Karlsruhe (West Germany). Institut fuer Experimentelle Kernphysik). June 1965. 26p. (CONF-650437-2). Dep. mn.

From Cyclotron Colloquium, Eindhoven, Netherlands.

A general survey of the applications of AVF-cyclotrons is presented. Specific applications are reviewed for elastic and inelastic α scattering and coincidence experiments. (M.O.W.)

4498 (LA-3419) QUARTERLY STATUS REPORT ON THE MEDIUM-ENERGY PHYSICS PROGRAM FOR PERIOD ENDING SEPTEMBER 30, 1965. (Los Alamos Scientific Lab., Univ. of California, N. Mex.). Oct. 1965. Contract W-7405-eng-36. 75p. Dep. mn; CFSTI $3.00 cy, $0.50 mn.

Design and development activities connected with an 800-Mev, 1-ma average current, 6 to 12% duty-cycle, variable-energy proton linac are reported. (T.F.H.)

4499 (LNF-65/26) ADONE—THE FRASCATI 1.5 Gev ELECTRON POSITRON STORAGE RING. Note No. 285. (Laboratori Nazionali di Frascati, Comitato Nazionale per l'Energia Nucleare (Italy)). Aug. 30, 1965. 9p. (CONF-650923-17). Dep. mn.

From 5th International Conference on High Energy Accelerators, Frascati, Italy.

A status report on the Frascati 1.5-Bev Storage Ring is presented. Brief descriptions of the machine components are given. The expected performance of the machine is discussed. (M.O.W.)

4500 (LNF-65/27) THE TRANSVERSE RESISTIVE WALL INSTABILITY OF EXTREMELY RELATIVISTIC BEAMS OF ELECTRONS AND POSITRONS. Note No. 286. Ferlenghi, E.; Pellegrini, C.; Touschek, B. (Laboratori Nazionali di Frascati, Comitato Nazionale per l'Energia Nucleare (Italy)). Aug. 30, 1965. 22p. Dep. mn.

A brief account of the physical principles underlying the transverse instability of high energy beams is presented. A theoretical treatment of the transverse resistive wall instability of relativistic electron beams is presented in terms of a kinematical description of the electrons, the fields, forces on electrons and positrons, the one beam instability for an unbunched beam, and for extremely bunched beams. (M.O.W.)

4501 (LNF-65/34) ON THE GENERALITY OF THE STABILITY CRITERION AGAINST THE TRANSVERSE WALL INSTABILITY OF RELATIVISTIC BEAMS. Internal Note No. 291. Ferlenghi, E. (Comitato Nazionale per l'Energia Nucleare, Rome (Italy)). Oct. 6, 1965. 6p. Dep. mn.

It is shown that stability criteria (but not instability rise-times) are independent of the material properties of the wall, for the situation in which a relativistic particle beam interacts with the resistive walls of the vacuum tank of an accelerator. The production of coherent transverse instabilities is given particular attention. (T.F.H.)

4502 (NIRL/R/92) FURTHER EXTRACTION STUDIES FOR THE HARWELL VARIABLE ENERGY CYCLOTRON. Mayhook, A. R. (National Inst. for Research in Nuclear Science, Chilton (England). Rutherford High Energy Lab.). Mar. 1965. 26p. Dep. mn.

An account is given of computations on which the design of the extraction system for the cyclotron was based. Two alternative systems were considered consisting of two electrostatic deflectors followed by either a magnetic wedge or a magnetic channel. Three different ions were considered each at a different field level. The investigation covered the change of shape of particle orbits in the deflectors, the effect of changing extractor parameters on the position and direction of the emerging beam, and an estimate of the quality of the extracted beam. (auth)

4503 (NP-15340) SUR UNE METHODE D'ETUDE DE LA DYNAMIQUE DES PARTICULES DANS UN ACCELERATEUR LINEAIRE [These]. (On a Method of Study of Particle Dynamics in a Linear Accelerator [Thesis]). Ferat, Alain (Lyon Univ. (France). Institut de Physique Nucleaire). Apr. 29, 1965. 84p. Dep. mn.

A method for the study of the particle dynamics in linear accelerators that is adapted to numerical calculations was

perfected. The principle of the Alvarez linear accelerator is reviewed and the new principles proposed with respect to the structure and the focusing are discussed. A method of numerical study, based on the systematic development of all the variable quantities as a function of successive powers of some infinitely small variables each corresponding to a well determined effect was proposed. The method makes it possible to appreciate neglected terms when the study is limited to the given order and to know the relative influence of various effects. The study is made by means of reduced variables which gives it a great generality and avoids the necessity of choosing systems of use. (J.S.R.)

4504 (NP–15420) SEVENTH ANNUAL REPORT FOR THE PERIOD OCTOBER 1, 1963–SEPTEMBER 30, 1964. (National Inst. for Research in Nuclear Science, Chilton (England). Rutherford High Energy Lab. National Inst. for Research in Nuclear Science, Daresbury (England). Daresbury Nuclear Physics Lab.). 43p. Dep. mn.

A review of research work carried out during the past year is presented. Discussions include; recent developments in elementary particle physics and the role of Nimrod, recent developments in medium energy nuclear physics and the role of the proton linear accelerator, the Daresbury Nuclear Physics Laboratory, and the Atlas Computer Laboratory. (M.O.W.)

4505 (ORNL-P–1738) THEORETICAL METHODS IN THE DOSIMETRY OF HIGH-ENERGY PARTICLES. Turner, J. E. (Oak Ridge National Lab., Tenn.). Oct. 1965. Contract W-7405-eng-26. 26p. (CONF-651109–4). Dep. mn; CFSTI $2.00 cy, $0.50 mn.

From 1st Symposium on Accelerator Radiation Dosimetry and Experience, Upton, N. Y.

Specific nuclear reactions relevant to high-energy particle dosimetry are described and the results of several calculations of dose at high energies are reviewed. For health physics personnel monitoring under normal operating conditions in the vicinity of a high-energy accelerator, neutrons, gamma photons, and muons will generally constitute the most important radiation outside shields. The reactions that give rise to these radiations are described. A summary is given of an ICRP task group report on the estimation of absorbed dose and dose-equivalent for nucleons with energies up to 400 Mev. The calculations treat explicitly nuclear cascade and evaporation processes and multiple nuclear interactions arising from secondary and higher-order reaction products. Pion production was not treated and hence the calculations were applied to nucleons with energies not above 400 Mev. The new estimated flux densities of protons that deliver 2.5 millirem/hr are, for normally incident protons, lower than those given in the Report of ICRP Committee IV (1953–1959) for energies lower than about 215 Mev. At higher energies the newer flux densities for normal incidence are greater than the older ones by factors of about 2 to 3. The newer and older estimates agree well for isotropically incident protons. For neutrons the newer estimates give fluxes that are greater than those given in the previous report by factors of 2 to 3. Figures summarizing these results were prepared. A study is being made of the possible change in absorbed dose and dose equivalent from high-energy nucleons at an interface of soft tissue and bone. Some preliminary results from this work are presented. (M.O.W.)

4506 (PPAD–569E) THE RADIATIONS MEASUREMENTS GROUP AT THE PRINCETON-PENNSYLVANIA 3 Gev PROTON SYNCHROTRON. Awschalom, M.; Larsen, F. L.; Sass, R. E. (Princeton-Pennsylvania Accelerator, Princeton, N. J.). Oct. 13, 1965. Contract AT(30-1)-2137. 41p. (CONF-651109–3). Dep. mn; CFSTI $2.00 cy, $0.50 mn.

From 1st Symposium on Accelerator Radiation Dosimetry and Experience, Upton, N. Y.

A brief description of the Princeton–Pennsylvania 3-Bev Proton Synchrotron is presented. A survey of the experiments carried out in the areas of routine health physics and radiation studies is presented. (M.O.W.)

4507 (PPAD–2137-560) DRIFT TUBE RF SYSTEM. Bertuccio, T. D. (Princeton-Pennsylvania Accelerator, Princeton, N. J.). July 26, 1965. Contract AT(30-1)-2137. 81p. Dep. mn; CFSTI $3.00 cy, $0.75 mn.

The characteristics and operating roles of the components in the drift tube system of the Princeton-Pennsylvania Accelerator are described in detail. Circuit diagrams are included. The overall characteristics and uses of the drift tube system are discussed. (T.F.H.)

4508 (RPI–328-40) LINEAR ACCELERATOR PROJECT. Progress Report, July–September 1965. (Rensselaer Polytechnic Inst., Troy, N. Y.). Contract AT(30-3)-328. 74p. Dep. mn; CFSTI $3.00 cy, $0.50 mn.

Separate abstracts were prepared for 4 of the 5 included sections. The other section contained two brief summaries of research work on electron radiation effects on germanium and silicon. (M.O.W.)

For abstracts of individual sections see: 4246, 4806, 4807, and 4846.

4509 (UCRL–14343) AN OPTICAL SYSTEM FOR MODERATE-RIGIDITY CHARGED-PARTICLE BEAMS. Sherwood, W. A. (Lawrence Radiation Lab., Univ. of California, Livermore). Aug. 18, 1965. Contract W-7405-eng-48. 5p. Dep. mn; CFSTI $1.00 cy, $0.50 mn.

An unconventional electromagnetic beam transport and conditioning system is described. This system is capable of handling nonparaxial beams. The usual restrictive assumptions used for transport system element design can be greatly relaxed. The system components are steering coils, conventional focusing coil lenses and quadrupole lenses. Great flexibility in beam handling is obtained simply by allowing the focusing coil lenses and/or the quadrupole lenses to have one or two degrees of controlled mechanical freedom around or perpendicular to a required axis. Beam matching then becomes an empirical exercise (knob twisting and observation). It should be emphasized that charged-particle trajectories through the proposed system are still amenable to computation and analog determination. (auth)

4510 (UCRL–16016) A GUIDE FOR DESIGNING ELECTRICAL CONTROLS OF ACCELERATORS. Harris, C. A. (Lawrence Radiation Lab., Univ. of California, Berkeley). Mar. 24, 1965. Contract W-7405-eng-48. 63p. Dep. mn; CFSTI $3.00 cy, $0.75 mn.

A large variety of engineering principles must be applied in the design of a control system for an accelerator, large or small, linear or circular. A general but unified set of procedures to be followed by engineers designing accelerator controls are presented in order that such controls may have some degree of consistency. The included information not only supplements the national and local sets of mechanical and safety codes that may be applicable to any given accelerator, but it also includes areas not covered specifically in the safety codes. (auth)

4511 (UCRL–16242) CAVITY RESONATOR SYSTEMS FOR SUPPORTING NONSINUSOIDAL PERIODIC WAVEFORMS. Kerns, Quentin A. (Lawrence Radiation Lab., Univ. of California, Berkeley). June 30, 1965. Contract W-7405-eng-48. 17p. (CONF-650923–21). Dep. mn; CFSTI $1.00 cy, $0.50 mn.

From 5th International Conference on High Energy Accelerators, Frascati, Italy.

The phenomenon of resonance allows a modest power flow to build up a large-amplitude wave. Although resonators are commonly designed for waves varying sinusoidally in time, any waveform describable as a Fourier series can be supported by designing the metallic enclosure for the wave so that resonance occurs at all integer multiples of the fundamental frequency. The principle is not limited to standing-wave resonators; it can be applied to traveling-wave cavities as well, by incorporating

a suitable circulator between output and input ports of the cavity. Several experimental superposition resonators constructed in the course of the Berkeley Accelerator Study are described, together with their r-f driving circuits. Potential applications include, on one hand, continuously operating devices such as sawtooth wave-form bunchers or cavities providing specialized waveforms for particle acceleration, separation, or extraction. Pulsed cavities, on the other hand, by the accumulation of large energy over a period of time for later rapid discharge, can provide fast-rising, shaped pulses of high peak power for track or discharge chambers. (auth)

4512 (UCRL-16243) DESIGN OF LONG STRAIGHT SECTIONS FOR SYNCHROTRONS. Garren, A. A. (Lawrence Radiation Lab., Univ. of California, Berkeley). Sept. 2, 1965. Contract W-7405-eng-48. 18p. (CONF-650923-18). Dep. mn; CFSTI $1.00 cy, $0.50 mn.

From 5th International Conference on High Energy Accelerators, Frascati, Italy.

A number of variations of long straight section insertions are available for synchrotron design. Collins-type (two quadrupole) insertions may be lengthened by altering the lengths of neighboring magnets and gaps. The momentum compaction increase of Collins-type insertions can be eliminated by pairing them. Another type of insertion using four quadrupoles and having a phase advance of π radians permits drift lengths several times greater than does the Collins-type insertion. The momentum compaction increase of these π insertions is reduced or eliminated by inclusion of bending magnets without gradient. (auth)

4513 (UCRL-16440) INSTABILITIES OF RELATIVISTIC PARTICLE BEAMS. Sessler, Andrew M. (Lawrence Radiation Lab., Univ. of California, Berkeley). Oct. 4, 1965. Contract W-7405-eng-48. 42p. (CONF-650923-22). Dep. mn; CFSTI $2.00 cy, $0.50 mn.

From 5th International Conference on High Energy Accelerators, Frascati, Italy.

A general review of instabilities exhibited by relativistic particle beams is presented. The experimental information presently available, with emphasis upon the degree to which it confirms or disagrees with theory, is discussed. (M.O.W.)

4514 (UCRL-16445) ACCELERATOR RADIATION MONITORING AND SHIELDING. Patterson, H. Wade (Lawrence Radiation Lab., Univ. of California, Berkeley). Aug. 2, 1965. Contract W-7405-eng-48. 14p. (CONF-651109-2). Dep. mn; CFSTI $1.00 cy, $0.50 mn.

From 1st Symposium on Accelerator Radiation Dosimetry and Experience, Upton, N. Y.

Radiation measurements and shielding studies were made on the 60-inch cyclotron, the 184-inch cyclotron, the electron synchrotron, the electron linear accelerator, the Bevatron, the heavy-ion linear accelerator, the proton linear accelerator, and the 88-inch cyclotron. Measurements were mostly made with the purpose of identifying the various components of the radiation field and determining their energy distribution. A general rule that has emerged from these studies is that fast neutrons (0.1 to 10 Mev) dominate the biological hazard of the radiation field existing near a well-shielded particle accelerator by contributing more than half the total rem dose. Gamma rays and low-energy neutrons contribute 10 to 20%, and high-energy neutrons make up the balance. The development and use of neutron detectors that allow one to estimate the neutron spectrum were emphasized. Neutron detectors most effective are moderated slow-neutron detectors, threshold reaction detectors, emulsion, and the polyethylene-lined proportional counter. Techniques of measurement, application of specific detectors to certain problems, and practical illustrative examples of monitoring problems and their solutions are given in some detail. (M.O.W.)

4515 DETERMINATION OF THE EQUIVALENT LENGTH OF THE ELECTRODES OF PARTICLE SEPARATORS. Durand, Alain (Univ. Paris, Rennes, France). Compt. Rend., 261: 1948-51(Aug. 30, 1965). (In French).

The electric field on the axis of the separator is calculated by using a Schwarz transformation. The equivalent length of the separator electrodes follows from it. (tr-auth)

4516 THE SACLAY VARIABLE-ENERGY CYCLOTRON. Thirion, Jacques (CEN, Saclay, France). Ind. At., 9: No. 7-8, 45-56(1965). (In French).

The Saclay variable-energy cyclotron (maximum energy 29 Mev protons) went into service a year ago. A brief description is given of the characteristics of this new type of accelerator and of the implantation of experiments. One of the essential purposes of these constructions was to have polarized protons available from a special source in operation for several months. This polarized source merited detailed description. The use of the beams so obtained has begun; the program and the corresponding results are outlined. (auth)

4517 DESIGN EVOLUTION OF THE SL 75 LINEAR ACCELERATOR FOR SUPER VOLTAGE THERAPY. Atherton, L. Medicamundi, 10: 77-89(1965).

The development and production of linear accelerators over the past sixteen years are briefly discussed. The medical aspects of the optimum accelerator machine for radiotherapy are summarized. The principles of operation, isocentric mounting principle, evolution of the 360° rotation design, x-ray head design, and patient support couch are described. The relative merits of supervoltage and high energy electron treatments are discussed. The design of the accelerating structure, electron gun, and associated components are treated in the appendix. (L.B.S.)

4518 ELECTRON ACCELERATION IN HELICAL FIELDS. Eicker, H.; Krudewig, W. (Technische Hochschule, Aachen). Z. Physik, 188: 290-302(1965). (In German).

An electron accelerator with a betatronlike air core accelerating field and with helical stabilizing fields is described. It consists of a glass torus having a medium radius of 20 cm which is surrounded by three coils generating the following magnetic fields: a betatronlike accelerating field, a toroidal field (B_z-field) and a helical quadrupole field. Electrons are injected into the torus by a spark discharge at a gas pressure of less than 10^{-5} mm Hg. In a B_z-field of 18,000 gauss electrons were accelerated up to 6 Mev, as measured with a 1.5 l bubble chamber, and up to 10 Mev, as measured with scintillation counters. In the energy range of 0.5 to 1.6 Mev, depending on experimental conditions, electron currents between 100 and 1000 amps were observed, independently by Rogowsky-belt measurements and by determining the bremsstrahlung intensity. Considering the superposition of various drift velocities, stability conditions are derived for the motion of the electrons. (auth)

4519 SOURCE OF POLARIZED IONS FOR CYCLOTRON. Kult, K.; Bejsovec, V.; Mares, J.; Trejbal, Z.; Marek, M.; Vincour, J. (Inst. of Nuclear Research, Czechoslovak Academy of Sciences, Rez). pp 248-53 of Physics and Techniques of Low Temperatures. Prague, Publishing House of the Czechoslovak Academy of Sciences, 1964.

A polarized ion source for a cyclotron is described. The principal scheme of the source is shown and discussed. The design of the dissociator is described. Optimum yields of 4×10^{17} atoms/sec were obtained at a pressure of 0.25 mm Hg and a frequency of 13.5 MHz. The dependence of the intensity of the atomic beam on the frequency of the high-frequency generator is shown. The separation magnet is discussed and its characteristics shown. High-frequency polarization is discussed and the course of the field and gradient in the air slit of the 4-pole magnet is given. The inverse magnetron is also considered for ionization of the atomic beam. The energy distribution of ionization products in this inverse magnetron is shown. (J.F.P.)

4520 PROTON DEPOLARIZATION IN CYCLOTRONS. Pliss, Yu. A.; Soroko, L. M. (Joint Inst. for Nuclear Research, Dubna, USSR). pp 254-8 of Physics and Techniques of Low Temperatures. Prague, Publishing House of the Czechoslovak Academy of Sciences, 1964.

A table is shown in which depolarization is given for resonances taking place in a proton synchrocyclotron. In order to analyze the effect of phase oscillations upon depolarization, a case was analyzed when the second derivative of the exponential index vanishes to zero. It is shown that phase oscillations do not change the results of the calculation. Calculation of proton depolarization in a relativistic cyclotron was performed on the basis of the project topography of the magnetic field and was aimed at determining the requirements of shimming accuracy of the magnetic field. (J.F.P.)

Astrophysics and Cosmology

Refer also to abstract 4750.

4521 (AD-618222) RESEARCHES IN SOLAR PHYSICS DURING 1964. Rosseland, Svein (Oslo Univ. (Norway). Dept. of Astrophysics). Jan. 30, 1965. Contract AF61(052)-743. 25p. (SR-1; AFCRL-65-363). CFSTI $1.00 cy, $0.50 mn.

The structure of storm bursts in the meter wave region and their interrelations were studied. Individual bursts in a shower appear to be independent. Occasional bursts sometimes show an approach to regular periodicity, but irregular distributions of bursts are more common. Studies of the band 310-340 Mc showed very few bursts which might be ascribed to a solar origin. A comparison of meter wave observations of the sun at Oslo with NERA (The Netherlands) and Tokyo indicated that the Oslo data have a high degree of reliability and stability, even over a 10 year period. Some progress is reported in a study of the new type of bursts named flash-bursts. A study of the lifetime of sunspot groups and of magnetic properties of sunspot groups led to the discovery of several new tendencies of the sun to display secular variations, different from one cycle to the next. The transparency properties of sunspot models are discussed. Some current models fail to stand up to the test in this respect. The continuation of Maltby's work on Evershed effect and wiggles was continued with fair success, in spite of the low solar activity. In this connection Brahde made a theoretical study of the instrumental width of spectral lines taken with the large spectrograph of the solar tower. (auth)

4522 (CNIE-PE-5) FISICA DEL ESPACIO INTERPLANETARIO. Publicacion Especial No. 5. (Physics of the Interplanetary Medium. Special Publication No. 5). Webber, W. R. (Comision Nacional de Investigaciones Espaciales, Buenos Aires (Argentina)). July 1964. 63p. Dep. mn.

The following four aspects of interplanetary physics are discussed; experimental evidence about the interplanetary medium, theoretical models to explain the observed characteristics of this medium, experimental evidence concerning cosmic ray time variations, and theoretical models to explain the cosmic ray variations in terms of the interplanetary medium. The general properties and characteristics of the interplanetary medium are discussed. Theories relating to the solar corona and the interplanetary medium are discussed. (M.O.W.)

4523 (COO-818-63) PROPOSED ν_e TELESCOPE TO DETECT SOLAR NEUTRINOS BY ELASTIC SCATTERING ON e^-. Reines, Frederick (Case Inst. of Tech., Cleveland, Ohio. Dept. of Physics). [1965]. Contract AT(11-1)-818. 8p. (CONF-650111-6). Dep. mn; CFSTI $1.00 cy, $0.50 mn.

From CERN Informal Neutrino Conference, Geneva.

An experiment is discussed which will be used to detect solar neutrinos and for observation of the scattering process $\nu_e + e^- \rightarrow \nu_e + e^-$. A telescope utilizing the Cherenkov effect is discussed. (M.O.W.)

4524 HARMONIC STRUCTURE AND BAND SPLITTING OF TYPE II SOLAR RADIO BURSTS. Krishnamurthi, M.; Sastry, G. Sivarama; Rao, T. Seshagiri (Osmania Univ., Hyderabad, India). Australian J. Phys., 18: 473-8 (Oct. 1965).

An analysis of single-frequency records of type II solar radio bursts at 29 Mc was made. Such characteristic features as harmonic structure and band splitting due to coronal magnetic fields were identified. Calculations indicate that the shock fronts generating the type II bursts experience a deceleration as they move outwards. Existing theories are used to estimate the magnetic field strengths, which come out to be of the order of 3-8 G at a height of 0.7 solar radius above the photosphere at the time of occurrence of these bursts. (auth)

4525 SPACE TRAVEL AND EXPLORATION. Massey, Sir Harrie (Univ. of London). Contemp. Phys., 6: 321-37(June 1965).

Since a large part of the space program is involved with manned space travel, which has special difficulties associated with highly developed organisms, and since many opportunities are opened for biological research, this aspect of space travel and exploration is discussed. Exobiology, involving extra-terrestrial organisms, is discussed including automatic methods for the biological assay of planetary environments, the sterilization of space vehicles, and environmental studies of living organisms in space. Human beings in space are also considered. Topics include risks arising from meteor impact, and risks arising from energetic particle radiation. Previous manned orbital flights are discussed including technical aspects of the Russian flights, the American manned space flight program, the Mercury and Gemini programs, and the Apollo project. Manned orbital laboratories and flights to the planets are also mentioned. (J.F.P.)

4526 EXTINCT ^{129}I AND TRACE ELEMENTS IN CHONDRITES. Turner, G. (Univ. of California, Berkeley). J. Geophys. Res., 70: 5433-45(Nov. 1, 1965).

I-Xe formation intervals for the Bjurböle chondrite and the dark and light fractions of the Pantar meteorite were measured by activation techniques with the correlated release method. On the basis of the uniform synthesis model the intervals obtained are (60 ± 2), (68 ± 3), and (60 ± 8), m.y. The similarity of these and other recently measured values gives added confidence in the validity of the method. Other models of nucleosynthesis are considered. I, Te, Ba, Br, and Se abundances were also obtained, and the light fraction of Pantar is found to be strongly depleted in I, Te, and Br with respect to both the dark fraction and the ordinary chondrites. Current ideas on the formation of the gas-rich meteorites are considered in the light of this evidence. (auth)

4527 INTERPLANETARY MAGNETIC EFFECTS OF SOLAR FLARES: EXPLORER 18 AND PIONEER 5. Greenstadt, E. W. (TRW Space Technology Labs., Redondo Beach, Calif.). J. Geophys. Res., 70: 5451-2 (Nov. 1, 1965).

It is reported that the behavior of the ambient field at Explorer 18, 33 hours after the flare of 0922 UT December 13, is consistent with effects recorded statistically and in detail during the flight of Pioneer 5, and may confirm relations tentatively indicated by previous data. The uniqueness of this flare makes it a plausible source of the anomalous disturbance recorded on December 14. If a moderate flare was responsible for the perturbation field of 15 gammas, it is speculated that lower bounds of 7 to 50 for interplanetary disturbances, estimated from Pioneer 5's single component measurements, represented 50% or less of the total disturbed field magnitudes, and that fields of 20 to 100 gammas are common during intervals of intense solar activity. (J.F.P.)

4528 THE STRUCTURE OF THE SOLAR CHROMOSPHERE. I. IDENTIFICATION OF SPICULES ON THE DISK. Bhavilai, Rawi (Commonwealth Scientific and Industrial Research Organization, Sydney). Mon. Notic. Roy. Astron. Soc., 130: 411-22(1965).

Spicules were studied in the Hα line with a 1/8 Å tunable filter, and a 3/4 Å filter equipped with a beam splitter yielding simultaneous photographs in opposite wings. Spicules were traced from outside the solar limb on to the chromospheric disk just inside the limb, where they appear as bright emission features. On the disk, they appear as mottles which are bright at all positions across the line profile. The well-known dark mottles, although merging to form the general chromosphere at the limb, do not extend beyond as spicules. However, there is a close association between the dark and bright mottles, the latter being found in the central parts of the well-known chains of the chromospheric network or of clusters of dark mottles. A three-dimensional model of some of these structures is described. (auth)

4529 INTERPLANETARY MAGNETIC FIELD. Axford, W. I. (Cornell Univ., Ithaca, N. Y.). New Scientist, 27: 262-4(July 29, 1965).

Recent observations made with Mariner and Imp spacecraft confirm predictions about the magnetic field of the solar system, based on the behavior of cosmic rays. The field extends in a spiral form and rotates with the sun. A description of the structure and behavior of the field is given. Also a description of cosmic ray phenomena including diurnal variation, correlation with solar flares, and the effect on cosmic rays of the co-rotation of the interplanetary magnetic field with the sun. The freezing of magnetic field lines with the fluid material in which they are imbedded is also described. (J.F.P.)

4530 PHOTON-INDUCED BETA DECAY IN STELLAR INTERIORS. Shaw, P. B.; Clayton, D. D.; Michel, F. C. (Rice Univ., Houston, Tex.). Phys. Rev., 140: B1433-41 (Dec. 6, 1965).

Because of the astrophysical importance of beta-decay lifetimes in stellar interiors, the rate of photon-induced beta decay (photobeta decay) is calculated. In the photobeta process the photon can be considered to decay virtually into an electron-positron pair, with the positron being absorbed by the nucleus. The photobeta process is in competition with normal beta decay (if energetically possible), excited-state beta decay, and free-positron capture. An infrared divergence problem for exothermic photobeta decay is discussed, although the exothermic photobeta rate is too small to enhance most spontaneous beta decays. Applications are discussed in the driven decay of stable nuclei. As an example, the photobeta lifetime of a nucleus stable by 200 kev drops from 3×10^{10} yr at 3×10^{8}°K, to 10^{5} yr at 1.2×10^{9}°K for a nuclear transition matrix-element characterized by log ft = 6. The competition between the photobeta process and excited-state beta decay is discussed. (auth)

4531 NEUTRON STARS. I. PROPERTIES AT ABSOLUTE ZERO TEMPERATURE. Bahcall, John N.; Wolf, Richard A. (California Inst. of Tech., Pasadena). Phys. Rev., 140: B1445-51(Dec. 6, 1965).

The properties of a neutron star at absolute zero temperature are discussed. The problem of determining the ground state of a neutron star is formulated in a general way and the conditions are described under which it might reasonably be hoped that an individual-particle model is valid. The effects of the strong interactions on the number densities and production thresholds of the various hadrons are illustrated with several examples. The modification of the energy spectrum of neutrons and protons in a neutron star is calculated using an effective-mass approximation adapted from the theory of nuclear matter. Crude estimates are made of the contributions of hadrons other than nucleons to the equation of state and specific heat. (auth)

4532 NEUTRON STARS. II. NEUTRINO-COOLING AND OBSERVABILITY. Bahcall, John N.; Wolf, Richard A. (California Inst. of Tech., Pasadena). Phys. Rev., 140: B1452-66(Dec. 6, 1965).

Calculations of the rates of the cooling reactions $n + n \rightarrow n + p + e^{-} + \nu_e$ and $n + \pi^{-} \rightarrow n + e^{-} + \nu_e$ are presented; the rates of the closely related muon-producing reactions and the four inverse processes are also given. Several different arguments are used to obtain estimates of the relevant matrix elements. The nucleons are assumed to form a normal Fermi fluid with a continuous excitation spectrum. The calculated cooling rates indicate that a neutron star containing quasifree pions would cool within a few days to a temperature so low that the star would be unobservable. The surface of a star that does not contain quasifree pions would cool to 10^{7}°K in a few months and would reach 4×10^{6}°K in about 100 years. The calculated cooling rates strongly indicate that the discrete x-ray sources located in the direction of the galactic center are not neutron stars. (auth)

4533 SELECTED TOPICS IN MODERN THEORETICAL PHYSICS. Chiu, H. Y. pp 225-91 of Lectures in Theoretical Physics. Vol. VI. Boulder, Colo., The University of Colorado Press, 1964.

The overall stellar processes and properties are reviewed. Stellar structure equations are derived, and neutrino processes are discussed for stellar energy dissipation without involving photons. The iron-helium phase transition at about 6×10^{9} °K, which is a process important in supernova collapse, is considered. Other topics covered are dynamical collapse of a star, static structure of neutron stars, and the dynamic collapse of over-sized neutron stars. (J.F.P.)

4534 NUCLEAR AND NEUTRINO PROCESSES IN STARS AND SUPERNOVAE. Vogl, Joseph L.; Fowler, William A. pp 379-458 of Lectures in Theoretical Physics. Vol. VI. Boulder, Colo., The University of Colorado Press, 1964.

In discussing nuclear and neutrino processes in stars and supernovae several facets of the phenomena are covered. Among these is the origin of the nuclear species, in which the universal or cosmic abundance curve is considered. A few of the many cosmologies are briefly discussed primarily to indicate that the view that heavy elements are produced in stellar interiors can be accommodated within the framework of practically all of the various cosmological theories. A brief review is given of stellar structure, and stellar evolution is discussed. Other topics considered are nuclear reaction rates under stellar conditions, hydrogen and helium burning, and neutrinos in the equilibrium process. (J.F.P.)

Atomic Physics

Refer also to abstracts 4215 and 4708.

4535 (ANL–7081, pp 128-9) ATOMIC-BEAM RESEARCH. Childs, W. J.; Goodman, L. S.; Dalman, J. (Argonne National Lab., Ill.).

A brief review of research carried out during the past year with the Mark II atomic-beam magnetic-resonance apparatus is presented. Results are presented for a resonance in the $^{4}F_{\frac{5}{2}}$ metastable atomic state of ^{51}V. (M.O.W.)

4536 (COO–818-61) THE ELECTRON LIFETIME. AN EXPERIMENTAL TEST OF CHARGE CONSERVATION [Thesis]. Moe, Michael K. (Case Inst. of Tech., Cleveland, Ohio). 1965. Contract AT(11-1)-818. 75p. Dep. mn; CFSTI $3.00 cy, $0.75 mn.

New lower limits on the electron lifetime were set by a series of experiments sensitive to two different conditions for non-charge-conserving electron decay processes. The lifetime of iodine K electrons for a process without photons among the decay products was shown to be $\tau_e > 4 \times 10^{21}$ year compared to the earlier limit of $\tau_e > 10^{18}$ year set by der Mateosian and Goldhaber. The lower limit on the lifetime for the process $e^{-} \rightarrow \nu_e + \gamma$ was raised from a previous best value of $\tau_e' > 10^{19}$ year to $\tau_e' > 5 \times 10^{22}$ year. These results were interpreted in terms of their implications with respect to the law of charge conservation. (auth)

4537 (NP–15576) SELF-CONSISTENT PERTURBATION METHOD. I. CALCULATION OF DIPOLE POLAR-

IZABILITY AND SHIELDING FACTOR. Lahiri, J.; Mukherji, A. (Saha Inst. of Nuclear Physics, Calcutta (India)). [1965]. 20p. Dep. mn.

A variation method was described which yields self-consistent wave function for an atom or molecule subjected to a perturbing field. With a determinantal wave function, energy expression up to the second order is derived in terms of perturbed one electron orbitals. Functions which are self-consistent up to the first order are obtained by energy minimization through successive approximation. It is possible to increase the accuracy of this method by considering higher order terms in the energy expression. This variation method was applied very satisfactorily, within the limits of the Hartree-Fock approximation, to the solution of first order perturbation of atomic orbitals in an external electric field. Dipole polarizability and shielding factor of several atoms and ions were calculated. (M.O.W.)

4538 (NP–15577) SELF-CONSISTENT PERTURBATION. II. CALCULATION OF QUADRUPOLE POLARIZABILITY AND SHIELDING FACTOR. Lahiri, J.; Mukherji, A. (Saha Inst. of Nuclear Physics, Calcutta (India)). [1964]. 15p. Dep. mn.

Quadrupole polarizability and shielding factors for 2- and 4-electron closed shell ions were computed following the self-consistent perturbation method. The results are accurate up to first order in the wave functions under the fully coupled Hartree-Fock approximation. The importance of choosing proper representation for perturbed orbitals is discussed. (auth)

4539 (UCRL–11444) UNITS FOR ATOMIC AND SUBATOMIC PHYSICS. Barkas, Walter H. (Lawrence Radiation Lab., Univ. of California, Berkeley). May 11, 1964. Contract W-7405-eng-48. 8p. Dep. mn; CFSTI $1.00 cy, $0.50 mn.

The consequences are examined of setting h = 1 and c = 1, while retaining the electron-volt. The system of units thus defined is simple and practical for atomic and subatomic physics. A convention is also suggested which permits any quantity to be expressed by a number near unity. (auth)

4540 (UCRL–14364) THE KIRZHNITS CORRECTIONS TO THE THOMAS-FERMI EQUATION OF STATE. McCarthy, Shaun L. (Lawrence Radiation Lab., Univ. of California, Livermore). Aug. 26, 1965. Contract W-7405-eng-48. 62p. Dep. mn; CFSTI $3.00 cy, $0.75 mn.

The derivation of the quantum and exchange corrections to the Thomas-Fermi model is outlined. An equation of state is discussed. Expressions dealing in atomic number are given for the pressure, energy, and their quantum and exchange corrections. Numerical results of computer calculations appear in the appendix for scaled temperatures $10^{-2} \leq kT/z^{4/3} \leq 10^{5}$ ev. Polynomial approximations to the Fermi-Dirac integrals $I_{1/2}(\eta)$, $I'_{1/2}(\eta)$, and $I''_{1/2}(\eta)$ used in the calculation of the equation of state were evaluated. The equation of state of lead according to the TF, TFD, and TFC (quantum and exchanges corrected) models are compared with a Mie-Gruneisen semi-empirical equation of state from high-pressure Soviet experimental data. The comparison indicates that the TFC zero-temperature isotherm approaches the experimental Mie-Gruneisen results more closely than the other statistical models. However, the operator expansion of the electron distribution used to evaluate the corrections in the TFC model appears to be asymptotic near normal densities and low temperatures ($kT/z^{4/3} < 10^{-2}$ ev), yielding over-correction to the pressure and energy. First-order terms become smaller with the increase of temperature and density. (auth)

4541 (UCRL-16405) SECONDARY ELECTRON DISTRIBUTION FOR HEAVY IONS. Oda, Nobuo; Lyman, John T. (Lawrence Radiation Lab., Univ. of California, Berkeley). Sept. 15, 1965. Contract W-7405-eng-48. 21p. (CONF-650924-6). Dep. mn; CFSTI $1.00 cy, $0.50 mn.

From Workshop Conference on Space Radiation Biology, Berkeley, Calif.

Two approaches for examining the contribution of delta rays to the radiation effect of heavy ions are discussed. They are the space-averaged picture and the extended-track picture. The fundamental quantity for the space-averaged picture is the differential flux ϕ_δ (E) of δ rays. Experimental results on the low-energy part of ϕ_δ (E) are presented. (M.O.W.)

4542 MEASUREMENTS OF BALMER LINE RADIATION FROM SELF-SUSTAINED TOWNSEND DISCHARGES IN HYDROGEN. Nygaard, Kaare J. (Norges Tekniske Hoegskole Trondheim, Norway). Appl. Sci. Res., Sect. B, 12: 91-100(1965).

Absolute radiation intensities of the Hα and Hβ lines emitted from self-sustained Townsend discharges in hydrogen were measured by means of interference filters and a photomultiplier tube. The radiation intensity was in all cases found to be proportional to the discharge current, i.e., the radiation was produced in single encounter electronic excitation processes. The excitation coefficient, corrected for quenching of the radiation, was determined absolutely for E/p = 65–250 v/torr × cm. Finally, some possible production mechanisms are discussed. (auth)

4543 THE EXCITATION BY ELECTRON IMPACT OF STRONGLY IONIZED IONS OF p^2 CONFIGURATION. Bely, Francoise; Bely, Oleg; Lan, Vo Ky (Observatoire Paris-Meudon, France). Compt. Rend., 261: 1189-91 (Aug. 2, 1965). (In French).

The problem of the excitation by electron collision of levels with the p^2 configuration in strongly ionized ions is considered. The ion is superposed by intermediary coupling and the exchange processes between the ion and the electron are not taken into consideration. The coupling potentials intervene in the coupled equations obtained and are given in a very simple form. (tr-auth)

4544 STUDY OF THE TRANSFERS BETWEEN HYPERFINE LEVELS OF ODD ISOTOPES OF MERCURY IN THE 6^3P_1 STATE UNDER THE EFFECT OF COLLISIONS WITH RARE GASES. Barrat, Jean-Pierre; Cojan, Jean-Louis; Lacroix-Desmazes, Francois (Univ. Paris, Caen, France). Compt. Rend., 261: 1627-30(Aug. 18, 1965). (In French).

The transfer cross section between hyperfine levels of odd isotopes of mercury by collisions with different rare gases was measured, and it was found that within the experimental error this cross section is identical to that which provokes the enlargement of the magnetic resonance lines of even isotopes. (tr-auth)

4545 ELASTIC SCATTERING AND POLARIZATION OF ELECTRONS BY ATOM IN SECOND BORN APPROXIMATION. Chatterjee, G.; Sil, N. C. (Indian Assoc. for the Cultivation of Science, Calcutta). Indian J. Phys., 39: 239-47(May 1965).

The differential cross section of scattering and the asymmetry after double scattering for electrons of energy 121 kev by screened field of the gold atom were calculated by the Born method in second approximation, the theoretical findings were compared with the exact results obtained by numerical computation. The comparison allows us to re-examine the degree of validity of the Born method in scattering process. It is found that the second Born approximation gives fairly good results for scattering cross section of 121-kev electrons, but for polarization effect, the second approximation is inadequate. (auth)

4546 SPUTTERING AT ACUTE INCIDENCE. Cheney, Kenneth B.; Pitkin, Edward T. (Marquardt Corp., Van Nuys, Calif.; Univ. of Connecticut, Storrs). J. Appl. Phys., 36: 3542-4(Nov. 1965).

Experimental sputtering yields obtained for incidence angles from 2 to 90° (normal) with incident ion energies of 1.5 to 30 kev are reported. These data were obtained by bombardment of copper, molybdenum, and tungsten sur-

faces with xenon and argon ions. Brief surveys of low- and high-temperature surface effects are also reported. (auth)

4547 INFLUENCE OF ANISOTROPIC SCATTERING ON STOPPING BY ELASTIC COLLISIONS. Baroody, E. M. (Battelle Memorial Inst., Columbus, Ohio). J. Appl. Phys., 36: 3565-73(Nov. 1965).

Calculations of spatial moments $\langle z^n \rangle$ for particles from a plane source in an infinite medium of randomly located target atoms are extended to a scattering cross section which is a product of factors depending on energy and angle separately. It is shown that expressions for Laplace transforms of moments of the flux $f_{nl}(s)$ which were used before for isotropic scattering continue to be valid, provided the definition of the functions $G_l(s)$ is broadened in a natural way. For classical scattering by several inverse power repulsive potentials, and for various ratios of target mass to fast particle mass, spatial moments at zero energy have been calculated through n = 4. Deviations of distributions from the Gaussian form prove to be moderate, and Edgeworth expansions may be used to give approximate curves. With certain additional approximations the results can be applied for scattering by a Thomas–Fermi potential. A few comparisons are made with published Monte Carlo results and with measurements on range distributions of kilovolt ions in gases. (auth)

4548 ION EXPLOSION SPIKE MECHANISM FOR FORMATION OF CHARGED-PARTICLE TRACKS IN SOLIDS. Fleischer, R. L.; Price, P. B.; Walker, R. M. (General Electric Co., Schenectady, N. Y.). J. Appl. Phys., 36: 3645-52(Nov. 1965).

Massive charged particles create regions of intense damage (tracks) by passing through bulk samples of insulating materials. These tracks are shown to result from the positively charged region created by ionization. An approximate model of an "ion explosion spike" is proposed in which the mutual repulsion of the positive ions ejects them into the surrounding lattice. This model is shown to be generally consistent with a wide range of experimental fact. An additional damage mechanism appears to apply to polymers, in some of which tracks are produced by light projectiles such as α particles. The data here are shown to be consistent with tracks consisting primarily of broken bonds caused by decay of directly excited electrons. (auth)

4549 INELASTIC SCATTERING OF ELECTRONS FROM HYDROGEN. Faisal, Farhad (Univ. of Dacca, Pakistan); Harun-ar-Rashid, A. M. J. Nat. Sci. Math., 5: 15-24(Apr. 1965).

With the improvement of experimental techniques, the study of elastic and inelastic scattering of electrons from hydrogen has made considerable progress recently. The classical Born approximation calculations of Massey et al., are however found inadequate and improved methods like that of the impulse approximation are being tried. In this calculation certain inelastic transitions are calculated using, for the evaluation of the exchange integrals, the parametric method of Feynman. Evaluation of the differential cross-sections is also given. (auth)

4550 A GENERAL FORMULA FOR THE CALCULATION OF ABSORPTION CROSS SECTIONS FOR FREE-FREE TRANSITIONS IN THE FIELD OF POSITIVE IONS. Peach, G. (University Coll., London). Mon. Notic. Roy. Astron. Soc., 130: 361-77(1965).

A general formula is derived by assuming that the free electron is moving in a central field. The approximate initial and final free state wave functions are chosen so that they have exact asymptotic forms, the phases being obtained by extrapolating the quantum defects of the observed energy levels into the continuum. The relevant free-free transition integrals were computed and, from the tables given, the free-free absorption cross section for an electron in the field of a positive ion can be readily calculated, provided that the experimental data permits a reliable extrapolation to positive energies. Use is made of the tables to compute cross sections for helium, and it is shown that the simple hydrogenic approximation can be considerably in error. (auth)

4551 CHARGE CONSERVATION AND THE LIFETIME OF THE ELECTRON. Moe, M. K.; Reines, F. (Case Inst. of Tech., Cleveland). Phys. Rev., 140: B992-8(Nov. 22, 1965). (TID-22285).

New lower limits on the electron lifetime were set by experiments sensitive to two kinds of noncharge-conserving decay processes for orbital electrons. The lifetime of the K electrons in iodine for a process without photons among the decay products has been shown to be $>2 \times 10^{21}$ yr and the lifetime for the process $e^- \rightarrow \nu_e + \gamma$ to be $>4 \times 10^{22}$ yr. (auth)

4552 APPROXIMATE CROSS SECTIONS FOR OPTICALLY DISALLOWED EXCITATION OF ATOMS BY ELECTRONS. Vriens, L. (Univ., Utrecht). Physica, 31: 1333-6(Aug. 1965).

Formulas for approximate calculation of excitation cross sections for optically disallowed transitions are discussed. It is shown that the formula previously given by Drawin can be used in a different manner, which seems to give reasonably accurate cross sections for small energies of the incident electrons, and gives the correct high energy limit. A comparison is made between approximate cross sections and Born cross sections. (auth)

4553 TRANSITION PROBABILITIES IN HIGHLY IONIZED p^2 AND p^4 CONFIGURATIONS. Malville, J. McKim; Berger, Richard A. (Univ. of Michigan, Ann Arbor). Planet. Space Sci., 13: 1131-6(Nov. 1965).

Line strengths of magnetic dipole and electric quadrupole transitions in the configurations $2p^2$, $2p^4$, $3p^2$ and $3p^4$ are calculated using interpolated values of spin-orbit interaction parameters and unperturbed energies of the levels. Probabilities of the important ground state transitions are tabulated in the four isoelectronic sequences through the following net charges: $17(2p^2)$, $13(2p^4)$, $15(3p^2)$, $13(3p^4)$. (auth)

4554 SIMULTANEOUS MEASUREMENT OF HYPERFINE STRUCTURE, STARK EFFECT, AND ZEEMAN EFFECT OF $^{133}Cs^{19}F$ WITH A MOLECULAR BEAM RESONANCE APPARATUS. Graeff, G.; Runolfsson, O. Z. Physik, 187: 140-50(1965). (In German).

An electric molecular beam resonance spectrometer was used to measure simultaneously the Zeeman- and Stark-effect splitting of the hyperfine structure of $^{133}Cs^{19}F$. Electric four pole lenses served as focusing and refocusing fields of the spectrometer. A homogeneous magnetic field (Zeeman field) was superimposed on the electric field (Stark field) in the transition region of the apparatus. Electrically induced ($\Delta m_J = \pm 1$)-transitions were measured in the J = 1 rotational state, v = 0, 1 vibrational state. The obtained quantities are: The electric dipole moment μ_{el} of the molecule for v = 0, 1; the rotational magnetic dipole moment μ_J for v = 0, 1; the anisotropy of the magnetic shielding ($\sigma_\perp - \sigma_\parallel$) by the electrons of both nuclei as well as the anisotropy of the molecular susceptibility ($\xi_\perp - \xi_\parallel$), the spin rotational interaction constants c_{C_s} and c_F, the scalar and the tensor part of the nuclear dipole-dipole interaction, the quadrupole interaction eqQ for v = 0, 1. (auth)

4555 AXIAL ELECTRON DENSITY OF H_2^+ IN THE GROUND STATE AND IN EXCITED STATES. Dunken, H.; Friedrich, V. (Universitaet, Jena, Ger.). Z. Physik. Chem. (Leipzig), 29: 299-304(1965). (In German).

The results of the calculation of the axial electron density of H_2^+ in the states $1s\sigma$, $2s\sigma$, $3s\sigma$, and $3d\sigma$ were reported for several different nuclear distances. The results are shown graphically. The method used for the numerical calculation for the axial electron density is described. (J.S.R.)

4556 SECONDARY ION ENERGIES IN CHARGE EXCHANGE REACTIONS [Thesis]. Slanger, Tom George. Los Angeles, Univ. of California, 1965. 145p.

Measurements were made of the energies of secondary ions produced in certain resonant and near-resonant charge exchange reactions. The reactions studied were Ar^+Ar (signifying $Ar^+ + Ar \rightarrow Ar + Ar^+$), Ne^+Ne, $N_2^+N_2$, N_2^+Ar, and Ar^+H_2. A magnetically confined plasma was used to produce the ions, a mass spectrometer assured a pure ion beam, and the beam energy used for the study was 1 to 2 kev. The measured energies are interpreted in terms of space charge and focusing effects to give values for the kinetic energy possessed by the ions just after formation. The ion energies are related to the interaction potentials for ions such as Ar_2^+ and Ne_2^+, which are then compared to the experimental and theoretical results of other investigators. The probability for charge exchange does not appear to be very dependent on the molecular states of the species formed during the exchange, which for Ar_2^+ and Ne_2^+ are $^2\Sigma$ and $^2\pi$ states. The interaction potentials observed for these species are 0.64 ev for Ar_2^+ and 0.36 ev for Ne_2^+. Charge exchange cross sections were measured for a considerable number of reactions, and the anomalously low value observed for Ar^+N_2, and its apparently high secondary ion energy are discussed. A method was devised for measuring the surface effects, and it is shown that there are at least two separate phenomena. There is an effect that has an equilibration time of 15–30 minutes, in which time the surface is charged to 0.5–1.0 volts; and there is a very rapid effect, equilibrating in seconds or less, which charges the surface to a saturated value of 0.35 volts. The similarity of these phenomena to observations made with semiconductors is discussed, and it is concluded that there is a thin semiconducting layer on the metal surfaces used in the apparatus. (Dissertation Abstr.)

4557 AN INVESTIGATION OF BETA SOURCE IONIZATION CURRENTS IN GASEOUS MEDIA [Thesis]. Garte, Samuel M. New York, New York Univ., 1964. 168p.

An instrument was designed and constructed for the measurement of ionization currents in gasses as a function of temperature, pressure, and applied voltage. Operating temperatures up to 125°C may be employed so that compounds of low volatility can be measured in the vapor state up to pressures in the range of one atmosphere. Two ionization chambers, differing in active volumes, were tested. An external source consisting of 100 curies of Pm-147 was used. Measurements were made on the following substances: water, air, nitrogen, oxygen, helium, hydrogen, argon, methane, ethane, ethylene, acetylene, propane, propylene, cyclopropane, 1-butene, isobutylene, 1,3-butadiene, n-butane, isobutane, n-hexane, 2,3-dimethyl butane, 2,2,4-trimethyl pentane, cyclohexane, cyclohexene, benzene, methyl chloride, methyl bromide, methyl iodide, methylene chloride, chloroform, carbon tetrachloride, ethyl chloride, dichloroethane, dimethyl ether, methanol, ethanol, diethyl ether, diacetyl, acetone, formaldehyde, and acetaldehyde. It was found that the low pressure region of the current pressure curve is nearly linear. The current at some arbitrarily chosen low pressure was found to be very nearly a constitutive property of the molecule. Excellent agreement with the Otvos and Stevenson theory of ionization cross-section of molecules was obtained. At higher pressures the shape of the current-pressure curve is sensitive to the nature of the gas. Experiments with gas mixtures demonstrated the feasibility of this technique as an analytical tool for the determination of the composition of gas mixtures. (Dissertation Abstr.)

4558 CALCULATIONS OF THE ENERGY AND ANGULAR DISTRIBUTION OF ELECTRONS EJECTED FROM HELIUM BY PROTONS [Thesis]. Oldham, William Jennings Bryan Jr. College Station, Tex., Texas Agricultural and Mechanical Univ., 1965. 129p.

Calculations from the Born approximation of cross sections for ejection of secondary electrons of various energies and various angles from helium bombarded by 50-, 100-, and 150-kev protons are presented. The range of angles investigated is 10 to 160°, and the range of electron energies is 2 to 300 ev. The results are presented from three calculations, which differ from each other by the choice of functions used to approximate the ground state and continuum wave functions of helium. In the first calculation, hydrogen-like wave functions are used to approximate the helium wave functions. In the second, an analytical approximation to the Hartree–Fock ground state wave function is used, but the hydrogen-like continuum wave functions are retained. In the third calculation, the ground state wave function of the second calculation is used, but the L = 1 part of the hydrogen-like continuum wave is replaced by a Hartree–Fock type wave function. It is found that the results of all three calculations predict the general trend of the cross sections as functions of both electron energy and ejection angle. The cross sections appear to be more sensitive to the choice of the ground state wave function than they are to the choice of the continuum wave function. (Dissertation Abstr.)

4559 OPTICAL PROPERTIES OF ATOMIC HYDROGEN BEAM. Trejbal, Zdenek (Inst. of Nuclear Research, Czechoslovak Academy of Sciences, Rez). pp 259-65 of Physics and Techniques of Low Temperatures, Prague, Publishing House of the Czechoslovak Academy of Sciences, 1964.

Important focusing characteristics of a multipole, with invariable shape of the pole pieces along the beam axis, were obtained, from general considerations, as a function of the parameters of the magnet and the focused beam. The calculation is performed for an atomic hydrogen beam. The focusing effects of a four- and six-pole magnet were considered with assumed course of the magnetic field strength as a function of the distance from the magnet axis. The focusing effect for a four-pole magnet was mathematically verified by the Monte Carlo method. Some important characteristics of the focused beam were obtained from general considerations, assuming that the azimuthal velocities of the atoms are zero. (J.F.P.)

Cosmic Radiation

See also Elementary Particles and Radiations
Nuclear Properties and Reactions

Refer also to abstracts 4522 and 4729.

4560 (AD-618562) GEOPHYSICAL ASPECTS OF COSMIC RAYS. Final Report. Sandstrom, A. E. (Uppsala Univ. (Sweden)). Apr. 15, 1965. 22p. (AFCRL-65-418). CFSTI $1.00 cy, $0.50 mn.

A short survey is given of research on cosmic ray intensity variations during 1964 and a study of atmospheric effects on cosmic ray records from plastic scintillator monitors at Uppsala by A. E. Sandstrom and L. Ekstrom. Data recorded during the first 18 months performance of the plastic scintillator meson monitors are given. (P.C.H.)

4561 (COO-818-64) INTERACTION OF MUONS PRODUCED BY ATMOSPHERIC NEUTRINOS. Reines, F.; Crouch, M. F.; Jenkins, T. L.; Kropp, W. R.; Gurr, H. (Case Inst. of Tech., Cleveland, Ohio); Sellschop, J. P. F.; Meyer, B. (University of the Witwatersrand, Johannesburg (South Africa)). [1965]. Contract AT(11-1)-818. 5p. (CONF-650111-7). Dep. mn; CFSTI $1.00 cy, $0.50 mn.

From CERN Informal Neutrino Conference, Geneva.

An experiment to detect the high energy neutrinos produced in the earth's atmosphere by the interaction of primary cosmic rays is discussed. A rock target was used, and the muons produced in the rock were detected by a large area scintillation detector. A brief discussion of the experimental facilities is presented. (M.O.W.)

4562 (MIT-2098-174) X-RAY AND γ-RAY ASTRONOMY. Oda, Minoru (Massachusetts Inst. of Tech., Cambridge. Dept. of Physics; Massachusetts Inst. of Tech., Cambridge. Lab. for Nuclear Science; Institute for Nuclear Study, Tokyo Univ. (Japan)). [1965]. Contract AT(30-1)-2098. 57p. (CONF-650948-1). Dep. mn; CFSTI $3.00 cy, $0.50 mn.

From 9th International Conference on Cosmic Rays, London.

A review of observational facts and related arguments concerning x and γ rays of cosmic origin is presented. Observational methods are briefly summarized. A review of the many unexpected results of observational facts of cosmic x rays in the 1 to 10 kev range is presented. Physical processes of x-ray generation in discrete x-ray sources are briefly discussed. While the discovered discrete x-ray sources are in the galactic plane, an isotropic component which is likely of extragalactic origin seems to exist. Observations of radiation from several tens of kev up to γ-ray energies are reviewed. Though no γ-rays of proven cosmic origin have been detected, upper limits set for various suspected discrete sources and the isotropic component have considerable physical significance. (auth)

4563 THE UPPER LIMITING PRIMARY RIGIDITY OF THE COSMIC RAY SOLAR ANISOTROPY. Jacklyn, R. M. (Dept. of External Affairs, Melbourne; Univ. of Tasmania, Australia); Humble, J. E. Australian J. Phys., 18: 451-71(Oct. 1965).

A method of determining the upper limiting rigidity of the solar diurnal variation of the cosmic ray primaries in free space is described. It involves a comparison of the response to the anisotropy of neutron monitors at sea level and of meson telescopes underground. Making use of the model for the free-space first harmonic proposed by Rao, McCracken, and Venkatesan, the annual average value for the upper limiting rigidity (R_u) in 1958 is estimated to have been 95 Bv with an error of estimate of about 10–20 Bv. Changes in the observed annual mean daily variation between 1958 and 1962 indicate that R_u may have decreased by about 20–40 Bv over this period, but a more refined analysis is needed to confirm this. Changes in R_u could also influence a sidereal daily variation as observed at the earth. Evidence is presented for such an effect, from the observations underground at Hobart. It is shown that the annual average pressure-corrected solar diurnal variation observed at a depth of 40 mwe must be largely under the control of the solar anisotropy. The most significant evidence presented comes from observations in three different directions underground at Hobart during 1961 and 1962. The first harmonics of the solar daily variations observed in these directions have been found to be broadly compatible with the model for the anisotropy proposed by Rao, McCracken, and Venkatesan. The results of an investigation of the response of an underground telescope to generalized free-space first and second harmonics, for different approximations to the geomagnetic field and for small and large sets of arrival directions are also presented. (auth)

4564 ON THE ORIGIN OF COSMIC RAYS. Haar, D. Ter (Magdalen Coll., Oxford). Contemp. Phys., 6: 338-48(June 1965).

A brief survey is given of the various physical, astronomical, and radioastronomical data pertaining to cosmic ray nuclei with energies above 1 Bev. A theory is then outlined, the details of which are due to Ginzburg and Syrovatskii, in which it is suggested that these cosmic rays are produced in supernovae and that their properties—such as chemical composition, energy spectrum, and spatial distribution—are determined partly by their acceleration in and ejection from the sources and partly by various physical processes occurring during the passage of the cosmic rays from their sources to the earth. (auth)

4565 SOLAR MODULATION OF THE LOW-ENERGY GALACTIC HELIUM SPECTRUM AS OBSERVED ON THE IMP 1 SATELLITE. Gloeckler, George (Univ. of Chicago). J. Geophys. Res., 70: 5333-43(Nov. 1, 1965).

The time variations in the low-energy cosmic-ray helium of galactic origin were studied over a continuous period of 5.5 months near the minimum of the present solar activity cycle. It was found that during this time the helium flux in the 30- to 90-Mev per nucleon energy interval increased by (65 ± 22)% while the flux in the 250- to 500-Mev per nucleon energy range increased by (30 ± 8)%. The increase in the flux of primaries >3 Bev in rigidity, as derived from the Climax neutron monitor intensity, was only ~5% in this time interval. It is shown from these observed increases that the modulation of the galactic cosmic radiation at these low energies is dependent on the velocity of the galactic particle rather than on its rigidity and that it is well described by the theory of Parker. The nature of the spectrum outside the solar system is discussed. The time-averaged modulated galactic helium spectrum in early 1964 which has now been extended down to 7 Mev per nucleon can be approximated by $dJ/dE = 3 \times 10^{-6} E^{1.65}$ helium/m^2 sec ster-Mev, with total kinetic energy E measured in Mev, over the energy range 7 to 90 Mev per nucleon. The evidence for helium of solar system origin below ~50 Mev per nucleon in the "27-day" recurrent regions which are already known to contain large fluxes of low-energy protons is reported. The measurements were made on the Imp 1 (Explorer 18) satellite over the continuous period from November 27, 1963, to May 15, 1964. The instrument used was a four-element charged particle telescope, capable of measuring the energy loss and the total energy of low-energy proton and helium nuclei. (auth)

4566 LOW-ENERGY SPECTRUM OF COSMIC RAYS AS AN INDICATOR OF PRIMARY SOURCE CHARACTERISTICS AND INTERSTELLAR PROPAGATION. Balasurrahmanyan, V. K.; Boldt, E.; Palmeira, R. A. R. (Goddard Space Flight Center, Greenbelt, Md.). Phys. Rev., 140: B1157-61(Nov. 22, 1965).

The low-energy spectra of protons and helium nuclei, recently measured by McDonald and Ludwig, and by Fan, Gloeckler, and Simpson are corrected for solar modulation according to Parker's model and for diffusive passage through interstellar matter. The resulting source spectrum is exhibited and compared with the spectrum of accelerated particles inferred from high-energy data and from an energy-equipartition argument due to Syrovatskii. This analysis yields a transmission function for the source environment which is similar in form to the velocity-dependent solar modulation of low-energy particles. (auth)

4567 IQSY-EQEX COSMIC-RAY EXPEDITION TO INDIA. Korff, Serge A. (New York Univ., New York). Phys. Today, 18: 21-4(June 1965).

The experiments carried out by the joint Indo-American IQSY equatorial expedition (EQEX) are described. The cosmic-ray research program involved a series of balloon flights over southern India, whose latitude is one which restricts the incident radiation to the band of incident primary energies in excess of 15 Bev (Stoermer cutoff). The problems studied include fast-neutron production by cosmic radiation, gammas or x rays from outer space, high-energy photons, and the high-energy portion of the heavy primary spectra. The ballooning operations and instruments are briefly described. (L.B.S.)

4568 THE PROPAGATION IN SPACE OF COSMIC-RAY HELIUM NUCLEI AND THE SLOPE OF THEIR ENERGY SPECTRUM. Apparao, M. V. Krishna (Inst. of Fundamental Research, Bombay). Proc. Indian Acad. Sci., Sect. A, 62: 78-89(Aug. 1965).

Cosmic helium nuclei, along with heavier nuclei, traverse interstellar and interplanetary matter during their propagation from their "source" to the earth. Ionization and spallation losses during this traversal modify the energy spectra with which they started. Taking these effects into account, a calculation was made of the abundance of helium nuclei relative to that of heavier nuclei (charge $Z \geq 6$) as a function of energy and the amount of matter traversed. A comparison of the results with the experimental observations suggests that the exponents of the energy spectra of the helium and heavier nuclei should differ by ~0.25 at the "source." (auth)

4569 PRIMARY COSMIC RAY ENERGY SPECTRA [Thesis]. Schrautemeier, Bernard Edward. St. Louis, Washington Univ., 1964. 174p.

At a time of relative solar calm during the summer of 1962, nuclear emulsions were flown by high altitude balloons over Alamogordo, New Mexico and Calvinia, South

Africa in order to measure (by means of multiple Coulomb scattering) some details of the energy spectra of the multiply charged components of the primary cosmic radiation. The New Mexico alpha particle flux was found to be 80 ± 7 particles/(m^2 sec sterad). It was found (by means of a maximum likelihood calculation) that the average values of the eastern and the western (sharp) kinetic energy cut-offs, in the respective 0–45° intervals of projected zenith angles, were 1.6 ± 0.1 and 1.35 ± 0.1 Bev/n, respectively, for the New Mexico data. The corresponding effective (blunt) cut-off values for South Africa were 2.35 ± 0.1 and 1.85 ± 0.1 Bev/n, respectively. The average kinetic energy cut-off values for each entire sample of tracks (east and west components considered together) were 1.5 ± 0.1 Bev/n for New Mexico (sharp cut-off) and 2.05 ± 0.1 Bev/n for South Africa (blunt cut-off). All of the measured values of the cut-off energies were consistent with the cut-off energies and penumbral structures calculated by means of a sixth order harmonic expansion of the earth's magnetic field (assuming no external sources). Also, the experimentally measured asymmetries in the number of tracks incident from the east and from the west at kinetic energies below 2.0–2.5 Bev/n were in agreement with the values predicted by the theoretical calculations involving the magnetic field configuration and the shape of the energy spectrum. The integral energy spectrum was found to be of the form $W^{-\nu}$ for total energies/nucleon, W, of 3.5–10.0 Bev. The values found for the constant ν (1.7 ± 0.15 for New Mexico and 1.45 ± 0.15 for South Africa) were found to be the same (within the errors of measurement) as found near solar maximum. (Dissertation Abstr.)

Direct Energy Conversion

Refer also to abstract 4359.

4570 (AD–614592) THERMIONIC EMITTER MATERIALS RESEARCH PROGRAM. Final Technical Summary Report, October 1, 1963–November 30, 1964. Kitrilakis, S. S.; Weinstein, J. H.; Gunther, B. (Thermo Electron Engineering Corp., Waltham, Mass.). Contract Nonr356300. 93p. (TE74-65). CFSTI $3.00 cy, $0.75 mn.

The accomplishments during the first and second years of the three-year Thermionic Materials Research Program are summarized. The development of an advanced test vehicle using a collector guard ring and other improvements is described. Collector work function data obtained with a niobium collector and a rhenium collector are described and analyzed. The results are compared with earlier results of molybdenum collectors. Power output data using each of the collector materials were also taken and analyzed. Again a comparison was made between power output from similar emitters opposite rhenium, niobium, and molybdenum collectors. It was concluded that no significant difference in optimum converter performance resulted from the difference in collector material. The relationship between collector work function and converter performance is shown to be more complex than previously predicted, and further study is recommended to determine the actual relationship. Earlier work on electron cooling and interelectrode radiation values was confirmed using the guarded collector test vehicle. (auth)

4571 (AD–618037) 300 WATT PORTABLE THERMOELECTRIC GENERATOR. Monthly Progress Report No. 9 for Period Ending June 1965. Carlton, R. D. (Minnesota Mining and Mfg. Co., St. Paul). Contract N600-61533-62758. 5p. CFSTI $1.00 cy, $0.50 mn.

Over 1000 hours of stable performance has been accumulated on a 5-couple test module. A 9-couple module verified the predicted electrical and thermal performance of the thermopile design. (TAB)

4572 (EUR–2283.d) UNTERSUCHUNGEN UEBER EMITTERSUBSTANZEN FUER THERMIONIC-KONVERTER. EINFLUSS VON CsF AUF DIE ELEKTRONENAUSTRITTSARBEIT VON W, Ta UND Mo. (Investigations on Emission Materials for Thermionic Converter Influence of CsF on Electron Work Functions of W, Ta and Mo). Minor, A.; Langpape, R. (Brown, Boveri und Cie A. G., Heidelberg (West Germany)). 1965. 26p. Dep. mn.

The influence of the addition of cesium fluoride in a cesium thermionic converter was investigated. The electron emission of W, Ta and Mo was measured under free field conditions in the presence of CsF vapor at various pressures and various emitter temperatures. From this, the work function was calculated using the Richardson equation. The results show an increase of the work function with increasing CsF vapor pressure but only above a certain CsF vapor pressure which depends on the emitter temperature. In the same way the work function of Mo was determined in a mixture of Cs and CsF vapor. An independent variation of the Cs and CsF vapor pressures was accomplished. The results demonstrate that the Cs vapor pressure required to lower the work function to a certain value could be considerably decreased if a sufficiently high CsF vapor pressure in the cesium diode could be permanently maintained. The measured results cannot be described with the theory of Rasor and Warner. (auth)

4573 CURRENT SUPPLY SYSTEM WITH LIQUID METAL CIRCULATION. Menke, H.; Pegel, K. Raumfahrtforschung, 9: 138-44(July-Sept. 1965). (In German).

The power needs for electric space drives are given. The properties of liquid metals that make them suitable as heat transfer media and as thermodynamic working media are reported. Energy conversion systems with using liquid metals and the construction of MHD cells are described. (J.S.R.)

4574 USE OF EXTENDED SURFACES IN THERMIONIC CONVERTERS [Thesis]. Quintella, Sergio Geraldo. Urbana, Ill., Univ. of Illinois, 1965. 98p.

The use of extended surface electrodes in thermionic converters is investigated. The governing equations are derived with the use of methods from irreversible thermodynamics. These equations are linearized and their solution provides useful analytical expressions for the study of the problem of simultaneous electron and heat transfer. Several fin profiles are studied with special emphasis on the rectangular and triangular fins. It was found that the finned system, in general, has a higher current density and a higher efficiency than the conventional thermionic converter. A comparison between the rectangular and triangular-finned systems favors the latter. The ineffectiveness of previous experimental configurations of serrated anode, sawtooth cathode, box converter, and slotted cathode is explained from the basic relations. Optimum configurations are discussed. (Dissertation Abstr.)

4575 2nd ANNUAL ENERGY CONVERSION AND STORAGE CONFERENCE, PROCEEDINGS, Oct. 12–13, 1964. Linville, Bill (ed.). Stillwater, Okla., Oklahoma State Univ., [1964]. 72p. $5.00. (CONF-641014).

The conference included 10 complete papers. A separate abstract was prepared for one paper. One paper appeared previously in NSA as 19: 16464. Topics covered in the remaining papers are storage as an economic alternative to peaking power, the Taum Sauk Project for energy storage by hydraulic means, the economics of energy storage, the use of one or more three-phase bridges for conversion in d-c power transmission, fuel cell research, and high-energy electrochemical power system, the fuel cell power plant for the electric utility industry, and the need for basic research in energy conversion. (J.F.P.)

For an abstract of the individual paper see: 4992.

4576 IMPROVEMENTS RELATING TO THE THERMIONIC GENERATION OF ELECTRICITY FROM NUCLEAR FUEL HEAT. (to Babcock and Wilcox Co.). British Patent 1,008,541. Oct. 27, 1965. Filed July 21, 1961.

A cell adapted for electricity generation thermionically from the heat of neutron-irradiated nuclear fuel includes a pair of conversion units. Each unit includes cathodes in lamina form on respective sides of a charge of nuclear fuel and in heat relation with it and anodes in lamina form

adapted to be fluid cooled and arranged for receiving thermionically emitted electrons from the cathodes across inter-electrode spaces. A number of cell assemblies each made up of a number of cell units having a single cell arranged between each pair of adjacent spaced elongated parallel plates is proposed for inclusion in the core of a liquid moderated and cooled heterogeneous reactor core. (B,L,M.)

Elementary Particles and Radiations

See also Field Theory, Scattering Theory, and Symmetries

Refer also to abstracts 4504, 4536, 4551, 4848, and 4849.

4577 (AD-618067) HIGH ENERGY PHYSICS RESEARCH USING A 460 Mev SYNCHROCYCLOTRON. Final Report. Anderson, Herbert L. (Enrico Fermi Inst. for Nuclear Studies, Univ. of Chicago, Ill.). July 14, 1965. Contract N60ri02022). 15p. CFSTI $1.00 cy, $0.50 mn.

Doctoral dissertations are listed for students who conducted their research with the cyclotron. Also given is a chronological list of published research. (TAB)

4578 (AD-618660) ETA PHOTOPRODUCTION IN THE REGION FROM THRESHOLD TO 900 Mev. Prepost, R.; Lundquist, D.; Quinn, D. (Stanford Univ., Calif. High-Energy Physics Lab.). May 1965. Contract Nonr22567. 16p. (HEPL-384). CFSTI $1.00 cy, $0.50 mn.

Measurements of the differential cross section of the process $\gamma + p$ to $\eta^0 + p$ were made in approximately 50 Mev intervals from threshold to 900 Mev. The yield of recoil protons was measured at a fixed momentum and angle as a function of the bremsstrahlung end point energy, and η production was seen as a step in the proton yield at the appropriate threshold energy. The differential cross section at 90 degrees was characterized by a sharp rise near threshold reaching a maximum value of 1 microbarn/sr at 760 Mev, and then falling off to a value of 0.3 microbarn/sr at 900 Mev. A measurement of the differential cross section for 3 different angles at 790 Mev indicated that the cross section is isotropic in the center of mass at this energy. The interpretation of these results in terms of possible contributing partial waves is discussed. (auth)

4579 (AD-618661) PION-PAIR PHOTOPRODUCTION BELOW 1 Bev. Allaby, J. V.; Lynch, H. L.; Ritson, D. M. (Stanford Univ., Calif. High-Energy Physics Lab.). May 1965. Contract Nonr22567. 17p. (HEPL-385). CFSTI $1.00 cy, $0.50 mn.

Measurements of the differential cross section for the reaction $\gamma + p$ to $\pi^- + \pi^+ + p$ were made at several angles for photon energies in the range 550-1000 Mev, using the Stanford Mark III linear accelerator. The π^- were detected and momentum analyzed using a 90 degree magnetic spectrometer. It was found that the reaction was dominated by the pseudo-2-body photoproduction $\gamma + p$ to $\pi^- + N^*$ (1238) especially near the threshold for this process. At low momenta, the π^- were identified by range. At high momenta (>250 Mev/c), the contaminating electrons were eliminated by using a lead and scintillation-counter sandwich system. The yields of both π^- and π^+ off hydrogen were measured and the normalization was obtained by comparing with the known cross sections for $\gamma + p$ to $\pi^+ + n$. Computer calculations of the shapes of the yield curves expected from 2-body and 3-body production enabled the data to be separated into the two possible states $\gamma + p$ to $\pi^- + N^*$ (1238) and $\gamma + p$ to $\pi^- + \pi^+ + p$. Angular distributions and total cross sections are presented. (auth)

4580 (AD-618662) EXPERIMENTAL EVIDENCE FOR A POSSIBLE MESON-EXCHANGE CONTRIBUTION TO ELASTIC ELECTRON-DEUTERON SCATTERING. Buchanan, C. D.; Yearian, M. R. (Stanford Univ., Calif. High-Energy Physics Lab.). June 1965. Contract Nonr22567. 16p. (HEPL-386). CFSTI $1.00 cy, $0.50 mn.

Measurements of magnetic (elastic) electron-deuteron cross sections at q-sq = 6.0, 7.0, 8.0, and 12.0 1/F-sq. Electric scattering was also observed in these q-sq values, as well as at one additional point (q-sq = 20.0 1/F-sq). An analysis of the data definitely indicates that the simple impulse approximation model of the deuteron, incorporating the best possible values for the nucleon form factors, is inadequate to explain the experimental results. (TAB)

4581 (AD-618663) REPORT ON THE INELASTIC ELECTRON SCATTERING PROGRAM AT STANFORD. Lynch, H.; Allaby, J. V.; Ritson, D. (Stanford Univ., Calif. High-Energy Physics Lab.). June 1965. Contract Nonr22567. 20p. (HEPL-387). CFSTI $1.00 cy, $0.50 mn.

A program for measuring the inelastic electron scattering cross section from protons over the range of electron energies available at Stanford is presently being pursued. Of the final products only the electron's momentum and scattering angle are observed. The process is schematically described where the electron emits a photon of four-momentum q; the photon is absorbed and a composite system of mass M is formed (e.g., a proton and a π^0 meson or a π-N resonance). (TAB)

4582 (JINR-P-2361) ISSLEDOVANIE REAKTSII $\pi^- p \rightarrow m\,\pi^0 + n$ PRI IMPUL'SE π^--MEZONOV 4 Gev/c. (Investigation of Reactions $\pi^- p \rightarrow m\,\pi^0 + n$ at the π^- Momentum of 4 Gev/c). Grishin, V. G.; Kistenev, E. P.; Kopylova, D. K.; Kriventsova, A. G.; Mu Chun; Ryabtsov, V. D.; Sil'vestrov, L. V. (Joint Inst. for Nuclear Research, Dubna (USSR). Lab. of High Energy). 1965. 20p. Dep. mn.

The π^0 production was investigated in the reactions of the type $\pi^- p \rightarrow m\pi^0 + n$ (m = 1,2,3...) at the π^- meson momentum of 3.97 + 0.06 Bev/c. A 24-liter propane chamber was used. Events having two and more number of γ quanta were analyzed. In the effective mass spectrum of two γ quanta there is a sharp π^0 peak. The average number of π^0 mesons per interaction is 1.9 ± 0.2. The angular momentum distributions of π^0 mesons were obtained. The charge exchange cross section was found to be $\sigma(\pi^- p \rightarrow \pi^0 n) = 0.17 \pm 0.06$ mb. (auth)

4583 (JINR-P-2371) METODIKA OPREDELENIYA IMPUL'SA ZARYAZHENNOI CHASTITSY V NEODNORODNOM MAGNITNOM POLE. (A Determination of Charged Particle Momentum in an Inhomogeneous Magnetic Field). Malyshev, R. V. (Joint Inst. for Nuclear Research, Dubna (USSR)). 1965. 14p. Dep. mn.

A method is described of determining the particle momentum by its trajectory in a cloud chamber with a magnetic field having a considerable inhomogeneity. The least squares method is used to determine the parameters of a system of differential equations which describes the experimental trajectory. The particle momentum is found as one of the parameters of this system. The method was applied in the program for processing the V^0-events in studying the K_2^0 decaying properties. (auth)

4584 (JINR-P-2380) O VOSSTANOVLENII AMPLITUDY REAKTSII ROZHDENIYA VEKTORNOGO MEZONA $\pi + N \rightarrow N + \omega\,(\rho)$. (On Reconstruction of the Amplitude of the Vector Meson Production Reactions $\pi + N \rightarrow N + \omega\,(\rho)$). Doan-Nhuong (Joint Inst. for Nuclear Research, Dubna (USSR). Lab. of Theoretical Physics). 1965. 10p. Dep. mn.

A complete set of experiments is considered which is necessary for a direct reconstruction of the amplitude of the vector meson $\omega(\rho)$ production reactions. It is shown that these experiments are the polarization effects of the target and recoil nucleons and of the vector meson. (auth)

4585 (SLAC-43) SPIN AND PARITY ANALYSIS IN TWO-STEP DECAY PROCESSES. Berman, S. M.;

Jacob, M. (Stanford Linear Accelerator Center, Stanford Univ., Calif.). May 1965. Contract AT(04-3)-515. 37p. Dep. mn; CFSTI $2.00 cy, $0.50 mn.

Results are given for applying the helicity formalism to spin and parity analysis of a certain class of resonances decaying into another resonance and a non-resonant particle with the subsequent decay of the intermediate resonance into non-resonant particles. Integer and half integer cases are treated separately. (auth)

4586 (TID-22315) MEASUREMENTS OF POSITIVE KAON PRODUCTION IN PROTON-PROTON COLLISIONS AT 2.85 AND 2.40 Bev [Thesis]. Reed, James Theodore (Rochester Univ., N. Y. Dept. of Physics and Astronomy). [1965]. Contract AT(30-1)-875. 146p. Dep. mn; CFSTI $4.00 cy, $0.75 mn.

An experiment is described in which protons from the external beam of the BNL Cosmotron were directed onto a liquid hydrogen target, and the doubly differential cross sections $d^2\sigma/d\Omega dp$ for the production of positive kaons were measured. These measurements were made at incident proton kinetic energies of 2.85 and 2.40 Bev and at laboratory angles of 0°, 17°, and 32°. The kaon data are presented in the form of five laboratory and five center-of-mass spectra. The results of integrating these spectra over momentum are given, i.e., $d\sigma/d\Omega$. A further integration over angles yields a total cross section for production of K^+ of $\sigma = 279 \pm 56$ μ barns. An enhancement is seen in the 0° spectra, at or near the maximum kaon momentum. Possible explanations for the peak are advanced in terms of a lambda-proton bound state, resonance, and final state interaction. The possibility of a bound state is shown to be unlikely. The peak would correspond to a Q value of 4 ± 8 Mev/c^2 for the Λ-p system. From a Breit-Wigner fit, one finds $\Gamma/2 = 17^{+\infty}_{-10}$. Using the S-wave scattering formalism, the peak can be fitted by "a" = +3 ± 1f and "r_0" ≤ 2f. (auth)

4587 (UCRL-11495) A DYNAMICAL FORMULA FOR THE SLOPE OF THE POMERANCHUK TRAJECTORY. Chew, Geoffrey F.; Teplitz, Vigdor L. (Lawrence Radiation Lab., Univ. of California, Berkeley). June 11, 1964. Contract W-7405-eng-48. 7p. Dep. mn; CFSTI $1.00 cy, $0.50 mn.

An approximate dynamical relation is derived between the slope of the Pomeranchuk trajectory at zero energy. This relation is: $\alpha_P(0) \approx (1/64\pi^2)(m_\rho/\Gamma_\rho)(\sigma_{\pi\pi})$ where m_ρ is the mass, Γ_ρ is the full width of the meson (ρ), and $\sigma_{\pi\pi}$ is the asymptotic meson (π)-meson (π) total cross section at high energy. The derivation is based on a version of the strip approximation which ignores branch points in angular momentum but does not neglect inelastic scattering, even in the low energy resonance region. The shape and rate of shrinking of the high-energy diffraction peak is also considered. (J.F.P.)

4588 (UCRL-11565) POLARIZATION PARAMETER IN PROTON-PROTON SCATTERING FROM 328 TO 736 Mev [Thesis]. Betz, Frederick William (Lawrence Radiation Lab., Univ. of California, Berkeley). Aug. 11, 1964. Contract W-7405-eng-48. 90p. Dep. mn; CFSTI $3.00 cy, $0.75 mn.

The polarization parameter in elastic proton-proton scattering was measured at several energies and angles. The unpolarized external proton beam from the 184-inch synchrocyclotron was made incident upon a polarized target. The full energy of the beam was degraded by means of copper absorber to obtain beams with laboratory kinetic energies of 328, 614, 679, and 736 Mev. The elastic proton-proton scatterings were kinematically separated from background events by detection of both protons in coincidence with the use of scintillation counters. Measurements were made in the center-of-mass angular region from 33 to 110 degrees (at smaller angles the slower proton lacked sufficient range to emerge from the target). The target was polarized by means of a technique called dynamic nuclear orientation. Its polarization was measured by monitoring the nuclear magnetic resonance signal of the free protons in the target. This signal was calibrated in terms of absolute magnitude of polarization by measurement of the temperature of the proton system and the frequency of its resonance when the polarization of the target was unenhanced. The experimental procedure was to count the number of elastic scatterings into a solid angle with the polarization of the target parallel to the normal to the scattering plane and then, under identical conditions, to count the elastic scatterings with the direction of the polarization of the target reversed. The measured values of the polarization parameter are presented as a function of angle for each incident proton energy. (auth)

4589 (UCRL-11754) AN ATTEMPT TO OBSERVE A POSITIVE-STRANGENESS BARYON. Lyons, Louis; Dahl, Orin I. (Lawrence Radiation Lab., Univ. of California, Berkeley). Nov. 3, 1964. Contract W-7405-eng-48. 15p. Dep. mn; CFSTI $1.00 cy, $0.50 mn.

An experiment was performed in order to detect a +1 strangeness baryon (Z^+). Film taken in the course of a systematic study of 1.5 to 4.2 Bev/c π^-p interactions in the LRL 72 inch hydrogen bubble chamber was scanned for Z^+. Negative results are reported. The possible decay modes of Z^+ are discussed. (M.O.W.)

4590 (UCRL-11926) NUCLEON-NUCLEON POLARIZATION AT 700, 600, 500, AND 400 Mev [Thesis]. Cheng, David (Lawrence Radiation Lab., Univ. of California, Berkeley). July 1, 1965. Contract W-7405-eng-48. 105p. Dep. mn; CFSTI $4.00 cy, $0.75 mn.

The polarization parameters for the two-nucleon systems were measured at the 184-in. cyclotron at beam energies of 700, 600, 500, 400 and 310 Mev. They are measured for both the pp and pn systems by means of a polarized proton beam initially produced by scattering the external proton beam on a carbon target at ±6 deg, and then scattered in a liquid hydrogen target or a liquid deuterium target. The asymmetry is measured by reversing the sign of the beam polarization by reversing the pC scattering angle. The angular range treated is between 30 and 150 deg in the center-of-mass system, and involves measurements at eight angular positions at each energy. In order to calibrate the beam polarization, the polarization parameter for pC is also measured at the above energies in the forward direction between 6 and 14 deg in the laboratory frame. When fitting both the differential cross section, I_0, and polarization, P, with all the data available in this energy region, in terms of power series, the differential cross sections in both the pp and pn systems were found to vary with energy to a greater extent than the polarization parameters. From these fits, I_0 and P, for the isotopic spin singlet (I = 0) state of the 2-nucleon system is also calculated. (M.O.W.)

4591 (UR-875-108) MUON-PROTON SCATTERING AT HIGH MOMENTUM TRANSFERS [Thesis]. Ellsworth, Robert Waldo (Rochester Univ., N. Y.). 1965. Contract AT(30-1)-875. 130p. Dep. mn; CFSTI $4.00 cy, $1.00 mn.

A measurement was made of the cross section for muon-proton elastic scattering at 4-momentum transfers between 700 and 1100 Mev/c. A purified beam of muons, with momenta between 1.5 and 6.0 Bev/c, was constructed at the Brookhaven AGS. A liquid hydrogen target, 6 feet long and 18 inches in diameter was exposed to the beam, and recoil particles detected in an array of counters and spark chambers. Photographs of the spark chambers were used to reconstruct the scattering events. The cross section, computed from a total of 496 events, is compared with corresponding data from other measurements of electron-proton scattering. The two sets of data show the same dependence on 4-momentum transfer. Although the absolute μ-p cross section is slightly lower than the absolute e-p cross section, no significant difference between e-p and μ-p scattering is found. (auth)

4592 ANALYTICAL WAVE FUNCTIONS AND PHOTODISINTEGRATION OF THE DEUTERON. Haemaelaeinen, R. M. K. (Univ. of Helsinki). Ann. Acad. Sci. Fennicae, Ser. A VI, 1-7(1965).

The photodisintegration of the deuteron at gamma energy

of 77.3 Mev is investigated with the aim of studying analytical wave functions of the deuteron ground state. The calculations show that the shape of the wave functions plays an essential role in the problem. (auth)

4593 UNITARY SOLUTION TO THE THREE CHANNEL N/D EQUATIONS IN A POLE APPROXIMATION. Auvil, P. R.; Brehm, J. J. (Northwestern Univ., Evanston, Ill.). Ann. Phys., (N.Y.), 34: 505-12(Oct. 6, 1965).

The N/D equations are treated for three, two body channels where the force is approximated by a simple pole. An explicit, unitary solution for the T matrix is found. This solution is then used to study the coupled (π N), ($\pi N^*_{\frac{3}{2}}$), and ($fN^*_{\frac{3}{2}}$) channels. A resonance corresponding to the $N^*_{\frac{3}{2}}$ (1920) is found, and by varying the coupling we are able to fit its mass and branching ratio to the (π N) channel. The full width is too small in this approximation but additional inelastic couplings might improve this result. (auth)

4594 SINGLE PHOTON ANNIHILATION OF THE ^3S STATE OF A NEGATON-POSITON PAIR. Khanna, K. M. (Indian Inst. of Tech., Kharagpur). Indian J. Pure Appl. Phys., 3: 311-12(Aug. 1965).

Bogoliubov canonical transformation was used to study the annihilation of a negaton-positon pair in the ^3S state surrounded by virtual negaton-positon pairs. The dynamics of the γ-ray production was replaced by the simple assumption that the average number of γ rays produced is equal to the average number of negaton-positon pairs in the ground state of the hamiltonian describing the system. In order to conform to the energy and momentum conservation laws in the decay of a negaton-positon pair into a single photon, the production of a neutral particle of the same mass as that of an electron or positon and of spin 0, 1, or 2 was postulated. Such a particle is hitherto unknown and it is conjectured that its lifetime will be very large and it will be much less interactive. (auth)

4595 MEASUREMENT OF POLARIZATION IN ELASTIC PROTON-DEUTERON SCATTERING AT 155 Mev. Kuroda, K.; Michalowicz, A.; Poulet, M. (Universite de Paris, Orsay, France). J. Phys. (Paris), 26: 303-4(June 1965). (In French).

Polarization in elastic p-d scattering at 155 Mev was measured from 7.5 to 82° c.m. An analyzing magnet was used to separate the elastic peak from the inelastic contribution. Polarization of the scattered protons was measured using an analyzing polarimeter. Values found are about 20% lower than those found at Harvard by Postma and Wilson. (auth)

4596 ALPHA-PARTICLE-INDUCED BREAKUP OF THE DEUTERON. Nagatani, K.; Tombrello, T. A.; Bromley, D. A. (Yale Univ., New Haven). Phys. Rev., 140: B824-34(Nov. 22, 1965).

Alpha-particle-induced deuteron breakup reactions were studied in single-counter measurements at incident alpha-particle energies of 41.6 and 29.3 Mev. Simultaneous differential and total cross-section measurements were carried out on protons, deuterons, and alpha particles. Unambiguous evidence for final-state resonance effects in the alpha-nucleon interactions was obtained, particularly from the proton energy spectra; the $p_{\frac{3}{2}}$ alpha-nucleon resonances corresponding to the ^{5}He and ^{5}Li ground states play important roles. As anticipated, phase-space-factor and zero-range Born-approximation calculations failed to reproduce the observed energy spectra. A more exact analysis which explicitly includes the alpha-nucleon interactions, represented by Gammel-Thaler phenomenological potentials, does provide good agreement with the experimental results both in spectrum shape and in total breakup cross section. (auth)

4597 DIRECT NUMERICAL INTEGRATION OF THE TWO-NUCLEON SCHROEDINGER EQUATION WITH TENSOR FORCES. Lovitch, Lionel (Istituto Nazionale di Fisica Nucleare, Pisa, Italy); Rosati, Sergio. Phys. Rev., 140: B877-82(Nov. 22, 1965).

The technique of middle-point matching accompanied by an iterative application of suitable correction formulas for trial values of corresponding parameters is considered in integrating a two-channel Schrödinger equation. In the case of the deuteron wave equations, when tensor forces are taken into account, a correction formula for improving an initial energy value is used in obtaining the binding energy and the corresponding wave functions, the formula giving quadratic convergence. The extension of the method to nucleon-nucleon scattering states is straightforward and the variable quantities are, in that case, the parameters of a phenomenological potential. (auth)

4598 DASHEN-LEE SUM RULES FOR MAGNETIC MOMENTS. Bietti, Amilcare (California Inst. of Tech., Pasadena). Phys. Rev., 140: B908-10(Nov. 22, 1965). (CALT-68-45).

The importance is stressed of the contribution of an isotopic-spin-$\frac{1}{2}$ meson (π) nucleon intermediate state for the Dashen-Lee sum rules which are obtained from the commutation relations between various combinations of the isoscalar and isovector magnetic-moment operators M^S and M^V. In particular, it is shown that the $M^S - M^V$ sum rule can be brought into agreement with experiment by introducing this contribution. Furthermore, it does not have much influence on the "good" $M^V - M^V$ sum rule $(\mu_p^2/2m)^2 = \langle r\rangle_p^2/6$, where μ_p, m, and $\langle r\rangle_p$ are the total magnetic moment, mass, and charge radius of the proton, respectively. The implications of these results for the commutation relations between space components of current densities are also discussed. (auth)

4599 M(12) PREDICTIONS FOR pp SCATTERING. Freund, P. G. O.; Lo, S. Y. (Univ. of Chicago). Phys. Rev., 140: B927-8(Nov. 22, 1965). (COO-264-265).

The relations $A = -R'$, $A' = R$, $C_{KP} = 0$, $C_{PP} = C_{KK}$ and $C_{NN}(\theta) = D(\theta) + D(\pi - \theta) - 1$ between the standard parameters of pp scattering are derived from M(12) invariance and compared with experiment. The applicability of M(12) invariance to scattering processes is discussed. (auth)

4600 CLASSIFICATION OF ALL C-NONINVARIANT ELECTROMAGNETIC INTERACTIONS AND THE POSSIBLE EXISTENCE OF A CHARGED, BUT C = 1, PARTICLE. Lee, T. D. (Columbia Univ., New York). Phys. Rev., 140: B959-66(Nov. 22, 1965). (TID-22048).

Assuming that the strong interaction H_{st} is invariant under the particle-antiparticle conjugation C, it is shown that all possible C-noninvariant electromagnetic interactions H_γ can be classified according to the anticommutator between C and the charge operator Q into two types: (1) $\{C,Q\} = 0$ and (2) $\{C,Q\} \neq 0$. Discussions of the first type C-noninvariant minimal electromagnetic interaction were already given previously. If $\{C,Q\} \neq 0$, then the operator C must be different from what is normally called the "charge-conjugation operator" C_γ which, by definition, changes any state of charge Q to that of $-Q$. Thus, $\{C_\gamma, Q\} = 0$ and $C \neq C_\gamma$. As a consequence, there must exist, at least, a charged particle a^+ which is an eigenstate of C; its eigenvalue can always be chosen to be +1. Furthermore, in the framework of a Lorentz-invariant local-field theory, H_{st} and H_γ are invariant under $C_\gamma PT$, but not CPT. The $C_\gamma PT$ invariance requires the existence of another charged particle a^- which has the same mass as a^+ but the opposite charge. The a^- is also an eigenstate of C. The existence of such $a^\pm$ particles necessitates not only the C nonconservation of H_γ, but also the T noninvariance of H_{st}. The general algebraic relations between H_{st}, H_γ, and these symmetry operators are studied, and the properties of the particles $a^\pm$ are discussed. An explicit spin-$\frac{1}{2}$ model of $a^\pm$ based on the principle of minimal electromagnetic interaction is given. A possible unifying view connecting the present C, T noninvariance with the well-known C, P nonconservation of the weak interaction is discussed. (auth)

4601 MINIMAL ELECTROMAGNETIC INTERACTION AND C, T NONINVARIANCE. Lee, T. D. (Columbia Univ., New York). Phys. Rev., 140: B967-76(Nov. 22, 1965). (TID-22049).

It is well known that the principle of minimal electromagnetic interaction determines a unique electromagnetic-interaction form for a spin-0 or spin-½ charged particle. It is shown that the same principle, when applied to a spin-1 charged particle, leads to a minimal electromagnetic interaction that depends on two arbitrary real parameters: the charge and the magnetic moment. It is further shown that the minimal electromagnetic interaction of a system of N spin-1 particles of the same charge depends on the charge ϵ and an $(N \times N)$ Hermitian matrix, called the magnetic-moment matric M. Such a minimal electromagnetic interaction can be noninvariant under C and T. The general condition of C, T invariance, or noninvariance is analyzed. These considerations are extended to a system of N neutral spin-1 particles, assuming that the minimal electromagnetic interaction of such a system is not zero. Application to the observed ϕ^0, ρ^0, and ω^0 particles gives a C, T noninvariant minimal electromagnetic interaction, which, however, is invariant under P and CT. By making a further assumption concerning its transformation property under SU_3, this C, T noninvariant interaction assumes a simple and unique form. Some of its experimental consequences are discussed. (auth)

4602 COMPARISON OF FORWARD DISPERSION RELATIONS WITH EXPERIMENTS AROUND 10 Gev. Lautrup, B. (NORDITA, Copenhagen); Nielsen, P. Moeller; Olesen, P. Phys. Rev., 140: B984-9(Nov. 22, 1965).

Using the recent experimental data on the real part of the forward π^+-p amplitude around 10 Bev, a comparison is made of forward dispersion relations with experiments in the high-energy region. In this work a new method for testing forward dispersion relations which involves no assumptions whatsoever about the unknown cross sections above 20 Bev is proposed. On account of the large systematic errors in the measured real parts, no definite conclusion can be drawn as to the validity of forward dispersion relations. In estimating the standard deviations in the dispersion integrals, a Monte Carlo method was used. (auth)

4603 ASYMPTOTIC BEHAVIOR OF THE FORWARD-SCATTERING AMPLITUDE. Banerjee, Haridas (Univ. of Delhi). Phys. Rev., 140: B989-91(Nov. 22, 1965).

It is argued on the basis of unitarity and analyticity properties of the scattering amplitude that the total cross section in high-energy scattering should be bounded by $s^{-\frac{1}{4}}\ln^{\frac{1}{2}}s$, where s is the square of the center-of-mass energy. The high-energy accelerator data on $\bar{p}p$ scattering and cosmic-ray data on pp scattering are quite consistent with the law $\sigma_{tot} \propto s^{-\frac{1}{4}}$ asymptotically. If it is further assumed that in the asymptotic limit particle and antiparticle cross sections are identical, the ratio α of the real and the imaginary parts of the forward scattering amplitude in the asymptotic limit is obtained as the value $\alpha \approx -0.4$, which is in fairly good agreement with the results of recent experiments on pp scattering. (auth)

4604 DIFFERENTIAL CROSS SECTION FOR TRIDENT PRODUCTION. Johnson, Eric G. Jr. (Harvard Univ., Cambridge, Mass.). Phys. Rev., 140: B1005-8(Nov. 22, 1965).

The different cross section for pair production by electron scattering off an arbitrary fixed potential (trident) is discussed. This cross section assumes that the three outcoming electrons' energies are to be measured. A modified version of the Monte Carlo procedures is used to obtain the cross section. Three cases were evaluated on an IBM 7090 computer, to obtain a standard deviation of about 4 to 9%. (auth)

4605 COMPARISON OF NUCLEON-NUCLEON SCATTERING DATA WITH THE PREDICTIONS OF $SU(12)_q$. Kantor, P. B.; Kuo, T. K.; Peierls, Ronald F.; Trueman, T. L. (Brookhaven National Lab., Upton, N. Y.). Phys. Rev., 140: B1008-12(Nov. 22, 1965). (BNL-9295).

The form of the nucleon-nucleon scattering amplitude is determined subject to the restriction that baryon-baryon scattering be invariant under $SU(12)_q$ transformations. The results are found to disagree with experiment. The possibility that $SU(12)_q$ may be a "leading approximation" to a true S-matrix theory is discussed briefly. (auth)

4606 REGGE POLES, OPTICAL MODEL, AND HIGH-ENERGY CHARGE-EXCHANGE REACTIONS. Arnold, Richard C. (Argonne National Lab., Lemont, Ill.). Phys. Rev., 140: B1022-5(Nov. 22, 1965).

An optical-model viewpoint, with a Regge-pole form for the absorptive energy-dependent potential, is shown to imply an absorptive correction to Regge-pole formulas for charge-exchange scattering amplitudes. At the same time a closed form for high-energy elastic-scattering amplitudes is obtained incorporating cuts in the angular-momentum plane. Numerical estimates illustrate the difference between these predictions and the uncorrected poles. The power law for large-momentum-transfer behavior is shown to be easily obtainable. (auth)

4607 SIMULTANEOUS BOOTSTRAP OF THE ρ AND f^0 IN $\pi\pi$ SCATTERING. Balazs, L. A. P.; Vaidya, S. M. (Tata Inst. of Fundamental Research, Bombay). Phys. Rev., 140: B1025-6(Nov. 22, 1965).

A self-consistent calculation of the parameters of the ρ and f^0 resonances is carried out, using an effective-potential approach. The exchange of these resonances in $\pi\pi$ scattering is used to construct a lowest order effective potential at each energy. This is sufficient to produce these same resonances in the scattering process. The requirement that the masses and reduced widths of these output resonances be the same as those of the exchanged resonances can then be used to fix these parameters. With 10% self-consistency, mass ≈600 Mev, width ≈100 Mev for the ρ, and mass ≈1100 Mev, and width ≈90 Mev for the f^0 were obtained. The width of the ρ thus comes out considerably narrower than in the usual calculations which ignore the f^0. (auth)

4608 ANTIHYPERON PRODUCTION IN ANTIPROTON-PROTON REACTIONS AT 3.7 Bev/c. Baltay, C. (Yale Univ., New Haven); Sandweiss, J.; Taft, H. D.; Culwick, B. B.; Kopp, J. K.; Louttit, R. I.; Shutt, R. P.; Thorndike, A. M.; Webster, M. S. Phys. Rev., 140: B1027-38(Nov. 22, 1965). (BNL-9276).

Results on the production of antihyperons in the reactions of 3.7 Bev/c antiprotons with protons are presented. Examples were observed of the production of the antiparticles of all the baryons with hypercharge 0 and 1, several of which had not been observed prior to this experiment. The mass and lifetime of the $\bar{\Lambda}$ and the lifetimes of the $\bar{\Sigma}^{\pm}$ were measured and are consistent with the corresponding quantities of the Λ and $\Sigma^{\pm}$, as required by CPT invariance. In the two-body $\Lambda\bar{\Lambda}$, $\Lambda\bar{\Sigma}^0$, $\bar{\Lambda}\Sigma^0$, and $\Sigma^+\bar{\Sigma}^-$ final states the antihyperons displayed a very sharply forward peaked angular distribution. The production of the three-body final states $Y\bar{Y}\pi$ and $\Lambda\bar{N}K$ or $\bar{\Lambda}NK$ tend to proceed through the $Y\bar{Y}^*$ or $\bar{Y}Y^*$ intermediate states, where the Y^* is either the Y_1^* (1385), the Y_0^* (1405), or the Y_0^* (1520). The four-body $\Lambda\bar{\Lambda}\pi^+\pi^-$ final state is dominated by the pair production of the Y_1^* (1385) hyperon isobar. (auth)

4609 STUDY OF THE K^+ DECAY PROBABILITY. Fitch, V. L. (Princeton Univ., N. J.); Quarles, C. A.; Wilkins, H. C. Phys. Rev., 140: B1088-91(Nov. 22, 1965).

The mean life of the K^+ meson was measured with particular attention paid to whether the decay obeys the exponential law. No evidence is found for nonexponential decay. The data give a χ^2 of 365 with 379 degrees of freedom when fitted to a pure exponential between 2.5 and 7.3 mean lives from production. The mean life is found to be 12.443 ± 0.038 nsec. (auth)

4610 SPIN-1 MESON PHOTOPRODUCTION. Harun-ar-Rashid, A. M. (Pakistan Atomic Energy Commission, Dacca, East Pakistan); Moravcsik, Michael J. Phys. Rev., 140: B1123-31(Nov. 22, 1965). (UCRL-12162).

Production of a spin-1 boson from a spin-½ fermion by a photon is discussed. First, general formulas are given for the number of invariant amplitudes in a reaction involving two particles in both the initial and final states.

They give, with parity conservation, 12 amplitudes for the process under discussion. These 12 amplitudes are enumerated and grouped in a way which emphasizes the similarities between this process and photoproduction of spin-0 mesons. Expressions are given for all 64 physical observables which can be measured when the meson polarization is averaged over. It is shown that the measurement of the recoil-nucleon polarization and the differential cross section from polarized nucleon targets is here not sufficient to determine the parity of the meson produced (as it was in the case of spin-0 photoproduction), but this measurement instead allows a distinction of spin-0 and spin-1 photoproduction (independent of the parity) in case the spin of the meson produced is unknown. Finally a one-particle-exchange calculation of the vector-meson production process is given, using as intermediate particles a nucleon, a pion, and one or several kinds of vector mesons. (auth)

4611 RADIATIVE LEPTON PRODUCTION BY A NEUTRINO BEAM. Adams, J. Barclay (Stanford Univ., Calif.; Brandeis Univ., Waltham, Mass.). Phys. Rev., 140: B1131-40(Nov. 22, 1965).

The reaction $\nu + n \rightarrow \mu + p + \gamma$ is considered. To an extensive perturbation-theory type model for the nonradiative reaction ($\nu + n \rightarrow \mu + p$) are added electromagnetic interactions of the particles involved. Total and differential cross sections are computed for several neutrino energies in the Bev range. Results when normalized to the nonradiative cross sections are found to be insensitive to parameters in the model except the nucleon anomalous moments. For high-energy neutrinos, the effect of the anomalous moments is manifest as a striking peak in the photon spectrum when displayed as $d\sigma/d\ln k$ versus $\ln k$. This offers the possibility of testing for the excitation of higher nucleon resonances in the reaction. (auth)

4612 ELECTRON AND POSITRON SCATTERING AND THE ANAPOLE. Bergstrom, J. C. (Univ. of Saskatchewan, Saskatoon); Margolis, B.; Robertson, D. Phys. Rev., 140: B1141-4(Nov. 22, 1965).

Electron-electron, electron-positron, and electron-nucleus scattering are calculated in first Born approximation, including an anomalous interaction which defines the "anapole" and violates charge conjugation and parity conservation. An anapole produces longitudinal polarization in electron-nucleus scattering. Polarization effects in $e^- - e^\pm$ scattering are not calculated. The effect of anomalous electric and magnetic dipole moments are discussed briefly. The results are equally valid for muon scattering if the electron mass is replaced by the muon mass. (auth)

4613 EXPLICIT WAVE FUNCTIONS FOR ANY SPIN. Frishman, Y. (Weizmann Inst., Rehovoth, Israel); Gotsman, E. Phys. Rev., 140: B1151-6(Nov. 22, 1965). (IA-1040).

A general method is given for calculating the exact form of the helicity eigenstates of a wave function for any spin. Explicit expressions of the wave functions for spin S = 1, $\frac{3}{2}$, 2, and $\frac{5}{2}$ are listed. Examples of helicity amplitudes for the production of $S = \frac{3}{2}^+$ and $S = \frac{5}{2}^+$ isobars in proton-proton scattering are computed. (auth)

4614 CALCULATIONS OF NEUTRON-DEUTERON SCATTERING. Aaron, R. (Northeastern Univ., Boston); Amado, R. D.; Yam, Y. Y. Phys. Rev., 140: B1291-1300 (Dec. 6, 1965).

Exact three-body calculations using separable two-body interactions were carried out for the neutron-deuteron system at low and intermediate energies. Binding energies, scattering lengths, angular distributions, and total cross sections for n-d scattering and the total break-up cross sections for n + d → n + n + p were obtained. These agree well with experimental data where available, indicating that nucleon exchange is the dominant mechanism at these energies. Other theoretical results presented are the partial-wave scattering amplitudes, phase shifts, and angular distributions for the quartet and doublet spin states of the n-d system. Diffraction scattering is noted in the doublet state, and its development as a function of energy is traced. Further refinements and future calculations are discussed and outlined. (auth)

4615 ANTIPROTON-NUCLEON ANNIHILATION AT REST INTO TWO MESONS AND SU(6) SYMMETRY. Konuma, Michiji (Scuola Normale Superiore, Pisa, Italy; Centro Ricerche Fisica e Matematica, Pisa, Italy); Remiddi, Ettore. Phys. Rev., 140: B1318-23(Dec. 6, 1965).

Two-meson production processes in antiproton-nucleon annihilation at rest are discussed extensively on the SU(6) model. For the orbital angular momenta in the initial and final states the s and the p wave, respectively, are taken. The effects of the SU(3)-invariant interaction and of the first-order SU(3)-breaking interaction are taken into account. All the transition amplitudes are expressed in terms of five SU(6)-invariant amplitudes [seven in the case when the SU(3)-breaking effect is included]. These expressions could give a very convenient tool for a systematic analysis of the experimental results. The relations between transition amplitudes are derived, and several useful relations such as $\sigma(\bar{p}n \rightarrow \pi^0\pi^-)/k_\pi = 2\sigma(\bar{p}n \rightarrow K^0K^-)/k_K$, $\sigma(\bar{N}N \rightarrow \eta\omega)/k_{\eta\omega} = (9/25)\sigma(\bar{N}N \rightarrow \eta\rho)/k_{\eta\rho}$, and $\sigma(\bar{N}N \rightarrow \pi\varphi) = \sigma(\bar{N}N \rightarrow \pi\varphi) = \sigma(\bar{N}N \rightarrow \rho\varphi) = \sigma(\bar{N}N \rightarrow \omega\varphi) = 0$ are discussed, where use is made of the usual ω-φ mixing parameter and k is the relative momentum of the final two mesons. (auth)

4616 Σ RADIATIVE DECAY AND THE ANGULAR MOMENTUM OF Σ PIONIC DECAY. Bazin, M. (Princeton Univ., N. J.); Blumenfeld, H.; Nauenberg, U.; Seidlitz, L.; Plano, R. J.; Marateck, S.; Schmidt, P. Phys. Rev., 140: B1358-64(Dec. 6, 1965). (PPAD-2137-554).

The pion spectrum in the $\Sigma^\pm \rightarrow n + \pi^\pm + \gamma$ decay was studied in order to determine the angular-momentum channel of the Σ pionic decay. The results from measurements of a sample of 14,800 $\Sigma^+ \rightarrow \pi^+ + n$ decays and 25,000 $\Sigma^- \rightarrow \pi^- + n$ decays are discussed. After subtraction of the background, 26 Σ^+ radiative decays and 28 Σ^- radiative decays with $P_{cm} < 166$ Mev/c are found. The combination $\Sigma^+ \rightarrow \pi^+ + n$ decays via P wave and $\Sigma^- \rightarrow \pi^- + n$ decays via S wave is 45 times more likely than the combination $\Sigma^+ \rightarrow \pi^+ + n$ decays via S wave and $\Sigma^- \rightarrow \pi^- + n$ decays via P wave. This means that the result is 2.7 standard deviations in favor of the first combination. (auth)

4617 EVALUATION OF THE I = 0 PION-PION SCATTERING LENGTH USING A FORWARD-SCATTERING DISPERSION RELATION. Rothe, Heinz J. (Univ. of California, Berkeley). Phys. Rev., 140: B1421-6(Dec. 6, 1965). (UCRL-16234).

The I = 0 ππ scattering length is evaluated with a forward-direction elastic-scattering dispersion relation. The high-energy contribution to the dispersion integral is obtained on the assumption that the high-energy behavior of the forward scattering amplitude is dominated by a few leading crossed-channel Regge poles, while any available experimental information on total ππ cross sections is used to compute the low-energy contribution. The scattering length is found to be negative, with a calculated value of $-1.7^{+1}_{-0.5}\cdot\frac{1}{3}$ (in pion Compton wavelengths). Evaluation of the I = 1 amplitude at threshold yields the value −0.4, which is found to be consistent with zero; this indicates that the method used in the evaluation of the scattering length is not unreasonable. (auth)

4618 MEASUREMENT OF THE K^+ BRANCHING RATIO INTO THE τ MODE. De Marco-Trabucco, A.; Grosso, C.; Rinaudo, G. (Istituto Nazionale di Fisica Nucleare, Turin; Univ., Turin). Phys. Rev., 140: B1430-2(Dec. 6, 1965).

A determination of the K^+ decay branching ratio into the mode $K^+ \rightarrow \pi^+\pi^+\pi^-$ is obtained in a H_2 bubble chamber with a beam of stopping K^+. With a total τ^+ count of 2186, the branching ratio obtained is (5.71 ± 0.15)%. The estimated world average is (5.54 ± 0.075)%. (auth)

4619 GEOMETRIC THEORY OF NEUTRINOS. Inomata, Akira; McKinley, William A. (Rensselaer Polytechnic Inst., Troy, N. Y. Phys. Rev., 140: B1467-73 (Dec. 6, 1965).

A theory of neutrinos is constructed within the present scheme of geometrodynamics. First, a special class of c-number Heisenberg fields is considered, and a plane-wave-like solution of the covariant neutrino equation is obtained in the two-component limit. It is shown that the special class of neutrinos forms a Rainich null geometry. Conversely, a geometry suitable for the special neutrino-dynamics is distinguished from general null geometries by imposing the condition that the null eigenvector of geometry is the gradient of the neutrino complexion. Finally, the geometrical parallelism between gravito-electrodynamics and gravito-neutrinodynamics is discussed. (auth)

4620 THE PHYSICS OF ELEMENTARY PARTICLES. MODERN STATUS AND PROSPECTS. Tamm, I. E. Priroda, No. 6, 6-16(June 1965). (In Russian).

A brief review is given of the present status of the physics of elementary particles. The experimental discoveries made in this field and the concept of resonances and other systematics are discussed. The inherent degrees of freedom in the theory of relativity, symmetry analysis, and possible future theories are indicated. The possible applications of the physics of elementary particles are discussed. (J.S.R.)

4621 RADIATION OF ELECTROMAGNETIC WAVES BY AN ELECTRON BEAM MOVING ABOVE A DIFFRACTION GRADIENT. Tretyakov, O. A.; Tretyakova, S. S.; Shestopalov, V. P. Radiotekhn. i Elektron., 10: 1233-43 (July 1965). (In Russian).

An electron at rest over a diffraction grating and its image represent a dipole with a definite dipole moment. If the electron is displaced parallel to the lattice plane at a constant velocity, the dipole moment will vary periodically, and radiation will be emitted that is similar to Cherenkov radiation in nature. The emitted radiation is represented in the form of a Fourier series. The unknown Fourier coefficients are found by analyzing the boundary conditions. The boundary problem is solved by means of Riemann-Gilbert equations. The solution is given in the form of an infinite system of linear algebraic equations with respect to the Fourier coefficients. This set of equations is very suitable for calculations on a computer. The energy characteristics of the radiation are analyzed. (TTT)

4622 RADIATION OF A CHARGED PARTICLE MOVING ABOVE A DIFFRACTION GRID. Tretyakov, O. A. Radiotekhn. i Elektron., 10: 1343-6(July 1965). (In Russian).

A solution for the emission of electromagnetic waves occurring during the motion of a charged point particle over an ideally-conducting grid is obtained in general form. The conditions for the occurrence of radiation are established. The electromagnetic field is found. The direction and wavelength of the radiation are determined. The results can be generalized to the case, where an electron bunch of finite dimensions moves over the grid. The charge density of the particle is represented by a Fourier series, whose coefficients are determined. (TTT)

4623 TRANSIENT AND CHERENKOV RADIATION OF ELECTRON SHEETS. Groshev, I. N. Radiotekhn. i Elektron., 10: 1346-8(July 1965). (In Russian).

Electron sheets with a frequency ω strike an ideally-conducting metallic surface a × b in area. The current falling on a small area ds is expressed in the form of a Fourier series. The power of the n-th conversion harmonic is given as follows: $P_n = 2.4\, j_n \beta^2\, ab\, \lambda^2 (\sin^2 \theta_m/\cos\theta_m)$. With j_n = 1 amp/cm^2, a = b = 5 cm, λ = 1 mm, $\sin^2 \theta_m/\cos\theta_m \sim 1$, β = 0.4 (u = 40 kv), the value of p_n is ~9.6×10^{-2} watts. The Cherenkov emission in watts is given by the following expression: $P_e = 94\, j_n^2\, l^2\, (\sin^2 \theta_m/\cos\theta_m)$. It is difficult to estimate the value of P_e because l is indefinite (l is the distance over which the Cherenkov emission takes place). However, it can be assumed that $l \ll \lambda$. Here the wavelength of the emitted radiation is λ. (TTT)

4624 OBTAINING ELECTRON SHEETS. Goroshev, I. N. Radiotekhn. i Elektron., 10: 1348-9(July 1965). (In Russian).

Coherent radiation by means of electron sheets can be obtained by injecting an electron beam of thickness h into a high-frequency (ω) field with amplitude E. The electron velocity along the x-axis is v_e. At large transit angles the form of the electron beam is close to the form of a sheet on the axis at y = 0. The design parameters are the beam thickness δ in the x-direction, and the term $\zeta = v_\theta/c$, where v_θ is the translational velocity of the point of contact of the beam with the plane x = x'; c is the velocity of light. In order to obtain coherent radiation it is necessary that $\delta \ll \lambda$, where λ is the wavelength of the emitted radiation. The term ζ determines the direction of the radiation. Expressions are given relating the term ζ at the point (x', y) with the strength of the electric field E. For the case of conversion radiation it is necessary that $\zeta > 1$, and two deflecting systems are presented where $\xi > 1$. Both deflection schemes can be realized on resonators of the type of a Fabry-Perot interferometer. An expression is given for the relative widening of the beam in the x-direction. (TTT)

4625 THEORY OF EMISSION OF A CHARGE PASSING THROUGH AN ELECTRICALLY INHOMOGENEOUS MEDIUM. Bass, F. G.; Yakovenko, V. M. Usp. Fiz. Nauk, 86: 189-230(June 1965). (In Russian).

Radiation emitted by a charged particle passing through a dielectrically inhomogeneous medium is reviewed. The major topics covered are as follows: transition radiation of a charge passing through a boundary between two media, radiation of a charged particle passing through a moving boundary, transition radiation as a result of a charge obliquely incident on a boundary, transition radiation with spatial dispersion of the dielectric constant taken into account, radiation of a point charge passing through a plate, radiation of a particle moving in a medium with periodically varying properties, radiation of a particle in a medium with fluctuating dielectric constant, and radiation of a particle in the presence of obstacles. The review is based on 131 papers. (ATD)

4626 KAON DECAY INTO TWO PIONS AND POSSIBLE CP NONCONSERVATION. Terent'ev, M. V. Usp. Fiz. Nauk, 86: 231-62(June 1965). (In Russian).

The physical consequences of the important observation of the decay of a meson (K) into two pions by a group at Princeton (J. Christenson et al., Phys. Rev. Letts., 13: 138(1964)), and its bearing on the various parity conservation laws is discussed. The $K \to 2\pi$ decay is accepted as an undisputed fact. A general treatment of the phenomena of decay and interference in a K-meson beam is given. The nature of the information which follows from the data of the Princeton group is described. Along with the existence of the $K \to 2\pi$ decay, the smallness of the observed effect is explained, since the decay of the long-lived component of the meson (K) beam (K_L) is 4×10^{-3} of the short-lived component (K_S). There is a discussion of attempts to explain the experiment on the basis of a hypothesis of the existence in nature of new fields whose forces have a macroscopic range. It is assumed here that CP is rigorously conserved. Attempts to explain the experiment on the basis of various mechanisms of breakdown of CP invariance are reported. Although all the models considered are regarded as too speculative to describe correctly the actual situation, it is believed that their consideration is important for indicating various specific lines to follow in further experimental study of the problem. Interference phenomena is considered which may arise if the long-lived component K_L can decay into two mesons (π) and the amplitudes for the $K_S \to 2\pi$ and $K_L \to 2\pi$ decays are coherent, since the resultant interference leads to new features of the time dependence of two-meson decay. Various experiments are enumerated whose performance is necessary in the future in connection with the $K_L \to 2\pi$ decay and the nonconservation of CP. (ATD)

4627 POLARIZATION OF RECOIL NUCLEONS IN π^0-PHOTOPRODUCTION ON PROTONS BELOW 500 Mev. I. Muellensiefen, A. (Technische Hochschule, Karlsruhe, Ger.). Z. Physik, 188: 199-219(1965).

Using the model of meson (π) photoproduction recently

discussed by Ball and Schmidt a prediction for the polarization of the recoil protons is given for unpolarized photons. The strong dependence on the assumed values of E_{0+} and M_{1-} is shown. Taking into account this result and assuming that M_{1+} and the higher multipoles are sufficiently known, the possibility of determining the small multipoles from measurements is discussed. (auth)

4628 POLARIZATION EFFECTS IN PION-PHOTOPRODUCTION ON PROTONS BELOW 500 Mev. II. Muelensiefen, A. (Technische Hochschule, Karlsruhe, Ger.). Z. Physik, 188: 238-51(1965).

Using the same model as in previous work a prediction for the polarization of the recoil protons is given in case of polarized photons. The determination of E_{0+} and E_{1+} from measurements is discussed. Furthermore the influence of the $\pi\pi$-interaction on polarization is considered. In the case of π^+-production the polarization of the recoil neutrons is investigated and the dependence of the cross section on the polarization state of the target protons is discussed. (auth)

4629 EFFECTS OF THE WEAK VECTOR BOSON IN CERTAIN RADIATIVE WEAK DECAYS [Thesis]. Ginsberg, Edward Stephen. Stanford, Calif., Stanford Univ., 1965. 92p.

The effects of an intermediate vector boson in certain (radiative) weak decays are systematically investigated. The feasibility of using these reactions as a test of the intermediate vector boson hypothesis is discussed. A simple model of the W-boson, which allows for arbitrary anomalous magnetic and quadrupole moments, is assumed. The results of a numerical calculation of the decay $K \rightarrow \mu + \nu + \gamma$ indicate that the W-boson will have observable effects if its mass is not too great. The dependence of these effects on the mass and magnetic moment of the W-boson is discussed in detail. It is noted that photon polarization phenomena are quite sensitive to the presence of the W-boson. This sensitivity is also evident in the related decay $K \rightarrow \mu + \nu + e^+ + e^-$, in which the photon internally converts into an electron-positron pair. Investigation of this process shows that the presence of the W-boson can have a striking effect on the orientation of the plane of the Dalitz pair relative to the decay plane. Sample distributions in the momentum and energy separation of the Dalitz pair are given. The effect of a W-boson with arbitrary anomalous electromagnetic properties is also investigated for radiative muon decay. Radiative corrections to the muon polarization from pi-decay (K-decay), $\pi(K) \rightarrow \mu + \nu$, are also calculated. The muon polarization is no longer complete owing to the emission of soft photons. The correction, which is very small in the usual V-A theory, is not affected by the presence of the W-boson. These conclusions apply a fortiori to the electron modes of these decays. (Dissertation Abstr.)

4630 POSITRON-PROTON SCATTERING [Thesis]. Browman, Andrew Arnold. Stanford, Calif., Stanford Univ., 1965. 146p.

The importance of two-photon exchange contributions to elastic electron-proton scattering was investigated using positron and electron beams. The ratio of elastic electron-proton to elastic positron-proton scattering was measured with momentum transfers as large as 0.76 $(Bev/c)^2$. This ratio, with radiative corrections subtracted, would be expected to be one if two-photon exchanges were negligible. The theoretical calculation of the two-photon contribution has not been made at high momentum transfers, but a knowledge of this contribution is desirable due to the interest in electron-proton scattering. Positron and electron beams from the Stanford Mark III Linear Accelerator were momentum analyzed and scattered from one foot of liquid hydrogen. The first experiment detected the recoil proton in coincidence with the recoil positron or electron using counters with no analyzing magnets. In the second experiment the recoil positrons and electrons were detected after being momentum analyzed. Checks were performed to ensure that the experimental conditions were the same for positrons and electrons. Corrections were made for contamination of the elastic scattering events by meson production processes. The data indicate that there are two-photon effects present at the higher momentum transfer points. More precise measurements will be necessary to determine the size of the effect. (A.G.W.)

4631 A MEASUREMENT OF THE K_{MU3} DECAY SPECTRUM OF THE K_2^0 MESON [Thesis]. Carpenter, Dwight William. Urbana, Ill., Univ. of Illinois, 1965. 82p.

An experiment was performed to observe the energy spectrum of the $K_{\mu 3}^0$ decay ($K_2^0 \rightarrow \pi^{\pm} + \mu^{\mp} + \nu$). The interaction was found to be vector, rather than tensor or scalar, in agreement with the V-A theory of weak interactions. This conclusion is obtained even when energy-dependent form factors are considered. The two form factors of the vector interaction are observed to vary with the energy of the π. The variations are consistent with the predictions obtained by assuming a sharp J = 1 intermediate K-π state of mass 460^{+80}_{-20} Mev. The results are also consistent with the assumption of linearly varying form factors. If the form factors are assumed to be constant, their ratio is found to be $f_-/f_+ \equiv \xi = 2.1 \pm 0.5$, but the goodness of fit is significantly lower than that obtained with variable form factors. The data consist of 1372 events obtained from 40,000 pictures of a spark chamber detection system. The system was located in a 30° neutral beam at the Brookhaven AGS. The useful decays occur in a vacuum pipe. The charged decay products are observed in a set of foil plate spark chambers around the pipe in a magnetic field. The μ is identified in a second set of chambers by its ability to pass through several interaction lengths of material. (Dissertation Abstr.)

4632 PROPERTIES OF THE Ξ^- [Thesis]. Westgard, James Blake. Syracuse, N. Y., Syracuse Univ., 1964. 122p.

An experiment was performed to measure the mass, lifetime, spin, and decay parameters α, β, and γ of the negative cascade hyperon. The data were obtained from a 300,000-picture exposure of the 20-in. BNL liquid hydrogen bubble chamber to the 2.3 Bev/c K^- beam at the Brookhaven A.G.S. The cascade mass was determined by standard methods to be 1321.0 ± .05 Mev. The lifetime was determined to be $1.74^{+.18}_{-.18} \times 10^{-10}$ sec by a modification of the Bartlett method. A tentative measurement of the cascade spin by means of the Lee-Yang test functions yielded inconclusive results, but are in agreement with spin ½. The decay parameters were determined from the various angular correlations to be $\alpha = +.57 \pm .15$, $\beta = +0.0 \pm .24$, and $\gamma = +.82^{+.09}_{-.13}$ in agreement with other recent measurements. These results indicate strong parity nonconservation and are consistent with the requirements of time reversal invariance. The effects of final state interactions are discussed and indicate violation of charge conjugation invariance. (Dissertation Abstr.)

4633 I. PHENOMENOLOGICAL ANALYSIS OF THE NEW RESONANCES. II. SPIN EFFECTS IN THE REGGE POLE APPROACH TO HIGH ENERGY COLLISIONS. Jacob, M. (Centre d'Etudes Nucleaires, Saclay, France). pp 97-127 of Elementary Particle and High Energy Physics. New York, Gordon and Breach Science Publishers, 1965.

A phenomenological review is given of the new resonances which appeared during the last three years. First the baryon resonances are considered, and then the meson (π)-hyperon resonances. In the discussion of spin effects in the Regge pole method for high-energy interactions, the topics considered are Regge poles in high-energy physics, spin complication in the Regge pole formalism, proton-proton interactions, Regge formalism for particles with spins, and meson (π)-nucleon scattering. (J.F.P.)

4634 PHENOMENOLOGICAL STUDY OF WEAK INTERACTIONS. SELECTED TOPICS. Meyer, Ph. (Universite, Paris). pp 326-62 of Elementary Particle and High Energy Physics. New York, Gordon and Breach Science Publishers, 1965.

A rapid survey of the phenomenology of weak interactions is given. Emphasis is placed on the weak interac-

tions of strange particles, others are mentioned only for completeness. The topics discussed include the leptonic and semi-leptonic hamiltonian, nonleptonic decay, construction of the weak interaction hamiltonian, and the weak interaction hamiltonian with the intermediate boson. (J.F.P.)

4635 REMARKS ON THE $\Delta I = \frac{1}{2}$ RULE IN WEAK INTERACTIONS. Nuyts, Jean. pp 169-89 of Lectures in Theoretical Physics. Vol. VI. Boulder, Colo., The University of Colorado Press, 1964.

Theoretical and experimental problems in the weak interactions of elementary particles are considered. Then topics related to the $|\Delta I| = \frac{1}{2}$ rule are discussed. A definition of this rule is given. The leptonic interaction with strongly interacting particles and change of strangeness in analogy with the case of no change of strangeness is treated. The general model for weak decays of hyperons is described, and it is shown that a general analysis along this line is not yet possible. Nonleptonic decays of mesons (K) in the three meson (π) mode are also considered. (J.F.P.)

4636 THE METHOD OF COMPLEX ANGULAR MOMENTA IN RELATIVISTIC QUANTUM THEORY. Freund, Peter G. O. pp 459-512 of Lectures in Theoretical Physics. Vol. VI. Boulder, Colo., The University of Colorado Press, 1964.

An exposition of the method of complex angular momenta and its applications in high energy physics is given omitting any discussion of potential scattering, since this is insufficient for the treatment of the relativistic problem with particle production included. The general properties are reviewed for the Mandelstam representation and the interpolation problem for partial wave amplitudes. The scattering of two types of scalar particles with the same mass are considered. The nature of the singularities of the functions $f_l(t,l)$ are discussed in both variables. Other topics considered include the theory of Regge poles, the concept of elementary particles, and high-energy scattering. (J.F.P.)

4637 NEW POSSIBILITIES FOR INVESTIGATING NUCLEON, PION AND GAMMA-QUANTA REACTIONS ON POLARIZED HYDROGEN TARGETS. Lapidus, L. I. (Joint Inst. for Nuclear Research, Dubna, USSR). pp 232-6 of Physics and Techniques of Low Temperatures. Prague, Publishing House of the Czechoslovak Academy of Sciences, 1964.

A short survey is given of new experimental possibilities with elementary particles, especially at high energies, using polarized hydrogen targets. These new possibilities belong to an important branch of research, the investigation of polarization effects, a source of much new information difficult to obtain in any other way. Examples of such possibilities are discussed. One of these is elastic scattering in which the polarization of initially unpolarized particles is equal to the asymmetry in the scattering cross section on a polarized target, thus the cross section asymmetry, which is simpler, may be studied in order to find this polarization. Other examples include meson (π)-nucleon, nucleon-nucleon scattering, the scattering of γ quanta on protons and nuclei, and scattering of high-energy electrons on protons. (J.F.P.)

Field Theory, Scattering Theory, and Symmetries

See also Elementary Particles and Radiations

Refer also to abstract 4769.

4638 (AD-617965) EXTRAPOLATING ELECTROMAGNETIC FIELDS FROM VALUES IN A SPHERICAL REGION. Period Covered: October 1964–March 1965. Babb, D. D.; Granzow, K. D. (Dikewood Corp., Albuquerque, N. Mex.). June 1965. Contract AF29(601)-6634. 55p. (WL-TR-64-179). CFSTI $3.00 cy, $0.75 mn.

Methods were developed for extrapolating electromagnetic fields from values of the spherical harmonic expansion coefficients of the spherical components on a sphere surrounding a source region. The region outside the sphere is considered to be homogeneous, isotropic, source free, and nonconducting, except that application of the method of images allows the introduction of an infinitely conducting ground plane. Solutions of the scalar wave equation are made applicable by expressing the spherical harmonic expansion coefficients of the rectangular components in terms of the coefficients of the spherical components. Two methods were developed for obtaining time dependent solutions for fields at points outside the sphere without invoking Fourier analysis. One method resulted from inserting the expansions of the rectangular components into the Kirchhoff integral solution of the wave equation. The other method involved eliminating the explicit frequency dependence of the eigenfunction solution of the wave equation by introducing a differential operator to replace the Hankel function. These methods are useful when the source has a very wide-band frequency spectrum, so that it is best described in the time domain. This is the case with electromagnetic pulses from nuclear detonations. (auth)

4639 (IC/65/73) ON THE POSITION OF SINGULARITIES OF THE S-MATRIX IN UNIFIED THEORIES. DETERMINATION OF MASS RATIOS AND COUPLING CONSTANTS. Barut, A. O. (International Centre for Theoretical Physics, Trieste (Italy)). Aug. 1965. 21p. (CONF-650717-1). Dep. mn.

From Conference on Unified Field Theories, Feldafing, Ger.

It is argued that if all strongly interacting particles are intimately related consistency should result in a special distribution of singularities of the S-matrix. On the basis of two methods it is then shown how one can obtain, from the coincidence of certain singularities, all coupling constants and mass ratios in agreement with experiment. These coincidences of singularities are manifestations of some underlying dynamical mechanisms. (auth)

4640 (IC/65/75) BEHAVIOUR FOR LARGE k OF THE S-MATRIX FOR STRONGLY SINGULAR POTENTIALS. Limic, N. (International Centre for Theoretical Physics, Trieste (Italy)). Aug. 1965. 13p. Dep. mn.

The exact asymptotic behavior of the S-matrix for fixed λ and large k in the right half of the k-plane is obtained in the case of the scattering on strongly singular potentials. (auth)

4641 (IC/65/76) THE ROLE OF SYMMETRY PHYSICS. SOME CONCLUSIONS FROM THE OXFORD CONFERENCE, SEPTEMBER 1965. Salam, Abdus (International Centre for Theoretical Physics, Trieste (Italy)). 1965. 35p. (CONF-650945-2). Dep. mn.

From International Conference on Elementary Particles, Oxford.

The development and growth of symmetry physics is discussed. Discussions are presented on dynamical groups in general, lessons learned from the hydrogen atom problem conjectured rest symmetries, and the S-matrix. (M.O.W.)

4642 (IC/65/78) THE (56, $\overline{56}$) CONTRIBUTION TO THE NUCLEON FORM FACTORS. Delbourgo, R.; White, R. (International Centre for Theoretical Physics, Trieste (Italy)). Nov. 2, 1965. 10p. Dep. mn.

The contribution to the electromagnetic form factors of the nucleon from the next (-) parity multiplet, the (56, $\overline{56}$), are evaluated, assuming that the photon couples to the SU(6) 35 in the pole approximation. The resulting small correction, besides possessing other desirable features, succeeds in explaining for the first time the slope, which was determined experimentally from the e-n interaction. The phenomenological status of these form factors are recapitulated, and a sketch is given of the calculation and its detailed consequences. (J.F.P.)

4643 (INR–607/VI/PH) NUMERICAL CALCULATIONS IN THE STATISTICAL THEORY OF PARTICLE PRODUCTION IN ANGULAR MOMENTUM REPRESENTATION. Majewski, M. (Institute of Nuclear Research, Warsaw (Poland)). Feb. 1965. 36p. Dep.

The methods of numerical calculations in the statistical theory of multiple particle production taking into account the angular momentum conservation law was discussed. To classify the states with respect to the angular momenta of the particles the parameter $C = \sum l_i$, which for many reasons appears to be very convenient, is introduced. In the case of the decay of a meson cloud with the mass of 20 μ_μ into pions the amount of the calculations is estimated. The averaging of probabilities with respect to the initial values of the angular momenta is discussed. Finally an approximate method is proposed which allows to reduce the amount of the calculations and the calculation time by the order of magnitude. (auth)

4644 (JINR-P–2299) ELEKTROMAGNITNYE SVOISTVA MEZONOV V NARVSHENNEI SIMMETRII SU(6). (Electromagnetic Properties of Mesons in Broken Symmetry SU(6)). Babaev, Z. R.; Zamiralov, V. S.; Solov'ev, L. D. (Joint Inst. for Nuclear Research, Dubna (USSR). Lab. of Theoretical Physics). 1965. 6p. Dep. mn.

Relations were found between the probabilities of the radiative decays and the magnetic moments of the vector mesons under the symmetry. An account is taken of the medium strong interaction leading to the mass splitting in the unitary multiplets. (auth)

4645 (NP–15599) PROVERKA SLEDSTVII UNITARNOI SIMMETRII V REAKTSIYAKH ADRONOV (OBZOR). (Tests of the Consequences of Unitary Symmetry in Hadron-Production Reactions (Survey)). Dolgov, A. D.; Solovev, V. V. (Gosudarstvennyi Komitet po Ispol'zovaniyu Atomnoi Energii SSSR, Moscow. Institut Teoreticheskoi i Eksperimental'noi Fiziki). 1965. 100p. Dep. mn.

Some achievements of unitary symmetry and methods for constructing unitarily invariant amplitudes are summarized briefly. Predictions of SU(3) symmetry are compared with experimental results for: meson-baryon reactions with the formation of octet baryons or decuplet baryon resonances; proton-antiproton annihilation reactions; baryon-baryon scattering in the S-state; reactions with formation of the f^0 meson, assumed to be the SU(3) singlet; and hadron photoproduction reactions. (M.J.T.)

4646 (NYO–3399-40) CONCLUDING REMARKS AT THE INTERNATIONAL SEMINAR ON UNIFIED FIELD THEORIES AT FELDAFING ON STARNBERGERSEE NEAR MUNICH, JULY 1965. Sudarshan, E. C. G. (Syracuse Univ., N. Y. Dept. of Physics). Contract AT(30-1)-3399. 11p. (CONF-650717–2). Dep. mn; CFSTI $1.00 cy, $0.50 mn.

From Conference on Unified Field Theories, Feldafing, Ger.

The various topics discussed at the International Seminar on Unified Field Theories are briefly reviewed. (M.O.W.)

4647 (TID–22274) THREE-PARTICLE UNITARITY INTEGRAL. Technical Report No. 454. Li, Ming Chiang (Maryland Univ., College Park. Dept. of Physics and Astronomy). Apr. 1965. Contract AT(40-1)-2504. 62p. Dep. mn; CFSTI $3.00 cy, $0.75 mn.

The partial wave decomposition of the three-particle unitarity condition is studied. Using simple Feynman amplitude as an illustration, two three-particle unitarity integrals are constructed (crossed and non-crossed integrals). The partial-wave amplitudes and their energy dependence for these two cases are investigated. It is shown that the contribution from the non-crossed integral decreases faster than that from the crossed integral as the angular momentum increases. The effects of the unstable-particle width on the effective two-particle approximation of the three-particle unitarity integral are examined. (auth)

4648 PROBLEM OF A SPIN IN A TIME-DEPENDENT MAGNETIC FIELD. Montgomery, David; Ruijgrok, Th. W. (Rijksuniversiteit, Utrecht). Amer. J. Phys., 33: 946-9 (Nov. 1965).

The long-standing disagreement between the exact and perturbation solutions for the problem of a spin one-half particle in crossed, time-dependent, magnetic fields is resolved. The resolution is achieved by adapting the perturbation methods given by Krylov, Bogoliubov, and Mitropolskii for classical systems. (auth)

4649 OCTET ENHANCEMENT AND THE RECIPROCAL BOOTSTRAP. Gerstein, I. S.; Whippman, M. L. (Univ. of Pennsylvania, Philadelphia). Ann. Phys., (N.Y.), 34: 488-504(Oct. 6, 1965).

Perturbations of the masses of baryon and meson-baryon resonances due to the breaking of an internal symmetry group are studied in the static model. For particular assignments of particles to representations of SU(2) it is shown that the bootstrap condition for the baryon implies the enhancement of perturbations which transform like isotopic vectors. In the case of SU(3) the reciprocal bootstrap is used for the octet baryons and decuplet resonances and the relation between it and octet enhancement is shown. The results show in a simple way the manner in which the bootstrap equations make definite predictions about the transformation properties of mass perturbations. (auth)

4650 FIELDS AS OPERATOR-VALUED DISTRIBUTIONS IN RELATIVISTIC QUANTUM THEORY. Wightman, A. S.; Garding, L. (Princeton Univ., N. J.; Univ. of Lund, Sweden). Arkiv Fys., 28: 129-84(1965).

The essential mathematical construction in terms of which the notion of field is defined is operator-valued distribution. The operators are in general unbounded. An inductive derivation of the axioms is given starting from the basic notions of classical field theory and relativistic quantum theory. A general idea of what a field ought to be is set up. This is then refined until it reaches precise axiomatic form. Some examples of fields satisfying the preceding axioms are discussed, and the Wick polynomials in a free scalar field are discussed. These constitute precisely the equivalence class of a free field, thus it is important to show that they satisfy the axioms. (J.F.P.)

4651 ON THE DERIVATION OF THE COLLISION LIFETIME MATRIX. Gien, Tran Trong (Ohio Univ., Athens). Can. J. Phys., 43: 1978-84(Nov. 1965).

If the lifetime of a collision is defined as the difference between the times in which a particle moves in free space and under an interaction from a scattering center to the outside (or in the reverse direction), it is shown that exactly the same relation between the lifetime operator Q and the scattering matrix S as was found by Smith can be derived. This can be done in a natural way provided that the time operator is defined as $\phi = -i\hbar\,\partial/\partial E$ and the manifold of the asymptotic outgoing (or incoming) states is chosen to be the set of corresponding eigenstates. The part of the time needed for the particle moving freely from the scattering center to R is equal to R/v. (auth)

4652 A PARAMETRIC REPRESENTATION OF THE "KINETIC MOMENT" OPERATORS FOR THE GROUP SU(3). Gueret, Philippe (Institut Henri Poincare, Paris). Compt. Rend., 261: 1186-8(Aug. 2, 1965). (In French).

If a unitary representation in spherical coordinates is given of the group SU(3), operators having commutation properties of the kinetic moment operators can be constructed. In the basic representation these operators correspond to the matrices of Salam and Matthews. The operators corresponding to the U-spin and the V-spin are thus deduced. (tr-auth)

4653 A NONLOCAL EXTENSION OF THE UTIYAMA FORMALISM. Toro, Tiberiu I. (Univ., Timisoara, Romania). Compt. Rend., 261: 2593-6(Oct. 4, 1965). (In French).

The general formalism of the local invariants given by Utiyama is generalized for the nonlocal case. It is shown that this nonlocal extension contains the local formalism of Utiyama as well as a particular case. All the known local relations are also obtained. It is applied to the case of nonlocal gauge transformations. (tr-auth)

4654 PARAMETRIC REPRESENTATION OF "KINETIC MOMENT" OPERATORS FOR THE SU(4) GROUP. ASSOCIATED HARMONIC FUNCTIONS. Gueret, Philippe (Institut Henri Poincare, Paris). Compt. Rend., 261: 1469-72 (Aug. 9, 1965). (In French).

The operators of Cartan and the kinetic-moment operators are constructed, starting from a unitary representation in spherical coordinates of the SU(4) group; in the fundamental representation, linear combinations of Dirac matrices correspond to these operators. The harmonic functions associated with these operators are also obtained. (tr-auth)

4655 THEORY OF SCATTERING OF IDENTICAL PARTICLES. Rys, Franz (Univ., Geneva). Helv. Phys. Acta, 38: 457-68(1965).

The problem of a satisfactory formulation of the rigorous non-relativistic time-dependent scattering theory for systems with two identical particles is solved. (auth)

4656 GAUGE CO-ORDINATE GROUP OF PHYSICAL THEORY. Goodall, M. C. (Massachusetts Inst. of Tech., Cambridge). Nature, 207: 1286(Sept. 18, 1965).

A note is presented on the role of larger exceptional Lie groups in physical theory, namely automorphisms of Clifford algebras of the special form $\Gamma^{(m,n)} = Q_m \times Q_n$; the groups being F_4, E_6, E_7, E_8, for m = 3 and n = 0, 1, 2, 3. It is pointed out that the theory of strong interactions has required the enlargement of the gauge group to A_5, in which case a role might be expected for E_8 with the approximate splitting $E_8 \sim B_3 + A_5$. It is further pointed out that an interprepation of E_8 as the group of a classical phase space necessarily involves a cosmological model, that is, at least one of the invariants of the group must have a cosmological significance. (L.B.S.)

4657 NON-ABELIAN GAUGE FIELDS AND GOLDSTONE BOSONS. Fuchs, Norman (Univ. of Pennsylvania, Philadelphia). Phys. Rev., 140: B911-13(Nov. 22, 1965).

The theory of a massless, in general non-Abelian, gauge vector field is considered and the relation between the supplementary condition for the vector field and the condition for spontaneously broken symmetry is explored. Goldstone bosons are found to exist and their equations of motion are determined; the non-Abelian nature of the gauge group leads to interaction for the Goldstone bosons. The results are applied to the problems of broken isotopic and unitary symmetries. (auth)

4658 PHASE-SPACE CONSIDERATIONS FOR FOUR-PARTICLE FINAL STATES. Nyborg, P.; Song, H. S.; Kernan, W.; Good, R. H. Jr. (Ames Lab., Ames, Iowa). Phys. Rev., 140: B914-20(Nov. 22, 1965).

A discussion of four-particle phase space is given in terms of the invariant mass variables M_{12}^2, M_{34}^2, M_{14}^2, M_{124}^2, and M_{134}^2. Formulas are given for the boundary of the physically allowed region and for the distribution of states inside. Some of the simpler distributions, which result when integrations are made over some of the variables, are derived. (auth)

4659 PHASE-SPACE CONSIDERATIONS FOR FIVE-PARTICLE FINAL STATES. Nyborg, Per (Ames Lab., Ames, Iowa). Phys. Rev., 140: B921-5(Nov. 22, 1965). (IS-1158).

A detailed and explicit discussion of five-particle phase space is given in terms of invariant variables. The distribution of final states, after taking account of energy and momentum conservation, is integrated over orientations of the entire system and then expressed in terms of squares of invariant masses. The results permit analysis for two-, three-, and four-particle resonances. Formulas are given for the boundary of the allowed region in the eight dimensions and for the distribution of final states inside, together with several of the simpler distributions which result when integrations can be made over some of the invariant masses. (auth)

4660 ON GOLDSTONE'S THEOREM. Lopuszanski, Jan; Reeh, Helmut (Inst. for Advanced Study, Princeton, N. J.). Phys. Rev., 140: B926-7(Nov. 22, 1965).

An example is given which shows that a continuous symmetry property of the field does not necessarily imply the existence of particles of mass zero. (auth)

4661 OPERATOR ANALYSIS OF THE BETHE-SALPETER EQUATION. Ciafaloni, M.; Menotti, P. (Scuola Normale Superiore, Pisa, Italy; Istituto Nazionale di Fisica Nucleare, Pisa, Italy). Phys. Rev., 140: B929-46(Nov. 22, 1965).

The Bethe-Salpeter equation for equal-mass bosons interacting through the exchange of a scalar boson is analyzed by means of a spectral representation in the coupling constant. The connection between bound and antibound states is established. A mathematical treatment of the nonrelativistic limit is given for the case when the exchanged boson has a mass different from zero. An analysis of the physical acceptability of the solutions of the Bethe-Salpeter equation is given in terms of a normalization condition of the wave function. It is shown how the solutions that are odd in the relative time do not contribute to the S matrix, and how they give rise to inconsistencies with field theory. (auth)

4662 MULTIPLE POLES IN THE SCATTERING GREEN'S FUNCTION. Nakanishi, Noboru (Brookhaven National Lab., Upton, N. Y.). Phys. Rev., 140: B947-56 (Nov. 22, 1965). (BNL-9294).

A general theory of multiple poles in the scattering Green's function is developed. It is shown that their residues are determined by certain generalized Bethe-Salpeter equations apart from an over-all multiplicative factor. As an example of multiple poles, the zero-energy case is considered in the Wick-Cutkosky model. By means of an integral representation, the generalized Bethe-Salpeter equations are converted into simultaneous one-dimensional integral equations. Exact solutions are obtained to these equations of the first order. The results are compared with Heisenberg's dipole-ghost theory and with the quantum electrodynamics of Gupta and Bleuler. (auth)

4663 UNSUBTRACTED DISPERSION RELATIONS IN WEAK INTERACTIONS AND A PARTIALLY CONSERVED AXIAL-VECTOR CURRENT. Saito, Takesi (Univ. of California, Berkeley). Phys. Rev., 140: B957-8(Nov. 22, 1965). (UCRL-16224).

It is shown that a combined use of unsubtracted dispersion relations (UDR) in weak interactions with a partially conserved axial-vector current (PCAC) due to Nambu leads to a very small wave-function renormalization constant of the meson (π) field ($Z_3 \ll 1$), where an additional condition for PCAC is necessary to obtain the case $Z_3 = 0$. The pology version of PCAC due to Gell-Mann and others does not generally lead to such a conclusion. A model of PCAC ($\partial_\mu a_\mu = \text{const}\,\phi_\pi$) proposed by Gell-Mann and Lévy contradicts UDR for the π-μ decay amplitude. But their model can always be modified so as to be equivalent to the pology version or Nambu's version of PCAC. (auth)

4664 CLASSIFICATION OF ELEMENTARY PARTICLES BASED ON THE REPRESENTATION TYPES OF THE POINCARE GROUP INCLUDING SPACE, TIME, AND CHARGE REFLECTIONS. Tarimer, Niyazi (Middle East Technical Univ., Ankara). Phys. Rev., 140: B977-83 (Nov. 22, 1965).

It is argued that a type analysis of the Poincaré group including space, time, and charge reflections suffices to determine all the known quantum numbers of elementary particles in a way consistent with the superselection rules. The charged Poincaré group, defined as the direct product of the full Poincaré group with the involution group of charge conjugations, is studied, and its representation types are classified. It is shown that these representations can be grouped into multiplets. While there exist superselection rules separating the different multiplets, there is no superselection between the states of each multiplet.

The theory defines exactly three Dirac fields for massive spin-$\frac{1}{2}$ representations. One of these fields transforms like an ordinary Dirac field under C,P,T. The other two fields form a doublet where the charge conjugation has the significance of G parity. They are identified with the λ, p, and n quarks of Gell-Mann. The meaning of the SU_3 symmetries becomes self-evident after this identification. The leptons are assumed to have zero masses in the unitary-symmetry limit. The γ_5 invariance is exploited to choose a "neutral" type with trivial charge conjugations. The theory defines six neutral two-component fields, which are identified with the neutrinos, the left- and right-handed electron, and muon fields. The discrete symmetries lead in a natural way to the V – A coupling for the lepton-lepton interactions. Thus it is concluded that the lepton-lepton weak interactions preserve the space, time, and charge reflection symmetries of an unusual type of representation. (auth)

4665 MAGNETIC MOMENTS OF THE BARYONS. Pagels, Heinz (Stanford Univ., Calif.). Phys. Rev., 140: B999-1002(Nov. 22, 1965).

The anomalous magnetic moments of the baryon octet are calculated in broken SU(3) symmetry using low-energy pole dominance as a dynamical model and keeping only the lowest lying intermediate states, the pseudoscalar-meson-baryon states. By using dispersion theory, the anomalous moments are related to an energy integral over the $S_{\frac{1}{2}}$ and $P_{\frac{1}{2}}$ photomeson production amplitudes, which at low energy and for vanishing meson mass are exactly given by the pole terms. From this exact information the low-energy contribution to the anomalous moments are calculated, keeping all orders in baryon and meson mass splittings and using the SU(3)-symmetric strong-coupling constants. The dominant contribution to the proton and neutron magnetic moment is accounted for and it is found in addition, for an F/D ratio ~0.6, that K(Λ) ~ 0.4K (n), in agreement with the observed value. The SU(3) predictions for the other moments and the $\Sigma^0 \to \Lambda + \gamma$ transition moment are found to be more badly violated. (auth)

4666 DECAYS OF POSITIVE-PARITY BARYON RESONANCES IN A BROKEN $\tilde{U}(12)$. Harari, H. (Israel Atomic Energy Commission, Yavne); Horn, D.; Kugler, M.; Lipkin, H. J.; Meshkov, S. Phys. Rev., 140: B1003-5 (Nov. 22, 1965).

The simplest representations of SU(6) and $\tilde{U}(12)$ which are capable of describing the low-lying positive-parity baryon resonances are the three-quark representations. All particle states in these multiplets are eigenstates of W spin and $SU(6)_W$, the subgroup of $\tilde{U}(12)$ and $U(6) \times U(6)$ which remains invariant for two-body decay processes, even when kinetic-energy terms and derivative couplings are included in the calculations. It is shown that $SU(6)_W$ leads to various selection rules and to definite branching ratios for the decays of these resonances. The branching ratios for the decays of the spin-$\frac{3}{2}$, SU(3)-octet resonances in the 70 representation of SU(6) and $SU(6)_W$ are calculated. An attempt is made to include SU(3) symmetry-breaking effects in a calculation of the decay rates of the $\frac{3}{2}^+$ decuplet within the 56 of $SU(6)_W$. (auth)

4667 SHMUSHKEVICH'S METHOD FOR A CHARGE-INDEPENDENT THEORY. Pinski, G.; Macfarlane, A. J.; Sudarshan, E. C. G. (Syracuse Univ., N. Y.). Phys. Rev., 140: B1045-53(Nov. 22, 1965). (NYO-3399-24).

The Shmushkevich method for deducing consequences of charge independence is explained and discussed. This method, which avoids entirely the use of Clebsch-Gordan coefficients, generates linear equalities and inequalities among cross sections using only a simple counting procedure. A comprehensive list of such relations, applying to most elementary-particle reactions of interest which involve at least one pair of isospin-½ particles, is presented. A discussion of the various uses of these relations is given. (auth)

4668 NORMAL THRESHOLD SHEET STRUCTURE OF TWO-PARTICLE SCATTERING AMPLITUDES. Gross, David J.; Schwarz, John H. (Univ. of California, Berkeley). Phys. Rev., 140: B1054-67(Nov. 22, 1965). (UCRL-16193).

From the requirements of analyticity and unitarity, it is proven that certain normal threshold branch points are absent on unphysical sheets of certain other ones. Also the existence of complex thresholds corresponding to unstable particles is proven, and they are shown to have the discontinuities that would be expected on the basis of "nuclear democracy." To obtain these results it was necessary to derive certain elementary discontinuity formulas, to explicitly construct the inverse of an elastic n-particle-to-n-particle S matrix, and to prove the factorization theorem for the residues of poles in multiparticle amplitudes. (auth)

4669 SPONTANEOUS SYMMETRY BREAKDOWN IN A NONLINEAR BOSON FIELD: A MODEL FOR C VIOLATION. Marx, G. (Stanford Univ., Calif.). Phys. Rev., 140: B1068-78(Nov. 22, 1965).

A boson field with quartic self-coupling is discussed in the BCS approximation. For certain values of the coupling constant the transition from simple products to normal ordered products by a Bogolyubov transformation implies a spontaneous breakdown of the original symmetries in the lagrangian. In a real scalar field a discrete symmetry can be broken; in more complex fields mass splitting also occurs. If the boson is characterized by the assignment 0^{+-}, the nonvanishing vacuum expectation value of its field operator may result in tadpole diagrams, which offer an explanation of the C-violating transitions. The experimental consequences of different coupling schemes between the 0^{+-} meson and other particles are discussed in detail. The role of the $\rho\pi\eta$ and $\rho\pi X$ matrix elements is emphasized in explaining different C-violating transitions in SU(2)- and SU(3)-symmetric ways, respectively. (auth)

4670 FIELD THEORY OF THE TWO-PION SYSTEM (S AND D WAVES). Alexanian, Moorad (Univ. of California, Livermore); Wellner, Marcel. Phys. Rev., 140: B1079-87(Nov. 22, 1965).

Use is made of a recently developed series expansion, applying the procedure to S and D waves. With an input of (π mass) = 1, (ρ mass) = 5.53, the results for the isospin-T, spin-J scattering lengths a_J^T and the Chew-Mandelstam coupling constant λ are: $a_0^0 = -0.72$, $a_0^2 = -0.40$, $a_1^1 = +0.032$, $a_1^2 = +0.0032$, $a_2^2 = 0.0026$, and $\lambda = +0.22$. The results for $a_0^{0,2}$ and λ are improved by a higher order correction, but with little change from previous work; a_1^1 is as quoted previously, the $a_2^{0,2}$ are new results. The S-wave phase shifts δ_0^T are also calculated and it is found that δ_0^0 and δ_0^2 go through $-\frac{1}{2}\pi$ on the way down at energies of 760 and 630 Mev, respectively. Finally the D-wave phase shifts are calculated: The f^0 resonance is found at 1950 Mev, and a corresponding T = 2, D-wave resonance is found at 1520 Mev. The substantial discrepancy with experiment for the f_0 is attributed to the need for considering more terms in the expansion as energy increases, as well as to a diminished reliability of the $\lambda\phi^4$ model at high energy. (auth)

4671 NORMALIZATION OF BETHE-SALPETER WAVE FUNCTIONS. Lurie, D. (Dublin Inst. for Advance Studies); Macfarlane, A. J.; Takahashi, Y. Phys. Rev., 140: B1091-9(Nov. 22, 1965). (NYO-3399-25).

A brief and transparent derivation is presented which does not depend on the existence of a conserved quantity, of the normalization condition for Bethe-Salpeter bound-state wave functions. A comment on the structure of the condition is made. Application of the condition to the Bethe-Salpeter wave-function description of physical meson states in ordinary pseudoscalar-meson theory is also described in detail. (auth)

4672 COUPLED-EQUATIONS METHOD FOR THE SCATTERING OF IDENTICAL PARTICLES. Levin, F. S. (Brookhaven National Lab., Upton, N. Y.). Phys. Rev., 140: B1099-1109(Nov. 22, 1965). (BNL-9233).

The completely antisymmetric solution Ψ^A to the problem of the scattering of a fermion by a finite system of identical fermions is studied by means of the expansion $\Psi^A = \Sigma\varphi_\alpha\psi_\alpha$, where $\{\varphi_\alpha\}$ is a complete set of antisymmetric states for the target and ψ_α are one-particle functions. Coupled equations for the ψ_α are found that obey the proper boundary conditions. This is done by means of the integral equation for Ψ^A and the use of projection operators. The elastic-scattering (optical-model) wave function ψ_0 is shown to obey an inhomogeneous differential equation, rather than a Schroedinger equation. The homogeneous solution is identical to the elastic wave function obtained when the projectile is distinguishable, while the inhomogeneous solution is due entirely to exchange effects. The function ψ_0 is identical to the optical-model wave function found by Bell and Squires, who showed that ψ_0 obeys a Schroedinger equation with an optical potential containing direct and exchange contributions. It is shown that ψ_0 yields the exact elastic amplitude including direct and exchange contributions, and a phase-shift analysis of the exchange term is given. The more standard form of solution $\Psi^A = \Sigma\mathcal{A}\{\varphi_\alpha f_\alpha\}$, where $\mathcal{A}$ is an antisymmetrizer, is briefly discussed. The extension to the cases of inelastic scattering and deuteron elastic scattering is made. (auth)

4673 WEAK ELECTROMAGNETIC DECAYS OF HYPERONS IN SU(3). Graham, R. H.; Pakvasa, S. (Purdue Univ., Lafayette, Ind.). Phys. Rev., 140: B1144-50(Nov. 22, 1965).

Two-body and three-body weak radiative decays of hyperons are studied in context of the SU(3) scheme. The various sum rules that follow from T-L symmetries as well as those due to R invariance are derived. A pole model is set up for the two-body decays of both radiative and pionic type and is used to predict the amplitudes and decay rates for the photonic modes. In particular, the rate for $\Sigma^+ \rightarrow p + \gamma$ calculated in this model agrees with the recent experimental value. (auth)

4674 STRONG AND ELECTROMAGNETIC DECAY OF MESONS. Chan, Lai-Him (Harvard Univ., Cambridge, Mass.). Phys. Rev., 140: B1324-7(Dec. 6, 1965).

Partial widths of strong and electromagnetic decays of mesons are calculated within the framework of Schwinger's field theory of matter. Results are consistent with present experimental data. The model requires a two-photon–pseudoscalar-meson interaction and a direct four-pseudoscalar-meson interaction. The former is shown to be consistent with the $\pi \rightarrow \gamma e^+e^-$ form factor. The latter explains the $\delta \rightarrow \eta\pi\pi$ and $\eta \rightarrow \pi^+\pi^0\pi^-$ decays, and the coupling constant also agrees with the $\pi\pi$ S-wave coupling constant. Some justification in terms of the heavy scalar-meson nonet is given for the four-meson interaction. (auth)

4675 FADDEEV FORMALISM FOR FOUR-PARTICLE SYSTEMS. Mitra, A. N. (Univ. of Wisconsin, Madison); Gillespie, J.; Sugar, R.; Panchapakesan, Nargis. Phys. Rev., 140: B1336-8(Dec. 6, 1965).

From the four-particle Lippmann-Schwinger equation a set of equations of the Faddeev type with properly connected kernels is obtained. The kernels contain only the two- and three-particle scattering amplitudes and do not involve the potentials. (auth)

4676 SYMMETRIES AND DYNAMICS OF NONLEPTONIC DECAYS. Pati, Jogesh C.; Oneda, Sadao (Univ. of Maryland, College Park). Phys. Rev., 140: B1351-4 (Dec. 6, 1965).

It is shown that the strength of the $K_1 \rightarrow$ vacuum vertex, arising solely through medium-strong SU(3)-breaking interactions, is large and can provide a natural explanation for the octet enhancement of the parity-violating nonleptonic amplitudes. Furthermore, the sum rule $-A(\Lambda \rightarrow p + \pi^-) + 2A(\Xi^- \rightarrow \Lambda + \pi^-) = \sqrt{3}A(\Sigma^+ \rightarrow p + \pi^0)$ for parity-violating hyperon decays, derived on the basis of the λ_6 transformation, also holds if the amplitudes are dominated by any or all of the following: the baryon octet, baryon decuplet, or scalar- or vector-octet pole terms, arising through the K_1 tadpole. This is true even though the latter transforms like λ_7. Thus it is concluded that neither the forbiddenness of the K_1 tadpole in the limit of SU(3) nor the existence of the sum rule for the parity-violating decays on the basis of the λ_6 transformation provide any argument against a possible dynamical picture of octet enhancement in nonleptonic transitions. The dynamics considered should be important regardless of whether the octet transformation has a dynamical or primary origin. Comments are also made on some other directly related problems: (i) the possible effect of symmetry violation on an otherwise forbidden transition (especially $K_1 \rightarrow 2\pi$ decay), (ii) the meaning of enhancement of nonleptonic rates compared with leptonic ones, and (iii) the ratio of $\Gamma(K^+ \rightarrow \pi^+ + \pi^0)$ to $\Gamma(K_1 \rightarrow \pi^+ + \pi^-)$. (auth)

4677 BARYON-MESON VERTEX IN A RELATIVISTIC SU(6) THEORY. Barnes, K. J. (Cornell Univ., Ithaca, N. Y.). Phys. Rev., 140: B1355-8(Dec. 6, 1965).

A calculation is presented of the vector and pseudoscalar currents for the baryon-meson vertex within the context of a relativistic SU(6)-invariant S-matrix theory. This symmetry is not intrinsically broken and is exact in the limit of exact SU(6) symmetry. (auth)

4678 NEW SUM RULE FOR MESON-BARYON TOTAL CROSS SECTIONS AT HIGH ENERGY. Barger, V.; Rubin, M. H. (Univ. of Wisconsin, Madison). Phys. Rev., 140: B1365-6(Dec. 6, 1965). (TID–22142).

Under the assumption that the dominant underlying mechanism of high-energy meson-nucleon elastic scattering is the exchange of SU_3 octet meson states, a new sum rule relating meson-nucleon total cross sections is derived: $\sigma_t(K^-p) - \sigma_t(K^+p) = \sigma_t(K^-n) - \sigma_t(K^+n) + \sigma_t(\pi^-p) - \sigma_t(\pi^+p)$. Comparison of the sum rule with experiment indicates substantial agreement from 10 to 18 Bev/c. The f/d ratio for the charge coupling of the vector-meson octet to the baryon octet is also determined from ratios of total cross-section differences. (auth)

4679 SU(6) PREDICTIONS FOR s-WAVE BARYON-BARYON SCATTERING. Barger, V.; Rubin, M. H. (Univ. of Wisconsin, Madison). Phys. Rev., 140: B1366-7 (Dec. 6, 1965). (COO–30-101(Rev.)).

The predictions of the SU(6)-symmetry model for s-wave baryon-baryon scattering are derived and compared with some low-energy experimental data. (auth)

4680 SOME ASPECTS OF COMPLEX ANGULAR MOMENTUM AND THREE-PARTICLE STATES. Drummond, Ian T. (Univ. of California, Berkeley). Phys. Rev., 140: B1368-77(Dec. 6, 1965).

An attempt is made to gain some understanding of the problem of how complex singularities affect the continuation of multiparticle amplitudes to complex angular momentum J by examining a few simple pole contributions to a production amplitude. It is found that in order to compute the effect of a three-particle state on a two-particle amplitude of definite signature the unitarity integral has to be considerably reorganized. This has the result of requiring three different production amplitudes of definite signature to be considered, each of which provides a different continuation to complex J. It is found also that the phase-space integrations which occur in unitarity-like equations must be performed over suitably deformed contours when J is complex. For integer angular momentum, of course, the deformation has no effect. This situation is elucidated by introducing doubly projected partial-wave amplitudes in which both the total and a sub-angular momentum are projected out. (auth)

4681 MODEL OF C VIOLATION IN SEMISTRONG INTERACTIONS. Fujii, Y. (Stanford Univ., Calif.). Phys. Rev., 140: B1378-86(Dec. 6, 1965).

A simple model of C violation in semistrong interactions is proposed. The basic semistrong interaction is an equal mixture of C-invariant and -noninvariant parts. The former part is the coupling between two neutral vector mesons (Sakurai's interaction), and the latter is the coupling between neutral vector and scalar mesons. The nature of this particular interaction and the possible experimental

consequences are discussed. The small $K_2^0 \to 2\pi$ decay rate can be consistent with the model. Also the $\rho\eta\pi$ coupling and the C-violating effect in the $\Sigma^0 \to \Lambda e^+e^-$ decay are calculated. (auth)

4682 SOME CONSEQUENCES OF THE PROPOSED C AND T VIOLATIONS IN ELECTROMAGNETIC INTERACTIONS. Feinberg, G. (Columbia Univ., New York). Phys. Rev., 140: B1402-4(Dec. 6, 1965). (TID-22093).

The model in which C and T are violated in the electromagnetic interactions of hadrons is considered further. It is shown that in this model, the nucleons should have electric dipole moments of order 10^{-19} cm × e, comparable to the present upper limit for the neutron electric dipole moment. The effect of mixing between η^0 and $X^0(960)$ on the decays $\eta^0 \to \pi^0e^+e^-$, $X^0 \to \pi^0e^+e^-$, and $X^0 \to \eta^0e^+e^-$ is discussed, and some estimates for the branching ratios are presented. It is found that the branching ratios of these to all η^0 and X^0 decays may be about 1%. (auth)

4683 SU(6) AND DEVIATIONS FROM THE $\Delta I = \frac{1}{2}$ RULE IN THE NONLEPTONIC HYPERON DECAYS. Suzuki, Mahiko (Univ. of Wisconsin, Madison). Phys. Rev., 140: B1405-6(Dec. 6, 1965).

Deviations from the $\Delta I = \frac{1}{2}$ rule in the nonleptonic hyperon decays are investigated within the framework of SU(6) on the assumption that the weak interaction should be of the current × current type and CP-invariant. A remarkable result is obtained for parity-violating amplitudes: the deviation turns out to exist only in the Σ decay, not in the Λ nor Ξ decay. Experimental data are in good agreement with this prediction. (auth)

4684 ROLE OF SPIN IN THE MONOPOLE PROBLEM. Goldhaber, Alfred S. (Univ. of California, Berkeley). Phys. Rev., 140: B1407-14(Dec. 6, 1965).

The scattering of an electric charge from a magnetic monopole is discussed in a way which explicitly incorporates conservation of angular momentum. The Dirac quantization condition for the physical charges is derived from the correspondence principle and the requirement of rotational invariance. The same discussion shows that the initial and final states of the scattering reaction contain an extra spin, which can not be associated with either particle alone. In the classical nonrelativistic theory it is known that such an extra spin appears, and that it may be identified with the angular momentum of the electromagnetic field. A quantized version of this nonrelativistic spin theory is obtained and shown to be equivalent to the Dirac theory based on a singular vector potential. The spin approach gives an interesting perspective on the relativistic monopole problem. Among the standard S-matrix postulates, that of crossing symmetry must be modified or abandoned if a relativistic theory is to succeed. (auth)

4685 APPROXIMATE SUPERMULTIPLET MODEL CONSISTENT WITH RELATIVITY AND UNITARITY. Papastamatiou, N. J.; Taylor, J. C. (Oxford Univ.). Phys. Rev., 140: B1415-20(Dec. 6, 1965).

A relativistic model field theory which yields an approximate SU(6) invariance is constructed. The hamiltonian is $H_0 + H'$, where H_0 is invariant under an inhomogeneous SL(6) with 36 translation generators P_A. H' is small, but it does not commute with the 32 unphysical P_A; and so its presence abolishes the problem of giving them a physical interpretation. Because of H', physical states involve a wave function of the unphysical momenta which, to a zeroth approximation, has no spin-orbit mixing and gives pure SU(6) states. Treating the small spin-orbit term as a perturbation leads to deviations from SU(6) symmetry. Other qualitative predictions of the model are: (a) that matrix elements should have an approximate SL(6) structure except insofar as they are sensitive to the detailed spectrum of intermediate states; (b) that the matrix elements should include irregular terms even in zeroth-order approximation; and (c) that there should be excited states which behave like approximately degenerate sets of incomplete SU(6) multiplets, and whose presence as intermediate states makes the model consistent with unitarity. The model does not include a parity operation, but the possibility of generalization to an inhomogeneous $S\tilde{U}(12)$ group is briefly and incompletely discussed. The Wigner-Bargmann equations seem to arise naturally. (auth)

4686 POMERANCHUK REPULSION AND RESONANCE NARROWING. Chew, Geoffrey F. (Univ. of California, Berkeley). Phys. Rev., 140: B1427-30(Dec. 6, 1965). (UCRL-16245).

The contribution of the P (Pomeranchuk) and P′ trajectories to the generalized two-particle (low-energy) potential is shown to be repulsive and effectively of long range. A rough expression for the P potential is given in terms of the high-energy total cross section and associated diffraction peak. It is argued that Pomeranchuk repulsion represents the many-particle channels that dominate high energies and that have an important narrowing effect on resonance widths even though these channels are closed in the low-energy resonance region. (auth)

4687 EXISTENCE OF THE S MATRIX. Omnes, Roland (Centre de Recherches Nucleaires, Strasbourg). Phys. Rev., 140: B1474-?(Dec. 6, 1965).

An attempt is made to develop an analysis of collision experiments according to the method of Wittgenstein. It is shown that the probability amplitude of a two-particle collision is the matrix element of a unitary operator S. This derivation uses only the superposition principle and the probabilistic interpretation of quantum mechanics. It does not assume any microscopic notion of time nor the validity of the Schrödinger equation. (auth)

4688 ON NON-COMPACT GROUPS. III. THE LINEAR REPRESENTATIONS OF $S\tilde{U}_3$. Fronsdal, C. (International Centre for Theoretical Physics, Trieste). Proc. Roy. Soc. (London), Ser. A, 288: 98-112(Oct. 5, 1965).

The representations of a non-compact form $S\tilde{U}_3$ of SU_3 were studied, with emphasis on the unitary ones. Some of the representations, though infinite dimensional, appear to be eminently suitable for describing elementary particle multiplets. For baryons the only new particle of strangeness larger than −3 that is predicted is one with strangeness −2 and isotopic spin $\frac{3}{2}$. The most important companion to the "decuplet" resonance is a Y_2^*. It seems likely that many theoretical predictions of SU_3 are carried over to $S\tilde{U}_3$. (auth)

4689 ON NON-COMPACT GROUPS. IV. SOME REPRESENTATIONS OF $S\tilde{U}_4(NU_4^*)$. Fronsdal, C. (International Centre for Theoretical Physics, Trieste). Proc. Roy. Soc. (London), Ser. A, 288: 113-22(Oct. 5, 1965).

It was suggested previously that certain non-compact groups, among them $S\tilde{U}_{12}$, may be relevant for the theory of elementary particles. The non-compact subgroup $S\tilde{U}_4$, of $S\tilde{U}_{12}$ was studied. It was found that among several non-compact real forms of SU_4, only that which is isomorphic to the rotation group $R_{4.2}$ is of interest. For this group all the unitary irreducible representations for which the energy operator has a positive definite spectrum were determined. The relation between these representations and those of the Poincaré group were also studied. (auth)

4690 EFFECTIVE RANGE THEORY AND UNCOUPLED PHASE METHOD IN MULTICHANNEL REACTIONS [Thesis]. Nath, Pran. Stanford, Calif., Stanford Univ., 1965. 131p.

The uncoupled phase method is a formalism developed by Ross and Shaw, relating the uncoupled amplitudes describing n-1 channels to the actual amplitudes for all n channels. The uncoupled phase method was based on the model of an n × n potential matrix H_I coupling the n channels, which would yield agreement with experiment. These strong interactions were assumed to have a short well defined range and no hard core. It is demonstrated that the uncoupled phase method remains a quantitative procedure over a much wider range of conditions than originally anticipated. The

method is derived for interactions with hard cores. By performing a two-channel computer experiment, the method is seen to be quantitatively accurate for Yukawa interactions with hard cores; this holds for p-wave as well as s-wave orbital angular momenta, and in the case that one of the channels is closed as well as when both are open. The uncoupled phase method is compared with other methods that include the neglected channel as a perturbation and thus have a much more limited range of validity. The uncoupled phase method previously based on the potential model is extended to the relativistic problem by considering a set of n coupled N/D equations. The resulting relationships are exactly analogous to those derived from the potential model. The quantitative validity of the uncoupled phase method is tested for a variety of left hand singularities, by solving numerically a set of coupled ND^{-1} integral equations. Possible applications of the uncoupled phase method are discussed. An effective range theory in the N/D formalism is proposed, that has the same simple features of the multichannel effective range theory of Ross and Shaw in the potential model. (Dissertation Abstr.)

4691 A CALCULATION OF THE BARYON-VECTOR MESON MIXING PARAMETERS [Thesis]. Krisch, Jean Peck. Ithaca, N. Y., Cornell Univ., 1965. 51p.

By assuming pure unitary symmetry the mixing parameters in the vector meson-baryon Lagrangian $L = g_E\bar{B}((1-f_E)\underline{D} + f_E\underline{F})\gamma^a B \cdot V^a + g_M\bar{B}((1-f_M)\underline{D} + f_M\underline{F})\sigma_{ab}B \times \partial^a V^b - \partial^b V^a$ are calculated. By considering the process $\bar{B}B \rightarrow PP$, where P is the pseudoscalar meson octet and B the baryon octet f_{EM} is calculated. It is assumed that this process is dominated by intermediate vector mesons in the direct channel, and that the dominant forces come from baryon and baryon resonance exchange. Crossing symmetry is used to relate the crossed channels to the direct channels, in equating the residues of the direct and cross channel amplitudes. This gives an equation for the mixing parameters in terms of experimentally determinable parameters. The mixing parameters are found to be approximately $f_E = .4$ and $f_M = .8$. This implies that the magnetic (tensor) forces are produced almost entirely by baryon exchange. Baryon and baryon resonance exchange produce comparable forces in the elastic case. (Dissertation Abstr.)

4692 THE PION LIFE-TIME AND THE EIGHT-FOLD SYMMETRY [Thesis]. Welling, Daniel John. St. Louis, St. Louis Univ., 1963. 132p.

The eight-fold symmetry group introduced by Gell-Mann as a mathematical framework for the strong interactions is investigated with a view toward producing a possible theoretical basis for the decay of the pion. It has been shown that a sufficient condition for producing the correct formula is to have the divergence of an axial-vector current (a source), obtained from the strong Lagrangian, proportional to the pion field. The sources are constructed in the usual way by imposing certain infinitesimal transformations in the eight-space, which leave the interaction non-invariant. It is then found, using the eight-fold Lagrangian, that the effects from the interation terms on the source cannot be removed in a simple way. If, however, one assumes that it is sufficient to require that the source have the same quantum numbers as the pion field, then certain sources from the eight-dimensional theory are derived that do resemble the pion. These can be regarded as equivalently causing effects for which the pion is blamed. It is thus concluded that with this assumption the Gell-Mann strong interaction theory does satisfy, at least sufficiently, the conditions for a theory of pion-decay. (Dissertation Abstr.)

4693 STUDIES IN HAMILTONIAN THEORIES OF RELATIVISTIC INTERACTING PARTICLES, AND IN THE APPLICATION OF SYMMETRY GROUPS TO ELEMENTARY PARTICLE PHYSICS. (PARTS I AND II) [Thesis]. Mukunda, Narasimhaiengar. Rochester, N. Y., Univ. of Rochester, 1964. 276p.

Part I contains the construction of a two-channel Hamiltonian model of Lorentz invariant particle interactions. A Hilbert space of wave functions is set up to describe a non-interacting two-channel system with different thresholds, each channel containing two spinless particles. A unitary representation of the inhomogeneous Lorentz group is set up in this space by explicitly giving the forms of the (free) generators of this group. Interaction is introduced by the method of Moeller matrices (wave operators). The momentum and angular momentum operators are the same for the free and the interacting systems, and the wave operators break up into independent operators for each partial wave in the center of momentum frame. The form of the wave operators is determined from the scattering eigensolutions of a separable potential type two-channel Hamiltonian. The scattering amplitudes of the theory are calculated and shown to be manifestly Lorentz invariant functions. Some analytic properties of the scattering amplitudes in their energy and angular momentum dependence are studied. The model shows that in a multichannel situation with several thresholds and branch cuts, poles in the scattering amplitude, corresponding to physical resonances, need not appear on all unphysical sheets adjoining the physical sheet of the energy variable. In Part II, some properties of the second rank Lie group G_2 are studied first. Next the theory of representation mixing for SU_3, correct to first order in symmetry breaking interactions, is set up. Finally, some theorems concerning Clebsch-Gordan coefficients of arbitrary compact groups are proved, which allow the development of a generalized Shmushkevich method for any symmetry group. This is a simple device for deriving consequences of exact (or approximate) group invariance, for such quantities as decay widths and reaction cross sections. (A.G.W.)

4694 ANALYSIS OF THE EXPERIMENTAL EVIDENCE FOR THE STATISTICS OF ELEMENTARY PARTICLES [Thesis]. Von Baeyer, Hans Christian. Nashville, Vanderbilt Univ., 1964. 171p.

Means of determining the statistics of elementary particles without recourse to either the spin-statistics theorem or any assumption that limits the possible types of statistics are presented. In order to find the experimental consequences of statistics, the principle of indistinguishability and the permutation operators are discussed in detail. The mathematical formulations of the Pauli exclusion principle and the Bose-Einstein symmetry are derived. As a concrete example of anomalous statistics a complete but brief critical review of the subject of parastatistics is included. As a possible means for determining statistics a theorem is proved, which states that under certain assumptions it is possible to relate the statistics of unstable particles to those of their decay products. Other tests, independent of this theorem, are discussed for elementary particles. Some of these tests have been suggested previously, some are based on experiments that have been performed and some are suggestions for experiments that can be done in the future. Among these tests the most important new result pertains to pions: An examination of the selection rules for nonleptonic decays of kaons yields the conclusion that pions are bosons. (Dissertation Abstr.)

4695 ELEMENTARY PARTICLE AND HIGH ENERGY PHYSICS. 1963 Lectures Given at the Cargese Summer School of Theoretical Physics. Levy, M.; Meyer, Ph. (eds.). New York, Gordon and Breach Science Publishers, 1965. 367p. $7.95 paper; $14.50 cloth.

The book includes six complete papers. Separate abstracts were prepared for each of these. (J.F.P.)

For abstracts of individual papers see: 4633, 4634, and 4696–4699.

4696 STRONG INTERACTIONS AT VERY HIGH ENERGY. Van Hove, L. (CERN, Geneva). pp 1-48 of Elementary Particle and High Energy Physics. New York, Gordon and Breach Science Publishers, 1965.

Elastic and inelastic collisions of strongly interacting particles are considered in the multi-Bev region characterized by the approximate limit $E_{lab} \gtrsim 5$ Bev. In this region, all properties of the collisions seem to vary slowly with the incident energy. Since experimental knowledge is

very partial and theoretical knowledge is very primitive and fragmentary, only the establishment of a few logical connections between various conjectured aspects of the phenomena can be accomplished. Topics discussed include definitions of elastic and inelastic collisions, definitions and formulas of scattering theory, the behavior of various cross sections at high energy, isotopic spin considerations and the absence of charge exchange, the generalized Pomeranchuk theorem in dispersion relation analysis, and the Regge pole approach to high energy scattering. Other topics are the shadow scattering calculation, high energy collisions, and calculation of shadow scattering for a model. (J.F.P.)

4697 COMPLEX ANGULAR MOMENTUM THEORY OF PARTICLES WITH SPIN. Charap, J. M. (Imperial Coll. of Science and Tech., London). pp 49-96 of Elementary Particle and High Energy Physics. New York, Gordon and Breach Science Publishers, 1965.

A potential scattering model which is always restricted to two-particle states is studied. But the particles will, in general, have spins s_1 and s_2, and a multichannel problem is considered. After deriving enough to conclude, for a very wide class of potentials, that the partial waves are interconnected, and that no one can be arbitrarily changed, such that the subtraction problem is in principle solved, more stringent conditions are applied. Then the relativistic S-matrix theory is used. Dynamical branch cuts are suggested for solution of the equation. This would be a crucial breakdown to the analogy between the analytic properties of the scattering amplitude derived from potential theory and that needed for relativistic theory. (J.F.P.)

4698 UNITARY SYMMETRY—MODEL OF THE OCTET. Gourdin, M. (Universite, Paris). pp 127-88 of Elementary Particle and High Energy Physics. New York, Gordon and Breach Science Publishers, 1965. (In French).

An extension of the Lie algebra and an acceptable choice of physical conditions are proposed according to the following criteria: the charge is diagonal for all masses, and the values are multiples of the elementary charge. All members of the same supermultiplet have the same spin J and the same parity P. There are an equal number of baryons B. The result is that the total Lie algebra cannot be simple, the operator B commutes with all the other infinitesimal generators. But it does not necessarily follow that the symmetry group be produced directly. A simple model of symmetry is studied including isotopic spin, the mathematical basis for the unitary symmetry of which is the Lie algebra with matrices of dimension 3. (J.F.P.)

4699 QUANTUM THEORY OF GAUGE FIELDS. Schwinger, J. (Harvard Univ., Cambridge, Mass.). pp 189-325 of Elementary Particle and High Energy Physics. New York, Gordon and Breach Science Publishers, 1965.

Some recent work on the relativistic field theory is discussed, particularly some problems of quantization concerned with the idea of nonabelian gauge fields. The work leads to a satisfactory solution for the quantization of the gravitational field. Topics considered are the quantum action principle, the relativistic invariant gauge field, quantum variables and the gauge group, and the quantized gravitational field. A survey is given of the problems arising from these considerations. (J.F.P.)

4700 GROUP THEORETICAL PROPERTIES OF COMPLEX ANGULAR MOMENTA. Beltrametti, Enrico (Univ. of Genca). pp 155-68 of Lectures in Theoretical Physics. Vol. VI. Boulder, Colo., The University of Colorado Press, 1964.

An attempt is made to describe a complex angular momentum from a group theoretical point of view. It is found that the extension to complex angular momenta of Weyl's method leads to a definition of two sets of infinite matrices which can be defined in correspondence of the elements r or R_3, with some exceptions. Also it is seen that the product of two matrices does not always exist, but a typical structure is obtained which is able to describe the product rules of the rotations. Use is made of the homomorphism between the unitary unimodular group SU_2 and R_3. (J.F.P.)

4701 RECENT PROGRESS IN POTENTIAL SCATTERING THEORIES. Regge, Tullio. pp 373-8 of Lectures in Theoretical Physics. Vol. VI. Boulder, Colo., The University of Colorado Press, 1964.

A survey is given on potential scattering. The improvements made over the past two years in potential scattering theory from attempts to generalize previous results to more complicated cases are discussed. These improvements include relativistic extensions of the theory, extensions to the many-channel problem, the treatment of already known results, and the problem of dealing with three or more particle systems. (J.F.P.)

Fluid Physics and Thermodynamics

See also Plasma Physics and Thermonuclear Processes

4702 (AD-619094) GASDYNAMIC METHODS IN MHD FLOW. Final Administrative Report, January 1, 1963-December 31, 1964. Summary Report No. 1. Cap, Ferdinand; Kerer, G.; Herrnegger, F.; Lackner, F.; Skarics, R. (Innsbruck Univ. (Austria). Institut fuer Theoretische Physik). Contract AF61(052)-675. 42p. CFSTI $2.00 cy, $0.50 mn.

An investigation of the use of Crocco's theorem for plasmas was conducted with emphasis on conditions for potential flow in a plasma, application of the method of characteristics and others of gasdynamics for plasma flows. (TAB)

4703 (AD-619101) THE EFFECTS OF ELECTRICAL CONDUCTANCE OF WALL ON MAGNETOHYDRODYNAMIC CHANNEL FLOW WITH HEAT TRANSFER. Special Report No. 52. Hwang, Un-Pah; Tripp, Wilson; Hwang, Ching-Lai; Fan, Liang-tseng (Kansas Engineering Experiment Station, Manhattan). 1965. 64p. (AFOSR-65-1312). CFSTI $3.00 cy, $0.75 mn.

Kans. State Univ., Eng. Exp. Sta., Bull., Vol. 49, No. 3, March 1965.

A detailed as well as critical review of some mathematical and physical aspects of the MHD flow is presented. First, the details of the pioneering work by Hartmann and Lazarus on the subject of channel flow are described. The modified Hartmann flow with the electrical conductance of walls investigated by Chang and Lundgren, and by Chang and Yen are then reviewed. (TAB)

4704 (NASA-TN-D-3058) A SINGLE-COLLISION MODEL FOR ELECTRON-BEAM CURRENTS BETWEEN PLANE ELECTRODES. Goldstein, Charles M.; Goldstein, Arthur W. (National Aeronautics and Space Administration, Cleveland, Ohio. Lewis Research Center). Nov. 1965. 22p. CFSTI $1.00 cy, $0.50 mn.

Space-charge and potential distributions are calculated for the region between two plane electrodes. The effect of elastic, hard-sphere collisions between the electrons of the injected beam and the neutral gas molecules is incorporated into the analysis with the assumption that the electrons will suffer at most one scattering collision. The injected beam, itself, is assumed monoenergetic. Calculations of current as a function of voltage are compared with results from a multiple-collision model; very good agreement is found for an electrode-spacing to mean-free-path ratio of 0.1, and a maximum deviation of only 1.5% was observed for a ratio of 0.5. Current-voltage characteristics are also calculated for various values of emission current and electrode spacing. Collisions are found to have a pronounced influence on potential and density distributions, current, and region of time-independent operation. (auth)

4705 (NYO-1480-33) FINITE DIFFERENCE CALCULATIONS FOR HYDRODYNAMIC FLOWS CONTAINING

DISCONTINUITIES. Burstein, Samuel Z. (Courant Inst. of Mathematical Sciences, New York Univ., N. Y.). Sept. 1965. Contract AT(30-1)-1480. 43p. Dep. mn; CFSTI $2.00 cy, $0.50 mn.

The calculation of the steady hypersonic inviscid flow, including a detached shock, around a blunt body is presented. The steady flow is obtained as the limit for large time of time dependent flow, starting with plane flow impinging on the body. The transient flow is the solution of a mixed initial-boundary value problem for the partial differential equations of inviscid fluids which is solved by a difference scheme proposed by Lax and Wendroff. Calculations show that by itself this difference scheme tends to be unstable and does not converge to the steady flow; by adding an artificial viscosity term one succeeds in stabilizing the calculation. A theoretical explanation of this stabilizing effect and a new stability condition are discussed. Both plane and cylindrical symmetries are considered. (M.O.W.)

4706 (RPI-3036-1) WALL EFFECTS IN NON-EQUILIBRIUM STATISTICAL MECHANICS. Final Report. Hollinger, Henry B. (Rensselaer Polytechnic Inst., Troy, N. Y.). Oct. 1965. Contract AT(30-1)-3036. 50p. Dep. mn; CFSTI $2.00 cy, $0.50 mn.

An attempt is made to establish foundations for the non-equilibrium statistical mechanics of systems with containing walls, and to assess the effect of wall collisions on transport phenomena. A new formulation of the problem of irreversibility is given and a solution is proposed. The origin of irreversibility is identified and illustrated by the use of a generalized entropy. And the role of wall collisions is considered. A solution of problem of states is proposed. Also the analysis of the effects of wall collisions on transport phenomena in a dilute gas of rigid spheres is formulated, and the appropriate form of the molecular chaos assumption is derived. (J.F.P.)

4707 (UCRL-14318) A STUDY OF SIMPLE WAVES. Hardy, J. (Lawrence Radiation Lab., Univ. of California, Livermore). Aug. 10, 1965. Contract W-7405-eng-48. 14p. Dep. mn; CFSTI $1.00 cy, $0.50 mn.

A method for construction of simple waves is presented. Attention is focused on forward-facing compression waves, specifically at the points at which shocks develop, and predictions concerning shock strength, etc. Discussion is limited to γ-law gases, although the technique is general. (auth)

4708 (UCRL-14360, pp 50-73) THERMODYNAMIC PROPERTIES OF MATTER. (Lawrence Radiation Lab., Univ. of California, Livermore).

A method for determining the bound states in a short-range central potential was developed and applied to the Debye-Hückel and Wood-Saxon potentials. The binding energies of polyatomic ^{4}He molecules were investigated, and a method for obtaining information from power series expansions in thermodynamics and statistical mechanics was developed. Cell theories for hard particles were considered, and the equation of state for disks was determined over a wide range of densities. Fluid transport mechanisms in hard-sphere molecular systems were considered, and the radial distribution function for hard spheres was studied. The phase transitions of repulsive lattice gas models were investigated, and the properties and pair distribution of an electron gas were calculated. Calculations were made of solid-phase entropies, and a computer program was developed for determining equations of state. The flow characteristics in an explosive-driven shock tube were observed; and the electric conductivity of solid iodine, carbon tetrachloride, and alumina was measured at high pressures behind shock fronts. Shock-induced phase transitions were observed in single-crystal and pressed samples of Bi and KBr. The anomalous demagnetization of ceramic spinel nickel ferrite was studied further. (D.C.W.)

4709 MAGNETOHYDRODYNAMIC FLOW IN THE ENTRANCE REGION OF A PARALLEL-PLATE CHANNEL. Snyder, William T. (Univ. of Tennessee, Tullahoma). AIAA (Amer. Inst. Aeron. Astronaut.) J., 3: 1833-8(Oct. 1965).

A new method is presented for the analysis of MHD flow in the entrance region of a parallel-plate channel. The method, recently described by Sparrow, Lin, and Lundgren for non-MHD flows, involves a linearization of the inertia terms and the introduction of a stretched axial coordinate. A solution is obtained for the velocity distribution which is valid from the duct inlet to the fully developed region. From this solution results are obtained for the entrance length, the pressure distribution, and the wall shear stress for a range of Hartmann numbers. A comparison of the results from the present analysis is made with available analytical studies of the same problem by other methods. This comparison supports the validity of the present method for analyzing MHD channel flows in the entrance region. (auth)

4710 AN INVARIANCE PROPERTY OF THE FREE ELECTROMAGNETIC FIELD. Calkin, M. G. (Dalhousie Univ., Halifax, Nova Scotia, Can.). Amer. J. Phys., 33: 958-60(Nov. 1965).

In the absence of charges and currents, Maxwell's equations are invariant under the transformation $E' = E\cos\theta + B\sin\theta$, $B' = -E\sin\theta + B\cos\theta$. Using Noether's theorem, it is shown that the corresponding conserved quantity is proportional to the difference in the number of right and left circularly polarized photons in the field. (auth)

4711 HALL CURRENT EFFECT ON MAGNETOHYDRODYNAMIC WAVES IN ROTATING LIQUIDS. Nigam, P. D. Appl. Sci. Res., Sect. B, 12: 139-50(1965).

The effect of the Hall current on the directional distribution and attenuation of waves created by a localized periodic source in ionized, incompressible, rotating liquids in the presence of a uniform externally applied magnetic field was studied using a technique developed by Lighthill. It is found that the Hall current causes a radial expansion of Alfvén waves and radial contraction of Taylor waves. It also alters the modes of decay of these waves. (auth)

4712 THE RELATIVISTIC TRANSFORMATION OF TEMPERATURE. Guessous, Abdelmalek (Faculte des Sciences, Rabat, Maroc, France. Laboratoire Joliot-Curie de Physique Nucleaire, Orsay, France). Compt. Rend., 261: 1182-5(Aug. 2, 1965). (In French).

In a previous study (Compt. Rend., 260: 6811(1965)), the relativistic distribution function $F(\vec{x}, \vec{p}, t)$ of a perfect gas in equilibrium was determined and a kinetic definition of the temperature T that was analyzed in the physical sense was proposed. In the present study the transformation formula of T is established directly beginning with its definition. It is shown that the distribution function f of the gas is, in the more general sense, a relativistic invariant. The variants of the entropy S and the variation of the number of particles per unit volume are deduced. (tr-auth)

4713 STUDY OF THE DOPPLER TEMPERATURE IN A TOROIDAL DISCHARGE USING A MULTICHANNEL FABRY-PEROT INTERFEROMETER. Platz, Peter; Hirschberg, Joseph G. (C.N.R.S., Bellevue, France. Euratom-C.E.A., Fontenay-aux-Roses, France. Princeton Univ., N. J.). Compt. Rend., 261: 1207-10(Aug. 2, 1965). (In French).

A multichannel Fabry-Perot interferometer was used to measure the Doppler length of atomic rays and rays emitted by ions with multiple charge in an electric discharge with toroidal geometry. An atomic and an ionic temperature was deduced by taking into consideration various parasite effects. A possible process for the heating of the atom by the ions was indicated. The temperature of the ions with multiple charge (0^{4+}) in low proportion in the discharge was discussed. (tr-auth)

4714 METHOD FOR THE MEASUREMENT OF THE ELECTRON TEMPERATURE IN THE IONIZATION PHASE OF A PULSED DISCHARGE IN HYDROGEN. Breton, Claude; Schwob, Jean-Louis (Euratom-C.E.A., Fontenay-aux-Roses, France. C.N.R.S., Bellevue, France). Compt. Rend., 261: 1211-14(Aug. 2, 1965). (In French).

The evolution of the hydrogen rays during a discharge was studied theoretically using an ionization model that takes into consideration the dissociation of molecules and the reabsorption of atomic rays. The important role of the dissociation on the moment of the emission of the rays was noted. From this study a measurement of the electron temperature was deduced from the position in time of the intensity maximum of H_β. (tr-auth)

4715 CHANNEL FLOW OF A COMPRESSIBLE, ELECTRICALLY CONDUCTING FLUID UNDER THE ACTION OF A NON-UNIFORM MAGNETIC FIELD. Peyret, Roger (California Inst. of Tech., Pasadena). Compt. Rend., 261: 1591-4(Aug. 18, 1965). (In French).

The time-averaged two-dimensional flow in a progressive-wave plasma accelerator is considered, taking into account in particular the effect of the axial component of the magnetic field. The solution obtained by the linearization method makes it possible to calculate the acceleration of the fluid and gives evidence of a confinement effect. (tr-auth)

4716 A METHOD FOR SUSTAINING AN ASSIGNED CONDUCTING GAS FLOW IN A TRANSVERSE MAGNETIC FIELD. Bertinov, A. I.; But, D. A. Izv. Akad. Nauk SSSR, Energ. i Transp., No. 3, 94-5(May-June 1965). (In Russian).

The maintaining of an assigned isoparametric regime of magnetogasdynamic flow by using the correction of the profile of a transverse magnetic field was proposed. On the example of the isothermal uniform flow of an ideal conducting gas, the general method for the development of programming conditions, which can be expected on the basis of the calculation of systems of automatic control, was demonstrated. (tr-auth)

4717 ONE-DIMENSIONAL FLOW IN AN IONIZING GAS. Butler, D. S. (Univ. of Strathclyde, Glasgow). J. Fluid Mech., 23: 1-21(Sept. 1965).

In order to gain into the macroscopic behavior of gas interacting with electric and magnetic fields, while its degree of ionization is changing, the one-dimensional unsteady flow of gas with temperature-dependent conductivity is investigated. A simple continuum model is used for the gas. It is assumed to be compressible and to obey polytropic gas laws and its conductivity is supposed to change discontinuously at a critical temperature. Particular attention is devoted to the various types of transition boundaries which can occur as the conductivity changes, and it is shown that complete flow patterns can be constructed with these as elements. A wide variety of transitions is possible and some of these have remarkable properties. For example, it is shown that discontinuous deionizing fronts can exist and are expansive in nature. This contrasts sharply with the situation in conventional gas dynamics and magnetogasdynamics where only compressive discontinuities can exist. (auth)

4718 ON LARGE-AMPLITUDE MAGNETOHYDRODYNAMICS. Yih, Chia-Shun (Univ. of Michigan, Ann Arbor). J. Fluid Mech., 23: 261-71(Oct. 1965).

The flow of an inviscid, incompressible, and infinitely conducting fluid in a magnetic field is investigated. It is shown that all steady flows with magnetic lines coincident with streamlines are reducible to flows without a magnetic field. The possibility of a steady irrotational and current-free flow with coincident streamlines and magnetic lines is established. The flow of a fluid through a circular cylinder of radius R into a point sink with strength m is also investigated when the fluid carries a current density j_0 at infinity. It is shown that the condition of uniform flow at infinity is impossible to maintain if a dimensionless number $(kR)^2$ involving the current density j_0 exceeds the value $(3 \cdot 831)^2$, and that the current has the effect of concentrating the flow near the center line and of producing ring eddies which become longer as (kR^2) is increased. (L.B.S.)

4719 A LIMIT THEOREM ON MAGNETOFLUIDDYNAMICS. I. Arora, Kasturi L. (Univ. of Colorado, Boulder. Martin Marietta Corp., Denver). J. Math. Anal. Appl., 12: 122-34(Aug. 1965).

A theorem on the limit function of a sequence of solutions is proved for a nonlinear system of differential equations of magnetofluid dynamics, which contains terms quadratic in the first derivatives of the velocity and magnetic field. No assumptions are made on the divergence of the derivatives. The system contains three parameters, the coefficients of viscosity, heat conduction and electric conductivity, which converge to zero in the limit. (L.B.S.)

4720 A LIMIT THEOREM ON MAGNETOFLUIDDYNAMICS. II. Arora, Kasturi L. (Univ. of Colorado, Boulder). J. Math. Anal. Appl., 12: 135-47(Aug. 1965).

A theorem on the limit functions of a sequence of flows in magnetofluiddynamics is proved for a nonlinear differential system that contains terms quadratic in the first derivatives of the velocity and magnetic fields. The case is considered where the magnetic diffusity coefficient is allowed to converge to zero in the limit. (L.B.S.)

4721 THE BOLTZMANN EQUATION FOR THE DISTRIBUTION FOR PRIMARY ATOMS. Leibfried, Guenther; Mika, Klaus (Technische Hochschule, Aachen). Nukleonik, 7: 309-12(July 1965). (In German).

The equation formulated by Leibfried (Z. Physik 171: 1(1963)) for the distribution $W(r,v_0)$ of the final position r of primary atoms with an initial velocity v_0 has certain similarities with the linear Boltzmann equation known in the transport theory. This relation was investigated. For the density $n(r,b;v_0)$ in the position and velocity space, in addition to the Boltzmann equation in which v is variable, another transport equation was derived in which v_0 is a variable and v is a parameter. This (backward) equation is especially suitable for the derivation of the equation for $w(r,v_0)$ that was obtained by Leibfried on the basis of a random walk consideration. On the example of the mean value r^n, the relation between the distribution $w(r,v_0)$ and the Boltzmann equation $n(r,v;v_0)$ is explained. (tr-auth)

4722 ION DENSITY IN ELECTRON BEAMS. Callebaut, D. K. (Univ., Ghent). Physica, 31: 1177-92(Aug. 1965).

The charge trapped in electron or ion beams at pressures below breakdown may be determined from a general integro-differential equation. An approximation method to solve the latter is given. The method is particularly suitable for polynomials in x or in exp x. Some relevant exact solutions are considered. It is shown that Aitken's solution for constant beam density and ion production has much wider application. In the latter case the ion potential and the d-c part of the external potential add to a parabola, the coefficient of which may be determined, for all parameters involved, from a single unified curve (plotted). An upper and a lower limit are given for the potential to take account of the thermal velocity. Dimensionless quantities of invaluable help are introduced. (auth)

4723 EVOLUTION EQUATION FOR N RELATIVISTIC CHARGED PARTICLES. Hobson, A.; Leaf, B. (Kansas State Univ., Manhattan). Physica, 31: 1227-41(Aug. 1965).

The evolution equation, correct to second order in the charge, for N relativistic point charges in zero external field is derived. This is done by writing down the Liouville equation for the system of charges and fields, assuming appropriate initial conditions, and integrating the Liouville equation over the field variables. The initial conditions imply that the field has initially no statistical dispersion, and is the field of N stationary point charges. Renormalization is carried out, and the k integrals are performed. The evolution equation exhibits an explicit time dependence. It reaches its asymptotic form in the time necessary for light signals to connect the mean positions of all the charges. The results are checked by deriving the asymptotic evolution equation, to order $(v/c)^2$, by a different method, related to the Lorentz gauge analogue of the Coulomb gauge Darwin Hamiltonian. (auth)

4724 THERMAL DIFFUSION IN ISOTOPIC HYDROGEN AND HYDROGEN-HELIUM MIXTURES. I. THEORETICAL APPROACH. Los, J.; Slieker, C. J. G. Physica, 31: 1346-56(Aug. 1965).

In the thermal diffusion factors of isotopic mixtures of diatomic molecules, large anomalies are measured. These anomalies are due to different asymmetries for different isotopic molecules. Using an effective spherical symmetric potential, the discrepancies are explained only qualitatively, while the quantitative agreement is still unsatisfactory. A quantum mechanical derivation of an effective potential leads to the same results. However, this method eventually permits the use of Waldmann's theory, where the influence of the azimuthal momentum transport on the transport properties is accounted for. Moreover, inelastic collisions will result in a correction on the effective potential which will lead to a better quantitative agreement. (auth)

4725 VISCOUS MHD FLOW ABOUT A SPHERICAL MAGNETIC QUADRUPOLE. O'Brien, Vivian (John Hopkins Univ., Baltimore). Quart. Appl. Math., 23: 283-5(Oct. 1965).

The perturbation velocity field and the perturbation magnetic field due to the first-order interaction of the slow flow field of a conductive viscous fluid with an aligned quadrupole magnet were calculated. The drag increase can be computed from the perturbation stream function alone with an economy of effort compared to previous calculations for magnetized bodies. (auth)

4726 ELECTROSTATIC APPARATUS FOR REMOVAL OF DUST PARTICLES FROM A GAS STREAM. Allemann, Rudolph T.; Moore, Robert L.; Upson, U. L. (to U. S. Atomic Energy Commission). U. S. Patent 3,218,781. Nov. 23, 1965.

An apparatus is designed for removing particles entrained in a gas stream from the stream. It comprises first and second electrodes whose potentials are such that an electrical discharge exists therebetween. An enclosure is provided having an electrically conductive liquid contained therewithin and means for applying a potential to the liquid different from that of the electrodes. An electrically nonconductive enclosure is provided having a plurality of openings through the base. The base together with the openings is submerged in the liquid. The electrically nonconductive enclosure is disposed about electrodes and the space therebetween to effect electrical insulation between the electrodes and the liquid. Means are provided for passing the gas through the electrical discharge between the electrodes and then through the openings in the base of the electrically nonconductive enclosure into the liquid, the presence of the gas prohibiting passage of the liquid through the openings. (AEC)

Geophysics

4727 (AD-618054) ELECTRON TEMPERATURES IN THE D REGION. Dalgarno, A.; Henry, R. J. W. (Queen's Univ., Belfast (Northern Ireland). Dept. of Applied Mathematics). 1965. 23p. (AFCRL-65-482). CFSTI $1.00 cy, $0.50 mn.

Detailed estimates were made of the rates of energy loss of electrons moving in the D region and it is argued that the electron gas has a negligible non-thermal component. The Maxwellian velocity distribution of the thermal component is brought about by collisions with molecular nitrogen involving rotational transitions and the distribution is determined by the neutral particle gas temperature. (auth)

4728 (AD-618118) TWO-DIMENSIONAL CALCULATIONS OF MAGNETIC MICROPULSATION RESONANCES [Thesis]. Greenfield, Roy Jay (Massachusetts Inst. of Tech., Cambridge). June 21, 1965. 147p. CFSTI $4.00 cy, $1.00 mn.

Magnetic micropulsations in the period range of 5 to 45 seconds were interpreted as a resonant amplification of waves in the ionosphere. The wave involved is of the type which is not guided by the earth's magnetic field. A resonance can occur, because the wave energy is trapped by the rapid increase with height of the Alfven wave velocity above the F2 peak. Previous theoretical investigations of this resonance have been limited to models for the ionosphere in which the properties could only vary with height and not with horizontal position. Here the effect of horizontal variations is considered by examining the solutions of two-dimensional models. The first model simulates longitude independent propagation in a spherical earth-ionosphere. The horizontal variation is introduced by the inclusion of a dipole magnetic field. The second model is a cylindrical model. In this model the ionospheric parameters, such as the electron density, vary with the angular coordinate. Both two-dimensional models were solved by the use of finite difference methods. (TAB)

4729 (CNIE-PE-4) THE PRODUCTION AND REMOVAL OF IONIZATION IN THE UPPER ATMOSPHERE. Gassmann, G. J. (Comision Nazional de Investigaciones Espaciales, Buenos Aires (Argentina)). 1965. 125p. Dep. mn.

An extensive literature survey on ionization production and removal in the upper atmosphere is presented. Detailed information is presented in connection with atmospheric profiles, radiation input and production of ionization, and removal processes and the balance of ionization. (M.O.W.)

4730 (SC-DC-65-1797) A PRELIMINARY REPORT ON THE INTERACTION OF AN ELECTROMAGNETIC FIELD WITH A MISSILE HAVING AN IONIZED TRAIL. Harrison, Charles W. Jr.; Taylor, Clayborne D. (Sandia Corp., Albuquerque, N. Mex.); Ruquist, Richard D. (Gordon McKay Lab. of Applied Science, Harvard Univ., Cambridge, Mass.). Oct. 15, 1965. Contract AT(29-1)-789. 30p. Dep. mn; CFSTI $2.00 cy, $0.50 mn.

A missile with plume (ionized trail) in flight at relatively low altitudes is treated as an isolated cylindrical receiving antenna. One portion of the antenna is considered to be perfectly conducting and represents the missile; the other section of the antenna is assumed to be imperfectly conducting and represents the plume. In the present version of the theory no charge is permitted to build up between the portions of the antenna. The incident electromagnetic field is assumed to be a plane wave with the electric field polarized parallel to the axis of the missile and plume. The current distributions along both the missile and plume are obtained by solving the nonhomogeneous differential equations for the currents in the two antenna sections subject to appropriate boundary conditions. (auth)

4731 (UCRL-7659-T(Rev.1)) THE TRAPPED ELECTRON SPECTRA FROM THE STARFISH DETONATION AND FROM THE OUTER BELT IN THE FALL OF 1962. West, Harry I. Jr. (Lawrence Radiation Lab., Univ. of California, Livermore). Oct. 14, 1965. Contract W-7405-eng-48. 6p. (CONF-650816-3). Dep. mn; CFSTI $1.00 cy, $0.50 mn.

From Conference on Radiation Trapped in the Earth's Magnetic Field, Bergen, Norway.

A brief summary of some of the electron spectra measured in 1962 is presented. Measurements were made with a five-channel magnetic electron spectrometer covering the range of 325 to 3250 kev. (auth)

4732 (UCRL-14368-T(Rev.1)) SOME OBSERVATIONS OF THE TRAPPED ELECTRONS PRODUCED BY THE RUSSIAN HIGH-ALTITUDE NUCLEAR DETONATION OF OCTOBER 28, 1962. West, Harry I. Jr. (Lawrence Radiation Lab., Univ. of California, Livermore). Oct. 15, 1965. Contract W-7405-eng-48. 46p. (CONF-650816-4). Dep. mn; CFSTI $2.00 cy, $0.50 mn.

From Conference on Radiation Trapped in the Earth's Magnetic Field, Bergen, Norway.

The trapped electrons produced by the Russian high altitude nuclear detonation of October 28, 1962, were observed by a five-channel magnetic spectrometer covering the range

of 325 to 3250 kev. The results are presented in terms of energy spectra and pitch angle distributions. Mirror-point density distributions are derived which give an insight into the details of the injection of the trapped electrons into the earth's geomagnetosphere. (auth)

4733 (AI-Trans-201) DETERMINATION OF DISTRIBUTION OF AEROSOL PARTICLES ACCORDING TO SIZE BY DIFFUSION METHOD. Fuks, N. A.; Stechkina, I. B.; Staroselsky, V. A. Translated for Atomics International, Canoga Park, Calif., from Inzh.-Fiz. Zh., Akad. Nauk Belorussk. SSR, 5: No. 12, 100-3(1962). 8p. Dep. mn; CFSTI $1.00 cy, $0.50 mn; JCL $1.10 fs, $0.80 mf.

De Marcus' formula obtained for monodisperse aerosol was applied to polydisperse ones. For this purpose the law of a log-normal particle distribution was adopted, and De Marcus' formula was generalized by the inverse Laplace transformation. With the use of a computer the diffusion precipitation was calculated over the range of $\eta\Delta$ between 10^{-7} and 10^{-5} cm as well as standard geometric deviation of $\beta\Delta$ from 1 to 2.5. A plot is presented. The mean diameter of aerosol particles may be determined from three measured values of n/n_0 and y depicted in this plot. (auth)

4734 (N64-30079) ANALYTICAL REPRESENTATION OF THE GEOMAGNETIC FIELD AND THE SECULAR VARIATION. Kautzleben, Heinz. Translated from Abhandl. Geomagn. Inst. Observ. Potsdam-Neimagh, No. 32, (1963). 147p. (NASA-TT-F-8700). CFSTI $1.10 cy.

Topics discussed include representation of the vertical component on the terrestrial surface, representation of geomagnetic potential on the earth's surface, representation and analysis of total intensity and horizontal intensity, error in potential calculations, representation of the secular variation, formulas for spherical harmonics, and orthogonal polynomials for discrete distributions of value. (auth)

4735 STUDY OF FOCUSING INHOMOGENEITIES IN IONOSPHERE BY RADIOASTRONOMIC METHOD ON 13-54 Mgc FREQUENCIES. Erukhimov, L. M.; Rizhov, V. A. (Gor'kii State Univ., USSR). Geomagn. Aeronomiya, 5: 693-7(July-Aug. 1965). (In Russian).

It was shown that inhomogeneous electron densities of the ionosphere of the size of approximately 10 km have focusing properties. The evaluation of the fluctuation of the electron concentration $\Delta N/N$ for this inhomogeneity was derived. (tr-auth)

4736 ANOMALOUS IONIZATION OF THE LOWER IONOSPHERE OF THE TEMPERATE LATITUDES DURING THE WORLD MAGNETIC STORMS. Benediktov, E. A.; Korobkov, Yu. S.; Tolmacheva, A. V. (Gor'kii State Univ.). Geomagn. Aeronomiya, 5: 698-704(July-Aug. 1965). (In Russian).

During world magnetic storms in the temperate zones anomalous ionization of the lower ionosphere was observed, causing the appearance of supplementary absorption of radio waves. The analysis of the results of the measurement of the absorption of the cosmic radiation in the ionosphere on some fixed frequencies showed that anomalous ionization originated at high altitudes of approximately 50 km, and electron concentrations reached values of approximately 10^3 electrons/cm^3. The primary electron current necessary for the formation of the anomalous ionization was evaluated. (tr-auth)

4737 MECHANISM OF THE LOWER IONOSPHERE IONIZATION. Ivanov-Kholodnii, G. S. (Inst. of Applied Geophysics, Academy of Sciences, USSR). Geomagn. Aeronomiya, 5: 705-20(July-Aug. 1965). (In Russian).

Ionization at heights of 60 to 100 km during different activities of the calm sun and during solar flares was calculated. On the basis of the comparison of the results of these calculations with the results of measurements of $\underline{n}_e$ and α' it was concluded that the cosmic rays generated stronger ionization than solar radiation below approximately 75 km in periods of minimum solar activity and below approximately 65 km in periods of maximum activity. X radiation of the sun shorter than 10 to 20 Å can explain ionizations 85 to 95 km and longer wave lengths cause more long wave x rays and ultraviolet (approximately 1000 Å) radiation. At altitudes of 75 to 90 km the electron concentration during a solar cycle must fluctuate at 0.5 to 1 of the order of magnitude. The ionization at altitudes of 70 to 85 km is difficult to explain by the effects of L_α radiation of the sun. Rocket and sputnik data on the x radiation of the solar flares agree with ionization data on $\underline{n}_e$ and α' during ionospheric disturbances. At altitudes from 60 to 75 km it is necessary to assume the effect of the third principle of ionization of a sporadic character. (tr-auth)

4738 QUIET SOLAR-DAILY VARIATIONS OF GEOMAGNETIC FIELD DURING IGY. II. NONCYCLIC VARIATIONS IN MAGNETO-QUIET DAYS. SEASONAL CHANGES OF THE FIELD VALUE AT NIGHT. Fatkullin, M. N.; Feldstein, I. I. Geomagn. Aeronomiya, 5: 735-9 (July-Aug. 1965). (In Russian).

The cyclic variation (N_c) of the elements of the geomagnetic field in magneto-quiet days during three seasons of the IGY was investigated. The variability of the night levels composing the magnetic fields was discussed. (tr-auth)

4739 SOME PECULIARITIES OF GEOMAGNETIC VARIATIONS IN THE POLAR REGIONS. Mansurov, S. M.; Mansurova, L. G. Geomagn. Aeronomiya, 5: 740-4(July-Aug. 1965). (In Russian).

From data of high altitude stations of the southern hemisphere for the period of the IGY-IQSY, it was determined that the geographic distribution of the diurnal variations of the magnetic field in the international calm day (S_q) becomes significantly simpler if the field S_q is introduced in some effective system, the pole of which is inclined between geomagnetic poles and poles of the inclination. Also the effective discrepancy at amplitudes S_q at some high amplitude stations remain and these can be specified with the field of some supplementary zonal systems of the current. The question of the origin of the zonal currents was discussed. (tr-auth)

4740 THE LATITUDE OF AURORAL ACTIVITY DURING PERIODS OF ZERO AND VERY WEAK MAGNETIC DISTURBANCE. Stringer, W. J.; Belon, A. E.; Akasofu, s.-I. (Univ. of Alaska, College). J. Atmos. Terrest. Phys., 27: 1039-44(Oct. 1965).

It is shown that when there is complete magnetic calm in the dark sector, so that both K_p and the local K-indices are zero, the dipole (dp) latitude of auroral activity is above 74°. However, when even a very weak magnetic disturbance occurs, causing the local K to rise to the value 1 (even if K_p is still zero), the midnight auroral dp latitude abruptly decreases nearly to 67.5°, that of the statistical auroral zone. Characteristics of the aurora in the above two conditions are, however, different in several ways. (auth)

4741 ABNORMAL BEHAVIOR OF f_0F2 AT HUANCAYO IN MAGNETICALLY ACTIVE PERIODS OF IGY-IGC. Rastogi, R. G.; Rajaram, G. (Physical Research Lab., Ahmedabad, India). J. Atmos. Terrest. Phys., 27: 1097-1103(Oct. 1965).

The way in which f_0F2 near noon varies with magnetic activity at different epochs of solar activity is studied. In the American Zone, the normal equatorial increase in noon f_0F2 for disturbed days is replaced by a decrease in f_0F2 during the December solstice (local summer) of years with large solar and magnetic activity. (auth)

4742 A CLASSIFICATION OF THE DAILY GEOMAGNETIC VARIATIONS. Maeda, Hiroshi (High Altitude Observatory, Boulder, Colo.). J. Atmos. Terrest. Phys., 27: 1116-18(Oct. 1965).

A classification system together with symbols of the solar and lunar daily geomagnetic variations is proposed. (L.B.S.)

4743 A STATISTICAL METHOD FOR QUANTITATIVE ANALYSIS OF GEOMAGNETIC GIANT PULSATIONS. Paulson, K. V. (Kiruna Geophysical Observatory, Sweden);

Egeland, A.; Eleman, F. J. Atmospheric Terrest. Phys., 27: 943-67(Aug. 1965).

A method for quantitative analysis of geomagnetic giant pulsations is described in some detail since it was not used in previous geomagnetic investigations. This method gives a quantitative measure of the type and degree of polarization as well as the principal directions of the resultant vectors in each of three orthogonal planes. All giant pulsations recorded at the Kiruna Geophysical Observatory ($\phi = 67.8°N$, $\lambda = 20.4°E$) during 1963 were analyzed by this method. The phase differences between each orthogonal component were evaluated from crosscorrelation functions, while the mean period and bandwidth of the variations in each component were determined from autocorrelation functions. The principal results of the analysis of these giant pulsations can be summarized as follows: A high degree of polarization exists. The pulsations are confined to a very narrow frequency-band. The orientation of the mean vector in the horizontal plane is remarkably constant; the orientation of the mean vector in the magnetic meridian displays a considerable variation. The variance of the Z-component is of the same magnitude as the variances of either of the horizontal components. From the last result, it is concluded that any physical explanation of the phenomenon is inadequate if it is based solely on the field-line propagation of transverse hydromagnetic waves. (auth)

4744 SHOCK WAVES IN THE SOLAR WIND AND GEOMAGNETIC STORMS. Sturrock, P. A.; Spreiter, J. R. (Ames Research Center, Moffett Field, Calif.). J. Geophys. Res., 70: 5345-51(Nov. 1, 1965).

Certain geomagnetic storms exhibit, in addition to the usual initial sudden positive impulse, a subsequent sudden negative impulse. The former is normally ascribed to a shock wave in the interplanetary medium, and it was recently suggested that the latter may be ascribed to a reverse shock convected away from the sun by the solar wind. If the velocity of efflux of gas from a source is supersonic (with respect to the source), if the velocity is instantaneously increased, and if certain subsidiary conditions are met, a pair of shock waves will be produced which propagate away from the source. The 'fast' shock propagates away from the contact surface in the ambient gas (which was ejected from the source before the change in efflux velocity); the 'slow' shock propagates away from the contact surface in the driver gas but has an outward velocity when this velocity is measured relative to the source. This problem (which may be identified with a classical problem considered by Riemann) is discussed in its relation to the production of pairs of shock waves by the enhanced solar wind produced by a solar flare. The equations giving the relationship between the velocities of the shock waves and those of the ambient and driver gases become very simple in the strong-shock approximation. It is shown that the propagation times of the positive and negative impulses of the July 11, 1959, magnetic storm may be explained satisfactorily on the basis of this theory. (auth)

4745 RECURRENT GEOMAGNETIC STORMS AND THE SOLAR WIND. Hirshberg, Joan (Ames Research Center, Moffett Field, Calif.). J. Geophys. Res., 70: 5353-9(Nov. 1, 1965).

The structure that would be expected to develop when a fast stream in the solar wind is embedded in a slower ambient wind is discussed on the basis of gas dynamics. This structure is compared with that appearing in recurrent geomagnetic storms. It is found that the development of M-region storms follows the expected structure of the solar-wind stream. The sudden commencements on some M storms correspond to the shock that is expected to occur in the solar wind if the relative velocities of the fast stream face and the ambient wind are high enough. It is also shown that the typical quiet initial phase of the sudden commencement M storm corresponds to the relatively low-velocity region in space between the shock and the stream proper. The main phase corresponds to the high-velocity stream itself. In particular the fast M streams detected by Mariner 2 and their associated geomagnetic storms are discussed. (auth)

4746 ELECTRON-DENSITY VARIATIONS AT 1000 KILOMETERS. Dayharsh, Thomas I.; Farley IV, William W. (Stanford Research Inst., Menlo Park, Calif.). J. Geophys. Res., 70: 5361-8(Nov. 1, 1965).

Data gathered at Stanford University from the Alouette satellite were separated into seasonal, diurnal, and magnetic-activity groups. Two fundamental tests of statistical significance, the χ^2 test (testing the significance of the differences in the average distributions of the groups) and an analysis of variances (testing the relative variability of the groups), were applied to the data. Both tests indicated that separation of the data into the aforementioned groups was valid. Three phenomena are discussed: a significant depression of electron density at auroral latitudes under magnetically disturbed conditions, an apparent electron-density depletion over magnetic shells with a large range of L values on disturbed summer days, and a large nighttime trough centered about L = 4. (auth)

4747 GYRORESONANCE RADIATION PRODUCED BY PROTON AND ELECTRON BEAMS IN DIFFERENT REGIONS OF THE MAGNETOSPHERE. Gendrin, R. (Centre National d'Etudes des Telecommunications, Issy-les-Moulineaux, France). J. Geophys. Res., 70: 5369-83 (Nov. 1, 1965).

The gyroresonant interaction of an electron or proton beam with electromagnetic waves is studied at frequencies below the electron gyrofrequency ω_B. Attention is drawn to the two cases of double roots that occur in the equation giving the emitted frequencies for a proton beam interacting with a whistler wave (p, R interaction). The emitted frequencies are very near to half the electron gyrofrequency ($\omega_B/2$) and twice the proton gyrofrequency ($2\Omega_B$). Three preferred regions of interaction exist in the magnetosphere, one in the equatorial plane and two at low altitudes (<1200 km). It is suggested that the 'high' frequency radiation ($\omega \simeq \omega_B/2$) is part of the explanation of the enhanced radio noise recently observed near 0.7 Mc by spaceborne equipment. Assuming mean values for the ionospheric parameters, calculations are made of the emitted frequency, altitude of emission, and energy of the interacting particles, for two different latitudes. The possibility of reflection of both waves and particles near the ends of the magnetic lines of force is taken into account, and the results are shown to be quite different from those for the homogeneous case. Amplification coefficients for the two double roots ($\omega \simeq \omega_B/2$, $\omega \simeq 2\Omega_B$) and for asymptotic cases ($\omega \sim \omega_B$, $\omega \sim 0$) are calculated, and comparisons are made with the (e, L) interaction (electrons and left-hand wave). It is shown that, for interactions over some finite length l_c, protons are more efficient than electrons, and that the maximum amplification does not depend on the plasma parameters but only on the beam density n. Its value, $1.8 \times 10^{-3} n^{1/4} l_c$, in MKSA, is of the order of 5 db for realistic assumptions concerning n and l_c. (auth)

4748 AVERAGE EFFECT OF THE ATMOSPHERE ON TRAPPED PROTONS. Hassitt, A. (Univ. of California, San Diego, La Jolla). J. Geophys. Res., 70: 5385-94 (Nov. 1, 1965).

An efficient method of computing the average atmosphere encountered by particles trapped in the earth's magnetic field is described. An average height is defined. It is shown that this height is a slowly varying function of L (the magnetic shell parameter), B_m (the magnetic field at the mirror point), and μ (the inverse of the scale height). Coefficients for low-order-polynomial fits to the average height are given. Some models of the atmosphere are compared with measurements of trapped proton fluxes. (auth)

4749 EQUATORIAL GEOMAGNETIC ANOMALY AND ITS ASSOCIATED CURRENT SYSTEM. Goldberg, Richard A. (Goddard Space Flight Center, Greenbelt, Md.). J. Geophys. Res., 70: 5417-24(Nov. 1, 1965).

From a detailed study of the momentum transport equation for charged gaseous fluids moving through a neutral

gas, it is suggested that the equatorial F-region electron density distribution (the geomagnetic anomaly) is simply the natural steady-state distribution one would expect for charged fluids under the influence of gravitational, electric, and magnetic fields and production and loss, when interaction with the neutral medium is negligible. It is shown that this steady-state distribution maintains itself by means of a longitudinal current system, and a study of the properties of this longitudinal current system leads to a technique for its complete mapping in the upper F region of the ionosphere. Quite importantly, it is shown that the latitudinal electron-density distribution that characterizes the equatorial anomaly cannot exist when the longitudinal current system is absent. The study of the longitudinal current system also demonstrates the possibility of large errors in temperature calculations that utilize vertical density slope measurements to determine scale height, and a technique is suggested to correct such calculations. Finally, using cited measurements for support, it is possible to suggest the mechanisms responsible for the diurnal and asymmetric behavior of the anomaly. (auth)

4750 GEOMAGNETIC AND SOLAR DATA. Lincoln, J. Virginia, [ed.]. (National Bureau of Standards, Boulder, Colo). J. Geophys. Res., 70: 5447-9(Nov. 1, 1965).

Geomagnetic and solar data are presented for 1965. Sudden commencements, activity, and ranges are given. Geomagnetic and solar data are also presented for June 1965. Three-hour range indices are given. (J.F.P.)

4751 A 75-SECOND PERIODICITY IN AURORAL-ZONE X RAYS. Barcus, J. R.; Christensen, A. (Univ. of California, Berkeley). J. Geophys. Res., 70: 5455-9 (Nov. 1, 1965).

Further observations of an unusual set of auroral-zone x-ray pulsations are presented. Although the event is of smaller intensity, it is remarkable for a degree of spectral purity that is very high in comparison with previous results. The pulsations were encountered during a high-altitude balloon flight at 64.8° geographic latitude, 147.8° geographic longitude, at 0330 UT on June 20, 1964. Bremsstrahlung x rays of energy greater than 25 kev were detected by means of an NaI scintillator. The pulsations of interest occurred around 1600 UT, after the major precipitation activity. The pulsating character of the radiation over the interval 1545 to 1610 UT is shown. Though the amplitude of the variations is only less than 30% of the excess above cosmic-ray background, the repetitive nature is clearly evident. The distribution in temporal separation between 18 consecutive major pulsations is also shown. It indicates a most probable separation of about 75 seconds, which is in excellent agreement with the average value. An autocovariance and spectral analysis was also performed, and these results are shown. Possible sources of the pulsations are considered. (J.F.P.)

4752 TERRESTRIAL ALBEDO OF THE 40- TO 190-kev X RAYS. Brini, D.; Ciriegi, U.; Fuligni, F.; Gandolfi, A.; Moretti, E. (Bologna Univ., Italy). J. Geophys. Res., 70: 5460-3(Nov. 1, 1965).

The terrestrial albedo of the x rays of 40 to 200 kev was studied. The possibility of obtaining information about the degree of isotropy of x-ray production in the atmosphere by cosmic radiation was also considered. The detector consisted of a NaI(Tl) crystal on the bottom of a lead cylinder surrounded by a plastic scintillator. By extrapolating the data, the resulting vertical albedo intensity can be evaluated in the entire energy range from 40 to 190 kev. Since no substantial variations of the ratios with pressure and with orientation of the x-ray telescopes can be observed, the spectrum of the detected x rays may be considered independent both of pressure, in the interval 10–70 g/cm^3, and independent of the two directions of the x-ray emission. It is concluded that the results obtained with the omnidirectional detectors give upper limits of the albedo flux. (J.F.P.)

4753 PHOTOELECTRON ENERGY DISTRIBUTION IN THE F REGION. Hoegy, Walter R.; Fournier, Jean-Pierre; Fontheim, Ernest G. (Univ. of Michigan, Ann Arbor). J. Geophys. Res., 70: 5464-8(Nov. 1, 1965).

The results of computation of the photoelectron contribution to the high energy tail of the electron distribution in the ionosphere are presented. The photoelectrons are considered to be test particles, which are affected by the ambient particles, but which themselves do not alter the ambient distribution. When the initial energy of the photoelectrons is much higher than the average energy of the ambient electrons, it is possible to distinguish the photoelectron from the ambient electron. In that case the test particle assumption is valid and the high-energy distribution can be considered equal to the photoelectron distribution plus a Maxwellian distribution. Curves are drawn for the results obtained, and a discussion of them is given. (J.F.P.)

4754 THE ELECTRON DISTRIBUTION IN THE QUIET D-REGION DERIVED FROM ROCKET MEASUREMENTS OF LOW-FREQUENCY PROPAGATION. Hall, J. E.; Fooks, Jean (S.R.C. Radio and Space Research Station, Slough, Bucks., Eng.). Planet. Space Sci., 13: 1013-30(Nov. 1965).

The results of a 202 kc/s radio propagation experiment to determine the distribution of electron concentration in the D-region are presented. A transmitter on the ground was used to generate a wavefield in the lower ionosphere which was explored by means of a rocket carrying three orthogonal receiving aerials. The wavefield configurations for a series of model ionospheres were calculated using a full-wavefield theory and compared with the measured wavefield. The model producing the best fit was taken to represent the ionosphere at the time of the experiment. Results are presented for two rockets launched in quiet solar conditions; one in the daytime and one at night. (auth)

4755 IONOSPHERIC BACKSCATTER OBSERVATIONS AT MILLSTONE HILL. Evans, J. V. (Massachusetts Inst. of Tech., Lexington). Planet. Space Sci., 13: 1031-74(Nov. 1965).

Studies of the electron density, electron and ion temperatures in the F-region were made by means of ground-based radar observations at the Millstone Hill radar observatory. A 70 m parabolic antenna directed vertically and a 2.5 Mw pulse radar operating at 440 Mc/s were employed for the measurements which were conducted for periods of 30 hr at approximately weekly intervals. The results of observations extending over a period of one year from 1963 to 1964 are presented. The diurnal and seasonal variations of the density, electron and ion temperatures are discussed in some detail. It was found that the ratio T_e/T_i achieved a maximum value ~ 2.0–2.6 at a height of about 300 km soon after dawn irrespective of the season. There was little change in the height dependence in this ratio throughout the daylight hours, and at sunset the ratio fell with a time constant of the order of an hour. At night T_e/T_i was on occasion close to unity, but more often there remained a significant difference in the temperatures at all heights. The ion temperature was found to increase with height at all times, but at night above 500 km this may be due in part to the presence of an unknown amount of He^+ ions which considerably affects the interpretation of the signal spectra. The electron temperatures were largely independent of height above about 300 km. Evidence is presented of ionospheric heating during magnetically disturbed conditions, but it is shown that this is only of great importance at night. The results for the electron temperature are compared with results obtained using the Explorer VIII, Explorer XVII and Ariel satellites. Good agreement is obtained with the Explorer XVII results and it appears that the Ariel values are underestimates. (auth)

4756 THE INFLUENCE OF GEOMAGNETIC ACTIVITY ON POLAR CAP ABSORPTION. Leinbach, H. (Univ. of Iowa, Iowa City); Venkatesan, D.; Parthasarathy, R. Planet. Space Sci., 13: 1075-95(Nov. 1965).

Several polar cap absorption events, for which simultaneous riometer data exist for Thule, Greenland, and College, Alaska, are examined in detail in order to make a careful comparison of the ratio of absorption at the two

stations. In addition, comparison with other stations both to the south and north of College is made. It is verified that one can divide the polar cap into two regions. In the first, including latitudes to the north of geomagnetic 65° (L = 5.5), the progress of the PCA event is dominated by the time variations of the solar particle flux, and is essentially independent of the geomagnetic field variations. The ratio of absorption College/Thule is usually found to be 0.8 or greater throughout the event. In the second zone, extending from geomagnetic latitudes of about 64° down to about 55°, the characteristics of the PCA are largely dominated by the influence of the geomagnetic field. It is shown that at L = 4.3, the pre-magnetic storm value of the ratio Farewell/Thule is about 0.14. However, during the magnetic storm, the ratio tends to approach unity. At King Salmon (L = 3.3) it is seldom possible to identify PCA prior to the magnetic storm, although the post-storm value of the ratio King Salmon/Thule may approach unity for sufficiently large magnetic storms (maximum D_{st} > 200 γ). The results are compared with satellite studies of the solar particles and with the theoretical calculations of the absorption expected from protons with given exponential rigidity spectra. These results lead to the deduction of an effective cutoff at College of the order of 30 Mev or less, as has been observed directly by satellites in a small number of events. The magnetic activity is characterized by D_{st}. It is found that, in the second zone of PCA activity (the outer ring), the prestorm cutoffs are apparently restored at a greater D_{st} value than that corresponding to onset of the cutoff reduction at the beginning of the storm. The effect may be interpreted in terms of a progressive softening of the proton spectrum as the event progresses. (auth)

4757 SOME MORPHOLOGICAL ASPECTS OF GEOMAGNETIC SECULAR VARIATION. Slaucitajs, L.; Winch, D. E. (Univ. of Sydney). Planet. Space Sci., 13: 1097-1110(Nov. 1965).

Analysis of geomagnetic secular variation data, in the three elements X, Y and Z at five observatories distributed over the Earth, shows that amplitudes obtained for a 50 year cycle by harmonic analysis are highly significant. Amplitudes of higher order harmonics are found to be either not as significant or not significant, indeed, the cycle can be seen directly on the graphs of observational data. These results are confirmed by power spectrum analysis. Using phase angles obtained for the 50 year (semicentennial) cycle from different stretches of data, an improved value for the period is found to be 61 ± 6 years. The approximate semicentennial values are interesting in view of the theoretical possibility of an oscillation of an S_2^0 field of period 77 years superimposed on the main field. (auth)

4758 RECURRENT SI^+-SI^- IMPULSE PAIRS AND SHOCK STRUCTURE IN M-REGION BEAMS. Razdan, H.; Colburn, D. S.; Sonett, C. P. (Ames Research Center, Moffett Field, Calif.). Planet. Space Sci., 13: 1111-23 (Nov. 1965).

The worldwide positive-negative ($SI^+ - SI^-$) impulse pair observed on geomagnetic records is found in several instances to be recurrent and associated with M-region disturbances. From this is deduced an extension of the model where an interplanetary shock ensemble consisting of a forward and reverse pointing shock strongly convected outward in the solar wind was postulated as the source of the $SI^+ - SI^-$ pair. It is shown that the same general shock ensemble can be invoked but with the shocks highly oblique to the wind streaming direction. A narrower choice of mechanisms for the production of the impulse pair appears possible for the recurrent phenomenon than in the instance of the pair associated with a solar flare. The observed separation between the shocks is small compared to the total beam width, and the pair is expected to bracket the leading edge of the beam. The model considered has many similarities to that proposed by Dessler and Fejer. (auth)

4759 LOSS OF He^+ IONS IN THE UPPER ATMOSPHERE. Stebbings, R. E.; Rutherford, J. A.; Turner, B. R. (General Atomic Div., General Dynamics Corp., San Diego, Calif.). Planet. Space Sci., 13: 1125-9(Nov. 1965).

Charge transfer between He^+ ions and molecules of nitrogen and oxygen was investigated in a crossed beam experiment within the energy range 3 to 600 ev. Interpolation between these data and the 300°K results of afterglow measurements is made to provide cross sections for these processes at collision energies pertinent to the Earth's upper atmosphere. The results so obtained are in marked disagreement with those inferred from atmospheric data. (auth)

4760 RECENT STUDIES OF THE IONOSPHERE BY SPACE VEHICLES. Boyd, R. L. F. (Univ. of London). Proc. Roy. Inst. G. Brit., 40: 129-42(1964).

Measurements made by the satellites Ariel I and Alouette are considered: mass spectrum of the ions and temperature of the electrons by instruments carried on Ariel, and measurement of electron concentration by the method of topside sounding employed on Alouette. A diagram shows the concentration of the various ions obtained in terms of relative composition over the surface of the globe. Concentration of oxygen ions is given as a percentage of the mixture of oxygen and helium ions occurring at 1000-km altitude and is plotted as contours of constant composition. The data reveal features which show the important part played by the earth's magnetic field, or which demonstrate that the energy to maintain the electrons at a higher temperature than the ambient gas comes primarily from solar electromagnetic radiation during the day but that fast charged particles, produced within the atmosphere and possibly also coming from without, also play a part in keeping the electron gas warm. As seen with positive ions, so even more for the electrons the temperature rises from the equator toward the poles. It is shown that the amount by which the electron temperature exceeds the ion temperature increases with latitude and hence explains, in part at least, the rising temperature with latitude. The various parameters of the topside ionosphere, such as electron temperature, ion temperature, ion mass spectrum and electron concentration are closely connected. Certain unsuspected enhancements of ionization associated in a regular way with the earth's magnetic field were discovered. The data indicate that ionospheric electrons are trapped by the earth's magnetic field in a manner similar to the way in which the much more energetic particles of the Van Allen belts are trapped. (TCO)

4761 AN INVESTIGATION OF IONOSPHERE-PROTONSPHERE COUPLING [Thesis]. Geisler, John Edmund. Urbana, Ill., Univ. of Illinois, 1965. 265p.

The physical processes that govern the distribution and thermal state of the ionization in the F2-layer of the ionosphere and in the protonosphere are discussed in detail. Calculations of the rate of exchange of ionization and of thermal energy between these two regions are presented. Effects of this exchange on the distribution and the thermal state of the ionization in both regions are described. The investigation begins with a calculation of the relation between the whistler dispersion, the temperature of the protonosphere, and the ionization content of a protonospheric field tube. A steady-state model of the F2-layer is set up in order to obtain an estimate of the magnitude of the flow of ionization into or out of the topside of the layer that is required to produce a significant effect on the structure of the layer. This is followed by a study of the processes that account for this flow of ionization. The solution of a form of the steady-state continuity equation for ionized hydrogen is obtained, and it is shown that a flow of ionization sufficient to affect the structure of the daytime F2-layer cannot be maintained by diffusive transport of hydrogen ions. The solution of the continuity equation for ionized hydrogen is then combined with the observed diurnal variation of electron density at the F2-layer maximum to formulate a steady-state model describing the diurnal exchange of ionization between the F2-layer and the protonosphere. The processes that heat and cool the ionosphere are discussed in detail. An expression is derived

for the rate of heat input to the topside ionosphere, which includes the contribution from photoelectrons that originate at and below the F2-layer maximum. Daytime electron and ion temperatures are obtained over the altitude range between 120 and 1000 km from solutions of the steady-state heat conduction equation. The theory developed for the rate of heat input to the topside ionosphere is extended to derive the rate of heat input to the ionization contained within a protonospheric field tube by photoelectrons which originate at F2-layer heights. The temperature profile along the length of the field tube is calculated. Nighttime electron and ion temperature profiles are derived under the assumption that thermal energy stored in the protonosphere is the only source of heat input to the nighttime ionosphere. (Dissertation Abstr.)

Gravitation, Quantum Mechanics, and Relativity Theory

Refer also to abstracts 4619, 4699, and 4712.

4762 OPERATOR GAUGE TRANSFORMATIONS. Corinaldesi, E.; Roman, P. (Boston Univ.). Amer. J. Phys., 33: 939-42(Nov. 1965).

The Gupta-Bleuler formulation of the subsidiary condition of quantum electrodynamics in the interaction picture is reviewed. This formalism is used to construct a simple proof of the invariance of the S-matrix under q-number gauge transformations $A'_\mu = A_\mu + \partial_\mu F(\Box)\partial^\nu A$ or, equivalently, under certain well-known modifications of the photon propagator. (auth)

4763 NEUTRINOS AND PURE SINGULAR FIELDS OF SPIN 1 AND OF SPIN 2. Moret-Bailly, Francoise (Univ. Paris, Dijon, France). Compt. Rend., 261: 1607-9(Aug. 18, 1965). (In French).

A tensor field $H_{\alpha\beta,\lambda\mu}$ having the properties of a pure gravitational field is constructed from 2 pure singular electromagnetic fields or from 4 spinor fields describing the neutrinos. (tr-auth)

4764 ON AN ITERATIVE METHOD OF RESOLUTION OF CERTAIN INTEGRAL EQUATIONS. Guy, Jean; Sales, Andre; Joly-Cabaret, Francoise (Laboratoire des Recherches Physique, Sorbonne, France). J. Phys. (Paris), 26: 335-8(June 1965). (In French).

Equations of the form $\Delta U = f(M) + g(M) \cdot U(M)$ appear frequently in physics (especially in perturbation problems). These equations can be changed into integral equations of Fredholm type, when limit-conditions are given. Unfortunately, the Liouville-Neumann series solutions of these integral equations, are often divergent. In order to find the desired solutions, a more general iterative process is established. It is possible by this method to set up convergent sequences, after a suitable choice of some a priori arbitrary functions, introduced in the analytical formulation. (auth)

4765 INFRARED DIVERGENCE IN QUANTUM ELECTRODYNAMICS. Chung, Victor (Univ. of California, Berkeley). Phys. Rev., 140: B1110-22(Nov. 22, 1965). (UCRL-16202).

The infrared divergences of quantum electrodynamics are eliminated to all orders of perturbation theory in the matrix elements by an appropriate choice of initial and final soft photon states. The condition for this cancellation restricts these states to representations of the canonical commutation rules which are unitarily inequivalent to the usual Fock representation. (auth)

4766 QUALITATIVE ASPECTS OF THE N-BODY PROBLEM FOR APPROXIMATELY RELATIVISTIC EQUATIONS OF MOTION. Hoffman, Richard B.; Havas, Peter (Lehigh Univ., Bethlehem, Pa.). Phys. Rev., 140: B1162-73(Nov. 22, 1965).

Following the pioneering work of Jacobi, numerous qualitative results were obtained for dynamical systems, especially on the asymptotic time development of such systems. All these studies were based on Newtonian concepts and the basic equations treated as mathematically exact, whereas even within classical theory they only represent approximations to relativistic equations. The question of generalizing known Newtonian theorems is investigated for the N-body problem on the basis of the Einstein-Infeld-Hoffmann (EIH), Coulomb, and Darwin approximate equations of motion. Proofs of two theorems are given in a manner pointing the way to further generalization in higher order approximations. Two additional theorems are considered for the EIH case utilizing the method of continuous induction; the reason for the failure to prove one of them is discussed, as is the question of whether some Newtonian results are invalidated if the basic equations cannot be considered as exact. A number of theorems previously proved for general dynamical systems are shown to hold for the three cases considered before as well as for the canonical formalism of special-relativistic particle interactions, and some limitations of the applicability of such results are discussed. (auth)

4767 SINGULARITIES IN BOOTSTRAP GRAVITATIONAL GEONS. Brans, Carl H. (Loyola Univ., New Orleans). Phys. Rev., 140: B1174-?(Nov. 22, 1965).

The solution to the empty-space, time-symmetric Einstein initial-value problem recently given by Komar as representing a bootstrap gravitational geon is shown to display singular behavior along portions of an axis in the regions in which the solution deviates from the standard Schwarzschild solution. This difficulty is in addition to the problems explicitly studied by Komar related to the jumps in the derivatives of the metric and seems to correspond more closely to the essential, delta-function type of singularity in the Schwarzschild solution at the origin. A direct analysis in terms of Cartesian coordinates seems to cast doubt on the likelihood that Komar's metric is even C^0 in any topologically trivial manifold. (auth)

4768 EQUATIONS OF MOTION WITHOUT INFINITE SELF-ACTION TERMS IN GENERAL RELATIVITY. Carmeli, Moshe (Temple Univ., Philadelphia). Phys. Rev., 140: B1441-4(Dec. 6, 1965).

The role of the Bianchi identity in obtaining the equations of motion in general relativity is further discussed in connection with the problem of the infinite self-action terms. It is shown that because of this identity and under certain assumptions (concerning the type of singularity of the Christoffel symbols near the particle), there is a possibility of obtaining an equation of motion, free of infinite self-action terms, without referring to any renormalization procedure. This is the Infeld equation of motion which describes the motion of a particle of finite mass and in which the time coordinate is taken to be the independent parameter. Besides that, however, the Bianchi identity imposes certain constraints that the field functions have to satisfy in addition to the equation of motion. (auth)

4769 OLD AND NEW FASHIONS IN FIELD THEORY. Dyson, Freeman J. (Univ. of California, San Diego). Phys. Today, 18: 21-4(June 1965).

The history of quantum electrodynamics is briefly reviewed in the sense that during the period from 1949 to the present the history has repeated that of gravitation theory developed thirty years earlier. The view on the field theory and S-matrix theory approaches are discussed. Two important achievements are mentioned to point out the relevance of quantum electrodynamics to particle physics, namely, Dashen's explanation of the mass difference between the neutron and proton, and the experiment on wide-angle pair production carried out at the Harvard–MIT accelerator. (L.B.S.)

4770 CRITIQUE OF A NEW THEORY OF GRAVITATION. Deser, S. (Brandeis Univ., Waltham, Mass.); Pirani, F. A. E. Proc. Roy. Soc. (London), Ser. A, 288: 133-45(Oct. 5, 1965).

Hoyle and Narlikar (1964d) have developed a new theory

of gravitation, for which they claim that it is a direct interparticle theory, that it "is equivalent to that of Einstein in the description of macroscopic phenomena, and hence the situation is the same so far as the classical tests of general relativity are concerned," that the sign of the gravitational constant is correctly determined, and that it has other advantages over Einstein's theory such as implying the absence of solutions representing an empty universe. It is shown that these claims are largely unsubstantiated. (auth)

4771 THE GRAVITATION THEORY OF HOYLE AND NARLIKAR. Majumdar, S. Datta (Indian Inst. of Tech., Kharagpur); Banerji, Skriranjan. Sci. Cult. (Calcutta), 31: 331-4(July 1965).

The development of gravitation theory is briefly reviewed. The Hoyle-Narlikar theory is outlined, and its departures from the Einstein theory are pointed out. The cosmological models associated with these theories are also considered. (D.C.W.)

4772 SOME ASPECTS OF THE LIQUID HELIUM PROBLEM. Parry, W. E. (Oriel Coll., Oxford). pp 190-224 of Lectures in Theoretical Physics. Vol. VI. Boulder, Colo., The University of Colorado Press, 1964.

The present state of the theory of liquid helium is described, and a direction for future research is suggested. The emphasis is placed on numerical results, although an introduction is given to some of the formal techniques employed. Topics considered include experimental properties of liquid helium, the Bogoliubov prescription, the use of Green functions, approximate calculations for the self-energy parts, spectral functions and sum rules, further approximate results, and coordinate space considerations. (J.F.P.)

Low Temperature Physics

Refer also to abstracts 4417 and 4426.

4773 (COO-1198-306) PROPERTIES OF ^{3}He AT LOW TEMPERATURES. Wheatley, John C. (Illinois Univ., Urbana). [1965]. Contract AT(11-1)-1198. 96p. (CONF-651030-2). Dep. mn; CFSTI $3.00 cy, $0.75 mn.

From German Physical Society, Annual Meeting, Frankfurt, Ger.

An extensive survey of the low temperature properties of liquid ^{3}He was made. Experiments were performed to measure at low temperatures the heat capacity, the magnetic susceptibility and self-diffusion coefficient, the velocity and attenuation of sound, the thermal conductivity, and the transfer of energy across the surface between a solid and liquid ^{3}He. Superfluidity in ^{3}He is also discussed. (M.O.W.)

4774 (IS-T-22) THE SUPERCONDUCTING PROPERTIES OF HIGH PURITY NIOBIUM [Thesis]. Stromberg, Thorsten Fredrick (Ames Lab., Iowa State Univ. of Science and Tech.). July 1965. Contract W-7405-eng-82. 107p. Dep. mn; CFSTI $4.00 cy, $0.75 mn.

The superconducting properties of high purity niobium were investigated throughout the temperature range from 1.1°K to the transition temperature at 9.25°K. The results of these measurements show that niobium exhibits a reversible, but broad magnetic transition like that found in type-II superconductors. Analysis of the niobium data shows that H_c, the thermodynamic critical field, is linear in T^2 to one percent with $T_c = 9.25$°K and $H_0 = 1990$ gauss. The free energy shows approximate agreement with the BCS prediction. From low temperature H_c data a value for γ, the normal state electronic specific heat coefficient, is found to be 1.80×10^{-3} cal/mole°K^2. The temperature dependence of H_{c1} follows the function $H_{c1}(t) = 1735(1 - t^{2.14})$ to 1%. The magnetic moment in the region near H_{c1} is a continuous function of applied field with a slope ten times smaller than the demagnetizing slope. Consequently, the transition is of second order. H_{c2} fits a function of the following form: $H_{c2}(t) = (1 - t^2/1 + t^2)$ to 5%. The GLAG theory of superconductivity predicts a temperature dependence at $T = 0$ for H_{c2} which is 30% smaller than the measured values. Presumably this discrepancy is due to the fact that niobium does not satisfy the locality condition ($\xi_0 \ll \lambda$) required by the GLAG theory. Only in a very restricted temperature range near T_c, where the locality condition can be satisfied, is there any agreement with theory. (auth)

4775 (UCRL-16376) AN INORGANICALLY INSULATED SUPERCONDUCTING SOLENOID FOR OPERATION AT 1 deg K. Hintz, R. E. (Lawrence Radiation Lab., Univ. of California, Berkeley); Laverick, C. (Argonne National Lab., Ill.). Aug. 30, 1965. Contract W-7405-eng-48. 9p. (CONF-650922-20). Dep. mn; CFSTI $1.00 cy, $0.50 mn.

From 1st International Symposium on Magnet Technology, Stanford, Calif.

An inorganically insulated 30-kG 2-in.-bore Nb-25% Zr solenoid for operation at 1°K is described. The thickness of the copper plating and the thermal environment prevented serious current degradation at 1°K. The insulation was sufficient to allow for a high charge rate with low heat input to the 1°K bath. (auth)

4776 CONSTRUCTION AND OPERATION OF A ^{3}He REFRIGERATOR. Quadros, Carlos; de Oliveira, Nei F. Jr. (Universidade de Sao Paulo, Brazil). Anais Acad. Brasil. Cienc., 36: 403-6(1964).

A ^{3}He refrigerator was built that can run for a long time with a small loss of liquid ^{4}He. The refrigerator is built inside a vacuum chamber kept at 4°K by a surrounding liquid ^{4}He bath at atmospheric pressure. The ^{3}He is condensed by liquid ^{4}He in a small reservoir inside the chamber where the pressure can be lowered by a mechanical pump. (auth)

4777 FLUXOID STRUCTURE IN SUPERCONDUCTING FILMS. Maki, Kazumi (Univ. of Chicago). Ann. Phys., (N.Y.), 34: 363-76(Oct. 6, 1965). (COO-264-238).

In the framework of the Ginzburg-Landau theory a detailed study was made of the fluxoid structure in a superconducting film in the presence of a perpendicular magnetic field. It is established that the fluxoid structure is a stable solution of the Ginzburg-Landau equations if the film thickness d is sufficiently smaller than λ the penetration depth independently of κ the Ginzburg-Landau parameter. The explicit expressions of the free energy as well as the magnetic induction are obtained at some limiting cases. (auth)

4778 TOPOLOGY OF THE STRUCTURE OF INTERMEDIATE STATES OF SUPERCONDUCTORS OF TYPE I AND MEASUREMENTS OF SURFACE ENERGY. Haenssler, Fr.; Rinderer, L. (Univ., Lausanne, Switzerland). Helv. Phys. Acta, 38: 448-54(1965). (In French).

The intermediate state in circular indium disks placed in a perpendicular magnetic field was made visible by the superconducting powder technique. A fundamental topological difference is observed between the structure resulting from the different ways of entering the intermediate state. It is shown that only the patterns resulting from normal-intermediate state transitions can be used for determining the surface energy parameter according to the various existing intermediate state models. (auth)

4779 USE OF THE POMERANCHUK EFFECT TO OBTAIN INFRALOW TEMPERATURES. Anufriev, Yu. D. (Vavilov Inst. of Physics Problems, Academy of Sciences, USSR). JETP Lett. (USSR) (Engl. Transl.), 1: 155-7 (June 15, 1965).

For observation of the Pomeranchuk effect an apparatus was developed to reduce the volume in which the helium-3 is contained without releasing any heat, since this solves a problem of adiabatic transfer of pressure to helium-3. The design of this apparatus is described. The operation of the apparatus for the Pomeranchuk effect for infralow temperature attainment is also described. Experiments on the adiabatic crystallization of helium-3 showed that the

Pomeranchuk effect can yield with assurance temperatures of 0.02°K, although the temperature achieved was probably lower than this. (J.F.P.)

4780 THERMAL AND MAGNETIC PROPERTIES OF LIQUID ^{3}He AT LOW PRESSURE AND AT VERY LOW TEMPERATURES. Abel, W. R.; Anderson, A. C.; Black, W. C.; Wheatley, J. C. (Univ. of Illinois, Urbana). Physics, 1: 337-87 (July-Aug. 1965). (COO-1198-252).

A brief review of the experimental and theoretical properties of low pressure liquid ^{3}He as related to this work is given. This is followed by a discussion of the magnetic cooling method as applied to cooling ^{3}He using both nuclear and electronic paramagnetics. A number of possible metals for nuclear cooling are suggested, while cerium magnesium nitrate (CMN) is taken to be the best electronic paramagnetic known for the present purposes. The spin-bath thermal resistance is discussed in both cases. In the case of CMN recent work on the spin-bath resistance, due to a phonon bottleneck, shows it to be remarkably low. This is borne out in the experiments. It is concluded that for temperatures in the millidegree range CMN is the best possibility. A careful discussion is given of the techniques developed for obtaining and maintaining temperature below 0.010°K for many hours in an apparatus of moderate size using superconducting magnets. Details are given of the method of using epoxy resins for producing apparatus for using ^{3}He with application to the measurement of heat capacity and magnetic properties. The method of executing the experiments is presented together with a thermodynamic analysis of the effectiveness of the final cooling process. New measurements of the heat capacity of a mixture of low pressure ^{3}He and CMN are presented down to a magnetic temperature of 0.004°K. No anomalous results are obtained. The experimental technique is analyzed and criticized. The results are compared with earlier data. The limiting value of C/nRT still cannot be precisely assessed but seems to be in the range 3.0 to 3.2°K^{-1}. Detailed comparison is made of the present work with that of Peshkov, whose results are interpreted in terms of an experimental effect. The thermal boundary resistance from epoxy walls to ^{3}He compares favorably with previous work. Measurements by the spin-echo method of the self-diffusion coefficient, D, and the susceptibility, χ, of the ^{3}He are presented down to a temperature of 0.0035°K. No anomalous behavior is observed. D obeys the law $D = 1.36 \times 10^{-6}$ T°$^{-2}$cm^2°K^{2}sec^{-1} to below 0.005°K. If an experimental effect is corrected for, χ appears to be temperature independent. Assuming that D defines the Kelvin temperature by $T \propto D^{-\frac{1}{2}}$, the work measures χ vs T without recourse to an auxiliary thermometer. The same assumption leads to the conclusion that the Kelvin and magnetic temperatures differ by only 0.0001°K at 0.0035°K. The ^{3}He spin-lattice relaxation time, measured down to 0.004°K where it is about 2 sec in the present cell, decreases with decreasing T but without a well defined temperature dependence. (auth)

4781 SUPERCONDUCTIVITY IN NONMETALLIC SYSTEMS. Keldysh, L. V. Usp. Fiz. Nauk, 86: 327-33 (June 1965). (In Russian).

The status of research in superconductivity is reviewed with special emphasis on practical applications and the difficulties brought about by the very low temperature required and by the destruction of superconductivity in relatively weak magnetic fields. The main ideas advanced by W. A. Little (Scientific American, 212(2): 21(1965)) are reviewed where the possibility of synthesizing of organic materials capable of conducting electricity without resistance is discussed. The objections to Little's hypothesis both from the point of view of the principles involved and from the point of view of the deductions, are reviewed, particularly the objection that Little's result contradicts the known theorem that a phase transition into an ordered state is impossible in a one-dimensional system such as the hypothetical superconducting molecule proposed by Little. In view of this major objection, the proposal made by Ginzburg and Kirzhnits for effecting surface superconductivity is mentioned. Superconductivity in semiconductors, especially in $SrTiO_3$, which was theoretically first considered by Gurevich, Larkin, and Firsov, and which is free of the main obstacle to superconductivity (Coulomb repulsion of electrons), is also discussed in detail. It is stated in the conclusion that the possibility of obtaining a superconductor with sufficiently high critical temperature (at least on the order of 100°K) is still the major obstacle to be overcome in this research, but there are hopes of obtaining superconductors which differ greatly from ordinary metals. (ATD)

4782 ULTRASONIC ATTENUATION IN SUPERCONDUCTING LEAD [Thesis]. Love, Roy Edward. Troy, N. Y., Rensselaer Polytechnic Inst., 1964. 105p.

The ultrasonic pulse technique was used to measure the absorption of ultra sound in normal and superconducting single crystal lead. Longitudinal sound waves were propagated in the 100, 110, and 111 crystallographic directions at frequencies between 10 and 70 mc. Attempts were made to measure the temperature dependence as well as the anisotropy of the superconducting energy gap. Sufficiently reliable data at low temperatures to do the latter could not be obtained with the present apparatus. However, reliable data at low temperatures to do the latter could not be obtained with the present apparatus. However, reliable values of the temperature dependence of the average energy gap were obtained. The best estimate of the zero temperature energy gap is $2\Delta(0) = (4.1 \pm 2)\ kT_c$. The attenuation was found to be amplitude-dependent in the superconducting state while at the same temperature in the normal state it was amplitude-independent. The empirical nature of the effect and its consequences in relation to determining the energy gap in lead are extensively discussed. The possibility is pointed out that disagreements between energy gap temperature dependencies predicted by BCS theory and those derived from ultrasonic measurements in elements other than lead may be due to this effect. (Dissertation Abstr.)

4783 INSTABILITIES OF THE DOMAIN STRUCTURE IN THE INTERMEDIATE STATE OF SUPERCONDUCTORS [Thesis]. Lalevic, Bogoljub. Philadelphia, Temple Univ., 1964. 203p.

The investigation of the instabilities of the domain structure was performed by studying the patterns of the resistance fluctuations and related phenomena as a function of temperature, current, and applied magnetic field. The experiments were performed for the current-induced intermediate state, the magnetically induced intermediate state where the external field was slowly and continually varied while the specimen current was kept constant, and the magnetically induced intermediate state in a fixed magnetic field while the specimen current varied. Information was obtained about the domain size, the velocity of normal or superconducting boundary propagation and the metastable energy states of a domain configuration as a function of temperature, current, and field. Evidence for the existence of the resistance levels was found in both the current and magnetically induced intermediate states. The resistance levels are related to the metastable energy states of a domain configuration. Since the phenomena related to the instability of a domain structure are time dependent, present theories of the intermediate state based on equilibrium conditions cannot be applied or compared directly with the experimental results. However, by making certain simplifying assumptions certain conclusions were drawn about the mechanism of collapse of superconducting domains, resistance fluctuations, and resistance levels. It was found that the best agreement with experimental results is obtained if one assumes that the mechanism of collapse of superconducting domains in the intermediate state corresponds to a longitudinal, rather than radial, contraction. It is concluded that under certain conditions superconducting domains, initially expanding, would contract, come to some equilibrium size, expand, and repeat the same process. Such pulsation of superconducting domains would be responsible for the appearance of resistance fluctuations. (Dissertation Abstr.)

4784 FLUX QUANTIZATION AND GENERALIZED PAIRING IN SUPERCONDUCTING CYLINDERS [Thesis]. Schwartz, Brian Benjamin. Providence, Brown Univ., 1964. 115p.

The observation that flux is quantized in units of ch/2e in multiply connected superconductors can be understood if the paired electrons in the ground state wavefunction have identical angular momentum. It is possible, however, to generalize the pairing condition and obtain a superconductor in which the ground-state paired electrons have different momentum. Under these circumstances, the relation betwen superconductivity and flux quantization is obscured, and this question is reinvestigated. The normal constant momentum pairing incorporates a dynamical assumption (the pairing) as weil as a symmetry property: the translational (rotational) invariance of the electron-electron interaction. These two, however, are logically independent. In this development, the concept of pairing is retained by introducing a one-to-one mapping of the complete set of up-spin states onto those of down spin. The particular pairing is determined by minimizing the Gibbs' function of the system with respect to the mapping and can contain pair states of different momentum. The Gibbs' function per unit volume of the superconductor can be decomposed into three parts: (1) a magnetic term given by $(H_e - H)^2R_1^2/8\pi(R_2^2 - R_1^2)$, where H_e and H are the external and internal fields and R_1 is the radius of the hole; (2) a kinetic term, which after suitable averaging, is found to be independent of Φ; and (3) the superconducting correlation energy, which is periodic in the enclosed flux with minima at integral multiples of ch/2e. Flux quantization in units of ch/2e occurs when the correlation term changes more rapidly than the magnetic term. By choosing an appropriate sample the magnetic energy might be made to dominate in the Gibbs' function. Then one would expect a breakdown of quantization with the flux approaching that due to the external field. Nonintegral flux values would correspond to states of mixed pairing. In such a situation, it might be possible that thin cylinders would be superconductors but would not support persistent currents. (Dissertation Abstr.)

4785 MAGNETIC TRANSITION OF THIN SUPERCONDUCTING FILMS [Thesis]. Chang, George Kuei-cheng. New Brunswick, N. J., Rutgers Univ., 1965. 67p.

Magnetization curves were obtained for thin superconducting films when the plane of the film is perpendicular to a uniform applied magnetic field. The magnetization was recorded in a slowly varying field by means of a vibrating sample magnetometer. Data were obtained for various thicknesses of pure indium, pure tin, and alloys of tin in indium, bismuth in indium, and indium in tin. The values of the field, $H_T(T)$, at which the magnetic moment vanishes were determined as a function of the temperature, T. For pure indium, it was found that H_T at a given temperature was a minimum for a film thickness of about 9000 Å. For films of thickness much less than this value, the Ginzburg-Landau parameter K(T) can be calculated from $H_T(T)$. At the transition temperature, T_c, $K(T_c)$ varies linearly with the electrical resistivity of the films. The rate of variation is, however, about 50% less than in bulk alloy specimens. It was also found that the form of the temperature dependence of K(T) depends sensitively on the resistivity and thus on the electron mean free path. For long mean free paths, K(T) is given by the two-fluid model. As the mean free path is reduced, K(T) approaches the dependence derived by Gor'kov. No existing theory accounts for the variation of K(T) with mean free path. (Dissertation Abstr.)

4786 SPECIFIC HEAT OF TYPE II SUPERCONDUCTORS IN A MAGNETIC FIELD [Thesis]. McConville, George Terrence Jr. New Brunswick, N. J., Rutgers State Univ., 1965. 72p.

The specific heats of niobium, a niobium-tantalum alloy, and an indium-bismuth alloy were measured as a function of temperature in several constant magnetic fields. The values of the magnetic fields and the temperature ranges were chosen in such a way that the transitions at H_{c1}, the lower critical field, and H_{c2} the upper critical field, could be observed. The four niobium specimens and the In + 1.9 at % Bi specimen all had a Ginzburg-Landau $\kappa \sim 1$. The κ of the 50% Nb + 50% Ta was ~4. When the specimens were heated in a constant magnetic field, the heat capacity exhibited a very large peak at a low temperature followed by a leveling off and then an abrupt drop to the normal state at a higher temperature. The peak occurs at a temperature where the applied field $H_a \sim H_{c1}$. The abrupt drop is the second-order transition at H_{c2}. The evidence presented suggests that a first-order transition takes place at H_{c1} for materials of small κ. The magnitudes of the specific heat discontinuities at H_{c2} were compared with the prediction of the Abrikosov theory of Type II superconductors. The measurements on two alloys that have short electron mean free paths are in agreement with the theory. The measurements on Nb are not in agreement with the theory of Abrikosov. The magnitudes of the measured discontinuities only approached the theoretical value at T_c. At lower temperatures the measured values were about a factor of two too small. Thus, although Nb shows the qualitative features exhibited by other Type II superconductors, there are clear quantitative differences that must originate in the long electron mean free path of pure Nb. (Dissertation Abstr.)

4787 THE INTERACTION OF FREE ELECTRONS WITH LIQUID HELIUM [Thesis]. Sommer, Warren Thomas. Stanford, Calif., Stanford Univ., 1965. 73p.

An investigation of the behavior of electrons that impinge on the free surface of liquid helium is described. It is shown that the liquid is an energy barrier to the electrons. Measurements indicate that the height of the energy barrier is about 1.3 electron volts. Since low-energy electrons are not able to pass through the liquid surface, it is possible to form an electron-charge layer of a unique type upon the liquid surface. The mobility of these surface charges was investigated to determine the extent of the interaction between the electrons and the liquid. The mobility was found to be lower, by about a factor of 3, than the calculated mobility of a free electron in the vapor. It is suggested that this result may be interpreted in terms of the properties of the electron wave function that would be formed on an incompressible dielectric with a plane surface. A further investigation of the interaction of the surface charge and the liquid was made with radiation from a helium vapor discharge impinging on the charged surface. It was found that under these conditions a considerable number of electrons were able to enter the liquid in spite of the barrier. It is believed that this is the result of excitation of surface atoms, which subsequently capture electrons from the surface charge. A brief review is given of the experiments involving electrons in liquid helium carried out by others and of the models for the negative ion structure. It is shown that the discovery of the surface barrier constitutes strong evidence for what is known as the cavity or bubble model of the electron in the liquid. The experimental results stemming from the studies of the electron within the liquid are reconsidered, and it is shown that these results are also consistent with the cavity model when appropriately analyzed. (Dissertation Abstr.)

4788 THE MOBILITY OF ELECTRONS IN DENSE HELIUM GAS AT LOW TEMPERATURES [Thesis]. Levine, James Lewis. Minneapolis, Univ. of Minnesota, 1965. 136p.

The mobility of electrons in helium gas was measured at liquid helium temperatures. The electrons were injected in short pulses from a photocathode and the drift velocity in an applied electric field was deduced by a time-of-flight technique. The mobility was taken to be the ratio of drift velocity to field strength in the limit of zero field. Measurements were made at temperatures in the range 2.2–4.2°K and at pressures between approximately .05 atm and the saturated vapor pressure. The mobility was found to be an extremely strong function of density, and a weak function of pressure and temperature at constant density. At high densities ($\gtrsim 1.5 \times 10^{21}$ atoms/cm^3) the mobilities were four orders of

magnitude lower than the values expected for a free electron and were characteristic of a large and/or massive ion. As the density was decreased below this value, the mobility was found to increase sharply, approaching asymptotically the values expected for a free electron. The possibility that a region of low gas density might form around an electron because of the repulsive interaction is considered in detail. It is shown that under the experimental conditions the electron-helium interaction may be approximated by a continuous repulsive potential proportional to the gas density. A self-consistent calculation of the electron wave function and the form of the gas density disturbance is given. At high densities, the states are found to be highly localized, with the electron confined to a region approximately 20 Å in radius which is almost devoid of helium atoms. It argued that the "hole" must follow the average motion of the electron. An approximate calculation of the mobility of such an entity is given, and the results are found to be in reasonable agreement with experiment at high densities. It is also shown that free-electron-like states can exist at all densities. It is found that these non-localized states become thermodynamically more favorable below a critical density of approximately 1.5×10^{21} atoms/cm^3. The mobility is expected to rise sharply at lower densities, as observed experimentally. The calculated critical density is in excellent agreement with experiment, lending support to the basic validity of the model. (A.G.W.)

4789 THEORY OF SUPERFLUIDS. Valatin, J. G. (Univ. of Birmingham, Eng.). pp 292-372 of Lectures in Theoretical Physics. Vol. VI. Boulder, Colo., The University of Colorado Press, 1964.

A discussion is given on superconductors at thermal equilibrium, and a discussion of similar methods in application to boson systems which brings out some of the similarities and differences between fermion and boson superfluids. The starting point for superconductivity theory is an assumption of some effective two-body forces between the electrons. The interaction of the electrons with a phonon field is not discussed. The analogous matrix equations for bosons, and variations on the use of the quasi-particle techniques are also given. A review is given of the equations for the theory of superconductivity at T = 0. Superconductors at thermal equilibrium are considered including the statistical operator, the partition function, nonintegrating fermions, the temperature dependent Hartree-Fock method, quasi-particle ensembles, the model with constant matrix element interaction, matrix equations, and the two-fluid model for the Meissner effect. Boson systems are also discussed including the variational principle and quasi-particle variables, the momentum representation and a simple model, matrix equations, and the temperature dependent description. (J.F.P.)

4790 PHYSICS AND TECHNIQUES OF LOW TEMPERATURES. Proceedings of the 3rd Regional Conference Held in Prague 1963. Kaczer, Jan (ed.). Prague, Publishing House of the Czechoslovak Academy of Sciences, 1964. 270p. (CONF-630913).

The conference included 43 papers. Separate abstracts were prepared for 20 papers. Other papers included experimental investigations of spin-wave spectrum in antiferromagnetic carbonates, investigation of properties of conduction electrons in metals at microwave frequencies, theoretical investigation into the fundamentals of thermodynamics, linear magnetostriction of antiferromagnetic CoF_2, antiferromagnetic resonance in hematite, mobility and magnetoresistivity of Cd_3As_2 at temperatures between 1.6 and 300°K, magnetoresistance of constantan, combined resonance in InSb, the influence of plastic deformation on thermal and electric conductivity of electrolytic copper at 18 to 80°K, and the residual resistivity of quenched platinum. Other papers were an investigation into austenite and martensite at very low temperatures, methods of obtaining helium temperatures, studies on neon, the liquefaction of helium in a cycle with expansion turbines, the Cryogenic Laboratory of the Joint Institute of Nuclear Research, a helium level indicator, the measurement of thermal conductivity at 4 to 100°K, an adiabatic vacuum calorimeter for measuring small quantities of substances, and the thermosiphon as a heat transferring element in the low temperature range. Also included were studies on cryopumps at 78 and 28°K, heats of absorption at low temperatures, new types of metal high vacuum valves, and effective thermal insulation for low-boiling liquids. (J.F.P.)

For abstracts of individual papers see: 4037, 4257, 4453, 4489, 4490, 4519, 4520, 4559, 4637, 4791—4798, 4932, 4933, and 5021.

4791 REVIEW OF THE THEORY OF SUPERCONDUCTING ALLOYS. Abrikosov, A. A. (Inst. for Physical Problems, Moscow). pp 11-16 of Physics and Techniques of Low Temperatures. Prague, Publishing House of the Czechoslovak Academy of Sciences, 1964.

The modern theory of superconductivity of Bardeen, Cooper, Schrieffer, and Bogolyubov, according to which the electrons in superconductors are coupled in pairs, is reviewed. The new theory of superconductivity explains the surface energy between the normal and superconducting phases. It is noted that if no surface energy existed the field transition of a massive cylinder in a longitudinal field could not be a transition of the first kind. The critical current, of which recent data indicate that nonuniformity of alloys is the main cause, is also considered. (J.F.P.)

4792 SUPERCONDUCTIVE PROPERTIES OF Nb–Zr ALLOYS. Bychkov, J. F.; Goncharov, I. N.; Kuzmin, V. I.; Litomiskii, M.; Khukhareva, I. S. (Joint Inst. for Nuclear Research, Dubna, USSR). pp 53-9 of Physics and Techniques of Low Temperatures. Prague, Publishing House of the Czechoslovak Academy of Sciences, 1964.

Niobium-zirconium alloys with Zr content from 0 to 80% are studied. Particular attention is paid to alloys with Zr as the basic material (from 65% Zr), and these are studied before and after the various thermal treatments. The alloys were studied in the β state of solid solution which was produced in the alloys with less than 75% Zr content by quick cooling of the samples on the copper underlay. Voltage contacts were constructed in the center of the sample, and the temperature of the superconductive transition and the critical current density were measured for fields up to 27 kOe at 4.2°K. The results are shown for the superconductive properties of alloys that were not thermally treated, and for those that were thermally treated. These results are shown graphically and discussed. (J.F.P.)

4793 SUPERCONDUCTING HOLLOW CYLINDERS MADE OF Nb_3Sn AS PERSISTENT MAGNETS AT 14 deg K. Lange, F. (Lab. of Low Temperature Physics, Dresden). pp 60-5 of Physics and Techniques of Low Temperatures. Prague, Publishing House of the Czechoslovak Academy of Sciences, 1964.

Hollow cylinders in longitudinal magnetic fields are studied for values of the mean current density in such cylinders as a function of the surrounding field. Since this is a measurement without contacts, the sample may be sintered after each measurement. Also the troublesome influence of contact resistances is eliminated. Such investigations were made in magnetic fields up to 25 kOe in the temperature range accessible for liquid hydrogen. The most favorable sintering conditions were determined and used for the samples tested. The occurrence of flux jumps was found, and the tendency of these jumps to occur was investigated. The individual samples were studied at 14, 15, 16, and 17°K. The investigation showed that the tendency to flux jumps decreases with increasing sintering time. Thus a general connection between the tendency to flux jumps and the quality was assumed and investigated. A field of 15 kOe was trapped into a sample at 14°K. This corresponds to about 70% to the trapped field which would be possible if no flux jumps occurred. The mean current density with a trapped field of 14 kOe is found to be more than 2.2×10^4 amp/cm^2. (J.F.P.)

4794 CHANGE OF MAGNETIC INDUCTION DISTRIBUTION WITH TEMPERATURE IN CYLINDRICAL

SPECIMEN AT DESTRUCTION OF SUPERCONDUCTIVITY BY CURRENT. Makiej, B.; Freud, R.; Sulkowski, C. (Inst. of Physics, Polish Academy of Sciences, Wroclaw). pp 66-70 of Physics and Techniques of Low Temperatures. Prague, Publishing House of the Czechoslovak Academy of Sciences, 1964.

Since deviations of the experimental curves from the theoretical ones occurring in the border region of the intermediate state core and normal state sheath only negligibly exceeded the mean error of experimental results, a closer examination of this inconsistency is made. The distribution of magnetic induction in a specimen at a fixed current I = 25.8 amp was determined for several temperatures of the specimen, since at a temperature increase the border region sheath-core shifts toward the axis of the specimen, and it is possible in the region in question to avoid the disturbing influence of the border effect of the slot in the specimen. The specimen was a polycrystalline tin cylinder whose slot was measured by means of a magnetoresistance bismuth probe carefully fixed so that its movement would not cause variable mechanical tensions. Resistivity measurements of the probe are shown and the calculation given. It is found that the temperature increase is accompanied by a decrease in the radius of the intermediate state core, and the experimental points in the border region sheath-core do not lie on the theoretical curves. (J.F.P.)

4795 SOME SUPERCONDUCTING AND OTHER PROPERTIES OF Sn- AND In-WHISKERS. Grohman, Antoni (Inst. of Physics, Polish Academy of Sciences, Wroclaw). pp 71-80 of Physics and Techniques of Low Temperatures. Prague, Publishing House of the Czechoslovak Academy of Sciences, 1964.

Some results of investigations undertaken to explain the practical possibilities of using Sn and In whiskers in the field of superconductivity are reported. The methods of obtaining the whiskers and the methods of mounting them are described. Their superconducting properties are discussed. These include their resistance ratio, transition temperature, characteristics of their critical magnetic fields, the penetration depth of the magnetic field, and the transition temperature maximum shift for Sn whiskers. The phenomenon of diffusion is considered in which the Sn whisker effuses toward the thin In layer, bringing about a reduction of diameter of the whisker, or even its failure. Also the transition of β Sn to α Sn and the instantaneous disintegration of a part of the whisker were observed. (J.F.P.)

4796 NEUTRONOGRAPHIC INVESTIGATIONS OF SOLID OXYGEN. Alikhanov, R. (Inst. for Physical Problems, Moscow). pp 127-31 of Physics and Techniques of Low Temperatures. Prague, Publishing House of the Czechoslovak Academy of Sciences, 1964.

Neutronographic investigations were made in solid oxygen for the purpose of using the diffraction of neutrons to study the crystalline and magnetic properties of solid oxygen at low temperatures. The new cryostat model used has the important feature that an additional screen takes the temperature of the bath, besides the oxygen-filled appendix. The introduction of this screen ensures that the temperature of the sample stably follows the temperature of the bath. Measurements of neutron diffraction on oxygen were performed with the bath filled with liquid neon, hydrogen, and helium. The neutronogram obtained at 27°K, that is, in the β phase of oxygen, is given. The position of the diffraction lines is described well by a rhombohedral lattice. The relations of the intensities of the reflection maxima correspond to the D^5_{3d}. It is found that the neutronogram contains an additional contribution to the refraction (111) and (110) compared with the nuclear one. The nature of this contribution seems to be magnetic. (J.F.P.)

4797 LARGE LABORATORY HYDROGEN LIQUEFIER VO 2 FOR USE WITH LARGE LIQUID HYDROGEN BUBBLE CHAMBERS. Zeldovich, A. G.; Pilipenko, Yu. K. (Joint Inst. of Nuclear Research, Dubna, USSR). pp 172-8 of Physics and Techniques of Low Temperatures. Prague, Publishing House of the Czechoslovak Academy of Sciences, 1964.

A description is given of a hydrogen liquefier. The cooling cycle in the liquefier is realized by the expansion of highly compressed hydrogen with the pre-cooling of hydrogen in two baths of liquid nitrogen boiling under atmospheric and lowered pressure. A subsidiary collector is used for the cooling regime and for the production of para-hydrogen in the liquefier. A diagram of this liquefier is shown. Reasons for choosing this apparatus and the fundamental working conditions are discussed. Calculations based on experimental results from the liquefier performance show that it is capable of working with 1500 m^3/hr of compressed hydrogen and hence can produce 460 l/hr or normal and 280 l/hr of para-hydrogen. For this case a few modifications must be made. (J.F.P.)

4798 HELIUM LIQUEFACTION IN THE NUCLEAR RESEARCH INSTITUTE. Prusak, Jan (Inst. of Nuclear Research, Czechoslovak Academy of Sciences, Rez). pp 179-82 of Physics and Techniques of Low Temperatures. Prague, Publishing House of the Czechoslovak Academy of Sciences, 1964.

The arrangement of the floor space of the building for containing a combined helium and hydrogen liquefier is described. The purpose of this arrangement is firstly to ensure the safety of the performance and secondly to isolate the dynamical effects of heavy compressors and pumps for the foundations of the pavilion in which measurements on sensitive instruments are performed. The design and performance of this liquefier are also described. It is a cascade type liquefier, pre-cooled by liquid nitrogen and liquid hydrogen, using the throttling of compressed helium. The hydrogen and helium circuits are analogous, the gas, which is stored under pressure in steel cylinders, is let into a gas-holder. From there it is sucked up by a compressor and compressed; and after cooling by water and the oil separated, the gas enters the exchangers of the liquefier and passes to the throttling valve. After some modifications in the design, the output of the liquefier was 12 liters of liquid helium and 15 liters of liquid hydrogen per hour. (J.F.P.)

4799 METHOD FOR INCREASING THE CRITICAL CURRENT OF SUPERCONDUCTING ALLOYS. Kneip, G. D.; Betterton, J. O.; Easton, D. S.; Scarbrough, J. O. (to U. S. Atomic Energy Commission). U. S. Patent 3,215,569. Nov. 2, 1965.

A method is described for increasing the critical current of a hard superconducting alloy, which comprises annealing the alloy within a multiphase region of its equilibrium phase diagram below a substantially homogeneous solid phase for a period of time sufficient to induce precipitation of a secondary phase, quenching the annealed alloy to retain said secondary phase, and them subjecting the alloy to a magnetic field below its critical magnetic field at or below its critical temperature. (AEC)

Neutron Physics

See also REACTOR TECHNOLOGY — Criticality Studies

Refer also to abstract 5200.

4800 (AE-198) MEASURED AND PREDICTED NEUTRON FLUXES IN, AND LEAKAGE THROUGH, A CONFIGURATION OF PERFORATED Fe PLATES IN D_2O. Aalto, E. (Aktiebolaget Atomenergi, Stockholm (Sweden)). Oct. 1965. 24p. Dep. mn.

Detailed neutron flux measurements were performed in a 48 cm thick configuration of thin regions of Fe and D_2O (30% of total thickness Fe), both when the Fe regions are massive and when they are penetrated by 15 cm dia. D_2O channels. It was found that the total leakage of neutrons through the configuration was increased by 25% in the latter case. It is shown that this increase and the de-

tailed flux distribution on a duct axis can be satisfactorily predicted by a one-dimensional shielding code when the duct is calculated as a pure D_2O layer and a radial buckling term is used for the <1 ev neutrons when penetrating the Fe regions. Another calculation through the massive part of Fe is to be performed in the usual way. It is believed that this 2-component method is usable in a wider range of similar configurations. A calculation with regions where the Fe and the D_2O ducts were homogenized into a single material overestimates the increase in leakage, and the relative error is greater than that in the 2-component calculation. (auth)

4801 (GA-6634) INTEGRAL NEUTRON THERMALIZATION. Quarterly Progress Report for the Period Ending June 30, 1965. Beyster, J. R.; Carriveau, G.; Crosbie, K.; Koppel, J. U.; Naliboff, Y. D.; Neill, J. M.; Russell, J. L. Jr.; Young, J. A.; Young, J. C. (General Atomic, San Diego, Calif. John Jay Hopkins Lab. for Pure and Applied Science). July 30, 1965. Contract AT(04-3)-167. 75p. Dep. mn; CFSTI $3.00 cy, $0.75 mn.

Research for the development of well tested thermal scattering kernels and the understanding of thermalization and transport phenomena is presented. The approach used is to develop a theoretical scattering model for each moderator, develop a good engineering type code to generate a scattering kernel from that model, and test the calculations against measurements of neutron spectra and single differential cross sections. The scattering kernels can be tested either by comparing calculated and measured neutron spectra, which are of more direct interest to reactor design, or by comparing calculated and measured single differential scattering cross sections $d\sigma/d\Omega$, which are more sensitive to the details of the scattering model. Considerable analysis was made of scattering measurements made previously on H_2O, D_2O, and $ZrH_{1.85}$. For the spectral studies, measurements with more sensitivity to the scattering kernel are also sought. In the infinite medium spectral studies in H_2O at elevated temperatures, resonance absorbers (erbium and gadolinium) were used. These absorbers are of interest in reactor design as burnable poisons, gadolinium because of its high cross section, and erbium due to its resonances overlapping those of ^{239}Pu and ^{241}Pu. These measurements also serve to check out the scattering kernel for water at temperatures closer to reactor operating conditions. In addition, spectral studies were continued in heterogeneous systems to develop measuring and analyzing techniques for the determination of cell spectra. Preliminary measurements were made across a single fuel rod assembly. Further measurements and analyses were performed on polyethylene slab cells. (M.O.W.)

4802 (IDO-17115) LIMITED-ENERGY NEUTRON SOURCES PRODUCED BY THE DECAY OF EXCITED NUCLEI [Thesis]. King, E. A. (Phillips Petroleum Co. Idaho Falls, Idaho. Atomic Energy Div.). Sept. 1965. Contract AT(10-1)-205. 61p. Dep. mn; CFSTI $3.00 cy, $0.75 mn.

Three phenomena are considered as sources of neutrons. Nitrogen-17 and fission product delayed neutron precursors are considered and several systems for their use in MTR are proposed. Radionuclide gamma ray bombardment of beryllium and deuterium is reviewed. Several reactions not previously considered in the literature are included. Neutron-capture gamma rays are considered as gamma ray sources. Several (n,γ) and (γ,n) targets are considered. Systems for their use in MTR are proposed. Reactions using alpha particles emitted from radionuclides are considered as sources. Some usable radionuclide alpha particle sources are listed, nuclides with usable reaction thresholds are tabulated, and a bibliography of alpha-neutron sources is included. (auth)

4803 (INR-630/IX-A/PR) TABLES OF THE FUNCTIONS $X(c,-\nu)$ AND $X^2(c_1,c_2)$ FOR THE NUMERICAL SOLUTION OF SLAB GEOMETRY NEUTRON TRANSPORT PROBLEMS. PART I. Kowalska, K. (Institute of Nuclear Research Warsaw (Poland)). May 1965. 252p. Dep.

Tables of the characteristic functions appearing in the solution of slab geometry neutron transport problems, based on the expansion into eigenfunctions, were prepared. The mean number of secondary neutrons per collision is a variable parameter. (auth)

4804 (KAPL-3098) LINK. A COMBINED SLOWING-DOWN AND THERMALIZATION PROGRAM WITH A THERMAL CUTOFF OF 3.06 ev. Bollacasa, D.; Goldman, D. T. (Knolls Atomic Power Lab., Schenectady, N. Y.). May 19, 1965. Contract W-31-109-eng-92. 35p. Dep. mn; CFSTI $2.00 cy, $0.50 mn.

The joining of a neutron slowing-down program, FOMENT, with a thermalization program, SWAK, to form a continuous unit, LINK is described. The effect of changing the value of the maximum energy of the thermalization portion to include more of the upscattering contribution is presented. The thermalization program is available as 32-point (0.625 ev), 36-point (0.835), and 78-point (3.06 ev) versions, complete with full scattering kernels to these energies. Results of calculations for sample problems are given, both as average group constants and as detailed flux spectra. The advantage in including upscattering to higher energies is manifest. (auth)

4805 (ORNL-TM-1245) SPCTRM. AN 05R MONTE CARLO ANALYSIS ROUTINE FOR CALCULATING THE NEUTRON ENERGY SPECTRUM. Morrison, G. W.; Mihalczo, J. T.; Irving, D. C. (Oak Ridge National Lab., Tenn.). Aug. 26, 1965. Contract W-7405-eng-26. 17p. Dep. mn; CFSTI $1.00 cy, $0.50 mn.

SPCTRM is a FORTRAN subroutine for analyzing the collision tapes from the 05R Monte Carlo neutron transport code to obtain the energy spectrum of neutrons crossing a boundary, of neutrons in the medium, and of source neutrons, using equal energy intervals or equal logarithmic energy intervals. It also computes the fraction of neutrons leaking from the system and the average number of collisions before the neutrons are lost. The standard deviations of the neutron spectra are also determined. (auth)

4806 (RPI-328-40, pp 1-42) NEUTRON THERMALIZATION. (Rensselaer Polytechnic Inst., Troy, N. Y.).

Several neutron experiments were carried out. The following papers are presented for each; test of the zirconium scatterer technique for scalar flux extraction, spatially dependent spectra in a multiplying medium, resonance capture by the pulsed technique, the feasibility of measuring resonance absorption by the pulsed source technique, time-dependent spectra in small Be assemblies, infinite medium H_2O steady state spectrum, reactor kinetics; non 1/V thermalization parameters, time dependent spectra in the P-N approximation, calculation of time dependent spectra in D_2O, and the analysis of spatially dependent asymptotic spectra measurements in water. (M.O.W.)

4807 (RPI-328-40, pp 56-66) LOW ENERGY NEUTRON INELASTIC SCATTERING (LENIS). (Rensselaer Polytechnic Inst., Troy, N. Y.).

Research carried out on low energy neutron scattering is presented. Summaries of papers on inelastic scattering (filter method) and LENIS (chopper method) are included. (M.O.W.)

4808 (UCRL-14432-T) NEUTRON SELF SHIELDING IN INTERMEDIATE SYSTEMS [Thesis]. Doyas, Richard J. (Lawrence Radiation Lab., Univ. of California, Livermore). Aug. 6, 1965. Contract W-7405-eng-48. 74p. Dep. mn; CFSTI $3.00 cy, $0.75 mn.

A general equation is derived for the neutron self-shielding of a heterogeneously distributed pure absorber; it is shown to reduce in the appropriate limiting situations to equations which were demonstrated to be correct for isolated-slab monoenergetic and resonance absorbers, respectively. Reduction to other geometries is made. It is pointed out that the equation, if taken to the limit of large group and isotropic flux, is equivalent to the procedure of Nordheim if absorber scatter is neglected in the latter formulation, although the basic assumption

seems superficially quite different. It is further demonstrated (with the use of Monte Carlo calculations) that the P_1 incident flux prescription from diffusion theory is not valid for slab lattices whose separations fall below several moderator mean free paths, and that the cause is a strong change in the anisotropy of the incident angular neutron current. Therefore, the commonly used separability assumption (i.e., that the flux distribution internal to an absorber, and hence the self-shielding factor, $\overline{\varphi}_i/\varphi_s$, is independent of the moderator properties) is invalid below separations of this magnitude. The need for a better method of predicting the shape of the incident flux for small absorber separations is indicated. (auth)

4809 ON THE THEORY OF MAGNETIC SCATTERING OF SLOW NEUTRONS BY ANTIFERROMAGNETS. Seidov, Yu. M.; Emirov, M. B. Izv. Akad. Nauk Azerbaidzh. SSR, Ser. Fiz.-Tekhn. Mat. Nauk, No. 1, 75-9 (1965). (In Russian).

A calculation is made of the effect of the field of crystallographic anisotropy of the nuclear magnetic moment on the differential cross section of inelastic magnetic scattering of slow nonpolarized neutrons by antiferromagnets. The method of two time-dependent Green functions is used. (M.J.T.)

4810 INELASTIC NEUTRON SCATTERING FROM PRESSURIZED ETHANE. Straker, E. A. (Univ. of Michigan, Ann Arbor). J. Chem. Phys., 43: 4134-40 (Dec. 1, 1965).

Motions of the ethane molecule were investigated at room temperature by inelastic neutron scattering techniques. Ethane targets were observed both in the gas and liquid phases by means of pressure variation. A four-rotor mechanical monochromator was used to obtain data at scattering angles of 90 and 22° for neutron energies in the range from 0.046 to 0.020 ev. Triple-axis-crystal spectrometer measurements were also made at 0.035 and 0.064 ev as verification. These data indicated that there is no significant difference in the scattering properties of ethane in the gas and liquid state. Effects of the torsional motion of the two methyl groups about the C–C bond can be seen in the forward-angle data. Comparison of experiment with theory indicated that a Krieger-Nelkin model, which included a harmonic-oscillator representation of the torsional motion, approximately predicts the observed data. The influence of multiple scattering on the final energy distribution was observed and is discussed. (auth)

4811 COMPLETE CONTINUITY OF THE FREE GAS SCATTERING OPERATOR IN NEUTRON THERMALIZATION THEORY. Montagnini, Bruno; Demuru, Maria Luisa (Univ. of Milan). J. Math. Anal. Appl., 12: 49-57(Aug. 1965).

The integrodifferential equation describing the motion of neutrons in an absorbing and scattering homogeneous medium is treated. Some properties of the collision operators, and related operators, are studied within the scheme of the free gas model. (L.B.S.)

4812 ON THE USE OF THE POINCARE-BERTRAND FORMULA IN NEUTRON TRANSPORT THEORY. Kuscer, I.; McCormick, N. J. (Univ., Ljubljana, Yugoslavia). Nucl. Sci. Eng., 23: 304(Dec. 1965).

It is shown that a consistent system of formulas for neutron transport theory can be constructed using two versions of the Poincare-Bertrand formula. (L.B.S.)

4813 AN ATTEMPT TO MEASURE DIRECTLY THE SLOWING DOWN AGE OF (D,D) NEUTRONS IN PARAFFIN. Grimeland, B.; Seierstad, G. (Univ., Oslo). Nucl. Sci. Eng., 23: 339-43(Dec. 1965).

Small crystals of NaI(Tl) were exposed to (D,D) neutrons slowed down in a paraffin moderator. The crystals were either enclosed in cadmium or placed inside a small cadmium box filled with the moderator material. The activities induced in iodine at different positions were measured. Now let the normalized activities obtained with the detectors enclosed in cadmium be A_1 and let those obtained with the detectors placed inside the cadmium box be A_2. It is assumed that the difference A_2-A_1 is proportional to q(0.5 ev)–the slowing down density at an energy of 0.5 ev–and from the measured quantities $A_2(r)$ and $A_1(r)$ the slowing down age is determined. Bare crystals were also irradiated and the induced activities measured. Let these activities be A_3. Then the difference A_3-A_1 will give a measure of the density of thermal neutrons and the migration area can be determined. With migration area and slowing down age known, the diffusion length of thermal neutrons is determined. The result obtained was $L = (2.86 \pm 0.16)$ cm compared to a calculated value of (2.60 ± 0.01) cm. The discrepancy might indicate that the neutron temperature in the paraffin is about 400°K. (auth)

4814 POLARIZATION EFFECTS ON NEUTRON TRANSPORT. Bell, George I.; Goad, Walter B. (Los Alamos Scientific Lab., N. Mex.). Nucl. Sci. Eng., 23: 380-91(Dec. 1965). (LA-DC-6742).

A theory of neutron transport which includes polarization effects is developed. In particular, the polarization of fast neutrons is treated that results when they are scattered by unpolarized nuclei–an effect explained by a neutron-nucleus spin-orbit interaction. The polarization of neutrons is described by a quantum-mechanical polarization vector. The change of this vector in scattering is examined and a general transport theory is formulated in terms of two coupled transport (Boltzmann) equations for the scalar neutron flux and the vector polarization flux. For plane or spherical geometry it is shown that the polarization vector is always normal to the $(\hat{r},\Omega)$ plane and two coupled scalar transport equations are obtained for the flux and this one component of the polarization flux. A spherical harmonics solution is developed wherein the neutron flux is expanded in Legendre polynomials and the polarization flux is expanded in associated Legendre functions of the first kind. In the P_1 approximation the effect of polarization on the neutron flux is obtained by simply increasing the transport cross section. The polarization flux is then proportional to the neutron current (as a function of position) times sin θ with $\cos\theta = \hat{r}\cdot\Omega$, as usual. Higher-order spherical-harmonics values are found for the asymptotic diffusion length, and numerical results are calculated for neutrons scattered from uranium. It is concluded that the P_1 theory can be used to obtain a reasonable estimate of the polarization effects and that the changes in diffusion length due to polarization are generally small, but may be a few percent for the energy range where the p wave scattering is important. The polarization of neutrons in a multiplying assembly should be experimentally observable. (auth)

4815 DECAY CONSTANT OF A NEUTRON PULSE INSIDE A FINITE SOLID MODERATOR ASSEMBLY. Kothari, L. S. (Univ., Delhi). Nucl. Sci. Eng., 23: 402-3(Dec. 1965).

An attempt is made to explain why the experimental values of the decay constant–(λ) for large assembly buckling (B^2) are found to be larger than the mathematical bound limit λ_{min}. (L.B.S.)

4816 DECAY CONSTANT OF A NEUTRON PULSE. Corngold, Noel (Brookhaven National Lab., Upton, N. Y.). Nucl. Sci. Eng., 23: 403-4(Dec. 1965).

A qualitative explanation is given for the observed exponential decrease characterized by $\lambda > \lambda^* = (\nu\Sigma)$ min in pulsed-neutron experiments. A quantitative agreement is given by treating the leakage of neutrons by diffusion theory. (L.B.S.)

4817 DETERMINATION OF THE DIFFUSION CONSTANTS D(E_0,T) AND Dv(T) OF THERMAL NEUTRONS IN H_2O, PHENYLENE, $ZrH_{1.92}$, AND D_2O BY MEASUREMENT OF THE SCATTERING ANGULAR DISTRIBUTION $(4\pi/\sigma)\cdot(d\sigma/d\Omega)$. III. BENZENE, DIPHENYL, o-, m-, AND p-TERPHENYL. Hofmeyr, Christoph (Technische Hochschule, Munich). Nukleonik, 7: 286-95(July 1965). (In German).

Monochromatic neutrons with energies of 0.0225, 0.044,

0.071, and 0.105 ev were scattered on thin layers of benzene, diphenyl ($C_{12}H_{10}$), o-, m-, and p-terphenyl at various temperatures for the determination of the differential scattering cross section $4\pi/\sigma\ d\sigma/d\Omega(\theta)$. From the scattering angular distribution the mean scattering cosmic μ and the diffusion constant D were calculated in dependence on the neutron energy and the sample temperature. The averaging of $D(E_0)$ over a Maxwell spectrum at corresponding neutron and moderator temperature gave the mean diffusion constant $\overline{Dv}$ at various temperatures. For diphenyl at 85°C and benzene at 21 ± 1°C good agreement with the theory of Pál was obtained. Only agreement with the measurement of Brown for diphenyl for 85°C was obtained with the experimental values. For the $\overline{Dv}\rho$ at 21°C (ρ is a substance density) the following values were determined: 45,250 ± 700 g cm^{-1} sec^{-1} for benzene, 50,800 ± 930 g cm^{-1} sec^{-1} for diphenyl, 55,000 ± 1000 g cm^{-1} sec^{-1} for m-terphenyl, and 55,550 ± 1000 g cm^{-1} sec^{-1} for p-terphenyl. The maxima that were found for $d\sigma/d\Omega(\theta)$, for the substances investigated, could be explained by intermolecular interference. (tr-auth)

4818 NEUTRON THERMALIZATION IN GRAPHITE. [PART] II. **Young, James A.; Wikner, N. F.; Parks, D. E. (General Atomic Div., General Dynamics Corp., San Diego, Calif.). Nukleonik, 7: 295-300(July 1965).**

A review of the lattice dynamics of graphite and a description of the phonon spectra are presented. A comparison is made with differential neutron measurements and the integral properties of the phonon spectra are given. Calculations are made of the integral properties of the scattering kernel. A brief description of the calculated neutron spectrum using scattering kernels obtained on the basis of the phonon spectra discussed is presented. (J.S.R.)

4819 COHERENT SCATTERING OF SLOW NEUTRONS BY LIQUID ARGON. **Singwi, K. S. (Argonne National Lab., Ill.). Physica, 31: 1257-85(Aug. 1965).**

Some calculations are reported of both quasi-elastic and inelastic scattering of slow neutrons by liquid argon near its triple point. The calculations are based on a phenomenological theory. It is shown what role the coherence parameter R plays in determining the scattering. The width of the quasi-elastic scattering is calculated as a function of momentum transfer, which exhibits a characteristic oscillatory behavior. A formula for the inelastic differential scattering cross section in one-phonon approximation is derived and is shown to reduce in a certain limit to that given by Egelstaff. The scattering function $S(\alpha,\beta)$ was calculated as a function of α for various values of β. For small values of β, the general shape of $S(\alpha,\beta)$ is nearly the same as given by the convolution approximation but for large values of β there is a significant difference. (auth)

4820 THE SPHERICAL HARMONICS APPROXIMATION IN GENERAL GEOMETRY WITH APPLICATIONS TO THE THERMAL EQUIVALENT CELL PROBLEM [Thesis]. **Dudley, Thomas Edward. Troy, N. Y., Rensselaer Polytechnic Inst., 1964. 155p.**

The multidimensional spherical harmonics approximation is presented, and discussed in terms of the geometrical effects of neutron transport that this theory predicts. The stationary, one-group Boltzmann equation in the constant cross section approximation with isotropic scattering, is considered. Sources are also isotropic and region-wise constant. Geometry-induced transients excited by sudden changes in the geometry, such as corners, are investigated. These transients do not appear in the more usual slab or spherical geometry P_L equations and therefore, are little known. Particular attention is paid to a transient in the neutron current, which represents a divergence-less component unrelated operationally to the scalar flux. The general formulation of the spherical harmonics equations is obtained and applied to the two-dimensional thermal cell problem. The spatial moments are expanded in a Fourier-Bessel series, which satisfies the boundary conditions along all of the sides of the cell except one. With a cylindrical geometrical representation, the interface conditions for this two-region cell can be evaluated analytically. The boundary conditions along the one remaining side cannot be satisfied rigorously by the finite spatial expansion, but rather are evaluated at a finite number of points along this boundary. The characteristics and convergence properties of the P_1, P_2, and P_3 approximations are compared with the one-dimensional case. The results of this first analytical treatment of the multidimensional P_L equations are used to investigate the validity of the Wigner-Seitz approximation for small cells in neutron transport calculations, and to investigate the transport effects in these small two-dimensional cells. (Dissertation Abstr.)

Nuclear Properties and Reactions

Refer also to abstracts 3947, 4233, 4248, 4255, 4504, 4539, 4802, and 5018.

4821 (ANL-7081, pp 2-21) RESEARCH AT THE REACTORS CP-5 AND JUGGERNAUT. (Argonne National Lab., Ill.).

Summaries of work done by members of the Physics Division at the reactors CP-5 and Juggernaut are presented. The work includes; instrumentation for measurements of the symmetry properties of neutron decay, electron-neutron interaction, neutron resonances, thermal-neutron capture gamma ray studies, precision measurements of high-energy neutron capture gamma rays, study of radiation widths of low-energy nuclear states by resonance scattering of neutron capture gamma rays, and high-resolution studies of thermal neutron capture. (M.O.W.)

4822 (ANL-7081, pp 22-35) RESEARCH AT THE 4.5-Mev VAN DE GRAAFF ACCELERATOR. (Argonne National Lab., Ill.).

Experiments with fast neutrons are emphasized, especially measurements of the polarization of scattered neutrons. Other experiments performed include pulsed-beam measurements of the lifetimes of excited states, studies of Coulomb excitation by heavy ions, studies of nuclear reactions induced by charged particles, and measurements of total neutron cross sections. Brief discussions of these experiments are presented. (M.O.W.)

4823 (ANL-7081, pp 36-69) RESEARCH AT THE 12-Mev TANDEM VAN DE GRAAFF. (Argonne National Lab., Ill.).

Summaries of experiments using the 12-Mev accelerator are presented. Research on the following is reported; pulsed-beam experiments, charged-particle reactions, dependence of the angular distribution of direct reactions on the total angular momentum transfer, research with the magnetic spectrograph, radiative-capture studies of the giant dipole resonance, and sources for the production of polarized ions. (M.O.W.)

4824 (ANL-7081, pp 70-7) RESEARCH AT THE 60-IN. CYCLOTRON. (Argonne National Lab., Ill.).

Experiments using the Argonne 60-inch Cyclotron are summarized. They include; nucleon-capture reactions, scattering of 45 Mev α-particles by ^{208}Pb, shell-model selection rules and excitation of 4^+ states in the $Ti(\alpha,\alpha')$ reaction, collective excitations in the Zr isotopes, wide-angle scattering of 43-Mev α-particles by ^{58}Ni, angular distributions of the $^{25}Mg(^3He,\alpha)$ reaction, pickup reactions, ^3He scattering from even Ni isotopes, and delayed proton emission. (M.O.W.)

4825 (ANL-7081, pp 81-93) OTHER NUCLEAR EXPERIMENTS. (Argonne National Lab., Ill.).

Several experimental investigations carried out by the Physics Division are reported. These include experiments on the decay schemes of radionuclides, levels populated by beta decay, muonic x-rays, radiation-damage effects in lithium-drifted silicon detectors bombarded by heavy particles, pattern recognition for nuclear events, and microscopic location of ^{17}O, ^{18}O, and ^{15}N. (M.O.W.)

4826 (ANL–7081, pp 121-7) MOESSBAUER MEASUREMENTS. (Argonne National Lab., Ill.).

Research concerning the Mössbauer effect in hexagonal cobalt, xenon compounds, ^{133}Cs, V–Fe alloys, and in ^{40}K produced by an accelerator is briefly discussed. Other brief discussions included are; ratio of the quadrupole moment of the first excited state of ^{129}Xe to that of the ground state of ^{131}Xe, quadrupole moment of the first excited state in ^{127}I, comparison of I and Xe compounds, variation of the ^{57}Fe isomer shift with atomic size in laves phases, and the computation of Mössbauer spectra. (M.O.W.)

4827 (CEA-Bib-60) DIFFRACTION DANS LES REACTIONS NUCLEAIRES A MOYENNE ENERGIE. (Diffraction in Medium-Energy Nuclear Reactions). Longequeue, Nicole (Commissariat a l'Energie Atomique, Saclay (France). Centre d'Etudes Nucleaires). Aug. 1965. 20p. Dep. mn.

The diffraction model used for nuclear reactions which involve particles having energies of from 10 to 30 Mev often give satisfactory results. However, since the simple diffraction theory does not take into account the spin-orbit coupling, it cannot explain recent experimental results indicating the dependence of the spin on the final state for the angular distributions. An attempt to introduce this spin-orbit coupling was recently made. (auth)

4828 (COO–818-60) SEARCH FOR THE DOUBLE BETA DECAY OF ^{150}Nd [Thesis]. East, Larry V. (Case Inst. of Tech., Cleveland, Ohio). 1965. Contract AT (11-1)-818. 99p. Dep. mn; CFSTI $3.00 cy, $0.75 mn.

A search for the double beta decay of ^{150}Nd was carried out using thin plastic scintillation detectors immersed in a 500 gallon liquid scintillation anticoincidence shield. Approximately 43 g of ^{150}Nd in the form of Nd_2O_3 was used as a source. The experiment was performed 585 meters underground in the relatively low radioactive background environment of a salt mine. The count rates observed allow a lower limit of $\geq 3 \times 10^{17}$ years to be placed on half-life of the decay $^{150}Nd \rightarrow {}^{150}Sm + 2e^- + 2\tilde{\nu}$ and a lower limit of $>3 \times 10^{18}$ years for the half-life of $^{150}Nd \rightarrow {}^{150}Sm + 2e^-$. A discussion is given of the possible interpretation of these results in terms of lepton conservation. (auth)

4829 (GEMP–173(Suppl.1)) NINE AND SIXTEEN GROUP CROSS SECTIONS FOR REACTOR ANALYSIS, Supplement No. 1. Bermanis, H. L.; Henderson, W. B.; Robertson, C. S. Jr. (General Electric Co., Cincinnati, Ohio. Nuclear Materials and Propulsion Operation). Sept. 29, 1965. Contract AT(40-1)-2847. 11p. Dep. mn; CFSTI $1.00 cy, $0.50 mn.

Additions and modifications to the sixteen group cross sections listed in the first edition of GEMP-173 dated January 18, 1963, are reported. (auth)

4830 (GEMP–384) A NEUTRON CROSS SECTION LIBRARY FOR MONTE CARLO CODES FMC-N, 18-0, AND 18-1. Burns, L. S. (General Electric Co., Cincinnati, Ohio. Nuclear Materials and Propulsion Operation). Aug. 23, 1965. Contract AT(40-1)-2847. 104p. Dep. mn; CFSTI $4.00 cy, $0.75 mn.

Neutron cross sections for a number of materials were prepared in a format acceptable to GE-NMPO Monte Carlo Programs FMC-N, 18-0, and 18-1. Cross sections are presented for H, Be, B-10, C, O, Al, Cr, Fe, Ni, Nb, Mo, Ta, W, U-235, and U-238. A brief summary of the processing procedure and the sources of the data are also included. (auth)

4831 (HEPL–272) MAGNETIC ELECTRON SCATTERING. Walecka, J. D.; Pratt, R. H. (Stanford Univ., Calif. Dept. of Physics). Aug. 10, 1962. 8p.

The formula for the differential cross section for an electron to scatter through a certain angle and at the same time take a nucleus from the state $J_i \rightarrow J_f$ given in the Born approximation is considered. From this an equation is derived which is identical with the formula derived previously for the scattering of an electron from a point system with a certain charge and magnetic moment. Some characteristics of this equations are noted, and its comparison with the Rosenbluth formula is discussed. Calculations of the M1 form factor for fluorine-19 are also given since this is one of two points which, within the experimental error, do not agree with the theory using the static magnetic moment. The results give a 30% reduction of the theoretical cross section and bring it to the edge of the experimental error. (J.F.P.)

4832 (IAE–901) ANALIZ POLYARIZATSII V PUCHKE NEITRONOV RASSEYANIEM NA KULONOVSKOM POLE YADRA. (Analysis of Polarization in a Neutron Beam by Scattering on the Coulomb Field of the Nucleus). Lebedeva, N. S. (Institut Atomnoi Energii, Gosudarstvennyi Komitet po Ispol'zovaniyu Atomnoi Energii SSSR, Moscow). 1965. 4p. Dep. mn.

An expression for the Coulomb scattering amplitude is given, obtained previously by Schwinger, assuming that the small-angle elastic scattering amplitude is independent of neutron spin and that the imaginary part of the small-angle nuclear scattering amplitude can vary for forward scattering. This expression is used to derive an equation for the polarization of neutrons scattered on the Coulomb field of a heavy nucleus, which gives polarization in terms of the total cross section and the differential cross section at two points. (M.J.T.)

4833 (IS-T-43) PHOTONUCLEAR DETERMINATION OF THE YIELD CURVE AND CROSS SECTION CURVE FOR THE PRODUCTION OF ^{13}N IN ^{16}O [Thesis]. Tuhy, Richard Michael (Ames Lab., Iowa State Univ. of Science and Tech.). Aug. 1965. Contract W-7405-eng-82. 34p. Dep. mn; CFSTI $2.00 cy, $0.50 mn.

The cross section for the production of ^{13}N in ^{16}O by nuclear photon absorption was measured between 25 and 65 Mev. The yield curve for the reaction was measured using bremsstrahlung. Compressed boric acid samples were used as the oxygen target. It was assumed that the only significant reactions were $^{16}O(\gamma,n)^{15}O$ and $^{16}O(\gamma,x)^{13}N$, where x represents three possible products (t, nd, and p2n) leading to ^{13}N. The contribution from each individual reaction was separated from the total activity, measured by NaI(Tl) scintillation crystals, by the Brookhaven decay curve analysis program. The cross section was obtained from the yield curve by use of the least-structures technique. Using this technique, resonance peaks at 30.5, 40.5, 47.2, and 55.4 Mev were discovered in the cross section for production of ^{13}N. (auth)

4834 (JINR–E–2360) A NEW ISOTOPE, ^{174}W. Demeter I., Sil, Kim Hon; Nadjakov, E.; Zaitseva, N. G. (Joint Inst. for Nuclear Research, Dubna (USSR). Lab. of Nuclear Problems). 1965. 16p. Dep. mn.

The isotope ^{174}W is obtained after irradiation of an erbium target with ^{12}C ions. ^{174}W is identified using its genetic relation with ^{174}Ta. The half-life of ^{174}W is measured to be 31 ± 2 min. (auth)

4835 (JINR-P–2287) ISSLEDOVANIE CHUVSTVITEL'NOSTI NEKOTORYKH YADERNYKH KHARAKTERISTIK K PARAMETRAM MODELI PROMEZHUTOCHNOI SVYAZI. (An Investigation of Sensitivity of Some Nuclear Characteristics to the Intermediate Coupling Parameters). Boyarkina, A. N.; Zhusupov, M. A.; Rotter, I. (Joint Inst. for Nuclear Research, Dubna (USSR). Lab. of Theoretical Physics). 1965. 14p. Dep. mn.

Several cases of angular correlations in resonance and direct reactions and nucleon reduced widths are investigated in the framework of the shell model, the intermediate coupling parameters being widely used. Different variants of exchange forces are included. The results are compared with experiment. The intermediate coupling model turns out, in the main, to be close to experiment than extreme cases of LS and jj-couplings. It is confirmed that the choice of the model parameters made from the analysis of other data is correct. (auth)

4836 (JINR-P-2298) K VOPROSU OB UGLOVOM RASPREDELENII PRODUKTOV REAKTSII PEREDACHI. (On the Angular Distribution of the Transfer Reaction

Products). Kalinkin, B. N.; Grabovskii, Ya. (Joint Inst. for Nuclear Research, Dubna (USSR). Lab. of Theoretical Physics). 1965. 8p. Dep. mn.

The consequences of the quasiclassical theory of the angular distribution of the transfer reaction products were considered. The results are consistent with the experimental data. (auth)

4837 (JINR-P-2310) K VOPROSU O KORREKTNOSTI METODA EDINOI TEORII YADERNYKH REAKTSII. (On Correctness of the Method for Unified Theory of Nuclear Reactions). Amirkhanov, I.; Zastavenko, L. G.; Zakhar'ev, B. N. (Joint Inst. for Nuclear Research, Dubna (USSR). Lab of Theoretical Physics). 1965. 15p. Dep. mn.

The problem concerning the motion of a complex particle in an external field is considered. A method previously suggested for investigating the convergence of the expansion of the function of the whole system in a complete set of the eigenfunctions of the internal motion of the complex particle is generalized to the three-dimensional case. It is shown that the population of the higher virtual excited states decreases rapidly with the excitation energy. The neglect of the states higher than that of S introduces an error tending to zero with the increase of the S-state energy. (auth)

4838 (JINR-P-2314) O POZITRONNOM RASPADE ^{145}Eu. (On Positron Decay of ^{145}Eu). Zhelev, Zh.; Muziol, G. (Joint Inst. for Nuclear Research, Dubna (USSR). Lab. of Nuclear Problems). 1965. 13p. Dep. mn.

Measurements were made of the triple coincidences between the 511-511 kev γ-quanta and the quanta of the whole β-spectrum at a scintillation γ-spectrometer. A measurement was also made of the positron spectrum at a β-spectrometer with a threefold focusing. It was established from these measurements that the positron spectrum arising by the ^{145}Eu decay consists of two components. Their boundary energies are 1740 ± 40 and 800 ± 40 kev. These two components populate the main level and the 893.3 kev level with intensities of 1% and 0.35% per decay, respectively. The decay energy of ^{145}Eu → ^{145}Sm is 2760 ± 40 kev. According to the data obtained and those from other papers an analysis was made of the γ-transition intensities in the ^{145}Eu → ^{145}Sm decay scheme. (auth)

4839 (JINR-P-2333) O MATRICHNYKH ELEMENTAKH DLYA NEUPRUGOGO RASSEYANIYA TYAZHELYKH CHASTITS. I. (On Matrix Elements for Inelastic Scattering of Heavy Particles. [Part] I.). Kalinkin, B. N.; Grabovskii, Ya. (Joint Inst. for Nuclear Research, Dubna (USSR). Lab. of Theoretical Physics). 1965. 16p. Dep. mn.

The structure of matrix elements of inelastic scattering of heavy particles (at $E > V_B$) was analyzed. It is shown that it is possible to make their calculation much simpler by using the quasiclassical approximation. The role of distortions introduced by nuclear forces is cleared up. (auth)

4840 (LAL-1140) ELASTIC ELECTRON SCATTERING BY MAGNETIC AND ELECTRIC MOMENTS. Goldemberg, J. (Laboratoire de l'Accelerateur Lineaire, Univ. de Paris, Orsay (France)). July 1965. 18p. (CONF-651030-1). Dep. mn.

From German Physical Society Annual Meeting, Frankfurt, Ger.

The measurement and interpretation of the electric quadrupole moments and form factors as well as the corresponding information for magnetic moments are discussed. As an example, previous results for ^{10}B and ^{11}B are presented. A discussion is presented on the problem of measuring form factors in nuclei which have an exchange current contribution to the magnetic moment and the possibility that the normal and exchange currents have different form factors. (M.O.W.)

4841 (NAA-SR-Memo-11511) A WIDE RANGE STUDY OF THE EFFECTIVE RESONANCE INTEGRAL AND DOPPLER EFFECT IN ^{197}Au. PART I. Beller, L. S.; Farrar IV, H. (Atomics International, Canoga Park, Calif.). July 8, 1965. Contract AT(11-1)-Gen-8. 22p. (CONF-650602-78). Dep. mn; CFSTI $1.00 cy, $0.50 mn.

From American Nuclear Society 11th Annual Meeting, Gatlinburg, Tenn.

Combined measurements of the effective resonance integral and Doppler effect in ^{197}Au were undertaken in order to provide detailed comparisons between analytical calculations and experiment over a wide range in surface/mass ratios. Quantitative investigations of the effects of reactor spectrum variations, materials of the in-core capsule, and cadmium covering were made. Detailed corrections for gamma-ray self-shielding, activity distribution, and counting geometry were found for each surface/virgule mass ratio. The results are compared with calculation. (auth)

4842 (NASA-TN-D-3116) OPTIMUM TARGET ORIENTATION IN NUCLEAR REACTION EXPERIMENTS. Need, John L. (National Aeronautics and Space Administration, Cleveland, Ohio. Lewis Research Center). Nov. 1965. 25p. CFSTI $2.00 cy, $0.50 mn.

The conditions are examined under which the energy spread in outgoing particles from a nuclear reaction due to finite target thickness is minimized. Physical restrictions on the angle of incidence and emission are explicitly considered, and it is shown that the minimum in energy spread does not always occur at the limits. Targets are considered both in transmission and in reflection. A FORTRAN IV program embodying these results is described. The program determines the optimum target angle for each of a sequence of angles of observation and calculates the energy spread. (auth)

4843 (NP-15456) DETERMINATIONS OF NUCLEAR DECAY ENERGIES AND CONVERSION COEFFICIENTS USING COINCIDENCE TECHNIQUES [Thesis]. Lewin, Walter Hendrik Gustav (Technische Hogeschool, Delft (Netherlands)). 1965. 103p. Dep. mn.

Coincidence methods were applied in the determination of conversion coefficients and electron capture decay energies. The various methods leading to conversion coefficients using a beta ray spectrometer are discussed. Special attention is paid to several types of coincidence methods and to the required determination of the beta ray spectrometer efficiency. The way is shown in which the latter quantity can successfully be determined using coincidence techniques too. A detailed description is given of coincidence measurements of K-conversion coefficients of unhindered pure E2 groundstate transitions in ^{198}Hg, ^{200}Hg, and ^{194}Pt, using the radioactive nuclides ^{198}Au, ^{200}Tl, and ^{194}Au respectively. The coincidence techniques applied were adjusted to the special properties of these nuclides. The results obtained are all in agreement with the theoretical predictions. To demonstrate the general validity of the coincidence method introduced, the relative electron capture transition probability from ^{202}Tl to the groundstate of ^{202}Hg was determined experimentally. In order to find out why recent values for the conversion coefficient of the 412 kev transition in ^{198}Hg obtained from the use of the peak-to-beta spectrum method are persistently lower than theory, the spectrum shape of the 962 kev beta branch in ^{198}Au was reinvestigated. This shape was found to be very nearly statistical, in disagreement with all shapes reported so far. Consequently the earlier results obtained from the use of the peak-to-beta spectrum method should be increased; the corrected results come very close to theory now. Experimental data on decay energies in beta radioactivity are of use for beta decay theory. Conflicting results were previously reported for electron capture decay energies in ^{203}Pb and ^{202}Tl. These decay energies were studied by means of coincidence techniques; the results obtained clarify the situation. (auth)

4844 (ORNL-TM-1234) THE HAUSER-FESHBACH NUCLEAR SCATTERING COMPUTER CODE LIANA. Smith, William R. (Oak Ridge National Lab., Tenn.). Sept. 20, 1965. Contract W-7405-eng-26. 28p. Dep. mn; CFSTI $2.00 cy, $0.50 mn.

The FORTRAN code LIANA computes the scattering angular distribution and integrated cross section for any two-particle nuclear reaction. The input and output are essentially the same as that for the code described previously, but the present calculation is more general and, in addition, includes a nonlocal potential and a Porter-Thomas width-fluctuation correction. A listing of the program is included. (auth)

4845 (ORNL-TM-1318) HALF-LIVES AND SPECIFIC ACTIVITIES OF COMMON RADIONUCLIDES. Goldstein, Gerald; Reynolds, S. A. (Oak Ridge National Lab., Tenn.). Nov. 8, 1965. Contract W-7405-eng-26. 16p. Dep. mn; CFSTI $1.00 cy, $0.50 mn.

A compilation was made of the half lives, decay constants, and specific activities of radionuclides with half lives greater than 1 day, including the transuranium elements. (auth)

4846 (RPI-328-40, pp 43-8) NEUTRON CROSS SECTIONS. (Rensselaer Polytechnic Inst., Troy, N. Y.).

Brief discussions of 4 papers on neutron cross section measurements are presented. The papers are fast neutron total cross section measurements, cryostat and spark chamber experiments, neutron capture cross section measurements, and resonance capture gamma-ray spectra. (M.O.W.)

4847 (UCRL-12085(Pt.1)) UNDERGROUND NEUTRINO EXPERIMENT. I. INVERSE BETA DECAY. Colgate, S. A. (Lawrence Radiation Lab., Univ. of California, Livermore). July 1965. Contract W-7405-eng-48. 6p. Dep. mn; CFSTI $1.00 cy, $0.50 mn.

An experiment is outlined to observe the inverse β-decay reaction as a preliminary step in the measurement of the electron-neutrino scattering cross section. It is proposed to detect the neutrinos from the superallowed β-decays of fission fragments produced in an underground nuclear detonation, by means of a disposable Cd-loaded scintillator 1 m^3 in volume. The detector will be located as close to the nuclear device as possible (~100 ft) to take advantage of solid angle gains. Estimates are given for the neutrino detection probability as a function of time. (auth)

4848 (UCRL-12085(Pt.2)) UNDERGROUND NEUTRINO EXPERIMENT. II. NEUTRINO-ELECTRON SCATTERING. Colgate, S. A. (Lawrence Radiation Lab., Univ. of California, Livermore). July 1965. Contract W-7405-eng-48. 5p. Dep. mn; CFSTI $1.00 cy, $0.50 mn.

A discussion is presented on possible neutrino sources and detection systems for the observation of the inverse β-decay reaction. Arguments based on the dependence of detector efficiency on energy and the value of the scattering cross section on type of electron suggest the use of the superallowed decay of ^{12}N as the neutrino source. Considerations of the needed mass of detector and allowed detection time indicate the use of liquid scintillators or bubble chambers as detection systems. The relative merits of these systems are discussed. (auth)

4849 (UCRL-14360, pp 1-50) NUCLEAR AND ATOMIC PHYSICS. (Lawrence Radiation Lab., Univ. of California, Livermore).

The experimental and theoretical studies carried out during the period in elementary-particle and nuclear physics are summarized, together with observations on the magnetic properties of KO_2, PuO_2, NiSe, NiS, and FeTe. (D.C.W.)

4850 A SOLUBLE SEMICLASSICAL PARTICLE TRANSFER PROBLEM. Breit, G. (Yale Univ., New Haven). Ann. Phys., (N.Y.), 34: 377-99(Oct. 6, 1965). (YALE-1807-25).

The one dimensional semiclassical transfer problem presented by two δ-function potentials approaching each other with uniform velocities before a certain time and receding from each other again with uniform velocities in the infinite future admits of an exact solution. A systematic iterative construction is described and the properties of the solution are compared with those of solutions obtained by two approximate methods. The first of these is the "energy matrix" approximation used by Breit and Ebel in calculations on the $^{14}N(^{14}N, {}^{13}N)^{15}N$ reaction. The second is similar to it in that only two out of an infinity of expansion functions are used in the expansion of the time dependent wave function. Instead of employing linear combinations of adiabatic wave functions, however, the second method of approximation employs expansion functions which are eigenfunctions for each of the two potentials in its own Galilean frame. The exact solution gives transition probabilities in reasonable agreement with the approximations within limits explicable by the character of the approximations. The form of the exact answer shows that a symmetrization of the semiclassical three dimensional transfer problem regarding initial and final states which has been used in data analysis has definite limitations regarding accuracy, a similar symmetrization leading to an answer differing from the exact one in the one dimensional case. (auth)

4851 APPLICATIONS OF THE EXACTLY SOLUBLE ONE DIMENSIONAL MODEL OF TRANSFER REACTIONS. Herling, G. H.; Nishida, Y. (Yale Univ., New Haven). Ann. Phys., (N.Y.), 34: 400-14(Oct. 6, 1965). (YALE-1807-26).

An attempt is made to apply the one dimensional exactly soluble model of transfer reactions proposed by Breit in 1960 and discussed by him in the preceding paper to the consideration of nucleon tunneling calculations made in the semiclassical approximation employing the energy matrix formulation of Breit and Ebel. The exact expression for the transfer probability in the case of one fixed potential reversing its motion is arranged in combined powers of the barrier penetrabilities of the two regions of negative kinetic energy around each of the potentials. Through an application of different Galilean transformations to the elementary solutions entering the problem just mentioned before and after the reversal of the motion, a solution corresponding to the assumption of equal masses of the heavy nuclear aggregates throughout the process is worked out and the series for the transition probability is rearranged in powers of barrier penetrability as in the first problem. Different ways of adjusting the parameters of the model to those of the actual three dimensional problem are tried in the case of the $^{14}N(^{14}N, {}^{13}N)^{15}N$ and of the $^{24}Mg(^{14}N, {}^{13}N)^{25}Mg$ reactions. Parametrizations based on simulating barrier penetrability effects lead to fair although not perfect agreement with the energy matrix calculations. (auth)

4852 THE ONE DIMENSIONAL SOLUBLE PARTICLE TRANSFER PROBLEM AND THE MODIFIED ENERGY MATRIX METHOD. Nishida, Y. (Yale Univ., New Haven). Ann. Phys., (N.Y.), 34: 415-23(Oct. 6, 1965).

The comparison of the modified energy matrix treatment of the particle transfer problem with the exact solution available in a special one dimensional case which has been made by Breit is analyzed and carried out by an alternative procedure with the same conclusion. The analysis includes the consideration of effects of the continuum of the energy spectrum of each of the two δ-function potentials and of the effects of these parts of the spectra on the transition probability. These effects are found small in the case considered. The exact solutions are put into a form especially suitable for the comparisons made. The modified energy matrix method is made use of to estimate the effect of the finiteness of the range of force and to analyze the location in space of contributions to the transfer amplitude. (auth)

4853 ON THE LAW OF CONSERVATION OF NUCLEONS. Alvaeger, T.; Martinson, I.; Ryde, H. (Univ. of Stockholm; Nobel Inst. of Physics, Stockholm). Arkiv Fys., 28: 185-9(1965).

The law of conservation of nucleons was tested with emphasis on such processes which correspond to a reverse continual creation of matter, i.e., continual extinction of matter. The mean life for an extinction of a nucleon in a complex nucleus is found to be larger than 3×10^{20} years. (auth)

4854 GAMMA TRANSITIONS BETWEEN EVEN-PARITY STATES IN ^{16}O. Fujii, S.; Rose, M. E. (Univ. of Virginia, Charlottesville). Can. J. Phys., 43: 2045-51 (Nov. 1965).

The large transition rates in the rotational band based on the 0^+ state at 6.05 Mev in ^{16}O are studied using Eisenberg, Spicer, and Rose's model for the even-parity states. The transition rates from low-lying 4^+ states to low-lying 2^+ states and from these 2^+ states to the first excited 0^+ state are calculated. The calculated values are much smaller than the experimental ones. (auth)

4855 COMPOSITION OF MATTER IN NUCLEAR STATISTICAL EQUILIBRIUM AT HIGH DENSITIES. Tsuruta, Sachiko; Cameron, A. G. W. (Inst. for Space Studies, New York). Can. J. Phys., 43: 2056-77(Nov. 1965).

Various properties of dense matter in nuclear statistical equilibrium are studied for densities and temperatures in the range $10^6 \leq \rho \leq 10^{12}$g/cm^3 and $2 \times 10^9 \leq T \leq 10^{10}$ °K. With increasing density the stability shifts to more and more neutron-rich nuclei. With increasing temperature the general tendency is that nuclei of smaller charge become more abundant, and the abundances of nuclei near a peak tend to become nearly as large as that of the peak nucleus. The shifting of the most stable region with change of density or temperature takes place rather abruptly from one neutron closed shell region to the next. For densities $\leq \sim 10^6$ g/cm^3, the ordinary iron group nuclei are most stable until the temperature becomes about 5×10^9 °K; for higher temperatures matter in equilibrium consists of almost pure helium. For higher density, this transition to a helium phase takes place at a somewhat higher temperature, and the equilibrium configuration for temperatures below the helium transition point shifts to the neutron-rich side of the valley of beta stability. When $T \leq 10^{10}$ °K, matter consists of almost pure neutrons at all densities. Rates of beta reactions and neutrino emission generally increase with increase of density and temperature. At a typical temperature of about 5×10^9 °K, the neutrino energy emission rate increases from about 2×10^{11} ergs/g sec at $\rho \sim 10^6$g/cm^3 to about 2×10^{17} erg/g sec at $\rho \sim 3 \times 10^{11}$ g/cm^3. (auth)

4856 THE BINDING ENERGY OF THE DEUTERON. Prestwich, W. V.; Kennett, T. J.; Hughes, L. B.; Fiedler, J. (McMaster Univ., Hamilton, Ont.). Can. J. Phys., 43: 2086-7(Nov. 1965).

Using the recent precision measurements for the ^{24}Mg and ^{60}Ni gamma-ray transitions (Murray et al. 1965) and the electron rest mass (Cohen et al. 1962), the energy of the gamma ray resulting from the reaction H(n,γ)D was determined. The measurement was undertaken to improve the precision of the deuteron binding energy and to resolve the discrepancy of 5 kev existing between the NaI(Tl) results of Monahan et al. and the crystal spectrometer results of Knowles. (auth)

4857 HYPERFINE STRUCTURES OF GROUND LEVELS OF TERBIUM. SIGN AND NUCLEAR QUADRUPOLAR MOMENT OF ^{159}Tb. Arnould, Claire; Gerstenkorn, Simon (CNRS, Bellevue, France; Commissariat a l'Energie Atomique, Paris). Compt. Rend., 261: 1488-91 (Aug. 9, 1965). (In French).

The study of the hyperfine structures of the first three levels $^8G_{11/2}$, $^8G_{13/2}$, and $^8G_{15/2}$ of the configuration $f^6\,ds^2$ of Tb I, using a photoelectric Fabry-Perot spectrometer, and the knowledge of the wave functions of these levels deduced from the classification of the arc spectrum made it possible by using the value of the magnetic moment given by Bleaney, to determine the values $\langle a_0^3/r^3\rangle_4 f$ and $\langle a_0^3/r^3\rangle_5 d$ as equal to 8.30 ± 0.08 and 2.82 ± 0.4, respectively. The value of the quadrupole moment calculated by this method was found to be 1.26 ± 0.12 b. (tr-auth)

4858 STUDY OF THE EXCITATION CURVES OF THE (t,α) REACTION ON ^{16}O BETWEEN 1 AND 3 Mev. Gerardin, Claude; Wery, Michel; Seltz, Raymond; Magnac-Valette, Denise (CRN, Strasbourg). Compt. Rend., 261: 1512-14 (Aug. 9, 1965). (In French).

The excitation curves of the reaction $^{16}O(t,\alpha_0)^{15}N$ + 7.687 Mev were studied with incident tritons at energies between 1.4 and 3.4 Mev. Among the maxima detected, the ^{19}F resonances obtained in ^{18}O + P by Scherrer were found. (tr-auth)

4859 ANALYSIS OF THE ELASTIC SCATTERING OF α PARTICLES ON LIGHT NUCLEI USING OPTICAL POTENTIALS. Fayard, Claude; Lamot, Georges-Henri; El-Baz, Edgard; Lafoucriere, Joseph (Institut de Physique Nucleaire, Lyon). Compt. Rend., 261: 1663-6(Aug. 18, 1965). (In French).

In order to determine the optical potential parameters for the elastic scattering of α particles, the angular distributions obtained on ^{16}O, ^{20}Ne, ^{24}Mg, ^{28}Si at 28.5 Mev were analyzed. The curves were optimized by a χ^2 method. (tr-auth)

4860 LIGHT ISOTOPES OF POLONIUM PRODUCED BY NUCLEAR REACTIONS OF ^{12}C IONS ON PLATINUM. Brun, Colette; le Beyec, Yvon; Lefort, Marc (Univ. Paris, Orsay, France). Compt. Rend., 261: 1667-9 (Aug. 18, 1965). (In French).

The 199 to 202 isotopes of polonium were produced by reactions of accelerated carbon ions, C^{4+}, on a Pt target. It was shown that the α rays of 5.67 and 5.77 Mev come from the 201 isotope for which two isomeric levels were detected. From the comparison of the cross sections it was found that an average energy from 5 to 6 Mev per neutron emitted was necessary to obtain the most favorable conditions for a (C, xn) reaction. (tr-auth)

4861 DECAY OF ^{192}Re. Blachot, Jean; Monnand, Edouard; Moussa, Andre (Centre d'Etudes Nucleaires, Grenoble, France). Compt. Rend., 261: 1835-8(Aug. 23, 1965). (In French).

The rhenium-192 produced by the nuclear reaction $^{192}Os(n, p)\,^{192}Re$ with neutrons at 14 to 15 Mev was studied by γ spectrometry. The γ spectrum of the deexcitation of ^{192}Os was obtained, and the half life of ^{192}Re was measured as $T_{1/2} \cong 6.2 \pm 0.8$ sec. (tr-auth)

4862 DECAY OF ^{183}Hf. Blachot, Jean; Nobar, Youssef Motavalledi; Berthier, Jean (Centre d'Etudes Nucleaires, Grenoble, France). Compt. Rend., 261: 1956-9(Aug. 30, 1965). (In French).

^{183}Hf, produced by the reaction $^{186}W(n,\alpha)\,^{183}Hf$, was studied by scintillation and coincidence β and γ spectrometry. The existence of γ rays at 140, 165, 210, 280, 320, 405, 465, 610, 720, 820, and 900 kev was shown. The β spectrum shows 3 branches with maximum energies at 1570 kev (25%), 1200 kev (50%), and 650 kev (25%). (tr-auth)

4863 NUCLEAR MATRIX ELEMENTS OF THE TRANSITION $^{42}K(2^-) \xrightarrow{\beta} {}^{42}Ca(2^+)$. Andre, Stephane; Menet, Jacques; Depommier, Pierre (Univ., Grenoble, France; Centre d'Etudes Nucleaires, Grenoble, France). Compt. Rend., 261: 2087-90(Sept. 6, 1965). (In French).

The 6 nuclear matrix elements of the transition $^{42}K(2^-) \xrightarrow{\beta} {}^{42}Ca(2^+)$ were determined from measurements of the shape of the β spectrum, the β-γ directional correlation, and the polarized β-γ correlation. The results can not be explained by a pure $n(f_{7/2}) \rightarrow p(d_{3/2})$ transition. For one of the zones of solutions, the ratio $\int\vec{r}/\int i\vec{\alpha}$ is in agreement with the value predicted by the conserved vector current theory. (tr-auth)

4864 ELASTIC SCATTERING OF 1.12 Mev GAMMA-RAYS FROM PLATINUM AND TANTALUM. Anand, S.; Singh, M.; Sood, B. S. (Punjab Univ., Chandigarh, India). Curr. Sci. (India), 34: 581(Oct. 20, 1965).

Elastic scattering cross sections were estimated for 1.12-Mev gamma rays on platinum and tantalum at various angles and were compared with other theoretical and experimental results. The method of estimation consists in plotting the scattering amplitudes for mercury at different momentum transfers, from which the index of the Z-dependence is obtained. The results calculated from the Z-dependence relation for the elastic scattering cross sections are tabulated for platinum and tantalum. (L.B.S.)

4865 DECAY SCHEME AND DIRECTIONAL CORRELATIONS OF GAMMA RAYS FROM ^{182}Ta. Venkata

Reddy, K.; Venkatapathi Raju, B. B.; Rama Mohan, R. V.; Jnanananda, Swami (Andhra Univ., Waltair, India). Indian J. Pure Appl. Phys., 3: 284-7(Aug. 1965).

A slow-fast triple coincidence spectrometer was assembled and tested for directional correlation measurement of gamma rays, using the well-known ^{60}Ni cascade. From directional correlation studies using this instrument, the correlation coefficients A_2 and A_4 of the correlation function of the type $W(\theta) = 1 + A_2P_2 \cos\theta + A_4P_4 \cos\theta$ were evaluated for nine cascades (67-1222, 67-1122, 67-264, 100-1250, 100-229, 100-1122, 1222-152, 1122-152 and 229-1003 kev.), in the decay of ^{182}Ta. It was found that for ^{182}W there is a ground state rotational band consisting of the 0, 100, and 329-kev levels with spins of 0, 2, and 4 respectively. The spins of the excited states and multipolarities of the gamma transitions evaluated from angular correlation measurements are in good agreement with those obtained from measurements using conventional methods. (auth)

4866 ON THE PROPERTIES OF LEPTON IRRADIATION PRODUCED BY NEUTRINO REACTION WITH A SUBSTANCE. Shishkin, G. V. (Inst. of Heat and Mass Exchange, Academy of Sciences, USSR). Izv. Vyssh. Ucheb. Zavendenii, Fiz., No. 4, 166-71(1965). (In Russian).

The properties of leptons produced by the interaction of neutrinos with matter were investigated. The probability for the formation of lepton radiation was calculated with consideration of their longitudinal and transverse polarization status for (V, A) variants of weak tetrafermion interactions. Special consideration was given to the case where vectors of polarization (and therefore the vector of the degree of transverse and longitudinal polarization) forming the leptons do not depend upon the constant of the bond GV and GA of weak interactions and all leptons of the beam produce polarization. (tr-auth)

4867 NUCLEAR QUADRUPOLE SPECTRA IN VERY ASYMMETRIC FIELD GRADIENTS. Alexander, S.; Ganiel, U. (Weizmann Inst. of Science, Rehovoth, Israel). J. Chem. Phys., 43: 4060-4(Dec. 1, 1965).

Pure nuclear quadrupole resonance spectra in asymmetric field gradients are discussed. Contrary to the usual approach, the fully asymmetric case ($\eta = 1$) was taken as a starting point. It is shown that in this case the Hamiltonian has an important symmetry property, which gives information on the energy-level spectrum and relations between the eigenfunctions. Closed solutions in terms of quadratic equations can be obtained for spins up to $\frac{9}{2}$. A perturbation expansion around $\eta = 1$, which seemed to converge very well, is also described. (auth)

4868 FAST NEUTRON CAPTURE IN RHENIUM. Stupegia, D. C.; Schmidt, M.; Madson, A. A. (Argonne National Lab., Ill.). J. Nucl. Energy: Pt. A and B, 19: 767-73(Oct. 1965).

Using an activation method, the neutron capture cross section of ^{185}Re and ^{187}Re, and the cross section for the production of the 18.7-min state of ^{188}Re were measured as a function of neutron energy between 4 kev and 2.6 Mev. (auth)

4869 STUDY OF THE SECOND STEP OF THE REACTION ^{7}Li(d,n)^{8}Be; ^{8}Be = 2α. Lemeille, C. (Centre d'Etudes Nucleaires, Saclay, France); Marquez, L.; Saunier, N.; Steyaert, J. J. Phys. (Paris), 26: 330-4 (June 1965). (In French).

The energy spectra of the alpha particles coming from the two step reaction d + ^{7}Li = n + ^{8}*Be, ^{8}*Be = 2α were measured. The measurements were made at incident energies between 3 and 7 Mev and angles between 30 and 90°. The observed spectra can be explained quantitatively if it is assumed that the intermediate level in ^{8}*Be is the level at 16.63 Mev excitation and if the angular distribution of the neutrons has a stripping shape. (auth)

4870 STUDY OF ^{16}O(d,α_0), ^{16}O(d,p_0) AND ^{16}O(d,p_1) REACTIONS AT 300 kev TO 1 Mev. EXPERIMENTAL RESULTS. Longequeue, N.; Beaumevieille, H.; Ligeon, E.; Longequeue, J. P.; Sandon, M. (Universite et Centre d'Etudes Nucleaires, Grenoble, France). J. Phys. (Paris), 26: 367-72 (June 1965). (In French).

The reactions ^{16}O(d,α_0), ^{16}O(d,p_0) and ^{16}O(d,p_1) were studied in the energy range 300 kev-1 Mev. The experimental results for α_0 and p_0 suggest the two ^{18}F* levels: E_d = 480 and 650 kev. The angular distributions for p_1 suggest that at very low energy the reaction ^{16}O(d,p_1) proceeds by Coulomb stripping. (auth)

4871 TIME PARITY NONCONSERVATION IN STRONG INTERACTIONS. Lobov, G. A. JETP Lett. (USSR) (Engl. Transl.), 1: 157-9(June 15, 1965).

The correlation of the pulses of two cascade gamma quanta are calculated for the general case when both gamma transitions are mixed. The polarized nucleus is allowed to go from an excited state with a certain momentum and polarization to a state with a different momentum by emitting a mixed gamma quantum of multipolarity, followed by transition to another state by emission of another quantum. (J.F.P.)

4872 STRUCTURAL BASIS OF NEUTRON AND PROTON MAGIC NUMBERS IN ATOMIC NUCLEI. Pauling, Linus. Nature, 208: 174(Oct. 9, 1965).

It was found that the magic numbers have a very simple structural significance: 2 and 8 correspond to the closed shells $1s^2$ and $1s^21p^6$, and the others to a closed-shell core with an outer layer (the mantle of the nucleus) containing the number of spherons (helion, helium-4, tritons, helium-3, or dineutrons) required to surround the core in closest packing. The magic-number structures of atomic nuclei are given. It is concluded that the stability that characterizes the magic numbers results from the completion of shells for a single layer (2,8) or two layers (20) of spherons, or, for the larger magic numbers (50, 82, 126), for the core layers, the mantle having a completed shell plus a completed sub-sub-shell. (J.F.P.)

4873 EXPLANATION OF THE BETA DECAY OF ^{32}P IN TERMS OF A CANCELLATION EFFECT IN THE ALLOWED MATRIX ELEMENT. Coussement, R. (Univ., Louvain, Belg.). Nucl. Phys., 75: 1-9(1965).

Taking into account configuration mixing, high ft values for allowed transitions can be explained by a cancellation effect in the allowed matrix element, and the non-linear spectrum shape by the interference term of the second-forbidden matrix element $\int\alpha \times r$ with the allowed $\int\sigma$. (auth)

4874 COMPARATIVE HALF-LIVES OF $\Delta I = 3$, NO BETA TRANSITIONS, IN EVEN NUCLEI. Brahmavar, S. M. (Panjab Univ., Chandigarh, India). Nucl. Phys., 75: 79-80(1965).

The quantity $\log f_0^3t = \log(\langle S_0^3\rangle f_0t)$, which takes into account the dependence of the shape factor S_0^3 in the integration over the spectrum, is expected to be a better constant for $\Delta I = 3$, no beta transitions, than the usual ft value. A survey and analysis of all such transitions indicates anomalies for two transitions in ^{26}Al. (auth)

4875 ELECTRON CAPTURE RATIOS IN THE DECAY OF ^{202}Tl. Leutz, H.; Schulz, G.; Wenninger, H. (Univ., Heidelberg). Nucl. Phys., 75: 81-100(1965).

The following electron capture ratios in ^{202}Tl leading to the ground state (index 0), to the 440-kev level, and to the 965-kev level of ^{202}Hg were determined with NaI(Tl) scintillation crystals containing ^{202}Tl as a constituent of the crystal lattice: $(P_L/P_K)_0 = 0.22^{+0.07}_{-0.015}$, $(P_L/P_K)_{440} = 0.196 \pm 0.002$, $(P_L/P_K)_{965} = 0.305 \pm 0.020$, $(P_M/P_L)_{440} = 0.269 \pm 0.007$, $(P_{N+} \ldots /P_M)_{440} = 0.3 \pm 0.1$. A transition energy of 1237 ± 20 kev was calculated from the $(P_L/P_K)_{440}$ and $(P_L/P_K)_{965}$ ratios if no electron exchange correction was taken into account and the influence of matrix elements for first non-unique forbidden transitions was neglected. The largest electron exchange correction which is consistent with the $(P_L/P_K)_{440}$ and $(P_L/P_K)_{965}$ capture ratios, amounts to 1.5%. With external ^{202}Tl sources and NaI(Tl) and CsI(Tl) scintillation crystals the relative intensities of 965, 525, and 440 kev gamma quanta and the relative intensity of electron capture decay to the ground state were determined to be $I_{965}/I_{440} = (0.13 \pm 0.03)\%$, $I_{525}/I_{440} =$

$(1.0 \pm 0.3)\%$, and $I_0/(I_0 + I_{440}) = (5 \pm 1)\%$. The measured decay curve of ^{202}Tl yields a half-life of 12.4 ± 0.1 d. (auth)

4876 ON THE SPONTANEOUS FISSION OF NUCLEI. Urin, M. G. (Inst. of Physics and Engineering, Moscow); Zaretskii, D. F. Nucl. Phys., 75: 101-8(1965).

Spontaneous fission half lives are analyzed in terms of the superfluid model of nuclei. The effect of the pair correlation on the parameters determining the potential barrier penetrability for fission is analyzed. The difference in the spontaneous fission period for even nuclei and odd-mass nuclei is interpreted. Periods versus nuclear excitation are investigated. The empirical Swiatecki formula is substantiated for even nuclei. (auth)

4877 HALF-LIVES OF THE FIRST EXCITED STATES IN ^{182}W AND ^{170}Yb. Rao, B. V. Narasimha; Jnanananda, Swami (Andhra Univ., Waltair, India). Nucl. Phys., 75: 109-12(1965).

The half-lives of the first excited states of ^{182}W and ^{170}Yb are measured with a fast time-to-amplitude converter. The half-life of the 100 kev level of ^{182}W is 1.43 ± 0.05 ns and that of the 84 kev level of ^{170}Yb is 1.6 ± 0.05 ns. Experimental internal conversion coefficients are calculated using the present values of the lifetime measurements and the published data of the Coulomb-excitation B(E2) values. Comparison with the theoretical internal conversion coefficients show an agreement within 1.5%. (auth)

4878 STUDY OF THE REACTION $^{12}C(n,n')3\,\alpha$. Moesner, Juergen; Schmidt, Guenter; Schintlmeister, Josef (Zentralinstitut fuer Kernforschung, Rossendorf, Ger.). Nucl. Phys., 75: 113-27(1965). (In German).

The reaction $^{12}C(n,n')3\alpha$ was studied in a CO_2 filled expansion cloud chamber operated at 200 torr in the state of expansion. A total of 1267 events were accepted for analysis. It was found that all events could be interpreted as cascade decays via the levels 7.65, 9.63, 10.1, 10.8, 11.2, 11.82 and 12.73 Mev of ^{12}C or 2.43 Mev of ^{9}Be and further via the ground state or the 2.9 Mev level of ^{8}Be or the ground state of ^{5}He. The relative cross sections of the different decay modes are given. The spin and parity of the 11.81 and 12.73-Mev levels of ^{12}C should be 2^- and 1^+, respectively. The inelastic scattered neutrons, which leave ^{12}C in the 9.63 Mev level, have an angular distribution symmetrical to 90° in the centre-of-mass system. The angular correlation of the α-particles emitted by ^{12}C in the 9.63 Mev level may be fitted by assuming the assignment $J = 3^-$ for the 9.63 Mev level. (auth)

4879 NUCLEAR REACTIONS IN NUCLEAR MATTER. Thouless, D. J. (Cambridge Univ., Eng.). Nucl. Phys., 75: 128-44(1965).

A number of topics in nuclear reaction theory are examined from the point of view of the liquid drop model. It is shown that, although the absolute value of the nucleon strength function at low energies has significance for high-energy experiments, it cannot be deduced from low-energy elastic scattering experiments, since the energy-dependence and the non-locality of the optical potential cannot be distinguished. The depth of the optical potential for a deuteron in the interior of a nucleus should be at least as great as the sum of the neutron and proton optical potential depths (minus the binding energy of a deuteron), or else the deuteron will dissociate in the interior. A simple inelastic interaction is considered and it is shown that, although the absolute value of the nucleon strength function again cannot be determined, the coefficients of the Bogoliubov-Valatin quasiparticle transformation can, under reasonable conditions, be deduced from such an experiment. The absorption of a nucleon in the nuclear surface is considered and it is shown that, in the absence of pairing, the surface absorption, like the volume absorption, goes to zero as $(E - E_F)^2$ when the energy E approaches the Fermi energy E_F. (auth)

4880 SOME ABSOLUTE BETA POLARIZATION MEASUREMENTS. van Klinken, J. (State Univ., Groningen, Ger.). Nucl. Phys., 75: 145-60(1965).

The longitudinal beta polarization of several transitions was investigated for energies varying from 46 to 261 kev. The beta polarization was first converted from longitudinal to transverse by deflection of the electrons in an electric field, after which the transversely polarized electrons were analyzed with the aid of a calibrated Mott analyzer. Results are reported for beta rays from ^{32}P, ^{60}Co, ^{114}In, ^{147}Pm, ^{147}Nd, ^{153}Sm and ^{198}Au. For energies larger than 100 kev, no large deviations from the expected value $P = -v/c$ were observed. At lower energies there exist deviations, which may partly be explained as an effect of screening, according to calculations of Bühring. Much attention was given to the effect of depolarization in sources of finite thickness, the influence of which increases towards lower energies. (auth)

4881 DOUBLE SCATTERING OF ELECTRONS. van Klinken, J. (State Univ., Groningen, Ger.). Nucl. Phys., 75: 161-88(1965).

The Mott asymmetry function for electrons with energies from 26 to 261 kev was investigated with an improved arrangement for double scattering of accelerated electrons. First, a beam of singly scattered electrons with a reproducible and well defined degree of transverse polarization was obtained by performing a double scattering experiment with identical scattering conditions for polarizer and analyzer. In this experiment scattering angles of 105° and gold foils of a standard thickness were used. The beam of singly scattered electrons was then used for calibration of a rotatable Mott analyzer, consisting of a second scattering foil and four scintillation counters. Two counters were set at large scattering angles for detection of the asymmetry due to polarization and two were set at 45° for simultaneous observation and elimination of instrumental asymmetries. It is shown that the 45°-zero measurement is very effective in reducing the influence of several instrumental effects. The calibrated analyzer can be used for polarization detection of other electron beams with a relatively large efficiency. The ratio of the numbers of incident and scattered electrons is about 0.6×10^{-3}. The instrument yields the absolute degree of transverse polarization of the incoming electrons with an accuracy of better than 1% in favorable cases. Measurements are reported of the energy dependence of the Mott function S at 45° and 105° and of its angular dependence at 121 kev. The results agree with those of Mikaélyan et al. but have higher accuracy. Qualitatively the present results show the energy and angular dependence of S predicted by theory. Measurements at small angles show a change of sign, as to the calculations. However, quantitative agreement is often poor. Especially at low energies and small angles the calculated S values are significantly larger than the observed values. (auth)

4882 ON THE THEORY OF NUCLEAR REACTIONS. I. SHELL-MODEL CALCULATIONS IN THE CONTINUUM. Weidenmueller, Hans A. (Univ., Heidelberg). Nucl. Phys., 75: 189-208(1965).

By a generalization of a method due to Fano, a theory of nuclear reactions is developed which applies to the elastic and inelastic scattering of nucleons. The method determines the positions and the total and partial widths of the resonances directly in terms of the eigenvalues and properties of a complex symmetric matrix. This matrix is the generalization of the usual shell-model matrix to resonant states. The formalism incorporates the exclusion principle exactly and without complication of the theory. Particular attention is paid to the description of threshold effects and to the possibility of obtaining simultaneously the eigenvalues of bound states and of resonant states. Single-particle resonances are easily incorporated into the formalism without our having to introduce projection operators. The S-matrix is decomposed into a slowly varying background term plus pole terms. For the latter a centre-of-gravity theorem is proved. A relationship is established which connects the sum over all the poles of the partial widths for a given channel with the total coupling strength of all the states with the continuum (corresponding to that channel). (auth)

4883 GAMMA DECAY OF ^{102}Tc AND ^{104}Tc. Zander, Arlen R.; Gray, Peter R.; Ebrey, Thomas G. (Phillips Petroleum Co., Bartlesville, Okla.). Nucl. Phys., 75: 209-14(1965).

The decay schemes of ^{102}Tc and ^{104}Tc were investigated by gamma spectroscopy coincidence methods. A new level at 2.705 Mev is assigned to ^{102}Ru, and decay schemes for both ^{102}Tc and ^{104}Tc are shown. (auth)

4884 STUDY OF THE INVERSE PHOTODEUTERON REACTION IN ^{11}B AND ^{16}O IN THE GIANT RESONANCE ENERGY REGION. Suffert, M. (Centre de Recherches Nucleaires, Strasbourg). Nucl. Phys., 75: 226-40(1965).

The radiative capture of deuterons by ^{9}Be and ^{14}N was studied in the energy range 0.5 Mev < E_d < 5.5 Mev using direct observation of the ground state gamma transition of about 20 Mev energy. After a short description of the experimental method the results of the measurements are given in the form of excitation curves and angular distributions. For the ^{9}Be(d,γ_0)^{11}B reaction the excitation curve shows no structure with a total peak cross section of about 8 μb. The results may be interpreted by direct E_1 capture besides the asymmetry of the angular distributions. For the ^{14}N(d,γ_0)^{16}O reaction, where the isospin selection rule forbids the E_1 transition, the excitation curve shows a peak at 22.7 Mev excitation energy with a total peak cross section of about 6 μb. The angular distribution at this energy has a predominantly dipole characteristic but also displays asymmetry. The peak cannot be identified with any peak of the giant E_1 resonance of ^{16}O. There are also indications for peaks at 22.2 and 24.5 Mev excitation energy. The possible interpretations for the ^{14}N(d,γ_0)^{16}O cross section are given. (auth)

4885 HARMONIC GENERATION IN A PLASMA DUE TO A VELOCITY-DEPENDENT COLLISION FREQUENCY. Krenz, J. H. (Univ. of Colorado, Boulder). Phys. Fluids, 8: 1871-5(Oct. 1965).

Harmonic components associated with the plasma electron velocity distribution function often result from a strong radio-frequency field. In this analysis, an expression is obtained for the third harmonic current which is a result of a velocity-dependent collision frequency. By introducing a low-collision frequency approximation and a collision frequency of the form $\nu = \kappa v^{\mu}$, the successive integrations necessary to obtain the third harmonic current are readily performed. As a result of this approximation which is valid for typical harmonic generation experiments, the third harmonic current is then shown to depend only upon various moments of the static isotropic part of the electron velocity distribution function. An estimate of this current is obtained by assuming a Maxwellian distribution. It is then shown that for a typical discharge configuration the third harmonic obtained due to this mechanism is small although not negligible compared to that observed experimentally. (auth)

4886 STUDY OF THE FORMATION OF α SUBSTRUCTURES ON THE SURFACE OF LANTHANUM NUCLEI BY MEASUREMENT OF THE CROSS SECTIONS OF ISOMERIC STATES OF ^{135}Cs PRODUCED IN THE REACTION ^{139}La (p,pα)^{135}Cs. Nguyen-Long-Den (Universite de Paris, Orsay, France). Phys. Letters, 18: 158-60(Aug. 15, 1965). (In French).

The different coupling configurations of nucleons in the lanthanum nucleus are examined. (J.S.R.)

4887 EUROPIUM-144. Messlinger, R.; Morinaga, H.; Signorini, C. (Max Planck Institut fuer Kernphysik, Heidelberg). Phys. Letters, 19: 133-4(Oct. 1, 1965).

A short lived activity which was assigned to europium-144, was found in measurements of (p,n) cross sections on N = 82 nuclei. The newly found activity is analogous to the ground state decay of praseodymium-140 and promethium-142. The activity was produced by bombarding a samarium-144 target with a proton beam. The decay curve measured with a silicon detector biased against low energy background radiation is shown. The value of the half life obtained from a number of measurements is 10.5 ± 0.3 seconds. Beta rays were observed with a plastic scintillator, but a search for gamma rays did not indicate the existence of any line of appreciable intensity. The threshold for the production of the activity was also measured. It was found to be 7.16 ± 0.03 Mev, which corresponds to 5.30 ± 0.03 Mev for the end point of the ground-state beta transition, in good agreement with the direct beta measurements. The log ft value of the ground state transition is obtained as 4.5, ignoring possible weak beta branching to excited states. The results confirm the assignments to the activity to ^{144}Eu. Also the reported 18 minute half life was investigated by bombarding ^{144}Sm by a 9.72-Mev proton beam. No evidence was found of this activity being due to a higher spin isomer. (J.F.P.)

4888 HYPERFINE STRUCTURE IN THE 2084-kev STATE OF ^{140}Ce. Levy, R. M.; Shirley, D. A. (Univ. of California, Berkeley). Phys. Rev., 140: B811-15(Nov. 22, 1965). (UCRL-11922).

Differential perturbed angular-correlation measurements were made on the 2084-kev state of ^{140}Ce in aqueous solution at room temperature, and in lanthanum metal both at room temperature and at 77°K. The derived g factor of +1.014 ± 0.038 is compared with Rho's theory and with other experimental values. The advantages of working with metals and at low temperatures are discussed. An upper limit of approximately 200°K is set on the quantity ΔE, where $\Delta E/k$ is the energy spacing between Γ_7 and Γ_8 for Ce^{3+} in La metal. An approximate value of 4.1 ± 0.4 atomic units is derived for $\langle r^{-3} \rangle$ of the cerium 4f electron, using the above upper limit for ΔE. (auth)

4889 DECAY OF THE 185-μsec ISOMER IN ^{166}Ho. Bjoernholm, S. (Univ., Copenhagen); Borggreen, J.; Frahm, H. J.; Hansen, N. J. Sigurd; Schult, O. Phys. Rev., 140: B816-20(Nov. 22, 1965).

The 185-μsec isomer in ^{166}Ho was produced by the ^{165}Ho (d,p) reaction and the delayed radiation studied with γ scintillation spectrometers and a magnetic β spectrometer. The results were combined with high-resolution measurements of the γ rays from thermal-neutron capture in ^{165}Ho, using a curved-crystal spectrometer. A $K^{\pi} = 3^+$ level at 190.90 kev decays by two K-forbidden E1 transitions of 19 and 136.66 kev to the 3^- and 2^- members, respectively, of the $K^{\pi} = 0^-$ ground-state rotational band of ^{166}Ho. (auth)

4890 NUCLEAR SPIN AND MAGNETIC MOMENT OF ^{37}Ar. Robertson, M. M. (Univ. of Wisconsin, Madison); Mack, J. E.; Cohen, V. W. Phys. Rev., 140: B820-3 (Nov. 22, 1965).

The hyperfine structure of the $3p^54s$-$3p^54p$ lines of ^{37}ArI, studied in an electrodeless discharge, was used to determine the nuclear spin $I(^{37}Ar) = 3/2$, and the nuclear magnetic moment $\mu(^{37}Ar) = (+0.95 \pm 0.20)$ nm. The ^{37}Ar-^{40}Ar isotope shift, which was completely resolved for only one line, tends generally to confirm earlier work. (auth)

4891 EXCITED-CORE MODEL IN ^{27}Al AND INELASTIC SCATTERING OF 14.2-Mev NEUTRONS. Bonazzola, G. C. (Univ., Turin; Istituto Nazionale di Fisica Nucleare, Turin); Chiavassa, E.; Bressani, T. Phys. Rev., 140: B835-7(Nov. 22, 1965).

Differential cross sections for 14.2-Mev neutron inelastic scattering to the first levels in ^{27}Al were measured at forward angles using a time-of-flight spectrometer. The experimental values agree with the predictions of the excited-core model; mixing between the ground state and the $5/2^+$ excited state must be allowed for, the square of the mixing parameter being $A^2 = 0.82 \pm 0.07$. (auth)

4892 (^{3}He,α) PICKUP REACTIONS IN ^{58}Ni AND ^{60}Ni. Brussel, M. K.; Rundquist, D. E.; Yavin, A. I. (Univ. of Illinois, Urbana). Phys. Rev., 140: B838-44(Nov. 22, 1965).

(^{3}He,α) pickup reactions in ^{58}Ni and ^{60}Ni were studied using 24.5-Mev $(^3He)^{2+}$ ions. Several new energy levels in ^{57}Ni were found. Angular distributions for l = 1 neutron transfer were found to be similar to one another, but different from angular distributions for l = 3 neutron trans-

fer. A j dependence of the angular distributions is suggested by the data, and some new spin assignments are proposed. (auth)

4893 NUCLEAR RECOIL AND SIMPLE NUCLEAR REACTIONS. Benioff, Paul A.; Person, Lucy Wu (Argonne National Lab., Ill.). Phys. Rev., 140: B844-62 (Nov. 22, 1965).

The nuclear-recoil properties of simple nuclear reactions are studied in the distorted-wave impulse approximation. Calculations of the differential recoil cross section $d^2\sigma/d\Omega_K dT_K$, and the recoil angular distribution $d\sigma/d\Omega_K$, for the $^{12}C(p,pn)^{11}C$ and $^{58}Ni(p,pn)^{57}Ni$ reactions at 450 Mev are presented and discussed. Relativistic kinematics are used and the calculations are not limited to coplanar events: they are valid for any type of kinematically allowed event. Harmonic-oscillator and exponential radial wave functions are used along with a complex, energy-dependent, Woods-Saxon optical potential. The calculations show appreciable differences between the exponential and harmonic-oscillator forms and also between distorted- and plane-wave calculations. In general, curves of $d^2\sigma/d\Omega_K dT_K$ plotted as a function of T_K for fixed θ_K, show steeper narrower peaks and larger flatter tails at $\theta_K = 90°$ than at $\theta_K = 0°$ or 180°. Comparison of the recoil angular distribution for outlying target neutron shells (1p in ^{12}C and 2p in ^{58}Ni) and interior shells (1s in ^{12}C and 1 f in ^{58}Ni) shows a definite sideways peaking for the outlying shells which is lacking for the interior shells. This effect is explained as being a result of the equatorial localization of reaction sites which is greater for outer shells than for inner shells. Comparison with the small number of experiment data available indicates satisfactory agreement, except possibly for sideways recoil angles where, according to Remsberg, another reaction mechanism may be contributing. (auth)

4894 MASS- AND CHARGE-DISTRIBUTION STUDIES IN THE FISSION OF ^{197}Au BY INTERMEDIATE-ENERGY HELIUM IONS. Lisman, F. L.; Brandhorst, H. W. Jr.; Cobble, J. W. (Purdue Univ., Lafayette, Ind.). Phys. Rev., 140: B863-70(Nov. 22, 1965).

The absolute fission yields of twelve nuclides from the helium-ion-induced fission of ^{197}Au were determined radiochemically at 40.0, 37.0, and 33.5 Mev. The mass yield distributions were observed to be symmetric, and an upper limit of approximately 0.03% for an asymmetric fission mode was obtained. Independent and cumulative yield data were best correlated with the constant-charge-ratio postulate, although the charge distribution about Z_p was Gaussian and similar to those observed by others in heavier-element nuclides. The width of the mass distributions was invariant over the energy range studied, and fewer neutrons appear to be emitted than was previously reported. The total fission cross sections are in good agreement with those obtained by others using purely instrumental techniques. (auth)

4895 POLARIZATION OF NEUTRONS FROM THE D(d,n)^{3}He REACTION. Purser, F. O. Jr.; Sawers, J. R. Jr.; Walter, R. L. (Duke Univ., Durham, N. C.). Phys. Rev., 140: B870-6(Nov. 22, 1965).

Angular distributions of the polarization of neutrons from the D(d,n)^{3}He reaction were obtained at several deuteron energies from 1.9 to 3.7 Mev. The polarization at 45° cm ranged from -0.109 ± 0.013 at 1.9 Mev to -0.027 ± 0.015 at 3.7 Mev. Similar measurements presently available in the literature are reviewed and shown to fall into two conflicting sets, one of which is confirmed by the present measurement. All presently available angular distributions of the differential polarization were fitted to the expansion $P_1(\theta)\sigma(\theta) = \Sigma_n a_n \sin 2n\theta$, and except for a previous measurement at 0.375 Mev, there is no evidence for terms of higher order than n = 2 in the expansion. The coefficients of this expansion were tabulated to permit interpolation of the differential polarization over deuteron energy and reaction angle. (auth)

4896 (n,d) REACTION STUDIES ON ^{58}Ni, ^{63}Cu, AND ^{64}Zn. Wang, W. N.; Winhold, E. J. (Rensselaer Polytechnic Inst., Troy, N. Y.). Phys. Rev., 140: B882-7 (Nov. 22, 1965).

Studies were made of (n,d) pickup reactions on ^{58}Ni, ^{63}Cu, and ^{64}Zn initiated by 14-Mev neutrons. Deuteron spectra at a series of forward angles were measured using a counter telescope, and distorted-wave Born-approximation fits were made to the data. For ^{63}Cu, the 1.17-Mev 2+ state in ^{62}Ni is excited with a cross section of 0.5 that of the ^{62}Ni ground state. For ^{64}Zn, transitions to the ground and 0.67-Mev states of ^{63}Cu involve p-particle pickup. Transitions to the 0.96-Mev $5/2^-$-state are not observed, indicating that the $f_{5/2}$ proton component in the ^{64}Zn ground state is small. Strong transition strength to the 1.33-Mev $1/2^-$-level suggests that this state has a significant $(f_{5/2})^{-1}$ proton single-particle component, in addition to the core excitations included in recent calculations. In ^{58}Ni, excitation of the 1.37-Mev level with S = 0.6 implies a significant 2p proton admixture in the ^{58}Ni ground state. (auth)

4897 QUANTITATIVE NUCLEAR EVAPORATION THEORY. II. PROTON EVAPORATION. Beard, David B.; McLellan, Alden (Univ. of California, Davis). Phys. Rev., 140: B888-97(Nov. 22, 1965).

The transmission of protons into an infinitely absorbing Eckart-Bethe diffuse-nuclear-potential well was calculated exactly as a function of nuclear size, proton energy, and angular momentum. The transmission varies by an order of magnitude from that computed by others in the critical energy range where the peak of the evaporated proton spectrum occurs. The computed transmission is used to calculate the spectra of protons emitted from excited nuclei and the reaction cross sections for (p,pn), (p,2n), and (p,2p) processes. The fit with experimental data is excellent. (auth)

4898 NUCLEAR SIZE DETERMINATION BY NEUTRAL-PION PHOTOPRODUCTION. Schrack, Roald A. (National Bureau of Standards, Washington, D. C.). Phys. Rev., 140: B897-904(Nov. 22, 1965).

The angular distributions of neutral mesons (π) produced by 166-Mev bremsstrahlung on Li, Be, C, O, Mg, Al, Si, S, Ca, and Cu were obtained by coincident detection of the meson (π) decay photons. The density distributions of nuclear matter were inferred from the experimental data by means of a Monte Carlo synthesis based on an impulse-approximation elastic-coherent-production model. (auth)

4899 LOW-LYING LEVELS IN ^{50}V AND ^{58}Co STUDIED WITH THE (p,d) REACTION. Ball, J. B.; Sweet, R. F. (Oak Ridge National Lab., Tenn.). Phys. Rev., 140: B904-7(Nov. 22, 1965). (ORNL-P-1433).

The low-lying levels in the odd-odd nuclei ^{50}V and ^{58}Co were studied by means of the (p,d) reaction produced with 22-Mev protons from the ORNL 86-inch cyclotron. The deuteron spectra were obtained with a magnetic-spectrograph system having an overall energy resolution of about 30 kev. The levels observed in ^{50}V are compared with recent calculations on $f_{7/2}$ shell nuclei. The levels observed in ^{58}Co are used to calculate the expected level scheme for ^{56}Co. (auth)

4900 TRANSVERSE POLARIZATION OF K-CONVERSION ELECTRONS FOLLOWING THE β DECAY OF ^{198}Au. Rasera, R. L.; Steffen, R. M. (Purdue Univ., Lafayette, Ind.). Phys. Rev., 140: B1177-81(Dec. 6, 1965). (COO-1420-116).

The degree of transverse polarization $P_{||}(\theta) = K_K(\nu/c)\sin\theta$ of the K-conversion electrons following the beta decay of ^{198}Au was measured with a view to the determination of the particle parameter $b_{1,||}$ (E2). The experimental result was obtained using a lens spectrometer to focus the conversion electrons on a thin gold foil, and measuring the Mott-scattering asymmetry δ of the counts in coincidence with those detected in a beta detector placed opposite the source at an angle θ of 90° with the spectrometer axis. The measured asymmetry of $\delta = -0.044 \pm 0.013$ yields a value of

$K_K = +0.43 \pm 0.17$, with all instrumental corrections applied. Given the beta-decay angular correlation coefficient $A_1(\beta)$ known from beta circularly polarized gamma correlations, the particle parameter is found to be $b_{1,||}(E2) = -1.0 \pm 0.4$. This value, although in disagreement with previous measurements, agrees with the value calculated by Becker and Rose. (auth)

4901 INFLUENCE OF MULTIPLE VIRTUAL TRANSITIONS ON THE REORIENTATION EFFECT IN COULOMB EXCITATION. Masso, J. F.; Lin, D. L. (Yale Univ., New Haven). Phys. Rev., 140: B1182-90(Dec. 6, 1965). (YALE-1807-29).

Calculations of the reorientation effect in Coulomb excitation of the first 2^+ state of even-even nuclei are extended by employing the semiclassical approximation to take into account second- and third-order virtual E2 transitions to higher excited states. Deviations from first-order perturbation theory in the excitation probability are investigated numerically as a function of the bombarding energy and the scattering angle for heavy-ion projectiles. Results are presented for rotational and vibrational nuclei as a guide in the selection of conditions suitable for the determination of the static quadrupole moment of the lowest 2^+ state. Conditions for the practical convergence of the perturbation expansion are discussed. (auth)

4902 QUADRUPOLE DEFORMATION IN ^{7}Li. Kurath, Dieter (Argonne National Lab., Ill.). Phys. Rev., 140: B1190-2(Dec. 6, 1965).

The quadrupole deformation of ^{7}Li is calculated by generating many-particle wave functions from deformed single-particle orbitals. In order to account for the E2 properties of ^{7}Li and retain the dominance of the basic shell-model configuration, excitation of the $(1s)^4$ core must be included. The admixtures of higher configurations are appreciable. (auth)

4903 VALIDITY OF THE ξ APPROXIMATION FOR THE $^7/_2^-(\beta)\,^7/_2^+$ DECAY IN $^{141}_{58}$Ce. Rao, W. V. S.; Rao, V. S.; Sastry, D. L.; Jnanananda, S. (Andhra Univ., Waltair, India). Phys. Rev., 140: B1193-6(Dec. 6, 1965).

The energy dependence of the beta-gamma directional correlation was measured for the $^7/_2^-(\beta)^7/_2^+(\gamma)^5/_2^+$ beta-gamma cascade in the decay of ^{141}Ce with a slow-fast scintillation assembly in the beta energy region 165.5 to 422.5 kev. Results from the integral correlation showed that the correlation coefficient ϵ_4 was zero within experimental errors, while those from the differential correlation experiment showed that the coefficient ϵ_2 was small throughout the energy range, and the results were in accordance with the use of the ξ approximation to explain the inner beta transition of ^{141}Ce. (auth)

4904 ^{7}Li QUADRUPOLE MOMENT. [PART] III. Morris, B. M.; Present, R. D. (Univ. of Tennessee, Knoxville). Phys. Rev., 140: B1197-8(Dec. 6, 1965).

The electric-quadrupole moment Q of the ^{7}Li nucleus was calculated on the basis of the Wigner supermultiplet theory with configuration mixing that preserves the partition symmetry and LS coupling. The experimental value of Q can be obtained with an ad hoc mixture of configurations in which the p shell alone is excited and in which the ground configuration is predominant (65%). The linearly independent symmetrized seven-nucleon wave functions for the ^{2}P[4 + 3] states arising from the $1s^31p^31d$ configuration were constructed and the matrix elements of Q evaluated. The experimental value of Q can be obtained with ad hoc mixtures of $1s^41p^3$, $1s^41p^22P$, $1s^41p^31f$, and $1s^31p^31d$ in which the proportion of the ground configuration is over 85%. All of the electromagnetic and beta-decay properties of the A = 7 nuclei are explained on this model. (auth)

4905 STUDIES OF ELECTROMAGNETIC TRANSITIONS IN ^{15}N AND ^{15}O. Warburton, E. K.; Olness, J. W.; Alburger, D. E. (Brookhaven National Lab., Upton, N. Y.). Phys. Rev., 140: B1202-25(Dec. 6, 1965). (BNL-9360).

Electromagnetic transitions in ^{15}N and ^{15}O were investigated following the population of the bound levels of these nuclei by ^{14}N + d, ^{14}O + d, ^{13}C + ^{3}He, and ^{16}O + ^{3}He with bombarding energies from 1.9 to 6.7 Mev. Gamma-ray angular distributions and relative intensities were determined using a three-crystal pair spectrometer. Gamma-ray branching ratios in ^{15}N were determined through measurements of proton-gamma coincidence spectra following the ^{14}N(d,p)^{15}*N and ^{13}C(^{3}He,p)^{15}*N reactions. The ratios of radiative width to total width for the unbound 10.45- and 10.81-Mev levels of ^{15}N were obtained as $\Gamma_\gamma/\Gamma > 0.7$ and $\Gamma_\gamma/\Gamma = 0.55^{+0.25}_{-0.15}$, respectively. Gamma-ray branching ratios in ^{15}N and ^{15}O were determined from measurements of gamma-gamma coincidence spectra using ^{14}N + d, ^{14}C + d, and ^{16}O + ^{3}He. Evidence was found for an excitation energy for the sixth excited state of ^{15}O of 7.284 ± 0.007 Mev, rather than 7.17 ± 0.05 Mev as previously reported. Singles gamma-ray spectra were measured from all four targets using a lithium-drifted germanium detector. In these measurements, gamma-ray cascades to the 5.3-Mev doublet of ^{15}N were separated, and it was determined that all the bound levels of ^{15}N and ^{15}O except the ^{15}N 5.270- and ^{15}O 5.240-Mev levels have mean lifetimes less than 5×10^{-13} sec. An intermediate-image magnetic spectrometer was used to study the angular correlation of internal pairs for ten ground-state transitions in ^{15}N and ^{15}O. From this work it was determined that the ^{15}N 8.57-Mev level has $J^\pi = 3/2^+$, the ^{15}N 9.06- and 10.07-Mev levels have $J^\pi = 1/2^+$ or $3/2^+$, the 9.76- and 9.93-Mev levels are most probably $J^\pi = 1/2^+$ or $3/2^+$, and the 9.16-Mev level is most probably $J^\pi = 5/2^-$. For the remaining levels the measurements serve to restrict the range of possible spin-parity assignments. The correspondence between mirror levels in ^{15}N and ^{15}O is discussed, and a comparison with theoretical predictions is made. (auth)

4906 ELASTIC SCATTERING OF 160-Mev PROTONS FROM ^{9}Be, ^{40}Ca, ^{58}Ni, ^{120}Sn, AND ^{208}Pb. Roos, Philip G.; Wall, N. S. (Massachusetts Inst. of Tech., Cambridge; Univ. of Maryland, College Park). Phys. Rev., 140: B1237-44(Dec. 6, 1965).

A good-resolution total-energy scintillation spectrometer was used to measure the elastic-scattering differential cross sections of 160-Mev protons from ^{9}Be, ^{40}Ca, ^{58}Ni, ^{120}Sn, and ^{208}Pb. Optical-model analyses of the data were made and the pertinent parameters are given. The most significant result of the analyses is that the extent of the imaginary part of the optical potential has a radius of the order of 10^{-13} cm greater than that of the real part, independent of atomic weight. (auth)

4907 STUDIES ON ^{19}F IN THE ^{18}O(p,γ)^{19}F REACTION. Allen, J. P. (Yale Univ., New Haven); Howard, A. J.; Bromley, D. A.; Olness, J. W. Phys. Rev., 140: B1245-57(Dec. 6, 1965).

Studies of the ^{18}O(p,γ)^{19}F reaction at the 849-kev resonance established decay schemes for the 8.76-Mev resonance level and also for the 3.91-Mev level which is populated through de-excitation of the former by an 18% branch. Angular-correlation measurements establish a $J = 3/2$ assignment for the 3.91-Mev level. A level of this spin assignment is not predicted by the intermediate-coupling shell models, but all collective models which were applied to ^{19}F and which imply a strong prolate deformation of the nucleus predicted a $3/2^+$ state in this energy region. Selection rules based on the asymptotic Nilsson model provide an excellent description of the de-excitation branching ratios for both the 8.76- and the 3.91-Mev states demonstrating the utility of these rules even in so light a nucleus. Additional measurements at the 1169-kev resonance determined the decay scheme for the 9.07-Mev resonance level, which de-excites strongly through the 2.79-Mev level. The limitation $J = 5/2$ or $9/2$ on possible spin assignments for the 2.79-Mev level is confirmed; however, simple angular-distribution measurements can not distinguish between these two possibilities. (auth)

4908 STUDY OF THE ^{19}F(^{3}He,d)^{20}Ne REACTION. Siemssen, R. H. (Argonne National Lab., Ill.); Lee, L. L. Jr.; Cline, Douglas. Phys. Rev., 140: B1258-66 (Dec. 6, 1965).

The reaction $^{19}F(^3He,d)^{20}Ne$ was studied at ^3He energies of 9.5 and 10.0 Mev. Angular distributions were measured for deuteron groups leading to final states in ^{20}Ne up to an excitation of 7.43 Mev. The elastic scattering of 9.0-Mev ^3He on ^{19}F was also measured. The reaction data were analyzed by use of the zero-range distorted-wave Born approximation and spectroscopic information was extracted. Angular distributions characteristic of a stripping mechanism were observed for the reactions to the ground state ($l_p = 0$), 1.63-Mev state ($l_p = 2$), 5.80-Mev state ($l_p = 1$), 6.72 Mev state ($l_p = 0$), and 7.43-Mev state ($l_p = 2$). The reactions to the 4.25-, 4.97-, 5.63-, and 7.02-Mev excited states had small cross sections with little angular structure and were probably excited by other reaction mechanisms. The results are in reasonable agreement with the predictions of both the Nilsson model and the extreme SU(3) classification of the shell model that assumes a dominant long-range quadrupole residual interaction. (auth)

4909 SMALL-ANGLE SCATTERING OF NEUTRONS BY NUCLEI. Redmond, Robert F. (Battelle Memorial Inst., Columbus, Ohio). Phys. Rev., 140: B1267-72 (Dec. 6, 1965).

The partial-wave phase shifts for the scattering of neutrons by nuclei are considered with some emphasis on large values of orbital angular momentum l. It is shown that a rather simple general approximation technique for obtaining the phase shifts follows from the scattering integral equation for the partial-wave amplitudes. This method is used to study the electromagnetic scattering of neutrons by nuclei. It is shown that the first-order approximation for the phase shifts gives a small but non-negligible correction to the Born approximation (zero order) even for large l. However, it is shown that higher order approximations tend to reduce the correction significantly. The interference effects between the electromagnetic scattering and the nuclear scattering are also considered. For large l the scattering tends to be dominated by the electromagnetic scattering. However it is found that if the nuclear spin-orbit interaction is sufficiently strong then the nuclear scattering can become important even for large l. It is suggested that this effect may be significant in explaining the anomalous small-angle scattering of neutrons by Th, U, and Pu nuclei. (auth)

4910 CALCULATION OF THE (π^-,π^0) REACTION ON COMPLEX NUCLEI. Kaufman, Sheldon B.; Hower, Charles O. (Princeton Univ., N. J.). Phys. Rev., 140: B1272-6(Dec. 6, 1965). (PPAD-2137-544).

The excitation function for the reaction $_zA(\pi^-,\pi^0)_{z-1}A$ was calculated using the Fermi-gas model of the nucleus and the impulse approximation. Experimental data on the differential cross section of the free-particle reaction $\pi^- + p \rightarrow \pi^0 + n$ was used, and the effect of the momentum distribution of the nucleons on the kinematics was included. The predicted cross section shows a minimum near 200 Mev and maxima near 100 and 350 Mev. This structure, if confirmed experimentally, would lend support to this simple model, which is frequently used to interpret high-energy nuclear reactions. (auth)

4911 FAST-NEUTRON CAPTURE CROSS SECTION OF ^{64}Ni. Grench, H. A. (Lockheed Palo Alto Research Labs., Calif.). Phys. Rev., 140: B1277-82(Dec. 6, 1965).

The fast-neutron capture cross section of ^{64}N was measured by the activation technique at 18 neutron energies between approximately 0.2 and 2.0 Mev. The measurements were made relative to the $^{197}Au(n,\gamma)^{198}Au$ cross section. The results are interpreted in terms of the statistical theory of nuclear reactions and the Fermi-gas level-spacing model. A good fit to the data was obtained with the adjustment of a single free parameter. A value of 0.34 ev was obtained for the average radiation width of the $\frac{1}{2}$+ levels in ^{65}Ni at the neutron binding energy. (auth)

4912 LEVELS IN ^{57}Ni FROM THE $^{58}Ni(^3He,\alpha)^{57}Ni$ REACTION. Fou, Cheng-Ming; Zurmuehle, Robert W. (Univ. of Pennsylvania, Philadelphia). Phys. Rev., 140: B1283-90(Dec. 6, 1965).

Levels in ^{57}Ni were studied by detecting the α particles from the $^{58}Ni(^3He,\alpha)^{57}Ni$ reaction in a 24-in. dia scattering chamber using surface-barrier solid-state detectors. The Q value of the reaction was measured to be 8.40 ± 0.05 Mev. Excited levels in ^{57}Ni at 0.75, 1.05, 2.55, 3.25, 3.70, 3.85, 4.25, 4.55, 4.95, 5.25, 5.57, 5.85, 6.05, 6.97, 7.15, 7.85 Mev were observed. Angular distributions of elastically scattered ^3He, as well as those of α particles leading to ground, 0.75-, 1.05-, 2.55-, 3.25-, 5.25-, 5.57-, and 6.05-Mev states were measured. Gamma rays, in coincidence with the reaction α particles, were also observed with a 3 in. × 4 in. NaI(Tl) crystal and analyzed with a 2-parameter pulse-height analyzer to study the decay scheme of the excited states. Distorted-wave analysis, using the JULIE computer code, yielded the following spin assignments: ground state, $l = 1$; 0.75-Mev state, $l = 3$; 1.05-Mev state, $l = 1$; 2.55-, 3.25-, 5.25-, 5.57-Mev states, all $l = 3$; 6.05-Mev state, either $l = 2$ or $l = 3$. Relative spectroscopic factors of these states were extracted. (auth)

4913 DIVISION OF NUCLEAR CHARGE DEDUCED FROM X-RAY MEASUREMENTS IN THE SPONTANEOUS FISSION OF ^{252}Cf. Glendenin, L. E.; Unik, J. P. (Argonne National Lab., Ill.). Phys. Rev., 140: B1301-9(Dec. 6, 1965).

The variation of nuclear charge with mass in the spontaneous fission of ^{252}Cf was investigated by simultaneous measurement of the masses and characteristic K x-ray energies associated with the fission fragments. The K x rays were detected by a thin NaI(Tl) scintillator or by an argon-filled proportional counter in coincidence with a pair of solid-state detectors for the complementary fission fragments. The yield and energy of K x rays emitted in the first centimeter (~1 nsec) of fragment flight were determined as a function of fragment mass. The yield of K x rays per fragment is a pronounced function of mass, rising from 0.04 in the region of mass (after neutron emission) below 98 ($N < 59$) to a maximum of 0.13 near the center of the light group, falling to 0.05 in the mass region 131-135 ($Z \approx 50$, $N \approx 82$), rising to 0.15 near the center of the heavy group, and then increasing rapidly beyond mass 145 (region of deformed nuclei) to a peak of 1.0 around mass 154. The observed correlation of K x-ray energies with fragment mass leads to a most probable nuclear-charge (Z_p) function in better agreement with the empirical rule of equal charge displacement (ECD) than with other postulates for charge division in nuclear fission. (auth)

4914 EMISSION OF K X RAYS AND DIVISION OF NUCLEAR CHARGE IN THE SPONTANEOUS FISSION OF ^{252}Cf. Kapoor, S. S.; Bowman, H. R.; Thompson, S. G. (Univ. of California, Berkeley). Phys. Rev., 140: B1310-17(Dec. 6, 1965). (UCRL-16208).

Measurements of the energies of the prompt K x rays emitted by the fragments in the spontaneous fission of ^{252}Cf were made which give information concerning the division of nuclear charge in fission. The kinetic energies of the pairs of fragments and the coincident K x rays emitted along the direction of fragment motion were recorded event by event, using a multiparameter analyzer. The energies of the fragments were measured by two semiconductor detectors, and the x-ray energies were measured with a lithium-drifted silicon detector operated at dry-ice temperature. The energy resolution of the x-ray detector as measured in terms of the full width at half-maximum of the 59.57-kev line of ^{241}Am was 3.5 kev. The data were analyzed to obtain (a) the most probable charge versus the fragment mass, (b) the x-ray yield per fragment versus the fragment mass and charge, and (c) the average half life for x-ray emission versus the fragment mass and charge. The measured x-ray emission times and the variation of the x-ray yield per fragment with the fragment mass are found to be consistent with the view that these x rays are emitted as a result of the internal-conversion process during the de-excitation of the fragment nuclei. In the heavy group, the abrupt rise in the x-ray yield at fragment mass 144 appears to be connected with the onset of large stable nuclear deformations of fragment nuclei at neutron number about 88. The

measured x-ray yield from the light-fragment group suggests that most of these nuclei make up a new region of deformation. The observed variation of the most probable charge with the fragment-mass ratio over a limited mass region is found to be very similar to that obtained in radiochemical studies of the thermal fission of ^{235}U. (auth)

4915 COUPLING CONSTANTS IN MUON CAPTURE. Foldy, L. L. (Case Inst. of Tech., Cleveland); Walecka, J. D. Phys. Rev., 140: B1339-50(Dec. 6, 1965).

The measured capture rate of muons in ^{12}C leading to the ground state of ^{12}B, in combination with other data, is employed as a basis for a determination of the weak-interaction coupling constants associated with muon capture. The study of this transition has the advantages: (1) that the rate depends only weakly on the vector, induced pseudoscalar, and (possible) tensor coupling constants, but not at all on a possible scalar coupling constant; (2) that empirical information from inelastic electron scattering on ^{12}C leading to the excitation of the 15.1-Mev level, the M1 lifetime of this level, and the $ft_{½}$ value for the beta decay of ^{12}B allows the required nuclear matrix elements of major importance (as well as some of minor importance) to be determined in practically a model-independent way. The capture rate can thus be expressed in terms of the axial vector coupling constant and the weak-magnetism coupling constants. If the validity of the conserved-vector-current hypothesis (CVC) is assumed, and $5 < C_p < 28$, it is found that $F_A^u/F_A^p = 1.04^{+0.07}_{-0.10}$. On the other hand, if $F_A^u = F_A^p$ is assumed, one obtains for the isotopic vector magnetic moment of the nucleon (at the appropriate momentum transfer) $\mu(\nu^2) = 5.7^{+1.1}_{-1.6}$ nuclear magnetons, which is consistent with the CVC prediction of 4.60 nm and can be considered as evidence for weak magnetism in muon capture. (auth)

4916 NATURAL RADIOACTIVITY OF ^{40}K, ^{87}Rb, AND ^{176}Lu. Brinkman, G. A.; Aten, A. H. W. Jr.; Veenboer, J. Th. (Instituut voor Kernphysisch Onderzoek, Amsterdam). Physica, 31: 1305-19(Aug. 1965).

The radioactive isotopes ^{40}K and ^{87}Rb were calibrated by $4\pi\beta$ liquid scintillation counting. ^{176}Lu was calibrated by β-γ coincidence counting, by means of a calibrated NaI crystal and by the "sum peak" method. The following values were found: ^{40}K: 29.2 ± 0.5 βps/gK; ^{87}Rb: 826 ± 25 dps/g Rb or $T_{½} = (5.22 \pm 0.15) \times 10^{10}$ years; ^{176}Lu: β-γ coincidence: 55.7 ± 0.8 dps/g Lu or $T_{½} = (3.54 \pm 0.05) \times 10^{10}$ years, calibrated γ crystal: 56.2 ± 2.2 dps/g Lu or $T_{½} = (3.50 \pm 0.14) \times 10^{10}$ years, sum peak method: 53.6 ± 0.8 dps/g Lu or $T_{½} = (3.68 \pm 0.06) \times 10^{10}$ years. (auth)

4917 METHODS OF MEASURING EXTREMELY SHORT LIFETIMES OF NUCLEI IN EXCITED STATES. Balanda, Andrzej (Jagellonian Univ., Krakow). Postepy Fiz., 16: 247-56(1965). (In Polish).

Five methods of measuring ultrashort decay times of excited nuclei are reviewed. The delayed coincidence method, in which the number of coincidences of a two-particle (or, gamma-ray) cascade is plotted as a function of delay time from one of the particle detectors, is useful for decay times greater than 5×10^{-11} seconds. Several methods of analyzing the coincidence curves are presented. The microwave method is useful for decay times longer than 10^{-12} sec. It utilizes two beta spectrometers and a microwave accelerating field that is associated with each spectrometer. The coincidence count rate from a cascade type decay of two conversion electrons is analyzed as a function of the relative phase of the two microwave fields. In the case where a nucleus has been excited by a heavy-particle bombardment (or following a heavy-particle decay), the emission of gammas or betas can be measured as a function of path length of the recoil nucleus in gas or vacuum with the aid of collimators and counters. This method is useful for lifetimes greater than 10^{-14} seconds. The method of gamma resonance absorption, which utilizes the Doppler shift of gammas as a function of velocity, the recoil nucleus and of angle with respect to the direction of motion, is applicable for decay times shorter than 10^{-5} sec. In Coulomb excitation of gamma line, lifetimes greater than 10^{-12} sec can be deduced from measurements of Coulomb excitation cross sections. (TTT)

4918 THE CLOSE-PACKED-SPHERON THEORY AND NUCLEAR FISSION. Pauling, Linus (Center of Democratic Insts., Santa Barbara, Calif.). Science, 150: 297-305(Oct. 15, 1965).

The close-packed theory of nuclear structure is described as a refinement of the shell model and the liquid-drop model in which the geometric consequences of the effectively constant volumes of nucleons, aggregated into spherons, are considered. The spherons are assigned to concentric layers, the mantle, outer core, inner core, and innermost core, by using a packing equation. This assignment is related to the principal quantum number of the shell model. The theory is applied in the discussion of the sequence of sub-subshells, magic numbers, the proton-neutron ratio, prolate deformation of nuclei, and symmetric and asymmetric fission. (J.F.P.)

4919 THE DECAY OF ^{40}K. Leutz, H.; Schulz, G.; Wenninger, H. (Universitaet, Heidelberg). Z. Physik, 187: 151-64(1965). (In German).

The half life and branching ratios of potassium-40 decay are redetermined. High accuracy for these values is desirable since they are used in the determination of the ages of minerals. Specific β^- activity as well as specific γ activity of natural uranium are important in mineral age determination. Two methods were used for these activity determinations. Cubic KI(Tl)-scintillation crystals were used to evaluate the specific β^- activity and the specific γ activity. The specific γ activity was also measured with five well-type scintillation crystals. The results gave a half life value with an error of ±0.6% and a branching ratio value with an error of ±2%. Applying the results the error of mineral age due to the error of nuclear data is restricted to about ±2%. (J.F.P.)

4920 CONVERSION OF THE 238.6-kev γ LINE OF ThB AND COMPARISON WITH THE TABLES OF SLIV AND OF ROSE. Daniel, H.; Jahn, P.; Spannagel, G. (Max-Planck-Institut fuer Kernphysik, Heidelberg). Z. Physik, 188: 252-5(1965). (In German).

The conversion ratios K/L_I and K/L_{II} of the 238.6 kev γ transition of ThB were measured with the new Heidelberg $\pi/2\sqrt{13}$ β-ray spectrometer. For this transition there are great discrepancies between the values as given by Sliv and Band, and by Rose. The experimental results $K/L_I = 5.96 \pm 0.26$ and $K/L_{II} = 60.3 \pm 7.1$ are in excellent agreement with the values of Sliv and Band. (auth)

4921 ON THE ISOMERISM OF ^{197}Tl. Schmidt-Ott, W.-D.; Smend, F.; Weirauch, W.; Flammersfeld, A. (Univ., Goettingen, Ger.). Z. Physik, 188: 282-9(1965). (In German).

The isomer ^{197m}Tl was produced by the $(\alpha,4n)$ reaction on ^{197}Au using 49-Mev α particles. The following results were obtained: Half life $T_{½} = (0.55 \pm 0.02)$ sec; energy of the isomeric level (607 ± 4) kev, determined directly by summing up the cascade transitions in a well-type scintillator; energy of the isomeric transition (222 ± 2) kev; conversion coefficients of this transition $\alpha_{K222} = 0.41 \pm 0.05$ and $\alpha_{tot222} = 2.1 \pm 0.2$, indicating an E3 multipolarity; energy of the second transition (385 ± 3) kev; conversion coefficients $\alpha_{K385} = 0.09 \pm 0.03$ and $\alpha_{tot385} < 0.1$. This transition was identified as E2 with a M1 admixture of 20 to 30%. Spins and parities are $½^+$, $3/2^+$, and $9/2^-$ for the ground state, the 385 kev state and the 607 kev isomeric state, respectively, in disagreement with the extreme single-particle model. If this model were correct, another M1 transition should appear. No further M1 transition having an energy greater than the L-shell binding energy of Tl was observed. (auth)

4922 ISOMERIC CROSS SECTION RATIOS FOR THE $^{44,44m}Sc$ SYSTEM [Thesis]. Keedy, Curtis Russell. Madison, Wis., Univ. of Wisconsin, 1965. 140p.

The absolute cross sections and isomeric cross section ratios were determined for the ^{41}K $(\alpha,n)^{44,44m}Sc$ reaction for alpha energies from 7.50 to 12.50 Mev. These and other

experimental isomer ratios were compared to calculated values obtained using three variations of the nuclear statistical model with the transmission coefficients obtained from optical model calculations. The possibility of (α,p) and (α,α') competing reaction modes was included in the theoretical calculations. It was found that, in order to reproduce the experimental isomer ratios, a nuclear moment of inertia was needed that was less than the rigid body value at low excitation energies, but which increased rapidly to that value as the excitation energy approached 20 Mev. This behavior was best approximated by the superconductor statistical model. The (α,p) and (α,α') competing reactions were a significant part of the compound nucleus decays but had only small effects on the isomer ratios. The nuclear temperature also had little effect on the isomer ratios. Calculations based on high-energy neutrons, which left the excitation energy of the residual nucleus below the separation energy of the next neutron, gave isomer ratios that became constant for incident alpha-particle energies of 22 Mev and above, but the experimentally observed decline of isomer ratios above 26 Mev could not be reproduced, and was thus assumed to result from a direct interaction mechanism. (Dissertation Abstr.)

4923 FINE STRUCTURE NEAR ISOBARIC ANALOGUE RESONANCES [Thesis]. Richard, Patrick. Tallahassee, Florida State Univ., 1964. 90p.

Measurements were made on the 5.3- and 5.92-Mev S-wave resonances in ^{92}Mo(p,p) and ^{90}Zr(p,p) excitation functions. In both cases the neutron exit channel is closed and the other competing reactions are relatively unimportant. It is found that the magnitude of the fluctuations becomes about 25% of the Rutherford scattering cross section on resonance and fades away off resonance. The variation of the magnitude of the fluctuations with energy is asymmetric with respect to the observed resonance energy. The cross section averaged over the fine structure was analyzed using a Coulomb plus single level formula. It is found that both resonances exhibit a spreading width "W," which is a measure of the absorption of protons out of the pure state, characterized by isobaric spin $T = T_t + \frac{1}{2}$, into the more abundant states of isobaric spin $T = T_t - \frac{1}{2}$, where $T_t = \frac{1}{2}(N - Z)$ represents the isobaric spin of the target nucleus. The asymmetry of the fluctuations away from the average is explained in terms of the "external" mixing of states of different isobaric spin. This mixing occurs in a region of radial space near the nucleus for $r > a_c$ where a_c is the charge radius of the nucleus. This explanation leads to the conclusion that relative isobaric spin is pure for the region of radial space $r < a_c$. (Dissertation Abstr.)

4924 THE GAMMA-RAY DECAY OF ^{165}Tm, ^{176m}Lu, AND ^{175}Ta [Thesis]. Staehle, George Gardner. Columbus, Ohio, Ohio State Univ., 1964. 180p.

The decays of ^{165}Tm, ^{176m}Lu, ^{176}Ta, and ^{175}Ta were studied by the method of gamma-ray spectrometry. The results of gamma-gamma coincidence measurements and the relative numbers of K x rays and observed gamma rays are given. Energy levels in ^{165}Er and ^{176}Hf are proposed, including decay branching ratios and relative transition probabilities. Tentative energy levels are proposed for ^{175}Hf. A review of collective model systematics is presented, including a chart showing the trends of particle states in the odd-N rare-earth nuclides. The general methods of analysis used in gamma-ray spectroscopy are presented with details on sum-peak analysis and decay-point determination for counting times comparable to the half life being measured. (A.G.W.)

4925 THE STUDY OF (^{3}He,n) REACTIONS [Thesis]. Din, Ghias Ud. Houston, Tex., Rice Univ., 1964. 244p.

Six (^{3}He,n) reactions were studied in the range of bombarding energies from 1.3 to 5.8 Mev. The nuclei bombarded were ^{7}Li, ^{9}Be, ^{11}B, ^{12}C, ^{13}C, and ^{18}O. In the case of ^{9}Be and ^{18}O targets the neutron groups leading to the ground state and the first excited state of the residual nuclei were studied. For the other four target nuclei only the neutron groups leading to the ground states of the residual nuclei were investigated. The neutron detector for the ^{12}C(^{3}He,n)^{14}O reaction was a BF_3 counter embedded in paraffin. For the other five reactions the neutron detector was a stilbene crystal coupled to a photomultiplier tube. Pulse-shape discrimination was used to eliminate gamma-ray events or beta-decay electrons in the crystal. The total cross section for ^{12}C(^{3}He,n)^{14}O was determined by measuring both the yield of beta particles from the radioactive ^{14}O that is produced and the yield of gamma rays of 2.31 Mev that accompanies this decay. Nineteen excitation functions at 0°, 90°, and the backward angle, and 73 angular distributions were measured. The excitation functions show broad resonant structure, especially at 0°. The angular distributions show changes in shape with energy, especially at lower energies. At the lowest bombarding energy these are either nearly isotropic or nearly symmetric about 90°. The angular distributions for some reactions show peaks in the backward direction as the bombarding energy is increased. At the higher bombarding energies dominant forward peaks and relatively small yields in the backward direction are common to all reactions. The reactions are discussed in terms of both direct interaction theory and compound nucleus theory. It is suggested that both mechanisms are operative. (Dissertation Abstr.)

4926 (p,γ) ANGULAR CORRELATIONS IN ^{48}Ti [Thesis]. Humes, Richard Martin. Columbus, Ohio, Ohio State Univ., 1964. 102 p.

Absolute double-differential cross section measurements were made for the inelastic scattering of protons from the 0.99-Mev first excited state of ^{48}Ti. The measurements were made in the plane formed by k_p and $k_p \times k_{p'}$ at ten energies between 4.14 and 6.08 Mev. In addition, extensive measurements to test symmetry predictions were made both in and out of the scattering plane at 4.63 and 5.25 Mev. The experimental data are compared with the statistical compound nucleus model predictions. The agreement between experiment and theory is good qualitatively, if not quantitatively, in the k_p, $k_p \times k_{p'}$ plane except at peaks in the excitation curve above the Coulomb barrier where measurements at forward proton scattering angles show much stronger variation than predicted. The agreement in other planes at 4.63 Mev and 5.25 Mev is poor, while the variation with azimuthal angle is drastically underpredicted. (Dissertation Abstr.)

4927 A HIGH RESOLUTION STUDY OF THE ^{18}O(p,n)^{18}F REACTION [Thesis]. Beard, Percy Morris Jr. Durham, N. C., Duke Univ., 1965. 137p.

A gas handling and recovery system was developed for use in conjunction with the windowless cryogenic gas target chamber. It permits the employment of a limited quantity of rare gas where, during each run, the entire amount is cycled through the target chamber and then recovered with a minimum of loss or contamination. A liter (NTP) of oxygen gas, 65% enriched in ^{18}O, was used to study the relative total yield of the ^{18}O(p,n) reaction from threshold to 3.290 Mev proton energy. With a total effective proton energy spread of about $\frac{1}{11000}$, a previously unreported resonance was observed and improved values of widths and energies were obtained for the other resonances. Through a method by which neutron and proton energies are measured simultaneously a Q-value for the reaction was determined at -2439 ± 1.0 kev, which places threshold at 2576 ± 1.0 kev. In addition, ^{18}O(p,n) neutrons were used in a series of transmission measurements to test the resolution capability of the gas target as a neutron source. Results were in general agreement with resolution predictions. Total neutron energy spreads were 250 and 500 ev at neutron energies of 30 and 525 kev respectively. In view of the successful performance of the ^{18}O(p,n) gas target, the feasibility of using a ^{3}T(p,n) gas target as a neutron source is discussed. (Dissertation Abstr.)

4928 INVESTIGATION OF THE INTERACTIONS OF ^{3}He AND d WITH ^{237}Np [Thesis]. Polishuk, Paul. Columbus, Ohio, Ohio State Univ., 1964. 146p.

Investigations of the reactions of ^{3}He and deuterons with ^{237}Np were intended to determine fission products and direct reactions produced in the ^{3}He and d bombardments

of ^{237}Np. A total of four bombardments of ^{237}Np oxide target were performed in the Ohio State University cyclotron. Two were with ^{3}He projectiles and the others were with deuterons. No reactions were observed in the ^{237}Np + ^{3}He reactions except for the ^{16}O(^{3}He,p)^{18}F reaction. Deuteron reactions produced both fission products and direct reactions. A total of 12 fission products were identified and 5 other possible products determined. Techniques used included scintillation spectroscopy and the use of lithium drifted silicon and germanium solid state detectors. One- and two-millimeter-thick lithium drifted germanium detectors were used to analyze the reaction products of ^{237}Np + d reactions. Operation and fabrication of the solid state detector system is discussed as well as the design of equipment used in scintillation spectroscopy aspects. (Dissertation Abstr.)

4929 INTERACTION OF 31 Mev PROTONS WITH DEUTERIUM [Thesis]. Bunch, Stanley Marion. Los Angeles, Univ. of Southern California, 1965. 139p.

Differential cross sections were obtained for protons elastically scattered from deuterium over an angular range of 10° to 170° in the center-of-mass system. The protons were detected with NaI(Tl) and CsI(Tl) detectors, and the spectra were displayed on a 100-channel analyzer. Minima in the angular distribution occurred at 13.5° cms where the cross section was 54.4 ± 3.5 mb/sr and at 129.5° cms where the cross section was 2.27 ± .10 mb/sr. A maximum was observed at 23.9° cms where the cross section was 64.7 ± 1.7 mb/sr. The cross section at backward angles became quite large and at 170° cms had a value of 40 mb/sr. The present results were compared with the experimental angular distributions obtained at other energies from 5.6 to 146 Mev, and the over-all agreement with the data of the other experimenters is quite good if one takes into account the general decrease of cross section at a fixed angle with the beam energy. It was noted that, for an increase in bombarding energy, the first minimum becomes more pronounced and shifts toward smaller angles, and the second minimum, which is broad at low energies, becomes sharp at 31 Mev but becomes quite flat again at 146 Mev. The differential cross section for the D(p,2p)n reaction was determined for coincident protons emitted in the plane of the incident beam with one detector kept fixed at a laboratory angle of 35°, while the other was varied from 25° to 65°. The experimental results showed a pronounced peak in the angular distribution at ~40° in the laboratory system with a cross section at the maximum of 54 ± 10 mb/sr^2. The peak fell off quite sharply on both sides of the maximum and had a full width at half of the maximum of ~17°. The experimental results for the breakup reaction were compared with the spectator model of Kuckes, Wilson, and Cooper. (Dissertation Abstr.)

4930 BETA-DECAY OF HYPERNUCLEI [Thesis]. Chen-tsai, Ching-tang. St. Louis, Washington Univ., 1964. 157p.

A formalism for treating the beta decay of hypernuclei is developed. Derived are the general expressions for the angular distributions of decay particles and formulas for β-β and β-correlations. Specific shell model calculations for some light hypernuclei on the branching ratio of the partial decay rate (decay of a hypernucleus to the ground state of the final nucleus) to the total decay rate (decay of the hypernucleus to all kinematically accessible states of the final nucleon system) are made. The results of the calculations, when tested with experiment, provide some information on the spin-dependent property of Λ-nucleon forces and the structure of the hypernuclei. A few predictions of the isobaric selection rules, $\Delta S = \Delta Q$ and $\Delta I = 1/2$ of leptonic weak interactions are also made from some hypernucleon beta-decay processes. Finally the total cross sections for some inverse beta-decay processes, i.e., the processes of the production of hypernuclei induced by neutrino beams, are evaluated by shell model calculation. (Dissertation Abstr.)

4931 PULSED NUCLEAR MAGNETIC RESONANCE IN RAPIDLY ROTATING SOLIDS [Thesis]. Kessemeier, Horst. St. Louis, Washington, Univ., 1964. 157p.

The method of high-speed mechanical sample rotation was improved and applied to a nuclear magnetic resonance investigation of various metal phosphides and aluminum metal. It is demonstrated, both theoretically and experimentally, that the transverse and longitudinal nuclear relaxation times increase by subjecting the solid to rapid rotation at the "magic angle" $\theta = 54.7°$ (θ is the angle between the applied magnetic field and the axis of rotation) provided that rotationally non-invariant interactions (e.g., magnetic dipole-dipole coupling) dominate or contribute to nuclear relaxation. (Dissertation Abstr.)

4932 THE ANISOTROPY OF THE MOESSBAUER EFFECT IN β-Sn SINGLE CRYSTALS AT 4.2°K. Alekseevski, N. E.; Kiryanov, A. P.; Samarski, Yu. A. (Inst. for Physical Problems, Moscow). pp 96-101 of Physics and Techniques of Low Temperatures. Prague, Publishing House of the Czechoslovak Academy of Sciences, 1964.

The anisotropy of Moessbauer effect at 4.2°K is investigated. Resonance absorption was measured on an experimental set-up ensuring the movement of the absorber with a constant velocity with respect to the gamma ray source. The absorber was in direct contact with a helium bath. The resonance absorption in β Sn single crystals was measured at temperatures of 4.2 and 80 to 200°K. The absorbers used had the form of plates cut from a monocrystalline block of metallic tin enriched in ^{120}Sn, the ^{118}Sn content was equal to 1.7%. The resonance absorption spectra for plates of orientation (001) and (110) at 4.2°K are shown. These curves are not symmetrical because of the quadrupole splitting. Data on the strength of the resonance absorption varying with the temperature of the absorber at resonance velocity are given in dimensionless units. The areas of the experimental absorption curves and the velocities are also given. The Lamb-Moessbauer factor was found to be 0.31 ± 0.06 at 80°K and 0.42 ± 0.06 at 4.2°K. (J.F.P.)

4933 ORIENTED NUCLEI AND BETA DECAY. Vinduska, M.; Janouch, F. (Inst. of Nuclear Research, Czechoslovak Academy of Sciences, Rez). pp 237-45 of Physics and Techniques of Low Temperatures. Prague, Publishing House of the Czechoslovak Academy of Sciences, 1964.

The problems of nuclear β decay are discussed, and some directions are shown in which investigations with oriented nuclei should be very fruitful. The experimental set ups are also discussed. First the present situation in weak interactions and especially in β decay is recapitulated. Topics discussed include the conserved vector current (CVC) hypothesis in weak interactions, and the assumption of T invariance in β decay. It is noted that two experiments which can only be performed using oriented nuclei are β-γ correlations of oriented nuclei, and e-ν correlations of oriented nuclei. (J.F.P.)

Plasma Physics and Thermonuclear Processes

See also Fluid Physics and Thermodynamics

4934 (AD-619093) ELECTRON DENSITY IONIZATION RATE AND APPROACH TO THERMAL EQUILIBRIUM BEHIND SHOCK WAVES BY MEANS OF MICROWAVE TECHNIQUES. Final Scientific Report. Low, W. (Hebrew Univ., Jerusalem (Israel). Dept. of Physics). Oct. 1964. Contract AF61(052)-401. 27p. (AFOSR-65-1138). CFSTI $2.00 cy, $0.50 mn.

Information is included on: improvement in the microwave diagnostics of shock waves; time dependence and shape of microwave attenuation in shocks of air at pressures of 1 and 5mm of Hg; effects of constrictions and taper sections on the shock speed and on the microwave

attenuation; experiments with an electrical discharge shock tube; construction of a 4mm Fabry-Perot interferometer; and testing a 4mm carcinotron. Measurements were made on the peak microwave attenuation of shock waves in argon and neon. (TAB)

4935 (AFCRL-65-556) OBSERVATION OF NON-QUASISTATIC PLASMA SURFACE WAVES. Scientific Report No. 83. Granatstein, V. L.; Schlesinger, S. P. (Columbia Univ., New York. Dept. of Electrical Engineering). June 25, 1965. Contract AF19(628)-2461. 21p. (CU-12-65-AF-2461-EE). CFSTI $1.00 cy, $0.50 mn.

Surface waves were launched from a waveguide onto a glass-clad plasma column of moderate size ($2\pi R \approx \lambda_0$), in order to test the validity of quasistatic analysis when the small column condition ($2\pi R \ll \lambda_0$) is not satisfied. Resonances were observed in an open microwave cavity, and dispersion of both the circularly-symmetric surface wave and the dipole surface wave was determined from experimental data. The two waves exhibit regions of backward-wave and forward-wave propagation. The observed positive slope of the dipole mode dispersion curve near $\omega/k_z = c$ is contrary to the predictions of quasistatic analysis, and is shown to agree quantitatively with the results of a more rigorous analysis. (auth)

4936 (ANL-7081, pp 130-3) HIGH-FREQUENCY PLASMAS. (Argonne National Lab., Ill.).

Research on three aspects of h-f plasmas is briefly discussed. These include plasmas in uniform r-f electric fields, multipacting suppression, and plasmas in nonuniform (cavity) electromagnetic fields. (M.O.W.)

4937 (IAE-907) VLIYANIE VINTOVOGO POLYA NA OMICHESKII NAGREV PLAZMY V USTANOVKE S-1. (The Effect of a Helical Field on Ohmic Heating of Plasma in an S-1 Apparatus). Blinov, P. I.; Gavrilov, B. I.; Cheremnykh, P. A.; Yashin, N. M. (Institut Atomnoi Energii, Gosudarstvennyi Komitet po Ispol'zovaniyu Atomnoi Energii SSSR, Moscow). 1965. 36p. Dep. mn.

The effect of a helical magnetic field, formed by a triple spiral winding, on the development of the discharge, the value of the plasma conductivity, and the stabilization of the position of the plasma column was studied. It was shown that the helical field in a well-compensated magnetic system does not evidence any special effect on the stabilization of the plasma column. Values of $T_e = 20$ to 30 ev and $T_i = 10$ ev were obtained, corresponding to a conductivity of the order of 10^{15} in cgs units. (tr-auth)

4938 (IAE-909) ISSLEDOVANIE STRUKTURY FRONTA SIL'NOI MAGNITO-ZVUKOVOI VOLNY V RAZREZHENNOI PLAZME. (Study of the Structure of the Front of a Strong Magneto-sonic Wave in a Rarefied Plasma). Zagorodnikov, S. P.; Rudakov, L. I.; Smolkin, G. E.; Sholin, G. V. (Institut Atomnoi Energii, Gosudarstvennyi Komitet po Ispol'zovaniyu Atomnoi Energii SSSR, Moscow). 1965. 8p. Dep. mn.

The structure of the front of a strong cylindrical magnetoacoustic wave, spreading across a magnetic field, was studied in a plasma with density from $\sim 0.5 \times 10^{12}$ to $\sim 6 \times 10^{13}$ cm^{-3}. The profile of the magnetic field of the wave in the plasma found in the experiment (with accuracy up to the cylindricality effect) agrees with the profile calculated in the work of Adlam and Allen (Proc. Phys. Soc. (London), 75: 640(1960)) for the nondetermined motion of a magnetic piston in a rarefied plasma. The width of the forward part of the front coincides within about 50% with the theoretically calculated width on the scale c/ω_{pe} (taking into account nonstationary behavior). (auth)

4939 (IAE-911) MAGNITNO-ZVUKOVOI NAGREV PLAZMY. (Magneto-sonic Heating of Plasma). Kovan, I. A.; Podgornyi, I. M.; Rusanov, V. D.; Smirnov, V. P.; Spektor, A. M.; Frank-Kamenetskii, D. A. (Institut Atomnoi Energii, Gosudarstvennyi Komitet po Ispol'zovaniyu Atomnoi Energii SSSR, Moscow). 1965. 20p. Dep. mn.

Results are presented of a study of the excitation, diffusion, and absorption of magnetoacoustic waves in a plasma. The experiments were performed with the goal of investigating plasma heating using oblique waves and magnetoacoustic resonance. It was shown that at large values of the amplitude of the high-frequency magnetic field nonlinear absorption effects are observed. These effects can be explained by collisionless mechanisms of dissipation of the waves in the plasma. (tr-auth)

4940 (IAE-932) DLINNOVOLNOVYE ELEKTRONNYE KOLEBANIYA V SISTEME PUCHOK-PLAZMA. (Longwave Electron Oscillations in a Beam-Plasma System). Nezlin, M. V.; Sapozhnikov, G. I.; Solntsev, A. M. (Institut Atomnoi Energii, Gosudarstvennyi Komitet po Ispol'zovaniyu Atomnoi Energii SSSR, Moscow). 1965. 29p. Dep. mn.

Long-wave electron oscillations excited by an electron beam in a rarified plasma in the presence of a strong longitudinal magnetic field were studied experimentally. The plasma is formed as a result of ionization of the gas by the beam, with the gas pressure $p \simeq 10^{-5}$ mm Hg and the plasma density commensurable with the density of the beam. The oscillations observed in the experiment do not appear to be Langmuir oscillations; their spectrum consists of a series of harmonics, whose wavelengths λ_n obey the relation $\lambda_n = 2L/n$ (where n is the number of the harmonic and L is the beam length) and whose frequencies ω_n are determined by the electron beam velocity v and the wavelength according to $\omega_n \sim k_n v$, where $k_n = 2\pi/\lambda n$. It is shown that the conditions of excitation of the oscillations and their spectral characteristics are in good agreement with theories of longitudinal electron oscillations in a homogeneous beam-plasma system with bounded longitudinal and transverse dimensions. (tr-auth)

4941 (LA-DC-7290) PLASMA COMPRESSION BY EXPLOSIVELY PRODUCED MAGNETIC FIELDS. Thomson, D. B.; Caird, R. S.; Garn, W. B.; Fowler, C. M. (Los Alamos Scientific Lab., Univ. of California, N. Mex.). [1965]. Contract W-7405-eng-36. 51p. (CONF-650937-3). Dep. mn; CFSTI $3.00 cy, $0.50 mn.

From Conference on Megagauss Magnetic Field Generation by Explosives and Related Experiments, Frascati, Italy.

Early attempts to apply multi-megagauss fields obtained by cylindrical explosive compression to plasma compression are reported. Two approaches are discussed. In the first method, a slotted liner is used, so that the initial field may be applied rapidly and plasma is produced by a fast θ-pinch, prior to implosion. This method has the advantage that the initial plasma may be made quite hot, i.e., 200-800 ev, but has the disadvantage of requiring a cylindrical insulator, such as Pyrex, to hold the vacuum, thereby limiting the effective implosion field to the range of ½ to 1 megagauss. In the second method, an unslotted resistive cylinder is used to hold the vacuum, thereby allowing the implosion fields to reach measured values as high as 4 megagauss. Here, the initial magnetic field diffuses through the cylinder so that the initial plasma is heated by a slow θ-pinch with the disadvantage that the initial temperatures were low, about 5-15 ev. Implosion shots have resulted in very small ($<10^4$) neutron yields for the first method, and zero yields for the second method. Hitherto the first method was hindered by field asymmetries and by marginally low fields. A review of results and improvements to date is presented, and future plans are indicated. (auth)

4942 (MATT-372) PLASMA CONFINEMENT IN LOW-DENSITY C STELLARATOR DISCHARGES. Stodiek, W.; Grove, D. J.; Kessler, J. O. (Princeton Univ., N. J. Plasma Physics Lab.). Sept. 1965. Contract AT(30-1)-1238. 23p. (CONF-650935-39). Dep. mn; CFSTI $1.00 cy, $0.50 mn.

From 2nd IAEA Conference on Plasma Physics and Controlled Nuclear Fusion Research, Culham, Eng.

Theoretical work has suggested that anomalously high plasma loss rates (pumpout) may be due to ohmic heating currents. Previous experiments however showed that pumpout persists even when the currents (normally re-

quired to prevent cooling and recombination) are much below the critical values for ion wave instabilities. Experiments are reported on the C stellarator which extend the measurements to zero ohmic heating currents. They were performed at low initial pressures ($2 - 3 \times 10^{-6}$ torr) of hydrogen, at low electron densities of 5×10^9 to 2×10^{11} cm^{-3} and at electron temperatures of 1 to 3 ev. The confining field was usually 12.3 kG; a few measurements were made at 35 kG. A rotational transform of 0.75 π was provided by l = 2 and l = 3 helical windings. In these low-density, low-temperature experiments an anomalous loss rate exists in the C stellarator for four operating conditions: ohmic heating, electron cyclotron resonance heating, resistive microwave heating, and no heating at all. It is concluded that neither the presence of an axial current of small magnitude nor density variations in the range $5 \times 10^9 < n_e < 2 \times 10^{11}$ cm^{-3} seem to affect the transport time constant τ_p for plasma loss across the magnetic confining field. The observed loss rate cannot be accounted for in terms of a lack-of-equilibrium model associated with finite resistivity. The overall plasma decay time is consistent within a factor 2 with the relation $\tau_p = 0.9\ B/T_e$ milliseconds (B in kG, T_e in ev; plasma radius = 5 cm) observed by Hinnov and Bishop at densities near 10^{13} cm^{-3}, higher temperatures, and higher ohmic heating currents. (auth)

4943 (MATT-379) MICROWAVE ABSORPTION IN A HOT PLASMA NEAR THE SECOND HARMONIC OF THE ELECTRON CYCLOTRON FREQUENCY. Arunasalam, V.; Gurnee, M. N.; Meservy, E. B.; Davidson, R. C. (Princeton Univ., N. J. Plasma Physics Lab.). Oct. 1965. Contract AT(30-1)-1238. 14p. (CONF-650806-17). Dep. mn; CFSTI $1.00 cy, $0.50 mn.

From 7th International Conference on Phenomena in Ionized Gases, Belgrade.

Analysis is presented of 4-mm microwave propagation in the extraordinary mode (for propagation angles of 75, 90, and 105° to the magnetic field), near the second harmonic of the electron cyclotron frequency, across a reasonably uniform, highly ionized plasma of approximately 10 cm diameter confined in a homogeneous (0.05%) magnetic field in the Model C stellarator. Reasonably good agreement with the predictions of the conventional hot plasma theory is obtained. The 75 and 105° measurements show another small absorption resonance, possibly due to electrons bouncing off the wall-sheaths. (auth)

4944 (ORNL-3871) THE ELECTRON-PHONON, ELECTRON-PLASMON, PLASMON-PHONON, AND PLASMON-PLASMON INTERACTIONS AND SOME INSTABILITIES THAT THEY LEAD TO. Harris, E. G. (Oak Ridge National Lab., Tenn.). Nov. 1965. Contract W-7405-eng-26. 19p. Dep. mn; CFSTI $2.00 cy, $0.50 mn.

The electron-phonon and electron-plasmon interaction hamiltonians previously found by Pines and Schrieffer are derived. Then a plasmon-phonon interaction hamiltonian is derived. This is used to discuss a "wave vector space" instability found by Vedenov and Rudakov. Plasmons may interact by exchanging phonons. The plasmon-plasmon interaction hamiltonian is derived. It is used to discuss the instability of a plasmon gas which was also found by Vedenov and Rudakov. (auth)

4945 (ORNL-TM-1306) REPORT ON A MEETING HELD IN THE OLD LECTURE ROOM AT CHRIST CHURCH COLLEGE, OXFORD, AT 9 P.M. ON THURSDAY, SEPTEMBER 9, 1965. Alexeff, I.; Getty, W.; Malein, A.; Seidl, M. (Oak Ridge National Lab., Tenn.). Oct. 25, 1965. Contract W-7405-eng-26. 7p. Dep. mn; CFSTI $1.00 cy, $0.50 mn.

Several reports on beam-plasma interaction were given. An experiment in which two Penning ion sources produced counter streaming beams parallel to a 10 kG field was discussed. A strong charge-exchange process was evident. Measurements were made of the frequency spectrum up to 5 mc. A large oscillation was detected. Next a mirror machine was described. The instabilities of the electron gas produced by an electron gun were studied. Another discussion was given on the propagation and instabilities of waves examined in a plasma where the transverse boundaries and temperature were important. The next experiment described was that in which a beam injected into a magnetized plasma along field lines, diverged. The non-linear theory of the beam plasma interaction was examined and the normal Doppler effect instabilities were suggested as most plausible. Helicon waves were then described. These are known as whistlers in plasmas. Experiments were then described demonstrating ion-electron coupling with no magnetic field. A possible process was suggested whereby directed beam energy could be converted to random ion motion. After this, an elegant experiment involving a 19-kev beam of noble gas ions directed onto a copper plate was discussed. Lastly, plasma phenomena were considered in an experiment in which a 10-kev electron beam was injected into a mirror field forming a tenuous plasma. (J.F.P.)

4946 (ORNL-TM-1307) REPORT OF AN INFORMAL STRIATION MEETING HELD AT THE SEVENTH INTERNATIONAL CONFERENCE ON PHENOMENA IN IONIZED GASES, BELGRADE, YUGOSLAVIA, AUGUST 22-27, 1965. Alexeff, I.; Jones, W. D. (Oak Ridge National Lab., Tenn.). Oct. 25, 1965. Contract W-7405-eng-26. 7p. Dep. mn; CFSTI $1.00 ct, $0.50 mn.

A list of delegates who attended the session, as well as a brief summary of discussions given by various delegates concerning their work on striations, is included. (auth)

4947 (SU-IPR-13) BEAM-PLASMA INTERACTION IN A WARM PLASMA. Crawford, F. W. (Stanford Univ., Calif. Inst. for Plasma Research). May 1965. Contract AT(04-3)-326. 30p. (CONF-650930-1). Dep. mn; CFSTI $1.00 cy, $0.50 mn.

From International Conference on the Microwave Behavior of Ferrimagnetics and Plasmas, London.

Electron beam/plasma interaction is investigated in planar geometry for both finite and infinite beams in an infinite, uniform warm plasma. In the finite beam case, the question of appropriate boundary conditions to use at the beam edge arises. For cold plasmas, the Hahn approximation involving postulation of an equivalent surface charge at the beam edge is usually applied. In the case of a warm plasma, it is unlikely that this approximation would describe accurately the plasma behavior, though it may still be appropriate for the beam. Suitable boundary conditions are suggested, and computed curves are presented comparing the complex solutions of the resulting dispersion relation with the cold plasma solutions for the same geometry. For typical experimental conditions a substantial reduction of gain is indicated when nonzero electron temperature is taken into account. (auth)

4948 (TID-22179, pp 85-175) PLASMA DYNAMICS. (Massachusetts Inst. of Tech., Cambridge. Research Lab. of Electronics).

Research and development are reported on plasma physics, plasma electronics, plasma magnetohydrodynamics, and energy conversion. (J.R.D.)

4949 (UCRL-14360, pp 85-94) RADIATION PHYSICS. (Lawrence Radiation Lab., Univ. of California, Livermore).

The dependence of the solutions of the Schroedinger equation on the dielectric constant in the complete screened Coulomb potential was studied, and a systematic method was developed for calculating the free energy and all other thermodynamic functions of an ionized gas mixture. A quantum theory of the pair distribution function of a high-temperature plasma was developed, and a secular-equation method was used to calculate the energies and wave functions of doubly excited two-electron atoms. Nonlinear laser noise and coherence were analyzed, and effective fluorescent lifetimes were calculated for a variety of sizes of laser ruby rods. The effect of ionizing radiation on the conductivity of air, nitrogen, and oxygen at atmospheric pressure was also calculated. The computer program FOTRAC for photon transport calculations was provided with its own source generator, and a Monte Carlo method

was developed for calculating the energy and angular distributions of photons from photon reactions with an atom. (D.C.W.)

4950 (UCRL-Trans-1261(L)) A PLASMA WITH RELATIVISTIC ELECTRONS IN A TRAP WITH MAGNETIC MIRRORS. Budker, G. I.; Volosov, V. I.; Moiseev, S. S.; Pal'chikov, V. E.; Tsel'nik, F. A. Translated for Univ. of California Lawrence Radiation Lab., Livermore, from Russian paper CN-21/217 presented at the Conference on Plasma Physics and Controlled Nuclear Fusion Research, Culham, England, September 6-10, 1965. 22p. Dep. mn; CFSTI $1.00 cy, $0.50 mn; JCL $2.60 fs, $0.86 mf.

Various uses of relativistic electrons in connection with magnetic mirror plasmas are discussed. Plasma stability is discussed from the standpoint of injecting relativistic electrons. Separate discussions are presented on heating of the plasma ions, magnetic bremsstrahlung, and the problem of relativistic electron injection. (M.O.W.)

4951 EXPERIMENTS ON THE STARTING PROCESS OF A ROTATING PLASMA. Bergstroem, J.; Holmberg, S.; Lehnert, B. (Royal Inst. of Tech., Stockholm). Arkiv Fys., 28: 191-204(1965).

An experiment is made with a rotating plasma by starting a discharge at right angles to a magnetic field. After some time a short-circuit is applied across the discharge and the stored angular momentum of the plasma is measured. Further, the azimuthal plasma current is recorded by means of a Rogowski coil and the angular momentum is estimated from the radial balance of forces. The measurements indicate that the plasma becomes completely ionized within the confinement region, as soon as the critical level of the power input is exceeded. (auth)

4952 THE STARTING PROCESS OF A ROTATING PLASMA. Lehnert, Bo (Royal Inst. of Tech., Stockholm). Arkiv Fys., 28: 205-14(1965).

The momentum balance of a partially ionized, rotating plasma is considered as a function of the ionization degree and the power input from an external source. The macroscopic fluid velocity of the charged particles relative to the neutral gas is assumed to be limited during the transition from a partially to a completely ionized state. The latter can only be reached if the power input exceeds a certain critical level. The results apply also to a plasma structure which consists of a number of radial spokes. (auth)

4953 FREE-WHEELING OF A ROTATING PLASMA. Bergstroem, J.; Holmberg, S.; Lehnert, B. (Royal Inst. of Tech., Stockholm). Arkiv Fys., 28: 231-2(1965).

A rotating plasma is released from its energy source and the corresponding decay times of the plasma voltage and the azimuthal plasma current are measured. A strong azimuthal current balances the centrifugal force during the entire period of free-wheeling. Further, the decay time of the voltage increases with the magnetic field strength and approaches a saturation level of about 310 microseconds. Its behavior can be explained by a transverse momentum loss due to viscous forces and a longitudinal loss caused by particles which escape to the end insulators. (auth)

4954 THE NONLINEAR INTERACTION OF A RADIO-FREQUENCY WAVE WITH AN INHOMOGENEOUS PLASMA SLAB. II. NONLINEAR REFLECTION AND TRANSMISSION COEFFICIENTS OF AN INHOMOGENEOUS PLASMA SLAB. Papa, Robert J.; Case, Carl T. (Air Force Cambridge Research Labs., Bedford, Mass.). Can. J. Phys., 43: 2036-44(Nov. 1965).

When a radio-frequency plane wave is incident upon an inhomogeneous, lossy plasma slab, part of the electromagnetic energy is reflected, part is absorbed by the plasma medium, and part is transmitted. At sufficiently high power levels (about 1 watt cm^2 at X-band frequencies), the equation of state of the plasma is altered, which produces a change in the effective dielectric constant of the medium. In the high-frequency limit, the effective dielectric constant of the medium is expressed as a function of the electron density and an effective collision frequency. The electron density and effective collision frequency at each point in the medium are functions of the electron temperature. The electron temperature (T_e) at each point (z) in the slab is expressed in terms of the local value of E^2/ω^2, where E = electric field amplitude and ω = signal frequency, i.e., $T_e = T_e(z, E^2/\omega^2)$. Using the predetermined functional dependence of T_e on z and E^2/ω^2, the electromagnetic field distribution and the net reflection and transmission coefficients of the plasma slab are computed by employing the Runge-Kutta technique to integrate Maxwell's equations numerically step by step. For each value of ω, relatively small changes in the reflection and transmission coefficient are produced as E^2_{inc}/ω^2 is increased up to a critical value of E^2_{inc}/ω^2, where E_{inc} = incident electric field amplitude. For values of E^2_{inc}/ω^2 greater than this critical value, there is a sharp increase in the reflection coefficient and a sharp drop in the transmission coefficient. (auth)

4955 SIMPLE METHOD FOR MEASUREMENT OF THE ELECTRON DENSITY AND THE COLLISION FREQUENCY OF A PLASMA USING A HIGH-FREQUENCY RESONANCE SPHERICAL PROBE. Lepechinsky, Dimitri; Rolland, Paul; Taillet, Joseph (Centre d'Etudes Nucleaires, Saclay, France). Compt. Rend., 261: 663-4(July 19, 1965). (In French).

A simple method for measurement of the electron density and the collision frequency of a plasma, beginning with the resonance peak of the probe current of a spherical probe exposed to a high frequency potential with variable frequency, is described. It gives these two parameters without it being necessary to know the thickness of the sheath. (tr-auth)

4956 PROPAGATION OF THE DIPOLAR MODE ALONG A PLASMA COLUMN. Leprince, Philippe (Univ. Paris, Orsay, France). Compt. Rend., 261: 665-7 (July 19, 1965). (In French).

The dispersion curve of a plasma guide for the dipolar mode was measured and calculated. The good agreement between theory and experiment indicates that the hypothesis of a homogeneous plasma, although inexact a priori, gives correct results unless it is necessary to know the attenuation of the waves. (tr-auth)

4957 THE KINETIC THEORY OF PLASMAS. Diener, Gerhard (Institut Henri Poincare, Paris). Compt. Rend., 261: 1204-6(Aug. 2, 1965). (In French).

A generalization of the adiabatic hypothesis of Bogoliubov for a completely ionized plasma susceptible to unstable oscillations on slightly damped oscillations is proposed. (tr-auth)

4958 LOCAL ANALYSIS BY ELECTRIC PROBE OF A CESIUM PLASMA PRODUCED BY CONTACT IONIZATION. Felden, Marceau; Haug, Robert; Patou, Claude (Faculte des Sciences, Nancy). Compt. Rend., 261: 1215-18(Aug. 2, 1965). (In French).

The parameters of an alkaline plasma obtained by contact ionization was studied locally with two types of probes. Difficulties were encountered in obtaining the characteristics of usable probes. Some possible solutions for this problem are discussed. (tr-auth)

4959 A PROPERTY OF CORRELATION IN A PLASMA DURING EQUILIBRIUM. Yvon, Jacques; Laval, Guy (Euratom-C.E.A., Fontenay-aux-Roses, France). Compt. Rend., 261: 1219-22(Aug. 2, 1965). (In French).

The hypothesis of the disappearance of correlations between remote particles is exploited. Then by the use of recurrence equations on reduced phase densities, integral relations for correlation functions are deduced. A closed system of two equations on the densities in simple and double phase in the linearized Kirkwood approximation is described. (tr-auth)

4960 ELECTRIC CONDUCTIVITY OF PLASMAS WHERE THE CHARGE CARRIERS APPEAR OR DISAPPEAR IN SPACE. Dolique, Jean-Michel (Faculte des

Sciences, Grenoble, France. E.I.E., Grenoble, France). Compt. Rend., 261: 1223-6(Aug. 2, 1965). (In French).

In a preceding study an Ohm law was established for partially ionized plasmas that was more rigorous and more general than that given by Cowling. The results of that study are extended to plasmas where, because of inelastic collisions, charge carriers appear or disappear in space. (tr-auth)

4961 CALCULATION OF THE ELECTRON DISTRIBUTION FUNCTION OF A HOMOGENEOUS LORENTZIAN PLASMA BY A SUCCESSIVE APPROXIMATION METHOD. Jancel, Raymond (Institut Henri Poincare, Paris). Compt. Rend., 261: 2169-72(Sept. 13, 1965). (In French).

The solutions of the infinite system of equations verified by the Fourier components of the electron distribution function of a homogeneous Lorentzian plasma were investigated using following successive powers of a small parameter characterizing the nonlinearity of the plasma. (tr-auth)

4962 CALCULATION OF THE NON-LINEAR EFFECTS BOUND TO THE PROPAGATION OF THE ELECTROMAGNETIC WAVES IN A HOMOGENEOUS AND ISOTROPIC LORENTZIAN PLASMA. Basu, Diptendu; Jancel, Raymond; Kahan, Theo (Groupe de Recherches Ionospheriques, Saint-Maur-des-Fosses, France; Institut Henri Poincare, Paris). Compt. Rend., 261: 2302-5(Sept. 20, 1965). (In French).

The results obtained previously (Compt. Rend. 260: 3877(1965) and 258: 837(1964)) were applied to the calculation of various nonlinear effects appearing during the propagation of electromagnetic waves in a homogeneous Lorentzian plasma. The demodulation (or self-modulation) of an amplitude-modulated wave and the effect of increased modulation (or Luxembourg effect) of this first wave on another non-modulated carrier wave were studied. In order to simplify the study the calculations were made in the absence of a magnetic field (isotropic plasma), but the results obtained can be extended without difficulty to the case of an isotropic plasma. (tr-auth)

4963 THE FIRST APPROXIMATIONS OF THE KINETIC THEORY FOR AN UNSTABLE PLASMA. Diener, Gerhard (Institut Henri Poincare, Paris). Compt. Rend., 261: 1473-5(Aug. 9, 1965). (In French).

The first approximations of a kinetic theory for a homogeneous and unstable plasma, obtained previously by generalizing the Bogolioubov method, are discussed. (tr-auth)

4964 STUDY OF THE REABSORPTION OF L_β AND H_α RAYS IN A PULSED DISCHARGE IN HYDROGEN. Schwob, Jean-Louis; Breton, Claude (CNRS, Bellevue, France; EURATOM-CEA, Fontenay-aux-Roses, France). Compt. Rend., 261: 1476-9(Aug. 9, 1965). (In French).

The ratio R_M of the mean transmission coefficients of the L_β and the H_α rays in the vicinity of their intensity maxima is studied theoretically as a function of the initial atomic density N and the electron temperature T_e. The results obtained are compared to the measurements made on a pulsed toroidal discharge. It is noted that the measurement of the ratio R_M and the transit time by the intensity maximum of the rays permits an evaluation of N and T_e. (tr-auth)

4965 STUDY OF THE OSCILLATORY REGIMES OF A CESIUM PLASMA MACHINE. Felden, Marceau; Haug, Robert; Patou, Claude (Univ. Paris, Nancy). Compt. Rend., 261: 1480-3(Aug. 9, 1965). (In French).

Some results obtained with a cesium plasma machine by contact ionization at variable geometry and operating at low cesium pressure (10^{-6} torr) are reported. The emphasis of the experimental study was on the variation of frequency and amplitude of the oscillations as a function of the temperature of the emitter, the applied voltage, and the continually variable emitter-collector distance. (tr-auth)

4966 THE ADIABATIC HYPOTHESIS IN THE QUASI-LINEAR THEORY OF PLASMAS. Diener, Gerhard (Institut Henri Poincare, Paris). Compt. Rend., 261: 1619-21(Aug. 18, 1965). (In French).

The adiabatic hypothesis of Bogolyubov is generalized for an inhomogeneous plasma, and the equivalence with the multitime scale method used by Frieman and Rutherford is shown. (tr-auth)

4967 ON MEASUREMENT OF ELECTRON DENSITY OF PLASMA. Ghoshal, A. K.; Sen, S. K.; Basu, J. (Univ. of Calcutta). Indian J. Phys., 39: 248-50(May 1965).

In order to assess the accuracy of the results and for comparison with the results given by the perturbation and admittance methods for a typical plasma, a more accurate method termed the exact method is developed for determining the electron density in a plasma. With the plasma placed coaxially in it, the cylindrical cavity operating in the TM_{010} mode is tuned. Maxwell's equations for the different media in the cavity, viz. plasma, its container, and air (air assumed equivalent to free space), are solved. The transcendental equations relating the operating frequency and the electron density are obtained by applying proper boundary conditions. Experiments were carried out on a typical mercury discharge plasma column. Electron densities at various discharge currents were determined by the perturbation, admittance, and exact methods using the derived equations. The electron density at the maximum current was found to be of the order of 1.7×10^{11} per cc, corresponding to $N/Nc \approx 1.5$. A comparison of the results of the first two methods with those of the exact method showed that the perturbation method is somewhat more accurate. (J.F.P.)

4968 THEORY OF THE DOUBLE PROBE AT HIGH GAS PRESSURE. Cozens, J. R.; von Engel, A. (Oxford Univ.). Int. J. Electron (1), 19: 61-8(1965).

It is shown that the mean electron energy in a uniform steady plasma at high gas pressure can be obtained from the analysis of a plane double probe curve. If the motion of charges to the boundary is controlled by diffusion and mobility, their production by single electron collisions and their loss by charge neutralization on the wall, the electron temperature is found from a relation which is similar to that for probes at low pressure. The mechanism of selection of electrons of different energy by a probe at low gas pressure is contrasted with that at high pressure and the application of the theory to various physical systems is discussed. (auth)

4969 ON CENTIMETER WAVE DETECTION IN GAS-DISCHARGE PLASMA. Sobol, G. A. Izv. Vysshikh Uchebn. Zavedenii, Radiofiz., 8: 420-1(1965). (In Russian).

Graphs were constructed of probe $I_p = f_1(V_s)$ and detector $I_d = f_2(V_s)$ characteristics for a glow discharge at three frequencies (50, 10^9, 10^{10} Hz), at neon pressure 1 mm Hz. Correlation of the three detector characteristics for identical discharge conditions showed that detector properties are inherent to plasma at a wide range of frequencies and can be utilized (at 20 to 10^{10} Hz) in plasma detectors. (R.V.J.)

4970 SPATIALLY AND TEMPORALLY RESOLVED ELECTRON AND ATOM CONCENTRATIONS IN AN AFTERGLOW GAS DISCHARGE. Gerardo, J. B.; Verdeyen, J. T.; Gusinow, M. A. (Univ. of Illinois, Urbana). J. Appl. Phys., 36: 3526-34(Nov. 1965).

The use of a modified laser interferometer to measure the temporal and spatial behavior of a medium density (10^{13}–10^{14} electrons/cc) afterglow plasma is described. The plasma was located inside the laser cavity. The presence of the plasma changes the laser frequency (within the Doppler-broadened transition) and this frequency shift was determined by coupling an external cavity to the laser. This modification of the interferometer preserves the high sensitivity of using the transverse modes in the external cavity and has a spatial resolution in the medium being studied of less than 1 mm^2. Two optical wavelengths, $\lambda_0 = 0.6328\ \mu$ and $\lambda_0 = 1.1523\ \mu$, and two microwave wavelengths, $\lambda = 4$, 8 mm, were used and

excellent agreement was obtained between measurements. It is shown that there is a strong migration of the gas atoms away from the discharge vessel axis due to the localized heating during the active discharge. Electron loss processes in such plasmas are discussed. Because of the excellent spatial resolution, the rate of loss of electrons by diffusion can be measured directly, and hence the electron temperature can be estimated. Electron temperatures obtained in this manner agree to within a factor of two with that obtained by the double-probe technique. (auth)

4971 MICROWAVE PLASMA DENSITY MEASUREMENTS. Thomassen, K. I. (Stanford Univ., Calif.). J. Appl. Phys., 36: 3642-4(Nov. 1965).

To make plasma density measurements on a cylindrical column with a microwave cavity requires a precise curve of cavity frequency versus density. In practice, one uses the measured cavity frequency (without a plasma) and the initial slope of this curve. An analysis is made for the TM_{010} mode to determine the effects of nonuniformity (a parabolic density) and of the holes in the cavity where the plasma column is admitted. It is shown that both effects result in a smaller slope so that one underestimates the density if they are not taken into account. (auth)

4972 DENSITY WAVES IN LOW-PRESSURE PLASMA COLUMNS. Woods, L. C. (Balliol Coll., Oxford). J. Fluid Mech., 23: 315-23(Oct. 1965).

Density waves in low-pressure arc discharges have been observed traveling toward the anode with speeds near $(\kappa T_e/M)^{1/2}$. A dispersion relation for these waves is developed, taking into account the boundary effects, namely, the continuous loss of ions to the containing walls. This theory is in fair agreement with experiment, except in its prediction of a rather high value for the wave damping. However, by allowing for the effect of electrostatic instabilities on anode-approaching waves, due to electron drift, this discrepancy is satisfactorily explained. (auth)

4973 EXPERIMENTAL STUDIES OF THE CONTINUUM EMISSION OF HYDROGEN. Hamberger, S. M.; Johnson, A. W. (Univ. of Oklahoma, Norman). J. Quant. Spectros. Radiative Transfer, 5: 683-95(Sept.-Oct. 1965).

The absolute intensity of continuum radiation emitted from a transient hydrogen plasma was measured for the wavelength range 3000-8000 Å, and found to agree closely with that theoretically predicted by considering all the significant radiating processes. The various particle densities and the temperatures needed for the comparison were spectroscopically obtained from the line radiation and independently of the continuum; the necessary assumption of local thermal equilibrium is discussed. The plasma was produced in an electrically driven shock tube, and observed close behind the shock front where impurity radiation was found to be unimportant. The measured electron densities were in the range 3×10^{16}–1.1×10^{17} cm^{-3}, and temperatures 11,000–18,000°K. Under some conditions both the atomic and negative ion free-bound and free-free spectra were important, while the experimental accuracy was insufficient to distinguish any contribution due to H_2^+ formation. (auth)

4974 AN EXPERIMENTAL STUDY OF THE EFFECTS OF ABSORPTION ON SPECTRAL LINES FROM A PLASMA. Bickel, William S.; Scoboria, Raymond (Pennsylvania State Univ., University Park). J. Quant. Spectros. Radiative Transfer, 5: 729-33(Sept.-Oct. 1965).

The progressive effects of absorption on the shape of a spectral line as a function of source intensity are experimentally demonstrated. Studies of a partially resolved helium triplet, using the relative intensities of the components, half widths and degrees of absorption, show that the question "when is a plasma optically thin" is indeed a subtle one. (auth)

4975 THE IMPEDANCE FORMULA FOR A PARTIALLY IONIZED, COLLISION-DOMINATED PLASMA. Okuda, Takayoshi; Yamamoto, Kenzo. Mem. Fac. Eng., Nagoya Univ., 16: 39-54(Nov. 1964).

The impedance formula for a partially ionized, collision-dominated plasma is derived on the basis of the transport equation, taking the temperature perturbation into account. Several attempts are made. In the first attempt, the density perturbation is completely neglected but the inertia term is retained. The second is based on the ignorance of all space derivatives of the quantities involved. The third attempt is made by use of the quasi-steady approximation, but without exception of the term related to the space charge field. The fourth corresponds to the quasi-steady treatment of the second case. (auth)

4976 NOTE ON SHEATH FORMATION. Miyajima, Shigeki. Mem. Fac. Eng., Nagoya Univ., 16: 55-67(Nov. 1964).

A plasma-sheath transition is discussed as a function of the electric current delivered to the sheath, using a one-dimensional, collisionless model and a set of macroscopic equations. When the conditions $\gamma^2 = \Sigma_{e,i} m_s v_{s0}^2 / \Sigma_{e,i} kT_s = 1$ and $E_0 = 0$, (where the subscript s stands for e (electron) and i (ion), m_s is the mass of a particle, v_{s0} the velocity at the plasma-sheath boundary, T_s the temperature and E_0 the electric field at the boundary, for $m_i v_{i0}^2/kT_i > 1$ (or $m_e v_{e0}^2/kT_e < 1$) the pure ion sheath is formed without any local excess of electron space charge, for $m_i v_{i0}^2/kT_i = 1$ (or $m_e v_{e0}^2/kT_e = 1$) any sheath is not established and for $m_i v_{i0}^2/kT_i < 1$ (or $m_e v_{e0}^2/kT_e > 1$) the pure electron sheath is developed. When $\gamma^2 \neq 1$ and $E_0 = 0$ or $\neq 0$, then the formation of sheath is much complicated. Thus the conditions $\gamma = 1$ and $E_0 = 0$ lead to the establishment of much simple sheaths among the various sheaths and are including the familiar Bohm criterion when $v_{s0} \to 0$. Furthermore, one may find that the ideal Langmuir probe curve, in which the conditions $\gamma^2 = 1$ and $E_0 = 0$ are imposed, deviates from the classical probe theory. (auth)

4977 EXPERIMENTAL OBSERVATIONS ON THE STRUCTURE OF COLLISIONLESS SHOCK WAVES IN A MAGNETIZED PLASMA. Paul, J. W. M.; Holmes, L. S.; Parkinson, M. J.; Sheffield, J. (U. K. Atomic Energy Authority Research Group, Culham Lab., Abingdon, Eng.). Nature, 208: 133-5(Oct. 9, 1965).

Measurements of the structure of shock waves propagating through a plasma in a direction perpendicular to an initial magnetic field are reported. The shock wave is produced by a fast linear Z pinch between electrodes. The applied electric field produces an axial current, which is driven by pinch forces radially inwards at a velocity exceeding the Alfvén velocity for the undisturbed plasma. This rapid radial compression generates an imploding shock wave which propagates ahead of the driving current layer. At low Mach numbers ($M_A < 3$) the results indicate that a resistive shock is formed which probably involves collisionless turbulence. Above the predicted critical $M_A(\sim 3)$ the observed change of structure is interpreted as due to an additional, but unidentified, collisionless mechanism. None of the present theories of shock structure gives convincing agreement over the range of observations, but some can be eliminated. (J.F.P.)

4978 NONLINEAR ALFVEN WAVES IN A VLASOV PLASMA. Bell, T. F. (Technical Univ. of Denmark, Lyngby). Phys. Fluids, 8: 1829-39(Oct. 1965).

Stationary solutions to the nonlinear Vlasov-Boltzmann equations are considered which represent one-dimensional electromagnetic waves in a hot magnetoplasma. These solutions appear in arbitrary reference frames as circularly polarized, sinusoidal waves of unlimited amplitude, i.e., as nonlinear Alfvén waves. Solutions are found implicitly by deriving a set of integral dispersion relations which link the wave characteristics with the particle distribution functions. A physical discussion is given of the way in which the Alfvén waves can trap particles, and it is shown that the presence of "cyclotron-trapped" particles introduces a boundary condition which no set of isotropic distribution functions can satisfy. An application of these solutions to theories of very low frequency emissions is briefly discussed. (auth)

4979 FINITE GYRO-RADIUS CORRECTIONS TO THE HYDROMAGNETIC EQUATIONS FOR A VLASOV PLASMA. Macmahon, Alan (Univ. of California, Berkeley). Phys. Fluids, 8: 1840-5(Oct. 1965). (UCRL–11634).

Velocity moments of the Vlasov equation are expanded systematically in m/e and equations obtained giving the fluid velocity transverse to B through second order. These equations include all "finite gyro-radius" effects. No a priori form is imposed on the velocity distribution. The transverse electric field $E_\perp$ is allowed to be large. For straight field lines the equations for purely transverse motion are closed. For weak instabilities ($E_\perp$ small) closed equations are obtained only for low plasma pressure. (auth)

4980 LONGITUDINAL OSCILLATIONS IN UNBOUNDED ONE-DIMENSIONAL NONUNIFORM PLASMAS. Harker, Kenneth J. (Stanford Univ., Calif.). Phys. Fluids, 8: 1846-52(Oct. 1965).

A study is made of the oscillations in a one-dimensional nonuniform plasma by use of the linearized Boltzmann-Vlasov equation. Particular attention is given to static potential distributions varying as x^n. An integral equation is derived for the radio-frequency electric field. Examination of the kernel of this equation reveals that Landau damping can only occur when there are unperturbed electron orbits whose periods are some odd multiple of the period of the applied field. Since all the unperturbed orbits in the case of parabolic static potential distributions have the same period, it is clear that in general there will be no Landau damping with this configuration. For the case of a parabolic state potential, the resonances of the plasma are obtained by solving numerically for the eigenvalues of the integral equation. For certain frequencies it is also possible to evaluate the kernel of the integral equation in closed form. (auth)

4981 MICROINSTABILITY OF A MIRROR-CONFINED PLASMA. Guest, G. E.; Dory, R. A. (Oak Ridge National Lab., Tenn.). Phys. Fluids, 8: 1853-9(Oct. 1965). (ORNL-P-1257).

Infinite uniform magnetized plasmas with non-Maxwellian particle distributions are subject to electrostatic longitudinal instabilities of the type discussed by Harris. Mirror confinement leads to depletion of low energy ion populations and thus to the Rosenbluth-Post "maser" instability at frequencies $\omega \gg \omega_{ci}$, the ion gyrofrequency, and to the flute-like instability of Dory, Guest, and Harris with $\omega \simeq \omega_{ci}$ and wave vector normal to the external magnetic field. This study is concerned with unstable waves which propagate obliquely with $\omega \simeq \omega_{ci}$ and wavelength $\lesssim \rho_g$, ion gyroradius. For their appearance it is necessary that ω_{pe}/ω_{ci} exceed a threshold value of order $n(1\ 8a^2v_{\|e}^2/v_{\perp i}^2)^{1/2}$, where n is the harmonic number of the unstable wave, and $v_{\|e}$ and $v_{\perp i}$ are the components of electron and ion thermal velocity, parallel and perpendicular to the external magnetic field. Over a wide range of interesting conditions, the parameter a lies between 2 and 3. Furthermore, the plasma is stable if $n\omega_{ci} \lesssim ak_\| v_{\|e}$ or if $\omega_{pe} \lesssim ak_\| v_{\|e}$, where $k_\|$ is the parallel component of the wave propagation vector and ω_{pe} is the electron plasma frequency. These waves are not fully stabilized by increasing ion temperature parallel to the field as are the anisotropy modes in a two-temperature Maxwellian plasma. (auth)

4982 ENHANCED BREMSSTRAHLUNG FROM PLASMAS CONTAINING NONTHERMAL ELECTRONS. Tidman, Derek A. (Univ. of Maryland, College Park); Dupree, Thomas H. Phys. Fluids, 8: 1860-70(Oct. 1965).

The bremsstrahlung emitted from thermal plasmas which coexist with a flux of energetic (suprathermal) electrons is calculated. It is found that under some circumstances the radiation emitted can be greatly increased compared to the emission from a Maxwellian plasma with no energetic particles present. The enhanced emission occurs at the fundamental and second harmonic of the electron plasma frequency. (auth)

4983 NUMERICAL MODEL OF AN ION-CYCLOTRON WAVE EXPERIMENT. Hamilton, Gordon W. (Univ. of California, Berkeley). Phys. Fluids, 8: 1876-85(Oct. 1965). (UCRL–11619(Rev.1)).

A numerical model is constructed to demonstrate the propagation and absorption of ion-cyclotron waves in a previously reported experiment. Ion-cyclotron waves in a deuterium plasma induced by a radially applied 8.3-Mc electric field propagate in a magnetic-mirror field to a resonance region where the ion-cyclotron frequency approaches the wave frequency. The numerical model considers the wave propagation in the nonuniform divergenceless magnetic field with spatially nonuniform plasma parameters, subject to boundary conditions modeled after the experiment. The model is based on the macroscopic equation of motion, the generalized Ohm's law, the wave equation, an equivalent resistivity representing the effect of ion-cyclotron damping, and damping by collisions between deuterons and other particle species. The equations are solved numerically by a single-line block over-relaxation technique. The numerical results are compared with the experimental wave measurements and also provide information regarding current distributions, wave polarizations, evanescent compressional waves, and reflections from the resonance under certain conditions. (auth)

4984 OPTIMUM GENERATION OF ION-CYCLOTRON WAVES IN A CYLINDRICAL TWO-ION PLASMA. Chung, K.; Rothman, M. A.; Sinclair, R. M.; Yoshikawa, S. (Princeton Univ., N. J.). Phys. Fluids, 8: 1886-9(Oct. 1965). (MATT–343).

Ion-cyclotron waves were generated in a hydrogen-deuterium plasma (previously formed by Ohmic heating) contained in the Model C stellarator, using an induction coil of finite wavelength. The conditions for optimum generation of waves, found experimentally, were in good agreement with theoretical predictions. (auth)

4985 OSCILLATIONS OF A PLASMA COLUMN. Landau, R. W.; Schmidt, G. (Stevens Inst. of Tech., Hoboken, N. J.). Phys. Fluids, 8: 1890-5(Oct. 1965).

Oscillations in plasma columns exhibit many interesting features not found in infinite uniform plasmas. A study is made on the effects due to retardation of the electromagnetic field which gives rise to a curious behavior of the static mode for long wavelengths and a radiating branch of electrostatic plasma oscillations. The principal aim of this study is to gain an understanding of the physical mechanisms underlying these phenomena. The transition from the finite column to the infinite uniform plasma case is also discussed. (auth)

4986 NONLINEAR OSCILLATIONS IN A HOT ELECTRON PLASMA. Nayfeh, Ali Hasan (Heliodyne Corp., Los Angeles). Phys. Fluids, 8: 1896-8(Oct. 1965).

The derivative-expansion method is applied to the longitudinal nonlinear traveling oscillations in a hot electron plasma. The frequency and wavenumber shifts obtained by using the above method agree with those obtained by using the Krylov-Bogoliubov-Mitropolsky perturbation method. (auth)

4987 CLASSIFICATION OF INSTABILITIES FROM THEIR DISPERSION RELATIONS. Sudan, R. N. (Cornell Univ., Ithaca, N. Y.). Phys. Fluids, 8: 1899-1904(Oct. 1965).

Necessary and sufficient criteria are derived for classifying waves in complex media into evanescent, propagating, and growing waves (or instabilities). An absolute or nonconvective instability is shown to exist only if the complex group velocity $d\omega/dk$ vanishes at some point in the upper half of the frequency plane. A physical interpretation of this result is given. The analysis is extended to include slowly varying inhomogeneous media. (auth)

4988 CLASSICAL COLLISION INTEGRALS FOR THE REPULSIVE SCREENED COULOMB POTENTIAL. Smith, Francis J. (Queen's Univ., Belfast); Mason, E. A.; Munn, R. J. Phys. Fluids, 8: 1907-8(Oct. 1965).

Classical transport collision integrals are presented for a screened Coulomb potential. These are written in the

form $\phi(r) = \phi_0(\rho/r)e^{-r/\rho}$ where ϕ_0 and ρ are positive constants. The results are given as calculated numerically. The results resemble those for the repulsive exponential at low temperatures. For high temperatures the screened Coulomb potential is a more realistic model because of its behavior near r = 0. (J.F.P.)

4989 GROWING WAVES IN A NONGYROTROPIC PLASMA. Sudan, R. N. (Cornell Univ., Ithaca, N. Y.). Phys. Fluids, 8: 1915-18(Oct. 1965).

A collisionless electron plasma in a uniform field $B_0\hat{e}_z$ which possesses an unperturbed distribution function f^0 for the electrons that cannot be considered isotropic in the v_x, v_y plane of velocity space, is treated, that is, a nongyrotropic plasma defined by $\partial f^0/\partial\phi \neq 0$, $\phi = \tan^{-1}(v_y/v_x)$, the azimuthal angle made by the velocity vector v. Such situations may arise in proposed schemes that involve the injection of fast neutrals into confining magnetic fields. To keep the analysis from becoming too unwieldly, the positive ions are assumed to be completely immobile and uniformly distributed to neutralize the zero-order electron charge. (J.F.P.)

4990 TOTAL THERMAL CONDUCTIVITY OF PARTIALLY AND FULLY IONIZED GASES. Ahtye, Warren F. (Ames Research Center, Moffett Field, Calif.). Phys. Fluids, 8: 1918-20(Oct. 1965).

Problems which arose in previous attempts to calculate the total thermal conductivity within the framework of the Chapman-Enskog formulation for partially and fully ionized gases are circumvented by the method presented. The approach for a binary plasma is extended to obtain closed form expressions for the total thermal conductivity of a partially ionized plasma and a fully ionized ternary plasma, e.g., a mixture of singly and doubly ionized atoms and electrons. The crux of this approach is not to separate the forcing potential d, into $\partial x/\partial r$ and E components, but to solve for this quantity directly by making use of the conservation of the net flux for each species, which was previously mentioned. Physically this means that an arbitrary value of the charge separation field will result in a readjustment of the concentration gradients so that the net flux is conserved. Therefore, the combined effect in the form of d is a more logical variable than its components. (J.F.P.)

4991 NOISE AND CORRELATION STUDIES OF MICROWAVE RESONANCES OF A PLASMA COLUMN IN A MAGNETIC FIELD [Thesis]. Oetzel, George Norton. Stanford, Calif., Stanford Univ., 1965. 145p.

Recent observations of strong resonances at the harmonics of the electron cyclotron frequency in the noise emission from low-temperature plasmas have raised the question of whether the harmonics were being generated in the volume of the plasma or in the sheath. Conclusive evidence is presented that the observed harmonic effects can be explained satisfactorily in terms of electrostatic oscillations in the plasma volume, and that they cannot be explained in terms of effects in the sheath. The methods used included observations of noise emission, wave propagation measurements, and a new type of noise measurement, which is called a two-frequency correlation measurement. The two-frequency correlation measurement was also a major object of investigation. It consists of irradiating the plasma at one frequency with a transmitted microwave signal and observing the heating effects of the transmitted signal with a receiver at a different frequency. Very good agreement with the calculated dispersion relation for the electrostatic oscillations was obtained in noise measurements. Transmission parallel to the magnetic field and plasma column was observed, an effect which cannot be explained in terms of the plasma sheath. Resonant heating in the cyclotron harmonic modes was observed, and the resonances satisfied the calculated dispersion relation very well. The noise signals generated by heating the column in the fundamental and second harmonic modes were also observed to propagate along the magnetic field and plasma column. Observations of noise emission, wave propagation, and resonances in modes other than the cyclotron harmonic modes are also presented. A theoretical discussion of the two-frequency correlation experiment and a further exploration of its experimental properties are given. (Dissertation Abstr.)

4992 PROBLEMS AND PROGRESS IN CONTROL OF THERMONUCLEAR FUSION FOR ELECTRICAL POWER PRODUCTION. Dougal, Arwin A. (Univ. of Texas [Austin]). pp 9.1-8 of 2nd Annual Energy Conversion and Storage Conference. Stillwater, Okla., Oklahoma State Univ., [1964].

The basic principles of controlled thermonuclear fusion are summarized. A discussion is given of two promising experimental approaches: research on ion cyclotron resonances and waves in thermonuclear plasmas, and research on theta-pinch thermonuclear plasmas. A new plasma diagnostic technique using Faraday rotation for infrared masers is also described. The fundamental problems in controlling the nuclear fusion reaction are the heating of an ultrapure, low-density, deuterium plasma to super-high temperatures in the $10^{8\circ}$K range, the containment of the high-temperature plasma stably and adequately by an electromagnetic field for a sufficiently long time for the nuclei to fuse, and the conversion of the energy released for useful electric power. These problems are also discussed. (J.F.P.)

4993 PARTICLE INJECTING DEVICE. Leboutet, Hubert; Dube, R. Georges (to Compagnie Generale de Telegraphie Sans Fil). U. S. Patent 3,212,974. Oct. 19, 1965. Filed May 31, 1960.

A plasma injecting device is provided that mixes the high energy ions with electrons prior to injection into the confining device. The high energy ion beam is passed through the inside of a tubular electron beam that is made to converge in such a manner that the mixing occurs in the neighborhood of the axis of the injector and forms the high energy plasma. The confining means is comprised of a magnetic bottle inside the evacuated vessel. (B.L.M.)

4994 METHOD AND APPARATUS FOR PRODUCING A MAGNETICALLY CONFINED HOT DENSE PLASMA. Ehler, Arthur W. (to U. S. Atomic Energy Commission). U. S. Patent 3,218,235. Nov. 16, 1965.

A device and method are described for producing plasmas confined within a magnetic field or "bottle." The method comprises injecting atoms of the isotope ^{6}He into an evacuated chamber wherein ^{6}He decays to ^{6}Li with the emission of a relativistic electron. The electron is trapped in the magnetic field and interacts to form an energetic plasma with hydrogen gas used to purge the Li ions. Other neutral gas particles may be injected and ionized in the plasma which may then be compressed to produce a highly energetic plasma. (AEC)

4995 PLASMA CONFINEMENT APPARATUS EMPLOYING A HELICAL MAGNETIC FIELD CONFIGURATION. Furth, Harold P. (to U. S. Atomic Energy Commission). U. S. Patent 3,219,534. Nov. 23, 1965.

A device is designed for stably confining a plasma employing a helically non-axially symmetric magnetic field having closed magnetic flux surfaces. The magnetic field is composed of three magnetic field components and is established by energizing a solenoidal coil in the form of a toroid to establish an axial magnetic field component. An azimuthal magnetic field component is generated by energizing a center conductor supported insulatingly apart from and coaxially with the solenoidal coil. The center conductor energizing current is directed in the same direction as the axial magnetic field component lines. Two parallel wound diametrically opposed helical coils are supported insulatingly apart from and coaxially with the solenoidal coil and are energized by oppositely flowing current to establish a transverse helically rotating magnetic field component. The mutual interaction of the magnetic field components produces a resultant magnetic field comprised of nested magnetic flux surfaces defined by infinitesimal magnetic flux tubes with the surfaces of flux tubes of larger volumes per unit flux being encircled by surfaces of flux tubes having smaller volumes per unit flux. Certain hydromagnetical instabilities are minimized by the defined configuration. (AEC)

Shielding

Refer also to abstracts 4299, 4406, 5181, and 5183.

4996 (AWRE-O-79/65) A 12 GROUP SET OF PHOTON CROSS SECTIONS FOR USE IN ANISOTROPIC S_n CALCULATIONS OF PHOTON TRANSPORT. Kerr, W. M. M.; Parker, K.; Williams, D. V. J.; Wilton, Patricia M. (Atomic Weapons Research Establishment, Aldermaston (England)). Oct. 1965. 38p. Dep.; BIS $1.10; HMSO 5s. 6d.

The 12 group set 2 photon cross sections calculated for use in STRAINT and other programs in which anisotropic scattering can be taken into account is described. All the numbers required are given in the form of SC4020 prints so that the cross sections can be used in other programs. (auth)

4997 (EUR-2494.d) ABSCHIRMUNGSEXPERIMENTE AM FORSCHUNGSREAKTOR GEESTHACHT—JAHRESBERICHT 1964. (Shielding Experiments at the Reactor Station Geesthacht—Annual Report, 1964). Bagge, E.; Fischer, E. (Gesellschaft fuer Kernenergieverwertung in Schiffbau und Schiffahrt m.b.H., Hamburg (West Germany)). 1965. 175p. Dep. mn.

The experimental rigs ESTAKOS, ESTAGROP I and ESTAGROP II were used for several tests. The ESTAKOS group carried out various tests to check the measuring accuracy as well as measuring the radiation field on 5 shield arrays and determining the effective relaxation values of a number of materials. A start was made on tests to verify the accuracy with which ESTAKOS measuring results can be used to predict the measuring results obtained on other experimental devices. In Pool IV of the FRG (ESTAGROP I) the temperature rise resulting from radiation absorption in a 5 cm steel plate was investigated. It was shown that the temperature increase was everywhere proportional to the gamma dose-rate, the neutrons playing only a small part in the heating effect. On conclusion of these tests, the first experiments were carried out on shield penetrations. Studies were made on gamma-permeability at a penetration in a 20 cm-thick iron slab and at an S-shaped penetration in concrete. The measurements provided basic data for the design of the main steam duct penetration in the secondary shielding of the research ship. Shielding tests were performed with layered shielding assemblies for the purpose of defining the optimum shielding design for mobile reactors. It proved possible to deal with 12 different shielding setups. A start was made on the first shielding experiments in the large irradiation-channel of the FRS (ESTAGROP II). The radiation field was measured in a water-filled irradiation space (thermal, epithermal and fast neutron flux and gamma dose-rate). The work aimed at the elaboration of measuring devices covered basically the further development of a recoil proton spectrometer and tests intended to provide data concerning the possibility of using semi-conductor spectrometers for neutron spectrometry in shielding rigs. Indications are given of the difficulties arising as a result of interference reactions in the silicon of the semiconductor diodes. The theoretical group performed rough calculations for shield penetrations while continuing its work connected with the setting-up of comparative calculations for the experiments with flat assemblies. The computation programs MENDIP-65, COGA, and SHIGA made it possible to estimate group constants from microscopic data. A new method for radiation shielding optimization was devised with which layered shields including their material components, in flat, cylindrical and sphero-symmetrical geometry, can be optimized. Furthermore, new mathematical methods were evolved in connection with neutron transport theory. (auth)

4998 (JINR-P-2359) PROKHOZHDENIE NEITRONOV VYSOKIKH ENERGII V ZHELEZOVODNYKH SMESYAKH. (Passage of High Energy Neutrons in Iron-Aqueous Mixtures). Sychev, B. S.; Mal'kov, V. V.; Komochkov, M. M.; Zaitsev, L. N. (Joint Inst. for Nuclear Research, Dubna (USSR)). 1965. 14p. Dep. mn.

The accumulation of slowed down neutrons (E < 1 Mev) was determined experimentally and theoretically when high energy protons pass in iron and iron-aqueous mixtures. The data obtained allow to construct a shielding of heavy concrete and iron–cement mixtures. It is established that the use of iron for accelerator's shielding without adding hydrogen is not expedient. (auth)

4999 (ORNL-2599) AIRCRAFT NUCLEAR PROPULSION PROJECT SEMIANNUAL PROGRESS REPORT FOR PERIOD ENDING SEPTEMBER 30, 1958. (Oak Ridge National Lab., Tenn.). Feb. 5, 1959. Contract W-7405-eng-26. 220p. Dep. mn; CFSTI $6.00 cy, $1.25 mn.

Melting, purification, and fabrication of niobium were studied, and conclusions are drawn. Studies were conducted to determine the solubility of lithium nitride and lithium oxide in lithium. Static corrosion tests of niobium tubing were conducted. A series of seesaw-furnace tests of various systems is described. Static corrosion tests of Be in Li showed Be to be quite resistant to attack by static Li in all Be systems. A survey of phase diagrams of refractory-metal base binary systems revealed several promising brazing alloys. Equipment was developed for tensile and creep tests of materials in controlled environments at temperatures up to 2500°F. Creep and rupture properties of Inconel were investigated in tubes with both internal pressure and axial stress. Dynamic load tests on Inconel rods and tubes are described. Small batches of zirconium boride were synthesized for incorporation into BeO bodies. Several additives were tested as means for increasing the density of BeO. Tests were run to determine the oxidation resistance of various borides when added to high-density BeO. Non-destructive testing techniques are discussed. A semicircular heat exchanger was examined metallographically to determine the location and effects of leaks that caused termination of operation. Experimental information was obtained regarding a tentative procedure for purifying lithium metal by extracting oxide, nitride, and carbide impurities with a eutectic mixture of lithium halide salts. The method for the determination of oxygen in fluoride salts with $KBrF_4$ was successfully applied. A cryostat for studying radiation effects on semiconductors was constructed with a temperature range of –200 to 350°C. Radiation effects on a grown-junction silicon diode were determined. Attempts were made to alloy indium and germanium at low temperatures. Pump testing is described. Experimental studies of the effect of thermal-stress cycling on structural materials were conducted with the pulse-pump system. Analyses of data obtained from a mercury system in the study of heat transfer in a liquid metal with internal heat generation were completed. A survey was made of various types of auxiliary power units suitable for use in satellites. A calculation was performed to obtain predicted pulse-height spectra of capture and inelastic scattering gamma rays. The Oracle Monte Carlo code was used to calculate the primary gamma heating in a slab shield. Neutron dose-rate distributions beyond water slabs were calculated for plane monodirectional, monoenergetic sources incident on the slabs at angles of 0, 30, 60, and 75°. Shielding studies and measurements in the Lid Tank Shielding Facility, Bulk Shielding Facility, and Tower Shielding Facility are reported. The latest design of the TSR-II and several studies supporting the design are presented. (W.D.M.)

5000 (ORNL-IIC-5, pp 91-8) BREMSSTRAHLUNG FROM ^{90}Sr–^{90}Y IN THIN ABSORBERS. Bustard, Thomas S.; (Hittman Associates, Inc., Baltimore, Md.); Silverman, Joseph (Maryland Univ., College Park. Dept. of Chemical Engineering).

The bremsstrahlung yields from targets ranging in atomic number from 13 to 73 with a thin, point source of ^{90}Sr–^{90}Y are presented. A novel method of obtaining these yields was used, the bremsstrahlung spectra being measured as they are built up and attenuated through tar-

gets whose mass thicknesses are less than the range of the ^{90}Y maximum-energy beta particle. The resulting bremsstrahlung yields were then compared to those calculable from the Evans (Evans, R. D., The Atomic Nucleus, 1955) approximation to thick target theory. (auth)

5001 (ORNL-RSIC-9) A COMPARISON OF THREE METHODS USED TO CALCULATE GAMMA-RAY TRANSPORT IN IRON. Trubey, D. K.; Penny, S. K.; Lathrop, K. D. (Oak Ridge National Lab., Tenn.). Oct. 1965. Contract W-7405-eng-26. 57p. Dep. mn; ORNL Free.

Calculations of the gamma-ray energy spectra, dose rate, and heating in a sphere of iron were made using the Monte Carlo and S_n methods and the data from a moments method calculation (Goldstein-Wilkins). The source was taken to be isotropic and distributed uniformly within a sphere with an energy distribution proportional to $e^{-1.1E}$, where E is the energy in Mev. The results of all calculations were in very good agreement. (auth)

5002 TEMPERATURE DISTRIBUTION IN GAMMA SHIELDING. Osanov, D. P. (Moscow Inst. of Biophysics). Inzh.-Fiz. Zh., 8: 807-14(June 1965). (In Russian).

A method is presented for calculating the temperature distribution in the shielding against gamma radiation based on the solution of a steady-state heat conduction equation with boundary conditions of the third kind. The temperature distribution is obtained for plane isotropic and plane monodirectional radiation sources in concrete shieldings of various thicknesses. It was found that boundary conditions have a substantial effect on the temperature distribution within the shielding. Scattering of gamma rays inside the concrete shielding results in an increase of temperature. The γ beam geometry has a lesser effect on temperature distribution. The increase in the thickness of the shielding worsens the heat removal from interior portions of the shielding block. The results obtained make it possible to evaluate approximate safety conditions for concrete shielding. (ATD)

Solid State Physics

See also CHEMISTRY — Inorganic and Physical Chemistry
METALS, CERAMICS, AND OTHER MATERIALS — Properties and Structure

Refer also to abstracts 3914, 3947, 4008, 4796, and 4809.

5003 (CEA-R-2875) OBSERVATION DES DISLOCATIONS DANS LES CRISTAUX PAR TRANSMISSION DES RAYONS X ET DES ELECTRONS [Theses]. (Observation of Dislocations in Crystals Using X-ray and Electron Transmission [Thesis]). Morlevat, Jean-Pierre (Commissariat a l'Energie Atomique, Grenoble (France). Centre d'Etudes Nucleaires). Oct. 1965. 28p. Dep. mn.

Two approaches to the dynamical theory of diffraction (Ewald's and Anthier's) are briefly reviewed. The information on crystal dislocations that may be gained through the application of these theories, using both electron and x-ray diffraction, is then considered. (P.C.H.)

5004 (IAE-927) O PRIRODE ZAVISIMOSTI ENERGII IZLUCHENIYA V MESSBAUER-EFFEKTE OT TEMPERATURY. (The Nature of the Relationship of Energy Emission in the Moessbauer Effect to Temperature). Morozov, V. M. (Institut Atomnoi Energii, Gosudarstvennyi Komitet po Ispol'zovaniyu Atomnoi Energii SSSR, Moscow). 1965. 8p. Dep. mn.

An explanation for the decrease of the average energy of radiation in the Mössbauer effect with an increase of the temperature of the solid by the so-called transverse Doppler effect is considered. It is shown that the Doppler effect does not explain the observed dependence of the average radiation energy on the temperature, since, in spite of a widespread delusion, the Doppler effect leads to a growth of the average radiation energy with an increase of the mean square velocity of the displacement of the radiator. It is noted that the absence of the thermal Doppler effect in the Mössbauer effect excludes the representation of the oscillations of atoms in a crystalline lattice like a classical pendulum. (tr-auth)

5005 (IAE-928) O FONONNOM SPEKTRE RESHETKI BELOGO OLOVA. (The Phonon Spectrum of the Lattice of White Tin). Brovman, E. G.; Kagan, Yu. (Institut Atomnoi Energii, Gosudarstvennyi Komitet po Ispol'zovaniyu Atomnoi Energii SSSR, Moscow). 1965. 29p. Dep. mn.

A consistent discussion of the dynamic problem of lattice oscillations of white tin in the framework of the Born-Karmann model is carried out. All the force constants entering into the full dynamic matrix of oscillations for the first three coordinate spheres are used; interactions with the following three coordinate spheres are approximated by two force constants each. The dispersion curves along the symmetry directions, the function of the frequency distribution of the phonon spectum, the thermal capacity, and the probability of the Mössbauer effect are found. A comparison of these values with experimental data is carried out. In the framework of the obtained results, a successful explanation is made of the observed anomalies in the heat capacity at low temperatures and the anomalous sign of the Mössbauer-effect anisotropy in the temperature range 77 to 400°K. It is found that as $T \to 0$ the anisotropy practically disappears or even changes sign. (tr-auth)

5006 (ORNL-3870, pp 50-5) SOLID-STATE AND MOLECULAR THEORY. Faulkner, J. S. (Oak Ridge National Lab., Tenn.).

Calculations of the magnetic properties of rare-earth germanomolybdates were consistent with experiment. The sublattice magnetization of α-Fe_2O_3 can be explained by antiferromagnetic spin-wave theory if the long-wavelength approximation is not used. A FORTRAN code was written to calculate the energy levels and eigenvectors of the d^2 and d^8 configurations in crystalline electric fields of arbitrary symmetry within the framework of the point charge model. The convergence of the one-center expansion for H_2^+ was investigated, several highly excited states of He and He^- were examined, and attempts were made to determine the shape and size of CH_4^+. Large-scale calculations on the lithium atom were made using approximate wave functions with angular interelectronic coordinates. A simple energy-calibrated molecular orbital technique was developed and applied to correlate ionization potentials in several groups of related compounds. The connection between the Green's-function method and the transfer-matrix method for investigating the electronic states of disordered systems was clarified. A nontrivial extension of the Green's-function method is being developed and applied to liquid metals. Questions concerning the utility of the one-center expansion in relation to energy and molecular geometry calculations were studied. For certain problems, multicenter calculations promise greater accuracy. (W.L.G.)

5007 (UCRL-14398) A THEORETICAL STUDY OF THE SECOND-ORDER RAMAN SPECTRA OF THE CESIUM HALIDES. Hardy, J. R.; Karo, A. M.; Morrison, I. W. (Lawrence Radiation Lab., Univ. of California, Livermore). Sept. 6, 1965. Contract W-7405-eng-48. 19p. Dep. mn; CFSTI $1.00 cy, $0.50 mn.

The results of recent calculations of the second-order Raman spectra of CsCl, CsBr, and CsI are reported. For the last two crystals experimental results are available, and the calculations can be compared with the observed spectra. It was found that the spectra derived by allowing for the polarizability and overlap deformation of the ions were in much better agreement with the experimental results than those derived by treating the ions as rigid point charges. In fact, in the first case the overall agreement was remarkably close, even though no allowance was made for the wavevector dependence of the Raman polarizability tensor. The probable reason for this agreement seems to be that the main peaks in the theoretical spectra arise

from superpositions of critical points in the two-phonon dispersion curves which occur along symmetry axes. Because of this, matrix elements were averaged over, and therefore agreement in shape with the experimental curves was not too surprising. The results tend to support the view that the observed Raman spectra provide a reasonably close mapping of the two-phonon density of states and can be used both to test and refine theoretical calculations of the dynamical matrix. Also, if the computed spectra are reliable, it is apparent that low-temperature, high-resolution spectra should reveal considerably more detail than is currently available from room-temperature measurements. (auth)

5008 (ORNL-tr-872) TRANSITION RADIATION AND THE OPTICAL PROPERTIES OF MATERIALS. Frank, I. M. (Akademiya Nauk SSSR, Moscow. Institut Fiziki). Translated for Oak Ridge National Lab., Tenn., from Perekhodnoe Lzluchenie i Opticheskie Svoistva Veshchestva. 39p. Dep. mn; CFSTI $2.00 cy, $0.50 mn; JCL $3.60 fs, $1.37 mf.

The theory of transition radiation for charged particles is presented. A special case is considered with the charged particle being an electron. A survey of experimental data is presented, and the characteristics of the optical part of the spectrum of transition radiation of relativistic particles are discussed. (M.O.W.)

5009 (UCRL-Trans-1227) A CONTRIBUTION TO THE INVESTIGATION OF RECIPROCAL LATTICES OF SINGLE CRYSTALS BY MEANS OF KIKUCHI-PATTERNS. Riecke, W. D.; Sakaki, Y. Translated for Univ. of California Lawrence Radiation Lab., Berkeley, from Z. Physik, 156: 534-54(1959). 36p. Dep. mn; JCL $3.60 fs, $1.28 mf.

A new method was developed for the examination of the reciprocal lattice of single crystals by means of Kikuchi patterns. The Kikuchi bands belonging to a zone axis may be used to locate the lattice points lying within the reciprocal lattice plane, which is orthogonal to this axis and passes through the origin. For the investigation of the whole reciprocal lattice, a series of reflection patterns is taken at different orientations of the specimen. Each group of Kikuchi bands belonging to a zone axis is used to locate the reciprocal lattice points in a section orthogonal to the respective zone axis. The angles between the section planes are obtained by recording the angle of rotation between successive exposures and by considering the inclinations of the zone axes relative to the primary beam. In a perspective drawing the reciprocal lattice region near the origin is then composed of these sections. (auth)

5010 DETERMINATION OF RELATIVE INTENSITY IN X-RAY REFLECTION STUDY. Feng, C. (Martin Co., Baltimore). J. Appl. Phys., 36: 3432-5(Nov. 1965).

An analysis is made of the loss of x-ray intensity for the reflection technique with respect to geometric arrangement of the specimen. Good agreement was obtained between the analysis and experimental data from various materials of different lattice structures. The relative loss of intensity was found decreasing with higher index planes, i.e., shorter d spacings. This is considered advantageous in comparison with the transmission techniques of which the loss of intensity is greater for higher index planes. (auth)

5011 PIEZOELECTRIC RESPONSE OF Z-CUT TOURMALINE TO SHOCKS OF UP TO 21 KILOBARS. Hearst, J. R.; Irani, G. B.; Geesaman, L. B. (Univ. of California, Livermore). J. Appl. Phys., 36: 3440-4(Nov. 1965). (UCRL-14169).

The piezoelectric sensitivity of Z-cut tourmaline was measured for plane shocks with amplitudes up to 21 kbar. No evidence of hysteresis or significant effects due to mounting was found. Two straight lines provided the best fit to the data. (auth)

5012 ULTRASONIC STUDIES OF THE NONLINEAR BEHAVIOR OF SOLIDS. Breazeale, M. A.; Ford, Joseph (Oak Ridge National Lab., Tenn.). J. Appl. Phys., 36: 3486-90(Nov. 1965). (ORNL-P-1292).

The non-Hookeian behavior of a solid is studied using the distortion of an initially sinusoidal ultrasonic wave. The nonlinear differential equation describing the propagation of a finite amplitude ultrasonic wave in a cubic crystal is shown to take the same form as that describing a fluid. The propagation distance required for discontinuity in the particle velocity is calculated for various directions in the crystal. It is shown that in a typical experiment the path length can be appreciably less than the discontinuity distance, so that the distortion can be represented as a linear increase of second harmonic content with path length. Experimental results are given for copper single crystals which have been annealed or neutron irradiated. (auth)

5013 THERMOELECTRIC AND ELECTRICAL MEASUREMENTS IN THE Er–Se SYSTEM. Haase, D. J.; Steinfink, H. (Univ. of Texas, Austin). J. Appl. Phys., 36: 3490-5(Nov. 1965).

An evaluation of the electrical conductivity and thermoelectric power for compounds in the Er–Se system shows that they are degenerate semiconductors. In order to explain the observations in the intrinsic region the number of carriers must be considered as a function of the concentration of the erbium atoms in the compound. Two temperature-dependent processes take place; the activation of impurity levels and the high-temperature activation of localized energy levels associated with the number of erbium atoms present. (auth)

5014 NARROW-LINE SOURCE FOR ^{119}Sn MOESSBAUER SPECTROSCOPY. Herber, R. H. (Rutgers Univ., New Brunswick, N. J.); Spijkerman, J. J. J. Chem. Phys., 43: 4057-9(Dec. 1, 1965). (TID-22042).

A dilute solution of metallic tin in palladium was found to be useful as a source in ^{119m}Sn Mössbauer spectroscopy. A 3% Sn–97% Pd matrix was studied in detail and gave rise to single-line resonance spectra with single-line absorbers (e.g., β-Sn, Mg_2Sn, etc.). The zero-absorber-thickness extrapolated linewidth obtained with the Pd(Sn) source at 297°K and β-tin absorbers at 77°K was found to be 0.77 ± 0.02 mm sec^{-1}. The recoil-free fraction for the Pd(Sn) source was ~0.42 at 297°K. The observed Pd(Sn)–SnO_2 isomer shift was 1.46 ± 0.04 mm sec^{-1} at room temperature and the corresponding Pd(Sn)–Mg_2Sn isomer shift was 0.35 ± 0.02 mm sec^{-1}. Palladium-tin matrices with up to ~10% by weight of tin can be successfully used as narrow line, large recoil-free fraction sources for Mössbauer spectroscopy at room temperature. (auth)

5015 CHARACTERISTIC ENERGY LOSSES OF ELECTRONS IN SOLIDS. Pradal, F. (Faculte des Sciences, Toulouse); Gout, C.; Fabre, D. J. Phys. (Paris), 26: 372-84(June 1965). (In French).

Recent developments related to the characteristic energy losses of electrons in solids are surveyed. Some data are given on energy analyzers and on their performance. The interaction phenomena giving rise to characteristic losses are briefly described. The energy loss function which determines the energy transfer from incident electrons to the electron gas of the solid is defined, and the correlation between energy losses and the ultraviolet optical constants is shown. The conditions for the excitation of a plasmon are discussed. The cases of aluminum, silver, semiconductors and alkali halides are specially studied. It is shown that data drawn from characteristic spectra are in good agreement with optical experiments. This proves the validity of the theoretical approximations. Finally, the recent results concerning the radiation emission by solids under electron bombardment are reported. They are a decisive proof of the the existence of plasmons, whose energy may then be accurately measured. (auth)

5016 EFFECTS OF PARTICLE SIZE ON THE EXTINCTION OF NEUTRON DIFFRACTION. Sizov, R. A.; Yamzin, I. I. (Inst. of Crystallography, Academy of Sciences, USSR). Soviet Phys.-Cryst. (Engl. Transl.), 10: 346(Nov.-Dec. 1965).

Translated from Kristallografiya, 10: 423-4(May-June 1965).

A direct experimental investigation was made of the effects of particle size on the extinction of neutron dif-

fraction, using powders of the hexagonal ferrite $BaCo_{1.0}Fe_{1.0}{}^{2+}Fe_{16}{}^{3+}O_{27}$. The ground material was passed through various sieves to give six specimens. Measurements made with a two-coordinate diffractometer are reported. (L.B.S.)

5017 TRANSITION RADIATION, BREMSSTRAHLUNG, AND PLASMA RADIATION. Boersch, H.; Dobberstein, P.; Fritsche, D.; Sauerbrey, G. (Technische Universitaet, Berlin). Z. Physik, 187: 97-118(1965). (In German).

The visible and ultraviolet radiation emitted from electron bombarded metal targets was investigated for normal and oblique electron incidence in the range of primary energies E = 6 ... 40 kev. For normal incidence the observed spectra could be separated in transition radiation and bremsstrahlung because of their different energy dependences. When silver targets were bombarded at oblique incidence a third radiation was observed which is peaking near λ = 3500 Å (half width $\Delta\lambda$ = 200 ... 300 Å). For grazing incidence (α = 0.5° against the target surface) under UHV conditions the peak intensity is 100 times greater than transition radiation at normal incidence. Due to the wavelength, the dependence on the angle of incidence, and the strong dependence on surface contaminations this radiation is assumed to be caused by surface plasmon excitation in the silver target. (auth)

5018 SOLID STATE AND NUCLEAR RESULTS FROM MOESSBAUER STUDIES WITH ^{129}I [Thesis]. Hafemeister, David Walter. Urbana, Ill., Univ. of Illinois, 1965. 80p.

The Mössbauer effect of the 26.8-kev transition in ^{129}I was studied in a number of iodine compounds. The isomeric shifts for the alkali iodides were found to be linearly dependent on the number of 5p holes in the iodine ion. From this dependency, a calibration of the isomeric shift scale in terms of the 5s-electron density was obtained. The s and p populations inferred from these data are in sharp disagreement with those predicted by the simple theory of electronegativity. An explanation for this discrepancy is given. From the above calibration, a relative change of nuclear radius $\Delta R/R = R_{26.8} - R_{gnd}/R_{gnd} = 3 \times 10^{-5}$ is computed. The isomeric shifts for some iodates indicate that their 5s-electron density is about 18% larger than that of the iodides. This increase is caused by the partial removal of 5p electrons from iodine in the I–O bonds, which results in reduced screening of the 5s electrons. The charge removed per I–O bond calculated from the isomeric shifts of the iodates and periodate is 0.61 e. The quadrupole splitting of KIO_3 was used to determine the ^{129}I quadrupole ratio, $Q_{26.8}/Q_{gnd} = 1.23 \pm 0.02$. The asymmetry of the iodate spectrum and the sign of quadrupole moment show that the sign of the iodate field gradient is negative. The values of the quadrupole coupling constant, eqQ, at 80°K for KIO_3 and NH_4IO_3 are in agreement with NMR results and eqQ_{127} = 1030 ± 20 Mc/sec for $Ba(IO_3)_2$. The mean life, τ = 26.8 ± 1.5 nsec, of the 26.8 kev state of ^{129}I was determined. This value corresponds to a retardation factor of 140 when compared to the single particle M1 estimate. An extrapolation of the absorption line width to zero thickness gives a value of 20 nsec for the mean life. This should be considered as a lower limit because of the possibility of solid state broadening. The recoilless fraction f was found to deviate from 0.26 by less than 25% for all alkali iodides at 80°K. (Dissertation Abstr.)

5019 ELECTRON-SPIN RESONANCE STUDIES OF IRRADIATED GLASSES [Thesis]. Lee, Sook. Providence, Brown Univ., 1964. 191p.

Electron-spin resonance (ESR) spectra were observed for boron oxide, various types of alkali borate, and borosilicate glasses exposed to x-ray, γ-ray or thermal-neutron irradiations. The irradiated alkali borate glasses (Li_2O-B_2O_3, Na_2O-B_2O_3, K_2O-B_2O_3, Cs_2O-B_2O_3, and Rb_2O-B_2O_3) containing less than approximately 25 molar percent alkali oxide exhibit spectra consisting of five major absorption lines at an operating frequency in the vicinity of 9.2 KMcps, an X-band microwave frequency. The same five-line resonance was also observed in the irradiated boron oxide and borosilicate glasses. Irradiated alkali borate glasses containing more than roughly 25 molar percent alkali oxide exhibit spectra partially resolved into four absorption lines and the X-band frequency. All of the irradiated glasses display a structureless, anisotropic resonance, regardless of the type and composition of the glasses. In addition to the five-line and structureless, anisotropic resonances, ESR spectra observed for the borosilicate glasses exposed to neutron irradiations or high dose γ-ray irradiations exhibit a sharp, intense resonance absorption line, which was not produced in the irradiated borate glasses. It is concluded that the five-line resonance can be explained satisfactorily as arising from an axially symmetric hyperfine interaction of a hole with a ^{11}B nucleus (spin I of $\frac{3}{2}$), whereas the four-line resonance can be attributed to an isotropic hyperfine interaction of a hole with a ^{11}B nucleus. The structureless, anisotropic resonance appears to be due to a hole trapped on a non-bridging oxygen ion, while the sharp, intense resonance observed only in the irradiated borosilicate glasses can be attributed to electrons trapped on oxygen vacancies of the SiO_2 network. In order to correlate the structure of the alkali borate glasses with those of the alkali borate crystalline compounds, ESR investigations were also made on several types of crystalline alkali borates. (Dissertation Abstr.)

5020 SPIN-LATTICE RELAXATION OF TETRAVALENT PROTACTINIUM IN A CUBIC CRYSTAL [Thesis]. Raubenheimer, Louis Johannes. Urbana, Ill., Univ. of Illinois, 1965. 112p.

The paramagnetic relaxation time is investigated for Pa^{4+} in the cubic matrix $Cs_2(Zr,Pa)Cl_6$ between 1.4 and 4.2°K, using the pulse saturation method. A theory, developed for materials in which the electrostatic crystal potential is described by a few crystal field parameters, has been used quite successfully in predicting the relaxation behavior of salts containing rare earth ions. It is the purpose of this study to determine whether the same theory can be extended to an actinide ion, where the effects of the spin-orbit interaction are comparable to the effects of the crystal field interaction. Experimental data fit the expression $1/T_1 = A'T + C'T^9$, with $A' = 3.5 \pm 0.7$ sec^{-1} deg^{-1} and $C' = (5.1 \pm 1.5) \times 10^{-5}$ sec^{-1} deg^{-9}. For the purpose of calculating $1/T_1$ theoretically, static crystal field parameters $A_4^0\langle r^4\rangle$ and $A_6^0\langle r^6\rangle$ are used to predict the corresponding dynamic parameters $a_4^m\langle r^4\rangle$ and $a_6^m\langle r^6\rangle$. Second degree coupling coefficients $a_2^m\langle r^2\rangle$ are treated in terms of a single parameter $a_2^0\langle r^2\rangle$, which is considered unknown in the calculations, as is the phonon velocity, v. A comparison of the resulting theoretical expressions for A' and C' with the corresponding experimental values results in two nonlinear equations in $a_2^0\langle r^2\rangle$ and v. These equations are found to be consistent with a measured phonon velocity of 4.5×10^5 cm/sec and a value of $a_2^0\langle r^2\rangle$ = 24,000 cm^{-1}, calculated from a dynamic point charge model consistent with the values of $a_4^0\langle r^4\rangle$ and $a_6^0\langle r^6\rangle$. In Appendix A the relaxation behavior of the rare earth ion, Ho^{3+}, in yttrium ethyl sulfate is treated. Experimental results show a dependence of $1/T_1$ on the concentration of holmium ions. This may be explained by assuming the relaxation to be phonon-limited. (Dissertation Abstr.)

5021 THE DYNAMIC POLARIZATION OF PROTONS IN A ROTATING CRYSTAL OF LANTHANUM-MAGNESIUM NITRATE. Luschykov, V. I.; Neganov, B. S.; Parfenov, L. B.; Taran, J. V. (Joint Inst. of Nuclear Research, Dubna, USSR). pp 266-8 of Physics and Techniques of Low Temperatures. Prague, Publishing House of the Czechoslovak Academy of Sciences, 1964.

Experiments for observing the dynamic polarization of protons in a rotating crystal of lanthanum magnesium nitrate were performed in fields from 2 to 5 kOe at saturation frequencies from 60 to 170 Mc, and for uniform rotation of the crystal in the range of 30 to 550 rev/min. The experiments were carried out at a temperature of about 1.3°K, using the method of forced transitions similar to the "effet solide" method. It was ascertained that the polarization increases for the decrease in cerium content from 2 to 0.2%, the temperature dependence of the amplification

coefficient of polarization is analogous to the dependence observed for the simple "effet solide," the amplification coefficient rapidly increases with speed of revolution in the range from 30 to 100 rev/min and then slowly decreases, if the power applied to the sample was 1 watt and the circuit quality about 16, then the intensity of the radio-frequency field was small for gaining saturation, and the amplification coefficient of polarization obtained in individual experiments reached a value of 70 for an irradiation time of 30 to 40 min. (J.F.P.)

5022 TEMPERATURE-SENSITIVE X-RAY SMALL ANGLE SCATTERING FROM MELT-CRYSTALIZED POLYETHYLENE. Schultz, J. M.; Pound, G. M.; Robinson, W. H. (Carnegie Inst. of Tech., Pittsburgh). 42p. (CONF-641118-2). ORINS. Gmelin, AED-CONF-64-229-12.

From Pittsburgh Diffraction Conference, Pittsburgh.

The temperature dependence of x-ray small angle scattering from fractionated linear polyethylene crystallized from the melt was measured experimentally over a range of temperatures from room temperature to the melting point of the various polymer fractions used. For each temperature selected in this range a specimen of a given molecular weight produced a peak in the small angle scattering whose angular position was proportional to the reciprocal of the thickness of the crystalline unit of the polymer and whose intensity was proportional to the square of the thickness of the amorphous layer separating the crystalline units. It was found that for temperatures between room temperature and the temperature at which the specimen was crystallized the small angle peak intensity change reversibility with temperature while its angular position remained unchanged. At temperatures higher than the crystallization temperature, the peak position shifted discontinuously to lower angles, finally disappearing altogether over a certain small temperature range. It was concluded from these data that the region separating the crystalline units is comprised of a defect that is in thermodynamic equilibrium with the crystalline regions and is the principal thermally sensitive defect in the material and that the polymer chains of which the defect is composed must be attached to at least one of its neighboring crystallites. The molecular mechanism of secondary crystallization and the surface free energy of the crystalline unit as a function of molecular weight could be determined from x-ray small angle data. (auth)

REACTOR TECHNOLOGY

General

Refer also to abstracts 4104, 4183, 4311, and 4829.

5023 (IITRI-578P21/15) STUDIES OF REACTOR CONTAINMENT. Progress Report, August 1–September 30, 1965. Eichler, J. B.; Gallagher, E. V.; Lieberman, P.; Singer, T. (IIT Research Inst., Chicago, Ill.). Contract AT(11-1)-578. 59p. Dep. mn; CFSTI $3.00 cy, $0.75 mn.

The dynamic pressure-volume and pressure-time characteristics of sugar-pine wood samples under shock-wave loading are measured. Experiments in a water shock tube, designed for studies of pressure loadings associated with gross failures of reactor primary cooling systems, are also reported. (T.F.H.)

5024 (ORNL–3870, pp 261-5) REACTOR EVALUATION. Douglas, D. A. Jr. (Oak Ridge National Lab., Tenn.).

As part of broad studies on the total cost of producing nuclear power, fabrication costs and fuel element performance were examined as they relate to fuel cycle and other cost areas. The methodology of calculating fabrication costs and the major variables that can affect such costs are reported along with brief analyses of selected fuel element concepts. (auth)

5025 (WAPD-T–1832) IN-PLANT TEACHING OF NUCLEAR REACTOR PLANT KINETICS AND CONTROL TO GRADUATE ENGINEERS AND SCIENTISTS. Bean, W. C. (Bettis Atomic Power Lab., West Mifflin, Pa.). July 1965. Contract AT-11-1-GEN-14. 33p. (CONF-650917–3). Dep. mn; CFSTI $2.00 cy, $0.50 mn.

From International Conference on Industrial Electronics and Control Instrumentation, Philadelphia.

A training program is described that is intended to indoctrinate specialists having a wide variety of backgrounds in the techniques and theory of operation of dual-cycle steam-producing pressurized-water power reactors. The training is initially of a general nature, and presents an introduction to analysis and design before any realistic reactor problems are studied. (T.F.H.)

5026 EVALUATION OF THERMOCOUPLE THERMAL-LOADING ERRORS FOR A SURFACE-ATTACHED THERMOCOUPLE ON A FLAT-PLATE FUEL ELEMENT. Brindley, J. H. (Atomics International, Canoga Park, Calif.). Nucl, Sci. Eng., 23: 313-28(Dec. 1965).

Flat-plate fuel-element surface temperatures in the Organic Moderated Reactor Experiment were monitored by 0.005-in. (0.013-cm)-dia chromel-alumel thermocouple wires, spot-welded to the stainless-steel fuel-plate surface. The thermocouple assembly, being exposed to the coolant stream, is subject to thermal-loading errors; as a result, thermocouple-calibration tests were performed in a forced-convection heat-transfer loop with Santowax O-M flowing over an electrically heated test plate containing typical thermocouple specimens. The tests were conducted under the following simulated reactor conditions: coolant temperatures from 300 to 600°F (149 to 316°C), coolant velocities from 10 to 20 ft/sec (3.1 to 6.1 m/sec), and heat fluxes ranging from 0.50×10^5 to 1.6×10^5 Btu/(h ft^2) (15.77 to 50.46 w/cm^2). Test results demonstrate that at reactor operating conditions, 600°F organic coolant flowing at 17.5 ft/sec (5.34 m/sec), the observed fuel-plate surface temperature is 700°F (371°C), while, in reality, the actual surface temperature is 750°F (399°C). The thermocouple thermal-loading errors were found to be a function of the coolant Reynolds and Prandtl numbers. Heat flux had no effect on the calibration. Excellent agreement was obtained between the experimental and predicted (Dittus-Boelter) heat-transfer coefficients for the organic coolant. Thermocouple-calibration factors for correction of observed surface temperatures over a wide range of operating conditions, are presented as a function of the organic-coolant heat-transfer coefficient on the fuel-plate surface. (auth)

5027 THE GROWTH OF REACTOR SAFETY CRITERIA IN THE UNITED KINGDOM. Farmer, F. R. Paper No. 9 of Anglo-Spanish Nuclear Power Symposium. Vol. 1. [Risley, Eng., United Kingdom Atomic Energy Authority, 1965]. 8p.

An extensive study and critical evaluation were made of the safety of all reactors in the United Kingdom. The gradual development of safety criteria is illustrated, which was based on extensive operational experience and a supporting program of nuclear safety research. (L.B.S.)

5028 SIMULATED FUEL ASSEMBLY. Savino, Joseph M.; Lanzo, Chester D. (to U. S. Atomic Energy Commission). U. S. Patent 3,205,141. Sept. 7, 1965.

A method is described for measuring the flow of fluid through a flow passage having known overall pressure drop versus flow rate characteristics and the flow of cooling water into areas occupied by fuel assemblies in a nuclear reactor. A simulated fuel assembly containing flow measuring apparatus that has been adapted to be mounted in a reactor core is used to produce the requisite flow characteristics. (AEC)

5029 APPARATUS FOR CANNING NUCLEAR REACTOR FUEL ELEMENTS. Nicoll, David; Hedgecock, J. L. (to U. S. Atomic Energy Commission). U. S. Patent 3,216,174. Nov. 9, 1965.

An apparatus is designed for canning nuclear reactor fuel elements, which includes a shielded fluid tight container for receiving an elongated container in alignment with a sealable opening in one wall and means for releasably supporting the container in alignment with the opening. Means are provided for supporting and moving a cap to a position over the container and for heating the cap for brazing to close the container subsequent to insertion of a fuel element through said opening. (AEC)

Auxiliaries and Components

Refer also to abstract 4800.

5030 (AHSB(S)R–86) POST INCIDENT COOLING OF A P.W.R. CORE. Edwards, A. R.; Hunt, D. L. (Authority Health and Safety Branch, United Kingdom Atomic Energy Authority, London (England)). 1965. 26p. Dep.; BIS $0.80; HMSO 4s. 0d.

Present designs of PWR are not able to withstand, without damage to the core (leading to a release of fission product), a depressurization accident following a wide range of break sizes. It is shown that, for a typical 1500-Mw(t) reactor, a low pressure flooding system will not protect the reactor from break sizes in the range ½ to 16 in. dia. Methods of protecting the reactor from breaks in this range are discussed. They are: circulating pumps capable of handling two-phase entry conditions, a variable displacement injection pump, or an in-core spray either pumped or supplied from a high pressure reservoir. (auth)

5031 (BAW–1280-32) SODIUM-HEATED STEAM GENERATOR DEVELOPMENT. Quarterly Progress Report, July–September 1965. (Babcock and Wilcox Co., Alliance, Ohio. Research Center). Oct. 15, 1965. Contract AT(11-1)-1280. 29p. Dep. mn; CFSTI $2.00 cy, $0.50 mn.

The preliminary design of the prototype steam generator is complete. Fabrication of the prototype is proceeding. Coiling of tubes for the superheater bundle was started. Overall fabrication of the steam generator is approximately 20% complete. (auth)

5032 (EURAEC–1477) THE STEADY STATE AND DYNAMIC BEHAVIOUR OF A BOILING WATER REACTOR. Quarterly Progress Report XVII, January 1, 1965–April 1, 1965. (Technische Hogeschool, Eindhoven (Netherlands)). Apr. 1965. Contract P-313. 15p. (EUR–2398; WW016-R83). Dep. mn; CFSTI $1.00 cy, $0.50 mn.

Work Performed under United States–Euratom Joint Research and Development Program.

An outline is given of test-system components, instruments, and experimental results in studies of the steady-state and dynamic characteristics of boiling-water reactors. (T.F.H.)

5033 (GA–6588) SAFE-PCRS. A COMPUTER PROGRAM FOR THE STRESS ANALYSIS OF COMPOSITE BODIES OF REVOLUTION. INPUT INSTRUCTIONS. Cornell, D. C. (General Atomic, San Diego, Calif. John Jay Hopkins Lab. for Pure and Applied Science). Aug. 1, 1965. Contract AT(04-3)-167. 43p. Dep. mn; CFSTI $2.00 cy, $0.50 mn.

The SAFE-PCRS computer program is described as a procedure for numerically determining the stress and strain distribution within either homogeneous or heterogeneous thick-walled bodies of revolution. The program is written in the FORTRAN IV language and compiled for the IBM 7044 digital computer. This program employs the finite element method in the solution of elastic boundary value problems. It is oriented toward the analysis of heterogeneous structures such as reinforced and/or pressurized concrete vessels. The assumptions and present limitations are that deformations must be small, that is within the elastic limit of the materials being considered, only bodies of revolution and axisymmetric loading conditions are analyzed, the program size is 2400 degrees of freedom, and the finite element method used is an approximate method. (J.F.P.)

5034 (NOLTR–63-140) EXPLOSION CONTAINMENT LAWS FOR NUCLEAR REACTOR VESSELS. Wise, W. R. Jr.; Proctor, J. F. (Naval Ordnance Lab., White Oak, Md.). Aug. 16, 1965. 173p. Dep. mn; CFSTI $5.00 cy, $1.00 mn.

The location of power reactors in urban areas increases the need for containment of the maximum credible nuclear accident. Such an accident could possibly involve a large and rapid energy release in the core region due to a nuclear excursion. To contain the energy release (and any subsequent release of fission products), the integrity of the reactor primary vessel is very important. To investigate this integrity, extensive theoretical and experimental analyses were performed, and basic explosion containment laws for water-filled right-circular cylinders were formulated and verified for a wide range of vessel materials and sizes. These laws express explosive charge weight as a function of vessel geometry and conventional material properties. The basic containment laws were amplified to characterize the response of reactor primary vessels to a large spectrum of postulated nuclear accidents. Included in the study are experimental data on the effects upon containment of weldments, nozzles, and end constraints. (auth)

5035 (ORNL-TM–1278) DIMENSIONAL LOCATION OF REACTOR COMPONENTS BY OPTICAL TOOLING. Abbatiello, A. A. (Oak Ridge National Lab., Tenn.). Sept. 23, 1965. Contract W-7405-eng-26. 14p. Dep. mn; CFSTI $1.00 cy, $0.50 mn.

An optical tooling system that consists of surveying-type instruments and a coordinate grid provides for remote point location. Optical tooling was applied to measurements of four reactors in five situations. It has particular advantages where the points to be located are visible but not physically accessible due to radioactivity, water, etc., as in pool-type reactors. Measurements in remote areas are highly precise, with an accuracy of up to 5 parts per million attainable under ideal conditions. The system is now in routine use. (auth)

5036 (RL-SA–47) MEASUREMENT OF FILTER EFFICIENCY WITH A CONDENSATION NUCLEI COUNTER. Smith, M. L. (General Electric Co., Richland, Wash. Hanford Atomic Products Operation). July 23, 1965. Contract AT(45-1)-1350. 2p. (CONF-651101–34). Dep. mn; CFSTI $1.00 cy, $0.50 mn.

From 13th Conference on Remote Systems Technology, Washington, D. C.

A new technique using condensation nuclei was developed which permits the measurement of the efficiency of the reactor confinement filter system while it is in service. This method was compared with the uranine dye and dioctyl phthalate methods. (M.O.W.)

5037 OPERATIONAL MONITORING OF REACTOR INSTRUMENTATION. Wehrle, G.; Reichert, W. (Siemens and Halske AG, Karlsruhe, Ger.). Atomwirtschaft, 10: 511-15(Oct. 1965). (In German).

An electronic safety system with automatic testing of the signal width in a 2-to-3 value system was described. It has the task of monitoring the process and of introducing safety operations during perturbations to the installation. In addition to this automatic testing of safety system, a routine testing for the counter tube and ionization chamber measurement channels is of importance. A special monitoring method for routine testing was described. (tr-auth)

5038 NUCLEAR REACTOR. Hackney, Stanley (to United Kingdom Atomic Energy Authority). British Patent 1,007,207. Oct. 13, 1965. Filed Oct. 11, 1963.

A nuclear reactor of the type having the fuel of its core contained in company with a circulatable heat transfer fluid within clustered tubes exposed externally to a reactor coolant is described. In the reactor the tubes in both a central zone and a surrounding outer zone of the cluster are divided into two groups: a first group for flow of the heat transfer fluid in one direction, and a second group for fluid flow in the opposite direction. The two groups in each zone are interconnected at the same end of the cluster while at the other end the first group in one zone is connected to the second group in the other zone. Connections are provided from the inlet and outlet of the pump means for circulating the heat transfer fluid to complete a closed circuit for the fluid. (B.L.M.)

5039 NUCLEAR REACTOR. Hackney, Stanley (to United Kingdom Atomic Energy Authority). British Patent 1,007,208. Oct. 13, 1965. Filed Sept. 9, 1964.

A coolant pressurizer is provided for a reactor of the type employing a liquid coolant that is pressurized for control of its boiling. The pressurizer includes a number of separate units disposed within the pressure vessel boundaries and each having space for a trapped volume of gaseous medium to impart its pressure to a free surface presented by the liquid coolant within the vessel. Each unit includes a chamber, a freely movable abutment substantially impervious to the coolant and gas and separating two portions of the chamber, and connections for the admission of coolant and gas to the two chamber portions. The travel of the movable abutment, such as a piston, is limited in the direction from the gas portion towards the coolant portion. If the vessel is cylindrical in shape, the pressurizer units, each in an elongated form, are distributed in upright positions around the inner side walls of the vessel. (B.L.M.)

5040 IMPROVEMENTS RELATING TO NUCLEAR REACTOR SERVICING APPARATUS. Long, Everett (to English Electric Co. Ltd.). British Patent 1,007,974. Oct. 22, 1965. Filed Feb. 1, 1961.

Servicing apparatus is described for providing access to a group of fuel elements in the core of a reactor that includes a fixed access duct penetrating the biological shield opposite the group of fuel channels. The apparatus includes a charge chute having a cross section substantially smaller than that of the access duct and mounted rotatably at least partly within the duct. The chute axis is displaced sideways by a substantial amount relative to the cross sectional dimensions of the duct. The chute has an opening at the inner end displaced from the axis of the charge chute by the maximum amount that will still permit withdrawal of the charge chute from the access duct. The apparatus also includes an assembly of fixed fuel element guide tubes adjacent to the

servicing end of the fuel channels. Each guide tube is aligned at one end with one of the fuel channels within the group, and the other end is positioned so that by rotation of the charge chute access may be obtained to any desired fuel channel within the group through the opening in the guide chute and the guide tube. (B.L.M.)

5041 IMPROVEMENTS RELATING TO NUCLEAR REACTOR SERVICING APPARATUS. Greaves, Thomas Cyril; Orszak, Peter; Long, Everett; Knight, William John (to English Electric Co.). British Patent 1,007,975. Oct. 22, 1965. Filed Jan. 31, 1962.

A servicing apparatus is described for providing access to a group of fuel elements in the core of a reactor that includes an access duct penetrating the biological shielding. The apparatus includes a charge chute arranged to be rotatably mounted in the access duct and carrying a guide member movable angularly with respect to the axis of the charge chute. An assembly of fixed fuel-element guide tubes is positioned adjacent to the servicing ends of the fuel channels. One end of each guide tube is aligned with one of the channels within the group, and the other ends of the guide tubes are positioned on a number of radii struck from a point in alignment with the axis of the charge chute. A cam track is arranged on the guide tube assembly, and cam follower means is operatively coupled to or forms a part of the guide member. The cam track is so shaped as to impart to the guide member an appropriate angular movement between two of the radii in response to rotation of the chute to provide access by way of the charge chute, guide member, and fixed guide tube to any fuel channel within the group. (B.L.M.)

5042 IMPROVEMENTS IN VALVES FOR FLUID FLOW CONTROL. Bussi, Jean; Lichevallier, Maurice (to Commissariat a l'Energie Atomique). British Patent 1,008,000. Oct. 22, 1965. Priority date May 13, 1963, France.

A gate-valve is described that comprises an obturating member that is adapted to move within a conduit so as to close off the conduit at will irrespective of the direction of the forces exerted on the obturating member by the fluid present in the conduit. The valve is particularly applicable to the coolant gas circuits in a nuclear reactor. The shut-off valve has two coaxial annular seats located symmetrically at a predetermined axial distance from each other and a single obturator flap that can be applied axially and in leak-tight manner against either one or the other of the valve seats. Means are also provided for guiding and operating the flap so as to permit it to move into position in which it is located parallel to the axes of both valve seats and either one of the positions in which it is brought to bear against one valve seat. This means is adapted to impart to the flap a movement of translation that is substantially at right angles to the valve seats at least at the time of application of the flap against a valve seat or at the time of release of the flap from the valve seat. (B.L.M.)

5043 FUEL ELEMENT CHARGING ARRANGEMENTS FOR NUCLEAR REACTORS. (to Societe des Forges et Ateliers du Creusot). British Patent 1,008,506. Oct. 27, 1965. Priority date Nov. 14, 1961, France.

A fuel element charging device of the type having an axial tube and a tubular arm articulated on the tube is described. The lower end of the arm is adapted to be indexed onto any one of a number of fuel element channels in the core by rotation of the axial tube and the tubular arm as a whole about the tube axis and angular movement of the tubular arm about an articulation axis transverse to the axis of rotation. The means for angular movement of the tubular arm includes a member axially movable with respect to the axial tube and that is responsive to rotation of the axial tube by a threaded connection between the member driven in unison with the axial tube and a pivot housing adapted to be secured against rotation when engaged in a cooperating recess of the reactor core. The member is resiliently coupled against axial movement with respect to the housing and has a one-way abutment connection with the axial tube. (B.L.M.)

5044 NUCLEAR REACTOR CONTROL ROD ASSEMBLY WITH IMPROVED DRIVING MECHANISM. Macomber, John W. (to U. S. Atomic Energy Commission). U. S. Patent 3,198,709. Aug. 3, 1965.

A nuclear reactor control rod assembly is designed which includes an improved driving mechanism. The assembly is composed of a plurality of elongated control rods extending vertically through the reactor core and arranged in substantial juxtaposition with the fuel elements. The control rods are made up of a first section, at least one other section adjacent to the first section, and an assembly means for selectively securing the first section to the other section. A driving means is mounted below the reactor for selectively raising the first control rod section into the reactor core to increase the power level and lowering the section out of the core to decrease the power. Also included in the control rod assembly are a connecting means for operably connecting the driving means to the control rod, a disassembly device for releasing the first control rod section from the second control rod section independently of the operation of the connecting means, and a disengaging device responsive to an increase in the reactor power level above a predetermined maximum value which would enable the first control rod section to fall away from the core. (AEC)

5045 THERMOMETER DEVICES. Franklin, Ernest (to United Kingdom Atomic Energy Authority). U. S. Patent 3,211,002. Oct. 12, 1965. Priority date Dec. 12, 1959, Great Britain.

A thermometer device applicable in measuring reactor temperatures includes a coaxial transmission line having a shorted end and an unshorted end and a rectangular hysteresis loop ferromagnetic core located on the inner conductor of the line adjacent to the shorted end. The core has at least two sections having different Curie temperatures. A discontinuous train of substantially rectangular current pulses of alternate polarity are applied to the unshorted end to saturate the core in alternate directions of magnetization. Means are provided for integrating the voltage pulses appearing at the unshorted end as a result of reflections from the shorted end. (B.L.M.)

5046 SERVOMECHANICAL FLUID CHARGING AND VOLUME CONTROL SYSTEM FOR A NUCLEAR REACTOR. Brown, Eugene H. C. (to Westinghouse Electric Corp.). U. S. Patent 3,211,622. Oct. 12, 1965. Filed Mar. 5, 1963.

A completely automatic coolant volume and charging control system is described for a reactor having a main fluid coolant line with a pressurizer connected to the line. The system includes a let-down flow path and a make-up flow path connected together through a low pressure tank and bridging the main coolant line. Means are provided for detecting and controlling the flow rate in each path and the level of fluid in the pressurizer. An input signal is produced by each detecting means, and comparator means generate an error signal in response to the input signal from the detecting means. The error signal is delivered to the controlling means so as to maintain the fluid level in the pressurizer fairly constant. (B.L.M.)

5047 NUCLEAR REACTOR CONTROL DEVICES. White, William Paul; Eickhoff, Keith Guy (to United Kingdom Atomic Energy Authority). U. S. Patent 3,212,976. Oct. 19, 1965. Priority date May 17, 1961, Great Britain.

An emergency control device for insertion into a vertical channel of a reactor, particularly a gas cooled reactor, is described. A number of freely linked bodies of neutron-absorbing material are housed in a container. A retaining member holds the bodies in a compact folded form in the housing. In case of an emergency, the retaining member is ejected, and the bodies fall under gravity into a dispersed position. The bodies may be plates loosely hinged together or hollow cones interconnected by non-pivotal links, such as flexible wires. (B.L.M.)

5048 CONTROL ROD POSITION INDICATING APPARATUS AND METHOD. Campbell, Ronald Hugh (to United Kingdom Atomic Energy Authority). U. S. Patent

3,212,977. Oct. 19, 1965. Priority date July 6, 1959, Great Britain.

Apparatus for monitoring the position of a number of adjustable members, particularly reactor control rods, includes means for adjusting the positions of the members individually and simultaneously and means operatively connected to each member for producing an electrical output signal indicative of the position of the member. The electrical signal is received by a receiver means where an error signal proportional to the difference between the signal and a reference is generated. Selector switch means serially connects each signal producing means with the receiver means to cyclically monitor the rods' positions. Means are provided for sensing the error signal generated by the receiver means, for varying the receiver means reference to eliminate the error signal, and for actuating an alarm signal when the error signal exceeds a predetermined magnitude. (B.L.M.)

5049 NUCLEAR REACTOR CORE SUPPORT STRUCTURE. Short, Vincent R.; Stevens, Glenn (to Westinghouse Electric Corp.). U. S. Patent 3,212,978. Oct. 19, 1965. Filed Apr. 18, 1961.

A core structure is described for heterogeneous reactors having an upright annular wall structure. A top core plate is supported on a flange in the wall and a bottom core plate is attached to support members provided by the guide tubes for the control rods. The core plates serve to position the fuel elements. A guide tube support plate is located above the top core plate and bears the load of the fuel elements rather than the thin core plate to eliminate the need for an upper core support barrel. (B.L.M.)

5050 CORE SUPPORT STRUCTURE. Silverblatt, Bernard L. (to Westinghouse Electric Corp.). U. S. Patent 3,212,979. Oct. 19, 1965. Filed Apr. 18, 1961.

A support structure for fuel elements located within the pressure vessel of a reactor includes an apertured relatively thin core plate forming a part of the bottom of the core assembly for positioning and supporting the elements. A relatively rigid primary support member is spaced below the core plate and suspended from the walls of the vessel. Means extend from the support member for supporting the main body of the core plate and the assembly from the support member. The support member is a shroud tube, and the lower shroud tubes are incorporated between the relatively thin core supporting plate and a grid member so that they provide a column type reinforcing support for the core plate and associated fuel elements. The connecting means between the lower support grid and the lower core support is provided by tie rods so that the shroud rods are rigidly connected to hold the tie rods in tension and the shroud tubes in compression to provide added support for the lower core supporting plate. (B.L.M.)

5051 RELEASABLE COUPLING MECHANISM. Kmonk, Stanley; Widmer, Thomas F. (Westinghouse Electric Corp.). U. S. Patent 3,212,980. Oct. 19, 1965. Filed Nov. 16, 1961.

A releasable coupling device is provided for joining a driving member to a driven member, particularly for joining the drive shaft in a bottom mounted control rod drive mechanism to its associated control rod in the reactor. For use of the coupling mechanism the driven member is arranged adjacent to the driving member for movement along a prescribed path, and the mechanism includes at least one latch pivotally secured to the driven member. Cooperating means on the latch and on the driving member are provided for releasably engaging the latch to the driving member, and the latch may be locked in an engaged position with the driving member. Both members are surrounded by an enclosure that includes means for producing a predetermined relative movement between the locking means and the latch to disengage the locking means from the latch at a predetermined position of the driving member. The coupling device is described for particular application to pressurized water reactors. (B.L.M.)

5052 NUCLEAR REACTORS. Tollet, Louis Henri Joseph; Maldague, Pierre Edmond Jules Marie (to Societe Anglo-Belge Vulcain, Societe Anonyme). U. S. Patent 3,212,981. Oct. 19, 1965. Priority date Mar. 9, 1961, Belgium.

Actuating mechanism for reactor shut-down or control rods is described that is operated by differences of pressure normally met inside the vessel enclosing the reactor core or in circuits connected to the reactor. A hollow cylindrical housing extends outwardly from the vessel and has one end in open communication with the interior of the vessel and the cooling fluid contained in the vessel. A control member of substantially the same length is slidably mounted in the housing and has an annular form for its entire length. Spring means in the interior of the annular portion operatively connected to the control member normally bias the control member in an extended position within the vessel. A telescoping, double-action piston is coaxial with the control member and is mounted within the annular portion. One end of the piston is exposed to the high pressure fluid within the vessel, and the other end is subjected to fluid pressure from a second source. Latch means connect the piston to the control member, and a bellows connected to the latch means and exposed to fluid from a second source causes the latch means to extend and retract in response to pressure changes from this second fluid. The spring means normally bias the bellows means to maintain the latch means in a retracted position. (B.L.M.)

5053 METHOD OF VARYING THE MODERATION IN A NUCLEAR REACTOR. Tollet, Louis Henri Joseph; Maldague, Pierre Edmond Jules Marie (to Societe Anglo-Belge Vulcain, Societe Anonyme). U. S. Patent 3,212,984, Oct. 19, 1965. Priority date May, 24, 1961, Belgium.

A method is provided for modifying the moderator properties in a reactor by subdividing the enclosure(s) provided within the core for containing the moderator into two or more sub-chambers filled with different moderating fluids. By modifying the volume of one or more of the sub-chambers, the quantities of each of the fluids vary; and the resulting moderator has different moderating characteristics. (B.L.M.)

5054 MOUNTING OF FUEL TUBE IN REACTOR SHIELDING. Bunch, Wilbur L. (to U. S. Atomic Energy Commission). U. S. Patent 3,216,903. Nov. 9, 1965.

The way in which the outer portion of a reactor fuel tube is associated with a reactor shield through which it passes is described. The outer portion of the fuel tube is loosely received in a conical portion of a sleeve in the shield and fairly closely fits a cylindrical portion of the sleeve, whereby the fuel tube may move laterally and the void spaces between shield and tube are kept to a minimum. Beyond the shield the fuel tube has an external shoulder facing and overlapping the outer end of the sleeve, whereby any beam of radiation between the sleeve and fuel tube is stopped. (AEC)

Criticality Studies

Refer also to abstracts 4801 and 5200.

5055 (BNWL–146) RED CROSS. A CODE TO COMPUTE RESONANCE SHIELDED, TEMPERATURE DEPENDENT CROSS SECTIONS FOR FAST REACTOR ANALYSIS. Little, W. W. Jr.; Hardie, R. W. (Battelle-Northwest, Richland, Wash. Pacific Northwest Lab.). Aug. 1965. Contract AT(45-1)-1830. 75p. Dep. mn; CFSTI $3.00 cy, $0.75 mn.

A code is described which uses extensive Russian data to compute resonance shielded, temperature dependent, 26-group cross sections. The output (printed or punched) is in a format suitable for fast reactor analyses using the corrected transport approximation. (auth)

5056 (CONF-654–22) APPLICATION OF MULTICHANNEL SYNTHESIS TO 2-D DEPLETION CALCULA-

TIONS. Turner, W. H.; Merriman, F. C.; Hansen, E. C. (Knolls Atomic Power Lab., Schenectady, N. Y.). [nd]. Contract W-31-109-eng-52. 15p. Dep. mn; CFSTI $1.00 cy, $0.50 mn.

From American Nuclear Society Meeting, San Francisco, Nov.-Dec. 1964.

A multichannel neutron-flux synthesis program is described that carries out a two-dimensional neutron diffusion calculation at approximately the same cost that a one-dimensional calculation would cost if carried out by conventional techniques. The program is part of a reactor design procedure, which is incorporated into the SPRITE program system. (T.F.H.)

5057 (GA–6540) GAMBLE-4. A PROGRAM FOR THE SOLUTION OF THE MULTIGROUP NEUTRON-DIFFUSION EQUATIONS IN TWO DIMENSIONS, WITH ARBITRARY GROUP SCATTERING, FOR THE IBM-7044 FORTRAN IV SYSTEM. Dorsey, J. P. (General Atomic, San Diego, Calif. John Jay Hopkins Lab. for Pure and Applied Science). July 1, 1965. Contract AT(04-3)-167. 50p. Dep. mn; CFSTI $2.00 cy, $0.50 mn.

GAMBLE-4 is an IBM-7044 FORTRAN IV chain program that finds, over a nonuniform rectangular mesh imposed upon a rectangular area of either the x-y or the r-z plane, a discrete numerical solution to the multigroup, time-independent, neutron diffusion equations for a heterogeneous reactor. The solution is obtained over as many as 300 macroscopic determining regions, using from two to ten lethargy groups and up to 20,000 mesh points. (M.O.W.)

5058 (JINR-P–2335) KORRELYATSIONNAYA TEORIYA REAKTORA S OTRAZHATELEM. (Correlation of Neutrons in a Reflected Reactor). Kozik, B. (Joint Inst. for Nuclear Research, Dubna (USSR). Lab. of Neutron Physics). 1965. 18p. Dep. mn.

The statistical theory of neutron multiplication is applied to a stationary reflected reactor. Exact and approximate expressions are obtained for the correlation functions, for variations of detector counts for a time Δt in the Feynman method, for the recording probability of correlated neutron pairs in the Rossi's method and for the spectral power densities. In turns out that if the mean probability of the neutron transfer from the reactor into the reflector is not very small and the ratio of the neutron lifetimes in the reactor and the reflector is sufficiently great, then the reflected reactor can be considered as a simple linear dynamical system. Then all statistical correlation measurements in the reactor can be replaced by those in the reflector. The spectral density frequencies should be limited to a certain condition fulfilled in usual thermal reactors. (auth)

5059 (RT/FIMA(65)–1) CYRCO PROGRAMMA PER IL CALCOLO DI CRITICITA DI REATTORI CILINDRICI TOTALMENTE RIFLESSI. (CYRCO—Program for the Calculation of a Totally Reflected Cylindrical Reactor Design). Azzoni, P.; Casali, F.; Poli, P. (Comitato Nazionale per l'Energia Nucleare, Rome (Italy)). June 1965. 69p. Dep. mn.

The CYRCO code is a two-group, two-core totally reflected cylindrical reactor design program. Tensorial properties of the diffusion coefficients were considered. The code also includes the calculation of the axial and radial adjoint fluxes. The CYRCO program is written in FORTRAN-II language for IBM-704 and IBM-7094 computers. (auth)

5060 (TID–22357) PROGRESS REPORT OF NORA PROJECT, JULY 1–SEPTEMBER 30, 1965. (Institutt for Atomenergi, Kjeller (Norway)). Oct. 1965. Contract AT(30-1)-3498. 38p. (NC–72). Dep. mn; CFSTI $2.00 cy, $0.50 mn.

Uniform H_2O cores with a lattice pitch of 2.314 cm were studied. The noise measurements were continued, and the reactivity worths of control rods were investigated experimentally and theoretically. The intracell thermal-neutron density distribution in the H_2O core was measured. Computer programs and methods for the analysis of temperature reactivity coefficients and of lattice experiments were evaluated. (D.C.W.)

5061 (ZFK-RN–22) EIN EINFACHER REAKTIVITAETSMESSER HOHER EMPFINDLICHKEIT. (A Simple Reactivity Meter of High Sensitivity). Ebersbach, Hans-Georg; Liewers, Peter; Scholz, Josef (Zentralinstitut fuer Kernphysik, Rossendorf bei Dresden (East Germany)). Oct. 1963. 23p. Dep. mn.

The reactivity meter described is based on the simulator principle. It computes the value of the reactivity due to the time variation of the neutron density. For ionization chamber currents in the range of $10^{-8}-10^{-3}$ A reactivities of $10^{-5}-10^{-1}$ are measurable. The accuracy in the range $\rho = 10^{-4}-10^{-2}$ is about 1%. Comparisons with conventional measuring methods showed a correspondence within 3%. The reactivity meter may be used for many purposes, especially for quick critical adjustments of reactors, for accurate and quick calibration of control rods, for the determination of power- and temperature-coefficients etc. (auth)

5062 REACTIVITY APPROXIMATION. Carpenter, Donald G.; Alme, Marvin L. (U. S. Air Force Academy, Colorado). Amer. J. Phys., 33: 961(Nov. 1965).

A two-term approximation is proposed for computing reactivity in the intermediate range. As an example to illustrate the merits of the approximation, a graph is presented of reactivity versus period for a spherical homogeneous reactor using ^{235}U as a fuel and H_2O as moderator in a molar ratio of 1 : 400. (L.B.S.)

5063 MULTIPOLES IN A SQUARE CELL REACTOR LATTICE. Amin, M. (Univ. of Eng. of Tech., Lahore). J. Nat. Sci. Math., 5: 105-10(Apr. 1965).

The problem of multipoles in a simple square cell reactor lattice is discussed. It is shown that only the lattices of multipoles of order 2^{4m} can contribute to the flux and thermal utilization in the case of a square cell lattice. The lattice of multipoles of order 2^4 and its effect on flux and thermal utilization are fully treated. (auth)

5064 THE REACTIVITY EFFECT OF VOID AND HOLE. Sugimoto, Osamu (Chugoku Electric Power Co., Hiroshima). J. Nucl. Sci. Technol. (Tokyo), 2: 277-84 (Aug. 1965).

The reactivity loss caused by a hole introduced in a reactor is calculated by using the two group perturbation theory based on neutron balance. It is shown that better agreement with experimental results is obtained by the use of a more reasonable probability function than those of Marti and Schneeberger. The reactivity loss by the presence of a void is calculated by the same method, and results are obtained for several cases: When void volume is below a certain limit, $\Delta k(z)$ is independent of z and proportional to the void volume; in the limit of small void, $\Delta k(z)$ is proportional to the square of flux. From these results the mechanism of reactivity loss is discussed. In order to justify the discussion, a comparison is made of the theoretical results with experiments on JRR-2. (auth)

5065 COUPLED REACTOR KINETICS. II. THEORY. Kawai, Toshio (Central Research Lab., Hitachi Ltd., Ozenji, Tokyo). J. Nucl. Sci. Technol. (Tokyo), 2: 285-95 (Aug. 1965).

Two methods, modal expansion and invariant imbedding, can be applied to derive a weak coupling reactor kinetics model. The criteria for weak coupling are examined, and coupling constants obtained. The resulting transfer functions and the inhour equation are compared with ordinary space independent cases. (auth)

5066 THEORY OF STATISTICAL FLUCTUATIONS IN NEUTRON DISTRIBUTIONS. Saito, Keiichi; Otsuka, Masuhiko (Japan Atomic Energy Research Inst., Tokyo). J. Nucl. Sci. Technol. (Tokyo), 2: 304-14(Aug. 1965).

Statistical fluctuations in neutron and precursor distributions in a reactor are investigated in a continuous phase space. The theory is constructed on the basis of Ramak-

rishman's product density and of the concept of "detectrons". The basic equations for the product densities of degree 2 are derived and solved. The space-time correlation function for the outputs of neutron detectors and a generalized formula for the Feynman-α experiment are obtained. (auth)

5067 TEMPERATURE COEFFICIENT OF WATER LATTICES. Wajima, J. Tsunetaka; Yamamoto, Kazuko (Hitachi, Ltd., Kawasaki-shi, Japan). J. Nucl. Sci. Technol. (Tokyo), 2: 331-9(Sept. 1965).

Temperature coefficients of slightly enriched UO_2-H_2O lattices were measured in the Ozenji Critical Facility and analyzed in terms of critical parameters. The lattices studied were mainly those of 2.5% enriched UO_2, 10 mm in diameter and clad in 0.8 mm thick Al tube, and with water to fuel volume ratios of 2.5 and 1.5. Analyses were made with Deutsch's four factor critical equation and also with three group one dimensional diffusion calculations. The result shows the importance of the influence of the reflector, which is the largest positive contribution to the temperature coefficient, being about 1×10^{-4} $\Delta k/k/°C$. This was experimentally demonstrated by measuring the coefficient for a core with an inner reflector water gap. Analyses also show that the discrepancy between experiment and calculation, which increases from 0.2 to 0.7×10^{-4} $\Delta k/k/°C$ as the water to fuel volume ratio decreases, may be mostly resolved by applying corrections for the space-dependent spectrum within the cell using the THERMOS code and for the effect of Dancoff factor with the TUZ-ZUT code. Calculation with these corrections applied reproduces experiment within an accuracy of about 0.2×10^{-4} $\Delta k/k/°C$ over the temperature range of 20 to 70°C. (auth)

5068 THE COMPARATIVE STUDY OF THE SODIUM LOSS REACTIVITY EFFECT OF LARGE Pu-U AND Pu-Th FAST REACTORS. Ohta, Masao (Kyoto Univ.). J. Nucl. Sci. Technol. (Tokyo), 2: 340-8(Sept. 1965).

Fast reactors having a 3,000 l core volume fueled with ceramic Pu-U and Pu-Th are compared with each other for their reactivity effects due to large-scale loss of coolant. Using a one-dimensional multi-group calculation, the maximum volume fractions of fuel for both fast systems are determined on the assumption that total loss of sodium in the core should not result in positive reactivity effect. It is concluded that Pu-Th fast reactors can be charged with more than several volume percent of fuel above the limit applicable to Pu-U fast reactors. (auth)

5069 EVALUATION AND CORRECTION OF THE ERROR DUE TO COARSE MESH ADJACENT TO ABSORBING REGIONS IN DIFFUSION CODE CALCULATIONS. Aisu, Hideo (Mitsubishi Atomic Power Industries, Inc., Japan). J. Nucl. Sci. Technol. (Tokyo), 2: 349-54(Sept. 1965).

A simple correction formula is analytically desired to reduce the error due to coarse mesh adjacent to absorbing regions in diffusion code calculations. The formula is derived by equating the neutron current, obtained by the three point difference equation with a finite mesh size, with the true value corresponding to zero mesh size. The formula is numerically confirmed to be quite satisfactory in practical two dimensional critical calculations with quite coarse mesh size. When a transitional fine mesh region is adopted to represent the geometrical heterogeneity in the vicinity of the absorber region, the error is almost entirely determined by the mesh size in the transitional region and the correction is only necessary for the mesh size therein if the region thickness is above one and a half times the diffusion length. (auth)

5070 A GENERALIZED ANALYSIS OF ROSSI-α EXPERIMENT. Ukai, Seiji; Takeda, Seishi; Yamada, Shusaku (Kyoto Univ.). J. Nucl. Sci. Technol. (Tokyo), 2: 355-62 (Sept. 1965).

A generalized theory of the Rossi-α method is shown and is applied to the analysis of an experiment made with a remotely subcritical system. Starting from the neutron transport equation, a general expression for the probability of detecting correlated neutrons is given, which is a function of the positions and sensitivities of the neutron detectors used in the experiment. Some numerical examples for this expression are also given under the one-group diffusion approximation for comparison with the experiment. The agreement between them is satisfactory. (auth)

5071 STUDY OF A SLIGHTLY ENRICHED UO_2 LATTICE WITH H : U = 0.42—MEASUREMENT AND ANALYSIS. Baer, W.; Hardy, J. Jr.; Klein, D.; Volpe, J. J.; Palowitch, B. L.; Frantz, F. S. Jr. (Westinghouse Electric Corp., Pittsburgh). Nucl. Sci. Eng., 23: 361-7(Dec. 1965). (WAPD-T-1631).

Parameter measurements in a 1.3% enriched UO_2 lattice with H : U = 0.42 were performed. The measurements are an extension of an experimental program in the TRX critical facility of the Bettis Atomic Power Laboratory. Earlier measurements were made for a wide range of water-to-uranium (H_2O : U) volume ratios (1 : 1 to 8 : 1) using 4-ft (1.2-m)-high slightly enriched, 0.387-in. (0.98-cm)-diam uranium metal or oxide fuel rods clad with aluminum. The new data were compared with current analytic techniques, using both P-1 and P-3 multigroup analysis in the epithermal-neutron energy range and Monte Carlo multigroup methods for thermal neutrons. This extremely undermoderated lattice provides a very stringent test for both the computational methods and the neutron cross sections used. The quantities measured were: the ratio of epithermal-to-thermal radiative captures in ^{238}U (ρ^{28}); the ratio of captures in ^{238}U to fissions in ^{235}U (the modified conversion ratio, CR*); the ratio of ^{238}U fissions to ^{235}U fissions (δ^{28}); and the ratio of epithermal-to-thermal ^{235}U fissions (δ^{25}). In addition, activations were obtained with thermal-neutron detectors of widely different spectral response. The results indicate that the calculational methods predict the parameters very well, except for δ^{28}. The discrepancy in δ^{28} may be due to inadequate ^{238}U inelastic scattering cross sections, but this conclusion requires additional study. Monte Carlo calculations of thermal-neutron detector activations show that use of either the Nelkin or Koppel kernel gives results that agree with the data. (auth)

5072 DOPPLER COEFFICIENT MEASUREMENTS FOR ^{235}U IN FAST-REACTOR SPECTRA. Amundson, P. I.; Gasidlo, J. M. (Argonne National Lab., Idaho Falls, Idaho). Nucl. Sci. Eng., 23: 392-3(Dec. 1965).

The Doppler coefficient of ^{235}U was measured in the ZPR II Assembly 45A, a zoned reactor containing a central region whose composition represents a large sodium-cooled fast power-breeder reactor having ^{239}Pu-^{238}U mononocarbide fuel. The reactor regional parameters are tabulated. The reactivity coefficient was found to be approximately $+3 \times 10^{-6}$/°C. (L.B.S.)

5073 THERMAL DISADVANTAGE FACTORS IN VERY UNDERMODERATED WATER-URANIUM OXIDE LATTICES. Boynton, Allen R. (Argonne National Lab., Ill.). Nucl. Sci. Eng., 23: 393-5(Dec. 1965).

Previous measurements of the thermal disadvantage factors in five High Conversion Critical Experiment lattices that had water-to-uranium oxide ratios of 0.96 to 0.16 are compared with calculated values using the THERMOS and B692/RP codes. Two disagreements are noted: firstly, THERMOS values are larger than experimental disadvantage factors except for the tightest lattice; and secondly, the experimental values increase at lower values of water-to-uranium oxide volume than about 0.5, while the calculations show the disadvantage factor to be monotonically decreasing with smaller lattice pitch. It is not concluded whether the discrepancy between experiment and theory results from errors of experimental or computational origin. (L.B.S.)

5074 EQUIVALENCE OF THE TIME OPTIMAL AND MINIMAX SOLUTIONS TO THE XENON SHUTDOWN PROBLEM. Roberts, John J.; Smith, Harold P. Jr. (Univ. of California, Berkeley). Nucl. Sci. Eng., 23: 397-9(Dec. 1965).

It is shown that a solution for the time optimum case is also a solution to the minimax case. The discrepancy between the solution and those of Rosztoczy and Weaver and

Ash are examined. It is shown that if the minimax criterion is applied during, as well as after, the shutdown program, their solutions are not always optimum. A specific case is presented to demonstrate this point. (L.B.S.)

5075 A NOTE ON THE ADJOINT FUNCTION IN THE TIME OPTIMAL XENON SHUTDOWN PROBLEM. Lewins, Jeffery (Univ. of Washington, Seattle). Nucl. Sci. Eng., 23: 404-5(Dec. 1965).

The Pontryagin theorem was recently applied to time optimal xenon shutdown. One aspect of the adjoint functions used in the analysis is pointed out in respect to the reversed-time problem. (L.B.S.)

5076 A COMMON THEORY FOR NEUTRONIC NOISE ANALYSIS EXPERIMENTS IN NUCLEAR REACTORS. Borgwaldt, Horst; Stegemann, Dieter (Kernforschungszentrum Karlsruhe, Ger.). Nukleonik, 7: 313-25(July 1965).

A common basic formula is developed for the description of neutronic noise analysis experiments in nuclear reactors. From this formula specific expressions are derived for techniques, such as frequency analysis of noise, Rossi-α-experiments, variance-determinations, and the analysis of counting statistics. Proposals for new techniques are included which seem advantageous from theoretical and experimental considerations. Although the basic theoretical formulas are of general validity and include space- and energy-dependence as well as delayed neutrons, the point-reactor model approximation was used for the derivation of most specific expressions. The possibility of using noise analysis experiments for investigating the kinetics of coupled reactor systems is also discussed. (auth)

5077 A BOLTZMANN INTEGRAL EQUATION TREATMENT OF RESONANCE ABSORPTION IN REACTOR LATTICES [Thesis]. Lewis, Elmer Eugene. Urbana, Ill., Univ. of Illinois, 1965. 129p.

A method was developed for calculating resonance effects in nuclear reactor lattices without the two widely used assumptions that the neutron flux is spatially independent within each region of the lattice cell, and that the flux recovers an asymptotic 1/E form between resonances. The neutron slowing down problem is formulated in terms of a Boltzmann integral equation, and the correct transport kernel is derived for a Wigner-Seitz equivalent cell with isotropic scattering in the laboratory system. A new method of polynomial approximations is then used to reduce the transport problem to matrix form. From this there results a set of integral equations in energy for the neutron flux at a number of discrete ordinates. These equations are numerically integrated to obtain the neutron flux as a function of space and energy. A set of FORTRAN codes was written, which used the above method to calculate flux distributions and reaction rates for the resolved resonances of fertile and fissile nuclides in cylindrical lattices. Resolved resonance integrals are calculated for a number of ^{238}U-graphite lattices with both metal and oxide rods. Where comparisons are made, the results are in excellent agreement with accurate Monte Carlo calculations. Both the flat flux and flux recovery assumptions are found to cause significant overestimates of the resonance integrals, the errors increasing with the rod radii. The temperature coefficients, however, are less sensitive to these assumptions. It is also found that the usual linear relationships of the resonance integrals of $\sqrt{S/M}$, the square root of the fuel element surface to mass ratio, are invalid for $\sqrt{S/M} < .2$. The codes are also used to study the lack of flux recovery between the low-lying resonances of ^{232}Th, to calculate epithermal fission and capture rates for enriched uranium rods, and to study the errors introduced by the isotropic scattering assumption in a heavy water lattice. (Dissertation Abstr.)

Design and Feasibility

5078 (GAMD-6676) CORE. A COMPUTER CODE FOR THE DESIGN OF A GAS-COOLED REACTOR CORE. Schultz, G. M. (General Atomic, San Diego, Calif. John Jay Hopkins Lab. for Pure and Applied Science). Aug. 27, 1965. Contract AT(04-3)-167. 47p. Dep. mn; CFSTI $2.00 cy, $0.50 mn.

The computer program CORE, in FORTRAN IV for the IBM 7044, will design a gas-cooled reactor core and calculate its fuel-cycle costs as a function of the specified independent variables and constraint functions. The analytical models and the iterative technique used by the program are described. (D.C.W.)

5079 (NP-15572) PRELIMINARY DESIGN WORK OF THE 100 MWt EXPERIMENTAL FAST REACTOR. Tamura, Tetsuo; Sako, Kiyoshi; Inoue, Teruji (Japan Atomic Energy Research Inst., Tokyo). Sept. 1, 1965. 28p. Dep. mn.

A summary of the preliminary design work of the experimental fast reactor is presented. An emphasis is placed on the flexibility to alter the core volume and shape. The thermal design criteria adopted are as follows: sodium inlet temperature is 250°C, 150% power of the rated power will not make sodium boiling at the hot spot, the maximum fuel temperature on the operation at the hot spot does not reach the melting point, the total pressure drop of the coolant in the primary loop shall not be exceeded 5 kg/cm^2, and orifices will be provided in the blanket region, etc. YOM-16 group constants were used for the nuclear calculations. The code used is a one dimensional diffusion code. The temperature in the cold clean state will be 250°C, and the densities adopted for UO_2, S.S. 316, 347, and sodium are 10,3, 7.82 and 0.893 (g/cc) respectively. (auth)

5080 NUCLEAR REACTOR. Woods, William John (to United Kingdom Atomic Energy Authority). British Patent 1,007,206. Oct. 13, 1965. Filed Sept. 22, 1964.

A core module for a liquid moderated reactor in which the moderator acts as a coolant is made up of a number of elongated fuel elements clustered in parallel spaced relation to surround a vacancy. A filler element without a fissile content and of moderator material having a neutron slowing-down power less than that of the coolant is centrally located in the vacancy. A shroud tube is disposed in the vacancy and encircles the filler element with clearance for the insertion of a hollow neutron-absorbing element with an open end foremost into the shroud tube. The other end of the hollow tube has only a restricted opening for the coolant flow. (B.L.M.)

5081 GASEOUS NUCLEAR REACTOR. Rom, Frank E. (to U. S. Atomic Energy Commission). U. S. Patent 3,202,582. Aug. 24, 1965.

A gaseous nuclear reactor is designed that is composed of an outer shell, a heating cell contained within the outer shell, a nozzle device for injecting a gaseous fissile material into the heating cell, a first toroidal nozzle means for injecting a primary quantity of propellant concentric to the injected gaseous fissile material, a second toroidal nozzle means for injecting a secondary quantity of propellant concentrically adjacent to the injected primary quantity of propellant and the injected gaseous fissile material, a neutron reflector-moderator, a device for cooling the reflector-moderator, and a device for controlling the fission power level of the injected gaseous fissile material within the heating cell. (AEC)

5082 HETEROGENEOUS BREEDER OR CONVERTER TYPE NEUTRONIC REACTOR. Creagan, Robert J. (to Westinghouse Electric Corp.). U. S. Patent 3,211,621. Oct. 12, 1965. Filed Sept. 29, 1960.

A core arrangement for a converter type heterogeneous reactor includes three groups of uniformly elongated fuel element assemblies supported within the core structure. The first group of fuel assemblies is arranged in a parallel array in the center region of the core; the second group is arranged outside of and surrounding the first group; and the third group is outside and surrounding the second group. The second group of fuel elements contain either natural U or natural Th, and the first and third groups contain fissile material having a relatively low uniform enrichment of from 1 to 10% and contain sufficient fissile material at least initially to sustain a chain reaction. (B.L.M.)

5083 NEUTRONIC REACTOR AND FUEL ELEMENT THEREFOR. Tower, Stephen N. (to Westinghouse Electric Corp.). U. S. Patent 3,211,623. Oct. 12, 1965. Filed Apr. 22, 1960.

A reactor of the pressure tube variety is described in which ready access is afforded for refueling; control is effected by varying the moderating and reflecting capabilities, by a control rod arrangement, or by a combination of the two; and an improved arrangement is included for circulating the coolant through the pressure tubes and for recycling the fuel in each pressure tube or among the array of pressure tubes. The moderator is preferably a liquid, and the reactor can be operated at atmospheric pressure without moderator boiling. A fuel element is patented also that permits ready insertion or withdrawal relative to the corresponding pressure tubes, alignment within the pressure tubes, and a continuity of flow passage through the tubes. Allowance is also made for differential thermal expansions among the components of each fuel element. (B.L.M.)

5084 METHOD AND MEANS FOR CONTROLLING THE START OF A HOMOGENEOUS NUCLEAR REACTOR. Widell, Bjoern (to Allmanna Svenska Elektriska Aktiebolaget). U. S. Patent 3,211,624. Oct. 12, 1965. Priority date Sept. 25, 1962, Sweden.

A method is described for controlling the start of a homogeneous reactor in which the fuel is dissolved or dispersed in a liquid coolant from which steam is produced and the heat content of the coolant is carried off during condensation of the steam in a primary steam circuit. The reactor vessel with a conduit is placed in free liquid transport communication with a subcritical collecting vessel arranged at a lower level having a sufficiently large volume to contain at shutdown of the reactor a fuel composition necessary for operation of the reactor. The collecting vessel with another conduit is in communication with a subcritical storage vessel arranged at the same level as the reactor. Before the start the fuel is stored in the collecting vessel; and a pressure difference between the gas phases on the two sides of the reactor vessel and the other vessels forces the fuel into the reactor vessel. Suitable control of the pressure on the gas phases and the communicating conduits permits control of the fuel composition with a minimum of movable parts in contact with the fuel. (B.L.M.)

5085 BOILING REACTOR WITH SUPER HEAT. Setterwall, Max (to Allmanna Svenska Elektriska Aktiebolaget). U. S. Patent 3,211,625. Oct. 12, 1965. Priority date Sept. 7, 1962, Sweden.

A boiling reactor with nuclear superheating consists of the core, a guide and support structure above the core, and a steam dome arranged above the guide and support structure. Each tube for generating steam from the reactor coolant is arranged with part of its length in the core and part in the guide and support structure. The tubes for superheating the steam generated in the first tubes are arranged with a part of their length in the reactor core and a part in the guide and support structure and contain fuel elements at least in the parts arranged in the core and have inlet ports for the steam in the part that is in the guide and support structure. The guide and support structure form a closed vessel, and the tubes for steam generation have outlet ports for a mixture of steam and liquid from the reactor coolant above the support structure within the steam dome. At least one steam channel has an inlet port arranged above the outlet ports of the steam generating tubes in the steam dome and an outlet port into the guide and support structure so that the steam dome is in communication with the guide and support structure and with the superheating tubes. (B.L.M.)

5086 NEUTRONIC REACTOR. Kornbichler, Heinz (to Licentia Patent-Verwaltungs-GmbH.). U. S. Patent 3,212,983. Oct. 19, 1965. Priority date Dec. 5, 1957.

A heterogeneous liquid moderated reactor is described in which hot spots are reduced or completely eliminated to permit operation at a higher overall output. The reactor core is made up of a number of fuel assemblies with a number of elements in each assembly arranged in sections. The joints between sections are composed of non fissionable structural material having interspaces filled by the moderator. An end zone is adjacent to each joint, and a main zone extends beyond the end zone. When water is the moderator, each end zone contains H_2O, Zr, and UO_2 of an isotropic ratio occurring in nature, and each main zone consists of H_2O, Zr, and UO_2 initially having a 1.2% enrichment of fissionable material. (B.L.M.)

5087 NUCLEAR REACTOR WITH EMERGENCY COOLANT CROSS FLOW. Silvester, Austin G. (to U. S. Atomic Energy Commission). U. S. Patent 3,215,606. Nov. 2, 1965.

A nuclear reactor is designed wherein the coolant is arranged to flow across as well as along the fuel rods to equalize the internal pressure as well as temperature distribution within the core. The system comprises a plurality of fuel elements having shroud means with inlet and outlet parts midway along the shroud to permit cross flow of current. The plurality of fuel rods within the shroud are arranged to define zones, beginning proximate the bottom portion of the rod with a fissile fuel zone, a moderator and cross flow zone immediately above the fissile fuel zone, a top exit zone immediately above the moderator and cross flow zone with a top shield zone defined by the top portion of the fuel rods immediately above the top cross flow zone. (AEC)

Fuels

Refer also to abstracts 3969, 4102, 4376, and 4576.

5088 (EURAEC–1337) NUCLEAR VAPOTRON. Annual Report. (Compagnie Francaise Thomson-Houston, Paris). Oct. 30, 1964. Contract 034-63-11-TEEC(RD). 160p. (EUR–2313). Dep. mn; CFSTI $5.00 cy, $1.00 mn.

Work Performed under United States–Euratom Joint Research and Development Program.

Thermal tests are reported on full-size "nuclear vapotron" fuel cans in a test loop capable of operating at pressures up to 70 bar. The improvements made in the test loop and test cell; the safety devices developed and used; and the operating conditions are reviewed. An outline is given of the geometric configurations of the cans tested, the measurements and observations carried out, the results, and the conclusions reached. The major part of the effort is devoted to determining the burnout flows as a function of the flow rate and enthalpy at the cell inlet. (T.F.H.)

5089 (GA–6181) ADVANCED, GRAPHITE-MATRIX, DISPERSION-TYPE FUEL SYSTEMS AND RESEARCH ON GRAPHITE. Quarterly Progress Report for the Period Ending February 14, 1965. Bokros, J. C.; Goeddel, W. V.; Lonsdale, H. K.; Price, R. J.; White, J. L.; Zumwalt, L. R. (General Atomic, San Diego, Calif. John Jay Hopkins Lab. for Pure and Applied Science). Feb. 15, 1965. Contract AT(04-3)-167. 64p. Dep. mn; CFSTI $3.00 cy, $0.75 mn.

Pyrolytic-carbon coating studies were extended from 1900 to 2400°C. The densities of the structures deposited increased uniformly with deposition temperature. Both isotropic and granular structures were deposited; low methane concentrations, high temperatures, and small surface areas favored deposition of granular structures. Mechanical property measurements performed on the high-temperature deposits showed that the modulus, fracture stress, and fracture strain increase with increasing deposition temperature for granular structures. Isotropic and transition structures showed a slight decrease in modulus and fracture stress with increasing deposition temperature. Newly developed x-ray scattering techniques were applied to carbons deposited at 1400°C from 5 and 40% methane. Measurement of the physical and mechanical properties of annealed laminar structures, which were deposited at

1400°C under various conditions, showed that while various properties respond differently to annealing, the order of annealability between structures remains the same. In general, the annealability increases with a decrease in the amount of single layers in a structure. Tracer-level diffusion studies conducted on granular pyrolytic carbon structures using ^{228}Th as the diffusive species showed that the diffusion coefficients for this type structure are about a factor of 10 greater than for laminar pyrolytic carbon. These results confirmed that the diffusion coefficient is strongly dependent on the structure of the pyrolytic carbon. Studies of the influence of additives dispersed within a graphite matrix on the hot-working process and on the properties of the hot-worked bodies resulted in the development of unique carbide-graphite cermets. These new materials were prepared by hot-working carbide-bearing graphite bodies at temperatures such that the dispersed carbide phase is in the liquid state. Hot-working of graphite bodies containing MoC or ZrC in the liquid state resulted in large increases in compressive strengths parallel to the direction of hot-working, and modest increases in the perpendicular direction. The helium permeability of these carbide-graphite cermets is near the limit of detection with existing apparatus ($<10^{-6}$ cm^2/sec). (P.C.H.)

5090 CREEP BOWING OF A FUEL ELEMENT AGAINST A CONTINUOUS RESTRAINT. Blackburn, W. S. (International Research and Development Co. Ltd., Newcastle upon Tyne, Eng.). J. Nucl. Energy: Pt. A and B, 19: 753-66(Oct. 1965).

The behavior of fuel elements with initial bows of various forms and ends either held in a pin-jointed manner in the center of the channel or allowed to tilt across it is investigated for up to 100 doubling times after intermediate contact occurs, and the displacements and forces at points of contact are evaluated. The maximum horizontal force up to 100 doubling times was found to be about sixteen times the vertical load times the ratio of the effective clearance to the length of the element, for a variety of different forms of initial bow and end condition. Small deviations in the shape of an initial bow in general had no significant effects on the shape after an appreciable number of doubling times. (auth)

5091 AXIAL HEAT CONDUCTION IN REACTOR FUEL ELEMENTS. Thorpe, J. F. (Univ. of Kentucky, Lexington). Nucl. Sci. Eng., 23: 329-34(Dec. 1965).

An approximate method is developed for determining the axial and transverse heat-flux distributions in reactor-fuel elements. The method is analogous to the Karman-Pohlhausen method of boundary-layer theory. When the results of the approximate method are compared with those of known exact solutions, the agreement is found to be excellent. Two examples are given in which the approximate method gives values that agree with the exact solutions to within about 2%. (auth)

5092 RESONANCE CAPTURE AND DOPPLER COEFFICIENT IN CYLINDRICAL URANIUM FUEL ELEMENTS. Beynon, T. D. (Woolwich Polytechnic, London); Grant, I. S. Nucl. Sci. Eng., 23: 368-79(Dec. 1965).

Double P_0 diffusion theory is shown to be a sufficiently accurate representation for calculating resonance absorption and its temperature coefficient. The theory is formulated to allow for non-uniform temperature distributions and spatial variation of neutron cross sections. It is applied to uranium rods in graphite-moderated reactors, assuming a parabolic fuel-temperature distribution. Volume and surface temperature coefficients for absorption are defined. The energy distributions of these coefficients in strongly absorbing resonances are shown to differ significantly. It is found that the total volume coefficient exceeds the total surface coefficient by 15% at normal operating temperatures. At higher temperatures the total volume coefficient is larger by 5%. Rowlands' formula for the effective uniform temperature is shown to be reliable for calculating the resonance integral and the volume temperature coefficient, but not for the surface coefficient. (auth)

5093 NON-DESTRUCTIVE EXAMINATION OF IRRADIATED NUCLEAR FUEL FOR BURN-UP AND FISSION PRODUCT MIGRATION BY GAMMA SCANNING. Fudge, A. J.; Causer, R.; Murphy, L. (Atomic Energy Research Establishment, Harwell, Eng.). pp 101-10 of International Symposium on Working Methods in High Activity Hot Laboratories. Vol. I. Paris, Organization for Economic Cooperation and Development, 1965.

The distribution of burnup and the migration of fission products within irradiated nuclear fuel is of primary importance in design considerations. Gamma scanning is a direct and nondestructive technique by which the abundance and distribution of certain fission-product nuclides can be obtained. Collimation and distance are used to reduce the activity to levels acceptable by the detectors. Spectral resolution is obtained by pulse height analysis. Continuous and stepwise scanning is used for both horizontal and vertical movement of the specimens. The data can be obtained in either analog or digital format for relative comparison or absolute calibration. Cracks, fuel breakdown, fuel inhomogeneity, and fission-product migration were confirmed by subsequent destructive examination. (auth)

5094 UNITED KINGDOM EXPERIENCE OF MAGNOX FUEL ELEMENTS. Franklin, N. L.; Edge, T.; Jones, F. R. R. Paper No. 3 of Anglo-Spanish Nuclear Power Symposium. Vol. 1. [Risley, Eng., United Kingdom Atomic Energy Authority, 1965]. 20p.

Some of the principal features of the U.K. experience in the design, development, manufacture, and performance of uranium-magnox fuel elements are outlined. Drawings are shown of typical examples. (L.B.S.)

5095 IMPROVEMENTS IN OR RELATING TO FUELLING ARRANGEMENTS FOR NUCLEAR REACTORS. Wills, Stanley Charles Frederick (to Strachan and Henshaw Ltd.). British Patent 1,008,956. Nov. 3, 1965. Filed Mar. 17, 1961.

A replacement head is provided for a reactor fuel element from which the normal head has become detached while the element is situated in a reactor channel. The replacement head has an upper end provided with a head part for coupling engagement by normal fuel element handling equipment and a lower end formed as a cap member having depending jaws arranged about an axis. The jaws house slidably arranged dogs positioned in grooves sloping longitudinally downward toward the axis. The jaws are adapted to engage the outside of the upper end of the fuel element and lock onto it when the device is lifted by the normal fuel element handling means. (B.L.M.)

5096 NEUTRONIC REACTOR FUEL ELEMENT AND MEMBER THEREFOR. Nerenstone, Marc A.; Charland, Telesphore L. (to Westinghouse Electric Corp.). U. S. Patent 3,211,626. Oct. 12, 1965. Filed Dec. 3, 1959.

A fuel element for a nuclear reactor consists of an elongated cladding tube containing a number of porous members inserted in tandem in the tube and substantially filling the tube. The porous member has the porous central region with the outer region being infiltrated with a metal having a higher heat conductivity and a lower melting point than the fissile material and having a relatively low thermal neutron cross section. The metal is selected from the group consisting of Al, Fe, Si, Ti, Zr, and Mo. (B.L.M.)

5097 FUEL ELEMENT FOR A COOLANT-MODERATOR NUCLEAR REACTOR. Thorp II, Arthur G. (to Westinghouse Electric Corp.). U. S. Patent 3,211,627. Oct. 12, 1965. Filed Feb. 5, 1962.

A fuel element for a heterogeneous coolant-moderator reactor is formed with varying cross section and a varying amount of fuel along its length. The element is made up of a hollow cladding means of differing cross sectional sizes with the fissile material in the form of suitably sized pellets contained in the cladding. A plug serves to retain the fissile material in the hollow cladding means, and a single plug is associated with adjacent cladding members to secure the members together in an end-to-end relation. Each plug has a flange projecting outwardly between the adjacent cladding members, and the adjacent members and the plug

flange are bonded together. The cross sectional size of the fuel element decreases over its entire length. Several such fuel elements may be arranged upstandingly in an array between upper and lower core support plates. (B.L.M.)

5098 PROCESS OF ASSEMBLING A TEMPERATURE MEASURING DEVICE WITHIN AN APERTURE OF A FUEL ELEMENT. Noakes, Michael Lesney (to United Kingdom Atomic Energy Authority). U. S. Patent 3,212,178. Oct. 19, 1965. Priority date Dec. 16, 1960, Great Britain.

A process is described whereby a temperature measuring device may be incorporated within a fuel element produced by multiple rolling operations. A wire is inserted in a prepared aperture comprising a longitudinal slot machined in the fuel core before the first rolling operation. The wire is removed after the first rolling operation, and the steps are repeated with wires of gradually decreasing diameter until after the penultimate rolling stage, the device is inserted, and the member rolled to the final thickness. The process is particularly applicable to sheathed fuel plates. (B.L.M.)

5099 FUEL ELEMENT FOR NUCLEAR REACTORS. Ringot, Claude. U. S. Patent 3,212,988. Oct. 19, 1965. Priority date July 18, 1961, France.

A fuel element for gas cooled reactors is composed of a fuel substance, either UO_2 or UC, covered by a first sheath 0.04 to 0.08 in. thick selected from the group of materials consisting of Zr, Al, and Be. Discs of the same material are integrally attached to the ends of the sheath. The sheathed fuel material is enclosed with a sheath of another material that is compatible with the cooling gases at temperatures up to 1100°F. The outer cylindrical sheath is not more than 0.004 in. thick and is composed of austenitic steel, molybdenum refractory steel, or a Ni–Cr refractory alloy. (B.L.M.)

5100 FUEL ELEMENT CLUSTER. Murtha, Bruce E. (to Combustion Engineering, Inc.). U. S. Patent 3,212,990. Oct. 19, 1965. Filed Nov. 21, 1961.

A fuel element cluster assembly is made up of a number of elongated, parallel casing members having both hollow and solid portions. The fissionable material is contained in the hollow portions. The solid portions alternate with the hollow ones and provide a fluid tight separation of the hollow portions. The elements are arranged in bidirectional rows, and means are provided for maintaining the elements in fixed, spaced relation. Elongated rigid support members extend laterally of the rows and are received in aligned openings in the solid portions of the elements. The support members are joined to the elements in some manner, e.g., brazing, to prevent relative movement. (B.L.M.)

5101 NUCLEAR FUEL ELEMENT CASING. Salesse, Marc; Stohr, Jacques Andre (to Commissariat a l'Energie Atomique). U. S. Patent 3,212,992. Oct. 19, 1965. Priority date Mar. 17, 1960, France.

A finned sheath structure is provided for the cylindrical body of a fuel element in which the flow of coolant is parallel to the axis of the fuel element. The fins form a number of series of portions of helices disposed transversely to the longitudinal axis of the sheath. The entire surfaces of the fins are helicoidal elements having the same longitudinal axis as the sheath and are raised above the sheath. Each of the series have an opposite direction to the next adjacent series. (B.L.M.)

5102 MULTI-REGION NEUTRONIC FUEL ELEMENT. Lackey, M. (to U. S. Atomic Energy Commission). U. S. Patent 3,215,607. Nov. 2, 1965.

A fuel element for a nuclear reactor is described which comprises a jacket of nonfissionable material surrounding a uranium bearing core portion having uniform thermal and chemical properties throughout. The nuclear properties of the core portion vary, however, in that the fissionable uranium isotope is in greater abundance in the core region adjacent the jacket than throughout the remainder of the uranium bearing core portion. (AEC)

5103 NUCLEAR REACTOR CORE CLAMPING SYSTEM. Guenther, Ralph W. (to U. S. Atomic Energy Commission). U. S. Patent 3,215,608. Nov. 2, 1965.

Devices for holding fuel elements together to form a unified core are designed. The system comprises parallel spaced torsion rods aligned circumjacent the bundle of fuel elements and having upper and lower moment arms proximate each end of the rod, each arm bearing in opposite rotational direction against shoes fitted to bear against the bundle of fuel elements. (AEC)

Power and Power-Breeder Reactors

Refer also to abstracts 4305, 4313, 4331, and 5034.

5104 (ACNP–65006) ESH–4 TEST PROGRAM. REPORT ON FUEL ELEMENTS IRRADIATED IN THE E-SADE LOOP OF THE VALLECITOS BOILING WATER REACTOR. Wick, E. A.; Patterson, D. A. (comps.) (Allis-Chalmers Mfg. Co., Bethesda, Md. Atomic Energy Div.). Div.). Oct. 1, 1965. Contract AT(11-1)-1123. 117p. Dep. mn; CFSTI $4.00 cy, $0.75 mn.

The design, fabrication, and in-pile irradiation performance of nine superheater fuel elements in the E-SADE loop of VBWR are described. Each element consists of a seven-rod cluster of low-enrichment UO_2, operating at 1000 psi inlet pressure, 61 kw maximum power, and 1250°F maximum steady-state temperature. (T.F.H.)

5105 (ACNP–65544(Vol.I)) LA CROSSE BOILING-WATER REACTOR—SAFEGUARDS REPORT FOR OPERATING AUTHORIZATION. VOLUME I. (Allis-Chalmers Mfg. Co., Bethesda, Md. Atomic Energy Div.). July 1965. Contract AT(11-1)-850. 303p. Dep. mn; CFSTI $7.00 cy, $2.00 mn.

Descriptions of the reactor and site are presented along with descriptions of the primary cooling system and auxiliary systems including waste disposal. Design features of the containment building are also described along with the power plant. (J.R.D.)

5106 (ACNP–65544(Vol.II)) LA CROSSE BOILING-WATER REACTOR—SAFEGUARDS REPORT FOR OPERATING AUTHORIZATION. VOLUME II. (Allis-Chalmers Mfg. Co., Bethesda, Md. Atomic Energy Div.). July 1965. Contract AT(11-1)-850. 476p. Dep. mn; CFSTI $7.76 cy, $2.25 mn.

Information is included on instrumentation and control, electrical distribution, shielding, operating principles and safeguards, environmental survey, administrative and operational procedures, safeguards evaluation, and plant evaluation procedures. (J.R.D.)

5107 (ACNP–65589) PATHFINDER ATOMIC POWER PLANT TECHNICAL PROGRESS REPORT, OCTOBER 1964–DECEMBER 1964. (Allis-Chalmers Mfg. Co., Milwaukee, Wis. Atomic Energy Div.). Oct. 1965. Contract AT(11-1)-589. 37p. Dep. mn; CFSTI $2.00 cy, $0.50 mn.

Test 303 (Full Core Loading and Criticality) was completed for the full core 96 2.2 w/o boiler elements and 409 superheater elements. In this test, control rod bank and group critical heights, rod differential worths, and total and most reactive single rod full out shutdown margins were determined as a function of the number of boron-stainless steel poison shims in the core. Data taken during the tests are included. Test 312 (Cold Core Superheater Flooding and Control Rod Calibration) was completed. In this test the reactivity effect was determined for partial and full flooding with water of the superheater steam passages. The superheater control rods were also calibrated. The results of this test are included. A description of this test are included. A description of Test 313 (Full Core Boration and Flux Mapping) is presented. (M.O.W.)

5108 (AD–618376) PM–1 ANNUAL SUMMARY REPORT, 1 NOVEMBER 1963–31 OCTOBER 1964. Wester-

meir, James T.; Belson, John D.; Singleton, John L. (Air Force Weapons Lab., Kirtland AFB, N. Mex.). July 1965. 139p. (WL-TR-65-91). CFSTI $4.00 cy, $1.00 mn.

An evaluation of PM-1 nuclear power plant operations during the period 1 November 1963 to 31 October 1964 is presented. All phases of plant operations are included. Recommendations are made with the dual objective of cost reduction and improved availability. Weaknesses in several subsystems are discussed. A proposed reorganization of plant personnel is presented, and, based upon this, plant supply procedures are re-evaluated. Finally, the high cost of power generation is discussed. Supporting data for all recommendations have been included either in the text or as appendixes. (TAB)

5109 (AECL–2360) RUPTURED FUEL LOCATION WITH HIGH RESOLUTION GAMMA-RAY SPECTROMETERS. Lipsett, J. J. (Atomic Energy of Canada Ltd., Chalk River (Ontario). Chalk River Nuclear Labs.). Oct. 1965. 32p. Dep.; AECL $1.00.

Specific fission products are measurable in the coolant flow of power reactors with a lithium-drifted germanium γ-ray spectrometer. A channel containing ruptured fuel could be identified in a pressure-tube reactor by γ-scanning the channel outlets. Such a location system would be less elaborate than those involving continuously metered sample side streams, gas separation, iodine accumulation, etc. Calculations show that such a location system is feasible if short lived fission product release rates are adequate, or if long lived fission products which are released at high rates can be rapidly removed from the recirculating coolant system. The release must be measured against a background from uranium contamination on the fuel channel surfaces. The effect of activation products must also be considered. The lithium-germanium γ-ray spectrometer has resolutions of 3.5 and 7 kev at 1.17 Mev on single sources with full-energy-peak efficiencies of 50 and 0.2% at these energies. Double-escape-peak efficiency has a maximum of 0.5% at 4 Mev. Many specific γ-emitting fission products are identifiable in mixed sources, in the energy range from 80 kev to 4 Mev. The γ-spectra of mixed fission products were measured in NRX loop experiments using intentionally punctured UO_2 fuel. Test results on fission products appearing in organic coolant after a sudden puncture and immediate reactor shut-down and release of fission products through a 0.33 mm drilled puncture in highly-rated fuel in pressurized water are included. (auth)

5110 (AES–4) TEKNISK UPPHANDLING INOM REAKTOROMRADET. (Engineering Purchases within the Reactor Area). Jonson, Erik (Aktiebolaget Atomenergi, Stockholm (Sweden)). Nov. 1963. 63p. Dep. mn.

The engineering purchases for the Agesta reactor were described. The work area, work area responsibility, general purchasing procedures, technical specifications, bids, contracts, contract approval, and purchase control systems were considered. (J.S.R.)

5111 (AI-PC–710) HNPF POST CRITICAL TEST PROCEDURE. WET EXCESS FUEL LOADING. (Atomics International, Canoga Park, Calif.). May 25, 1963. Contract AT(11-1)-Gen-8. 103p. Dep. mn; CFSTI $4.00 cy, $0.75 mn.

The test was performed in order to present the sequence to be followed for installing an operational loading of fuel in the HNPF sodium filled reactor. The following reactor parameters were established in this test; the excess reactivity composing the operational loading of fuel, the shutdown margin available to the reactor, the total worth of the control rods in the reactor, the reactivity worth of the sodium in the reactor, and the reactivity effect of moving the source element from the normal core position to the peripheral channel in a partially loaded core, and inserting a fuel element in the original source position. (M.O.W.)

5112 (CEND–507) NUCLEAR ANALYSIS OF THE ELK RIVER REACTOR. Turner, S. E. (Combustion Engineering, Inc., Dunedin, Fla. Nuclear Div.). Oct. 1964. Contract AT(11-1)-651. 69p. Dep. mn; CFSTI $3.00 cy, $0.75 mn.

The results of a theoretical analysis of the nuclear characteristics of the Elk River Reactor are presented. For the present analysis, primary emphasis was placed on predicting, theoretically, the position of the control rods under different operating conditions. In any operating reactor, the one operating parameter which can be accurately observed at all times is the position of the control blades. Additional information concerning the core nuclear characteristics can be inferred from reactor period measurements under different conditions. The calculational procedure used for the analysis of the Elk River Reactor is given. Fortunately, the mode of operation chosen for the reactor specifies the use of banked control rods; either all 13 rods banked or 12 rods banked with the central rod remaining inserted until the 12 rod bank is fully withdrawn. This mode of operation simplifies the analytical procedures considerably. The basic analyses were performed with the TURFO code, a three-group diffusion theory code, with isotopic depletion, including options to select isotopic depletion, steam void calculations, and a rod position search routine. The majority of the calculations were performed in the axial direction, correcting the results with a small radial weighting factor. Results of these calculations are summarized. (auth)

5113 (CONF-650602–59) STATUS OF NUCLEAR SUPERHEAT DEVELOPMENT. Erb, D. E. (Division of Reactor Development and Technology (AEC), Washington, D. C.). [1965]. 11p. Dep. mn; CFSTI $1.00 cy, $0.50 mn; Gmelin, AED-CONF-65-125-78.

From American Nuclear Society 11th Annual Meeting, Gatlinburg, Tenn.

A sketch is given of the materials, concepts, economics, environmental contamination, and fuel performance for direct-cycle central-station nuclear superheat reactors using water. (T.F.H.)

5114 (CRRP–1221) A PRELIMINARY ASSESSMENT OF THORIUM AS A FUEL FOR THERMAL REACTORS. Duret, M. F.; Halsall, M. J. (Atomic Energy of Canada Ltd., Chalk River (Ontario)). Aug. 1965. 42p. (AECL–2290). Dep.; AECL $1.00.

A preliminary survey of the contributing factors to total fuel cost is presented for a variety of potentially economic fuel cycles. Uranium-238 and thorium-232 are considered as fertile materials with enrichments of ^{235}U, ^{233}U and plutonium. The total fuel cost comprises a fuel supply cost which is derived from a manufacturing cost and the fuel burnup, a spent fuel credit, and inventory charges. The interrelation of these three factors and their dependence on reactor flux, fuel burnup, the heat rating of the fuel and the interest rate are considered for each combination of fertile and fissile material. Results show that inventory charges, spent fuel credit (hence processing costs) and fabrication costs have an important effect on the fuelling cost. In addition, using highly rated thorium-based fuels will affect reactor capital costs. Further, more detailed studies of reactor design, fuel design and fuel management schemes are now required to verify the attraction of using thorium as a reactor fuel. (auth)

5115 (GA–4967) EXPERIMENTAL BERYLLIUM OXIDE REACTOR PROGRAM. Quarterly Progress Report for the Period Ending December 31, 1963. (General Atomic, San Diego, Calif. John Jay Hopkins Lab. for Pure and Applied Science). Jan. 29, 1964. Contract AT(04-3)-187. 46p. Dep. mn; CFSTI $2.00 cy, $0.75 mn.

Studies are reported of the effects of in-pile irradiation on BeO, BeO–MgO, BeO–MgO–Al_2O_3, and Dy_2O_3–Al_2O_3 at 1000 to 1600°F; BeO development for Experimental Beryllium Oxide Reactor (EBOR); in-pile radiation effects on EBOR fuels; EBOR development; and other topics related to the development of beryllium-oxide power reactors. (T.F.H.)

5116 (GA–5618) TARGET—A PROGRAM FOR A 1000-Mw(e) HIGH-TEMPERATURE GAS-COOLED REAC-

TOR. Quarterly Progress Report for the Period Ending August 31, 1964. (General Atomic, San Diego, Calif. John Jay Hopkins Lab. for Pure and Applied Science). Sept. 25, 1964. Contract AT(04-3)-167. 132p. Dep. mn; CFSTI $4.00 cy, $1.00 mn.

The preliminary design of the 1000-Mw(e) and the prototype plant is presented. Related research and development is reported in terms of advanced fuel development, turbocirculator development, fuel cycle development, alternate materials of construction, helium purification systems, and component development. (M.O.W.)

5117 (GA–5866) TARGET. A PROGRAM FOR A 1000-Mw(e) HIGH-TEMPERATURE GAS-COOLED REACTOR. Quarterly Progress Report for the Period Ending November 30, 1964. (General Atomic, San Diego, Calif. John Jay Hopkins Lab. for Pure and Applied Science). Dec. 31, 1964. Contract AT(04-3)-167. 139p. Dep. mn; CFSTI $4.00 cy, $1.00 mn.

Optimization programs were developed, and the fuel element development work progressed to the selection of the nonpurged packed-bed concept as the tentative reference design fuel elements. Irradiation and vibration tests of fuel elements were performed, as well as irradiation studies of carbon-coated fuel particles. Fission-product release and transport were stressed. Studies were made of fission product sorption and diffusion in graphite and of beryllium oxide-graphite compatibility. Preliminary investigations for the helium purification system were carried out including fission-product deposition and trapping studies and a study of hydrogen adsorption on activated carbon from high-pressure helium. Preliminary calculations of the gamma activities and the dose rates from ^{232}U daughter products in fuel were performed. Fuel cycle costs were analyzed, and methods for physics analyses were developed. A computer program for analyzing the prestressed concrete reactor structure was completed, and the liner for the first concrete model was tested. A theoretical investigation of thermal insulation for the TARGET prestressed concrete reactor structure was carried out. (D.C.W.)

5118 (GA–6647) 40-MW(E) PROTOTYPE HIGH-TEMPERATURE GAS-COOLED REACTOR POSTCONSTRUCTION RESEARCH AND DEVELOPMENT PROGRAM. Fifth Quarterly Progress Report for Period Ending July 31, 1965. (General Atomic, San Diego, Calif. John Jay Hopkins Lab. for Pure and Applied Science). Aug. 31, 1965. Contract AT(04-3)-314. 39p. Dep. mn; CFSTI $2.00 cy, $0.50 mn.

The analyses that were performed during the period are summarized, particularly those related to the continuation of zero-power testing. For tests at power, preliminary calculations were made to determine the character of the proposed rod scram transient tests. The techniques and instrumentation developed for measuring flux and power distributions are described, and the test procedures are summarized. (D.C.W.)

5119 (GA–6732) SAFETY CHARACTERISTICS OF LARGE GAS-COOLED FAST POWER REACTORS. Fortescue, Peter; Shanstrom, R.; Broido, J.; Stein, J. M.; Baxter, A.; Fenech, H. (General Atomic, San Diego, Calif. John Jay Hopkins Lab. for Pure and Applied Science). Oct. 8, 1965. Contract AT(04-3)-167. 81p. (CONF-651009–5). Dep. mn; CFSTI $3.00 cy, $0.75 mn.

From Conference on Safety, Fuels and Core Design in Large Fast Power Reactors, Argonne, Ill.

After a brief description of the reference design, analyses of the effects of coolant loss, introduction of water into the core, control-rod withdrawal, and fuel assembly insertion at cold critical are summarized, together with a stability analysis and maximum energy release studies. (D.C.W.)

5120 (GEAP–4799) SOUTHWEST EXPERIMENTAL FAST OXIDE REACTOR DEVELOPMENT PROGRAM. Third Quarterly Report, October 1964–January 1965. Horst, K. M. (ed.) (General Electric Co., San Jose, Calif. Atomic Power Equipment Dept.). Feb. 1965. Contract AT(04-3)-540. 150p. Dep. mn; CFSTI $4.00 cy, $1.00 mn.

Activities during the quarter are summarized dealing with planning of the experimental program, fuel development, development of instrumentation for the experimental program, mockup tests of the core assembly, development of equipment for inducing reactivity variations, development of fuel handling equipment and procedures, and core design. The reactivity effects of axial fuel expansion and sodium loss were calculated, and Doppler coefficients were compared for several design variations. (D.C.W.)

5121 (HIT–3459-11(Vol.1)) ANALYTICAL INVESTIGATION OF NUCLEAR AND THERMAL-HYDRAULIC DESIGN CHARACTERISTICS OF SM-1A, CORE 3. VOLUME I. (Hittman Associates, Inc., Baltimore, Md.). Mar. 1965. Contract AT(30-1)-3459. 80p. (HIT–161(Vol.1)). Dep. mn; CFSTI $3.00 cy, $0.75 mn.

The method and results of a detailed nuclear and thermal-hydraulic analysis of the SM-1A Core 3 are described. These two analyses were conducted in conjunction with each other to yield an overall evaluation of the design limitations of the core throughout life. The nuclear analysis is in good agreement with the as-built SM-1A Core 3 cold critical experiment; critical bank positions, bank-rod worth, excess reactivity, temperature defect, flux and power distributions are predicted within experimental error. The nuclear analysis applied to the hot operating condition and lifetime characteristics predicts an initial excess reactivity of 3.51% Δ k at 435°F, equilibrium xenon; a maximum reactivity after 12 Mw-Yrs of operation; a lifetime of $32\pm\frac{1}{2}$ Mw-Yrs; a capability of shutdown throughout life with any two rods withdrawn. The thermal-hydraulic analysis indicates that the core may be operated safely at 120 percent of its design power of 20.2 Mw(t) with the set points currently in use. Under these conditions, the minimum DNB ratio is 2.67, the maximum coolant enthalpy is 45 Btu/lb below saturation, and the pressure drop versus flow rate curve has a positive slope for each channel of every element. A brief study of operation at higher power levels was made. This study indicated that stable hydraulic conditions exist at 29 Mw(t), but that operation at still higher power levels may lead to hydraulic instabilities. The analysis at higher power levels did not consider all aspects and a more complete analysis would be required before any operation at power levels above 24.4 Mw(t), the 120 percent set point. (auth)

5122 (HIT–3459-11(Vol.2)) ANALYTICAL INVESTIGATION OF NUCLEAR AND THERMAL-HYDRAULIC DESIGN CHARACTERISTICS OF SM-1A, CORE 3. VOLUME II. (Hittman Associates, Inc., Baltimore, Md.). Mar. 1965. Contract AT(30-1)-3459. 112p. (HIT–161(Vol.2)). Dep. mn; CFSTI $4.00 cy, $0.75 mn.

The SM-1A core 3 is described in detail, and the techniques used in the nuclear physics and thermal-hydraulic analyses of the core are summarized, together with the results. The results of the nuclear physics analysis are compared with SM core measurements. (D.C.W.)

5123 (HPR–61) HBWR QUARTERLY PROGRESS REPORT, JANUARY TO MARCH 1965. (Institutt for Atomenergi, Halden (Norway). OECD Halden Reaktor Prosjekt). May 1965. 96p. Dep. mn.

Developments at the Halden Boiling Water Reactor are summarized. Information is included concerning operation, heavy water status, plant performance and plant engineering. Research efforts resulted in development of two macroscopic programs for solution of neutron diffusion equations using the Gier computer. In other work, a charge assembly with an estimated burnup of 4180 Mwd/t U was prepared for isotopic composition analysis. Developments in reactor fuel elements, test equipment and data handling equipment are summarized along with fuel irradiation work. (J.R.D.)

5124 (NYO–3250-4) TITLE I AND TITLE II: DESIGN AND ENGINEERING. Annual Report, July 1964–June

1965. (Connecticut Yankee Atomic Power Co., Haddam). Aug. 1965. Contract AT(30-1)-3250. 75p. Dep. mn; CFSTI $3.00 cy, $0.75 mn.

Commercial operation in October, 1967, at 490 megawatts electric is still the realistic project completion date. Design is progressing well. Approximately 80 percent of the work covered by the AEC design assistance contract is now complete. Slack time was consumed in many areas; however, no obstacle to the scheduled completion is foreseen. Developments during this period are reported. (auth)

5125 (NYO–10732) LIQUID FLUIDIZED BED REACTOR PROGRAM. Wise, Jules (New York Operations Office (AEC), N. Y.). Oct. 1964. 223p. Dep. mn; CFSTI $6.00 cy, $1.25 mn.

The planned scopes, and contractual arrangements for the various phases of work are presented. The work completed is summarized, and unresolved problem areas, as indicated by the results of the work performed, are discussed. Brief descriptions are presented of the work performed in the following areas: concept feasibility; development of abrasion resistant fuel; evaluation of alternative critical experiment concepts; critical experiment–description and experimental operation; economic evaluation and scope of operation for a reactor experiment. (auth)

5126 (ORNL–3870, pp 293–9) BONUS REACTOR SUPPORT PROGRAM. Cunningham, J. E. (Oak Ridge National Lab., Tenn.).

A superheater assembly that had failed prematurely in the Boiling Nuclear Superheat (BONUS) Reactor was examined in the hot cells to determine the nature and cause of failure. Two damaged Inconel-clad UO_2 fuel rods were found in the 32-rod assembly. One rod contained a 13-in.-long cladding rupture, while the other showed gross evidence of swelling. The cause of these failures was definitely traced to defective welding during fabrication. Improved welding techniques were devised and specifications modified to prevent failures of this nature from occurring in the future. (auth)

5127 (ORNL-P–1698) RESPONSE OF A HELIUM-COOLED FAST REACTOR TO CHANGES IN COOLANT FLOW AND REACTIVITY. Carlsmith, R. S.; Delene, J. G. (Oak Ridge National Lab., Tenn.). [1964]. Contract W-7405-eng-26. 24p. (CONF-651009–4). Dep. mn; CFSTI $1.00 cy, $0.50 mn.

From Conference on Safety, Fuels and Core Design in Large Fast Power Reactors, Argonne, Ill.

The ORNL design of a helium-cooled fast reactor was studied with respect to its response to various types of accident conditions. These accident conditions included step and ramp reactivity insertions and loss of coolant pressure and flow. The objective was to determine what kind of accidents this reactor could withstand before fuel melting began, without regard to questions of accident credibility. A Doppler coefficient, T dk/dT of -0.0053 and total helium loss coefficient of $+0.0051$ δk were calculated for this reactor. These coefficients proved adequate to prevent melting for a step reactivity addition of less than 29 cents, if no scram occurs, and a step change of $1.35 if a power-level scram occurs. For reasonable rates of coolant loss (half life in the vicinity of 20 sec), the reactor would not approach prompt criticality at any time during the transient. The ability of the reference reactor to remove delayed fission product heat in the event of two loss-of-coolant accidents was determined. (auth)

5128 (TID–22225) THE DESIGN AND EVALUATION OF A 1000 MW(e) CENTRAL STATION POWER-PLANT WITH A CIRCULATING FUEL GASEOUS CORE REACTOR. A Study Carried Out as Part of the First Graduate Nuclear Engineering Design Seminar, June 15–August 7, 1964. Arcella, F. G.; Foad, H. Y.; Habegger, L. J.; Hochreiter, L. E.; Nardi, A. J.; Prickett, W. Z. (Purdue Univ., Lafayette, Ind. Dept. of Nuclear Engineering). Contract AT(11-1)-1373. 304p. Dep. mn; CFSTI $7.00 cy, $1.50 mn.

The overall view of the plant including the circulating fuel gaseous core reactor is extensively discussed. The following analyses were performed; economic, nuclear, thermodynamic, chemical and materials, and structures and safety. Extensive results from these studies are presented. (M.O.W.)

5129 (TID–22328) 237 MW KRB NUCLEAR POWER PLANT. Quarterly Report No. 8, January 1–March 31, 1965. (Kernkraftwerk RWE-Rayerwerk G.m.b.H., Gundremmingen (West Germany)). 136p. (KRB–1965/1). Dep. mn; CFSTI $4.00 cy, $1.00 mn.

Development progress made during the period Jan. through March 1965 is reported. Construction progress, preliminary tests, diagrammatical representation of construction status, status of total project, work schedule, personnel employed on site, photographs, financing, and contracts awarded are summarized. (M.O.W.)

5130 (TID–22355) HALLAM NUCLEAR POWER FACILITY MONTHLY OPERATING REPORT NO. 37, AUGUST 1965. (Consumers Public Power District, Hallam, Nebr.). Contract AT(11-1)-513. 29p. Dep. mn; CFSTI $2.00 cy, $0.50 mn.

The reactor remained shutdown for the moderator replacement program. Significant operating activities during the month are summarized, together with plant performance through the month. Water was observed in the four fuel storage thimbles; an attempt was made to determine the source of the water. During the moderator element examination program, it was noted that one element failed due to a mechanical gouge in the skin. An attempt was made to determine the cause of the gouge. (D.C.W.)

5131 (UNC–5135) PERFORMANCE EVALUATION OF HEAT EXCHANGERS FOR SODIUM-COOLED REACTORS. Quarterly Technical Progress Report, July 1–September 30, 1965. Dischinger, R. H. (United Nuclear Corp., White Plains, N. Y. Development Div.). Oct. 20, 1965. Contract AT(11-1)-1452. 47p. Dep. mn; CFSTI $2.00 cy, $0.50 mn.

Reports, drawings, and other documents relating to the design, manufacture, and test of the heat exchangers were reviewed. Knowledge of the installation and instrumentation of these exchangers in the Sodium Components Test Installation was acquired from reports, drawings, and discussions with the test operator, Atomics International. Methods were established for transmitting and processing the test data. Procedures were prepared to derive actual performance from the test data and to calculate predicted performance consistent with the test conditions and in accordance with the component designer's methods and assumptions. Formats were developed for comparison of predicted and observed performance. Several inconsistencies found in the heat exchanger design reports were resolved. (auth)

5132 (WAPD-MRP–113) PRESSURIZED WATER REACTOR PROJECT. Technical Progress Report, April 24, 1965–July 23, 1965. (Bettis Atomic Power Lab., Pittsburgh, Pa.). Contract AT-11-1-GEN-14. 120p. Dep. mn; CFSTI $2.50 cy, $0.75 mn.

Prior to initial power operation, core thermocouples were calibrated and reactor flow distribution was measured, with the results showing that the thermocouples were in general within the anticipated range and that the flow distribution confirmed predictions within the accuracy of the measurements. During initial power operation, the data taken by means of the core thermocouples showed cluster coolant temperature rises in agreement with prediction, and that no significant radial power asymmetry was present in the core. A data reduction code has been placed in operation to process data obtained during PWR Core 2 Seed 1 operation. Evaluation of core inlet water temperatures has shown that the effect of gamma heating in the reactor components upstream of the core cannot be detected. PWR-2 Seed 2 fuel test plates in the MTR VH3 loop continue to exhibit normal irradiation behavior. However, a grossly bulged compartment was observed in plate BETT 63-119 during a regularly scheduled examination of

the X-3-0 test elements. No cladding rupture occurred. Radiochemical analyses showed that the bulge occurred at 15.3×10^{20} fissions/cc maximum exposure. Fission gas release values ranged from 6.5 to 7.4% for all compartments, respectively. Metallographic examination revealed, as expected, grossly overheated fuel in the bulged compartment. No fuel or cladding abnormalities were observed in the remaining compartments. Poison elements containing end hooks that are reference design in rod support plates of Seed 2 clusters have been irradiated to full depletion of ^{10}B atoms in a proof test. Modest dimensional changes in both defected and non-defected plates were noted, and gas release values are less than 0.3%. The most highly depleted MCO plate was removed because of gross bulging after reaching a burnup of 75×10^{20} fissions/cc (compartment). Additional examinations of Core 1 components have been completed with all data confirming anticipated performance. The re-analysis of PWR Core 1, Seeds 1 and 2, using TNT02 synthesis, has been completed and calculations have been completed to obtain the materials composition of the blanket fuel rods removed after each of these seed lives. In general, the results show improvement over previous calculations. The hot, clean, beginning-of-life physics tests for PWR Core 2 Seed 1 were completed during this report period. Power operation commenced on May 1, 1965. Results of physics tests conducted during power operation until the present time (~1050 EFPH) are reported herein. In general, Core 2 is performing in a satisfactory manner consistent with design calculations. There has been a small deviation in core activity relative to the calculations. This deviation appears to have reached a constant value so that at about 1000 EFPH the reactivity difference is about 0.5% $\Delta\rho$. Additional seed fuel zoning studies were completed for Seed 2 of Core 2. These consisted of a minor revision to the fuel zoning arrangement in each subassembly in order to provide additional thermal capability at end-of-life. (auth)

5133 (WAPD-PWR-TE-151) EVALUATION OF CORE THERMAL AND HYDRAULIC DATA OBTAINED DURING THE OPERATION OF PWR CORE-1 WITH THE FOURTH SEED (DLCS-33801, DLCS-18201, DLCS-24301, DLCS-36201), JANUARY 1963–FEBRUARY 1964. Smeltzer, P. (Bettis Atomic Power Lab., West Mifflin, Pa.). Dec. 1964. Contract AT(11-1)-Gen-14. 105p. Dep. mn; CFSTI $4.00 cy, $0.75 mn.

An evaluation of data obtained from four tests performed during the operation of PWR Core 1 with the fourth seed installed is presented. The four tests were: periodic intercalibration of temperature sensing elements, calibration of core flow instrumentation, flow distribution across the core, and reactivity lifetime test. The results of the intercalibration of the core temperature sensing elements indicate an appreciable short-term shift occurred in the readout error of the thermocouple monitoring system early in seed life. The July, 1963 correction factors that compensate for the exit water temperature readout error were found to be approximately 2°F lower than those obtained from the January, 1963 calibration data. The third calibration test performed in November, 1963, at 500°F, resulted in an increase of approximately 1°F in the correction factors at the 500°F level. Nine transmitters of the core flow instrumentation train were calibrated in January of 1963. As-found data were obtained for six of the differential pressure cells indicating that the six cells were not within the acceptable limits of ±1.25 percent of full scale. Five cells monitoring flow at F-4, J-12, L-8, H-8, and H-9 were recalibrated successfully. Four cells monitoring the flow at G-11, I-5, D-8, and H-7 were calibrated but were outside the limits at the sixty percent flow level. The inability to calibrate the four D/P cells was ascribed to non-linearities in the range spring and bellows assembly. Adjustment at the D/P cell coil and the Data Acquisition System could not totally compensate for the non-linear characteristics. Reference curves were established to aid in the accurate determination of flow. The core flow distribution test was performed in January, 1963 with four main coolant pumps operating at fast speed and with the reactor coolant temperature and pressure stabilized at 500°F and 1785 psig respectively. The calibrated instrumentation monitoring the seed region flow indicated clusters F-4 and J-12 had flow rates that were within two percent of the design value for the region. Clusters D-8 and L-8 had low flow indications; however, it was concluded from an evaluation of the thermal data and calibration history that adequate flow was also present at the latter two locations. The flow to the blanket fuel assemblies, including the special test assemblies located in the central portion of the core, was found to be within acceptable limits. The evaluation of the data obtained during the reactivity lifetime test includes a brief discussion of the power correction factors derived from the specially instrumented seed clusters F-4 and D-8. The reactivity lifetime test data shows the trend in the power history curves of the seed assemblies to have been in reasonable agreement with those obtained from the TNT calculations. The major differences between the calculated and experimental measurements of power in the seed region were assignable to instrumentation location and the consequent inability to accurately measure the assembly average coolant temperature. (auth)

5134 (WCAP-3269-12) LARGE CLOSED-CYCLE WATER REACTOR RESEARCH AND DEVELOPMENT PROGRAM. Progress Report, January 1–March 31, 1965. (Westinghouse Electric Corp., Pittsburgh, Pa. Atomic Power Div.). Contract AT(30-1)-3269. 90p. Dep. mn; CFSTI $3.00 cy, $0.75 mn.

Discussions and results are presented on the following areas of the large closed-cycle water reactor research and development program; light water physics methods development, local power distributions, instrumentation systems, mechanical and physical properties of Zircaloy, hydriding studies of Zircaloy fuel element cladding, fabrication of advanced RCC fuel assembly, biaxial strain fatigue of cladding materials, stress corrosion of fuel element cladding, irradiation proof testing of advanced fuel assembly prototypes, irradiation testing of advanced fuel assembly with improved grids, fuel swelling studies, development of advanced fuel assembly, advanced RCC canless fuel assembly design, reactor evaluation channel operation and special equipment maintenance, out-of-pile corrosion testing, in-pile chemistry testing, chemical studies of soluble neutron poisons, chemical shim experiments, system stability and control studies, and reactor hazards analysis. (M.O.W.)

5135 (WCAP-3269-40) AN EXPERIMENTAL EVALUATION OF THE POWER COEFFICIENT IN SLIGHTLY ENRICHED PWR CORES. Sha, W. T. (Westinghouse Electric Corp., Pittsburgh, Pa. Atomic Power Div.). Apr. 1965. Contract AT(30-1)-3269. 46p. Dep. mn; CFSTI $2.00 cy, $0.50 mn.

A correlation of the effective fuel pellet (UO_2) temperature (T_{eff}) for the Doppler broadening of U-238 resonance which is based on the experimental power coefficient data from Yankee, Saxton, BR-3, and Selni is presented. The correlation can predict the total power defect of reactivity from hot zero power to full power within experimental uncertainties and T_{eff} at any power level within ±80°F, a magnitude which constitutes no more than ±6% of the value at full power for current PWR design. With the ±80°F uncertainty in T_{eff}, the power coefficient of reactivity can vary as much as ±30% in the low power region and ±20% in the high power region. This study indicates the temperature drop in the gap between the pellet and clad to be much lower than the value calculated for it in the past. (auth)

5136 (WCAP-5554) REMOTE UNDERWATER DEVICES FOR THE EVALUATION AND REDUCTION OF SPENT YANKEE FUEL ASSEMBLIES. Kitzes, Arnold S.; Miner, Daniel; Santavy, John A. (Westinghouse Electric Corp., Pittsburgh, Pa. Atomic Power Div.). June 1965. Contract AT(30-1)-3017. 4p. (CONF-651101-1). Dep. mn; CFSTI $1.00 cy, $0.50 mn.

From 13th Conference on Remote Systems Technology, Washington, D. C.

A brief discussion is presented on the development of devices used in determining the dimensional stability of entire fuel assemblies and the removal of individual fuel rods for the evaluation and reduction of spent Yankee fuel assemblies. (M.O.W.)

5137 (JPRS-31193) THE BN-350 ATOMIC POWER STATION. Lepunskii, A. I. Translated from pp 1-30 of Atomnaya Stantsiya BN-350, April 1965. 29p. (TT-65-31690). CFSTI $2.00 cy, $0.50 mn.

The sodium-cooled, 1000-Mwt fast power reactor is described as well as the analyses and tests on which it is based. (D.C.W.)

5138 THE MZFR NUCLEAR POWER STATION WITH A MULTI-PURPOSE REACTOR. Sauerwald, Karl J. (Siemens-Schuckertwerke AG, Erlangen, Ger.). At. Strom., 11: 106-15(Sept.-Oct. 1965). (In German).

The MZFR nuclear station with an electrical output of 57 Mw is the prototype of the D_2O natural uranium line which has been developed by the Siemens-Schuckert company. So that the wide requirements for test facilities under reactor conditions could be met besides the generation of power, the reactor was fitted with additional devices which convert it into an efficient test reactor without limiting the operation as a power generator. (auth)

5139 FIRST PRACTICAL EXPERIENCE ON THE CONSTRUCTION OF THE 252 MW NUCLEAR POWER STATION AT LINGEN. Deublein, Otmar (Kernkraftwerks Lingen GmbH, Dortmund, Ger.); Schmoczer, Ruediger. At. Strom, 11: 116-20(Sept.-Oct. 1965). (In German).

A description is given of the location, construction, and basic circuit of the power station, the preparation of the site and the commencement of the civil engineering work. Finally an account is given of the procedure for legal approval from the atomic and hydraulic points of view. (auth)

5140 ECONOMIC VIEW POINTS ON THE MEASUREMENT AND CONTROL TECHNOLOGY IN NUCLEAR POWER PLANTS. Merz, L. (Technische Hochschule, Munich). Atomwirtschaft, 10: 500-1(Oct. 1965). (In German).

In addition to the need to use good control engineering properties to maintain the net frequency, economic viewpoints are also valid. The task of automatic control systems is therefore to make possible a contribution to the maintenence of the net frequency in addition to its base load operation. In addition to safeguarding the security of the reactor, the safety system in the future must prevent unwarranted shutdowns for economic reasons. The automatic operation can increase the utility of the installation. (J.S.R.)

5141 PRESENT STATE AND FUTURE DEVELOPMENTS OF MEASUREMENT TECHNOLOGY IN NUCLEAR POWER PLANTS. Costantin, P. (AEG Allgemeine Elektricitaets-Gesellschaft, Frankfurt am Main). Atomwirtschaft, 10: 506-10(Oct. 1965). (In German).

The high requirements placed on instrumentation by power reactors has lead to considerable advances in reactor measurement techniques. The developments trends include complete transistorization of the electronic devices, transmitters with uniform output for nuclear physical measurement magnitudes, improvement of nuclear measurement methods, fail-safe reactor protection systems with a semiconductor basis, process operation and automation using program-controlling digital computers, and reduced observation in connection with low-current control. (tr-auth)

5142 STEAM GENERATING HEAVY WATER REACTOR. Engineer, 220: 122-3(July 23, 1965).

The Steam Generating Heavy Water Reactor (SGHWR) being built at Winfrith, the first water-moderated power reactor projected by the U.K. Atomic Energy Authority, is described and illustrated. It has a nominal design power output of 100 Mw(e) and is intended as a prototype capable of yielding design and operating experience relevant to a large commercial station. The fuel is UO_2 contained in pressure tubes cooled by light water and moderated by heavy water in a cylindrical tank surrounding the pressure tubes. The reactor is due to be completed in 1967. Advantages of the SGHWR system are enumerated. The reactor core consists of a bank of pressure tubes which pass through vertical tubes in a cylindrical tank containing the heavy water moderator. Fuel is contained in the pressure tubes and the heat generated is removed by light water passing up these tubes and being partially vaporized. Fuel elements for the boiling channels are 36 rod clusters, with each rod 12 ft long (the full length of the core). The elements are canned in zirconium alloy. The fuel clusters can be loaded and discharged with the reactor on-load. Detailed specifications of the reactor are given. Fabrication of the tank surrounding the pressure tubes is described in detail. (TCO)

5143 THE CHANGING PATTERN OF PROBLEMS IN THE USE OF HEAVY WATER IN NUCLEAR REACTORS. Dolle, Lucien (CEN, Saclay, France). Ind. At., 9: No. 7-8, 57-69(1965). (In French).

The physico-chemical behavior of heavy water in nuclear reactors is closely linked with the effects of ionizing rays and with any possible interaction with the containing walls. Its isotopic purity is responsible for its fine moderating qualities. Experience with heavy-water reactors has made it possible to understand this behavior and its connection with a certain number of incidents that took place during operations. The advent of heavy-water powered reactors, expected shortly, does, on the one hand, benefit from the knowledge so far obtained, but it also raises fresh problems. The most important one is that of controlling the reactivity by soluble poisons, for this brings in simultaneously all the phenomena taking place in the moderator under the effect of the resulting chemical pollution. (auth)

5144 THE HEAVY-WATER REACTOR TANK EL-4. Peuchmaur, Alphonse (Societe Indatom, Paris). Ind. At., 9: No. 7-8, 71-4(1965). (In French).

The tank of the EL-4 reactor, which is described, has a very important part in the structure of the reactor. This tank, located inside of concrete shielding, receives the heavy water and supports the fuel cans. It is also the point of convergence for the control rods, for the tubes for feeding the gas coolant, and for the pipes containing the heavy water. It is surrounded by insulation, which reduces the heat flux on the concrete to an acceptable value. The geometry, materials, temperature, and pressure are given for this tank. The various studies and tests carried out are described. The construction of the tank is also described. (J.F.P.)

5145 DIMENSIONING OF THE OVERPRESSURE DISCHARGE SYSTEM OF THE PRO REACTOR MODERATED AND COOLED BY ORGANIC LIQUID. Merli, E. (CNEN, Rome). Ing. Nucl., 6: 135-52(May-June 1965). (In Italian).

The pressure transition caused by an incident in the heat exchanger with inlet of water into the primary circuit is examined. The dimensions of the apparatus constituting the discharge system for the overpressure are determined. (tr-auth)

5146 APPLICATION OF THE PRESSURE-SUPPRESSION SYSTEM FOR CONTAINMENTS IN NUCLEAR POWER PLANTS. Roemer, W. (Technische Ueberwachungsvereins Bayern e.V., Munich). Kerntechnik, 7: 330-2(July 1965). (In German).

The rapid increase of power output of boiling and pressurized water reactors makes it necessary due to constructural problems and costs, to look for new methods in designing of containments. The pressure suppression system of the Humboldt Bay Reactor and the experiments to develop this system are described. The basic concept of design of a full power containment is shown to see the tendency of development. (auth)

5147 ENGINEERING PROBLEMS OF POWER REACTOR FUEL. II. LIGHT-WATER REACTOR FUEL. Imai, Ryukichi (Japan Atomic Power Co., Tokyo). Nippon Genshiryoku Gakkaishi., 7: 579-85(1965).

The engineering implications of power reactor fuel problems, based investigations on light-water reactor fuel technology for the Tsuruga Power Station, are considered. The reliability of available basic UO_2 data, Zircaloy corrosion and hydrogen pickup, fabrication cost considerations in design optimization, mechanical design including vibration problems, fretting corrosion due to spacer design, burnout considerations, and various modes of possible fuel failure are discussed. (auth)

5148 HINKLEY POINT NUCLEAR POWER STATION. ENGINEERING PROBLEMS ASSOCIATED WITH THE CONSTRUCTION OF CURRENT NUCLEAR POWER STATIONS. Reed, D. (English Electric Co., Ltd., Whetstone, Eng.). Nucl. Energy, 272-83(Sept. 1965).

The design and development of the Hinkley Point Power Station are discussed. The station has an output of 500 Mw(e) from two reactors of the graphite-moderated, gas-cooled type, fueled with natural uranium. Topics discussed include the choice of site, the program of construction, civil engineering problems, including the reactor foundations, biological shield, turbine house, cooling water system, and concrete control. The pressure vessel is discussed including the choice of material, inspection of material, welding procedures, fabrication, welding inspection, erection, stress relief, and pressure testing. The steam raising units, gas ducts, reactor core, pile cap, fueling machinery, discharge of fuel, testing, fueling and commissioning are also discussed. (J.F.P.)

5149 PERSPECTIVES OF ATOMIC HEAT AND POWER PLANTS. Gorshkov, A. S.; Loginov, A. A.; Sokolov, E. Ya. Teploenergetika, No. 9, 44-7(Sept. 1965). (In Russian).

Because of the wide development of central power stations where both heat and electricity are produced it is necessary that nuclear power stations produce heat in order to make a significant contribution to the overall fuel-energy balance. At present electric energy comprises only 15% of the total energy needs. This figure will rise to 25% in the future. The deficit of organic fuels is rising in the European part of Russia, and this unbalance can be corrected with the proper use of nuclear fuel. A uranium-graphite reactor can supply steam at 130 atm and 565°C, which can be used to produce both hot water for heating purposes and electricity in units of 50,000 to 100,000 kilowatts. Nuclear reactors can also economically produce potable water by distillation at a reactor power of 2,000,000 kilowatts with the simultaneous production of electricity. Thus, a reactor can be designed with an electrical power of 840,000 kw to give 16,000 m^3/hr of distilled water. Reactors producing heat and electricity, or electricity and distilled water have a promising outlook. (TTT)

5150 ELEVENTH ANNUAL REPORT FOR THE PERIOD, 1st APRIL, 1964–31st MARCH, 1965. London, Her Majesty's Stationery Office, 1965. 110p. 8 shillings.

A general survey is given of the second nuclear power program in the United Kingdom. Topics considered include finance, accounts, and contracts, production plants and commercial activities, the reactor development program, research on reactor systems, general research and development, plasma physics, and fusion research. Other topics are nuclear weapons and test detection, isotope production and research, relations with industry and universities, health and safety, information services, and international relations. (J.F.P.)

5151 FACT BOOK ON U. S. NUCLEAR POWER PROJECTS. Seventh Edition. New York; Washington, D. C., Electric Companies Public Information Program, 1965. 92p.

A collection of background information is presented on the development of nuclear electric power in the United States and of fact sheets on all United States nuclear power projects. This is a complete revision of the fact sheets first published in December 1958, and revised annually since then. The data were checked with the organizations involved. Topics covered include pressurized-water, boiling-water, sodium-cooled, organic-cooled, and gas-cooled reactors. Nuclear power development, non-investor-owned utilities, electric company participation in this development, electric industry development, research and study projects, and reactor classification are also discussed. (J.F.P.)

5152 ATOM, 1965. An Illustrated Summary of the Eleventh Annual Report, 1st April 1964 to 31st March 1965, London, Her Majesty's Stationery Office, 1965. 38p. 2s. 6d.

The second nuclear power program in the United Kingdom is surveyed. This general review includes the assessment of various reactors, collaboration with industry and universities, reactor fuel development, isotope research, and health and safety. (J.F.P.)

5153 OPERATIONAL EXPERIENCE IN THE DOUNREAY BETA-GAMMA HOT CELLS. Edmonds, E. (United Kingdom Atomic Energy Authority, Caithness, Scotland). pp 857-68 of International Symposium on Working Methods in High Activity Hot Laboratories. Vol. II. Paris, Organization for Economic Cooperation and Development, 1965.

The high-activity beta-gamma facility at Dounreay is described. The major role of the cells was to provide a rapid feed back of information to the reactor operators on the behavior and conditions of fuel elements in the Dounreay Fast Reactor. Many modifications were made in the light of experience gained during operation and some of these are described. Cell decontamination, contamination control, and specific rig handling problems are also discussed. (auth)

5154 ANGLO-SPANISH NUCLEAR POWER SYMPOSIUM, PROCEEDINGS, MADRID, NOVEMBER, 1964. ENGLISH EDITION. VOL. 1. [Risley, Eng., United Kingdom Atomic Energy Authority, 1965]. 160p. (CONF-641125 (Vol.1)).

Nine papers are included; separate abstracts are prepared for each. (L.B.S.)

For abstracts of individual papers see: 4081, 5027, 5094, and 5155–5160.

5155 NUCLEAR DEVELOPMENT IN THE U. K. Stewart, J. C. C. Paper No. 1 of Anglo-Spanish Nuclear Power Symposium. Vol. 1. [Risley, Eng., United Kingdom Atomic Energy Authority, 1965]. 9p.

Summaries are presented on the development of gas-cooled graphite-moderated reactors with natural uranium magnox-clad fuel elements and with uranium dioxide stainless-steel clad fuel elements, the second British nuclear power program for construction of stations of 5000 Mw nuclear generating capacity for commissioning during 1970 to 1975, the fast reactor program, and other reactor developments in the field of water-moderated reactors, plutonium-fuel fast reactors and nuclear desalination. (L.B.S.)

5156 LATEST OPERATING EXPERIENCE OF MAGNOX STATIONS. Fair, D. R. R.; Murfitt, R. H. Paper No. 2 of Anglo-Spanish Nuclear Power Symposium. Vol. 1. [Risley, Eng., United Kingdom Atomic Energy Authority, 1965]. 13p.

A brief description is given of the Berkeley and Bradwell commercial nuclear power stations; the general parameters of the two stations are tabulated along with corresponding data for Calder Hall and Oldbury. The commissioning procedures, staffing and training requirements, and performance during the first two years to June 1964 of Bradwell and Berkeley are summarized. A brief discussion is also presented on operating experience, including on-load refueling, operational convenience, and reactor incidents. (L.B.S.)

5157 THE CURRENT AND FUTURE DEVELOPMENT OF THE MAGNOX REACTOR. Vaughan, R. D.; Joss, J. O. Paper No. 4 of Anglo-Spanish Nuclear Power Symposium. Vol. 1. [Risley, Eng., United Kingdom Atomic Energy Authority, 1965]. 15p.

The effects of extending reactor operating parameters, improvements in engineering design, and increasing reactor size on the economics of the natural-uranium magnox reactor of the Oldbury type are discussed. A comparison is made of reactor dimensions for the Oldbury 300 Mw design and for an advanced 500 Mw design, which shows where the largest gains are expected. (L.B.S.)

5158 PROBLEMS IN THE INTRODUCTION OF NUCLEAR POWER STATIONS IN SPAIN. Antonanzas, J. L.; Bosch, F.; Fustel, E. Paper No. 6 of Anglo-Spanish Nuclear Power Symposium. Vol. 1. [Risley, Eng., United Kingdom Atomic Energy Authority, 1965]. 18p.

A general analysis is given of the most important problems involved in the introduction of nuclear power stations in Spain on nuclear fuels, economics, design and construction, operation, safety and legislation, and public relations. Consideration is given to the need for the incorporation of nuclear energy into the traditional means of production of electric energy. (L.B.S.)

5159 THE ADVANTAGES OF THE MAGNOX REACTOR TO SPANISH INDUSTRY AND ECONOMY. Ghalib, S. A. Paper No. 7 of Anglo-Spanish Nuclear Power Symposium. Vol. 1. [Risley, Eng., United Kingdom Atomic Energy Authority, 1965]. 8p.

Considerations are made on the past and present uranium fuel supply and the power demand in the U.K. The availability of fuel in Spain and considerations of the electricity supply industry are briefly discussed. A comparison is made of the economics of water and gas-cooled reactors, and tables are presented to illustrate the bases of economic evaluation 300 Mw(e), generation costs, and foreign currency expenditure assuming toll enrichment. The advantages of adopting the natural-uranium gas-cooled reactor are summarized. (L.B.S.)

5160 THE SELECTION OF THE TYPE OF REACTOR AND INFLUENCE THEREOF IN THE SPANISH ECONOMIC AND SOCIAL DEVELOPMENT PLAN. Saiz de Bustamente, A. Paper No. 8 of Anglo-Spanish Nuclear Power Symposium. Vol. 1. [Risley, Eng., United Kingdom Atomic Energy Authority, 1965]. 7p.

Three 300 Mw(e) nuclear power plants are envisaged in the Spanish economic and social development plan. The influence of the selection of the nuclear reactor on the overall economy of the country and the degree of participation of Spanish industry in the construction are considered. The main components of a nuclear power plant with a magnox reactor are listed showing the corresponding percentage of Spanish manufacture. (L.B.S.)

5161 ANGLO-SPANISH NUCLEAR POWER SYMPOSIUM, PROCEEDINGS, MADRID, NOVEMBER 1964. ENGLISH EDITION. VOL. 2. [Risley, Eng., United Kingdom Atomic Energy Authority, 1965]. 155p. (CONF-641125(Vol.2)).

Five papers are included; a separate abstract has been prepared for each. (L.B.S.)

For abstracts of individual papers see: 5162–5165, and 5207.

5162 THE DON PROJECT. Pascaul Martinez, F. Paper No. 10 of Anglo-Spanish Nuclear Power Symposium. Vol. 2. [Risley, Eng., United Kingdom Atomic Energy Authority, 1965]. 12p.

The major design parameters of the 30 Mw(e) prototype DON heavy-water moderated, organic-cooled, natural-uranium fueled reactor are tabulated. Brief descriptions are given of the reactor complex, fuel elements, control rods and drives, process systems, instrumentation and control and nuclear characteristics. The main areas covered by the research and development program aimed at clarifying specific problems of the reactor are discussed. (L.B.S.)

5163 THE STEAM GENERATING HEAVY WATER REACTOR. Moore, R. V.; Firth, A. Paper No. 11 of Anglo-Spanish Nuclear Power Symposium. Vol. 2. [Risley, Eng., United Kingdom Atomic Energy Authority, 1965]. 19p.

The general characteristics are given of the steam-generating heavy-water reactor under study in Britain with a 100 Mw(e) prototype reactor. The reasons for the choice of the heavy water system are discussed. Descriptions are given of the size, program, and state of construction, main design features, primary circuit, fuel element assembly, fuel handling, reactivity control, nuclear design, thermal performance, and engineering and development of the prototype reactor. The main parameters are tabulated and diagrams are included. (L.B.S.)

5164 ADVANCED GAS-COOLED REACTORS. Moore, R. V.; Thorn, J. D. Paper No. 12 of Anglo-Spanish Nuclear Power Symposium. Vol. 2. [Risley, Eng., United Kingdom Atomic Energy Authority, 1965]. 19p.

The development of the advanced gas-cooled reactor toward a commercial power reactor is considered from the standpoint of four areas: the direct experience of operating the Windscale AGR; the accumulation of graphite irradiation data over the ranges of irradiation dose, pressures, and temperatures of interest in AGR's; the development and proving of a fuel element that will give low fuel costs; and extent to which capital and generating costs can be reduced by the designer with the use of high temperature fuel elements. (L.B.S.)

5165 FAST REACTOR DEVELOPMENT. Kronberger, H.; Frame, A. G. Paper No. 13 of Anglo-Spanish Nuclear Power Symposium. Vol. 2. [Risley, Eng., United Kingdom Atomic Energy Authority, 1965]. 17p.

A brief introduction is given on the physics of fast and thermal reactors. The main parameters and the principal features of the Dounreay fast reactor are given. A description is given of the main aspects of the development program for a prototype power reactor which include core and fuel design, physics problems, engineering aspects, and control and safety. (L.B.S.)

5166 ATOMIC POWER: A REVIEW. Papers Presented at the Symposium held at the University of New South Wales on November 7, 1963. Kensington, N. S. W., Univ. of New South Wales [1964]. 110p. 1 pound. (CONF-631109).

The conference included 8 complete papers. Separate abstracts were prepared for 5 papers. One of the papers previously appeared in NSA as 19: 653. The two papers not abstracted are summarized as follows: "The Role of the Nuclear Engineer" presents a summary of nuclear engineering qualifications and problems. "Radioisotopes" presents general comments on advances since 1954 in the study of the formation, measurement, and uses of radioisotopes. (J.F.P.)

For abstracts of individual papers see: 4069, 4270, 4313, 5167, and 5168.

5167 TEN YEARS OF NUCLEAR PROGRESS: A SURVEY. Baxter, J. P. (Univ. of New South Wales, Kensington). pp 11-17 of Atomic Power: A Review. Kensington, N. S. W., Univ. of New South Wales [1964].

The rapid progress of nuclear development is surveyed. Progress in nuclear power is discussed generally, and the progress in several countries is mentioned. A list is given of world nuclear power stations. Progress in international cooperation is discussed especially that resulting from the work of the International Atomic Energy Agency; its goals and history are given. Future progress is considered. This includes ship propulsion, nuclear explosives for excavation, desalination, and also the use of radioisotopes. The progress of the nuclear growth in Australia is also considered. (J.F.P.)

5168 NUCLEAR POWER STATIONS—TYPES AND ECONOMICS. Griffiths, D. R. (Australian Atomic Energy Commission). pp 39-56 of Atomic Power: A Review. Kensington, N. S. W., Univ. of New South Wales [1964].

A discussion is given of the developed systems for nuclear power which show promise of producing economic power; variations and possible lines for future development are also considered. These reactor types are graphite moderated and gas-cooled, light water moderated and cooled, heavy water moderated, sodium cooled systems, and fast breeder reactors. The economics of reactors is considered. It is noted that there is a downward trend in costs with development. It is also noted that no two stations of the same design are yet built; and design changes account for a significant part of the total cost. (J.F.P.)

5169 IMPROVEMENTS IN OR RELATING TO NUCLEAR POWER PLANT. Taylor, Anthony James; Walker, Alexander (to Babcock and Wilcox Ltd.). British Patent 1,008,712. Nov. 3, 1965. Filed Dec. 20, 1961.

A vapor generator and a circulator for circulating coolant in a closed circuit are disposed in series within the pressure vessel or an extension of the pressure vessel of a nuclear power plant. A section of the heat exchange surface is included within the pressure vessel, and the coolant is led from the circulator past the section to the coolant entry side of the section through at least one space between the inner surface of the pressure vessel and partitioning of the section where the section is widely spaced from the pressure vessel. A valve for the control of coolant flow is also disposed within the pressure vessel. (B.L.M.)

5170 IMPROVEMENTS IN NUCLEAR REACTOR HEAT GENERATING AND UTILIZING PLANT. Taylor, Anthony James (to Babcock and Wilcox Ltd.). British Patent 1,008,713. Nov. 3, 1965. Filed Dec. 23, 1960.

A regulating means for a heat generating and utilizing plant of the kind having a gas cooled reactor and means for circulating the coolant under super-atmospheric pressure through the reactor and through a pressure vessel containing the heat exchanger is described. The regulating means regulates the coolant temperature at the inlet to the reactor and includes a by-pass means extending through a central space between parts of the heat exchange means or through a respective central space between parts of the heat exchange means in relation to which the coolant is to be bypassed. (B.L.M.)

5171 NUCLEAR POWER SYSTEM. Acklin, Leo (to Sulzer Freres, Societe Anonyme). U. S. Patent 3,210,943. Oct. 12, 1965. Priority date Aug. 19, 1960, Switzerland.

In a steam power plant having a nuclear reactor as a source of heat, two boilers are provided. The pressure in the first boiler is maintained at a higher value than in the second boiler. A steam channel extends in heat exchange relation with the source, with the first and second boilers successively and then ultimately to a load. Steam from the high pressure boiler is expanded to the pressure of the lower-pressured boiler, and the energy from the steam is recovered. The expanded steam and the steam from the lower-pressured boiler is then delivered to the channel upstream of at least two passages of the channel in heat exchange of the source. (B.L.M.)

5172 BOILING WATER NUCLEAR REACTOR OPERATING WITH PRIMARY AND SECONDARY COOLANT. Hackney, Stanley (to United Kingdom Atomic Energy Authority). U. S. Patent 3,212,985. Oct. 19, 1965. Priority date July 15, 1960, Great Britain.

A reactor operating with primary and secondary coolant includes fuel elements housed in fuel tubes, a liquid neutron-moderating primary coolant within the fuel tubes, and a secondary coolant passing outside the fuel tubes in heat transfer relationship through the tubes with the primary coolant in the tubes. An unfueled extension tube is connected in series with each fuel tube, and the extension tubes are exposed to the secondary coolant for heat transfer from the primary coolant to the secondary coolant. Preferably the reactor uses water coolants, the primary coolant being pressurized water and the secondary coolant being boiling water. (B.L.M.)

Process Heat Reactors

Refer also to abstract 3916.

5173 (ORNL–3870, pp 191-3) DESALINATION. Douglas, D. A. Jr. (Oak Ridge National Lab., Tenn.).

Efforts were divided into three general categories: calculating fuel fabrication costs, developing fabrication processes for thin titanium tubing for evaporator-condensors, and evaluating fuel performance. Computer codes for fuel fabrication costs were extended to include the coextrusion of Zircaloy cladding with thorium, thorium–uranium alloy, or uranium. Metal fuel performance was surveyed to help define applications of metal fuels for large desalination reactors. Methods of producing fluted titanium tubing by roll forming, tube drawing, isostatic pressing, high-energy-rate forming, and press forming were evaluated. (auth)

Production Reactors

5174 (ORNL–3870, pp 214-29) HIGH FLUX ISOTOPE REACTOR. Adamson, G. M. Jr. (Oak Ridge National Lab., Tenn.).

Fuel elements for the reactor startup and prototypes for nonnuclear testing were successfully produced. With only minor exceptions, all elements conformed with the proposed specifications. The plate spacing for the reactor elements was held within ±3 mils for the average channel cross section and within ±6 mils for any individual spot, both of which are only about half of the permitted variations. Machining and welding techniques were developed and shown to be capable of the extremely close dimensional tolerances required. More difficulty than had been previously experienced was encountered with dimensional variations, homogeneity, and nonbond on the reactor element. These problems were not inherent in the technique but resulted principally from excessive moisture in the aluminum powder. An acceptable boron distribution was obtained, which was a reproducible function of both the length and width coordinates of the plates. The x-ray attenuation technique for determining fuel homogeneity was demonstrated on a production basis. It showed differences in the fabricability of oxides produced by various vendors. Considerable assistance was given to the commercial fuel element fabricator. Preliminary development was completed and plate production was started. Two complete sets of the very complex HFIR control rods were fabricated for use in reactor startup. With the large dispersion plates containing four discrete composition regions, close dimensional tolerances were met during both roll bonding and explosive forming. To avoid rupturing the brittle europium oxide–aluminum dispersion, the inner cylinder was formed under a compressive load. The 5-ft-long 18-in.-dia cylinder containing four longitudinal welds was held within a ±15-mil tolerance for the combination of diameter and straightness. Specimens of the europium oxide–aluminum dispersion did not swell during 1 year in the ORR. (auth)

5175 (ORNL–3870, pp 230-7) HIGH FLUX ISOTOPE REACTOR TARGET DEVELOPMENT. Douglas, D. A. Jr. (Oak Ridge National Lab., Tenn.).

Design, fabrication, and assembly in three simulated cells for mockup testing some 54 items that will be used to remotely fabricate the target elements were completed. Procedures were written for operation, disassembly, and reassembly of each unit. Four prototype capsules were irradiated and performed satisfactorily. The one designed to operate continuously at a heat flux equivalent to the maximum instantaneous hot spot showed no detectable swelling and very little fission-gas escape from the pellets. Substantial reaction between the PuO_2 and the Al powder had no serious consequences. Additional elements were fabricated and are being irradiated at Savannah River. A dummy assembly of 31 elements was fabricated for hydraulic tests. (auth)

Propulsion and Space

See also ENGINEERING — Space Propulsion

Refer also to abstracts 4262, 4299, and 4999.

5176 (EUR–2468.e) NUCLEAR ANALYSES AND NUCLEAR POWER COST OF THE NERO CORE REFERENCE DESIGN. Luidinga, F. (Reactor Centrum Nederland, The Hague). 1965. 86p. Dep. mn.

The zone enrichment ratio, the zone volume ratio and the H_2O to UO_2 volume ratio of a two zone core of a pressurized light water reactor are varied to study their influences on fuel cycle cost. Attention is paid to the influences of different use charges, Pu prices and fabrication charges on minimum fuel cycle costs and resulting core lifetime. (auth)

5177 (LA–3381) FORTRAN IV HYDROGEN PROPERTY TABULAR CODES. Farmer, O. A.; Springer, T. E.; Fisher, B. B. (Los Alamos Scientific Lab., Univ. of California, N. Mex.). Sept. 15, 1965. Contract W-7405-eng-36. 27p. Dep. mn; CFSTI $2.00 cy, $0.50 mn.

A two-dimensional interpolation is used to compute hydrogen properties from two independent parameters. A grid network keeps the deviation from source data below a specified error. FORTRAN IV subroutines compute sets of eight properties approximately 28,000 times per minute (based on IBM-7094). (auth)

5178 (NAA-SR–11303) ARGON GENERATION IN NaK-COOLED REACTORS. Rosen, S. L. (Atomics International, Canoga Park, Calif.). Nov. 10, 1965. Contract AT-11-1-GEN-8. 13p. Dep. mn; CFSTI $1.00 cy, $0.50 mn.

^{41}Ar, a gamma emitter, was experimentally observed in the primary coolant system of the SNAP 8 Experimental Reactor. A fast-neutron reaction with the potassium-41 in the NaK-78 eutectic alloy coolant is believed to be the mechanism for the generation of the ^{41}Ar. This mechanism leads to the prediction of the presence of ^{39}Ar. This prediction is verified experimentally. (auth)

5179 (NAA-SR-Memo–6484) EFFECT OF DIMENSIONAL TOLERANCES ON POWER OUTPUT OF A RADIATION COOLED THERMOELECTRIC CONVERTER. Cooper, J. C. (Atomics International, Canoga Park, Calif.). June 6, 1961. Contract AT(11-1)-Gen-8. 6p. Dep. mn; CFSTI $1.00 cy, $0.50 mn.

Previous work indicated the dimensional tolerances of the Pbte thermoelements cause the major part of the variations of electric and thermal resistance of the SNAP-10A converter. Variations of these parameters are partially compensated by a corresponding change in radiator temperature. An analysis was performed to assess the effect on power output of the same tolerances on the Pbte as those assumed in the previous work. (auth)

5180 (NAA-SR-Memo–11604) THE EFFECT OF TEMPERATURE AND MICROSTRUCTURE OF SINTERED BERYLLIUM OXIDE ON THE SCATTERING CROSS SECTION FOR A SNAP REACTOR. Ottewitte, E. H. (Atomics International, Canoga Park, Calif.). Aug. 25, 1965. Contract AT(11-1)-Gen-8. 6p. Dep. mn; CFSTI $1.00 cy, $0.50 mn.

The maximum possible effects of the temperature and microstructure dependence of the BeO scattering cross sections are estimated. The estimates are conservative because the effects would be less for the neutron energy spectrum of SNAP 8 which is harder than the Maxwellian-spectrum which was used. The maximum possible temperature contribution during a BeO-reflected SNAP 8 rise to power would be a gain of 24¢. As this contribution is both small and positive, it need not be considered in the reflector design. The maximum contribution to the temperature coefficient is estimated as +2.4¢ per 100°F, constant over the range 68 to 981°F. The maximum possible effects caused by method of fabrication and grain size should be 3.5 and 17¢, respectively. (auth)

5181 (ORNL–3029) AIRCRAFT NUCLEAR PROPULSION PROJECT SEMIANNUAL PROGRESS REPORT FOR PERIOD ENDING OCTOBER 31, 1960. (Oak Ridge National Lab., Tenn.). Dec. 22, 1960. Contract W-7405-eng-26. 125p. Dep. mn; CFSTI $4.00 cy, $0.75 mn.

The reactions of Nb and Nb alloys with low-pressure gases at high temperatures were investigated, and the compatibility of Nb-Zr alloys with UO_2 was tested. The effects of oxygen contamination and Li on the tensile properties of Nb and Nb–Zr alloy were studied, as was the corrosion of oxygen-contaminated Nb and Ta by Li. Mass transfer of carbon and nitrogen from stainless steel to Nb and Nb–Zr alloy in NaK was also investigated; and tests were performed on the corrosion of Haynes alloy 15, 316 stainless steel, and Inconel by boiling potassium. Studies were continued on the effects of small amounts of surface contamination on the aging behavior of Nb–Zr alloys. The effects of hydrogen, nitrogen, and oxygen on the mechanical properties of Nb were investigated. Exceptionally pure Nb–Zr alloys were prepared by electron-beam melting; and the purification of Mo, Ta, W, and V by electron-beam melting was demonstrated. It was also demonstrated that electron-beam welding maintains the purity of Nb–Zr alloy, and an electron-beam furnace was modified for the melting of large ingots. Methods for the production and purification of BeO were studied, as well as radiation effects on BeO. A method was developed for determining He in irradiated BeO. The effects of neutron bombardment on the times to rupture of Inconel and 304 stainless steel were investigated, as were phase relations in BeO-metal oxide systems. The fabrication of components for the boiling-potassium heat transfer system continued, and the thermal conductivity of pure Li and of a Li–Ag alloy was measured. Critical experiments were performed on the TSR-II core; and flux, power, and flow distributions in the core were investigated. Static and dynamic tests were performed on the BSR-II core at the SPERT-I facility. The gamma response of CsI and NaI crystals was investigated, as well as line widths in NaI(Tl) spectrometers. The BSF gamma spectrometer was completed, and methods for unscrambling spectra and obtaining response functions for spectrometers were studied. The use of silicon surface-barrier detectors in fast-neutron detection and spectroscopy was investigated; the energy distribution of alpha-triton pairs from the $^{6}Li(n,\alpha)T$ reaction in ^{6}LiF was calculated. The preliminary design of a neutron-chopper spectrometer for Bulk Shielding Facility was completed, and corrections to thermal-neutron flux measurements in water by gold activation were studied further. The investigation of the spectrum of prompt gamma rays from thermal-neutron fission of ^{235}U continued; the response function of the gamma pair spectrometer was determined. Computer programs for shielding calculations were developed, and the angular distributions of neutrons emerging from hydrogenous slabs and lead slabs were measured. Shielding calculations for space vehicles were also considered. Additionally, the gamma and neutron dose rates in the crew compartment of a nuclear aircraft were analyzed; and gamma and neutron attenuation in lithium hydride-uranium shielding was studied experimentally, together with secondary gamma production in the shielding. The shield configuration proposed for the ML-1 reactor was evaluated in a series of experiments at the Lid Tank Shielding Facility. Optimization calculations were made for the design of a reactor shadow shield. (D.C.W.)

5182 (ORNL–P–1721) MPRE RADIATOR DEVELOPMENT TESTS. Fraas, A. P. (Oak Ridge National Lab., Tenn.). [1965]. Contract W-7405-eng-26. 31p. (CONF-651026–3). Dep. mn; CFSTI $2.00 cy, $0.50 mn.

From 1st AIAA Rankine Circle Space Power System Specialists Conference, Cleveland.

Six tapered tube direct condensing radiators were built and operated in the course of the system development test program at ORNL, and a number of tests were run with individual tubes. The bases for the design of these units and the more significant results of the test program are

summarized, and some implications relative to future design work are discussed. (auth)

5183 (ORNL-P-1736) THE SNAP SHIELDING PROGRAM AT ORNL. Clifford, C. E.; Lewin, J. (Oak Ridge National Lab., Tenn.). [nd]. Contract W-7405-eng-26. 6p. (CONF-651026-2). Dep. mn; CFSTI $1.00 cy, $0.50 mn.

From 1st AIAA Rankine Circle Space Power System Specialists Conference, Cleveland.

Experimental and theoretical research carried out at ORNL toward the SNAP Shielding Program is reviewed. Various experiments that have been performed are briefly discussed. Theoretical work for the future is pointed out. (M.O.W.)

5184 (ORNL-P-1740) EXPERIENCE WITH TURBINE-DRIVEN POTASSIUM BOILER-FEED PUMPS FOR THE MEDIUM POWER REACTOR EXPERIMENTS. Wilson, L. V.; Young, H. C.; Smith, A. M. (Oak Ridge National Lab., Tenn.). [1965]. Contract W-7405-eng-26. 32p. (CONF-651026-4). Dep. mn; CFSTI $2.00 cy, $0.50 mn.

From 1st AIAA Rankine Circle Space Power System Specialists Conference, Cleveland.

A series of potassium vapor turbine driven boiler feed pumps with potassium lubricated bearings was designed, built and tested for a total of 2000 hr of operation at high temperatures. The problems that have arisen in the course of the design, fabrication, and operation of these units are summarized. Approaches to the thermal expansion problems, provisions for lubricant flow to the bearings, speed pickups, and maintenance of moving parts installed in hermetically sealed systems are discussed. Test experience with the units operated with steam and water is related to the test experience obtained in potassium systems. The problems encountered in fabricating tungsten carbide parts, difficulties both with the brittleness of TZM molybdenum alloy and its tendency to gall and seize, together with solutions that were found effective for coping with these problems are outlined. (auth)

5185 (UCRL-13095(Vol.1)) DESIGN OF TORY IIC VERNIER AND SHIM ACTUATOR SYSTEMS. VOLUME I. Final Technical Report, April 1, 1962-September 30, 1963. (Bendix Corp., Southfield, Mich. Research Labs. Div.). Contract AT(29-2)-705. (BC/RLD-2801(Vol 1)). Dep. mn; CFSTI $6.00 cy, $1.50 mn.

Research on the design of vernier and shim actuator systems for the Tory IIC ground test reactor is presented. Separate sections are included giving detailed information on the description of Tory IIC control rod actuator systems, planetary transmission, torque-limiting clutch, refinement of 1200°F electropneumatic servo valve, and the scram system. (M.O.W.)

5186 (UCRL-13095(Vol.2)) DESIGN OF TORY IIC VERNIER AND SHIM ACTUATOR SYSTEMS. VOLUME II. Final Technical Report, April 1, 1962-September 30, 1963. (Bendix Corp., Southfield, Mich. Research Labs. Div.). Contract AT(29-2)-705. 188p. (BC/RDL-2801 (Vol.2)). Dep. mn; CFSTI $5.00 cy, $1.00 mn.

Research on the design of vernier and shim actuator systems for the Tory IIC ground test reactor is discussed. Detailed information is included on electric cables, cooling tests of the Tory IIC actuator drive train, H.A.B.S. (Hot Air Blowdown System) tests of upgraded model 1240 vernier actuator and breadboard shim actuator systems, and reliability criteria. (M.O.W.)

5187 AN INVESTIGATION OF OPTIMUM CONTROL FOR NUCLEAR ROCKETS [Thesis]. Haag, Fred George. Troy, N. Y., Rensselaer Polytechnic Inst., 1964. 177p.

The methods of optimum control theory are applied to nuclear reactor control. The optimum control of both reactor power and reactor temperature is considered. A simplified form of the reactor kinetics equations is derived, which is suitable for application of optimization techniques. The start-up problem is cast into a "quasi-linear" form by introduction of a logarithmic power variable. The mechanization of the simplified reactor kinetics equations requires a logarithmic amplifier, a period meter, and a division circuit, which are already available. The optimization problem in which (a) the desired input is piece-wise continuous, (b) the system is described by an n^{th} order set of linear constant coefficient differential equations and (c) the minimization is with respect to an integrated squared error criterion, is considered. A relatively simple closed form optimum controller specialized to a nuclear reactor desired start-up program of constant period followed by operation at constant power is obtained. The closed form optimum controller is shown to be superior to the switching system in certain particulars. The closed form optimum control system is derived by the Pontryagin maximum principle, calculus of variations and dynamic programming. The same optimum system results for all derivations. Although the optimum system is based on a one delay group model, the resulting controller can be adjusted to the actual six delay group model. The compensation of temperature and pressure reactivity feedback is considered. A bifurcated control system is defined in which power control and temperature control are decoupled. The relationship of transient temperature to thermal stress is considered. It is shown that the distributed parameter equations for temperature may be reduced to a form suitable for application of the closed form optimum controller by use of Laplace transforms. (Dissertation Abstr.)

Research and Test Reactors

Refer also to abstracts 3909, 4821, and 4997.

5188 (AERE-R-4932) THE SAFETY OF DAPHNE. England, C. J.; Kenward, C. J.; Parsons, N. A. (Atomic Energy Research Establishment, Harwell (England)). July 1965. 69p. Dep.; BIS $1.80; HMSO 9s. 0d.

A brief description is given of the reactor, its control and safety systems, and the operating procedures used. A number of computer studies were made of the transient behavior of the reactor following a reactivity addition, and the results of these studies are discussed in relation to the credible reactivity addition processes. It is concluded that the degree of hazard associated with operation of the reactor is negligible. (auth)

5189 (ANL-6929) SAFETY ANALYSIS REPORT FOR THE ARGONNE ADVANCED RESEARCH REACTOR CRITICAL EXPERIMENT. Kelber, C. N.; Groh, E. F.; Plumlee, K. E. (Argonne National Lab., Ill.). June 1965. Contract W-31-109-eng-38. 59p. Dep. mn; CFSTI $3.00 cy, $0.75 mn.

The hazards of zero-power critical experimentation utilizing a core of the proposed design of the Argonne Advanced Research Reactor are reported. The design includes a central, hexagonal water-filled flux trap (each side 6 cm long) inside a modified fuel annulus containing 13.5 to 70.3 kg of highly enriched uranium, plus water moderator and stainless steel. A beryllium radial reflector is included. No unsafe condition or undue hazard is associated with this facility. (auth)

5190 (ANL-7106) FARET CORE I FUEL IRRADIATION PROGRAM AND REFERENCE DESIGN. Persiani, P. J.; Bump, T. R.; Kann, W. J. (Argonne National Lab., Ill.). Oct. 1965. Contract W-31-109-eng-38. 26p. Dep. mn; CFSTI $2.00 cy, $0.50 mn.

The Fast Reactor Test Facility FARET will be used in the testing and verification of fast reactor fuel elements typical of those likely to be used in future large, fast, prototype power reactors. A detailed study of the reference core to be used in FARET is presented. Included are the basic core plan, thermal considerations, instrumented fuel subassemblies and fuel element design, core composition and configuration, critical experiments, and the experimental program. (M.O.W.)

5191 (AWRE-R-4/65) MEASUREMENT OF THE NEUTRON SPECTRUM IN HERALD THERMAL COLUMN.

Reichelt, J. M. A. (Atomic Weapons Research Establishment, Aldermaston (England)). Oct. 1965. 10p. Dep.; BIS $0.30; HMSO 1s. 9d.

A thermal column neutron spectrum measurement by time-of-flight using a slow chopper is described. The experimental spectrum is in fair agreement with a Maxwellian distribution at the higher energies and shows at low energies intensity peaks due to the crystalline properties of the moderator. (auth)

5192 (BNWL-SA-251) FFTF DRIVER FUEL: PuO_2–STAINLESS STEEL CERMET. Bailey, W. J.; Hennig, R. J.; de Halas, D. R.; Skavdahl, R. E. (Battelle-Northwest, Richland, Wash. Pacific Northwest Lab.). Nov. 3, 1965. Contract AT(45-1)-1830. 26p. Dep. mn; CFSTI $2.00 cy, $0.50 mn.

The design characteristics, operating conditions, and nucleonic and thermal performance of FFTF driver elements (PuO_2–stainless steel cermet pins, clad in stainless steel) are described. Radiation effects on UO_2–stainless steel, PuO_2–stainless steel, and $(U,Pu)O_2$–stainless steel cermets and $(U,Pu)O_2$ in various environments are reviewed. Fuels for the FTR (Fast Flux Test Reactor) associated with the FFTF (Fast Flux Test Facility) are investigated. (T.F.H.)

5193 (DP-967) THE INITIAL CRITICAL AND ZERO POWER TESTING OF THE HWCTR. Gorrell, Thomas C. (Du Pont de Nemours (E. I.) and Co., Aiken, S. C. Savannah River Lab.). Oct. 1965. Contract AT(07-2)-1. 49p. Dep. mn; CFSTI $2.00 cy, $0.50 mn.

The initial lattice of the Heavy Water Components Test Reactor (HWCTR) was assembled and was made critical without incident. The reactivity worth of the control system and the reactivity effects of temperature were measured in a series of zero power tests. The axial and radial flux distributions were measured for several control rod complements. The results of the complete set of tests demonstrated that the operating behavior of the reactor could be predicted with consistency, and provided the basis for proceeding to full-power operation. (auth)

5194 (DP-971) PERFORMANCE OF HWCTR SAFETY ROD AND CONTROL ROD DRIVE SYSTEMS. Kigler, Eugene O.; Kale, Stephen H. (Du Pont de Nemours (E. I.) and Co., Aiken, S. C. Savannah River Lab.). Oct. 1965. Contract AT(07-2)-1. 42p. Dep. mn; CFSTI $2.00 cy, $0.50 mn.

The Heavy Water Components Test Reactor (HWCTR) is a pressurized, D_2O reactor that has 18 control rods and six safety rods, each driven by an electric motor through a rack and pinion gear train. Racks, pinions, and bearings are located inside individual pressure housings which penetrate through floating ring labyrinth seals. The drives are mounted on the top head of the reactor vessel. Safety rods have electromagnetic clutches and drop into the reactor when it is scrammed. The reliability and performance of the rod drives were very good, from initial critical on March 3, 1962, to termination of operation on December 1, 1964. Seal leakage was well within design limits. Inspection of seals and control rod parts showed no evidence of deposit buildup or stress corrosion cracking of type 17-4 PH stainless steel components. The accident potential of the system is acceptably low. (auth)

5195 (HW-68082) RADIOLOGICAL BACKGROUND STUDY OF THE PLUTONIUM RECYCLE TEST REACTOR SITE, AUGUST–OCTOBER 1960. Williams, L. D. (General Electric Co., Richland, Wash. Hanford Atomic Products Operation). Dec. 29, 1960. Contract AT(45-1)-1350. 29p. Dep. mn; CFSTI $1.00 cy, $0.50 mn.

A preoperational radiological background study was undertaken in the vicinity of the Plutonium Recycle Test Reactor (PRTR). This study was confined almost entirely to the immediate area surrounding the PRTR since the routine environmental monitoring program for the Hanford plant provided adequate data on conditions at greater distances. The results of this study are presented. (auth)

5196 (IS-1200(Sect. R)) REACTOR DIVISION. (Ames Lab., Iowa State Univ. of Science and Tech.). 54p.

Development and operation of the Ames Research Reactor (ALRR) are summarized. Information is included on ALRR modications, operational testing, and determination of ALRR characteristics. Information is also included on developments in support of experiments. (J.R.D.)

5197 (JUL-239-RE) UNTERSUCHUNG DER ABSCHALTINSTRUMENTIERUNG SOWIE DER ABSCHALTBEDINGUNGEN BEI RAMPENFOERMIGEN REAKTIVITAETSSTOERUNGEN FUER DEN 10 MW-BETRIEB DES FRJ-2 (DIDO). (Study of the Safety Instrumentation by Means of Safety Conditions in Ramp Forming Reactivity Perturbations for the 10 MW Operation of the FRJ-2 (DIDO)). Kalker, K. J. (Kernforschungsanlage, Juelich (West Germany). Institut fuer Physikalische Chemie). July 1965. 37p. Dep. mn.

Perturbation analyses were made for the 10 Mw operation of the FRJ-2 reactor using an analog computer. The fast and slow period meters installed in the safety system during the operation and the power shutdown amplifier were coupled with an analog computer simulating the reactor in order to investigate its behavior in ramp-forming reactivity perturbations. The time available for the begining of the steering arm was determined for which a given shutdown condition with respect to the surface temperature of the fuel element plates can be maintained. From these data the region from the ramp steepness and the maximum reactivity can be given within which the power excursions can be kept through the use of the present safety instrumentation. A graphic representation of this region is given. (J.S.R.)

5198 (ORNL-TM-1290) OAK RIDGE RESEARCH REACTOR QUARTERLY REPORT, APRIL, MAY, AND JUNE OF 1965. Tabor, W. H.; Hurt III, S. S. (Oak Ridge National Lab., Tenn.). Oct. 6, 1965. Contract W-7405-eng-26. 33p. Dep. mn; CFSTI $2.00 cy, $0.50 mn.

The ORR operated a record 90.7% of the time for the quarter. There was one major shutdown terminating operating cycle 59. The total number of shutdowns was slightly above the average for recent report periods because of several shutdowns following low-power experiments. The first of the miniature fission chambers was replaced after 33 months of service. These miniature chambers installed at the poolside represent a considerable improvement over the former counting channel components installed in the subpile room and extending to the bottom of the core which were extremely troublesome due to the effect of the control rods and radiation damage. The south bank of absolute filters in the pressurizable off-gas system were replaced after testing proved them to be slightly below tolerance (DOP test). The iodine-removal efficiency of the building ventilation filter system was found to be 99.71% (average of two tests). A boiling detection experiment was conducted utilizing a special orificed fuel element in core position B-3. The analysis of the data accumulated is incomplete; however, preliminary indications are that bulk boiling was produced and detected with little or no indication of nucleate or film boiling beforehand. (auth)

5199 (ORNL-TM-1328) EVALUATION OF OFF-GAS SYSTEM FOR THE CP-ORR CAPSULE EXPERIMENT. Adams, R. E.; Browning, W. E. Jr. (Oak Ridge National Lab., Tenn.). Nov. 12, 1965. Contract W-7405-eng-26. 14p. Dep. mn; CFSTI $1.00 cy, $0.50 mn.

The performance of the off-gas system of the CP-ORR (Coated Particle-Oak Ridge Research Reactor) Capsule Experiment is evaluated both with and without an activated charcoal trap by computing the possible atmospheric radiation doses that would result from a fission product release and comparing these doses with permissible atmospheric doses. Both continuous release and instantaneous release of accumulated fission products from the UC_2 fuel particles were considered. By the addition of the charcoal trap it is

demonstrated that a possible total body radiation dose of 273 mR may be reduced to 3 mR which is 30% of the permissible ORNL atmospheric dose. It is concluded that the activated charcoal trap, as designed, will process released fission products satisfactorily and no undue atmospheric radiation hazard will be produced. (auth)

5200 (TID-3571(Suppl.1)) PULSED REACTORS AND PULSED CRITICAL ASSEMBLIES. A Literature Search. Smith, Richard J. (comp.) (Division of Technical Information Extension (AEC), Oak Ridge, Tenn.). Nov. 1965. 51p. Dep. mn; CFSTI $3.00 cy, $0.50 mn.

A total of 246 subject-arranged annotated references is presented to reports, published literature, and patents concerning the technology of pulsed neutron facilities. Personal author and report number-availability indexes are provided. (auth)

5201 ASSESSMENT OF THE EFFICIENCY OF VENTILATION OF ATOMIC REACTORS OF IRT-2000 TYPE. Moiseitsev, P. I.; Seredin, Yu. V. (Inst. of Industrial Hygiene and Occupational Disease, Moscow). Gigiena i Sanit., No. 6, 100-2(June 1965). (In Russian).

Engineering and health physics tests of the ventilation of the IRT-2000 type reactor showed prohibited changes in the standard design plan and a low quality of assembly work. As a result separate ventilation systems were installed resulting in a marked excess of supply above air extraction and entailing the breakdown in a normal ventilation operation. In preventive and present monitoring for ventilation of reactors it is necessary to give special attention to quality controls for the assembly, repair, and the exploitation of the ventilation system. In the design of the control of the air exchange in a room of the reactor building in which there is a possible influx of radioactive substances, it is necessary to provide excess exhaust over inflow of 20 to 30% (or some unspecified solution using special technological effects). It is necessary to consider possibilities of alternative operations and a series of exhaust systems. (tr-auth)

5202 THE NEUTRON AND GAMMA HEATING IN THE EXPERIMENTAL CHANNELS OF THE FRJ-2 REACTOR. Leyers, H. J. (Zentralinstitut fuer Reaktorexperimente, Juelich, Ger.). Nukleonik, 7: 300-9(July 1965). (In German).

The nuclear heating rate of Mg, graphite, and polyethylene were determined in the vertical channels of the FRJ-2 reactor in a non-poisoned reactor core with adiabatic calorimeters. It was shown that on the basis of these parameters for a given irradiation species in the reactor, and at given reactor powers, the heating rate of a random material can be obtained with an accuracy of approximately 10%. A numerical example is given. The measurements gave some indications of the flux spectrum in the FRJ-2 reactor. (tr-auth)

5203 UNDERWATER RADIOGRAPHY OF IRRADIATED SPECIMENS. Sayag, C.; Nauche, R. (Communaute Europeenne de l'Energie Atomique, Pays-Bas, Netherlands). pp 41-55 of International Symposium on Working Methods in High Activity Hot Laboratories. Vol. I. Paris, Organization for Economic Cooperation and Development, 1965. (In French).

Equipment was developed for underwater radiography of irradiated specimens in the HFR reactor at the Petten Nuclear Center (The Netherlands). The choice of the film emulsion, the utilization of special screens, techniques for film treatment, magnification, and the influence of the gamma veil were studied. The immersed mechanical system is described. (auth)

5204 DEMOUNTING WORK ON IRRADIATED EXPERIMENTS AT THE HFR. Sayag, C. (Communaute Europeenne de l'Energie Atomique, Pays-Bas, Netherlands). pp 289-302 of International Symposium on Working Methods in High Activity Hot Laboratories. Vol. I. Paris, Organization for Economic Cooperation and Development, 1965. (In French).

Special tools and equipment, together with the associated operating procedures, for dismantling of experiments irradiated in the HFR reactor at Petten are described. Ideas for underwater dismantling, which precedes the in-cell operations are considered. The working procedures and equipment used are described. (auth)

5205 THE DISMANTLING CELLS ASSOCIATED WITH THE C.E.A. RESEARCH REACTORS. Caramaux, G. (CEN, Grenoble, France); Baas, C.; Briffaud, G. pp 303-14 of International Symposium on Working Methods in High Activity Hot Laboratories. Vol. I. Paris, Organization for Economic Cooperation and Development, 1965. (In French).

Methods of operation in use in the dismantling cells associated with the research reactors are described. Disassembly, cutting, and shearing are the three major processes in current use. Practical examples of dismantling are described. (auth)

WASTE DISPOSAL AND PROCESSING

See also BIOLOGY AND MEDICINE — Ecology
CHEMISTRY — Radiochemistry
CHEMISTRY — Separation Processes and Procedures
HEALTH AND SAFETY

5206 THE REMOVAL OF RADIONUCLIDES FROM WATER AND WASTE-WATER BY MANGANESE DIOXIDE [Thesis]. Touhill, Charles Joseph Jr. Troy, N. Y., Rensselaer Polytechnic Inst., 1964. 238p.

The extent and mechanism of removal of radionuclides from aqueous solution by hydrous manganese dioxide for a variety of process conditions were investigated. The extent of removal of radionuclides was correlated with pH and with one of the electrokinetic properties of solutions containing colloidal hydrous manganese dioxide. The property measured was the electrophoretic mobility of the colloidal particles. Cesium-137, iodine-131, cerium-144 (with the praseodymium-144 daughter), strontium-90, and yttrium-90 were the radionuclides whose adsorption was correlated with electrophoretic mobility and pH. Three chemical reactions for precipitating manganese dioxide were investigated to determine which would be suitable for use in a water or waste-water treatment process. The well-known Guyard reaction and the reaction in which manganous ion is oxidized by oxygen in the presence of alkali produced satisfactory slurries of manganese dioxide. Reduction of permanganate with hydrogen peroxide was not satisfactory. The dependence of electrophoretic mobility on pH provided fundamental information about the nature of the manganese dioxide micelle and the extent of adsorption of anions, especially hydroxyl ions. A micelle model was developed from the correlation of electrophoretic mobility with pH. This model was extended using the results of radionuclide adsorption and was used to interpret the observed adsorption phenomena. Use of hydrous manganese dioxide in a treatment plant for removing radionuclides from water and waste-water would seem to be feasible. (A.G.W.)

5207 SOME CONSIDERATIONS IN THE DESIGN AND ENGINEERING OF ACTIVE EFFLUENT TREATMENT PLANTS. Spalding, E. G.; Ayre, D. J. Paper No. [9] of Anglo-Spanish Nuclear Power Symposium. Vol. 2. 30p. [Risley, Eng., United Kingdom Atomic Energy Authority, 1965].

The nature of the effluent treatment problem is considered in reference to discharge limits and probable arisings of solid, liquids, and gaseous wastes from various types of nuclear facilities. Emphasis is given to research establishment and power reactor wastes. Treatment methods are discussed, which include segregation, storage, and dilution; filtration; floc treatment; ion exchange; and evaporation. A brief outline is given on the application of treatment methods; emphasis is given to aqueous wastes, but mention is made of nonaqueous arisings. The design and construction of effluent treatment plants are also considered. Discharge limits are tabulated for some nuclear facilities. (L.B.S.)

5208 PROCESS FOR THE DESTRUCTION OF CELLULOSE-CONTAINING MATERIAL CONTAMINATED WITH RADIOACTIVE MATERIAL. Jacobson, Cecil Felix; Larsen, Ib (to Atomenergikommissionen). British Patent 1,007,212. Oct. 13, 1965. Priority date Sept. 24, 1963, Denmark.

A process for the destruction of cellulose-containing material contaminated with radioactive material by means of concentrated sulfuric acid consists of suspending the material in cold concentrated sulfuric acid and conducting the suspension down below the surface of concentrated sulfuric acid maintained at a temperature of 300–330°C. A catalyst, such as selenium, is added to promote oxidation of the cellulose-containing material to CO_2 and H_2O. According to the process the destruction proceeds without the formation of large volumes of gas and smoke that entrain the radioactive material as suspended particles. (B.L.M.)

5209 METHOD OF SEALING REFRACTORY VESSEL CONTAINING RADIOACTIVE WASTES. Heinemann, Heinz; Kraus, John W.; Spector, Marshall L. (to Pullman Inc.). U. S. Patent 3,213,031. Oct. 19, 1965. Filed Aug. 28, 1961.

A method is described for sealing a refractory vessel containing a solid fixation mixture of a radioactive component and non-radioactive components. The fixation mixture is fed through an entrance port of a vessel. After the entrance port is sealed, the vessel is submerged in a sealant mixture contained in a second larger container. The sealant mixture is made up of a metal oxide selected from the group consisting of oxides of Cr, Co, and Fe and an elemental metal selected from the group consisting of Al, B, Zr, and Si. The sealant mixture is heated to its ignition temperature to provide a seal around the vessel that is resistant to erosion and thermal degradation. (B.L.M.)

5210 RECOVERY OF STRONTIUM VALUES FROM SULFATE-CONTAINING WASTE SOLUTIONS. Davis, W.; Yee, W. (to U. S. Atomic Energy Commission). U. S. Patent 3,218,123. Nov. 16, 1965.

A method is presented for recovering strontium values from sulfate-containing waste solutions. A nitric acid solution containing strontium values and values of other metals which precipitate as sulfates in the precipitation of strontium nitrate is contacted with a stoichiometric excess of ferric ions for formation of ferric sulfate. The nitric acid concentration is then raised to between 55 to 60 weight per cent whereby ferric sulfate is selectively precipitated. The precipitate is subsequently separated from the solution and the strontium values recovered from the aqueous solution by precipitation as strontium nitrate from greater than 18 molar nitric acid solution at a temperature of 50° to 75°C. (AEC)

GENERAL AND MISCELLANEOUS

5211 (ANL–7087) ARGONNE NATIONAL LABORATORY PUBLICATIONS, JULY 1, 1964–JUNE 30, 1965. (Argonne National Lab., Ill.). Aug. 1965. Contract W-31-109-eng-38. 333p. Dep. mn; CFSTI $7.00 cy, $1.50 mn.

Approximately 1500 references are given to publications of ANL from July 1964 to June 1965. Included are items published as journal articles, technical reports, books, etc. Separate author and subject indexes are included. (P.C.H.)

5212 (BNL–930) CHEMICAL CRYSTALLOGRAPHY. Brookhaven Lecture Series Number 47. Hamilton, Walter C. (Brookhaven National Lab., Upton, N. Y.). May 12, 1965. Contract AT(30-2)-Gen-16. 15p. Dep. mn; CFSTI $1.00 cy, $0.50 mn.

The use of molecular structure in determining crystal structure is discussed. Experiments and examples are cited. (P.C.H.)

5213 (IS–1200) ANNUAL SUMMARY RESEARCH REPORT OF CHEMISTRY, ENGINEERING, METALLURGY, PHYSICS AND REACTOR DIVISIONS, JULY 1, 1964–JUNE 30, 1965. (Ames Lab., Iowa State Univ. of Science and Tech.). Aug. 1965. Contract W-7405-eng-82. 487p. Dep. mn; CFSTI $7.87 cy, $2.25 mn.

Research and development progress is summarized in five sections. Separate abstracts were prepared for each. (J.R.D.)

For abstracts of individual sections see: 3863, 4077, 4297, 4476, and 5196.

5214 (IS-T–33) FORTRAN SIMULATION OF A DIGITAL DIFFERENTIAL ANALYZER [Thesis]. Blumenberg, Wayne Edward (Ames Lab., Iowa State Univ. of Science and Tech.). July 1965. Contract W-7405-eng-82. 92p. Dep. mn; CFSTI $3.00 cy, $0.75 mn.

FORDAN is a programming system by which a digital computer can be programmed using the analog programming method. The programmer only needs to be concerned with the relationships between inputs and outputs of basic computational components. The components used are similar to the standard components of analog computers and digital differential analyzers. FORDAN is written entirely in Fortran. Therefore, it can be used on any computer which has a Fortran compiler. The system may be applied to boundary value and frequency response problems, to the initial value problems ordinarily solved on analog computers, to non-linear problems, and to control problems involving transport delay. (auth)

5215 (SC-TM–65-448) AT-25 TELEMETRY BAND TRACKING ANTENNA. Gutscher, W. D.; Varnado, S. G. (Sandia Corp., Albuquerque, N. Mex.). Oct. 1965. Contract AT(29-1)-789. 34p. Dep. mn; CFSTI $2.00 cy, $0.50 mn.

A technique is described by which a large telemetry band tracking antenna can be positioned with greater accuracy than is usually found in such a system. In addition, the technique provides a means of removing the inevitable errors of the large mount. The output has the capability of an angular accuracy in the region of 3 minutes or better. Automatic acquisition capabilities should be able to function over most of a hemisphere. (auth)

5216 (SC-TM–65-457) SEMICONDUCTOR PRESSURE TRANSDUCERS. Wright, R. R. (Sandia Corp., Albuquerque, N. Mex.). Sept. 1965. Contract AT(29-1)-789. 98p. Dep. mn; CFSTI $3.00 cy, $0.75 mn.

Several types of phenomena in semiconductors that could possibly be utilized in the design of pressure transducers are reviewed, namely absorption, photoelasticity, Hall effect, piezoelectric effect, piezoresistivity, and junction properties of semiconductors. The effects of hydrostatic pressure on the electric characteristics of tunnel diodes are considered in some detail and conclusions are drawn based on experimental studies of germanium, silicon, and gallium arsenide diodes. (auth)

5217 (TID–21169) THE EFFECT OF HYDROCORTISONE ON ALKALINE PHOSPHATASE IN CULTURED CANCER CELLS. Erwin, Virgel G.; Whitehead, Richard W. (Colorado Univ., Denver. Dept. of Pharmacology). [1963]. Contract AT(11-1)-394. 4p. Dep. mn; CFSTI $1.00 cy, $0.50 mn.

The low level of alkalino phosphatase activity in normal HeLa cells was markedly increased when the cells were grown in the presence of hydrocortisone. Conversely, the level of activity is very high in normal J111 cells and is greatly decreased by exposure to hydrocortisone. Likewise, the alkaline phosphatase activity which is relatively high in normal H.Ep2 cells is lowered significantly by hydrocortisone. The histochemical determinations of alkaline phosphatase were conducted on all the above cells in order to localize the areas of altered enzyme activity. The results were not clear cut due to a high level of enzymatic activity and concomitant dye concentration. However, the histochemical findings were in agreement, quantitatively, with the enzymatic determinations; high concentrations of the dye were observed in preparations showing high levels of the enzyme and vice versa. (auth)

5218 (TID–21991) IMPROVEMENT IN PULSE TRANSMISSION ON COAXIAL TRANSMISSION LINES BY REDUCTION OF SKIN EFFECT. Final Scientific Report. Evans, C. M.; Whicker, L. R. (Purdue Univ., Lafayette, Ind. School of Electrical Engineering). Aug. 1963. Contract AT(29-1)-1183. 72p. Dep. mn; CFSTI $3.00 cy, $0.75 mn.

For Edgerton, Germeshausen and Grier, Inc., Las Vegas, Nev.

The response at a load at one end of a transmission line to a pulse source at the other end is determined from the response to an impulse source by transform methods, assuming isolated source and load. Skin effects are taken into account, and means for their reduction are analyzed. (T.F.H.)

5219 (TID–22372) ELECTRON MICROSCOPIC AND BIOCHEMICAL CHARACTERIZATION OF FRACTION I PROTEIN. Haselkorn, R.; Fernandez-Moran, H.; Kieras, F. J.; van Bruggen, E. F. J. (Chicago Univ., Ill. Dept. of Biophysics). [1965]. Contract AT(11-1)-1344. 12p. Dep. mn; CFSTI $1.00 cy, $0.50 mn.

High resolution electron micrographs of Fraction I protein from Chinese cabbage leaves were obtained. The protein, which has ribulose 1, 5-diphosphate carboxylase activity, appears to be a cube with edge of about 120 Å. Substructure can be seen in individual particles, consistent with a model having 24 subunits, the number prescribed by the available physical and chemical data. (auth)

5220 (UCRL–13185) DYNAMIC PERFORMANCE OPTIMIZATION FOR NUMERICAL CONTROL SYSTEMS. Snow, J. A.; Wang, J. C.; Costanza, J. L. (California Univ., Berkeley. Inst. of Engineering Research). Aug. 1965. Contract W-7405-eng-48. 107p. (MD–65-6). Dep. mn; CFSTI $4.00 cy, $0.75 mn.

Research was conducted on the subject of performance optimization of numerically controlled machine tools. The salient results of this study are included. Discussions are presented for systems analysis, computer program, and simulation results. (M.O.W.)

5221 (UCRL–14228) A NUMERICAL CALCULATION OF TWO-DIMENSIONAL STEADY-STATE DETONATIONS BY THE METHOD OF CHARACTERISTICS. Richards, Gerald T. (Lawrence Radiation Lab., Univ. of California, Livermore). May 26, 1965. Contract W-7405-eng-48. 107p. Dep. mn; CFSTI $4.00 cy, $0.75 mn.

A method is presented for finding the state of the detonation products for a plane detonation wave utilizing the two-dimensional steady-state hydrodynamics equations and the method of characteristics. It is shown that in those cases where the equation of state gives pressure along the adiabat as a function of density (only), the characteristic equations can be solved analytically in velocity space for the plane problem. A numerical method for the solution in coordinate space is then developed using the solution in velocity space in conjunction with the geometric relationship between characteristic curves in the two spaces. In this manner the difficulty encountered due to the coincidence of the detonation front and two characteristic curves in coordinate space is overcome. The derivations involved are included as appendices. The application of the technique is described for an ideal gas equation of state and for an equation of state developed by Mark Wilkins. A further application is described in which this solution is used to start a solution for a steady state detonation in cylindrical geometry. The results are reported for PBX 9404 in the form of graphs produced by the computing facilities on a cathode ray tube from the computer programs described. (auth)

5222 (UCRL–14505) THE CALCULATION OF TREATMENT SCHEDULES FOR CANCER CHEMOTHERAPY. Merkle, T. C.; Stuart, R. N.; Gofman, J. W. (Lawrence Radiation Lab., Univ. of California, Livermore). Oct. 13, 1965. Contract W-7405-eng-48. 19p. Dep. mn; CFSTI $1.00 cy, $0.50 mn.

A model of the growth process in simple neoplastic tissues and a model of growth processes in rapidly multiplying host tissues were used in calculations of the dynamic response of neoplastic and host tissues to the administration of chemotherapeutic agents. A computer system was developed for the rapid evaluation of selected treatment schedules. The rationale of the model is discussed and some typical examples of computational results obtained using data from tissue culture studies are included. (79 references) (C.H.)

5223 (UCRL–16303) GIBBS ENERGIES, ENTROPIES, AND HEATS OF FORMATION FROM DROP CALORIMETRY: THE SILVER–LEAD SYSTEM [Thesis]. Sommelet, Pierre-Hubert (Lawrence Radiation Lab., Univ. of California, Berkeley). Sept. 1965. Contract W-7405-eng-48. 43p. Dep. mn; CFSTI $2.00 cy, $0.50 mn.

A thermodynamic study was made of silver-lead alloys by use of a diphenyl-ether drop calorimeter. Corrections for deviation from equilibrium of the final solid state were derived and applied so that heats of formation of liquid alloys and two phase alloys could be calculated. By the use of the Oelsen technique, Gibbs energies and entropies were also found. Corrections for non-equilibrium were of considerable importance. (auth)

5224 INVESTIGATIONS ON ESTIMATION OF THE COMPOSITION OF HAM IN LIVE AND SLAUGHTERED PIGS BY MEANS OF X RAYS. Kliesch, J.; Horst, P. (Technische Univ., Berlin). Zeuchtsungskunde, 36: 76-86(Feb. 1964). (In German).

An x ray method was developed to evaluate the muscle content of ham. Earlier investigations showed the close correlation between chemical analysis, results from dissection, and the density of ham on the one hand and the corresponding value of the whole carcass. The correlation coefficients vary between $r = 0.77$ and $r = 0.97$. Investigations in 38 hogs and 52 sows of the Improved Landrace variety showed that the results of dissection of the knuckle give a good indication of the portion of muscle, fat, rind, and bone in the ham. To examine these relations in live pigs, estimates were made of the composition of the knuckle by x ray photos to find out if these values are related to the composition of the ham. Ultrasonic measurements were found unsuitable for this purpose. In preliminary studies x ray measurements were taken in the pig carcass. To evaluate the photos, areas of muscle, fat, and bone in the region of the tibia were outlined and the corresponding areas determined planimetrically. The x ray values found were related to various chemical analytic and dissection results. There were distinct relations in results for knuckle and ham. The correlation between the quotient of the muscle and fat areas in the knuckle and the amount of fat in the ham was $r = -0.65$ in hogs and $r = -0.55$ in sows. It is concluded that the method described offers a means for objective estimation of the ham contents and, at the same time, for a rough selection for the breeding pigs by objective measurements. (BBB)

5225 RANGE INDICATING SYSTEM. Roeschke, C. W. (to U. S. Atomic Energy Commission). U. S. Patent 3,216,010. Nov. 2, 1965.

A range indicating system is designed for aircraft. As the distance between the system and an object, such as the earth, closes, a signal of predetermined frequency is transmitted towards said object. A reflected signal from the object is received by the system 180° out of phase with the transmitted signal. When the distance is closed by one-half, the reflected signal is 90° out of phase. At this half distance from the object the modulated frequency is doubled, thus again placing the reflected signal 180° out of phase with the transmitted signal. This procedure is repeated until a desired frequency level is attained which indicates the desired distance from the object. (AEC)

5226 F.M. RADAR SYSTEM. Kabell, L. J.; Roeschke, C. U. (to U. S. Atomic Energy Commission). U. S. Patent 3,217,322. Nov. 9, 1965.

A simplified distance determining system is designed wherein wave frequency is varied, frequency of transmitted and reflected waves is compared, and upon attainment of a preselected frequency difference which corresponds to a preselected distance an indication is furnished. (AEC)

5227 ULTRASONIC INSPECTION METHOD FOR INACCESSIBLE PIPE AND TUBING. Worlton, Daniel C. (to U. S. Atomic Energy Commission). U. S. Patent 3,218,845. Nov. 23, 1965.

An ultrasonic method is described for detecting flaws in a metal pipe. A transducer is mounted at a pre-determined angle with respect to the surface of the pipe in a first plane passing through the longitudinal axis thereof. A coupling medium is interposed between the transducer and the pipe. The transducer is positioned at an angle with respect to the longitudinal axis of the pipe in a second plane passing through the longitudinal axis normal to the first plane. The transducer is moved back and forth a short distance along the longitudinal axis of the pipe while holding the angular position of the transducer constant. The transducer is excited so as to generate ultrasonic plane waves therefrom, the ultrasonic plane waves impinging on the surface of the pipe to cause Lamb waves to be excited therein which travel along the pipe in a helical path. Flaws in the pipe cause reflections of the Lamb waves, which reflections are detected to denote the presence of flaws in the pipe. (AEC)

CORPORATE AUTHOR INDEX

This index contains entries for this period for all report literature and, in addition, for certain published literature items for which it is felt that a corporate approach is especially desirable, e.g., symposia, conference proceedings, and meetings.

Each entry under a corporate author is a shortened version of the title of the publication, followed by the *NSA* volume and abstract number. Report numbers are given in parentheses.

The phrase "Progress report" is abbreviated as "Prog. rpt.," permitting a more rapid and complete alphabetical arrangement of the titles without changing the location of the progress report titles in relation to the other titles.

A

AEROJET-GENERAL NUCLEONICS, SAN RAMON, CALIF.
Prog. rpt. on fissiochemical development, semiannual, 1–6/65, 20: 3982 (AGN-8156)
RISE. Radioisotope submersible engine, 20: 4276 (AGN-8128)

AIR FORCE MATERIALS LAB., WRIGHT-PATTERSON AFB, OHIO.
Prog. rpt. on rare earth W bronzes, 8/64–1/65, 20: 4362 (AD-620033)

AIR FORCE WEAPONS LAB., KIRTLAND AFB, N. MEX.
Prog. rpt. on PM-1, annual, 11/63–10/64, 20: 5108 (AD-618376)

AIX-MARSEILLES UNIV. (FRANCE). FACULTE DES SCIENCES.
Contribution to microcalorimetric study of characteristics of radioelements, 20: 3866 (CEA-R-2630)

AKADEMIYA NAUK SSSR, MOSCOW. INSTITUT FIZIKI.
Transition radiation and optical properties of materials, 20: 5008 (ORNL-tr-872)

AKTIEBOLAGET ATOMENERGI, STOCKHOLM (SWEDEN).
Engineering purchases within reactor area, 20: 5110 (AES-4)
Measured and predicted neutron fluxes in, and leakage through, configuration of perforated Fe plates in D_2O, 20: 4800 (AE-198)
Study of tensile strength in soft steel, 20: 4365 (AES-3)

ALBUQUERQUE OPERATIONS OFFICE (AEC), N. MEX.
Relationship between quality control and quality assurance, 20: 4113 (TID-22358)

ALLIS-CHALMERS MFG. CO., BETHESDA, MD. ATOMIC ENERGY DIV.
ESH-4 test program. Report on fuel elements irradiated in E-SADE Loop of VBWR, 20: 5104 (ACNP-65006)
La Crosse boiling-water reactor—safeguards report for operating authorization, 20: 5105 (ACNP-65544(Vol.I))
La Crosse boiling-water reactor—safeguards report for operating authorization, 20: 5106 (ACNP-65544(Vol.II))

ALLIS-CHALMERS MFG. CO., MILWAUKEE, WIS. ATOMIC ENERGY DIV.
Prog. rpt. on Pathfinder power plant, 10–12/64, 20: 5107 (ACNP-65589)

AMERICAN SOCIETY FOR TESTING AND MATERIALS, PHILADELPHIA, PA.
Conference on radiation effects in electronics, Syracuse 10/64, 20: 4266
Symposium on physics in testing materials, Philadelphia, 2/64, 20: 4116

AMES LAB., IOWA STATE UNIV. OF SCIENCE AND TECH.
Annual summary research report of Chemistry, Engineering, Metallurgy, Physics and Reactor Divisions, July 1, 1964–June 30, 1965, 20: 5213 (IS-1200)
Application of Gibbs-Duhem equation to binary vapor-liquid equilibrium data of metal systems using Newton's interpolation formulae, 20: 4375 (IS-1241)
Catalog of nuclear quadrupole interactions and resonance frequencies in solids. II., 20: 3973 (IS-1222)
Chemistry Division, 20: 3863 (IS-1200(Sect. C))
Engineering Division, 20: 4077 (IS-1200(Sect.E))
FORTRAN simulation of digital differential analyzer, 20: 5214 (IS-T-33)
Metallurgy Division, 20: 4297 (IS-1200(Sect. M))
Photonuclear determination of yield curve and cross section curve for production of ^{13}N in ^{16}O, 20: 4833 (IS-T-43)
Physics Division, 20: 4476 (IS-1200(Sect.P))
Reactor Division, 20: 5196 (IS-1200(Sect.R))
Simultaneous equilibria of D2EHPA and TBP with $Pr(NO_3)_3$ and $Nd(NO_3)_3$ solutions, 20: 3875 (IS-T-37)
Superconducting properties of high purity niobium, 20: 4774 (IS-T-22)

ARGONNE CANCER RESEARCH HOSPITAL, CHICAGO, ILL.
Radioisotopic device for measuring bone mineral, 20: 3803 (ORNL-IIC-5, pp 257-76)

ARGONNE NATIONAL LAB., ILL.
Argonne National Laboratory publications, July 1, 1964–June 30, 1965, 20: 5211 (ANL-7087)
Atomic-beam research, 20: 4535 (ANL-7081, pp 128-9)
Collected algorithms 1900–1963 from communications of the Association for Computing Machinery, 20: 4286 (ANL-7054)
Consolidation of lanthanon fission products in alloys, 20: 3865 (ANL-7064)
Development of variable-energy cyclotron HIVEC, 20: 4491 (ANL-7081, pp 78-80)
Developments in portable x-ray fluorescence instrument using radioisotope excitation sources, 20: 3883 (ORNL-IIC-5, pp 154-81)
Faret Core I fuel irradiation program and reference design, 20: 5190 (ANL-7106)
High-frequency plasmas, 20: 4936 (ANL-7081, pp 130-3)
In vivo measurement of bone mineral content by transmission technique, 20: 3886 (ORNL-IIC-5, pp 290-4)
Inorganically insulated superconducting solenoid for operation at 1°K, 20: 4775 (UCRL-16376)
Mass-spectrometric investigations, 20: 4215 (ANL-7081, pp 134-49)
Moessbauer measurements, 20: 4826 (ANL-7081, pp 121-7)
Other nuclear experiments, 20: 4825 (ANL-7081, pp 81-93)
Prog. rpt. on physics, annual, 4/64–3/65, 20: 4474 (ANL-7081)
Research at Reactors CP-5 and Juggernaut, 20: 4821 (ANL-7081, pp 2-21)
Research at 12-Mev tandem Van de Graaff, 20: 4823 (ANL-7081, pp 36-69)
Research at 4.5-Mev Van de Graaff Accelerator, 20: 4822 (ANL-7081, pp 22-35)
Research at 60-in. cyclotron, 20: 4824 (ANL-7081, pp 70-7)
Safety analysis for AARR critical experiment, 20: 5189 (ANL-6929)
Theoretical physics, 20: 4475 (ANL-7081, pp 95-119)

ATOMIC ENERGY ESTABLISHMENT, INSHAS (EGYPT).
Prog. rpt. on ^{90}Sr contained in marine animals following possible release of radioactive waste, final, 1963–64, 20: 3659 (NP-15156)

ATOMIC ENERGY ESTABLISHMENT, TROMBAY (INDIA). CHEMISTRY DIV.
Diffusion of copper in nickel, 20: 4363 (AEET/CD/31)

ATOMIC ENERGY OF CANADA LTD., CHALK RIVER (ONTARIO).
Further geometrical factors affecting dryout heat flux in vertical, internally heated annuli cooled by steam/water mixtures at 1000 psi, 20: 4099 (AECL-2333)
Portable tritium–air monitor, 20: 4235 (AECL-2283)
Preliminary assessment of thorium as fuel for thermal reactors, 20: 5114

ATOMIC ENERGY OF CANADA LTD., CHALK RIVER (ONTARIO). CHALK RIVER NUCLEAR LABS.
Ruptured fuel location with high resolution gamma-ray spectrometers, 20: 5109 (AECL-2360)

ATOMIC ENERGY RESEARCH ESTABLISHMENT, HARWELL (ENGLAND).
Drying of oxide powder samples for neutron transmission measurements, 20: 3914 (AERE-M-1654)
Gas evolution from solid plutonium-bearing residues during storage, 20: 4364 (AERE-M-1644)
Safety of Daphne, 20: 5188 (AERE-R-4932)
Uses of reactors in neutron activation analysis, 20: 3864 (AERE-L-166)

ATOMIC WEAPONS RESEARCH ESTABLISHMENT, ALDERMASTON (ENGLAND).
Blast loading on right circular cylinder, 20: 4132 (AWRE-O-93/65)
Measurement of neutron spectrum in Herald thermal column, 20: 5191 (AWRE-R-4/65)
New long-period vertical-component seismometer, 20: 4216 (AWRE-O-70/65)
Permeation and diffusion of H isotopes through stainless steels. II., 20: 4366 (AWRE-O-90/65)
12 group set of photon cross sections for use in anisotropic Sn calculations of photon transport, 20: 4996 (AWRE-O-79/65)
ATOMICS INTERNATIONAL, CANOGA PARK, CALIF.
Argon generation in NaK-cooled reactors, 20: 5178 (NAA-SR-11303)
CAT—concentration and temperature code describing simultaneous heat and mass transfer for an infinite cylinder, 20: 4103 (NAA-SR-Memo-11099)
Effect of dimensional tolerances on power output of radiation cooled thermoelectric converter, 20: 5179 (NAA-SR-Memo-6484)
Effect of temperature and microstructure of sintered beryllium oxide on scattering cross section for SNAP reactor, 20: 5180 (NAA-SR-Memo-11604)
Effective resonances integral and Doppler effect in ^{197}Au. I., 20: 4841 (NAA-SR-Memo-11511)
HNPF wet excess fuel loading, 20: 5111 (AI-PC-710)
Least square determination of diffusion coefficients of gases in spherical solids, 20: 4377 (NAA-SR-Memo-10741)
Metallography of zirconium-base alloy hydrides, 20: 4341 (NAA-SR-Memo-10927)
X-ray diffraction data for $ZrC.ZrH_2$, 20: 4378 (NAA-SR-Memo-11542)
AUTHORITY HEALTH AND SAFETY BRANCH, UNITED KINGDOM ATOMIC ENERGY AUTHORITY, LONDON (ENGLAND).
Post incident cooling of P.W.R. core, 20: 5030 (AHSB(S)R-86)

B

BABCOCK AND WILCOX CO., ALLIANCE, OHIO. RESEARCH CENTER.
Corrosion of croloy 2¼ steel in products of a sodium–water reaction, 20: 4317 (BAW-1280-30)
Prog. rpt. on Na-heated steam generator, 7–9/65, 20: 5031 (BAW-1280-32)
BABCOCK AND WILCOX CO., BARBERTON, OHIO. BOILER DIV.
Sodium-heated steam generator development, 20: 4100 (BW-67-2(a))
BATTELLE-NORTHWEST, RICHLAND, WASH. PACIFIC NORTHWEST LAB.
Distribution and excretion of technetium in humans, 20: 3663 (TID-22318)
Fabrication costs for Pu fuel elements. D., 20: 4339 (BNWL-131D)
Fatty acid synthesis by subcellular fractions of lung tissue, 20: 3656 (BNWL-SA-225)
FFTF driver fuel: PuO_2–stainless steel cermet, 20: 5192 (BNWL-SA-251)
Prog. rpt. on W–Tc alloys, 7–10/65, 20: 4367 (BNWL-162)
Pulmonary clearance of $^{59}Fe_2O_3$ and $^{51}Cr_2O_3$ in rats and dogs exposed to cigarette smoke, 20: 3655 (BNWL-SA-224)
RED CROSS. Code to compute resonance shielded, temperature dependent cross sections for fast reactor analysis, 20: 5055 (BNWL-146)
BENDIX CORP., SOUTHFIELD, MICH. RESEARCH LABS. DIV.
Design of TORY IIC vernier and shim actuator systems, 20: 5185 (UCRL-13095(Vol.I))
Design of TORY IIC vernier and shim actuator systems, 20: 5186 (UCRL-13095(Vol.2))
BETTIS ATOMIC POWER LAB., PITTSBURGH, PA.
Extension of hot-1 to treat Neumann boundary conditions—with applications to certain vibration problems, 20: 4080 (WAPD-TM-535)
Prog. rpt. on PWR project, 4/24–7/23/65, 20: 5132 (WAPD-MRP-113)
BETTIS ATOMIC POWER LAB., WEST MIFFLIN, PA.
Evaluation of core thermal and hydraulic data obtained during the operation of PWR Core-1 with the fourth seed (DLCS-33801, DLCS-18201, DLCS-24301, DLCS-36201). January 1963–February 1964, 20: 5133 (WAPD-PWR-TE-151)
In-plant teaching of nuclear reactor plant kinetics and control to graduate engineers and scientists, 20: 5025 (WAPD-T-1832)
BLUME (JOHN A.) AND ASSOCIATES RESEARCH DIV., SAN FRANCISCO, CALIF.
Structural response of residental-type test structures in close proximity to underground nuclear detonation. Salmon event—Project Dribble, 20: 4189 (VUF-1030)
Structural response of tall industrial and residential structures to underground nuclear detonation. Salmon event—Project Dribble, 20: 4190 (VUF-1031)
BROOKE GENERAL HOSPITAL, FORT SAM HOUSTON, TEX.
Prog. rpt. on chromosomal damage in humans by x-irradiation, annual, 1964, 20: 3705 (AD-617601)
BROOKHAVEN NATIONAL LAB., UPTON, N. Y.
Brookhaven radio frequency beam separator, 20: 4493 (BNL-9642)
Calibration and response of personnel monitoring film dosimeters to synchrotron stray radiations, 20: 4237 (BNL-9665)
Chemical crystallography, 20: 5212 (BNL-930)
Comments on deflectors with eccentric beam hole, 20: 4492 (BNL-9640)
Health physics program for Brookhaven National Laboratory synchrotrons, 20: 4175 (BNL-9650)
Linear energy transfer spectra and effective quality factors in stray radiation areas at Brookhaven National Laboratory proton synchrotrons, 20: 4176 (BNL-9684)
Thermoluminescence induced by low energy alpha particles, 20: 3983 (BNL-9589)
Thermoluminescent neutron dosimetry system, 20: 4236 (BNL-9605)
Water budget of a forest damaged by ionizing radiation, 20: 3653 (BNL-8466)
BROWN, BOVERI UND CIE A. G., HEIDELBERG (WEST GERMANY).
Investigations on emission materials for thermionic converter influence of CsF on electron work functions of W, Ta, and Mo, 20: 4572 (EUR-2283.d)
BRUSSELS UNIV. (BELGIUM).
Prog. rpt. on diagnosis and treatment by methods derived from nuclear techniques, annual, 1963, 20: 3658 (EUR-2414.f.i)
BUREAU OF MINES, WASHINGTON, D. C.
Contamination resulting from use of nuclear explosives for stimulating petroleum production, 20: 4082 (BM-RI-6684)

C

CALIFORNIA INST. OF TECH., PASADENA.
Improvement of Caltech 1.5 Bev electron synchrotron, 20: 4495 (CONF-650923-16)
CALIFORNIA UNIV., BERKELEY. INST. OF ENGINEERING RESEARCH.
Dynamic performance optimization for numerical control systems, 20: 5220 (UCRL-13185)
Malfunction detection and diagnosis, 20: 4222 (UCRL-13186)
CALIFORNIA UNIV., DAVIS. COLL. OF ENGINEERING.
Bibliography on deformation, vibration, and stability of shells, 20: 4079 (UCRL-13187)
CARBORUNDUM CO., NIAGARA FALLS, N. Y.
Prog. rpt. on U–Pu monoxides, 7–9/65, 20: 4327 (UNC-5138)
CASE INST. OF TECH., CLEVELAND, OHIO.
Electron lifetime. Experimental test of charge conservation, 20: 4536 (COO-818-61)
Interaction of muons produced by atmospheric neutrinos, 20: 4561 (COO-818-64)
Search for double beta decay of ^{50}Nd, 20: 4828 (COO-818-60)
CASE INST. OF TECH., CLEVELAND, OHIO. DEPT. OF PHYSICS.
Proposed ν_e telescope to detect solar neutrinos by elastic scattering on e^-, 20: 4523 (COO-818-63)
CENTRE D'ETUDE DE L'ENERGIE NUCLEAIRE, MOL (BELGIUM).
Prog. rpt. on imperfections in metals. II., 4–6/65, 20: 4319 (EURAEC-1457)
Prog. rpt. on reprocessing of irradiated fuels, 7/1–9/30/64, 20: 4046 (EURAEC-1340)
Studies on separation of ^{137}Cs and ^{90}Sr from fission products in acid medium on mineral ion exchangers, 20: 3871 (EUR-2497.e)
CHICAGO UNIV., ILL. DEPT. OF BIOPHYSICS.
Electron microscopic and biochemical characterization of fraction I protein, 20: 5219 (TID-22372)
CHICAGO UNIV., ILL. DEPT. OF RADIOLOGY.
Radioisotopic device for measuring bone mineral, 20: 3803 (ORNL-IIC-5, pp 257-76)
CLEREMONT-FERRAND UNIV. (FRANCE). FACULTE DES SCIENCES.
Heavy liquid bubble chamber, 20: 4244 (NP-15416)
COLORADO UNIV., DENVER. DEPT. OF PHARMACOLOGY.
Effect of hydrocortisone on alkaline phosphatase in cultured cancer cells, 20: 5217 (TID-21169)
COLUMBIA UNIV., NEW YORK. DEPT. OF ELECTRICAL ENGINEERING.
Observation of nonquasistatic plasma surface waves, 20: 4935 (AFCRL-65-556)
COLUMBIA UNIV., NEW YORK. ENGINEERING RESEARCH LABS.
Critical heat flux for large diameter, internally heated annuli in forced convection boiling at 1000 psia, 20: 4105 (TID-22321)
COMBUSTION ENGINEERING, INC., DUNEDIN, FLA. NUCLEAR DIV.
Nuclear analysis of Elk River reactor, 20: 5112 (CEND-507)
COMBUSTION ENGINEERING, INC., WINDSOR, CONN. NUCLEAR DIV.
Prog. rpt. on correlations between sensitization and stress corrosion cracking of 300 series stainless steels, 7–9/65, 20: 4370 (CEND-3256-250)
COMISION NACIONAL DE ENERGIA ATOMICA, BUENOS AIRES (ARGENTINA).
Biosynthetic preparation of ^{75}Se-methionine and ^{75}Si-cystine. Its incorporation and distribution in mice, 20: 3661 (NP-15594)
Prog. rpt. on improvement of renogram techniques, final, 20: 3800 (NP-

15150)
Standardization of capture of ^{131}I by thyroid in accordance with recommendations of O.I.E.A., 20: 3660 (NP-15528)

COMISION NACIONAL DE INVESTIGACIONES ESPACIALES, BUENOS AIRES (ARGENTINA).
Physics of interplanetary medium, 20: 4522 (CNIE-PE-5)
Production and removal of ionization in upper atmosphere, 20: 4729 (CNIE-PE-4)

COMITATO NAZIONALE PER L'ENERGIA NUCLEARE, ROME (ITALY).
CRYO—Program for calculation of totally reflected cylindrical reactor design, 20: 5059 (RT/FIMA(65)-1)
Generality of stability criterion against transverse wall instability of relativistic beams, 20: 4501 (LNF-65/34)
Technology of liquid metals, 20: 4330 (ORNL-tr-854)

COMMISSARIAT A L'ENERGIE ATOMIQUE, CHUSCLAN (FRANCE). CENTRE DE PRODUCTION DE PLUTONIUM DE MARCOULE.
Contribution to microcalorimetric study of characteristics of radioelements, 20: 3866 (CEA-R-2630)

COMMISSARIAT A L'ENERGIE ATOMIQUE, FONTENAY-AUX-ROSES (FRANCE). CENTRE D'ETUDES NUCLEAIRES.
Analytical methods used in cycles for plutonium purification by trilaurylamine, 20: 3868 (CEA-R-2860)
Comparison of spectrographic methods of analysis of plutonium and its compounds, 20: 3869 (CEA-R-2869)
Experimental contamination of pink shrimps by ^{137}Cs, 20: 3657 (CEA-R-2818)
Radiochemical determination of ^{90}Sr in large volumes of drinking water, 20: 3867 (CEA-R-2844)
Survey of uranium–carbon–nickel ternary diagram, 20: 4368 (CEA-R-2845)
Vapor pressure studies of uranium dioxide (UO_2) by effusion method, 20: 4369 (CEA-R-2871)

COMMISSARIAT A L'ENERGIE ATOMIQUE, GRENOBLE (FRANCE). CENTRE D'ETUDES NUCLEAIRES.
Effect of fractionating 100 R hard x-ray doses on haemogram and proteinogram of rabbit, 20: 3709 (CEA-R-2865)
Observation of dislocations in crystals using x-ray and electron transmission, 20: 5003 (CEA-R-2875)

COMMISSARIAT A L'ENERGIE ATOMIQUE, SACLAY (FRANCE). CENTRE D'ETUDES NUCLEAIRES.
Cesium-137 decontamination of concentrated fission product solutions, 20: 3874 (EUR-2535.f)
Critical study of some soft-tissue equivalent material. Sensitivity to neutrons of 1 kev to 14 Mev, 20: 3708 (CEA-R-2833)
Diffraction in medium-energy nuclear reactions, 20: 4827 (CEA-Bib-60)
Noble gas compounds, 20: 3915 (CEA-Bib-61)
Study of some transversal motions of electron beam in linear accelerator, 20: 4494 (CEA-R-2843)

COMPAGNIE FRANCAISE THOMSON–HOUSTON, PARIS.
Prog. rpt. on nuclear vapotron annual, 10/64, 20: 5088 (EURAEC-1337)

CONNECTICUT YANKEE ATOMIC POWER CO., HADDAM.
Prog. rpt. on design and engineering, 7/64–6/65, 20: 5124 (NYO-3250-4)

CONSUMERS PUBLIC POWER DISTRICT, HALLAM, NEBR.
Prog. rpt. on operation of HNPF, 8/65, 20: 5130 (TID-22355)

COSMIC, INC., WASHINGTON, D. C.
Charged colloid generating system for electric propulsion, 20: 4133 (N64-25007)

COURANT INST. OF MATHEMATICAL SCIENCES, NEW YORK UNIV., N. Y.
Finite difference calculations for hydrodynamic flows containing discontinuities, 20: 4705 (NYO-1480-33)

D

DARTMOUTH COLL., HANOVER, N. H. DEPT. OF GEOLOGY.
Thermoluminescence induced by low energy alpha particles, 20: 3983 (BNL-9589)

DAVID SARNOFF RESEARCH CENTER, PRINCETON, N. J.
Prog. rpt. on photomultiplier investigation, 5/15–8/14/65, 20: 4218 (NYO-3421-4)

DEPARTMENT OF MINES AND TECHNICAL SURVEYS (CANADA). MINES BRANCH.
Effect of U additions on corrosion behavior of AISI type 430 stainless steel, 20: 4325 (TB-58)

DIKEWOOD CORP., ALBUQUERQUE, N. MEX.
Extrapolating electromagnetic fields from values in spherical region, 20: 4638 (AD-617965)

DIVISION OF OPERATIONAL SAFETY (AEC), WASHINGTON, D. C.
Operational accidents and radiation exposure experience within United States Atomic Energy Commission, 1943–1964, 20: 4188 (TID-22268)

DIVISION OF REACTOR DEVELOPMENT AND TECHNOLOGY (AEC), WASHINGTON, D. C.
Status of nuclear superheat development, 20: 5113 (CONF-650602-59)

DIVISION OF TECHNICAL INFORMATION EXTENSION, (AEC), OAK RIDGE, TENN.
Bibliography on pulsed reactors and pulsed critical assemblies, 20: 5200 (TID-3571(Suppl.1))

DU PONT DE NEMOURS (E. I.) & CO., AIKEN, S. C. SAVANNAH RIVER LAB.
Initial critical and zero power testing of HWCTR, 20: 5193 (DP-967)
Performance of HWCTR safety rod and control rod drive systems, 20: 5194 (DP-971)
Radioactive cobalt for heat sources, 20: 4277 (DP-1012)

E

EDGERTON, GERMESHAUSEN AND GRIER, INC., SANTA BARBARA, CALIF.
Flashing light satellite system for SNAP radiation environments, 20: 4262 (NP-15610)

EDSEL B. FORD INST. FOR MEDICAL RESEARCH, DETROIT, MICH.
X-ray absorptiometry with beta-stimulated x-ray sources, 20: 3882 (ORNL-IIC-5, pp 51-71)

ENRICO FERMI INST. FOR NUCLEAR STUDIES, UNIV. OF CHICAGO, ILL.
High energy physics research using 460 Mev synchrocyclotron, 20: 4577 (AD-618067)

EUROPEAN ATOMIC ENERGY COMMUNITY.
Bibliographical survey on facilities and processes for radioactive milk decontamination, 20: 3872 (EUR-2507.d)
Cesium-137 decontamination of concentrated fission product solutions, 20: 3874 (EUR-2535.f)
Computer analysis of tensile tests, 20: 4371 (EUR-2514.e)
Determination of sulfur in terphenyl by neutron activation, 20: 3873 (EUR-2523.i)
Efficiency of semiconductor sandwich detector in flux of fission neutrons from disk source, 20: 4238 (EUR-2487.e)
Investigations on emission materials for thermionic converter influence of CsF on electron work functions of W, Ta, and Mo, 20: 4572 (EUR-2283.d)
Measurement of radioactivity by scintillation in liquid medium: biological uses, 20: 3870 (EUR-2459.f)
Nuclear analyses and nuclear power cost of Nero core reference design, 20: 5176 (EUR-2468.e)
Prog. rpt. on atomic energy in agriculture, annual, 1964, 20: 3710 (EUR-2493.e)
Prog. rpt. on diagnosis and treatment by methods derived from nuclear techniques, annual, 1963, 20: 3658 (EUR-2414.f.i)
Prog. rpt. on shielding experiments at reactor station Geesthacht, annual, 1964, 20: 4997 (EUR-2494.d)
Results of environmental radioactivity measurements in community countries in 1964, 20: 4155 (EUR-2516.d,f,i,n)
SAHYB: program for solution of initial and boundary value problems, 20: 4287 (EUR-2519.e)
Synthesis of products akin to polyphenyls, 20: 3972 (EUR-2528.f)

EUROPEAN ATOMIC ENERGY COMMUNITY, ISPRA (ITALY). EUROPEAN SCIENTIFIC DATA PROCESSING CENTER.
SAHYB: program for solution of initial and boundary value problems, 20: 4287 (EUR-2519.e)

EUROPEAN ATOMIC ENERGY COMMUNITY, ISPRA (ITALY). JOINT NUCLEAR RESEARCH CENTER.
Computer analysis of tensile tests, 20: 4371 (EUR-2514.e)
Determination of sulfur in terphenyl by neutron activation, 20: 3873 (EUR-2523.i)
Efficiency of semiconductor sandwich detector in flux of fission neutrons from disk source, 20: 4238 (EUR-2487.e)
SAHYB: program for solution of initial and boundary value problems, 20: 4287 (EUR-2519.e)

EUROPEAN NUCLEAR ENERGY AGENCY, PARIS (FRANCE).
Prog. rpt. on chemical processing of irradiated fuels, 1962–64, 20: 4048 (NP-15406)

F

FRANKFORD ARSENAL, PHILADELPHIA, PA.
Steady disturbances to viscous, highly conducting laminar boundary layer flow over nonconducting wall with parallel magnetic field, 20: 4098 (AD-614633)

G

GENERAL ATOMIC, SAN DIEGO, CALIF. JOHN JAY HOPKINS LAB. FOR PURE AND APPLIED SCIENCE.
CORE, computer code for design of GCR core, 20: 5078 (GAMD-6676)
Description and results of P9 coated particle irradiation experiment, 20: 4458 (GA-6485)
GAMBLE-4. Program for solution of multigroup neutron-diffusion equations

in two dimensions, 20: 5057 (GA-6540)
Prog. rpt. on advanced, graphite-matrix, dispersion type fuel systems and research on graphite, 11/15/64–2/14/65, 20: 5089 (GA-6181)
Prog. rpt. on effect of substructure on irradiation stability of ASTM A302 grade B steel, 10/65, 20: 4372 (GA-6724)
Prog. rpt. on experimental beryllium oxide reactor program, 10–12/63, 20: 5115 (GA-4967)
Prog. rpt. on integral neutron thermalization, 4–6/65, 20: 4801 (GA-6634)
Prog. rpt. on TARGET, program for 1000 Mw(c) HTGCR, 9–11/64, 20: 5117 (GA-5866)
Prog. rpt. on TARGET, program for 1000 Mw(e) high temperature GCR, 6–8/64, 20: 5116 (GA-5618)
Prog. rpt. on 40-Mw(e) HTGCR, 6/65, 20: 5118 (GA-6647)
SAFE-PCRS. Computer program for stress analysis of composite bodies of revolution, 20: 5033 (GA-6588)
Safety characteristics of large gas-cooled fast power reactors, 20: 5119 (GA-6732)
Stress analysis of axisymmetric disk with variable thickness, 20: 4075 (GA-6267)

GENERAL ELECTRIC CO., CINCINNATI, OHIO. NUCLEAR MATERIALS AND PROPULSION OPERATION.
Neutron cross section library for Monte Carlo codes FMC-N, 18-0, and 18-1, 20: 4830 (GEMP-384)
Nine and sixteen group cross sections for reactor analysis, 20: 4829 (GEMP-173(Suppl.1))

GENERAL ELECTRIC CO., CINCINNATI, OHIO. SPACE POWER AND PROPULSION SECTION.
Material specifications for advanced refractory alloys, 20: 4380 (NASA-CR-54761)

GENERAL ELECTRIC CO., RICHLAND, WASH. HANFORD ATOMIC PRODUCTS OPERATION.
Critically safe flat bed contactor for processing solid fissile materials, 20: 4049 (RL-SA-52)
Maximum temperatures in flat-plate fuel elements with fuel-clad bonding defects, 20: 4102 (HW-SA-3640)
Measurement of filter efficiency with condensation nuclei counter, 20: 5036 (RL-SA-47)
Radiological background study of plutonium recycle test reactor site, August–October 1960, 20: 5195 (HW-68082)

GENERAL ELECTRIC CO., SAN JOSE, CALIF. ATOMIC POWER EQUIPMENT DEPT.
High-temperature tensile properties of selected alloys after prolonged thermal exposure, 20: 4373 (GEAP-4794)
Irradiation performance of UO_2 produced by alternate fabricating processes, 20: 4459 (GEAP-4850)
Prog. rpt. on SEFOR development, 10/64–1/65, 20: 5120 (GEAP-4799)

GEOLOGICAL SURVEY, DENVER, COLO.
Geology and surface effects, handcar event, 20: 4144 (PNE-810F)

GESELLSCHAFT FUR KERNENERGIEVERWERTUNG IN SCHIFFBAU UND SCHIFFAHRT m.b.H., HAMBURG (WEST GERMANY).
Prog. rpt. on shielding experiments at reactor station Geesthacht, annual, 1964, 20: 4997 (EUR-2494.d)

GORDON MCKAY LAB. OF APPLIED SCIENCE, HARVARD UNIV., CAMBRIDGE, MASS.
Preliminary report on interaction of electromagnetic field with missile having ionized trail, 20: 4730 (SC-DC-65-1797)

GOSUDARSTVENNYI KOMITET PO ISPOL'ZOVANIYU ATOMNOI ENERGII SSSR, MOSCOW. INSTITUT TEORETICHESKOI I EKSPERIMENTAL'NOI FIZIKI.
Tests of consequences of unitary symmetry in Hadron-Production Reactions (Survey), 20: 4645 (NP-15599)

H

HAYES INTERNATIONAL CORP., HUNTSVILLE, ALA.
Plane thermal stress analysis of thick-wall cylinders, 20: 4076 (HIC-1-1564-3(Vol.2))

HEBREW UNIV., JERUSALEM (ISRAEL). DEPT. OF PHYSICS.
Electron density ionization rate and approach to thermal equilibrium behind shock waves by means of microwave techniques, 20: 4934 (AD-619093)

HITTMAN ASSOCIATES, INC., BALTIMORE, MD.
Analytical investigation of nuclear and thermal-hydraulic design characteristics of SM-1A, Core 3. I., 20: 5121 (HIT-3459-11(Vol.1))
Analytical investigation of nuclear and thermal-hydraulic design characteristics of SM-1A, Core 3. II., 20: 5122 (HIT-3459-11(Vol.2))
Bremsstrahlung from ^{90}Sr–^{90}Y in thin absorbers, 20: 5000 (ORNL-IIC-5, pp 91-8)

I

IIT RESEARCH INST., CHICAGO, ILL.
Prog. rpt. on reactor containment, 8–9/65, 20: 5023 (IITRI-578P21-15)
Prog. rpt. on yield point occurrence in polycrystalline alpha-Zr, 9/64–8/65, 20: 4374 (IITRI-578-P27-12)

ILLINOIS UNIV., URBANA.
Properties of ^3He at low temperatures, 20: 4773 (COO-1198-306)

INNSBRUCK UNIV. (AUSTRIA). INSTITUT FUER THEORETISCHE PHYSIK.
Gasdynamic methods in MHD flow, 20: 4702 (AD-619094)

INSTITUT ATOMNOI ENERGII, GOSUDARSTVENNYI KOMITET PO ISPOL'ZOVANIYU ATOMNOI ENERGII SSSR, MOSCOW.
Analysis of polarization in a neutron beam by scattering on Coulomb field of nucleus, 20: 4832 (IAE-901)
Differential gaseous Cherenkov counter, 20: 4239 (IAE-900)
Effect of helical field on ohmic heating of plasma in S-1 apparatus, 20: 4937 (IAE-907)
Longwave electron oscillations in beam-plasma system, 20: 4940 (IAE-932)
Magneto-sonic heating of plasma, 20: 4939 (IAE-911)
Nature of the relationship of energy emission in the Moessbauer effect to temperature, 20: 5004 (IAE-927)
Phonon spectrum of lattice of white tin, 20: 5005 (IAE-928)
Static characteristics of voltage stabilizer in electromagnetic isotope separator, 20: 4281 (IAE-926)
Structure of front of strong magneto-sonic wave in rarefied plasma, 20: 4938 (IAE-909)

INSTITUTE FOR NUCLEAR STUDY, TOKYO UNIV. (JAPAN).
X-ray and γ-ray astronomy, 20: 4562 (MIT-2098-174)

INSTITUTE OF NUCLEAR RESEARCH, WARSAW (POLAND).
Numerical calculations in statistical theory of particle production in angular momentum representation, 20: 4643 (INR-607/VI/PH)
Tables of functions $X(c,\nu)$ and $X^{\pm}(c_1,c_2)$ for numerical solution of slab geometry neutron transport problems, 20: 4803 (INR-630/IX-A/PR)

INSTITUTE OF OCEANOGRAPHY (EGYPT).
Prog. rpt. on ^{90}Sr contained in marine animals following possible release of radioactive waste, final, 1963–64, 20: 3659 (NP-15156)

INSTITUTT FOR ATOMENERGI, HALDEN (NORWAY). OECD HALDEN REAKTOR PROSJEKT.
Prog. rpt. on HBWR, 1–3/65, 20: 5123 (HPR-61)

INSTITUTT FOR ATOMENERGI, KJELLER (NORWAY).
Prog. rpt. on NORA project, 7–9/65, 20: 5060 (TID-22357)

INSTITUUT VOOR TOEPASSING VAN ATOOMENERGIE IN DE LANDBOUW, WAGENINGEN (NETHERLANDS).
Prog. rpt. on atomic energy in agriculture, annual, 1964, 20: 3710 (EUR-2493.e)

INTERNATIONAL ATOMIC ENERGY AGENCY, VIENNA (AUSTRIA).
Radioisotope sources of low-energy electromagnetic radiation and their use in analysis and measurement of coating thickness, 20: 4219 (ORNL-IIC-5, pp 182-205)

INTERNATIONAL CENTRE FOR THEORETICAL PHYSICS, TRIESTE (ITALY).
Behavior for large k of S-matrix for strongly singular potentials, 20: 4640 (IC/65/75)
Contribution to nucleon form factors, 20: 4642 (IC/65/78)
Position of singularities of S-matrix in unified theories, 20: 4639 (IC/65/73)
Role of symmetry physics, 20: 4641 (IC/65/76)

ISTITUTO SUPERIORE DI SANITA', ROME (ITALY). LABORATORI DI FISICA.
Determination of tritium content in samples, 20: 3876 (ISS-65/8)

J

JAPAN ATOMIC ENERGY RESEARCH INST., TOKYO.
Determination of radioactive fallout from nuclear weapon tests. Detection and determination of radioactive nuclides in rain water, 20: 4177 (JAERI-1083)
Preliminary design work on 100 MWt experimental fast reactor, 20: 5079 (NP-15572)

JOHNS HOPKINS UNIV., BALTIMORE, MD.
Medical applications of low-energy x-ray and gamma radiation sources, 20: 3802 (ORNL-IIC-5, pp 239-42)

JOINT INST. FOR NUCLEAR RESEARCH, DUBNA (USSR).
Determination of charged particle momentum in inhomogeneous magnetic field, 20: 4583 (JINR-P-2371)
Passage of high energy neutrons in iron-aqueous mixtures, 20: 4998 (JINR-P-2359)

JOINT INST. FOR NUCLEAR RESEARCH, DUBNA (USSR). LAB OF HIGH ENERGY.
Electrostatic field of wire electrodes for spark chamber, 20: 4241 (JINR-P-2364)
Inflatable gaskets for JINR large-volume hydrogen bubble chambers, 20: 4242 (JINR-P-2376)
Investigation of reactions π^- p yields m π^0 + n at the π^- momentum of 4 Bev/c, 20: 4582 (JINR-P-2361)
Measurement of energy and angular characteristics of electrons and γ-

quanta in propane bubble chamber, 20: 4240 (JINR-P-2277)
Multiple acceleration system for high energy particle electrodynamic separator, 20: 4496 (JINR-P-2375)
JOINT INST. FOR NUCLEAR RESEARCH, DUBNA (USSR). LAB. OF NEUTRON PHYSICS.
Correlation of neutrons in reflected reactor, 20: 5058 (JINR-P-2335)
JOINT INST. FOR NUCLEAR RESEARCH, DUBNA (USSR). LAB OF NUCLEAR PROBLEMS.
New isotope, ^{174}W, 20: 4834 (JINR-E-2360)
β positron decay of ^{145}Eu, 20: 4838 (JINR-P-2314)
JOINT INST. FOR NUCLEAR RESEARCH, DUBNA (USSR). LAB OF THEORETICAL PHYSICS.
Angular distribution of transfer reaction products, 20: 4836 (JINR-P-2298)
Correctness of method for unified theory of nuclear reactions, 20: 4837 (JINR-P-2310)
Electromagnetic properties of mesons in broken symmetry, 20: 4644 (JINR-P-2299)
Matrix elements for inelastic scattering of heavy particles. I., 20: 4839 (JINR-P-2333)
On reconstruction of the amplitude of the vector meson production reactions $\pi + N$ yields ω (ρ), 20: 4584 (JINR-P-2380)
Sensitivity of some nuclear characteristics to intermediate coupling parameters, 20: 4835 (JINR-P-2287)

K

KANSAS ENGINEERING EXPERIMENT STATION, MANHATTAN.
Effects of electrical conductance of wall on magnetohydrodynamic channel flow with heat transfer, 20: 4703 (AD-619101)
KERNFORSCHUNGSANLAGE, JUELICH (WEST GERMANY). INSTITUT FUER PHYSIKALISCHE CHEMIE.
Study of safety instrumentation by means of safety conditions in ramp forming reactivity perturbations of FRJ-2 (DIDO), 20: 5197 (JUL-239-RE)
KERNFORSCHUNGSANLAGE, JUELICH (WEST GERMANY). INSTITUT FUER REAKTORENTWICKLUNG.
Physical properties of fused fluoride salts, special application to MOSEL reactor concept, 20: 4376 (JUL-268-RG)
KERNFORSCHUNGSANLAGE, JUELICH (WEST GERMANY). ZENTRALABTEILUNG STRAHLENSCHUTZ.
Environmental radioactivity of the Nuclear Research Center, Juelich, 20: 4178 (JUL-284-ST)
KERNFORSCHUNGSZENTRUM, KARLSRUHE (WEST GERMANY). INSTITUT FUER EXPERIMENTELLE KERNPHYSIK.
Use of AVF-cyclotrons for nuclear physics, 20: 4497 (KFK-310)
KERNKRAFTWERK RWE-BAYERWERK G.M.B.H., GUNDREMMINGEN (WEST GERMANY).
Prog. rpt. on KRB nuclear power plant, 1–3/65, 20: 5129 (TID-22328)
KNOLLS ATOMIC POWER LAB., SCHENECTADY, N. Y.
Application of multichannel synthesis to 2-D depletion calculations, 20: 5056 (CONF-654-22)
Combined slowing-down and thermalization program with a thermal cutoff of 3.06 ev, 20: 4804 (KAPL-3098)

L

LABORATOIRE DE L'ACCELERATEUR LINEAIRE, UNIV. DE PARIS, ORSAY (FRANCE).
Elastic electron scattering by magnetic and electric moments, 20: 4840 (LAL-1140)
Utilization of semiconductor detectors with high-energy accelerator. I and II., 20: 4243 (LAL-1102)
LABORATORI NAZIONALI DI FRASCATI, COMITATO NAZIONALE PER L'ENERGIA NUCLEARE (ITALY).
ADONE—Frascati 1.5 Bev electron positron storage ring, 20: 4499 (LNF-65/26)
Transverse resistive wall instability of extremely relativistic beams of electrons and positrons, 20: 4500 (LNF-65/27)
LABORATORIO DE FISICA E ENGENHARIA NUCLEARES, JUNTA DE ENERGIA NUCLEAR, SACAVEM (PORTUGAL).
Improvement and utilization of nuclear fuels, 20: 4047 (LFEN-32)
LAWRENCE RADIATION LAB., UNIV. OF CALIFORNIA, BERKELEY.
Accelerator radiation monitoring and shielding, 20: 4514 (UCRL-16445)
Analysis of elliptically polarized light, 20: 4480 (UCRL-11802)
Attempts to observe a positive-strangeness baryon, 20: 4589 (UCRL-11754)
Cavity resonator systems for supporting nonsinusoidal periodic waveforms, 20: 4511 (UCRL-16242)
Design of long straight sections for synchrotrons, 20: 4512 (UCRL-16243)
Dynamical formula for slope of Pomeranchuk trajectory, 20: 4587 (UCRL-11495)
Gibbs energies, entropies, and heats of formation from drop calorimetry, 20: 5223 (UCRL-16303)
Guide for designing electrical controls of accelerators, 20: 4510 (UCRL-16016)
Inorganically insulated superconducting solenoid for operation at 1°K, 20: 4775 (UCRL-16376)
Instabilities of relativistic particle beams, 20: 4513 (UCRL-16440)
Nucleic acid content of chloroplasts of spinach isolated by a non-aqueous technique, 20: 3649 (UCRL-11475)
Nucleon-nucleon polarization at 700, 600, 500, and 400 Mev, 20: 4590 (UCRL-11926)
Polarization parameter in proton-proton scattering from 328 to 736 Mev, 20: 4588 (UCRL-11565)
Secondary electron distribution for heavy ions, 20: 4541 (UCRL-16405)
Some uses and characteristics of MOS transistors for health physics applications, 20: 4250 (UCRL-16446)
Structure and high strength metals, 20: 4399 (UCRL-16301)
Three types of 4π neutron spectrometers, 20: 4249 (UCRL-16311)
Units for atomic and subatomic physics, 20: 4539 (UCRL-11444)
LAWRENCE RADIATION LAB., UNIV. OF CALIFORNIA, LIVERMORE.
Bibliography on deformation, vibration, and stability of shells, 20: 4079 (UCRL-13187)
Calculation of treatment schedules for cancer chemotherapy, 20: 5222 (UCRL-14505)
CRT plotting routines in use at LRL-Livermore, 20: 4292 (UCRL-14427-T)
Effect of high velocity translation on photon correlations in laser interferometers, 20: 4223 (UCRL-14345)
Electronic scheme for measurement of exploding wire energy, 20: 4481 (UCRL-14170)
Fluid and hydrodynamics, 20: 4153 (UCRL-14360, pp 73-85)
Kirzhnits corrections to Thomas-Fermi equation of state, 20: 4540 (UCRL 14364)
Logarithmic current-to-voltage amplifier with high sensitivity, stability, and dynamic range, suitable for field application, 20: 4221 (UCRL-12394-T)
Mathematical and computational methods, 20: 4290 (UCRL-14360, pp 94-7)
Neutron self shielding in intermediate systems, 20: 4808 (UCRL-14432-T)
Nuclear and atomic physics, 20: 4849 (UCRL-14360, pp 1-50)
Numerical calculation of two-dimensional steady-state detonations by method of characteristics, 20: 5221 (UCRL-14228)
Optical system for moderate-rigidity charged-particle beams, 20: 4509 (UCRL-14343)
PLOT3D: FORTRAN subroutine for three-dimensional plotting, 20: 4291 (UCRL-14425)
Prog. rpt. on physics, 2–5/65, 20: 4482 (UCRL-14360)
Quartz pressure transducer package, 20: 4224 (UCRL-14448)
Radiation physics, 20: 4949 (UCRL-14360, pp 85-94)
Study of simple waves, 20: 4707 (UCRL-14318)
Theoretical study of second-order Raman spectra of cesium halides, 20: 5007 (UCRL-14398)
Thermodynamic properties of matter, 20: 4708 (UCRL-14360, pp 50-73)
Trapped electron spectra from Starfish detonation and from outer belt in fall of 1962, 20: 4731 (UCRL-7659-T(Rev.1))
Trapped electrons produced by Russian high-altitude nuclear detonation of October 28, 1962, 20: 4732 (UCRL-14368-T(Rev.1))
Underground neutrino experiment. I., 20: 4847 (UCRL-12085(Pt.1))
Underground neutrino experiment. II., 20: 4848 (UCRL-12085(Pt.2))
LIBRARY OF CONGRESS, WASHINGTON, D. C. SCIENCE AND TECHNOLOGY DIV.
World outlook for food irradiation, 20: 4271 (WASH-1063)
LOCKHEED MISSILES AND SPACE CO., PALO ALTO, CALIF.
Space materials handbook, 20: 4312
LOS ALAMOS SCIENTIFIC LAB., UNIV. OF CALIFORNIA, N. MEX.
Arc spray powder feeder for ultra-fine particles with wide range of densities, 20: 4298 (LA-DC-7275)
Cylindrical explosive flux-compression system, 20: 4477 (LA-DC-7289)
Determination of low level plutonium activity; autoradiographic techniques vs. scintillation counting, 20: 3877 (LA-DC-7483)
FORTRAN IV hydrogen property tabular codes, 20: 5177 (LA-3381)
Iodine-131 sampling with activated charcoal and charcoal-impregnated filter paper, 20: 4179 (LA-3363)
Plasma compression by explosively produced magnetic fields, 20: 4941 (LA-DC-7290)
Prog. rpt. on medium-energy physics program, 7–9/65, 20: 4498 (LA-3419)
Structure, chemistry, and instability of detonation in homogeneous, low density fluids—gases, 20: 3918 (LA-DC-7276)
Thermodynamic-transport and related properties of para-hydrogen from 36 to 5000°R at pressures to 5000 psia, 20: 3917 (LA-3405)
LYON UNIV. (FRANCE). INSTITUT DE PHYSIQUE NUCLEAIRE.
Method of study of particle dynamics in linear accelerator, 20: 4503 (NP-15340)

Microdetermination of oxygen in metals by radioactive reagents and by activation with fast neutrons at 14 Mev, 20: 3878 (LYCEN-6524)

M

MARTIN CO., BALTIMORE, MD. NUCLEAR DIV.
SNAP technology conceptual design 100-watt thermoelectric generator heat transfer analysis, 20: 4278 (MND-P-2229)
MARYLAND UNIV., COLLEGE PARK. DEPT. OF CHEMICAL ENGINEERING.
Bremsstrahlung from ^{90}Sr–^{90}Y in thin absorbers, 20: 5000 (ORNL-IIC-5, pp 91-8)
MARYLAND UNIV., COLLEGE PARK. DEPT. OF PHYSICS AND ASTRONOMY.
Three-particle unitarity integral, 20: 4647 (TID-22274)
MASCHINENFABRIK AUGSBURG-NUERNBERG A. G., NUREMBERG (WEST GERMANY).
Prog. rpt. on research into critical heat flux in boiling H_2O, 1–3/65, 20: 4101 (EURAEC-1354)
MASSACHUSETTS INST. OF TECH., CAMBRIDGE.
Two-dimensional calculations of magnetic micropulsation resonances, 20: 4728 (AD-618118)
MASSACHUSETTS INST. OF TECH., CAMBRIDGE. DEPT. OF MECHANICAL ENGINEERING.
Effect of nonuniform axial heat flux distribution, 20: 4104 (NP-15622)
MASSACHUSETTS INST. OF TECH., CAMBRIDGE. DEPT. OF METEOROLOGY.
Eddy fluxes and biennial oscillation in stratosphere, 20: 4150 (MIT-2241-7)
Stratospheric wind temperature and isobaric height conditions during IGY period. III., 20: 4151 (MIT-2241-14)
MASSACHUSETTS INST. OF TECH., CAMBRIDGE. DEPT. OF PHYSICS.
X-ray and γ-ray astronomy, 20: 4562 (MIT-2098-174)
MASSACHUSETTS INST. OF TECH., CAMBRIDGE. LAB. FOR NUCLEAR SCIENCE.
X-ray and γ-ray astronomy, 20: 4562 (MIT-2098-174)
MASSACHUSETTS INST. OF TECH., CAMBRIDGE. RESEARCH LAB. OF ELECTRONICS.
General physics, 20: 4479 (TID-22179, pp 1-83)
Plasma dynamics, 20: 4948 (TID-22179, pp 85-175)
Quarterly progress report No. 78, 20: 4478 (TID-22179)
MASSACHUSETTS UNIV., AMHERST. DEPT. OF ZOOLOGY.
Prog. rpt. on inhibition of synthesis of macromolecules by ultraviolet radiation, 1965, 20: 3686 (TID-22352)
MICHAEL REESE HOSPITAL, CHICAGO, ILL.
In vivo measurement of bone mineral content by transmission technique, 20: 3886 (ORNL-IIC-5, pp 290-4)
MINNESOTA MINING AND MFG. CO., ST. PAUL.
Prog. rpt. on fabrication of W alloy tubing, 7/1–10/22/65, 20: 4340 (COO-1518-1)
Prog. rpt. on portable thermoelectric generator, 6/65, 20: 4571 (AD-618037)
MINNESOTA UNIV., MINNEAPOLIS. DEPT. OF BOTANY.
Water budget of a forest damaged by ionizing radiation, 20: 3653 (BNL-8466)
MOUND LAB., MIAMISBURG, OHIO.
Prog. rpt., 5/65, 20: 3879 (MLM-1266)
MRD DIV., GENERAL AMERICAN TRANSPORTATION CORP., NILES, ILL.
Close-in effects from surface burst, 20: 4143 (AD-619969)
MSA RESEARCH CORP., CALLERY, PA.
Prog. rpt. on measurement of impurities in Na, 7–9/65, 20: 3880 (MSAR-65-150)

N

NARMCO RESEARCH AND DEVELOPMENT DIV., WHITTAKER CORP., SAN DIEGO, CALIF.
Prog. rpt. on silica fiber/core-sheath fiber, final, 2/64–6/65, 20: 4338 (AD-620055)
NATIONAL AERONAUTICS AND SPACE ADMINISTRATION, CLEVELAND, OHIO. LEWIS RESEARCH CENTER.
Optimum target orientation in nuclear reaction experiments, 20: 4842 (NASA-TN-D-3116)
Single-collision model for electron-beam currents between plane electrodes, 20: 4704 (NASA-TN-D-3058)
NATIONAL HEALTH SERVICE, COPENHAGEN (DENMARK).
Danish laws and regulations relating to radiation hygiene, 20: 4180 (NP-15571)
NATIONAL INST. FOR RESEARCH IN NUCLEAR SCIENCE, CHILTON (ENGLAND). RUTHERFORD HIGH ENERGY LAB.
Further extraction studies for Harwell variable energy cyclotron, 20: 4502 (NIRL/R/92)
Prog. rpt., annual, 1963–1964, 20: 4504 (NP-15420)
NATIONAL INST. FOR RESEARCH IN NUCLEAR SCIENCE, DARESBURY (ENGLAND). DARESBURY NUCLEAR PHYSICS LAB.
Prog. rpt., annual, 1963–1964, 20: 4504 (NP-15420)
NAVAL CIVIL ENGINEERING LAB., PORT HUENEME, CALIF.
Feasibility of modeling run-up effects of dispersive water waves, 20: 4142 (AD-619053)
Shallow-buried model arches subjected to traveling-wave load, 20: 4131 (AD-622552)
NAVAL ORDNANCE LAB., WHITE OAK, MD.
Application of anticoincidence-shielded scintillation spectrometer to study of $^{14}N(p,\gamma)^{15}O$ reaction, 20: 4233 (AD-618676)
Explosion containment laws for nuclear reactor vessels, 20: 5034 (NOLTR-63-140)
Physics of base surge, 20: 4141 (AD-618733)
NAVAL RADIOLOGICAL DEFENSE LAB., SAN FRANCISCO, CALIF.
Analysis of local and systemic effects of ionizing radiation on bone growth, 20: 3707 (AD-623641)
Charged particle tracks in polymers. I., 20: 4251 (USNRDL-TR-917)
Evidence for humoral mediation of radiation-induced motivation obtained from parabiont rats, 20: 3706 (AD-623365)
Influence of temperature on radiation-induced surface effects in transistors, 20: 4261 (AD-623078)
Influence of weather on salt distributions and aerosols on beaches, 20: 4148 (AD-623515)
Physical and radiochemical properties of fallout particles, 20: 4156 (USNRDL-TR-899)
Size analysis of –44 micron dust particles, 20: 4149 (AD-623639)
NEW BRUNSWICK LAB. (AEC), N. J.
Spectrophotometric determination of gallium in plutonium–gallium alloy, 20: 3881 (NBL-228)
NEW YORK OPERATIONS OFFICE (AEC), N. Y.
Liquid fluidized bed reactor program, 20: 5125 (NYO-10732)
NIJVERHEIDSORGANISATIE (TNO), THE HAGUE (NETHERLANDS).
Prog. rpt. on determination of brittle-ductile transition in steel, 4–9/65, 20: 4457 (EURAEC-1474)
NUCLEAR MATERIALS AND EQUIPMENT CORP., APOLLO, PA.
Prog. rpt. on UO_2–PuO_2–ZrO_2 fuel development, 7–9/65, 20: 4382 (NUMEC-3505-8)
NUCLEAR METALS, INC., WEST CONCORD, MASS.
Prog. rpt. on methods to control grain size, purity and texture in Be and Be alloys, 4–5/65, 20: 4381 (NMI-8001.4)

O

OAK RIDGE NATIONAL LAB., TENN.
Army reactors program, 20: 4305 (ORNL-3870, pp 187-90)
Bibliography on tracer diffusion in metals. II., 20: 4383 (ORNL-3795 (Pt.2))
Body composition by differential absorption of monochromatic x rays, 20: 3885 (ORNL-IIC-5, pp 277-89)
Bonus reactor support program, 20: 5126 (ORNL-3870, pp 293-9)
Bremsstrahlung from ^{90}Sr–^{90}Y in thin absorbers, 20: 5000 (ORNL-IIC-5, pp 91-8)
Characterization and behavior of accident-released fission products, 20: 4185 (ORNL-3843, pp 169-234)
Comparison of three methods used to calculate gamma-ray transport in iron, 20: 5001 (ORNL-RSIC-9)
Conference on low-energy x- and gamma sources and applications, Chicago, 10/64, 20: 4111 (ORNL-IIC-5)
Crystal physics, 20: 3919 (ORNL-3870, pp 3-6)
Deformation of crystalline solids, 20: 4384 (ORNL-3870, pp 7-14)
Desalination, 20: 5173 (ORNL-3870, pp 191-3)
Developments in portable x-ray fluorescence instrument using radioisotope excitation sources, 20: 3883 (ORNL-IIC-5, pp 154-81)
Diffusion in solids, 20: 4385 (ORNL-3870, pp 15-19)
Dimensional location of reactor components by optical tooling, 20: 5035 (ORNL-TM-1278)
Electron microscopy, 20: 4386 (ORNL-3870, pp 20-6)
Electron-phonon, electron-plasmon, plasmon-phonon, and plasmon-plasmon interactions, 20: 4944 (ORNL-3871)
Electronic properties of metals and alloys, 20: 3920 (ORNL-3870, pp 27-37)
Evaluation of off-gas system for CP-ORR capsule experiment, 20: 5199 (ORNL-TM-1328)
Experience with stainless steel sheathed Chromel–Alumel thermocouples in irradiated experiments, 20: 4263 (ORNL-TM-1320)
Experience with turbine-driven potassium boiler-feed pumps for medium power reactor experiments, 20: 5184 (ORNL-P-1740)
Filtration and adsorption under accident conditions, 20: 4086 (ORNL-3843, pp 137-67)
Fuel element development, 20: 4342 (ORNL-3870, pp 85-101)
Gas-cooled reactor program, 20: 4306 (ORNL-3870, pp 194-213)
Generation and practical use of monoenergetic x rays from alpha-

emitting isotopes, 20: 4268 (ORNL-IIC-5, pp 353-73)
Half-lives and specific activities of common radionuclides, 20: 4845 (ORNL-TM-1318)
Hauser-Feshbach nuclear scattering computer code LIANA, 20: 4844 (ORNL-TM-1234)
High flux isotope reactor, 20: 5174 (ORNL-3870, pp 214-29)
High flux isotope reactor target development, 20: 5175 (ORNL-3870, pp 230-7)
High-temperature materials, 20: 4301 (ORNL-3870, pp 102-35)
In vivo measurement of bone mineral content by transmission technique, 20: 3886 (ORNL-IIC-5, pp 290-4)
Industrial analysis of ^{147}Pm x rays for radiography and imaging readout, 20: 3801 (ORNL-IIC-5, pp 222-38)
Materials compatibility, 20: 4321 (ORNL-3870, pp 136-9)
Mechanical properties, 20: 4460 (ORNL-3870, pp 140-5)
Medical applications of low-energy x-ray and gamma radiation sources, 20: 3802 (ORNL-IIC-5, pp 239-42)
Medium power reactor experiment, 20: 4307 (ORNL-3870, pp 238-42)
Metallography, 20: 4309 (ORNL-3870, pp 300-4)
Molten-salt reactor program, 20: 4308 (ORNL-3870, pp 243-60)
MPRE radiator development tests, 20: 5182 (ORNL-P-1721)
Nondestructive test development, 20: 4110 (ORNL-3870, pp 146-54)
Nuclear safety information, 20: 4186 (ORNL-3843, pp 235-44)
Ore and coal analysis using radioisotope techniques, 20: 3884 (ORNL-IIC-5, pp 206-21)
Physical ceramic studies, 20: 4387 (ORNL-3870, pp 38-43)
Physical properties, 20: 4388 (ORNL-3870, pp 44-9)
Portable devices for isotope chest radiography and other applications, 20: 3804 (ORNL-IIC-5, pp 309-28)
Preparation, coating, evaluation, and irradiation testing of sol-gel oxide microspheres, 20: 4344 (ORNL-P-1725)
Preparation of thoria and mixed-oxide microspheres, 20: 3922 (ORNL-TM-1281)
Prog. rpt. for physical properties group, 10/65, 20: 4310 (ORNL-P-1699)
Prog. rpt. on ANP project, semiannual, 9/58, 20: 4999 (ORNL-2599)
Prog. rpt. on ANP project, semiannual, 10/60, 20: 5181 (ORNL-3029)
Prog. rpt. on ANP project, semiannual, 3/59, 20: 4299 (ORNL-2711)
Prog. rpt. on metals and ceramics, annual, 6/30/65, 20: 4300 (ORNL-3870)
Prog. rpt. on nuclear safety, semiannual, 1–6/65, 20: 4182 (ORNL-3843)
Prog. rpt. on research reactor, 4–6/65, 20: 5198 (ORNL-TM-1290)
Promethium-147 radiation measurements of one-watt, prototype heat source, 20: 4279 (ORNL-TM-1177)
Radioisotope sources of low-energy electromagnetic radiation and their use in analysis and measurement of coating thickness, 20: 4219 (ORNL-IIC-5, pp 182-205)
Radioisotopic device for measuring bone mineral, 20: 3803 (ORNL-IIC-5, pp 257-76)
Reactor evaluation, 20: 5024 (ORNL-3870, pp 261-5)
Release and transport of fission products upon in-pile destruction of reactor fuels, 20: 4183 (ORNL-3843, pp 2-70)
Release and transport behavior of fission products in containment systems, 20: 4184 (ORNL-3843, pp 71-135)
Report of an informal striation meeting held at the seventh international conference on phenomena in ionized gases, Belgrade, Yugoslavia, August 22-27, 1965, 20: 4946 (ORNL-TM-1307)
Report on a meeting held in the old lecture room at Christ Church College, Oxford, at 9 p.m. on Thursday, September 9, 1965, 20: 4945 (ORNL-TM-1306)
Response of helium-cooled fast reactor to changes in coolant flow and reactivity, 20: 5127 (ORNL-P-1698)
Review of ORNL Electromagnetic Separations Program, 20: 4282 (ORNL-3861)
SALINE: a FORTRAN computer program for process design of saline water conversion plants using the multi-stage, flash-evaporation process, 20: 3923 (ORNL-TM-1299)
SNAP shielding program at ORNL, 20: 5183 (ORNL-P-1736)
SNAP-50 corrosion studies, 20: 4323 (ORNL-3870, pp 308-11)
SNAP-8 corrosion studies, 20: 4322 (ORNL-3870, pp 305-7)
Solid-state and molecular theory, 20: 5006 (ORNL-3870, pp 50-5)
SPCTRM. 05R Monte Carlo analysis routine for calculating neutron energy spectrum, 20: 4805 (ORNL-TM-1245)
Spectroscopy of ionic media, 20: 3921 (ORNL-3870, pp 56-60)
Structure of metals, 20: 4389 (ORNL-3870, pp 61-4)
Superconducting materials, 20: 4390 (ORNL-3870, pp 65-9)
Surface reactions of metals, 20: 4320 (ORNL-3870, pp 70-4)
Synthesis of 3,9-diethyltridecyl-6-amine, 20: 3974 (ORNL-TM-1314)
Theoretical methods in dosimetry of high-energy particles, 20: 4505 (ORNL-P-1738)
Thermally compensated closure for liquid density autoclave, 20: 4087 (ORNL-TM-1293)
Thorium utilization, 20: 4343 (ORNL-3870, pp 266-89)
Tungsten metallurgy, 20: 4302 (ORNL-3870, pp 155-63)
Uranium nitride, 20: 4303 (ORNL-3870, pp 164-70)
Use of digital computer in time-of-flight experiments, 20: 4245 (ORNL-P-1723)
X-ray absorptiometry with beta-stimulated x-ray sources, 20: 3882 (ORNL-IIC-5, pp 51-71)
X-ray diffraction, 20: 4391 (ORNL-3870, pp 75-82)
Zirconium metallurgy, 20: 4304 (ORNL-3870, pp 171-83)

OESTERREICHISCHE STUDIENGESELLSCHAFT FUER ATOMENERGIE G.M.B.H., SEIBERSDORF.
Operating experience with Seibersdorf inhomogeneous sector field isotope separator, 20: 4283 (SGAE-PH-27/1965)

OHIO STATE UNIV. RESEARCH FOUNDATION, COLUMBUS.
Thermal and electrical conductivities of Mo–Re alloys in superconducting and normal states, 20: 4361 (AD-619719)

ORGANIZATION FOR ECONOMIC CO-OPERATION AND DEVELOPMENT, PARIS (FRANCE).
Symposium on high activity hot laboratories, Vol. I and II, Grenoble, 6/65, 20: 4040

OSLO UNIV. (NORWAY). DEPT. OF ASTROPHYSICS.
Researches in solar physics during 1964, 20: 4521 (AD-618222)

P

PARAMETRICS, INC., WALTHAM, MASS.
Generation and practical use of monoenergetic x rays from alpha-emitting isotopes, 20: 4268 (ORNL-IIC-5, pp 353-73)

PARIS UNIV. (FRANCE). INSTITUT DE DROIT COMPARE.
International regulation of transport of radioactive materials, 20: 4181 (NP-15620)

PARIS UNIV. (FRANCE). LABORATOIRE CURIE.
Measurement of radioactivity by scintillation in liquid medium: biological uses, 20: 3870 (EUR-2459.f)

PHILLIPS PETROLEUM CO. IDAHO FALLS, IDAHO., ATOMIC ENERGY DIV.
Application of nuclear heat to production of ammonia, 20: 3916 (CONF-650902-20)
Limited-energy neutron sources produced by decay of excited nuclei, 20: 4802 (IDO-17115)

PICKER X-RAY CORP., CLEVELAND, OHIO.
Industrial analysis of ^{147}Pm x rays for radiography and imaging readout, 20: 3801 (ORNL-IIC-5, pp 222-38)

PISA UNIV. (ITALY).
Prog. rpt. on diagnosis and treatment by methods derived from nuclear techniques, annual, 1963, 20: 3658 (EUR-2414.f.i)

PRATT AND WHITNEY AIRCRAFT, MIDDLETOWN, CONN. CONNECTICUT ADVANCED NUCLEAR ENGINEERING LAB.
Alkali metal corrosion. I., 20: 4318 (CNLM-5359)
Compressive creep of UC and UN. I., 20: 4396 (PWAC-482(Pt.1))
High temperature titanium alloy development, 20: 4393 (PWAC-472)
Low pressure oxidation of pure columbium, 20: 4324 (PWAC-460)
Phase diagram of Cb–Zr–C system at 1538°C and 1092°C, 20: 4392 (PWAC-461)
Self diffusion of nitrogen in uranium mononitride, 20: 4394 (PWAC-477)
Stability of carbon strengthened columbium–zirconium alloys at elevated temperature in ultra-high vacuum, 20: 4397 (TIM-955)
Thermodynamic properties of uranium monocarbide, 20: 4395 (PWAC-478)
Users report for pump impeller codes, 20: 4088 (TIM-949)

PRINCETON–PENNSYLVANIA ACCELERATOR, PRINCETON, N. J.
Drift tube rf system, 20: 4507 (PPAD-2137-560)
Radiations measurements group at Princeton-Pennsylvania 3 Bev proton synchrotron, 20: 4506 (PPAD-569E)

PRINCETON UNIV., N. J. PLASMA PHYSICS LAB.
A-c response of spirally wound capacitors, 20: 4217 (MATT-378)
Microwave absorption in hot plasma near the second harmonic of electron cyclotron frequency, 20: 4943 (MATT-379)
Plasma confinement in low-density C stellarator discharges, 20: 4942 (MATT-372)

PRODUCTION GROUP, UNITED KINGDOM ATOMIC ENERGY AUTHORITY, ANNON (SCOTLAND).
Biology of the Solway firth in relation to movement and accumulation of radioactive materials. IV., 20: 3662 (PG-Report-650)

PRODUCTION GROUP, UNITED KINGDOM ATOMIC ENERGY AUTHORITY, SELLAFIELD (ENGLAND).
Determination of radio-ruthenium in reactor fuel processing plant solutions, 20: 3887 (PG-Report-677)

PURDUE UNIV., LAFAYETTE, IND. DEPT. OF NUCLEAR ENGINEERING.
Design and evaluation of 1000 Mw(e) central station power-plant with a circulating fuel gaseous core reactor, 20: 5128 (TID-22225)

PURDUE UNIV., LAFAYETTE, IND. SCHOOL OF ELECTRICAL ENGINEERING.
Improvement in pulse transmission on coaxial transmission lines by reduction of skin effect, 20: 5218 (TID-21991)

Q

QUEEN'S UNIV., BELFAST (NORTHERN IRELAND). DEPT. OF APPLIED MATHEMATICS.
Electron temperatures in D region, 20: 4727 (AD-618054)

R

RADIATION EFFECTS INFORMATION CENTER, BATTELLE MEMORIAL INST., COLUMBUS, OHIO.
Radiation effects on propellants and explosives: annotated bibliography, 20: 4461 (REIC-Memo-28)
RADIO CORP. OF AMERICA, LANCASTER, PA. DIRECT ENERGY CONVERSION DEPT.
Prog. rpt. on thermionic converters, emitter shell phase, final, 7/63–2/65, 20: 4359 (AD-618923)
RAND CORP., SANTA MONICA, CALIF.
Nuclear explosions in cavities, 20: 4167 (RM-3727(RAND))
REACTOR CENTRUM NEDERLAND, THE HAGUE.
Nuclear analyses and nuclear power cost of Nero core reference design, 20: 5176 (EUR-2468.e)
REACTOR GROUP, UNITED KINGDOM ATOMIC ENERGY AUTHORITY, RISLEY (ENGLAND).
Ageing of chromel–alumel thermocouples, 20: 4398 (TRG-Report-1021)
RENSSELAER POLYTECHNIC INST., TROY, N. Y.
Low energy neutron inelastic scattering (LENIS), 20: 4807 (RPI-328-40, pp 56-66)
Neutron cross sections, 20: 4846 (RPI-328-40, pp 43-8)
Neutron thermalization, 20: 4806 (RPI-328-40, pp 1-42)
New instrumentation programs (primarily for neutron cross section measurements), 20: 4246 (RPI-328-40, pp 49-55)
Prog. rpt. on linear accelerator project, 7–9/65, 20: 4508 (RPI-328-40)
Prog. rpt. on wall effects in non-equilibrium statistical mechanics, final, 1965, 20: 4706 (RPI-3036-1)
RESEARCH GROUP, UNITED KINGDOM ATOMIC ENERGY AUTHORITY, WANTAGE (ENGLAND).
Irradiation of carbon dioxide–methane system, 20: 3981 (AERE-R-5051)
Ore and coal analysis using radioisotope techniques, 20: 3884 (ORNL-IIC-5, pp 206-21)
Silt movement investigation in oxcars spoil ground, firth of forth using radioactive tracers, 1961 and 1964, 20: 4166 (AERE-R-4980)
ROCHESTER UNIV., N. Y.
Muon-proton scattering at high momentum transfers, 20: 4591 (UR-875-108)
Prog. rpt. on skeletal metabolism in man, final, 1965, 20: 3664 (TID-22324)
ROCHESTER UNIV., N. Y. DEPT. OF PHYSICS AND ASTRONOMY.
Measurements of positive Kaon production in proton-proton collisions at 2.85 and 2.40 Bev, 20: 4586 (TID-22315)
ROCKY FLATS DIV., DOW CHEMICAL CO., GOLDEN, COLO.
FORTRAN II data reduction program for gas phase radiolysis studies, 20: 3985 (RFP-624)
ROSCOE B. JACKSON MEMORIAL LAB., BAR HARBOR, MAINE.
Prog. rpt. on genetic control of aging and radiation-induced life shortening of mice, 1/1–9/30/65, 20: 3711 (NYO-3314-2)

S

SAHA INST. OF NUCLEAR PHYSICS, CALCUTTA (INDIA).
Self-consistent perturbation. I., 20: 4537 (NP-15576)
Self-consistent perturbation. II., 20: 4538 (NP-15577)
SANDIA CORP., ALBUQUERQUE, N. MEX.
A digital computer program for the simulation of sampled data systems, 20: 4288 (SC-DR-65-312)
Aero heating results from RFD-2 flight test, 20: 4280 (SC-DC-65-1601)
AT-25 telemetry band tracking antenna, 20: 5215 (SC-TM-65-448)
Craters from a single row of charges buried beneath the craters from parallel rows of charges, 20: 4083 (SC-RR-65-478)
Digital computer simulation as experimental tool in evaluation of sampled-data systems, 20: 4289 (SC-DR-65-318)
Launch hazards assessment program. Report on Atlas/Centaur abort, 20: 4187 (SC-RR-65-333)
Preliminary report on interaction of electromagnetic field with missile having ionized trail, 20: 4730 (SC-DC-65-1797)
Semiconductor pressure transducers, 20: 5216 (SC-TM-65-457)
Shock springs and pulse shaping on impact shock machines, 20: 4112 (SC-TM-65-443)
Thin-film, field-effect devices, 20: 4220 (SC-TM-65-424)
SOCIETE D'ETUDES, DE RECHERCHES ET D'APPLICATIONS POUR L'INDUSTRIE, BRUSSELS (BELGIUM).
Synthesis of products akin to polyphenyls, 20: 3972 (EUR-2528.f)
SOUTHWEST RESEARCH INST., SAN ANTONIO, TEX.
Prog. rpt. on liquid-metal lubricated journal bearings, 4–7/65, 20: 4078 (SWRI-1228-67)
SPINDLETOP RESEARCH, LEXINGTON, KY.
Investigation of pyrolytic products of irradiated cigarettes, 20: 3984 (ORO-633)
STANFORD LINEAR ACCELERATOR CENTER, STANFORD UNIV., CALIF.
Compact photomultiplier-tube base, 20: 4247 (TID-21362)
Spin and parity analysis in two-step decay processes, 20: 4585 (SLAC-42)
STANFORD RESEARCH INST., MENLO PARK, CALIF.
Feasibility of cavity pressure and temperature measurements for decoupled nuclear explosion, 20: 4084 (VUF-3017)
STANFORD UNIV., CALIF. DEPT. OF PHYSICS.
Magnetic electron scattering, 20: 4831 (HEPL-272)
STANFORD UNIV., CALIF. HIGH-ENERGY PHYSICS LAB.
Eta photoproduction in region from threshold to 900 Mev, 20: 4578 (AD-618660)
Experimental evidence for possible meson-exchange contribution to elastic electron-deuteron scattering, 20: 4580 (AD-618662)
Pion-pair photoproduction below 1 Bev, 20: 4579 (AD-618661)
Report on inelastic electron scattering program at Stanford, 20: 4581 (AD-618663)
STANFORD UNIV., CALIF. INST. FOR PLASMA RESEARCH.
Beam-plasma interaction in warm plasma, 20: 4947 (SU-IPR-13)
STANFORD UNIV., CALIF. STANFORD ELECTRONICS LABS.
Semitoroidal reflex discharge as propulsion device, 20: 4134 (SEL-63-120)
SYRACUSE UNIV., N. Y. DEPT. OF PHYSICS.
Concluding remarks at international seminar on unified field theories at Feldafing on Starnbergersee near Munich, July 1965, 20: 4646 (NYO-3399-40)

T

TECHNICAL OPERATIONS RESEARCH, BURLINGTON, MASS.
Prog. rpt. on modification of photometric measurement assemblies, final, 1/4–5/3/65, 20: 4234 (AD-619177)
TECHNISCHE HOGESCHOOL, DELFT (NETHERLANDS).
Determinations of nuclear decay energies and conversion coefficients using coincidence techniques, 20: 4843 (NP-15456)
TECHNISCHE HOGESCHOOL, EINDHOVEN (NETHERLANDS).
Prog. rpt. on steady state and dynamic behavior of BWR, 1–4/65, 20: 5032 (EURAEC-1477)
THERMO ELECTRON ENGINEERING CORP., WALTHAM, MASS.
Thermionic emitter materials research program, 20: 4570 (AD-614592)
TITANIUM METALS CORP. OF AMERICA, NEW YORK.
Prog. rpt. on development of stable-beta Ti alloy, 7–9/64, 20: 4360 (AD-619399)
TRACERLAB/WEST, RICHMOND, CALIF.
Survey and recommendations for radioisotope applications pertinent to U. S. Naval Civil Engineering Laboratory operations, 20: 4089 (TLW-1055A)
TRAVELERS RESEARCH CENTER, INC., HARTFORD, CONN.
Prog. rpt. on influence of local winds on fallout, semiannual, 10/15/64–4/15/65, 20: 4154 (AD-620003)
TRW EQUIPMENT LABS., THOMPSON RAMO WOOLDRIDGE INC., CLEVELAND, OHIO.
Corrosion of super-alloys by lithium fluoride in cyclic high temperature environment, 20: 4326 (TRW-ER-6561)

U

UNITED NUCLEAR CORP., WHITE PLAINS, N. Y. DEVELOPMENT DIV.
Electrochemical oxygen meter operating manual, 20: 3889 (UNC-5113)
Prog. rpt. on performance evaluation of heat exchangers for Na-cooled reactors, 7–9/65, 20: 5131 (UNC-5135)
Prog. rpt. on U–Pu monoxides, 7–9/65, 20: 4327 (UNC-5138)
UNITED STATES–EURATOM JOINT RESEARCH AND DEVELOPMENT PROGRAM.
Prog. rpt. on correlations between sensitization and stress corrosion cracking of 300 series stainless steels, 7–9/65, 20: 4370 (CEND-3256-250)
Prog. rpt. on determination of brittle-ductile transition in steel, 4–9/65, 20: 4457 (EURAEC-1474)
Prog. rpt. on effect of substructure on irradiation stability of ASTM A302 grade B steel, 10/65, 20: 4372 (GA-6724)
Prog. rpt. on imperfections in metals. II., 4–6/65, 20: 4319 (EURAEC-1457)
Prog. rpt. on nuclear vapotron annual, 10/64, 20: 5088 (EURAEC-1337)
Prog. rpt. on reprocessing of irradiated fuels, 7/1–9/30/64, 20: 4046 (EURAEC-1340)
Prog. rpt. on research into critical heat flux in boiling H_2O, 1–3/65,

20: 4101 (EURAEC-1354)
Prog. rpt. on steady state and dynamic behavior of BWR, 1–4/65, 20: 5032 (EURAEC-1477)
Prog. rpt. on U–Pu monoxides, 7–9/65, 20: 4327 (UNC-5138)
Prog. rpt. on UO_2–PuO_2–ZrO_2 fuel development, 7–9/65, 20: 4382 (NUMEC-3505-8)
Prog. rpt. on yield point occurrence in polycrystalline alpha-Zr, 9/64–8/65, 20: 4374 (IITRI-578-P27-12)

UNIVERSITY OF THE WITWATERSRAND, JOHANNESBURG (SOUTH AFRICA).
Interaction of muons produced by atmospheric neutrinos, 20: 4561 (COO-818-64)

UPPSALA UNIV. (SWEDEN).
Geophysical aspects of cosmic rays, 20: 4560 (AD-618562)

V

VANDERBILT UNIV., NASHVILLE, TENN.
Extension of internal-external conversion method to lens beta-ray spectrometer by measurement of 662 kev conversion line of ^{137}Ba, 20: 4248 (TID-22333)

VERMONT UNIV., BURLINGTON.
Thermodynamics of non-aqueous electrolytic solutions, 20: 3926 (TID-22374)

VERMONT UNIV., BURLINGTON. DEPT. OF CHEMISTRY.
Thermodynamic properties of ions in aqueous and non-aqueous solutions at various temperatures, 20: 3924 (TID-22366)
Thermodynamic properties of non-aqueous solutions. II., 20: 3925 (TID-22366, App. B)

VERSUCHS- UND FORSCHUNGSANSTALT FUER MILCHWIRTSCHAFT, KIEL (WEST GERMANY).
Bibliographical survey on facilities and processes for radioactive milk decontamination, 20: 3872 (EUR-2507.d)

VIENNA UNIV. (AUSTRIA). ANALYTISCHES INSTITUT.
Ion exchange separation of uranium and thorium in mixed and non-aqueous solvents, 20: 3888 (TID-22402)

VISO CORP., DETROIT, MICH.
Portable devices for isotope chest radiography and other applications, 20: 3804 (ORNL-IIC-5, pp 309-28)

W

WEATHER BUREAU, LAS VEGAS, NEV.
Early-time cloud rise from chemical high explosive detonations, 20: 4152 (TID-22266)

WESTINGHOUSE ELECTRIC CORP., LIMA, OHIO. AEROSPACE ELECTRICAL DIV.
Magnetic, electrical conductor, electrical insulation, and bore seal materials, 20: 4379 (NASA-CR-54091)

WESTINGHOUSE ELECTRIC CORP., PITTSBURGH, PA.
Prog. rpt. on growth and characterization of single crystals of rare earth compounds, 20: 4358 (AD-438516)

WESTINGHOUSE ELECTRIC CORP., PITTSBURGH, PA. ATOMIC POWER DIV.
Experimental evaluation of power coefficient in slightly enriched PWR cores, 20: 5135 (WCAP-3269-40)
Physical and mechanical properties of Zircaloy 2 and 4, 20: 4400 (WCAP-3269-41)
Prog. rpt. on Water Reactors, 1–3/65, 20: 5134 (WCAP-3269-12)
Remote underwater devices for evaluation and reduction of spent Yankee fuel assemblies, 20: 5136 (WCAP-5554)
Stress corrosion in alloys for fuel element cladding—stainless steel and Zircaloy, 20: 4328 (WCAP-3269-50)

WISCONSIN UNIV., MADISON.
Body composition by differential absorption of monochromatic x rays, 20: 3885 (ORNL-IIC-5, pp 277-89)

Z

ZENTRALINSTITUT FUER KERNPHYSIK, ROSSENDORF BEI DRESDEN (EAST GERMANY).
Simple reactivity meter of high sensitivity, 20: 5061 (ZFK-RN-22)

PERSONAL AUTHOR INDEX

Each entry after an author's name is a shortened version of the title of the report or article, followed by the *NSA* volume and abstract number. Report numbers are given in parentheses.

The phrase "Progress report" is abbreviated as "Prog. rpt.," permitting a more rapid and complete alphabetical arrangement of the titles without changing the location of the progress report titles in relation to the other titles.

Because of problems involving the mechanical preparation of this index, all accent marks are omitted. The following changes in spelling have been introduced to reduce some of the confusion which might result from omitting the accents:

ä	becomes	ae
ö		oe
ø		oe
ü		ue (except in transliterated Chinese names)

A

AALTO, E., Measured and predicted neutron fluxes in, and leakage through, configuration of perforated Fe plates in D_2O, 20: 4800 (AE-198)

AARON, R., Calculations of neutron-deuteron scattering, 20: 4614

ABBATIELLO, A. A., Dimensional location of reactor components by optical tooling, 20: 5035 (ORNL-TM-1278)

ABBATT, John D., Malignancy and other late effects following administration of Thorotrast, 20: 3753

ABBES, M., Biologic and hormonal results of destruction of pituitary by ^{90}Y, 20: 3809

ABE, Ryuji, Gradual increase of coercive field of x-irradiated Rochelle salt, 20: 3995

ABEL, W. R., Thermal and magnetic properties of liquid ^3He at low pressure and at very low temperatures, 20: 4780

ABRIKOSOV, A. A., Review of theory of superconducting alloys, 20: 4791

ACCARY, A., Morphology and mechanism of atmospheric corrosion of uranium monocarbide, 20: 4336

ACKER, Ellsworth G., Fine sized powders of thoria, urania, and mixtures thereof and methods for their preparation, 20: 3969

ACKLIN, Leo, Nuclear power system, 20: 5171

ADAMS, J. Barclay, Radiative lepton production by neutrino beam, 20: 4611

ADAMS, R. E., Evaluation of off-gas system for CP-ORR capsule experiment, 20: 5199 (ORNL-TM-1328)

ADAMSON, G. M. Jr., Army reactors program, 20: 4305 (ORNL-3870, 187-90)

ADAMSON, G. M. Jr., Fuel element development, 20: 4342 (ORNL-3870, pp 85-101)

ADAMSON, G. M. Jr., High flux isotope reactor, 20: 5174 (ORNL-3870, pp 214-29)

ADAMSON, G. M. Jr., Medium power reactor experiment, 20: 4307 (ORNL-3870, pp 238-42)

ADDE, Robert, Study of NO_3 radical in sodium nitrate irradiated at 77°K, 20: 3988

ADDINK, N. W. H., X-ray irradiation of the metalloprotein carbonic anhydrase, 20: 3693

AFANAS'EV, Yu. A., Thermochemistry of cerium(IV) nitrates, 20: 3954

AGARWALA, R. P., Diffusion of copper in nickel, 20: 4363 (AEET-CD-31)

AHTYE, Warren F., Total thermal conductivity of partially and fully ionized gases, 20: 4990

caval anastomosis, 20: 3681

AIMARD, G., Experimental study of the clearance of colloidal ^{198}Au, 20: 3680

AISU, Hideo, Evaluation and correction of error due to coarse mesh adjacent to absorbing regions in diffusion code calculations, 20: 5069

AKASOFU, S. I., Latitude of auroral activity during periods of zero and very

AIMARD, G., Clearance of radioactive colloidal gold in dog with portoweak magnetic disturbance, 20: 4740

AKIMUNE, Hideo, Dielectric properties of irradiated paraffin wax, 20: 3989

ALBURGER, D. E., Studies of electromagnetic transitions in ^{15}N and ^{15}O, 20: 4905

ALCONE, J. M., Malfunction detection and diagnosis, 20: 4222 (UCRL-13186)

ALEKPEROV, R. A., Extraction of cerium and yttrium by naphthenates, 20: 4051

ALEKSEEVSKI, N. E., Anisotropy of the Moessbauer effect in β-Sn single crystals at 4.2°K, 20: 4932

ALEXANDER, Peter, Murine leukemia cell lines of different radiosensitivity in vitro, 20: 3736

ALEXANDER, S., Nuclear quadrupole spectra in very asymmetric field gradients, 20: 4867

ALEXANIAN, Moorad, Field theory of two-pion system (S and D waves), 20: 4670

ALEXEFF, I., Report on a meeting held in the old lecture room at Christ Church College, Oxford, at 9 p.m. on Thursday, September 9, 1965, 20: 4945 (ORNL-TM-1306)

ALEXEFF, I., Report of an informal striation meeting held at the seventh international conference on phenomena in ionized gases, Belgrade, Yugoslavia, August 22–27, 1965, 20: 4946 (ORNL-TM-1307)

ALIBERT, A., Cholinesterase activities in mouse liver and kidney during experimental intoxication with uranyl nitrate, 20: 3670

ALIKHANOV, R., Neutronographic investigations of solid oxygen, 20: 4796

ALIX, Denise, Effect of fractionating 100 R hard x-ray doses on hemogram and proteinogram of rabbit, 20: 3709 (CEA-R-2865)

ALLABY, J. V., Pion-pair photoproduction below 1 Bev, 20: 4579 (AD-618661)

ALLABY, J. V., Report on inelastic electron scattering program at Stanford, 20: 4581 (AD-618663)

ALLEMANN, Rudolph T., Electrostatic apparatus for removal of dust particles from gas stream, 20: 4726

ALLEN, Harvey F., Radioactive cobalt for heat sources, 20: 4277 (DP-1012)

ALLEN, J. P., Studies on ^{19}F in $^{18}O(p,\gamma)^{19}F$ reaction, 20: 4907

ALLGOOD, J. R., Shallow-buried model arches subjected to traveling-wave load, 20: 4131 (AD-622552)

ALLINSON, J. D., Compatibility of some refractory metals with UC–ZrC, 20: 4335

ALLIO, R. J., Corrosion and hydriding of Zircaloy-4 under heat transfer conditions, 20: 4331

ALLIO, R. J., Stress corrosion in alloys for fuel element cladding—stainless steel and Zircaloy, 20: 4328 (WCAP-3269-50)

ALME, Marvin L., Reactivity approximation, 20: 5062

ALVAEGER, T., Law of conservation of nucleons, 20: 4853

AMADO, R. D., Calculations of neutron-deuteron scattering, 20: 4614

AMAR, Arjan D., Demonstration of vesicoureteral reflux without radiation exposure, 20: 3834

AMAR, Arjan D., Double dose contrast medium in excretory urography, 20: 3857

AMAURY, Paul, Improvements in or relating to methods of and apparauts for transferring liquids under remote control, 20: 4095

AMEMIYA, Ayao, Relative radiation stability of some para-polyphenyls, 20: 3991

AMIEL, J.-L., Comparison of reactivity against host of thymocytes and semiallogenic lymph node cells, 20: 3777

AMIN, M., Multipoles in square cell reactor lattice, 20: 5063

AMIRKHANOV, I., Correctness of method for unified theory of nuclear reactions, 20: 4837 (JINR-P-2310)
AMIS, E. S., Exchange reactions involving uranium and neptunium ions solvent, salt and ion effects temperature coefficients, 20: 3964
AMSEL, G., Utilization of semiconductor detectors with high-energy accelerator. I and II., 20: 4243 (LAL-1102)
AMUNDSON, P. I., Doppler coefficient measurements for ^{235}U in fast-reactor spectra, 20: 5072
ANAND, M. S., Diffusion of copper in nickel, 20: 4363 (AEET/CD/31)
ANAND, S., Elastic scattering of 1.12 Mev γ rays from platinum and tantalum, 20: 4864
ANCELLIN, Jacques, Experimental contamination of pink shrimps by ^{137}Cs, 20: 3657 (CEA-R-2818)
ANDERSEN, J., Prog. rpt. on U–Pu monoxides, 7–9/65, 20: 4327 (UNC-5138)
ANDERSON, A. C., Thermal and magnetic properties of liquid ^{3}He at low pressure and at very low temperatures, 20: 4780
ANDERSON, Daniel Harvie, Uranium–Th–Pb ages of zircons and feldspars, 20: 4169
ANDERSON, Herbert L., High energy physics research using 460 Mev synchrocyclotron, 20: 4577 (AD-618067)
ANDRAE, K., Contributions to chemistry of 4 and 6 valent U, 20: 3961
ANDRE, Stephane, Nuclear matrix elements of transition $^{42}K(2^-) \rightarrow {}^{42}Ca(2^+)$, 20: 4863
ANDREAS, R. D., Digital computer simulation as experimental tool in evaluation of sampled-data systems, 20: 4289 (SC-DR-65-318)
ANDREEVA, N. I., Thiophene ^{35}S, 20: 3976
ANGERMAN, Carl L., Radioactive cobalt for heat sources, 20: 4277 (DP-1012)
ANGHILERI, L. J., Biosynthetic preparation of ^{75}Se-methionine and ^{75}Si-cystine. Its incorporation and distribution in mice, 20: 3661 (NP-15594)
ANSELIN, Francois, Survey of uranium–carbon–nickel ternary diagram, 20: 4368 (CEA-R-2845)
ANTHONY, John W., Crystal morphology of thorium-bearing synthetic monazite, 20: 4174
ANTOKU, Shigetoshi, Radiation dose received by mother and fetus x-ray examination, 20: 3823
ANTON, H. F., Charged colloid generating system for electric propulsion, 20: 4133 (N64-25007)
ANTONANZAS, J. L., Problems in introduction of nuclear power stations in Spain, 20: 5158
ANUFRIEV, Yu. D., Use of Pomeranchuk effect to obtain infralow temperatures, 20: 4779
AOKI, Hatsue, Genetically significant radiation dose from dental x-ray diagnosis. I., 20: 4195
AOYAMA, Takeshi, On recovery-promoting chemicals after gamma-ray irradiation to mouse strain L cells cultured in vitro, 20: 3791
APELGOT, S., Measurement of radioactivity by scintillation in liquid medium: biological uses, 20: 3870 (EUR-2459.f)
APPARAO, M. V. Krishna, Propagation in space of cosmic-ray He nuclei, 20: 4568
ARCELLA, F. G., Design and evaluation of 1000 MW(e) central station power-plant with a circulating fuel gaseous core reactor, 20: 5128 (TID-22225)
ARMSTRONG, F. E., Contamination resulting from use of nuclear explosives for stimulating petroleum production, 20: 4082 (BM-RI-6684)
ARMSTRONG, Robert H., Early-time cloud rise from chemical high explosive detonations, 20: 4152 (TID-22266)
ARNOLD, Richard C., Regge poles, optical model, and high energy charge-exchange reactions, 20: 4606
ARNOULD, Claire, Hyperfine structures of ground levels of terbium, 20: 4857
ARORA, Kesturi L., Limit theorem on magnetofluid-dynamics. I., 20: 4719
ARORA, Kesturi L., Limit theorem on magnetofluid-dynamics. II., 20: 4720
ARTHUR, C. E., Contamination resulting from use of neuclear explosives for stimulating petroleum production, 20: 4082 (BM-RI-6684)
ARUNASALAM, V., Microwave absorption in hot plasma near the second harmonic of electron cyclotron frequency, 20: 4943 (MATT-379)
ASKILL, John, Bibliography on tracer diffusion in metals. II., 20: 4383 (ORNL-3795(Pt.2))
ASPIN, N., Gonadal x-ray dose to children from diagnostic radiographic technics, 20: 3854
ATEN, A. H. W. Jr., Natural radioactivity of ^{40}K, ^{87}Rb, and ^{176}Lu, 20: 4916
ATHERTON, L., Design evolution of SL 75 linear accelerator for super voltage therapy, 20: 4517
ATKINSON, P. W. M., Sintering of uranium mononitride, 20: 4349
ATTERMO, R., Study of tensile strength in soft steel, 20: 4365 (AES-3)
ATWATER, H. A., EPR measurements of radiation immunization in PMMA, 20: 4036
AUBERTIN, Ch., ^{137}Cs decontamination of concentrated fission product solutions, 20: 3874 (EUR-2535.f)
AUSKOVA, R., Calciferol estimation in irradiated yeast and mycelia, 20: 3690
AUVIL, P. R., Unitary solution to three channel N/D equations in pole approximation, 20: 4593
AWSCHALOM, M., Radiations measurements group at Princeton-Pennsylvania 3 Bev proton synchrotron, 20: 4506 (PPAD-569E)
AXFORD, W. I., Interplanetary magnetic field, 20: 4529
AYRE, D. J., Some considerations in design and engineering of active effluent treatment plants, 20: 5207
AZARY, Z., Flashing light satellite system for SNAP radiation environments, 20: 4262 (NP-15610)
AZEVEDO, A. E. G., Magnetic susceptibility of some samarium salts between 1.2 and 4°K, 20: 3930
AZZONI, P., CYRCO—program for calculation of totally reflected cylindrical reactor design, 20: 5059 (RT/FIMA(65)-1)

B

BAAS, C., Dismantling cells associated with C.E.A. research reactors, 20: 5205
BABAEV, Z. R., Electromagnetic properties of mesons in broken symmetry, 20: 4644 (JINR-P-2299)
BABB, D. D., Extrapolating electromagnetic fields from values in spherical region, 20: 4638 (AD-617965)
BACIK, Z., Calciferol estimation in irradiated yeast and mycelia, 20: 3690
BADACSONYI, Tivador, Measurement of particle residence times in fluidized bed with isotopes, 20: 4106 (BNL-tr-43)
BADER, B. E., Launch hazards assessment program, report on Atlas/Centaur abort, 20: 4187 (SC-RR-65-333)
BAER, W., Study of slightly enriched UO_2 lattice with H : U = 0.42—measurement and analysis, 20: 5071
BAETSLE, L. H., Studies on separation of ^{137}Cs and ^{90}Sr from fission in acid medium on mineral ion exchangers, 20: 3871 (EUR-2497.e)
BAGGE, E., Prog. rpt. on shielding experiments at reactor station Geesthacht, annual, 1964, 20: 4997 (EUR-2494.d)
BAHCALL, John N., Neutron stars. I., 20: 4531
BAHCALL, John N., Neutron stars. II., 20: 4532
BAILEY, W. J., FFTF driver fuel: PuO_2–stainless steel cermet, 20: 5192 (BNWL-SA-251)
BAIN, R. L., Isotopic exchange reactions in thionyl chloride and sulfuryl chloride, 20: 3965
BAIR, W. J., Pulmonary clearance of $^{59}Fe_2O_3$ and $^{51}Cr_2O_3$ in rats and dogs exposed to cigarette smoke, 20: 3655 (BNWL-SA-224)
BAKER, D. G., Studies of corneal graft reaction: effect of x-irradiation of donor tissue, 20: 3719
BAKER, Philip S., Conference on low-energy x- and gamma sources and applications, Chicago, 10/64, 20: 4111 (ORNL-IIC-5)
BALANDA, Andrzej, Methods of measuring extremely short lifetimes of nuclei in excited states, 20: 4917
BALASURRAHMANYAN, V. K., Low-energy spectrum of cosmic rays, 20: 4566
BALAZS, L. A. P., Simultaneous bootstrap of the ρ and f^0 in $\pi\pi$ scattering, 20: 4607
BALDWIN, W. F., Mutants of parasitic wasp Dahlbrominus fuscipennis (ZETT.) (Hymenoptera: eulophidae), 20: 3733
BALL, J., Industrial analysis of ^{147}Pm x rays for radiography and imaging readout, 20: 3801 (ORNL-IIC-5, pp 222-38)
BALL, J. B., Low-lying levels in ^{50}V and ^{58}Co studied with the (p,d) reaction, 20: 4899
BALTAY, C., Antihyperon production in antiproton-proton reactions at 3.7 Bev/c, 20: 4608
BANDGAARD LARSEN, F., Transfer through alpha-gamma barriers in Risoe hot cells, 20: 4042
BANERJEE, Haridas, Asymptotic behavior of forward scattering amplitude, 20: 4603
BANERJI, Sriranjan, Gravitation theory of Hoyle and Narlikar, 20: 4771
BANK, S., Malignant Zollinger-Ellison syndrome in Bantu woman with prolonged remission after gastric radiotherapy, 20: 3821
BANVILLE, B., Portable tritium-in-air monitor, 20: 4235 (AECL-2283)
BARANOW, S., Coating for niobium, 20: 4355
BARCUS, J. R., 75-second periodicity in auroral-zone x rays, 20: 4751
BARENDREGT, T. J., Economic problems in processing of irradiated fuel materials, 20: 4050
BARGER, V., New sum rule for meson-baryon total cross sections at high energy, 20: 4678
BARGER, V., SU(6) predictions for s-wave baryon-baryon scattering, 20: 4679
BARKAS, Walter H., Units for atomic and subatomic physics, 20: 4539 (UCRL-11444)
BARNA, Arpad, Compact photomultiplier-tube base, 20: 4247 (TID-21362)
BARNES, K. J., Baryon-meson vertex in relativistic SU(6) theory, 20: 4677
BARNES, R. G., Catalog of nuclear quadrupole interactions and resonance

frequencies in solids. II., 20: 3973 (IS-1222)
BAROCH, C. J., Irradiation performance of UO_2 produced by alternate fabricating processes, 20: 4459 (GEAP-4850)
BARODDY, E. M., Influence of anisotropic scattering on stopping by elastic collisions, 20: 4547
BARR, William L., Angled plate scanning interferometer, 20: 4232
BARRAT, Jean-Pierre, Transfers between hyperfine levels of odd isotopes of mercury in 6^3P_1 state under effect of collisions with rare gases, 20: 4544
BARSKI, G., Chromosomal number and radiosensitivity of experimental tumors, 20: 3751
BARUT, A. O., Position of singularities of S-matrix in unified theories, 20: 4639 (IC/65/73)
BASMAJIAN, J. A., Effect of yttrium on the recrystallization and grain growth of tantalum, 20: 4424
BASS, C. D., Infrared spectrum and vibrational analysis of dibromoborane and dibromoborane-d, 20: 3940
BASS, F. G., Theory of emission of charge passing through electrically inhomogeneous medium, 20: 4625
BASTIDE, P., Cholinesterase activities in mouse liver and kidney during experimental intoxication with uranyl nitrate, 20: 3670
BASU, Diptendu, Calculation of non-linear effects bound to propagation of electromagnetic waves in plasma, 20: 4962
BASU, J., Measurement of electron density of plasma, 20: 4967
BASU, P. K., Studies of corneal graft reaction: effect of x-irradiation of donor tissue, 20: 3719
BATSAKIS, John G., Carcinoma of thyroid gland in children and adolescents, 20: 3739
BATZENSCHLAGER, A., Cancers of bile duct in thorotrastosis of liver, 20: 3722
BAUDET, C., Synthesis of products akin to polyphenyls, 20: 3972 (EUR-2528.f)
BAUMGAERTEL, F., Decontamination of radioactive reservoir waters, 20: 4068
BAXTER, A., Safety characteristics of large gas-cooled fast power reactors, 20: 5119 (GA-6732)
BAXTER, J. P., Ten years of nuclear progress: a survey, 20: 5167
BAYLY, John G., Apparatus for determining quantity of contaminant in substance, 20: 3970
BAZIN, M., Σ radiative decay and angular momentum of Σ pionic decay, 20: 4616
BEACH, A. D., New long-period vertical-component seismometer, 20: 4216 (AWRE-O-70/65)
BEAN, W. C., In-plant teaching of nuclear reactor plant kinetics and control to graduate engineers and scientists, 20: 5025 (WAPD-T-1832)
BEARD, D. W., Industrial analysis of ^{147}Pm x rays for radiography and imaging readout, 20: 3801 (ORNL-IIC-5, pp 222-38)
BEARD, David B., Quantitative nuclear evaporation theory. II., 20: 4897
BEARD, Percy Morris Jr., High resolution study of the $^{18}O(p,n)^{18}F$ reaction, 20: 4927
BEASLEY, T. M., Distribution and excretion of technetium in humans, 20: 3663 (TID-22318)
BEAUFAIT, L. J. Jr., Survey and recommendations for radioisotope applications pertinent to U. S. Naval Civil Engineering Laboratory Operations, 20: 4089 (TLW-1055A)
BEAUMEVIEILLE, H., Study of $^{16}O(d,\alpha_0)$, $^{16}O(d,p_0)$, and $^{16}O(d,p_1)$ reactions at 300 kev to 1 Mev, 20: 4870
BECKER, J. F., Infrared properties of 40-60 Mev electron-irradiated germanium, 20: 4468
BEGUIN, Claude, Process for production of tantalum or niobium in hydrogen plasma jet, 20: 4314
BEIL, Hans, Study of some transversal motions of electron beam in linear accelerator, 20: 4494 (CEA-R-2843)
BEILHARZ, Rolf George, Genetic analysis of behavior traits in swine, 20: 3784
BEJSOVEC, V., Source of polarized ions for cyclotron, 20: 4519
BELAI, G. E., Investigation of cerium distribution in cast iron by means of electron probe, 20: 4414
BELL, George I., Polarization effects on neutron transport, 20: 4814
BELL, T. F., Nonlinear Alfven waves in Vlasov plasma, 20: 4978
BELL, T. K., Annular counting of radioisotopes in large liquid volumes on well type scintillation crystal of sodium iodide, 20: 3817
BELL, W. A., Review of ORNL electromagnetic separations program, 20: 4282 (ORNL-3861)
BELLER, L. S., Effective resonance integral and Doppler effect in ^{197}Au. I., 20: 4841 (NAA-SR-Memo-11511)
BELON, A. E., Latitude of auroral activity during periods of zero and very weak magnetic disturbance, 20: 4740
BELONOGOV, A. V., Expansion mechanism of 40 cm hydrogen bubble chamber of JINR, 20: 4257
BELSON, John D., Prog. rpt. on PM-1, annual, 11/63–10/64, 20: 5108 (AD-618376)
BELTRAMETTI, Enrico, Group theoretical properties of complex angular momenta, 20: 4700
BELY, Francoise, Excitation by electron impact of strongly ionized ions of p^2 configuration, 20: 4543
BELY, Oleg, Excitation by electron impact of strongly ionized ions of p^2 configuration, 20: 4543
BENAKSAS, D., Utilization of semiconductor detectors with high-energy accelerator. I and II., 20: 4243 (LAL-1102)
BENAROYA, R., Development of variable-energy cyclotron HIVEC, 20: 4491 (ANL-7081, pp 78-80)
BENDER, H., Oxidation resistant coatings on niobium, 20: 4315
BENEDIKTOV, E. A., Anomalous ionization of lower ionosphere of temperate latitudes during world magnetic storms, 20: 4736
BENIOFF, Paul A., Nuclear recoil and simple nuclear reactions, 20: 4893
BENTON, E. V., Charged particle tracks in polymers. 1., 20: 4251 (USNRDL-TR-917)
BERG, S., Radiation-induced electronic phenomena in polyethylene, 20: 4035
BERGER, Harold, Neutron radiography. Methods, capabilities, and applications, 20: 4115
BERGER, Richard A., Transition probabilities in highly ionized p^2 and p^4 configurations, 20: 4553
BERGERE, Roland, Study of some transversal motions of electron beam in linear accelerator, 20: 4494 (CEA-R-2843)
BERGSTROEM, J., Experiments on starting process of rotating plasma, 20: 4951
BERGSTROEM, J., Free-wheeling of rotating plasma, 20: 4953
BERGSTROM, J. C., Electron and positron scattering and anapole, 20: 4612
BERLAND, R. F., CAT—concentration and temperature. Code describing simultaneous heat and mass transfer for an infinite cylinder, 20: 4103 (NAA-SR-Memo-11099)
BERMAN, S. M., Spin and parity analysis in two-step decay processes, 20: 4585 (SLAC-43)
BERMANIS, H. L., Nine and sixteen group cross sections for reactor analysis, 20: 4829 (GEMP-173(Suppl.1))
BERNARD, Jean, Chromosomes and leukemia, 20: 3730
BERNARD, W., Equivalence of stress- and radiation-induced defects in degenerate p-n junctions, 20: 4264
BERNDT, A. F., Some intermediate phases in thorium–technetium and uranium–technetium systems, 20: 4428
BERNDT, Alan F., Preferred orientation in sheet of alpha-rolled plutonium, 20: 4407
BERTHEL, K. H., Electrical resistivity of W single crystals, 20: 4453
BERTHIER, Jean, Decay of ^{183}Hf, 20: 4862
BERTINOV, A. I., Method for sustaining assigned conducting gas flow in transverse magnetic field, 20: 4716
BERTOLOTTI, M., Electron microscope observation of high-energy-neutron-irradiated germanium, 20: 4467
BERTUCCIO, T. D., Drift tube rf system, 20: 4507 (PPAD-2137-560)
BESSON, Jean, Hydrolysis of thorium dicarbide, 20: 3937
BESSONOV, A. F., Kinetics of oxidation of uranium by air, oxygen, and carbon dioxide, 20: 4329 (CEA-tr-R-1868)
BESSONOV, A. F., Oxide systems for measuring electric resistance and x-ray analysis of specimens, 20: 3953
BESSONOV, A. F., Studies of uranium dioxide oxidation by means of high-temperature electroconductivity, x-ray phase studies, and continuous weighing, 20: 3952
BETTERTON, J. O., Electronic properties of metals and alloys, 20: 3920 (ORNL-3870, pp 27-37)
BETTERTON, J. O., Method for increasing critical current of superconducting alloys, 20: 4799
BETZ, Frederick William, Polarization parameter in proton-proton scattering from 328 to 736 Mev, 20: 4588 (UCRL-11565)
BEWLEY, D. K., Effect of fractionation on four day survival of mice after whole-body neutron irradiation, 20: 3728
BEYNON, T. D., Resonance capture and doppler coefficient in cylindrical uranium fuel elements, 20: 5092
BEYSTER, J. R., Prog. rpt. on integral neutron thermalization, 4–6/65, 20: 4801 (GA-6634)
BHATIA, C. R., Effect of nitric oxide on x-ray sensitivity of Crotalaria intermedia seeds, 20: 3759
BHAVILAI, Rewi, Structure of solar chromosphere. 1., 20: 4528
BIBRING, Herve, Examination by electron microscope of niobium contaminated at high temperature by interstitial elements, 20: 4401 (ANL-Trans-218)
BICKEL, William S., Experimental study of effects of absorption on spectral lines from plasma, 20: 4974
BIEFER, G. J., Effect of U additions on corrosion behavior of AISI type 430 stainless steel, 20: 4325 (TB-58)
BIETTI, Amilcare, Dashen-Lee sum rules for magnetic moments, 20: 4598
BIGGINS, J., Nucleic acid content of chloroplasts of spinach isolated by a nonaqueous technique, 20: 3649 (UCRL-11475)
BILLION, Marc, Recrystallization, grain growth, and preferred orientations

of zirconium purified by zone fusion, 20: 4413
BISHOP, Stanley R., Logarithmic current-to-voltage amplifier with high sensitivity, stability, and dynamic range, suitable for field application, 20: 4221 (UCRL-12394-T)
BISHOP, W., Thermoluminescent neutron dosimetry system, 20: 4236 (BNL-9605)
BITEAU, J., Dismantling workshop for Orgel fuel elements, 20: 4064
BJOERNHOLM, S., Decay of 185-μsec isomer in ^{166}Ho, 20: 4889
BLACHOT, Jean, Decay of ^{192}Re, 20: 4861
BLACHOT, Jean, Decay of ^{183}Hf, 20: 4862
BLACK, Elizabeth G., Radioisotope osteogram in rickets, 20: 3672
BLACK, W. C., Thermal and magnetic properties of liquid ^{3}He at low pressure and at very low temperatures, 20: 4780
BLACKBURN, W. S., Creep bowing of fuel element against continuous restraint, 20: 5090
BLACKER, H. Martin, Case of aseptic meningitis secondary to intrathecal injection of ^{131}I human serum albumin, 20: 3843
BLAND, William H., Nuclear medicine, 20: 3860
BLINOV, P. I., Effect of helical field on ohmic heating of plasma in S-1 apparatus, 20: 4937 (IAE-907)
BLOCK, Arthur D., Method and apparatus for measuring hydrogenous material, 20: 3913
BLOOMSTER, C. H., Fabrication costs for Pu fuel elements. D., 20: 4339 (BNWL-131D)
BLUM, Pierre, Hydrolysis of thorium dicarbide, 20: 3937
BLUMENBERG, Wayne Edward, Fortran simulation of digital differential analyzer, 20: 5214 (IS-T-33)
BLUMENFELD, H., Σ radiative decay and angular momentum of Σ pionic decay, 20: 4616
BOEHME, G., Transfer procedures used in alpha-gamma hot laboratory at Karlsruhe, 20: 4209
BOENIG, Herman V., Investigation of pyrolytic products of irradiated cigarettes, 20: 3984 (ORO-633)
BOERMAN, D. J., Computer analyses of tensile tests, 20: 4371 (EUR-2514.e)
BOERSCH, H., Transition radiation, bremsstrahlung and plasmastrahlung, 20: 5017
BOHNE, F., Studies of radiation biology of T5 receptor, 20: 3787
BOKROS, J. C., Prog. rpt. on advanced, graphite-matrix, dispersion type fuel systems and research on graphite, 11/15/64–2/14/65, 20: 5089 (GA-6181)
BOLDT, E., Low-energy spectrum of cosmic rays, 20: 4566
BOLLACASA, D., LINK. Combined slowing-down and thermalization program with a thermal cutoff of 3.06 ev, 20: 4804 (KAPL-3098)
BOLLIGER, Theodore T., Use of ^{99m}Tc pertechnetate in cardiac scanning, 20: 3831
BONAMOUR, Anne-Marie, Improvements in grafted copolymers and methods of obtaining them, 20: 4038
BONAZZOLA, G. C., Excited-core model in ^{27}Al, 20: 4891
BONDARENKO, D. V., Thermal electronic properties of tungsten–hafnium system, 20: 4405 (K-Trans-9)
BONNET, G., Machining and dismantling methods in high activity cells at Ispra, 20: 4125
BONNET, Jacques, Study of resistivity of solid phases of lutetium–hydrogen system, 20: 3934
BONNET, P., Computer analyses of tensile tests, 20: 4371 (EUR-2514.e)
BOON-LONG, P., Absorption of 200 kv x rays and ^{60}Co γ rays in the human body, 20: 4207
BORGGREEN, J., Decay of 185-μsec isomer in ^{166}Ho, 20: 4889
BORGWALDT, Horst, Common theory for neutronic noise analysis experiments in nuclear reactors, 20: 5076
BORISOV, N. G., Multiple acceleration system for high energy particle electrodynamic separator, 20: 4496 (JINR-P-2375)
BORLAI, Oszkar, Measurement of particle residence times in fluidized bed with isotopes, 20: 4106 (BNL-tr-43)
BORY, Louis, Is skin a screen for cosmic radiation? 20: 3731
BORY, Philippe, Is skin a screen for cosmic radiation? 20: 3731
BOSCH, F., Problems in introduction of nuclear power stations in Spain, 20: 5158
BOSE, S., Deuterium isotope effects in cytology, 20: 3651
BOSSHARD, R., Utilization of semiconductor detectors with high-energy accelerator. I and II., 20: 4243 (LAL-1102)
BOUCHARD, J., Treatment of Mikulicz's disease with radiation therapy, 20: 3826
BOUDETTE, W. V., Roentgen study of soft tissues of pregnancy, 20: 3825
BOURQUE, J. M., Users report for pump impeller codes, 20: 4088 (TIM-949)
BOWMAN, H. R., Emission of K x rays and division of nuclear charge in spontaneous fission of ^{252}Cf, 20: 4914
BOX, W. D., ^{147}Pm—radiation measurements of one-watt, prototype heat source, 20: 4279 (ORNL-TM-1177)
BOYARKINA, A. N., Sensitivity of some nuclear characteristics to intermediate coupling parameters, 20: 4835 (JINR-P-2287)
BOYARSKI, Adam, Compact photomultiplier-tube base, 20: 4247 (TID-21362)
BOYD, R. L. F., Recent studies of ionosphere by space vehicles, 20: 4760
BOYNTON, Allen R., Thermal disadvantage factors in very undermoderated water-uranium oxide lattices, 20: 5073
BRADFORD, D., Prog. rpt. on silica fiber/core-sheath fiber, final, 2/64–6/65, 20: 4338 (AD-620055)
BRADLEY, Edward L., Arc spray powder feeder for ultra-fine particles with a wide range of densities, 20: 4298 (LA-DC-7275)
BRADLEY, M. J., Chemical disintegration and recovery of uranium from sintered graphite–uranium compacts, 20: 4074
BRAHMAVAR, S. M., Comparative half-lives of Δ I = 3, no β transitions in even nuclei, 20: 4874
BRANDHORST, H. W. Jr., Fission of ^{197}Au by intermediate-energy He ions, 20: 4894
BRANEMARK, P. I., Regeneration of bone marrow, 20: 3789
BRANS, Carl H., Singularities in bootstrap gravitational geons, 20: 4767
BREAULT, Eugene A., Ion-exchange resin separation and flame photometric determination of sodium, potassium, magnesium, calcium, and strontium, 20: 4053
BREAZEALE, M. A., Ultrasonic studies of the nonlinear behavior of solids, 20: 5012
BREHM, J. J., Unitary solution to three channel N/D equations in pole approximation, 20: 4593
BREINE, U., Regeneration of bone marrow, 20: 3789
BREIT, G., Soluble semiclassical particle transfer problem, 20: 4850
BRESSANI, T., Excited-core model in ^{27}Al, 20: 4891
BRETON, Claude, Method for measurement of electron temperature in ionization phase of pulsed discharge in hydrogen, 20: 4714
BRETON, Claude, Reabsorption of L_β and H_α rays in pulsed discharge in hydrogen, 20: 4964
BREZIN, Colette, Comparison of reactivity against host of thymocytes and semi-allogenic lymph node cells, 20: 3777
BRIFFAUD, G., Dismantling cells associated with C.E.A. research reactors, 20: 5205
BRIFFAUD, G., Radioscopy and radiography equipment for irradiated fuel elements, 20: 4117
BRINDLEY, J. H., Evaluation of thermocouple thermal-loading errors for surface-attached thermocouple on flat-plate fuel element, 20: 5026
BRINI, D., Terrestrial albedo of 40- to 190-kev x rays, 20: 4752
BRINKMAN, G. A., Natural radioactivity of ^{40}K, ^{87}Rb, and ^{176}Lu, 20: 4916
BRINKMANN, G., Use of standardized, movable, in-cell boxes, 20: 4093
BRITTIN, Wesley E., Lectures in theoretical physics, 20: 4487
BRODE, H. L., Nuclear explosions in cavities, 20: 4167 (RM-3727RAND))
BROIDO, J., Safety characteristics of large gas-cooled fast power reactors, 20: 5119 (GA-6732)
BROMLEY, D. A., Alpha-particle-induced breakup of deuteron, 20: 4596
BROMLEY, D. A., Studies on ^{19}F in ^{18}O(p,γ)^{19}F reaction, 20: 4907
BROOKS, R. O., Shock springs and pulse shaping on impact shock machines, 20: 4112 (SC-TM-65-443)
BROYMAN, E. G., Phonon spectrum of lattice of white tin, 20: 5005 (IAE-928)
BROWMAN, Andrew Arnold, Positron-proton scattering, 20: 4630
BROWN, Eugene H. C., Servomechanical fluid charging and volume control system for nuclear reactor, 20: 5046
BROWN, F. L., Remote metrology and examination techniques on irradiated fuel materials, 20: 4124
BROWN, James Barrett, High-energy electron injury from accelerator machines, 20: 3724
BROWN, W. Lynn, Possible artifact in cyclic variations in radiosensitivity, 20: 3766
BROWNELL, Arnold S., Ultraviolet light inhibition of galactoside permease induction, 20: 3688
BROWNING, W. E. Jr., Evaluation of off-gas system for CP-ORR capsule experiment, 20: 5199 (ORNL-TM-1328)
BRUBAKER, C. H. Jr., Electron-exchange reaction between $SbCl_3$ and $SbCl_5$ in carbon tetrachloride, 20: 3962
BRUN, Colette, Light isotopes of polonium produced by nuclear reactions of ^{12}C ions on platinum, 20: 4860
BRUNERIE, D., Experimental study of the clearance of colloidal ^{198}Au, 20: 3680
BRUNST, V. V., Effects of ionizing radiation on development of amphibians, 20: 3773
BRUSSEL, M. K., (^{3}He,α) Pickup reactions in ^{58}Ni and ^{60}Ni, 20: 4892
BUCHANAN, C. D., Experimental evidence for possible meson-exchange contribution to elastic electron-deuteron scattering, 20: 4580 (AD-618662)
BUCHHEIM, W., Bibliographical survey on facilities and processes for radioactive milk decontamination, 20: 3872 (EUR-2507.d)
BUCK, K. E., RISE. Radioisotope submersible engine, 20: 4276 (AGN-8128)
BUDKER, G. I., Plasma with relativistic electrons in trap with magnetic mirrors, 20: 4950 (UCRL-Trans-1261(L))
BUETON, Milton, Luminescence phenomena in gamma-irradiated pure alkane glasses, 20: 3990

BULLIER, Denise, Radiochemical determination of ^{90}Sr in large volumes of drinking water, 20: 3867 (CEA-R-2844)
BUMP, T. R., Faret core I fuel irradiation program and reference design, 20: 5190 (ANL-7106)
BUNCH, Stanley Marion, Interaction of 31 Mev protons with deuterium, 20: 4929
BUNCH, Wilbur L., Mounting of fuel tube in reactor shielding, 20: 5054
BUNDE, E., Absorption of x rays in body equivalent phantom, 20: 3816
BURGESS, Thomas J., Effect of high velocity translation on photon correlations in laser interferometers, 20: 4223 (UCRL-14345)
BURGET, J., Dynamic polarization of protons and nuclei of fluorine in irradiated polymers, 20: 4037
BURKO, Jakub, Method of preparing uranic oxide in granulated form, 20: 3971
BURLEY, Harvey, Method and apparatus for measuring hydrogenous material, 20: 3913
BURNETT, J. R., Flashing light satellite system for SNAP radiation environments, 20: 4262 (NP-15610)
BURNIE, Glen, Fine sized powders of thoria, urania, and mixtures thereof and methods for their preparation, 20: 3969
BURNS, L. S., Neutron cross section library for Monte Carlo codes FMC-N, 18-0, and 18-1, 20: 4830 (GEMP-384)
BURSTEIN, Samuel Z., Finite difference calculations for hydrodynamic flows containing discontinuities, 20: 4705 (NYO-1480-33)
BURTON, R. A., Prog. rpt. on liquid-metal lubricated journal bearings, 4–7/65, 20: 4078 (SWRI-1228-67)
BURTON, Rodney L., Ejection of pinched plasma from axial orifice, 20: 4138
BURUSHINA, T. N., Free radicals of γ irradiated olefinoorganic silicates, 20: 4012
BUSCHKE, Franz, Progress in radiation therapy: introduction, 20: 3849
BUSCHOW, K. H. J., Phase relations and intermetallic compounds in the systems neodymium–aluminium and gadolinium–aluminium, 20: 4427
BUSER, W. H., Influence of weather on salt distributions and aerosols on beaches, 20: 4148 (AD-623515)
BUSHMER, Charles P., Effect of neutron bombardment on kinetics of some reconstructive phase transformations, 20: 4462
BUSSI, Jean, Improvements in valves for fluid flow control, 20: 5042
BUSTARD, Thomas S., Bremsstrahlung from ^{90}Sr–^{90}Y in thin absorbers, 20: 5000 (ORNL-IIC-5, pp 91-8)
BUT, D. A., Method for sustaining assigned conducting gas flow in transverse magnetic field, 20: 4716
BUTLER, D. S., One-dimensional flow in ionizing gas, 20: 4717
BYCHKOV, J. F., Superconductive properties of Nb–Zr alloys, 20: 4792
BYRD, B. L., Bone scanning with ^{68}Ga: carrier effect, 20: 3676
BYRNE, John J., Effect of ionizing irradiation on developing maxilla and mandible, 20: 3808

C

CABELL, M. J., Uses of reactors in neutron activation analysis, 20: 3864 (AERE-L-166)
CAIRD, R. S., Cylindrical explosive flux-compression system, 20: 4477 (LA-DC-7289)
CAIRD, R. S., Plasma compression by explosively produced magnetic fields, 20: 4941 (LA-DC-7290)
CAIRNS, R. C., Recovery of spent nuclear fuels: processing, 20: 4069
CALAIS, Daniel, Survey of uranium–carbon–nickel ternary diagram, 20: 4368 (CEA-R-2845)
CALDWELL, Richard L., Calibration of radioactive well logging system, 20: 4171
CALKIN, M. G., Invariance property of free electromagnetic field, 20: 4710
CALLCUT, V. A., Ageing of Chromel–Alumel thermocouples, 20: 4398 (TRG-Report-1021)
CALLEBAUT, D. K., Ion density in electron beams, 20: 4722
CALNE, R. Y., Selective lymphopenia by use of intralymphatic ^{198}Au and splenectomy, 20: 3729
CALVERT, H. T., Dermatomyositis following treatment of cancer, 20: 3847
CAMERON, A. G. W., Composition of matter in nuclear statistical equilibrium at high densities, 20: 4855
CAMERON, J. F., Radioisotope sources of low-energy electromagnetic radiation and their use in analysis and measurement of coating thickness, 20: 4219 (ORNL-IIC-5, pp 182-205)
CAMERON, J. R., Body composition by differential absorption of monochromatic x rays, 20: 3885 (ORNL-IIC-5, pp 277-89)
CAMPBELL, Evan E., Determination of low level plutonium activity; autoradiographic techniques vs. scintillation counting, 20: 3877 (LA-DC-7483)
CAMPBELL, Ronald Hugh, Control rod position indicating apparatus and method, 20: 5048
CAP, Ferdinand, Gasdynamic methods in MHD flow, 20: 4702 (AD-619094)
CARAMAUX, G., Dismantling cells associated with C.E.A. research reactors, 20: 5205
CARLSMITH, R. S., Response of helium-cooled fast reactor to changes in coolant flow and reactivity, 20: 5127 (ORNL-P-1698)
CARLTON, J. E., Bone scanning with ^{68}Ga: carrier effect, 20: 3676
CARLTON, R. D., Prog. rpt. on portable thermoelectric generator, 6/65, 20: 4571 (AD-618037)
CARMELI, Moshe, Equations of motion without infinite self-action terms in general relativity, 20: 4768
CARPENTER, Donald G., Reactivity approximation, 20: 5062
CARPENTER, Dwight William, Measurement of the $K_{\mu 3}$ decay spectrum of the K_2^0 meson, 20: 4631
CARPER, H. J., Prog. rpt. on liquid-metal lubricated journal bearings, 4–7/65, 20: 4078 (SWRI-1228-67)
CARR, W. J., Geology and surface effects, handcar event, 20: 4144 (PNE-810F)
CARRIVEAU, G., Prog. rpt. on integral neutron thermalization, 4–6/65, 20: 4801 (GA-6634)
CARROLL, H. W., Evidence for humoral mediation of radiation-induced motivation obtained from parabiont rats, 20: 3706 (AD-623365)
CARROLL, Keith J., Elastic constants of niobium from 4.2° to 300°K, 20: 4422
CARTA, J. S., Low pressure oxidation of pure columbium, 20: 4324 (PWAC-460)
CASALI, F., CYRCO—program for calculation of totally reflected cylindrical reactor design, 20: 5059 (RT/FIMA(65)-1)
CASE, Carl T., Nonlinear interaction of r-f wave with inhomogeneous plasma slab. II., 20: 4954
CASSEDANNE, Jeannine, Study of equilibrium diagram of La_2O_3–PbO, 20: 3931
CATHCART, J. V., Surface reactions of metals, 20: 4320 (ORNL-3870, pp 70-4)
CAUSER, R., Non-destructive examination of irradiated nuclear fuel, 20: 5093
CAUWE, J., Machining and dismantling methods in high activity cells at Ispra, 20: 4125
CAVALLARO, Leonardo, Stress analysis of axisymmetric disk with variable thickness, 20: 4075 (GA-6267)
CAYOLLA DA MOTTA, L., Malignancy and other late effects following administration of Thorotrast, 20: 3753
CAZALIS, J. P., Special procedure for alpha–beta–gamma transfers of large pieces of equipment, 20: 4210
CEDERQUIST, Ebbe, Whole-body counting of ^{85}Sr and ^{47}Ca in patients with widespread malignant skeletal disease, 20: 3805
CERVERA, J., Problems of supply of electrical energy in Spain, 20: 4081
CESARANO, C., Decontamination experience at hot laboratory of Casaccia, 20: 4211
CESARANO, C., Techniques for dismantling irradiated rigs, 20: 4092
CHABAL, J., Clearance of radioactive colloidal gold in dog with portocaval anastomosis, 20: 3681
CHAMBERS, H. L., Influence of operating conditions on radiation damage to transistor gain, 20: 4267
CHAMPAGNE, Robert J., Calibration and response of personnel monitoring film dosimeters to synchrotron stray radiations, 20: 4237 (BNL-9665)
CHAMPAGNE, Robert J., Linear energy transfer spectra and effective quality factors in stray radiation areas at Brookhaven National Laboratory proton synchrotrons, 20: 4176 (BNL-9684)
CHAN, Loi-Him, Strong and electromagnetic decay of mesons, 20: 4674
CHANDRASEKHAR, S., Higher order virial equations and their applications to equilibrium and stability of rotating configurations, 20: 4295
CHANG, George Kuei-chang, Magnetic transition of thin superconducting films, 20: 4785
CHAPIRO, Adolphe, Improvements in grafted copolymers and methods of obtaining them, 20: 4038
CHAPPELL, Willard R., Lectures in theoretical physics, 20: 4487
CHAPUT, Michel, Comparison of spectrographic methods of analysis of plutonium and its compounds, 20: 3869 (CEA-R-2869)
CHARAP, J. M., Complex angular momentum theory of particles with spin, 20: 4697
CHARLAND, Telesphore L., Neutronic reactor fuel element and member therefor, 20: 5096
CHARLESBY, A., Radiation-induced crosslink formation in polyethylene. I., 20: 4002
CHARLESBY, A., Recent development in irradiation treatment of polymers, 20: 4033
CHASE, Lawrence P., Radiation-induced changes in epithelium of Buccal mucosa, 20: 3744
CHATTERJEE, G., Elastic scattering and polarization of electrons by atom in second Born approximation, 20: 4545
CHAU, Paul M., Radiotherapeutic management of malignant tumors of vagina, 20: 3848
CHEN, Kuo-chun, Genetics of Sordaria brevicollis, 20: 3783
CHENEY, Kenneth B., Sputtering at acute incidence, 20: 4546

CHENG, David, Nucleon-nucleon polarization at 700, 600, 500, and 400 Mev, 20: 4590 (UCRL-11926)
CHEN-TSAI, Ching-tang, Beta-decay of hypernuclei, 20: 4930
CHEREMNYKH, P. A., Effect of helical field on ohmic heating of plasma in S-1 apparatus, 20: 4937 (IAE-907)
CHEW, Geoffrey F., Dynamical formula for slope of Pomeranchuk trajectory, 20: 4587 (UCRL-11495)
CHEW, Geoffrey F., Pomeranchuk repulsion and resonance narrowing, 20: 4686
CHIAVASSA, E., Excited-core model in ^{27}Al, 20: 4891
CHILDS, W. J., Atomic-beam research, 20: 4535 (ANL-7081, pp 128-9)
CHIU, H. Y., Selected topics in modern theoretical physics, 20: 4533
CHOQUET, Claudine, Comparison of reactivity against host of thymocytes and semi-allogenic lymph node cells, 20: 3777
CHOU, Chin, Critical shear stress of Mo single crystal, 20: 4445
CHRISTENSEN, A., 75-second periodicity in auroral-zone x rays, 20: 4751
CHRISTOPHER, S. S., Prog. rpt. on correlations between sensitization and stress corrosion cracking of 300 series stainless steels, 7–9/65, 20: 4370 (CEND-3256-250)
CHUIKO, A. A., Free radicals of γ irradiated olefinoorganic silicates, 20: 4012
CHUN, Mu, Investigation of reactions $\pi^- p \to n \pi^0 + n$ at the π^- momentum of 4 Bev/c, 20: 4582 (JINR-P-2361)
CHUNG, K., Optimum generation of ion-cyclotron waves in cylindrical two-ion plasma, 20: 4984
CHUNG, Victor, Infrared divergence in quantum electrodynamics, 20: 4765
CHWOJNIK, A., Prog. rpt. on improvement of renogram techniques, final, 20: 3800 (NP-15150)
CIAFALONI, M., Operator analysis of Bethe-Salpeter equation, 20: 4661
CIRIC, Ivan, Analysis of 96 abnormal brain scans using ^{99m}Tc (pertechnetate form), 20: 3824
CIRIEGI, U., Terrestrial albedo of 40- to 190-kev x rays, 20: 4752
CLARK, A. J. Jr., AERO heating results from RFD-2 flight test, 20: 4280 (SC-DC-65-1601)
CLARK, G. W., Crystal physics, 20: 3919 (ORNL-3870, pp 3-6)
CLAYTON, D. D., Photon-induced beta decay in stellar interiors, 20: 4530
CLEARY, R. E., Alkali metal corrosion. I., 20: 4318 (CNLM-5359)
CLIFFORD, C. E., Snap shielding program at ORNL, 20: 5183 (ORNL-P-1736)
CLINE, Douglas, Study of ^{19}F(^{3}He,d)^{20}Ne reaction, 20: 4908
CLINTON, S. D., Preparation of thoria and mixed-oxide microspheres, 20: 3922 (ORNL-TM-1281)
CLOUSTON, J. G., Industrial applications of radiation, 20: 4270
COBBLE, J. W., Fission of ^{197}Au by intermediate-energy He ions, 20: 4894
COHEN, Gerald, Light scattering of water, deuterium oxide, and other pure liquids, 20: 3941
COHEN, Jules Bernard, Effects of ionizing radiation on aqueous solutions of detergent alkylbenzenesulfonate and several lower homologs, 20: 4025
COHEN, V. W., Nuclear spin and magnetic moment of ^{37}Ar, 20: 4890
COJAN, Jean-Louis, Transfers between hyperfine levels of odd isotopes of mercury in 6^3P_1 state under effect of collisions with rare gases, 20: 4544
COLBURN, D. S., Recurrent Si^+–Si^- impulse pairs and shock structure in M-region beams, 20: 4758
COLEMAN, E. W., Industrial analysis of ^{147}Pm x rays for radiography and imaging readout, 20: 3801 (ORNL-IIC-5, pp 222-38)
COLGATE, S. A., Underground neutrino experiment. I., 20: 4847 (UCRL-12085(Pt.1))
COLGATE, S. A., Underground neutrino experiment. II., 20: 4848 (UCRL-12085(Pt.2))
COLLIER, J. G., Further geometrical factors affecting dryout heat flux in vertical, internally heated annuli cooled by steam/water mixtures at 1000 psi, 20: 4099 (AECL-2333)
COLLINS, H., X-ray absorptiometry with beta-stimulated x-ray sources, 20: 3882 (ORNL-IIC-5, pp 51-71)
COLLVER, M. M., Charged particle tracks in polymers. 1., 20: 4251 (USNRDL-TR-917)
COLSON, C., Effect of γ rays on serum albumin, 20: 3687
COLVETT, D., Thermoluminescent neutron dosimetry system, 20: 4236 (BNL-9605)
COMETS, Jean-Claude, Study of effect of electron irradiation on piezoelectric quartz films, 20: 4463
COMPRELLI, F. A., High-temperature tensile properties of selected alloys after prolonged thermal exposure, 20: 4373 (GEAP-4794)
CONTAMIN, Ghislaine, Noble gas compounds, 20: 3915 (CEA-Bib-61)
COOBS, J. H., Gas-cooled reactor program, 20: 4306 (ORNL-3870, pp 194-213)
COOBS, J. H., Preparation, coating, evaluation, and irradiation testing of sol-gel oxide microspheres, 20: 4344 (ORNL-P-1725)
COOKE, J. W., Prog. rpt. for physical properties group, 10/65, 20: 4310 (ORNL-P-1699)
COOPER, J. C., Effect of dimensional tolerances on power output of radiation cooled thermoelectric converter, 20: 5179 (NAA-SR-Memo-6484)
CORDISCHI, D., Radiation-induced polymerization of 1,2-cyclohexene oxide, 20: 3992
CORELLI, J. C., Infrared properties of 40-60 Mev electron-irradiated germanium, 20: 4468
CORINALDESI, Alberto, Modifications of iliac and lumboaortic lymphographic findings, following irradiation, 20: 3852
CORINALDESI, E., Operator gauge transformations, 20: 4762
CORLESS, James T., Determination of calcium in sea water, 20: 3902
CORNELL, D. C., SAFE-PCRS. Computer program for stress analysis of bodies of revolution, 20: 5033 (GA-6588)
CORNELL, R. M., Behavior of fission product gases in uranium dioxide, 20: 4435
CORNGOLD, Noel, Decay constant of neutron pulse, 20: 4816
CORNIE, James A., Phase diagram of Cb–Zr–C system at 1538C and 1092C, 20: 4392 (PWAC-461)
CORTI, F., Determination of tritium content in samples (a review). Part I., 20: 3876 (ISS-65/8)
CORWIN, W. C., Internal friction in ZrO_2 containing CaO, 20: 3945
COSTANTIN, P., Measurement technology in nuclear power plants, 20: 5141
COSTANZA, J. L., Dynamic performance optimization for numerical control systems, 20: 5220 (UCRL-13185)
COSTANZA, J. L., Malfunction detection and diagnosis, 20: 4222 (UCRL-13186)
COUSSEMENT, R., Explanation of beta decay of ^{32}P, 20: 4873
COWAN, Frederick P., Health physics program for Brookhaven National Laboratory synchrotrons, 20: 4175 (BNL-9650)
COZENS, J. R., Theory of double probe at high gas pressure, 20: 4968
CRAWFORD, F. W., Beam-plasma interaction in warm plasma, 20: 4947 (SU-IPR-13)
CREAGAN, Robert J., Heterogeneous breeder or converter type neutronic reactor, 20: 5082
CRESPI, H. L., Deuterium isotope effects in cytology, 20: 3651
CRISS, Cecil M., Thermodynamic properties of ions in aqueous and non-aqueous solutions at various temperatures, 20: 3924 (TID-22366)
CRISS, Cecil M., Thermodynamic properties of non-aqueous solutions. II., 20: 3925 (TID-22366, App. B)
CROCKER, G. R., Physical and radiochemical properties of fallout particles, 20: 4156 (USNRDL-TR-899)
CROOKS, D. D., Mechanical property evaluation of Be-38% Al alloy from –320 to 800F, 20: 4440
CROSBIE, K., Prog. rpt. on integral neutron thermalization, 4–6/65, 20: 4801 (GA-6634)
CROUCH, M. F., Interaction of muons produced by atmospheric neutrinos, 20: 4561 (COO-818-64)
CROZY, A., Study of complex and covalent iron compounds using ^{57}Fe Moessbauer effect, 20: 3927 (AERE-Trans-1026)
CULWICK, B. B., Antihyperon production in antiproton-proton reactions at 3.7 Bev/c, 20: 4608
CUNDALL, R. B., Energy transfer effects in irradiation of benzene + butene-2 mixtures, 20: 4014
CUNNINGHAM, J. E., Bonus reactor support program, 20: 5126 (ORNL-3870, pp 293-9)

D

DADD, A. H., Studies on induced mutants of corynebacterium fascians, 20: 3723
D'AGOSTINO, J. P., Geology and surface effects, handcar event, 20: 4144 (PNE-810F)
DA GRAGNANO, V. L., Influence of weather on salt distributions and aerosols on beaches, 20: 4148 (AD-623515)
DAHL, Oris I., Attempt to observe a positive-strangeness baryon, 20: 4589 (UCRL-11754)
DALGARNO, A., Electron temperatures in D region, 20: 4727 (AD-618054)
DALMAN, J., Atomic-beam research, 20: 4535 (ANL-7081, pp 128-9)
DALRYMPLE, Glenn V., Effect of massive doses of 32 Mev protons and ^{60}Co radiation on primates, 20: 3692
DANFORTH, John P., Method and apparatus for measuring hydrogenous material, 20: 3913
DANIEL, H., Conversion of 238.6-kev γ line of ThB and comparison with the tables of Sliv and of Rose, 20: 4920
DANIELSSON, Ingvar, Scattering of x rays in aqueous solutions of sodium caprylate, 20: 4483
DAOU, Joseph N., Metastable equilibrium of lanthanum–hydrogen system, 20: 3936
DAOU, Joseph N., Study of resistivity of solid phases of lutetium–hydrogen system, 20: 3934
DARBY, J. B. Jr., Some intermediate phases in thorium–technetium and uranium–technetium systems, 20: 4428
DA SILVA HORTA, J., Malignancy and other late effects following administration of Thorotrast, 20: 3753
DARTE, John M., Radiation therapy in childhood, 20: 3850

DASTUGUE, G., Cholinesterase activities in mouse liver and kidney during experimental intoxication with uranyl nitrate, 20: 3670
DAUNT, J. G., Thermal and electrical conductivities of Mo–Re alloys in superconducting and normal states, 20: 4361 (AD-619719)
DAVIDSON, R. C., Microwave absorption in hot plasma near the second harmonic of electron cyclotron frequency, 20: 4943 (MATT-379)
DAVIS, H. M., Reaction of liquid titanium with some refractory compounds, 20: 3929
DAVIS, Hubert G., Detection of volatile ^{14}C labeled compounds by modified gas chromatography-ionization chamber technique, 20: 3899
DAVIS, R. E., Geology and surface effects, handcar event, 20: 4144 (PNE-810F)
DAVIS, Roger T., Size constancy as function of ageing and x-ray irradiation in rhesus monkeys, 20: 3721
DAVIS, W., Recovery of strontium values from sulfate-containing waste solutions, 20: 5210
DAYHARSH, Thomas I., Electron-density variations at 1000 kilometers, 20: 4746
DEBENETTI, Alessandro, Changes of permeability of isolated frog heart irradiated with x rays, 20: 3794
DE CRESCENTE, M. A., Compressive creep of UC and UN. I., 20: 4396 (PWAC-482(Pt.1))
DE CRESCENTE, M. A., Self diffusion of nitrogen in uranium mononitride, 20: 4394 (PWAC-477)
DE CRESCENTE, M. A., Thermodynamic properties of uranium monocarbide, 20: 4395 (PWAC-478)
DEELEY, T. J., Effects of radiation of normal rectum, 20: 3734
DEGROSSI, O., Standardization of capture of ^{131}I by thyroid in accordance with recommendations of O.I.E.A., 20: 3660 (NP-15528)
DE HALAS, D. R., FFTF driver fuel: PuO_2–stainless steel cermet, 20: 5192 (BNWL-SA-251)
DEILY, G. J., Methods used in United States for transferring materials through radiation barriers, 20: 4043
DE KERVILER, Herve, Critical study of some soft-tissue equivalent material. Sensitivity to neutrons of 1 kev to 14 Mev, 20: 3708 (CEA-R-2833)
DE KOCK, Carroll Wayne, Heats of dilution of some aqueous rare-earth chloride solutions at 25°C, 20: 3956
DELBOURGO, R., (56, 56) contribution to nucleon form factors, 20: 4642 (IC/65/78)
DELENE, J. G., Response of helium-cooled fast reactor to changes in coolant flow and reactivity, 20: 5127 (ORNL-P-1698)
DELGROSSO, E. J., High temperature titanium alloy development, 20: 4393 (PWAC-472)
DELGROSSO, E. J., Low pressure oxidation of pure columbium, 20: 4324 (PWAC-460)
DELGROSSO, Eugene J., Phase diagram of Cb–Zr–C system at 1538C and 1092C, 20: 4392 (PWAC-461)
DELIMARSKII, Yu. K., Solubility of metal oxides in fused borax, 20: 3951
DEL LITTO, Bernard, Hydrolysis of thorium dicarbide, 20: 3937
DE MARCO-TRABUCCO, A., Measurement of K^+ branching ratio into τ mode, 20: 4618
DEMETER, I., New isotope, ^{174}W, 20: 4834 (JINR-E-2360)
DEMURU, Maria Luisa, Complete continuity of free gas scattering operator in neutron thermalization theory, 20: 4811
DENHARDT, David T., Process of infection with bacteriophage ϕX174. V., 20: 3748
DENHARDT, David T., Process of infection with bacteriophage ϕX174. VI., 20: 3749
DE OLIVEIRA, Noi F. Jr., Construction and operation of ^3He refrigerator, 20: 4776
DEPOMMIER, Pierre, Nuclear matrix elements of transition $^{42}K(2^-) \rightarrow {}^{42}Ca(2^+)$, 20: 4863
DERBYSHIRE, R. T. P., Development of active radiographic inspection techniques at Harwell, 20: 4119
DESER, S., Critique of new theory of gravitation, 20: 4770
DETMER, Don E., Case of aseptic meningitis secondary to intrathecal injection of ^{131}I human serum albumin, 20: 3843
DEUBLEIN, Otmar, First practical experience on construction of 252 MW nuclear power station at Iingen, 20: 5139
DE VAN, J. H., Materials compatibility, 20: 4321 (ORNL-3870, pp 136-9)
DE VILLIERS, Arnoldus Jakobus, Morphologic changes induced in lungs of hamsters and rats by external radiation (x-rays), 20: 3785
DEVINE, R. T., Influence of weather on salt distributions and aerosols on beaches, 20: 4148 (AD-623515)
DEWEY, W. C., Radiosensitivity of normal and 5-bromodeoxyuridine treated mammalian cells during different phases of cell cycle, 20: 3737
DE WIJN, H. W., Microwave rotational spectra of thallium mono-chloride, 20: 3947
DEXTER, Arthur H., Radioactive cobalt for heat sources, 20: 4277 (DP-1012)
D'HOOP, H., SAHYB: program for solution of initial and boundary value problems, 20: 4287 (EUR-2519.e)
DIAMOND, J. J., Vapor pressure and heat of sublimation of tungsten, 20: 4438
DIAMOND, Milton J., Method and apparatus for measuring hydrogenous material, 20: 3913
DI COLA, G., Calculation of differential fast-neutron spectra from threshold-foil activation data by least-squares series expansion methods, 20: 4256
DIEHN, Bodo, Reactions of recoil carbon atoms in acetamide system, 20: 4026
DIENER, Gerhard, Adiabatic hypothesis in quasilinear theory of plasmas, 20: 4966
DIENER, Gerhard, First approximations of kinetic theory for unstable plasma, 20: 4963
DIENER, Gerhard, Kinetic theory of plasmas, 20: 4957
DILLEY, J. V., Pulmonary clearance of $^{59}Fe_2O_3$ and $^{51}Cr_2O_3$ in rats and dogs exposed to cigarette smoke, 20: 3655 (BNWL-SA-224)
DIN, Ghias Ud, Study of $(^3He,n)$ reactions, 20: 4925
DISCHINGER, R. H., Prog. rpt. on performance evaluation of heat exchangers for Na-cooled reactors, 7–9/65, 20: 5131 (UNC-5135)
DISTENFELD, C., Thermoluminescent neutron dosimetry system, 20: 4236 (BNL-9605)
DIXIT, R. M., Fluorescence spectrum of uranyl ion contained in some rare-earth chlorides, 20: 3948
DJURLE, S., Procedures for non-destructive testing of fuel rods, 20: 4123
DJURLE, S., Storage of radioactive material in Studsvik hot laboratory, 20: 4041
DOAN-NHUONG, On reconstruction of the amplitude of the vector meson production reactions $\pi + N \rightarrow \omega (\varphi)$, 20: 4584 (JINR-P-2380)
DOBBERSTEIN, P., Transition radiation, bremsstrahlung and plasma-strahlung, 20: 5017
DO GOER, A. M., Thermal conductivity of beryllium oxide at 1.5 to 300°K, 20: 4433
DOLGOV, A. D., Tests of consequences of unitary symmetry in Hadron-production reactions (survey), 20: 4645 (NP-15599)
DOLIQUE, Jean-Michel, Electric conductivity of plasmas where charge carriers appear or disappear in space, 20: 4960
DOLLE, Lucien, Changing pattern of problems in use of heavy water in nuclear reactors, 20: 5143
DORSEY, J. P., GAMBLE-4. Program for solution of multigroup neutron-diffusion equations in two dimensions, 20: 5057 (GA-6540)
DORY, R. A., Microinstability of mirror-confined plasma, 20: 4981
DOSE, K., Amino acid changes in cattle insulin by uv-irradiation, 20: 4016
DOUGAL, Arwin A., Thermonuclear fusion for electrical power production, 20: 4992
DOUGLAS, D. A. Jr., Desalination, 20: 5173 (ORNL-3870, pp 191-3)
DOUGLAS, D. A. Jr., High flux isotope reactor target development, 20: 5175 (ORNL-3870, pp 230-7)
DOUGLAS, D. A. Jr., Reactor evaluation, 20: 5024 (ORNL-3870, pp 261-5)
DOUGLAS, D. A. Jr., Thorium utilization, 20: 4343 (ORNL-3870, pp 266-89)
DOULAT, J., Thermal conductivity of beryllium oxide at 1.5 to 300°K, 20: 4433
DOWNEY, J. W., Some intermediate phases in thorium–technetium and uranium–technetium systems, 20: 4428
DOYAS, Richard J., Neutron self shielding in intermediate systems, 20: 4808 (UCRL-14432-T)
DRAGANIC, Zorica, Irradiation possibilities in 2 kilocurie ^{60}Co radiation unit at Boris Kidric Institute at Vinca, 20: 4272 (JPRS-32813)
DRAPER, Lawrence R., Roles of liver and appendix in serum hemolysin response in rabbits, 20: 3746
DREYFUS, B., Thermal conductivity of beryllium oxide at 1.5 to 300°K, 20: 4433
DRUMMOND, Ian T., Some aspects of complex angular momentum and three-particle states, 20: 4680
DUBE, R. Georges, Particle injecting device, 20: 4993
DUBROVA, S. E., Comparative study of result of radiation after-effects on chromosomal non-divergence, 20: 3715 (JPRS-31514, pp 59-64)
DUBROVSKAYA, L. B., Temperature and composition effects on electric conductivity of tantalum–carbon β and γ phases, 20: 4415
DUDLEY, Thomas Edward, Spherical harmonics approximation in general geometry, 20: 4820
DUMMER, J. E. Jr., ^{131}I sampling with activated charcoal and charcoal-impregnated filter paper, 20: 4179 (LA-3363)
DUNCAN, W., Malabsorption syndrome following radiotherapy, 20: 3851
DUNKEN, H., Axial electron density of H_2^+ in ground state and in excited states, 20: 4555
DUNNING, D. N., Effect of yttrium on the recrystallization and grain growth of tantalum, 20: 4424
DURAND, Alain, Determination of equivalent length of electrodes of particle separators, 20: 4515
DURCZOK, H., Breast tumor treatment by radical operation including preopemtive x irradiation, 20: 3861
DURET, M. F., Preliminary assessment of thorium as fuel for thermal reactors, 20: 5114 (CRRP-1221)

DVORNIK, Igor, Gamma radiation sources at Rudjer Boskovic Institute. I., 20: 4090 (JPRS-32842)
DWORKIN, Howard J., Efficiency of molecular iodine removal from air, 20: 3673
DYACHKOV, E. I., Expansion mechanism of 40 cm hydrogen bubble chamber of JINR, 20: 4257
D'YACHKOVA, R. A., Tributyl phosphate extraction of Pa. II., 20: 4058
D'YACHKOVA, R. A., Tributyl phosphate extraction of Pa. I., 20: 4057
DYAD'KIN, I. G., Fast convergence in Monte Carlo method of resolving problems of radioactive logging, 20: 4168
DYSON, Freeman J., Old and new fashions in field theory, 20: 4769

E

EAST, Larry V., Search for double beta decay of ^{150}Nd, 20: 4828 (COO-818-60)
EASTMAN, G. Y., Prog. rpt. on thermionic converters, emitter shell phase, final, 7/63–2/65, 20: 4359 (AD-618923)
EASTON, D. S., Method for increasing critical current of superconducting alloys, 20: 4799
EBERLE, A. R., Differential spectrophotometric determination of boron with diaminochrysazin, 20: 3892
EBERSBACH, Hans-Georg, Simple reactivity meter of high sensitivity, 20: 5061 (ZFK-RN-22)
EBREY, Thomas G., Gamma decay of ^{102}Tc and ^{104}Tc, 20: 4883
EDGE, T., United Kingdom experience of magnox fuel elements, 20: 5094
EDMONDS, E., Operational experience in Dounreay beta-gamma hot cells, 20: 5153
EDSALL, Pamela C., Effect of near ultraviolet and green radiations on plant growth, 20: 3769
EDWARDS, A. R., Post incident cooling of P.W.R. core, 20: 5030 (AHSB(S)R-86)
EFENDIEV, G. Kh., Extraction of cerium and yttrium by naphthenates, 20: 4051
EGELAND, A., Statistical method for quantitative analysis of geomagnetic giant pulsations, 20: 4743
EGUISA, F., Effect of gamma radiation on reproductive potential of Mexican fruit fly, 20: 3745
EHLER, Arthur W., Method and apparatus for producing magnetically confined hot dense plasma, 20: 4994
EICHELBERGER, J. F., Prog. rpt., 5/65, 20: 3879 (MLM-1266)
EICHLER, J. B., Prog. rpt. on reactor containment, 8–9/65, 20: 5023 (IITRI-578P21-15)
EICKER, H., Electron acceleration in helical fields, 20: 4518
EICKHOFF, Keith Guy, Nuclear reactor control devices, 20: 5047
EISENBERG, Henryk, Light scattering of water, deuterium oxide, and other pure liquids, 20: 3941
EISENBERG, Henryk, Refractive indices and piezo-optic coefficients of deuterium oxide, methanol, and other pure liquids, 20: 4484
EL-BAZ, Edgard, Analysis of elastic scattering of α particles on light nuclei using optical potentials, 20: 4859
ELDER, Michael, Crystal structure of technetium(IV) chloride, 20: 3932
ELDER, S. Thomas, Effects of whole-body x-irradiation on vr-3 food reinforced bar-pressing, 20: 3772
ELEKES, Istvan, Fat absorption tests performed with ^{131}I-labeled triolein combined with whole-body irradiation, 20: 3754
ELEMAN, F., Statistical method for quantitative analysis of geomagnetic giant pulsations, 20: 4743
ELISEEVA, G. D., Geochemistry and analytical chemistry of rare earth elements. I., 20: 4146
ELLIOTT, D. M., Prog. rpt. on fissiochemical development, semiannual, 1–6/65, 20: 3982 (AGN-8156)
ELLIOTT, R. A., Drying of oxide powder samples for neutron transmission measurements, 20: 3914 (AERE-M-1654)
ELLSWORTH, Robert Waldo, Muon-proton scattering at high momentum transfers, 20: 4591 (UR-875-108)
EMIROV, M. B., Theory of magnetic scattering of slow neutrons by antiferromagnets, 20: 4809
ENDO, Kuminori, Effect of oxygen on mechanical properties of high purity zirconium, 20: 4416
ENGEL, A. E. J., Potassium, rubidium, strontium, thorium, uranium, and ratio of ^{87}Sr to ^{86}Sr in oceanic tholeiitic basalt, 20: 4145
ENGESET, Arnfinn, Irradiation of lymph nodes and vessels, 20: 3718
ENGLAND, C. J., Safety of DAPHNE, 20: 5188 (AERE-R-4932)
ENGLISH, J., Recent advances in ultraviolet irradiation: photosensitivity tests, 20: 3767
EPSTEIN, Ervin, Dermatologic radiotherapy 1965, 20: 3812
ERB, D. E., Status of nuclear superheat development, 20: 5113 (CONF-650602-59)
ERICKSON, George F., Ceramic to metal bonding process, 20: 4354
ERMISCHER, W., On phase transformations of U_3O_8, 20: 4429
ERUKHIMOV, L. M., Study of focusing inhomogeneities in ionosphere by radioastronomic method on 13-54 Mgc frequencies, 20: 4735
ERWIN, Virgel G., Effect of hydrocortisone on alkaline phosphatase in cultured cancer cells, 20: 5217 (TID-21169)
ETTINGER, H. J., ^{131}I sampling with activated charcoal and charcoal-impregnated filter paper, 20: 4179 (LA-3363)
ETTMAYER, P., Contribution to system mercury–thorium, 20: 4441
EVANS, Albert E. Jr., Application of anticoincidence-shielded scintillation spectrometer to study of ^{14}N(p,γ)^{15}O reaction, 20: 4233 (AD-618676)
EVANS, C. M., Improvement in pulse transmission on coaxial transmission lines by reduction of skin effect, 20: 5218 (TID-21991)
EVANS, E. B., Scaling of yttrium in air, 20: 4334
EVANS, J. A., Permeation and diffusion of H isotopes through stainless steels. II., 20: 4366 (AWRE-O-90/65)
EVANS, J. V., Ionospheric backscatter observations at Millstone Hill, 20: 4755

F

FABRE, D., Characteristic energy losses of electrons in solids, 20: 5015
FAIR, D. R. R., Latest operating experience of magnox stations, 20: 5156
FAISAL, Farhad, Inelastic scattering of electrons from hydrogen, 20: 4549
FAN, Liang-tseng, Effects of electrical conductance of wall on magneto-hydrodynamic channel flow with heat transfer, 20: 4703 (AD-619101)
FARLEY IV, William W., Electron-density variations at 1000 kilometers, 20: 4746
FARMER, F. R., Growth of reactor safety criteria in United Kingdom, 20: 5027
FARMER, O. A., Fortran IV hydrogen property tabular codes, 20: 5177 (LA-3381)
FARMER, Otis A., Thermodynamic-transport and related properties of para-hydrogen from 36 to 5000°R at pressures to 5000 psia, 20: 3917 (LA-3405)
FARRAR IV, H., Effective resonance integral and Doppler effect in ^{197}Au. I., 20: 4841 (NAA-SR-Memo-11511)
FASSLER, M. H., Compressive creep of UC and UN. I., 20: 4396 (PWAC-482(Pt.1))
FATKULLIN, M. N., Quiet solar-daily variations of geomagnetic field during IGY. II., 20: 4738
FAUDROWICZ, Adam, Some new ideas in application of radioisotopes for measuring thickness and density, 20: 4273
FAULKNER, J. S., Solid-state and molecular theory, 20: 5006 (ORNL-3870, pp 50-5)
FAYARD, Claude, Analysis of elastic scattering of α particles on light nuclei using optical potentials, 20: 4859
FEDER, Harold M., Regeneration of nuclear fuel, 20: 4073
FEDORKO, Yu. P., Radioactive instruments—their application in industry, 20: 4275
FEDOROV, Yu. K., Thermodynamic properties of deuterium and tritium substituted non-linear triatomic hydrides, 20: 3950
FEINBERG, G., Some consequences of proposed C and T violations in electromagnetic interactions, 20: 4682
FEINE, U., DNA synthesis and radiation effects, 20: 3701
FELDEN, Marceau, Local analysis by electric probe of cesium plasma produced by contact ionization, 20: 4958
FELDEN, Marceau, Oscillatory regimes of cesium plasma machine, 20: 4965
FELDEN, Marceau, Study of effect of electron irradiation on piezoelectric quartz films, 20: 4463
FELDMAN, M., Studies on immune unresponsiveness induced by radiation, 20: 3738
FELDSTEIN, I. I., Quiet solar-daily variations of geomagnetic field during IGY. II., 20: 4738
FENECH, H., Safety characteristics of large gas-cooled fast power reactors, 20: 5119 (GA-6732)
FENG, C., Determination of relative intensity in x-ray reflection study, 20: 5010
FENG, Paul Y., Behavior of materials exposed to radiation, 20: 4464
FENN, R. W. Jr., Mechanical property evaluation of Be-38% Al alloy from –320 to 800F, 20: 4440
FERAT, Alain, Method of study of particle dynamics in linear accelerator, 20: 4503 (NP-15340)
FERGUSON, K. R., United States practices in control and containment of radioactive contamination, 20: 4214
FERGUSON, W. E., Effect of yttrium on the recrystallization and grain growth of tantalum, 20: 4424
FERLENGHI, E., Generality of stability criterion against transverse wall instability of relativistic beams, 20: 4501 (LNF-65/34)
FERLENGHI, E., Transverse resistive wall instability of extremely relativistic beams of electrons and positrons, 20: 4500 (LNF-65/27)
FERNANDEZ-MORAN, H., Electron microscopic and biochemical characterization of fraction I protein, 20: 5219 (TID-22372)
FERRIS, L. M., Chemical disintegration and recovery of uranium from sintered graphite–uranium compacts, 20: 4074

FERRO, A., Effect of crystalline structure on fatigue, 20: 4443
FEUERBACHER, John Larry, Extension of internal-external conversion method to lens beta-ray spectrometer by measurement of 662 kev conversion line of ^{137}Ba, 20: 4248 (TID-22333)
FIEDLER, J., Binding energy of the deuteron, 20: 4856
FIORE, C., Amino acid changes in cattle insulin by uv-irradiation, 20: 4016
FIRTH, A., Steam generating heavy water reactor, 20: 5163
FISCHER, E., Prog. rpt. on shielding experiments at reactor station Geesthacht, annual, 1964, 20: 4997 (EUR-2494.d)
FISCHER, John J., Vanadium–gallium system in region of V_3Ga, 20: 4426
FISH, Stewart A., Environmental teratogens and birth defects, 20: 3747
FISHER, B. B., Fortran IV hydrogen property tabular codes, 20: 5177 (LA-3381)
FITCH, V. L., Study of K^+ decay probability, 20: 4609
FITZSIMMONS, B. W., Reactions of thorium tetrachloride with o-phenanthroline and triphenylphosphine, 20: 3933
FLAMMERSFELD, A., Isomerism of ^{197}Tl, 20: 4921
FLATT, J. P., Study of formation of hemolytic antibodies in rabbit, 20: 3689
FLAUMENHAFT, E., Deuterium isotope effects in cytology, 20: 3651
FLEISCHER, E. S., Methods used in United States for transferring materials through radiation barriers, 20: 4043
FLEISCHER, R. L., Ion explosion spike mechanism for formation of charged-particle tracks in solids, 20: 4548
FLORKOWSKI, T., Radioisotope sources of low-energy electromagnetic radiation and their use in analysis and measurement of coating thickness, 20: 4219 (ORNL-IIC-5, pp 182-205)
FLUCK, Ekkehard, Study of complex and covalent iron compounds using ^{57}Fe Moessbauer effect, 20: 3927 (AERE-Trans-1026)
FLYNN, P. W., Prog. rpt. on effect of substructure on irradiation stability of ASTM A302 grade B steel, 10/65, 20: 4372 (GA-6724)
FOAD, H. Y., Design and evaluation of 1000 MW(e) central station power-plant with a circulating fuel gaseous core reactor, 20: 5128 (TID-22225)
FOEEX, Marc, High-temperature study of allotropic transformations of sesquioxides of yttrium, erbium, and thulium, 20: 3939
FOELSCHE, H. W. J., Brookhaven radio frequency beam separator, 20: 4493 (BNL-9642)
FOLDY, L. L., Coupling constants in muon capture, 20: 4915
FONTHEIM, Ernest G., Photoelectron energy distribution in F region, 20: 4753
FOOKS, Jean, Rlectron distribution in quiet d-region, 20: 4754
FORBES, R. L., Prog. rpt. on U–Pu monoxides, 7–9/65, 20: 4327 (UNC-5138)
FORCHER, H., Standardization of capture of ^{131}I by thyroid in accordance with recommendations of O.I.E.A., 20: 3660 (NP-15528)
FORD, Joseph, Ultrasonic studies of the nonlinear behavior of solids, 20: 5012
FORD, Judith D., CRT plotting routines in use at LRL-Livermore, 20: 4292 (UCRL-14427-T)
FORMANN, E., Operating experience with Seibersdorf inhomogeneous sector field isotope separator, 20: 4283 (SGAE-PH-27/1965)
FORTESCUE, Peter, Safety characteristics of large gas-cooled fast power reactors, 20: 5119 (GA-6732)
FOU, Cheng-Ming, Levels in ^{57}Ni from $^{58}Ni(^3He,\alpha)^{57}Ni$ reaction, 20: 4912
FOURCY, Andre, Determination of metals in vegetable products using neutron activation analysis, 20: 3901
FOURNIER, Jean-Pierre, Photoelectron energy distribution in F region, 20: 4753
FOWLER, C. M., Cylindrical explosive flux-compression system, 20: 4477 (LA-DC-7289)
FOWLER, C. M., Plasma compression by explosively produced magnetic fields, 20: 4941 (LA-DC-7290)
FOWLER, William A., Nuclear and neutrino processes in stars and supernovae, 20: 4534
FOX, P. G., Analysis of xenon and krypton using omegatron, 20: 3908
FRAAS, A. P., MPRE radiator development tests, 20: 5182 (ORNL-P-1721)
FRAHM, H. J., Decay of 185-μsec isomer in ^{166}Ho, 20: 4889
FRAME, A. FG., Fast reactor development, 20: 5165
FRANCOIS, B., Clearance of radioactive colloidal gold in dog with portocaval anastomosis, 20: 3681
FRANCOIS, B., Experimental study of the clearance of colloidal ^{198}Au, 20: 3680
FRANK, I. M., Transition radiation and optical properties of materials, 20: 5008 (ORNL-tr-872)
FRANK, Max, Influence of operating conditions on radiation damage to transistor gain, 20: 4267
FRANK, R. G., Material specifications for advanced refractory alloys, 20: 4380 (NASA-CR-54761)
FRANK-KAMENETSKII, D. A., Magneto-sonic heating of plasma, 20: 4939 (IAE-911)
FRANKLIN, Ernest, Thermometer devices, 20: 5045
FRANKLIN, N. L., United Kingdom experience of magnox fuel elements, 20: 5094
FRANTZ, F. S. Jr., Study of slightly enriched UO_2 lattice with H : U = 0.42—measurement and analysis, 20: 5071
FRASER, R. T. M., Electron exchange reactions mediated by oxyanions, 20: 3967
FREDRIKSSON, Lars, Enrichment of forage vegetation in Sr and Cs, 20: 3665 (CEA-tr-X-619)
FREILING, E. C., Physical and radiochemical properties of fallout particles, 20: 4156 (USNRDL-TR-899)
FREUD, R., Magnetic induction distribution in cylindrical specimen, 20: 4794
FREUND, Harry, Determination of titanium and zirconium in molybdenum base alloys by ion exchange, 20: 3896
FREUND, P. G. O., M(12) predictions for pp scattering, 20: 4599
FREUND, Peter G. O., Method of complex angular momenta in relativistic quantum theory, 20: 4636
FRIEDRICH, V., Axial electron density of Hf in ground state and in excited states, 20: 4555
FRIESE, K., Amelioration of adhesive properties of polyethylene foils, 20: 4029
FRISHMAN, Y., Explicit wave functions for any spin, 20: 4613
FRITSCHE, D., Transition radiation, bremsstrahlung and plasmastrahlung, 20: 5017
FRONSDAL, C., On non-compact groups. III., 20: 4688
FRONSDAL, C., On non-compact groups. IV., 20: 4689
FRYER, Minot P., High-energy electron injury from accelerator machines, 20: 3724
FUCHS, Norman, Non-abelian gauge fields and Goldstone bosons, 20: 4657
FUDGE, A. J., Non-destructive examination of irradiated nuclear fuel, 20: 5093
FUGELSO, L. E., Close-in effects from surface burst, 20: 4143 (AD-619969)
FUHRMAN, N., Prog. rpt. on U–Pu monoxides, 7–9/65, 20: 4327 (UNC-5138)
FUJII, S., Gamma transitions between even-parity states in ^{16}O, 20: 4854
FUJII, Taro, Effects of 14-Mev neutrons in heterozygotic Einkorn wheat, 20: 3762
FUJII, Y., Model of C violation in semistrong interactions, 20: 4681
FUJIWARA, Yoshisada, On recovery-promoting chemicals after gamma-ray irradiation to mouse strain L cells cultured in vitro, 20: 3791
FUKS, N. A., Determination of distribution of aerosol particles according to size by diffusion method, 20: 4733 (AI-Trans-201)
FUKUDA, Takashi, Crosslinking in polyethylene single crystals by ^{60}Co γ-ray irradiation, 20: 3998
FULIGNI, F., Terrestrial albedo of 40- to 190-kev x rays, 20: 4752
FULLAM, H. T., Critically safe flat bed contactor for processing solid fissile materials, 20: 4049 (RL-SA-52)
FULLER, R. K., Size analysis of –44 micron dust particles, 20: 4149 (AD-623639)
FULL-SCHARRER, G., Problem of malignant degeneration long after previous x irradiation, 20: 3841
FUNABASHI, Koichi, Luminescence phenomena in gamma-irradiated pure alkane glasses, 20: 3990
FURNAS, T. C., Industrial analysis of ^{147}Pm x rays for radiography and imaging readout, 20: 3801 (ORNL-IIC-5, pp 222-38)
FURTH, Harold P., Plasma confinement apparatus employing helical magnetic field configuration, 20: 4995
FUSTEL, E., Problems in introduction of nuclear power stations in Spain, 20: 5158

G

GAINES, Richard V., Moctezumite, new lead uranyl tellurite, 20: 4173
GALLAGHER, E. V., Prog. rpt. on reactor containment, 8–9/65, 20: 5023 (IITRI-578P21-15)
GALLIVAN, J. B., Evidence for dissociative electron attachment in γ-irradiated hydrocarbon glasses, 20: 4013
GALLO, C. F., Anomalous thermal conductivity of rare earth metals, 20: 4419
GALLO, K. M., Possible artifact in cyclic variations in radiosensitivity, 20: 3766
GANDOLFI, A., Terrestrial albedo of 40- to 190-kev x rays, 20: 4752
GANDOLFO, J. M., Working methods in use at transplutonium complex, 20: 4065
GANIEL, U., Nuclear quadrupole spectra in very asymmetric field gradients, 20: 4867
GANS, P., Reactions of thorium tetrachloride with o-phenanthroline and triphenylphosphine, 20: 3933
GARCIA DEL RIO, H., Prog. rpt. on improvement of renogram techniques, final, 20: 3800 (NP-15150)
GARDING, L., Fields as operator-valued distributions in relativistic quantum theory, 20: 4650
GARDNER, Andrew S., Angled plate scanning interferometer, 20: 4232
GARFINKLE, M., Reaction of liquid titanium with some refractory com-

pounds, 20: 3929
GARN, W. B., Cylindrical explosive flux-compression system, 20: 4477 (LA-DC-7289)
GARN, W. B., Plasma compression by explosively produced magnetic fields, 20: 4941 (LA-DC-7290)
GARREN, A. A., Design of long straight sections for synchrotrons, 20: 4512 (UCRL-16243)
GARRIC, C., Dismantling workshop for Orgel fuel elements, 20: 4064
GARTE, Samuel M., Investigation of beta source ionization currents in gaseous media, 20: 4557
GASIDLO, J. M., Doppler coefficient measurements for ^{235}U in fast-reactor spectra, 20: 5072
GASSER, R. P. H., Interaction of carbon monoxide with tantalum, 20: 4444
GASSMANN, G. J., Production and removal of ionization in upper atmosphere, 20: 4729 (CNIE-PE-4)
GAVRILOV, B. I., Effect of helical field on ohmic heating of plasma in S-1 apparatus, 20: 4937 (IAE-907)
GEESAMAN, L. B., Piezoelectric response of z-cut tourmaline to shocks of up to 21 kilobars, 20: 5011
GEISLER, John Edmund, Investigation of ionosphere-protonsphere coupling, 20: 4761
GEISSLER, G., Modifications of crystalline sugars by roentgen radiation, 20: 4020
GEL'D, P. V., Temperature and composition effects on electric conductivity of tantalum–carbon β and γ phases, 20: 4415
GENDRIN, R., Gyroresonance radiation produced by proton and electron beams in different regions of magnetosphere, 20: 4747
GENTILE, Arthur C., Effects of near ultraviolet and green radiations on plant growth, 20: 3769
GERARD, J., Determination of uranium in its alloys, 20: 3890 (AEC-tr-6617)
GERARDIN, Claude, Study of excitation curves of (t,α) reaction on ^{16}O between 1 and 3 Mev, 20: 4858
GERARDO, J. B., Electron and atom concentrations in afterglow gas discharge, 20: 4970
GERIG, John Sebastian, Induction coupled superconducting bolometer, 20: 4229
GERRARD, Martha, Conference on low-energy x- and gamma sources and applications, Chicago, 10/64, 20: 4111 (ORNL-IIC-5)
GERRITY, Joseph P. Jr., Prog. rpt. on influence of local winds on fallout, semiannual, 10/15/64–4/15/65, 20: 4154 (AD-620003)
GERSTEIN, I. S., Octet enhancement and reciprocal bootstrap, 20: 4649
GERSTENKORN, Simon, Hyperfine structures of ground levels of terbium, 20: 4857
GERVING, Martha A., Radioprotective action of RNA in mice, 20: 3792
GETTY, W., Report on a meeting held in the old lecture room at Christ Church College, Oxford, at 9 p.m. on Thursday, September 9, 1965, 20: 4945 (ORNL-TM-1306)
GHALIB, S. A., Advantages of the magnox reactor to Spanish industry and economy, 20: 5159
GHEZZI, E., Decontamination experience at hot laboratory of Casaccia, 20: 4211
GHEZZI, E., Techniques for dismantling irradiated rigs, 20: 4092
GHIDONI, John J., Effect of massive doses of 32 Mev protons and ^{60}Co radiation on primates, 20: 3692
GHOSHAL, A. K., Measurement of electron density of plasma, 20: 4967
GIBALA, Ronald, Clustering of oxygen in solid solution in niobium, 20: 4449
GIBSON, R., Permeation and diffusion of H isotopes through stainless steels. II., 20: 4366 (AWRE-O-90/65)
GIEN, Tran Trong, Derivation of collision lifetime matrix, 20: 4651
GIERDALSKI, Jerzy, Some new ideas in application of radioisotopes for measuring thickness and density, 20: 4273
GIGNOUX, D., Charged colloid generating system for electric propulsion, 20: 4133 (N64-25007)
GILLESPIE, J., Faddeev formalism for four-particle systems, 20: 4675
GILLET, C., Restoration of cytoplasmic streaming as soon as possible after irradiation, 20: 3698
GILMOUR, B. A., Radiation effects on propellants and explosives: annotated bibliography, 20: 4461 (REIC-Memo-28)
GINSBERG, Edward Stephen, Effects of weak vector boson in certain radiative weak decays, 20: 4629
GINSBURG, Theo, Peaceful applications of nuclear explosions, 20: 4085
GIRARD, Francois, Examination by electron microscope of niobium contaminated at high temperature by interstitial elements, 20: 4401 (ANL-Trans-218)
GLENDENIN, L. E., Division of nuclear charge deduced from x-ray measurements in spontaneous fission of ^{252}Cf, 20: 4913
GLOECKLER, George, Solar modulation of low-energy galactic helium spectrum as observed on IMP I satellite, 20: 4565
GLUKHOVA, L. P., Determination of small amounts of U(VI) in presence of large amounts of U(IV), 20: 3903
GOAD, Walter B., Polarization effects on neutron transport, 20: 4814
GODEL, Dieter, Crystal structure of phases AgSm, Ag_5Sm, 20: 4447
GOEDDEL, W. V., Prog. rpt. on advanced, graphite-matrix, dispersion type fuel systems and research on graphite, 11/15/64–2/14/65, 20: 5089 (GA-6181)
GOETZEL, Claus G., Space materials handbook, 20: 4312
GOFMAN, J. W., Calculation of treatment schedules for cancer chemotherapy, 20: 5222 (UCRL-14505)
GOHAR, H. A. F., Prog. rpt. on ^{90}Sr contained in marine animals following possible release of radioactive waste, final, 1963–64, 20: 3659 (NP-15156)
GOLDBERG, Richard A., Equatorial geomagnetic anomaly and its associated current system, 20: 4749
GOLDEMBERG, J., Elastic electron scattering by magnetic and electric moments, 20: 4840 (LAL-1140)
GOLDEN, J. H., Degradation of polytetramethylene oxide. II., 20: 3999
GOLDENBERG, Gerald J., Murine leukemia cell lines of different radiosensitivity in vitro, 20: 3736
GOLDHABER, Alfred S., Role of spin in monopole problem, 20: 4684
GOLDMAN, D. T., LINK. Combined slowing-down and thermalization program with a thermal cutoff of 3.06 ev, 20: 4804 (KAPL-3098)
GOLDSTEIN, Arthur W., Single-collision model for electron-beam currents between plane electrodes, 20: 4704 (NASA-TN-D-3058)
GOLDSTEIN, Charles M., Single-collision model for electron-beam currents between plane electrodes, 20: 4704 (NASA-TN-D-3058)
GOLDSTEIN, Gerald, Half-lives and specific activities of common radionuclides, 20: 4845 (ORNL-TM-1318)
GOLIKOV, V. Ya., Individual dosimetric control technique, 20: 4198
GOLOVANOV, L. B., Hundred-and-fifty centimeter hydrogen target, 20: 4490
GOLUB, C. N., Launch hazards assessment program, report on Atlas/Centaur abort, 20: 4187 (SC-RR-65-333)
GONCHAROV, I. N., Superconductive properties of Nb–Zr alloys, 20: 4792
GOOD, R. H. Jr., Phase-space considerations for four-particle final states, 20: 4658
GOODALL, M. C., Gauge co-ordinate group of physical theory, 20: 4656
GOODMAN, L. S., Atomic-beam research, 20: 4535 (ANL-7081, pp 128-9)
GOODMAN, Leonard S., In vivo measurement of bone mineral content by transmission technique, 20: 3886 (ORNL-IIC-5, pp 290-4)
GOODRICH, Jack K., Isotope encephalogram in brain tumor diagnosis, 20: 3830
GOOLDEN, A. W. G., Radiation cancer of pharynx. Case reports, 20: 3806
GORMAN, J., Biology of the Solway firth in relation to movement and accumulation of radioactive materials. IV., 20: 3662 (PG-Report-650)
GORNYI, G. Ya., Geochemistry and analytical chemistry of rare earth elements. I., 20: 4146
GORRELL, Thomas C., Initial critical and zero power testing of HWCTR, 20: 5193 (DP-967)
GORSHKOV, A. S., Perspectives of atomic heat and power plants, 20: 5149
GOTSMAN, E., Explicit wave functions for any spin, 20: 4613
GOTTA, H., Prog. rpt. on improvement of renogram techniques, final, 20: 3800 (NP-15150)
GOTTLOB, P., Transfer procedures used in alpha-gamma hot laboratory at Karlsruhe, 20: 4209
GOURDIN, M., Unitary symmetry—model of octet, 20: 4698
GOUT, C., Characteristic energy losses of electrons in solids, 20: 5015
GOWGIEL, Joseph M., Eruption of irradiation-produced rootless teeth in monkeys, 20: 3743
GOWGIEL, Joseph M., Experimental radio-osteonecrosis of jaws, 20: 3742
GRABOVSKII, Ya., Angular distribution of transfer reaction products, 20: 4836 (JINR-P-2298)
GRABOVSKII, Ya., Matrix elements for inelastic scattering of heavy particles. I., 20: 4839 (JINR-P-2333)
GRAEFF, G., Simultaneous measurement of hyperfine structure, Stark effect, and Zeeman effect of $^{133}Cs^{19}F$ with molecular beam resonance apparatus, 20: 4554
GRAF, G., Lung changes after irradiation with 180 kv x rays, fast electrons and ^{60}Co γ rays, 20: 3700
GRAF, P., Dismantling and machining methods used in hot cells and workshops, 20: 4127
GRAF, P., Transfer methods for irradiation rigs and fuel elements, 20: 4063
GRAHAM, R. H., Weak electromagnetic decays of hyperons in SU(3), 20: 4673
GRANATSTEIN, V. L., Observation of nonquasistatic plasma surface waves, 20: 4935 (AFCRL-65-556)
GRANGER, Roger, Phase diagram of Cb–Zr–C system at 1538C and 1092C, 20: 4392 (PWAC-461)
GRANT, I. S., Resonance capture and doppler coefficient in cylindrical uranium fuel elements, 20: 5092
GRANZOW, K. D., Extrapolating electromagnetic fields from values in spherical region, 20: 4638 (AD-617965)
GRAY, Peter R., Gamma decay of ^{102}Tc and ^{104}Tc, 20: 4883
GRAY, R. J., Metallography, 20: 4309 (ORNL-3870, pp 300-4)

GREAVES, Thomas Cyril, Improvements relating to nuclear reactor servicing apparatus, 20: 5041
GREBESHOVA, R. N., Biochemical characteristics of aspergillus uv mutants, 20: 3756
GREBESHOVA, R. N., Some physiological peculiarities of ultraviolet-induced mutants of aspergillus, 20: 3755
GREEN, Allen E., Radiotherapeutic management of malignant tumors of vagina, 20: 3848
GREEN, Anthony, Tracking cobalt project, 20: 3842
GREEN, Farno L., Portable devices for isotope chest radiography and other applications, 20: 3804 (ORNL-IIC-5, pp 309-28)
GREENBERG, Joseph, Locus for radiation sensitivity in Escherichia coli B_{m}, 20: 3757
GREENBERG, Joseph, Radiation sensitivity in Escherichia coli, some properties of radiation-sensitive Hfr K12 mutant, PAM 401, 20: 3758
GREENE, Richard George, Anion exchange separations of rare earths in nonaqueous solvents, 20: 4067
GREENFIELD, Peter, Improvements relating to heat treatment processes for magnesium alloys, 20: 4456
GREENFIELD, Roy Jay, Two-dimensional calculations of magnetic micropulsation resonances, 20: 4728 (AD-618118)
GREENSTADT, E. W., Interplanetary magnetic effects of solar flares: Explorer 18 and Pioneer 5, 20: 4527
GREENWOOD, F. C., Growth hormone in acromegaly, 20: 3828
GREENWOOD, G. W., Non-destructive testing of fuel elements at Berkeley, 20: 4121
GRENCH, H. A., Fast-neutron capture cross section of ^{64}Ni, 20: 4911
GRENCH, R. E., Collected algorithms 1900–1963 from communications of the association for computing machinery, 20: 4286 (ANL-7054)
GRIFFITH, W. L., Saline: a FORTRAN computer program for process design of saline water conversion plants using the multi-stage, flash-evaporation process, 20: 3923 (ORNL-TM-1299)
GRIFFITHS, D. R., Nuclear power stations—types and economics, 20: 5168
GRIFFITHS, P. A., Energy transfer effects in irradiation of benzene + butene-2 mixtures, 20: 4014
GRILLMAIER, R. E., Biophysical studies of persons with deposits of radionuclides of natural Th series, 20: 3683
GRIMELAND, B., Attempt to measure directly slowing down age of (d,d) neutrons in paraffin, 20: 4813
GRIN, M., Computer analyses of tensile tests, 20: 4371 (EUR-2514.e)
GRISHIN, V. G., Investigation of reactions $\pi^- p \to m\,\pi^0 + n$ at the π^- momentum of 4 Bev/c, 20: 4582 (JINR-P-2361)
GRISHIN, V. G., Measurement of energy and angular characteristics of electrons and γ-quants in propane bubble chamber, 20: 4240 (JINR-P-2277)
GRODEL, Mar'yan, Radioluminescence of styrene-methylmethacrylate copolymers, 20: 4001
GROH, E. F., Safety analysis for AARR critical experiment, 20: 5189 (ANL-6929)
GROHMAN, Antoni, Some superconducting and other properties of Sn- and In-whiskers, 20: 4795
GROSHEV, I. N., Obtaining electron leaves, 20: 4624
GROSHEV, I. N., Transient and Cherenkov radiation of electrons leaves, 20: 4623
GROSS, David J., Normal threshold sheet structure of two-particle scattering amplitudes, 20: 4668
GROSSO, C., Measurement of K^+ branching ratio into τ mode, 20: 4618
GROVE, D. J., Plasma confinement in low-density C stellarator discharges, 20: 4942 (MATT-372)
GROVE, G. R., Prog. rpt., 5/65, 20: 3879 (MLM-1266)
GRUBESSICH, J., Oxidation resistant coatings for Nb and Nb alloys, 20: 4357
GRUENEWALD, T., Dose distribution for irradiations with Van de Graaff electron accelerators, 20: 4204
GRUNE, Werner N., Effects of high energy ionizing radiation on colloidal systems and suspensions, 20: 4015
GUELFI, J., Cancer and geography, 20: 4193
GUENTHER, Ralph W., Nuclear reactor core clamping system, 20: 5103
GUERET, Philippe, Parametric representation of the "kinetic moment" operators for group SU(3), 20: 4652
GUERET, Philippe, Parametric representation of "kinetic moment" operators for SU(4) group, 20: 4654
GUERIN, M.-Th., Binding of radiocalcium (^{47}Ca) and radiostrontium (^{85}Sr) with serum proteins, 20: 3697
GUERIN, R. A., Binding of radiocalcium (^{47}Ca) and radiostrontium (^{85}Sr) with serum proteins, 20: 3697
GUERY, A., Studies on separation of ^{137}Cs and ^{90}Sr from fission in acid medium on mineral ion exchangers, 20: 3871 (EUR-2497.e)
GUESSOUS, Abdelmalek, Relativistic transformation of temperature, 20: 4712
GUEST, G. E., Microinstability of mirror-confined plasma, 20: 4981
GUITTARD, MICHELINE, Regions of homogeneity of NaCl type formed by monosulfates of rare earths, 20: 3938
GUMM, Barbara, PLOT3D: FORTRAN subroutine for three-dimensional plotting, 20: 4291 (UCRL-14425)
GUNTHER, B., Thermionic emitter materials research program, 20: 4570 (AD-614592)
GUREVICH, Ya. B., Effect of hot plastic deformation on structure and properties of molybdenum, niobium, and titanium, 20: 4403 (JPRS-32317)
GURNEE, M. N., Microwave absorption in hot plasma near the second harmonic of electron cyclotron frequency, 20: 4943 (MATT-379)
GURR, H., Interaction of muons produced by atmospheric neutrinos, 20: 4561 (COO-818-64)
GURSKY, S., Examinations of radiation reactions of liver by means of ^{131}I bengal rose tests, 20: 3774
GUSINOW, M. A., Electron and atom concentrations in afterglow gas discharge, 20: 4970
GUTHRIE, J. E., Occurrence of ^{22}Na in some species of Canadian biota, 20: 4161
GUTSCHER, W. D., AT-25 telemetry band tracking antenna, 20: 5215 (SC-TM-65-448)
GUY, Jean, Iterative method of resolution of certain integral equations, 20: 4764
GWIN, R., Use of digital computer in time-of-flight experiments, 20: 4245 (ORNL-P-1723)
GYORGYI, S., Excretion of isotopically labeled glucose and thioglucose in rat, 20: 3678

H

HAAG, Fred George, An investigation of optimum control for nuclear rockets, 20: 5187
HAAR, D. Ter, Origin of cosmic rays, 20: 4564
HAAS, Paul A., Preparation of thoria and mixed-oxide microspheres, 20: 3922 (ORNL-TM-1281)
HAASE, D. J., Thermoelectric and electrical measurements in Er–Se system, 20: 5013
HABEGGER, L. J., Design and evaluation of 1000 MW(e) central station powerplant with a circulating fuel gaseous core reactor, 20: 5128 (TID-22225)
HABISH, H. A., Studies of induced mutants of corynebacterium fascians, 20: 3723
HACKNEY, Stanley, Boiling water nuclear reactor operating with primary and secondary coolant, 20: 5172
HACKNEY, Stanley, Nuclear reactor, 20: 5039
HACKNEY, Stanley, Nuclear reactor, 20: 5038
HAEMAELAEINEN, R. M. K., Analytical wave functions and photodisintegration of deuteron, 20: 4592
HAENSSLER, Fr., Topology of structure of intermediate states of superconductors of type I, 20: 4778
HAFEMEISTER, David Walter, Solid state and nuclear results from Moessbauer studies with ^{129}I, 20: 5018
HAGHIRI, F., Reducing uptake of ^{90}Sr by plants on contaminated Ohio soils, 20: 3679
HAGHIRI, F., ^{90}Sr, ^{95}Zr, and ^{137}Cs accumulation in corn plants as influenced by soil temperature, 20: 3668
HAHN, H., Brookhaven radio frequency beam separator, 20: 4493 (BNL-9642)
HAHN, H., Comments on deflectors with eccentric beam hole, 20: 4492 (BNL-9640)
HALAMA, H. J., Brookhaven radio frequency beam separator, 20: 4493 (BNL-9642)
HALIK, Jaroslav, Working hazard in radon spas, 20: 3798
HALL, J. E., Electron distribution in quiet d-region, 20: 4754
HALLIWELL, Robert S., Effects of gamma irradiation on symptom expression of barley stripe mosaic virus disease and on two viruses in vivo, 20: 3768
HALSALL, M. J., Preliminary assessment of thorium as fuel for thermal reactors, 20: 5114 (CRRP-1221)
HAMANOUE, Kunso, Radiation-induced copolymerization of carbon monoxide with α-olefines, such as propylene, butene-1, and isobutylene, 20: 3997
HAMBERGER, S. M., Experimental studies of continuum emission of hydrogen, 20: 4973
HAMBLING, P. G., Effect of uniaxial compression upon transformation of metastable delta-phase plutonium, 20: 4434
HAMILL, W. H., Evidence for dissociative electron attachment in γ-irradiated hydrocarbon glasses, 20: 4013
HAMILTON, Gordon W., Numerical model of ion-cyclotron wave experiment, 20: 4983
HAMILTON, Walter C., Chemical crystallography, 20: 5212 (BNL-930)
HAMLING, B. H., Prog. rpt. on fissiochemical development, semiannual, 1–6/65, 20: 3982 (AGN-8156)
HANSEN, E. C., Application of multichannel synthesis to 2-D depletion calculations, 20: 5056 (CONF-654-22)
HANSEN, N. J. Sigurd, Decay of 185-μsec isomer in ^{166}Ho, 20: 4889

HAMSMANN, M., Studies of ^{144}Ce metabolism in liver cells of rats, 20: 3682
HARARI, H., Decays of positive-parity baryon resonances in broken U(12), 20: 4666
HARDIE, R. W., RED CROSS. Code to compute resonance shielded, temperature dependent cross sections for fast reactor analysis, 20: 5055 (BNWL-146)
HARDY, J., Study of simple waves, 20: 4707 (UCRL-14318)
HARDY, J. Jr., Study of slightly enriched UO_2 lattice with H : U = 0.42—measurement and analysis, 20: 5071
HARDY, J. R., Theoretical study of second-order Raman spectra of cesium halides, 20: 5007 (UCRL-14398)
HARIHARAN, Alleppey V., Process of preparing thorium metal from oxide, 20: 4316
HARKER, Kenneth J., Longitudinal oscillations in unbounded one-dimensional nonuniform plasmas, 20: 4980
HARMS, I., Treatment of irradiation reaction of mucosa, 20: 3840
HARMS, W. O., Gas-cooled reactor program, 20: 4306 (ORNL-3870, pp 194-213)
HARMS, W. O., High-temperature materials, 20: 4301 (ORNL-3870, pp 102-35)
HARMS, W. O., Tungsten metallurgy, 20: 4302 (ORNL-3870, pp 155-63)
HARMS, W. O., Uranium nitride, 20: 4303 (ORNL-3870, pp 164-70)
HARRIS, C. A., Guide for designing electrical controls of accelerators, 20: 4510 (UCRL-16016)
HARRIS, E. G., Electron-phonon, electron-plasmon, plasmon-phonon, and plasmon-plasmon interactions, 20: 4944 (ORNL-3871)
HARRIS, F., Radioisotope osteogram in rickets, 20: 3672
HARRIS, G. M., Reactions of hexachlororhodium(III) and pentachloraquorhodium(III) ions in aqueous acid solutions, 20: 3966
HARRISON, Charles W. Jr., Preliminary report on interaction of electromagnetic field with missile having ionized trail, 20: 4730 (SC-DC-65-1797)
HART, James L., Removal of vanadium from aqueous solutions, 20: 4071
HART, Ralph James, Improvements in or relating to apparatus for controlling small rates of flow of gases, 20: 4230
HARUN-AR-RASHID, A. M., Inelastic scattering of electrons from hydrogen, 20: 4549
HARUNAR-RASHID, A. M., Spin-1 meson photoproduction, 20: 4610
HARVEY, G. G., Prog. rpt., 3–5/65, 20: 4478 (TID-22179)
HASELKORN, R., Electron microscopic and biochemical characterization of fraction I protein, 20: 5219 (TID-22372)
HASHISH, S. E. E., Prog. rpt. on ^{90}Sr contained in marine animals following possible release of radioactive waste, final, 1963–64, 20: 3659 (NP-15156)
HASSAN, A., Prog. rpt. on ^{90}Sr contained in marine animals following possible release of radioactive waste, final, 1963–64, 20: 3659 (NP-15156)
HASSITT, A., Average effect of atmosphere on trapped protons, 20: 4748
HAUG, Robert, Local analysis by electric probe of cesium plasma produced by contact ionization, 20: 4958
HAUG, Robert, Oscillatory regimes of cesium plasma machine, 20: 4965
HAUG, Robert, Study of effect of electron irradiation on piezoelectric quartz films, 20: 4463
HAUSER, H., Determination of radioactivity of reactor cooling H_2O, 20: 3909
HAUSER, O., On phase transformations of U_3O_8, 20: 4429
HAUSER, William N., Analysis of 96 abnormal brain scans using ^{99m}Tc (pertechnetate form), 20: 3824
HAVAS, Peter, Qualitative aspects of N-body problem for approximately relativistic equations of motion, 20: 4766
HAYAKAWA, Sohachiro, Oxygen effect and temperature dependence of fluorescence intensity in naphthalene scintillators, 20: 3994
HAYES, R. L., Bone scanning with ^{68}Ga: carrier effect, 20: 3676
HAYET, L., Decontamination procedures and frequencies in $\alpha\,\beta\,\gamma$ metallurgical hot cells, 20: 4213
HAZEL, J., Treatment of Mikulicz's disease with radiation therapy, 20: 3826
HAZI, Endre, Measurement of particle residence times in fluidized bed with isotopes, 20: 4106 (BNL-tr-43)
HEARNE, J. A., Irradiation of carbon dioxide-methane system, 20: 3981 (AERE-R-5051)
HEARST, J. R., Electronic scheme for measurement of exploding wire energy, 20: 4481 (UCRL-14170)
HEARST, J. R., Piezoelectric response of z-cut tourmaline to shocks of up to 21 kilobars, 20: 5011
HECHTL, E., Operating experience with Seibersdorf inhomogeneous sector field isotope separator, 20: 4283 (SGAE-PH-27/1965)
HEDGE, C. E., Potassium, rubidium, strontium, thorium, uranium, and ratio of ^{87}Sr to ^{86}Sr in oceanic tholeiitic basalt, 20: 4145
HEDGECOCK, J. L., Apparatus for canning nuclear reactor fuel elements, 20: 5029
HEINEMANN, Heinz, Method of sealing refractory vessel containing radioactive wastes, 20: 5209
HELD, Robert Paul, Thermodynamics of non-aqueous electrolytic solutions, 20: 3926 (TID-22374)
HELTEMES, E. C., Behavior of materials at cryogenic temperatures, 20: 4417
HENDERSON, Dale J., Developments in portable x-ray fluorescence instrument using radioisotope excitation sources, 20: 3883 (ORNL-IIC-5, pp 154-81)
HENDERSON, W. B., Nine and sixteen group cross sections for reactor analysis, 20: 4829 (GEMP-173(Suppl.1))
HENGLEIN, A., γ Radiolysis of hydrogen sulfides in all aggregate states, 20: 4017
HENKE, R. P., Charged particle tracks in polymers. 1., 20: 4251 (USNRDL-TR-917)
HENNIG, R. J., FFTF driver fuel: PuO_2—stainless steel cermet, 20: 5192 (BNWL-SA-251)
HENRY, R. J. W., Electron temperatures in D region, 20: 4727 (AD-618054)
HENRY, W. M., Germanium diode to determine C in steels by measurement of prompt γ-radiation, 20: 3894
HERBER, R. H., Narrow-line source for ^{119}Sn Moessbauer spectroscopy, 20: 5014
HERLEY, Patrick J., Luminescence phenomena in gamma-irradiated pure alkane glasses, 20: 3990
HERLING, G. H., Applications of exactly soluble one dimensional model of transfer reactions, 20: 4851
HERNANDEZ-VERELA, J. L., Problems of supply of electrical energy in Spain, 20: 4081
HERRNEGGER, F., Gasdynamic methods in MHD flow, 20: 4702 (AD-619094)
HERZMANN, Hermann, Kieselgel as support in tritium labeling of cardiac glycosides, 20: 3810
HEYNE, L., Effect of reactor irradiation on electrical polarization and conductivity of high polymers, 20: 4030
HILGNER, Wilfried, Multiple scattering of medium fast electrons in films, 20: 4485
HINTZ, R. E., Inorganically insulated superconducting solenoid for operation at 1°K, 20: 4775 (UCRL-16376)
HIRAI, T., Mechanism of pyrolytic graphite formation, 20: 4348
HIRAI, T., Microstructure and density of pyrolytic graphite, 20: 4431
HIRASAWA, Yoshihei, Metabolic studies on experimental nephrosis. I., 20: 3666
HIRSCHBERG, Joseph G., Doppler temperature in toroidal discharge using multichannel Fabry-Perot interferometer, 20: 4713
HIRSCHI, Hans, Radioactivity of few swiss rocks. I., 20: 4157 (ORNL-tr-702)
HIRSHBERG, Joan, Recurrent geomagnetic storms and solar wind, 20: 4745
HO, Tsing, Critical shear stress of Mo single crystal, 20: 4445
HOBSON, A., Evolution equation for N relativistic charged particles, 20: 4723
HOCHREITER, L. E., Design and evaluation of 1000 MW(e) central station powerplant with a circulating fuel gaseous core reactor, 20: 5128 (TID-22225)
HODKIN, D. J., Gas evolution from solid plutonium-bearing residues during storage, 20: 4364 (AERE-M-1644)
HOEGY, Walter R., Photoelectron energy distribution in F region, 20: 4753
HOELZER, B., Demonstration of immunological differences between graffi and gross leukemias, 20: 3694
HOFFENBERG, R., Radioisotope osteogram in rickets, 20: 3672
HOFFMAN, Richard B., Qualitative aspects of N-body problem for approximately relativistic equations of motion, 20: 4766
HOFMEYR, Christoph, Diffusion constants of thermal neutrons in H_2O, phenylene, $ZrH_{1.92}$, and D_2O. III., 20: 4817
HOGAN, J. F., Stability of carbon strengthened columbium–zirconium alloys at elevated temperature in ultra-high vacuum, 20: 4397 (TIM-955)
HOLLENDER, Lars, Radiation doses in oral radiography. IV., 20: 3846
HOLLINGER, Henry B., Prog. rpt. on wall effects in non-equilibrium statistical mechanics, final, 1965, 20: 4706 (RPI-3036-1)
HOLMAN, W. P., Medical examination of radiation workers, 20: 4199
HOLMBERG, S., Experiments on starting process of rotating plasma, 20: 4951
HOLMBERG, S., Free-wheeling of rotating plasma, 20: 4953
HOLMES, J. R., Applications of radioactive isotopes in veterinary medicine, 20: 3859
HOLMES, L. S., Structure of collisionless shock waves in magnetized plasma, 20: 4977
HOLSOPPLE, H. L., Synthesis of 3,9-diethyltridecyl-6-amine, 20: 3974 (ORNL-TM-1314)
HOLTZHAUER, R., Dose measurements from Ra needles, 20: 4205
HOOTEN, B. W., Germanium diode to determine C in steels by measurement of prompt γ-radiation, 20: 3894
HORN, D., Decays of positive-parity baryon resonances in broken U(12), 20: 4666
HORNSEY, Shirley, Effect of fractionation on four day survival of mice after whole-body neutron irradiation, 20: 3728
HORSLEY, R. J., ^{60}Co simulator for treatment planning, 20: 3827

HORST, K. M., Prog. rpt. on SEFOR development, 10/64–1/65, 20: 5120 (GEAP-4799)
HORST, P., Composition of ham in live and slaughtered pigs by means of x rays, 20: 5224
HOWARD, A. J., Studies on ^{19}F in $^{18}O(p,\gamma)^{19}F$ reaction, 20: 4907
HOWER, Charles O., Calculation of (π^-,π^0) reaction on complex nuclei, 20: 4910
HRABOVSZKY, Zoltan, Question of dose using chaoul irradiation tube, 20: 3838
HSU, Y. C., Prog. rpt. on liquid-metal lubricated journal bearings, 4–7/65, 20: 4078 (SWRI-1228-67)
HUBAUX, A., Computer analyses of tensile tests, 20: 4371 (EUR-2514.e)
HUDGINS, A. C. Jr., Magnetocaloric effect in dysprosium, 20: 4420
HUDSON, C. B., Synthesis of [carboxyl-^{14}C]3,4-dehydro-DL-proline, 20: 3975
HUEGEL, F. J., Compressive creep of UC and UN. I., 20: 4396 (PWAC-482(Pt.1))
HUGHES, L. B., Binding energy of the deuteron, 20: 4856
HUMBERT, J., Decanning problems in hot laboratories and attempted solutions, 20: 4962
HUMBLE, J. E., Upper limiting primary rigidity of cosmic ray solar anisotropy, 20: 4563
HUMES, Richard Martin, (p,γ) angular correlations in ^{48}Ti, 20: 4926
HUMPHREY, R. M., Radiosensitivity of normal and 5-bromodeoxyuridine treated mammalian cells during different phases of cell cycle, 20: 3737
HUNT, D. L., Post incident cooling of P.W.R. core, 20: 5030 (AHSB(S)R-86)
HUNT, E. L., Evidence for humoral mediation of radiation-induced motivation obtained from parabiont rats, 20: 3706 (AD-623365)
HUNTER, D. B., Prog. rpt. on development of stable-beta Ti alloy, 7–9/64, 20: 4360 (AD-619399)
HURT III, S. S., Prog. rpt. on research reactor, 4–6/65, 20: 5198 (ORNL-TM-1290)
HUSMANN, O. K., Characteristics of porous tungsten ionizers, 20: 4135
HUYS, D., Studies on separation of ^{137}Cs and ^{90}Sr from fission products in an acid medium on mineral ion exchangers, 20: 3871 (EUR-2497.e)
HWANG, Ching-Lai, Effects of electrical conductance of wall on magneto-hydrodynamic channel flow with heat transfer, 20: 4703 (AD-619101)
HWANG, Un-Poh, Effects of electrical conductance of wall on magneto-hydrodynamic channel flow with heat transfer, 20: 4703 (AD-619101)

I

IIDA, Shoji, Electrical properties of non-stoichiometric uranium dioxide, 20: 4439
IKEJIRI, Joji, Experimental studies on x rays and leukemia. IA., 20: 3765
IMAI, Ryukichi, Engineering problems of power reactor fuel. II., 20: 5147
IMAMURA, Masashi, γ-Ray-induced oxidation of liquid methanol, 20: 4011
INGE-VECHTOMOV, S. G., Comparison of specificity of action of ultra-violet rays and x-rays on mutability of yeast, 20: 3717 (JPRS-31514, pp 77-91)
INGLE, R., Use of digital computer in time-of-flight experiments, 20: 4245 (ORNL-P-1723)
INOMATA, Akira, Geometric theory of neutrinos, 20: 4619
INOUE, Teruji, Preliminary design work of 100 MWt experimental fast reactor, 20: 5079 (NP-15572)
IRANI, G. B., Piezoelectric response of z-cut tourmaline to shocks of up to 21 kilobars, 20: 5011
IRVING, D. C., SPCTRM. 05R Monte Carlo analysis routine for calculating neutron energy spectrum, 20: 4805 (ORNL-TM-1245)
ISHIHARA, Shinichi, Effects of ^{60}Co γ-ray on pharmaceutical powders. II., 20: 4019
ISHIKAWA, Mamoru, Genetically significant radiation dose from dental x-ray diagnosis. I., 20: 4195
ITO, Isamu, Radiation-induced graft copolymerization of methylmethacrylate on polyethylene in an emulsion system, 20: 3996
IVANOV-KHOLODNII, G. S., Mechanism of lower ionosphere ionization, 20: 4737
IVANTISHIN, M. N., Geochemistry and analytical chemistry of rare earth elements. I., 20: 4146

J

JACKLYN, R. M., Upper limiting primary rigidity of cosmic ray solar anisotropy, 20: 4563
JACOB, M., Analysis of new resonances and Regge pole approach to high energy collisions, 20: 4633
JACOB, M., Spin and parity analysis in two-step decay processes, 20: 4585 (SLAC-43)
JACOBS, H., Environmental radioactivity of the Nuclear Research Center, Juelich, 20: 4178 (JUL-284-ST)
JACOBS, S. E., Studies on induced mutants of corynebacterium fascians, 20: 3723
JACOBSON, Cecil Felix, Process for destruction of cellulose-containing material contaminated with radioactive material, 20: 5208
JAHN, P., Conversion of 238.6-kev γ line of ThB and comparison with the tables of Sliv and of Rose, 20: 4920
JAHN, Robert G., Ejection of pinched plasma from axial orifice, 20: 4138
JANCEL, Raymond, Calculation of electron distribution function of homogeneous Lorentzian plasma by successive approximation method, 20: 4961
JANCEL, Raymond, Calculation of non-linear effects bound to propagation of electromagnetic waves in plasma, 20: 4962
JANOUCH, F., Oriented nuclei and beta decay, 20: 4933
JANSSEN, O., Radiolysis of Cs_2, 20: 4028
JANSSON, L., Rig demounting and machining processes for in-cell use, 20: 4351
JARVIS, Stephen Jr., Steady disturbances to viscous, highly conducting laminar boundary layer flow over nonconducting wall with parallel magnetic field, 20: 4098 (AD-614633)
JEANMAIRE, Lucien, Radiochemical determination of ^{90}Sr in large volumes of drinking water, 20: 3867 (CEA-R-2844)
JEANRENAUD, A., Radiological effects at a distance after selective irradiation of lymphatic organs, 20: 3775
JEFFERSON, Sidney, Improvements in or relating to entrance arrangements for irradiation cell, 20: 4096
JELINEK, V., Calciferol estimation in irradiated yeast and mycelia, 20: 3690
JENKINS, T. L., Interaction of muons produced by atmospheric neutrinos, 20: 4561 (COO-818-64)
JICHA, J., SNAP technology conceptual design 100-watt thermoelectric generator heat transfer analysis, 20: 4278 (MND-P-2229)
JIRACEK, V., Excretion of isotopically labeled glucose and thioglucose in rat, 20: 3678
JNANANANDA, S., Validity of ξ approximation for the $\frac{5}{2}^-$ (β) $\frac{1}{2}^+$ decay in $^{141}_{58}Ce$, 20: 4903
JNANANANDA, Swami, Decay scheme and directional correlations of γ rays from ^{182}Ta, 20: 4865
JNANANANDA, Swami, Half-lives of first excited states in ^{182}W and ^{170}Yb, 20: 4877
JOHANSSON, B., Regeneration of bone marrow, 20: 3789
JOHNSON, A. W., Experimental studies of continuum emission of hydrogen, 20: 4973
JOHNSON, Eric G. Jr., Differential cross section for trident production, 20: 4604
JOHNSON, Ernest Walter, Vaporization of Sr sulfide, La monosulfide, and some La–Ag alloys, 20: 3957
JOHNSON, Fred M., Laser as potential tool for cell research, 20: 3741
JOHNSON, J. E., Separation and measurement of ^{137}Cs in precipitation, 20: 4159
JOHNSON, K. W., Development of variable-energy cyclotron HIVEC, 20: 4491 (ANL-7081, pp 78-80)
JOHNSON, Noye M., Thermoluminescence induced by low energy alpha particles, 20: 3983 (BNL-9589)
JOHNSON, R. H., Prog. rpt. on modification of photometric measurement assemblies, final, 1/4–5/3/65, 20: 4234 (AD-619177)
JOLY-CABARET, Francoise, Iterative method of resolution of certain integral equations, 20: 4764
JONES, Carolyn, Radioprotective action of RNA in mice, 20: 3792
JONES, E. W., Influence of weather on salt distributions and aerosols on beaches, 20: 4148 (AD-623515)
JONES, F. R. R., United Kingdom experience of magnox fuel elements, 20: 5094
JONES, I. R., Transfer of radiostrontium from cows' feed to milk, 20: 4162
JONES, J. Benton Jr., Reducing uptake of ^{90}Sr by plants on contaminated Ohio soils, 20: 3679
JONES, L. V., Prog. rpt., 5/65, 20: 3879 (MLM-1266)
JONES, P. M. S., Permeation and diffusion of H isotopes through stainless steels. II., 20: 4366 (AWRE-O-90/65)
JONES, W. D., Report on an informal striation meeting held at the seventh international conference on phenomena in ionized gases, Belgrade, Yugoslavia, August 22–27, 1965, 20: 4946 (ORNL-TM-1307)
JONSON, Erik, Engineering Purchases within reactor area, 20: 5110 (AES-4)
JORDAAN, Jan M. Jr., Feasibility of modeling run-up effects of dispersive water waves, 20: 4142 (AD-619053)
JOSEPH, J. Walter Jr., Radioactive cobalt for heat sources, 20: 4277 (DP-1012)
JOSS, J. O., Current and future development of magnox reactor, 20: 5157
JOUANNAUD, Claude, Method of preparing uranic oxide in granulated form, 20: 3971
JOUFFREY, Bernard, Examination by electron microscope of niobium contaminated at high temperature by interstitial elements, 20: 4401 (ANL-Trans-218)
JUNGER, J. M., Machining and dismantling methods in high activity cells at Ispra, 20: 4125

JUST, Richard, Improvements in or relating to radiation detectors, 20: 4258
JUZA, Robert, Ferrimagnetism of Mn_4N and of some mixed crystals of Mn_4N, 20: 4402 (ANL-Trans-230)

K

KABELL, L. J., F.M. radar system, 20: 5226
KACZER, Jan, Conference on low temperatures, Prague, 63, 20: 4790
KAERCHER, K. H., Appearance of isoenzymes of various enzymes during irradiation therapy, 20: 3845
KAERCHER, K. H., Results of clinical radiation enzymology, 20: 3763
KAERCHER, K. H., Treatment of irradiation reaction of mucosa, 20: 3840
KAGAN, Yu., Phonon spectrum of lattice of white tin, 20: 5005 (IAE-928)
KAHAN, Theo, Calculation of non-linear effects bound to propagation of electromagnetic waves in plasma, 20: 4962
KAHN, B., Transfer of radiostrontium from cows' feed to milk, 20: 4162
KAHN, S., Prog. rpt. on fissiochemical development, semiannual, 1–6/65, 20: 3982 (AGN-8156)
KAIDO, J., Determination of radioactive fallout from nuclear weapon tests. Detection and determination of radioactive nuclides in rain water, 20: 4177 (JAERI-1083)
KALE, Stephen H., Performance of HWCTR safety rod and control rod drive systems, 20: 5194 (DP-971)
KALINKIN, B. N., Angular distribution of transfer reaction products, 20: 4836 (JINR-P-2298)
KALINKIN, B. N., Matrix elements for inelastic scattering of heavy particles. I., 20: 4839 (JINR-P-2333)
KALKER, K. J., Study of instrumentation conditions in ramp forming reactivity perturbations FRJ-2 (DIDO), 20: 5197 (JUL-239-RE)
KAMINSKY, J. J., High temperature titanium alloy development, 20: 4393 (PWAC-472)
KANAGAWA, Akira, Isotope separation by concurrent gas centrifuge, 20: 4285
KANAMORI, Hitoshi, High-voltage waveforms and abnormal voltages in single-phase x-ray units, 20: 4091
KANGOS, James D., Prog. rpt. on influence of local winds on fallout, semiannual, 10/15/64–4/15/65, 20: 4154 (AD-620003)
KANN, J., X-ray absorptiometry with beta-stimulated x-ray sources, 20: 3882 (ORNL-IIC-5, pp 51-71)
KANN, W. J., Faret core I fuel irradiation program and reference design, 20: 5190 (ANL-7106)
KANTOR, P. B., Comparison of nucleon-nucleon scattering data with the predictions of SU(12)$_L$, 20: 4605
KAPOOR, S. S., Emission of K x rays and division of nuclear charge in spontaneous fission of ^{252}Cf, 20: 4914
KARLAN, Mitchell S., Late small bowel obstruction secondary to post-radiation enteritis, 20: 3732
KARO, A. M., Theoretical study of second-order Raman spectra of cesium halides, 20: 5007 (UCRL-14398)
KARTTUNEN, John O., Developments in portable x-ray fluorescence instrument using radioisotope excitation sources, 20: 3883 (ORNL-IIC-5, pp 154-81)
KATO, H. T., Appearance of isoenzymes of various enzymes during irradiation therapy, 20: 3845
KATO, H. T., Results of clinical radiation enzymology, 20: 3763
KATZ, J. J., Deuterium isotope effects in cytology, 20: 3651
KAUFMAN, Sheldon B., Calculation of (π^-,π^0) reaction on complex nuclei, 20: 4910
KAUTSKY, H., Method of determination of radioactive isotopes ^{55}Fe and ^{59}Fe in sea water, 20: 3891 (CEA-tr-A-1838)
KAUTZLEBEN, Heinz, Analytical representation of geomagnetic field and secular variation, 20: 4734 (N64-30079)
KAWAI, T., Radiation-induced crosslink formation in polyethylene. I., 20: 4002
KAWAI, T., Radiation-induced crosslink formation in polyethylene. II., 20: 4003
KAWAI, T., Radiation-induced crosslink formation in polyethylene. IV., 20: 4005
KAWAI, T., Radiation-induced crosslinking in polyethylene. V., 20: 4006
KAWAI, Toshio, Coupled reactor kinetics, II., 20: 5065
KAWAMURA, Fumio, Protection mechanisms of non-malignant and malignant cell against ionizing radiation. II., 20: 3796
KAZIYAMA, H., Determination of radioactive fallout from nuclear weapon tests. Detection and determination of radioactive nuclides in rain water, 20: 4177 (JAERI-1083)
KEANE, B. E., Image contrast and radiation protection. II., 20: 3815
KEEDY, Curtis Russell, Isomeric cross section ratios for $^{44,44m}Sc$ system, 20: 4922
KEILING, R., Cancers of bile duct in thorotrastosis of liver, 20: 3722
KELBER, C. N., Safety analysis for AARR critical experiment, 20: 5189 (ANL-6929)
KELDYSH, L. V., Superconductivity in nonmetallic systems, 20: 4781
KELLER, A., Radiation-induced crosslink formation in polyethylene. I., 20: 4002
KELLER, A., Radiation-induced crosslink formation in polyethylene. II., 20: 4003
KELLER, A., Radiation-induced crosslink formation in polyethylene. IV., 20: 4005
KELLER, A., Radiation-induced crosslinking in polyethylene. V., 20: 4006
KELLER, R. M., Saline: a FORTRAN computer program for process design of saline water conversion plants using the multi-stage, flash-evaporation process, 20: 3923 (ORNL-TM-1299)
KELLOGG, R. B., Extension of hot-1 to treat Neumann boundary conditions—with applications to certain vibration problems, 20: 4080 (WAPD-TM-535)
KELLY, Roger, Study of inert-gas diffusion in ionic crystals and sinters, 20: 3944
KENNADY, J. C., Albumin macroaggregates for brain scanning: experimental basis and safety in primates, 20: 3832
KENNETT, T. J., Binding energy of the deuteron, 20: 4856
KENWARD, C. J., Safety of DAPHNE, 20: 5188 (AERE-R-4932)
KEPPLER, E., Frequency of chlorophyll mutations after x irradiation of heterzygous M_2-seed stock of barley, 20: 3782
KERER, G., Gasdynamic methods in MHD flow, 20: 4702 (AD-619094)
KERLER, Werner, Study of complex and covalent iron compounds using ^{57}Fe Moessbauer effect, 20: 3927 (AERE-Trans-1026)
KERNAN, W., Phase-space considerations for four-particle final states, 20: 4658
KERNS, Quentin A., Cavity resonator systems for supporting nonsinusoidal periodic waveforms, 20: 4511 (UCRL-16242)
KERR, R. C., Enhancement of radiosensitivity of skin of patients by high pressure oxygen, 20: 3727
KERR, W. M. M., 12 Group set of photon cross sections for use in anisotropic S_n calculations of photon transport, 20: 4996 (AWRE-O-79/65)
KESSEMEIER, Horst, Pulsed nuclear magnetic resonance in rapidly rotating solids, 20: 4931
KESSLER, J. O., Plasma confinement in low-density C stellarator discharges, 20: 4942 (MATT-372)
KESSLER, Joachim, Multiple scattering of medium fast electrons in films, 20: 4485
KHANNA, K. M., Single photon annihilation of ^3S state of negaton-positon pair, 20: 4594
KHLEBNEKOVA, V. N., Thermodynamic properties of deuterium and tritium substituted non-linear triatomic hydrides, 20: 3950
KHLEBNIKOV, V. P., Tributyl phosphate extraction of Pa. I., 20: 4057
KHLEBNIKOV, V. P., Tributyl phosphate extraction of Pa. II., 20: 4058
KHOE, T. K., Development of variable-energy cyclotron HIVEC, 20: 4491 (ANL-7081, pp 78-80)
KHRPPOVA, V. I., Comparative study of mutagenic action of different types of radiation and ethyleneimine on alga chlorella, 20: 3716 (JPRS-31514, pp 65-76)
KHUKHAREVA, I. S., Superconductive properties of Nb–Zr alloys, 20: 4792
KIERAS, F. J., Electron microscopic and biochemical characterization of fraction I protein, 20: 5219 (TID-22372)
KIGLER, Eugene O., Performance of HWCTR safety rod and control rod drive systems, 20: 5194 (DP-971)
KIKINDAI, Tivadar, Chemical and kinetic study of reaction between sulfur dioxide and uranium hexafluoride, 20: 3935
KIKUCHI, Atsushi, Genetically significant radiation dose from dental x-ray diagnosis. II., 20: 4196
KIKUCHI, Chihiro, Thermal-neutron-induced recoil defects in cadmium sulfide, 20: 4000
KIKUCHI, Atsushi, Genetically significant radiation dose from dental x-ray diagnosis. I., 20: 4195
KIMELDORF, D. J., Analysis of local and systemic effects of ionizing radiation on bone growth, 20: 3707 (AD-623641)
KIMELDORF, D. J., Evidence for humoral mediation of radiation-induced motivation obtained from parabiont rats, 20: 3706 (AD-623365)
KING, E. A., Limited-energy neutron sources produced by decay of excited nuclei, 20: 4802 (IDO-17115)
KINOSHITA, Hideo, Studies on uranium refinery, 20: 4052
KINOSHITA, Tsuneo, Effects of physical treatments on infectivity of Myc. lepraemurium, 20: 3752
KINOSHITA, Yasutomi, Metabolic studies on experimental nephrosis. I., 20: 3666
KIRKBRIDE, L. D., Effect of yttrium on the recrystallization and grain growth of tantalum, 20: 4424
KIRYANOV, A. P., Anisotropy of the Moessbauer effect in β-Sn single crystals at 4.2°K, 20: 4932
KISTENEV, E. P., Investigation of reactions $\pi^-p \to n\pi^0 + n$ at the π^- momentum of 4 Bev/c, 20: 4582 (JINR-P-2361)
KISTENEV, E. P., Measurement of energy and angular characteristics of

electrons and γ-quanta in propane bubble chamber, 20: 4240 (JINR-P-2277)
KITABATAKE, Takeshi, Survey on death rate and causes of death in x-ray technicians, 20: 3760
KITE, F. D., Launch hazards assessment program, report on Atlas/Centaur abort, 20: 4187 (SC-RR-65-333)
KITRILAKIS, S. S., Thermionic emitter materials research program, 20: 4570 (AD-614592)
KITZES, Arnold S., Remote underwater devices for evaluation and reduction of spent yankee fuel assemblies, 20: 5136 (WCAP-5554)
KLEBANOV, Yu. D., Differential gaseous Cherenkov counter, 20: 4239 (IAE-900)
KLEIN, D., Study of slightly enriched UO_2 lattice with H : U = 0.42—measurement and analysis, 20: 5071
KLEIN, Richard M., Effects of near ultraviolet and green radiations on plant growth, 20: 3769
KLEINERT, H., Treatment of irradiation reaction of mucosa, 20: 3840
KLENER, Vladislav, Biological effect of small doses of ionizing radiation on human organism, 20: 3770
KLIESCH, J., Composition of ham in live and slaughtered pigs by means of x rays, 20: 5224
KLING, H. P., Oxidation resistant coatings on niobium, 20: 4315
KLINGMUELLER, Walter, Inactivation and mutation rate of x- and γ-irradiated Neurospora Crassa conidia, 20: 3780
KMONK, Stanley, Releasable coupling mechanism, 20: 5051
KNEIP, G. D., Method for increasing critical current of superconducting alloys, 20: 4799
KNIGHT, William John, Improvements relating to nuclear reactor servicing apparatus, 20: 5041
KNIGHTON, J. B., Consolidation of lanthanon fission products in alloys, 20: 3865 (ANL-7064)
KNIGHTON, James B., Process of preparing thorium metal from oxide, 20: 4316
KNIGHTON, James B., Regeneration of nuclear fuel, 20: 4073
KNOBLOCH, E., Calciferol estimation in irradiated yeast and mycelia, 20: 3690
KNODEL, W., Radiation sensitivity of DNA synthesis, 20: 3702
KNOOP, E., Bibliographical survey on facilities and processes for radioactive milk decontamination, 20: 3872 (EUR-2507.d)
KOBAYASHI, Jindo, Protection mechanisms of non-malignant and malignant cell against ionizing radiation. II., 20: 3796
KOBAYASHI, Koinosuke, Changes of polymer crystals due to irradiation with electrons accelerated at various voltages, 20: 3987
KOBAYASHI, Shigeo, Oxygen effect and temperature dependence of fluorescence intensity in naphthalene scintillators, 20: 3994
KOENNE, W., Construction of concrete containers, 20: 4406 (ORNL-tr-873)
KOFSKY, I. L., Prog. rpt. on modification of photometric measurement assemblies, final, 1/4–5/3/65, 20: 4234 (AD-619177)
KOHL, J., Survey and recommendations for radioisotope applications pertinent to U. S. Naval Civil Engineering Laboratory Operations, 20: 4089 (TLW-1055A)
KOKUBU, Nobuhide, Simultaneous ultraviolet spectrophotometric determination of niobium and tantalum by hydrogen peroxide method, 20: 3904
KOLOUSEK, J., Excretion of isotopically labeled glucose and thioglucose in rat, 20: 3678
KOMAREK, E. E., Thin-film, field-effect devices, 20: 4220 (SC-TM-65-424)
KOMIYAMA, Kihachiro, Survey on death rate and causes of death in x-ray technicians, 20: 3760
KOMOCHKOV, M. M., Passage of high energy neutrons in iron–aqueous mixtures, 20: 4998 (JINR-P-2359)
KONDO, Teruo, On recovery-promoting chemicals after gamma-ray irradiation to mouse strain L cells cultured in vitro, 20: 3791
KONUMA, Michiji, Antiproton-nucleon annihilation at rest into two mesons and SU(6) symmetry, 20: 4615
KOPCEWICZ, T., Determining air contamination at earth surface by stratospheric radioactive substances, 20: 4158
KOPP, J. K., Antihyperon production in antiproton-proton reactions at 3.7 Bev/c, 20: 4608
KOPPEL, J. U., Prog. rpt. on integral neutron thermalization, 4–6/65, 20: 4801 (GA-6634)
KOPYLOVA, D. K., Investigation of reactions $\pi^- p \to n \pi^0 + n$ at the π^- momentum of 4 Bev/c, 20: 4582 (JINR-P-2361)
KORENKOV, I. P., Individual dosimetric control technique, 20: 4198
KORFF, Serge A., IQSY-EQEX cosmic-ray expedition to India, 20: 4567
KORKISCH, J., Ion exchange separation of uranium and thorium in mixed and nonaqueous solvents, 20: 3888 (TID-22402)
KORNBICHLER, Heinz, Neutronic reactor, 20: 5086
KOROBKOV, Yu. S., Anomalous ionization of lower ionosphere of temperate latitudes during world magnetic storms, 20: 4736
KOROLEVA, I. I., Thermochemistry of cerium(IV) nitrates, 20: 3954
KORST, William L., X-ray diffraction data for ZrC · ZrH_2, 20: 4378 (NAA-SR-Memo-11542)
KOSANIC, Miroslav, Irradiation possibilities in 2 kilocurie ^{60}Co radiation unit at Boris Kidric Institute at Vinca, 20: 4272 (JPRS-32813)
KOSKI, W. S., Intermediates in isotopic exchange reactions involving diborane, 20: 3963
KOTHARI, L. S., Decay constant of neutron pulse inside finite solid moderator assembly, 20: 4815
KOVALENKO, N. F., Thermodynamic properties of deuterium and tritium substituted non-linear triatomic hydrides, 20: 3950
KOVALENKO, V., Safeguarding food products and water from agents of mass destruction, 20: 4192 (JPRS-32686)
KOVAN, I. A., Magneto-sonic heating of plasma, 20: 4939 (IAE-911)
KOWALSKA, K., Tables of functions $x(c,\nu)$ and $\pm (c_1,c_2)$ for numerical solutions of slab geometry neutron transport problems. I., 20: 4803 (INR-630/IX-A/PR)
KOZHIN, S. A., Comparison of specificity of action of ultra-violet rays and x-rays on mutability of yeast, 20: 3717 (JPRS-31514, pp 77-91)
KOZIK, B., Correlation of neutrons in refleoted reactor, 20: 5058 (JINR-P-2335)
KOZIOL, J. J., Prog. rpt. on correlations between sensitization and stress corrosion cracking of 300 series stainless steels, 7–9/65, 20: 4370 (CEND-3256-250)
KRASIK, V. P., Physics and techniques of strong magnetic fields, 20: 4486
KRAUS, John W., Method of sealing refractory vessel containing radioactive wastes, 20: 5209
KRENZ, J. H., Harmonic generation in plasma due to velocity-dependent collision frequency, 20: 4885
KRISCH, Jean Peck, Calculation of the baryon-vector meson mixing parameters, 20: 4691
KRISHNAMURTHI, M., Harmonic structure and band splitting of type II solar radio bursts, 20: 4524
KRISTAPSON, Yu. Zh., Radiation physics. III., 20: 4008
KRIVENTSOVA, A. G., Investigation of reactions $\pi^- p \to n \pi^0 + n$ at the π^- momentum of 4 Bev/c, 20: 4582 (JINR-P-2361)
KRIVOV, M. A., Influence of x radiation on electrophysical properties of Ge and Ge p-n transitions. I., 20: 4465
KRONBERGER, H., Fast reactor development, 20: 5165
KRONGAUS, A. N., Ruler to determine relative deep doses and selection of proper conditions for irradiation by telegamma-units, 20: 3839
KROPP, W. R., Interaction of muons produced by atmospheric neutrinos, 20: 4561 (COO-818-64)
KRUCHININ, S. P., Differential gaseous Cherenkov counter, 20: 4239 (IAE-900)
KRUDEWIG, W., Electron acceleration in helical fields, 20: 4518
KRUGER, O. L., Heat pulse measurements of uranium compounds, 20: 3943
KRUSE, D., Irradiation of patients during extra-oral radiography of teeth and jaw, 20: 4206
KSYCKI, Joecile, Effects of chlorpromazine on radioiodine uptake and metabolism in C-57 brown mice, 20: 3677
KUESER, P. E., Magnetic, electrical conductor, electrical insulation, and bore seal materials, 20: 4379 (NASA-CR-54091)
KUGLER, M., Decays of positive-parity baryon resonances in broken U(12), 20: 4666
KUHN, Peter, Study of complex and covalent iron compounds using ^{57}Fe Moessbauer effect, 20: 3927 (AERE-Trans-1026)
KUL'SKAYA, O. A., Geochemistry and analytical chemistry of rare earth elements. I., 20: 4146
KULT, K., Source of polarized ions for cyclotron, 20: 4519
KUNDEL, Harold L., Effect of massive doses of 32 Mev protons and ^{60}Co radiation on primates, 20: 3692
KUNTZMAN, F., Cancers of bile duct in thorotrastosis of liver, 20: 3722
KUO, T. K., Comparison of nucleon-nucleon scattering data with the predictions of $SU(12)_L$, 20: 4605
KURATH, Dieter, Quadrupole deformation in ^7Li, 20: 4902
KURIMURA, Yoshimi, Radiation-induced oxidation of Sb(III) in aqueous solution. III., 20: 4009
KURODA, K., Measurement of polarization in elastic proton-deuteron scattering at 155 Mev, 20: 4595
KURODA, Tadashi, Preparation of high purity uranium metal by the electrolysis of fused uranium tetrachloride, 20: 4346
KURODA, Tadashi, Production of high purity uranium by fused salt electrolysis, 20: 4347
KUSCER, I., Use of Poincare-Bertrand formula in neutron transport theory, 20: 4812
KUTKA, J., Production of uranium single crystals, 20: 4350
KUZMIN, V. I., Superconductive properties of Nb–Zr alloys, 20: 4792
KVITKO, K. V., Comparative study of mutagenic action of different types of radiation and ethyleneimine on alga chlorella, 20: 3716 (JPRS-31514, pp 65-76)
KVOKOVA, I. M., Electrolytic deposition of thick and reguline rhenium layers, 20: 4404 (JPRS-32773)

L

LABROCHE, Claude, Improvements in or relating to methods of and apparatus for transferring liquids under remote control, 20: 4095

LACKEY, M., Multi-region neutronic fuel element, 20: 5102

LACKNER, F., Gasdynamic methods in MHD flow, 20: 4702 (AD-619094)

LACROIX-DESMAZES, Francois, Transfers between hyperfine levels of odd isotopes of mercury in 6^3P_1 state under effect of collisions with rare gases, 20: 4544

LAFOUCRIERE, Joseph, Analysis of elastic scattering of α particles on light nuclei using optical potentials, 20: 4859

LAHIRI, J., Self-consistent perturbation. I., 20: 4537 (NP-15576)

LAHIRI, J., Self-consistent perturbation. II., 20: 4538 (NP-15577)

LALEVIC, Bogoljub, Intermediate state of superconductors, 20: 4783

LAMOT, Georges-Henri, Analysis of elastic scattering of α particles on light nuclei using optical potentials, 20: 4859

LAN, Vo Ky, Excitation by electron impact of strongly ionized ions of p^2 configuration, 20: 4543

LANDAU, R. W., Oscillations of plasma column, 20: 4985

LANGE, F., Superconducting hollow cylinders made of Nb_3Sn as persistent magnets at 14°K, 20: 4793

LANGERON, Jean-Paul, Recrystallization, grain growth, and preferred orientations of zirconium purified by zone fusion, 20: 4413

LANGPAPE, R., Investigations on emission materials for thermionic converter influence of CsF on electron work functions of W, Ta and Mo, 20: 4572 (EUR-2283.d)

LANGSTON, Ruble, Effects of gamma irradiation on symptom expression of barley stripe mosaic virus disease and on two viruses in vivo, 20: 3768

LANZL, Lawrence H., Radioisotopic device for measuring bone mineral, 20: 3803 (ORNL-IIC-5, pp 257-76)

LANZO, Chester D., Simulated fuel assembly, 20: 5028

LAPIDUS, L. I., New possibilities for investigating nucleon, pion and gamma-quanta reactions on polarized hydrogen targets, 20: 4637

LARIN, I. K., Method and equipment for investigations of electric field effect on radiolysis of gases, 20: 4022

LARSEN, F. L., Radiations measurements group at Princeton-Pennsylvania 3 Bev proton synchrotron, 20: 4506 (PPAD-569E)

LARSEN, Ib, Process for destruction of cellulose-containing material contaminated with radioactive material, 20: 5208

LATHROP, K. D., Comparison of three methods used to calculate gamma-ray transport in iron, 20: 5001 (ORNL-RSIC-9)

LAURO, M., Decontamination experience at hot laboratory of Casaccia, 20: 4211

LAURO, M., Techniques for dismantling irradiated rigs, 20: 4092

LAUTRUP, B., Comparison of forward dispersion relations with experiments around 10 Bev, 20: 4602

LAVAL, Guy, Property of correlation in plasma during equilibrium, 20: 4959

LAVERICK, C., Inorganically insulated superconducting solenoid for operation at 1°K, 20: 4775 (UCRL-16376)

LAWRENCE, Walter Jr., Functional capacity of canine bone marrow implants in the spleen, 20: 3652

LAYNER, V. I., Electrolytic deposition of thick and reguline rhenium layers, 20: 4404 (JPRS-32773)

LEAF, B., Evolution equation for N relativistic charged particles, 20: 4723

LEBEDEV, R. M., Inflatable gaskets for JINR large-volume hydrogen bubble chambers, 20: 4242 (JINR-P-2376)

LEBEDEVA, N. S., Analysis of polarization in a neutron beam by scattering on Coulomb field of nucleus, 20: 4832 (IAE-901)

LE BEYEC, Yvon, Light isotopes of polonium produced by nuclear reactions of ^{12}C ions on platinum, 20: 4860

LEBOUTET, Hubert, Particle injecting device, 20: 4993

LEE, D. Y., Influence of temperature on radiation-induced surface effects in transistors, 20: 4261 (AD-623078)

LEE, L. L. Jr., Study of $^{19}F(^3He,d)^{20}Ne$ reaction, 20: 4908

LEE, Sook, Electron-spin resonance studies of irradiated glasses, 20: 5019

LEE, T. D., Minimal electromagnetic interaction and C, T noninvariance, 20: 4601

LEE, T. D., Possible existence of a charged, but C = 1, particle, 20: 4600

LEFEVRE, I., ^{137}Cs decontamination of concentrated fission product solutions, 20: 3874 (EUR-2535.f)

LEFEVRE, Jean, Improvements in or relating to zirconium phosphate preparation, 20: 3968

LEFEVRE, Jean, Treatment of solutions of products formed by fission of U–Mo alloys, 20: 4070

LEFORT, G., Transfer in high activity chemistry cell, 20: 4044

LEFORT, Marc, Light isotopes of polonium produced by nuclear reactions of ^{12}C ions on platinum, 20: 4860

LEHNERT, B., Experiments on starting process of rotating plasma, 20: 4951

LEHNERT, B., Free-wheeling of rotating plasma, 20: 4953

LEHNERT, Bo, Starting process of rotating plasma, 20: 4952

LEIBFRIED, Guenther, Boltzmann equation for distribution for primary atoms, 20: 4721

LEINBACH, H., Influence of geomagnetic activity on polar cap absorption, 20: 4756

LEMEILLE, C., Study of the second step of the reaction $^7Li(d,n)^8Be$; $^8Be \rightarrow 2\alpha$, 20: 4869

LENGEMANN, F. W., Factors affecting iodine concentration in bovine milk, 20: 3674

LENZI, M., Radiation-induced polymerization of 1,2-cyclohexene oxide, 20: 3992

LEONARD, J. C., Malabsorption syndrome following radiotherapy, 20: 3851

LEPECHINSKY, Dimitri, Measurement of electron density and collision frequency of plasma, 20: 4955

LEPETIT, Henri, Microdetermination of oxygen in metals by radioactive reagents and by activation with fast neutrons at 14 Mev, 20: 3878 (LYCEN-6524)

LEPILOVA, L. I., Measurement of energy and angular characteristics of electrons and γ-quanta in propane bubble chamber, 20: 4240 (JINR-P-2277)

LEPRINCE, Philippe, Propagation of dipolar mode along plasma column, 20: 4956

LEPUNSKII, A. I., BN-350 atomic power station, 20: 5137 (JPRS-31193)

LERNER, Bernard J., Reductive chlorination of activated ores containing high melting metals, 20: 4072

LERNER, E., Thermal and electrical conductivities of Mo–Re alloys in superconducting and normal states, 20: 4361 (AD-619719)

LERNER, M. W., Differential spectrophotometric determination of boron with diaminochrysazin, 20: 3892

LESINSKI, J., Reasons of work instability of G-M counters excitation pulses, 20: 4254

LEUTZ, H., Decay of ^{40}K, 20: 4919

LEUTZ, H., Electron capture ratios in decay of ^{202}Tl, 20: 4875

LEV, I. E., Investigation of cerium distribution in cast iron by means of electron probe, 20: 4414

LEVER, R. C., Coating for niobium, 20: 4355

LEVIN, Bertram, In vivo measurement of bone mineral content by transmission technique, 20: 3886 (ORNL-IIC-5, pp 290-4)

LEVIN, F. S., Coupled-equations method for scattering of identical particles, 20: 4672

LEVIN, Gilbert V., Rapid microbiological determinations with radioisotopes, 20: 3667

LEVIN, Ira W., Vibrational spectra and potential function for SnH_4 and SnD_4, 20: 3942

LEVINE, James Lewis, Mobility of electrons in dense helium gas at low temperatures, 20: 4788

LEVY, M., Elementary particle and high energy physics, 20: 4695

LEVY, M. E., Propellant triggered gas discharges in pulsed plasma engines, 20: 4136

LEVY, R. M., Hyperfine structure in 2084-kev state of ^{140}Ce, 20: 4888

LEWIN, J., Snap shielding program at ORNL, 20: 5183 (ORNL-P-1736)

LEWIN, Walter Hendrik Gustav, Determination of nuclear decay energies and conversion coefficients using coincidence techniques, 20: 4843 (NP-15456)

LEWINS, Jeffery, Adjoint function in time optimal xenon shutdown problem, 20: 5075

LEWIS, Elmer Eugene, Boltzmann integral equation treatment of resonance absorption in reactor lattices, 20: 5077

LEYERS, H. J., Neutron and gamma heating in experimental channels of FRJ-2 reactor, 20: 5202

LI, Ming Chiang, Three-particle unitarity integral, 20: 4647 (TID-22274)

LICHEVALLIER, Maurice, Improvements in valves for fluid flow control, 20: 5042

LIEBENDOERFER, Helmut, Flexible system for collecting and recording of information, 20: 4226

LIEBERMAN, P., Prog. rpt. on reactor containment, 8–9/65, 20: 5023 (IITRI-578P21-15)

LIEWERS, Peter, Simple reactivity meter of high sensitivity, 20: 5061 (ZFK-RN-22)

LIGEON, E., Study of $^{16}O(d,\alpha_0)$, $^{16}O(d,p_0)$, and $^{16}O(d,p_1)$ reactions at 300 kev to 1 Mev, 20: 4870

LIMIC, N., Behavior for large k of S-matrix for strongly singular potentials, 20: 4640 (IC/65/75)

LIMONCELLI, E. A., Stability of carbon strengthened columbium–zirconium alloys at elevated temperature in ultra-high vacuum, 20: 4397 (TIM-955)

LIN, D. L., Influence of multiple virtual transitions on reorientation effect in Coulomb excitation, 20: 4901

LINCOLN, J. Virginia, Geomagnetic and solar data, 20: 4750

LINDSAY, Ian R., Effect of massive doses of 32 Mev protons and ^{60}Co radiation on primates, 20: 3692

LINFOOT, J. A., Growth hormone in acromegaly, 20: 3828

LINGUET, Roger, Improvements in or relating to neutron detectors,

20: 4260
LINVILLE, Bill, Conference on energy conversion and storage, Stillwater, 10/64, 20: 4575
LIPKIN, H. J., Decays of positive-parity baryon resonances in broken U(12), 20: 4666
LIPSETT, J. J., Ruptured fuel location with high resolution gamma-ray spectrometers, 20: 5109 (AECL-2360)
LISENENKOV, A. T., Fast convergence in Monte Carlo method of resolving problems of radioactive logging, 20: 4168
LISMAN, F. L., Fission of ^{197}Au by intermediate-energy He ions, 20: 4894
LITOMISKII, M., Superconductive properties of Nb–Zr alloys, 20: 4792
LITOMISKII, Miroslav, Solenoids for strong magnetic fields, 20: 4489
LITTLE, W. W. Jr., RED CROSS. Code to compute resonance shielded, temperature dependent cross sections for fast reactor analysis, 20: 5055 (BNWL-146)
LIVINGOOD, J. J., Development of variable-energy cyclotron HIVEC, 20: 4991 (ANL-7081, pp 78-80)
LLOYD, Lowell T., Preferred orientation in sheet of alpha-rolled plutonium, 20: 4407
LO, S. Y., M(12) predictions for pp scattering, 20: 4599
LOBASHEV, M. E., Studies in genetics, 20: 3712 (JPRS-31514)
LOBOV, G. A., Time parity nonconservation in strong interactions, 20: 4871(T)
LOCKETT, Clodovie, Effects of chlorpromazine on radioiodine uptake and metabolism in C-57 brown mice, 20: 3677
LOEBE, J., Examinations of radiation reactions of liver by means of ^{131}I bengal rose tests, 20: 3774
LOGINOV, A. A., Perspectives of atomic heat and power plants, 20: 5149
LOMBARD, Paul, Crystalline and magnetic properties of mixed garnets of dysprosium and ceric earths, 20: 4411
LONG, Everett, Improvements relating to nuclear reactor servicing apparatus, 20: 5040
LONG, Everett, Improvements relating to nuclear reactor servicing apparatus, 20: 5041
LONGEQUEUE, J. P., Study of $^{16}O(d,\alpha_0)$, $^{16}O(d,p_0)$, and $^{16}O(d,p_1)$ reactions at 300 kev to 1 Mev, 20: 4870
LONGEQUEUE, N., Study of $^{16}O(d,\alpha_0)$, $^{16}O(d,p_0)$, and $^{16}O(d,p_1)$ reactions at 300 kev to 1 Mev, 20: 4870
LONGEQUEUE, Nicole, Diffraction in medium-energy nuclear reactions, 20: 4827 (CEA-Bib-60)
LONSDALE, H. K., Prog. rpt. on advanced, graphite-matrix, dispersion type fuel systems and research on graphite, 11/15/64–2/14/65, 20: 5089 (GA-6181)
LOOMIS, T. C., X-ray spectroscopy as analytical tool, 20: 3911
LOPEZ, D. F., Effect of gamma radiation on reproductive potential of Mexican fruit fly, 20: 3745
LOPUSZANSKI, Jan, Goldstone's theorem, 20: 4660
LORENZ, A., Prog. rpt. on physics, 2–5/65, 20: 4482 (UCRL-14360)
LORIERS, Jean, Crystalline and magnetic properties of mixed garnets of dysprosium and ceric earths, 20: 4411
LOS, J., Thermal diffusion in isotopic hydrogen and hydrogen–helium mixtures, 20: 4724
LOURO, Jose M., Prog. rpt. on chromosomal damage in humans by x-irradiation, annual, 1964, 20: 3705 (AD-617601)
LOUTTIT, R. I., Antihyperon production in antiproton-proton reactions at 3.7 Bev/c, 20: 4608
LOUW, J. H., Malignant Zollinger-Ellison syndrome in Bantu woman with prolonged remission after gastric radiotherapy, 20: 3821
LOVE, L. O., Review of ORNL electromagnetic separations program, 20: 4282 (ORNL-3861)
LOVE, Roy Edward, Ultrasonic attenuation in superconducting lead, 20: 4782
LOVE, William D., Isotope technics in clinical cardiology, 20: 3818
LOVELACE, William E., Size constancy as function of ageing and x-ray irradiation in rhesus monkeys, 20: 3721
LOVITCH, Lionel, Direct numerical integration of two-nucleon Schroedinger equation with tensor forces, 20: 4597
LOW, Charles A. Jr., Electrostatic propulsion system with direct nuclear electro generator, 20: 4140
LOW, W., Electron density ionization rate and approach to thermal equilibrium behind shock waves by means of microwave techniques, 20: 4934 (AD-619093)
LOZINA, L. A., Differential gaseous Cherenkov counter, 20: 4239 (IAE-900)
LUBY, C. S., Description and results of P9 coated particle irradiation experiment, 20: 4458 (GA-6485)
LUCAS, Jacques, Chemical and kinetic study of reaction between sulfur dioxide and uranium hexafluoride, 20: 3935
LUGMAIR, G., Operating experience with Seibersdorf inhomogeneous sector field isotope separator, 20: 4283 (SGAE-PH-27/1965)
LUIDINGA, F., Nuclear analyses and nuclear power cost of nero core reference design, 20: 5176 (EUR-2468.e)
LUKENS, H. R. Jr., Elemental survey analysis by neutron activation: simplified estimation of upper limits, 20: 3898
LUKSHA, Eugene, Thermodynamic properties of non-aqueous solutions. II., 20: 3925 (TID-22366, App. B)
LUNDQUIST, D., Eta photoproduction in region from threshold to 900 Mev, 20: 4578 (AD-618660)
LUNDY, T. S., Diffusion in solids, 20: 4385 (ORNL-3870, pp 15-19)
LUNG, Chi-wei, Critical shear stress of Mo single crystal, 20: 4445
LUPPOV, G. M., Development of methods of defectoscopy of metals with application of gamma radiation, 20: 4114 (AD-621784)
LURIE, D., Normalization of Bethe-Salpeter wave functions, 20: 4671
LUSCHYKOV, V. I., Polarization of protons in La–Mg nitrate, 20: 5021
LYMAN, John T., Secondary electron distribution for heavy ions, 20: 4541 (UCRL-16405)
LYNCH, H., Report on inelastic electron scattering program at Stanford, 20: 4581 (AD-618663)
LYNCH, H. L., Pion-pair photoproduction below 1 Bev, 20: 4579 (AD-618661)
LYNDS, L., Infrared spectrum and vibrational analysis of dibromoborane and dibromoborane-d, 20: 3940
LYONS, Louis, Attempt to observe a positive-strangeness baryon, 20: 4589 (UCRL-11754)
LYTTON, J. L., Effects of C and W on flow stress recovery of Mo, 20: 4409

M

MACDONALD, I. P. L., Further geometrical factors affection dryout heat flux in vertical, internally heated annuli cooled by steam/water mixtures at 1000 psi, 20: 4099 (AECL-2333)
MACFARLANE, A. J., Normalization of Bethe-Salpeter wave functions, 20: 4671
MACFARLANE, A. J., Shmushkevich's method for charge-independent theory, 20: 4667
MACK, J. E., Nuclear spin and magnetic moment of ^{37}Ar, 20: 4890
MACMAHON, Alan, Finite gyro-radius corrections to hydromagnetic equations for Vlasov plasma, 20: 4979
MACOMBER, John W., Nuclear reactor control rod assembly with improved driving mechanism, 20: 5044
MADSON, A. A., Fast neutron capture in rhenium, 20: 4868
MAEDA, Hiroshi, Classification of daily geomagnetic variations, 20: 4742
MAGALOTTI, Marion F., Radiation-induced changes in epithelium of Buccal mucosa, 20: 3744
MAGNAC-VALETTE, Denise, Study of excitation curves of (t,α) reaction on ^{16}O between 1 and 3 Mev, 20: 4858
MAILLET, P., Clearance of radioactive colloidal gold in dog with porto-caval anastomosis, 20: 3681
MAILLET, P., Experimental study of the clearance of colloidal ^{198}Au, 20: 3680
MAJEWSKI, M., Numerical calculations in statistical theory of particle production in angular momentum representation, 20: 4643 (INR-607/VI/PH)
MAJUMDAR, S. Datta, Gravitation theory of Hoyle and Narlikar, 20: 4771
MAKI, Kazumi, Fluxoid structure in superconducting films, 20: 4777
MAKIEJ, B., Magnetic induction distribution in cylindrical specimen, 20: 4794
MAKOV, N. N., Extraction of cerium and yttrium by naphthenates, 20: 4051
MALAISE, E. P., Chromosomal number and radiosensitivity of experimental tumors, 20: 3751
MALDAGUE, Pierre Edmond Jules Marie, Method of varying moderation in nuclear reactor, 20: 5053
MALDAGUE, Pierre Edmond Jules Marie, Nuclear reactors, 20: 5052
MALEIN, A., Report on a meeting held in the old lecture room at Christ Church College, Oxford, at 9 p.m. on Thursday, September 9, 1965, 20: 4945 (ORNL-TM-1306)
MALET, P., Cholinesterase activities in mouse liver and kidney during experimental intoxication with uranyl nitrate, 20: 3670
MAL'KOV, V. V., Passage of high energy neutrons in iron–aqueous mixtures, 20: 4998 (JINR-P-2359)
MALOY, J. O., Improvement of Caltech 1.5 Bev electron synchrotron, 20: 4495 (CONF-650923-16)
MALVILLE, J. McKim, Transition probabilities in highly ionized p^2 and p^4 configurations, 20: 4553
MALYANOV, S. V., Influence of x radiation on electrophysical properties of Ge and Ge p-n transitions. I., 20: 4465
MALYSHEV, R. V., Determination of charged particle momentum in inhomogeneous magnetic field, 20: 4583 (JINR-P-2371)
MANCINI, R. A., Consolidation of lanthanon fission products in alloys, 20: 3865 (ANL-7064)
MANSUROV, S. M., Some peculiarities of geomagnetic variations in polar regions, 20: 4739
MANSUROVA, L. G., Some peculiarities of geomagnetic variations in polar regions, 20: 4739
MARATECK, S., Σ radiative decay and angular momentum of Σ pionic decay, 20: 4616

MARCQ, A., Synthesis of products akin to polyphenyls, 20: 3972 (EUR-2528.f)
MARCUS, C. Silber, Comparison of intestinal discrimination between ^{47}Ca, ^{85}Sr, and ^{133}Ba, 20: 3669
MARDON, P. G., Gas evolution from solid plutonium-bearing residues during storage, 20: 4364 (AERE-M-1644)
MAREK, M., Source of polarized ions for cyclotron, 20: 4519
MARES, J., Source of polarized ions for cyclotron, 20: 4519
MARGOLIS, B., Electron and positron scattering and anapole, 20: 4612
MARIN, Jean-Francois, Application of α spectrometry to measurement of low diffusion coefficients; case of uranium dioxide, 20: 4412
MARKS, I. N., Malignant Zollinger-Ellison syndrome in Bantu woman with prolonged remission after gastric radiotherapy, 20: 3821
MARQUES, R. O., Biosynthetic preparation of ^{75}Se-methionine and ^{75}Si-cystine. Its incorporation and distribution in mice, 20: 3661 (NP-15594)
MARQUES VIDEIRA, F. H., Improvemeat and utilization of nuclear fuels, 20: 4047 (LFEN-32)
MARQUEZ, L., Study of the second step of the reaction $^{7}Li(d,n)^{8}Be$; $^{8}Be \rightarrow 2\alpha$, 20: 4869
MARTIN, Velorie C., Blast loading on right circular cylinder, 20: 4132 (AWRE-O-93/65)
MARTINSON, I., Law of conservation of nucleons, 20: 4853
MARUYAMA, Yosh, Studies of LSA ascites lymphoma of C57BL mice. I., 20: 3750
MARX, G., Spontaneous symmetry breakdown in a nonlinear boson field, 20: 4669
MASON, E. A., Classical collision integrals for repulsive screened Coulomb potential, 20: 4988
MASSEY, Sir Harrie, Space travel and exploration, 20: 4525
MASSO, J. F., Influence of multiple virtual transitions on reorientation effect in Coulomb excitation, 20: 4901
MATHE, G., Comparison of reactivity against host of thymocytes and semi-allogenic lymph node cells, 20: 3777
MATHES, H., Radiation measurements of porphyries in region of Sarr-Nahe basin, 20: 4165
MATSUDA, Kiyoshi, Simultaneous ultraviolet spectrophotometric determination of niobium and tantalum by hydrogen peroxide method, 20: 3904
MATSUMURA, Yoshitake, Determination of uranium in bomb waste by emission spectrochemical method, 20: 3906
MATSUURA, Niro, Radiation-induced oxidation of Sb(III) in aqueous solution. III., 20: 4009
MATSUZAWA, Michio, Relative radiation stability of some para-polyphenyls, 20: 3991
MATSUZAWA, Taiju, Survival time in germfree mice after lethal whole body x-irradiation, 20: 3778
MATVEENKO, I. I., Temperature and composition effects on electric conductivity of tantalum–carbon β and γ phases, 20: 4415
MATYUSHIN, A. T., Electrostatic field of wire electrodes for spark chamber, 20: 4241 (JINR-P-2364)
MATYUSHIN, V. T., Electrostatic field of wire electrodes for spark chamber, 20: 4241 (JINR-P-2364)
MATZKE, Hansjoachim, Study of inert-gas diffusion in ionic crystals and sinters, 20: 3944
MATZNER, Bruce, Critical heat flux for large diameter, internally heated annuli in forced convection boiling at 1000 psia, 20: 4105 (TID-22321)
MAURICE, P. A., Radiological effects at a distance after selective irradiation of lymphatic organs, 20: 3775
MAY, Virgil R. Jr., Simultaneous bilateral intracapsular fractures of hips, 20: 3856
MAYHOOK, A. R., Further extraction studies for Harwell variable energy cyclotron, 20: 4502 (NIRL/R/92)
MAYINGER, F., Prog. rpt. on research into critical heat flux in boiling H_2O, 1–3/65, 20: 4101 (EURAEC-1354)
MAZZETTI, P., Effect of crystalline structure on fatigue, 20: 4443
MC CALL, John R., PLOT3D: FORTRAN subroutine for three-dimensional plotting, 20: 4291 (UCRL-14425)
MC CARTHY, Shaun L., Kirzhnits corrections to Thomas-Fermi equation of state, 20: 4540 (UCRL-14364)
MC CARTHY, Walter C., Potential radiation protective agents. III., 20: 3790
MC CASLIN, Joseph B., Some uses and characteristics of Mos transistors for health physics applications, 20: 4250 (UCRL-16446)
MC CLUNG, R. W., Nondestructive test development, 20: 4110 (ORNL-3870, pp 146-54)
MC CONVILLE, George Terrence Jr., Specific heat of type II superconductors in magnetic field, 20: 4786
MC CORMICK, N. J., Use of Poincare-Bertrand formula in neutron transport theory, 20: 4812
MC DOWELL, A. A., Possible artifact in cyclic variations in radiosensitivity, 20: 3766
MC ELROY, D. L., Physical properties, 20: 4388 (ORNL-3870, pp 44-9)
MC GHIE, R. D., Bibliography on deformation, vibration, and stability of shells, 20: 4079 (UCRL-13187)
MC HARGUE, C. J., Structure of metals, 20: 4389 (ORNL-3870, pp 61-4)
MC KENNA, Virgil V., Size constancy as function of ageing and x-ray irradiation in rhesus monkeys, 20: 3721
MC KINLEY, William A., Geometric theory of neutrinos, 20: 4619
MC LAREN, J. R., Sintering of uranium mononitride, 20: 4349
MC LEISH, J. A., Predicting irradiation-growth in uranium, 20: 4470
MC LELLAN, Alden, Quantitative nuclear evaporation theory. II., 20: 4897
MC MANUS, G. M., Short-range order in some nickel-base alloys, 20: 4421
MEAD, K. F., Blast loading on right circular cylinder, 20: 4132 (AWRE-O-93/65)
MECKSTROTH, George R., Effects of whole-body x-irradiation on vr-3 food reinforced bar-pressing, 20: 3772
MEGERTH, F. H., Irradiation performance of UO_2 produced by alternate fabricating processes, 20: 4459 (GEAP-4850)
MEISELS, G. G., Prog. rpt. on fissiochemical development, semiannual, 1–6/65, 20: 3982 (AGN-8156)
MEISSNER, G., γ Radiolysis of hydrogen sulfides in all aggregate states, 20: 4017
MELAMED, Myron, Functional capacity of canine bone marrow implants in the spleen, 20: 3652
MELE, A., Radiation-induced polymerization of 1,2-cyclohexene oxide, 20: 3992
MENET, Jacques, Nuclear matrix elements of transition $^{42}K(2^-)^{g}$, $^{42}Ca(2^+)$, 20: 4863
MENKE, H., Current supply system with liquid metal circulation, 20: 4573
MENOTTI, P., Operator analysis of Bethe-Salpeter equation, 20: 4661
MERKLE, T. C., Calculation of treatment schedules for cancer chemotherapy, 20: 5222 (UCRL-14505)
MERLI, E., Dimensioning of overpressure discharge system of PRO reactor, 20: 5145
MERRILL, H. E. Jr., New electron probe x-ray microanalyzers, 20: 3912
MERRIMAN, F. C., Application of multichannel synthesis to 2-D depletion calculations, 20: 5056 (CONF-654-22)
MERZ, L., Economic view points on measurement and control technology in nuclear power plants, 20: 5140
MESERVY, E. B., Microwave absorption in hot plasma near the second harmonic of electron cyclotron frequency, 20: 4943 (MATT-379)
MESHKOV, S., Decays of positive-parity baryon resonances in broken U(12), 20: 4666
MESSLINGER, R., Europium-144, 20: 4887
MESTER, H., X-ray generators, 20: 4228
METAIS, B., Clearance of radioactive colloidal gold in dog with portocaval anastomosis, 20: 3681
MEYER, B., Interaction of muons produced by atmospheric neutrinos, 20: 4561 (COO-818-64)
MEYER, H. N. Jr., Relationship between quality control and quality assurance, 20: 4113 (TID-22358)
MEYER, Ph., Elementary particle and high energy physics, 20: 4695
MEYER, Ph., Phenomenological study of weak interactions. Selected topics, 20: 4634
MEYER, R. E., Rotating disk study of dissolution of zirconium in $HF-H_2SO_4$, 20: 4055
MICELI, Roberto, Modifications of iliac and lumbosortic lymphographic findings, following irradiation, 20: 3852
MICHALOWICZ, A., Measurement of polarization in elastic proton-deuteron scattering at 155 Mev, 20: 4595
MICHAUD, Henri, Application of α spectrometry to measurement of low diffusion coefficients; case of uranium dioxide, 20: 4412
MICHEL, F. C., Photon-induced beta decay in stellar interiors, 20: 4530
MICHON, Georges, Experimental contamination of pink shrimps by ^{137}Cs, 20: 3657 (CEA-R-2818)
MICKELSON, William R., Electrostatic propulsion system with direct nuclear electro generator, 20: 4140
MIHALCZO, J. T., SPCTRM. 05R Monte Carlo analysis routine for calculating neutron energy spectrum, 20: 4805 (ORNL-TM-1245)
MIKA, Klaus, Boltzmann equation for distribution for primary atoms, 20: 4721
MIKETTA, D. N., Material specifications for advanced refractory alloys, 20: 4380 (NASA-CR-54761)
MIKHAILOV, V. A., Solubility of tributylphosphate in aqueous solution $UO_2(NO_3)_2$, 20: 3955
MILLER, C. S., Prog. rpt. on modification of photometric measurement assemblies, final, 1/4–5/3/65, 20: 4234 (AD-619177)
MILLER, Gordon H., Feasibility study of use of antimatter as rocket propellant, 20: 4137
MILLER, R. G., Electron exchange reactions mediated by oxyanions, 20: 3967
MILLER, R. I., Prog. rot. on fissiochemical development, semiannual, 1–6/65, 20: 3982 (AGN-8156)
MILLER, Robert W., Environmental agents in cancer, 20: 3779
MILLO, Aldo, Changes of permeability of isolated frog heart irradiated with x rays, 20: 3794
MILNER, A., Prog. rpt. on fabrication of W alloy tubing, 7/1–10/22/65,

20: 4340 (COO-1518-1)
MINER, Daniel, Remote underwater devices for evaluation and reduction of spent yankee fuel assemblies, 20: 5136 (WCAP-5554)
MINOR, A., Investigations on emission materials for thermionic converter influence of CsF on electron work functions of W, Ta and Mo, 20: 4572 (EUR-2283.d)
MINUSHKIN, B., Electrochemical oxygen meter operating manual, 20: 3889 (UNC-5113)
MITRA, A. N., Faddeev formalism for four-particle systems, 20: 4675
MITROFANOV, Yu. A., Effect of culture density on frequency of chromosome aberrations in mouse fibroblasts under normal conditions and under x irradiation of 35 r, 20: 3691
MIYAJIMA, Shigeki, Note on sheath formation, 20: 4976
MIYOSHI, Katsuhiko, 14-Mev neutron-activation analysis unit for oxygen determination, 20: 3907
MOCHIZUKI, Ken, Alloys of nickel with lithium, barium, and strontium, 20: 4442
MOE, M. K., Charge conservation and lifetime of electron, 20: 4551
MOE, Michael K., Electron lifetime. Experimental test of charge conservation, 20: 4536
MOECK, E. O., Further geometrical factors affecting dryout heat flux in vertical, internally heated annuli cooled by steam/water mixtures at 1000 psi, 20: 4099 (AECL-2333)
MOERS, Kurt, Investigations on salt-like nature of lithium hydride, 20: 3928 (UCRL-Trans-1254(L))
MOESNER, Juergen, Study of reaction $^{12}C(n,n')3\alpha$, 20: 4878
MOGENSEN, H. P., Development of variable-energy cyclotron HIVEC, 20: 4491 (ANL-7081, pp 78-80)
MOISEEV, S. S., Plasma with relativistic electrons in trap with magnetic mirrors, 20: 4950 (UCRL-Trans-1261(L))
MOISEITSEV, P. I., Assessment of the efficiency of ventilation of atomic reactors of IRT-2000 type, 20: 5201
MONCASTER, Michael Edward, Radiation monitor, 20: 4259
MONCELON, Bernard, Chemical and kinetic study of reaction between sulfur dioxide and uranium hexafluoride, 20: 3935
MONNAND, Edouard, Decay of ^{192}Re, 20: 4861
MONTAGNINI, Bruno, Complete continuity of free gas scattering operator in neutron thermalization theory, 20: 4811
MONTALENTI, G., Effect of crystalline structure on fatigue, 20: 4443
MONTEROSSO, R., SAHYB: program for solution of initial and boundary value problems, 20: 4287 (EUR-2519.e)
MONTGOMERY, David, Problem of spin in time-dependent magnetic field, 20: 4648
MOORE, R. V., Advanced gas-cooled reactors, 20: 5164
MOORE, R. V., Steam generating heavy water reactor, 20: 5163
MOORE, Robert L., Electrostatic apparatus for removal of dust particles from gas stream, 20: 4726
MORAVCSIK, Michael J., Spin-1 meson photoproduction, 20: 4610
MORET-BAILLY, Francoise, Neutrinos and pure singular fields of spin 1 and of spin 2, 20: 4763
MORETTI, E., Terrestrial albedo of 40- to 190-kev x rays, 20: 4752
MORGAN, C. S., Physical ceramic studies, 20: 4387 (ORNL-3870, pp 38-43)
MORGAN, D. J., Retention of inhaled radioactive vapors by human subjects, 20: 4202
MORGAN, R. L., Radiation cancer of pharynx. Case reports, 20: 3806
MORGAN, Rowland L., Therapeutic possibilities of high-energy charged particles, 20: 3735
MORINAGA, H., Europium-144, 20: 4887
MORLEVAT, Jean-Pierre, Observation of dislocations in crystals using x-ray and electron transmission, 20: 5003 (CEA-R-2875)
MOROZ, V. I., Measurement of energy and angular characteristics of electrons and γ-quanta in propane bubble chamber, 20: 4240 (JINR-P-2277)
MOROZOV, V. M., Nature of the relationship of energy emission in Moessbauer effect to temperature, 20: 5004 (IAE-927)
MOROZOV, V. P., Thermodynamic properties of deuterium and tritium substituted non-linear triatomic hydrides, 20: 3950
MORRIS, B. M., ^{7}Li quadrupole moment. III., 20: 4904
MORRIS, J., Recent developments in irradiation treatment of polymers, 20: 4033
MORRISON, G. W., SPCTRM. 05R Monte Carlo analysis routine for calculating neutron energy spectrum, 20: 4805 (ORNL-TM-1245)
MORRISON, I. W., Theoretical study of second-order Raman spectra of cesium halides, 20: 5007 (UCRL-14398)
MORTER, W. F., Demounting and machining techniques in hot cells at Berkeley, 20: 4128
MOSER, J. B., Heat pulse measurements of uranium compounds, 20: 3943
MOSS, William D., Determination of low level plutonium activity; autoradiographic techniques vs. scintillation counting, 20: 3877 (LA-DC-7483)
MOULOKHIA, K., Prog. rpt. on ^{90}Sr contained in marine animals following possible release of radioactive waste, final, 1963–64, 20: 3659 (NP-15156)
MOUSSA, Andre, Decay of ^{192}Re, 20: 4861
MOWAT, J. Richard, Analysis of elliptically polarized light, 20: 4480 (UCRL-11802)
MRAZ, Josef, Some observations in experimental transplantation of bone marrow, 20: 3795
MUELLENSIEFEN, A., Polarization effects in pion-photoproduction on protons below 500 Mev. II., 20: 4628
MUELLENSIEFEN, A., Polarization of recoil nucleons in π^0-photoproduction on protons below 500 Mev. I., 20: 4627
MUELLER, Erwin W., Initial oxidation of tantalum observed in field ion microscope, 20: 4332
MUELLER, J. H., Metabolic effects of therapeutic use of radiocolloids on the reticuloendothelial system, 20: 3822
MUENTER, John Stuart, Study of isotope effects on molecular dipole moments, 20: 3977
MUENZEL, F., Irradiation of cellulose and its derivatives, 20: 4034
MUKHERJI, A., Self-consistent perturbation. I., 20: 4537 (NP-15576)
MUKHERJI, A., Self-consistent perturbation. II., 20: 4538 (NP-15577)
MUKUNDA, Narasimhaiengar, Studies in Hamiltonian theories of relativistic interacting particles, 20: 4693
MULLER, Rolf H., Analysis of elliptically polarized light, 20: 4480 (UCRL-11802)
MUNN, R. J., Classical collision integrals for repulsive screened Coulomb potential, 20: 4988
MURAI, Takeo, Genetically significant radiation dose from dental x-ray diagnosis. I., 20: 4195
MURAI, Takeo, Genetically significant radiation dose from dental x-ray diagnosis. II., 20: 4196
MURANO, Robert, Bulk calibration of ^{99m}Tc eluate from BNL ^{99}Mo cow, 20: 4269
MURAOKA, Shinye, Effects of physical treatments on infectivity of Myc. lepraemurium, 20: 3752
MURARKA, S. P., Diffusion of copper in nickel, 20: 4363 (AEET/CD/31)
MURATA, Toshifumi, Preliminary experiment on radial distribution of ^{137}Cs, $^{89,90}Sr$, and ^{95}Zr in sintered uranium dioxide pellet, 20: 4472
MURFITT, R. H., Latest operating experience of magnox stations, 20: 5156
MURGATROYD, R. J., Radioactivity in atmosphere, 20: 4163
MURPHY, L., Non-destructive examination of irradiated nuclear fuel, 20: 5093
MURPHY, W. F., Remote metrology and examination techniques on irradiated fuel materials, 20: 4124
MURTHA, Bruce E., Fuel element cluster, 20: 5100
MUSSET, Edmond E., Homopolar generator, 20: 4231
MUZIOL, G., Positron decay of ^{145}Eu, 20: 4838 (JINR-P-2314)
MYERS, Rupert H., Production of nuclear fuels, 20: 4313

N

NACHTIGAL, D., Studies on immune unresponsiveness induced by radiation, 20: 3738
NADJAKOV, E., New isotope, ^{174}W, 20: 4834 (JINR-E-2360)
NAFTULIN, S. M., Static characteristics of voltage stabilizer in electromagnetic isotope separator, 20: 4281 (IAE-926)
NAGASAKI, Ryukichi, Effect of oxygen on mechanical properties of high purity zirconium, 20: 4416
NAGASAKI, Ryukichi, Effect of grain size on tensile properties of Magnox AL80, 20: 4437
NAGATANI, K., Alpha-particle-induced breakup of deuteron, 20: 4596
NAGY, Eva J., Fat absorption tests performed with ^{131}I-labeled triolein combined with whole-body irradiation, 20: 3754
NAGY, Gyorgy, Problems and results of radiophosphorus therapy of polycythemia vera, 20: 3837
NAKAGAWA, Shigeru, Radiation dose received by mother and fetus x-ray examination, 20: 3823
NAKAJIMA, Kentaro, Production of high purity uranium by fused salt electrolysis, 20: 4347
NAKAMURA, Masahiro, Effects of physical treatments on infectivity of Myc. lepraemurium, 20: 3752
NAKAMURA, Shogo, Initial oxidation of tantalum observed in field ion microscope, 20: 4332
NAKAMURA, Tadashi, Genetically significant radiation dose from dental x-ray diagnosis. I., 20: 4195
NAKAMURA, Tadashi, Genetically significant radiation dose from dental x-ray diagnosis. II., 20: 4196
NAKANISHI, Nobuo, Multiple poles in scattering Green's function, 20: 4662
NALIBOFF, Y. D., Prog. rpt. on integral neutron thermalization, 4–6/65, 20: 4801 (GA-6634)
NANBERG, R., Storage of radioactive material in Studsvik hot laboratory, 20: 4041
NARAIN, L., Studies of corneal graft reaction: effect of x-irradiation of donor tissue, 20: 3719
NARDI, A. J., Design and evaluation of 1000 MW(e) central station powerplant with a circulating fuel gaseous core reactor, 20: 5128 (TID-22225)

NATH, Pran, Effective range theory and uncoupled phase method in multichannel reactions, 20: 4690

NAUCHE, R., Underwater radiography of irradiated specimens, 20: 5203

NAUENBERG, U., Σ radiative decay and angular momentum of Σ pionic decay, 20: 4616

NAYFEH, Ali Hasan, Nonlinear oscillations in hot electron plasma, 20: 4986

NAZARCHUK, M. M., Flow of gas in channels in presence of heat transfer, 20: 4107 (NASA-TT-F-262)

NAZARENKO, G. D., Solubility of metal oxides in fused borax, 20: 3951

NEALE, E. J. E., Dermatomyositis following treatment of cancer, 20: 3847

NEED, John L., Optimum target orientation in nuclear reaction experiments, 20: 4942 (NASA-TN-D-3116)

NEGANOV, B. S., Polarization of protons in La–Mg nitrate, 20: 5021

NEILL, J. M., Prog. rpt. on integral neutron thermalization, 4–6/65, 20: 4801 (GA-6634)

NEIMAN, A. S., Mechanical property evaluation of Be-38% Al alloy from –320 to 800F, 20: 4440

NELP, W. B., Distribution and excretion of technetium in humans, 20: 3663 (TID-22318)

NELP, Wil B., Bulk calibration of ^{99m}Tc eluate from BNL ^{99}Mo cow, 20: 4269

NELSON, Frederick, Ion-exchange procedures. VIII., 20: 4054

NEMODRUK, A. A., Determination of small amounts of U(VI) in presence of large amounts of U(IV), 20: 3903

NERENSTONE, Marc A., Neutronic reactor fuel element and member therefor, 20: 5096

NEUIMIN, A. D., Studies of uranium dioxide oxidation by means of high-temperature electroconductivity, x-ray phase studies, and continuous weighing, 20: 3952

NEUMEISTER, K., Examinations of radiation reactions of liver by means of ^{131}I bengal rose tests, 20: 3774

NEUWIRTH, Wolfgang, Study of complex and covalent iron compounds using ^{57}Fe Moessbauer effect, 20: 3927 (AERE-Trans-1026)

NEWELL, Reginald E., Eddy fluxes and biennial oscillation in stratosphere, 20: 4150 (MIT-2241-7)

NEZLIN, M. V., Longwave electron oscillations in beam-plasma system, 20: 4940 (IAE-932)

NGUYEN-LONG-DEN, Study of formation of α substructures α on the surface of lanthanum nuclei, 20: 4886

NGUYEN VAN DONG, Disordered regions induced in Ge by fast-neutron bombardment, 20: 4466

NICOLL, David, Apparatus for canning nuclear reactor fuel elements, 20: 5029

NIELSEN, P. Moeller, Comparison of forward dispersion relations with experiments around 10 Bev, 20: 4602

NIGAM, P. D., Hall current effect on magnetohydrodynamic waves in rotating liquids, 20: 4711

NIKL, Istvan, Question of dose using chaoul irradiation tube, 20: 3838

NISHIDA, Y., Applications of exactly soluble one dimensional model of transfer reactions, 20: 4851

NISHIDA, Y., One dimensional soluble particle transfer problem and modified energy matrix method, 20: 4852

NISHIHARA, Kiyokado, Determination of uranium in bomb waste by emission spectrochemical method, 20: 3906

NISHIKAWA, Kazuyuki, Studies on uranium refinery, 20: 4052

NISHIYAMA, Ronald H., Carcinoma of thyroid gland in children and adolescents, 20: 3739

NOAKES, Michael Lesney, Process of assembling temperature measuring device within aperture of fuel element, 20: 5098

NOBAR, Youssef Motevalledi, Decay of ^{183}Hf, 20: 4862

NOGUEIRA, E. D., Reprocessing of irradiated MTR type fuels at Spanish J.E.N., 20: 4066

NOLLET, Patrick, Method of preparing uranic oxide in granulated form, 20: 3971

NORRIS, T. H., Isotopic exchange reactions in thionyl chloride and sulfuryl chloride, 20: 3965

NORTHROP, David Covell, Radiation monitor, 20: 4259

NOUVERTNE, W., Preparation of ^{3}H labeled amino acids, 20: 3978

NOWAK, A., Transfer procedures used in alpha-gamma hot laboratory at Karlsruhe, 20: 4209

NOWELL, Peter C., Prognostic value of marrow chromosome studies in human preleukemia, 20: 3650

NOZIN, A. G., Solubility of tributylphosphate in aqueous solution $UO_2(NO_3)_2$, 20: 3955

NUCKOLLS, M. J., Size analysis of –44 micron dust particles, 20: 4149 (AD-623639)

NUYTS, Jean, Remarks on $\Delta I = \frac{1}{2}$ rule in weak interactions, 20: 4635

NYBORG, P., Phase-space considerations for four-particle final states, 20: 4658

NYBORG, Per, Phase-space considerations for five-particle final states, 20: 4659

NYGAARD, Keare J., Measurements of Balmer line radiation from self-sustained Townsend discharges in hydrogen, 20: 4542

NYIRE NYA, E. U., Influence of whole body irradiation on loir (Glis glis), 20: 3703

NYIRO, Laszlo, Fat absorption tests performed with ^{131}I-labeled triolein combined with whole-body irradiation, 20: 3754

O

OBINATA, Ichiji, Alloys of nickel with lithium, barium, and strontium, 20: 4442

O'BRIEN, H. A. Jr., ^{147}Pm—radiation measurements of one-watt, prototype heat source, 20: 4279 (ORNL-TM-1177)

O'BRIEN, Joseph F., Quartz pressure transducer package, 20: 4224 (UCRL-14448)

O'BRIEN, Vivian, Viscous MHD flow about spherical magnetic quadrupole, 20: 4725

O'CONNOR, J. D., Physical and radiochemical properties of fallout particles, 20: 4156 (USNRDL-TR-899)

ODA, Minoru, X-ray and γ-ray astronomy, 20: 4562 (MIT-2098-174)

ODA, Nobuo, Secondary electron distribution for heavy ions, 20: 4541 (UCRL-16405)

OEHLKERS, Friederich, Developmental history of mutants of Funaria hygrometrica L. induced by x irradiation, 20: 3781

OESTBERG, G., Study of tensile strength in soft steel, 20: 4365 (AES-3)

OETZEL, George Norton, Noise and correlation studies of microwave resonances of plasma column in magnetic field, 20: 4991

OHSE, Roland W., Vapor pressure studies of uranium dioxide (UO_2) by effusion method, 20: 4369 (CEA-R-2871)

OHTA, Masao, Comparative study of the sodium loss reactivity effect of large Pu–U and P–Th fast reactors, 20: 5068

OKAMOTO, Takao, Ultrastructure of epithelial cells of lens and ciliary body in beta irradiation cataract, 20: 3761

OKANE, Isao, Rupture properties to HT 70 steel for pressure vessels. II., 20: 4446

OKUDA, Takayoshi, Impedance formula for partially ionized, collision-dominated plasma, 20: 4975

OLANDER, Donald R., Solubility of helium in uranium dioxide, 20: 3946

OLDHAM, William Jennings Bryan Jr., Electrons ejected from He by protons, 20: 4558

OLESEN, P., Comparison of forward dispersion relations with experiments around 10 Bev, 20: 4602

OLIVARIA, A., Prog. rpt. on improvement of renogram techniques, final, 20: 3800 (NP-15150)

OLLIVIER, Jean, Improvements in or relating to zirconium phosphate preparation, 20: 3968

OLNESS, J. W., Studies of electromagnetic transitions in ^{15}N and ^{15}O, 20: 4905

OLNESS, J. W., Studies on ^{19}F in ^{18}O(p,γ)^{19}F reaction, 20: 4907

OLSON, Robert S., Laser as potential tool for cell research, 20: 3741

OLSSON, Per O. M., Laplace transform of product of two Whittaker functions, 20: 4293

OMNES, Roland, Existence of S matrix, 20: 4687

ONEDA, Sadao, Symmetries and dynamics of nonleptonic decays, 20: 4678

OPPELT, Jiri, Radioisotope flowmeter, 20: 4227

ORMEROD, M. G., Radiation-induced crosslink formation in polyethylene. I., 20: 4002

ORMEROD, M. G., Radiation-induced crosslink formation in polyethylene. III., 20: 4004

ORSZAK, Peter, Improvements relating to nuclear reactor servicing apparatus, 20: 5041

ORZHEKHOVSKII, V. L., Effect of hot plastic deformation on structure and properties of molybdenum, niobium, and titanium, 20: 4403 (JPRS-32317)

OSANOV, D. P., Temperature distribution in gamma shielding, 20: 5002

OSAWA, Yasutaka, Fission gas release from nuclear fuels. II., 20: 4471

OSBORNE, R. L., Malfunction detection and diagnosis, 20: 4222 (UCRL-13186)

OSTERHOLTZ, F. D., Prog. rpt. on fissiochemical development, semi-annual, 1–6/65, 20: 3982 (AGN-8156)

OSTERTAG, Werner, Prog. rpt. on rare earth W bronzes, 8/64–1/65, 20: 4362 (AD-620033)

OSWALD, Robert B. Jr., Thermal-neutron-induced recoil defects in cadmium sulfide, 20: 4000

OSWALD, Robert Bernard Jr., Thermal neutron induced recoil defects in cadmium sulfide, 20: 4027

OTSUKA, Masahiko, Theory of statistical fluctuations in neutron distributions, 20: 5066

OTTAVI, Henri, Study of spectrometer sensitive to weak transverse static fields, 20: 4255

OTTEWITTE, E. H., Effect of temperature and microstructure of sintered beryllium oxide on scattering cross section for SNAP reactor, 20: 5180 (NAA-SR-Memo-11604)

OTTO, W. H., Prog. rpt. on silica fiber/core-sheath fiber, final, 2/64–6/65, 20: 4338 (AD-620055)

OWEN, Joe D., Hydrogen index and gamma ray well logging, 20: 4170
OWENS, Thomas Charles, Simultaneous equilibria of D2EHPA and TBP with $Pr(NO_3)_3$ and $Nd(NO_3)_3$ solutions, 20: 3875 (IS-T-37)
OZIAS, Yves, Contribution to microcalorimetric study of characteristics of radioelements, 20: 3866 (CEA-R-2630)

P

PACE, F. C., Protection against nuclear weapon fallout in emergency health services units, 20: 3797
PACKARD, J. R., Behavior of materials at cryogenic temperatures, 20: 4417
PAGELS, Heinz, Magnetic moments of baryons, 20: 4665
PAGES, Lucien, Critical study of some soft-tissue equivalent material. Sensitivity to neutrons of 1 kev to 14 Mev, 20: 3708 (CEA-R-2833)
PAILLAUD, A., Biologic and hormonal results of destruction of pituitary by ^{90}Y, 20: 3809
PAKVASA, S., Weak electromagnetic decays of hyperons in SU(3), 20: 4673
PAL'CHIKOV, V. E., Plasma with relativistic electrons in trap with magnetic mirrors, 20: 4950 (UCRL-Trans-1261(L))
PALEI, P. N., Determination of small amounts of U(VI) in presence of large amounts of U(IV), 20: 3903
PALMEIRA, R. A. R., Low-energy spectrum of cosmic rays, 20: 4566
PALMER, George J. Jr., Behavioral factors in disaster situations, 20: 4200
PALMER, H. E., Distribution and excretion of technetium in humans, 20: 3663 (TID-22318)
PALOWITCH, B. L., Study of slightly enriched UO_2 lattice with H : U = 0.42—measurement and analysis, 20: 5071
PANCHAPAKESAN, Nargis, Faddeev formalism for four-particle systems, 20: 4675
PAPA, Robert J., Nonlinear interaction of r-f wave with inhomogeneous plasma slab. II., 20: 4954
PAPA, T., Electron microscope observation of high-energy-neutron-irradiated germanium, 20: 4467
PAPASTAMATIOU, N. J., Approximate supermultiplet model consistent with relativity and unitarity, 20: 4685
PAPATHANASSOPULOS, K., Diffusion of ^{133}Xe in UC nuclear fuel as a function of composition and radiation dose, 20: 4450
PAPWORTH, M. P., Enhancement of radiosensitivity of skin of patients by high pressure oxygen, 20: 3727
PARFENOV, L. B., Polarization of protons in La–Mg nitrate, 20: 5021
PARISH, R. W., Development of active radiographic inspection techniques at Harwell, 20: 4119
PARK, R. B., Nucleic acid content of chloroplasts of spinach isolated by a nonaqueous technique, 20: 3649 (UCRL-11475)
PARKER, E. R., Structure and high strength metals, 20: 4399 (UCRL-16301)
PARKER, K., 12 Group set of photon cross sections for use in anisotropic S_n calculations of photon transport, 20: 4996 (AWRE-O-79/65)
PARKINSON, M. J., Structure of collisionless shock waves in magnetized plasma, 20: 4977
PARKS, D. E., Neutron thermalization in graphite. II., 20: 4818
PARNELL, C. J., Effect of fractionation on four day survival of mice after whole-body neutron irradiation, 20: 3728
PARRY, W. E., Some aspects of liquid helium problem, 20: 4772
PARSON, T. V., Silt movement investigation in oxcars spoil ground, firth of forth, using radioactive tracers, 1961 and 1964, 20: 4166 (AERE-R-4980)
PARSONS, N. A., Safety of DAPHNE, 20: 5188 (AERE-R-4932)
PARTHASARATHY, R., Influence of geomagnetic activity on polar cap absorption, 20: 4756
PASCAUL MARTINEZ, F., Don project, 20: 5162
PASKHALOV, V. V., Extraction of cerium and yttrium by naphthenates, 20: 4051
PASSEFORT, Jean-Claude, Survey of uranium–carbon–nickel ternary diagram, 20: 4368 (CEA-R-2845)
PASSELL, T. O., Feasibility of cavity pressure and temperature measurements for decoupled nuclear explosion, 20: 4084 (VUF-3017)
PASTERNAK, G., Demonstration of immunological differences between graffi and gross leukemias, 20: 3694
PATI, Jogesh C., Symmetries and dynamics of nonleptonic decays, 20: 4678
PATOU, Claude, Local analysis by electric probe of cesium plasma produced by contact ionization, 20: 4958
PATOU, Claude, Oscillatory regimes of cesium plasma machine, 20: 4965
PATTENDEN, N. J., Drying of oxide powder sampler for neutron transmission measurements, 20: 3914 (AERE-M-1654)
PATTERSON, D. A., ESH-4 test program. Report on fuel elements irradiated in E-SADE loop of VBWR, 20: 5104 (ACNP-65006)
PATTERSON, H. Wade, Accelerator radiation monitoring and shielding, 20: 4514 (UCRL-16445)
PATTI, Francois, Radiochemical determination of ^{90}Sr in large volumes of drinking water, 20: 3867 (CEA-R-2844)
PAUL, J. W. M., Structure of collisionless shock waves in magnetized plasma, 20: 4977
PAUL, T. M., Studies of inhibition of intestinal absorption of radioactive Sr. IV., 20: 3671
PAULING, Linus, Close-packed-spheron theory and nuclear fission, 20: 4918
PAULING, Linus, Structural basis of neutron and proton magic numbers in atomic nuclei, 20: 4872
PAULSON, K. V., Statistical method for quantitative analysis of geomagnetic giant pulsations, 20: 4743
PAVLOVIC, A. S., Magnetocaloric effect in dysprosium, 20: 4420
PEACH, G., Absorption cross sections for free-free transitions in field of positive ions, 20: 4550
PEARCE, R. J., Thermal expansion of UAl_3 in temperature range 20 to 750°C, 20: 4436
PECK, P. F., Germanium diode to determine C in steels by measurement of prompt γ-radiation, 20: 3894
PECORINI, V., Prog. rpt. on improvement of renogram techniques, final, 20: 3800 (NP-15150)
PEGEL, K., Current supply system with liquid metal circulation, 20: 4573
PEIERLS, Ronald F., Comparison of nucleon-nucleon scattering data with the predictions of $SU(12)_L$, 20: 4605
PEIFFER, M., SNAP technology conceptual design 100-watt thermoelectric generator heat transfer analysis, 20: 4278 (MND-P-2229)
PEIXOTO CABRAL, J. M., Improvement and utilization of nuclear fuels, 20: 4047 (LFEN-32)
PELLEGRINI, C., Transverse resistive wall instability of extremely relativistic beams of electrons and positrons, 20: 4500 (LNF-65/27)
PENFOLD, Bruce R., Crystal structure of technetium(IV) chloride, 20: 3932
PENG, Li, Stratospheric wind temperature and isobaric height conditions during IGY period. III., 20: 4151 (MIT-2241-14)
PENNY, S. K., Comparison of three methods used to calculate gamma-ray transport in iron, 20: 5001 (ORNL-RSIC-9)
PERAY, R., Decanning problems in hot laboratories and attempted solutions, 20: 4062
PEREZ, B. Lopez, Reprocessing of irradiated MTR type fuels at Spanish J.E.N., 20: 4066
PEREZ, Jean-Jacques, Analytical methods used in cycles for plutonium purification by trilaurylamine, 20: 3868 (CEA-R-2860)
PERKINS, E. J., Biology of the Solway firth in relation to movement and accumulation of radioactive materials. IV., 20: 3662 (PG-Report-650)
PERKINS, W. E., Effect of yttrium on the recrystallization and grain growth of tantalum, 20: 4424
PERSIANI, P. J., Faret core I fuel irradiation program and reference design, 20: 5190 (ANL-7106)
PERSON, Lucy Wu, Nuclear recoil and simple nuclear reactions, 20: 4893
PESENTI, P., Special procedure for alpha–beta–gamma transfers of large pieces of equipment, 20: 4210
PETERS, D. E., Electron exchange reactions mediated by oxyanions, 20: 3967
PETERSON, P. J., Methods used in United States for transferring materials through radiation barriers, 20: 4043
PETERSON, Sigfred, Prog. rpt. on metals and ceramics, annual, 6/30/65, 20: 4300 (ORNL-3870)
PETERSON, W. D., Extension of hot-1 to treat Neumann boundary conditions—with applications to certain vibration problems, 20: 4080 (WAPD-TM-535)
PETRANYI, Gyula, Problems and results of radiophosphorus therapy of polycythemia vera, 20: 3837
PETRICEK, V., Dynamic polarization of protons and nuclei of fluorine in irradiated polymers, 20: 4037
PEUCHMAUR, Alphonse, Heavy-water reactor tank EL-4, 20: 5144
PEYRET, Roger, Channel flow of compressible electrically conducting fluid under action of non-uniform magnetic field, 20: 4715
PFEIFER, W., Dosage problems of radioiodide treatment of thyroid gland disorders, 20: 3853
PHAKLIDES, G. D., A digital computer program for the simulation of sampled data systems, 20: 4288 (SC-DR-65-312)
PHILIPPOT, Jean, Effects of ultraviolet and visible radiations on microorganisms, 20: 3726
PHILLIPS, Leigh F., Calibration and response of personnel monitoring film dosimeters to synchrotron stray radiations, 20: 4237 (BNL-9665)
PHILLIPS, Leigh F., Linear energy transfer spectra and effective quality factors in stray radiation areas at Brookhaven National Laboratory proton synchrotrons, 20: 4176 (BNL-9684)
PHILLIPS, R. D., Analysis of local and systemic effects of ionizing radiation on bone growth, 20: 3707 (AD-623641)
PICIU, Doina, Radioactivity of some forms of vegetation studied in neighborhood of city of Cluj, 20: 3654
PICKLESIMER, M. L., Superconducting materials, 20: 4390 (ORNL-3870,

pp 65-9)
PICKLESIMER, M. L., Zirconium metallurgy, 20: 4304 (ORNL-3870, pp 171-83)
PIERCE, T. B., Germanium diode to determine C in steels by measurement of prompt γ-radiation, 20: 3894
PIETRA, R., Determination of sulfur in terphenyl by neutron activation, 20: 3873 (EUR-2523.i)
PIETRI, C. E., Spectrophotometric determination of gallium in plutonium–gallium alloy, 20: 3881 (NBL-228)
PIGACHE, D. R., Semitoroidal reflex discharge as propulsion device, 20: 4134 (SEL-63-120)
PIGEOT, Alain, Method of preparing uranic oxide in granulated form, 20: 3971
PIGFORD, Thomas H., Solubility of helium in uranium dioxide, 20: 3946
PILIPENKO, Yu. K., Large laboratory hydrogen liquefier VO 2 for use with large liquid hydrogen bubble chambers, 20: 4797
PILKINGTON, E. S., Influence of polynuclear zirconium species on direct titration of zirconium with EDTA 20: 3893
PINCET, J., Cancer and geography, 20: 4193
PINSKI, G., Shmushkevich's method for charge-independent theory, 20: 4667
PIRANI, F. A. E., Critique of new theory of gravitation, 20: 4770
PITKIN, Edward T., Sputtering at acute incidence, 20: 4546
PITMAN, R. S., Gas evolution from solid plutonium-bearing residues during storage, 20: 4364 (AERE-M-1644)
PLANO, R. J., Σ radiative decay and angular momentum of Σ pionic decay, 20: 4616
PLANTE, E. R., Vapor pressure and heat of sublimation of tungsten, 20: 4438
PLASKON, D., Prog. rpt. on silica fiber/core-sheath fiber, final, 2/64–6/65, 20: 4338 (AD-620055)
PLATZ, Peter, Doppler temperature in toroidal discharge using multichannel Fabry-Perot interferometer, 20: 4713
PLISS, Yu. A., Proton depolarization in cyclotrons, 20: 4520
PLUMLEE, K. E., Safety analysis for AARR critical experiment, 20: 5189 (ANL-6929)
PLYASHKEVICH, N. N., Multiple acceleration system for high energy particle electrodynamic separator, 20: 4496 (JINR-P-2375)
PODGORNYI, I. M., Magneto-sonic heating of plasma, 20: 4939 (IAE-911)
POLACKI, Zenon, Radioluminescence of styrene-methylmethacrylate copolymers, 20: 4001
POLI, P., CYRCO—program for calculation of totally reflected cylindrical reactor design, 20: 5059 (RT/FIMA(65)-1)
POLISHUK, Paul, Investigation of interactions of ^{3}He and d with ^{237}Np, 20: 4928
POLSTER, G., Environmental radioactivity of the Nuclear Research Center, Juelich, 20: 4178 (JUL-284-ST)
POMRANING, G. C., Method for computing $\int_{-1}^{1} dx\ P_k^l(x)P_n^m(x)$, 20: 4294
PONYATOV, G. I., Fast convergence in Monte Carlo method of resolving problems of radioactive logging, 20: 4168
PORTER, C. R., Transfer of radiostrontium from cows' feed to milk, 20: 4162
POTTER, L. C., Effects of C and W on flow stress recovery of Mo, 20: 4409
POULET, M., Measurement of polarization in elastic proton-deuteron scattering at 155 Mev, 20: 4595
POUND, G. M., Temperature-sensitive x-ray small angle scattering from melt-crystallized polyethylene, 20: 5022
POWERS, E. L., Some recent advances in radiation biology of bacteria, 20: 3776
PRADAL, F., Characteristic energy losses of electrons in solids, 20: 5015
PRATT, R. H., Magnetic electron scattering, 20: 4831 (HEPL-272)
PREPOST, R., Eta photoproduction in region from threshold to 900 Mev, 20: 4578 (AD-618660)
PRESENT, R. D., ^{7}Li quadrupole moment. III., 20: 4904
PRESTWICH, W. V., Binding energy of the deuteron, 20: 4856
PRETTY, William Edward, Radiation monitor, 20: 4259
PREUSS, Luther E., X-ray absorptiometry with beta-stimulated x-ray sources, 20: 3882 (ORNL-IIC-5, pp 51-71)
PRICE, K. R., Electron-exchange reaction between $SbCl_3$ and $SbCl_5$ in carbon tetrachloride, 20: 3962
PRICE, P. B., Ion explosion spike mechanism for formation of charged-particle tracks in solids, 20: 4548
PRICE, R. H., ^{60}Co simulator for treatment planning, 20: 3827
PRICE, R. J., Prog. rpt. on advanced, graphite-matrix, dispersion type fuel systems and research on graphite, 11/15/64–2/14/65, 20: 5089 (GA-6181)
PRICEMAN, S., Protective coatings for niobium and its alloys, 20: 4356
PRICKETT, W. Z., Design and evaluation of 1000 MW(e) central station powerplant with a circulating fuel gaseous core reactor, 20: 5128 (TID-22225)
PROBST, Hubert B., Behavior of materials at high temperatures, 20: 4418
PROBST, Hubert B., Vanadium–gallium system in region of V_3Ga, 20: 4426
PROCTOR, J. F., Explosion containment laws for nuclear reactor vessels, 20: 5034 (NOLTR-63-140)
PROSPECT, Jacques, Improvements in or relating to zirconium phosphate preparation, 20: 3968
PROVOOST, F., Gamma irradiation polymerization of acrylonitrile in presence of solid additives, 20: 4007
PRUSAK, Jan, Helium liquefaction in nuclear research institute, 20: 4798
PSHEZHETSKII, S. Ya., Kinetics and sensitization of ammonia radiolysis in gaseous phase under fast electron irradiation, 20: 4021
PURSER, F. O. Jr., Polarization of neutrons from D(d,n)^{3}He reaction, 20: 4895
PYCHLAU, P., Absorption of x rays in body equivalent phantom, 20: 3816

Q

QUADROS, Carlos, Construction and operation of ^{3}He refrigerator, 20: 4776
QUADROS, Carlos, Magnetic susceptibility of some samarium salts between 1.2 and 4°K, 20: 3930
QUARLES, C. A., Study of K^+ decay probability, 20: 4609
QUINN, D., Eta photoproduction in region from threshold to 900 Mev, 20: 4578 (AD-618660)
QUINN III, James L., Analysis of 96 abnormal brain scans using ^{99m}Tc (pertechnetate form), 20: 3824
QUINTELLA, Sergio Geraldo, Use of extended surfaces in thermionic converters, 20: 4574

R

RABITZSCH, Georg, Kieselgel as support in tritium labeling of cardiac glycosides, 20: 3810
RABWIN, Marcus H., Late small bowel obstruction secondary to post-radiation enteritis, 20: 3732
RAGGENBASS, A., ^{137}Cs decontamination of concentrated fission product solutions, 20: 3874 (EUR-2535.f)
RAGGENBASS, Andre, Treatment of solutions of products formed by fission of U–Mo alloys, 20: 4070
RAINES, John Arthur, Radiation monitor, 20: 4259
RAJARAM, G., Abnormal behavior of f_0F2 at Huancayo in magnetically active periods of IGY-IGC, 20: 4741
RAKOVIC, Miloslav, Problems of interference in neutron activation analysis, 20: 3900
RAMALHO, A. J., Improvement and utilization of nuclear fuels, 20: 4047 (LFEN-32)
RAMA MOHAN, R. V., Decay scheme and directional correlations of γ rays from ^{182}Ta, 20: 4865
RAMANUJAM, H. R., Malfunction detection and diagnosis, 20: 4222 (UCRL-13186)
RAMLER, W. J., Development of variable-energy cyclotron HIVEC, 20: 4491 (ANL-7081, pp 78-80)
RAMOS, J. G. P., Magnetic susceptibility of some samarium salts between 1.2 and 4°K, 20: 3930
RAMSTEDT, C. F., Influence of temperature on radiation-induced surface effects in transistors, 20: 4261 (AD-623078)
RAMUZ, A., Control of radioactivity in food products in America, 20: 4201
RAO, B. V. Narasimha, Half-lives of first excited states in ^{182}W and ^{170}Yb, 20: 4877
RAO, D., Malfunction detection and diagnosis, 20: 4222 (UCRL-13186)
RAO, T. Seshagiri, Harmonic structure and band splitting of type II solar radio bursts, 20: 4524
RAO, V. S., Validity of ξ approximation for the $\frac{7}{2}^-$ (β) $\frac{5}{2}^+$ decay in ^{141}Ce, 20: 4903
RAO, W. V. S., Validity of ξ approximation for the $\frac{7}{2}^-$ (β) $\frac{5}{2}^+$ decay in ^{141}Ce, 20: 4903
RARING, L. M., High temperature titanium alloy development, 20: 4393 (PWAC-472)
RASERA, R. L., Transverse polarization of K-conversion electrons following β decay of ^{198}Au, 20: 4900
RASTOGI, R. G., Abnormal behavior of f_0F2 at Huancayo in magnetically active periods of IGY-IGC, 20: 4741
RAUBENHEIMER, Louis Johannes, Spin-lattice relaxation of tetravalent protactinium in cubic crystal, 20: 5020
RAUSCHENBACH, P., Isotope studies of biochemistry of fructose metabolism and gluconeogenesis in liver, 20: 3684
RAYMOND, J. W., Metallography of zirconium-base alloy hydrides, 20: 4341 (NAA-SR-Memo-10927)
RAZDAN, H., Recurrent Si^+–Si^- impulse pairs and shock structure in M-region beams, 20: 4758
REDMOND, Robert F., Small-angle scattering of neutrons by nuclei, 20: 4909
REED, D., Hinkley point nuclear power station, 20: 5148
REED, James Theodore, Measurements of positive kaon production in proton-proton collisions at 2.85 and 2.40 Bev, 20: 4586 (TID-22315)

REEH, Helmut, Goldstone's theorem, 20: 4660
REGGE, Tullio, Recent progress in potential scattering theories, 20: 4701
REHNBORG, Carl Samuel, Effects of x-irradiation on physico-chemical properties of serum lipoproteins, 20: 3704
REICHELT, J. M. A., Measurement of neutron spectrum in herald thermal column, 20: 5191 (AWRE-R-4/65)
REICHERT, W., Operational monitoring of reactor instrumentation, 20: 5037
REINERS, W. A., Water budget of a forest damaged by ionizing radiation, 20: 3653 (BNL-8466)
REINES, F., Charge conservation and lifetime of electron, 20: 4551
REINES, F., Interaction of muons produced by atmospheric neutrinos, 20: 4561 (COO-818-64)
REINES, Frederick, Proposed ν_e telescope to detect solar neutrinos by elastic scattering on e^-, 20: 4523 (COO-818-63)
REISLER, Emil, Refractive indices and piezo-optic coefficients of deuterium oxide, methanol, and other pure liquids, 20: 4484
REMIDDI, Ettore, Antiproton-nucleon annihilation at rest into two mesons and SU(6) symmetry, 20: 4615
REUSSER, Robert E., Removal of vanadium from aqueous solutions, 20: 4071
REYNOLDS, S. A., Half-lives and specific activities of common radionuclides, 20: 4845 (ORNL-TM-1318)
RHODE, R. H., Effect of gamma radiation on reproductive potential of Mexican fruit fly, 20: 3745
RHODES, J. R., Ore and coal analysis using radioisotope techniques, 20: 3884 (ORNL-IIC-5, pp 206-21)
RHYS-LEWIS, R. D. S., Radiotherapy in herpes zoster, 20: 3836
RIBOTTA, Roland, Study of spectrometer sensitive to weak transverse static fields, 20: 4255
RICARD, A., Low pressure oxidation of pure columbium, 20: 4324 (PWAC-460)
RICCABONA, G., ^{126}I in clinical evaluation of thyroid disease, 20: 3844
RICHARD, Patrick, Fine structure near isobaric analogue resonances, 20: 4923
RICHARDS, Gerald T., Numerical calculation of two-dimensional steady-state detonations by method of characteristics, 20: 5221 (UCRL-14228)
RICHTER, Wendy, Enhancement of radiosensitivity of skin of patients by high pressure oxygen, 20: 3727
RIECKE, W. D., Contribution to investigation of reciprocal lattices of single crystals by means of Kikuchi-patterns, 20: 5009 (UCRL-Trans-1227)
RIGAL, M. Th., Cholinesterase activities in mouse liver and kidney during experimental intoxication with uranyl nitrate, 20: 3670
RIMONDI, Carlo, Modifications of iliac and lumboaortic lymphographic findings, following irradiation, 20: 3852
RINAUDO, G., Measurement of K^+ branching ratio into τ mode, 20: 4618
RINDERER, L., Topology of structure of intermediate states of superconductors of type I, 20: 4778
RINDNER, W., Equivalence of stress- and radiation-induced defects in degenerate p-n junctions, 20: 4264
RINGOT, Claude, Fuel element for nuclear reactors, 20: 5099
RITCHIE, A. B., Dismantling and machining operations on high activity rigs at Harwell, 20: 4126
RITCHIE, A. B., Transfer of radioactive sources, 20: 4208
RITSON, D., Report on inelastic electron scattering program at Stanford, 20: 4581 (AD-618663)
RITSON, D. M., Pion-pair photoproduction below 1 Bev, 20: 4579 (AD-618661)
RITTENHOUSE, John B., Space materials handbook, 20: 4312
RIVIERE, J. C., Compatibility of some refractory metals with UC–ZrC, 20: 4335
RIVIERE, J. C., Surface potential of oxygen on thorium, 20: 4410
RIZHOV, V. A., Study of focusing inhomogeneities in ionosphere by radio-astronomic method on 13-54 Mgc frequencies, 20: 4735
ROBB, W., Reactions of hexachlororhodium(III) and pentachloraquo-rhodium(III) ions in aqueous acid solutions, 20: 3966
ROBERTS, John J., Equivalence of time optimal and minimax solutions to xenon shutdown problem, 20: 5074
ROBERTS, Merritt E., Radioprotective action of RNA in mice, 20: 3792
ROBERTSON, A. V., Synthesis of [carboxyl-^{14}C]3,4-dehydro-DL-proline, 20: 3975
ROBERTSON, C. S. Jr., Nine and sixteen group cross sections for reactor analysis, 20: 4829 (GEMP-173(Suppl.1))
ROBERTSON, D., Electron and positron scattering and anapole, 20: 4612
ROBERTSON, M. M., Nuclear spin and magnetic moment of ^{37}Ar, 20: 4890
ROBICHET, Jacques, Comparison of spectrographic methods of analysis of plutonium and its compounds, 20: 3869 (CEA-R-2869)
ROBINSON, Mark T., Radiation damage displacement cascade, 20: 4473
ROBINSON, W. H., Temperature-sensitive x-ray small angle scattering from melt-crystallized polyethylene, 20: 5022
RODIER, Georges, Improvements in or relating to neutron detectors, 20: 4260
ROECKERT, H., Regeneration of bone marrow, 20: 3789
ROEMER, W., Application of pressure-suppression system for containments in nuclear power plants, 20: 5146
ROESCHKE, C. U., F.M. radar system, 20: 5226
ROESCHKE, C. W., Range indicating system, 20: 5225
ROGER, Joel, Improvements in or relating to neutron detectors, 20: 4260
ROHSENOW, Warren M., Effect of nonuniform axial heat flux distribution, 20: 4104 (NP-15622)
ROLLAND, Paul, Measurement of electron density and collision frequency of plasma, 20: 4955
ROM, A. M., Thermally compensated closure for liquid density autoclave, 20: 4087 (ORNL-TM-1293)
ROM, Frank E., Gaseous nuclear reactor, 20: 5081
ROMAN, P., Operator gauge transformations, 20: 4762
ROOS, Philip G., Elastic scattering of 160-Mev protons from ^{9}Be, ^{40}Ca, ^{58}Ni, ^{120}Sn, and ^{208}Pb, 20: 4906
ROOT, John Walter, Recoil tritium reactions with alkanes, 20: 4024
RORO, Tiberiu I., Nonlocal extension of Utiyama formalism, 20: 4653
ROSE, M. E., Gamma transitions between even-parity states in ^{16}O, 20: 4854
ROSEN, S. L., Argon generation in NaK–cooled reactors, 20: 5178 (NAA-SR-11303)
ROSENBLUM, Earl, Radiation injury to intestinal tract, 20: 3720
ROSSELAND, Svein, Researches in solar physics during 1964, 20: 4521 (AD-618222)
ROSUMNY, M. R., Industrial analysis of ^{147}Pm x rays for radiography and imaging readout, 20: 3801 (ORNL-IIC-5, pp 222-38)
ROTA, A., Calculation of differential fast-neutron spectra from threshold-foil activation data by least-squares series expansion methods, 20: 4256
ROTH, H., Equivalence of stress- and radiation-induced defects in degenerate p-n junctions, 20: 4264
ROTHE, Heinz J., Evaluation of the I = 0 pion-pion scattering length, 20: 4617
ROTHMAN, M. A., Optimum generation of ion-cyclotron waves in cylindrical two-ion plasma, 20: 4984
ROTTER, I., Sensitivity of some nuclear characteristics to intermediate coupling parameters, 20: 4835 (JINR-P-2287)
ROUDEIX, Henri, Processes of radiation chemistry modifying natural and synthetic textile fibers, 20: 4032
ROULLET, Robert, Heavy liquid bubble chamber, 20: 4244 (NP-15416)
ROUNDS, Donald E., Laser as potential tool for cell research, 20: 3741
ROUSSET, P., Morphology and mechanism of atmospheric corrosion of uranium monocarbide, 20: 4336
ROWE, D. S., Maximum temperatures in flat-plate fuel elements with fuel-clad bonding defects, 20: 4102 (HW-SA-3640)
ROWENHORST, D. D., Prog. rpt. on fabrication of W alloy tubing, 7/1–10/22/65, 20: 4340 (COO-1518-1)
ROY, Rustum, Effect of neutron bombardment on kinetics of some reconstructive phase transformations, 20: 4462
ROYLANCE, P. J., Regeneration of bone marrow, 20: 3789
RUBIN, M. H., New sum rule for meson-baryon total cross sections at high energy, 20: 4678
RUBIN, M. H., SU(6) predictions for s-wave baryon-baryon scattering, 20: 4679
RUBIN, S., Feasibility of cavity pressure and temperature measurements for decoupled nuclear explosion, 20: 4084 (VUF-3017)
RUBRIGHT, M. M., Corrosion of Croloy 2¼ steel in products of a sodium–water reaction, 20: 4317 (BAW-1280-30)
RUDAKOV, L. I., Structure of front of strong magneto-sonic wave in rarefied plasma, 20: 4938 (IAE-909)
RUEDENAUER, F., Operating experience with Seibersdorf inhomogeneous sector field isotope separator, 20: 4283 (SGAE-PH-27/1965)
RUELLE, D., Rigorous results in statistical mechanics, 20: 4488
RUFEH, Firooz, Solubility of helium in uranium dioxide, 20: 3946
RUGH, Roberts, Radiation and radiomimetic chlorambucil and fetal retina, 20: 3725
RUIJGROK, Th. W., Problem of spin in time-dependent magnetic field, 20: 4648
RUNDQUIST, D. E., (^{3}He,α) Pickup reactions in ^{58}Ni and ^{60}Ni, 20: 4892
RUNOLFSSON, O., Simultaneous measurement of hyperfine structure, Stark effect, and Zeeman effect of ^{133}Cs^{19}F with molecular beam resonance apparatus, 20: 4554
RUQUIST, Richard D., Preliminary report on interaction of electromagnetic field with missile having ionized trail, 20: 4730 (SC-DC-65-1797)
RUSANOV, V. D., Magneto-sonic heating of plasma, 20: 4939 (IAE-911)
RUSSELL, J. L. Jr., Prog. rpt. on integral neutron thermalization, 4–6/65, 20: 4801 (GA-6634)
RUTHERFORD, J. A., Loss of He^+ ions in the upper atmosphere, 20: 4759
RYABININ, A. I., Thermochemistry of cerium(IV) nitrates, 20: 3954
RYABTSOV, V. D., Investigation of reactions $\pi^- p \to m\,\pi^0 + n$ at the π^- momentum of 4 Bev/c, 20: 4582 (JINR-P-2361)
RYDE, H., Law of conservation of nucleons, 20: 4853
RYDIN, R. A., Efficiency of semiconductor sandwich detector in flux of

fission neutrons from disk source, 20: 4238 (EUR-2487.e)
RYE, Merrill M., Effects of whole-body x-irradiation on vr-3 food reinforced bar-pressing, 20: 3772
RYS, Franz, Theory of scattering of identical particles, 20: 4655

S

SABBIONI, E., Determination of sulfur in terphenyl by neutron activation, 20: 3873 (EUR-2523.i)
SACHA, J., Dynamic polarization of protons and nuclei of fluorine in irradiated polymers, 20: 4037
SAENKO, A. P., Multiple acceleration system for high energy particle electrodynamic separator, 20: 4496 (JINR-P-2375)
SAGOT, Marcel, Improvements in or relating to neutron detectors, 20: 4260
ST. JOHN, C. F., Grain size dependence of fracture in α-uranium, 20: 4430
SAITO, Keiichi, Theory of statistical fluctuations in neutron distributions, 20: 5066
SAITO, Takesi, Unsubtracted dispersion relations in weak interactions, 20: 4663
SAITOV, I. S., Inflatable gaskets for JINR large-volume hydrogen bubble chambers, 20: 4242 (JINR-P-2376)
SAIZ DE BUSTAMENTE, A., Selection of type of reactor and influence thereof in Spanish economic and social development plan, 20: 5160
SAKAKI, Y., Contribution to investigation of reciprocal lattices of single crystals by means of Kikuchi-patterns, 20: 5009 (UCRL-Trans-1227)
SAKAOKU, Kiichiro, Changes of polymer crystals due to irradiation with electrons accelerated at various voltages, 20: 3987
SAKO, Kiyoshi, Preliminary design work of 100 MWt experimental fast reactor, 20: 5079 (NP-15572)
SALAM, Abdus, Role of symmetry physics, 20: 4641 (IC/65/76)
SALES, Andre, Iterative method of resolution of certain integral equations, 20: 4764
SALESSE, Marc, Nuclear fuel element casing, 20: 5101
SALLERON, Claude, International regulation of transport of radioactive materials. Present trends, 20: 4181 (NP-15620)
SALVADOR, L. Ramos, Reprocessing of irradiated MTR type fuels at Spanish J.E.N., 20: 4066
SAMA, L., Oxidation resistant coatings on niobium, 20: 4315
SAMA, L., Oxidation resistant coatings for Nb and Nb alloys, 20: 4357
SAMA, L., Protective coatings for niobium and its alloys, 20: 4356
SAMARSKI, Yu. A., Anisotropy of the Moessbauer effect in β-Sn single crystals at 4.2°K, 20: 4932
SAMSONOV, G. V., Rare elements and rare earths in technology, 20: 4451
SANCHEZ, Moises G., Fine sized powders of thoria, urania, and mixtures thereof and methods for their preparation, 20: 3969
SANDIFER, C. W., Flashing light satellite system for SNAP radiation environments, 20: 4262 (NP-15610)
SANDON, M., Study of $^{16}O(d,\alpha_0)$, $^{16}O(d,p_0)$, and $^{16}O(d,p_1)$ reactions at 300 kev to 1 Mev, 20: 4870
SANDSTROM, A. E., Geophysical aspects of cosmic rays, 20: 4560 (AD-618562)
SANDWEISS, J., Antihyperon production in antiproton-proton reactions at 3.7 Bev/c, 20: 4608
SANNES, F., Portable tritium-in-air monitor, 20: 4235 (AECL-2283)
SANTAVY, JOHN A., Remote underwater devices for evaluation and reduction of spent yankee fuel assemblies, 20: 5136 (WCAP-5554)
SANTIAGO, ARTURO, Intraoral stent for the direction of radiation beam therapy, 20: 3833
SAPOZHNIKOV, G. I., Longwave electron oscillations in beam-plasma system, 20: 4940 (IAE-932)
SASS, R. E., Radiations measurements group at Princeton-Pennsylvania 3 Bev proton synchrotron, 20: 4506 (PPAD-569E)
SASTRY, D. L., Validity of ξ approximation for the $\frac{1}{2}^-$ (β) $\frac{1}{2}^+$ decay in ^{141}Ce, 20: 4903
SASTRY, G. Sivarama, Harmonic structure and band splitting of type II solar radio bursts, 20: 4524
SATER, V. E., Application of Gibbs-Duhem equation to binary vapor-liquid equilibrium data of metal systems using Newton's interpolation formula, 20: 4375 (IS-1241)
SATOW, T., Mechanism of pyrolytic graphite formation, 20: 4348
SATOW, T., Microstructure and density of pyrolytic graphite, 20: 4431
SAUERBREY, G., Transition radiation, bremsstrahlung and plasmastrahlung, 20: 5017
SAUERWALD, Kurt J., MZFR nuclear power station with multi-purpose reactor, 20: 5138
SAUNIER, N., Study of the second step of the reaction $^7Li(d,n)^8Be$; $^8Be \rightarrow 2\alpha$, 20: 4869
SAVAGE, H. Wesley, Technology of liquid metals, 20: 4330 (ORNL-tr-854)
SAVINO, Joseph M., Simulated fuel assembly, 20: 5028
SAWAYAMA, Toshiko, On recovery-promoting chemicals after gamma-ray irradiation to mouse strain L cells cultured in vitro, 20: 3791
SAWERS, J. R. Jr., Polarization of neutrons from D(d,n)^{3}He reaction, 20: 4895
SAYAG, C., Demounting work on irradiated experiments at HFR, 20: 5204
SAYAG, C., Underwater radiography of irradiated specimens, 20: 5203
SCALSKY, Edward D., Linear energy transfer spectra and effective quality factors in stray radiation areas at Brookhaven National Laboratory proton synchrotrons, 20: 4176 (BNL-9684)
SCARBROUGH, J. O., Method for increasing critical current of superconducting alloys, 20: 4799
SCHAD, O., Prog. rpt. on research into critical heat flux in boiling H_2O, 1–3/65, 20: 4101 (EURAEC-1354)
SCHELLER, Walter, Process for production of tantalum or niobium in hydrogen plasma jet, 20: 4314
SCHENCK, G. F., Alkali metal corrosion. I., 20: 4318 (CNLM-5359)
SCHENK, M., On phase transformations of U_3O_8, 20: 4429
SCHENK, W., Use of standardized, movable, in-cell boxes, 20: 4093
SCHENKEL, J., Irradiation of cellulose and its derivatives, 20: 4034
SCHINTLMEISTER, Josef, Study of reaction $^{12}C(n,n')3\alpha$, 20: 4878
SCHLESINGER, S. P., Observation of nonquasistatic plasma surface waves, 20: 4935 (AFCRL-65-556)
SCHLEWITZ, J. H., Spectrophotometric determination of zirconium with 8-hydroxyquinoline, 20: 3895
SCHMIDT, G., Oscillations of plasma column, 20: 4985
SCHMIDT, Guenter, Study of reaction $^{12}C(n,n')3\alpha$, 20: 4878
SCHMIDT, M., Fast neutron capture in rhenium, 20: 4868
SCHMIDT, P., Σ radiative decay and angular momentum of Σ pionic decay, 20: 4616
SCHMIDT, Robert W., Carcinoma of thyroid gland in children and adolescents, 20: 3739
SCHMIDT-KUESETER, W. J., Symposium of federal ministers for scientific research, Lindau/Bodensee, July 8–10, 1964, 20: 4274
SCHMIDT-OTT, W.-D., Isomerism of ^{197}Tl, 20: 4921
SCHMITT, D. E., Method of determination of radioactive isotopes ^{55}Fe and ^{59}Fe in sea water, 20: 3891 (CEA-tr-A-1838)
SCHNITZEL, R. H., Strengthening of tungsten at intermediate test temperatures from 300 to 1600 C, 20: 4408
SCHOLZ, Josef, Simple reactivity meter of high sensitivity, 20: 5061 (ZFK-RN-22)
SCHOPPER, H., Use of AVF-cyclotrons for nuclear physics, 20: 4497 (KFK-310)
SCHOTT, Garry L., Structure, chemistry, and instability of detonation in homogeneous, low density fluids-gases, 20: 3918 (LA-DC-7276)
SCHRACK, Roald A., Nuclear size determination by neutral-pion photoproduction, 20: 4898
SCHRAUTEMEIER, Bernard Edward, Primary cosmic ray energy spectra, 20: 4569
SCHUETT, Klaus, Process for production of tantalum or niobium in hydrogen plasma jet, 20: 4314
SCHULT, O., Decay of 185-μsec isomer in ^{166}Ho, 20: 4889
SCHULTE, J. W., Methods used in United States for transferring materials through radiation barriers, 20: 4043
SCHULTZ, G. M., CORE, computer code for design of GCR core, 20: 5078 (GAMD-6676)
SCHULTZ, J. M., Temperature-sensitive x-ray small angle scattering from melt-crystallized polyethylene, 20: 5022
SCHULZ, G., Decay of ^{40}K, 20: 4919
SCHULZ, G., Electron capture ratios in decay of ^{202}Tl, 20: 4875
SCHULZ, W., Use of standardized, movable, in-cell boxes, 20: 4093
SCHULZE, E., Lipomatosis interna of descending colon with appearance of radiation injury, 20: 3820
SCHULZE, R. C., Corrosion of superalloys by lithium fluoride in cyclic high temperature environment, 20: 4326 (TRW-ER-6561)
SCHWALB, A. J., Propellant triggered gas discharges in pulsed plasma engines, 20: 4136
SCHWARTZ, Brian Benjamin, Flux quantization and generalized pairing in superconducting cylinders, 20: 4784
SCHWARZ, Eberhard, Processes of radiation chemistry modifying natural and synthetic textile fibers, 20: 4032
SCHWARZ, Harold A., Radiation chemistry, 20: 3986
SCHWARZ, John H., Normal threshold sheet structure of two-particle scattering amplitudes, 20: 4668
SCHWINGER, J., Quantum theory of gauge fields, 20: 4699
SCHWOB, Jean-Louis, Method for measurement of electron temperature in ionization phase of pulsed discharge in hydrogen, 20: 4714
SCHWOB, Jean-Louis, Reabsorption of L_β and H_α rays in pulsed discharge in hydrogen, 20: 4964
SCOBORIA, Raymond, Experimental study of effects of absorption on spectral lines from plasma, 20: 4974
SCOTT, D. B., Physical and mechanical properties of Zircaloy 2 and 4, 20: 4400 (WCAP-3269-41)
SCOTT, Walter P., Tumor/air ratio calculators, 20: 3855
SEABOLD, R. H., Shallow-buried model arches subjected to traveling-wave load, 20: 4131 (AD-622552)
SEALY, R., Malignant Zollinger-Ellison syndrome in Bantu woman with prolonged remission after gastric radiotherapy, 20: 3821

SEELEY, F. G., Synthesis of 3,9-diethyltridecyl-6-amine, 20: 3974 (ORNL-TM-1314)
SEGEL, S. L., Catalog of nuclear quadrupole interactions and resonance frequencies in solids. II., 20: 3973 (IS-1222)
SEIDL, M., Report on a meeting held in the old lecture room at Christ Church College, Oxford, at 9 p.m. on Thursday, September 9, 1965, 20: 4945 (ORNL-TM-1306)
SEIDLITZ, L., Σ radiative decay and angular momentum of Σ pionic decay, 20: 4616
SEIDOV, Yu. M., Theory of magnetic scattering of slow neutrons by antiferromagnets, 20: 4809
SEIERSTAD, G., Attempt to measure directly slowing down age of (d,d) neutrons in paraffin, 20: 2813
SEKI, Hiroshi, γ-Ray-induced oxidation of liquid methanol, 20: 4011
SEKI, Jisuke, Analytical application of fluoric ion. III., 20: 4059
SEKI, Jisuke, Analytical application of fluoric ion. IV., 20: 4060
SEKI, Jisuke, Analytical application of fluoric ion. V., 20: 3905
SELECKI, A., Natural isotopes. III., 20: 4284 (CEA-tr-X-617)
SELIGA, Mojmir, Problems of technological parameters of radiochemical apparatus, 20: 3993
SELLERS, Bach, Generation and practical use of monoenergetic x rays from alpha-emitting isotopes, 20: 4268 (ORNL-IIC-5, pp 353-73)
SELLS, S. B., Behavioral factors in disaster situations, 20: 4200
SELLSCHOP, J. P. F., Interaction of muons produced by atmospheric neutrinos, 20: 4561 (COO-818-64)
SELTZ, Raymond, Study of excitation curves of (t,α) reaction on ^{16}O between 1 and 3 Mev, 20: 4858
SEMENYUSHKIN, I. N., Multiple acceleration system for high energy particle electrodynamic separator, 20: 4496 (JINR-P-2375)
SEN, S. K., Measurement of electron density of plasma, 20: 4967
SEREDIN, Yu. V., Assessment of the efficiency of ventilation of atomic reactors of IRT-2000 type, 20: 5201
SERRELS, G. A., Dismantling and machining operations on high activity rigs at Harwell, 20: 4126
SESSLER, Andrew M., Instabilities of relativistic particle beams, 20: 4513 (UCRL-16440)
SETTE, D., Electron microscope observation of high-energy-neutron-irradiated germanium, 20: 4467
SETTERWALL, Max, Boiling reactor with super heat, 20: 5085
SHA, W. T., Experimental evaluation of power coefficient in slightly enriched PWR cores, 20: 5135 (WCAP-3269-40)
SHAGIMARDANOV, N. Sh., Ruler to determine relative deep doses and selection of proper conditions for irradiation by telegamma-units, 20: 3839
SHAIKH, Hafazuddin, Effects of irradiation on infective larvae of Nippostrongylus brasiliensis (travassos, 1914) lane, 1923, in rats, 20: 3786
SHAKASHIRO, Mouffac, Determination of titanium and zirconium in molybdenum base alloys by ion exchange, 20: 3896
SHAKED, H., Simple theory for release of fission gas from powders, 20: 4432
SHALYGIN, V. A., Thiophene ^{35}S, 20: 3976
SHANSTROM, R., Safety characteristics of large gas-cooled fast power reactor, 20: 5119 (GA-6732)
SHARPE, B. F., Demounting and machining techniques in hot cells at Berkeley, 20: 4128
SHARPE, B. F., Non-destructive testing of fuel elements at Berkeley, 20: 4121
SHARPE, R. S., Development of active radiographic inspection techniques at Harwell, 20: 4119
SHAVER, E., Mutants of parasitic wasp Dahlbominus fuscipennis (ZETT.) (Hymenoptera: eulophidae), 20: 3733
SHAW, P. B., Photon-induced beta decay in stellar interiors, 20: 4530
SHAW, Trevor, Heat exchange unit spacer grids, 20: 4109
SHEA, J. J., Charged colloid generating system for electric propulsion, 20: 4133 (N64-25007)
SHEFFIELD, J., Structure of collisionless shock waves in magnetized plasma, 20: 4977
SHEPHERD, George Henry, Improvements in or relating to entrance arrangements for irradiation cell, 20: 4096
SHERWOOD, W. A., Optical system for moderate-rigidity charged-particle beams, 20: 4509 (UCRL-14343)
SHESTOPALOV, V. P., Radiation of electromagnetic waves by electron beam moving above diffractional rate, 20: 4621
SHINOHARA, Kenichi, Crosslinking of polyethylene by high energy radiation, 20: 4010
SHIRAISHI, Kensuke, Effect of grain size on tensile properties of Magnox AL80, 20: 4437
SHIRLEY, D. A., Hyperfine structure in 2084-kev state of ^{140}Ce, 20: 4888
SHISHKIN, G. V., Properties of lepton irradiation produced by neutrino reaction with substance, 20: 4866
SHISHOV, Yu. A., Inflatable gaskets for JINR large-volume hydrogen bubble chambers, 20: 4242 (JINR-P-2376)
SHOLIN, G. V., Structure of front of strong magneto-sonic wave in rarefied plasma, 20: 4938 (IAE-909)
SHOOP, D. T., Metallography of zirconium-base alloy hydrides, 20: 4341 (NAA-SR-Memo-10927)
SHORT, Vincent R., Nuclear reactor core support structure, 20: 5049
SHRIMAL, S. K., Determination of micro quantities of niobium in uranium, 20: 3897
SHUTT, R. P., Antihyperon production in antiproton-proton reactions at 3.7 Bev/c, 20: 4608
SIEBERT, W., Amino acid changes in cattle insulin by uv-irradiation, 20: 4016
SIEGERT, W., Frequency of chlorophyll mutations after x irradiation of heterzygous M_2-seed stock of barley, 20: 3782
SIEMSSEN, R. H., Study of $^{19}F(^3He,d)^{20}Ne$ reaction, 20: 4908
SIGNORINI, C., Europium-144, 20: 4887
SIL, Kim Hon, New isotope, ^{174}W, 20: 4834 (JINR-E-2360)
SIL, N. C., Elastic scattering and polarization of electrons by atom in second Born approximation, 20: 4545
SILBER, W., Malignant Zollinger-Ellison syndrome in Bantu woman with prolonged remission after gastric radiotherapy, 20: 3821
SILINI, Giovanni, Studies of LSA ascites lymphoma of C57BL mice. I., 20: 3750
SILVERBLATT, Bernard L., Core support structure, 20: 5050
SILVERMAN, Joseph, Bremsstrahlung from $^{90}Sr-^{90}Y$ in thin absorbers, 20: 5000 (ORNL-IIC-5, pp 91-8)
SILVERMAN, L., Diffusion board for filtering high pressure gases, 20: 4097
SILVESTER, Austin G., Nuclear reactor with emergency coolant cross flow, 20: 5087
SIL'VESTROV, L. V., Investigation of reactions $\pi^- p \to n\pi^0 + n$ at the π^- momentum of 4 Bev/c, 20: 4582 (JINR-P-2361)
SIMECK, Charles M., Efficiency of molecular iodine removal from air, 20: 3673
SIMON, George, Dangers of x rays to physiotherapist, 20: 4203
SINCLAIR, R. M., Optimum generation of ion-cyclotron waves in cylindrical two-ion plasma, 20: 4984
SINGER, T., Prog. rpt. on reactor containment, 8–9/65, 20: 5023 (IITRI-578P21-15)
SINGH, M., Elastic scattering of 1.12 Mev γ rays from platinum and tantalum, 20: 4864
SINGLETARY, John B., Space materials handbook, 20: 4312
SINGLETON, John L., Prog. rpt. on PM-1, annual, 11/63–10/64, 20: 5108 (AD-618376)
SINGWI, K. S., Coherent scattering of slow neutrons by liquid argon, 20: 4819
SINSHEIMER, Robert L., Process of infection with bacteriophage φX174. V., 20: 3748
SINSHEIMER, Robert L., Process of infection with bacteriophage φX174. VI., 20: 3749
SIZOV, R. A., Effects of particle size on extinction of neutron diffraction, 20: 5016
SKAREDOFF, Ludmila, Radiation and radiomimetic chlorambucil and fetal retina, 20: 3725
SKARICS, R., Gasdynamic methods in MHD flow, 20: 4702 (AD-619094)
SKAVDAHL, R. E., FFTF driver fuel: PuO_2–stainless steel cermet, 20: 5192 (BNWL-SA-251)
SKINNER, J., Examination of irradiated ceramic fuel elements at Windscale, 20: 4130
SKORYNA, Stanley C., Studies of inhibition of intestinal absorption of radioactive Sr. IV., 20: 3671
SLANGER, Tom George, Secondary ion energies in charge exchange reactions, 20: 4556
SLANSKY, Cyril M., Application of nuclear heat to production of ammonia, 20: 3916 (CONF-650902-20)
SLATTERY, G. F., Predicting irradiation-growth in uranium, 20: 4470
SLAUCITAJS, L., Some morphological aspects of geomagnetic secular variation, 20: 4757
SLIEKER, C. J. G., Thermal diffusion in isotopic hydrogen and hydrogen–helium mixtures, 20: 4724
SLOTNICK, H., Stability of carbon strengthened columbium–zirconium alloys at elevated temperature in ultra-high vacuum, 20: 4397 (TIM-955)
SMELTZER, P., Evaluation of core thermal and hydraulic data obtained during the operation of PWR core-1 with the fourth seed (DLCS-33801, DLCS-18201, DLCS-24301, DLCS-36201), January 1963–February 1964, 20: 5133 (WAPD-PWR-TE-151)
SMEND, F., Isomerism of ^{197}Tl, 20: 4921
SMID, Antonin, Some observations in experimental transplantation of bone marrow, 20: 3795
SMIRNOV, V. P., Magneto-sonic heating of plasma, 20: 4939 (IAE-911)
SMIT, J. Van R., Purification of rubidium compounds from traces of cesium, 20: 4056
SMITH, A. M., Experience with turbine-driven potassium boiler-feed pumps medium power reactor experiments, 20: 5184 (ORNL-P-1740)

SMITH, B. C., Reactions of thorium tetrachloride with o-phenanthroline and triphenylphosphine, 20: 3933
SMITH, B. E., X-ray study of fission fragment damage in steels, 20: 4469
SMITH, Colin Charles, Improvements relating to heat treatment processes for magnesium alloys, 20: 4456
SMITH, D. B., Silt movement investigation in oxcars spoil ground, firth of forth, using radioactive tracers, 1961 and 1964, 20: 4166 (AERE-R-4980)
SMITH, Francis J., Classical collision integrals for repulsive screened Coulomb potential, 20: 4988
SMITH, G. P., Spectroscopy of ionic media, 20: 3921 (ORNL-3870, pp 56-60)
SMITH, H. M. Jr., Prog. rpt. on photomultiplier investigation, 5/15–8/14/65, 20: 4218 (NYO-3421-4)
SMITH, Harold P. Jr., Equivalence of time optimal and minimax solutions to xenon shutdown problem, 20: 5074
SMITH, M. L., Measurement of filter efficiency with condensation nuclei counter, 20: 5036 (RL-SA-47)
SMITH, Richard K., Effects of whole-body x-irradiation on vr-3 food reinforced bar-pressing, 20: 3772
SMITH, William R., Hauser-Feshbach nuclear scattering computer code LIANA, 20: 4844 (ORNL-TM-1234)
SMOLKIN, G. E., Structure of front of strong magneto-sonic wave in rarefied plasma, 20: 4938 (IAE-909)
SNOW, J. A., Dynamic performance optimization for numerical control systems, 20: 5220 (UCRL-13185)
SNYDER, William T., Magnetohydrodynamic flow in entrance region of parallel-plate channel, 20: 4709
SOBOL, G. A., Centimeter wave detection in gas-discharge plasma, 20: 4969
SOBOLEVSKII, M. A., Individual dosimetric control technique, 20: 4198
SOKOLOV, E. Ya., Perspectives of atomic heat and power plants, 20: 5149
SOLNTSEV, A. M., Longwave electron oscillations in beam-plasma system, 20: 4940 (IAE-932)
SOLOV'EV, L. D., Electromagnetic properties of mesons in broken symmetry, 20: 4644 (JINR-P-2299)
SOLOVEV, V. V., Tests of consequences of unitary symmetry in Hadron-production reactions (survey), 20: 4645 (NP-15599)
SOMMELET, Pierre-Hubert, Gibbs energies, entropies, and heats of formation from drop calorimetry, 20: 5223 (UCRL-16303)
SOMMER, Warren Thomas, Interaction of free electrons with liquid helium, 20: 4787
SONETT, C. P., Recurrent $Si^{+}-Si^{-}$ impulse pairs and shock structure in M-region beams, 20: 4758
SONG, H. S., Phase-space considerations for four-particle final states, 20: 4658
SOOD, B. S., Elastic scattering of 1.12 Mev γ rays from platinum and tantalum, 20: 4864
SORENSON, James A., Body composition by differential absorption of monochromatic x rays, 20: 3885 (ORNL-IIC-5, pp 277-89)
SOROKIN, Yu. S., Kinetics and sensitization of ammonia radiolysis in gaseous phase under fast electron irradiation, 20: 4021
SOROKO, L. M., Proton depolarization in cyclotrons, 20: 4520
SOTA, Susumu, Leukemogenesis of mouse leukemia by x irradiation. I., 20: 3696
SOWMAN, H. G., Prog. rpt. on fabrication of W alloy tubing, 7/1–10/22/65, 20: 4340 (COO-1518-1)
SPALDING, E. G., Some considerations in design and engineering of active effluent treatment plants, 20: 5207
SPALTHOFF, W., Installation for non-destructive x-ray tests of irradiated fuel elements, 20: 4118
SPANIER, J., Extension of hot-1 to treat Neumann boundary conditions—with applications to certain vibration problems, 20: 4080 (WAPD-TM-535)
SPANNAGEL, G., Conversion of 238.6-kev γ line of ThB and comparison with the tables of Sliv and of Rose, 20: 4920
SPECTOR, Marshall I., Method of sealing refractory vessel containing radioactive wastes, 20: 5209
SPEIGLER, G., Image contrast and radiation protection. II., 20: 3815
SPEKTOR, A. M., Magneto-sonic heating of plasma, 20: 4939 (IAE-911)
SPICER, B. R., Effect of uniaxial compression upon transformation of metastable delta-phase plutonium, 20: 4434
SPIJKERMAN, J. J., Narrow-line source for ^{119}Sn Moessbauer spectroscopy, 20: 5014
SPITSYN, Vikt. I., Tributyl phosphate extraction of Pa. I., 20: 4057
SPITSYN, Vikt. I., Tributyl phosphate extraction of Pa. II., 20: 4058
SPREITER, J. R., Shock waves in solar wind and geomagnetic storms, 20: 4744
SPRINGER, T. E., Fortran IV hydrogen property tabular codes, 20: 5177 (LA-3381)
SRB, Vladimir, Effect of x-ray radiation on mitokinetic apparatus of cell, 20: 3764
STAEHLE, George Gardner, Gamma-ray decay of ^{165}Tm, ^{176m}Lu, and ^{178}Ta, 20: 4924
STANEK, Floyd J., Plane thermal stress analysis of thick-wall cylinders. II., 20: 4076 (HIC-1-1564-3(Vol.2))
STAROSELSKY, V. A., Determination of distribution of aerosol particles according to size by diffusion method, 20: 4733 (AI-Trans-201)
STAROZ, Claude, Improvements in or relating to zirconium phosphate preparation, 20: 3968
STAUFFER, M., Dismantling and machining methods used in hot cells and workshops, 20: 4127
STAUFFER, M., Transfer methods for irradiation rigs and fuel elements, 20: 4063
STEARNS, E. H., Remote metrology and examination techniques on irradiated fuel materials, 20: 4124
STEBBINGS, R. F., Loss of He^{+} ions in the upper atmosphere, 20: 4759
STECHKINA, I. B., Determination of distribution of aerosol particles according to size by diffusion method, 20: 4733 (AI-Trans-201)
STEEB, Siegfried, Crystal structure of phases $AgSm$, Ag_3Sm, 20: 4447
STEFFEN, R. M., Transverse polarization of K-conversion electrons following β decay of ^{198}Au, 20: 4900
STEGEMANN, Dieter, Common theory for neutronic noise analysis experiments in nuclear reactors, 20: 5076
STEIN, J. M., Safety characteristics of large gas-cooled fast power reactors, 20: 5119 (GA-6732)
STEINER III, Pinckney Alston, Stark effect studies of CH_3F, CD_3F, CH_3CN, and CD_3CN, 20: 3958
STEINFINK, H., Thermoelectric and electrical measurements in Er–Se system, 20: 5013
STEPANOVICH, A. S., Radioactive instruments—their application in industry, 20: 4275
STEPANYUK, V. L., Multiple acceleration system for high energy particle electrodynamic separator, 20: 4496 (JINR-P-2375)
STEUNENBERG, R. K., Consolidation of lanthanon fission products in alloys, 20: 3865 (ANL-7064)
STEUNENBERG, Robert K., Regeneration of nuclear fuel, 20: 4073
STEVENS, Glenn, Nuclear reactor core support structure, 20: 5049
STEVENS, William H., Apparatus for determining quantity of contaminant in substance, 20: 3970
STEVENSON, F. D., Application of Gibbs-Duhem equation to binary vapor-liquid equilibrium data of metal systems using Newton's interpolation formula, 20: 4375 (IS-1241)
STEWART, J. C. C., Nuclear development in the U. K., 20: 5155
STEYAERT, J., Study of the second step of the reaction $^{7}Li(d,n)^{8}Be$; $^{8}Be \rightarrow 2\alpha$, 20: 4869
STIEGLER, J. O., Electron microscopy, 20: 4386 (ORNL-3870, pp 20-6)
STILL, Edwin T., Effect of massive doses of 32 Mev protons and ^{60}Co radiation on primates, 20: 3692
STOCKSCHLAEDER, F., Use of standardized, movable, in-cell boxes, 20: 4093
STODDARD, Stephen D., Arc spray powder feeder for ultra-fine particles with a wide range of densities, 20: 4298 (LA-DC-7275)
STODIEK, W., Plasma confinement in low-density C stellarator discharges, 20: 4942 (MATT-372)
STOHR, Jacques Andre, Nuclear fuel element casing, 20: 5101
STOKES, Stuart K., Effects of whole-body x-irradiation on vr-3 food reinforced bar-pressing, 20: 3772
STOLLER, D. R., Effect of yttrium on the recrystallization and grain growth of tantalum, 20: 4424
STOLTZE, D., Film dosimetric studies of convergence irradiation of cerebral tumors, 20: 3862
STORER, John B., Prog. rpt. on genetic control of aging and radiation-induced life shortening of mice, 1/1–9/30/65, 20: 3711 (NYO-3314-2)
STRAKER, E. A., Inelastic neutron scattering from pressurized ethane, 20: 4810
STRANDJORD, Nels, Radioisotopic device for measuring bone mineral, 20: 3803 (ORNL-IIC-5, pp 257-76)
STRATTON, T. F., High current steady state coaxial plasma accelerators, 20: 4139
STRAUB, C. P., Transfer of radiostrontium from cows' feed to milk, 20: 4162
STREKALOVSKII, V. N., Studies of uranium dioxide oxidation by means of high-temperature electroconductivity, x-ray phase studies, and continuous weighing, 20: 3952
STRINGER, John, Effect of nitrogen on oxidation of tantalum at high temperatures, 20: 4333
STRINGER, W. J., Latitude of auroral activity during periods of zero and very weak magnetic disturbance, 20: 4740
STROMBERG, Thorsten Fredrick, Superconducting properties of high purity niobium, 20: 4774 (IS-T-22)
STUART, R. N., Calculation of treatment schedules for cancer chemotherapy, 20: 5222 (UCRL-14505)
STUCKENRATH, Robert Jr., ^{14}C and the unwary archaeologist, 20: 4147
STUPEGIA, D. C., Fast neutron capture in rhenium, 20: 4868
STURIALE, T. J., Self diffusion of nitrogen in uranium mononitride, 20: 4394 (PWAC-477)

STURROCK, P. A., Shock waves in solar wind and geomagnetic storms, 20: 4744
SUDAN, R. N., Classification of instabilities from their dispersion relations, 20: 4987
SUDAN, R. N., Growing waves in nongyrotropic plasma, 20: 4989
SUDARSHAN, E. C. G., Concluding remarks at international seminar on unified field theories at Feldafing on Starnbergersee near Munich, July 1965, 20: 4646 (NYO-3399-40)
SUDARSHAN, E. C. G., Shmushkevich's method for charge-independent theory, 20: 4667
SUFFERT, M., Study of inverse photodeuteron reaction in ^{11}B and ^{16}O in the giant resonance energy region, 20: 4884
SUGAR, R., Faddeev formalism for four-particle systems, 20: 4675
SUGIMOTO, Osamu, Reactivity effect of void and hole, 20: 5064
SUITA, Tokuo, Dielectric properties of irradiated paraffin wax, 20: 3989
SULKOWSKI, C., Magnetic induction distribution in cylindrical specimen, 20: 4794
SUSSDORF, Dieter H., Roles of liver and appendix in serum hemolysin response in rabbits, 20: 3746
SUZUKI, Mahiko, SU(6) and deviations from the $\Delta I = \frac{1}{2}$ rule in nonleptonic hyperon decays, 20: 4683
SWALLOW, A. J., Basic radiation chemistry with reference to application of radiation in textile industry, 20: 4031
SWANSON, K. M., Non-destructive testing of fuel in Dounreay alpha-gamma hot cells, 20: 4120
SWEET, R. F., Low-lying levels in ^{50}V and ^{58}Co studied with the (p,d) reaction, 20: 4899
SWENSON, Paul A., Prog. rpt. on inhibition of synthesis of macromolecules by ultraviolet radiation, 1965, 20: 3686 (TID-22352)
SWIFT, L. M., Feasibility of cavity pressure and temperature measurements for decoupled nuclear explosion, 20: 4084 (VUF-3017)
SYBENGA, J., Effect of nitric oxide on x-ray sensitivity of Crotalaria intermedia seeds, 20: 3759
SYCHEV, B. S., Passage of high energy neutrons in iron–aqueous mixtures, 20: 4998 (JINR-P-2359)
SZABO, A., Radioactivity of some forms of vegetation studied in neighborhood of city of Cluj, 20: 3654
SZWARC, R., Vapor pressure and heat of sublimation of tungsten, 20: 4438

T

TABATA, Yoneho, Radiation-induced copolymerization of carbon monoxide with α-olefines, such as propylene, butene-1, and isobutylene, 20: 3997
TABOADA, A., Molten-salt reactor program, 20: 4308 (ORNL-3870, pp 243-60)
TABOADA, A., SNAP-8 corrosion studies, 20: 4322 (ORNL-3870, pp 305-7)
TABOADA, A., SNAP-50 corrosion studies, 20: 4323 (ORNL-3870, pp 308-11)
TABOR, W. H., Prog. rpt. on research reactor, 4–6/65, 20: 5198 (ORNL-TM-1290)
TABUCHI, Akira, Radiation dose received by mother and fetus x-ray examination, 20: 3823
TAFT, H. D., Antihyperon production in antiproton-proton reactions at 3.7 Bev/c, 20: 4608
TAILLET, Joseph, Measurement of electron density and collision frequency of plasma, 20: 4955
TAKADLECEK, Ludvik, Some observations in experimental transplantation of bone marrow, 20: 3795
TAKAHASHI, Tomoo, Effects of ^{60}Co γ-ray on pharmaceutical powders. I., 20: 4018
TAKAHASHI, Tomoo, Effects of ^{60}Co γ-ray on pharmaceutical powders. II., 20: 4019
TAKAHASHI, Y., Normalization of Bethe-Salpeter wave functions, 20: 4671
TAKASHIMA, Yoichi, Isotope separation by concurrent gas centrifuge, 20: 4285
TAKEDA, Seishi, Generalized analysis of rossi-α experiment, 20: 5070
TAKEUCHI, Yo, Alloys of nickel with lithium, barium, and strontium, 20: 4442
TAKIZAWA, Masao, Radiation-induced oxidation of Sb(III) in aqueous solution. III., 20: 4009
TAL'ROZE, V. L., Method and equipment for investagations of electric field effect on radiolysis of gases, 20: 4022
TAMM, I. E., Physics of elementary particles. Modern status and prospects, 20: 4620
TAMURA, Tetsuo, Preliminary design work of 100 MWt experimental fast reactor, 20: 5079 (NP-15572)
TANG, Yi-nao, Recoil tritium reactions with chlorocarbons, 20: 4023
TANKINS, Edwin S., An examination of Henry's law in liquid metal systems with infinitely dilute solutions of oxygen, 20: 4454
TANZER, J., Chromosomes and leukemia, 20: 3730
TAPLIN, G. V., Albumin macroaggregates for brain scanning: experimental basis and safety in primates, 20: 3832
TARAN, J. V., Polarization of protons in La–Mg nitrate, 20: 5021
TARAN, Yu. N., Investigation of cerium distribution in cast iron by means of electron probe, 20: 4414
TARDY-JOUBERT, Philippe, Critical study of some soft-tissue equivalent material. Sensitivity to neutrons of 1 kev to 14 Mev, 20: 3708 (CEA-R-2833)
TARIMER, Niyazi, Classification of elementary particles, 20: 4664
TATSUMOTO, M., Potassium, rubidium, strontium, thorium, uranium, and ratio of ^{87}Sr to ^{86}Sr in oceanic tholeiitic basalt, 20: 4145
TAULBEE, C. D., Influence of operating conditions on radiation damage to transistor gain, 20: 4267
TAYLOR, Albert Major, Improvements relating to heat treatment processes for magnesium alloys, 20: 4456
TAYLOR, Anthony James, Improvements in or relating to nuclear power plant, 20: 5169
TAYLOR, Anthony James, Improvements in nuclear reactor heat generating and utilizing plant, 20: 5170
TAYLOR, Clayborne D., Preliminary report on interaction of electromagnetic field with missile having ionized trail, 20: 4730 (SC-DC-65-1797)
TAYLOR, Derek, Heat exchange unit spacer grids, 20: 4109
TAYLOR, J. C., Approximate supermultiplet model consistent with relativity and unitarity, 20: 4685
TAYLOR, K., Prog. rpt. on U–Pu monoxides, 7–0/65, 20: 4327 (UNC-5138)
TEGHTSOONIAN, E., Grain size dependence of fracture in α-uranium, 20: 4430
TENNEY, F. H., AC response of spirally wound capacitors, 20: 4217 (MATT-378)
TENNSTEDT, K., Isotope exchange studies with metal-organic compounds of Tl using ^{204}Tl, 20: 3960
TEPLITZ, Vigdor L., Dynamical formula for slope of Pomeranchuk trajectory, 20: 4587 (UCRL-11495)
TERENT'EV, M. V., Kaon decay into two pions and possible CP nonconservation, 20: 4626
TEREPKA, A. Raymond, Prog. rpt. on skeletal metabolism in man, final, 1965, 20: 3664 (TID-22324)
TERRY, L. E., Thin-film, field-effect devices, 20: 4220 (SC-TM-65-424)
TERZ, Jose J., Functional capacity of canine bone marrow implants in the spleen, 20: 3652
THACHER, H. C. Jr., Collected algorithms 1900–1963 from communications of the association for computing machinery, 20: 4286 (ANL-7054)
THERIAULT, A. J., Prog. rpt. on modification of photometric measurement assemblies, final, 1/4–5/3/65, 20: 4234 (AD-619177)
THIRION, Jacques, Saclay variable-energy cyclotron, 20: 4516
THOMAS, G., Structure and high strength metals, 20: 4399 (UCRL-16301)
THOMAS, K. C., Corrosion and hydriding of Zircaloy-4 under heat transfer conditions, 20: 4331
THOMAS, K. C., Stress corrosion in alloys for fuel element cladding—stainless steel and Zircaloy, 20: 4328 (WCAP-3269-50)
THOMAS, R. J., Electronic scheme for measurement of exploding wire energy, 20: 4481 (UCRL-14170)
THOMASSEN, K. I., Microwave plasma density measurements, 20: 4971
THOMPSON, R. D., Separation and measurement of ^{137}Cs in precipitation, 20: 4159
THOMPSON, S. G., Emission of K x rays and division of nuclear charge in spontaneous fission of ^{252}Cf, 20: 4914
THOMSON, D. B., Cylindrical explosive flux-compression system, 20: 4477 (LA-DC-7289)
THOMSON, D. B., Plasma compression by explosively produced magnetic fields, 20: 4941 (LA-DC-7290)
THORN, J. D., Advanced gas-cooled reactors, 20: 5164
THORNDIKE, A. M., Antihyperon production in antiproton-proton reactions at 3.7 Bev/c, 20: 4608
THORP II, Arthur G., Fuel element for coolant-moderator nuclear reactor, 20: 5097
THORPE, J. F., Axial heat conduction in reactor fuel elements, 20: 5091
THOULESS, D. J., Nuclear reactions in nuclear matter, 20: 4879
THURBER, W. C., High-temperature materials, 20: 4301 (ORNL-3870, pp 102-35)
THURBER, W. C., Medium power reactor experiment, 20: 4307 (ORNL-3870, pp 238-42)
THURBER, W. C., Tungsten metallurgy, 20: 4302 (ORNL-3870, pp 155-63)
THURBER, W. C., Uranium nitride, 20: 4303 (ORNL-3870, pp 164-70)
THWAITES, R., Interaction of carbon monoxide with tantalum, 20: 4444
TIDMAN, Derek A., Enhanced bremsstrahlung from plasmas containing nonthermal electrons, 20: 4982
TIKHOMIROV, V. B., Polymer coatings in nuclear techniques, 20: 3979
TIKHOMIROVA, M. M., Comparative study of result of radiation after-effects on chromosomal non-divergence, 20: 3715 (JPRS-31514, pp 59-64)
TIKHOMIROVA, M. M., Non-divergence of chromosomes under the influence of x-rays of varied hardness and intensity, 20: 3714 (JPRS-31514, pp 44-58)
TODREAS, Neil E., Effect of nonuniform axial heat flux distribution, 20: 4104 (NP-15622)

TOLLET, Louis Henri Joseph, Method of varying moderation in nuclear reactor, 20: 5053
TOLLET, Louis Henri Joseph, Nuclear reactors, 20: 5052
TOLMACHEVA, A. V., Anomalous ionization of lower ionosphere of temperate latitudes during world magnetic storms, 20: 4736
TOMBRELLO, T. A., Alpha-particle-induced breakup of deuteron, 20: 4596
TOMBROPOULOS, E. G., Fatty acid synthesis by subcellular fractions of lung tissue, 20: 3656 (BNWL-SA-225)
TOMNOVEC, F. M., Influence of weather on salt distributions and aerosols on beaches, 20: 4148 (AD-623515)
TOPPING, G., Infra-red assignments and force constants in metal–nitrato complexes, 20: 3949
TOTHILL, P., The retention by body of ^{131}I-polyvinylpyrrolidone and its effect on radiation dose, 20: 3675
TOTO, Patrick D., Radiation-induced changes in epithelium of Buccal mucosa, 20: 3744
TOUHILL, Charles Joseph Jr., Removal of radionuclides from water and waste-water by manganese dioxide, 20: 5206
TOURYAN, K. J., Ablation mechanism for impregnated tungsten, 20: 4108
TOUSCHEK, B., Transverse resistive wall instability of extremely relativistic beams of electrons and positrons, 20: 4500 (LNF-65/27)
TOWER, Stephen N., Neutronic reactor and fuel element therefor, 20: 5083
TOY, C. H., Spectrophotometric determination of zirconium with 8-hydroxyquinoline, 20: 3895
TRAUB, Eugene F., Squamous cell epithelioma, 20: 3811
TRAUGER, D. B., Experience with stainless steel sheathed chromel–alumel thermocouples in irradiated experiments, 20: 4263 (ORNL-TM-1320)
TRAVERSE, Jean-Pierre, High-temperature study of allotropic transformations of sesquioxides of yttrium, erbium, and thulium, 20: 3939
TREJBAL, Z., Source of polarized ions for cyclotron, 20: 4519
TREJBAL, Zdenek, Optical properties of atomic hydrogen beam, 20: 4559
TRETYAKOV, O. A., Radiation of electromagnetic waves by electron beam moving above diffractional rate, 20: 4621
TRETYAKOV, O. A., Radiation of charged particle moving above diffractional grid, 20: 4622
TRETYAKOVA, S. S., Radiation of electromagnetic waves by electron beam moving above diffractional rate, 20: 4621
TRIPP, Wilson, Effects of electrical conductance of wall on magnetohydrodynamic channel flow with heat transfer, 20: 4703 (AD-619101)
TROZERA, T. A., Prog. rpt. on effect of substructure on irradiation stability of ASTM A302 grade B steel, 10/65, 20: 4372 (GA-6724)
TRUBEY, D. K., Comparison of three methods used to calculate gamma-ray transport in iron, 20: 5001 (ORNL-RSIC-9)
TRUEMAN, T. L., Comparison of nucleon-nucleon scattering data with the predictions of SU(12)$_L$, 20: 4605
TSEL'NIK, F. A., Plasma with relativistic electrons in trap with magnetic mirrors, 20: 4950 (UCRL-Trans-1261(L))
TSIVILEV, M. P., Engineering and rescue operations at site of atomic strike, 20: 4191 (JPRS-31014)
TSUCHIDA, T., Magnetic characteristics of lanthanide elements combined with tin, lead, and indium, 20: 4423
TSUKROV, F. G., Thermal electronic properties of tungsten–hafnium system, 20: 4405 (K-Trans-9)
TSURUTA, Sachiko, Composition of matter in nuclear statistical equilibrium at high densities, 20: 4855
TUBIANA, M., Chromosomal number and radiosensitivity of experimental tumors, 20: 3751
TUHY, Richard Michael, Photonuclear determination of yield curve and cross section curve for production of ^{13}N in ^{16}O, 20: 4833 (IS-T-43)
TURCHINI, J.-P., Cholinesterase activities in mouse liver and kidney during experimental intoxication with uranyl nitrate, 20: 3670
TURK, R., Characteristics of porous tungsten ionizers, 20: 4135
TURNER, B. R., Loss of He$^+$ ions in the upper atmosphere, 20: 4759
TURNER, G., Extinct ^{129}I and trace elements in chondrites, 20: 4526
TURNER, J. E., Theoretical methods in dosimetry of high-energy particles, 20: 4505 (ORNL-P-1738)
TURNER, S. E., Nuclear analysis of Elk River reactor, 20: 5112 (CEND-507)
TURNER, W. H., Application of multichannel synthesis to 2-D depletion calculations, 20: 5056 (CONF-654-22)
TUTOR, Forrest T., Isotope encephalogram in brain tumor diagnosis, 20: 3830
TZUNG, Mu, Measurement of energy and angular characteristics of electrons and γ-quanta in propane bubble chamber, 20: 4240 (JINR-P-2277)

U

UEDA, Masao, Genetically significant radiation dose from dental x-ray diagnosis. I., 20: 4195
UENO, K., Determination of radioactive fallout from nuclear weapon tests. Detection and determination of radioactive nuclides in rain water, 20: 4177 (JAERI-1083)
UKAI, Seiji, Generalized analysis of rossi-α experiment, 20: 5070
ULANOVSKII, B. Ye., Engineering and rescue operations at site of atomic strike, 20: 4191 (JPRS-31014)
UNGAR, E. W., Ablation mechanism for impregnated tungsten, 20: 4108
UNGER, E., Effect of x-irradiation on take and growth of Guerin-tumor, I., 20: 3695
UNIK, J. P., Division of nuclear charge deduced from x-ray measurements in spontaneous fission of ^{252}Cf, 20: 4913
UPPARD, J. E., Blast loading on right circular cylinder, 20: 4132 (AWRE-O-93/65)
UPSON, U. L., Electrostatic apparatus for removal of dust particles from gas stream, 20: 4726
URABE, Masayoshi, Crosslinking in polyethylene single crystals by ^{60}Co γ-ray irradiation, 20: 3998
URIARTE, A., Reprocessing of irradiated MTR type fuels at Spanish J.E.N., 20: 4066
URIN, M. G., Spontaneous fission of nuclei, 20: 4876
USOV, N. A., Engineering and rescue operations at site of atomic strike, 20: 4191 (JPRS-31014)
USTENKO, E. P., Inflatable gaskets for JINR large-volume hydrogen bubble chambers, 20: 4242 (JINR-P-2376)
UST'YANTSEV, V. M., Oxide systems for measuring electric resistance and x-ray analysis of specimens, 20: 3953
UST'YANTSEV, V. M., Studies of uranium dioxide oxidation by means of high-temperature electroconductivity, x-ray phase studies, and continuous weighing, 20: 3952
UTIGER, Robert D., Radioimmunoassay of human plasma thyrotropin, 20: 3829

V

VAETH, Jerome, Radiation-induced myelitis, 20: 3771
VAGIN, V. A., Multiple acceleration system for high energy particle electrodynamic separator, 20: 4496 (JINR-P-2375)
VAIDYA, S. M., Simultaneous bootstrap of the ρ and f^0 in $\pi\pi$ scattering, 20: 4607
VALATIN, J. G., Theory of superfluids, 20: 4789
VALENTIN, A., Decontamination procedures and frequencies in $\alpha\,\beta\,\gamma$ metallurgical hot cells, 20: 4213
VALLELY, J., Examination of irradiated ceramic fuel elements at Windscale, 20: 4130
VAN BRUGGEN, E. F. J., Electron microscopic and biochemical characterization of fraction I protein, 20: 5219 (TID-22372)
VAN DE GEIJN, J., Construction of individualized intensity modifying filters in ^{60}Co teletherapy, 20: 3814
VAN DEN BRENK, H. A. S., Enhancement of radiosensitivity of skin of patients by high pressure oxygen, 20: 3727
VAN DER WERF-MESSING, B., Treatment of carcinoma of bladder with radium, 20: 3819
VAN DEYCK, D., Studies on separation of ^{137}Cs and ^{90}Sr from fission products in acid medium on mineral ion exchangers, 20: 3871 (EUR-2497.e)
VAN ELST, H. C., Prog. rpt. on determination of brittle-ductile transition in steel, 4–9/65, 20: 4457 (EURAEC-1474)
VAN HOVE, L., Determination of uranium in its alloys, 20: 3890 (AEC-tr-6617)
VAN HOVE, L., Strong interactions at very high energy, 20: 4696
VANIK, Milton C., Fine sized powders of thoria, urania, and mixtures thereof and methods for their preparation, 20: 3969
VAN KLINKEN, J., Double scattering of electrons, 20: 4881
VAN KLINKEN, J., Some absolute beta polarization measurements, 20: 4880
VAN SANTEN, R. T., Spectrophotometric determination of zirconium with 8-hydroxyquinoline, 20: 3895
VARDE, M. S., Determination of micro quantities of niobium in uranium, 20: 3897
VARELA, J. E., Prog. rpt. on improvement of renogram techniques, final, 20: 3800 (NP-15150)
VARNADO, S. G., AT-25 telemetry band tracking antenna, 20: 5215 (SC-TM-65-448)
VATISTAS, S., Effect of fractionation on four day survival of mice after whole-body neutron irradiation, 20: 3728
VATTI, K. V., Induced mutation process—effect of high temperature after irradiation on the frequency of occurrence of lethal mutations and chromosomal breaks, 20: 3713 (JPRS-31514, pp 29-43)
VAUGHAN, G. A., Examination of irradiated ceramic fuel elements at Windscale, 20: 4130
VAUGHAN, R. D., Current and future development of magnox reactor, 20: 5157
VEENBOER, J. Th., Natural radioactivity of ^{40}K, ^{87}Rb, and ^{176}Lu, 20: 4916
VENABLES, J. H., Gas release methods used in Harwell metallurgical post-irradiation laboratory, 20: 4452
VENKATAPATHIY RAJU, B. B., Decay scheme and directional correla-

tions of γ rays from ^{182}Ta, 20: 4865
VENKATA REDDY, K., Decay scheme and directional correlations of γ rays from ^{182}Ta, 20: 4865
VENKATESAN, D., Influence of geomagnetic activity on polar cap absorption, 20: 4756
VENKATRAMANA BHAT, K., Potential radiation protective agents. III., 20: 3790
VERDEYEN, J. T., Electron and atom concentrations in afterglow gas discharge, 20: 4970
VERKERK, B., Chemical considerations in the selection of reactor fuels, 20: 4345
VEYSSIERE, Andre, Study of some transversal motions of electron beam in linear accelerator, 20: 4494 (CEA-R-2843)
VIALLARD, Rodolphe, Metastable equilibrium of lanthanum–hydrogen system, 20: 3936
VIEHBOECK, F. P., Operating experience with Seibersdorf inhomogeneous sector field isotope separator, 20: 4283 (SGAE-PH-27/1965)
VILLERS, Gerard, Crystalline and magnetic properties of mixed garnets of dysprosium and ceric earths, 20: 4411
VILQUIN, Alain, Experimental contamination of pink shrimps by ^{137}Cs, 20: 3657 (CEA-R-2818)
VINCOUR, J., Source of polarized ions for cyclotron, 20: 4519
VINDUSKA, M., Oriented nuclei and beta decay, 20: 4933
VITALI, G., Electron microscope observation of high-energy-neutron-irradiated germanium, 20: 4467
VLASOV, V. G., Kinetics of oxidation of uranium by air, oxygen, and carbon dioxide, 20: 4329 (CEA-tr-R-1868)
VOGL, Joseph L., Nuclear and neutrino processes in stars and supernovae, 20: 4534
VOGT, K. J., Environmental radioactivity of the Nuclear Research Center, Juelich, 20: 4178 (JUL-284-ST)
VOLKOV, I. D., Engineering and rescue operations at site of atomic strike, 20: 4191 (JPRS-31014)
VOLODIN, V. D., Multiple acceleration system for high energy particle electrodynamic separator, 20: 4496 (JINR-P-2375)
VOLOSOV, V. I., Plasma with relativistic electrons in trap with magnetic mirrors, 20: 4950 (UCRL-Trans-1261(L))
VOLPE, J. J., Study of slightly enriched UO_2 lattice with H : U = 0.42—measurement and analysis, 20: 5071
VON BAEYER, Hans Christian, Analysis of experimental evidence for statistics of elementary particles, 20: 4694
VON ENGEL, A., Theory of double probe at high gas pressure, 20: 4968
VON JASKOWSKY, Woldemar, Ejection of pinched plasma from axial orifice, 20: 4138
VORNHUSEN, H. W., Physical properties of fused fluoride salts, special application to MOSEL reactor concept, 20: 4376 (JUL-268-RG)
VORTMAN, L. J., Craters from a single row of charges buried beneath the craters from parallel rows of charges, 20: 4083 (SC-RR-65-478)
VOTAVA, E., Effect of purity on mechanical properties of niobium, 20: 4425
VOZZELLA, P. A., Thermodynamic properties of uranium monocarbide, 20: 4395 (PWAC-478)
VRIENS, L., Approximate cross sections for optically disallowed excitation of atoms by electrons, 20: 4552
VYAZOVSKAYA, L. M., Extraction of titanium and zirconium from sulfuric acid solutions, 20: 4061

W

WACHTMAN, J. B. Jr., Internal friction in ZrO_2 containing CaO, 20: 3945
WAGNER, Henry N. Jr., Medical applications of low-energy x-ray and gamma radiation sources, 20: 3802 (ORNL-IIC-5, pp 239-42)
WAJIMA, J. Tsunetake, Temperature coefficient of water lattices, 20: 5067
WALDRON-EDWARD, Deirdre, Studies of inhibition of intestinal absorption of radioactive Sr. IV., 20: 3671
WALECKA, J. D., Coupling constants in muon capture, 20: 4915
WALECKA, J. D., Magnetic electron scattering, 20: 4831 (HEPL-272)
WALENTA, Kurt, Hallimondite, a new uranium mineral from Michael mine near Reichenbach (Black Forest, Germany), 20: 4172
WALKER, Alexander, Improvements in or relating to nuclear power plant, 20: 5169
WALKER, R. M., Ion explosion spike mechanism for formation of charged-particle tracks in solids, 20: 4548
WALL, N. S., Elastic scattering of 160-Mev protons from ^{9}Be, ^{40}Ca, ^{58}Ni, ^{120}Sn, and ^{208}Pb, 20: 4906
WALLACE, John M., Eddy fluxes and biennial oscillation in stratosphere, 20: 4150 (NIT-2241-7)
WALLACE, Roger, Three types of 4π neutron spectrometers, 20: 4249 (UCRL-16311)
WALLACE, W. E., Magnetic characteristics of lanthanide elements combined with tin, lead, and indium, 20: 4423
WALLINE, Robert Elm, Intermetallic compounds of lanthanide metals with Ni, Cu, and Ag, 20: 4448
WALRAVE, W. K. A., Equipment for non-destructive examination, 20: 4122
WALTER, R. L., Polarization of neutrons from D(d,n)^{3}He reaction, 20: 4895
WALY, Adnan, Improvements in or relating to radiation detectors, 20: 4258
WANG, J. C., Dynamic performance optimization for numerical control systems, 20: 5220 (UCRL-13185)
WANG, W. N., (n,d) Reaction studies on ^{58}Ni, ^{63}Cu, and ^{64}Zn, 20: 4896
WARBURTON, E. K., Studies of electromagnetic transitions in ^{15}N and ^{18}O, 20: 4905
WARD, G. M., Separation and measurement of ^{137}Cs in precipitation, 20: 4159
WASLEY, Richard J., Quartz pressure transducer package, 20: 4224 (UCRL-14448)
WASSEF, Marguerite A., Reactions of thorium tetrachloride with o-phenanthroline and triphenylphosphine, 20: 3933
WASSERMAN, R., Prog. rpt. on photomultiplier investigation, 5/15–8/14/65, 20: 4218 (NYO-3421-4)
WASSERMAN, R. H., Comparison of intestinal discrimination between ^{47}Ca, ^{85}Sr, and ^{133}Ba, 20: 3669
WATABE, Yoshikazu, Metabolic studies on experimental nephrosis. I., 20: 3666
WATANABE, Masaharu, Alloys of nickel with lithium, barium, and strontium, 20: 4442
WATANABE, T., Standardization of capture of ^{131}I by thyroid in accordance with recommendations of O.I.E.A., 20: 3660 (NP-15528)
WATANABE, Tsutomu, Radiation-induced graft copolymerization of methylmethacrylate on polyethylene in an emulsion system, 20: 3996
WATTS, G. H., Mechanical property evaluation of Be-38% Al alloy from –320 to 800F, 20: 4440
WEBB, C. G., Transfer of radioactive sources, 20: 4208
WEBB, D. M., Launch hazards assessment program, report on Atlas/Centaur abort, 20: 4187 (SC-RR-65-333)
WEBB, S. J., Effect of relative humidity and light on air-dried organisms, 20: 3740
WEBBER, W. R., Physics of interplanetary medium, 20: 4522 (CNIE-PE-5)
WEBSTER, M. S., Antihyperon production in antiproton-proton reactions at 3.7 Bev/c, 20: 4608
WEHRLE, G., Operational monitoring of reactor instrumentation, 20: 5037
WEIDENMUELLER, Hans A., Theory of nuclear reactions. I., 20: 4882
WEINSTEIN, D., Prog. rpt. on yield point occurrence in polycrystalline alpha-Zr, 9/64–8/65, 20: 4374 (IITRI-578-P27-12)
WEINSTEIN, J. H., Thermionic emitter materials research program, 20: 4570 (AD-614592)
WEIR, J. R. Jr., Mechanical properties, 20: 4460 (ORNL-3870, pp 140-5)
WEIRAUCH, W., Isomerism of ^{197}Tl, 20: 4921
WEISNER, L., Symposium of federal ministers for scientific research, Lindau/Bodensee, July 8–10, 1964, 20: 4274
WEISS, E., Prog. rpt. on research into critical heat flux in boiling H_2O, 1–3/65, 20: 4101 (EURAEC-1354)
WEISS, F. J., World outlook for food irradiation, 20: 4271 (WASH-1063)
WELLING, Daniel John, Pion life-time and eight-fold symmetry, 20: 4692
WELLNER, Marcel, Field theory of two-pion system (S and D waves), 20: 4670
WELLS, H., Decontamination procedures for high activity cells at A.E.R.E. Harwell, 20: 4212
WELSH, Marilyn J., CRT plotting routines in use at LRL-Livermore, 20: 4292 (UCRL-14427-T)
WENNINGER, H., Decay of ^{40}K, 20: 4919
WENNINGER, H., Electron capture ratios in decay of ^{202}Tl, 20: 4875
WENZEL, A. W., Spectrophotometric determination of gallium in plutonium–gallium alloy, 20: 3881 (NBL-228)
WERKEMA, G. J., FORTRAN II data reduction program for gas phase radiolysis studies, 20: 3985 (RFP-624)
WERVERS, H. J., Remotely controlled universal milling machine construction and operational experience, 20: 4129
WERY, Michel, Study of excitation curves of (t,α) reaction on ^{16}O between 1 and 3 Mev, 20: 4858
WEST, Harry I. Jr., Trapped electron spectra from Starfish detonation and from outer belt in fall of 1962, 20: 4731 (UCRL-7659-T(Rev.1))
WEST, Harry I. Jr., Trapped electrons produced by Russian high-altitude nuclear detonation of October 28, 1962, 20: 4732 (UCRL-14368-T(Rev.))
WEST, Wilk O., Treatment of bone marrow failure with massive androgen therapy, 20: 3793
WESTERMEIR, James T., Prog. rpt. on PM-1, annual, 11/63–10/64, 20: 5108 (AD-618376)
WESTGARD, James Blake, Properties of the Ξ^-, 20: 4632
WESTLAKE, D. G., Examination by electron microscope of niobium contaminated at high temperature by interstitial elements, 20: 4401 (ANL-Trans-218)
WESTON, L. W., Use of digital computer in time-of-flight experiments, 20: 4245 (ORNL-P-1723)
WEXLER, S., Mass spectrometric investigations of isotopic exchange reactions of gaseous hydrocarbon ions, 20: 3980

WHEATLEY, J. C., Thermal and magnetic properties of liquid ^{3}He at low pressure and at very low temperatures, 20: 4780
WHEATLEY, John C., Properties of ^{3}He at low temperatures, 20: 4773 (COO-1198-306)
WHEELER, J. R., Selective lymphopenia by use of intralymphatic ^{198}Au and splenectomy, 20: 3729
WHICKER, L. R., Improvement in pulse transmission on coaxial transmission lines by reduction of skin effect, 20: 5218 (TID-21991)
WHIPPMAN, M. L., Octet enhancement and reciprocal bootstrap, 20: 4649
WHITE, J. L., Prog. rpt. on advanced, graphite-matrix, dispersion type fuel systems and research on graphite, 11/15/64–2/14/65, 20: 5089 (GA-6181)
WHITE, J. S., Effect of uniaxial compression upon transformation of metastable delta-phase plutonium, 20: 4434
WHITE, R., (56, 56) contribution to nucleon form factors, 20: 4642 (IC/65/78)
WHITE, R. K., Possible artifact in cyclic variations in radiosensitivity, 20: 3766
WHITE, Roderick E., Detection of volatile ^{14}C labeled compounds by modified gas chromatography-ionization chamber technique, 20: 3899
WHITE, W. F., Selective lymphopenia by use of intralymphatic ^{198}Au and splenectomy, 20: 3729
WHITE, William Paul, Nuclear reactor control devices, 20: 5047
WHITEHEAD, Richard W., Effect of hydrocortisone on alkaline phosphatase in cultured cancer cells, 20: 5217 (TID-21169)
WHITEHOUSE, Walter M., Precautions in radiography of female patients, 20: 3858
WICK, E. A., ESH-4 test program. Report on fuel elements irradiated in E-SADE loop of VBWR, 20: 5104 (ACNP-65006)
WIDELL, Bjoern, Method and means for controlling start of homogeneous nuclear reactor, 20: 5084
WIDMER, Thomas F., Releasable coupling mechanism, 20: 5051
WIGHTMAN, A. S., Fields as operator-valued distributions in relativistic quantum theory, 20: 4650
WIKHAMMER, G. A., Further geometrical factors affecting dryout heat flux in vertical, internally heated annuli cooled by steam/water mixtures at 1000 psi, 20: 4099 (AECL-2333)
WIKNER, N. F., Neutron thermalization in graphite. II., 20: 4818
WILHELEM, A., Dismantling workshop for Orgel fuel elements, 20: 4064
WILIP, Elmar K., Ferrimagnetism of Mn_4N and of some mixed crystals of Mn_4N, 20: 4402 (ANL-Trans-230)
WILKES, A., Mutants of parasitic wasp Dahlbominus fuscipennis (ZETT.) (Hymenoptera: eulophidae), 20: 3733
WILKINS, H. C., Study of K^{+} decay probability, 20: 4609
WILLIAMS, B. R. H., Biology of the Solway firth in relation to movement and accumulation of radioactive materials. IV., 20: 3662 (PG-Report-650)
WILLIAMS, D. V. J., 12 Group set of photon cross sections for use in anisotropic S_n calculations of photon transport, 20: 4996 (AWRE-O-79/65)
WILLIAMS, J. D., Thin-film, field-effect devices, 20: 4220 (SC-TM-65-424)
WILLIAMS, John Llewellyn, Improvements in or relating to apparatus for controlling small rates of flow of gases, 20: 4320
WILLIAMS, L. D., Radiological background study of plutonium recycle test reactor site, August–October 1960, 20: 5195 (HW-68082)
WILLIAMS, R. O., Deformation of crystalline solids, 20: 4384 (ORNL-3870, pp 7-14)
WILLIAMSON, G. K., Behavior of fission product gases in uranium dioxide, 20: 4435
WILLS, Stanley Charles Frederick, Improvements in or relating to fueling arrangements for nuclear reactors, 20: 5095
WILSON, D. W., Separation and measurement of ^{137}Cs in precipitation, 20: 4159
WILSON, L. V., Experience with turbine-driven potassium boiler-feed pumps for medium power reactor experiments, 20: 5184 (ORNL-P-1740)
WILSON, M. T., Methods used in United States for transferring materials through radiation barriers, 20: 4043
WILSON, Raphael, Development of atypical secondary disease in x-irradiated germfree mice treated with allogenic and syngenic bone marrow, 20: 3788
WILSON, W., Influence of polynuclear zirconium species on direct titration of zirconium with EDTA, 20: 3893
WILTON, Patricia M., 12 Group set of photon cross sections for use in anisotropic S_n calculations of photon transport, 20: 4996 (AWRE-O-79/65)
WINCH, D. E., Some morphological aspects of geomagnetic secular variation, 20: 4757
WINHOLD, E. J., (n,d) Reaction studies on ^{58}Ni, ^{63}Cu, and ^{64}Zn, 20: 4896
WINSLOW, P. M., Corrosivity of cesium, 20: 4337
WINTERHOFF, D. H., Effect of ^{60}Co γ radiation on respiration of aerobic bacteria, 20: 3699
WIRRIES, H., Determination of Cl and Fe complexing in molten salts, 20: 3959
WISE, JULES, Liquid fluidized bed reactor program, 20: 5125 (NYO-10732)
WISE, W. R. Jr., Explosion containment laws for nuclear reactor vessels, 20: 5034 (NOLTR-63-140)
WITCOFSKI, Richard L., Use of ^{99m}Tc pertechnetate in cardiac scanning, 20: 3831
WITT, Dorothy M., Ultraviolet light inhibition of galactoside permease induction, 20: 3688
WITTING, Thorolf, Scattering of x rays in aqueous solutions of sodium caprylate, 20: 4483
WOLF, Richard A., Neutron stars. I., 20: 4531
WOLF, Richard A., Neutron stars. II., 20: 4532
WOLFGANG, Richard, Hot atom chemistry, 20: 4039
WOLFRAM, T., Infrared spectrum and vibrational analysis of dibromoborane and dibromoborane-d, 20: 3940
WOLSCHRIJN, R. A., Preliminary experiment on radial distribution of ^{137}Cs, $^{89,90}Sr$, and ^{95}Zr in sintered uranium dioxide pellet, 20: 4472
WOOD, Constance A. P., Treatment of malignant disease of face and jaws by radiation, 20: 3813
WOODLEY, Robert G., Thermoluminescence induced by low energy alpha particles, 20: 3983 (BNL-9589)
WOODS, L. C., Density waves in low-pressure plasma columns, 20: 4972
WOODS, William John, Nuclear reactor, 20: 5080
WOODWELL, G. M., Water budget of a forest damaged by ionizing radiation, 20: 3653 (BNL-8466)
WORK, Richard N., Photographic storage of pulse-height information in scintillation experiments, 20: 4253
WORLTON, Daniel C., Ultrasonic inspection method for inaccessible pipe and tubing, 20: 5227
WOTKE, H., Operating experience with Seibersdorf inhomogeneous sector field isotope separator, 20: 4283 (SGAE-PH-27/1965)
WRIGHT, R. R., Semiconductor pressure transducers, 20: 5216 (SC-TM-65-457)
WUERDINGER, H., Dosage problems of radioiodide treatment of thyroid gland disorders, 20: 3853
WYMER, R. G., Preparation, coating, evaluation, and irradiation testing of sol-gel oxide microspheres, 20: 4344 (ORNL-P-1725)
WYNNE, Griffith G., Stomach cancer and soil, 20: 4197

Y

YAJIMA, S., Mechanism of pyrolytic graphite formation, 20: 4348
YAJIMA, S., Microstructure and density of pyrolytic graphite, 20: 4431
YAKEL, H. L., X-ray diffraction, 20: 4391 (ORNL-3870, pp 75-82)
YAKOVENKO, V. M., Theory of emission of charge passing through electrically inhomogeneous medium, 20: 4625
YAM, Y. Y., Calculations of neutron-deuteron scattering, 20: 4614
YAMADA, Shusaku, Generalized analysis of rossi-α experiment, 20: 5070
YAMAMOTO, Akira, Genetically significant radiation dose from dental x-ray diagnosis. II., 20: 4196
YAMAMOTO, Kazuko, Temperature coefficient of water lattices, 20: 5067
YAMAMOTO, Kenzo, Impedance formula for partially ionized, collision-dominated plasma, 20: 4975
YAMAOKA, Y., Determination of radioactive fallout from nuclear weapon tests. Detection and determination of radioactive nuclides in rain water, 20: 4177 (JAERI-1083)
YAMZIN, I. I., Effects of particle size on extinction of neutron diffraction, 20: 5016
YANOOSH, I. M., Comparative study of result of radiation after-effects on chromosomal non-divergence, 20: 3715 (JPRS-31514, pp 59-64)
YANOOSH, I. M., Induced mutation process—effect of high temperature after irradiation on the frequency of occurrence of lethal mutations and chromosomal breaks, 20: 3713 (JPRS-31514, pp 29-43)
YASHIN, N. M., Effect of helical field on ohmic heating of plasma in S-1 apparatus, 20: 4937 (IAE-907)
YATSENKO, A. I., Investigation of cerium distribution in cast iron by means of electron probe, 20: 4414
YAVIN, A. I., $(^{3}He,\alpha)$ Pickup reactions in ^{58}Ni and ^{60}Ni, 20: 4892
YEARIAN, M. R., Experimental evidence for possible meson-exchange contribution to elastic electron-deuteron scattering, 20: 4580 (AD-618662)
YEE, W., Recovery of strontium values from sulfate-containing waste solutions, 20: 5210
YIH, Chia-Shun, Large-amplitude magnetohydrodynamics, 20: 4718
YOFFEY, J. M., Regeneration of bone marrow, 20: 3789
YOSHIKAWA, S., Optimum generation of ion-cyclotron waves in cylindrical two-ion plasma, 20: 4984
YOSHINAGA, Haruma, Radiation dose received by mother and fetus x-ray examination, 20: 3823
YOSHIZAKI, Tsutae, Protection mechanisms of non-malignant and malignant cell against ionizing radiation. II., 20: 3796
YOUNG, George A., Physics of base surge, 20: 4141 (AD-618733)
YOUNG, H. C., Experience with turbine-driven potassium boiler-feed pumps for medium power reactor experiments, 20: 5184 (ORNL-P-1740)
YOUNG, J. A., Prog. rpt. on integral neutron thermalization, 4–6/65, 20: 4801 (GA-6634)
YOUNG, J. C., Prog. rpt. on integral neutron thermalization, 4–6/65,

20: 4801 (GA-6634)
YOUNG, James A., Neutron thermalization in graphite. II., 20: 4818
YOUNG, W. A., Least square determination of diffusion coefficients of gases in spherical solids, 20: 4377 (NAA-SR-Memo-10741)
YUST, C. S., Physical ceramic studies, 20: 4387 (ORNL-3870, pp 38-43)
YVON, Jacques, Property of correlation in plasma during equilibrium, 20: 4959

Z

ZACK, J. F. Jr., Radiation-induced electronic phenomena in polyethylene, 20: 4035
ZACKAY, V. F., Structure and high strength metals, 20: 4399 (UCRL-16301)
ZAGORITES, H. A., Influence of temperature on radiation-induced surface effects in transistors, 20: 4261 (AD-623078)
ZAGORODNIKOV, S. P., Structure of front of strong magneto-sonic wave in rarefied plasma, 20: 4938 (IAE-909)
ZAITSEV, L. N., Passage of high energy neutrons in iron–aqueous mixtures, 20: 4998 (JINR-P-2359)
ZAITSEV, V. I., Multiple acceleration system for high energy particle electrodynamic separator, 20: 4496 (JINR-P-2375)
ZAITSEVA, N. G., New Isotope, ^{174}W, 20: 4834 (JINR-E-2360)
ZAJDE, C., Utilization of semiconductor detectors with high-energy accelerator. I and II., 20: 4243 (LAL-1102)
ZAKHAR'EV, B. N., Correctness of method for unified theory of nuclear reactions, 20: 4837 (JINR-P-2310)
ZAKHAROV, I. A., Comparative study of mutagenic action of different types of radiation and ethyleneimine on alga chlorella, 20: 3716 (JPRS-31514, pp 65-76)
ZAMIRALOV, V. S., Electromagnetic properties of mesons in broken symmetry, 20: 4644 (JINR-P-2299)
ZANDER, Arlen R., Gamma decay of ^{102}Tc and ^{104}Tc, 20: 4883
ZANDER, K., Influence of nuclear radiation on electrical properties of semiconductor parts, 20: 4265
ZANDER, K., Requirements on nuclear electronics, 20: 4225
ZARETSKII, D. F., Spontaneous fission of nuclei, 20: 4876
ZASTAVENKO, L. G., Correctness of method for unified theory of nuclear reactions, 20: 4837 (JINR-P-2310)
ZEC, Ursula, Gamma radiation sources at Rudjer Boskovic Institute. I., 20: 4090 (JPRS-32842)
ZELDOVICH, A. G., Expansion mechanism of 40 cm hydrogen bubble chamber of JINR, 20: 4257
ZELDOVICH, A. G., Large laboratory hydrogen liquefier VO 2 for use with large liquid hydrogen bubble chambers, 20: 4797
ZEL'VENSKII, Ya. D., Thiophene ^{35}S, 20: 3976
ZETTL, Sandra Massey, Rotating disk study of dissolution of zirconium in $HF–H_2SO_4$, 20: 4055
ZHAROVSKII, F. G., Extraction of titanium and zirconium from sulfuric acid solutions, 20: 4061
ZHELEV, Zh., Positron decay of ^{145}Eu, 20: 4838 (JINR-P-2314)
ZHUSUPOV, M. A., Sensitivity of some nuclear characteristics to intermediate coupling parameters, 20: 4835 (JINR-P-2287)
ZIEGLER, C. A., Generation and practical use of monoenergetic x rays from alpha-emitting isotopes, 20: 4268 (ORNL-IIC-5, pp 353-73)
ZIFFER, Herman, Vibrational spectra and potential function for SnH_4 and SnD_4, 20: 3942
ZIMMERMANN, Bodo, Study of complex and covalent iron compounds using ^{57}Fe Moessbauer effect, 20: 3927 (AERE-Trans-1026)
ZIMMERMANN, H. J., Prog. rpt., 3–5/65, 20: 4478 (TID-22179)
ZUBELDIA, J. M., Problems of supply of electrical energy in Spain, 20: 4081
ZUMWALT, L. R., Prog. rpt. on advanced, graphite-matrix, dispersion type fuel systems and research on graphite, 11/15/64–2/14/65, 20: 5089 (GA-6181)
ZURMUEHLE, Robert W., Levels in ^{57}Ni from $^{58}Ni(^3He,\alpha)^{57}Ni$ reaction, 20: 4912

SUBJECT INDEX

Main entries in this index are generally specific materials, things, and processes. These are followed by modifiers that describe the properties of, and processes applied to, the main entries.

The number preceding the colon is the *NSA* volume number, and the number following is the abstract number. The designation (R) following the abstract number indicates that the abstract is of a progress report; (P) indicates a patent; and (T) indicates a translation. Abstracts for reports other than progress reports carry no letter designation. References to report numbers, where appropriate, are included after the abstract number of the citation. Published literature (journal article or book) is identifiable by the absence of a report number.

The user should bear in mind that the ideas presented in the original literature, rather than key words, have been indexed. The indexers have tried to select what seemed the most probable and logical place to look for typical information. Since it is not possible to anticipate where a user would look for information, numerous cross references are included in cumulative indexes to assist him in his search.

Experience in using an index of this type will be the best guide in obtaining the desired information, and a consideration of synonymous or closely related terms will prove valuable.

Information must be so indexed as to be of the greatest use to the greatest number of users. This requires that a topic be indexed to headings that most specifically describe it and not ordinarily to the headings that describe its ultimate use, nor to the general class headings that include the specific headings. For example, information on the treatment of thyroid disease with I-131 would be indexed under Thyroid Gland and under Iodine Isotopes I-131, but not necessarily under Radiotherapy. A study of the effects of x radiation on hair would be indexed under both X Radiation and Hair. However, the information would not be indexed under the experimental animal, e.g., Rats, unless the report discusses the effects on rat hair as compared with the effect on the hair of other animals.

The broad, general class headings are used only for general information or for comprehensive reports or articles.

Subject Heading Styles

Generally, the direct form of subject entry is used rather than inverted headings, e.g., Amino Acids rather than Acids, Amino; Helium Isotopes He-4 rather than Helium—isotopes He-4 or Helium—He-4 isotopes. Note, however, that in some cases parenthetic modifying terms or inverted headings of the form Neutrons, Fast are used in preference to a direct entry that would result in the scattering of information. Organic compounds are usually entered in the index in the inverted form so that substituted compounds can be listed near the parent compound; e.g., Benzene, Bromo- rather than Bromobenzene. In general, the style of nomenclature used is that of Chemical Abstracts, except that some items listed in that publication as subheadings are elevated to form part of the main heading; e.g., Butyric Acid, Methyl Ester rather than Butyric Acid—methyl ester.

Alphabetization

Main headings are alphabetized word-by-word. A parenthetic qualifier following a main heading is disregarded in alphabetizing unless there are two or more headings identical except for the parenthetic qualifier, in which case the qualifier determines the order. Headings involving Greek letters are arranged as if the names of the letters were spelled out.

Examples:

M-Capture
  see Electron Capture
Magnesium
Magnesium Alloys
Manganese Fluorides
Manganese(II) Fluorides
Mesons
Mesons (π)
Mesons (ρ)
3-Pentanol, 2,4-Dimethyl-
2-Pentanol, 2-Methyl-
2-Pentanol, 4-Methyl-

Nomenclature of Inorganic Compounds

Inorganic compounds are indexed in the direct form, listing cations in the order of increasing valence in the case of polycationic salts of varying valence and in alphabetic order for polycationic salts in which all cations have the same valence; e.g., Sodium Aluminum Silicates and Potassium Sodium Sulfates.

Multicomponent Alloys and Other Systems

Multicomponent alloys, except well-known trade names are indexed under a main heading in the form "element alloy" for each element in the alloy. The modifier begins with element symbols for each component arranged alphabetically as if the English name for the element were spelled out.

Example: Copper-Gold Alloy is indexed
  Copper Alloys
    Cu-Au...
  Gold Alloys
    Cu-Au...

Well-known alloys such as Zircaloy-2 are indexed directly to the trade name; cross references referring from each component of the alloy to the entry for the trade name appear in cumulative indexes.

Multicomponent systems of non-metallic elements are indexed in a manner similar to alloys except the main heading used contains the word "Systems" in place of "Alloys."

Example: Silicon–Tungsten Systems are indexed
  Silicon Systems
    Si-W...
  Tungsten Systems
    Si-W...

Multicompound systems and mixtures of compounds are indexed under the main heading for each component com-

pound; the modifiers begin with an alphabetical listing of compound formulas.

Example: Lead Titanate–Lead Zirconate is indexed
Lead Titanates
$PbTiO_3$-$PbZrO_3$...
Lead Zirconates
$PbTiO_3$-$PbZrO_3$...

A mixed system of compounds and elements is indexed using a combined form of the above conventions, e.g., a dispersion of copper and alumina would be indexed

Aluminum Oxides
Al_2O_3-Cu...
Copper Systems
Al_2O_3-Cu..

Physical States and Configurations of Materials

Specification of the physical state, if other than normal, or geometric configuration of the material is included in the modifying phrase, i.e., liquid metals would be indexed to the metal with "liquid" in the modifier, and carbon crucibles would be indexed to Carbon with "crucibles" appropriately placed in the modifier and also to Crucibles if appropriate.

Modifying Phrases

The modifiers appearing under a main heading are written specifically to describe the relation of the item being indexed to that main heading. The modifier, therefore, will generally contain more useful information about that relation than will a title or a phrase written to be used under every main heading assigned to the item. Effort is exerted to begin the modifier with the word judged to be of greatest use to the greatest number of users; this, however, does not obviate the need to consider all modifiers under the main heading(s) of interest.

Modifiers are usually intended to form a meaningful phrase when combined with the main heading. Some are intended to be read following the main heading, e.g., the entry Hydrogen—sorption by charcoal is read "hydrogen sorption by charcoal"; however, as a result of placing the important word first, many modifiers must be arranged for smooth reading, e.g., Formaldehyde—yields in radiolysis of ethyl ether, effects of deuterium on is read "effects of deuterium on formaldehyde yields in radiolysis of ethyl ether" and Uranium—crystal structure of, effect of cooling rate on allotropic transformations in is read "effect of cooling rate on allotropic transformations in crystal structure of uranium." Prepositions are sometimes omitted if no ambiguity results.

Special characters are added to modifiers in the field of physics; if the modifier does not establish the experimental or theoretical character of a reference, a symbol (E), (T), or (E/T) is placed immediately after the modifying phrase and before the journal reference number. The value of this identification has been established by the American Institute of Physics.

A

ABDOMEN
radiosensitivity of, in man, 20: 3851
ABSORPTION SPECTRA
radiation effects on uv, in aqueous solutions of serum albumin, γ, 20: 3687
ABSTRACTS
on pulsed neutron facilities, 20: 5200 (TID-3571(Suppl.1))
on shell deformation, stability, and vibration, 20: 4079 (UCRL-13187)
ACCELERATORS
beam deflectors for, analysis of eccentric hole, (T), 20: 4492 (BNL-9640)
beam instabilities in, review of relativistic, 20: 4513 (UCRL-16440)
beam stability in, effects of resistive walls on, 20: 4501 (LNF-65/34)
beam transverse resistive wall instability in, electron and positron, (T), 20: 4500 (LNF-65/27)
cavity resonators for, design of, 20: 4511 (UCRL-16242)
control circuitry of, guide for designing, 20: 4510 (UCRL-16016)
design and performance of Frascati Adone, 20: 4499 (LNF-65/26)
design and performance of electron, 20: 4518
design evolution of SL 75, for radiotherapy, 20: 4517
radiation dosimetry around, methods for high-energy, 20: 4505 (ORNL-P-1738)
radiation monitoring and shielding of, 20: 4514 (UCRL-16445)
shielding of, development of cement-iron mixtures for, 20: 4998 (JINR-P-2359)
ACCIDENTS
assessment of launch hazards of Atlas-Centaur abort, 20: 4187 (SC-RR-65-333)
fission product release in reactor, model of, 20: 4183(R) (ORNL-3843, pp 2-70)
reactor, facility for analyzing primary-cooling-system, (E), 20: 5023(R) (IITRI-578P21-15)
review of AEC, 1943 through 1964, 20: 4188 (TID-22268)
ACETAMIDE
reactions with carbon atom, recoil, 20: 4026
ACETAMIDE, N-METHYL-
yields in reaction of recoil carbon atoms with acetamide, 20: 4026
ACETIC ACID
hypersonic and ultrasonic velocities in, effects of relaxation on, 20: 4479(R) (TID-22179, pp 1-83)
ACETIC ACID, (ETHYLENEDIAMINE)TETRA-
analytical use in determination of zirconium, 20: 3893
ACETONE
hypersonic and ultrasonic velocities in, effects of relaxation on, 20: 4479(R) (TID-22179, pp 1-83)
yields in reaction of recoil carbon atoms with acetamide, 20: 4026
ACETONITRILE
molecular dipole moments of deuterated and normal, 20: 3958
radioinduced production of, G-values and mechanisms of, 20: 3982(R) (AGN-8156)
yields in reaction of recoil carbon atoms with acetamide, 20: 4026
CH_3CN–HCN, radioinduced reactions of, G-values and mechanisms of, 20: 3982(R) (AGN-8156)
ACETYLENE
dipole moments of, effects of deuterium substitution on, 20: 3977
ACIDS
content in smoke from irradiated cigarettes, 20: 3984 (ORO-633)
ACOUSTIC WAVES
amplification and production in plasma, 20: 4479(R) (TID-22179, pp 1-83)
ACRYLONITRILES
radioinduced polymerization of, at 26 and –78°C, effects of solid additives on, 20: 4007
acrylonitrile–styrene, radioinduced graft copolymerization with chloroethylene, 20: 4038
ACTINIUM ISOTOPES Ac-227
separation from waste solution by cation exchange, 20: 3879(R) (MLM-1266)
ACTIVATION ANALYSIS
development, 20: 3863(R) (IS-1200(Sect. C))
methods of, use of reactors in, 20: 3864 (AERE-L-166)
sensitivity of neutron, interferences in, 20: 3900
sensitivity of, estimation of upper limits of, 20: 3898
ACTIVATION DETECTORS
data from, calculation of differential fast-neutron spectra from, 20: 4256
ADENOSINEPHOSPHORIC ACIDS
radiation effects on synthesis of, in *E. coli*, uv, 20: 3726
ADHESIVES
development for use in space vehicles, 20: 4312
AERODYNAMICS
materials development for use in, 20: 4312
AEROSOLS
composition of, from reactor accidents, 20: 4183(R) (ORNL-3843, pp 2-70)
filtration of, diffusion board for, 20: 4097(P)
metabolism in human body of radioactive, apparatus for determining, 20: 4202
particle distribution according to size, diffusion method for determination of, 20: 4733(T) (AI-Trans-201)
production and properties of simulated reactor-accident, 20: 4086(R) (ORNL-3843, pp 137-67)
sampling of fuel-meltdown, performance of diffusion tubes for, 20: 4185(R) (ORNL-3843, pp 169-234)
use in reactor filter efficiency measurements, 20: 5036 (RL-SA-47)
AGE
effects on visual discrimination in irradiated and nonirradiated monkeys, 20: 3721
AGE ESTIMATION
carbon-14 methods of, sources of error in, 20: 4147
feldspar and zircon, northeastern Minnesota, 20: 4169
AGING
effects on fission products from reactor loss-of-coolant accidents, 20: 4183(R) (ORNL-3843, pp 2-70)
effects on incidence of chromosome aberrations in mouse liver, 20: 3711(R) (NYO-3314-2)
AGRICULTURE
nuclear techniques for studies of, development of, 20: 3710(R) (EUR-2493.e)
strontium-90 uptake by plants, effects of species, soil type, and agronomy practices on, 20: 3679
AIR
corrosive effects on yttrium at 1100°C, 20: 4334
gamma dose rates in, single-scattering approximation to, (T), 20: 5181(R) (ORNL-3029)
heat transfer by, in vortex flow, 20: 4999(R) (ORNL-2599)
neutron reactions with, gamma dose rate from, 20: 4999(R) (ORNL-2599)
radiation effects on electric conductivity of, 20: 4949(R) (UCRL-14360, pp 85-94)
reactions with uranium, kinetics of, 20: 4329(T) (CEA-tr-R-1868)
air–^{4}He, vapor pressure at 77°K, 20: 3879(R) (MLM-1266)
air–steam, iodine sorption from, by charcoal, 20: 4086(R) (ORNL-3843, pp 137-67)
AIRCRAFT
range indicating system for, design of, 20: 5225(P)
AIRCRAFT SHIELD TEST REACTOR
gamma dose rates from, 20: 4999(R) (ORNL-2599)
neutron fluxes and dose rates from, 20: 4999(R) (ORNL-2599)
ALASKA
sodium-22 content in natives of, 20: 4161
sodium-22 content in food from, 20: 4161
ALBUMINS
binding of calcium-47 and strontium-85 by blood serum, 20: 3697
physiological reaction to subarachnoid injection of iodine-131-labeled human serum, 20: 3843
radiation effects on content in rabbit blood, x, 20: 3709 (CEA-R-2865)
radiation effects on serum, γ, 20: 3687
ALCOHOLS
solvent properties for titanium and zirconium, 20: 4061
ALDEHYDES
molecular structure of propyl carbox-, 20: 3863(R) (IS-1200(Sect. C))
ALGAE
effects of ethyleneimine on Chlorella, genetic, 20: 3716(T) (JPRS-31514, pp 65-76)
growth of, effects of wavelength of light on, 20: 3769
niobium-95 content of, in Solway Firth, 20: 3662 (PG-Report-650)
radiation effects on cyclosis in Nitella, recovery from x, 20: 3698
radiation effects on Chlorella, genetic, x, 20: 3716(T) (JPRS-31514, pp 65-70)
radiation effects on Chlorella, genetic, uv, 20: 3716(T) (JPRS-31514, pp 65-76)
ruthenium-106 content of, in Solway Firth, 20: 3662 (PG-Report-650)
zirconium-95 content of, in Solway Firth, 20: 3662 (PG-Report-650)
ALGINATES
sodium, effects on calcium-45 and strontium-89 uptake by rat bones, 20: 3671
ALKALI METAL BORATES
radiation effects on, ESR studies of, 20: 5019
ALKALI METAL HALIDES
book: *Radiation Physics. III. Ionic Crystals*, 20: 4008
color center luminescence in, effects of pressure on, (E/T), 20: 4476(R) (IS-1200(Sect.P))
electron energy losses in, characteristic, (T), 20: 5015
ALKALINE EARTH HALIDES
vapor pressure, 20: 4297(R) (IS-1200(Sect.M))
ALKANES
reactions of gaseous, with recoil tritium atoms, 20: 4024

ALLOYS
development for use in space vehicles, 20: 4312
superconducting critical currents of, method for increasing, 20: 4799(P)
superconductivity theory for, review of, (T), 20: 4791
tensile properties of, review on, 20: 4399 (UCRL-16301)
ALPHA BEAMS
effects on lead diffusion in silver, 20: 4385(R) (ORNL-3870, pp 15-19)
ALPHA PARTICLES
clustering in lanthanum-139, (T), 20: 4886
effects of, from deposited Thorotrast, carcinogenic, 20: 3722
effects on thermoluminescence of calcium carbonates and fluorides at low energies, 20: 3983 (BNL-9589)
energy distribution from neutron reactions (n,α) with lithium-6, 20: 5181(R) (ORNL-3029)
energy spectra of, from beryllium-8 decay, (E), 20: 4869
interactions with deuterons at 29.3 and 41.6 Mev, deuteron breakup from, (E), 20: 4596
reactions (α,n) with oxygen-17 and oxygen-18 at 5 to 12 Mev, cross sections for, (E), 20: 4849(R) (UCRL-14360, pp 1-50)
reactions (α,n) with nuclei, performance as neutron source, (E), 20: 4802 (IDO-17115)
reactions (α,n) with potassium-41, isomeric cross section ratios for, 20: 4922
reactions (α, 4n) with gold-197 at 49 Mev, thallium-197 isomer from, (E), 20: 4921
reactions with nuclei, angular momentum transfer, cross sections, and level studies from, 20: 4823(R) (ANL-7081, pp 36-69)
scattering by nuclei, angular distributions and excitation from, 20: 4824(R) (ANL-7081, pp 70-7)
scattering by oxygen-18 at 21.4, inelastic, (E), 20: 4849(R) (UCRL-14360, pp 1-50)
scattering on light nuclei at 28.5 Mev, optical potentials in elastic, (E/T), 20: 4859
use in thickness measurement, 20: 3982(R) (AGN-8156)
ALPHA SOURCES
preparation for spectrometric analysis, 20: 3879(R) (MLM-1266)
x-ray emission by, monoenergetic, 20: 4268 (ORNL-IIC-5, pp 353-73)
ALPHA SPECTROMETERS
use in diffusion measurements on alpha emitters, 20: 4412
ALUMINUM
analysis for oxygen, methods for, 20: 3878 (LYCEN-6524)
bremsstrahlung reactions (γ,π^0) at 166 Mev, angular distributions from, (E), 20: 4898
bremsstrahlung yields from, with incorporated strontium-90–yttrium-90, 20: 5000 (ORNL-IIC-5, pp 91-8)
dissolution using sodium hydroxide, flowsheet for, 20: 4048(R) (NP-15406)
effects on copper oxidation, 20: 4320(R) (ORNL-3870, pp 70-4)
effects on phase transformation of delta–plutonium, 20: 4434
electron energy losses in, characteristic, (T), 20: 5015
fatigue of, effects of notches and stress on, 20: 4297(R) (IS-1200 (Sect.M))
fiber textures, effects of deformation bands on formation of, 20: 4389(R) (ORNL-3870, pp 61-4)
fission fragment ranges in, 20: 3982(R) (AGN-8156)
gamma reactions at 0.01 to 10 Mev, cross sections for, 20: 4996 (AWRE-O-79/65)
grain boundary migration in, effects of copper impurities on, 20: 4389(R) (ORNL-3870, pp 61-4)
heat of fusion, 20: 4297(R) (IS-1200(Sect.M))
magnetic resonance shifts at 4.2 to 450°K, (E), 20: 4476(R) (IS-1200 (Sect.P))
meson (μ^-) transitions in mesic atoms of, energy of, 20: 4825(R) (ANL-7081, pp 81-93)
neutron cross sections for, 20: 4830 (GEMP-384)
nuclear magnetic resonance in rapidly rotating, (E), 20: 4931
separation from silver by partition chromatography, 20: 4054
tensile tests on, computer analyses of, 20: 4371 (EUR-2514.e)
thickness measurement by alpha energy degradation, 20: 3982(R) (AGN-8156)
use of promethium-147-excited, as source in x-ray fluorescence analysis, 20: 3883 (ORNL-IIC-5, pp 154-81)
ALUMINUM ALLOYS
deposition on niobium and niobium alloys for oxidation protection, 20: 4356(P)
deposition on niobium–titanium alloy for oxidation protection, 20: 4315(P)
radiation effects of mechanical properties of type 6061, neutron, 20: 4460(R) (ORNL-3870, pp 140-5)
sorptive properties of types 1199 and 6061, for hydrogen from water, 20: 4342(R) (ORNL-3870, pp 85-101)
tensile tests on, computer analyses of, 20: 4371 (EUR-2514.e)
Al–Be, mechanical properties at −320 to 800°F, 20: 4440
Al–Co–Fe–Ti–V, properties of aged, 20: 4360(R) (AD-619399)
Al–Cr–Co–Mo–Ni–Ti, corrosion of Udimet 500 by lithium fluoride in cyclic high-temperature environment, 20: 4326 (TRW-ER-6561)
Al–Cr–Ge–Ti–V, properties of aged, 20: 4360(R) (AD-619399)
Al–Cr–Ti–V, properties of aged, 20: 4360(R) (AD-619399)
Al–Fe, electric conductivity, 20: 4297(R) (IS-1200(Sect.M))
Al–Fe, plasticity of, effects of composition and temperature on, 20: 4297(R) (IS-1200(Sect.M))
Al–Fe–Mo–Ti–V, properties of aged, 20: 4360(R) (AD-619399)
Al–Fe–Ti–V, properties of aged, 20: 4360(R) (AD-619399)
Al–Gd, phase diagram, 20: 4427
Al–Mg, dissolution using sulfuric acid, flowsheets for, 20: 4048(R) (NP-15406)
Al–Mg, solvent properties for rare earth elements in molten chloride salts, 20: 3865 (ANL-7064)
Al–Mn–Ti–V, properties of aged, 20: 4360(R) (AD-619399)
Al–Nb, properties as coating for refractory metals, 20: 4418
Al–Nb–Ti–W–V–Zr, properties for use to 1200°F, 20: 4393 (PWAC-472)
Al–Nd, phase diagram, 20: 4427
Al–Sn, deposition on niobium for oxidation protection, 20: 4355(P)
Al–Sn, deposition on niobium and niobium alloys for oxidation protection, 20: 4357(P)
Al–Ta, mechanical properties of dispersions of, 20: 5174(R) (ORNL-3870, pp 214-29)
Al–Ta, properties as coating for refractory metals, 20: 4418
Al–Ti–V, corrosion by cesium at 400°C, 20: 4337
Al–Ti–W–V–Zr, properties for use to 1200°F, 20: 4393 (PWAC-472)
Al–U, preparation of intermetallic compound UAl_3, 20: 4342(R) (ORNL-3870, pp 85-101)
Al–U, thermal expansion of intermetallic compound UAl_3 at 20 to 750°C, 20: 4436
Al–U, uses as sintering aid for uranium mononitride, 20: 4342(R) (ORNL-3870, pp 85-101)
Al–Y, corrosion by water at 200°C, effects of yttrium content on, 20: 4320(R) (ORNL-3870, pp 70-4)
Al–Y, crystal structure of beta-phase, 20: 4297(R) (IS-1200(Sect.M))
Nb–Zr, creep properties, effects of cold working and annealing on, 20: 4301(R) (ORNL-3870, pp 102-35)
ALUMINUM CHLORIDES
$AlCl_3$–Bi–NaCl, spectra of reaction products of, absorption, 20: 3921(R) (ORNL-3870, pp 56-60)
$AlCl_3$–NaCl, density equations for molten, 20: 3921(R) (ORNL-3870, pp 56-60)
ALUMINUM ISOTOPES Al-26
beta transitions in, comparative half lives of $\Delta I = 3$, (T), 20: 4874
ALUMINUM ISOTOPES Al-27
neutron inelastic scattering at 14.2 Mev, differential cross sections for, (E), 20: 4891
ALUMINUM NITRATES
$Al(NO_3)_3$–HNO_3, separation of thorium from, by solvent extraction using TBP, 20: 4060
ALUMINUM OXIDES
cadmium, cerium, cobalt, neptunium, uranium, and zinc distribution between molten chloride and gamma-, 20: 3959
corrosion by cesium at 400°C, 20: 4337
diffusion of rare gases in, 20: 3944
effects on creep rate in thoria, 20: 4387(R) (ORNL-3870, pp 38-43)
electric conductivity at high pressures, 20: 4708(R) (UCRL-14360, pp 50-73)
properties as barrier shell for thermionic energy converters, (E), 20: 4359(R) (AD-618923)
properties as coating for refractory metals, 20: 4418
radiation effects on electrostatic charge in colloids of, x, 20: 4015
Al_2O_3–BeO–MgO, radiation effects on, in-pile, (E), 20: 5115(R) (GA-4967)
Al_2O_3–Dy_2O_3, radiation effects on, in-pile, (E), 20: 5115(R) (GA-4967)
ALUMINUM SYSTEMS
Al–Cr–Si–Ti–V, properties of aged, 20: 4360(R) (AD-619399)
Al–C–Ti, properties for use to 1200°F, 20: 4393 (PWAC-472)
Al–C–Ti, properties for use to 1200°F, 20: 4393 (PWAC-472)
Al–Eu_2O_3, radioinduced swelling of dispersions of, fast and thermal neutron, 20: 5174(R) (ORNL-3870, pp 214-29)
ALUMINUM, TRIPHENYL-
crystal structure, 20: 3863(R) (IS-1200(Sect. C))
AMERICIUM ISOTOPES Am-241
separation from other transplutonium elements, design of hot cells for, 20: 4065
AMERICIUM ISOTOPES Am-243
separation from other transplutonium elements, design of hot cells for, 20: 4065
AMERICIUM OXIDES
preparation of microspheres of, by sol-gel process, 20: 4344 (ORNL-P-1725)

AMES RESEARCH REACTOR
development and operation, July 1964 to June 1965, 20: 5196(R) (IS-1200(Sect.E))
AMIDE POLYMERS
radioinduced crosslinking, 20: 4031
AMINES
effects on methyl iodide retention by charcoal, 20: 4185(R) (ORNL-3843, pp 169-234)
3,9-diethyltridecyl-6-, preparation of, 20: 3974 (ORNL-TM-1314)
AMINO ACIDS
labeling with tritium, 20: 3978
radiation effects on, in cattle insulin, 20: 4016
radiation effects on serum albumin, γ, 20: 3687
storage of tritium-labeled, 20: 3978
AMMONIA
production by nuclear heat, economics and method for, 20: 3916 (CONF-650902-20)
radiolysis of gaseous, effects of propylene and rare gases on kinetics of, 20: 4021
ammonia–benzene, radioinduced reactions, 20: 3982(R) (AGN-8156)
AMMONIUM COMPOUNDS, QUATERNARY
solvent properties for plutonium, 20: 4048(R) (NP-15406)
AMMONIUM FLUOTECHNETATES
crystallography, 20: 4391(R) (ORNL-3870, pp 75-82)
AMMONIUM HYDROXIDES
preparation of tetrabutyl, 20: 3863(R) (IS-1200(Sect. C))
AMMONIUM URANATES
use in preparation of uranium(VI) oxides, 20: 3971(P)
AMMONIUM URANYL NITRATES
preparation and thermal decomposition, 20: 4052
AMMONIUM VANADATES
analytical use in determination of uranium IV by titration, 20: 3903
AMPHIBIANS
radiation effects on development of, bibliography, 20: 3773
AMPLIFIERS
design and performance of logarithmic, for field uses, 20: 4221 (UCRL-12394-T)
design for semiconductor detectors, 20: 4243 (LAL-1102)
AMYLASES
radiation effects on production in Aspergillus of, uv, 20: 3755(T)
AMYLOSES
crystal structure of potassium acetate complexes of, 20: 3863(R) (IS-1200(Sect. C))
ANEMIA
bone marrow failure induced by, treatment with massive androgen therapy, 20: 3793
in radiation sickness, etiology of, 20: 3658(R) (EUR-2414.f,i)
radioinduced, etiology in man, 20: 3851
ANILINE
separation of nitro-substituted, by reversed-phase chromatography, 20: 3863(R) (IS-1200(Sect. C))
ANIMAL CELLS
cerium-144 distribution in rat liver, following intravenous injection, model for, 20: 3682
effects of 2-mercaptoethylamine and antitumor drugs on tumor cells in culture, morphological, 20: 3796
radiation effects on, review of, 20: 4464
radiation effects on tritiated-thymidine metabolism in Yoshida ascites sarcoma, 20: 3702
radiation effects on mitosis in, 20: 3764
radiation injuries in cultured, protective effects of inosine against, γ, 20: 3791
radiosensitivity of, in tissue culture, γ, 20: 3737
radiosensitivity of mouse tumor, effects of anoxia induced by transplantation on, 20: 3750
ANIMAL RESPIRATION
measurement using nuclear image amplifier with technetium-99m and xenon-133, 20: 3802 (ORNL-IIC-5, pp 239-42)
ANIMALS
metabolism in, tracer studies, 20: 3685
radiation effects on hypothalamus pituitary system in normal and hibernating, 20: 3703
radiation effects on, bibliography, 20: 3773
ANOXIA
radiosensitivity effects of, in transplanted tumors cells in mice, 20: 3750
ANTENNAS
tracking, technique for positioning, 20: 5215 (SC-TM-65-448)
ANTHRAQUINONE, 1,8-DIHYDROXY-
analytical use for determination of boron, 20: 3892
ANTIBODIES
formation in mice injected with virus-induced leukemia, 20: 3694
production in rabbits of, role of appendix and liver in, 20: 3746
radiation effects on formation of, in rabbits, 20: 3689
radiation effects on production in rabbits, x, 20: 3738
ANTIFERROMAGNETIC MATERIALS
energy levels and spectra of, effects of spin wave interactions on, (E/T), 20: 4476(R) (IS-1200(Sect.P))
neutron inelastic magnetic scattering by, cross section of slow, (T), 20: 4809
properties of chromium-base, at 95 to 300°K, (E), 20: 4476(R) (IS-1200 (Sect.P))
ANTIGENS
immune reactions to, role of appendix and liver in, 20: 3746
ANTIHYPERONS (Λ)
production in antiproton-proton interactions at 3.7 Bev/c, lifetime and mass from, (E), 20: 4608
ANTIHYPERONS (Σ^-)
production in antiproton-proton interactions at 3.7 Bev/c, lifetime and mass from, (E), 20: 4608
ANTIHYPERONS (Σ^+)
production in antiproton-proton interactions at 3.7 Bev/c, lifetime and mass from, (E), 20: 4608
ANTIMONY
separation from low grade ores, reductive chlorination process for, 20: 4072(P)
ANTIMONY ALLOYS
Sb–In, Hall coefficient in, effects of magnetic fields and temperature variations on, 20: 4479(R) (TID-22179, pp 1-83)
Sb–Mg, solvent properties for rare earth elements in molten chloride salts, 20: 3865 (ANL-7064)
ANTIMONY CHLORIDES
chlorine-36 exchange with thionyl chloride and sulfuryl chloride, 20: 3965
electron exchange between trivalent and pentavalent effects of hydrochloric acid on, 20: 3962
ANTIMONY IONS
radioinduced oxidation of trivalent, in aqueous solutions, 20: 4009
ANTIMONY ISOTOPES Sb-116
beta decay, 20: 4825(R) (ANL-7081, pp 81-93)
ANTIMONY ISOTOPES Sb-124
beta decay of, gamma polarization from, (E), 20: 4476(R) (IS-1200 (Sect.P))
ANTIMONY ISOTOPES Sb-125
content in Canadian biota, 20: 4161
ANTIMONY SYSTEMS
Sb–Cr–Te, magnetic structure of CrSb–CrTe in, 20: 4358(R) (AD-438516)
ANTINEUTRINOS
interactions with protons, production of (3,3) resonance by, (T), (T), 20: 4476(R) (IS-1200(Sect.P))
interactions with neutrinos, pure gravitational tensor field from, (T), 20: 4763
ANTINUCLEONS
interactions with nucleons, potential model for, (T), 20: 4849(R) (UCRL-14360, pp 1-50)
ANTIPROTON BEAMS
separation from proton beams in JINR synchrocyclotron, 20: 4496 (JINR-P-2375)
ANTIPROTONS
interactions with protons at 2.7 Bev/c, final states of products from, (E), 20: 4476(R) (IS-1200(Sect.P))
interactions with protons, forward amplitude for, (T), 20: 4603
interactions with protons at 3.7 Bev/c, antihyperon production from, (E), 20: 4608
interactions with nucleons at rest, SU(6) symmetry in two-meson annihilation, (T), 20: 4615
use as rocket propellant, feasibility study of, (T), 20: 4137
APPENDIX
immune reactions in, of rabbits, 20: 3746
ARCHAEOLOGICAL SPECIMENS
age of, Carbon-14 method for estimation of, 20: 4147
ARGON
diffusion from stored solid plutonium residues, vacuum-drying effects on, 20: 4364 (AERE-M-1644)
diffusion in ionic crystals and sintered materials, 20: 3944
effects on sintering of uranium mononitride at 1700°C, 20: 4349
ejection of pinched plasma of, from axial orifice, 20: 4138
microwave resonance in plasma of, surface, (E), 20: 4935 (AFCRL-65-556)
neutron coherent scattering by liquid, slow, (T), 20: 4819
reactions with ions, charge-exchange, 20: 4556
reactions with mercury-199 and -201, hyperfine-level excitation in, (E), 20: 4544
shock waves in, microwave attenuation by, 20: 4934 (AD-619093)
ARGON IONS
reactions with argon, hydrogen, and nitrogen, charge-exchange, 20: 4556

sputtering on copper, molybdenum, and tungsten at 1.5 to 30 kev, (E), 20: 4546
ARGON ISOTOPES Ar-37
nuclear magnetic moment and spin of, (E), 20: 4890
ARGON ISOTOPES Ar-38
concentration by thermal diffusion, 20: 3879(R) (MLM-1266)
ARGON ISOTOPES Ar-39
production in potassium–sodium reactor cooling systems, (E), 20: 5178 (NAA-SR-11303)
ARGON ISOTOPES Ar-41
production in potassium–sodium reactor cooling systems, (E), 20: 5178 (NAA-SR-11303)
ARGONAUT REACTOR
kinetics of coupled, invariant imbedding and modal expansion for, (T), 20: 5065
ARGONNE ADVANCED RESEARCH REACTOR
critical facility for, safety analysis of, (E/T), 20: 5189 (ANL-6929)
ARGONNE FAST REACTOR EXPERIMENT TEST
fuel element testing, core design for, 20: 5190 (ANL-7106)
ARGONNE LOW POWER RESEARCH REACTOR
research at, 20: 4821(R) (ANL-7081, pp 2-21)
ARGONNE NATIONAL LAB., LEMONT, ILL.
bibliography of publications July 1964 to June 1965, 20: 5211 (ANL-7087)
ARGONNE RESEARCH REACTOR
research at, 20: 4821(R) (ANL-7081, pp 2-21)
ARMY REACTORS (ML-1)
shielding for, evaluation of, 20: 5181(R) (ORNL-3029)
ARMY REACTORS (PM-1)
fuel element quality in, examination of, 20: 4305(R) (ORNL-3870, pp 187-90)
operation, 20: 5108(R) (AD-618376)
ARMY REACTORS (PM-3)
fuel element quality in, examination of, 20: 4305(R) (ORNL-3870, pp 187-90)
ARMY REACTORS (SM-1)
core design for 1A, nuclear and thermal-hydraulic analyses of, 20: 5121 (HIT-3459-11(Vol.1))
kinetics analysis of SM-1A core 3, 20: 5122 (HIT-3459-11(Vol.2))
ARSENIC
determination in arsenic sulfide, volumetric, 20: 3863(R) (IS-1200 (Sect. C))
ARSENIC ISOTOPES As-75
neutron capture by, gamma energy and intensity in thermal, (E), 20: 4849(R) (UCRL-14360, pp 1-50)
ARSENIC SULFIDES
analysis for arsenic, volumetric, 20: 3863(R) (IS-1200(Sect. C))
ASTRONOMY
observation methods for gamma and x-ray, 20: 4562 (MIT-2098-174)
ATMOSPHERE
absorption spectra at 1.35 cm wavelength, of terrestrial, 20: 4479(R) (TID-22179, pp 1-83)
cosmic-ray reactions in, neutrino production from, 20: 4561 (COO-818-64)
effects on fission products in reactor loss-of-coolant accidents, 20: 4183(R) (ORNL-3843, pp 2-70)
effects on geomagnetically trapped protons, (T), 20: 4748
effects on structure of niobium by contamination at high temperatures, 20: 4401(T) (ANL-Trans-218)
electron density in, geomagnetic and temporal effects on, (E), 20: 4746
fallout monitoring in, near Cluj, Rumania, 20: 3654
helium–ion losses in upper, 20: 4759
interactions between electromagnetic fields and missiles in, (T), 20: 4730 (SC-DC-65-1797)
ionization production and removal in upper, 20: 4729 (CNIE-PE-4)
model for, 20: 4153(R) (UCRL-14360, pp 73-85)
radiation monitoring in German, 1965, 20: 4164
radioactivity measurements in, method for, 20: 4158
radioisotope distribution in, review of, 20: 4163
sampling device for, 20: 4148 (AD-623515)
separation of molecular iodine from, 20: 3673
shock structure in, 20: 4153(R) (UCRL-14360, pp 73-85)
sodium content in, effects of weather on, 20: 4148 (AD-623515)
x-ray albedo flux at 40 to 190 kev, (E), 20: 4752
x-ray flux in auroral zone of, periodicity in, (E), 20: 4751
ATMOSPHERE EXPOSURE CHAMBERS
for pulmonary clearance studies in cigarette smoking dogs, 20: 3655 (BNWL-SA-224)
ATOMIC BEAMS
focusing of hydrogen, four- and six-pole magnet for, 20: 4559
research with, 20: 4535(R) (ANL-7081, pp 128-9)
temperature effects on cesium, 20: 4479(R) (TID-22179, pp 1-83)
ATOMIC CLOUDS
formation from base surges from underwater explosions, (E/T), 20: 4141 (AD-618733)
ATOMIC ENERGY COMMISSION
accident review, 1943 through 1964, 20: 4188 (TID-22268)
ATOMIC EXPLOSIONS
book: *The Peaceful Applications of Nuclear Explosions; A Report on the Plowshare Program*, 20: 4085
electromagnetic waves from atmospheric, effects on missiles having ionized wakes, (T), 20: 4730 (SC-DC-65-1797)
engineering and rescue operations at site of, 20: 4191(T) (JPRS-31014)
fallout from, physical and radiochemical properties of, 20: 4156 (USNRDL-TR-899)
seismic waves from surface, propagation in rock of, 20: 4143 (AD-619969)
ATOMIC MODELS
potential in L-dependent, 20: 4476(R) (IS-1200(Sect.P))
ATOMIC PHYSICS
electron transitions in field of positive ions, absorption cross sections for free-free, 20: 4550
research, 20: 4535(R) (ANL-7081, pp 128-9)
units for, 20: 4539 (UCRL-11444)
ATOMIC WEAPONS
quality control of, relation of quality assurance to, 20: 4113 (TID-22358)
radiation protection measures against fallout from, 20: 3797
radiation protection measures against fallout from, 20: 3799
ATOMS
diffusion in gases, Boltzmann equation for, (T), 20: 4721
electron reactions with, cross sections for optically disallowed transitions transitions in, (T), 20: 4552
equation of state for, electron contribution corrections for, (T), 20: 4540 (UCRL-14364)
localized self-consistent-field orbitals in, theory of, 20: 3863(R) (IS-1200(Sect. C))
particle anisotropic scattering on, effect on stopping by elastic collisions, 20: 4547
photon reactions with, photon emission in, (T), 20: 4949(R) (UCRL-14360, pp 85-94)
polarizability and shielding factor for, perturbation theory calculation of dipole, 20: 4537 (NP-15576)
polarizability and shielding factor for, perturbation theory calculation of quadrupole, 20: 4538 (NP-15577)
reactions at high energies, classical collision integrals for Coulomb potential for, (T), 20: 4988
AURORAL STORMS
latitude and properties during zero and very weak magnetic disturbance, 20: 4740
AUTORADIOGRAPHY
techniques for determining radiosensitivity of DNA synthesis in Yoshida ascites sarcoma cells, 20: 3702
use for low-level plutonium determination, comparison of scintillation counting with, 20: 3877 (LA-DC-7483)
use in nondestructive testing of radioactive materials, 20: 4122

B

BACTERIA
identification of, use of labeled metabolites for, 20: 3667
radiation effects on β-galactosidase in, mechanism of uv inactivation, 20: 3686(R) (TID-22352)
radiation effects on oxygen consumption in aerobic, gamma, 20: 3699
radiation effects on growth in, gamma, 20: 3699
radiation effects on *Serratia marcescens*, lethal, uv and light, 20: 3740
radiation effects on infectious activity of *Mycobacterium lepraemurium*, uv, 20: 3752
radiation effects on infectious activity of *Mycobacterium lepraemurium*, thermal, 20: 3752
radiation effects on, review, 20: 3776
radioinduced mutations of *Corynebacterium fascians*, uv, 20: 3723
BACTERIOPHAGES
radiosensitivity of complexes with *Escherichia coli* of, β, 20: 3748
radiosensitivity of complexes with *Escherichia coli* of, uv, 20: 3749
BARIUM
content in chondrites, 20: 4526
diffusion in graphite, 20: 5117(R) (GA-5866)
diffusion of hydrogen in, 20: 4297(R) (IS-1200(Sect.M))
intestinal absorption of, tracer study in rats, 20: 3669
separation from silver by partition chromatography, 20: 4054
BARIUM ALLOYS
Ba–Ni, phase studies, 20: 4442
BARIUM COBALT IRON(II) FERRATE(III)
neutron diffraction by powdered, effects of particle size on, 20: 5016(T)
BARIUM FLUORIDES
diffusion of rare gases in, 20: 3944
BARIUM ISOTOPES Ba-137
internal conversion coefficients of 662-Mev line, 20: 4248 (TID-22333)

BARIUM OXIDES
dehydration to 600°C for neutron transmission measurements, 20: 3914 (AERE-M-1654)
BARIUM TITANATES
spectra of, temperature dependence of Raman, 20: 4479(R) (TID-22179, pp 1-83)
BARLEY
radiation effects on virus infections on leaves of, γ, 20: 3768
radioinduced chlorophyll mutations in, x, 20: 3782
BARYONS
electric dipole moments of, from C- and T-violating model for electromagnetic interactions, 20: 4682
interactions with baryons and mesons, SU(3) symmetry for hadron-production, 20: 4645 (NP-15595)
interactions with mesons, relativistic SU(6) theory for vertex in, 20: 4677
interactions with baryons, SU(6) model for S-wave, 20: 4679
magnetic moments of octet of, in broken SU(3), (T), 20: 4665
mass perturbations of, octet enhancement and reciprocal bootstrap for, 20: 4649
mass spectra of, formula for, (T), 20: 4476(R) (IS-1200(Sect.P))
mixing parameters for vector mesons and, calculation of, 20: 4691
production by interactions of particles with electromagnetic potentials, mass spectra of, (E/T), 20: 4476(R) (IS-1200(Sect.P))
symmetry models for, linear representations of non-compact SU(3), 20: 4688
BARYONS, RESONANCE
decay modes of positive-strangeness Z^*, 20: 4589 (UCRL-11754)
decay of, parity and spin analysis in two-step, (T), 20: 4585 (SLAC-42)
decays of positive-parity, in broken U(12), (T), 20: 4666
mass perturbations of, octet enhancement and reciprocal bootstrap for, 20: 4649
production in electron-proton inelastic scattering, 20: 4581 (AD-618663)
production of (1920), in meson (π^-)-proton interactions at 2.16 Bev, (T), 20: 4849(R) (UCRL-14360, pp 1-50)
production of N* (1238), in photon-proton interactions below 1 Bev, 20: 4579 (AD-618661)
production of $Z^*(1360)$ in meson (π^-)-proton interactions at 1.5 to 4.2 Bev/c, 20: 4589 (UCRL-11754)
properties of, phenomenological analysis of, (T), 20: 4633
wave functions for ⅗⁺ and ⅘⁺ isobars, (T), 20: 4613
BEACHES
sodium distribution on, device for measuring, 20: 4148 (AD-623515)
wave generation on, feasibility of modeling run-up effects of dispersive, (T), 20: 4142 (AD-619053)
BEAMS
separators of particle, equivalent length of electrodes of, (T), 20: 4515
BEHAVIOR
humoral mediation of, in parabiotic rats, 20: 3706 (AD-623365)
of populations during nuclear attack, 20: 4200
radiation effects on monkey visual discriminatory, effects of age on, x, 20: 3721
radiation effects on performance of learned response by rats, effects of nembutal on, x, 20: 3772
radiation effects on genetic analysis of, in swine, 20: 3784
BELGIAN REACTOR-3
fuel pellet temperature for Doppler broadening of uranium-238 resonance, 20: 5135 (WCAP-3269-40)
BELGIUM
fallout monitoring, 1964, 20: 4155 (EUR-2516.d,f,i,n)
BENZENE
effects on hydrogen yields from radiolysis of hydrogen sulfide, 20: 4017
hypersonic and ultrasonic velocities in, effects of relaxation on, 20: 4479(R) (TID-22179, pp 1-83)
neutron scattering by, angular distribution and diffusion constants from, (E), 20: 4817
ammonia–benzene, radioinduced reactions, 20: 3982(R) (AGN-8156)
benzene–2-butene, radioinduced isomerization of, energy transfer in gamma and fast-electron, 20: 4014
BENZENE, NITRO-
hypersonic and ultrasonic velocities in, effects of relaxation on, 20: 4479(R) (TID-22179, pp 1-83)
BERYLLIUM
analysis for oxygen, methods for, 20: 3878 (LYCEN-6524)
bremsstrahlung reactions (γ,π^0) at 166 Mev, angular distributions from, (E), 20: 4898
corrosion by lithium, 20: 4999(R) (ORNL-2599)
effects on niobium, additive, 20: 4299(R) (ORNL-2711)
electronic structure of atomic, in pair function approximation, 20: 3863(R) (IS-1200(Sect. C))
gamma reactions at 0.01 to 10 Mev, cross sections for, 20: 4996 (AWRE-O-79/65)
neutron cross sections for, 9- and 16-group, 20: 4829 (GEMP-173 (Suppl.1))
neutron cross sections for, 20: 4830 (GEMP-384)
neutron pulse decay constant in, (T), 20: 4815
nuclear magnetic resonance in, (E), 20: 4476(R) (IS-1200(Sect.P))
preparation by splatcooling and hot-pressing, 20: 4381(R) (NMI-8001.4)
separation from silver by partition chromatography, 20: 4054
BERYLLIUM ALLOYS
Al–Be, mechanical properties at −320 to 800°F, 20: 4440
Be–Cu, preparation by splatcooling and hot-pressing, 20: 4381(R) (NMI-8001.4)
Be–Fe, preparation by splatcooling and hot-pressing, 20: 4381(R) (NMI-8001.4)
Be–Nb, corrosion by lithium at high temperatures, 20: 4299(R) (ORNL-2711)
Be–Ni, preparation by splatcooling and hot-pressing, 20: 4381(R) (NMI-8001.4)
BERYLLIUM FLUORIDES
properties of molten, for use as reactor fuels, 20: 4376 (JUL-268-RG)
BeF_2–LiF–UF_4–ZrF_4, corrosive effects on type 304 stainless steel, 20: 4308(R) (ORNL-3870, pp 243-60)
BERYLLIUM ISOTOPES Be-6
energy levels, (E), 20: 4849(R) (UCRL-14360, pp 1-50)
BERYLLIUM ISOTOPES Be-8
decay of, alpha particle energy spectra from, (E), 20: 4869
BERYLLIUM ISOTOPES Be-9
deuteron reactions (d,γ) at 0.5 to 5.5 Mev, excitation curves and angular distributions from, (E), 20: 4884
gamma reactions (γ,n) at 1.6 to 3.1 Mev, cross sections for, (E), 20: 4802 (IDO-17115)
helium-3 reactions (He-3, n) at 1.3 to 5.8 Mev, (E), 20: 4925
proton elastic scattering at 160 Mev, differential cross sections for, (E/T), 20: 4906
BERYLLIUM ISOTOPES Be-10
beta transitions in, comparative half lives of $\Delta I = 3$, (T), 20: 4874
BERYLLIUM MODERATED REACTORS
development of beryllia-moderated power, (E), 20: 5115(R) (GA-4967)
BERYLLIUM OXIDE REACTOR EXPERIMENT
development, (E), 20: 5115(R) (GA-4967)
BERYLLIUM OXIDES
analysis of irradiated, for helium, 20: 5181(R) (ORNL-3029)
bonding to niobium or tantalum, method for, 20: 4354(P)
compatibility with graphite at high temperatures, 20: 5117(R) (GA-5866)
development for use in EBOR, 20: 5115(R) (GA-4967)
neutron scattering cross sections for, microstructure and temperature effects on, 20: 5180 (NAA-SR-Memo-11604)
neutron scattering by, differential cross section for thermal, (T), 20: 4801(R) (GA-6634)
production, 20: 5181(R) (ORNL-3029)
production of powders of, 20: 4299(R) (ORNL-2711)
properties as barrier shell for thermionic energy converters, (E), 20: 4359(R) (AD-618923)
radiation effects on, in-pile, (E), 20: 5115(R) (GA-4967)
radiation effects on, neutron, 20: 5181(R) (ORNL-3029)
radiation effects at high temperatures, 20: 4299(R) (ORNL-2711)
radiation effects on x-ray diffraction pattern of single-crystal, fast neutron, 20: 4391(R) (ORNL-3870, pp 75-82)
sintering, 20: 4299(R) (ORNL-2711)
thermal conductivity of sintered, at 1.5 to 300°K, effects of calcium oxide on, 20: 4433
Al_2O_3–BeO–MgO, radiation effects on, in-pile, (E), 20: 5115(R) (GA-4967)
BeO–CaO, crystallography of $Ca_{12}Be_{17}O_{29}$, 20: 4391(R) (ORNL-3870, pp 75-82)
BeO–CaO, phase studies of, 20: 5181(R) (ORNL-3029)
BeO–CeO_2, phase studies, 20: 5181(R) (ORNL-3029)
BeO–La_2O_3, phase studies, 20: 5181(R) (ORNL-3029)
BeO–MgO, phase studies, 20: 5181(R) (ORNL-3029)
BeO–MgO, radiation effects on, in-pile, (E), 20: 5115(R) (GA-4967)
BeO–ZrB_2, fabrication of hot-pressed blocks of, 20: 4999(R) (ORNL-2599)
BETA DECAY
detection of inverse, using underground explosion, (T), 20: 4847 (UCRL-12085(Pt.1))
detection of inverse, using underground explosions, 20: 4848 (UCRL-12085(Pt.2))
formalism for hypernucleus, 20: 4930
neutrino emission in, systems for detection of, 20: 4848 (UCRL-12085(Pt.2))
rates of photon-induced, in stellar interiors, (T), 20: 4530
theory for oriented nuclei, 20: 4933
BETA PARTICLES
dose estimations of, from therapeutic doses of injected gold-198 colloids,

20: 3822
dosimetry of, calibration of photographic film detectors for, 20: 4237 (BNL-9665)
effects on bacteriophage complexes with *Escherichia coli*, biological, 20: 3748
effects on blood picture in polycythemia patients, 20: 3837
effects on gases, measurements of ionization, 20: 4557
effects on germanium and silicon transistors, (E), 20: 4261 (AD-623078)
effects on hematopoietic system of, leukemogenic, 20: 3835
effects on hematopoietic system, leukemogenic, 20: 3730
effects on polycythemia of, from phosphorus-32, therapeutic, 20: 3835
effects on polycythemia, therapeutic, 20: 3837
effects on rabbit eyes, pathological, 20: 3761
effects on skin, effects of oxygen pressure on, 20: 3727
effects on skin, pathological, 20: 3724
effects on thyroid glands of therapeutic doses of, carcinogenic, 20: 3739
pituitary ablation induced by, from yttrium-90 implants, 20: 3809
therapy for polycythemia, leukemogenic effects of, 20: 3650

BETA SPECTROMETERS
design of semiconductor, 20: 4476(R) (IS-1200(Sect.P))
use for internal conversion coefficient measurements, correction factor for, 20: 4248 (TID-22333)

BIBLIOGRAPHIES
on Argonne National Laboratory publications, July 1964 to June 1965, 20: 5211 (ANL-7087)
on chemistry, instability, and structure of detonation in gases, 20: 3918 (LA-DC-7276)
on decontamination of milk, 20: 3872 (EUR-2507.d)
on determination of tritium content in samples, 20: 3876 (ISS-65/8)
on dissertation research using 460-Mev synchrocyclotron, 20: 4577 (AD-618067)
on halogen resonances in organic compounds, 20: 3973 (IS-1222)
on hot laboratories for handling activity of more than 1000 C, 20: 4045
on nuclear medicine, 20: 3860
on properties of magnetic materials for space power systems, 20: 4379 (NASA-CR-54091)
on pulsed neutron facilities, 20: 5200 (TID-3571(Suppl.1))
on radiation chemistry, 20: 3986
on radiation effects on explosives and propellants, 20: 4461 (REIC-Memo-28)
on radiation effects on living organisms, 20: 3773
on rare gas compounds, 20: 3915 (CEA-Bib-61)
on separation of rare earths, thorium, and uranium by ion exchange, 20: 3888 (TID-22402)
on shell deformation, stability, and vibration, 20: 4079 (UCRL-13187)
on tensile properties of high-strength materials, 20: 4399 (UCRL-16301)
on thermodynamics of non-aqueous electrolytic solutions, 20: 3926 (TID-22374)
on tracer diffusion in metals, 20: 4383 (ORNL-3795(Pt.2))

BILE DUCT
effects of deposited Thorotrast on, carcinogenic, 20: 3722

BIOLOGICAL MATERIALS
neutron reactions in, effects of element composition on kerma, 20: 3708 (CEA-R-2833)
radioactivity measurements in liquid media, scintillation method for, 20: 3870 (EUR-2459.f)

BIOLOGICAL MODELS
of growth processes in neoplastic tissues, 20: 5222 (UCRL-14505)
of growth processes in rapidly multiplying tissues, 20: 5222 (UCRL-14505)

BIOLOGICAL WARFARE
hazards of, review, 20: 4192(T) (JPRS-32686)

BIOLOGICAL WARFARE AGENTS
decontamination of food and water supplies of, 20: 4192(T) (JPRS-32686)

BIOPHYSICS
research programs at M.I.T. electronics lab., 20: 4478(R) (TID-22179)

BIOSYNTHESIS
radiation effects on DNA, in normal and neoplastic rat tissues, tracer study, 20: 3701

BIPHENYL
neutron scattering by, angular distribution and diffusion constants from, (E), 20: 4817

BISMUTH
phase transitions in, shock-induced, 20: 4708(R) (UCRL-14360, pp 50-73)
preparation of single-crystal, 20: 4077(R) (IS-1200(Sect. E))

BISMUTH ALLOYS
Bi–In, thermal capacity of superconducting, in magnetic fields, 20: 4786
Bi–Pb, wetting reactions with stainless steel, 20: 4077(R) (IS-1200 (Sect. E))
Bi–Sn, electric conductivity of liquid, 20: 4297(R) (IS-1200(Sect.M))
Bi–Sn, magnetic transitions of thin superconducting films of, 20: 4785

BISMUTH IONS
spectra in lithium chloride–potassium chloride eutectic, absorption, 20: 3921(R) (ORNL-3870, pp 56-60)

BISMUTH OXIDES
solubility in borax at 760 to 900°C, 20: 3951

BISMUTH SYSTEMS
$AlCl_3$–Bi–NaCl, spectra of reaction products of, absorption, 20: 3921(R) (ORNL-3870, pp 56-60)
Bi–NaCl–$ZnCl_2$, spectra of reaction products of, absorption, 20: 3921(R) (ORNL-3870, pp 56-60)

BLADDER
radiotherapy of carcinomas in human, rectal injuries following, 20: 3734
radiotherapy of carcinoma of, radium, 20: 3819

BLAST EFFECTS
from Salmon event on residential-type structures, 20: 4189 (VUF-1030)
from Salmon event on tall industrial and residential structures, 20: 4190 (VUF-1031)
from traveling-wave load in Operation Snowball on shallow-buried model arches, 20: 4131 (AD-622552)
on circular cylinders, (E/T), 20: 4132 (AWRE-O-93/65)

BLOOD
calcium-45 disapearance kinetics, computer calculation, 20: 3664(R) (TID-22324)
radiation effects on protein content in rabbit, x, 20: 3709 (CEA-R-2865)
radioinduced antimitotic factor in, of rats and rabbits, x, 20: 3775

BLOOD CELLS
effects of dimethyl myleran on murine leukemic, in culture, cytotoxic, 20: 3736
effects of nitrogen mustards on murine leukemic, in culture, cytotoxic, 20: 3736

BLOOD CIRCULATION
in brain measurement using krypton-85 as tracer, 20: 3658(R) (EUR-2414.f,i)
in heart and lungs, tracer studies, 20: 3818
in liver, effects on deposition of gold-198 colloids in dogs, 20: 3681
measurement in heart, tracer method for, 20: 3658(R) (EUR-2414.f,i)
measurement using nuclear image amplifier with technetium-99m and xenon-133, 20: 3802 (ORNL-IIC-5, pp 239-42)

BLOOD PICTURE
radiation effects on, in polycythemia patients, β, 20: 3837
radiation effects on, in rabbits, x, 20: 3709 (CEA-R-2865)
radiation effects on mouse, protective effects of chemicals against gamma, 20: 3792

BLOOD PLASMA
radiation effects on growth hormone content in, heavy particle, 20: 3828
radiation effects on lipids in mouse, x, 20: 3704
radioactivity in human, following injections of iodine-131-labeled, polyvinylpyrrolidone, 20: 3675
thyrotropin content in, radioimmunoassay method of measurement, 20: 3829
transport of iodides from, to milk in cattle, tracer study, 20: 3674

BLOOD SERUM
binding of calcium-47 and strontium-85 by proteins in, 20: 3697
radiation effects on lipoproteins in, x, 20: 3704

BOILERS
design and fabrication of sodium-heated, 20: 5031(R) (BAW-1280-32)
design of sodium-heated, effects of sodium–water reactions on, 20: 4100 (BW-67-2(a))

BOILING
burnout heat flux in Army Reactor (SM-1A) core 3, 20: 5122 (HIT-3459-11(Vol.2))
burnout heat flux in internally cooled tubes, effects on inlet flow conditions on, 20: 4101(R) (EURAEC-1354)
burnout heat flux for forced-convection, at 1000 psi in annuli, (E), 20: 4105 (TID-22321)
heat transfer in reactor channels during bulk, nonuniform axial, 20: 4104 (NP-15622)

BOILING REACTORS
containment systems for, pressure-suppression, 20: 5146
design using pressurized and boiling water, 20: 5172(P)
design using reactivity control by pressure difference between reactor vessel and fuel storage vessels, 20: 5084(P)
design using superheating, 20: 5085(P)
kinetics of, instrumentation for analyzing, 20: 5032(R) (EURAEC-1477)

BOLOMETERS
design and performance of induction-coupled superconducting, 20: 4229
development for detection of phonons in quartz and sapphire, 20: 4479(F) (TID-22179, pp 1-83)

BONDS
chemical, theory of, 20: 3863(R) (IS-1200(Sect. C))
dissociation energies for carbon-hydrogen, 20: 4024

BONE FRACTURES
incidence of bilateral hip, 20: 3856
pathology of bilateral hip, induced by radiotherapy of cervical cancer, 20: 3856

BONE MARROW
chromosomal aberrations in, use in leukemia diagnosis of, 20: 3650
distribution of transplants of homologous, tracer study in rats, 20: 3795
effects of injected, for treatment of radiation injuries, 20: 3789
growth of transplants of, in dog spleen, 20: 3652
metabolism of colloids of gold-198 in, 20: 3822
protective effects of homologous transplants of, against radiation injuries in rats, 20: 3795
radiation effects on immune reactions to transplants of, in mice, 20: 3777
radiation effects on immune reactions to injected, in germ-free mice, 20: 3788
regeneration of, cytology of, 20: 3789
stimulation of hematopoiesis in, by massive androgen therapy, 20: 3793
BONE TUMORS
radiodiagnosis of, using calcium-47 or strontium-85 as tracer and whole-counting, 20: 3805
BONES
calcium-45 and strontium-89 metabolism by rat, effects of sodium alginates on, 20: 3671
calcium-47 metabolism in, effects of rickets on, 20: 3672
gallium-68 uptake by rat, effects of carrier on, 20: 3676
radiation effects on growth of, in rats, x, 20: 3707 (AD-623641)
radiation effects on development of facial, in children, 20: 3808
radiography of swine knuckle, for estimation of composition of ham, 20: 5224
radioinduced necrosis in monkey jaw, effects of dose fractionation on x, 20: 3742
radiosensitivity of monkey jaw, x, 20: 3742
BORAL
neutron transmission through, 20: 4999(R) (ORNL-2599)
BORANE, DIBROMO-
spectra of, deuterium effects on vibrational, 20: 3940
BORANE, TRIMETHYL-
molecular structure, 20: 3863(R) (IS-1200(Sect. C))
BORAX
solvent properties of fused, for metal oxides at 760 to 900°C, 20: 3951
BORIC ACID
corrosive effects of aqueous solutions of, on inconel-600, 20: 5134(R) (WCAP-3269-12)
BORIDES
reactions with liquid titanium, 20: 3929
BORON
analysis for impurities by activation methods, 20: 3879(R) (MLM-1266)
determination using diaminochrysazin, spectrophotometric, 20: 3892
effects on neutron embrittlement of type 304 stainless steel, 20: 4460(R) (ORNL-3870, pp 140-5)
neutron cross sections for, 9- and 16-group, 20: 4829 (GEMP-173 (Suppl.1))
BORON COMPOUNDS
chemical properties as soluble reactor poison, 20: 5134(R) (WCAP-3269-12)
BORON HYDRIDES
isotopic exchange in, intermediates in self-, 20: 3963
molecular structure, 20: 3863(R) (IS-1200(Sect. C))
BORON ISOTOPES
exchange between diboranes, intermediates in, 20: 3963
BORON ISOTOPES B-9
energy levels from lithium-7 (He-3, n) reactions at 1.3 to 5.8 Mev, 20: 4925
BORON ISOTOPES B-10
electron elastic scattering by, form factors for, 20: 4840 (LAL-1140)
neutron cross sections for, 9- and 16-group, 20: 4829 (GEMP-173(Suppl.1))
neutron cross sections for, 20: 4830 (GEMP-384)
BORON ISOTOPES B-11
electron elastic scattering by, form factors for, 20: 4840 (LAL-1140)
helium-3 reactions (He-3, n) at 1.3 to 5.8 Mev, (E), 20: 4925
neutron cross sections for, 9- and 16-group, 20: 4829 (GEMP-173(Suppl.1))
BORON NITRIDES
crystal structure of hexagonal, 20: 4479(R) (TID-22179, pp 1-83)
spectra of hexagonal, infrared and Raman, 20: 4479(R) (TID-22179, pp 1-83)
BORON SYSTEMS
B–Ni–Si, brazing alloy for tungsten carbide–cobalt cermet to TZM molybdenum alloy, 20: 4307(R) (ORNL-3870, pp 238-42)
BOSONS
effects of weak vector, on radiative weak decays, 20: 4629
field theory for massless, non-Abelian gauge, 20: 4657
interactions of weak vector, (T), 20: 4634
interactions with bosons, operator analysis of Bethe-Salpeter equation for, (T), 20: 4661
photoproduction of spin-1, on fermions, (T), 20: 4610
scattering of identical, nonrelativistic time-dependent theory of, 20: 4655
symmetry spontaneous breakdown in nonlinear field of, C violation in, (T), 20: 4669
theory for superfluid systems of, (T), 20: 4789
theory of many-body systems of, 20: 4476(R) (IS-1200(Sect.P))
BRAIN
blood circulation in, use of krypton-85 as tracer for measuring, 20: 3658(R) (EUR-2414.f,i)
radiodiagnosis in monkeys using radioalbumin aggregates, safety of, 20: 3832
radiodiagnosis of tumors of, procedures for, 20: 3830
BRAIN TUMORS
radiodiagnosis of, using technetium-99 as tracer for external scanning, 20: 3824
BRAZING
development for use in lithium-cooled reactors, 20: 4299(R) (ORNL-2711)
BRAZING ALLOYS
corrosion by lithium at high temperatures, 20: 4999(R) (ORNL-2599)
BREASTS
radiotherapy of tumors of, prior to radical surgery, x, 20: 3861
BREATH
thorium-232 content in, from Thorotrast patients, 20: 3683
BREEDER REACTORS
core design for, with concentrically arranged parallel, elongated fuel assemblies, 20: 5082(P)
BREMSSTRAHLUNG
dose distribution in liquids and spherical samples, 20: 4204
dose rates from activated lithium, 20: 4299(R) (ORNL-2711)
emission from thermal plasma with energetic electron flux, enhanced, (T), 20: 4982
reactions (γ,π^0) with nuclei at 166 Mev, angular distributions from, (E), 20: 4898
BREMSSTRAHLUNG SOURCES
production from strontium-90–yttrium-90 in thin absorbers, 20: 5000 (ORNL-IIC-5, pp 91-8)
BRITISH REACTORS
development, 20: 5155
hazards analysis of DAPHNE, 20: 5188 (AERE-R-4932)
safety criteria, 20: 5027
BRITTANY POWER REACTOR (EL-4)
fuel elements for, equipment for testing irradiated, 20: 4117
tank design, construction, and testing for, 20: 5144
BROMINE
content in chondrites, 20: 4526
BROMINE ISOTOPES Br-79
nuclear magnetic resonances in organic compounds, catalog of, 20: 3973 (IS-1222)
BROMINE ISOTOPES Br-81
nuclear magnetic resonances in organic compounds, catalog of, 20: 3973 (IS-1222)
BROOKHAVEN ALTERNATING-GRADIENT SYNCHROTRON
beam deflectors for, analysis of eccentric hole, (T), 20: 4492 (BNL-9640)
beam separator for, design and performance of r-f, 20: 4493 (BNL-9642)
environs monitoring of, 20: 4175 (BNL-9650)
BROOKHAVEN SYNCHROTRON
environs monitoring of, 20: 4175 (BNL-9650)
BUBBLE CHAMBERS
development of freon-propane, 20: 4244 (NP-15416)
electron and gamma angular distributions and energy spectra in propane, (T), 20: 4240 (JINR-P-2277)
expansion mechanism design and performance for hydrogen, 20: 4257
gaskets for large hydrogen, design and performance of, 20: 4242 (JINR-P-2376)
hydrogen liquefier design and performance for, 20: 4797
performance for neutrino detection, 20: 4848 (UCRL-12085(Pt.2))
BUBBLES
growth in bubble chambers, (T), 20: 4244 (NP-15416)
BUILDING MATERIALS
diffusion board for filtering high pressure radioactive gases, 20: 4097(P)
BULK SHIELDING FACILITY
development of BSR-II, 20: 4299(R) (ORNL-2711)
gamma heating in shields at, 20: 4999(R) (ORNL-2599)
neutron fluxes and dose rates in nuclear heating experiment, 20: 4999(R) (ORNL-2599)
neutron fluxes in, thermal, (E/T), 20: 4299(R) (ORNL-2711)
radiation heating in laminated shields, 20: 4999(R) (ORNL-2599)
testing of BSR-II core, 20: 5181(R) (ORNL-3029)
1-BUTENE
radioinduced polymerization with carbon monoxide, 20: 3997
2-BUTENE
radiolysis of, mechanisms and yields of, 20: 3982(R) (AGN-8156)

benzene–2-butene, radioinduced isomerization of, energy transfer in gamma and fast-electron, 20: 4014

BUTYL PHOSPHATES
solubility in aqueous solutions of uranyl nitrate, 20: 3955
solvent properties for protactinium, 20: 4057
solvent properties for protactinium, 20: 4058
solvent properties for thorium, 20: 4059
solvent properties for titanium and zirconium, 20: 4061
solvent properties for uranium VI, 20: 3903
solvent properties for cerium(IV) nitrates, 20: 3954
solvent properties for thorium, 20: 3863(R) (IS-1200(Sect. C))
TBP–n-hexane, solvent properties for thorium, 20: 4060
di-(2-ethylhexyl) phosphoric acid–TBP, solvent properties for neodymium nitrate, 20: 3875 (IS-T-37)

C

CABLES
testing for Tory IIC, 20: 5186 (UCRL-13095(Vol.2))

CADARACHE REACTORS
fuel elements for Pegase, equipment for testing irradiated, 20: 4117

CADMIUM
distribution between γ-alumina and molten chlorides, 20: 3959
magnetic resonance shifts at 4.2 to 450°K, (E), 20: 4476(R) (IS-1200 (Sect.P))

CADMIUM ALLOYS
Cd–Mg, solvent properties for rare earth elements in molten chloride salts, 20: 3865 (ANL-7064)

CADMIUM ISOTOPES Cd-113
neutron capture in cadmium sulfides, recoil defects from thermal, 20: 4000

CADMIUM ISOTOPES Cd-114
recoil from (n,γ) reactions in cadmium sulfide, effects on physical properties, 20: 4027

CADMIUM OXIDES
dehydration to 600°C for neutron transmission measurements, 20: 3914 (AERE-M-1654)
solubility in borax at 760 to 900°C, 20: 3951

CADMIUM SULFIDES
radiation effects on physical properties of, thermal-neutron, 20: 4027
radioinduced recoil defects in, following thermal-neutron capture by cadmium-113, 20: 4000

CALCINATION
effects on gas evolution from solid plutonium residues in storage cans, 20: 4364 (AERE-M-1644)

CALCIUM
bremsstrahlung reactions (γ,π°) at 166 Mev, angular distributions from, (E), 20: 4898
determination by flame photometry, 20: 4053
determination in mixtures by x-ray fluorescence using promethium-147/aluminum and tritium/zirconium sources, 20: 3883 (ORNL-IIC-5, pp 154-81)
determination in sea water using calcium-45 tracer, 20: 3902
effects on crystal structure and physical properties of cerium phosphate, 20: 4174
elastic properties of single-crystal, 20: 4297(R) (IS-1200(Sect.M))
intestinal absorption of, tracer study in rats, 20: 3669
meson (μ⁻) transitions in mesic atoms of, energy of, 20: 4825(R) (ANL-7081, pp 81-93)
separation from other metal chlorides by ion exchange, 20: 4053

CALCIUM ALLOYS
Ca–Sn, preparation and properties of single-crystal, (E), 20: 4476(R) (IS-1200(Sect.P))
Ca–Yb, phase diagrams, 20: 4297(R) (IS-1200(Sect.M))
Ca–Zn, zinc vapor pressure over liquid and solid, 20: 4297(R) (IS-1200 (Sect.M))

CALCIUM CARBONATES
effects on radiation stability of thiamine hydrochlorides, 20: 4018
radioinduced thermoluminescence in, alpha, 20: 3983 (BNL-9589)

CALCIUM CHLORIDES
corrosive effects on failure of stainless steel under stress, 20: 4328 (WCAP-3269-50)
$CaCl_2$–$ThCl_4$, phase studies, 20: 4297(R) (IS-1200(Sect.M))

CALCIUM FLUORIDES
diffusion of rare gases in, 20: 3944
radioinduced thermoluminescence in, alpha, 20: 3983 (BNL-9589)

CALCIUM ISOTOPES Ca-40
photodisintegration at 28 to 60 Mev, cross sections for, (E), 20: 4476(R) (IS-1200(Sect.P))
proton elastic scattering at 160 Mev, differential cross sections for, (E/T), 20: 4906

CALCIUM ISOTOPES Ca-45
metabolism by rat bones, effects of sodium alginates on, 20: 3671
use as tracer in determination of calcium in sea water, 20: 3902
use as tracer, for skeletal metabolism studies, 20: 3664(R) (TID-22324)
use as tracer, for diagnosis of bone tumors, 20: 3805

CALCIUM ISOTOPES Ca-47
binding of, by blood serum proteins, 20: 3697
metabolism in bones of normal and rachitic children, effects of vitamin D on, 20: 3672
tracer uses for diagnosis of rickets in children, 20: 3672

CALCIUM OXIDES
effects on creep rate in thoria, 20: 4387(R) (ORNL-3870, pp 38-43)
effects on strontium-90 uptake by agricultural plants, 20: 3679
effects on thermal conductivity of beryllium oxide at 1.5 to 300°K, 20: 4433
BeO–CaO, crystallography of $Ca_{12}Be_{17}O_{29}$, 20: 4391(R) (ORNL-3870, pp 75-82)
BeO–CaO, phase studies of, 20: 5181(R) (ORNL-3029)
CaO–ThO_2, sintering of, material transport during, 20: 4387(R) (ORNL-3870, pp 38-43)
CaO–ZrO_2, internal friction, 20: 3945

CALCIUM PHOSPHATES
content in bones, x-ray transmission measurement of, 20: 3886 (ORNL-IIC-5, pp 290-4)
effects on radiation stability of thiamine hydrochloride, 20: 4018

CALCIUM SILICATES
radiation effects on phase transformations in, neutron, 20: 4462

CALDER HALL REACTORS
design and development of Hinkley Point Power Station, 20: 5148
design evaluation for advanced 500-Mw, 20: 5157
fuel element performance, 20: 5094
operation and performance of Berkeley and Bradwell, 20: 5156

CALIFORNIUM ISOTOPES Cf-252
fission fragment energy spectra of, 20: 3982(R) (AGN-8156)
fission of, nuclear-charge division in spontaneous, (E), 20: 4913
fission of, nuclear-charge division and x-ray emission in spontaneous, (E), 20: 4914

CALORIMETERS
design for high-temperature measurements, 20: 4297(R) (IS-1200(Sect.M))
design of, for measuring deformation energy of metals, 20: 4384 (ORNL-3870, pp 7-14)

CANADA
sodium-22 content in animal and plants from Manitoba, 20: 4161

CAPRYLIC ACID
sodium salt, x-ray scattering intensity in aqueous solutions of, (E), 20: 4483

CARBIDES
reactions with liquid titanium, 20: 3929

CARBOHYDRATES
radiation effects on metabolism of, in Aspergillus, 20: 3755(T)

CARBON
bremsstrahlung reactions (γ,π°) at 166 Mev, angular distributions from, (E), 20: 4898
deposition in fluidized beds at 1900 to 2400°C, properties and structure of pyrolytic, 20: 5089(R) (GA-6181)
deposition of pyrolytic, development of fluidized bed and rotary drum methods for, 20: 4343(R) (ORNL-3870, pp 266-89)
determination in steel by gamma spectroscopy, 20: 3894
diffusion of fission products from coatings of pyrolytic, on graphite disks, 20: 5089(R) (GA-6181)
diffusion of thorium-228 in, rates of, 20: 5089(R) (GA-6181)
effects on flow stress recovery of molybdenum, 20: 4409
effects on mechanical properties of niobium, 20: 4425
effects on stability of niobium–zirconium alloys at 2000°F, 20: 4397 (TID-955)
effects on tensile properties of tungsten, 20: 4408
effects on uranium mononitride lattice parameters, 20: 4303(R) (ORNL-3870, pp 164-70)
electric quadrupole and magnetic dipole transitions for isoelectric sequence of, (T), 20: 4553
gamma reactions at 0.01 to 10 Mev, cross sections for, 20: 4996 (AWRE-O-79/65)
graphitization of pyrolytic, effects of uranium carbide impurities on, 20: 4386(R) (ORNL-3870, pp 20-6)
mass transfer from stainless steel to niobium and niobium–zirconium alloy, in potassium–sodium alloy, 20: 5181(R) (ORNL-3029)
microstructure of pyrolytic, effects of deposition parameters on, 20: 4306(R) (ORNL-3870, pp 194-213)
neutron cross sections for, 20: 4830 (GEMP-384)
performance of coatings of pyrolytic, model for irradiation, 20: 4306(R) (ORNL-3870, pp 194-213)
properties and structure of pyrolytic deposits of, in fluidized beds at 1900 to 2400°C, 20: 5089(R) (GA-6181)
radiation effects on coatings of pyrolytic, on thorium and uranium carbide and oxide fuel particles, 20: 4458 (GA-6485)

structure of as-deposited and annealed pyrolytic, 20: 4386(R) (ORNL-3870, pp 20-6)
thermal stability of coatings of pyrolytic, on urania fuel particles, 20: 4306(T) (ORNL-3870, pp 194-213)
uses for oxygen removal from uranium nitride, 20: 4303(R) (ORNL-3870, pp 164-70)
CARBON (ACTIVATED)
efficiency for iodine-131 collection in stack effluents, 20: 4179 (LA-3363)
sorptive properties for iodine and iodides, factors affecting, 20: 4086(R) (ORNL-2843, pp 137-67)
CARBON DIOXIDES
diffusion from stored solid plutonium residues, vacuum-drying effects on, 20: 4364 (AERE-M-1644)
radiolysis of, yields from fission-fragment, 20: 3982(R) (AGN-8156)
reactions with uranium, kinetics of, 20: 4329(T) (CEA-tr-R-1868)
CO_2–methane, radiolysis of, formaldehyde yields in, 20: 3981 (AERE-R-5051)
CARBON ISOTOPES
effects on microwave spectra and structure of ethynylsilane, 20: 3977
CARBON ISOTOPES C-11
energy levels from beryllium-9 (He-3, n) reactions at 1.3 to 5.8 Mev, 20: 4925
incorporation in hydrocarbons by recoil, mechanisms of, 20: 3863(R) (IS-1200(Sect. C))
production from gamma reactions with oxygen-16 at 22 to 65 Mev, (E), 20: 4476(R) (IS-1200(Sect.P))
reactions with acetamide, recoil, 20: 4026
CARBON ISOTOPES C-12
decay of excited, 3α, (E), 20: 4878
deuteron reactions (d,n) and (d,p) with, angular distributions for, (E), 20: 4849(R) (UCRL-14360, pp 1-50)
gamma reactions (γ,n), at threshold to 65 Mev, cross sections for, (E), 20: 4476(R) (IS-1200(Sect.P))
gamma reactions (γ,p), energy spectra from, (E), 20: 4476(R) (IS-1200(Sect.P))
gamma reactions (γ,n) with, in liquid hydrocarbons, behavior of recoils in, 20: 3863(R) (IS-1200(Sect. C))
helium-3 reactions (He-3, n) at 1.3 to 5.8 Mev, (E), 20: 4925
meson (μ^-) capture by, coupling constants in, (T), 20: 4915
neutron reactions (n,nγ) at 13 to 18 Mev, 3α decay mode cross section for, (E), 20: 4878
proton reactions (p,pn) at 450 Mev, differential recoil from, (T), 20: 4893
reactions (C-12,xn) with platinum at 90 Mev, polonium production cross sections in, (E), 20: 4860
reactions with erbium, tungsten-174 from, (E), 20: 4834 (JINR-E-2360)
CARBON ISOTOPES C-13
determination in enriched methane by NMR, 20: 3879(R) (MLM-1266)
helium-3 reactions at 1.9 to 6.7 Mev, bound states from, (E), 20: 4905
helium-3 reactions (He-3, n) at 1.3 to 5.8 Mev, (E), 20: 4925
CARBON ISOTOPES C-14
deuteron reactions at 1.9 to 6.7 Mev, bound states from, (E), 20: 4905
distribution in glucose, 20: 3684
incorporation in pyroline-2-carboxylic acid, 20: 3975
production in radiolysis of methane–nitrogen mixtures, 20: 3982(R) (AGN-8156)
reactions with acetamide, recoil, 20: 4026
transmutation in liver of fructose-incorporated, 20: 3684
uptake from acetate by fatty acids in lungs of dogs, rabbits, and rats, mechanism of, 20: 3656 (BNWL-SA-225)
use in age estimations of archeological samples, 20: 4147
CARBON MONOXIDES
diffusion from stored solid plutonium residues, vacuum-drying effects on, 20: 4364 (AERE-M-1644)
effects on formaldehyde yields in electron radiolysis of carbon dioxide–methane, 20: 3981 (AERE-R-5051)
radioinduced polymerization with butene-1, isobutylene, and propylene, 20: 3997
sorption on tantalum, kinetics of, 20: 4444
yields from irradiation of polytetramethylene oxide, 20: 3999
CO–H–N, radioinduced reactions in, 20: 3982(R) (AGN-8156)
CARBON STEEL
corrosion by lead at 1100°F, 20: 4308(R) (ORNL-3870, pp 243-60)
diffusion of deuterium and hydrogen in EN58B, coefficients for, 20: 4366 (AWRE-O-90/65)
CARBON SULFIDES
effects on hydrogen yields from radiolysis of hydrogen sulfide, 20: 4017
hypersonic and ultrasonic velocities in, effects of relaxation on, 20: 4479(R) (TID-22179, pp 1-83)
radiolysis of liquid, G-values for polymer and sulfur in, 20: 4028
CARBON SYSTEMS
Al–C–Ti, properties for use to 1200°F, 20: 4393 (PWAC-472)
Al–C–Ti–Zr, properties for use to 1200°F, 20: 4393 (PWAC-472)
C–Hf–Ta–W, preparation and specifications for corrosion loop testing, 20: 4380 (NASA-CR-54761)
C–Mo–Nb–Ta–W–Zr, preparation and specifications for corrosion loop testing, 20: 4380 (NASA-CR-54761)
C–Mo–Ti–Zr, preparation and specifications for corrosion loop testing, 20: 4380 (NASA-CR-54761)
C–Nb–W–Zr, aging and recrystallization of D-43, 20: 4301(R) (ORNL-3870, pp 102-35)
C–Nb–W–Zr, corrosion of D-43, by potassium, 20: 4301(R) (ORNL-3870, pp 102-35)
C–Nb–W–Zr, corrosion of D-43, by lithium, effects of oxygen on, 20: 4301(R) (ORNL-3870, pp 102-35)
C–Nb–W–Zr, ductility of welds in D-43, effects of aging on bend, 20: 4301(R) (ORNL-3870, pp 102-35)
C–Nb–W–Zr, evaporation losses in high vacuum of D-43, 20: 4301(R) (ORNL-3870, pp 102-35)
C–Nb–W–Zr, preparation and specifications for corrosion loop testing, 20: 4380 (NASA-CR-54761)
C–Nb–W–Zr, tensile properties of welded plates of D-43, 20: 4301(R) (ORNL-3870, pp 102-35)
C–Nb–W–Zr, thermal conductivity of D-43, at 30 to 120°C, 20: 4301(R) (ORNL-3870, pp 102-35)
C–Nb–Zr, phase studies at 1092 and 1538°C, 20: 4392 (PWAC-461)
C–Ni–U, phase studies, 20: 4368 (CEA-R-2845)
C–N–O–Pu–U, corrosion by water at 550°F, 20: 4327(R) (UNC-5138)
C–N–O–Pu–U, preparation of single-phase compositions of, 20: 4327(R) (UNC-5138)
C–O–Pu–U, preparation of single-phase composition of, 20: 4327(R) (UNC-5138)
CARBON TETRACHLORIDE
effects on hydrogen yields from radiolysis of hydrogen sulfide, 20: 4017
electric conductivity at high pressures, 20: 4708(R) (UCRL-14360, pp 50-73)
hypersonic and ultrasonic velocities in, effects of relaxation on, 20: 4479(R) (TID-22179, pp 1-83)
CARBONITRIDES
ferromagnetic properties of manganese, 20: 4402(T) (ANL-Trans-230)
CARBONYLS
preparation and properties of bicyclic phosphite esters of, 20: 3863(R) (IS-1200(Sect. C))
CARCINOGENESIS
radioinduced in children by therapy, 20: 3850
radioinduced, by therapeutic doses of x, 20: 3841
radioinduced, in lungs of hamsters and rats, 20: 3785
radiotherapy of gonadal, effects on intestine of gamma, 20: 3732
CARCINOMAS
radioinduced thyroid, in adolescents and children, beta and x, 20: 3739
radioinduced, by therapeutic doses of x, 20: 3841
radioinduced, by therapy of skin epitheliomas, 20: 3811
radiotherapy of bladder, rectal injuries following x, 20: 3734
radiotherapy of bladder, using radium, 20: 3819
radiotherapy of cervical, effects on intestine of gamma, 20: 3720
radiotherapy of cervical, rectal injuries following gamma, 20: 3734
radiotherapy of cervical, methods for, 20: 3807
CASCADES
separation by, economics and engineering of, 20: 4284(T) (CEA-tr-X-617)
CAST IRON
cerium distribution in, 20: 4414
CATARACTS
radioinduced, in rabbit eyes, β, 20: 3761
CATHODE RAYS
effects on skin, pathological, 20: 3724
CATION EXCHANGE MATERIALS
preparation of granular zirconium phosphate, 20: 3968(P)
CATTLE
cesium-137 metabolism by grazing, 20: 3665(T) (CEA-tr-X-619)
immune reactions of rabbits to irradiated corneal grafts from, 20: 3719
secretion of iodine in milk of, factors affecting, tracer study, 20: 3674
strontium-89 metabolism in, effects of diet, 20: 4162
strontium-90 metabolism in, effects of diet, 20: 4162
strontium-90 metabolism by grazing, 20: 3665(T) (CEA-tr-X-619)
transport of iodides from plasma to milk in, tracer study, 20: 3674
CAVES
conference on high-activity, Grenoble, June 15 to 18, 1965, 20: 4040
decontamination of, radiation protection in, 20: 4211
decontamination of, at Harwell, 20: 4212
decontamination of alpha–beta–gamma, 20: 4213
design and operation of, for handling more than 1000 C, directory of, 20: 4045
design for decanning of irradiated fuel, 20: 4062
design for dismantling and machining processes in, 20: 4351
design for dismantling and machining fuels, fuel elements, and irradiation

capsules, 20: 4125
design for dismantling and machining irradiated materials, 20: 4127
design for examination of ceramic fuel elements, 20: 4130
design for handling irradiation capsules, 20: 5205
design for handling irradiated samples, 20: 4126
design for nondestructive testing of fuel elements, 20: 4121
design for separation of transplutonium elements, 20: 4065
design of alpha–gamma for nondestructive testing of fuels, 20: 4120
design of Cyrano, for processing irradiated fuel elements, 20: 4044
design of high-activity beta-gamma, 20: 5153
equipment loading in, under alpha-tight and gas-tight conditions, 20: 4209
equipment transfer from and to, procedures for, 20: 4210
equipment, materials, and personnel transfer through alpha-gamma barriers in, 20: 4042
glove box standardization for, 20: 4093
materials transfer in and out of, methods for, 20: 4043
materials transfer to, methods for, 20: 4208
radioactive material transfer to, equipment for, 20: 4044
radioactive materials transfer to, methods for, 20: 4209
shielding for, materials transfer through, 20: 4043
transfer systems for, design of, 20: 4063
waste collection in, from dismantling and machining processes, 20: 4351

CAVITY RESONATORS
design for nonsinusoidal periodic waveforms for accelerators, 20: 4511 (UCRL-16242)

CELLULOSE
destruction of radioactive, sulfuric acid process for, 20: 5208(P)
radiation effects on, 20: 4034
radioinduced halogenation of, for flameproofing, 20: 4033
radiolysis, 20: 4031

CELLULOSES
radioinduced polymerization of, in aqueous solutions and films, 20: 4034

CEMENTS
analysis by x-ray fluorescence using promethium-147/aluminum source, 20: 3883 (ORNL-IIC-5, pp 154-81)
development of iron-impregnated, for accelerator shielding, 20: 4998 (JINR-P-2359)

CENTRIFUGAL PUMPS
impeller design and analysis for, computer programs for, 20: 4088 (TIM-949)

CERAMIC CRUCIBLES
fabrication of ceria–zirconia, for uranium, 20: 4297(R) (IS-1200(Sect.M))

CERAMIC MATERIALS
bonding to metals, method for, 20: 4354(P)
development for use in space vehicles, 20: 4312
properties for use in space vehicles, 20: 4312
research programs at ORNL on, 20: 4300(R) (ORNL-3870)
tensile properties of, review on, 20: 4399 (UCRL-16301)

CERIUM
determination in hydrochloric acid or methanol–nitric acid media, spectrophotometric, 20: 3888 (TID-22402)
determination in mixtures by x-ray fluorescence using promethium-147/aluminum and tritium/zirconium sources, 20: 3883 (ORNL-IIC-5, pp 154-81)
distribution between γ-alumina and molten chlorides, 20: 3959
distribution in cast iron, 20: 4414
effects on proton polarization in lanthanum magnesium nitrate crystals, (E), 20: 5021
separation from aqueous solutions by solvent extraction using naphthenates, 20: 4051
separation from thorium by solvent extraction using tributyl phosphate, 20: 4059
solvent partition between magnesium alloys and magnesium–potassium–sodium chloride salt mixture, 20: 3865 (ANL-7064)

CERIUM ALLOYS
Ce–Nb, corrosion by lithium at high temperatures, 20: 4299(R) (ORNL-2711)
Ce–Pb, magnetic properties of, at 2 to 300°K, 20: 4423
Ce–Pu, transformation temperature of, effects of uniaxial compression on delta, 20: 4434
Ce–Sn, magnetic properties of, at 2 to 300°K, 20: 4423

CERIUM ISOTOPES Ce-137
content in Canadian biota, 20: 4161

CERIUM ISOTOPES Ce-140
energy levels of, hyperfine structure in 2084-kev, (E), 20: 4888

CERIUM ISOTOPES Ce-141
beta decay of, ξ approximation for β–γ directional correlation in, (E/T), 20: 4903

CERIUM ISOTOPES Ce-144
content in Canadian biota, 20: 4161
distribution in rat liver cells following intravenous injection, model for, 20: 3682
separation from reservoir water by coagulation with alumium and iron and fast filtration, 20: 4068
separation from waste solutions using manganese dioxide, 20: 5206

CERIUM NITRATES
thermodynamic properties of basic and neutral, in water and tributyl phosphate, 20: 3954

CERIUM OXIDES
BeO–CeO_2, phase studies, 20: 5181(R) (ORNL-3029)

CERIUM PHOSPHATES
crystal structure of, effects of calcium and thorium on, 20: 4174

CERIUM SULFIDES
homogeneity regions in, 20: 3938

CERMETS
corrosion by lithium at high temperatures, 20: 4299(R) (ORNL-2711)

CESIUM
corrosive effects on ceramics, alloys, and metals at 400°C, 20: 4337
diagnostics of contact ionization produced plasma of, electric probe method for, (E), 20: 4958
diffusion from liquid urania in containment mockup experiments, 20: 4184(R) (ORNL-3843, pp 71-135)
ionization on porous tungsten, 20: 4135
oscillations in contact-ionization plasma of, amplitude and frequency of, (E), 20: 4965
separation from ore, methods for, 20: 4297(R) (IS-1200(Sect.M))
separation from rubidium by ion exchange, 20: 4056
separation from solutions formed by dissolution of molybdenum–uranium fuel alloys, 20: 4070(P)
sorption on graphite, 20: 5117(R) (GA-5866)
sorption on stainless steel, 20: 4185(R) (ORNL-3843, pp 169-234)
thermionic emission by tungsten in, dependence on crystallographic direction and temperature, 20: 4948(R) (TID-22179, pp 85-175)

CESIUM BROMIDES
color centers in, (E/T), 20: 4476(R) (IS-1200(Sect.P))
spectra of, second-order Raman, (T), 20: 5007 (UCRL-14398)
thermodynamic properties in *N,N*-dimethylformamide and *N*-methylformamide solutions, 20: 3924 (TID-22366)
CsBr–$NiBr_2$, spectra of nickel(II) in melts of, absorption, 20: 3921(R) (ORNL-3870, pp 56-60)

CESIUM CHLORIDES
spectra of, second-order Raman, (T), 20: 5007 (UCRL-14398)
thermodynamic properties in *N,N*-dimethylformamide and *N*-methylformamide solutions, 20: 3924 (TID-22366)
thermodynamic properties in anhydrous *N*-methylformamide solutions, 20: 3925 (TID-22366, App. B)
thermodynamics of, in anhydrous *N*-methylformamide at 25°C, 20: 3926 (TID-22374)
CsCl–$NiCl_2$, density equations for molten, 20: 3921(R) (ORNL-3870, pp 56-60)
CsCl–$NiCl_2$, spectra of nickel(II) in melts of, absorption, 20: 3921(R) (ORNL-3870, pp 56-60)

CESIUM FLUORIDES
effects on electron emission in thermionic cells, 20: 4572 (EUR-2283.d)
hyperfine structure and Stark and Zeeman effects in, (E), 20: 4554
properties of molten, for use as reactor fuels, 20: 4376 (JUL-268-RG)

CESIUM IODIDES
response of crystals of, to gamma radiation, 20: 5181(R) (ORNL-3029)
spectra of, second-order Raman, (T), 20: 5007 (UCRL-14398)
thermodynamics of, in anhydrous *N,N*-dimethylformamide at 25°C, 20: 3926 (TID-22374)

CESIUM IONS
production using porous tungsten ionizers, 20: 4135

CESIUM ISOTOPES Cs-133
hyperfine structure and Stark and Zeeman effect in cesium fluorides, 20: 4554

CESIUM ISOTOPES Cs-134
beta decay of, gamma polarization from, (E), 20: 4476(R) (IS-1200 (Sect.P))

CESIUM ISOTOPES Cs-137
content in Canadian biota, 20: 4161
content in rain water, method for determining, 20: 4159
content in sintered uranium dioxide pellet, radial distribution of, 20: 4472
metabolism by forage plants of, effects of soil type and fertilizers on, 20: 3665(T) (CEA-tr-X-619)
metabolism by shrimp of, 20: 3657 (CEA-R-2818)
separation from fission product solutions, methods for, 20: 3874 (EUR-2535.f)
separation from other fission products by ion exchange, 20: 3871 (EUR-2497.e)
separation from waste solutions using manganese dioxide, 20: 5206
uptake by maize, effects of soil temperature on, 20: 3668

CESIUM PROTACTINIUM CHLORIDES

protactinium spin-lattice relaxation in, 20: 5020
CESIUM TRICHLOROCUPRATE(II)
crystal structure, 20: 3863(R) (IS-1200(Sect. C))
magnetic susceptibility, 20: 3863(R) (IS-1200(Sect. C))
CESIUM URANIUM NITRATES
spectra of, infrared, 20: 3949
CHARCOAL
performance as fission fragment filter, 20: 5199 (ORNL-TM-1328)
radioinduced ignition by fission products, 20: 4086(R) (ORNL-3843, pp 137-67)
reactions of chemically impregnated, with methyl iodide, 20: 4185(R) (ORNL-3843, pp 169-234)
sorptive properties for methyl iodide, effects of humidity and temperature on, 20: 4184(R) (ORNL-3843, pp 71-135)
sorptive properties for methyl iodide, factors affecting, 20: 4185(R) (ORNL-3843, pp 169-234)
CHARGED PARTICLE BEAMS
effects on pituitary gland, use for acromegaly therapy of, 20: 3828
kinetics in linear accelerators, method for determining, (T), 20: 4503 (NP-15340)
separators for, equivalent length of electrodes of, (T), 20: 4515
stability in accelerators, effects of resistive walls on, 20: 4501 (LNF-65/34)
stability of relativistic, review of, 20: 4513 (UCRL-16440)
transport system for, optical, 20: 4509 (UCRL-14343)
CHARGED PARTICLES
detection and measurement of tracks of, in polymers, (E), 20: 4251 (USNRDL-TR-917)
detection of, silicon single crystal for, 20: 4259(P)
electromagnetic wave emission by, moving above diffraction grid, 20: 4622
evolution equation for system of relativistic, 20: 4723
interactions of, collision lifetime matrix for, (T), 20: 4651
momentum of, determination in inhomogeneous magnetic fields, (T), 20: 4583 (JINR-P-2371)
radiation emission by, in dielectrically inhomogeneous media, (T), 20: 4625
reactions with solids in vacuum, transition radiation from, (E/T), 20: 5008(T) (ORNL-tr-872)
reactions with solids, ion-explosion spike mechanism for track formation in, 20: 4548
scattering in magnetic mirrors, comparison with magnetosphere, 20: 4948(R) (TID-22179, pp 85-175)
use in radiotherapy, review, 20: 3735
CHELATES
stability of rare earth, 20: 3863(R) (IS-1200(Sect. C))
CHELATION
reagents for rare earth, preparation of, 20: 3863(R) (IS-1200(Sect.C))
CHEMICAL ANALYSIS
book: *Geochemistry and Analytical Chemistry of Rare Earth Elements*, 20: 4146
electron probe x-ray microanalyzer for, 20: 3912
methods of, for fissiochemical reaction products, 20: 3982(R) (AGN-8156)
x-ray spectroscopic methods of, review of, 20: 3911
CHEMICAL WARFARE
hazards of, review, 20: 4192(T) (JPRS-32686)
CHEMICAL WARFARE AGENTS
decontamination of food and water supplies of, 20: 4192(T) (JPRS-32686)
CHEMICALS AND REAGENTS
preparation for chelation of rare earths, 20: 3863(R) (IS-1200(Sect. C))
CHEMISTRY
research programs at Ames Laboratory, July 1964–June 1965, 20: 5213(R) (IS-1200)
CHEMOTHERAPY
of tumors, computer calculation of drug treatment schedules, 20: 5222 (UCRL-14505)
CHERENKOV DETECTORS
construction and testing of differential gas, 20: 4239 (IAE-900)
description, 20: 4252(T) (FTD-TT-64-1228)
CHERENKOV RADIATION
emission by electron sheets, 20: 4623
production and properties of, review of, (E/T), 20: 5008(T) (ORNL-tr-872)
CHIMERAS
immune reactions of irradiated germ-free mouse, 20: 3788
CHLORAMBUCIL
effects on retinal development in human embryos, 20: 3725
CHLORIDE COMPLEXES
with rhodium, chemical properties of, tracer studies of, 20: 3966
CHLORIDES
effects on spectrophotometric determination of zirconium, 20: 3895
CHLORINE
determination in boreholes, calibration of equipment for, 20: 4171(P)
CHLORINE FLUORIDES
reactions with plutonia and uranía, 20: 4046(R) (EURAEC-1340)
CHLORINE ISOTOPES Cl-35
mass relative to chlorine-37, from thallium monochloride rotational spectra, 20: 3947
nuclear magnetic resonances in organic compounds, catalog of, 20: 3973 (IS-1222)
exchange between antimony pentachloride and thionyl chloride and sulfuryl chloride, 20: 3965
CHLORINE ISOTOPES Cl-37
mass relative to chlorine-35, from thallium monochloride rotational spectra, 20: 3947
CHLOROHYDROCARBONS
reactions with recoil tritium atoms, 20: 4023
CHLOROPHYLLS
radiation effects on mutation rates for barley, x, 20: 3782
CHLOROPLASTS
nucleic acid content of spinach, 20: 3649 (UCRL-11475)
CHOLINESTERASES
effects of uranium poisoning on activity of, in mouse liver, 20: 3670
effects of uranium poisoning on activity of, in mouse kidney, 20: 3670
CHROMATOGRAPHY
development for identification of radioiodine vapors, 20: 4185(R) (ORNL-3843, pp 169-234)
development of reversed-phase partition, 20: 3863(R) (IS-1200(Sect. C))
development of, for fissiochemical reaction products, 20: 3982(R) (AGN-8156)
CHROMIUM
diffusion of chromium-51 in, at 1500°C to melting point, 20: 4385(R) (ORNL-3870, pp 15-19)
ductility of, effects of dispersions on, 20: 4297(R) (IS-1200(Sect.M))
Fermi surfaces calculations for, 20: 4476(R) (IS-1200(Sect.P))
hardness of, effects of temperature on, 20: 4297(R) (IS-1200(Sect.M))
neutron cross sections for, 9- and 16-group, 20: 4829 (GEMP-173(Suppl.1))
neutron cross sections for, 20: 4830 (GEMP-384)
oxidation by chromium(III), 20: 3863(R) (IS-1200(Sect. C))
oxidation by vanadium(IV), 20: 3863(R) (IS-1200(Sect. C))
preparation of high-purity, 20: 4297(R) (IS-1200(Sect.M))
separation from low grade ores, reductive chlorination process for, 20: 4072(P)
separation from silver by partition chromatography, 20: 4054
CHROMIUM ALLOYS
analysis for rhenium, spectrophotometric, 20: 3863(R) (IS-1200(Sect. C))
antiferromagnetism at 95 to 300°K, (E), 20: 4476(R) (IS-1200(Sect.P))
ductility of, effects of grain size and heat treatments on, 20: 4297(R) (IS-1200(Sect.M))
Al–Cr–Co–Mo–Ni–Ti, corrosion of Udimet 500 by lithium fluoride in cyclic high-temperature environment, 20: 4326 (TRW-ER-6561)
Al–Cr–Ge–Ti–V, properties of aged, 20: 4360(R) (AD-619399)
Al–Cr–Ti–V, properties of aged, 20: 4360(R) (AD-619399)
Cr–Co, crystallography of intermetallic compound Co_3Cr, 20: 4391(R) (ORNL-3870, pp 75-82)
Cr–Fe–Mo–Ni–Nb–W, welding properties of Inco IN-102, 20: 4306(R) (ORNL-3870, pp 194-213)
Cr–Fe–Mo–V, properties of H-11 Steel for use in space electric power systems, 20: 4379 (NASA-CR-54091)
Cr–Hf, phase studies, 20: 4297(R) (IS-1200(Sect.M))
Cr–Ni, aging and thermoelectric power of Alumel–Chromel thermocouples, 20: 4398 (TRG-Report-1021)
Cr–Re, bonding in electrolytic deposition on copper and molybdenum, 20: 4404(T) (JPRS-32773)
Cr–U, corrosive effects of liquid, on niobium, 20: 4077(R) (IS-1200 (Sect. E))
Cr–U, corrosive effects of liquid, on tantalum and yttrium, 20: 4077(R) (IS-1200(Sect. E))
Cr–U, melting point of, effects of impurities on eutectic, 20: 4077(R) (IS-1200(Sect. E))
Cr–V, nuclear magnetic resonance of, (E), 20: 4476(R) (IS-1200(Sect.P))
CHROMIUM BROMIDES
thermal capacity, 20: 3863(R) (IS-1200(Sect. C))
CHROMIUM CHLORIDES
reduction by vanadium(II), mechanisms of, 20: 3863(R) (IS-1200(Sect. C))
CHROMIUM COMPLEXES
with hypophosphites, mechanisms of, 20: 3863(R) (IS-1200(Sect. C))
CHROMIUM IONS
aquation of chloropentaaquo-, effects of mercury(II) complexes on, 20: 3863(R) (IS-1200(Sect. C))
electron transfer between cobalt(III) and divalent oxyanions as bridging groups in, 20: 3967
electron transfer between (II) and (III), kinetics of, 20: 3863(R) (IS-1200 (Sect. C))
CHROMIUM ISOTOPES Cr-51

diffusion in chromium at 1500°C to melting point, 20: 4385(R) (ORNL-3870, pp 15-19)
use for measuring particle residence times in fluidized beds, 20: 4106(T) (BNL-tr-43)
CHROMIUM OXIDES
analysis by x-ray fluorescence using promethium-147/aluminum source, 20: 3883 (ORNL-IIC-5, pp 154-81)
electromagnetic waves in, propagation of, (E/T), 20: 4476(R) (IS-1200(Sect.P))
pulmonary excretion of, effects of chronic cigarette smoking on, tracer study in dogs, 20: 3655 (BNWL-SA-224)
vibration modes in single-crystal, (T), 20: 4476(R) (IS-1200(Sect.P))
CHROMIUM STEEL
corrosion by Croloy 9M by potassium–sodium, effects of hydrogen and oxygen on, 20: 4322(R) (ORNL-3870, pp 205-7)
corrosion by sodium hydroxide, 20: 4100 (BW-67-2(a))
corrosion of Croloy 2¼ by sodium hydroxide in aqueous solutions and in liquid sodium and sodium hydride, 20: 4317 (BAW-1280-30)
decarburization of Croloy 9M by potassium–sodium, 20: 4322(R) (ORNL-3870, pp 305-7)
tensile properties of stain-hardened, 20: 4100 (BW-67-2(a))
Cr–Mo, corrosion of Croloy 2¼, by lead, 20: 4308(R) (ORNL-3870, pp 243-60)
CHROMIUM SYSTEMS
Al–Cr–Si–Ti–V, properties of aged, 20: 4360(R) (AD-619399)
Sb–Cr–Te, magnetic structure of CrSb–CrTe in, 20: 4358(R) (AD-438516)
CHROMOSOMES
aberrations in bone marrow, use in leukemia diagnosis of, 20: 3650
effects of culture density on mouse fibroblast, aberrant, 20: 3691
radiation effects on mouse fibroblast in culture, x, 20: 3691
radiation effects on human, 20: 3705(R) (AD-617601)
radioinduced aberrations in mouse liver, effects of age, 20: 3711(R) (NYO-3314-2)
radioinduced aberrations in Drosophila, x, 20: 3713(T) (JPRS-31514, (pp 29-43)
radioinduced aberrations in Drosophila, x, 20: 3714(T) (JPRS-31514, pp 44-58)
radioinduced aberrations in Drosophila, x, 20: 3715(T) (JPRS-31514, pp 59-64)
radioinduced aberrations of leukocyte, relation to leukemogenesis, 20: 3730
radioinduced aberrations of, in animal cells in culture, γ, 20: 3737
radiosensitivity of, in Saccharomyces, 20: 3717(T) (JPRS-31514, pp 77-91)
CHYMOTRYPSIN
radiation effects on albumin sensitivity to, γ, 20: 3687
CITRIFLEX PROCESS
flowsheets for enriched fuels in, 20: 4048(R) (NP-15406)
CIVILIAN DEFENSE
engineering and rescue operations at site of nuclear strike, 20: 4191(T) (JPRS-31014)
measures against nuclear weapon fallout, 20: 3797
measures against nuclear weapon fallout, 20: 3799
CLOUD CHAMBERS
charged-particle momentum in, determination of, (T), 20: 4583 (JINR-P-2371)
COAL
analysis for oxygen by neutron activation methods, 20: 3907
analysis of, use of radioisotope methods for, 20: 3884 (ORNL-IIC-5, pp 206-21)
COATINGS
book: *Polymer Coatings in Atomic Techniques*, 20: 3979
deposition of metallic niobium or tantalum, on finely dispersed particles, process for, 20: 4314(P)
deposition of pyrolytic-carbon, development of fluidized bed and rotary drum methods for, 20: 4343(R) (ORNL-3870, pp 266-89)
deposition of, development of arc-spray powder feeder for, 20: 4298 (LA-DC-7275)
development for yttrium protection against oxidation, 20: 4077(R) (IS-1200(Sect. E))
effects of fuel-element, on fission products in reactor loss-of-coolant accidents, 20: 4183(R) (ORNL-3843, pp 2-70)
removal from fuel elements, equipment and procedures for, 20: 4048(R) (NP-15406)
thickness measurements on, developments in use of radioisotopes for, 20: 4219 (ORNL-IIC-5, pp 182-205)
COAXIAL CABLES
pulse transmission in, improvement by reduction of skin effects, 20: 5218 (TID-21991)
COBALT
determination in plants by neutron activation methods, 20: 3901
determination in platinum by neutron activation, 20: 3863(R) (IS-1200 (Sect. C))
distribution between γ-alumina and molten chlorides, 20: 3959
thermodynamic properties of oxygen in liquid, 20: 4454
transformations in, mechanisms of diffusionless, 20: 4297(R) (IS-1200 (Sect.M))
COBALT ALLOYS
Al–Co–Fe–Ti–V, properties of aged, 20: 4360(R) (AD-619399)
Al–Cr–Co–Mo–Ni–Ti, corrosion of Udimet 500 by lithium fluoride in cyclic high-temperature environment, 20: 4326 (TRW-ER-6561)
Co–Cu, thermodynamic properties of oxygen in liquid, 20: 4454
Co–Fe, plastic deformation of, effects of temperature on, 20: 4297(R) (IS-1200(Sect.M))
Co–Fe, properties of Hiperco 27 for use in space electric power systems, 20: 4379 (NASA-CR-54091)
Co–Fe, thermodynamic properties of oxygen in liquid, 20: 4454
Co–Fe–Mo–Ni, properties of Maraging Steel for use in space electric power systems, 20: 4379 (NASA-CR-54091)
Co–Fe–V, properties of Hiperco 50 and Supermendur for use in space electric power systems, 20: 4379 (NASA-CR-54091)
Co–Hf, phase studies, 20: 4297(R) (IS-1200(Sect.M))
Co–Ni, thermodynamic properties of oxygen in liquid, 20: 4454
Co–Ni–Ti–Zr, properties of Nivco in space electric power systems, 20: 4379 (NASA-CR-54091)
Co–Y, crystal structure, 20: 4297(R) (IS-1200(Sect.M))
Cr–Co, crystallography of intermetallic compound, 20: 4391(R) (ORNL-3870, pp 75-82)
COBALT COMPLEXES
radiolyses of, recoil processes from gamma, 20: 3863(R) (IS-1200 (Sect. C))
COBALT(III) COMPLEXES
reactions with iron(II), mechanisms of, 20: 3863(R) (IS-1200(Sect. C))
COBALT IONS
electron transfer between chromium(II), europium(II), titanium(III), and vanadium(II) and trivalent, 20: 3967
COBALT ISOTOPES Co-57
energy levels of, from neutron reactions (n,d) with nickel-58 at 14 Mev, (E), 20: 4896
COBALT ISOTOPES Co-58
energy levels of, from proton reactions (p,d) with cobalt-59 at 22 Mev, 20: 4899
production by cobalt-59 photonuclear reactions, 20: 3863(R) (IS-1200 (Sect. C))
COBALT ISOTOPES Co-59
proton reactions (p,d) at 22 Mev, energy levels from, (E), 20: 4899
COBALT ISOTOPES Co-60
beta transitions in, comparative half lives of $\Delta I = 3$, (T), 20: 4874
beta transitions in, polarization from, (E), 20: 4880
dosimetry of gamma radiation from, calculator for use with teletherapy unit, 20: 3839
dosimetry of gamma radiation from, in tumors, calculator for, 20: 3855
production and properties for use as heat source, 20: 4277 (DP-1012)
use in therapy of, treatment planning using simulator, 20: 3827
COBALT OXIDES
analysis by x-ray fluorescence using promethium-147/aluminum source, 20: 3883 (ORNL-IIC-5, pp 154-81)
COBALT SYSTEMS
Co–WC, brazing to TZM alloy, use of boron–nickel–silicon alloy for, 20: 4307(R) (ORNL-3870, pp 238-42)
COINCIDENCE COUNTERS
performance for conversion coefficient and decay energy measurements, 20: 4843 (NP-15456)
performance of plastic scintillator meson, 20: 4560 (AD-618562)
COLLOIDS
metabolism of injected, in man, 20: 3822
preparation of hydrophilic or organophilic uranium oxide and/or thorium oxide, 20: 3969(P)
production of charged, in system for electric propulsion, 20: 4133 (N64-25007)
COLUMBIA RIVER
sodium-22 content in fish from, 20: 4161
COMMUNICATION SYSTEMS
research programs at M.I.T. electronics lab., 20: 4478(R) (TID-22179)
COMMUNICATION THEORY
research programs at M.I.T. electronics lab., 20: 4478(R) (TID-22179)
COMPUTER PROGRAMS
ANGOPT, for target angle optimization for nuclear reactions, FORTRAN IV, 20: 4842 (NASA-TN-D-3116)
CAT, for simultaneous heat and mass transfer partial differential equations, FORTRAN II for IBM7090/7094, 20: 4103 (NAA-SR-Memo-11099)
CORE, for design of gas-cooled reactor cores, FORTRAN IV for IBM 7044, 20: 5078 (GAMD-6676)
CYRCO, for reactor design, in FORTRAN II for IBM 704 and 7094, 20: 5059 (RT/FIMA(65)-1)

DIAN, for digital simulation of analog operation, 20: 4077(R) (IS-1200 (Sect. E))
FABCOST 8, for calculating reactor fuel element fabrication costs, 20: 5173(R) (ORNL-3870, pp 191-3)
FMC-N, 18-0, and 18-1, neutron cross section library for, 20: 4830 (GEMP-384)
for algebraic manipulation, 20: 4290(R) (UCRL-14360, pp 94-7)
for analysis of axially symmetric reactor shields, 20: 5181(R) (ORNL-3029)
for analyzing particle reaction and scattering experiments, 20: 4849(R) (UCRL-14360, pp 1-50)
for analyzing pulse-height spectra, 20: 4849(R) (UCRL-14360, pp 1-50)
for calculating fast-neutron dose rates in crew compartment of nuclear aircraft, 20: 4299(R) (ORNL-2711)
for calculating gamma angular and energy distributions from sources in homogeneous isotropic media, 20: 4999(R) (ORNL-2599)
for calculating gamma distribution from sources in infinite homogeneous media, 20: 4299(R) (ORNL-2711)
for calculating neutron angular distributions from shielding, 20: 5181(R) (ORNL-3029)
for calculation of energy levels and eigenvectors of d-configurations in crystalline electric fields, FORTRAN, 20: 5006(R) (ORNL-3870, pp 50-5)
for calculation of calcium-45 blood disappearance, FORTRAN for IBM-7074, 20: 3664(R) (TID-22324)
for calculation of Christoffel symbols, 20: 4290(R) (UCRL-14360, pp 94-7)
for criticality studies of reactor matrices, 20: 5060(R) (TID-22357)
for data simulation for instrumentation system accuracy, FORTRAN for CDC 3600, 20: 4289 (SC-DR-65-318)
for expansion of hemispheric meteorological data in antisymmetric surface spherical harmonic series, 20: 4153(R) (UCRL-14360, pp 73-85)
for graphic display of diffusion coefficients of gases in spherical solids, FORTRAN IV, 20: 4377 (NAA-SR-Memo-10741)
for hydrogen propellant properties, FORTRAN IV for IBM 7094, 20: 5177 (LA-3381)
for integration of Gibbs–Duhem equation for gas–liquid equilibrium data of metal systems, FORTRAN for IBM-7040, 20: 4375 (IS-1241)
for neutron flux in reactor lattices, FORTRAN, 20: 5077
for prediction of corrosion and hydriding of Zircaloy-4 under heat-transfer conditions on IBM-7094, 20: 4331
for properties of electron gas, 20: 4708(R) (UCRL-14360, pp 50-73)
for pump impellers, FORTRAN-63 for CDC-1604B, 20: 4088 (TIM-949)
for stress wave propagation in rock from surface nuclear explosions, 20: 4143 (AD-619969)
for thermocouple data processing, 20: 4999(R) (ORNL-2599)
for two-dimensional neutron diffusion in reactors, (T), 20: 5056 (CONF-654-22)
FORDAN, for simulation of digital differential analyzers, in FORTRAN, 20: 5214 (IS-T-33)
FORK, for determining equations of state, 20: 4708(R) (UCRL-14360, pp 50-73)
FOTRAC, for photon transport calculations using Monte Carlo method, 20: 4949(R) (UCRL-14360, pp 85-94)
GAMBLE-4, for neutron diffusion in heterogeneous reactor, FORTRAN IV for IBM 7044, 20: 5057 (GA-6540)
GRINDER, for analyzing gamma scattering from cylinders, 20: 5181(R) (ORNL-3029)
GUTS, for bubble chamber data, 20: 4476(R) (IS-1200(Sect.P))
HETAL, for fuel-rod neutron absorption, 20: 5123(R) (HPR-61)
HOT-1, for Neumann boundary conditions, 20: 4080 (WAPD-TM-535)
LIANA, for two-particle nuclear reaction distribution and cross section, FORTRAN, 20: 4844 (ORNL-TM-1234)
LINK, for neutron slowing-down and thermalization, 20: 4804 (KAPL-3098)
PLOT3D, for three-dimensional data plotting, in FORTRAN II, 20: 4291 (UCRL-14425)
RADF, for analytical data reduction in gas phase radiolysis experiments, FORTRAN II, 20: 3985 (RFP-624)
RED CROSS, for cross sections for fast reactor analysis, in FORTRAN IV for IBM 7090, 20: 5055 (BNWL-146)
SAFE-PCRS, for stress analysis of composite bodies of revolution, FORTRAN IV for IBM 7044, 20: 5033 (GA-6588)
SAHYB, for solving boundary- and initial-value problems, in FAP and FORTRAN, 20: 4287 (EUR-2519.e)
SALINE, for cost, heat, and material balance calculations on saline water conversion plants, 20: 3923 (ORNL-TM-1299)
Sampled Data Simulator, for fixed-frequency sampling and reconstruction system simulating, FORTRAN for CDC 3600, 20: 4288 (SC-DR-65-312)
SPCTRM, for neutron energy spectra, FORTRAN, 20: 4805 (ORNL-TM-1245)
SPRITE, for two-dimensional neutron diffusion in reactors, (T), 20: 5056 (CONF-654-22)
subroutines for character, line, and point cathode ray tube plotting, in FORTRAN 400, 20: 4292 (UCRL-14427-7)
TRACER, for reduced cells in lattices, 20: 3863(R) (IS-1200(Sect. C))
ZAM, for weather prediction, 20: 4153(R) (UCRL-14360, pp 73-85)

COMPUTERS
algorithms for, tabulations of, 20: 4286 (ANL-7054)
language for, description of ALGOL, 20: 4286 (ANL-7054)
language optimizer for CDC 6600, FORTRAN, 20: 4290(R) (UCRL-14360 (pp 94-7))
performance and uses of, 20: 4296
performance of PDP-4C, for neutron time-of-flight calculations, 20: 4245 (ORNL-P-1723)
programming of digital, using DIAN code, 20: 4077(R) (IS-1200(Sect. E))
programming of, analog conversion for digital, 20: 5214 (IS-T-33)
use for machine tool system control, 20: 5220 (UCRL-13185)
use for tensile tests analyses, 20: 4371 (EUR-2514.e)
use in calculation of chemical treatment schedules for tumors, 20: 5222 (UCRL-14505)
uses for automatic detection and diagnosis of malfunctions in arbitrary systems, (T), 20: 4222 (UCRL-13186)

CONCRETES
gamma attenuation in s-shaped, (E), 20: 4997(R) (EUR-2494.d)
gamma attenuation in, temperature distribution from, (T), 20: 5002
stress analysis of pressure vessels of prestressed, computer program for, 20: 5033 (GA-6588)
use in containment structures, 20: 4406(T) (ORNL-tr-873)

CONFERENCES
see also introduction to Report Number Index
High Activity Hot Laboratories, International Symposium on Working Methods in, Vol. I and II. Grenoble, June 15 to 18, 1965, 20: 4040
Radioactive Isotopes in Textile Research and Industry, Symposium of Federal Ministers for Scientific Research on Uses of, Lindau/Bodensee, July 8 to 10, 1964, 20: 4274
Uses of Radioisotopes in Nutritional Sciences and of Ionizing Radiation in Food Technology, Strasbourg, Oct. 1962, 20: 3685

CONNECTICUT YANKEE POWER REACTOR
design and development, July 1964–June 1965, 20: 5124(R) (NYO-3250-4)

CONTACTORS
design of flat-bed, for processing solid fissile materials, 20: 4049 (RL-SA-52)

CONVECTION
of heat and water vapor in atmosphere, 20: 4153(R) (UCRL-14360, pp 73-85)
oscillation in stratosphere, biennial, 20: 4150 (MIT-2241-7)

CONVECTION (FORCED)
boiling burnout heat flux for, at 1000 psi in annuli, (E), 20: 4105 (TID-22321)

COPPER
analysis for oxygen by neutron activation methods, 20: 3907
brazing stainless-steel-clad fins of, to stainless steel tubes, technique for, 20: 4307(R) (ORNL-3870, pp 238-42)
bremsstrahlung reactions (γ,π^0) at 166 Mev, angular distributions from, (E), 20: 4898
coating with chromium–rhenium alloys by electrolytic deposition, bonding in, 20: 4404(T) (JPRS-32773)
corrosion by cesium at 400°C, 20: 4337
determination in mixtures by x-ray fluorescence using promethium-147/aluminum and tritium/zirconium sources, 20: 3883 (ORNL-IIC-5, pp 154-81)
determination in plants by neutron activation methods, 20: 3901
diffusion in nickel at 800 to 1050°C, 20: 4363 (AEET/CD/31)
effects on grain boundary migration in aluminum, 20: 4389(R) (ORNL-3870, pp 61-4)
electric conductivity of, effects of low temperature on, 20: 4417
meson (μ^-) transitions in mesic atoms of, energy of, 20: 4825(R) (ANL-7081, pp 81-93)
oxidation of, effects of aluminum, nickel, and silver additions on, 20: 4320(R) (ORNL-3870, pp 70-4)
properties of, effects of low temperature on, 20: 4417
radiation from promethium-147 beta excited, 20: 3882 (ORNL-IIC-5, pp 51-71)
separation from silver by partition chromatography, 20: 4054
slip in neutron-irradiated, activation energy and mechanism for, 20: 4384(R) (ORNL-3870, pp 7-14)
sputtering by argon ions at 1.5 to 30 kev, yields from, (E), 20: 4546
sputtering by xenon ions at 1.5 to 30 kev, yields from, (E), 20: 4546
texture of rolled, determination with inverse pole figures of, 20: 4384(R) (ORNL-3870, pp 7-14)
thermodynamic properties of oxygen in liquid, 20: 4454
ultrasonic wave propagation in annealed and neutron-irradiated single crystals of, (E), 20: 5012

COPPER ALLOYS
Be–Cu, preparation by splatcooling and hot-pressing, 20: 4381(R) (NMI-8001.4)
Co–Cu, thermodynamic properties of oxygen in liquid, 20: 4454
Cu–Mg, solvent properties for rare earth elements in molten chloride salts, 20: 3865 (ANL-7064)
Cu–Ni, thermal capacity of, effects of magnetic order on, 20: 4320(R) (ORNL-3870, pp 70-4)
Cu–rare earth, magnetic properties and structure, 20: 4448
Cu–Sn, use in thin-film bolometers, 20: 4479(R) (TID-22179, pp 1-83)
Cu–Tb–Zn, crystallography, 20: 4391(R) (ORNL-3870, pp 75-82)
COPPER CHLORIDES
magnetic susceptibility, 20: 3863(R) (IS-1200(Sect. C))
COPPER COMPLEXES
crystal structure of copper, decachlorobis (propyl alcohol) penta-, 20: 3863(R) (IS-1200(Sect. C))
COPPER COMPOUNDS
with manganese nitrides, ferromagnetic properties of, 20: 4402(T) (ANL-Trans-230)
COPPER ISOTOPES Cu-63
energy levels of, from neutron reactions (n,d) with zinc-64 at 14 Mev, (E), 20: 4896
neutron reactions (n,d) at 14 Mev, energy levels from, (E), 20: 4896
nucleon lifetime in, lower limits for bound, (E), 20: 4853
COPPER ISOTOPES Cu-65
nucleon lifetime in, lower limits for bound, (E), 20: 4853
COPPER MINERALS
analysis of, use of radioisotope methods for, 20: 3884 (ORNL-IIC-5, pp 206-21)
COPPER OXIDES
solubility in borax at 760 to 900°C, 20: 3951
CORROSION LOOPS
components of sodium, review on, 20: 4330(T) (ORNL-tr-854)
design of boiling-potassium, 20: 4301(R) (ORNL-3870, pp 102-35)
design of thermal-convection, for lead corrosion studies, 20: 4308(R) (ORNL-3870, pp 243-60)
material specifications for testing in potassium, 20: 4380 (NASA-CR-54761)
refluxing capsules in, method for sealing, 20: 4301(R) (ORNL-3870, pp 102-35)
tests of potassium–sodium and sodium, on stainless steel and other structural materials, 20: 4318 (CNLM-5359)
CORTISONE
effects on content of alkaline phosphatase in cultured cancer cells, 20: 5217 (TID-21169)
COSMIC ALPHA PARTICLES
energy spectra of low-energy, solar modulation of, (E), 20: 4565
energy spectra of, primary source and interstellar propagation characteristics from, (T), 20: 4566
flux over New Mexico in 1962, 20: 4569
COSMIC PARTICLES
abundances and energy spectra of helium nuclei in, (T), 20: 4568
interactions in upper atmosphere, ionization production from, 20: 4729 (CNIE-PE-4)
COSMIC PROTONS
energy spectra of, primary source and interstellar propagation characteristics from, (T), 20: 4566
COSMIC RADIATION
absorption by ionosphere during geomagnetic storms, analysis of, (E), 20: 4736
detection and measurement of, instruments for, 20: 4252(T) (FTD-TT-64-1228)
effects on lower ionospheric ionization, (E), 20: 4737
effects on materials in space vehicles, 20: 4312
energy spectra of primary, at high altitude, 20: 4569
intensity of, geophysical aspects of variations in, 20: 4560 (AD-618562)
intensity variations in interplanetary media, (E/T), 20: 4522 (CNIE-PE-5)
intensity variations of primary, rigidity for solar diurnal, (T), 20: 4563
interactions in upper atmosphere, ionization production from, 20: 4729 (CNIE-PE-4)
origin of gamma and x, 20: 4562 (MIT-2098-174)
production and properties of, review of, (T), 20: 4564
radiation dose to man from, 20: 3731
reactions in atmosphere, neutrino production from, 20: 4561 (COO-818-64)
research program of IQSY-EQEX Indo-American expedition, 20: 4567
sodium-22 content in, 20: 4161
COSMOLOGY
evolution of universe, 20: 4771
stellar elements in theories of, heavy, (T), 20: 4534
CRATERS
formation by single-, double-, and triple-row charges, comparison of, 20: 4083 (SC-RR-65-478)
nuclear explosions in, effects on reduction of seismic signals, 20: 4167 (RM-3727(RAND))
CRISTOBALITES
radiation effects on phase transformations, 20: 4462
CRITICAL ASSEMBLIES
accidents involving, review of AEC, 1943 through 1964, 20: 4188 (TID-22268)
criticality studies of SEFOR core in ZPR-III, 20: 5120(R) (GEAP-4799)
design for AARR, safety analysis of, (E/T), 20: 5189 (ANL-6929)
neutron production in pulsed, bibliography for, 20: 5200 (TID-3571 (Suppl.1))
reactivity temperature coefficient of uranium dioxide–water lattices in, (E), 20: 5067
uranium-235 Doppler coefficient in ZPR II 45-A, 20: 5072
CRITICALITY STUDIES
for Army Reactor (SM-1A) core 3, 20: 5122 (HIT-3459-11(Vol.2))
for BSR-II, 20: 4299(R) (ORNL-2711)
for Peach Bottom Power Reactor, 20: 5118(R) (GA-6647)
for SEFOR reactor, 20: 5120(R) (GEAP-4799)
for Tower Shielding Reactor-II, 20: 5181(R) (ORNL-3029)
for TSR-II, 20: 4999(R) (ORNL-2599)
for TSR-II, 20: 4299(R) (ORNL-2711)
in NORA research reactor, 20: 5060(R) (TID-22357)
of fluidized-bed reactors, 20: 5125 (NYO-10732)
CROSS SECTIONS
for analysis of space-vehicle shielding, 20: 5181(R) (ORNL-3029)
CRUSTACEA
metabolism of cesium-137 by shrimp, 20: 3657 (CEA-R-2818)
CRYOGENICS
helium and hydrogen liquefier design and performance, 20: 4798
helium-3 cooling using Pomeranchuk effect, apparatus for, (E), 20: 4779(T)
materials for, properties of, 20: 4417
physics and techniques of low temperatures, conference on, 20: 4790
CRYOSTATS
design and performance of helium-3, 20: 4776
design for studying radiation effects on semiconductor barriers, 20: 4999(R) (ORNL-2599)
CRYSTAL STRUCTURE
determination from molecular structure, review on, 20: 5212 (BNL-930)
lattice dynamics of, Kikuchi-patterns for reciprocal, 20: 5009(T) (UCRL-Trans-1227)
CRYSTALLOGRAPHY
inverse pole figures in, method for obtaining, 20: 4384(R) (ORNL-3870, pp 7-14)
molecular structure in, review on, 20: 5212 (BNL-930)
phase problems in x-ray, solution of, 20: 3863(R) (IS-1200(Sect. C))
pole figures in hcp metals, method for determining, 20: 4304(R) (ORNL-3870, pp 171-83)
CRYSTALS
book: *Radiation Physics. III. Ionic Crystals*, 20: 4008
color center aggregation in, effects of pressure on, (E/T), 20: 4476(R) (IS-1200(Sect.P))
dislocations in, electron and x-ray diffraction analyses of, (T), 20: 5003 (CEA-R-2875)
neutron diffraction by powdered, effects of particle size on, 20: 5016(T)
radiation effects on organic polymer, at 75 to 300 kev, 20: 3987
space charge and vibration modes in ionic, (T), 20: 4476(R) (IS-1200 (Sect.P))
structure of, relativistic electronic, (T), 20: 4476(R) (IS-1200(Sect.P))
CSREX PROCESS
x-ray reflection from lattices of, relative intensity in, (E), 20: 5010
CURIUM ISOTOPES Cm-244
separation from other transplutonium elements, design of hot cells for, 20: 4065
CURIUM OXIDES
preparation of microspheres of, by sol-gel process, 20: 4344 (ORNL-P-1725)
CUTTING TOOLS
design for irradiated materials, 20: 4129
design for use on radioactive materials, 20: 4351
CYANIDE COMPLEXES
with mercury, reactions of, 20: 3863(R) (IS-1200(Sect. C))
CYCLOPENTADIENYL COMPOUNDS
with iron and manganese carbonyl, crystal structure, 20: 3863(R) (IS-1200(Sect. C))
CYCLOTRON RADIATION
production in magnetically confined plasma by relativistic electrons, (T), 20: 4950(T) (UCRL-Trans-1261(L))
CYCLOTRONS
beam polarization in Saclay, 20: 4516
design and performance of Saclay variable-energy, 20: 4516
development of HIVRC, 20: 4491(R) (ANL-7081, pp 78-80)

ion source design and performance for, 20: 4519
proton depolarization table for resonances in, 20: 4520
research at 60", 20: 4824(R) (ANL-7081, pp 70-7)
uses of AVF, in nuclear physics, 20: 4497 (KFK-310)
CYLINDERS
blast effects on, (E/T), 20: 4132 (AWRE-O-93/65)
heat and mass transfer in, computer program for partial differential equations for simultaneous, 20: 4103 (NAA-SR-Memo-11099)
magnetic flux quantization and generalized pairing in superconducting, (T), 20: 4784
thermal stress analysis of thick-wall, (T), 29: 4076 (HIC-1-1564-3(Vol.2))
CYSTEINE
radiosensitivity effects on hypothalamus–pituitary system, 20: 3703
CYSTINE
incorporation of selenium-75 in, biosynthetic, 20: 3661 (NP-15594)
metabolism in mice, tracer study, 20: 3661 (NP-15594)
CYTOLOGY
of bone marrow during regeneration, 20: 3789
of radiation effects on onion roots, 20: 3764
of radiation injuries of oral epithelium, 20: 3744
CYTOPLASM
radiation effects on cyclosis in Nitella, x, 20: 3698

D

DATA RECORDING SYSTEMS
design of computer-based, (E/T), 20: 4476(R) (IS-1200(Sect.P))
development for HBWR, 20: 5123(R) (HPR-61)
performance of automatic, 20: 4226
DATA TABULATIONS
computer algorithms, 20: 4286 (ANL-7054)
decay constants, half lives, and specific activities of radioisotopes, 20: 4845 (ORNL-TM-1318)
gamma cross sections from 0.01 to 10 Mev, 12-group, 20: 4996 (AWRE-O-79/65)
gamma production cross sections in neutron reactions at 0.1 to 15 Mev, 20: 4849(R) (UCRL-14360, pp 1-50)
geomagnetic and solar data for April–June 1965, 20: 4750
neutron transport in slab geometry, tables of functions for, 20: 4803 (INR-630/IX-A/PR)
plotting of, computer program for three-dimensional, 20: 4291 (UCRL-14425)
proton depolarization for resonances in cyclotrons, 20: 4520
stratospheric isobaric height conditions and wind temperature during IGY, 20: 4151 (MIT-2241-14)
DECONTAMINATION
equipment and procedures for milk, bibliography on, 20: 3872 (EUR-2507.d)
methods of, for reservoir water, 20: 4068
DECONTAMINATION OF EQUIPMENT
methods of, at Harwell, 20: 4212
methods of, at KFA–Julich, 20: 4093
personnel radiation protection in, at Casaccia hot laboratory, 20: 4211
DEHYDROGENASES
radiation effects on content of isoenzymes of, in tumors undergoing therapy, 20: 3845
radiation effects on blood levels of lactic, in monkeys, γ, protons, and x, 20: 3692
DENMARK
radiation protection in, laws and regulations for, 20: 4180 (NP-15571)
DENSITOMETERS
design of optical, for charged-particle emulsion tracks, (E/T), 20: 4476(R) (IS-1200(Sect.P))
development of beta-absorption, 20: 4048(R) (NP-15406)
self-compensation system for, 20: 4273
DETERGENTS
radioinduced degradation of sulfonate, 20: 4025
DETONATION WAVES
calculation of two-dimensional steady-state, by method of characteristics, (T), 20: 5221 (UCRL-14223)
stability and structure of, in gases, 20: 3918 (LA-DC-7276)
DEUTERIUM
deuteron reactions (d,n) at 1.9 to 3.7 Mev, polarization angular distributions from, (E), 20: 4895
diffusion in EN58B low-carbon steel, coefficient for, 20: 4366 (AWRE-O-90-65)
effects on dipole moments of acetonitrile and fluoromethane, 20: 3958
effects on dipole moments of acetylene, 20: 3977
effects on infrared spectra of dibromoborane, 20: 3940
effects on infrared spectra of tin hydride, 20: 3942
effects on recoil tritium reactions with alkanes, 20: 4024
effects on thermodynamic properties of hydrogen selenide and hydrogen sulfide, 20: 3950
exchange between diboranes, intermediates in, 20: 3963
exchange with hydrogen in methane, 20: 3980
gamma reactions (γ,n) at 2.4 to 3.9 Mev, cross sections for, (E), 20: 4802 (IDO-17115)
ion cyclotron wave absorption and propagation in bounded plasma of, numerical model for, (T), 20: 4983
proton elastic scattering at 31 Mev, differential cross sections for, 20: 4929
DEUTERIUM SYSTEMS
D–H, ion cyclotron wave production in plasma of, optimum, (E/T), 20: 4984
DEUTERONS
angular distributions from fluorine-19 (He-3, d) reactions at 9.5 and 10 Mev, (E/T), 20: 4908
binding energy, (E), 20: 4856
interactions with deuterons, coupled equation for elastic, (T), 20: 4672
interactions with electrons, meson exchange in, (E), 20: 4580 (AD-618662)
interactions with gamma rays at 77.3 Mev, analytical wave functions for ground state from disintegration, (T), 20: 4592
interactions with protons at 155 Mev, polarization in elastic, (E), 20: 4595
interactions with alpha particles at 29.3 and 41.6 Mev, deuteron breakup from, (E), 20: 4596
interactions with neutrons, binding energies and cross sections for, (T), 20: 4614
interactions with protons at 31 Mev, cross sections for, 20: 4929
production of polarized, 20: 4823(R) (ANL-7081, pp 36-69)
reactions (d,α_0), (d,p_0), and (d,p_1) with oxygen-16 at 300 to 1,000 kev, fluorine-18 energy levels from, (E), 20: 4870
reactions (d,γ) with beryllium-9 and nitrogen-14 at 0.5 to 5.5 Mev, excitation curves and angular distributions from, (E), 20: 4884
reactions (d,He-3) with nuclei, level studies from, 20: 4824(R) (ANL-7081, pp 70-7)
reactions (d,n) and (d,p) with carbon-12, angular distributions for, (E), 20: 4849(R) (UCRL-14360, pp 1-50)
reactions (d,n) with lithium-7, alpha spectra from beryllium-8 breakup in, (E), 20: 4869
reactions (d,n) with deuterium at 1.9 to 3.7 Mev, polarization angular distributions from, (E), 20: 4895
reactions (d,p) with magnesium-25 at 7 and 8 Mev, (E), 20: 4849(R) (UCRL-14360, pp 1-50)
reactions (d,p) with holmium-165, holmium-166 energy levels from, (E), 20: 4889
reactions (d,p) with nuclei at 10 to 30 Mev, spin-orbit coupling in, (T), 20: 4827 (CEA-Bib-60)
reactions with carbon-14 and nitrogen-14 at 1.9 to 6.7 Mev, bound states from, (E), 20: 4905
reactions with neptunium-237, products of, 20: 4928
reactions with nuclei, cross sections and level studies from, 20: 4822(R) (ANL-7081, pp 22-35)
reactions with nuclei, angular momentum transfer, cross sections, and level studies from, 20: 4823(R) (ANL-7081, pp 36-69)
reactions with nuclei, optical potential for, (T), 20: 4879
wave equations for, tensor forces in Schroedinger, (T), 20: 4597
wave functions for ground-state, (T), 20: 4592
DIARRHEA
radioinduced, etiology in man, 20: 3851
DIDO REACTORS
gamma and neutron heating of graphite, magnesium, and polyethylene, in channels of FRJ-2, 20: 5202
reactivity perturbation in FRJ-2, safety instrumentation response to, 20: 5197 (JUL-239-RE)
DIET
of cattle, effects on strontium-89 and strontium-90 metabolism, 20: 4162
radiosensitivity effects of, in rats, 20: 3766
DIFFERENTIAL EQUATIONS
solution of boundary- and initial-value problems, computer program for, 20: 4287 (EUR-2519.e)
solution of second-order partial, 20: 4999(R) (ORNL-2599)
solution of simultaneous heat and mass transfer partial, computer program for, 20: 4103 (NAA-SR-Memo-11099)
DIFFRACTION
theory of electron and x-ray, by crystal dislocations, 20: 5003 (CEA-R-2875)
DIFFUSION
measurement of, use of alpha spectrometry for, 20: 4412
tracer solutes in metals, bibliography on, 20: 4383 (ORNL-3795(Pt.2))
DIGITOXIN
incorporation of tritium in, use of carriers for, 20: 3810
DILATOMETRY

equipment for thermal, 20: 4476(R) (IS-1200(Sect.P))
DIODES
radiation effects on silicon, 20: 4999(R) (ORNL-2599)
radiation effects on silicon, 20: 4299(R) (ORNL-2711)
radiation effects on computer and rectifier, in SNAP environment, 20: 4262 (NP-15610)
radiation effects on electric properties of, role of doping in, 20: 4265
use of germanium, for gamma spectrometric determination of carbon in steel, 20: 3894
use of semiconductor tunnel, as pressure transducers, 20: 5216 (SC-TM-65-457)
DIOXANE
dioxane–$Sn(ClO_4)_3$, magnetic susceptibility of hydrated, (E), 20: 3930
DIRECT ENERGY CONVERSION DEVICES
conference, 20: 4575
DISASTERS
behavior of population during, 20: 4200
DISCONNECTS
design for control rods and drive mechanism, 20: 5051(P)
DISEASES
effects of rachitic, on calcium-47 metabolism in bones, 20: 3672
DISKS
stress analysis of axisymmetric, with variable thickness, (T), 20: 4075 (GA-6267)
DISPLACEMENT GAGES
design for reactor control rods, 20: 5048(P)
DODECYLAMINE
solvent properties for plutonium, 20: 4048(R) (NP-15406)
DOGS
deposition of gold-198 colloids in liver of, 20: 3680
deposition of gold-198 colloids in liver of, 20: 3681
fatty acid synthesis in lung tissue of, tracer study, 20: 3656 (BNWL-SA-225)
pulmonary excretion of particles in, effects of chronic cigarette smoking on, 20: 3655 (BNWL-SA-224)
radiation effects on immune reactions to renal transplants in, γ, 20: 3729
respiration in, measurement using nuclear image amplifier with technetium-99m and xenon-133, 20: 3802 (ORNL-IIC-5, pp 239-42)
tissue transplants in, growth of bone marrow in spleen, 20: 3652
DOORS
design for irradiation facility, 20: 4096(P)
DOSIMETERS
design of phosphate glass, 20: 4258(P)
development of thermoluminescent, for gammas and neutrons, 20: 4236 (BNL-9605)
DOUNREAY FAST REACTOR
design and performance of, 20: 5165
fuel elements for, design of facility for testing, 20: 5153
DROPS
formation of, effects of time on, 20: 4077(R) (IS-1200(Sect. E))
DROSOPHILA
radiation effects on, genetic, x, 20: 3713(T) (JPRS-31514, pp 29-43)
radiation effects on, genetic, x, 20: 3714(T) (JPRS-31514, pp 44-58)
radiation effects on, genetic, x, 20: 3715(T) (JPRS-31514, pp 59-64)
DRUGS
antitumor, effects on tumor cells in culture, morphological, 20: 3796
effects on human embryos, teratogenic, 20: 3747
use of cytotoxic, for treatment of polycythemia, 20: 3835
DRYING
methods for sample, for neutron transmission measurements, 20: 3914 (AERE-M-1654)
DUSTS
particle size in, method for determining, 20: 4149 (AD-623639)
removal from gas stream, design of electrostatic apparatus for, 20: 4726(P)
DYES
dose of Hypaque, effects on radiation dose reduction in urography, 20: 3857
DYSPROSIUM
determination in hydrochloric acid or methanol–nitric acid media, spectrophotometric, 20: 3888 (TID-22402)
magnetocaloric effect in, (E), 20: 4420
thermal conductivity, (E/T), 20: 4419
DYSPROSIUM CHLORIDES
crystal structure, 20: 3863(R) (IS-1200(Sect. C))
phase studies, 20: 3863(R) (IS-1200(Sect. C))
DYSPROSIUM OXIDES
use in thermal neutron detector, 20: 4260(P)
Al_2O_3–Dy_2O_3, radiation effects on, in-pile, (E), 20: 5115(R) (GA-4967)
Dy_2O_3–Fe_2O_3, crystal structure and magnetic properties, 20: 4411
DYSPROSIUM SULFIDES
homogeneity regions in, 20: 3938

E

ECOLOGY
radiation effects on water balance of forests, 20: 3653 (BNL-8466)
ELECTRIC CHARGES
interactions with magnetic monopoles, spin angular momentum in, (T), 20: 4684
ELECTRIC CONDENSERS
impedance of spirally wound, calculations of, (T), 20: 4217 (MATT-378)
radiation effects on, in SNAP environment, 20: 4262 (NP-15610)
ELECTRIC CONDUCTIVITY
effects of wall, on MHD channel flow with heat transfer, (T), 20: 4703 (AD-619101)
ELECTRIC DISCHARGE
effects on gas flow in sample transport lines, (E), 20: 4476(R) (IS-1200(Sect.P))
plasma acceleration by, semitoroidal system for, 20: 4134 (SEL-63-120)
plasma production by, in helical magnetic field, (E), 20: 4937 (IAE-907)
striations in, properties of, 20: 4946 (ORNL-TM-1307)
ELECTRIC FIELDS
effects on radiolysis of gases, equipment and method for investigation of, 20: 4022
effects on solidification of metals, 20: 4297(R) (IS-1200(Sect.M))
plasma oscillations in nonuniform static, (T), 20: 4980
ELECTRIC GENERATORS
design of homopolar, with improved efficiency and power capacity, 20: 4231(P)
ELECTRIC INSULATORS
testing for Tory IIC, 20: 5186 (UCRL-13095(Vol.2))
ELECTRIC POWER
production and distribution in Spain, 20: 4081
production using thermonuclear reactions, (E/T), 20: 4992
ELECTRIC PROBES
performance for plasma diagnostics, characteristics for, (E), 20: 4969
use for cesium plasma diagnostics, (E), 20: 4958
ELECTRICITY
production using thermionic cells and reactors, 20: 4576(P)
ELECTRODES
design for thermionic converters, use of extended surfaces in, 20: 4574
electron beam currents between plane, single-collision model for, 20: 4704 (NASA-TN-D-3058)
properties of niobium and rhenium thermionic collector, 20: 4570(R) (AD-614592)
ELECTRODYNAMICS
evolution equation for system of relativistic charged particles in, 20: 4723
ELECTROMAGNETIC FIELDS
effects on oscillation retardation in plasma columns, (T), 20: 4985
extrapolation from values of spherical harmonic expansion coefficients in spherical region, (T), 20: 4638 (AD-617965)
interactions of pure singular, gravitational tensor field from, (T), 20: 4763
interactions with missiles having ionized wakes, (T), 20: 4730 (SC-DC-65-1797)
theory of free, invariance of Maxwell's equations in, 20: 4710
ELECTROMAGNETIC LENSES
development for moderate-rigidity charged-particle beams, 20: 4509 (UCRL-14343)
performance for antiproton-proton beam separation, 20: 4496 (JINR-P-2375)
ELECTROMAGNETIC PUMPS
design for sodium, 20: 4077(R) (IS-1200(Sect. E))
ELECTROMAGNETIC SEPARATION
operation of sector field separator at Seibersdorf, 20: 4283 (SGAE-PH-27/1965)
program at ORNL for, review of, 20: 4282 (ORNL-3861)
ELECTROMAGNETIC WAVES
amplification of ionospheric, resonance, (T), 20: 4728 (AD-618118)
emission by charged particles moving above diffraction grid, 20: 4622
emission by electron beams moving over diffraction gradient, 20: 4621
interactions with electrons and protons in magnetosphere gyroresonance radiation from, (T), 20: 4747
propagation in chromium oxides, equations for, (E/T), 20: 4476(R) (IS-1200(Sect.P))
propagation in homogeneous, Lorentzian plasma, nonlinear effects in, (T), 20: 4962
propagation in hot magnetoplasma, Boltzmann-Vlasov equation for, (T), 20: 4978
propagation of dipolar, along plasma column, (E/T), 20: 4956
use in materials testing, conference on, 20: 4116
ELECTROMAGNETISM
theory of magnetoelectric effect symmetry, 20: 4476(R) (IS-1200(Sect.P))

ELECTRON BEAMS
current between plane electrodes, single-collision model for, 20: 4704 (NASA-TN-D-3058)
deflection by high-frequency fields, production of coherent radiation by, 20: 4624
dose distribution of, inhomogeneity of, 20: 4204
dose distribution in liquids and spherical samples, 20: 4204
effects on germanium tunnel diodes, equivalence of stress and, 20: 4264
effects on infrared properties of germanium at 40 to 60 Mev, (E), 20: 4468
effects on rat lungs, effects of dose fractionation on histological, 20: 3700
electromagnetic wave emission by, moving over diffraction gradient, 20: 4621
interactions with plasma, (E), 20: 4945 (ORNL-TM-1306)
interactions with warm plasmas, (T), 20: 4947 (SU-IPR-13)
interactions with plasma, computer study of, 20: 4948(R) (TID-22179, pp 85-175)
interactions with plasma, long-wave electron oscillations in, (E), 20: 4940 (IAE-932)
ion density in, in gases, 20: 4722
scattering by gold at 26 to 261 kev, Mott asymmetry function for double, (E), 20: 4881
stability in accelerator storage rings, transverse resistive, (T), 20: 4500 (LNF-65/27)
trapping by magnetic fields, mechanisms of, 20: 4948(R) (TID-22179, pp 85-175)
use in chemical analysis, equipment for, 20: 3912
use in oral tumor therapy, device for beam direction in, 20: 3833
ELECTRON-DIFFRACTION ANALYSIS
methods for molecular structure of gases, 20: 3863(R) (IS-1200(Sect. C))
ELECTRON MICROSCOPY
sample preparation for, small highly radioactive, 20: 4386(R) (ORNL-3870, pp 20-6)
ELECTRON PAIRS
annihilation of ^3S state of, Bogoliubov canonical transformation for single photon, (T), 20: 4594
production in electron scattering by nuclei, differential cross section for trident, (T), 20: 4604
ELECTRON SOURCES
design and operation of plasma-producing, 20: 4948(R) (TID-22179, pp 85-175)
ELECTRONIC EQUIPMENT
design for energy measurements on exploding wires, (E), 20: 4481 (UCRL-14170)
development for use in space vehicles, 20: 4312
development in Germany, 20: 4225
operation in drift tube of Princeton-Pennsylvania Accelerator, (E), 20: 4507 (PPAD-2137-560)
radiation effects on, in SNAP environment, 20: 4262 (NP-15610)
ELECTRONICS
radiation effects in, conference on, 20: 4266
ELECTRONS
angular distributions and energy spectra in bubble chambers, (T), 20: 4240 (JINR-P-2277)
angular distribution and energy of, from proton reactions with helium, (T), 20: 4558
bremsstrahlung emission from energetic, in thermal plasma, (T), 20: 4982
Cherenkov radiation from moving sheets of, 20: 4623
decay of, charge conservation studies in, (E/T), 20: 4536 (COO-818-61)
decay of, lifetime from charge-nonconserving, 20: 4551
density and temperature variations in F region of ionosphere, (E), 20: 4755
density anomaly in ionospheric F region, from longitudinal current system, (T), 20: 4749
density distributions in ionospheric D region, (E/T), 20: 4754
density distribution and temperature in ionosphere, (E), 20: 4760
density distributions in Lorentzian plasma, calculation of, (T), 20: 4961
density in afterglow plasma, 20: 4970
density in atmosphere, geomagnetic and temporal effects on, (E), 20: 4746
density in hydrogen ion excited and ground states, numerical calculation for, (T), 20: 4555
density in plasma, laser interferometer measurement of, 20: 4948(R) (TID-22179, pp 85-175)
density in plasma, method for measuring, 20: 4955
density in plasma, method for determining, (E/T), 20: 4967
diffraction by crystal dislocations, theory and uses of, 20: 5003 (CEA-R-2875)
dosimetry of high-energy, methods for, (T), 20: 4505 (ORNL-P-1738)
effects on atomic equation of state, corrections for, (T), 20: 4540 (UCRL-14364)
effects on carbon disulfide, 20: 4028
effects on carbon dioxide–methane, carbon monoxide effects on formaldehyde yields in, 20: 3981 (AERE-R-5051)
effects on gaseous ammonia, 20: 4021
effects on isomerization of benzene-butene-2 mixtures, 20: 4014
effects on methane–nitrogen mixtures at 1 Mev, 20: 3982(R) (AGN-8156)
effects on monomers and polymers in production of textiles, 20: 4031
effects on organic polymer crystals at 75 to 300 kev, 20: 3987
effects on para-polyphenyls, π electron excitation cross section for, (T) 20: 3991
effects on paramagnetic centers in sodium nitrates, 20: 3988
effects on piezoelectric quartz films, 20: 4463
effects on polytetramethylene oxide, 20: 3999
emission from thermionic cathodes, cesium fluoride effects on, 20: 4572 (EUR-2283.d)
emission of δ-ray, from heavy ions reacting in matter, (T), 20: 4541 (UCRL-16405)
energy distribution in ionospheric F region, photoelectron contribution to, (T), 20: 4753
energy levels in diatomic molecules, 20: 3863(R) (IS-1200(Sect. C))
energy loss in ionospheric D region, 20: 4727 (AD-618054)
energy losses in solids, characteristic, (T), 20: 5015
energy spectra and pitch-angle distributions of geomagnetically trapped, from high-altitude explosions, 20: 4732 (UCRL-14368-T(Rev.1))
energy spectra of geomagnetically trapped, from Starfish detonation, 20: 4731 (UCRL-7659-T(Rev.1))
interaction frequency in plasma, third harmonic current generation from velocity-dependent, (T), 20: 4885
interactions with magnetically trapped plasma, relativistic, (T), 20: 4950(T) (UCRL-Trans-1261(L))
interactions with protons at 700 to 1100 Mev/c, cross sections for, (E/T), 20: 4591 (UR-875-108)
interactions with neutrinos, experiment for detecting, 20: 4848 (UCRL-12085(Pt.2))
interactions with phonons and plasmons in plasma, hamiltonian for, (T), 20: 4944 (ORNL-3871)
interactions with protons, polarized hydrogen target for, 20: 4637
interactions with magnetospheric electromagnetic waves, gyroresonance radiation from, (T), 20: 4747
interactions with deuterons, meson exchange in, (E), 20: 4580 (AD-618662)
interactions with protons, cross sections for inelastic, (E), 20: 4581 (AD-618663)
interactions with electrons first Born approximation including anapole for, (T), 20: 4612
interactions with positrons, first Born approximation including anapole for, (T), 20: 4612
interactions with protons, two-photon effects in elastic, 20: 4630
lifetime of K-shell, in iodine, (E), 20: 4536 (COO-818-61)
lifetime of K-shell, in iodine, (E), 20: 4551
mixing with high energy ions for plasma injection, device for, 20: 4993(P)
mobility in helium gas at 2.2 – 4.2°K, (E/T), 20: 4788
oscillations in hot plasma of, longitudinal nonlinear, (T), 20: 4986
pair distribution function of classical gas of, 20: 4708(R) (UCRL-14360, pp 50-73)
properties of gases of, computer program for calculating, 20: 4708(R) (UCRL-14360, pp 50-73)
reactions of free, with liquid helium, 20: 4787
reactions with atoms, cross sections for optically disallowed transitions in, (T), 20: 4552
reactions with germanium and silicon at 10 to 60 Mev, effects of, (E), 20: 4508(R) (RPI-328-40)
reactions with nuclei, first Born approximation including anapole for, (T), 20: 4612
reactions with solids in vacuum, transition radiation from, (E/T), 20: 5008(T) (ORNL-tr-872)
reactions with strongly ionized p^2 ions, excitation in, (T), 20: 4543
reflection from photon waves, 20: 3863(R) (IS-1200(Sect. C))
scattering by boron-10 and -11, form factors for elastic, 20: 4841 (LAL-1140)
scattering by germanium, gold, nickel, and silver films, differential cross sections for multiple, (E), 20: 4485
scattering by gold at 121 kev, Born approximation for differential cross section and polarization from elastic, (T), 20: 4545
scattering by hydrogen, differential cross sections and inelastic transitions for, (T), 20: 4549
scattering by metals at 6–40 kev, radiation spectra from, (E), 20: 5017
scattering by nuclei, magnetic, (T), 20: 4831 (HEPL-272)
scattering by nuclei, electric and magnetic moment effects on elastic, (T), 20: 4840 (LAL-1140)
scattering by nuclei, differential cross section for trident pair production from, (T), 20: 4604
scattering by silver, surface plasmon excitation radiation from, (E),

20: 5017
temperature in ionization phase of pulsed discharge in hydrogen, (E), 20: 4714
ELECTROSTATIC FIELDS
determination in spark chambers, (T), 20: 4241 (JINR-P-2364)
nuclear quadrupole spectra in asymmetric gradients of, (T), 20: 4867
ELECTROSTATIC LENSES
electrode equivalent length for charged-particle beams, (T), 20: 4515
ELECTROSTATIC PRECIPITATORS
design for removing dust particles from gas streams, 20: 4726(P)
ELEMENTARY PARTICLES
book: *Elementary Particle and High Energy Physics*, 20: 4695
classification of, Poincaré group for, (T), 20: 4664
decay of, dynamics and symmetries of nonleptonic, (T), 20: 4676
dosimetry of high-energy, methods for, (T), 20: 4505 (ORNL-P-1738)
field theory for zero mass, 20: 4660
field theory for, unified, 20: 4646 (NYO-3399-40)
interaction potentials of, resonance narrowing and Pomeranchuk repulsion for, (T), 20: 4686
interaction resonances of, inelastic effects in N/D calculations on, 20: 4849(R) (UCRL-14360, pp 1-50)
interactions and properties of, (T), 20: 4636
interactions and properties of, review of, 20: 4620
interactions at high energy, spin effects in Regge pole theory for, (T), 20: 4633
interactions in Bev range, elastic and inelastic strong, (T), 20: 4696
interactions of hadrons, C and T violation in electromagnetic, (T), 20: 4682
interactions of many-body systems of, review of, (T), 20: 4701
interactions of spin $\neq 0$, complex angular momentum theory for, (T), 20: 4697
interactions of, analysis using rotational invariance, 20: 4849(R) (UCRL-14360, pp 1-50)
interactions of, axial-vector current and dispersion relations in weak, (T), 20: 4663
interactions of, conservation laws for strong, (T), 20: 4849(R) (UCRL-14360, pp 1-50)
interactions of, collision lifetime matrix for, (T), 20: 4651
interactions of, complex angular momentum in three-particle states in, (T), 20: 4680
interactions of, classification of C-noninvariant electromagnetic, (T), 20: 4600
interactions of, C, T noninvariance in minimal electromagnetic, (T), 20: 4601
interactions of, C-violation model in semistrong, 20: 4681
interactions of, $|\Delta I| = \frac{1}{2}$ rule for weak, (T), 20: 4635
interactions of, effective range theory and uncoupled phase method in multichannel, 20: 4690
interactions of, explicit wave functions for any spin, (T), 20: 4613
interactions of, final-state expressions for five-, four-, and three-particle, (T), 20: 4476(R) (IS-1200(Sect.P))
interactions of, Faddeev formalism for four-body, (T), 20: 4675
interactions of, gauge coordinate group for strong, 20: 4656
interactions of, group theoretical properties of complex angular momenta for, (T), 20: 4700
interactions of, Hamiltonian theories and symmetry groups in, 20: 4693
interactions of, multiple poles in scattering Green function for, (T) 20: 4662
interactions of, parity determination by many-body, (T), 20: 4849(R) (UCRL 14360, pp 1-50))
interactions of, phenomenological study of weak, (T), 20: 4634
interactions of, phase-space for four-particle final states in, (T), 20: 4658
interactions of, phase space for five-particle final states in, (T), 20: 4659
interactions of, S-matrix from probability amplitude in two-body, 20: 4687
interactions of, structure of two-body amplitudes for, (T), 20: 4668
interactions of, Shmushkevich's method for charge-independent theory for, (T), 20: 4667
interactions of, three-body unitarity integral for, (T), 20: 4647 (TID-22274)
interactions with electromagnetic potentials, baryon mass spectra from, (E/T), 20: 4476(R) (IS-1200(Sect.P))
magnetic moments of, Dashen-Lee sum rules for, (T), 20: 4598
model for, relativity and unitarity in SU(6) supermultiplet, 20: 4685
motion of many-body systems of, relativistic equations for, (T), 20: 4766
photoproduction of, D-wave contributions to, (T), 20: 4849(R) (UCRL-14360, pp 1-50)
polarization of spin-one, theory of covariant, 20: 4476(R) (IS-1200 (Sect.P))
reactions with nuclei, unified theory for, 20: 4837 (JINR-P-2310)
resonance of spin one-half, in time-dependent magnetic field, (T), 20: 4648
scattering of identical, nonrelativistic time-dependent theory of, 20: 4655
scattering of, singularities of S-matrix for, (T), 20: 4640 (IC/65/75)
scattering of, solutions for two-body, (T), 20: 4476(R) (IS-1200(Sect.P))
scattering on atoms, effect on stopping by elastic collisions, 20: 4547
scattering solutions of the Biedenharn symmetric Dirac-Coulomb hamiltonian, (T), 20: 4476(R) (IS-1200(Sect.P))
scattering wave functions for Dirac, (E/T), 20: 4476(R) (IS-1200(Sect.P))
spin matrix equations of, analytic functions for, (T), 20: 4476(R) (IS-1200(Sect.P))
statistics of, determination of, 20: 4694
symmetries for, (T), 20: 4475(R) (ANL-7081, pp 95-119)
symmetries for, review of, (E/T), 20: 4641 (IC/65/76)
symmetry for, octet model for unitary, (T), 20: 4698
symmetry for, parametric representation of kinetic moment operators for SU(3), (T), 20: 4652
symmetry model for, parametric representation of kinetic-moment operators in SU(4), 20: 4654
symmetry models for, linear representations of non-compact $\bar{S}U(3)$, 20: 4688
symmetry models for, representations of $S\bar{U}_4(NU\frac{1}{2})$ in, 20: 4689
theories of relativistic single, position operators in, 20: 4476(R) (IS-1200(Sect.P))
theory for, nonabelian-gauge quantum field, 20: 4699
wave equations for spin one and three-halves, (T), 20: 4476(R) (IS-1200(Sect.P))
ELEMENTS
abundance curve for, cosmic, (T), 20: 4534
determination of, estimation of upper limits for activation methods of, 20: 3898
ELK RIVER POWER REACTOR
reactivity measurements in, (T), 20: 5112 (CEND-507)
EMBRYOS
effects of teratogens on human, 20: 3747
radiation effects on retinal development in, x, 20: 3725
viability of mouse, from x irradiated father, effects of genotype on, 20: 3711(R) (NYO-3314-2)
ENDOCRINE GLANDS
function of, effects of pituitary harmones on, 20: 3809
ENERGY
conversion and storage of, conference on, 20: 4575
deposition in fluids by fission fragments, calculation of, 20: 3982(R) (AGN-8156)
ENGINEERING
research programs at Ames Laboratory, July 1964–June 1965, 20: 5213(R) (IS-1200)
ENZYMES
radiation effects on induction of β-galactosidase and galactoside permease, mechanism for uv, 20: 3688
radiation effects in monkeys on blood levels of glutamic oxaloacetic transaminase, γ, protons, and x, 20: 3692
radiation effects on zinc in carbonic anhydrase, x, 20: 3693
radiation effects on content of, in blood of cancer patients during radiotherapy, 20: 3763
EPHEDRINE
preparation of mercapto analogs of, 20: 3790
radiosensitivity effects of mercapto analogs of, in mice, 20: 3790
EPITHELIUM
radiation effects on, of mouth, 20: 3744
radiosensitivity of, in rabbit eyes, β, 20: 3761
EQUATION OF STATE
determination of, computer program for, 20: 4708(R) (UCRL-14360, pp 50-73)
of plasmas, quantum theory of, 20: 4949(R) (UCRL-14360, pp 85-94)
of simple solids, 20: 4476(R) (IS-1200(Sect.P))
EQUIPMENT AND PROCEDURES
development for dismantling irradiated rigs, 20: 4092
development of automatic detection and diagnosis techniques for arbitrary systems, (T), 20: 4222 (UCRL-13186)
development of, for transfer of radioactive materials to and from hot cells, 20: 4210
ERBIUM
carbon-12 reactions with, tungsten-174 from, (E), 20: 4834 (JINR-E-2360)
determination in hydrochloric acid or methanol–nitric acid media, spectrophotometric, 20: 3888 (TID-22402)
ERBIUM ETHYL SULFATES
spectra of crystalline, magnetic effects on, (E), 20: 4476(R) (IS-1200(Sect.P))
ERBIUM ISOTOPES Er^{-165}
energy levels in, 20: 4924
ERBIUM OXIDES
phase studies at 1700 to 2400°C, 20: 3939

ERBIUM SELENIDES
properties of, electric and thermoelectric, (E), 20: 5013
ERBIUM SULFIDES
homogeneity regions in, 20: 3938
ERYTHROCYTES
radiation effects on, laser, 20: 3741
ESCHERICHIA COLI
effects of light on protein synthesis in, 20: 3726
radiation effects on protein synthesis in, uv, 20: 3726
radioinduced inhibition of enzyme induction in, mechanism for uv, 20: 3688
radiosensitivity of bacteriophage complexes with, β, 20: 3748
radiosensitivity of, gene locus for uv, 20: 3757
radiosensitivity of, gene locus for uv, 20: 3758
radiosensitivity of bacteriophage complexes with, uv, 20: 3749
ETHANE
neutron scattering by effects of gas and liquid states on inelastic, 20: 4810
yields from hydrogen isotope reactions with methane, 20: 3980
ETHANE, TRICHLORO-
effects on iodine-131 collection efficiency of activated charcoal, 20: 4179 (LA-3363)
ETHANETHIOL, 2-AMINO-
effects on permeation of rubidium-86, in x irradiated isolated frog heart, 20: 3794
effects on tumor cells in culture, morphological, 20: 3796
radiosensitivity effects on T5 receptor, 20: 3787
radiosensitivity effects in mice, gamma, 20: 3792
ETHANOL
determination in water using beta-excited x-ray sources, absorptiometric, 20: 3882 (ORNL-IIC-5, pp 51-71)
ETHERS
solvent properties for titanium and zirconium, 20: 4061
ETHYL ETHER
effects on serum lipoproteins, 20: 3604
hypersonic and ultrasonic velocities in, effects of relaxation on, 20: 4479(R) (TID-22179, pp 1-83)
ETHYLAMINE, 2,2'-DITHIOBIS-
radiosensitivity effects on T5 receptor, 20: 3787
ETHYLENE
molecular structure of deuterated and normal, 20: 3863(R) (IS-1200 (Sect. C))
radioinduced polymerization, 20: 4031
radiolysis of, yields from fission-fragment, 20: 3982(R) (AGN-8156)
yields from irradiation of polytetramethylene oxide, 20: 3999
ETHYLENE, CHLORO-
radioinduced graft copolymerization with acrylonitrile–styrene, 20: 4038
ETHYLENE, CHLORO- POLYMERS
radioinduced grafting of 4-vinylpyridine to, 20: 4032
ETHYLENE, DICHLORO-
mechanical properties for shock pulse generation on impact shock machines, 20: 4112 (SC-TM-65-443)
ETHYLENE POLYMERS
adhesive properties of, effects of methacrylic acid esters on, 20: 4029
gamma and neutron heating of, in experimental channels of FRJ-2 reactor, 20: 5202
mechanical properties for shock pulse generation on impact shock machines, 20: 4112 (SC-TM-65-443)
radiation effects on electric conductivity of, 20: 4035
radioinduced crosslinking of single crystals of, gamma, 20: 3998
radioinduced crosslinking in, effect of crystallization conditions on, 20: 4002
radioinduced crosslinking in, effect of crystallization conditions on, 20: 4003
radioinduced crosslinking in, effect of crystallization conditions on, 20: 4004
radioinduced crosslinking in, effect of crystallization conditions on, 20: 4005
radioinduced crosslinking in, effect of crystallization on, 20: 4006
radioinduced crosslinking of, effects of nitrous oxide on, 20: 4010
radioinduced polymerization of methylmethacrylate on, 20: 3996
radioinduced proton polarization in, neutron, (E), 20: 4037
x-ray scattering by melt-crystallized, 20: 5022
polyethylene–sodium acetate, determination of fractional composition by x-ray beam attenuation measurements, 20: 3885 (ORNL-IIC-5, pp 277-89)
ETHYLENE, TETRAFLUORO- POLYMERS
mechanical properties for shock pulse generation on impact shock machines, 20: 4112 (SC-TM-65-443)
radioinduced fluorine nuclei and proton polarization neutron in, (E), 20: 4037
ETHYLENIMINE
effects on Chlorella, genetic, 20: 3716(T) (JPRS-31514, pp 65-76)
EUROPIUM
determination in hydrochloric acid or methanol–nitric acid media, spectrophotometric, 20: 3888 (TID-22402)
determination in potassium carbonate, fluorometric, 20: 3863(R) (IS-1200 (Sect. C))
EUROPIUM IONS
electron transfer between cobalt(III) and divalent, oxyanions as bridging groups in, 20: 3867
EUROPIUM ISOTOPES Eu-144
beta decay of, half life for, (E), 20: 4887
production in proton reactions (p,n) with samarium-144, decay, half life, and threshold in, (E), 20: 4887
EUROPIUM ISOTOPES Eu-145
decay of, positron spectra from, (E), 20: 4838 (JINR-P-2314)
EUROPIUM MOLYBDATES
corrosion by water at 100 and 250°C, 20: 4305(R) (ORNL-3870, pp 187-90)
crystal structure of, effects of cooling rate on, 20: 4305(R) (ORNL-3870, pp 187-90)
phase transformations, 20: 4391(R) (ORNL-3870, pp 75-82)
reactions with stainless steel, 20: 4305(R) (ORNL-3870, pp 187-90)
EUROPIUM OXIDES
Al–Eu_2O_3, radioinduced swelling of dispersions of, fast and thermal neutron, 20: 5174(R) (ORNL-3870, pp 214-29)
Eu_2O_3–Fe_2O_3, crystal structure and magnetic properties, 20: 4411
EUROPIUM SULFIDES
grain growth and magnetic properties of, effects of lanthanum activation on, 20: 4358(R) (AD-438516)
EXHAUST SYSTEMS
development for radiological containment systems, 20: 4214
EXPLODING WIRE PHENOMENA
energy measurements in, electronic equipment for, (E), 20: 4481 (UCRL-14170)
EXPLOSION CLOUDS
dimensions of, photographic method for scaling, 20: 4152 (TID-22266)
rise rates of, relation of explosive yield to, 20: 4152 (TID-22266)
EXPLOSIONS
dust particles from ground surface of, method for size analysis of, 20: 4149 (AD-623639)
use for magnetic flux compression, 20: 4477 (LA-DC-7289)
EXPLOSIVES
radiation effects on, bibliography on, 20: 4461 (REIC-Memo-28)
EXTERNAL COMBUSTION ENGINES
design of radioisotope-fueled, for submersibles, 20: 4276 (AGN-8128)
EYES
corneal grafts of rabbit, effects of irradiation of graft material on take of, 20: 3719
effects of chlorambucil on retinal development in human embyos, 20: 3725
radiation effects on retinal development, x, 20: 3725
radiation effects on rabbit, pathological, β, 20: 3761

F

FALLOUT
deposition and transport of, effects of sea-breeze wind field on, 20: 4154(R) (AD-620003)
distribution in atmosphere, review of, 20: 4163
monitoring in Euratom countries, 1964, 20: 4155 (EUR-2516.d,f,i,n)
monitoring in Japan, 1961 and 1962, 20: 4177 (JAERI-1083)
monitoring in Rumania, 20: 3654
monitoring in U. S., by analysis of deciduous teeth, 20: 4160
monitoring stratospheric, in Uccle and Warsaw, 1959, 1962, and 1963, 20: 4158
properties of, physical and radiochemical, 20: 4156 (USNRDL-TR-899)
radiation protection measures against nuclear weapon, 20: 3797
radiation protection measures against, during radiological warfare, 20: 3799
size analysis of, method for, 20: 4149 (AD-623639)
sodium-22 content in, 20: 4161
FAST REACTORS
coolant flow and reactivity changes in helium-cooled, response to, 20: 5127 (ORNL-P-1698)
design of Russian BN-350 power, 20: 5137(T) (JPRS-31193)
design of 100 Mw(t), 20: 5079 (NP-15572)
development for power, 20: 5165
fuel development for Fast Flux Test Facility and Fast Flux Test Reactor, (E), 20: 5192 (BNWL-SA-251)
fuel development for, review of, 20: 4313
fuel element testing for, FARET reference core design for, 20: 5190 (ANL-7106)
neutron cross sections in, computer program for calculating, 20: 5055 (BNWL-146)

neutron spectra in, methods for calculating, (E/T), 20: 4801(R) (GA-6634)
reactivity coefficients of power-breeder, SEFOR program for determining Doppler, 20: 5120(R) (GEAP-4799)
reactivity sodium void effects on plutonium–thorium and plutonium–uranium fueled, 20: 5068
safety analysis for large gas-cooled power, 20: 5119 (GA-6732)
uranium-235 Doppler coefficient in, 20: 5072

FATS
sorptive properties for iodine-125 and -131, 20: 3658(R) (EUR-2414.f,i)
fats–muscles, determination of fractional composition by x-ray beam attenuation measurements, 20: 3885 (ORNL-IIC-5, pp 277-89)

FATTY ACIDS
radiation effects on absorption by rats of, tracer study, x, 20: 3754
synthesis of, tracer study in lungs of dogs, rabbits, and rats, 20: 3656 (BNWL-SA-225)

FECES
radioactivity in human, following injections of iodine-131-labeled polyvinylpyrrolidone, 20: 3675
thorium-232 content in, from Thorotrast patients, 20: 3683

FELDSPARS
age of northeastern Minnesota, estimations of, 20: 4169

FERMI FAST BREEDER REACTOR
shield plug response to TNT-simulated accident, 20: 5034 (NOLTR-63-140)

FERMIONS
interactions with fermion systems coupled-equation method for, 20: 4672
interactions with photons, spin-1 boson production from, (T), 20: 4610
scattering of identical, nonrelativistic time-dependent theory of, 20: 4655
theory for superfluid systems of, (T), 20: 4789

FERRITES
crystal growth rate variables, 20: 3919(R) (ORNL-3870, pp 3-6)

FERROMAGNETIC MATERIALS
correlation functions for Heisenberg, (T), 20: 4476(R) (IS-1200(Sect.P))
magnetic susceptibility of, de Hass–Van Alphen effects in, (E), 20: 4476(R) (IS-1200(Sect.P))

FERTILIZERS
effects of, on enrichment of forage vegetation on various soil type by cesium-137 and strontium-90, 20: 3665(T) (CEA-tr-X-619)
effects on strontium-90 uptake by agricultural plants, 20: 3679

FETUSES
radiation dose to, from diagnostic radiography during pregnancy, 20: 3832
radiation effects on retinal development in, x, 20: 3725

FIELD THEORY
coupling constants in, 20: 4849(R) (UCRL-14360, pp 1-50)
developments in, 20: 4769
elementary-particle interaction amplitudes in, 20: 4849(R) (UCRL-14360, pp 1-50)
extrapolation of electromagnetic fields from values in spherical region, (T), 20: 4638 (AD-617965)
formalism as operator-valued distributions in relativistic quantum theory, 20: 4650
formalism for S and D waves in meson (π) two-body system, 20: 4670
formalism for zero mass particles, 20: 4660
formalism of non-Abelian gauge, for massless bosons, 20: 4657
formalism of unified, for elementary particles, 20: 4646 (NYO-3399-40)
formulation of geometrodynamic neutrino, 20: 4619
formulation of relativistic, with approximate SU(6) invariance, 20: 4685
gauge coordinate groups in, 20: 4656
gauge transformations in, nonlocal extension of Utiyama formalism for, (T), 20: 4653
quantum theory of nonabelian gauge fields in, (T), 20: 4699
S-matrix in unified, singularities of, (T), 20: 4639 (IC/65/73)

FILMS
magnetic transitions of thin superconducting, 20: 4785

FILTERS
design for use in cobalt-60 teletherapy, 20: 3814
design of diffusion building board, for radioactive aerosols, 20: 4097(P)
development and testing for reactor-containment buildings, 20: 5196(R) (IS-1200(Sect.E))
efficiency of reactor cooling system, measurement of, 20: 5036 (RL-SA-47)
performance of absolute, for removal of arc-generated urania aerosols, 20: 4086(R) (ORNL-3843, pp 137-67)
performance of charcoal, for fission fragments, 20: 5199 (ORNL-TM-1328)
radiographic use of, evaluation of exposure time from, 20: 3815

FINNED TUBES
design, 20: 5101(P)

FIRES
control in radiological containment systems, 20: 4214

FISH
sodium-22 content in, in Columbia and Winnipeg River, 20: 4161

FISSION
theory of, close-packed-spheron, (T), 20: 4918

FISSION FRAGMENTS
beta decay of, detection of neutrino emission in, (T), 20: 4847 (UCRL-12085(Pt.1))
beta decay of, detection of neutrino emission from, 20: 4848 (UCRL-12085(Pt.2))
deposition in gaseous chemical reactions, monitoring methods for, 20: 3982(R) (AGN-8156)
effects on austenitic and ferritic steels, x-ray study of, 20: 4469
effects on ethylene, 20: 3982(R) (AGN-8156)
energy spectra of, from californium-252 and uranium-235, 20: 3982(R) (AGN-8156)
nuclear charge division of, from californium-252 spontaneous fission, (E), 20: 4913
nuclear charge division of, from californium-252 spontaneous fission, (E), 20: 4914
ranges in aluminum, gold, nickel, and silver, 20: 3982(R) (AGN-8156)
ranges in fuels, calculations of re-entering, 20: 3982(R) (AGN-8156)

FISSION PRODUCTS
behavior in reactor loss-of-coolant accidents, factors affecting, 20: 4183(R) (ORNL-3843, pp 2-70)
content in sintered uranium dioxide pellets, radial distribution of, (E), 20: 4472
detection and measurement in aerosols, methods for, 20: 4185(R) (ORNL-3843, pp 169-234)
determination in reactor cooling water, design of monitor for, 20: 3909
determination in rainwater collected in Japan, 20: 4177 (JAERI-1083)
diffusion from irradiated fuels, methods for measuring, 20: 4452
diffusion from low-dose, low-temperature irradiated fuels, (E), 20: 4471
diffusion in carbon-coated thorium carbide, uranium carbide, and uranium dioxide fuel particles, 20: 5117(R) (GA-5866)
diffusion in graphite, 20: 5117(R) (GA-5866)
diffusion in irradiated fuel elements, gamma scanning of, 20: 5093
diffusion in pyrolytic carbon coatings, 20: 5089(R) (GA-6181)
diffusion of gaseous, from powders, theory for, 20: 4432
diffusion of gaseous, from uranium mononitride, 20: 4303(R) (ORNL-3870, pp 164-70)
diffusion of rare-gas, in ionic crystals and sinters, 20: 3944
effects on charcoal filters, heating, 20: 4086(R) (ORNL-3843, pp 137-67)
production in deuteron reactions with neptunium-237, 20: 4928
properties and reactions of, in containment mockup experiments, 20: 4184(R) (ORNL-3843, pp 71-135)
reactions with water, effects of chemical agents on, 20: 4185(R) (ORNL-3843, pp 169-234)
separation from milk, review on equipment and procedures for, 20: 3872 (EUR-2507.d)
separation of cesium-137 and strontium-90 from, by ion exchange in acid media, 20: 3871 (EUR-2497.e)
separation of cesium-137 from, methods for, 20: 3874 (EUR-2535.f)
separation of ruthenium-106 from, by distillation from oxidizing medium, 20: 3887 (PG-Report-677)
sorption on reactor structures in accidents, 20: 4185(R) (ORNL-3843, pp 169-234)
transport behavior, pilot plant for study of, 20: 4184(R) (ORNL-3843, pp 71-135)
use in materials testing, conference on, 20: 4116
x-ray emission by, (E), 20: 4849(R) (UCRL-14360, pp 1-50)

FISSIONABLE MATERIAL
processing of solid, design of safe flat-bed contactor for, 20: 4049 (RL-SA-52)

FLAMES
spectra of elements in fuel-rich oxyacetylene, 20: 3863(R) (IS-1200 (Sect. C))

FLOWMETERS
calibration of magnetic, for sodium, 20: 4077(R) (IS-1200(Sect. E))
design for use in reactor fuel assembly, 20: 5028(P)
design of radiometric, 20: 4227

FLUID FLOW
acceleration in two-dimensional channel, in magnetic field, (T), 20: 4715
boiling burnout in forced-convection, at 1000 psi in annuli, (E), 20: 4105 (TID-22321)
distribution in annular fuel elements for TSR-II, 20: 4299(R) (ORNL-2711)
hydrodynamic discontinuities in, finite difference calculations for, 20: 4705 (NYO-1480-33)
in Army Reactor (SM-1A) core 3, 20: 5122 (HIT-3459-11(Vol.2))
in vortex tubes, 20: 4999(R) (ORNL-2599)
magnetohydrodynamic, large-amplitude, (T), 20: 4718
magnetohydrodynamic, limit theorem on, 20: 4719
magnetohydrodynamic, limit theorem on, (T), 20: 4720
magnetohydrodynamic viscous, about spherical magnetic quadrupoles, (T), 20: 4725
magnetohydrodynamic, in entrance region of parallel-plate channel, (T),

20: 4709
singularities in, motion of point, 20: 4153(R) (UCRL-14360, pp 73-85)
transport mechanisms in molecular, 20: 4708(R) (UCRL-14360, pp 50-73)
velocity of, use of radioisotopes for measuring, 20: 4227
FLUID FLOW (LAMINAR)
disturbance of viscous highly conducting, over nonconducting wall with parallel magnetic field, 20: 4098 (AD-614633)
FLUID PROPELLANTS
properties of hydrogen, computer program for, 20: 5177 (LA-3381)
radiation effects on, bibliography on, 20: 4461 (REIC-Memo-28)
FLUIDIZATION
particle residence times in fluidized beds, tracer measurement of, 20: 4106(T) (BNL-tr-43)
FLUIDS
nuclear magnetic resonance responses from flowing, spin-echo, 20: 4077(R) (IS-1200(Sect. E))
statistical mechanics of, wall effects in nonequilibrium, (T), 20: 4706(R) (RPI-3035-1)
wave propagation in, (T), 20: 4707 (UCRL-14318)
FLUORIDE IONS
analytical use in determination of thorium, 20: 3905
FLUORIDES
effects on spectrophotometric determination of zirconium, 20: 3895
properties of coolants and fuel salts of, for use in Molten Salt Epithermal Reactor, 20: 4376 (JUL-268-RG)
FLUORINE
determination in yttrium, methods for, 20: 4299(R) (ORNL-2711)
radioinduced polarization in polymers, neutron, (E), 20: 4037
reactions with plutonia and urania, 20: 4046(R) (EURAEC-1340)
FLUORINE ISOTOPES F-18
energy levels of, from deuteron reactions (d,α_0), (d,p_0), and (d,p_1) with oxygen-16 at 300 to 1,000 kev, (E), 20: 4870
FLUORINE ISOTOPES F-19
energy levels from oxygen-16 (t,α) reactions at 1.4 to 3.4 Mev, (E), 20: 4858
energy levels from oxygen-18 (p,γ) reactions, (E), 20: 4907
form factor for, M1, (T), 20: 4831 (HEPL-272)
helium-3 elastic scattering at 9.0 Mev, angular distributions from, (E), 20: 4908
helium-3 reactions (He-3, d) at 9.5 and 10 Mev, angular distributions from, (E/T), 20: 4908
hyperfine structure and Stark and Zeeman effect in cesium fluorides, 20: 4554
FOLIC ACID
radiation effects on intestinal absorption of, 20: 3851
FOOD
decontamination of, bacteriological, chemical, and radiological warfare agents, 20: 4192(T) (JPRS-32586)
radiation monitoring in German, 1965, 20: 4164
radiation processing of, 20: 3685
radiation processing of fruits and vegetables, effects on storage life, 20: 3710(R) (EUR-2493.e)
radioactive contamination of, monitoring systems in U. S. for determining, 20: 4201
radiosterilization of, world developments and outlook for, 20: 4271 (WASH-1063)
sodium-22 content in Alaskan, 20: 4161
FORESTS
radiation effects on water balance of, γ, 20: 3653 (BNL-8466)
FORMALDEHYDE
yields from radioinduced oxidation of methanol, 20: 4011
yields in electron radiolysis of carbon dioxide–methane, effects of carbon monoxide on, 20: 3981 (AERE-R-5051)
FORMAMIDE, *N,N*-DIMETHYL-
thermodynamic properties of alkali metal, gadolinium, and magnesium halides in solutions of, 20: 3924 (TID-22366)
FORMAMIDE, N-METHYL-
thermodynamic properties of alkali metal, gadolinium, and magnesium halides in solutions of, 20: 3924 (TID-22366)
thermodynamic properties of alkali metal halides in anhydrous, 20: 3925 (TID-22366, App. B)
FRANCE
fallout monitoring, 1964, 20: 4155 (EUR-2516.d,f,i,n)
radiation dose to population of Cotes-du-Nord, from uranium, radium, and radon in rocks and water supplies, 20: 4193
FRANCIUM ISOTOPES Fr-223
half life, 20: 3879(R) (MLM-1266)
separation from actinium-227 decay chain members by ion exchange, 20: 3879(R) (MLM-1266)
FREE RADICALS
content in smoke from irradiated cigarettes, 20: 3984 (ORO-633)
electron paramagnetic resonance spectra of, in irradiated silicoorganic compounds, 20: 4012
FROGS
radiation effects on rubidium-86 permeability of isolated heart of, x, 20: 3794
FRUCTOSE
radiation effects on crystal structure and melting point, 20: 4020
transmutation in liver of carbon-14-labeled, 20: 3684
FUNGI
growth of, effects of wavelength of light on, 20: 3769
radioinduced metabolic mutations in Aspergillus, characterization of, uv, 20: 3755(T)
radioinduced mutations in *Sordaria brevicollis*, uv, 20: 3783
radioinduced mutations of Aspergillus, uv, 20: 3756(T)
FURAN, TETRAHYDRO-, POLYMERS
radioinduced decomposition, 20: 3999
FURNACES
design for fluidized-bed and rotary-drum deposition of pyrolytic-carbon coating, 20: 4343(R) (ORNL-3870, pp 266-89)
design of high-pressure, for saturating uranium dioxide with helium, 20: 3946
design of 60-kw electron-beam, 20: 4297(R) (IS-1200(Sect.M))
use of electron-beam, in melting of ingots, 20: 5181(R) (ORNL-3029)
FUSED SALTS
thermal conductivity of molten fluoride, system for measuring, 20: 4310(R) (ORNL-P-1699)

G

GADOLINIUM
determination in hydrochloric acid or methanol–nitric acid media, spectrophotometric, 20: 3888 (TID-22402)
preparation of single-crystal, 20: 4077(R) (IS-1200(Sect. E))
thermal conductivity, (E/T), 20: 4419
GADOLINIUM ALLOYS
Al–Gd, phase diagram, 20: 4427
Gd–Fe, crystal structure, 20: 4297(R) (IS-1200(Sect.M))
Gd–Sn, magnetic properties of, at 2 to 300°K, 20: 4423
Gd–Th, electric conductivity in, (E), 20: 4476(R) (IS-1200(Sect.P))
GADOLINIUM CHLORIDES
magnetic susceptibility at 64 to 365°K, 20: 3863(R) (IS-1200(Sect. C))
magnetic susceptibility, 20: 4297(R) (IS-1200(Sect.M))
phase studies, 20: 3863(R) (IS-1200(Sect. C))
thermodynamics of, in anhydrous *N,N*-dimethylformamide and *N*-methylformamide at 25°C, 20: 3926 (TID-22374)
GADOLINIUM FLUORIDES
thermodynamic properties in *N,N*-dimethylformamide and *N*-methylformamide solutions, 20: 3924 (TID-22366)
GADOLINIUM IODIDES
phase studies, 20: 3863(R) (IS-1200(Sect. C))
GADOLINIUM ISOTOPES Gd-155
energy levels, (E), 20: 4476(R) (IS-1200(Sect.P))
GADOLINIUM ISOTOPES Gd-156
energy levels, (E), 20: 4476(R) (IS-1200(Sect.P))
GADOLINIUM OXIDES
magnetic susceptibility, 20: 3863(R) (IS-1200(Sect. C))
Gd_2O_3–SiO_2–Na_2O, glass forming temperature of, 20: 4077(R) (IS-1200 (Sect. E))
GADOLINIUM SULFIDES
homogeneity regions in, 20: 3938
GALACTOSE
radiation effects on crystal structure and melting point, 20: 4020
GALLIUM
determination in gallium–plutonium alloy, spectrophotometric, 20: 3881 (NBL-228)
determination in hydrochloric acid or methanol–nitric acid media, spectrophotometric, 20: 3888 (TID-22402)
effects on phase transformation of delta–plutonium, 20: 4434
electric conductivity of, effects of low temperature on, 20: 4417
Fermi surface of single-crystal, 20: 4479(R) (TID-22179, pp 1-83)
GALLIUM ALLOYS
Ga–Pu, analysis for gallium by spectrophotometry, 20: 3881 (NBL-228)
Ga–V, superconductivity, 20: 4426
GALLIUM ARSENIDES
properties of pressure transducers of, (E), 20: 5216 (SC-TM-65-457)
GALLIUM COMPOUNDS
metabolism in rats of gallium-68-labeled, effects of carrier on, 20: 3676
GALLIUM ISOTOPES Ga-68
metabolism in rats of citrate-incorporated, effects of carrier on, 20: 3676
GAMMA RADIATION
absorption in man and phantoms, measurements of, 20: 4207
angular distributions and energy spectra in bubble chambers, (T), 20: 4240 (JINR-P-2277)
attenuation and buildup in water collimator, 20: 4999(R) (ORNL-2599)
attenuation by lithium hydrides, 20: 5181(R) (ORNL-3029)

attenuation in concrete and iron, (E), 20: 4997(R) (EUR-2494.d)
detection and measurement in thermal-neutron flux, 20: 5060(R) (TID-22357)
detection and measurement of low-level, in large liquid volume, 20: 3817
detection of, silicon single crystal for, 20: 4259(P)
detection using cesium iodide and sodium iodide crystals, 20: 5181(R) (ORNL-3029)
distribution in phantom jaws, photographic film for determining, 20: 4205
distributions from sources in infinite homogeneous media, computer program for calculating, 20: 4299(R) (ORNL-2711)
dose rate from neutron reactions with air, 20: 4999(R) (ORNL-2599)
dose rates in air, single-scattering approximation to, (T), 20: 5181(R) (ORNL-3029)
dosimetry of, calculator for use with cobalt-60 teletherapy unit, 20: 3839
dosimetry of, calibration of photographic film detectors for, 20: 4237 (BNL-9665)
dosimetry of, development of thermoluminescent detectors for, 20: 4236 (BNL-9605)
dosimetry of, in tumors, calculator for, 20: 3855
dosimetry of, phosphate glass element for, 20: 4258(P)
effects on bacterial growth, 20: 3699
effects on beryllia-moderated-reactor materials, 20: 5115(R) (GA-4967)
effects on bones of, from radium implants used for cancer therapy, pathological, 20: 3856
effects on cells in culture, protective effects of inosine against, 20: 3791
effects on chemical systems, method of calculating parameters for, 20: 3993
effects on content of pyrolytic products in smoke from cigarettes, 20: 3984 (ORO-633)
effects on crosslinking of polyethylene single crystals, 20: 3998
effects on development of myelitis, 20: 3771
effects on dissociative electron attachment in hydrocarbon glasses, (E), 20: 4013
effects on electric conductivity and polarization of polymers, 20: 4030
effects on electronic equipment in SNAP environment, 20: 4262 (NP-15610)
effects on enzyme levels in monkey blood, 20: 3692
effects on explosives and propellants, bibliography on, 20: 4461 (REIC-Memo-28)
effects on fertility of Mexican fruit flies, effects of dose on, 20: 3745
effects on fluorescence of organic phosphors in naphthalene solutions, 20: 3994
effects on forest water balance, 20: 3653 (BNL-8466)
effects on germanium and silicon transistors, (E), 20: 4261 (AD-623078)
effects on glasses, ESR studies of, 20: 5019
effects on hematopoietic system, leukemogenic, 20: 3730
effects on human intestine following therapy of cervical carcinomas, 20: 3720
effects on hydrogen sulfides, 20: 4017
effects on immune reactions in dogs of, from injected gold-198 colloids, 20: 3729
effects on intestine following carcinoma therapy, injurious, 20: 3732
effects on isomerization of benzene-butene-2 mixtures, 20: 4014
effects on larvae of *Nippostrongylus brasiliensis* in rats, 20: 3786
effects on luminescence of alkane glasses at 77°K, 20: 3990
effects on mammalian cells in tissue culture, mitotic, 20: 3737
effects on methyl linoleate in presence of lactose, 20: 4019
effects on methyl methacrylate polymers, protective effects of organic additives against, 20: 4036
effects on mice, protective effects of chemicals against, 20: 3792
effects on monomers and polymers in production of textiles, 20: 4031
effects on *Neurospora conida*, biological, 20: 3780
effects on oxidation of antimony(III) in aqueous solutions, 20: 4009
effects on oxidation of methanol, 20: 4011
effects on oxygen consumption in aerobic bacteria, 20: 3699
effects on paraffin in air at 25°C, 20: 3989
effects on plutonia and urania ceramics and cermets, (E), 20: 5192 (BNWL-SA-251)
effects on polymerization of methylmethacrylate on polyethylene, 20: 3996
effects on polymerization of acrylonitrile in presence of solid additives, 20: 4007
effects on polymerization of methacrylic acid esters, 20: 4029
effects on polymerization of 1,2-cyclohexene oxide in liquid and solid state, 20: 3992
effects on rat lungs, effects of dose fractionation on histological, 20: 3700
effects on rectum following cervical carcinoma therapy, 20: 3734
effects on serum albumins, 20: 3687
effects on silicon transistor gain, effects of operating condition on, 20: 4267
effects on silicoorganic compounds, EPR study of, 20: 4012
effects on skin epitheliomas, late carcinogenic, 20: 3811
effects on skin of, post-operative therapeutic doses used for breast carcinoma, 20: 3847
effects on sulfonate detergents, 20: 4025
effects on thiamine hydrochloride in presence of calcium carbonate, dibasic calcium phosphate, and sodium chloride, 20: 4018
effects on TS receptor, factors affecting inactivation, 20: 3787
effects on virus infections of plants, 20: 3768
effects on wheat seeds, genetic, 20: 3762
emission in proton scattering by titanium-48, gamma-proton angular correlations in, (E/T), 20: 4926
energy distributions from neutron capture and inelastic scattering, 20: 4999(R) (ORNL-2599)
from fallout protective measures for, 20: 3799
interactions with protons, polarized hydrogen target for, 20: 4637
interactions with deuterons at 77.3 Mev, wave functions for ground state from, (T), 20: 4592
interactions with protons below 500 Mev, recoil proton polarization from, (T), 20: 4627
interactions with protons below 500 Mev, recoil-proton polarization from, (T), 20: 4628
penetration calculations for, using Monte Carlo method, 20: 5181(R) (ORNL-3029)
production in lead, 20: 4999(R) (ORNL-2599)
production in lithium hydride–uranium shields, 20: 5181(R) (ORNL-3029)
reactions (γ,n) with carbon-12 at threshold to 65 Mev, cross sections for, (E), 20: 4476(R) (IS-1200(Sect.P))
reactions (γ,n) with praseodymium-141 at threshold to 65 Mev, cross sections for, (E), 20: 4476(R) (IS-1200(Sect.P))
reactions (γ,n) with beryllium-9 and deuterium at 1.6 to 3.9 Mev, cross sections for, (E), 20: 4802 (IDO-17115)
reactions (γ,n) with oxygen-16, cross sections for, (E), 20: 4833 (IS-T-43)
reactions (γ,n) with lithium-6 at 8.0 to 32 Mev, cross sections for, (E), 20: 4849(R) (UCRL-14360, pp 1-50)
reactions (γ,n) with magnesium and magnesium-24 at 11 to 30 Mev, cross sections for, (E), 20: 4849(R) (UCRL-14360, pp 1-50)
reactions (γ,n) with zirconium-91, -92, and -93, cross sections for, (E), 20: 4849(R) (UCRL-14360, pp 1-50)
reactions (γ,n) with carbon-12, behavior of recoils in hydrocarbons, 20: 3863(R) (IS-1200(Sect. C))
reactions (γ,n) with oxygen-16, energy level transitions in, (E), 20: 4849(R) (UCRL-14360, pp 1-50)
reactions (γ,n) with oxygen-16 at threshold to 65 Mev, cross sections for, (E), 20: 4476(R) (IS-1200(Sect.P))
reactions (γ,p) with carbon-12, energy spectra from, (E), 20: 4476(R) (IS-1200(Sect.P))
reactions with calcium-40 at 28 to 60 Mev, cross sections for decomposition, (E), 20: 4476(R) (IS-1200(Sect.P))
reactions with graphite, magnesium, and polyethylene in channels of FRJ-2 reactor, heating from, 20: 5202
reactions with nuclei, neutron production in, (E), 20: 4802 (IDO-17115)
reactions with nuclei at 0.01 to 10 Mev, cross sections for, 20: 4996 (AWRE-O-79/65)
reactions with oxygen-16 at 22 to 65 Mev, production of carbon-11 and nitrogen-13 by, (E), 20: 4476(R) (IS-1200(Sect.P))
reactions with oxygen-16, nitrogen-13 production in, (E), 20: 4833 (IS-T-43)
scattering by platinum and tantalum at 1.12 Mev, cross sections for elastic, 20: 4864
scattering from cylinders, computer program for, 20: 5181(R) (ORNL-3029)
shielding for, temperature distribution in, (T), 20: 5002
spectra from neutron capture by nitrogen-14, 20: 4999(R) (ORNL-2599)
spectra from thermal-neutron fission of uranium-235, prompt, 20: 5181(R) (ORNL-3029)
spectra from thermal-neutron fission of uranium-235, 20: 4299(R) (ORNL-2711)
spectra from uranium-235 fission, (E), 20: 4849(R) (UCRL-14360, pp 1-50)
spectra of, least-squares analysis of scintillation, (E/T), 20: 4476(R) (IS-1200(Sect.P))
transport in iron, methods for calculating, (T), 20: 5001 (ORNL-RSIC-9)
transport of, cross sections for, 20: 4996 (AWRE-O-79/65)
use for therapy of bladder carcinoma of, from radium, 20: 3819
use in defectoscopy of metals, 20: 4114(T) (AD-621784)
use in therapy of, design of individualized shields for, 20: 3814

GAMMA SHIELDING
design for use in cobalt-60 telethempy, 20: 3814

GAMMA SOURCES
design and operation of, for physics, radiation chemistry, and radiobiology, 20: 4090 (JPRS-32842)

developments and uses of low-energy, conference on, 20: 4111 (ORNL-IIC-5)
use for therapy, simulator for cobalt-60 treatment planning, 20: 3827
GAMMA SPECTRA
analysis of scintillation, 20: 5181(R) (ORNL-3029)
GAMMA SPECTROMETERS
development for Bulk Shielding Facility, 20: 5181(R) (ORNL-3029)
development for Bulk Shielding Facility, 20: 4299(R) (ORNL-2711)
performance for directional correlation measurements, 20: 4865
performance of anticoincidence-shielded scintillation, for detecting nitrogen-14(p,γ)oxygen-15 reactions, 20: 4233 (AD-618676)
performance of bent-crystal, for analysis of scintillation spectra, 20: 4476(R) (IS-1200(Sect.P))
performance of lithium-drifted germanium, for locating ruptured fuel element, 20: 5109 (AECL-2360)
response matrix formulation for, 20: 5181(R) (ORNL-3029)
source positioning system for bent-crystal, (E), 20: 4476(R) (IS-1200 (Sect.P))
spectral line width in thallium-activated sodium iodide, 20: 5181(R) (ORNL-3029)
use in nondestructive testing of radioactive materials, 20: 4122
use in nondestructive testing of fuel rods, 20: 4123
use in nondestructive testing of irradiated fuel materials, 20: 4124
GARNETS
crystal structure and magnetic properties of mixed, 20: 4411
GAS ANALYZERS
development of, for fissiochemical reaction products, 20: 3982(R) (AGN-8156)
operation of oxygen, manual for, 20: 3889 (UNC-5113)
GAS CENTRIFUGES
development of countercurrent, for isotope separation, 20: 4285
GAS COOLED REACTORS
coolant circuits for, gate value for, 20: 5042(P)
coolant flow and reactivity changes in fast, response to, 20: 5127 (ORNL-P-1698)
coolant inlet temperature control, regulator design for, 20: 5170(P)
cooling system design for, 20: 5169(P)
core design for, computer program for, 20: 5078 (GAMD-6676)
development in U. K., 20: 5155
development of advanced, for commercial power, 20: 5164
development of Spanish Magnox, economic, 20: 5160
development of TARGET 1000-Mw(e) high-temperature, 20: 5117(R) (GA-5866)
development of 1000-Mw(e) TARGET, 20: 5116(R) (GA-5618)
economic evaluation of, for Spain, 20: 5159
fuel cycle costs for, computer program for calculating, 20: 5078 (GAMD-6676)
fuel cycle development for TARGET, 20: 5116(R) (GA-5618)
fuel development for, 20: 5116(R) (GA-5618)
fuel element design for high-temperature, double sheath, 20: 5099(P)
graphite properties for use in TARGET, 20: 5116(R) (GA-5618)
helium purification system development for TARGET, 20: 5116(R) (GA-5618)
thermocouples in, experience with stainless steel-clad Alumel–Chromel, 20: 4263 (ORNL-TM-1320)
use for ammonia production, economics and method for, 20: 3916 (CONF-650902-20)
GAS FLOW
book: *The Flow of Gas in Channels in the Presence of Heat Transfer*, (T), 20: 4107(T) (NASA-TT-F-262)
in tubes, vertical, 20: 4299(R) (ORNL-2711)
magnetic field effects on one-dimensional unsteady, transverse, (T), 20: 4717
magnetohydrodynamic, in transverse fields, (T), 20: 4716
particle entrainment in, electrostatic apparatus for removal of, 20: 4726(P)
GASEOUS DIFFUSION PROCESS
economic analysis of, 20: 4284(T) (CEA-tr-X-617)
GASEOUS FUEL REACTORS
chemical and materials analysis of 1000-Mw(e), (E/T), 20: 5128 (TID-22225)
design, 20: 5081(P)
performance for 1000-Mw(e) power stations, 20: 5128 (TID-22225)
safety analysis of 1000-Mw(e), 20: 5128 (TID-22225)
thermodynamic analysis of 1000-Mw(e), (E/T), 20: 5128 (TID-22225)
GASES
analysis using beta ionization currents, 20: 4557
atom distribution in Boltzmann equation for, (T), 20: 4721
composition of, from reactor accidents, 20: 4183(R) (ORNL-3843, pp 2-70)
compression wave propagation in, (T), 20: 4707 (UCRL-14318)
detonation in, chemistry, instability, and structure of, 20: 3918 (LA-DC-7276)
diffusion in spherical solids, least-square determination of coefficient of, 20: 4377 (NAA-SR-Memo-10741)
diffusion in spherical solids, computer program for graphic display of coefficients of, 20: 4377 (NAA-SR-Memo-10741)
dissociation, fragmentation, and ionization of molecular, mass spectrometric studies of, 20: 4215(R) (ANL-7031, pp 134-49)
electron beams in low-pressure, ion density in, 20: 4722
flow of, equipment for control of small rates of, 20: 4230(P)
ionization by beta particles, measurements of, 20: 4557
ionization of, effects of applied voltage and pressure on, 20: 3982(R) (AGN-8156)
pair distribution function of classical electron, 20: 4708(R) (UCRL-14360, pp 50-73)
preparation in vertical flow, 20: 4299(R) (ORNL-2711)
properties of electron, computer program for calculating, 20: 4708(R) (UCRL-14360, pp 50-73)
radiolysis of, computer program for data reduction in, 20: 3985 (RFP-624)
radiolysis of, equipment and method for study of electric field effects on, 20: 4022
temperature of, relativistic transformation for, (T), 20: 4712
transport from reactor to isotope separator, effects of electric discharge on, (E), 20: 4476(R) (IS-1200(Sect.P))
transport properties near a wall in dilute, molecular chaos assumption in, (T), 20: 4706(R) (RPI-3036-1)
gas–liquid, computer program for integration of Gibbs–Duhem equation for equilibrium in metal systems of, 20: 4375 (IS-1241)
GASKETS
design for large-volume hydrogen bubble chambers, 20: 4242 (JINR-P-2376)
GASTROINTESTINAL TRACT
discrimination between barium, calcium, and strontium by rat, tracer study, 20: 3669
radiation effects on human, following therapy of bladder and cervical carcinomas, gamma and x, 20: 3734
GEIGER-MUELLER TUBES
pulses in, formation mechanism for excitation, 20: 4254
GENES
locus for uv sensitivity of *Escherichia coli*, 20: 3757
locus for uv sensitivity of *Escherichia coli*, 20: 3758
GENETICS
analysis of radiation effects on swine behavior traits, 20: 3784
radiation effects on human chromosomes, 20: 3705(R) (AD-617601)
radiosensitivity effects in mice, leukemogenic, 20: 3765
GEOCHEMISTRY
book: *Geochemistry and Analytical Chemistry of Rare Earth Elements*, 20: 4146
GEOLOGY
of instrument holes in Handcar Project, 20: 4144 (PNE-810F)
GEOMAGNETIC FIELDS
effects on electron density in atmosphere, (E), 20: 4746
electron trapping in, from Starfish detonation, 20: 4731 (UCRL-7659-T (Rev.1))
electron trapping in, from high-altitude explosions, 20: 4732 (UCRL-14368-T(Rev.1))
intensity distributions and secular variations of, representation of, (T), 20: 4734 (N64-30079)
intensity variation on magneto-quiet days in IGY, cyclic, 20: 4738
intensity variation in night levels of, 20: 4738
intensity variations in polar regions, (T), 20: 4739
intensity variations of, secular, 20: 4757
interactions with missiles having ionized wakes, (T), 20: 4730 (SC-DC-65-1797)
origin, (T), 20: 4475(R) (ANL-7081, pp 95-119)
proton trapping in, average atmosphere traversed in, (T), 20: 4748
pulsation pairs in, correlation with shock structure in M-region beams, 20: 4758
pulsations in, statistical method for analysis of giant, (T), 20: 4743
variations of, classification of diurnal, 20: 4742
GEOMAGNETIC STORMS
data for April–June 1965, 20: 4750
effects on anomalous ionization of lower ionosphere, (E), 20: 4736
effects on PCA events, 20: 4756
solar wind shock effects on, (T), 20: 4744
solar wind shock effects on, (T), 20: 4745
GERMANIUM
electron scattering by films of, differential cross sections for multiple, (E), 20: 4485
microwave mobilities in p-type, (E/T), 20: 4476(R) (IS-1200(Sect.P))
performance of lithium-drifted, for locating ruptured fuel element, 20: 5109 (AECL-2360)
properties of pressure transducers of, (E), 20: 5216 (SC-TM-65-457)
purification by electrotransport, 20: 4297(R) (IS-1200(Sect.M))
radiation effects on electrophysical properties of, x, 20: 4465
radiation effects on thermal conductivity of, fast-neutron, 20: 4466

radiation effects on, electron-microscope observations of fast-neutron, 20: 4467
radiation effects on infrared properties of, electron, (E), 20: 4468
radiation effects on transistors of, (E), 20: 4261 (AD-623078)
radioinduced defects in, electron, (E), 20: 4508(R) (RPI-328-40)
radioinduced disordered regions in, fast-neutron, 20: 4466

GERMANIUM ALLOYS
Al–Cr–Ge–Ti–V, properties of aged, 20: 4360(R) (AD-619399)
Ge–Mg, sound velocities in intermetallic compound, (E/T), 20: 4476(R) (IS-1200(Sect.P))
Ge–Mg, thermal capacity of intermetallic compound in, 20: 3863(R) (IS-1200(Sect. C))

GERMANIUM ISOTOPES Ge-73
Mössbauer effects in, following Coulomb excitation, 20: 3920(R) (ORNL-3870, pp 27-37)

GERMANIUM JUNCTIONS
radiation- and stress-induced defects in, electron, 20: 4264

GERMANOMOLYBDATES
magnetic properties of rare earth, 20: 5006(R) (ORNL-3870, pp 50-5)
properties of lanthanide, 20: 3919(R) (ORNL-3870, pp 3-6)

GERMANOTUNGSTATES
properties of lanthanide, 20: 3919(R) (ORNL-3870, pp 3-6)

GERMANY
environs monitoring at Juelich Research Center, 1964, 20: 4178 (JUL-284-ST)
fallout monitoring, 1964, 20: 4155 (EUR-2516.d,f,i,n)
lead uranyl arsenate occurrence in Black Forest, 20: 4172
radiation monitoring in, 1965, 20: 4164
thorium and uranium content of porphyries in Saar-Nahe basin, 20: 4165

GLASS
properties of, effects of low temperature on, 20: 4417
radiation effects on luminescence of alkane, at 77°K, gamma, 20: 3990
radiation effects on, ESR studies of, 20: 5019

GLASS TEXTILES
preparation of, with composite core-sheath fibers, 20: 4338(R) (AD-620055)

GLOBULIN
binding of calcium-47 and strontium-85 by blood serum, 20: 3697
radiation effects on content of, in rabbit blood, x, 20: 3709 (CEA-R-2865)

GLOVE BOXES
decontamination of alpha-sealed, 20: 4213
design for transplutonium elements, 20: 4065
design standards and decontamination facility for, 20: 4093
development of high-activity, 20: 4048(R) (NP-15406)

GLUCOSE
carbon-14 distribution in, 20: 3684
effects on permeation of rubidium-86, in x irradiated isolated frog heart, 20: 3794
metabolism in rats of, effects of methionine sulfoximine on, tracer study, 20: 3678
metabolism of, tracer study, 20: 3658(R) (EUR-2414.f,i)
radiation effects on crystal structure and melting point, 20: 4020
radiation effects on metabolism in rats of, tracer study, x, 20: 3678

GLYCINE
ionization potential, 20: 3863(R) (IS-1200(Sect. C))

GLYOXIME, DIMETHYL- COMPLEXES
with copper and nickel, chemistry of, 20: 3863(R) (IS-1200(Sect. C))

GOITER
radiotherapy of, using iodine-131, 20: 3853

GOLD
electron elastic scattering at 121 kev, Born approximation for differential cross section and polarization from, (T), 20: 4545
electron scattering at 26 to 261 kev by foils of, Mott asymmetry function for double, (E), 20: 4881
electron scattering by films of, differential cross sections for multiple, (E), 20: 4485
fission fragment ranges in, 20: 3982(R) (AGN-8156)
thickness measurement by alpha energy degradation, 20: 3982(R) (AGN-8156)

GOLD ALLOYS
Au–rare earth, phase studies and solid solubilities of, 20: 4297(R) (IS-1200(Sect.M))

GOLD ISOTOPES Au-192
neon-20 reactions with, angular distributions of exchange products in, (T), 20: 4836 (JINR-P-2298)

GOLD ISOTOPES Au-197
alpha reactions (α, 4n) at 49 Mev, thallium-197 isomer from, (E), 20: 4921
helium ion fission at 33.5 to 40 Mev, absolute yields from, (E), 20: 4894
neon-20 inelastic scattering at 200 Mev, matrix elements for, (T), 20: 4389 (JINR-P-2333)
neutron reactions with, Doppler shifts and resonance integrals in, (E), 20: 4841 (NAA-SR-Memo-11511)

GOLD ISOTOPES Au-198
beta decay of, transverse polarization of K-conversion electrons from, (E), 20: 4900
beta transitions in, polarization from, (E), 20: 4880
deposition of colloids of, in dog liver, 20: 3680
deposition of colloids of, in dog liver, 20: 3681
effects of injected colloids of, on immune reactions in dogs, 20: 3729
radiation dose from injected colloids of, 20: 3822
use of colloids of, in cancer therapy, 20: 3822

GONADS
radiation dose measurements for female, during pregnancy, 20: 3823
radiation dose of, during diagnostic radiography of children, 20: 3854
radiation dose to, from dental radiography in Japan, 20: 4196
radiation dose to, from dental radiography, 20: 4206
radiation protection of female, during diagnostic radiography, 20: 3858
radiotherapy of carcinomas in, effects on intestine of gamma, 20: 3732

GRANITES
age of northeastern Minnesota, estimations of, 20: 4169
radioactivity of Swiss, petrographic–microscopic study of, 20: 4157(T) (ORNL-tr-702)

GRAPHITE
brazing to INOR-8, process development for, 20: 4308(R) (ORNL-3870, pp 243-60)
combustion in fuel processing plants, methods for, 20: 4048(R)(NP-15406)
compatibility with beryllium oxide at high temperatures, 20: 5117(R) (GA-5866)
density and microstructure of, effects of preparation conditions on, 20: 4431
diffusion of fission products in, 20: 5117(R) (GA-5866)
diffusion of thorium in pyrolytic, effects of structure on, 20: 4306(R) (ORNL-3870, pp 194-213)
dimensional stability of AGOT, 20: 4306(R) (ORNL-3870, pp 194-213)
gamma and neutron heating of, in experimental channels of FRJ-2 reactor, 20: 5202
impact resistance of fueled spheres of, 20: 4306(R) (ORNL-3870, pp 194-213)
neutron thermalization in, (T), 20: 4818
permeation of CGB, by molten sulfur, 20: 4308(R) (ORNL-3870, pp 243-60)
permeation of CGB, by xylene, 20: 4308(R) (ORNL-3870, pp 243-60)
preparation of pyrolytic, mechanisms for, 20: 4348
properties for use in TARGET, 20: 5116(R) (GA-5618)
properties of hot-pressed, containing molybdenum or zirconium carbides, 20: 5089(R) (GA-6181)
radiation effects on properties of fueled spheres of, fast neutron, 20: 4306(R) (ORNL-3870, pp 194-213)
radioinduced creep in, at 150 to 350°C, theoretical model for reactor, 20: 4306(R) (ORNL-3870, pp 194-213)
sorptive properties for cesium, 20: 5117(R) (GA-5866)
thermal conductivity of AGOT, 20: 4306(R) (ORNL-3870, pp 194-213)
C–MoC, properties and structure of hot-pressed, 20: 5089(R) (GA-6181)
C–ZrC properties and structure of hot-pressed, 20: 5089(R) (GA-6181)

GRAPHITE MODERATED REACTORS
development in U. K., 20: 5155
fuel element for, Doppler coefficient and resonance capture in uranium, 20: 5092

GRAPHITE SYSTEMS
graphite–U, separation of uranium from sintered, 20: 4074(P)

GRAVITATION
equations of motion without infinite self-action in general relativity theory, 20: 4768
field of, fusion of electromagnetic or neutrino fields for pure tensor, 20: 4763
geons in, singularities in bootstrap, (T), 20: 4767
quantization of field of, field theory for, (T), 20: 4699
theory, 20: 4771
theory of, direct interparticle action, 20: 4770

GREAT BRITAIN
nuclear power development and research program, 20: 5150

GRIGNARD REAGENTS
crystal structure of bromide, 20: 3863(R) (IS-1200(Sect. C))

GUIDED MISSILES
launch hazards assessment of Atlas Centaur abort, 20: 4187 (SC-RR-65-333)

GUNDREMMINGEN POWER REACTOR
development, Jan.-March 1965, 20: 5129(R) (TID-22328)

H

HAFNIUM
diffusion of hafnium-181 in beta-phase, 20: 4385(R) (ORNL-3870, pp 15-19)
separation from zirconium, chromatographic, 20: 3863(R) (IS-1200 (Sect. C))

HAFNIUM ALLOYS
Co–Hf, phase studies, 20: 4297(R) (IS-1200(Sect.M))
Cr–Hf, phase studies, 20: 4297(R) (IS-1200(Sect.M))
Hf–Mo, properties at high temperatures, 20: 4418
Hf–Nb–W–Y, evaporation losses in high vacuum of C-129Y, 20: 4301(R) (ORNL-3870, pp 102-35)
Hf–Ta, internal friction spectrum of, annealed at 2300°C, 20: 4301(R) (ORNL-3870, pp 102-35)
Hf–Ta–W, corrosion of T-111, by potassium, 20: 4301(R) (ORNL-3870, pp 102-35)
Hf–Ta–W, corrosion of T-111, by lithium, effects of oxygen on, 20: 4301(R) (ORNL-3870, pp 102-35)
Hf–Ta–W, evaporation losses in high vacuum of T-111, 20: 4301(R) (ORNL-3870, pp 102-35)
Hf–Ta–W, preparation and specifications for corrosion loop testing, 20: 4380 (NASA-CR-54761)
Hf–Ta–W, recovery and recrystallization of T-111, 20: 4301(R) (ORNL-3870, pp 102-35)
Hf–Ta–W, tensile properties of welded plates of T-111, 20: 4301(R) (ORNL-3870, pp 102-35)
Hf–Ta–W, thermal conductivity of T-111, at 30 to 120°C, 20: 4301(R) (ORNL-3870, pp 102-35)
Hf–W, emissivity properties of, 20: 4405(T) (K-Trans-9)
Hf–W, properties at high temperatures, 20: 4418
HAFNIUM IODIDES
phase studies, 20: 3863(R) (IS-1200(Sect. C))
HAFNIUM ISOTOPES Hf-175
energy levels in, 20: 4924
HAFNIUM ISOTOPES Hf-176
energy levels in, 20: 4924
HAFNIUM ISOTOPES Hf-181
diffusion in beta-phase hafnium, 20: 4385(R) (ORNL-3870, pp 15-19)
HAFNIUM ISOTOPES Hf-183
beta and gamma spectra, (E), 20: 4862
HAFNIUM SULFIDES
phase studies, 20: 3863(R) (IS-1200(Sect. C))
HAFNIUM SYSTEMS
C–Hf–Ta–W, preparation and specifications for corrosion loop testing, 20: 4380 (NASA-CR-54761)
HALDEN BOILING REACTOR
development and operation, Jan.–Mar. 1965, 20: 5123(R) (HPR-61)
HALL EFFECT
in indium antimonide, magnetic field and temperature effects on, 20: 4479(R) (TID-22179, pp 1-83)
HALLAM POWER REACTOR
criticality studies, 20: 5111 (AI-PC-710)
loading tests for, analysis of wet excess, 20: 5111 (AI-PC-710)
operation, Aug. 1965, 20: 5130(R) (TID-22355)
HALLIMONDITE
occurrence, in Black Forest, Germany, 20: 4172
HALOGENS
reactions of recoil, review of, 20: 4039
HAMSTERS
radiation effects on lungs of, x, 20: 3785
HANDBOOKS AND MANUALS
analytical procedures at Eurochemic plant, 20: 4048(R) (NP-15406)
for designing control circuitry of accelerators, 20: 4510 (UCRL-16016)
for training operators for pressurized-water power reactors, 20: 5025 (WAPD-T-1832)
of components in drift tube system of Princeton-Pennsylvania Accelerator, 20: 4507 (PPAD-2137-560)
on reactor containment, development of, 20: 4186(R) (ORNL-3843, pp 235-44)
HANDLING AND STORAGE
equipment for gas, liquid, and solid, at Eurochemic plant, 20: 4048(R) (NP-15406)
HARBORS
wave generation on, feasibility of modeling run-up effects of dispersive, (T), 20: 4142 (AD-619053)
HARWELL SYNCHROTRON
beam extraction system analysis, 20: 4502 (NIRL/R/92)
operation of Nimrod, 20: 4504(R) (NP-15420)
HASTELLOY F
tensile properties to 1300°F after prolonged thermal exposure, 20: 4373 (GEAP-4794)
HASTELLOY X
corrosion by lithium fluoride in cyclic high-temperature environment, 20: 4326 (TRW-ER-6561)
tensile properties to 1300°F after prolonged thermal exposure, 20: 4373 (GEAP-4794)
HAYNES 25 ALLOY
corrosion by cesium at 400°C, 20: 4337
corrosion by lithium fluoride in cyclic high-temperature environment, 20: 4326 (TRW-ER-6561)
corrosion by potassium at 980°C, 20: 4307(R) (ORNL-3870, pp 238-42)
HAYNES 56 ALLOY
corrosion by lithium fluoride in cyclic high-temperature environment, 20: 4326 (TRW-ER-6561)
HEALTH PHYSICS
measures for radiation personnel, 20: 4199
programs in Russia, instrumentation for, 20: 4198
HEART
blood circulation in, tracer methods for measuring, 20: 3658(R) (EUR-2414.f,i)
blood circulation in, tracer studies of, 20: 3818
radiation effects on rubidium-86 permeability of isolated frog, x, 20: 3794
radiodiagnosis of diseases of, using technetium-99m-labeled pertechnetates, 20: 3831
HEAT
sources of, production and properties of cobalt-60, 20: 4277 (DP-1012)
HEAT EXCHANGERS
design, 20: 4109(P)
design for Russian BN-350 power reactor, 20: 5137(T) (JPRS-31193)
performance testing for sodium-cooled reactors, 20: 5131(R) (UNC-5135)
HEAT EXCHANGERS (LIQUID-LIQUID)
thermal cycling of potassium–sodium, metallographic examination after failure, 20: 4999(R) (ORNL-2599)
HEAT-RESISTING ALLOYS
inspection of, development of methods for, 20: 4110(R) (ORNL-3870, pp 146-54)
HEAT TRANSFER
ablation mechanisms for copper-impregnated tungsten, 20: 4108
boiling burnout for forced-convection flows in annuli at 1000 psi, 20: 4105 (TID-22321)
book: *The Flow of Gas in Channels in the Presence of Heat Transfer*, (T), 20: 4107(T) (NASA-TT-F-262)
burnout heat flux in internally cooled tubes, effects on inlet flow conditions on, 20: 4101(R) (EURAEC-1354)
by air in vortex flow, 20: 4999(R) (ORNL-2599)
by boiling potassium, system for studying, 20: 5181(R) (ORNL-3029)
by liquid mercury in forced circulation, 20: 4999(R) (ORNL-2599)
by molten lithium, system for studying, 20: 4299(R) (ORNL-2711)
corrosion and hydriding of Zircaloy-4 under conditions of, 20: 4331
equations of simultaneous mass and, computer program for solving partial differential, 20: 4103 (NAA-SR-Memo-11099)
from annular fuel elements for TSR-II, 20: 4299(R) (ORNL-2711)
from packed-bed fuel elements, 20: 5117(R) (GA-5866)
heat flux dryout in steam-water mixtures in internally heated annuli, 20: 4099 (AECL-2332)
in Army Reactor (SM-1A) core 3, 20: 5122 (HIT-3459-11(Vol.2))
in flat-plate fuel elements with fuel-clad bonding defects, model for, (T) 20: 4102 (HW-SA-3640)
in MHD channel flow effects of wall electric conductivity on, (T), 20: 4703 (AD-619101)
in reactor channels under bulk boiling conditions, nonuniform axial flux distributions during, 20: 4104 (NP-15622)
HEAT TRANSFER SYSTEMS
fabrication of boiling-potassium, 20: 5181(R) (ORNL-3029)
HEAVY WATER REACTORS
coolant and moderator chemistry in, problems in, 20: 5143
design of DON power prototype, 20: 5162
shielding measurements for pressurized, 20: 4800 (AE-198)
HELIUM
abundance of cosmic, effects of spallation and ionization losses on, (T), 20: 4568
bound states of doubly excited, (T), 20: 4949(R) (UCRL-14360, pp 85-94)
crystal dynamics of, (E/T), 20: 4476(R) (IS-1200(Sect.P))
determination in irradiated beryllium oxide, method for, 20: 5181(R) (ORNL-3029)
diffusion in graphite, 20: 5117(R) (GA-5866)
diffusion in hot-pressed carbide–graphite cermets, 20: 5089(R) (GA-6181)
electron mobility in gaseous, at 2.2 – 4.2°K, (E/T), 20: 4788
electron reactions with liquid, 20: 4787
electron transitions in, absorption cross sections for free-free, 20: 4550
energy levels of excited states in, 20: 5006(R) (ORNL-3870, pp 50-5)
liquefaction of, equipment design and performance for, 20: 4798
proton reactions at 50–150 kev, electron angular and energy distributions from, (T), 20: 4558
purification in gas-cooled high-temperature reactor, 20: 5117(R) (GA-5866)
purification system development for TARGET, 20: 5116(R) (GA-5618)
reactions with mercury-199 and -201, hyperfine-level excitation in, (E), 20: 4544
specific heat of solid, anharmonic effects in, (E/T), 20: 4476(R)

(IS-1200(Sect.P))
spectral lines of plasma of, effects of absorption on, 20: 4974
theory of liquid, 20: 4772
HELIUM IONS
density distribution in ionosphere, (E), 20: 4760
detection and measurement of tracks of, in nitrocellulose, (E), 20: 4251 (USNRDL-TR-917)
energy levels of excited states in, 20: 5006(R) (ORNL-3870, pp 50-5)
reactions with gold-197 at 33.5 to 40 Mev, absolute fission yields from, (E), 20: 4894
reactions with nitrogen and oxygen at 3 to 600 ev, charge transfer in, 20: 4759
HELIUM ISOTOPES He-3
cooling of liquid, using Pomeranchuk effect, (E), 20: 4779(T)
performance in refrigerators, 20: 4776
properties at low pressure and very low temperatures, magnetic and thermal, (E/T), 20: 4780
properties of liquid, at low temperatures, 20: 4773 (COO-1198-306)
reactions (He-3,α) with nickel-58 and -60 at 24.5 Mev, energy levels from, (E), 20: 4892
reactions (He-3,α) with nickel-58 at 15 and 18 Mev, nickel-57 levels from, (E/T), 20: 4912
reactions (He-3,d) with fluorine-19 at 9.5 and 10 Mev, angular distributions from, (E/T), 20: 4908
reactions (He-3,n) and (He-3,p) with helium-4 at 25.5 Mev, 20: 4849(R) (UCRL-14360, pp 1-50)
reactions (He-3,n) with nuclei at 1.3 to 5.8 Mev, (E), 20: 4925
reactions with carbon-13 and oxygen-16 at 1.9 to 6.7 Mev, bound states from, (E), 20: 4905
reactions with neptunium-237, products of, 20: 4928
reactions with nuclei, angular momentum transfer, cross sections, and level studies from, 20: 4823(R) (ANL-7081, pp 36-69)
reactions with nuclei, angular distributions from, 20: 4824(R) (ANL-7081, pp 70-7)
reactions with nuclei, cross sections and level studies from, 20: 4822(R) (ANL-7081, pp 22-35)
scattering by fluorine-19 at 9.0 Mev, angular distributions from elastic, (E), 20: 4908
superfluidity, (E), 20: 4773 (COO-1198-306)
use in neutron spectrometers, 20: 4249 (UCRL-16311)
HELIUM ISOTOPES He-4
binding energies of polyatomic molecules of, (T), 20: 4708(R) (UCRL-14360, pp 50-73)
helium-3 reactions (He-3,n) and (He-3,p) at 25.5 Mev, (E), 20: 4849(R) (UCRL-14360, pp 1-50)
performance in refrigerators, 20: 4776
solubility in uranium dioxide, 20: 3946
air–^{4}He, vapor pressure at 77°K, 20: 3879(R) (MLM-1266)
HELIUM SYSTEMS
He–H, electric discharge in, Doppler temperature in toroidal, (E), 20: 4713
H–He, thermal diffusion in, effect of nonspherical potential field on, (T), 20: 4724
HEMATOPOIETIC SYSTEM
stimulation of, by androgens, 20: 3793
HEMOGLOBIN
radiation effects on oxygenated and reduced, spectral absorption curves of laser, 20: 3741
HEMOLYSIN
production of, role of appendix and liver in rabbits, 20: 3746
HETEROGENEOUS REACTORS
core design for breeder type, 20: 5082(P)
core support design for, 20: 5049(P)
core support design for, 20: 5050(P)
design, 20: 5086(P)
design using reactivity control by pressure difference between reactor vessel and fuel storage vessels, 20: 5084(P)
fuel element design for, 20: 5097(P)
neutron diffusion equations of, computer program for solving, 20: 5057 (GA-6540)
neutron spectra in, methods for calculatin, (E/T), 20: 4801(R) (GA-6634)
HETEROPOLY ACIDS
separation from other fission products by ion exchange, 20: 3871 (EUR-2479.e)
HEXANE
TBP–n-hexane, solvent properties for thorium, 20: 4060
HEXATRIENE, DIPHENYL-
radioinduced fluorescence of, in naphthalene, 20: 3994
HIBERNATION
radiosensitivity effects on hypotalamus pituitary system, 20: 3703
HIGH-ALTITUDE EXPLOSIONS
electromagnetic waves from nuclear, effects on missiles having ionized wakes, (T), 20: 4730 (SC-DC-65-1797)
electron production in Starfish, geomagnetic trapping of, 20: 4731 (UCRL-7659-T(Rev.1))
electron production in, geomagnetic trapping of, 20: 4732 (UCRL-14368-T(Rev.1))
HIGH ENERGY INJECTION DEVICES
design using electron-ion mixing, 20: 4993(P)
HIGH TEMPERATURE GAS COOLED REACTOR EXPERIMENT
fuel processing for, 20: 4048(R) (NP-15406)
HIGH TEMPERATURE SEPARATION PROCESSES
equipment for, 20: 4077(R) (IS-1200(Sect. E))
ion-pumped zone refining system for, 20: 3920(R) (ORNL-3870, pp 27-37)
HILSCH TUBES
mass flow in, 20: 4999(R) (ORNL-2599)
HISTAMINE
radiosensitivity effects in mice, gamma, 20: 3792
HOLMIUM
determination in hydrochloric acid or methanol–nitric acid media, spectrophotometric, 20: 3888 (TID-22402)
positron annihilation in single-crystal, (E/T), 20: 4476(R) (IS-1200 (Sect.P))
HOLMIUM CHLORIDES
heat of dilution of aqueous, at 25°C, 20: 3956
heat of solution at 25°C, aqueous, 20: 3956
HOLMIUM IONS
spin-lattice relaxation in yttrium ethyl sulfates, 20: 5020
HOLMIUM ISOTOPES Ho-165
deuteron reactions (d,p), holmium-166 energy levels from, (E), 20: 4889
HOLMIUM ISOTOPES Ho-166
decay of isomeric, (E), 20: 4889
HOLMIUM SULFIDES
homogeneity regions in, 20: 3938
HOMOGENEOUS REACTORS
reactivity of water-moderated, 20: 5062
HUMBOLDT BAY POWER REACTOR
containment design and development for, 20: 5146
HYDRAZINE
yields from radiolysis of gaseous ammonia, 20: 4021
HYDRIDES
binding energy of diatomic, chemical, 20: 3863(R) (IS-1200(Sect. C))
HYDROCARBONS
determination in earth formations, well logging instrument for, 20: 4170(P)
neutron reactions in, effects of element composition on kerma, 20: 3708 (CEA-R-2833)
radioinduced reactions with nitrogen, G-values and mechanisms of, 20: 3982(R) (AGN-8156)
reactions with recoil-carbon-11, mechanisms of, 20: 3863(R) (IS-1200 (Sect. C))
yields from irradiation of polytetramethylene oxide, 20: 3999
HYDROCHLORIC ACID
corrosive effects on stainless steel, effects of molybdenum and uranium on, 20: 4325 (TB-58)
effects on electron exchange between antimony trichloride and antimony pentochloride, 20: 3962
HYDROCYANIC ACID
production of, fissiochemical plant for, 20: 3982(R) (AGN-8156)
radioinduced production of, performance of nickel–urania fuel in, 20: 3982(R) (AGN-8156)
separation from fission products, methods for, 20: 3982(R) (AGN-8156)
CH_3CN–HCN, radioinduced reactions of, G-values and mechanisms of, 20: 3982(R) (AGN-8156)
HYDRODYNAMICS
of base surge and column formation in underwater explosions, (E/T), 20: 4141 (AD-618733)
solutions for flows containing discontinuities, finite difference, 20: 4705 (NYO-1480-33)
wave propagation in, (T), 20: 4707 (UCRL-14318)
HYDROFLUORIC ACID
corrosive effects on yttrium at high temperatures, 20: 4077(R) (IS-1200 (Sect. E))
HF–H_2SO_4, solvent properties for zirconium, 20: 4055
HYDROGEN
design and performance of radiation targets of liquid, 20: 4490
determination of combined, in nonhydrogenous material, by neutron thermalization, 20: 3913(P)
diffusion from stored, solid plutonium residues, vacuum-drying effects on, 20: 4364 (AERE-M-1644)
diffusion in barium, 20: 4297(R) (IS-1200(Sect.M))
diffusion in EN58B low-carbon steel, coefficient for, 20: 4366 (AWRE-O-90/65)
effects on Croloy 9M, INOR-8, and type 347 stainless steel corrosion by potassium–sodium, 20: 4322(R) (ORNL-3870, pp 305-7)
effects on mechanical properties of niobium, additive, 20: 5181(R) (ORNL-3029)

effects on plasticity of vanadium, 20: 4297(R) (IS-1200(Sect.M))
electric discharges in, Balmer line intensities from self-sustained Townsend, (E), 20: 4542
electric discharge in, atom density and electron temperature from x-ray reabsorption in, (E/T), 20: 4964
electric discharge in, electron temperature in ionization phase of pulsed, (E), 20: 4714
electron inelastic scattering by, differential cross sections and inelastic transitions for, (T), 20: 4549
focusing of atomic beams of, four- and six-pole magnets for, (T), 20: 4559
gamma reactions at 0.01 to 10 Mev, cross sections for, 20: 4996 (AWRE-O-79/65)
liquefaction of, equipment design and performance for, 20: 4797
liquefaction of, equipment design and performance for, 20: 4798
neutron cross sections for, 9- and 16-group, 20: 4829 (GEMP-173(Suppl.1))
neutron cross sections for, 20: 4830 (GEMP-384)
neutron reactions (n,γ), gamma spectra from, (E), 20: 4856
properties at 36 to 5000°R, thermodynamic-transport and related, 20: 3917 (LA-3405)
properties of propellants of, computer program for determination of, 20: 5177 (LA-3381)
reactions of recoil, review of, 20: 4039
reactions with ions, charge-exchange, 20: 4556
shock structure in magnetized plasma of, collisionless, (E), 20: 4977
sorption from water, by types 1199 and 6061 aluminum alloys, 20: 4342(R) (ORNL-3870, pp 85-101)
sorption on activated carbon, from helium, 20: 5117(R) (GA-5866)
spectra from plasma of, continuum emission, (E), 20: 4973
use of plasma jet of, in niobium or tantalum pentachlorides reduction to metal, 20: 4314(P)
use of polarized, in elementary particle reaction diagnostics, (T), 20: 4637
yields from irradiation of polytetramethylene oxide, 20: 3999
yields from radiolysis of hydrogen sulfides, 20: 4017
yields from radiolysis of ammonia, 20: 4021

HYDROGEN FERROCYANIDES
$H_4Fe(CN)_6$–Na_2MoO_4, ion exchange properties for cesium-137 and strontium-90, 20: 3871 (EUR-2497.e)
$H_4Fe(CN)_6$–Na_2WO_4, ion exchange properties for cesium-137 and strontium-90, 20: 3871 (EUR-2497.e)

HYDROGEN ION CONCENTRATION
effects on strontium-90 uptake by agricultural plants, 20: 3679

HYDROGEN IONS
binding of molecular, chemical, 20: 3863(R) (IS-1200(Sect. C))
bound states of doubly excited negative, (T), 20: 4949(R) (UCRL-14360, pp 85-94)
convergence in one-center expansion for ground state of, 20: 5006(R) (ORNL-3870, pp 50-5)
density distribution in ionosphere, (E), 20: 4760
electron density in excited and ground states of, numerical calculation for, (T), 20: 4555
ranges and stopping cross sections in organic compounds, recoil, 20: 4024
reactions with argon, charge-exchange, 20: 4556
Schroedinger equation with complete screened Coulomb potential, 20: 4949(R) (UCRL-14360, pp 85-94)

HYDROGEN ISOTOPES
thermal diffusion in, effect of nonspherical potential field on, (T), 20: 4724

HYDROGEN PEROXIDES
analytical use in determination of niobium and tantalum by spectrophotometry, 20: 3904

HYDROGEN SELENIDES
thermodynamic properties of, effects of deuterium and tritium on, 20: 3950

HYDROGEN SULFIDES
radiolysis of, yields of hydrogen and sulfur from gamma, 20: 4017
thermodynamic properties of, effects of deuterium and tritium on, 20: 3950

HYDROGEN SYSTEMS
CO–H–N, radioinduced reactions in, 20: 3982(R) (AGN-8156)
D–H, ion cyclotron wave production in plasma of, optimum, (E/T), 20: 4984
He–H, electric discharge in, Doppler temperature in toroidal, (E), 20: 4713
H–He, thermal diffusion in, effect of nonspherical potential field on, (T), 20: 4724
H–Lu, electric conductivity of solid phases of, 20: 3934
H–U, criticality studies of, 20: 5071

HYDROMAGNETIC WAVES
absorption and excitation of magnetoacoustic, in plasma, (E), 20: 4939 (IAE-911)
propagation along magnetic fields, stability of, 20: 4948(R) (TID-22179, pp 85-175)
propagation in rotating liquids, effect of Hall current on, (T), 20: 4711
propagation in Vlasov plasma, gyro-radius corrections to equations for, (T), 20: 4979
structure of front of magnetoacoustic, in rarefied plasma, (E), 20: 4938 (IAE-909)

HYPERFRAGMENTS
beta decay of, formalism for, 20: 4930
binding energies in light double, 20: 4849(R) (UCRL-14360, pp 1-50)
bound states of light double, (T), 20: 4849(R) (UCRL-14360, pp 1-50)
decay of heavy, (E), 20: 4476(R) (IS-1200(Sect.P))
decay of light, lifetime determinations from, (E), 20: 4476(R) (IS-1200(Sect.P))
research, (T), 20: 4475(R) (ANL-7081, pp 95-119)

HYPERONS
decay of, dynamics and symmetries of nonleptonic, (T), 20: 4676
decay of, SU(6) symmetry and $\Delta I = \frac{1}{2}$ rule in nonleptonic, (T), 20: 4683
decays of, model for weak, (T), 20: 4635
decays of, SU(3) for weak electromagnetic two- and three-body, (T) 20: 4673

HYPERONS (Λ)
binding energies in light double hypernuclei, (T), 20: 4849(R) (UCRL-14360, pp 1-50)

HYPERONS (Λ^0)
decay of, SU(6) symmetry and $\Delta I = \frac{1}{2}$ rule in nonleptonic, (T), 20: 4683

HYPERONS (Σ)
decay of, SU(6) symmetry and $\Delta I = \frac{1}{2}$ rule in nonleptonic, (T), 20: 4683

HYPERONS (Σ^-)
decays of, spectra in ($n\pi$) and ($n\pi\gamma$), (E), 20: 4616

HYPERONS (Σ^0)
decay of, C-violation model for ($\Lambda e^+ e^-$), 20: 4681

HYPERONS (Σ^+)
decays of, spectra in ($n\pi$) and ($n\pi\gamma$), (E), 20: 4616

HYPERONS (Ξ)
decay of, SU(6) symmetry and $\Delta I = \frac{1}{2}$ rule in nonleptonic, (T), 20: 4683

HYPERONS (Ξ^-)
properties of, determination of, (E), 20: 4632

HYPERTHYROIDISM
effects on thyrotropin content in plasma of patients, radioimmunoassay method of measurement, 20: 3829
radiotherapy of, using iodine-131, 20: 3853

HYPOPHOSPHITES
complex formation with chromium(III), mechanisms of, 20: 3863(R) (IS-1200(Sect. C))

HYPOTHYROIDISM
effects on thyrotropin content in plasma of patients, radioimmunassay method of measurement, 20: 3829
radiodiagnosis of, using iodine-125 as tracer, 20: 3844

I

IGNEOUS ROCKS
potassium, rubidium, strontium, thorium, and uranium content in oceanic theoleitic basalts, 20: 4145
strontium-87 to strontium-86 ratio in oceanic theoleitic basalts, 20: 4145

IMMUNE REACTIONS
of rabbits, to irradiated bovine corneal grafts, 20: 3718
radiation effects on, to sheep erythrocytes in rabbits, 20: 3689
radiation effects on rat, following lymph node irradiation, x, 20: 3718
radiation effects on, to renal transplants in dogs, γ, 20: 3729
radiation effects on, in rabbits, x, 20: 3738
radiation effects on, in rabbits, 20: 3746
radiation effects on, in tissue transplants in mice, 20: 3777
radiation effects on, to injected bone marrow in germ-free mice, 20: 3788
to leukemia transplants induced by two-virus strains, in mice, 20: 3694
to parasites in rats inoculated with irradiated larvae, 20: 3786

IMPACT SHOCK
tests on plastics, rubber, and springs, 20: 4112 (SC-TM-65-443)

IMPELLERS
computer programs for pump, 20: 4088 (TIM-949)

IN-PILE LOOPS
uses VBWR E-SADE, for testing superheater fuel elements, 20: 5104 (ACNP-65006)

INCOLOY
corrosion failure of Incoloy 800 in magnesium chloride solution, stress, 20: 4328 (WCAP-3269-50)
corrosion of 800, by lithium fluoride in cyclic high-temperature environment, 20: 4326 (TRW-ER-6561)
tensile properties of type-825, to 1300°F after prolonged thermal exposure, 20: 4373 (GEAP-4794)
thermal properties of type-801, to 1300°F after prolonged thermal exposure,

20: 4373 (GEAP-4794)
thermal properties of type-800, to 1300°F after prolonged thermal exposure, 20: 4373 (GEAP-4794)

INCONEL
corrosion by boiling potassium, effects on mechanical properties, 20: 5181(R) (ORNL-3029)
corrosion by cesium at 400°C, 20: 4337
corrosion by potassium at 870°C, 20: 4307(R) (ORNL-3870, pp 238-42)
corrosion of type 600, by partially neutralized boric acid solution, 20: 5134(R) (WCAP-3269-12)
creep and rupture properties, 20: 4999(R) (ORNL-2599)
radiation effects on stress-rupture properties of, 20: 4999(R) (ORNL-2599)
radiation effects on stress-rupture properties of, 20: 5181(R) (ORNL-3029)
radiation effects on stress-rupture at high temperatures, 20: 4299(R) (ORNL-2711)
tensile properties of type 718, to 1300°F after prolonged thermal exposure, 20: 4373 (GEAP-4794)
tensile properties of type 625, to 1300°F after prolonged thermal exposure, 20: 4373 (GEAP-4794)
thermal conductivity of type 702, 20: 4388(R) (ORNL-3870, pp 44-9)
thermal-stress cycling in fused salts, effects of, 20: 4999(R) (ORNL-2599)
thermal-stress cycling effects on, 20: 4299(R) (ORNL-2711)
welding properties of type 625, 20: 4306(R) (ORNL-3870, pp 194-213)

INCONEL X
corrosion of 750, by lithium fluoride in cyclic high-temperature environment, 20: 4326 (TRW-ER-6561)

INDEXES
keyword, to Ames Laboratory report, 20: 5213(R) (IS-1200)

INDIUM
determination in hydrochloric acid or methanol–nitric acid media, spectrophotometric, 20: 3888 (TID-22402)
magnetic transitions of thin superconducting films of, 20: 4785
nuclear magnetic resonance in, (E), 20: 4476(R) (IS-1200(Sect.P))
properties of, effects of low temperature on, 20: 4417
separation from silver by partition chromatography, 20: 4054
structure of intermediate state and surface energy of superconductors of, 20: 4778
superconducting properties of whiskers of, (E), 20: 4795

INDIUM ALLOYS
Bi–In, thermal capacity of superconducting, in magnetic fields, 20: 4786
Ce–In, magnetic properties of, at 2 to 300°K, 20: 4423
In–Ag–Tb, crystallography, 20: 4391(R) (ORNL-3870, pp 75-82)
In–Sn, magnetic transitions of thin superconducting films of, 20: 4785
In–Tl, elastic properties, 20: 4297(R) (IS-1200(Sect.M))
Sb–In, Hall coefficient in, effects of magnetic fields and temperature variations on, 20: 4479(R) (TID-22179, pp. 1-83)

INDIUM ISOTOPES In-114
beta transitions in, polarization from, (E), 20: 4880

INDIUM ISOTOPES In-116
energy levels of, parity and spin of, 20: 4825(R) (ANL-7081, pp 81-93)

INFECTIONS
associated with vesicouretheral reflux, diagnosis, 20: 3834
of *Escherichia coli* by bacteriophage, 20: 3748
of *Escherichia coli* by bacteriophage, 20: 3749
radiation effects on virus, of plants, γ, 20: 3768

INFLAMMATION
radioinduced myelitis, x, 20: 3771
radiotherapy of herpes zoster, 20: 3836
radiotherapy of Mikulicz's disease, x, 20: 3826

INOR-8
brazing to graphite, process development for, 20: 4308(R) (ORNL-3870, pp 243-60)
corrosion by lithium fluoride in cyclic high-temperature environment, 20: 4326 (TRW-ER-6561)
corrosion by nitrogen–oxygen mixtures at 1300 and 1400°F, 20: 4308(R) (ORNL-3870, pp 243-60)
corrosion by potassium–sodium at 1300 and 1400°F, effects of hydrogen and oxygen on, 20: 4322(R) (ORNL-3870, pp 305-7)
mechanical properties and microstructures of welds in, 20: 4308(R) (ORNL-3870, pp 243-60)
mechanical properties, effects of impurities on, 20: 4308(R) (ORNL-3870, pp 243-60)
radiation effects on mechanical properties of, neutron, 20: 4308(R) (ORNL-3870, pp 243-60)

INOSINE
radiosensitivity effects on cells in culture, γ, 20: 3791

INSECTS
radioinduced sterility in Mexican fruit flies, effects of dose on gamma, 20: 3745

INSTRUMENTATION
design for containment research installation, 20: 4184(R) (ORNL-3843, pp 71-135)
development for neutron cross section measurement, 20: 4246(R) (RPI-328-40, pp 49-55)
development for power reactors, 20: 5141
development for SEFOR experimental program, 20: 5120(R) (GEAP-4799)

INSTRUMENTS
book: *Radioactive Instruments–Their Application in Industry*, in Russian, 20: 4275
development for Eurochemic plant laboratory, 20: 4048(R) (NP-15406)
malfunction of, automatic detection and diagnosis of, (T), 20: 4222 (UCRL-13186)
performance of optical tooling, for dimensional location of reactor components, 20: 5035 (ORNL-TM-1278)
radiation effects on, review of, 20: 4464
requirements for radioisotope labs, 20: 4089 (TLW-1055A)
uses for automatic detection and diagnosis of malfunctions in arbitrary systems, (T), 20: 4222 (UCRL-13186)

INSULIN
radiation effects on amino acid changes in, uv, 20: 4016

INTERFEROMETERS
construction of 4-mm Fabry-Perot, 20: 4934 (AD-619093)
design and performance of laser, for plasma electron densities, 20: 4948(R) (TID-22179, pp 85-175)
design of angled-plate scanning, 20: 4232(P)
photon correlations in laser, effect of high-velocity translation on, (T), 20: 4223 (UCRL-14345)
use in Doppler temperature measurements in toroidal discharge, 20: 4713

INTERMETALLIC COMPOUNDS
heats of fusion of, high-temperature calorimeter for measuring, 20: 4297(R) (IS-1200(Sect.M))
properties and structure of rare earth, with copper, nickel, and silver, 20: 4448

INTERNAL CONVERSION
coefficients determination, (E), 20: 4476(R) (IS-1200(Sect.P))
coefficients of, beta spectrometer correction factor for measurement of, 20: 4248 (TID-22333)
measurement in rare earths using coincidence methods, (E/T), 20: 4476(R) (IS-1200(Sect.P))

INTESTINE
radiation effects on adsorptive function of, in man, 20: 3851
radiation effects on human, following therapy of cervical carcinomas, 20: 3720
radiation effects on, following carcinoma therapy, gamma, 20: 3732
radiation effects on absorption of fatty acids in, tracer study, x, 20: 3754
radiation effects on exteriorized rat, x, 20: 3775
radiation effects on exteriorized rabbit, x, 20: 3775
radiation injuries of, after radiotherapy of abdomen, 20: 3820
radiosensitivity of, 20: 3820
radiosensitivity of, 20: 3821

IODIDES
metabolism of iodine-132-labeled, apparatus for determining human, 20: 4202
transport of, from plasma to milk in cattle, tracer study, 20: 3674

IODINE
content in chondrites, 20: 4526
deposition in diffusion tubes, effects of temperature on, 20: 4185(R) (ORNL-3843, pp 169-234)
diffusion from liquid urania in containment mockup experiments, 20: 4184(R) (ORNL-3843, pp 71-135)
electric conductivity of solid, at high pressures, 20: 4708(R) (UCRL-14360, pp 50-73)
electron lifetime in, K-shell, (E), 20: 4536 (COO-818-61)
electron lifetime in K-shell, (E), 20: 4551
metabolism of, effects of content in atmosphere on, 20: 3673
metabolism of, in children, tracer studies, 20: 3844
properties of fission-product, in reactor accidents, 20: 4183(R) (ORNL-3843, pp 2-70)
radiation dosing from plasma, thyroidal, and urinary, after neutron activation, 20: 3658(R) (EUR-2414.f,i)
reactions of vaporous, with dioctylphthalate, 20: 4185(R) (ORNL-3843, pp 169-234)
reactions with organic vapors, 20: 4185(R) (ORNL-3843, pp 169-234)
secretion in cow's milk of, tracer study, 20: 3674
separation of molecular, from atmosphere, 20: 3673
sorption from air on activated charcoal, factors affecting, 20: 4086(R) (ORNL-3843, pp 137-67)

IODINE COMPOUNDS
chemical reactivity of radioactive vaporous, 20: 4185(R) (ORNL-3843, pp 169-234)
iodine-129 Mössbauer effect in, 20: 5018
sorption from air on activated charcoal, factors affecting, 20: 4086(R)

(ORNL-3843, pp 137-67)
IODINE ISOTOPES I-125
sorption by fats, 20: 3658(R) (EUR-2414.f,i)
use for diagnosis of thyroid diseases, 20: 3844
use for external measuring of renal excretion, 20: 3658(R) (EUR-2414.f,i)
use in x-ray unit for measuring mineral changes in bones, 20: 3803 (ORNL-IIC-5, pp 257-76)
IODINE ISOTOPES I-126
production by iodine-127 photonuclear reactions, 20: 3863(R) (IS-1200 (Sect. C))
IODINE ISOTOPES I-127
nuclear magnetic resonances in organic compounds, catalog of, 20: 3973 (IS-1222)
IODINE ISOTOPES I-129
energy levels of, mean life of 26.8-kev, 20: 5018
Mössbauer effect of 26.8-kev transition in, 20: 5018
IODINE ISOTOPES I-131
determination in radioisotope mixtures, microcalorimetric, 20: 3866 (CEA-R-2630)
dosage calculations of, for therapy of thyroid diseases, 20: 3853
metabolism in man of polyvinylpyrrolidone-incorporated, dose from, 20: 3675
metabolism in mice of, effects of chlorpromazine on, 20: 3677
metabolism in thyroid gland of man, effects of pathological conditions of pathological conditions of thyroid on, 20: 3660 (NP-15528)
monitoring in stack effluents using activated charcoal, 20: 4179 (LA-3363)
separation from waste solutions using manganese dioxide, 20: 5206
sorption by fats, 20: 3658(R) (EUR-2414.f,i)
use as label for rose bengal, for use in liver function tests, 20: 3774
use as tracer in clinical cardiology, 20: 3818
use for diagnosis of thyroid diseases, 20: 3844
use for therapy of thyroid diseases of, 20: 3853
use in radiodiagnosis of cancers, 20: 3658(R) (EUR-2414.f,i)
IODINE ISOTOPES I-132
metabolism of methyl iodide-incorporated, design of apparatus for determining, 20: 4202
ION EXCHANGE MATERIALS
properties of sodium molybdates and tungstates in ferrocyanic acid as, 20: 3871 (EUR-2497.e)
ION EXCHANGE PROCESSES
design of nonaqueous, for rare earths, 20: 4067
ION SOURCES
design and performance of, for cyclotrons, 20: 4519
development for polarized ions, 20: 4823(R) (ANL-7081, pp 36-69)
IONIZATION
production and removal in upper atmosphere, 20: 4729 (CNIE-PE-4)
radioinduced in gases, measurements of beta, 20: 4557
IONIZATION CHAMBERS
performance as personnel monitors in synchrotron area, 20: 4237 (BNL-9665)
testing of reactor, system for, 20: 5037
IONOSPHERE
electron and ion content in, distribution of, (E), 20: 4760
electron densities of, focusing properties of inhomogeneous, (E), 20: 4735
electron density anomaly in F region of, from longitudinal current system, (T), 20: 4749
electron density and temperature variations in F region of, (E), 20: 4755
electron distribution in D region of, (E/T), 20: 4754
electron energy distribution in F region of, photoelectron contribution to, (T), 20: 4753
electron energy loss rate in D region of, 20: 4727 (AD-618054)
frequency of F2 layer of, in IGY-IGC magnetically active periods, 20: 4741
geomagnetic effects on PCA events in, 20: 4756
geomagnetic variations in, classification of diurnal, 20: 4742
helium–ion losses in, 20: 4759
in temperature variations in F region of, (E), 20: 4755
ionization exchange between protonosphere and, (T), 20: 4761
ionization in lower, cosmic ray and solar effects on, (E), 20: 4737
ionization of lower, geomagnetic storm effects on anomalous, (E), 20: 4736
magnetic micropulsation resonance propagation in, (T), 20: 4728 (AD-618118)
solar burst and sunspot effects in, research on, 20: 4521 (AD-618222)
temperature of, processes affecting, (T), 20: 4761
IONS
density in electron beams in gases, 20: 4722
electron reactions with strongly ionized p^2, excitation in, (T), 20: 4543
mixing with electrons for plasma injection, device for, 20: 4993(P)
ordering in superconductors, (T), 20: 4476(R) (IS-1200(Sect.P))
polarizability and shielding factor for, perturbation theory calculation of dipole, 20: 4537 (NP-15576)
polarizability and shielding factor for, perturbation theory calculation of quadrupole, 20: 4538 (NP-15577)
production of polarized, 20: 4823(R) (ANL-7081, pp 36-69)
reactions in matter, δ-ray distributions from, (T), 20: 4541 (UCRL-16405)
scattering by even-even nuclei, reorientation effect in Coulomb excitation by, (T), 20: 4901
scattering by nuclei, matrix elements for inelastic, (T), 20: 4839 (JINR-P-2333)
temperature variations in F region of ionosphere, (E), 20: 4755
IRIDIUM
determination in platinum by neutron activation, 20: 3863(R) (IS-1200 (Sect. C))
IRIDIUM ALLOYS
Ir–Pt, corrosion by cesium at 400°C, 20: 4337
IRISH SEA
biology of Solway Firth, effects of fission products from waste solutions and fallout on, 20: 3662 (PG-Report-650)
IRON
analysis for nickel, spectrophotometric, 20: 3863(R) (IS-1200(Sect. C))
analysis for oxygen by neutron activation methods, 20: 3907
carburization of, mechanisms of, 20: 4297(R) (IS-1200(Sect.M))
determination in hydrochloric acid or methanol–nitric acid media, spectrophotometric, 20: 3888 (TID-22402)
determination in iron–nickel–uranium solutions, controlled-potential coulometric, 20: 3879(R) (MLM-1266)
determination in mixtures by x-ray fluorescence using promethium-147/aluminum and tritium/zirconium sources, 20: 3883 (ORNL-IIC-5, pp 154-81)
determination in plants by neutron activation methods, 20: 3901
gamma attenuation in slabs of, (E), 20: 4997(R) (EUR-2494.d)
gamma reactions at 0.01 to 10 Mev, cross sections for, 20: 4996 (AWRE-O-79/65)
gamma transport in, methods for calculating, (T), 20: 5001 (ORNL-RSIC-9)
magnetic effects in crystal whiskers of, (E), 20: 4476(R) (IS-1200 (Sect.P))
magnetic effects in, (E), 20: 4476(R) (IS-1200(Sect.P))
meson (μ^-) transitions in mesic atoms of, energy of, 20: 4825(R) (ANL-7081, pp 81-93)
neutron cross sections for, 9- and 16-group, 20: 4829 (GEMP-173(Suppl.1))
neutron cross sections for, 20: 4830 (GEMP-384)
neutron transport in, (E/T), 20: 4998 (JINR-P-2359)
radiation from promethium-147 beta excited, 20: 3882 (ORNL-IIC-5, pp 51-71)
reactions with cobalt(III) complexes, mechanisms of, 20: 3863(R) (IS-1200(Sect. C))
thermal capacity at 100 to 1300°C, 20: 4388(R) (ORNL-3870, pp 44-9)
thermal conductivity in Armco, at 30 to 1100°C, (E), 20: 4476(R) (IS-1200(Sect.P))
thermal conductivity to 900°C, method for calculating, 20: 4388(R) (ORNL-3870, pp 44-9)
thermodynamic properties of oxygen in liquid, 20: 4454
IRON ALLOYS
Al–Co–Fe–Ti–V, properties of aged, 20: 4360(R) (AD-619399)
Al–Fe, electric conductivity, 20: 4297(R) (IS-1200(Sect.M))
Al–Fe, plasticity of, effects of composition and temperature on, 20: 4297(R) (IS-1200(Sect.M))
Al–Fe–Mo–Ti–V, properties of aged, 20: 4360(R) (AD-619399)
Al–Fe–Ti–V, properties of aged, 20: 4360(R) (AD-619399)
Be–Fe, preparation by splatcooling and hot-pressing, 20: 4381(R) (NMI-8001.4)
Co–Fe, plastic deformation of, effects of temperature on, 20: 4297(R) (IS-1200(Sect.M))
Co–Fe, properties of Hiperco 27 for use in space electric power systems, 20: 4379 (NASA-CR-54091)
Co–Fe, thermodynamic properties of oxygen in liquid, 20: 4454
Co–Fe–Mo–Ni, properties of Maraging Steel for use in space electric power systems, 20: 4379 (NASA-CR-54091)
Co–Fe–V, properties of Hiperco 50 and Supermendur for use in space electric power systems, 20: 4379 (NASA-CR-54091)
Cr–Fe–Mo–Ni–Nb–W, welding properties of Inco IN-102, 20: 4306(R) (ORNL-3870, pp 194-213)
Cr–Fe–Mo–V, properties of H-11 Steel for use in space electric power systems, 20: 4379 (NASA-CR-54091)
Fe–Ni, thermodynamic properties of oxygen in liquid, 20: 4454
Fe–Ni–U, analysis for iron and uranium by controlled-potential coulometry, 20: 3879(R) (MLM-1266)
Fe–Rh, plastic deformation of, factors affecting, 20: 4297(R) (IS-1200(Sect.M))

corrosive effects on stainless steel, effects of molybdenum and uranium
Fe–Th, crystal structure, 20: 4297(R) (IS-1200(Sect.M))
Gd–Fe, crystal structure, 20: 4297(R) (IS-1200(Sect.M))
IRON(III) CHLORIDES
on, 20: 4325 (TB-58)
corrosive effects on failure of Zircaloy-4 under stress, 20: 4328 (WCAP-3269-50)
IRON COMPLEXES
iron-57 Mossbauer effect in, crystal lattice effects on, 20: 3927(T) (AERE-Trans-1026)
IRON COMPOUNDS
iron-57 Mossbauer effect in, crystal lattice effects on, 20: 3927(T) (AERE-Trans-1026)
IRON IODIDES
stability of, thermal, 20: 4185(R) (ORNL-3843, pp 169-234)
IRON IONS
effects of bivalent, on radioinduced polymerization of methylmethacrylate on polyethylene, 20: 3996
IRON ISOTOPES Fe-54
energy levels, 20: 4849(R) (UCRL-14360, pp 1-50)
proton scattering at 18.6 and 19.1 Mev, (E/T), 20: 4849(R) (UCRL-14360, pp 1-50)
IRON ISOTOPES Fe-55
separation from sea water by precipitation, method for, 20: 3891(T) (CEA-tr-A-1838)
IRON ISOTOPES Fe-56
energy levels, 20: 4849(R) (UCRL-14360, pp 1-50)
proton scattering at 18.6 and 19.1 Mev, (E/T), 20: 4849(R) (UCRL-14360, pp 1-50)
IRON ISOTOPES Fe-57
Mossbauer effect in iron complexes and covalent iron compounds, crystal lattice effects on, 20: 3927(T) (AERE-Trans-1026)
IRON ISOTOPES Fe-59
separation from sea water by precipitation, method for, 20: 3891(T) (CEA-tr-A-1838)
IRON OXIDES
pulmonary excretion of, effects of chronic cigarette smoking on, tracer study in dogs, 20: 3655 (BNWL-SA-224)
IRON(III) OXIDES
magnetization of, spin-wave theory for sublattice, 20: 5006(R) (ORNL-3870, pp 50-5)
radiation effects on electrostatic charge in colloids of, x, 20: 4015
solubility in borax at 760 to 900°C, 20: 3951
Dy_2O_3–Fe_2O_3, crystal structure and magnetic properties, 20: 4411
Eu_2O_3–Fe_2O_3, crystal structure and magnetic properties, 20: 4411
Fe_2O_3–La_2O_3, crystal structure and magnetic properties, 20: 4411
Fe_2O_3–Nd_2O_3, crystal structure and magnetic properties, 20: 4411
Fe_2O_3–Pr_2O_3, crystal structure and magnetic properties, 20: 4411
Fe_2O_3–Sm_2O_3, crystal structure and magnetic properties, 20: 4411
IRON SYSTEMS
Fe–D_2O, neutron fluxes and leakage through perforated laminates of, (E/T), 20: 4800 (AE-198)
Fe–H_2O, neutron transport in, (E/T), 20: 4998 (JINR-P-2359)
Fe–H_2O, proton reactions at 170 to 660 Mev, neutron production in, (T), 20: 4998 (JINR-P-2359)
Fe–Si, plastic deformation of, effects of atomic order on, 20: 4297(R) (IS-1200(Sect.M))
Fe–Si, properties of Cubex for use in space electric power systems, 20: 4379 (NASA-CR-54091)
IRRADIATION FACILITIES
design and operation of gamma, 20: 4090 (JPRS-32842)
design and uses of 2 kC cobalt-60, 20: 4272(T) (JPRS-32813)
door design for, 20: 4096(P)
ISOTOPE EFFECTS
deuterium and tritium, on thermodynamic properties of hydrogen selenides and sulfides, 20: 3950
on dipole moments of small organic molecules, 20: 3977
on spectra of tin hydride, 20: 3942
on vibrational spectra of dibromoborane, 20: 3940
ISOTOPE SEPARATION METHODS
development of gas-centrifuge, 20: 4285
electromagnetic, performance of Seibersdorf sector field, 20: 4283 (SGAE-PH-27/1965)
ISOTOPIC EXCHANGE
between deuterium or tritium and methane, 20: 3980
between inorganic and organic thallium compounds, 20: 3960
between polymeric tungstates, 20: 3863(R) (IS-1200(Sect. C))
between sulfur or sulfides and thiopene, 20: 3976
between sulfuryl and thionyl chlorides, 20: 3865
intermediates in self-, in diborane, 20: 3963
ITALY
fallout monitoring, 1964, 20: 4155 (EUR-2516.d,f,i,n)

J

JAPAN
fallout monitoring, 1961 and 1962, 20: 4177 (JAERI-1083)
gas centrifuge development in, for isotope separation, 20: 4285
radiation dose from dental radiography of population of, 20: 4195
radiography in, gonadal dose from dental, 20: 4196
JAWS
radiation dose distribution in phantom, photographic film for determining gamma, 20: 4205
radiation effects on development and eruption of teeth in, of monkeys, x, 20: 3743
radiation effects on development of bones of, in children, 20: 3808
radioinduced osteonecrosis in monkey, effects of dose fractionation on x, 20: 3742
JOURNAL BEARINGS
flow analysis of liquid-metal-lubricated, 20: 4078(R) (SWRI-1228-67)

K

KETONE, CYCLOPROPYL METHYL
molecular structure, 20: 3863(R) (IS-1200(Sect. C))
KIDNEYS
excretion by, use of iodine-125 for external measurement of, 20: 3658(R) (EUR-2414.f,i)
function tests of, using iodine-131 labeled serum albumin or Hippuran, 20: 3800(R) (NP-15150)
nephrosis of rat, induced by injected uranium nitrate or mercuric chloride, 20: 3666
radiography of, double-dose technique for contrast media in, 20: 3857
toxic effects of uranyl nitrate in mouse, 20: 3670
transplants in dogs, radiation effects on immune reactions to, 20: 3729
KRYPTON
determination using omegatron, 20: 3908
diffusion in graphite, 20: 5117(R) (GA-5866)
diffusion in ionic crystals and sintered materials, 20: 3944
diffusion in uranium dioxide, 20: 4435
reactions with mercury-199 and -201, hyperfine-level excitation in, (E), 20: 4544
KRYPTON ISOTOPES Kr-85
diffusion from pyrolytic carbon deposits, 20: 5089(R) (GA-6181)
use as tracer for measuring cerebral circulation, 20: 3658(R) (EUR-2414.f,i)
KRYPTON ISOTOPES Kr-86
concentration by thermal diffusion, 20: 3879(R) (MLM-1266)
KRYPTON ISOTOPES Kr-87
diffusion from pyrolytic carbon deposits, 20: 5089(R) (GA-6181)
KRYPTON ISOTOPES Kr-88
decay scheme, 20: 3982(R) (AGN-8156)
diffusion from pyrolytic carbon deposits, 20: 5089(R) (GA-6181)
KRYPTON ISOTOPES Kr-89
diffusion from pyrolytic carbon deposits, 20: 5089(R) (GA-6181)

L

LA CROSSE BOILING WATER REACTOR
design and operation procedures, 20: 5105 (ACNP-65544(Vol.I))
design and operating safeguards of, 20: 5106 (ACNP-65544(Vol.II))
LABORATORIES
conference on high-activity hot, Grenoble, June 15 to 18, 1965, 20: 4040
decontamination of radiometallurgical, 20: 4213
design and operation of hot, for handling more than 1000 C, directory of, 20: 4045
design for processing, storage, and transfer of radioactive materials, 20: 4041
design of Eurochemic, 20: 4048(R) (NP-15406)
design of radioisotope, considerations and economics for, 20: 4089 (TLW-1055A)
LABORATORY EQUIPMENT
coatings for, development of polymer, 20: 3979
decontamination of, at Harwell, 20: 4212
transport through alpha-gamma barriers in hot cells, 20: 4042
LACTASES
radiation effects on β-galactosidase in bacterial cells, mechanism of uv inactivation, 20: 3686(R) (TID-22352)
LACTOSE
effects on radioinduced decomposition of methyl linoleate, 20: 4019
LANTHANUM
determination in hydrochloric acid or methanol–nitric acid media, spectrophotometric, 20: 3888 (TID-22402)
effects on grain growth and magnetic properties of europium sulfide crystals, 20: 4358(R) (AD-438516)

solvent partition between magnesium alloys and magnesium–potassium–sodium chloride salt mixture, 20: 3865 (ANL-7064)
specific heat of fcc, (E), 20: 4476(R) (IS-1200(Sect.P))
superconductivity of, effects of crystal imperfections on, 20: 4297(R) (IS-1200(Sect.M))
transformations in, mechanisms of diffusionless, 20: 4297(R) (IS-1200 (Sect.M))

LANTHANUM ALLOYS
La–Ag, vaporization of, mass spectrometric studies of, 20: 3957
La–Ag–Tb, crystallography, 20: 4391(R) (ORNL-3870, pp 75-82)
La–W, preparation and properties of single-crystal, (E), 20: 4476(R) (IS-1200(Sect.P))

LANTHANUM CHLORIDES
heat of dilution of aqueous, at 25°C, 20: 3956

LANTHANUM HYDRIDES
phase studies, 20: 3936
phase studies, 20: 4297(R) (IS-1200(Sect.M))

LANTHANUM ISOTOPES La-139
alpha clustering structure on surface of, 20: 4886
proton reactions (p,pα) at 30 to 155 Mev, alpha cluster structure in, (T), 20: 4886

LANTHANUM OXIDES
BeO–La_2O_3, phase studies, 20: 5181(R) (ORNL-3029)
Fe_2O_3–La_2O_3, crystal structure and magnetic properties, 20: 4411
La_2O_3–PbO, phase studies, 20: 3931

LANTHANUM SULFIDES
homogeneity regions in, 20: 3938
vaporization of, mass spectrometric studies of, 20: 3957

LEAD
corrosive effects on carbon steel, Croloy 2¼, niobium–1 zirconium, and type 410 stainless steel, 20: 4308(R) (ORNL-3870, pp 243-60)
energy bands of, relativistic, (T), 20: 4476(R) (IS-1200(Sect.P))
gamma angular distributions and energy spectra in, calculation using Monte Carlo method, 20: 5181(R) (ORNL-3029)
gamma heating in slabs of, 20: 4999(R) (ORNL-2599)
gamma productivity in, secondary, 20: 4999(R) (ORNL-2599)
gamma reactions at 0.01 to 10 Mev, cross sections for, 20: 4996 (AWRE-O-79/65)
magnetic resonance shifts at 4.2 to 450°K, (E), 20: 4476(R) (IS-1200 (Sect.P))
magnetic susceptibility of, de Haas–Van Alphen effects in, (E) 20: 4476(R) (IS-1200(Sect.P))
neutron transmission by slabs of, angular distributions in, 20: 5181(R) (ORNL-3029)
properties of, effects of low temperature on, 20: 4417
radiation effects on diffusion in silver, alpha, 20: 4385(R) (ORNL-3870, pp 15-9)
separation from silver by partition chromatography, 20: 4054
ultrasonic attenuation in normal and superconducting, 20: 4782
use of shots of, in separation of vanadium from aqueous solutions, 20: 4071(P)

LEAD ALLOYS
Bi–Pb, wetting reactions with stainless steel, 20: 4077(R) (IS-1200 (Sect. E))
Ce–Pb, magnetic properties of, at 2 to 300°K, 20: 4423
Pb–Ag, thermodynamic properties of, 20: 5223 (UCRL-16303)
Pb–Mg, solvent properties for rare earth elements in molten chloride salts, 20: 3865 (ANL-7064)
Pb–Tl, elastic properties, 20: 4297(R) (IS-1200(Sect.M))
Pb–Y, phase diagrams, 20: 4297(R) (IS-1200(Sect.M))
Pb–Yb, phase diagrams, 20: 4297(R) (IS-1200(Sect.M))

LEAD FLUORIDES
properties of molten, for use as reactor fuels, 20: 4376 (JUL-268-RG)

LEAD IONS
spectra in lithium chloride–potassium chloride eutectic, absorption, 20: 3921(R) (ORNL-3870, pp 56-60)

LEAD ISOTOPES Pb-203
decay energies of, coincidence methods for determining, (E), 20: 4843 (NP-15456)

LEAD ISOTOPES Pb-205
analysis for polonium-209, counting systems for, 20: 3879(R) (MLM-1266)

LEAD ISOTOPES Pb-208
proton elastic scattering at 160 Mev, differential cross sections for, (E/T), 20 4906

LEAD ISOTOPES Pb-212
energy level transitions in, conversion ratios for 238, 6-kev, (E), 20: 4920

LEAD OXIDES
radiation effects on phase transformations in, neutron, 20: 4462
solubility in borax at 760 to 900°C, 20: 3951
La_2O_3–PbO, phase studies, 20: 3931

LEAD, TETRAETHYL-
determination in gasoline using beta-excited x-ray sources, absorptiometric, 20: 3882 (ORNL-IIC-5, pp 51-71)

LEAD URANIUM TELLURATES
crystal structure of, x-ray diffraction analysis of, 20: 4173
occurrence in Moctezuma, Sonora, Mexico, 20: 4173

LEAD URANYL ARSENATES
occurrence, in Black Forest, Germany, 20: 4172

LEAVES
composition and structure of Fraction I protein in Chinese cabbage, 20: 5219 (TID-22372)

LECTURES
book: *Elementary Particle and High Energy Physics*, 20: 4695
book: *Lectures in Theoretical Physics*. Vol. IV., 20: 4487

LEPTONS
interactions with strongly interacting particles, strangeness change in, (T), 20: 4635
production in neutrino reactions with matter, (T), 20: 4866

LEUKEMIA
antigenic characteristics of virus-induced mouse, 20: 3694
bone marrow failure induced by, treatment with massive androgen therapy, 20: 3793
diagnosis using aberrations in marrow chromosomes, 20: 3650
effects of dimethyl mylenan on cells of murine, in culture, cytotoxic, 20: 3736
effects on nitrogen mustards on cells of murine, in culture, cytotoxic, 20: 3736
etiology of, environmental factors, 20: 3779
immunological differences in virus-induced mouse, 20: 3694
incidence in Portugal, 20: 3753
radiation effects on antigen production by transplanted virus-induced, in mice, 20: 3694
radioinduced in man, incidence of, 20: 3779
radioinduced in mice, mechanism for x, 20: 3696
radioinduced in mice effects of, genotype, 20: 3765
radioinduced in polycythemia patients, incidence of β, 20: 3837
radioinduced, by phosphorus-32 used therapeutically, 20: 3835
radioinduced, etiology of, 20: 3730
radiosensitivity of cells of murine, in culture, 20: 3736

LEUKOCYTES
radioinduced chromosome aberrations in, relation to leukemogenesis, 20: 3730

LEVEL INDICATORS
development for extraction columns, 20: 4048(R) (NP-15406)

LID TANK FACILITY
gamma transmission by shielding configurations at, 20: 4999(R) (ORNL-2599)
neutron flux in water in, thermal, (E/T), 20: 4299(R) (ORNL-2711)
neutron transmission by shielding configurations at, 20: 4999(R) (ORNL-2599)

LIFE SPANS
radiation effects on mouse, effects of genotype on, 20: 3711(R) (NYO-3314-2)
radiation effects on, in mice with transplanted tumors, x, 20: 3751
radiation effects on, of x-ray technicians, x, 20: 3760
radiation effects on, of germ-free mice, 20: 3778

LIGHT
effects of wavelength of, on plant growth, 20: 3769
effects on protein synthesis in *E. coli*, 20: 3726
effects on *Serratia marcescens*, lethal, effects of humidity on, 20: 3740
scattering by pure liquids, Cabannes factor and Rayleigh ratio for, 20: 3941
polarization analysis of elliptically-polarized, (T), 20: 4480 (UCRL-11802)
scattering from plasma, incoherent, 20: 4948(R) (TID-22179, pp 85-175)

LINEAR ACCELERATORS
beam dynamics of, method for determining, (T), 20: 4503 (NP-15340)
beam motion in electron, transversal, (E), 20: 4494 (CEA-R-2843)
development for pulsed neutron sources, 20: 4508(R) (RPI-328-40)
development of variable-energy 800-Mev proton, (E), 20: 4498(R) (LA-3419)
operation of British proton, 20: 4504(R) (NP-15420)
radiation detector uses at Orsay, semiconductor, 20: 4243 (LAL-1102)

LINGEN POWER REACTOR
construction, 20: 5139
radiation effects on, in presence of lactose, 20: 4019

LIPIDS
effects of injected, on immune reactions in rabbits, 20: 3689
radiation effects on mouse plasma, x, 20: 3704

LIPOPROTEINS
properties of serum, effects of ethyl ether and incubation on physico-chemical on, 20: 3704
radiation effects on physico-chemical properties of serum, 20: 3704

LIQUEFIERS
design and performance of hydrogen, 20: 4797
design and performance of helium and hydrogen, 20: 4798

LIQUID FLOW
oscillation for fuel tube, contral equipment for, 20: 5123(R) (HPR-61)
LIQUID METAL COOLED REACTORS
heat exchangers for sodium, performance testing of, 20: 5131(R) (UNC-5135)
LIQUIDS
gas–liquid, computer program for integration of Gibbs–Duhem equation for equilibrium in metal systems of, 20: 4375 (IS-1341)
hydromagnetic waves in rotating, effect of Hall current on, (T), 20: 4711
light scattering by pure, Cabannes factor and Rayleigh ratio for, 20: 3941
radiation dosimetry in, electrons, 20: 4204
radioactivity measurements in, scintillation method for, 20: 3870 (EUR-2459.f)
transfer of noxious, remotely controlled apparatus for, 20: 4095(P)
LITHIUM
bremsstrahlung reactions (γ,π^0) at 166 Mev, angular distributions from, (E), 20: 4898
corrosive effects on brazing alloys at high temperatures, 20: 4999(R) (ORNL-2599)
corrosive effects on cermets at high temperatures, 20: 4299(R) (ORNL-2711)
corrosive effects on niobium, time dependence of, 20: 5181(R) (ORNL-3029)
corrosive effects on niobium, alloying effects on, 20: 4299(R) (ORNL-2711)
corrosive effects on niobium, 20: 4999(R) (ORNL-2599)
corrosive effects on beryllium, 20: 4999(R) (ORNL-2599)
corrosive effects on niobium- and tantalum-base alloys, effects of oxygen on, 20: 4301(R) (ORNL-3870, pp 102-35)
corrosive effects on tantalum, effects of oxygen content on, 20: 5181(R) (ORNL-3029)
determination in tungsten bronze, spectrographic, 20: 3863(R) (IS-1200 (Sect. C))
determination in yttrium, methods for, 20: 4299(R) (ORNL-2711)
effects on mechanical properties of 316 stainless steel, 20: 4299(R) (ORNL-2711)
effects on tensile properties of niobium and niobium–zirconium alloy, 20: 5181(R) (ORNL-3029)
equation of state, 20: 4476(R) (IS-1200(Sect.P))
heat-transfer coefficients for molten, system for determining, 20: 4299(R) (ORNL-2711)
purification, 20: 4999(R) (ORNL-2599)
purification by extraction with molten salts, 20: 4299(R) (ORNL-2711)
solvent properties for lithium nitride and lithium oxide, 20: 4999(R) (ORNL-2599)
solvent properties for lithium oxides, 20: 4299(R) (ORNL-2711)
thermal conductivity, 20: 5181(R) (ORNL-3029)
thermal conductivity of molten, 20: 4299(R) (ORNL-2711)
wave function calculation, antisymmetric, 20: 5006(R) (ORNL-3870, pp 50-5)
Li–Ag, thermal conductivity, 20: 5181(R) (ORNL-3029)
LITHIUM ALLOYS
Li–Ni, phase studies, 20: 4442
LITHIUM BROMIDES
thermodynamics of, in anhydrous *N,N*-dimethylformamide and *N*-methylformamide at 25°C, 20: 3926 (TID-22374)
LiBr–$NiBr_2$, spectra of nickel(II) in melts of, absorption, 20: 3921(R) (ORNL-3870, pp 56-60)
LITHIUM CHLORIDES
corrosive effects on failure of stainless steel under stress, 20: 4328 (WCAP-3269-50)
thermodynamic properties in anhydrous *N*-methylformamide solutions, 20: 3925 (TID-22366, App. B)
thermodynamic properties in *N*-methylformamide solutions, 20: 3924 (TID-22366)
thermodynamics of, in anhydrous *N,N*-dimethylformamide and *N*-methylformamide at 25°C, 20: 3926 (TID-22374)
LiCl–KCl, cadmium, cerium, cobalt, neptunium, uranium, and zinc distribution between γ-alumina and molten, 20: 3959
LiCl–KCl–$ZnCl_2$, oxidizing effects of liquid, on thorium, 20: 4297(R) (IS-1200(Sect.M))
LiCl–KCl–$ZnCl_2$, reactions with uranium carbide at 540 to 800°C, 20: 4297(R) (IS-1200(Sect.M))
LiCl–KCl, reactions of eutectic, with uranium hexafluoride, 20: 4046(R) (EURAEC-1340)
LiCl–KCl, spectra of bismuth, lead, and thallium ions in eutectic of, absorption, 20: 3921(R) (ORNL-3870, pp 56-60)
LiCl–$NiCl_2$, spectra of nickel(II) in melts of, absorption, 20: 3921(R) (ORNL-3870, pp 56-60)
$MgCl_2$–LiCl–KCl, solvent properties of liquid, for rare earths, 20: 4297(R) (IS-1200(Sect.M))
LITHIUM FLUORIDES
corrosive effects on superalloys in cyclic high-temperature environment, 20: 4326 (TRW-ER-6561)
performance for neutron dosimetry, 20: 4236 (ORNL-9605)
properties of molten, for use as reactor fuel, 20: 4376 (JUL-268-RG)
thermodynamic properties in *N,N*-dimethylformamide and *N*-methylformamide solutions, 20: 3924 (TID-22366)
BeF_2–LiF–UF_4–ZrF_4, corrosive effects on type 304 stainless steel, 20: 4308(R) (ORNL-3870, pp 243-60)
LiF–MgF_2–YF_3, analysis for magnesium and yttrium, 20: 4999(R) (ORNL-2599)
LiF–MgF_2–YF_3, analysis for oxygen, 20: 4299(R) (ORNL-2711)
LiF–YF_3, phase diagram, 20: 4999(R) (ORNL-2599)
LiF–YF_3, phase diagram, 20: 4299(R) (ORNL-2711)
UF_4–KCl–LiCl, electrolysis of fused, for production of high-purity uranium, 20: 4347
LITHIUM HYDRIDES
properties and salt-like nature of, 20: 3928(T) (UCRL-Trans-1254(L))
LITHIUM ISOTOPES
distribution in natural sources, 20: 3863(R) (IS-1200(Sect. C))
LITHIUM ISOTOPES Li-6
energy levels, (E), 20: 4849(R) (UCRL-14360, pp 1-50)
gamma reactions (γ,n) at 6.0 to 32 Mev, cross sections for, (E), 20: 4849(R) (UCRL-14360, pp 1-50)
neutron reactions (n,α) with, alpha and triton energy distributions from, 20: 5181(R) (ORNL-3029)
neutron reactions (n,α) at 1.2 to 8.0 Mev, cross section for, (E), 20: 4299(R) (ORNL-2711)
LITHIUM ISOTOPES Li-7
deuteron reactions (d,n) with, alpha spectra from beryllium-8 breakup in, (E), 20: 4869
helium-3 reactions (He-3,n) at 1.3 to 5.8 Mev, (E), 20: 4925
nuclear electric moment deformation of, quadrupole, (T), 20: 4902
nuclear electric quadrupole moment of, supermultiplet theory with configuration mixing for, 20: 4904
LITHIUM NITRATES
$LiNO_3$–methanol–HNO_3, use as solvent in ion-exchange separation of rare earths, 20: 4067
LITHIUM NITRIDES
solubility in lithium, 20: 4999(R) (ORNL-2599)
LITHIUM OXIDES
solubility in lithium, 20: 4999(R) (ORNL-2599)
solubility in lithium, 20: 4299(R) (ORNL-2711)
LITHIUM TUNGSTATES
electron spin resonance in, (E/T), 20: 4476(R) (IS-1200(Sect.P))
LIVER
cerium-144 distribution in cells of rat, following intravenous injection, model for, 20: 3682
deposition of gold-198 colloids in dog, 20: 3680
deposition of gold-198 colloids in dogs, 20: 3681
fructose metabolism in, tracer study, 20: 3684
function tests of, using iodine-131-rose bengal, 20: 3774
immune reactions in, of rabbits, 20: 3746
metabolism of colloids of gold-198 in, 20: 3822
radiation injuries of, function tests for determination of, 20: 3774
radioactivity in human, following injections of iodine-131-labeled polyvinylpyrrolidone, 20: 3675
radioinduced chromosome aberrations in mouse, effects of age, 20: 3711(R) (NYO-3314-2)
toxic effects of uranyl nitrate in mouse, 20: 3670
LOOPS
design and operation of fissiochemical, 20: 3982(R) (AGN-8156)
flow in liquid metal, measurement of, 20: 4077(R) (IS-1200(Sect. E))
LUBRICANTS
materials for space-vehicle, 20: 4312
LUMINESCENT DETECTORS
design of phosphate glass, 20: 4258(P)
LUNGS
fatty acid synthesis in tissue of, tracer study in dog, rabbit, and rat, 20: 3656 (BNWL-SA-225)
radiation dose to, of radon spa personnel, alpha, 20: 3798
radiation effects on rat, effects of dose fractionation on histological electron, γ, and x, 20: 3700
radiodiagnosis of diseases of, use of ytterbium-169 in portable device for, 20: 3804 (ORNL-IIC-5, pp 309-28)
radiodiagnosis of embolisms of, 20: 3818
radioinduced, in lungs of hamsters and rats, 20: 3785
LUTETIUM
determination in hydrochloric acid or methanol–nitric acid media, spectrophotometric, 20: 3888 (TID-22402)
separation from nitrogen and oxygen by electrotransport, 20: 4297(R) (IS-1200(Sect.M))
LUTETIUM HYDRIDES
electric conductivity of solid phases of, 20: 3934

LUTETIUM ISOTOPES Lu-175
energy levels, (E), 20: 4476(R) (IS-1200(Sect.P))
LUTETIUM ISOTOPES Lu-176
activity of, calibration of, 20: 4916
gamma decay, 20: 4924
LUTETIUM SYSTEMS
H–Lu, electric conductivity of solid phases of, 20: 3934
LUTETIUM SULFIDES
homogeneity regions in, 20: 3938
LYMPH CELLS
radiation effects on nodes and vessels in rat, x, 20: 3718
radiation effects on rat, x, 20: 3718
LYMPH SYSTEM
metabolism of colloids of gold-198 in, 20: 3822
radiation effects on immune reactions in dog, y, 20: 3729
radiation effects on, of rats and rabbits, x, 20: 3775
radiation effects on immunological activity of nodes of, in mice, 20: 3777
radiation injuries of, from therapeutic doses of x, 20: 3852

M

MACHINE TOOLS
design for radioactive materials, 20: 4126
development of, for irradiated fuel elements, 20: 4128
performance optimization of numerically controlled, 20: 5220 (UCRL-13185)
MAGNESIUM
analysis for oxygen, methods for, 20: 3878 (LYCEN-6524)
bremsstrahlung reactions (γ,π^0) at 166 Mev, angular distributions from, (E), 4898
determination by flame photometry, 20: 4053
determination in lithium fluoride–magnesium fluoride–yttrium fluoride, 20: 4999(R) (ORNL-2599)
determination in yttrium, methods for, 20: 4299(R) (ORNL-2711)
gamma and neutron heating of, in experimental channels of FRJ-2 reactor, 20: 5202
gamma reactions (γ,n) at 11 to 30 Mev, cross sections for, (E), 20: 4849(R) (UCRL-14360, pp 1-50)
meson (μ^-) transitions in mesic atoms of, energy of, 20: 4825(R) (ANL-7081, pp 81-93)
reactions with uranium tetrafluoride, determination of uranium in waste from, 20: 3906
separation from other metal chlorides by ion exchange, 20: 4053
separation from rare earths by extraction using fused chlorides, 20: 4297(R) (IS-1200(Sect.M))
separation from silver by partition chromatography, 20: 4054
Mg–Zr, dissolution using sulfuric acid, flowsheet for, 20: 4048(R) (NP-15406)
MAGNESIUM ALLOYS
Al–Mg, solvent properties for rare earth elements in molten chloride salts, 20: 3865 (ANL-7064)
Cd–Mg, solvent properties for rare earth elements in molten chloride salts, 20: 3865 (ANL-7064)
Cu–Mg, solvent properties for rare earth elements in molten chloride salts, 20: 3865 (ANL-7064)
Ge–Mg, sound velocities in intermetallic compound, (E/T), 20: 4476(R) (IS-1200(Sect.P))
Ge–Mg, thermal capacity of intermetallic compound in, 20: 3863(R) (IS-1200(Sect. C))
Mg–Ni, solvent properties for rare earth elements in molten chloride salts, 20: 3865 (ANL-7064)
Mg–rare earth, phase studies and solid solubilities of, 20: 4297(R) (IS-1200(Sect.M))
Mg–Sn, preparation and properties of single-crystal, (E), 20: 4476(R) (IS-1200(Sect.P))
Mg–Y, analysis for oxygen, 20: 4299(R) (ORNL-2711)
Mg–Y, enthalpies of formation and vapor pressures of, 20: 4297(R) (IS-1200(Sect.M))
Mg–Y, phase diagrams, 20: 4297(R) (IS-1200(Sect.M))
Mg–Yb, phase studies, 20: 4297(R) (IS-1200(Sect.M))
Mg–Zn, solvent properties for rare earth elements in molten chloride salts, 20: 3865 (ANL-7064)
Mg–Zr, dissolution using sulfuric acid, flowsheet for, 20: 4048(R) (NP-15406)
Mg–Zr, heat-treatment process for, 20: 4456(P)
Pb–Mg, solvent properties for rare earth elements in molten chloride salts, 20: 3865 (ANL-7064)
Sb–Mg, solvent properties for rare earth elements in molten chloride salts, 20: 3865 (ANL-7064)
MAGNESIUM CESIUM NITRATES
use for liquid helium-3 nuclear cooling, 20: 4780
MAGNESIUM CHLORIDES
corrosive effects on failure of Incoloy 800 and stainless steel under stress, 20: 4328 (WCAP-3269-50)
thermodynamics of, in anhydrous *N,N*-dimethylformamide and *N*-methylformamide at 25°C, 20: 3926 (TID-22374)
$MgCl_2$–KCl–NaCl, separation from rare earth fission products by solvent extraction using magnesium alloys, 20: 3865 (ANL-7064)
$MgCl_2$–LiCl–KCl, solvent properties of liquid, for rare earths, 22: 4297(R) (IS-1200(Sect.M))
$MgCl_2$–$NiCl_2$, spectra of nickel(II) in melts of, absorption, 20: 3921(R) (ORNL-3870, pp 56-60)
MAGNESIUM FLUORIDES
production by hydrofluorination of magnesium oxide, 20: 4999(R) (ORNL-2599)
thermodynamic properties in *N,N*-dimethylformamide and *N*-methylformamide solutions, 20: 3924 (TID-22366)
LiF–MgF_2–YF_3, analysis for magnesium and yttrium, 20: 4999(R) (ORNL-2599)
LiF–MgF_2–YF_3, analysis for oxygen, 20: 4299(R) (ORNL-2711)
MAGNESIUM ISOTOPES Mg-24
alpha elastic scattering at 28.5 Mev, optical potentials in, (E/T), 20: 4859
gamma reactions (γ,n) at 11 to 30 Mev, cross sections for, (E), 20: 4849(R) (UCRL-14360, pp 1-50)
nitrogen-14 reactions (N-14, N-13) with, particle transfer model for, 20: 4851
MAGNESIUM ISOTOPES Mg-25
deuteron reactions (d,p) at 7 and 8 Mev, (E), 20: 4849(R) (UCRL-14360, pp 1-50)
proton reactions (p,n) at 8.0 to 14 Mev, (E/T), 20: 4849(R) (UCRL-14360, pp 1-50)
MAGNESIUM ISOTOPES Mg-26
proton reactions (p,n) at 8.0 to 14 Mev, (E/T), 20: 4849(R) (UCRL-14360, pp 1-50)
MAGNESIUM LANTHANUM NITRATES
proton polarization in cerium-doped crystalline, dynamic, (E), 20: 5021
MAGNESIUM OXIDES
effects on polymorphism of zirconium oxide, 20: 3953
radiation effects on gas bubble formation in, fast neutrons, 20: 4387(R) (ORNL-3870, pp 38-43)
Al_2O_3–BeO–MgO, radiation effects on, in-pile, (E), 20: 5115(R) (GA-4967)
BeO–MgO, phase studies, 20: 5181(R) (ORNL-3029)
BeO–MgO, radiation effects on, in-pile, (E), 20: 5115(R) (GA-4967)
MgO–Y_2O_3–ZrO_2, phase studies of, on annealing and cooling, 20: 3953
MAGNESIUM SILICIDES
crystal structure of, determination of electronic structure from, (E/T), 20: 4476(R) (IS-1200(Sect.P))
electron spin resonance of Mn^{2+} in, (E/T), 20: 4476(R) (IS-1200(Sect.P))
thermal capacity, 20: 3863(R) (IS-1200(Sect. C))
MAGNET COILS
design for plasma containment, 20: 4995(P)
MAGNETIC FIELDS
book: *Physics and Techniques of Strong Magnetic Fields*, 20: 4486
charged-particle momentum in, determination of, (T), 20: 4583 (JINR-P-2371)
effect of helical, on ohmic heating of discharge plasma, (E), 20: 4937 (IAE-907)
effects of transverse, on one-dimensional ionized gas flow, (T), 20: 4717
effects on diffusion in plasma, 20: 4479(R) (TID-22179, pp 1-83)
effects on rare earth electric conductivity, (E/T), 20: 4476(R) (IS-1200(Sect.P))
flux compression in, cylindrical explosive systems for, 20: 4477 (LA-DC-7289)
flux density of solar, (T), 20: 4524
flux quantization in superconducting cylinders, (T), 20: 4784
gas flow in transverse, profile correction for sustaining, (T), 20: 4716
intensity of interplanetary, solar flare effects on, (E), 20: 4527
interactions with solar wind, 20: 4529
particle resonances in time-dependent, spin one-half, (T), 20: 4648
plasma compression by explosively produced, (E), 20: 4941 (LA-DC-7290)
plasma containment in helical, apparatus for stable, 20: 4995(P)
production of large, cylindrical explosive system for, 20: 4477 (LA-DC-7289)
properties and structure of interplanetary, 20: 4529
MAGNETIC MATERIALS
properties at 600 to 1400°F for use in space electric power systems, 20: 4379 (NASA-CR-54091)
MAGNETIC MIRROR MACHINES
particle scattering in, nonadiabatic, 20: 4948(R) (TID-22179, pp 85-175)
MAGNETIC MIRRORS
plasma containment by, stability of infinite uniform, (T), 20: 4981
plasma stability in, effect of relativistic electrons on, (T), 20: 4950(T) (UCRL-Trans-1261(L))
MAGNETIC MONOPOLES

interactions with electric charge, spin angular momentum in, (T), 20: 4684
MAGNETIC RESONANCE
propagation in cylindrical and spherical earth-ionosphere, micropulsations of, (T), 20: 4728 (AD-618118)
spectra of electron, in polystyrene, 20: 4479(R) (TID-22179, pp 1-83)
MAGNETIC SEPARATORS
voltage stabilizer in isotope, static characteristics of, 20: 4281 (IAE-926)
MAGNETIC SUSCEPTIBILITY
measurement by Faraday method, superconducting magnet design for, 20: 3919(R) (ORNL-3870, pp 3-6)
measurement of de Haas–Van Alphen effects in ferromagnetic metals, lead, and tungsten, (E), 20: 4476(R) (IS-1200(Sect.P))
MAGNETOHYDRODYNAMIC CELLS
condensing ejectors for liquid-metal, test facility for, 20: 4948(R) (TID-22179, pp 85-175)
design of coil system for induction-type, 20: 4948(R) (TID-22179, pp 85-175)
development of liquid metal, 20: 4573
MAGNETOHYDRODYNAMICS
flow of incompressible infinitely conducting fluid in, large-amplitude, (T), 20: 4718
flow of incompressible viscous fluid about spherical magnetic quadrupoles, (T), 20: 4725
fluid flow in entrance region of parallel-plate channel, (T), 20: 4709
fluid flow in nonuniform field, two-dimensional channel, (T), 20: 4715
fluid flow in, boundary-layer analysis of turbulent channel, 20: 4948(R) (TID-22179, pp 85-175)
fluid flow in, limit theorem for, 20: 4719
fluid flow in, limit theorem for, (T), 20: 4720
fluid flow in, steady disturbances in laminar boundary layer, 20: 4098 (AD-614633)
fluid flow with heat transfer in, effects of channel wall electric conductivity on, (T), 20: 4703 (AD-619101)
gas flow dynamics in, (T), 20: 4702 (AD-619094)
gas flow in transverse fields, method for sustaining, (T), 20: 4716
gas flow in, one-dimensional ionizing, (T), 20: 4717
wave propagation in rotating liquids, effect of Hall current on, 20: 4711
MAGNETOSPHERE
electron and proton reactions with electromagnetic waves in, gyroresonance radiation from, (T), 20: 4747
geomagnetic variations in, classification of diurnal, 20: 4742
particle scattering in, nonadiabatic, 20: 4948(R) (TID-22179, pp 85-175)
proton flow, 20: 4479(R) (TID-22179, pp 1-83)
MAGNETS
book: *Physics and Techniques of Strong Magnetic Fields*, 20: 4486
focusing effects of four- and six-pole, for atomic hydrogen beams, (T), 20: 4559
MAGNOX ALLOYS
tensile properties of AL80, grain-size effects on, (E), 20: 4437
MAIZE
cesium-137 uptake by, effects of soil temperature on, 20: 3668
strontium-90 uptake by, effects of soil temperature on, 20: 3668
zirconium-95 uptake by, effects of soil temperature on, 20: 3668
MAMMALS
sodium-22 content in muscles of Canadian, 20: 4161
MAN
blood circulation in, measurement using nuclear image amplifier with technetium-99m and xenon-133, 20: 3802 (ORNL-IIC-5, pp 239-42)
bone marrow regeneration in, cytology of, 20: 3789
compatibility with spacecraft materials, 20: 4312
induction of aseptic meningitis in, subarachnoid injection of iodine-131-labeled human serum albumin, 20: 3843
iodine metabolism in, tracer studies, 20: 3844
iodine-131 metabolism in thyroid of, measurements of, 20: 3660 (NP-15528)
metabolism of technetium in, tracer study, 20: 3663 (TID-22318)
radiation absorption by, during diagnostic radiography, x, 20: 3816
radiation dose determinations in, following injections of iodine-131-labeled polyvinylpyrrolidone, 20: 3675
radiation dose of, from cosmic radiation, 20: 3731
radiation dose to gonads of children, during diagnostic radiography, 20: 3854
radiation dosimetry in, using angle of incidence measurements, 20: 4207
radiation effects on herpes zoster inflammations in, x, 20: 3836
radiation effects on chromosomes in, 20: 3705(R) (AD-617601)
radiation effects on, low-dose, x, 20: 3779
radiation effects on development of jaw bones, in children, 20: 3808
radiation effects in, low-level, 20: 3770
radiation injuries in, biological methods for low-level, 20: 3770
radioinduced myelitis in, x, 20: 3771
radioinduced nutritional diseases in, 20: 3851
sodium-22 content in Alaskan, 20: 4161
MANGANESE
determination in mixtures by x-ray fluorescence using promethium-147/aluminum and tritium/zirconium sources, 20: 3883 (ORNL-IIC-5, pp 154-81)
determination in plants by neutron activation methods, 20: 3901
neutron cross sections for, 9- and 16-group, 20: 4829 (GEMP-173(Suppl.1))
separation from silver by partition chromatography, 20: 4054
MANGANESE ALLOYS
Al–Mn–Ti–V, properties of aged, 20: 4360(R) (AD-619399)
Mn–U, corrosive effects of liquid, on tantalum and yttrium, 20: 4077(R) (IS-1200(Sect. E))
Mn–U, melting point of, effects of impurities on eutectic, 20: 4077(R) (IS-1200(Sect. E))
MANGANESE CARBONYLS
with cyclopentadienyliron, crystal structure, 20: 3863(R) (IS-1200 (Sect. C))
MANGANESE ISOTOPES Mn-54
content in Canadian biota, 20: 4161
MANGANESE NITRIDES
ferromagnetic properties of, and its mixed crystals, 20: 4402(T) (ANL-Trans-230)
MANGANESE OXIDES
sorptive properties of hydrous, for radionuclides in waste solutions, 20: 5206
MARITIME REACTORS
economic and nuclear analyses of NERO, 20: 5176 (EUR-2468.e)
MASERS
use of infrared, in plasma diagnostics, 20: 4992
MASERS (OPTICAL)
diagnostic use for plasma electron densities, 20: 4948(R) (TID-22179, pp 85-175)
effects on erythrocytes, 20: 3741
effects on oxygenated and reduced hemoglobin, spectral absorption curves of, 20: 3741
fluorescence in ruby rods, 20: 4949(R) (UCRL-14360, pp 85-94)
photon correlations in laser interferometers, effect of high-velocity translation on, 20: 4223 (UCRL-14345)
spectral line width and intensity variations in, 20: 4949(R) (UCRL-14360, pp 85-94)
use in cytological research, 20: 3741
MASS SPECTROMETERS
design for vacuum fusion equipment, 20: 3863(R) (IS-1200(Sect. C))
physics research with, 20: 4215(R) (ANL-7081, pp 134-49)
source leak value design for, 20: 4230(P)
MASS TRANSFER
equations of simultaneous heat and, computer program for solving partial differential, 20: 4103 (NAA-SR-Memo-11099)
MATERIALS TESTING
development of nondestructive methods for, 20: 4110(R) (ORNL-3870, pp 146-54)
equipment for evaluating mechanical properties of niobium and niobium alloys, 20: 4299(R) (ORNL-2711)
facilities for nondestructive, of irradiated fuel elements, 20: 4118
machining methods in, for fuel elements, 20: 4128
methods for, conference on, 20: 4116
methods of, for irradiated ceramic fuel elements, 20: 4130
nondestructive gamma scanning methods of, for irradiated fuel elements, 20: 5093
nondestructive methods of, at Harwell, 20: 4119
nondestructive methods of, for fuels, at Dounreay, 20: 4120
nondestructive methods of, for fuel elements, 20: 4121
nondestructive methods of, for highly radioactive materials, 20: 4122
nondestructive methods of, for fuel rods, 20: 4123
nondestructive methods of, for irradiated fuel, 20: 4124
nondestructive, using x-ray-sensitive vidicon, 20: 4999(R) (ORNL-2599)
radiation sources in, low-energy gamma and x-ray, 20: 4111 (ORNL-IIC-5)
reference notches for, use of electrical discharge machining for producing, 20: 4110(R) (ORNL-3870, pp 146-54)
MATHEMATICS
elliptic integrals evaluation and reduction, 20: 4476(R) (IS-1200(Sect.P))
Fourier series of Gegenbauer's function, 20: 4476(R) (IS-1200(Sect.P))
gauge coordinate group of physical theory, 20: 4656
hypergeometric functions inequalities, 20: 4476(R) (IS-1200(Sect.P))
hypergeometric mean values in, definition of, 20: 4476(R) (IS-1200 (Sect.P))
input-output solution of optimal control problems, 20: 4948(R) (TID-22179, pp 85-175)
integral equations in, iterative methods of resolution of, (T), 20: 4764
Laplace transform of product of two Whittaker functions, (T), 20: 4293

recurrence relations for integrals involving products of Legendre functions, 20: 4294
spin matrix analytic function expansion, method for, 20: 4476(R) (IS-1200(Sect.P))
virial equations for stability of rotating configurations, higher order, 20: 4295
MATTER
properties of, in nuclear statistical equilibrium at high densities, (T), 20: 4855
thermodynamic properties, (T), 20: 4708(R) (UCRL-14360, pp 50-73)
MEATS
ham composition in live and slaughtered swine, estimation by radiography of knuckle, 20: 5224
MECHANICAL ENGINEERING
beam vibrations in, effects of water on, 20: 4080 (WAPD-TM-535)
HOT-1 extension to Neumann problem, 20: 4080 (WAPD-TM-535)
MECHANICS
central force problems in statistical, 20: 4488
many-body problem in, relativistic equations of motion for, (T), 20: 4766
MEDICAL PERSONNEL
radiation effects on life-span of x-ray technicians, 20: 3760
radiation hazards to physiotherapists, during patient radiography, 20: 4203
radiation protection measures for, 20: 4199
MEDICINE
book: *Nuclear Medicine*, 20: 3860
radiation sources in, low-energy gamma and x-ray, 20: 4111 (ORNL-IIC-5)
tracer techniques in veterinary, use of, 20: 3859
MERCAPTO GROUP
preparation of analogs of, ephedrine, 20: 3790
radiosensitivity effects of ephedrine analogs of, in mice, 20: 3790
MERCURY
heat transfer by liquid, in forced circulation, 20: 4999(R) (ORNL-2599)
solubility in organic compounds, tracer study of, 20: 3863(R) (IS-1200 (Sect. C))
thermal conductivity, 20: 4310(R) (ORNL-P-1699)
vapor pressure over mercury–thorium alloy, 20: 4441
MERCURY ALLOYS
Hg–Th, preparation and properties of intermetallic compounds in, 20: 4441
Hg–Th, vapor pressure of mercury over, 20: 4441
MERCURY IONS
effects on aquation of chloropentaaquochromium(III), 20: 3863(R) (IS-1200(Sect. C))
MERCURY ISOTOPES Hg-198
energy levels of, coincidence measurement of conversion coefficients for, 20: 4843(NP-15456)
internal conversion in, transverse polarization of K electrons from, (E), 20: 4900
MERCURY ISOTOPES Hg-199
rare-gas reactions with, hyperfine-level excitation in, (E), 20: 4544
MERCURY ISOTOPES Hg-200
energy levels of, coincidence measurement of conversion coefficients for, 20: 4843(NP-15456)
MERCURY ISOTOPES Hg-201
rare-gas reactions with, hyperfine-level excitation in, (E), 20: 4544
MERCURY ISOTOPES Hg-202
energy levels, (E), 20: 4875
MESIC ATOMS
energy level transitions in meson (μ^-), 20: 4825(R) (ANL-7081, pp 81-93)
MESON PAIRS
photoproduction on protons below 1 Bev, angular distributions and total cross sections for, 20: 4579 (AD-618661)
MESONS
decay of, C violation in, (T), 20: 4669
decay of, partial widths of electromagnetic and strong, (T), 20: 4674
electromagnetic properties of vector, in broken SU(6), (T), 20: 4644 (JINR-P-2299)
interactions with baryons and mesons, SU(3) symmetry for hadron-production, 20: 4645 (NP-15599)
interactions with baryons, relativistic SU(6) theory for vertex in, 20: 4677
interactions with nucleons at high energy, sum rule for cross sections of, (T), 20: 4678
mixing parameters for baryons and vector, calculation of, 20: 4691
photoproduction of spin-1, on nucleons, (T), 20: 4610
wave functions for bound states of, normalization of Bethe-Salpeter, (T), 20: 4671
MESONS, RESONANCE
decay of, parity and spin analysis in two-step, (T), 20: 4585 (SLAC-42)
mass perturbations of, octet enhancement and reciprocal bootstrap for, 20: 4649
MESONS (δ)
decay of, partial widths of electromagnetic and strong, (T), 20: 4674
MESONS (η)
interactions of, C-violation model for $\rho\eta\pi$ coupling in, 20: 4681
photoproduction on protons from threshold to 900 Mev, (E), 20: 4578 (AD-618660)
MESONS (η^0)
decay of, partial widths of electromagnetic and strong, (T), 20: 4674
decays of, C and T violation in mixing in leptonic, (T), 20: 4682
MESONS (H^0)
exchange in mesons (π) interactions, parameters for, (T), 20: 4607
MESONS (K)
decay of, dynamics and symmetries of nonleptonic, (T), 20: 4676
decay of, effects of weak vector bosons in, 20: 4629
decays of, 3π, (T), 20: 4635
MESONS (K^-)
interactions with protons at 5.0 Bev/c, (E), 20: 4476(R) (IS-1200(Sect.P))
interactions with protons at 2.00 Bev/c, charge exchange in, (E), 20: 4476(R) (IS-1200(Sect.P))
interactions with nucleons at high energy, sum rule for cross sections of, (T), 20: 4678
MESONS (K^0)
decay of K_2^0, (T), 20: 4849(R) (UCRL-14360, pp 1-50)
decay of K_2^0, spectra of $\pi\mu\nu$, 20: 4631
decay of K_S^0, method for analysis of, (T), 20: 4583 (JINR-P-2371)
decay of K_2^0, CP nonconservation in 2π, 20: 4626
decay of, C-violation model for 2π, 20: 4681
MESONS (K^+)
decay of, branching ratio for ($\pi^+\pi^+\pi^-$), (E), 20: 4618
decay probability, (E), 20: 4609
interactions with nucleons at high energy, sum rule for cross sections of, (T), 20: 4678
production in proton-proton interactions at 2.40 and 2.85 Bev, (E), 20: 4586 (TID-22315)
MESONS (K^0_{e3})
decay spectrum measurement, 20: 4631
MESONS (μ)
decay of, effects of weak vector bosons in, 20: 4629
interactions with protons at 700 to 1100 Mev/c, cross sections for, (E/T), 20: 4591 (UR-875-108)
production by neutrinos, experiment for detecting, 20: 4561 (COO-818-64)
production in neutrino interactions with neutrons, differential and total cross sections for, (T), 20: 4611
reactions with nuclei, first Born approximation including anapole for, (T), 20: 4612
MESONS (μ^-)
capture by thorium-232 and uranium-238, x-ray spectra from, 20: 4825(R) (ANL-7081, pp 81-93)
dosimetry of high-energy, methods for, (T), 20: 4505 (ORNL-P-1738)
interactions with mesons (μ^-), first Born approximation including anapole for, (T), 20: 4612
interactions with mesons (μ^+), first Born approximation including anapole for, (T), 20: 4612
reactions with carbon-12, coupling constants in capture, (T), 20: 4915
MESONS (μ^+)
dosimetry of high-energy, methods for, (T), 20: 4505 (ORNL-P-1738)
interactions with mesons (μ^-), first Born approximation including anapole for, (T), 20: 4612
interactions with mesons (μ^+), first Born approximation including anapole for, (T), 20: 4612
MESONS (ω)
production in meson (π)-nucleon interactions, amplitudes for, (T), 20: 4584 (JINR-P-2380)
MESONS (ω^0)
interactions of, C, T noninvariance in minimal electromagnetic, (T), 20: 4601
MESONS (ϕ)
interactions of, C, T noninvariance in minimal electromagnetic, (T), 20: 4601
MESONS (π)
decay of, effects of weak vector bosons in, 20: 4629
decay of, eight-fold symmetry in, (T), 20: 4692
dosimetry of high-energy, methods for, (T), 20: 4505 (ORNL-P-1738)
exchange in deuteron-electron elastic scattering, (E), 20: 4580 (AD-618662)
interactions of, C-violation model for $\rho\eta\pi$ coupling in, 20: 4681
interactions of, slope of Pomeranchuk trajectory for, (T), 20: 4587 (UCRL-11495)
interactions with protons, polarized hydrogen target for, 20: 4637
interactions with mesons (π), field theory for S and D waves in, (T), 20: 4670
interactions with nucleons, amplitude of vector meson production in, (T), 20: 4584 (JINR-P-2380)

interactions with nucleons, three-channel N/D equations in pole approximation for, 20: 4593
interactions with nucleons, Dashen-Lee sum rules for intermediate state in, (T), 20: 4598
interactions with mesons (π), ρ and f^0 resonances in, (T), 20: 4607
interactions with mesons (π), dispersion relation for I = 0 scattering length in, 20: 4617
photoproduction on protons below 1 Bev, angular distributions and total cross sections for, 20: 4579 (AD-618661)
production in angular momentum representation, statistics of multiple, (T), 20: 4643 (INR-607/VI/PH)
properties of, phenomenological analysis of, (T), 20: 4633

MESONS (π^-)
interactions with protons at 1.5 to 4.2 Bev/c, analysis of strangeness +1 baryon in, 20: 4589 (UCRL-11754)
interactions with nucleons, phase-shift analysis of, (T), 20: 4849(R) (UCRL-14360, pp 1-50)
interactions with protons at 2.16 Bev, 1920-Mev resonance in, (T), 20: 4849(R) (UCRL-14360, pp 1-50)
interactions with nucleons at high energy, sum rule for cross sections of, (T), 20: 4678
interactions with neutrons in neutron stars, neutrino cooling from, (T), 20: 4532
interactions with protons at 10 Bev, forward dispersion relations for, (T), 20: 4602
interactions with protons, forward amplitude for, (T), 20: 4603
interactions with protons, Regge poles in optical model for charge-exchange, 20: 4606
interactions with protons at 4 Bev/c, meson (π^0) production in, (E), 20: 4582 (JINR-P-2361)
photoproduction on protons below 1 Bev, angular distributions and total cross sections for pair, 20: 4579 (AD-618661)
reactions (π^-,π^0) on complex nuclei, excitation functions for, (T), 20: 4910
use in radiotherapy, feasibility of, 20: 3735

MESONS (π^0)
photoproduction on protons, recoil nucleon polarization from, (T), 20: 4627
photoproduction on nuclei, angular distributions from, (E), 20: 4898
production in meson (π^-)-proton interactions at 4 Bev/c, 20: 4582 (JINR-P-2361)

MESONS (π^+)
interactions with nucleons, phase-shift analysis of, (T), 20: 4849(R) (UCRL-14360, pp 1-50)
interactions with nucleons at high energy, sum rule for cross sections of, (T), 20: 4678
interactions with protons at 10 Bev, forward dispersion relations for, (T), 20: 4602
interactions with protons, forward amplitude for, (T), 20: 4603
photoproduction on protons below 1 Bev, angular distributions and total cross sections for pair, 20: 4579 (AD-618661)

MESONS (ρ)
exchange in mesons (π) interactions, parameters for, (T), 20: 4607
interactions of, C-violation model for $\rho\pi\eta$ coupling in, 20: 4681
production in meson (π)-nucleon interactions, amplitudes for, (T), 20: 4584 (JINR-P-2380)

MESONS (ρ^0)
interactions of, C, T noninvariance in minimal electromagnetic, (T), 20: 4601

MESONS (X^0)
decays of, C and T violation in mixing in leptonic, (T), 20: 4682

METABOLIC DISEASES
radiotherapy of acromegaly, heavy particle, 20: 3828

METABOLISM
effects of pituitary hormones on, 20: 3809
in tracer studies of animal, 20: 3685
models for, of phosphatides and proteins, 20: 3658(R) (EUR-2414.f,i)
of bacteria, use of labeled metabolites for rapid identification, 20: 3667
of glucose, tracer study, 20: 3658(R) (EUR-2414.f,i)
of skeleton, tracer studies in man during health and disease, 20: 3664(R) (TID-22324)

METAL SYSTEMS
gas–liquid equilibrium data for, computer program for integration of Gibbs–Duhem equation for, 20: 4375 (IS-1241)

METALLOGRAPHY
equipment and techniques used at ORNL, 20: 4309(R) (ORNL-3870, pp 300-4)

METALLURGY
research programs at Ames Laboratory, July 1964–June 1965, 20: 5213(R) (IS-1200)
research programs at ORNL on, 20: 4300(R) (ORNL-3870)

METALS
analysis for hydrogen, nitrogen, and oxygen, methods for, 20: 3863(R) (IS-1200(Sect. C))
analysis for rare earths, thorium, and uranium by ion exchange, review on, 20: 3888 (TID-22402)
analysis for tantalum and tungsten by neutron activation, 20: 3863(R) (IS-1200(Sect. C))
book: *Rare Elements and Rare Earths in Technology*, 20: 4451
defects in, gamma radiometric measurement of, 20: 4114(T) (AD-621784)
deformation of, calorimeter for measuring energy during, 20: 4384(R) (ORNL-3870, pp 7-14)
diffusion of solutes in, bibliography on, 20: 4383 (ORNL-3795(Pt.2))
diffusion of tracer solutes in, activation energies and frequency factors for, 20: 4383 (ORNL-3795(Pt.2))
distillation of liquid, surface concentration changes in, 20: 4077(R) (IS-1200(Sect. E))
electron reactions with vacuum-contained, transition radiation from, (E/T), 20: 5008(T) (ORNL-tr-872)
electron scattering by, at 6–40 kev, radiation spectra from, (E), 20: 5017
flow of liquid, in liquid-metal-lubricated journal bearings, 20: 4078(R) (SWRI-1228-67)
freezing point of, effects of electric fields on, 20: 4297(R) (IS-1200 (Sect.M))
heats of fusion of, high-temperature calorimeter for measuring, 20: 4297(R) (IS-1200(Sect.M))
liquid-vapor equilibrium in, measurement of, 20: 4077(R) (IS-1200 (Sect. E))
performance of liquid, in MHD cells, 20: 4573
phase transformation mechanisms, 20: 4297(R) (IS-1200(Sect.M))
properties for use in space vehicles, 20: 4312
properties of, effects of low temperature on, 20: 4417
radiation effects on, review of, 20: 4464
radiation effects on creep at high temperatures, 20: 4299(R) (ORNL-2711)
separation from rare earths by anion exchange, 20: 4067
technology of liquid, review on, 20: 4330(T) (ORNL-tr-854)
tensile properties of, review on, 20: 4399 (UCRL-16301)
theory of binding in, 20: 4476(R) (IS-1200(Sect.P))

METASTASES
radiation effects on rat sensitivity to pulmonary, following lymph node irradiation, x, 20: 3718
radiotherapy of, method for, 20: 3842

METEORITES
element abundances in Bjurböle, 20: 4526
iodine-xenon formation intervals for, (E), 20: 4526
production of gas-rich, (T), 20: 4526

METEOROLOGY
model of oceans in Northern Hemisphere, 20: 4153(R) (UCRL-14360, pp 73-85)
weather effects on sodium distribution in atmosphere and on beaches, 20: 4148 (AD-623515)
weather prediction, 20: 4153(R) (UCRL-14360, pp 73-85)

METHACRYLIC ACID, ESTERS
effects on adhesive properties of polyethylene, 20: 4029
radioinduced polymerization of, gamma, 20: 4029

METHACRYLIC ACID, METHYL ESTER
effects on hydrogen yields from radiolysis of hydrogen sulfide, 20: 4017
effects on radioluminescence of styrene, 20: 4001
radioinduced polymerization on polyethylene, 20: 3996
radioinduced polymerization with styrene, 20: 4001

METHACRYLIC ACID, METHYL ESTER POLYMERS
radiation damage in, protective effects of organic additives against x and gamma, 20: 4036

METHACRYLIC ACID POLYMERS
radiation effects on aerosols of, x, 20: 4015

METHANE
analysis for carbon-13 by NMR, 20: 3879(R) (MLM-1266)
diffusion from stored, solid plutonium residues, vacuum-drying effects on, 20: 4364 (AERE-M-1644)
isotopic exchange with deuterium and tritium, 20: 3980
molecular size and shape of CH_4^+, calculation of, 20: 5006(R) (ORNL-3870, pp 50-5)
radiolysis of, intermediate yields in, 20: 3982(R) (AGN-8156)
reactions with niobium at low pressures and high temperatures, 20: 5181(R) (ORNL-3029)
CH_4–N, radiolysis of, products from fission-fragment, 20: 3982(R) (AGN-8156)
CH_4–N_2, radiolysis of, products from electron, 20: 3982(R) (AGN-8156)
CO_2–methane, radiolysis of, formaldehyde yields in, 20: 3981 (AERE-R-5051)

METHANE, FLUORO-
molecular dipole moments of deuterated and normal, 20: 3958

METHANE, IODO-
preparation of labeled, 20: 4185(R) (ORNL-3843, pp 169-234)
reactions with chemically impregnated charcoal, 20: 4185(R) (ORNL-3843, pp 169-234)

sorption by activated charcoal, effects of humidity and temperature on, 20: 4086(R) (ORNL-3843, pp 137-67)
sorption by charcoal, effects of humidity and temperature on, 20: 4184(R) (ORNL-3843, pp 71-135)
sorption by coconut charcoal, factors affecting, 20: 4185(R) (ORNL-3843, pp 169-234)

METHANESULFONIC ACID, 1,4-DIMETHYLTETRAMETHYLENE ESTER
effects on leukemia cells, cytotoxic, 20: 3736

METHANOL
piezo-optic coefficients and refractive index, 20: 4484
radioinduced oxidation of, yields of formaldehyde in, 20: 4011
$LiNO_3$–methanol–HNO_3, use as solvent in ion-exchange separation of rare earths, 20: 4067

METHIONINE
incorporation of selenium-75 in, biosynthetic, 20: 3661 (NP-15594)
ionization potential, 20: 3863(R) (IS-1200(Sect. C))
metabolism in mice, tracer study, 20: 3661 (NP-15594)
sulfoximine, effects on glucose metabolism in rats, tracer study, 20: 3678

METROLOGY
use in nondestructive testing of fuel rods, 20: 4123
use in nondestructive testing of irradiated fuel materials, 20: 4124

MEXICO
lead uranyl tellurite occurrence in Moctezuma, Sonora, 20: 4173

MICE
immune reactions to virus-induced transplanted leukemias in, 20: 3694
metabolism of cystine in, tracer study, 20: 3661 (NP-15594)
metabolism of iodine in, effects of chloropromazine, tracer study, 20: 3677
metabolism of methionine in, tracer study, 20: 3661 (NP-15594)
neutron reactions in soft tissues of, effects of element composition on kerma, 20: 3708 (CEA-R-2833)
radiation and fasting effects on plasma lipids in, 20: 3604
radiation effects on life span of, effects of genotype on, 20: 3711(R) (NYO-3314-2)
radiation effects on, genetic, 20: 3711(R) (NYO-3314-2)
radiation effects in, mechanism for leukemogenic, x, 20: 3696
radiation effects on retinal development in embryos of, x, 20: 3725
radiation effects of dose fractionation on fast neutron, 20: 3728
radiation effects on survival of transplanted tumors in, x, 20: 3751
radiation effects on growth of tumor transplants in, x, 20: 3751
radiation effects on immune reactions in injected thymocytes and lymph node cells in, 20: 3777
radiation effects on germ-free, lethal, 20: 3778
radiation effects on, protective effects of chemicals against gamma, 20: 3792
radiation injuries of, protective effects of bone marrow injections in germ-free, 20: 3788
radiation injuries in, effects of mercapto analogs of ephedrine on, 20: 3790
radioinduced chromosomal aberrations in cultures of fibroblasts of, effects of culture density on x, 20: 3691
radioinduced leukemia in, effects of genotype on x, 20: 3765
toxic effects of uranyl nitrate in, 20: 3670
transplantation of ascites lymphoma cells from, 20: 3750

MICROORGANISMS
effects of water-d_2 on growth in, 20: 3651

MICROWAVE EQUIPMENT
development for Brookhaven AGS beam separator, 20: 4493 (BNL-9642)

MICROWAVES
absorption by plasma, analysis of, (E/T), 20: 4943 (MATT-379)
attenuation by shock waves in argon and neon, 20: 4934 (AD-619093)
propagation in argon plasma, resonance from, (E), 20: 4935 (AFCRL-65-556)
use for plasma density measurements, (T), 20: 4971
use in plasma noise measurements, 20: 4991
use in shock wave diagnostics, 20: 4934 (AD-619093)

MILK
content of iodine in cow's, factors affecting, tracer study, 20: 3674
decontamination of, review on equipment and procedures for, 20: 3872 (EUR-2507.d)
strontium-89 content in, effects of diet of cattle on, 20: 4162
strontium-90 content in, effects of diet of cattle on, 20: 4162

MINERALS
analysis for rare earths, thorium, and uranium by ion exchange, review on, 20: 3888 (TID-22402)
metabolism in bone, method of measuring, 20: 3803 (ORNL-IIC-5, 257-76)

MINNESOTA
feldspar and zircon ages in northeastern, 20: 4169

MISSILES
interactions with electromagnetic fields in atmosphere, (T), 20: 4730 (SC-DC-65-1797)

MITOSIS
effects of water-d_2 on, 20: 3651
radiation effects on, in animal cells, 20: 3764
radiation effects on, in plant cells, 20: 3764
radiosensitivity effects of, on animal cells in culture, γ, 20: 3737

MOCTEZUMITE
occurrence in Moctezuma, Sonora, Mexico, 20: 4173

MOLECULAR BEAMS
production of helium and nitrogen, 20: 4479(R) (TID-22179, pp 1-83)

MOLECULAR STRUCTURE
cell theory for hard particles, 20: 4708(R) (UCRL-14360, pp 50-73)
use in crystal structure determination, review on, 20: 5212 (BNL-930)

MOLECULES
binding energy of homonuclear diatomic, chemical, 20: 3863(R) (IS-1200 (Sect. C))
calculations of polyatomic, quantum mechanical, 20: 3863(R) (IS-1200 (Sect. C))
dissociation, fragmentation, and ionization of gases of, mass spectrometric studies of, 20: 4215(R) (ANL-7081, pp 134-49)
distribution function for system of hard spheres, radial, 20: 4708(R) (UCRL-14360, pp 50-73)
fluid transport mechanisms in hard-sphere systems, 20: 4708(R) (UCRL-14360, pp 50-73)
integrals in diatomic, coulomb and exchange, 20: 3863(R) (IS-1200 (Sect. C))
localized self-consistent-field orbitals in, theory of, 20: 3863(R) (IS-1200(Sect. C))
polarizability and shielding factor for, perturbation theory calculation of dipole, 20: 4537 (NP-15576)
polarizability and shielding factor for, perturbation theory calculation of quadrupole, 20: 4538 (NP-15577)

MOLLUSKS
metabolism of strontium-90 by *Nerita forskali*, 20: 3659(R) (NP-15156)

MOLTEN SALT REACTORS
coolants and fuels for MOSEL, properties of molten fluorides for use as, 20: 4376 (JUL-268-RG)

MOLYBDENUM
analysis for titanium and zirconium by ion exchange, 20: 3896
coating with chromium–rhenium and rhenium by electrolytic deposition, bonding in, 20: 4404(T) (JPRS-32773)
compatibility with uranium carbide–zirconium carbide system at 2000°C, 20: 4335
corrosion by cesium at 400°C, 20: 4337
creep and tensile properties at high temperatures, 20: 4999(R) (ORNL-2599)
deposition of, thermochemical, 20: 4342(R) (ORNL-3870, pp 85-101)
effects on corrosion resistance of stainless steel in acidic solutions, 20: 4325 (TB-58)
electron work functions for thermionic cathodes of, effects of cesium fluorides on, 20: 4572 (EUR-2283.d)
extrusion of alloy-clad billets of, 20: 4299(R) (ORNL-2711)
fatigue of, effect of crystal structure on, 20: 4443
Fermi surfaces calculations for, 20: 4476(R) (IS-1200(Sect.P))
mechanical properties of, effects of hot plastic deformation on, 20: 4403(T) (JPRS-32317)
neutron cross sections for, 9- and 16-group, 20: 4829 (GEMP-173(Suppl.1))
neutron cross sections for, 20: 4830 (GEMP-384)
properties at high temperatures, 20: 4418
purification by electron-beam melting, 20: 5181(R) (ORNL-3029)
radiation from promethium-147 beta excited, 20: 3882 (ORNL-IIC-5, pp 51-71)
reactions with low-melting metals, 20: 4077(R) (IS-1200(Sect. E))
separation from low grade ores, reductive chlorination process for, 20: 4072(P)
separation from solutions formed by dissolution of molydenum–uranium fuel alloys, 20: 4070(P)
shear stress of single crystals of, temperature dependence of critical, 20: 4445
sputtering by argon ions at 1.5 to 30 kev, yields from, (E), 20: 4546
sputtering by xenon ions at 1.5 to 30 kev, yields from, (E), 20: 4546
stress recovery of, effects of carbon and tungsten on flow, 20: 4409

MOLYBDENUM ALLOYS
Al–Cr–Co–Mo–Ni–Ti, corrosion of Udimet 500 by lithium fluoride in cyclic high-temperature environment, 20: 4326 (TRW-ER-6561)
Al–Fe–Mo–Ti–V, properties of aged, 20: 4360(R) (AD-619399)
Co–Fe–Mo–Ni, properties of Maraging Steel for use in space electric power systems, 20: 4379 (NASA-CR-54091)
Cr–Fe–Mo–Ni–Nb–W, welding properties of Inco IN-102, 20: 4306(R) (ORNL-3870, pp 194-213)
Cr–Fe–Mo–V, properties of H-11 Steel for use in space electric power systems, 20: 4379 (NASA-CR-54091)
Hf–Mo, properties at high temperatures, 20: 4418
Mo–Nb–V–Zr, corrosion of B-66, by lithium, effects of oxygen on,

20: 4301(R) (ORNL-3870, pp 102-35)
Mo–Nb–V–Zr, evaporation losses in high vacuum of B-66, 20: 4301(R) (ORNL-3870, pp 102-35)
Mo–Nb–V–Zr, tensile properties of welded plates of B-66, 20: 4301(R) (ORNL-3870, pp 102-35)
Mo–Ni, atomic structure of, short-range order and size-effect coefficients for, (E), 20: 4421
Mo–Re, electric and thermal conductivity of superconducting, 20: 4361 (AD-619719)
Mo–Ti, properties at high temperatures, 20: 4418
Mo–Ti–Zr, analysis for titanium and zirconium by ion exchange, 20: 3896
Mo–Ti–Zr, brazing tungsten carbide–cobalt cermet to TZM, use of boron–nickel–silicon for, 20: 4307(R) (ORNL-3870, pp 238-42)
Mo–Ti–Zr, corrosion of TZM, by potassium, 20: 4301(R) (ORNL-3870, pp 102-35)
Mo–Ti–Zr, creep properties of TZM, 20: 4301(R) (ORNL-3870, pp 102-35)
Mo–U, dissolution using nitric acid, equipment and procedures for, 20: 4048(R) (NP-15406)
Mo–U, processing reactor fuels of, 20: 4070(P)
Mo–W, stress recovery of, flow, 20: 4409
Mo–Zr, properties at low temperatures, 20: 3920(R) (ORNL-3870, pp 27-37)
Mo–Zr, properties at high temperatures, 20: 4418

MOLYBDENUM CARBIDES
C–MoC, properties and structure of hot-pressed, 20: 5089(R) (GA-6181)

MOLYBDENUM ISOTOPES Mo-92
proton reactions (p,p), fine structure near isobaric analog resonances in, 20: 4923

MOLYBDENUM ORES
processing by reductive chlorination, 20: 4072(P)

MOLYBDENUM OXIDES
dehydration to 600°C for neutron transmission measurements, 20: 3914 (AERE-M-1654)
solubility in borax at 760 to 900°C, 20: 3951

MOLYBDENUM SILICIDES
oxidation kinetics, 20: 4077(R) (IS-1200(Sect. E))

MOLYBDENUM STEEL
Cr–Mo, corrosion of Croloy 2¼, by lead, 20: 4308(R) (ORNL-3870, pp 243-60)

MOLYBDENUM SYSTEMS
C–Mo–Nb–Ta–W–Zr, preparation and specifications for corrosion loop testing, 20: 4380 (NASA-CR-54761)
C–Mo–Ti–Zr, preparation and specifications for corrosion loop testing, 20: 4380 (NASA-CR-54761)

MONAZITES
analysis for thorium by titration using fluoride ions, 20: 3905
crystal structure of, effects of calcium, thorium, and rare earth contents on, 20: 4174

MONKEYS
radiation effects on enzyme levels in blood of, γ, protons, and x, 20: 3692
radiation effects on retinal development in embryos of, x, 20: 3725
radiation effects on development and eruption of teeth in, x, 20: 3743
radiation effects on visual discrimination in, effects of age on, x, 20: 3721
radiodiagnosis in brain of, safety of radioalbumin aggregates for, 20: 3832
radioinduced osteonecrosis in jaws of, effects of dose fractionation on x, 20: 3742

MONTE CARLO METHOD
neutron cross section library for codes FMC-N, 18-0, and 18-1, 20: 4830 (GEMP-384)
use in analysis of neutron transmission by finite water slabs, 20: 4999(R) (ORNL-2599)
use in analyzing gamma scattering from cylinders, 20: 5181(R) (ORNL-3029)
use in analyzing photon emission in photon reactions with atoms, 20: 4949(R) (UCRL-14360, pp 85-94)
use in calculating gamma heating in shields, 20: 4999(R) (ORNL-2599)
use in calculating gamma response functions of cesium iodide and sodium iodide crystals, 20: 5181(R) (ORNL-3029)
use in calculating neutron angular distributions from shielding, 20: 5181(R) (ORNL-3029)
use in calculating fast-neutron dose rates in cylindrical compartment, 20: 4299(R) (ORNL-2711)
use in calculation of deep gamma penetrations, 20: 5181(R) (ORNL-3029)
use in well logging, 20: 4168

MÖSSBAUER EFFECT
energy emission in, temperature dependence of, (T), 20: 5004 (IAE-927)
in tin-120, anisotropy of, (E), 20: 4932
measurement in iron complexes and covalent iron compounds, crystal lattice effects on, 20: 3927(T) (AERE-Trans-1026)
research, 20: 4826(R) (ANL-7081, pp 121-7)

MOUTH
radiography of, hazards from, 20: 3846
radiosensitivity of mucosa of, 20: 3744
radiotherapy of cancer in, measures for preventing injuries from, 20: 3813

MUCOSA
radiosensitivity of, protective effects of rutin derivative, 20: 3840
radiosensitivity of oral, 20: 3744
radiosensitivity of intestinal, 20: 3821

MULTIPLICATION FACTOR
effects of holes and voids on, (T), 20: 5064

MUSCLES
composition of swine, estimated by radiography of knuckle, 20: 5224
fats–muscles, determination of fractional composition by x-ray beam attenuation measurements, 20: 3885 (ORNL-IIC-5, pp 277-89)

MUTATIONS
chemically induced by ethylenimine in Chlorella, 20: 3716(T) (JPRS-31514, pp 65-76)
radioinduced in Aspergillus, characterization of, uv, 20: 3755(T)
radioinduced in Aspergillus, uv, 20: 3756(T)
radioinduced in Chlorella, x, 20: 3716(T) (JPRS-31514, pp 65-76)
radioinduced in Chlorella, uv, 20: 3716(T) (JPRS-31514, pp 65-76)
radioinduced in Drosophila, effects of high temperature on x, 20: 3713(T) (JPRS-31514, pp 29-43)
radioinduced in Drosophila, effects of genotype on, x, 20: 3715(T) (JPRS-31514, pp 59-64)
radioinduced in *Escherichia coli*, gene locus for, uv, 20: 3757
radioinduced in *Escherichia coli*, gene locus for uv, 20: 3758
radioinduced in female Drosophila, effects of x ray voltage and high temperature on, 20: 3714(T) (JPRS-31514, pp 44-58)
radioinduced in *Funaria hygrometrica* plants, x, 20: 3781
radioinduced in Saccharomyces, x, 20: 3717(T) (JPRS-31514, pp 77-91)
radioinduced in Saccharomyces, uv, 20: 3717(T) (JPRS-31514, pp 77-91)
radioinduced in *Sordaria brevicollis*, uv, 20: 3783
radioinduced in wasps, genetic, 20: 3733
radioinduced plant, applications in breeding programs, 20: 3710(R) (EUR-2493.e)
radioinduced, etiology of human, 20: 3779
radioinduced, in barley, x, 20: 3782
radioinduced, in *Corynebacterium fascians*, uv, 20: 3723
radioinduced, in *Crotolaria intermedia*, x, 20: 3759
radioinduced, in wheat, 20: 3762

MZFR (SIEMENS REACTOR)
construction, 20: 5138

N

NAPHTHALENE
radioinduced fluorescence of organic phosphors in, 20: 3994

NAPHTHENIC ACIDS
solvent properties for cerium and yttrium, 20: 4051

NEMATODES
radiation effects on infectivity of *Nippostrongylus brasiliensis*, in rats, gamma, 20: 3786

NEODYMIUM
determination in hydrochloric acid or methanol–nitric acid media, spectrophotometric, 20: 3888 (TID-22402)

NEODYMIUM ALLOYS
Al–Nd, phase diagram, 20: 4427
Nd–Sn, magnetic properties of, at 2 to 300°K, 20: 4423

NEODYMIUM ISOTOPES Nd-147
beta transitions in, polarization from, (E), 20: 4880

NEODYMIUM ISOTOPES Nd-150
beta decay of, double, (E), 20: 4828 (COO-818-60)

NEODYMIUM NITRATES
separation from praseodymium nitrate by solvent extraction using di-(2-ethylhexyl) phosphoric acid and TBP, 20: 3875 (IS-T-37)

NEODYMIUM OXIDES
Fe_2O_3–Nd_2O_3, crystal structure and magnetic properties, 20: 4411

NEODYMIUM SULFIDES
homogeneity regions in, 20: 3938

NEON
diagnostics of plasma of, probe characteristics for, (E), 20: 4969
reactions with mercury-199 and -201, hyperfine-level excitation in, (E), 20: 4544
shock waves in, microwave attenuation by, 20: 4934 (AD-619093)

NEON IONS
reactions with neon, charge-exchange, 20: 4556

NEON ISOTOPES Ne-20
alpha elastic scattering at 28.5 Mev, optical potentials in, (E/T), 20: 4859

energy levels from fluorine-19 (He-3, d) reactions at 9.5 and 10 Mev, (E/T), 20: 4908
energy levels from oxygen-18 (He-3, n) reactions at 1.3 to 5.8 Mev, 20: 4925
gold-197 reactions with, angular distributions of exchange products in, (T), 20: 4836 (JINR-P-2298)
scattering by gold-197 at 200 Mev, matrix elements for inelastic, (T), 20: 4839 (JINR-P-2333)
separation from neon-22 by thermal diffusion, 20: 3879(R) (MLM-1266)
NEON ISOTOPES Ne-22
separation from neon-20 by thermal diffusion, 20: 3879(R) (MLM-1266)
NEPHROSIS
induced by injected mercuric chloride in rats, 20: 3666
pathology of, induced by injected uranium nitrate in rats, 20: 3666
NEPTUNIUM
distribution between γ-alumina and molten chlorides, 20: 3959
NEPTUNIUM IONS
reactions in pure and mixed solvents and in presence of inert salts, exchange, 20: 3964
NEPTUNIUM ISOTOPES Np-237
deuteron reactions with, products of, 20: 4928
helium-3 reactions with, products of, 20: 4928
NERVOUS SYSTEM
radiation effects on performance of learned response by rats, effects of nembutal on, x, 20: 3772
NETHERLANDS
fallout monitoring, 1964, 20: 4155 (EUR-2516.d,f,i,n)
NEUROLOGY
research programs at M.I.T. electronics lab., 20: 4478(R) (TID-22179)
NEUROSPORA
radiation effects on conida of, biological, γ and x, 20: 3780
NEUTRINOS
detection of cosmic-ray produced experiment for, 20: 4561 (COO-818-64)
detection of, cadmium-loaded scintillator for, 20: 4847 (UCRL-12085(Pt.1))
emission and interactions in stars, (T), 20: 4534
emission from fission fragments, detection of, (T), 20: 4847 (UCRL-12085(Pt.1))
emission from neutron stars, cooling rates from, (T), 20: 4532
emission in fission fragment beta decay, detection of, 20: 4848 (UCRL-12085(Pt.2))
emission in stellar processes, (T), 20: 4533
field theory for, geometrodynamic, 20: 4619
interactions with electrons, experiment for detecting, 20: 4848 (UCRL-12085(Pt.2))
interactions with antineutrinos, pure gravitational tensor field from, (T), 20: 4763
interactions with protons, production of (3,3) resonance by, (T), 20: 4476(R) (IS-1200(Sect.P))
interactions with neutrons, radiative meson (μ) production from, (T), 20: 4611
reactions with matter, lepton production in, (T), 20: 4866
NEUTRINOS (ν_e)
detection of solar, apparatus for, 20: 4523 (COO-818-63)
NEUTRON-ABSORPTION ANALYSIS
equipment and methods for hydrogenous material, 20: 3913(P)
NEUTRON BEAMS
depolarization by targets, calculation of, (T), 20: 4476(R) (IS-1200 (Sect.P))
NEUTRON CROSS SECTIONS
calculation for fast reactor analysis, computer program for, 20: 5055 (BNWL-146)
determination by activation and mass spectrometric methods, 20: 3864 (AERE-L-166)
library for Monte Carlo codes FMC-N, 18-0, and 18-1, 20: 4830 (GEMP-384)
measurement of, instrumentation development for, 20: 4246(R) (RPI-328-40, pp 49-55)
tabulation of 9- and 16-group, for reactor analysis, 20: 4829 (GEMP-173(Suppl.1))
NEUTRON-DIFFRACTION ANALYSIS
effects of particle size on scattering extinction in, 20: 5016(T)
sample drying for, 20: 3914 (AERE-M-1654)
use in materials testing, conference on, 20: 4116
NEUTRON PHOTOGRAPHY
book: *Neutron Radiography*, 20: 4115
NEUTRON SOURCES
development of limited-energy, produced by decay of excited nuclei, (E), 20: 4802 (IDO-17115)
development of pulsed, bibliography for, 20: 5200 (TID-3571 (Suppl.1))
performance of nitrogen-17, 20: 4802 (IDO-17115)
performance of oxygen-18 (p,n) gas target, 20: 4927
NEUTRON SPECTRA
calculation of differential fast, from threshold detector data, 20: 4256
calculation of epithermal and thermal, computer program for, 20: 4804 (KAPL-3098)
calculation of, computer program for, 20: 4805 (ORNL-TM-1245)
measurement in HERALD thermal column, (E), 20: 5191 (AWRE-R-4/65)
measurement in heterogeneous assemblies, methods for, (E/T), 20: 4801(R) (GA-6634)
measurement using nuclear emulsions, 20: 5196(R) (IS-1200(Sect.E))
NEUTRON SPECTROMETERS
data acquisition and processing system for time-of-flight, performance of computer, 20: 4245 (ORNL-P-1723)
design for Bulk Shielding Facility, 20: 5181(R) (ORNL-3029)
design of double, 20: 4476(R) (IS-1200(Sect.P))
efficiency of semiconductor-sandwich, (E), 20: 4238 (EUR-2487.e)
performance of emulsion, helium-3, and liquid scintillator 4π, 20: 4249 (UCRL-16311)
performance of proton-recoil, (E), 20: 4997(R) (EUR-2494.d)
performance of semiconductor, (E), 20: 4997(R) (EUR-2494.d)
use of silicon surface-barrier detectors in, for fast neutrons, 20: 5181(R) (ORNL-3029)
NEUTRON SPECTROSCOPY
data acquisition and processing system for time-of-flight, performance of computer, 20: 4245 (ORNL-P-1723)
measurement of, research on, 20: 4846(R) (RPI-328-40, pp 43-8)
NEUTRONS
absorption in reactor lattices, resonance integral calculation for, 20: 5077
attenuation by beryllium, pulse decay constant for, (T), 20: 4815
attenuation by lithium hydrides, 20: 5181(R) (ORNL-3029)
book: *Neutron Radiography*, 20: 4115
detection of, 4π spectrometers for, 20: 4249 (UCRL-16311)
diffraction by barium cobalt iron(II) ferrate(III) powders, effects of particle size on, 20: 5016(T)
diffusion equations for heterogeneous reactors, computer program for solving, 20: 5057 (GA-6540)
diffusion in reactors, two-dimensional codes for, (T), 20: 5056 (CONF-654-22)
diffusion in reactors, mesh size corrections for computer codes for, 20: 5069
dosimetry of high-energy, methods for, (T), 20: 4505 (ORNL-P-1738)
dosimetry of, calibration of photographic film detectors for, 20: 4237 (BNL-9665)
dosimetry of, development of thermoluminescent detectors for, 20: 4236 (BNL-9605)
effects on beryllia-moderated-reactor materials, 20: 5115(R) (GA-4967)
effects on beryllium oxides, 20: 5181(R) (ORNL-3029)
effects on electric conductivity and polarization of polymers, 20: 4030
effects on electronic equipment in SNAP environment, 20: 4262 (NP-15610)
effects on embrittlement of stainless steel, 20: 4460(R) (ORNL-3870, pp 140-5)
effects on explosives and propellants, bibliography on, 20: 4461 (REIC-Memo-28)
effects on mechanical properties of INOR-8, 20: 4308(R) (ORNL-3870, pp 243-60)
effects on performance of stainless steel-clad Alumel–Chromel thermocouples, in-pile, 20: 4263 (ORNL-TM-1320)
effects on phase transformations in calcium orthosilicate, cristobalite, lead oxide, quartz, and silicon oxide, 20: 4462
effects on plutonia and urania ceramics and cermets, (E), 20: 5192 (BNWL-SA-251)
effects on polarization of fluorine nuclei and protons in polymers, 20: 4037
effects on silicon diodes, 20: 4299(R) (ORNL-2711)
effects on stress-rupture properties of Inconel and 304 stainless steel, 20: 5181(R) (ORNL-3029)
effects on stress-rupture of Inconel at high temperatures, 20: 4299(R) (ORNL-2711)
effects on uranium expansion, 20: 4470
effects on wheat seeds, genetic, 20: 3762
flux and leakage through heavy water–iron laminates, (E/T), 20: 4800 (AE-198)
flux and thermal utilization in square cell reactor lattices, effects of multipoles on, (T), 20: 5063
flux distributions in reactors, meter design for measuring, 20: 5061 (ZFK-RN-22)
flux distributions in reactors, statistical fluctuations in, (T), 20: 5066
flux measurement of, performance of zirconium scatterer technique for, 20: 4806(R) (RPI-328-40, pp 1-42)
flux monitor development for, 20: 3982(R) (AGN-8156)
interactions with protons at 300 to 700 Mev, polarization parameters of, (E), 20: 4590 (UCRL-11926)
interactions with mesons (π^-) and neutrons in neutron stars, neutrino

cooling from, (T), 20: 4532
interactions with protons, Schroedinger equation with tensor forces for, (T), 20: 4597
interactions with neutrinos, radiative meson (μ) production from, (T), 20: 4611
interactions with deuterons, binding energies and cross sections for, (T), 20: 4614
kinetics in reactors, hole and void effects, (T), 20: 5064
kinetics in reactors, theory for experiments on noise from, (T), 20: 5076
lifetime in reactors, analysis of Rossi-α experiment on, (T), 20: 5070
multiplication in reflected reactors, correlation of, 20: 5058 (JINR-P-2335)
polarization in deuterium (d,n) reactions at 1.9 to 3.7 Mev, angular distributions of, (E), 20: 4895
polarization studies, 20: 4822(R) (ANL-7081, pp 22-35)
production by (α,n) and (γ,n) reactions with nuclei, (E), 20: 4802 (IDO-17115)
reactions (n,α) with lithium-6 at 1.2 to 8.0 Mev, cross sections for, 20: 4299(R) (ORNL-2711)
reactions (n,α) with lithium-6, alpha and triton energy distributions from, 20: 5181(R) (ORNL-3029)
reactions (n,d) with copper-63, nickel-58, and zinc-64 at 14 Mev, energy levels from, (E), 20: 4896
reactions (n,γ) with nuclei, level studies from, 20: 4821(R) (ANL-7081, pp 2-21)
reactions (n,γ) with hydrogen, gamma spectra from, (E), 20: 4856
reactions (n,n') with carbon-12 at 13 to 18 Mev, 3α decay mode cross section for, (E), 20: 4878
reactions (n,3n) with tritium at 14 Mev, cross section for, (E), 20: 4849(R) (UCRL-14360, pp 1-50)
reactions in tissue of, effects of neutron energy on, 20: 3708 (CEA-R-2833)
reactions with graphite, magnesium, and polyethylene in channels of FRJ-2 reactor, heating from, 20: 5202
reactions with nuclei, cross sections and polarization studies from, 20: 4822(R) (ANL-7081, pp 22-35)
reactions with nuclei at 0.1 to 15 Mev, gamma production cross sections for, 20: 4849(R) (UCRL-14360, pp 1-50)
reactions with uranium-238, effective temperature for Doppler broadening of resonances in, 20: 5135 (WCAP-3269-40)
resonance absorption measurement by pulsed source, feasibility of, 20: 4806(R) (RPI-328-40, pp 1-42)
scattering by aluminum-27 at 14.2 Mev, differential cross sections for inelastic, (E), 20: 4891
scattering by beryllium oxide, microstructure and temperature effects in, 20: 5180 (NAA-SR-Memo-11604)
scattering by ethane at 0.020 to 0.064 ev, inelastic, 20: 4810
scattering by nuclear Coulomb field, polarization determination from, (T), 20: 4832 (IAE-901)
scattering by nuclei, p-wave phase shifts in small-angle, (T), 20: 4909
scattering by plutonium-239, resonance, (E), 20: 4849(R) (UCRL-14360, pp 1-50)
scattering by water, cross sections for inelastic, (E), 20: 4807(R) (RPI-328-40, pp 56-66)
scattering in homogeneous medium, free-gas collision operator for, 20: 4811
scattering in moderators, decay constant for pulsed, 20: 4816
scattering in solids spectra from, (E), 20: 4476(R) (IS-1200(Sect.P))
shielding in heterogeneously distributed pure absorber, self-, (T), 20: 4808 (UCRL-14432-T)
slowing-down age in paraffin, 20: 4813
slowing-down and thermalization of, computer program for, 20: 4804 (KAPL-3098)
spectra in paraffin–zirconium oxide media, 20: 4806(R) (RPI-328-40, pp 1-42)
thermalization in graphite, (T), 20: 4818
thermalization of, research on, 20: 4806(R) (RPI-328-40, pp 1-42)
transmission by finite water slabs, 20: 4999(R) (ORNL-2599)
transmission by shielding, angular distributions in, 20: 5181(R) (ORNL-3029)
transmission through boral, 20: 4999(R) (ORNL-2599)
transmission through heterogeneous shields, 20: 4999(R) (ORNL-2599)
transport in iron and iron-water mixtures, (E/T), 20: 4998 (JINR-P-2359)
transport in slab geometry, tables of functions for, 20: 4803 (INR-630/IX-A/PR)
transport of, computer program for calculating energy spectra from, 20: 4805 (ORNL-TM-1245)
transport of, polarization effects in, (T), 20: 4814
transport theory for, spherical harmonics approximation in, 20: 4820
transport theory of, use of Poincare-Bertrand formula in, 20: 4812

NEUTRONS, FAST

detection and measurement in thermal-neutron flux, 20: 5060(R) (TID-22357)
detection and measurement using silicon surface-barrier detectors, 20: 5181(R) (ORNL-3029)
effects on coated thorium and uranium carbide and oxide fuel particles, 20: 4458 (GA-6485)
effects on dimensions of aluminum–europium oxide dispersions, 20: 5174(R) (ORNL-3870, pp 214-29)
effects on embrittlement of type 304 stainless steel, 20: 4460(R) (ORNL-3870, pp 140-5)
effects on embrittlement of types 304 and 304L stainless steels at 650 to 842°C, 20: 4460(R) (ORNL-3870, pp 140-5)
effects on embrittlement of type 304 stainless steel, role of grain boundary carbides in, 20: 4460(R) (ORNL-3870, pp 140-5)
effects on embrittlement of type 304 stainless steel, role of titanium additions in, 20: 4460(R) (ORNL-3870, pp 140-5)
effects on gas bubble formation in magnesium oxide, 20: 4387(R) (ORNL-3870, pp 38-43)
effects on germanium, electron-microscope observations of, 20: 4467
effects on mechanical properties of aluminum alloy 6061, 20: 4460(R) (ORNL-3870, pp 140-5)
effects on mice of, dose fractionation, biological, 20: 3728
effects on optical properties of zirconium oxide film, 20: 4304(R) (ORNL-3870, pp 171-83)
effects on pig skin, effects of dose fractionation on, 20: 3735
effects on properties of fueled graphite spheres, 20: 4306(R) (ORNL-3870, pp 194-213)
effects on silicon diodes, 20: 4999(R) (ORNL-2599)
effects on thermal conductivity of germanium, 20: 4466
effects on x-ray diffraction pattern of beryllia single crystals, 20: 4391(R) (ORNL-3870, pp 75-82)
performance in activation analyses, 20: 3863(R) (IS-1200(Sect. C))
reactions (n,γ) with nickel-64 at 0.2 to 2.0 Mev, cross sections for, (E/T), 20: 4911
reactions with gold-197, Doppler shifts and resonance integrals in, (E), 20: 4841 (NAA-SR-Memo-11511)
spectra of, calculation of differential, 20: 4256

NEUTRONS, FISSION

spectroscopy using semiconductor sandwich detectors, (E), 20: 4238 (EUR-2487.e)

NEUTRONS, THERMAL

capture by arsenic-75, gamma energy and intensity in, 20: 4849(R) (UCRL-14360, pp 1-50)
capture by cadmium-113 in cadmium sulfides, recoil defects from, 20: 4000
detection and measurement using dysprosium oxide, 20: 4260(P)
effects on dimensions of aluminum–europium oxide dispersions, 20: 5174(R) (ORNL-3870, pp 214-29)
effects on embrittlement of type 304 stainless steel, 20: 4460(R) (ORNL-3870, pp 140-5)
effects on embrittlement of types 304 and 304L stainless steels at 650 to 842°C, 20: 4460(R) (ORNL-3870, pp 140-5)
effects on embrittlement of type 304 stainless steel, role of grain boundary carbides in, 20: 4460(R) (ORNL-3870, pp 140-5)
effects on embrittlement of type 304 stainless steel, role of titanium additions in, 20: 4460(R) (ORNL-3870, pp 140-5)
effects on glasses, ESR studies of, 20: 5019
effects on mechanical properties of aluminum alloy 6061, 20: 4460(R) (ORNL-3870, pp 140-5)
effects on physical properties of cadmium sulfides, 20: 4027
flux distributions in Tower Shielding Reactor II, 20: 5181(R) (ORNL-3029)
flux in water in Lid Tank Facility, (E/T), 20: 4299(R) (ORNL-2711)
flux measurements in water using gold activation, corrections to, 20: 5181(R) (ORNL-3029)
flux measurements using gold activation, corrections to, 20: 4299(R) (ORNL-2711)
fluxes in Bulk Shielding Facility, (E/T), 20: 4299(R) (ORNL-2711)
fluxes in oil, at Lid Tank Facility, 20: 4999(R) (ORNL-2599)
performance in activation analyses, 20: 3863(R) (IS-1200(Sect. C))
scattering by antiferromagnets, cross section of inelastic magnetic, (T), 20: 4809
scattering by benzene, biphenyl, *m*-, *o*-, and *p*-terphenyl, angular distributions and diffusion constants from, (E), 20: 4817
scattering by beryllium oxides, differential cross sections for, (T), 20: 4801(R) (GA-6634)
scattering by liquid argon, coherent, (T), 20: 4819
scattering by water and zirconium hydrides, differential cross sections for, (E/T), 20: 4801(R) (GA-6634)

NEW MEXICO

cosmic-ray energy spectra at high altitude over, in 1962, 20: 4569

NICKEL

bremsstrahlung yields from, with incorporated strontium-90–yttrium-90, 20: 5000 (ORNL-IIC-5, pp 91-8)
corrosion by cesium at 400°C, 20: 4337

determination in iron, spectrophotometric, 20: 3863(R) (IS-1200(Sect. C))
determination in mixtures by x-ray fluorescence using promethium-147/aluminum and tritium/zirconium sources, 20: 3883 (ORNL-IIC-5, pp 154-81)
diffusion of copper in, at 800 to 1050°C, 20: 4363 (AEET/CD/31)
effects on copper oxidation, 20: 4320(R) (ORNL-3870, pp 70-4)
electron scattering by films of, differential cross sections for multiple, (E), 20: 4485
fission fragment ranges in, 20: 3982(R) (AGN-8156)
neutron cross sections for, 9- and 16-group, 20: 4829 (GEMP-173(Suppl.1))
neutron cross sections for, 20: 4830 (GEMP-384)
separation from silver by partition chromatography, 20: 4054
thermal capacity of, effects of magnetic order on, 20: 4320(R) (ORNL-3870, pp 70-4)
thermodynamic properties of oxygen in liquid, 20: 4454
thickness measurement by alpha energy degradation, 20: 3982(R) (AGN-8156)
Ni–UO_2, preparation of fibrous, for fissiochemical reactions, 20: 3982(R) (AGN-8156)

NICKEL ALLOY COUPLES
Alumel/Chromel, radiation effects on stainless steel-clad, 20: 4263 (ORNL-TM-1320)

NICKEL ALLOYS
corrosion by cesium at 400°C, 20: 4337
Al–Cr–Co–Mo–Ni–Ti, corrosion of Udimet 500 by lithium fluoride in cyclic high-temperature environment, 20: 4326 (TRW-ER-6561)
Alumel–Chromel, testing of thermocouples of, 20: 4299(R) (ORNL-2711)
Ba–Ni, phase studies, 20: 4442
Be–Ni, preparation by splatcooling and hot-pressing, 20: 4381(R) (NMI-8001.4)
Co–Fe–Mo–Ni, properties of Maraging Steel for use in space electric power systems, 20: 4379 (NASA-CR-54091)
Co–Ni, thermodynamic properties of oxygen in liquid, 20: 4454
Co–Ni–Ti–Zr, properties of Nivco in space electric power systems, 20: 4379 (NASA-CR-54091)
Cr–Fe–Mo–Ni–Nb–W, welding properties of Inco IN-102, 20: 4306(R) (ORNL-3870, pp 194-213)
Cr–Ni, aging and thermoelectric power of Alumel–Chromel thermocouples, 20: 4398 (TRG-Report-1021)
Cu–Ni, thermal capacity of, effects of magnetic order on, 20: 4320(R) (ORNL-3870, pp 70-4)
Fe–Ni, thermodynamic properties of oxygen in liquid, 20: 4454
Fe–Ni–U, analysis for iron and uranium by controlled-potential coulometry, 20: 3879(R) (MLM-1266)
Li–Ni, phase studies, 20: 4442
Mg–Ni, solvent properties for rare earth elements in molten chloride salts, 20: 3865 (ANL-7064)
Mo–Ni, atomic structure of, short-range order and size-effect coefficients for, (E), 20: 4421
Ni–rare earth, magnetic properties and structure, 20: 4448
Ni–Sr, phase studies, 20: 4442
Ni–Ta, atomic structure of, short-range order and size-effect coefficients for, (E), 20: 4421
Ni–W, atomic structure of, short-range order and size-effect coefficients for, (E), 20: 4421
Ni–Y, crystal structure, 20: 4297(R) (IS-1200(Sect.M))

NICKEL BROMIDES
CsBr–$NiBr_2$, spectra of nickel(II) in melts of, absorption, 20: 3921(R) (ORNL-3870, pp 56-60)
LiBr–$NiBr_2$, spectra of nickel(II) in melts of, absorption, 20: 3921(R) (ORNL-3870, pp 56-60)
$NiBr_2$–KBr, spectra of nickel(II) in melts of, absorption, 20: 3921(R) (ORNL-3870, pp 56-60)

NICKEL CATALYSTS
preparation of Raney, 20: 3974 (ORNL-TM-1314)

NICKEL CHLORIDES
density equations for molten mixtures of tri-n-butyl-benzylphosphonium chloride and, 20: 3921(R) (ORNL-3870, pp 56-60)
spectra of nickel(II) in mixtures of tri-n-butyl-benzylphosphonium chloride and, absorption, 20: 3921(R) (ORNL-3870, pp 56-60)
CsCl–$NiCl_2$, density equations for molten, 20: 3921(R) (ORNL-3870, pp 56-60)
CsCl–$NiCl_2$, spectra of nickel(II) in melts of, absorption, 20: 3921(R) (ORNL-3870, pp 56-60)
LiCl–$NiCl_2$, spectra of nickel(II) in melts of, absorption, 20: 3921(R) (ORNL-3870, pp 56-60)
$MgCl_2$–$NiCl_2$, spectra of nickel(II) in melts of, absorption, 20: 3921(R) (ORNL-3870, pp 56-60)
$NiCl_2$–KCl, spectra of nickel(II) in melts of, absorption, 20: 3921(R) (ORNL-3870, pp 56-60)
$NiCl_2$–NaCl, spectra of nickel(II) in melts of, absorption, 20: 3921(R) (ORNL-3870, pp 56-60)
$NiCl_2$–RbCl, spectra of nickel(II) in melts of, absorption, 20: 3921(R) (ORNL-3870, pp 56-60)

NICKEL COMPLEXES
magnetic interactions in, 20: 3863(R) (IS-1200(Sect. C))

NICKEL FERRATES (III)
magnetic properties of, shock effects on, 20: 4708(R) (UCRL-14360, pp 50-73)
magnetic properties of shock effects on, 20: 4708(R) (UCRL-14360, pp 50-73)

NICKEL IONS
effects on crystalline electric fields, method for calculating, 20: 5006(R) (ORNL-3870, pp 50-5)
spectra of divalent, in alkali halide melts, absorption, 20: 3921(R) (ORNL-3870, pp 56-60)

NICKEL ISOTOPES Ni-57
energy levels from nickel-58 (He-3, α) reactions at 15 and 18 Mev, (E/T), 20: 4912
energy levels of, from helium-3 reactions (He-3,α) with nickel-58, (E), 20: 4892

NICKEL ISOTOPES Ni-58
energy levels, 20: 4849(R) (UCRL-14360, pp 1-50)
helium-3 reactions (He-3,α) at 24.5 Mev, energy levels from, (E), 20: 4892
helium-3 reactions (He-3, α) at 15 and 18 Mev, nickel-57 levels from, (E/T), 20: 4912
neutron reactions (n,d) at 14 Mev, energy levels from, (E), 20: 4896
proton elastic scattering at 160 Mev, differential cross sections for, (E/T), 20: 4906
proton reactions (p,pn) at 450 Mev, differential recoil from, (T), 20: 4893
proton scattering at 18.6 and 19.1 Mev, (E/T), 20: 4849(R) (UCRL-14360, pp 1-50)

NICKEL ISOTOPES Ni-59
energy levels of, from helium-3 reactions (He-3,α) with nickel-60, (E), 20: 4892

NICKEL ISOTOPES Ni-60
energy levels, 20: 4849(R) (UCRL-14360, pp 1-50)
helium-3 reactions (He-3,α) at 24.5 Mev, energy levels from, (E), 20: 4892
proton scattering at 18.6 and 19.1 Mev, (E/T), 20: 4849(R) (UCRL-14360, pp 1-50)

NICKEL ISOTOPES Ni-61
Mössbauer effects in, following Coulomb excitation, 20: 3920(R) (ORNL-3870, pp 27-37)

NICKEL ISOTOPES Ni-62
energy levels, 20: 4849(R) (UCRL-14360, pp 1-50)
energy levels of, from neutron reactions with copper-63 at 14 Mev, (E), 20: 4896
proton scattering at 18.6 and 19.1 Mev, (E/T), 20: 4849(R) (UCRL-14360, pp 1-50)

NICKEL ISOTOPES Ni-64
neutron reactions (n,γ) at 0.2 to 2.0 Mev, cross sections for, (E/T), 20: 4911

NICKEL ISOTOPES Ni-65
energy levels from nickel-64 (n,γ) reactions at 0.2 to 2.0 Mev, radiation widths of, (E/T), 20: 4911

NICKEL OXIDES
solubility in borax at 760 to 900°C, 20: 3951

NICKEL SELENIDES
magnetic properties, (E), 20: 4849(R) (UCRL-14360, pp 1-50)

NICKEL SULFIDES
magnetic properties, (E), 20: 4849(R) (UCRL-14360, pp 1-50)
sulfur-35 exchange with thiopene, 20: 3976

NICKEL SYSTEMS
B–Ni–Si, brazing alloy for tungsten carbide–cobalt cermet to TZM molybdenum alloy, 20: 4307(R) (ORNL-3870, pp 238-42)
C–Ni–U, phase studies, 20: 4368 (CEA-R-2845)
Ni–ThO_2, corrosion by lithium fluoride in cyclic high-temperature environment, 20: 4326 (TRW-ER-6561)
Ni–ThO_2, properties at high temperatures, 20: 4418

NICOTINE
effects of chronic cigarette smoking, on pulmonary clearance in dogs, 20: 3655 (BNWL-SA-224)

NIOBIUM
bonding to beryllium oxide, method for, 20: 4354(P)
bremsstrahlung yields from, with incorporated strontium-90–yttrium-90, 20: 5000 (ORNL-IIC-5, pp 91-8)
coating with aluminum–tin alloy method for, 20: 4355(P)
coating with aluminum alloy, use of titanium as middle layer for, 20: 4356(P)
coating with aluminum–tin alloys, 20: 4357(P)
compatibility with uranium dioxide, 20: 5181(R) (ORNL-3029)
compatibility with uranium carbide–zirconium carbide system at 2000°C, 20: 4335

corrosion by liquid lithium, 20: 4999(R) (ORNL-2599)
corrosion by liquid chromium–uranium, 20: 4077(R) (IS-1200(Sect. E))
corrosion by lithium, time dependence of, 20: 5181(R) (ORNL-3029)
corrosion by lithium, alloying effects on, 20: 4299(R) (ORNL-2711)
corrosion by potassium–sodium alloys, 20: 5181(R) (ORNL-3029)
corrosion by potassium at 200, 600, and 815°C, effects of oxygen on, 20: 4321(R) (ORNL-3870, pp 136-9)
crystal structure of, effects of high-temperature contamination by atmosphere and nitrogen on, 20: 4401(T) (ANL-Trans-218)
crystal structure preferred orientation, 20: 4389(R) (ORNL-3870, pp 61-4)
deposition on finely dispersed particles, method for, 20: 4314(P)
determination of trace amounts of, in uranium and uranium alloys, 20: 3897
determination of, hydrogen peroxide method for spectrophotometric, 20: 3904
diffusion in tantalum at 900 to 2500°C, 20: 4320(R) (ORNL-3870, pp 70-4)
diffusion of niobium-95 and tantalum-182 in, 20: 4385(R) (ORNL-3870, pp 15-19)
diffusion of oxygen in, at 600 and 815°C, 20: 4321(R) (ORNL-3870, pp 136-9)
dislocation configuration in deformed foils of, 20: 4386(R) (ORNL-3870, pp 20-6)
elastic properties at 4.2 to 300°K, (E), 20: 4422
extrusion of alloy-clad billets of, 20: 4299(R) (ORNL-2711)
extrusion of arc-melted, 20: 4999(R) (ORNL-2599)
fatigue of, effect of crystal structure on. 20: 4443
mechanical properties of arc-cast, heat treatment effects on, 20: 4999(R) (ORNL-2599)
mechanical properties of, additive effects on, 20: 5181(R) (ORNL-3029)
mechanical properties of, effects of hot plastic deformation on, 20: 4403(T) (JPRS-32317)
mechanical properties of, effects of impurities on, 20: 4425
mechanical properties, 20: 4299(R) (ORNL-2711)
neutron cross sections for, 9- and 16-group, 20: 4829 (GEMP-173 (Suppl.1))
neutron cross sections for, 20: 4830 (GEMP-384)
oxidation at low pressures and high temperatures, 20: 5181(R) (ORNL-3029)
oxidation at low pressures at 870 to 3500°F, 20: 4324 (PWAC-460)
oxidation of, stress generation in surface layers during, 20: 4320(R) (ORNL-3870, pp 70-4)
preparation by reduction of pentachloride in hydrogen plasma jet, 20: 4314(P)
preparation of high-purity, 20: 4297(R) (IS-1200(Sect.M))
properties as collector in thermionic cells, 20: 4570(R) (AD-614592)
reactions with methane at low pressures and high temperatures, 20: 5181(R) (ORNL-3029)
reactions with nitrogen and oxygen at high temperatures, 20: 4299(R) (ORNL-2711)
separation from low grade ores, reductive chlorination process for, 20: 4072(P)
superconducting properties of high-purity, at 1.1 to 9.25°K, (E), 20: 4774 (IS-T-22)
superconductivity at 1 to 9.25°K, (E), 20: 4476(R) (IS-1200(Sect.P))
superconductivity of, effects of crystal imperfections on, 20: 4297(R) (IS-1200(Sect.M))
tensile properties of, effects of lithium and oxygen on, 20: 5181(R) (ORNL-3029)
thermal capacity of superconducting, in magnetic fields, 20: 4786
thermal conductivity, 20: 4299(R) (ORNL-2711)
welding, 20: 4299(R) (ORNL-2711)
welding techniques for, 20: 4999(R) (ORNL-2599)

NIOBIUM ALLOYS

coating with aluminum alloy, use of titanium as middle layer for, 20: 4356(P)
coating with aluminum–tin alloys, 20: 4357(P)
fabrication of tube shells by flow turning, process development for, 20: 4301(R) (ORNL-3870, pp 102-35)
oxidation at low pressures and high temperatures, 20: 5181(R) (ORNL-3029)
Al–Nb, properties as coating for refractory metals, 20: 4418
Al–Nb–Ti–W–V–Zr, properties for use to 1200°F, 20: 4393 (PWAC-472)
Be–Nb, corrosion by lithium at high temperatures, 20: 4299(R) (ORNL-2711)
Ce–Nb, corrosion by lithium at high temperatures, 20: 4299(R) (ORNL-2711)
Cr–Fe–Mo–Ni–Nb–W, welding properties of Inco IN-102, 20: 4306(R) (ORNL-3870, pp 194-213)
Hf–Nb–W–Y, evaporation losses in high vacuum of C-129Y, 20: 4301(R) (ORNL-3870, pp 102-35)
Mo–Nb–V–Zr, corrosion of B-66, by lithium, effects of oxygen on, 20: 4301(R) (ORNL-3870, pp 102-35)
Mo–Nb–V–Zr, evaporation losses in high vacuum of B-66, 20: 4301(R) (ORNL-3870, pp 102-35)
Mo–Nb–V–Zr, tensile properties of welded plates of B-66, 20: 4301(R) (ORNL-3870, pp 102-35)
Nb–Sn, crystal structure of intermetallic compounds in, 20: 4297(R) (IS-1200(Sect.M))
Nb–Sn, magnetic flux jumps and trapping in superconducting, (E), 20: 4793
Nb–Ta, thermal capacity of superconducting, in magnetic fields, 20: 4786
Nb–Ta, work hardening in tantalum-base, mechanisms of, 20: 4384(R) (ORNL-3870, pp 7-14)
Nb–Ta–V, development as brazing alloy for refractory metals, 20: 4301(R) (ORNL-3870, pp 102-35)
Nb–Ta–W–Zr, corrosion of FS-85, by lithium, effects of oxygen on, 20: 4301(R) (ORNL-3870, pp 102-35)
Nb–Ta–W–Zr, creep properties of FS-85, 20: 4301(R) (ORNL-3870, pp 102-35)
Nb–Ta–W–Zr, ductility of FS-85, effects of aging on bend, 20: 4301(R) (ORNL-3870, pp 102-35)
Nb–Ta–W–Zr, evaporation losses in high vacuum of FS-85, 20: 4301(R) (ORNL-3870, pp 102-35)
Nb–Ta–W–Zr, preparation and specifications for corrosion loop testing, 20: 4380 (NASA-CR-54761)
Nb–Ti, coating with aluminum alloy for oxidation protection, 20: 4315(P)
Nb–V, twinning in, relation of dislocation substructure to, 20: 4389(R) (ORNL-3870, pp 61-4)
Nb–W–Zr, corrosion of Cb-752, by lithium, effects of oxygen on, 20: 4301(R) (ORNL-3870, pp 102-35)
Nb–W–Zr, creep properties of Cb-752, 20: 4301(R) (ORNL-3870, pp 102-35)
Nb–Y, corrosion by lithium at high temperatures, 20: 4299(R) (ORNL-2711)
Nb–Zr, aging studies of, 20: 5181(R) (ORNL-3029)
Nb–Zr, aging studies on welds of, 20: 5181(R) (ORNL-3029)
Nb–Zr, brazing and welding of, 20: 5181(R) (ORNL-3029)
Nb–Zr, compatibility with uranium dioxide, 20: 5181(R) (ORNL-3029)
Nb–Zr, corrosion by potassium–sodium alloys, 20: 5181(R) (ORNL-3029)
Nb–Zr, corrosion by lead at 1400°F, 20: 4308(R) (ORNL-3870, pp 243-60)
Nb–Zr, corrosion by potassium–sodium eutectic, 20: 4323(R) (ORNL-3870, pp 308-11)
Nb–Zr, corrosion by lithium at high temperatures, 20: 4299(R) (ORNL-2711)
Nb–Zr, corrosion by potassium, 20: 4301(R) (ORNL-3870, pp 102-35)
Nb–Zr, corrosion by lithium, effects of oxygen on, 20: 4301(R) (ORNL-3870, pp 102-35)
Nb–Zr, creep properties, effects of cold working and annealing on, 20: 4301(R) (ORNL-3870, pp 102-35)
Nb–Zr, effects of lithium and oxygen on tensile properties of, 20: 5181(R) (ORNL-3029)
Nb–Zr, emissivity, effects of surface treatments on, 20: 4301(R) (ORNL-3870, pp 102-35)
Nb–Zr, evaporation losses in high vacuum, 20: 4301(R) (ORNL-3870, pp 102-35)
Nb–Zr, mechanical properties of, effects of oxygen on, 20: 4297(R) (IS-1200(Sect.M))
Nb–Zr, performance of superconducting solenoids of, 20: 4775 (UCRL-16376)
Nb–Zr, phase transformation kinetics, 20: 4390(R) (ORNL-3870, pp 65-9)
Nb–Zr, properties at low temperatures, 20: 3920(R) (ORNL-3870, pp 27-37)
Nb–Zr, purification by electron-beam melting, 20: 5181(R) (ORNL-3029)
Nb–Zr, sorptive properties for nitrogen, kinetics of, 20: 4301(R) (ORNL-3870, pp 102-35)
Nb–Zr, stability of carbon-strengthened, at 2000°F, 20: 4397 (TIM-955)
Nb–Zr, superconducting properties, 20: 4390(R) (ORNL-3870, pp 65-9)
Nb–Zr, superconducting properties, (E), 20: 4792
Nb–Zr, tube-burst tests on, 20: 5181(R) (ORNL-3029)

NIOBIUM BORIDES

preparation of polynuclear, 20: 3863(R) (IS-1200(Sect. C))

NIOBIUM CARBIDES

NbC–UC, diffusion of xenon-133 from low-dose, low-temperature irradiated fuels of, (E), 20: 4471

NIOBIUM CHLORIDES

preparation of polynuclear, 20: 3863(R) (IS-1200(Sect. C))
reduction to metal in hydrogen plasma jet, 20: 4314(P)
separation from tantalum chloride, methods for, 20: 4077(R) (IS-1200 (Sect. E))

NIOBIUM COMPOUNDS

molecular structure of $NbBr_4(CH_3CN)_2$, 20: 3863(R) (IS-1200(Sect. C))

NIOBIUM IODIDES
vaporization at 600 to 700°C, 20: 3863(R) (IS-1200(Sect. C))
NIOBIUM ISOTOPES Nb-95
content of, in brown algae of Solway Firth, 20: 3662 (PG-Report-650)
diffusion in niobium and tantalum, 20: 4385(R) (ORNL-3870, pp 15-19)
NIOBIUM ORES
processing by reductive chlorination, 20: 4072(P)
NIOBIUM OXYCHLORIDES
chlorination kinetics, 20: 4077(R) (IS-1200(Sect. E))
NIOBIUM SYSTEMS
C–Mo–Nb–Ta–W–Zr, preparation and specifications for corrosion loop testing, 20: 4380 (NASA-CR-54761)
C–Nb–W–Zr, aging and recrystallization of D-43, 20: 4301(R) (ORNL-3870, pp 102-35)
C–Nb–W–Zr, corrosion of D-43, by potassium, 20: 4301(R) (ORNL-3870, pp 102-35)
C–Nb–W–Zr, corrosion of D-43, by lithium, effects of oxygen on, 20: 4301(R) (ORNL-3870, pp 102-35)
C–Nb–W–Zr, ductility of welds in D-43, effects of aging on bend, 20: 4301(R) (ORNL-3870, pp 102-35)
C–Nb–W–Zr, evaporation losses in high vacuum of D-43, 20: 4301(R) (ORNL-3870, pp 102-35)
C–Nb–W–Zr, preparation and specifications for corrosion loop testing, 20: 4380 (NASA-CR-54761)
C–Nb–W–Zr, tensile properties of welded plates of D-43, 20: 4301(R) (ORNL-3870, pp 102-35)
C–Nb–W–Zr, thermal conductivity of D-43, at 30 to 120°C, 20: 4301(R) (ORNL-3870, pp 102-35)
C–Nb–Zr, phase studies at 1092 and 1538°C, 20: 4392 (PWAC-461)
Nb–O, oxygen clustering in solid solutions of, 20: 4449
Nb–O–Zr, phase studies, 20: 4297(R) (IS-1200(Sect.M))
NITRATE COMPLEXES
spectra of, determination of bidentate and unidentate from infrared, 20: 3949
NITRIC ACID
corrosive effects on stainless steel, effects of molybdenum and uranium on, 20: 4325 (TB-58)
separation of protactinium from, by solvent extraction using tributyl phosphate, 20: 4057
separation of protactinium from, by solvent extraction using tributyl phosphate, 20: 4058
solvent properties for plutonium, uranium, and uranium alloys, 20: 4948(R) (NP-15406)
$Al(NO_3)_3$–HNO_3, separation of thorium from, by solvent extraction using TBP, 20: 4060
$LiNO_3$–methanol–HNO_3, use as solvent in ion-exchange separation of rare earths, 20: 4067
NITROCELLULOSE
charged particle track analysis in, methods for, (E), 20: 4251 (USNRDL-TR-917)
NITROGEN
determination in boron by activation methods, 20: 3879(R) (MLM-1266)
determination in refractory metals by gas chromatography, 20: 3863(R) (IS-1200(Sect. C))
determination in steels by platinum-bath vacuum fusion, 20: 3863(R) (IS-1200(Sect. C))
determination in yttrium, methods for, 20: 4299(R) (ORNL-2711)
diffusion from stored solid plutonium residues, vacuum-drying effects on, 20: 4364 (AERE-M-1644)
diffusion in uranium mononitride, activation energy and rate of self-, 20: 4394 (PWAC-477)
effects on corrosion of niobium by lithium at high temperatures, 20: 4299(R) (ORNL-2711)
effects on ductility of vanadium, 20: 4297(R) (IS-1200(Sect.M))
effects on mechanical properties of niobium, additive, 20: 5181(R) (ORNL-3029)
effects on oxidation of tantalum at 600 to 925°C, 20: 4333
effects on structure of niobium by contamination at high temperatures, 20: 4401(T) (ANL-Trans-218)
gamma reactions at 0.01 to 10 Mev, cross sections for, 20: 4996 (AWRE-O-79/65)
helium–ion reactions at 3 to 600 ev, charge transfer in, 20: 4759
mass transfer from stainless steel to niobium and niobium–zirconium alloy, in potassium–sodium alloy, 20: 5181(R) (ORNL-3029)
radiation effects on electric conductivity of, 20: 4949(R) (UCRL-14360, pp 85-94)
radioinduced production of atomic, effects of nitric oxide on, 20: 3982(R) (AGN-8156)
radioinduced reactions with hydrocarbons, G-values and mechanisms of, 20: 3982(R) (AGN-8156)
reactions of atomic, with organics, 20: 3982(R) (AGN-8156)
reactions with ions, charge-exchange, 20: 4556
reactions with niobium at high temperatures, 20: 4299(R) (ORNL-2711)
separation from lutetium by electrotransport, 20: 4297(R) (IS-1200 (Sect.M))
solubility in uranium mononitride, 20: 4303(R) (ORNL-3870, pp 164-70)
sorption by niobium–1 zirconium alloy, kinetics of, 20: 4301(R) (ORNL-3870, pp 102-35)
yields from radiolysis of ammonia, 20: 4021
NITROGEN COMPOUNDS
spectra of, infrared, 20: 3863(R) (IS-1200(Sect. C))
NITROGEN IONS
reactions with argon and nitrogen, charge-exchange, 20: 4556
NITROGEN ISOTOPES N-13
energy levels from boron-11 (He-3, n) reactions at 1.3 to 5.8 Mev, 20: 4925
NITROGEN ISOTOPES N-14
deuteron reactions (d,γ) at 0.5 to 5.5 Mev, excitation curves and angular distributions from, (E), 20: 4884
deuteron reactions at 1.9 to 6.7 Mev, bound states from, (E), 20: 4905
neutron capture by, gamma spectra from, 20: 4999(R) (ORNL-2599)
nitrogen-14 reactions (N-14, N-13) with particle transfer model for, 20: 4851
proton reactions (p,γ) at 0.97 to 1.96 Mev, performance of anticoincidence shielded gamma spectrometer for detecting, (E), 20: 4233 (AD-618676)
NITROGEN ISOTOPES N-15
gamma transitions in, angular distributions and intensities of (E), 20: 4905
proton reactions (p,α) with, angular distributions for, (E), 20: 4849(R) (UCRL-14360, pp 1-50)
NITROGEN ISOTOPES N-17
production for use as neutron source, 20: 4802 (IDO-17115)
NITROGEN MUSTARDS
effects on bone marrow function in dogs, 20: 3652
effects on leukemia cells, cytotoxic, 20: 3736
NITROGEN OXIDES
effects on hydrogen yields from radiolysis of hydrogen sulfide, 20: 4017
effects on radioinduced crosslinking of polyethylene, 20: 4010
radiosensitivity effects of, on seeds, 20: 3759
NITROGEN SYSTEMS
CH_4–N, radiolysis of, products from fission-fragment, 20: 3982(R) (AGN-8156)
CH_4–N_2, radiolysis of, products from electron, 20: 3982(R) (AGN-8156)
C–N–O–Pu–U, corrosion by water at 550°F, 20: 4327(R) (UNC-5138)
C–N–O–Pu–U, preparation of single-phase compositions of, 20: 4327(R) (UNC-5138)
CO–H–N, radioinduced reactions in, 20: 3982(R) (AGN-8156)
N–O, corrosive effects on INOR-8 at 1300 and 1400°F, 20: 4308(R) (ORNL-3870, pp 243-60)
NOISE
measurement in plasma by two-frequency correlation method, 20: 4991
NORLEUCINE
ionization potential, 20: 3863(R) (IS-1200(Sect. C))
NOZZLES
effects on reactor accident containment, limiting, 20: 5034 (NOLTR-63-140)
plasma ejection from axial, pinched, 20: 4138
NRX REACTOR
fuel rupture in, location using gamma spectrometers, 20: 5109 (AECL-2360)
NUCLEAR AIRCRAFT
development, 20: 4999(R) (ORNL-2599)
development, 20: 5181(R) (ORNL-3029)
dose rates in crew compartment of, (T), 20: 5181(R) (ORNL-3029)
gamma dose rates in crew compartment of, 20: 4999(R) (ORNL-2599)
neutron dose rates in crew compartment, computer program for calculating fast, 20: 4299(R) (ORNL-2711)
neutron fluxes and dose rates in shield compartment of, 20: 4999(R) (ORNL-2599)
NUCLEAR AIRCRAFT POWER PLANTS
development, 20: 4999(R) (ORNL-2599)
development, 20: 5181(R) (ORNL-3029)
NUCLEAR EMULSIONS
use in cosmic-ray energy spectra measurements, 20: 4569
use in neutron spectrometers, 20: 4249 (UCRL-16311)
NUCLEAR MAGNETIC RESONANCE
detection using spectrometer sensitive to weak transverse static fields, 20: 4255
measurement in rapidly rotating solids, 20: 4931
NUCLEAR MATERIALS MANAGEMENT
burnup analysis by gamma scanning, 20: 5093
NUCLEAR MODELS
bound states in short-range central potentials, (T), 20: 4708(R) (UCRL-14360, pp 50-73)
description of close-packed-spheron, 20: 4918
theory of superfluid, for spontaneous fission, 20: 4876

NUCLEAR MODELS (DROP)
nuclear reaction theory from, 20: 4879
NUCLEAR MODELS (SHELL)
nucleon coupling parameters in, sensitivity of, 20: 4835 (JINR-P-2287)
NUCLEAR PHYSICS
research, (T), 20: 4475(R) (ANL-7081, pp 95-119)
research in England, 20: 4504(R) (NP-15420)
research in, 460-Mev synchrocyclotron, 20: 4577 (AD-618067)
units for, 20: 4539 (UCRL-11444)
NUCLEAR POWER
conference, 20: 5154
conference on, 20: 5161
development, 20: 5167
development and research program in United Kingdom, 20: 5150
development of, conference on, 20: 5166
research programs in U. S., 20: 5151
research programs in United Kingdom, 20: 5152
NUCLEAR POWER PLANTS
conference, 20: 5154
construction of MZFR, 20: 5138
construction of 252 Mw Lingen, 20: 5139
design and evaluation of 1000-Mw(e), with circulating fuel gaseous core reactor, 20: 5128 (TID-22225)
design using two differently pressured boilers, 20: 5171(P)
development and economics of, 20: 5168
development in Spain, problems in, 20: 5158
development of direct-cycle steam-superheating, 20: 5113 (CONF-650602-59)
development perspectives of Russian, 20: 5149
NUCLEAR QUADRUPOLE RESONANCE
spectra in asymmetric field gradients, (T), 20: 4867
NUCLEAR REACTIONS
angular correlations in direct and resonance, intermediate coupling parameters for, 20: 4835 (JINR-P-2287)
angular distributions and cross sections for two-particle, computer program for, 20: 4844 (ORNL-TM-1234)
diffraction in 10- to 30-Mev, spin-orbit coupling in, (T), 20: 4827 (CEA-Bib-60)
nucleon transfer in, mechanism of, (T), 20: 4850
nucleon transfer in, modified energy matrix method for one-dimensional model for, 20: 4852
polarization correlations in direct, (T), 20: 4849(R) (UCRL-14360, pp 1-50)
target orientation optimization for, computer program for, 20: 4842 (NASA-TN-D-3116)
theory for, shell-model calculations in continuum, (T), 20: 4882
theory from liquid drop model, 20: 4879
theory of, in stellar interiors, 20: 4534
theory of, unified, 20: 4837 (JINR-P-2310)
NUCLEAR STRUCTURE
nucleon magic numbers in, (T), 20: 4872
theory of, close-packed-spheron, (T), 20: 4918
NUCLEI
alpha reactions (α,n) with, performance as neutron source, (E), 20: 4802 (IDO-17115)
alpha scattering by, angular distributions and excitation from, 20: 4824(R) (ANL-7081, pp 70-7)
beta decay in stellar interiors, photon-induced, (T), 20: 4530
beta decay of oriented, problems in, (T), 20: 4933
charged-particle reactions with, cross sections and level studies from, 20: 4822(R) (ANL-7081, pp 22-35)
charged-particle reactions with, angular momentum transfer, cross sections, and level studies from, 20: 4823(R) (ANL-7081, pp 36-69)
deformation of, close-packed-spheron theory for, (T), 20: 4918
deuteron optical potential in, (T), 20: 4879
deuteron reactions (d,He-3) with, level studies from, 20: 4824(R) (ANL-7081, pp 70-7)
deuteron reactions (d,p) at 10 to 30 Mev, spin-orbit coupling in, (T), 20: 4827 (CEA-Bib-60)
electron elastic scattering by, electric and magnetic moment effects in, (T), 20: 4840 (LAL-1140)
electron magnetic scattering by, (T), 20: 4831 (HEPL-272)
electron reactions with, first Born approximation including anapole for, (T), 20: 4612
electron scattering by, differential cross section for trident electron pair production from, (T), 20: 4604
elementary particle reactions with, unified theory for, 20: 4837 (JINR-P-2310)
energy level transitions in, pulse correlation of two cascade quanta for mixed, (T), 20: 4871(T)
energy levels of deformed even-even, symmetry rules for, (E/T), 20: 4476(R) (IS-1200(Sect.P))
energy levels of, measurement of lifetimes of excited, (T), 20: 4917
fission half lives of, superfluid model for spontaneous, (T), 20: 4876
fission of, close-packed-spheron theory for, (T), 20: 4918
fission of, pair correlation effect on parameters for, (T), 20: 4876
gamma reactions with, neutron production in, (E), 20: 4802 (IDO-17115)
helium-3 reactions with, angular distributions from, 20: 4824(R) (ANL-7081, pp 70-7)
ion inelastic scattering by, matrix elements for, (T), 20: 4839 (JINR-P-2333)
ion scattering by even-even, reorientation effect in Coulomb excitation in, (T), 20: 4901
meson (μ) reactions with, first born approximations including anapole for, (T), 20: 4612
meson (π^-) reactions (π^-,π^0) on complex, excitation functions for, (T), 20: 4910
neutron reactions (n,γ) with, level studies from, 20: 4821(R) (ANL-7081, pp 2-21)
neutron reactions with, cross section and polarization studies from, 20: 4822(R) (ANL-7081, pp 22-35)
neutron scattering by Coulomb field of, polarization determination from, (T), 20: 4832 (IAE-901)
neutron scattering by, p-wave phase shifts in small-angle, (T), 20: 4909
nucleon magic numbers in, structural basis for, (T), 20: 4872
nucleon scattering by, shell-model calculations for, (T), 20: 4882
nucleon transfer reactions between, (T), 20: 4850
proton evaporation from excited, (T), 20: 4897
proton reactions (p,n) with $70 \leq A \leq 165$, Coulomb displacement energies from, (E), 20: 4849(R) (UCRL-14360, pp 1-50)
proton reactions (p,2n), (p,pn), and (p,2p), cross sections for, (T), 20: 4897
NUCLEONS
configuration in nuclei, magic numbers for, (T), 20: 4872
exchange in nuclear reactions, mechanism of, 20: 4850
exchange in nuclear reactions, one-dimensional tunneling model for, 20: 4851
exchange in nuclear reactions, modified energy matrix method for, 20: 4852
form factors of, (56,$\bar{5}6$) contribution to, (T), 20: 4642 (IC/65/78)
interactions with nucleons at 300 to 700 Mev, polarization parameters of, (E), 20: 4590 (UCRL-11926)
interactions with nucleons below 350 Mev, models for, (T), 20: 4849(R) (UCRL-14360, pp 1-50)
interactions with antinucleons, potential model for, (T), 20: 4849(R) (UCRL-14360, pp 1-50)
interactions with nucleons, phase-shift analysis of, (T), 20: 4849(R) (UCRL-14360, pp 1-50)
interactions with mesons ($\pi^\pm$), phase-shift analysis of, (T), 20: 4849(R) (UCRL-14360, pp 1-50)
interactions with mesons (π), amplitude of vector meson production in, (T), 20: 4584 (JINR-P-2380)
interactions with mesons (π), three-channel N/D equations in pole approximation for, 20: 4593
interactions with mesons (π), Dashen-Lee sum rules for intermediate state in, (T), 20: 4598
interactions with nucleons, SU(12) predictions for, (T), 20: 4605
interactions with photons, spin-1 meson production from, (T), 20: 4610
interactions with antiprotons at rest, SU(6) symmetry in two-meson annihilation, (T), 20: 4615
interactions with protons, polarized hydrogen target for, 20: 4637
interactions with mesons at high energy, sum rule for cross sections of, (T), 20: 4678
lifetime of bound, lower limits for, (E), 20: 4853
production of $N^*_{7/2}$ (1920) in mesons (π)-nucleon interactions, (T), 20: 4593
scattering by nuclei, shell-model calculations for, (T), 20: 4882
strength functions in nuclear matter, (T), 20: 4879
NUTRIENTS
distribution in soils of, tracer studies, 20: 3710(R) (EUR-2493.e)
metabolism of, tracer studies in animals of, 20: 3685
radiation effects on intestinal absorption of, in man, 20: 3851

O

OAK RIDGE NATIONAL LAB., TENN.
electromagnetic separations program at, review of, 20: 4282 (ORNL-3861)
OILS
neutron fluxes and dose rates in, 20: 4999(R) (ORNL-2599)
radiation effects on viscosity of, in rotary pump, 20: 4999(R) (ORNL-2599)
radiation effects on viscosity in rotary pumps, 20: 4299(R) (ORNL-2711)
OLEIC ACID, METHYL ESTER
radiosensitivity effects on mouse plasma lipids *in vivo*, 20: 3704
OPTICAL SYSTEMS
materials development for, for use in space vehicles, 20: 4312

performance for reactor components dimensional location, 20: 5035 (ORNL-TM-1278)
ORES
analysis of, use of radioisotope methods for, 20: 3884 (ORNL-IIC-5, pp 206-21)
ORGANIC ACIDS
molecular structure of cyclopropanecarboxylic acid chloride, 20: 3863(R) (IS-1200(Sect. C))
ORGANIC COMPOUNDS
determination of carbon-14-labeled, by gas chromatography-ionization chamber method, 20: 3899
halogen resonances in, catalog of, 20: 3973 (IS-1222)
radiation effects on, review of, 20: 4464
reactions of reactor-container-associated, with radioiodine, 20: 4185(R) (ORNL-3843, pp 169-234)
superconductivity in, (T), 20: 4781
ORGANIC COOLED REACTORS
design, 20: 5086(P)
design of DON power prototype, 20: 5162
ORGANIC MODERATED REACTOR EXPERIMENT
fuel-element surface temperature in, thermocouple analysis for, 20: 5026
ORGEL REACTOR
fuel elements for, design of facility for dismantling, 20: 4064
ORNL HIGH FLUX ISOTOPE REACTOR
control element fabrication for, 20: 5174(R) (ORNL-3870, pp 214-29)
fuel assembly machining and welding for, 20: 5174(R) (ORNL-3870, pp 214-29)
fuel plate fabrication for, description of, 20: 5174(R) (ORNL-3870, pp 214-29)
target element design, fabrication, and irradiation testing for, 20: 5175(R) (ORNL-3870, pp 230-7)
ORNL RESEARCH REACTOR
experimental facility for charcoal ignition in, 20: 4086(R) (ORNL-3843, pp 137-67)
fission fragment trapping for off-gas system of, performance of charcoal for, 20: 5199 (ORNL-TM-1328)
operation, April–June 1965, 20: 5198(R) (ORNL-TM-1290)
OSMIUM ISOTOPES Os-192
energy levels of, from rhenium-192 decay, (E), 20: 4861
OVENS
development of high-temperature, 20: 4048(R) (NP-15406)
7-OXABICYCLO[4.1.0]HEPTANE
radioinduced polymerization of, in liquid and solid state, 20: 3992
OXALATES
effects on spectrophotometric determination of zirconium, 20: 3895
OXAZOLE, DIPHENYL-
radioinduced fluorescence in naphthalene, 20: 3994
OXAZOLE, 2,2'-*p*-PHENYLENEBIS[5-PHENYL-
radioinduced fluorescence of, in naphthalene, 20: 3994
OXIDE SLURRIES
particle residence times in, tracer measurement of, 20: 4106(T) (BNL-tr-43)
OXIDES
analysis for oxygen by neutron activation methods, 20: 3907
OXIDIZING AGENTS
effects on methyl iodide retention by charcoal, 20: 4185(R) (ORNL-3843, pp 169-234)
OXYFLUORIDES
reactions in plutonium and uranium tetrafluorides, 20: 4046(R) (EURAEC-1340)
OXYGEN
bremsstrahlung reactions (γ,π^0) at 166 Mev, angular distributions from, (E), 20: 4898
clustering in niobium–oxygen solid solutions, 20: 4449
crystal structure and magnetic properties of solid, neutronographic study of, (E), 20: 4796
determination by neutron activation methods, equipment for, 20: 3907
determination in aluminum, beryllium, and magnesium, methods for, 20: 3878 (LYCEN-6524)
determination in fluoride salts, 20: 4999(R) (ORNL-2599)
determination in lithium fluoride–magnesium fluoride–yttrium fluoride, 20: 4299(R) (ORNL-2711)
determination in metals, emission spectrometric, 20: 3863(R) (IS-1200 (Sect. C))
determination in magnesium–yttrium alloy, 20: 4299(R) (ORNL-2711)
determination in potassium gettering-vacuum fusion method for, 20: 4321(R) (ORNL-3870, pp 136-9)
determination in refractory metals by gas chromatography, 20: 3863(R) (IS-1200(Sect. C))
determination in samarium and ytterbium by neutron activation, 20: 3863(R) (IS-1200(Sect. C))
determination in sodium, operating manual for gas analyzer for, 20: 3889 (UNC-5113)
determination in yttrium, methods for, 20: 4299(R) (ORNL-2711)
diffusion and reactions in tantalum, field-ion microscopic study of, 20: 4332
diffusion from stored solid plutonium residues, vacuum-drying effects on, 20: 4364 (AERE-M-1644)
diffusion in niobium at 600 and 815°C, 20: 4321(R) (ORNL-3870, pp 136-9)
effects on corrosion of tantalum by lithium, 20: 5181(R) (ORNL-3029)
effects on corrosion of niobium by lithium at high temperatures, 20: 4299(R) (ORNL-2711)
effects on Croloy 9M, INOR-8, and type 347 stainless steel corrosion by potassium–sodium, 20: 4322(R) (ORNL-3870, pp 305-7)
effects on ductility of vanadium, 20: 4297(R) (IS-1200(Sect.M))
effects on human embryos, teratogenic, 20: 3747
effects on mechanical properties of niobium, additive, 20: 5181(R) (ORNL-3029)
effects on mechanical properties of zirconium at 250 to 350°C, 20: 4416
effects on mechanical properties of niobium–zirconium alloy, 20: 4297(R) (IS-1200(Sect.M))
effects on niobium- and tantalum-base alloys corrosion by lithium, 20: 4301(R) (ORNL-3870, pp 102-35)
effects on niobium corrosion by potassium at 200, 600, and 815°C, 20: 4321(R) (ORNL-3870, pp 136-9)
effects on radioinduced fluorescence of organic phosphors in napthalene solutions, 20: 3994
effects on surface tension of sodium, 20: 3880(R) (MSAR-65-150)
electric quadrupole and magnetic dipole transitions for isoelectronic sequence of, (T), 20: 4553
gamma reactions at 0.01 to 10 Mev, cross sections for, 20: 4996 (AWRE-O-79/65)
helium–ion reactions at 3 to 600 ev, charge transfer in, 20: 4759
neutron cross sections for, 20: 4830 (GEMP-384)
radiation effects on electric conductivity of, 20: 4949(R) (UCRL-14360, pp 85-94)
radiation effects on uptake of, by aerobic bacteria, gamma, 20: 3699
radioinduced reactions with methanol, yields of formaldehyde from, 20: 4011
radiosensitivity effects on skin, β, 20: 3727
radiosensitivity effects on T5 receptor, 20: 3787
reactions with niobium and niobium alloys at low pressures and high temperatures, 20: 5181(R) (ORNL-3029)
reactions with niobium at high temperatures, 20: 4299(R) (ORNL-2711)
reactions with niobium at low pressures at 870 to 3500°F, 20: 4324 (PWAC-460)
reactions with tantalum at 600 to 925°C, effects of nitrogen on, 20: 4333
reactions with uranium, kinetics of, 20: 4329(T) (CEA-tr-R-1868)
separation from lutetium by electrotransport, 20: 4297(R) (IS-1200(Sect.M))
separation from uranium nitride, use of carbon for, 20: 4303(R) (ORNL-3870, pp 164-70)
sorption on thorium films, surface potential from, 20: 4410
thermodynamic properties of, in liquid metal systems, 20: 4454
OXYGEN IONS
density distribution in ionosphere, (E), 20: 4760
OXYGEN ISOTOPES O-14
energy levels from carbon-12 (He-3, n) reactions at 1.3 to 5.8 Mev, 20: 4925
OXYGEN ISOTOPES O-15
energy level lifetimes, (E), 20: 4233 (AD-618676)
energy levels from carbon-13 (He-3, n) reactions at 1.3 to 5.8 Mev, 20: 4925
gamma transitions in, angular distributions and intensities of, (E), 20: 4905
OXYGEN ISOTOPES O-16
alpha elastic scattering at 28.5 Mev, optical potentials in, (E/T), 20: 4859
deuteron reactions (d,α_0), (d,p_0), and (d,p_1) at 300 to 1,000 kev, fluorine-18 energy levels from, (E), 20: 4870
gamma reactions (γ,n) at threshold to 65 Mev, cross sections for, (E), 20: 4476(R) (IS-1200(Sect.P))
gamma reactions (γ,n) with, cross sections for, (E), 20: 4833 (IS-T-43)
gamma reactions with, nitrogen-13 production in, (E), 20: 4833 (IS-T-43)
gamma transitions between even parity states in, rates for, (T), 20: 4854
helium-3 reactions at 1.9 to 6.7 Mev, bound states from, (E), 20: 4905
photodisintegration at 22 to 65 Mev, production of carbon-11 and nitrogen-13 in, (E), 20: 4476(R) (IS-1200(Sect.P))
photon reactions (γ,n) with, energy level transitions in, (E), 20: 4849(R) (UCRL-14360, pp 1-50)
triton reactions (t,α) at 1.4 to 3.4 Mev, excitation curves of, (E), 20: 4858
OXYGEN ISOTOPES O-17
alpha reactions (α,n) at 5 to 12 Mev, cross sections for, (E), 20: 4849(R) (UCRL-14360, pp 1-50)
proton reactions (p,n) at 7.0 to 13.5 Mev, (E), 20: 4849(R) (UCRL-14360,

pp 1-50)
OXYGEN ISOTOPES O-18
alpha inelastic scattering at 21.4 Mev, (E), 20: 4849(R) (UCRL-14360, pp 1-50)
alpha reactions (α,n) at 5 to 12 Mev, cross sections for, (E), 20: 4849(R) (UCRL-14360, pp 1-50)
energy levels, (E), 20: 4849(R) (UCRL-14360, pp 1-50)
energy levels of, collective, (E), 20: 4849(R) (UCRL-14360, pp 1-50)
helium-3 reactions (He-3, n) at 1.3 to 5.8 Mev, (E), 20: 4925
proton reactions (p,n) at 7.0 to 13.5 Mev, (E), 20: 4849(R) (UCRL-14360, pp 1-50)
proton reactions (p,α) with, angular distributions for, (E), 20: 4849(R) (UCRL-14360, pp 1-50)
proton reactions (p,γ) with, fluorine-19 levels from, (E), 20: 4907
proton reactions (p,n) at threshold to 3.29 Mev, 20: 4927
OXYGEN SYSTEMS
C–N–O–Pu–U, corrosion by water at 550°F, 20: 4327(R) (UNC-5138)
C–N–O–Pu–U, preparation of single-phase compositions of, 20: 4327(R) (UNC-5138)
C–O–Pu–U, preparation of single-phase compositions of, 20: 4327(R) (UNC-5138)
Nb–O, oxygen clustering in solid solutions of, 20: 4449
Nb–O–Zr, phase studies, 20: 4297(R) (IS-1200(Sect.M))
N–O, corrosive effects on INOR-8 at 1300 and 1400°F, 20: 4308(R) (ORNL-3870, pp 243-60)

P

PALLADIUM
bremsstrahlung yields from, with incorporated strontium-90–yttrium-90, 20: 5000 (ORNL-IIC-5, pp 91-8)
determination in platinum by neutron activation, 20: 3863(R) (IS-1200 (Sect. C))
radiation from promethium-147-excited, 20: 3882 (ORNL-IIC-5, pp 51-71)
PALLADIUM ALLOYS
Pd–Ag–Tb, crystallography, 20: 4391(R) (ORNL-3870, pp 75-82)
Pd–Sn, tin-119 Mössbauer spectra in, 20: 5014
Pd–U, preparation for standard foils, 20: 3982(R) (AGN-8156)
PANCREAS
radiotherapy of Zollinger-Ellison syndrome induced by tumor of, 20: 3821
PARABIOSIS
humoral mediation of radioinduced motivation of rats during, 20: 3706 (AD-623365)
PARAFFIN
neutron slowing-down age in, 20: 4813
radiation effects on dielectric properties, gamma, 20: 3989
paraffin–ZrO_2, neutron spectra in, 20: 4806(R) (RPI-328-40, pp 1-42)
PARASITES
radiation effects on larvae of *Nippostrongylus brasiliensis*, in rats, gamma, 20: 3786
PARTICLE COLLECTORS
efficiency for molecular atmospheric iodine, 20: 3673
PARTICLE TRACKS
detection and measurement of, in polymers, (E), 20: 4251 (USNRDL-TR-917)
production mechanisms in solids, ion-explosion spike, 20: 4548
PARTICLES
mixing coefficients and residence times in fluidized beds, relation between, 20: 4106 (BNL-tr-43)
properties of, from reactor accidents, 20: 4183(R) (ORNL-3843, pp 2-70)
pulmonary excretion of, effects of chronic cigarette smoking on, tracer study in dogs, 20: 3655 (BNWL-SA-224)
removal from gas stream, design of electrostatic apparatus for, 20: 4726(P)
solidification of systems of, with repulsive forces, 20: 4708(R) (UCRL-14360, pp 50-73)
PEACH BOTTOM POWER REACTOR
development, 20: 5118(R) (GA-6647)
PEBBLE BED REACTORS
criticality studies, 20: 5125 (NYO-10732)
feasibility study for, 20: 5125 (NYO-10732)
fuel development for, 20: 5125 (NYO-10732)
PENTANE, 2-METHYL-
radiation effects on luminescence of glassy, at 77°K, gamma, 20: 3990
PENTANE, 3-METHYL-
radiation effects on luminescence of glassy, at 77°K, gamma, 20: 3990
toluene radiolysis at 77°K, γ, (E), 20: 4913
PENTOBARBITAL SODIUM
effects on performance of learned response in rats, 20: 3772
PERCHLORATES
effects on spectrophotometric determination of zirconium, 20: 3695
PERCHLORIC ACID
separation of protactinium from, by solvent extraction using tributyl phosphate, 20: 4058
PERSONNEL
accidents and radiation exposure of AEC, 1943 through 1964, 20: 4188 (TID-22268)
medical examination of, 20: 4199
radiation hazards to stray radiation areas at Brookhaven, LET and quality factors in, 20: 4176 (BNL-9684)
radiation hazards to, of radon spas, thoron, 20: 3798
radiation protection standards for Russian, 20: 4198
radiation protection of, in decontamination of hot cells, 20: 4211
training for dual-cycle PWR operation, manual on, 20: 5025 (WAPD-T-1832)
transport through alpha-gamma barriers in hot cells, 20: 4042
PERTECHNETATES
use in cardiac scanning of technetium-99m-labeled, 20: 3831
PERTURBATION THEORY
atomic dipole polarizability and shielding factor calculations in, 20: 4537 (NP-15576)
atomic quadrupole polarizability and shielding factor calculations in, 20: 4538 (NP-15577)
formalism of time-dependent, 20: 4476(R) (IS-1200(Sect. P))
integral equations in, iterative methods of resolution of, (T), 20: 4764
PETROLEUM
contamination of, when using nuclear explosions for production stimulation, 20: 4082 (BM-RI-6684)
PHANTOMS
design of body equivalent, 20: 3816
energy absorption in tissue-equivalent materials, as a function of neutron energy, 20: 3708 (CEA-R-2833)
of children, 20: 3854
preparation of pregnant woman, 20: 3823
radiation dose distribution in jaw, photographic film for determining γ, 20: 4205
radiation dosimetry in head, photographic film for, 20: 3862
radiation dosimetry in tissue equivalent, using angle of incidence measurements, 20: 4207
PHARMACEUTICALS
preparation of tritium-labeled digitoxin, 20: 3810
PHARNYX
radioinduced tumors of, after radiotherapy of thyrotoxicosis, 20: 3806
PHENANTHRENE
9-phenyl-, preparation and properties of, 20: 3972 (EUR-2528.f)
1,10-PHENANTHROLINE
reactions with thorium tetrachloride, effects of ethanol, ethyl acetate, and hydrochloric acid on, 20: 3933
PHENANTHROLINE COMPLEXES
with cadmium, hydrogen, and zinc, mechanisms of, 20: 3863(R) (IS-1200 (Sect. C))
PHENOLS
content in smoke from irradiated cigarettes, 20: 3984 (ORO-633)
separation by reversed-phase chromatography, 20: 3863(R) (IS-1200 (Sect. C))
PHENOTHIAZINE, 2-CHLORO-10-(3-DIMETHYLAMINOPROPYL)–
effects on metabolism of iodine in mice, tracer study, 20: 3677
PHONONS
amplitude of microwave-induced, calculation of, 20: 4479(R) (TID-22179, pp 1-83)
detection in quartz and sapphire, bolometer for, 20: 4479(R) (TID-22179, pp 1-83)
interactions with electrons and plasmons in plasma, hamiltonian for, (T), 20: 4944 (ORNL-3871)
propagation in x-cut quartz, 20: 4479(R) (TID-22179, pp 1-83)
PHOSPHATASES
content of alkaline, in cultured cancer cells, effects of hydrocortisone on, 20: 5217 (TID-21169)
radiation effects on content of isoenzymes of, in tumors undergoing therapy, 20: 3845
PHOSPHATE GLASS
properties as radiation dosimeter, 20: 4258(P)
PHOSPHATIDES
metabolism of, analog models of, 20: 3658(R) (EUR-2414.f,i)
PHOSPHIDES
nuclear magnetic resonance in rapidly rotating, (E), 20: 4931
PHOSPHINE, TRIPHENYL-
reactions with thorium tetrachloride, effects of ethanol, ethyl acetate, and hydrochloric acid on, 20: 3933
PHOSPHINE OXIDE, TRIPHENYL-
reactions with thorium tetrachloride in ethyl acetate, 20: 3933
PHOSPHINE OXIDES
molecular weights of tertiary, determination of, 20: 3863(R) (IS-1200 (Sect. C))
PHOSPHITES
preparation and properties of carbonyl complexes of, 20: 3863(R) (IS-

1200(Sect. C))
PHOSPHONIUM CHLORIDES
density equations for molten mixtures of nickel chloride and tri-n-butyl-benzyl-, 20: 3921(R) (ORNL-3870, pp 56-60)
spectra of nickel(II) in mixtures of nickel chloride and tri-n-butyl-benzyl-, absorption, 20: 3921(R) (ORNL-3870, pp 56-60)
PHOSPHORIC ACID, BIS(2-ETHYLHEXYL) ESTERS
solvent properties for rare earths, 20: 4077(R) (IS-1200(Sect. E))
di-(2-ethylhexyl) phosphoric acid–TBP, solvent properties for neodymium nitrate, 20: 3875 (IS-T-37)
PHOSPHORIMIDIC TRICHLORIDE, METHYL-
crystal structure of dimer of, 20: 3863(R) (IS-1200(Sect. C))
PHOSPHORS
performance of plastic, in cosmic ray monitors, 20: 4560 (AD-618562)
radioinduced fluorescence of organic, in naphthalene, 20: 3994
PHOSPHORUS
radiation effects on metabolism of, in Aspergillus, 20: 3755(T)
PHOSPHORUS ISOTOPES P-32
beta decay of, cancellation effect in allowed matrix element for, (T), 20: 4873
beta transitions in, polarization from, (E), 20: 4880
determination in radioisotope mixtures, microcalorimetric, 20: 3866 (CEA-R-2630)
effects on polycythemia, therapeutic, 20: 3837
incorporation in desoxyribonucleic acid, 20: 3748
use in therapy of polycythemia, 20: 3835
use in therapy of leukemia, 20: 3835
PHOTOELECTRIC CELLS
electron counts in maser-illuminated, 20: 4479(R) (TID-22179, pp 1-83)
PHOTOGRAPHIC FILM
protection against fogging by fallout, 20: 3799
protection from fogging by fallout, 20: 3797
use for storage of pulse-height information in scintillation experiments, 20: 4253
use in determining dose distributions in phantoms, 20: 4205
PHOTOGRAPHIC FILM DETECTORS
calibration for dosimetry, 20: 4237 (BNL-9665)
design, 20: 4237 (BNL-9665)
performance as personnel monitors in synchrotron area, 20: 4237 (BNL-9665)
use in dosimetry of head phantoms, 20: 3862
PHOTOGRAPHY
method of, for scaling cloud dimensions from chemical explosives, 20: 4152 (TID-22266)
use in nondestructive testing of radioactive materials, 20: 4122
use in nondestructive testing of fuel rods, 20: 4123
use in nondestructive testing of irradiated fuel materials, 20: 4124
PHOTOMETERS
design of differential filter, for determination of water in water–water-d_2 mixtures, 20: 3970(P)
PHOTOMETRY
equipment for use in Air Force KC-135 aircraft, modification of, 20: 4234(R) (AD-619177)
method of, for heavy water quality control, 20: 3970(P)
PHOTOMULTIPLIER TUBES
calibration of, description of system for, 20: 4110(R) (ORNL-3870, pp 146-54)
pulse-height stability, 20: 4218(R) (NYO-3421-4)
pulses in, origin of dark-current, 20: 4218(R) (NYO-3421-4)
tube base for, design of, 20: 4247 (TID-21362)
PHOTONS
dosimetry of high-energy, methods for, (T), 20: 4505 (ORNL-P-1738)
effects of two-photon exchanges in positron-proton scattering, 20: 4630
energy states of, infrared divergence in quantum electrodynamics from, (T), 20: 4765
interactions with protons from threshold to 900 Mev, meson (η) production in, (E), 20: 4578 (AD-618660)
interactions with protons below 1 Bev, angular distributions and total cross sections for meson (π^-) + (π^+) production in, 20: 4579 (AD-618661)
interactions with nucleons, spin-1 meson production from, (T), 20: 4610
interactions with fermions, spin-1 boson production from, (T), 20: 4610
properties of, review of basic, 20: 4476(R) (IS-1200(Sect. P))
reactions with atoms, photon emission in, (T), 20: 4949(R) (UCRL-14360, pp 85-94)
reactions with nuclei in stellar interiors, beta decay from, (T), 20: 4530
reflection of electrons by, 20: 3863(R) (IS-1200(Sect. C))
transport calculations using Monte Carlo method, computer program for, 20: 4949(R) (UCRL-14360, pp 85-94)
PHOTOSENSITIVITY
of *E. coli*, 20: 3726
of skin, relation to uv sensitivity, 20: 3767
PHTHALIC ACID, DIOCTYL ESTER
reactions with radioiodine, 20: 4185(R) (ORNL-3843, pp 169-234)
use for reactor filter efficiency measurements, 20: 5036 (RL-SA-47)
PHYSICS
book: *Elementary Particle and High Energy Physics*, 20: 4695
book: *Lectures in Theoretical Physics*. Vol. IV., 20: 4487
research, (E/T), 20: 4474(R) (ANL-7081)
research programs at Ames Laboratory, July 1964–June 1965, 20: 5213(R) (IS-1200)
research programs at M.I.T. electronics lab., 20: 4478(R) (TID-22179)
research progress at Lawrence Radiation Laboratory, 20: 4482(R) (UCRL-14360)
series expansions in statistical mechanics, 20: 4708(R) (UCRL-14360, pp 50-73)
PHYSIOLOGY
of nutrition, tracer studies, 20: 3685
PIPES
defects in, ultrasonic method for detecting, 20: 5227(P)
heat flux dryout in steam-water mixtures in internally heated annuli, 20: 4099 (AECL-2332)
pressure distributions in liquid sodium, 20: 4100 (BW-67-2(a))
PITUITARY GLAND
radiation effects on, physiological, effects of hibernation on, 20: 3703
radioinduced ablation of, heavy particle, 20: 3828
radioinduced ablation of, 20: 3809
PITUITARY HORMONES
content of thyrotropin in blood plasma, radioimmunoassay method of measurement, 20: 3829
effects of thyrotropin on iodine transfer from plasma to milk, 20: 3674
physiological effects of, 20: 3809
radiation effects on blood content of growth, heavy particle, 20: 3828
PLACENTA
radiographic localization of, 20: 3825
PLANETS
exploration of, development of equipment and methods for, 20: 4525
PLANT CELLS
nucleic acid content of spinach chloroplasts, 20: 3649 (UCRL-11475)
radiation effects on, review of, 20: 4464
radiation effects on cyclosis in Nitella, recovery from x, 20: 3698
radiation effects on *Allium cepa* root, x, 20: 3764
PLANTS
analysis for cobalt, copper, iron, manganese, potassium, and zinc by neutron activation methods, 20: 3901
cesium-137 metabolism by forage, effects of soil type and fertilizers on, 20: 3665(T) (CEA-tr-X-619)
compatibility with spacecraft materials, 20: 4312
composition and structure of Fraction I protein from Chinese cabbage leaves, 20: 5219 (TID-22372)
growth of, effects of wavelength of light on, 20: 3769
radiation effects on, genetic, 20: 3710(R) (EUR-2493.e)
radioactivity of, near Cluj, Rumania, 20: 3654
radioinduced mutations of *Funaria hygrometrica*, x, 20: 3781
strontium-90 metabolism by forage, effects of soil type and fertilizers on, 20: 3665(T) (CEA-tr-X-619)
uptake of strontium-90 by agricultural, effects of species, soil type, and agronomy practices on, 20: 3679
PLASMA
acceleration of high-current steady-state coaxial arc, model for, 20: 4139
atom electron and concentrations in afterglow, · 20: 4970
boundary dynamics, 20: 4948(R) (TID-22179, pp 85-175)
bremsstrahlung emission from thermal, with suprathermal electrons, (T), 20: 4982
collision frequency and electron density of, method for measuring, 20: 4955
compression by explosively produced magnetic fields, (E), 20: 4941 (LA-DC-7290)
containment in helical magnetic field, apparatus for stable, · 20: 4995(P)
containment in Stellarator C, loss rates from heating in, (E), 20: 4942 (MATT-372)
current generation in, velocity-dependent collision frequency for third harmonic, (T), 20: 4885
decay of rotating, free-wheeling, (E), · 20: 4953
density of cylindrical column of, microwave measurement of, (T), · 20: 4971
density waves in low-pressure cylindrical discharge, (T), · 20: 4972
diagnostics of contact ionization cesium, electric probe methods for, (E), · 20: 4958
diagnostics of high-pressure, theory of double probe for, · 20: 4968
diagnostics of, infrared maser technique for, · 20: 4992
diffusion in low-pressure arc discharges, magnetic effects on, 20: 4479(R) (TID-22179, pp 1-83)
ejection of pinched argon, from axial orifice, 20: 4138
electric conductivity of, Ohm's law for, (T), · 20: 4960
electric conductivity of partially ionized, collision-dominated, impedance formula for, (T), · 20: 4975

electric discharges in pulsed accelerators for, propellant triggered, 20: 4136
electromagnetic wave propagation in homogeneous, Lorentzian, nonlinear effects in, (T), 20: 4962
electromagnetic wave propagation in hot magneto-, Boltzmann-Vlasov equation for, (T), 20: 4978
electromagnetic-wave propagation along column of, dipolar, (E/T), 20: 4956
electron beam interactions with warm, (T), 20: 4947 (SU-IPR-13)
electron beam interactions with, computer study of, 20: 4948(R) (TID-22179, pp 85-175)
electron beam interactions with, (E), 20: 4945 (ORNL-TM-1306)
electron beam, interactions with, long-wave eletron oscillations in, (E), 20: 4940 (IAE-932)
electron cyclotron resonance discharge mechanisms of, 20: 4948(R) (TID-22179, pp 85-175)
electron cyclotron resonances in, noise and correlation studies of, 20: 4991
electron density in, laser interferometer measurement of, 20: 4948(R) (TID-22179, pp 85-175)
electron density in, method for determining, (E/T), 20: 4967
electron distribution function for homogeneous Lorentzian, successive approximation method for, (T), 20: 4961
electron interactions with magnetically confined, relativistic, (T), 20: 4950(T) (UCRL-Trans-1261(L))
flow in, magnetogasdynamics for, (T), 20: 4702 (AD-619094)
flute modes and rotation reversal in weakly ionized, 20: 4948(R) (TID-22179, pp 85-175)
heating of discharge, effect of helical magnetic field on ohmic, (E), 20: 4937 (IAE-907)
hydromagnetic equations for Vlasov, finite gyro-radius corrections to, (T), 20: 4979
injection into confining device, device for, 20: 4993(P)
ion beam reactions with, noble gas, (E), 20: 4945 (ORNL-TM-1306)
ion cyclotron wave absorption and propagation in bounded deuterium, numerical model for, (T), 20: 4983
ion cyclotron wave production in deuterium-hydrogen, optimum, (E/T), 20: 4984
ion reactions in, classical collision integrals for Coulomb potential for, (T), 20: 4988
kinetic theory for homogeneous unstable, 20: 4963
kinetics of completely ionized, Bogoliubov hypothesis generalization for, (T), 20: 4957
magnetoacoustic wave front structure in rarefied, (E), 20: 4938 (IAE-909)
magnetoacoustic wave excitation and absorption in, (E), 20: 4939 (IAE-911)
microwave absorption in hot, analysis of, (E/T), 20: 4943 (MATT-379)
microwave resonance in argon, surface, (E), 20: 4935 (AFCRL-65-556)
oscillations in contact-ionization cesium, amplitude and frequency of, (E), 20: 4965
oscillations in columns of, electromagnetic field retardation effects on, (T), 20: 4985
oscillations in hot electron, longitudinal nonlinear, (T), 20: 4986
oscillations in unbounded one-dimensional nonuniform, longitudinal, (T), 20: 4980
particle correlations during equilibrium, (T), 20: 4959
plasmon interactions with electrons, phonons, and plasmons in, hamiltonian for, (T), 20: 4944 (ORNL-3871)
probe characteristics in h-f discharge, method for measuring, (E), 20: 4969
production of completely ionized rotating, (E), 20: 4951
production of magnetically confined hot dense, device and method for, 20: 4994(P)
production of rotating, momentum balance in, (T), 20: 4952
production system designs, 20: 4948(R) (TID-22179, pp 85-175)
properties of h-f, research on, 20: 4936(R) (ANL-7081, pp 130-3)
radio wave reflection and transmission coefficients for nonlinear, (T), 20: 4954
recombination of rare gas, 20: 4479(R) (TID-22179, pp 1-83)
scattering of light from, incoherent, 20: 4948(R) (TID-22179, pp 85-175)
Schroedinger equation with complete screened Coulomb potential, 20: 4949(R) (UCRL-14360, pp 85-94)
sheath transition in, electric current dependence of, (T), 20: 4976
shock structure in magnetized hydrogen, collisionless, (E), 20: 4977
shock waves in, microwave diagnostics of, 20: 4934 (AD-619093)
sound wave amplification and production in, 20: 4479(R) (TID-22179, pp 1-83)
spectra of hydrogen, continuum, (E), 20: 4973
spectral lines of helium, effects of absorption on, 20: 4974
stability of infinite uniform mirror-confined, (T), 20: 4981
stability of, classification from dispersion relations, 20: 4987
stability of, interaction hamiltonians for, (T), 20: 4944 (ORNL-3871)
statistical mechanics of hot, equilibrium quantum, (T), 20: 4949(R) (UCRL-14360, pp 85-94)
striations in, properties of, 20: 4946 (ORNL-TM-1307)
thermal conductivity of fully and partially ionized, total, (T), 20: 4990
wave equations for inhomogeneous, Bogolyubov adiabatic hypothesis for, 20: 4966
waves in nongyrotropic, growing, (T), 20: 4989

PLASMA JETS
acceleration mechanism of coaxial arc, model for, 20: 4139
design and performance of semitoroidal reflex discharge, 20: 4134 (SEL-63-120)
development of arc-spray, for coating deposition, 20: 4298 (LA-DC-7275)
development of torch-type, 20: 4184(R) (ORNL-3843, pp 71-135)
ejection of pinched argon, from axial orifice, 20: 4138
electric discharges in pulsed, propellant triggered, 20: 4136
use of hydrogen, in preparation of niobium or tantalum metals, 20: 4314(P)

PLASTICS
development for use in space vehicles, 20: 4312
mechanical properties for shock pulse generation on impact shock machines, 20: 4112 (SC-TM-65-443)
properties of, effects of low temperature on, 20: 4417

PLATINUM
analysis for cobalt, iridium, palladium, and silver by neutron activation, 20: 3863(R) (IS-1200(Sect. C))
gamma elastic scattering at 1.12 Mev, cross sections for, (T), 20: 4864
thermal conductivity at 300 to 1300°K, (E), 20: 4476(R) (IS-1200(Sect.P))

PLATINUM ALLOYS
Ir–Pt, corrosion by cesium at 400°C, 20: 4337

PLATINUM COMPLEXES
with chloroamines, replacement of chloride ligands in, 20: 3863(R) (IS-1200(Sect. C))

PLATINUM ISOTOPES Pt-194
carbon-12 reactions (C-12,xn) at 90 Mev, polonium production cross sections in, (E), 20: 4860
energy levels of, coincidence measurement of conversion coefficients for, 20: 4843 (NP-15456)

PLATINUM ISOTOPES Pt-195
carbon-12 reactions (C-12,xn) at 90 Mev, polonium production cross sections in, (E), 20: 4860

PLATINUM ISOTOPES Pt-196
carbon-12 reactions (C-12,xn) at 90 Mev, polonium production cross sections in, (E), 20: 4860

PLOWSHARE PROJECT
book: *The Peaceful Applications of Nuclear Explosions; A Report on the Plowshare Program*, 20: 4085
crater formation by single-, double-, and triple-row charges, comparison of, 20: 4083 (SC-RR-65-478)
geology and surface effects of instrument holes in Handcar, 20: 4144 (PNE-810F)

PLUTONIUM
analysis for impurities, comparison of spectrographic methods for, 20: 3869 (CEA-R-2869)
crystal structure preferred orientation in alpha-, 20: 4407
determination by autoradiography and scintillation counting, comparison of, 20: 3877 (LA-DC-7483)
diffusion of gases from stored, solid residues of, vacuum-drying effects on, 20: 4364 (AERE-M-1644)
gamma reactions at 0.01 to 10 Mev, cross sections for, 20: 4996 (AWRE-O-79/65)
handling of irradiated, design of hot laboratories for, 20: 4213
neutron scattering by, p-wave phase shifts in small-angle, (T), 20: 4909
separation from impurities by solvent extraction using tridodecylamine, 20: 3868 (CEA-R-2860)
separation from irradiated fuels, 20: 4073(P)
separation from organic solutions by solvent extraction using trilaurylamine, 20: 4048(R) (NP-15406)
separation from spent fuels by solvent extraction, flowsheets for, 20: 4048(R) (NP-15406)
transformation temperature of delta-phase, effects of aluminum, gallium, and uniaxial compression on, 20: 4434

PLUTONIUM ALLOYS
diffusion of gases from stored, solid residues of, vacuum-drying effects on, 20: 4364 (AERE-M-1644)
Ce–Pu, transformation temperature of, effects of uniaxial compression on delta, 20: 4434
Ga–Pu, analysis for gallium by spectrophotometry, 20: 3881 (NBL-228)

PLUTONIUM COMPOUNDS
analysis for impurities, comparison of spectrographic methods for, 20: 3869 (CEA-R-2869)

PLUTONIUM(IV) FLUORIDES
preparation by plutonia hydrofluorination, 20: 4046(R) (EURAEC-1340)
reactions with oxygen and steam, pyrohydrolytic, 20: 4046(R) (EURAEC-1340)

PLUTONIUM ISOTOPES Pu-238
spectra of, alpha, 20: 3879(R) (MLM-1266)

PLUTONIUM ISOTOPES Pu-239
determination in mixture with plutonium-240, microcalorimetric, 20: 3866 (CEA-R-2630)
neutron scattering by, resonance, (E), 20: 4849(R) (UCRL-14360, pp 1-50)
spectra of, alpha, 20: 3879(R) (MLM-1266)

PLUTONIUM ISOTOPES Pu-240
determination in mixture with plutonium-239, microcalorimetric, 20: 3866 (CEA-R-2630)

PLUTONIUM ISOTOPES Pu-242
separation from transplutonium elements, design of hot cells for, 20: 4065

PLUTONIUM(IV) OXIDES
magnetic properties, (E), 20: 4849(R) (UCRL-14360, pp 1-50)
preparation and properties of carbon-coated sol-gel microspheres of, 20: 4344 (ORNL-P-1725)
preparation using depleted oxygen, method for, 20: 3879(R) (MLM-1266)
purification methods for, 20: 4046(R) (EURAEC-1340)
radiation effects on carbon-coated sol-gel microspheres of, 20: 4344 (ORNL-P-1725)
PuO_2–stainless steel, performance as fast-reactor driver fuel, (E), 20: 5192 (BNWL-SA-251)
PuO_2–stainless steel–UO_2, radiation effects on, in-pile, (E), 20: 5192 (BNWL-SA-251)
PuO_2–stainless steel, radiation effects on, in-pile, (E), 20: 5192 (BNWL-SA-251)
PuO_2–ThO_2, preparation and properties of carbon-coated sol-gel microspheres of, 20: 4344 (ORNL-P-1725)
PuO_2–ThO_2, radiation effects on carbon-coated sol-gel microspheres of, 20: 4344 (ORNL-P-1725)
PuO_2–UO_2, fabrication of fuel elements of, economics of, 20: 4339 (BNWL-131D)
PuO_2–UO_2, fluorination and hydrofluorination using chlorine trifluoride, 20: 4046(R) (EURAEC-1340)
PuO_2–UO_2, radiation effects on, in-pile, (E), 20: 5192 (BNWL-SA-251)
PuO_2–UO_2, reactivity sodium void effects on, in fast reactors, 20: 5068
PuO_2–UO_2–ZrO_2, properties for use in thermal reactors, 20: 4382(R) (NUMEC-3505-8)

PLUTONIUM RECYCLE TEST REACTOR
fuel element fabrication for, variable costs for, 20: 4339 (BNWL-131D)
radiation monitoring of, 20: 5195 (HW-68082)

PLUTONIUM SYSTEMS
diffusion of gases from stored, solid residues of, vacuum-drying effects on, 20: 4364 (AERE-M-1644)
C–N–O–Pu–U, corrosion by water at 550°F, 20: 4327(R) (UNC-5138)
C–N–O–Pu–U, preparation of single-phase compositions of, 20: 4327(R) (UNC-5138)
C–N–O–Pu–U, preparation of single-phase compositions of, 20: 4327(R) (UNC-5138)
C–O–Pu–U, preparation of single-phase compositions of, 20: 4327(R) (UNC-5138)

POLONIUM ISOTOPES Po-199
production in platinum (C-12,xn) reactions at 90 Mev, cross sections for, (E), 20: 4860

POLONIUM ISOTOPES Po-200
production in platinum (C-12,xn) reactions at 90 Mev, cross sections for, (E), 20: 4860

POLONIUM ISOTOPES Po-201
production in platinum (C-12,xn) reactions at 90 Mev, cross sections for, (E), 20: 4860

POLONIUM ISOTOPES Po-202
production in platinum (C-12,xn) reactions at 90 Mev, cross sections for, (E), 20: 4860

POLONIUM ISOTOPES Po-208
spectra of, alpha, 20: 3879(R) (MLM-1266)

POLONIUM ISOTOPES Po-209
decay and half life of, 20: 3879(R) (MLM-1266)
determination in lead-205, counting systems for, 20: 3879(R) (MLM-1266)
spectra of, alpha, 20: 3879(R) (MLM-1266)

POLONIUM ISOTOPES Po-210
determination in process solutions by ion exchange and gamma counting, 20: 3879(R) (MLM-1266)

POLYCYTHEMIA
radiotherapy of, efficiency of phosphorus-32 β, 20: 3837
radiotherapy of, using phosphorus-32, 20: 3835
therapy of, using cytotoxic drugs, 20: 3835

POLYMERS
book: *Polymer Coatings in Atomic Techniques*, 20: 3979
charged particle track analysis in, methods for, (E), 20: 4251 (USNRDL-TR-917)
development for use in space vehicles, 20: 4312
radiation effects on electric conductivity and polarization, 20: 4030
radiation effects on, in aqueous solutions and solid state, 20: 4033
radiation effects on crystals of organic, at 75 to 300 kev, 20: 3987
radiation effects on, review of, 20: 4464
radioinduced grafting of, in textile production, 20: 4031

POLYOXYMETHYLENES
radioinduced formation of crystalline fibriller, 20: 4033

POLYPHENYLS
alkyl, preparation and properties of, 20: 3973 (EUR-2528.f)
radiation stability of para-, electron, (T), 20: 3991

POPULATIONS
behavior of, during nuclear attack, 20: 4200
radiation burden in German, 1965, 20: 4164
radiation control of Mexican fruit fly, effects of dose on gamma, 20: 3745
radiation dose from dental radiography of Japanese, 20: 4195
tumor incidence in, of areas underlain with uraniferous rock, 20: 4193

PORPHYRIES
thorium and uranium content of, Saar-Nahe basin, Germany, 20: 4165

PORTUGAL
leukemia incidence in, 20: 3753
uranium ore processing in, 20: 4047

POSITRON BEAMS
stability in accelerator storage rings, transverse resistive, (T), 20: 4500 (LNF-65/27)

POSITRONS
annihilation in holmium single crystals, (E/T), 20: 4476(R) (IS-1200 (Sect.P))
interactions with electrons first Born approximation including anapole for, (T), 20: 4612
interactions with protons, two-photon effects in elastic, 20: 4630

POTASSIUM
analysis for oxygen, gettering-vacuum fusion method for, 20: 4321(R) (ORNL-3870, pp 136-9)
content in oceanic theoleitic basalts, 20: 4145
corrosive effects on Haynes 15 alloy, Inconel, and 316 stainless steel, effects on mechanical properties, 20: 5181(R) (ORNL-3029)
corrosive effects on D-43, T-111, TZM, and niobium–1 zirconium alloys, 20: 4301(R) (ORNL-3870, pp 102-35)
corrosive effects on Haynes 25 alloy, Inconel, and type 316 stainless steel at 870°C, 20: 4307(R) (ORNL-3870, pp 238-42)
corrosive effects on niobium at 200, 600, and 815°C, effects of oxygen on, 20: 4321(R) (ORNL-3870, pp 136-9)
determination by flame photometry, 20: 4053
determination in plants by neutron activation methods, 20: 3901
heat transfer by boiling, system for studying, 20: 5181(R) (ORNL-3029)
separation from other metal chlorides by ion exchange, 20: 4053

POTASSIUM ACETATES
complexes with cyclohexaamylose, crystal structure of, 20: 3863(R) (IS-1200(Sect. C))

POTASSIUM ALLOYS
K–Na, corrosive effects on niobium and niobium–zirconium alloy, 20: 5181(R) (ORNL-3029)
K–Na, corrosive effects on stainless steel and other structural materials, review on, 20: 4318 (CNLM-5359)
K–Na, corrosive effects on Croloy 9M, INOR-8, and type 347 stainless steel, 20: 4322(R) (ORNL-3870, pp 305-7)
K–Na, corrosive effects on niobium–1 zirconium and type 316 stainless steel, 20: 4323(R) (ORNL-3870, pp 308-11)

POTASSIUM BROMIDES
phase transitions in, shock-induced, 20: 4708(R) (UCRL-14360, pp 50-73)
thermodynamics of, in anhydrous *N,N*-dimethylformamide at 25°C, 20: 3926 (TID-22374)
$NiBr_2$–KBr, spectra of nickel(II) in melts of, absorption, 20: 3921(R) (ORNL-3870, pp 56-60)

POTASSIUM CARBONATES
analysis for europium and terbium, fluorometric, 20: 3863(R) (IS-1200 (Sect. C))

POTASSIUM CHLORIDES
diffusion of rare gases in, 20: 3944
thermodynamic properties in *N,N*-dimethylformamide and *N*-methylformamide solutions, 20: 3924 (TID-22366)
thermodynamic properties in anhydrous *N*-methylformamide solutions, 20: 3925 (TID-22366, App. B)
thermodynamics of, in anhydrous *N*-methylformamide at 25°C, 20: 3926 (TID-22374)
LiCl–KCl, cadmium, cerium, cobalt, neptunium, uranium, and zinc distribution between γ-alumina and molten, 20: 3959
LiCl–KCl–$ZnCl_2$, oxidizing effects of liquid, on thorium, 20: 4297(R) (IS-1200(Sect.M))
LiCl–KCl–$ZnCl_2$, reactions with uranium carbide at 540 to 800°C, 20: 4297(R) (IS-1200(Sect.M))
LiCl–KCl, reactions of eutectic, with uranium hexafluoride, 20: 4046(R) (EURAEC-1340)

LiCl–KCl, spectra of bismuth, lead, and thallium ions in eutectic of, absorption, 20: 3921(R) (ORNL-3870, pp 56-60)
$MgCl_2$–KCl–NaCl, separation from rare earth fission products by solvent extraction using magnesium alloys, 20: 3865 (ANL-7064)
$MgCl_2$–LiCl–KCl, solvent properties of liquid, for rare earths, 20: 4297(R) (IS-1200(Sect.M))
$NiCl_2$–KCl, spectra of nickel(II) in melts of, absorption, 20: 3921(R) (ORNL-3870, pp 56-60)

POTASSIUM FLUORIDES
properties of molten, for use as reactor fuels, 20: 4376 (JUL-268-RG)
UF_4–KCl–LiCl, electrolysis of fused, for production of high-purity uranium, 20: 4347

POTASSIUM IODATES
radiolysis of, recoil processes from gamma, 20: 3863(R) (IS-1200 (Sect. C))

POTASSIUM ISOTOPES K-40
activity of, calibration of, 20: 4916
decay of, branching ratio and half life for, (E), 20: 4919

POTASSIUM ISOTOPES K-41
alpha reactions (α,n) at 7.5 to 12.5 Mev, isomeric cross section ratios for, 20: 4922

POTASSIUM ISOTOPES K-42
beta decay of, matrix elements of $(2^-) \rightarrow (2^+)$, (T), 20: 4863

POTASSIUM MAGNESIUM FLUORIDES
spectra of crystalline, reflection, 20: 4479(R) (TID-22179, pp 1-83)

POTASSIUM NICKEL FLUORIDES
spectra of crystalline, reflection, 20: 4479(R) (TID-22179, pp 1-83)

POTASSIUM OXIDES
magnetic properties, (E), 20: 4849(R) (UCRL-14360, pp 1-50)

POTASSIUM PLATINUM CHLORIDES
spectra of, absorption, 20: 3863(R) (IS-1200(Sect. C))

POTASSIUM SODIUM TARTRATES
radiation effects on coercive magnetic field of, 20: 3995

POTATOES
radiation effects on virus infections on leaves of, γ, 20: 3768

POWDERS
diffusion of fission gases from, theory for, 20: 4432

POWER CYCLES
performance of Brayton, Rankine, and Stirling, for radioisotope-powered submersibles, 20: 4276 (AGN-8128)

POWER PLANTS
design studies of space, 20: 4299(R) (ORNL-2711)

POWER REACTORS
conference, 20: 5154
conference on, 20: 5161
containment overpressure discharge system dimensioning for PRO, 20: 5145
control systems for, economic aspects of, 20: 5140
design for fissiochemical plants, 20: 3982(R) (AGN-8156)
design of DON prototype, 20: 5162
development, 20: 5167
development and economics of, 20: 5168
development and research in U. S., 20: 5151
development in U. K., 20: 5155
development of advanced gas-cooled, 20: 5164
development of beryllia-moderated, (E), 20: 5115(R) (GA-4967)
development of fast, 20: 5165
development of Spanish Magnox, economic, 20: 5160
development of TARGET 1000-Mw(e) gas-cooled high-temperature, 20: 5117(R) (GA-5866)
development of, conference on, 20: 5166
economic evaluation of gas-cooled, for Spain, 20: 5159
fuel development for, review of, 20: 4313
fuel element testing for fast, FARET reference core design for, 20: 5190 (ANL-7106)
fuel rupture in, location using gamma spectrometers, 20: 5109 (AECL-2360)
instrumentation and measurement techniques for, development of, 20: 5141
operation of dual-cycle pressurized-water, training course for, 20: 5025 (WAPD-T-1832)
research programs in United Kingdom, 20: 5152
safety analysis for large gas-cooled fast, 20: 5119 (GA-6732)

PRASEODYMIUM
determination in hydrochloric acid or methanol–nitric acid media, spectrophotometric, 20: 3888 (TID-22402)
solvent partition between magnesium alloys and magnesium–potassium–sodium chloride salt mixture, 20: 3865 (ANL-7064)

PRASEODYMIUM ALLOYS
Pr–Sn, magnetic properties of, at 2 to 300°K, 20: 4423
Pr–Sn, tin-119 magnetic hyperfine in, (E/T), 20: 4476(R) (IS-1200 (Sect.P))

PRASEODYMIUM CHLORIDES
heat of dilution of aqueous, at 25°C, 20: 3956

PRASEODYMIUM ISOTOPES Pr-141
gamma reactions (γ,n) at threshold to 65 Mev, cross sections for, (E), 20: 4476(R) (IS-1200(Sect.P))

PRASEODYMIUM ISOTOPES Pr-144
energy levels, (E), 20: 4476(R) (IS-1200(Sect.P))
separation from waste solutions using manganese dioxide, 20: 5206

PRASEODYMIUM NITRATES
separation from neodymium nitrate by solvent extraction using di-(2-ethylhexyl) phosphoric acid and TBP, 20: 3875 (IS-T-37)

PRASEODYMIUM OXIDES
preparation of microspheres of, by sol-gel process, 20: 4344 (ORNL-P-1725)
Fe_2O_3–Pr_2O_3, crystal structure and magnetic properties, 20: 4411

PRASEODYMIUM SULFIDES
homogeneity regions in, 20: 3938

PREGNANCY
radiation dose to fetus from diagnostic radiography during, 20: 3823
radiation hazards from diagnostic radiography during, 20: 3858
radiation hazards from radiography during, 20: 3747
radiographic localization of placenta during, 20: 3825

PRESSURE
effects on magnetic properties of nickel ferrite, 20: 4708(R) (UCRL-14360, pp 50-73)
measurements in nuclear explosion cavities, 20: 4084 (VUF-3017)

PRESSURE GAGES
containers for quartz crystal transducers, development of, 20: 4224 (UCRL-14448)
design of semiconductor transducers, analysis for, 20: 5216 (SC-TM-65-457)
use in nuclear explosions, feasibility of, 20: 4084 (VUF-3017)

PRESSURE TRANSMITTERS
testing for use at high temperatures, 20: 4999(R) (ORNL-2599)

PRESSURE VESSELS
closure design for liquid density autoclave, thermally compensated, 20: 4087 (ORNL-TM-1293)
development of prestressed concrete, for gas-cooled high-temperature reactor, 20: 5117(R) (GA-5866)
evaluation of concrete, 20: 4406(T) (ORNL-tr-873)
failure of welded HT70 Steel properties, 20: 4446
response to reactor accidents, 20: 5034 (NOLTR-63-140)
shock wave effects on reactor, (E), 20: 5023(R) (IITRI-578P21-15)
stress analysis of, computer program for, 20: 5033 (GA-6588)

PRESSURIZED WATER REACTORS
containment systems for, pressure-suppression, 20: 5146
control rods of, releasable coupling design for, 20: 5051(P)
coolant loss accidents in, core damage prevention in, 20: 5030 (AHSB(S)R-8s)
design using pressurized and boiling water, 20: 5172(P)
economic and nuclear analyses of NERO, 20: 5176 (EUR-2468.e)
operation of dual-cycle power, training course for, 20: 5025 (WAPD-T-1832)
pressurizer design for, 20: 5039(P)
shielding measurements for heavy water, 20: 4800 (AE-198)

PRINCETON SYNCHROTRON
drift tube system of, component manual for, (E), 20: 4507 (PPAD-2137-560)
radiation doses from, during beam-on and beam-off conditions, 20: 4506 (PPAD-569E)

PROMETHIUM ISOTOPES Pm-147
beta transitions in, polarization from, (E), 20: 4880
gamma dose rates from 1-w heat source of, 20: 4279 (ORNL-TM-1177)
properties for use in imaging readout and radiography, 20: 3801 (ORNL-IIC-5, pp 222-38)
properties in x-ray source excitation, 20: 3882 (ORNL-IIC-5, pp 51-71)
properties in x-ray source excitation, 20: 3883 (ORNL-IIC-5, pp 154-81)

1,3-PROPANEDIONE, 1,3-DIPHENYL-
crystal structure, 20: 3863(R) (IS-1200(Sect. C))

PROPELLANTS
feasibility of antiproton annihilation reactions for rocket, (T), 20: 4137

PROPENE
effects on radiolysis of ammonia, 20: 4021
radioinduced polymerization with carbon monoxide, 20: 3997

PROPENE, 2-METHYL-
radioinduced polymerization with carbon monoxide, 20: 3997

PROPENE POLYMERS
mechanical properties for shock pulse generation on impact shock machines, 20: 4112 (SC-TM-65-443)
radioinduced proton polarization in, neutron, (E), 20: 4037

PROPIONAMIDE
yields in reaction of recoil carbon atoms with acetamide, 20: 4026

PROPULSION
electric system for, design of radioisotope, 20: 4140(P)

electric, design and performance of charged colloid generating system for, 20: 4133 (N64-25007)
electric, performance of tungsten ionizers for, 20: 4135
plasma accelerators for, performance of semitoroidal, (T), 20: 4134 (SEL-63-120)
PROTACTINIUM
separation from nitric acid by solvent extraction using tributyl phosphate, 20: 4057
separation of protactinium from, by solvent extraction using tributyl phosphate, 20: 4058
PROTACTINIUM IONS
spin-lattice relaxation of tetravalent, in cubic crystals, 20: 5020
PROTACTINIUM ISOTOPES Pa-231
spectra of, alpha, 20: 3879(R) (MLM-1266)
PROTEINS
binding of calcium-47 and strontium-85 by blood serum, 20: 3697
composition and structure of Fraction I, from Chinese cabbage leaves, 20: 5219 (TID-22372)
metabolism of, analog models of, 20: 3658(R) (EUR-2414.f,i)
radiation effects on synthesis of, in *E. coli*, uv, 20: 3726
PROTON BEAMS
effects on enzyme levels in monkey blood, 20: 3692
production up to 800 Mev, linac development for, (E), 20: 4498(R) (LA-3419)
separation from antiproton beams in JINR synchrocyclotron, 20: 4496 (JINR-P-2375)
PROTON SOURCES
design and performance of, for Saclay cyclotron, 20: 4516
PROTONS
dosimetry of high-energy, methods for, (T), 20: 4505 (ORNL-P-1738)
effects on carbon disulfide, 20: 4028
evaporation from excited nuclei, spectra of, (T), 20: 4897
interactions with antiprotons at 2.7 Bev/c, final states of products from, (E), 20: 4476(R) (IS-1200(Sect.P))
interactions with mesons (K^-) at 5.0 Bev/c, (E), 20: 4476(R) (IS-1200(Sect.P))
interactions with mesons (K^-) at 2.00 Bev/c, charge exchange in, (E), 20: 4476(R) (IS-1200(Sect.P))
interactions with antineutrinos and neutrinos, production of (3,3) resonance by, (T), 20: 4476(R) (IS-1200(Sect.P))
interactions with protons at 2.40 and 2.85 Bev, meson (K^+) production in, (E), 20: 4586 (TID-22315)
interactions with protons at 328 to 736 Mev, polarization parameter for, (E), 20: 4588 (UCRL-11565)
interactions with mesons (π^-) at 1.5 to 4.2 Bev/c, analysis of strangeness +1 baryon in, 20: 4589 (UCRL-11754)
interactions with protons at 300 to 700 Mev, polarization parameters of, (E), 20: 4590 (UCRL-11926)
interactions with neutrons at 300 to 700 Mev, polarization parameters of, (E), 20: 4590 (UCRL-11926)
interactions with electrons and mesons (μ) at 700 to 1100 Mev/c, cross sections for, (E/T), 20: 4591 (UR-875-108)
interactions with mesons (π^-) at 2.16 Bev, 1920-Mev resonance in, (T), 20: 4849(R) (UCRL-14360, pp 1-50)
interactions with electrons, mesons, and nucleons, polarized hydrogen target for, 20: 4637
interactions with magnetospheric electromagnetic waves, gyroresonance radiation from, (T), 20: 4747
interactions with photons at threshold to 900 Mev, meson (η) production in, (E), 20: 4578 (AD-618660)
interactions with electrons, cross sections for inelastic, (E), 20: 4581 (AD-618663)
interactions with deuterons at 155 Mev, polarization in elastic, (E), 20: 4595
interactions with neutrons, Schroedinger equation with tensor forces for, (T), 20: 4597
interactions with protons, M(12) predictions for, (T), 20: 4599
interactions with mesons (π^-) and (π^+) at 10 Bev, forward dispersion relations for, (T), 20: 4602
interactions with protons, forward amplitude for, (T), 20: 4603
interactions with mesons ($\pi^\pm$), forward amplitude for, (T), 20: 4603
interactions with antiprotons, forward amplitude for, (T), 20: 4603
interactions with mesons (π^-), Regge poles in optical model for charge-exchange, 20: 4606
interactions with antiprotons at 3.7 Bev/c, antihyperon production from, 20: 4608
interactions with protons, helicity amplitudes for $\frac{3}{2}^+$ and $\frac{1}{2}^+$ isobar production in, (T), 20: 4613
interactions with gamma rays below 500 Mev, recoil proton polarization from, (T), 20: 4627
interactions with gamma rays below 500 Mev, recoil-proton polarization from polarized, (T), 20: 4628
interactions with electrons and positrons, two-photon effects in elastic, 20: 4630
interactions with deuterons at 31 Mev, cross sections for, 20: 4929
interactions with photons below 1 Bev, angular distributions and total cross sections for meson (π^-) + (π^+) production in, (E), 20: 4579 (AD-618661)
interactions with mesons (π^-) at 4 Bev/c, meson (π^0) production in, (E), 20: 4582 (JINR-P-2361)
motion of geomagnetically trapped, average atmosphere traversed in, (T) 20: 4748
polarization in cerium-doped lanthanum magnesium nitrate crystals, dynamic, (E), 20: 5021
polarization table for resonances in cyclotrons, 20: 4520
radioinduced polarization in polymers, neutron, (E), 20: 4037
reactions (p,α) with nitrogen-15 and oxygen-18, angular distributions for, (E), 20: 4849(R) (UCRL-14360, pp 1-50)
reactions (p,d) with cobalt-59 and vanadium-51, at 22 Mev energy levels from, (E), 20: 4899
reactions (p,γ) on nitrogen-14 at 0.97 to 1.96 Mev, performance of anti-coincidence shielded gamma spectrometer for detecting, 20: 4233 (AD-618676)
reactions (p,γ) with oxygen-18, fluorine-19 levels from, (E), 20: 4907
reactions (p,n) with oxygen-17 and oxygen-18 at 7.0 to 13.5 Mev, (E), 20: 4849(R) (UCRL-14360, pp 1-50)
reactions (p,n) with magnesium-25 and magnesium-26 at 8.0 to 14 Mev, (E/T), 20: 4849(R) (UCRL-14360, pp 1-50)
reactions (p,n) with samarium-144 at 10 Mev, europium-144 production from, (E), 20: 4887
reactions (p,n) with nuclei with $70 \leq A \leq 165$, Coulomb displacement energies from, 20: 4849(R) (UCRL-14360, pp 1-50)
reactions (p,n) with oxygen-18 at threshold to 3.29 Mev, 20: 4927
reactions (p,pα) with lanthanum-139 at 30 to 155 Mev, alpha cluster structure in, (T), 20: 4886
reactions (p,pn) with carbon-12 and nickel-58 at 450 Mev, differential recoil from, (T), 20: 4893
reactions (p,p) with molybdenum-92 and Zirconium-90, fine structure near isobaric analog resonances in, 20: 4923
reactions (p,2n), (p,pα), and (p,2p) with excited nuclei, cross sections for, (T), 20: 4897
reactions in iron and iron-water systems at 170 to 660 Mev, neutron production in, (T), 20: 4998 (JINR-P-2359)
reactions with helium at 50–150 kev, electron angular and energy distributions from, (T), 20: 4558
reactions with nuclei, cross sections and level studies from, 20: 4822(R) (ANL-7081, pp 22-35)
reactions with nuclei, angular momentum transfer, cross sections, and level studies from, 20: 4823(R) (ANL-7081, pp 36-69)
scattering by deuterium at 31 Mev, differential cross sections for, 20: 4929
scattering by nuclei at 160 Mev, differential cross sections for elastic, (E/T), 20: 4906
scattering by titanium-48, gamma-proton angular correlations in inelastic, (E/T), 20: 4926
transfer between magnetosphere and transition regions, calculations of, 20: 4479(R) (TID-22179, pp 1-83)
PROTOZOA
growth of, effects of wavelength of light on, 20: 3769
PSEUDOUREA, 2-(2-AMINOETHYL)-2-THIO-
effects on absorption of fatty acids by irradiated rats, 20: 3754
radiosensitivity effects in mice, gamma, 20: 3792
PSYCHOLOGY
radiation effects on performance of learned response by rats, effects of nembutal on, x, 20: 3772
PUERTO RICO POWER REACTOR
fuel rod failure in, 20: 5126(R) (ORNL-3870, pp 293-9)
PULSE ANALYZERS
data analysis and storage using photographic film, 20: 4253
design for turbine flow meter signals, 20: 5123(R) (HPR-61)
PULSES
transmission in coaxial cables, improvement by reduction of skin effects, 20: 5218 (TID-21991)
PUMPS
fabrication for MPRE, 20: 5184 (ORNL-P-1740)
performance for post-accident cooling of PWR cores, 20: 5030 (AHSB(S)R-8s)
shaft seals for high-temperature, testing of face-type, 20: 4299(R) (ORNL-2711)
PUMPS (LIQUID METAL)
cavitation tests on centrifugal potassium–sodium, 20: 4999(R) (ORNL-2599)
testing of centrifugal potassium–sodium, 20: 4999(R) (ORNL-2599)
PUREX PROCESS
development, 20: 4948(R) (NP-15406)
PURINES

radiosensitivity effects in mice, gamma, 20: 3792
PYRIDINE, 4-VINYL-
radioinduced grafting to polyvinylchloride, 20: 4032
PYRIMIDINES
radiosensitivity effects in mice, gamma, 20: 3792
PYRROLIDONE, VINYL- POLYMERS
metabolism in man of iodine-131-labeled, dose from, 20: 3675
PYRROLINE-2-CARBOXYLIC ACID
labeling with carbon-14, 20: 3975

Q

QUALITY CONTROL
methods for, photometric, 20: 3970(P)
relation of quality assurance to, 20: 4113 (TID-22358)
QUANTUM ELECTRODYNAMICS
developments in, 20: 4769
infrared divergence from photon states in, (T), 20: 4765
operator gauge transformation in, 20: 4762
QUANTUM MECHANICS
bound states in short-range central potentials, (T), 20: 4708(R) (UCRL-14360, pp 50-73)
fields as operator-valued distributions in relativistic, (T), 20: 4650
oscillators in, SU(3) relations for three-dimensional isotropic, (T), 20: 4476(R) (IS-1200(Sect.P))
Schroedinger equation with complete screened Coulomb potential, 20: 4949(R) (UCRL-14360, pp 85-94)
statistical mechanics of hot plasma, (T), 20: 4949(R) (UCRL-14360, pp 85-94)
wave function calculations using one-center expansion, 20: 5006(R) (ORNL-3870, pp 50-5)
QUARTZ
containers for pressure transducers of, development of, 20: 4224 (UCRL-14448)
phonon detection in, bolometer for, 20: 4479(R) (TID-22179, pp 1-83)
phonon production in, amplitude of microwave induced, 20: 4479(R) (TID-22179, pp 1-83)
phonon propagation in x-cut, 20: 4479(R) (TID-22179, pp 1-83)
radiation effects on phase transformations, 20: 4462
radiation effects on piezoelectric films, electron, 20: 4463
QUARTZ FIBERS
preparation from fused melt at 1900 to 2300°C, 20: 4338(R) (AD-620055)
QUATERPHENYL
radioinduced fluorescence of, in naphthalene, 20: 3994
8-QUINOLINOL
analytical uses for determination of zirconium, 20: 3895

R

RABBITS
bone marrow regeneration in, cytology of, 20: 3789
fatty acid synthesis in lung tissue of, tracer study, 20: 3656 (BNWL-SA-225)
immune reactions of, to irradiated bovine corneal grafts, 20: 3719
radiation effects on immune reactions to sheet erythrocytes in, 20: 3689
radiation effects on blood picture in, x, 20: 3709 (CEA-R-2865)
radiation effects on blood protein content in, x, 20: 3709 (CEA-R-2865)
radiation effects on immune reactions in, x, 20: 3738
radiation effects on immune reactions in, 20: 3746
radiation effects on eyes of, pathological, β, 20: 3761
radiation effects on exteriorized intestine and spleen of, x, 20: 3775
sodium-22 content in muscles of Canadian, 20: 4161
RADAR
design for distance measurement, 20: 5226(P)
design for range indicating, 20: 5225(P)
RADIATION
detection of, field-effect transistor design and performance for, 20: 4250 (UCRL-16446)
dose of, from uranium, radium, and radon in rocks and water supplies in France, 20: 4193
dosimetry for cervical carcinoma therapy, 20: 3807
dosimetry in head phantoms, photographic film for, 20: 3862
effects in electronics, conference on, 20: 4266
effects on carbon-coated sol-gel microspheres of plutonium, thorium, and uranium dioxides and their mixtures, 20: 4344 (ORNL-P-1725)
effects on chromosome aberrations in leukocytes, relation to leukemogenesis, 20: 3730
effects on content of vitamin D_2 in yeast, 20: 3690
effects on crosslinking in ethylene polymers, 20: 4002
effects on crosslinking in ethylene polymers, 20: 4003
effects on crosslinking in ethylene polymers, 20: 4004
effects on crosslinking in ethylene polymers, 20: 4005
effects on crosslinking in ethylene polymers, 20: 4006
effects on crosslinking of polyethylene, 20: 4010
effects on development of amphibians, bibliography, 20: 3773
effects on DNA synthesis in normal and neoplastic rat tissue, tracer study, 20: 3701
effects on DNA synthesis, tracer study, 20: 3702
effects on electric conductivity of air, nitrogen, and oxygen, 20: 4949(R) (UCRL-14360, pp 85-94)
effects on electric conductivity of ethylene polymers, 20: 4035
effects on gases, equipment and method for investigations of electric field effects in, 20: 4022
effects on human embryos, teratogenic, 20: 3747
effects on hypothalamus pituitary system, effects of hibernation on, 20: 3703
effects on intestinal absorption of nutrients and vitamins, 20: 3851
effects on ionic crystals, 20: 4008
effects on living organisms, bibliography, 20: 3773
effects on man, low-level, 20: 3770
effects on materials, review of, 20: 4464
effects on nil ductility temperature and stress wave attenuation of steel, methods for determining, 20: 4457(R) (EURAEC-1474)
effects on plants, genetic, 20: 3710(R) (EUR-2493.e)
effects on polymerization of carbon monoxide with butene-1, isobutylene, and propylene, 20: 3997
effects on semiconductor electric properties, 20: 4265
effects on solids, influence of scattering law on displacement cascades in, 20: 4473
effects on squamous cell carcinomas, therapeutic, 20: 3807
effects on tritiated-thymidine metabolism in Yoshida ascites sarcoma cells, 20: 3702
effects on wasps, genetic, 20: 3733
emission by charged particles in dielectrically inhomogeneous media, (T), 20: 4625
emission by coherent, by electron sheets, 20: 4624
emission in electron scattering by silver, surface plasmon excitation, (E), 20: 5017
hazards to Brookhaven personnel from stray radiation fields, LET and quality factors in, 20: 4176 (BNL-9684)
use in industry, 20: 4270
RADIATION CHEMISTRY
data reduction in gas phase, computer program for, 20: 3985 (RFP-624)
equipment for, method of calculating parameters for, 20: 3993
facilities for hydrocyanic acid production by, 20: 3982(R) (AGN-8156)
hot-atom kinetics in, review of, 20: 4039
processes in, for use in textile industry, 20: 4031
processes in, review of, 20: 3986
RADIATION DETECTION INSTRUMENTS
design and manufacture of, for thermal neutrons, 20: 4260(P)
design for solar neutrinos, 20: 4523 (COO-818-63)
design of scintillation pulse-height analyzer with photographic storage, 20: 4253
development, 20: 5181(R) (ORNL-3029)
development of high-sensitivity whole-body, for high-speed measurements, 20: 3658(R) (EUR-2414.f,i)
survey for accelerator monitoring, 20: 4514 (UCRL-16445)
testing of reactor, system for, 20: 5037
RADIATION DETECTION INSTRUMENTS (PULSE TYPE)
design of scintillation, for low γ activity in large liquid volumes, 20: 3817
pulses in G-M, formation mechanism of excitation, 20: 4254
RADIATION DETECTORS
design and development, 20: 4048(R) (NP-15406)
design for use in determining human retention of radioactive vapors, 20: 4202
development of multiplate Moxon-Rae, for neutrons, 20: 4246(R) (RPI-328-40, pp 49-55)
evaluation for health physics programs in Russia, 20: 4198
performance for reactor neutrons, statistical fluctuations in, (T), 20: 5066
RADIATION INJURIES
detection in man, biological methods for low-level, 20: 3770
detection in personnel of, by medical examination, 20: 4199
incidence in AEC and contractor personnel of, 1943 through 1964, 20: 4188 (TID-22268)
induced in intestine by carcinoma therapy, 20: 3732
methods for preventing, from oral cancer therapy, 20: 3813
of developing teeth, histology of, 20: 3743
of liver, diagnosis using iodine-131-rose bengal function test, 20: 3774
of lymph system, induced by therapeutic doses of x radiation, 20: 3852
of skin, photosensitivity test for predicting uv, 20: 3767
pathology of intestinal, induced by radiotherapy of abdomen, 20: 3820
pathology of retinal, in developing fetuses, 20: 3725
pathology of skin, 20: 3724
pathology of skin, induced by cosmic radiation, 20: 3731

pathology of, in rabbit eyes, β, 20: 3761
pathology of, induced by radiotherapy, review, 20: 3849
protection against, effects of rutin derivative on mucosal, during radiotherapy, 20: 3840
protection against, effects of bone marrow injections in germ-free mice, 20: 3788
protection against, effects of injected bone marrow, 20: 3789
protection against, effects of mercapto analogs of ephedrine, 20: 3790
protection against γ, in cells in tissue culture, 20: 3791
protection against, effects of homologous bone marrow transplants in rats, 20: 3795
surgical repair of skin, 20: 3724

RADIATION MONITORING
equipment for accelerators, 20: 4514 (UCRL-16445)
in Germany, 1965, 20: 4164
of synchrotrons environs, 20: 4175 (BNL-9650)

RADIATION PROTECTION
development for manned space flight, 20: 4525
food monitoring programs in U. S. for, 20: 4201
in Denmark, laws and regulations for, 20: 4180 (NP-15571)
measures against nuclear weapon fallout, 20: 3797
measures against nuclear weapon fallout, 20: 3799
method for normal tissues during cancer therapy, 20: 3842
methods for normal tissues during vaginal tumor therapy, 20: 3848
of gonads during diagnostic radiography of females, 20: 3858
program of AEC, review, 20: 4188 (TID-22268)

RADIATION SICKNESS
anemia in, etiology of, 20: 3658(R) (EUR-2414.f,i)

RADIATION SOURCES
use in textile industry, 20: 4032
use in textile industry, 20: 4034
uses in industry, 20: 4275

RADIATION TARGET CANS
cutting of, design of milling machine for, 20: 4129
handling equipment for, 20: 5205
handling irradiated, design of equipment for, 20: 4127
handling of, design of hot cells for, 20: 4125
handling of, equipment for underwater, 20: 5204
machining and dismantling of, design of equipment for, 20: 4351
machining of, Harwell equipment for, 20: 4126

RADIATION TARGETS
design and performance of liquid hydrogen, 20: 4490
effects of orientation of, on nuclear reaction energy distributions, (T), 20: 4842(NASA-TN-D-3116)

RADIATORS
design for space power plants, 20: 4299(R) (ORNL-2711)
development for MPRE, 20: 5182 (ORNL-P-1721)

RADIO ASTRONOMY
equipment for, design of Haystack Research Facility, 20: 4479(R) (TID-22179, pp 1-83)
use in ionospheric electron density diagnostics, (E), 20: 4735

RADIO WAVES
emission by sun, harmonic structure and band splitting of type II, 20: 4524
interactions with missiles having ionized wakes, (T), 20: 4730 (SC-DC-65-1797)
interactions with inhomogeneous plasma slabs, reflection and transmission coefficients for nonlinear, (T), 20: 4954
sources of, mapping of astronomical, 20: 4479(R) (TID-22179, pp 1-83)

RADIOACTIVE CONTAMINATION
containment and control of, methods for, 20: 4214
levels of petroleum product, when using nuclear explosions for production stimulation, 20: 4082 (BM-RI-6684)

RADIOACTIVE MATERIALS
analysis of, engineering drawings of x-ray diffractometer modified for, 20: 3910
destruction of cellulose, sulfuric acid process for, 20: 5208(P)
handling and transfer to hot cells, methods for, 20: 4209
handling of, hot-cell transfer systems for, 20: 4063
handling of, method for sealing refractory vessel for, 20: 5209(P)
processing, storage, and transfer of, design of laboratory for, 20: 4041
testing of, nondestructive methods for, 20: 4122
transfer from shielded containers to hot cells, 20: 4208
transport into and from hot cells, methods for, 20: 4043
transport of, international regulations for, 20: 4181 (NP-15620)
transport through alpha-gamma barriers in hot cells, 20: 4042

RADIOACTIVE VOLTAGE GENERATORS
use with electrostatic rocket thruster for propulsion, 20: 4140(P)

RADIOACTIVE WATERS
hazards to personnel of radon in spas from thoron in, 20: 3798

RADIOACTIVITY
analysis of Swiss rocks, petrographic–microscopic, 20: 4157(T) (ORNL-tr-702)
measurement in liquid media, scintillation method for, 20: 3870 (EUR-2459.f)
monitoring of food, in U. S., 20: 4201
natural content in soils of, effects on incidence of stomach cancer, 20: 4197

RADIOAPPLICATORS
dose distribution from radium, photographic film for determining, 20: 4205

RADIOBIOLOGY
book: *Nuclear Medicine*, 20: 3860
review of bacterial, 20: 3776

RADIOCHEMICAL PROCESSING PLANTS
development of Eurochemic, 20: 4048(R) (NP-15406)

RADIOCHEMISTRY
hot-atom chemistry, review of, 20: 4039

RADIODERMATITIS
pathology of, 20: 3812
pathology of, in man, 20: 3724
pathology of, induced by cancer radiotherapy, 20: 3847

RADIODIAGNOSIS
book: *Nuclear Medicine*, 20: 3860
evaluation of methods of, for clinical cardiology, 20: 3818
procedures for brain scanning at University of Mississippi, 20: 3830
use of radioalbumin aggregates in, safety of, 20: 3832

RADIOFREQUENCY SPECTROMETERS
design and development of NMR, 20: 4476(R) (IS-1200(Sect,P))
development for NMR studies, 20: 4255

RADIOGRAPHY
book: *Neutron Radiography*, 20: 4115
contrast media for kidney, effects of double-dose technique on efficiency of, 20: 3857
development of gamma, 20: 4114(T) (AD-621784)
dose to gonads during dental, 20: 4206
dose to gonads from dental, in Japan, 20: 4196
equipment and methods development for, at Harwell, 20: 4119
equipment for underwater, in HFR reactor, 20: 5203
exposure unit for, design of shutter controlled, 20: 4094(P)
hazards from oral, Swedish survey of, 20: 3846
hazards to physiotherapists, 20: 4203
image contrast control during diagnostic, 20: 3815
of swine knuckle for estimation of ham composition for slaughtered animals, 20: 5224
of tumors, use of gamma therapy equipment and conditions for treatment planning, 20: 3827
of urinary tract, 20: 3800(R) (NP-15150)
radiation absorption by man, during diagnostic, x, 20: 3816
radiation dose from diagnostic, used for diagnosis of vesicoureteral reflux, 20: 3834
radiation dose from dental, of population of Japan, 20: 4195
radiation dose to gonads of children during diagnostic, 20: 3854
radiation dose to fetus from diagnostic, 20: 3823
radiation hazards to life-span of x-ray technicians, 20: 3760
radiation protection during diagnostic, 20: 3858
radiation protection during diagnostic, 20: 3815
technique for placenta localization, 20: 3825

RADIOISOTOPES
decay constants, half lives, and specific activities of, 20: 4845 (ORNL-TM-1318)
determination in mixtures, microcalorimetric, 20: 3866 (CEA-R-2630)
distribution in atmosphere, review of, 20: 4163
performance as power supply, for submersibles, 20: 4276 (AGN-8128)
preparation, 20: 4270
research programs in United Kingdom, 20: 5152
uptake by plants of, in Rumania, 20: 3654
use at U.S. Naval Civil Engineering Laboratory, recommendations for, 20: 4089 (TWL-1055A)
use for measuring velocity of fluid flow, 20: 4227
use in analysis and thickness measurements on coatings, review on, 20: 4219 (ORNL-IIC-5, pp 182-205)
use in industry, 20: 4270
use in measuring density and thickness, 20: 4273
use in textile research and industry, conference on, 20: 4274
use in veterinary medicine, 20: 3859
uses in industry, 20: 4275
uses of, industrial, 20: 4272(T) (JPRS-32813)

RADIOLOGICAL WARFARE
behavior of population during, 20: 4200
book: *Engineering and Rescue Operations at the Site of an Atomic Strike*, 20: 4191(T) (JPRS-31014)
hazards of, review, 20: 4192(T) (JPRS-32686)

RADIOLOGICAL WARFARE AGENTS
decontamination of food and water supplies of, 20: 4192(T) (JPRS-32686)

RADIOLOGY
equipment for chest, use of ytterbium-169 in portable, 20: 3804 (ORNL-

IIC-5, pp 309-28)
radiation hazards to technicians, survey on, 20: 3779
sources for, properties of promethium-147, 20: 3801 (ORNL-IIC-5, pp 222-38)
RADIOMETERS
modification of, for use in Air Force KC-135 aircraft, 20: 4234(R) (AD-619177)
performance of microwave, in measurement of water vapor in atmosphere, 20: 4479(R) (TID-22179, pp 1-83)
RADIOMETRIC ANALYSIS
methods for coal and ores, 20: 3884 (ORNL-IIC-5, pp 206-21)
radiation sources in, low-energy gamma and x-ray, 20: 4111 (ORNL-IIC-5)
RADIOPROTECTIVE COMPOUNDS
benadryl, effects in mice, gamma, 20: 3792
preparation and testing of mercapto analogs of ephedrine, 20: 3790
RADIOSENSITIVITY
effects of ploidy on tumor, x, 20: 3751
of *Escherichia coli*, gene locus for uv, 20: 3757
of rats, effects of fasting condition on, 20: 3766
RADIOSTERILIZATION
conference on food, 20 3685
development for food, world, 20: 4271 (WASH-1063)
RADIOTHERAPY
book: *Nuclear Medicine*, 20: 3860
dose calculations for gamma radiation for, 20: 3855
equipment design for, 20: 4517
hazards in pediatric, 20: 3850
method for cobalt tracking, 20: 3842
methods for vaginal tumor, 20: 3848
of oral tumors, electron beam, 20: 3833
of tumors, review of recent progress in, 20: 3849
use in pediatric malignancy, hazards from, 20: 3850
RADIUM
content in deciduous teeth, United States, 20: 4160
effects on bones of therapeutic doses, pathological, 20: 3856
separation from silver by partition chromatography, 20: 4054
RADON
diffusion of alpha-recoil, in ionic crystals and sinters, 20: 3944
RADON ISOTOPES Rn-220
contamination by, in radon spas, 20: 3798
content in thermal springs, 20: 3798
RAIN WATER
analysis for fission products of, collected in Japan, 20: 4177
cesium-137 content in, method for determining, 20: 4159
RAMAN EFFECT
in barium titanate, temperature dependence of, 20: 4479(R) (TID-22179, pp 1-83)
RARE EARTH ALLOYS
crystal structure of, Laves phases in, 20: 4297(R) (IS-1200(Sect.M))
Au–rare earth, phase studies and solid solubilities of, 20: 4297(R) (IS-1200(Sect.M))
Cu–rare earth, magnetic properties and structure, 20: 4448
Mg–rare earth, phase studies and solid solubilities of, 20: 4297(R) (IS-1200(Sect.M))
Ni–rare earth, magnetic properties and structure, 20: 4448
rare earth–Ag, magnetic properties and structure, 20: 4448
RARE EARTH CHLORIDES
physical and thermodynamic properties, 20: 3863(R) (IS-1200(Sect. C))
uranyl ion fluorescence spectra in, 20: 3948
RARE EARTH COMPLEXES
with ligand anions, stability, 20: 3863(R) (IS-1200(Sect. C))
RARE EARTH COMPOUNDS
book: *Rare Elements and Rare Earths in Technology*, 20: 4451
magnetic properties of germanomolybdates, 20: 5006(R) (ORNL-3870, pp 50-5)
properties of germanomolybdates, 20: 3919(R) (ORNL-3870, 3-6)
properties of germanotungstates, 20: 3919(R) (ORNL-3870, pp 3-6)
RARE EARTH ETHYL SULFATES
energy levels of hydrated, (E), 20: 4476(R) (IS-1200(Sect.P))
RARE EARTH MINERALS
book: *Geochemistry and Analytical Chemistry of Rare Earth Elements*, 20: 4146
RARE EARTH OXIDES
magnetic susceptibility, 20: 4297(R) (IS-1200(Sect.M))
preparation of nonstoichiometric, 20: 4297(R) (IS-1200(Sect.M))
RARE EARTH TUNGSTATES
preparation and electric and magnetic properties, 20: 4362(R) (AD-620033)
RARE EARTHS
analysis for tantalum, spectrophotometric, 20: 3863(R) (IS-1200(Sect. C))
book: *Geochemistry and Analytical Chemistry of Rare Earth Elements*, 20: 4146
book: *Rare Elements and Rare Earths in Technology*, 20: 4451
crystals of, polishing methods for, 20: 4297(R) (IS-1200(Sect.M))
determination in hydrochloric acid or methanol–nitric acid media, spectrophotometric, 20: 3888 (TID-22402)
effects on crystal structure of monazites, 20: 4174
effects on determination of uranium(IV) in presence of uranium(VI), 20: 3903
effects on niobium, additive, 20: 4299(R) (ORNL-2711)
electric conductivity of, effects of magnetic fields on, (E/T), 20: 4476(R) (IS-1200(Sect.P))
enthalpies at high temperatures, 20: 4297(R) (IS-1200(Sect.M))
magnetic properties, (E), 20: 4476(R) (IS-1200(Sect.P))
magnetic transitions and thermal hysteresis in, 20: 3863(R) (IS-1200 (Sect. C))
magnetostruction in, (E/T), 20: 4476(R) (IS-1200(Sect.P))
phase studies, 20: 4297(R) (IS-1200(Sect.M))
separation by anion exchange using nonaqueous solvents, 20: 4067
separation by ion exchange and solvent extraction, 20: 3863(R) (IS-1200 (Sect. C))
separation by solvent extraction using di(2-ethylhexyl) phosphoric acid, 20: 4077(R) (IS-1200(Sect. E))
separation from magnesium and thorium by extraction using fused chlorides, 20: 4297(R) (IS-1200(Sect.M))
separation from minerals, other metals, rocks, and sediments in mixed and nonaqueous solvents by ion exchange, 20: 3888 (TID-22402)
separation from thorium, 20: 3905
solvent properties for tantalum, 20: 4297(R) (IS-1200(Sect.M))
thermoelectric properties of single-crystal, (E), 20: 4476(R) (IS-1200(Sect.P))
RARE GAS COMPOUNDS
preparation and properties of, review on, 20: 3915 (CEA-Bib-61)
RARE GASES
diffusion in ionic crystals and sintered materials, 20: 3944
effects on radiolysis of ammonia, 20: 4021
reactions of ion beams of, with plasma, (E), 20: 4945 (ORNL-TM-1306)
recombination in plasmas of, 20: 4479(R) (TID-22179, pp 1-83)
RATE METERS
design for reactor reactivity determinations, 20: 5061 (ZFK-RN-22)
radiation injuries of, protective effects of homologous bone marrow transplants, 20: 3795
RATS
calcium-45 and strontium-89 metabolism by bones in, effects of sodium alginates on, 20: 3671
cerium-144 distribution in liver cells of, following intravenous injection, model for, 20: 3682
distribution of bone marrow transplants in, tracer study, 20: 3795
effects of methionine sulfoximine on glucose metabolism in, tracer study, 20: 3678
fatty acid synthesis in lung tissue of, tracer study, 20: 3656 (BNWL-SA-225)
gallium-68 metabolism in, effects of carrier on, 20: 3676
humoral mediation of behavior in parabiotic, 20: 3706 (AD-623365)
intestinal discrimination between barium, calcium, and strontium in, tracer study, 20: 3669
pathology of nephrosis induced by injected uranium nitrate in, 20: 3666
pathology of nephrosis induced by injected mercuric chloride in, 20: 3666
radiation effects on glucose metabolism in, tracer study, x, 20: 3678
radiation effects on growth of transplanted tumors in, 20: 3695
radiation effects on lungs in, effects of dose fractionation on histological electron, γ, and x, 20: 3700
radiation effects on DNA synthesis in normal and neoplastic tissues of, tracer study, 20: 3701
radiation effects on bone growth in, x, 20: 3707 (AD-623641)
radiation effects on retinal development in embryos of, x, 20: 3725
radiation effects on absorption of fatty acids in, tracer study, x, 20: 3754
radiation effects on performance of learned response by, effects of nembutal on, x, 20: 3772
radiation effects on exteriorized intestine and spleen of, x, 20: 3775
radiation effects on lungs of, x, 20: 3785
radiosensitivity of, effects of diet, 20: 3766
vaccination of, using irradiated *Nippostrongylus brasiliensis* larvae, 20: 3786
REACTOR COMPONENTS
containment systems development, (E), 20: 5023(R) (IITRI-578P21-15)
REACTOR CONTROL ELEMENTS
radiation effects on performance of alumina-dysprosia, 20: 5115(R) (GA-4967)
REACTOR CONTROL RODS
coupling to drive, design of releasable, 20: 5051(P)
drive mechanism for, design of, 20: 5044(P)
drive mechanism for, pressure operated, 20: 5052(P)
position indicator for, 20: 5048(P)
reactivity worths in NORA, 20: 5060(R) (TID-22357)

reactivity worths in Peach Bottom Power Reactor, 20: 5118(R) (GA-6647)
REACTOR CONTROL SYSTEMS
design for Russian BN-350 power reactor, 20: 5137(T) (JPRS-31193)
design of emergency shutdown, 20: 5047(P)
design of LCBWR, 20: 5106 (ACNP-65544(Vol.II))
design of rod assembly and driving mechanism, 20: 5044(P)
economic aspects of power reactor, 20: 5140
optimization of nuclear rocket, 20: 5187
REACTOR COOLANTS
bremsstrahlung dose rates from activated lithium, 20: 4299(R) (ORNL-2711)
flow of, method for measuring in-core, 20: 5028(P)
REACTOR COOLING SYSTEMS
coolant charging and volume control system for, design of servomechanical, 20: 5046(P)
design for liquid-moderated reactors, 20: 5038(P)
design of, with vapor generator and circulator included in pressure vessel, 20: 5169(P)
development for core protection in PWR coolant loss accidents, 20: 5030 (AHSB(S)R-8s)
failures of, analysis of accidents from, (E), 20: 5023(R) (IITRI-578P21-15)
fission product detection in, efficiency of filters for, 20: 5036 (RL-SA-47)
pressurizer design for, 20: 5039(P)
pump performance for post-accident cooling of PWR, 20: 5030 (AHSB(S)R-8s)
regulator design for, inlet temperature, 20: 5170(P)
REACTOR ENGINEERING
containment systems development, (E), 20: 5023(R) (IITRI-578P21-15)
development at Bettis Atomic Power Laboratory, 20: 5132(R) (WAPD-MRP-113)
REACTOR FUEL ELEMENTS
bowing against continuous restraint, (T), 20: 5090
burnup of, gamma scanning for determination of, 20: 5093
burnup profiles in, equipment for recording, 20: 4129
can design, fabrication, and performance, Magnox-, 20: 5094
cleaning and dismantling of, design of facility for, 20: 4064
design and development for advanced water reactors, 20: 5134(R) (WCAP-3269-12)
design of assembly of, for breeder reactors, 20: 5082(P)
design of clad, for improved heat transfer, 20: 5096(P)
design of clad, with heterogeneous enrichment, 20: 5102(P)
design of double sheathed, for high temperatures, 20: 5099(P)
design of finned, for improved heat transfer, 20: 5101(P)
design of rod-cluster, 20: 5100(P)
design of sheathed, with varying cross section, 20: 5097(P)
development and testing of "nuclear vapotron" canned, (E), 20: 5088(R) (EURAEC-1337)
development for gas-cooled high-temperature power reactor, 20: 5117(R) (GA-5866)
development for power reactors, engineering problems in, 20: 5147
development for Shippingport Pressurized Water Reactor, 20: 5132(R) (WAPD-MRP-113)
development of, review of, 20: 4313
diffusion of fission products from, methods for measuring, 20: 4452
fabrication costs of, economic study of, 20: 5024(R) (ORNL-3870, pp 261-5)
fabrication costs, computer program for calculating, 20: 5173(R) (ORNL-3870, pp 191-3)
fabrication of clad, process for, 20: 4353(P)
fabrication of, chemical aspects of, 20: 4345
failure detection by lithium-drifted germanium γ-spectrometers, 20: 5109 (AECL-2360)
fission product diffusion in, gamma scanning of, 20: 5093
handling irradiated, design of equipment for, 20: 4127
handling of defective, end-coupling device for in-pile, 20: 5095(P)
handling of, design of hot cells for, 20: 4125
heat transfer from annular, for TSR-II, 20: 4299(R) (ORNL-2711)
heat transfer in flat-plate, with fuel-clad bonding defects, (T), 20: 4102 (HW-SA-3640)
heat transfer in, axial, 20: 5091
machining and dismantling of, design of equipment for, 20: 4351
machining of irradiated, equipment for, 20: 4128
machining of, Harwell equipment for, 20: 4126
preparation and handling of, criticality safety in, 20: 4194
processing of irradiated, design of laboratory for, 20: 4041
processing of irradiated, design of Cyrano cell for, 20: 4044
processing of irradiated, design of hot cells for, 20: 4062
processing of irradiated MTR-type, design of pilot plant for, 20: 4066
radiation effects testing in HBWR, program summary, 20: 5123(R) (HPR-61)
radiography and radioscopy of irradiated, equipment for, 20: 4117
support design for, 20: 5049(P)
support design for, 20: 5050(P)
support structures for rod-cluster, design of, 20: 5103(P)
testing for fast power reactors, FARET reference core design for, 20: 5190 (ANL-7106)
testing for 1000-Mw(e) gas-cooled high-temperature reactor, 20: 5117(R) (GA-5866)
testing of irradiated, transfer methods for, 20: 4063
testing of irradiated, equipment for nondestructive, 20: 4118
testing of irradiated, nondestructive methods for, 20: 4124
testing of, design of high-activity beta-gamma facility for, 20: 5153
testing of, design of equipment for nondestructive, 20: 4121
testing of, Dounreay alpha–gamma hot cells for nondestructive, 20: 4120
testing of, nondestructive methods for, 20: 4122
REACTOR FUEL ELEMENTS (CERAMIC)
design, 20: 5123(R) (HPR-61)
development of plutonia–stainless steel cermet, (E), 20: 5192 (BNWL-SA-251)
fabrication costs of, economic study of, 20: 5024(R) (ORNL-3870, pp 261-5)
fabrication of plutonium dioxide–uranium dioxide for PRTR, variable cost of, 20: 4339 (BNWL-131D)
testing irradiated, design of caves for, 20: 4130
testing seven-rod-cluster urania, for steam superheating, 20: 5104 (ACNP-65006)
thermal conductivity of uranium dioxide pellets, 20: 5135 (WCAP-3269-12)
REACTOR FUEL ELEMENTS (DISPERSION)
development of graphite matrix-carbide, 20: 5089(R) (GA-6181)
fabrication of encapsulated, 20: 4352(P)
materials testing for nonbonds in, development of ultrasonic methods for, 20: 4110(R) (ORNL-3870, pp 146-54)
REACTOR FUEL ELEMENTS (THERMOELECTRIC)
design, 20: 4576(P)
REACTOR FUEL PINS
development of plutonia–stainless steel cermet, (E), 20: 5192 (BNWL-SA-251)
REACTOR FUEL PLATES
fuel content in, method for determining, 20: 4110(R) (ORNL-3870, pp 146-54)
temperature measuring device for sheathed, process of assembling, 20: 5098(P)
temperature of, thermocouple thermal-loading analysis for surface, 20: 5026
REACTOR FUEL RODS
development, fabrication, and performance of Magnox-clad, in U.K., 20: 5094
fuel homogeneity in, method for determining, 20: 4110(R) (ORNL-3870, pp 146-54)
neutron Doppler coefficient and resonance capture in uranium, in graphite-moderated reactors, (T), 20: 5092
radiation effects on uranium dioxide, produced by alternate fabrication processes, 20: 4459 (GEAP-4850)
testing of, procedures for nondestructive, 20: 4123
testing seven-rod-cluster urania, for steam superheating, 20: 5104 (ACNP-65006)
REACTOR FUEL TUBES
design and testing, 20: 5123(R) (HPR-61)
REACTOR FUEL WIRES
preparation of nickel–urania, for fissiochemical reactions, 20: 3982(R) (AGN-8156)
REACTOR FUELS
burnup in Shippingport Pressurized Water Reactor, 20: 5132(R) (WAPD-MRP-113)
burnup of, effects on fission-product behavior in loss-of-coolant accidents, 20: 4183(R) (ORNL-3843, pp 2-70)
development, 20: 5152
development and properties of plutonium dioxide–uranium dioxide–zirconium dioxide, 20: 4382(R) (NUMEC-3505-8)
development for fluidized-bed reactors, 20: 5125 (NYO-10732)
development for SEFOR, 20: 5120(R) (GEAP-4799)
development of plutonia–stainless steel cermet, (E), 20: 5192 (BNWL-SA-251)
development of, reviews of, 20: 4313
diffusion of fission products in carbon-coated thorium carbide, uranium carbide and uranium dioxide particles, 20: 5117(R) (GA-5866)
diffusion of xenon-133 from low-dose, low-temperature irradiated, (E), 20: 4471
fabrication costs, economic study of, 20: 5024(R) (ORNL-3870, pp 261-5)
machining of, design of hot cells for, 20: 4125
meltdown of, diffusion tube sampling of vapors from, 20: 4185(R) (ORNL-3843, pp 169-234)
performance of metallic, survey of, 20: 5173(R) (ORNL-3870, pp 191-3)

processing irradiated, for uranium and plutonium recovery, 20: 4073(P)
processing of irradiated, economics of, 20: 4050
processing of molybdenum–uranium, 20: 4070(P)
processing of spent, development of methods and techniques for, 20: 4069
processing spent, methods for, 20: 4046(R) (EURAEC-1340)
properties of, for various reactor types, 20: 4345
radiation effects on EBOR, 20: 5115(R) (GA-4967)
radiation effects on uranium dioxide, produced by alternate fabrication processes, 20: 4459 (GEAP-4850)

REACTOR MATERIALS
development for beryllia-moderated power reactors, 20: 5115(R) (GA-4967)
development of, review of, 20: 4313

REACTOR MATRICES
coolant flow through, method of measuring, 20: 5028(P)
criticality studies of, computer program for, 20: 5060(R) (TID-22357)
criticality studies of slightly enriched uranium dioxide, 20: 5071
neutron resonance absorption in, calculation of, 20: 5077
neutron thermal disadvantage factors in undermoderated water-uranium oxide, 20: 5073

REACTOR MODERATORS
neutron pulse decay constant in solid, (T), 20: 4815
radiation effects on beryllia and beryllia-mixture, 20: 5115(R) (GA-4967)
system design for fluid, for varying moderating characteristics, 20: 5053(P)

REACTOR OSCILLATORS
development for Ames Reactor, 20: 5196(R) (IS-1200(Sect.E))

REACTOR REFLECTORS
effects on temperature coefficients for uranium dioxide–water core, (E), 20: 5067

REACTOR SAFETY
analysis for large gas-cooled fast power reactors, 20: 5119 (GA-6732)
containment laws for, (E/T), 20: 5034 (NOLTR-63-140)
containment research facility design for, 20: 4184(R) (ORNL-3843, pp 71-135)
criteria for, in U.K., 20: 5027
evaluation of BSR-II, 20: 5181(R) (ORNL-3029)
fission product behavior in containment systems, 20: 4184(R) (ORNL-3843, pp 71-135)
fission product release in loss-of-coolant accidents, factors affecting, 20: 4183(R) (ORNL-3843, pp 2-70)
hazards analysis for 1000-Mw(e) gas-cooled high-temperature reactor, 20: 5117(R) (GA-5866)
instrumentation monitoring and operations for, system for, 20: 5037
research on filtration and sorption in accidents, 20: 4086(R) (ORNL-3843, pp 137-67)
safeguards report on LCBWR, 20: 5106 (ACNP-65544(Vol.II))
safeguards report on LCBWR, 20: 5105 (ACNP-65544(Vol.I))
transient accidents in TREAT, summary on simulated, 20: 4183(R) (ORNL-3843, pp 2-70)

REACTOR SHIELD VOIDS
tube mounting in, 20: 5054(P)

REACTOR SHIELDING
analysis of axially symmetric, computer program for, 20: 5181(R) (ORNL-3029)
design for TSR-II, 20: 4999(R) (ORNL-2599)
design of shadow, optimization of, 20: 5181(R) (ORNL-3029)
evaluation of ML-1, 20: 5181(R) (ORNL-3029)
gamma production in lithium hydride–uranium, 20: 5181(R) (ORNL-3029)
research at Geesthacht Reactor Station, (E), 20: 4997(R) (EUR-2494.d)

REACTOR SLURRIES
preparation of hydrophilic or organophilic uranium oxide and/or thorium oxide, 20: 3969(P)

REACTOR TUBES
design, 20: 5054(P)

REACTORS
accidents in, explosion containment laws for, (E/T), 20: 5034 (NOLTR-63-140)
auxiliaries of, dimensional location by optical tooling, (E), 20: 5035 (ORNL-TM-1278)
containment systems for, development of, (E), 20: 5023(R) (IITRI-578P21-15)
control rod actuator device for, pressure operated, 20: 5052(P)
core design for liquid-moderated, 20: 5080(P)
design of liquid-moderated, pressure-tube, 20: 5083(P)
design of two-core totally reflected cylindrical, computer program for, 20: 5059 (RT/FIMA(65)-1)
design with coolant cross flow, 20: 5087(P)
environs monitoring programs for, in U. S., 20: 4201
heat exchanger for, design of, 20: 4109(P)
heat transfer under bulk boiling conditions in, effects of nonuniform axial, 20: 4104 (NP-15622)
kinetics of coupled, invariant imbedding and modal expansion for, (T), 20: 5065
loading apparatus for, 20: 5040(P)
loading apparatus for, design of, 20: 5041(P)
loading device for, 20: 5043(P)
moderator system for, property variation using liquid, 20: 5053(P)
neutron cross sections for analysis of, 9- and 16-group, 20: 4829 (GEMP-173(Suppl.1))
neutron diffusion in, mesh size corrections for computer codes for, (T), 20: 5069
neutron flux and thermal utilization in square cell, effects of multipoles on, (T), 20: 5063
neutron flux distributions in, meter design for measuring, 20: 5061 (ZFK-RN-22)
neutron flux distributions in, statistical fluctuations in, (T), 20: 5066
neutron multiplication in reflected, correlation functions for, 20: 5058 (JINR-P-2335)
neutron noise in, theory for experiments on, (T), 20: 5076
neutron Rossi-α experiment in, generalized analysis of, (T), 20: 5070
neutron two-dimensional diffusion codes for design of, (T), 20: 5056 (CONF-654-22)
reactivity in, hole and void effects on, (T), 20: 5064
reactivity of, equation for, 20: 5062
reactivity of, meter design for determining, 20: 5061 (ZFK-RN-22)
shutdown of, adjoint function for optimal xenon, 20: 5075
shutdown of, time optimal and minimax solutions for xenon, 20: 5074
temperature measurement in, design of electromagnetic induction device for, 20: 5045(P)
use in neutron activation analysis, 20: 3864 (AERE-L-166)

REFRIGERATION
helium-3 refrigerator design and performance, 20: 4776

RELATIVITY THEORY
equations of motion without infinite self-action in general, Bianchi identity for, 20: 4768

REMOTE-CONTROL EQUIPMENT
design for dismantling and machining irradiated materials, 20: 4127
design for transfer of noxious liquids, 20: 4095(P)
design for transfer to and from hot cells, 20: 4210
development for fuel post-irradiation examination, 20: 5136 (WCAP-5564)

REMOTE-VIEWING EQUIPMENT
development for fuel post-irradiation examination, 20: 5136 (WCAP-5564)

RENÉ-41
corrosion by lithium fluoride in cyclic high-temperature environment, 20: 4326 (TRW-ER-6561)

RENÉ-62
tensile properties to 1300°F after prolonged thermal exposure, 20: 4373 (GEAP-4794)

RESEARCH REACTORS
experimental facilities for underwater radiography in HFR, 20: 5203
experimental facilities for underwater dismantling of irradiation experiments in HFR, 20: 5204
experimental facilities for, for dismantling irradiation capsules, 20: 5205
fuel development for Fast Flux Test Facility and Fast Flux Test Reactor, (E), 20: 5192 (BNWL-SA-251)
neutron production in pulsed, bibliography for, 20: 5200 (TID-3571 (Suppl.1))
neutron spectra from HERALD thermal column, measurement of, (E), 20: 5191 (AWRE-R-4/65)
research programs at Ames Laboratory, July 1964–June 1965, 20: 5213(R) (IS-1200)
shielding experiments at Geesthacht FRG, 20: 4997(R) (EUR-2494.d)

RESISTORS
radiation effects on, in SNAP environment, 20: 4262 (NP-15610)

RETICULO-ENDOTHELIAL SYSTEM
binding of gold-198 colloids by, in dog liver, 20: 3680
metabolism of colloids of gold-198 in, 20: 3822
stimulation of, effects on antibody formation in rabbits, 20: 3689

RHENIUM
compatibility with uranium carbide–zirconium carbide system at 2000°C, 20: 4335
deposition of, thermochemical, 20: 4342(R) (ORNL-3879, pp 85-101)
deposition on molybdenum, bonding in electrolytic, 20: 4404(T) (JPRS-32773)
determination in chromium alloys, spectrophotometric, 20: 3863(R) (IS-1200(Sect. C))
elastic properties of single-crystal, 20: 4297(R) (IS-1200(Sect.M))
neutron cross sections for, 9- and 16-group, 20: 4829 (GEMP-173(Suppl.1))
properties as collector in thermionic cells, 20: 4570(R) (AD-614592)

RHENIUM ALLOYS

Cr–Re, bonding in electrolytic deposition on copper and molybdenum, 20: 4404(T) (JPRS-32773)
Fe–Rh, plastic deformation of, factors affecting, 20: 4297(R) (IS-1200(Sect.M))
Mo–Re, electric and thermal conductivity of superconducting, 20: 4361 (AD-619719)
Re–Sn, nuclear magnetic resonance in, (E), 20: 4476(R) (IS-1200 (Sect.P))
Re–Ta–W, tensile strength at 3500°F, 20: 4455(P)
Re–U, phase studies, 20: 4297(R) (IS-1200(Sect.M))
Re–W, deposition of, thermochemical, 20: 4342(R) (ORNL-3870, pp 85-101)
Re–W, extrusion of, process development for, 20: 4301(R) (ORNL-2870, pp 102-35)
Re–W, fabrication and properties of tubes of, 20: 4340(R) (COO-1518-1)
Re–Zr, properties at low temperatures, 20: 3920(R) (ORNL-3870, pp 27-37)

RHENIUM ISOTOPES Re-185
neutron reactions (n,γ) at 4 kev to 2.6 Mev, cross sections for, 20: 4868

RHENIUM ISOTOPES Re-187
neutron reactions (n,γ) at 4 kev to 2.6 Mev, cross sections for, 20: 4868

RHENIUM ISOTOPES Re-188
energy levels from neutron reactions (n,γ) with rhenium 187, 20: 4868

RHENIUM ISOTOPES Re-192
beta decay of, gamma spectra and half life in, (E), 20: 4861

RHENIUM OXIDES
properties, 20: 4297(R) (IS-1200(Sect.M))

RHODIUM
reactions with sulfur, 20: 3863(R) (IS-1200(Sect. C))
separation from silver by partition chromatography, 20: 4054

RHODIUM ALLOYS
Rh–Tb, crystallography of intermetallic compound $TbRh_2$, 20: 4391(R) (ORNL-3870, pp 75-82)

RHODIUM COMPLEXES
chloride, chemical properties of, tracer studies of, 20: 3966

RIBONUCLEIC ACID
content in spinach chloroplasts, 20: 3649 (UCRL-11475)
radiation effects on synthesis of, in *E. coli*, uv, 20: 3726
radiosensitivity effects in mice, gamma, 20: 3792

RIBONUCLEIC ACID, DESOXY-
content in spinach chloroplasts, 20: 3649 (UCRL-11475)
incorporation of phosphorus-32 in, 20: 3748
radiation effects on synthesis of, in normal and neoplastic rat tissues, tracer study, 20: 3701
radiation effects on synthesis of, tracer study, 20: 3702
radiation effects on synthesis of, in *E. coli*, uv, 20: 3726
radiation effects on replication of, effects of 5-bromodeoxyuridine on, 20: 3737
radiation effects on synthesis of, from incorporated phosphorus-32, 20: 3748
radiosensitivity effects in mice, gamma, 20: 3792

ROCKET REACTORS
control of, optimum, 20: 5187
propellants for, computer program for determining properties of hydrogen, 20: 5177 (LA-3381)

ROCKET REACTORS (TORY)
control rod actuator drive train for IIC, cooling of, 20: 5186 (UCRL-13095(Vol.2))
control rod actuator system of IIC, clutch and transmission for, 20: 5185 (UCRL-13095(Vol.1))
electric cables for IIC, testing of, 20: 5186 (UCRL-13095(Vol.2))
scram system for IIC, design of, 20: 5185 (UCRL-13095(Vol.1))
servo valve for IIC, refinement of electropneumatic, 20: 5185 (UCRL-13095(Vol.1))

ROCKETS
propulsion by antiproton annihilation reactions, feasibility study of, (T), 20: 4137

ROCKS
analysis for rare earths, thorium, and uranium by ion exchange, review on, 20: 3888 (TID-22402)
radioactivity of Swiss, petrographic–microscopic study of, 20: 4157(T) (ORNL-tr-702)
seismic wave propagation in, from surface nuclear explosions, 20: 4143 (AD-619969)

ROENTGEN UNITS
relation to absorbed energy in man, 20: 3816

ROOTS
radiation effects on *Allium cepa*, x, 20: 3764

ROTARY PUMPS
radiation effects on rotary element of, 20: 4999(R) (ORNL-2599)
radiation effects, 20: 4299(R) (ORNL-2711)

RUBBER
mechanical properties for shock pulse generation on impact shock machines, 20: 4112 (SC-TM-65-443)

RUBIDIUM
content in oceanic theoleitic basalts, 20: 4145
separation from traces of cesium by ion exchange, 20: 4056

RUBIDIUM CHLORIDES
$NiCl_2$–RbCl, spectra of nickel(II) in melts of, absorption, 20: 3921(R) (ORNL-3870, pp 56-60)

RUBIDIUM FLUORIDES
properties of molten, for use as reactor fuels, 20: 4376 (JUL-268-RG)

RUBIDIUM ISOTOPES Rb-84
use as tracer in clinical cardiology, 20: 3818

RUBIDIUM ISOTOPES Rb-85
use as tracer for measuring coronary blood flow by external and internal counting, 20: 3658(R) (EUR-2414.f,i)

RUBIDIUM ISOTOPES Rb-86
permeability into isolated frog heart of, 20: 3794
use as tracer in clinical cardiology, 20: 3818

RUBIDIUM ISOTOPES Rb-87
activity of, calibration of, 20: 4916
use as tracer for measuring coronary blood flow by external and internal counting, 20: 3658(R) (EUR-2414.f,i)

RUBIDIUM ISOTOPES Rb-88
decay scheme, 20: 3982(R) (AGN-8156)

RUBIDIUM TUNGSTATES
superconductivity, (E), 20: 4476(R) (IS-1200(Sect.P))

RUBIDIUM URANYL NITRATES
spectra of, infrared, 20: 3949

RUBIES
fluorescence in rods of, laser, 20: 4949(R) (UCRL-14360, pp 85-94)

RUMANIA
fallout monitoring, 20: 3654

RUSSIAN REACTORS
design of BN-350 fast-power, 20: 5137(T) (JPRS-31193)
development for heat and power, 20: 5149
ventilation systems of IRT-2000, efficiency of, 20: 5201

RUTHENIUM
diffusion from liquid uranium in containment mockup experiments, 20: 4184(R) (ORNL-3843, pp 71-135)

RUTHENIUM ALLOYS
Ru–Zr, properties at low temperatures, 20: 3920(R) (ORNL-3870, pp 27-37)

RUTHENIUM ISOTOPES Ru-102
energy levels, 20: 4883

RUTHENIUM ISOTOPES Ru-104
energy levels, 20: 4883

RUTHENIUM ISOTOPES Ru-106
content in Canadian biota, 20: 4161
content of, in brown algae of Solway Firth, 20: 3662 (PG-Report-650)
separation from fission products by distillation from oxidizing medium, 20: 3887 (PG-Report-677)

RUTIN
protective effects of derivative of, against radiation injuries of mucosa in cancer patients, 20: 3840

S

SAFETY
activities at Nuclear Safety Information Center Jan.–June 1965, 20: 4186(R) (ORNL-3843, pp 235-44)
policies and programs of, Euratom, 20: 4048(R) (NP-15406)
procedures for fuel element preparation and handling, 20: 4194
program of AEC, review, 20: 4188 (TID-22268)
research programs on nuclear, 20: 4182(R) (ORNL-3843)

SAFETY HAZARDS
assessment of Atlas-Centaur abort, 20: 4187 (SC-RR-65-333)
evaluation of, in radiological containment systems, 20: 4214
of radiography, survey of oral, 20: 3846

SALTS
radiation effects on, review of, 20: 4464

SAMARIUM
analysis for oxygen by neutron activation, 20: 3863(R) (IS-1200(Sect. C))
determination in hydrochloric acid or methanol–nitric acid media, spectrophotometric, 20: 3888 (TID-22402)

SAMARIUM ALLOYS
Sm–Zn, phase diagrams, 20: 4297(R) (IS-1200(Sect.M))
Sm–Ag, crystal structure of intermetallic compounds AgSm and Ag_5Sm in, 20: 4447
Sm–Sn, magnetic properties of, at 2 to 300°K, 20: 4423

SAMARIUM ISOTOPES Sm-144
proton reactions (p,n) at 10 Mev, europium-144 production from, (E), 20: 4887

SAMARIUM ISOTOPES Sm-145
energy levels of, parity and spin of, (E), 20: 4838 (JINR-P-2314)

SAMARIUM ISOTOPES Sm-152
energy levels, (E), 20: 4476(R) (IS-1200(Sect.P))
SAMARIUM ISOTOPES Sm-153
beta transitions in, polarization from, (E), 20: 4880
SAMARIUM OXALATES
magnetic susceptibility of hydrated, (E), 20: 3930
SAMARIUM OXIDES
Fe_2O_3–Sm_2O_3, crystal structure and magnetic properties, 20: 4411
SAMARIUM PERCHLORATES
magnetic susceptibility of hydrated, (E), 20: 3930
dioxane–$Sn(ClO_4)_3$, magnetic susceptibility of hydrated, (E), 20: 3930
SAMPLING
equipment and method for atmospheric sodium, 20: 4148 (AD-623515)
equipment for nuclear safety pilot plant, 20: 4184(R) (ORNL-3843, pp 71-135)
methods for radioiodine vapor, diffusion-tube, 20: 4185(R) (ORNL-3843, pp 169-234)
of iodine-131, in stack effluents using activated charcoal, 20: 4179 (LA-3363)
simulation of fixed-frequency, computer program for, 20: 4288 (SC-DR-65-312)
SANDS
analysis for moisture by neutron thermalization, 20: 3913(P)
SAP (SINTERED ALUMINUM PRODUCTS)
tensile tests on, computer analyses of, 20: 4371 (EUR-2514.e)
SAPPHIRES
corrosion by cesium at 400°C, 20: 4337
phonon detection in, bolometer for, 20: 4479(R) (TID-22179, pp 1-83)
SARCOMAS
radiation effects on DNA synthesis in rat Yoshida, tracer study, 20: 3701
radiation effects on tritiated-thymidine metabolism in Yoshida ascites, 20: 3702
SATELLITES
power plants for, design studies of, 20: 4299(R) (ORNL-2711)
radiation effects on electronic equipment in flashing light, 20: 4262 (NP-15610)
SAVANNAH RIVER COMPONENTS TEST REACTOR
control and safety rod drive systems for, performance of, 20: 5194 (DP-971)
criticality and startup testing of, (E), 20: 5193 (DP-967)
SAXTON POWER REACTOR
control of, chemical studies of soluble-poison, 20: 5134(R) (WCAP-3269-12)
coolant fission product levels in, (E/T), 20: 5134(R) (WCAP-3269-12)
fuel pellet temperature for Doppler broadening of uranium-238 resonance, 20: 5135 (WCAP-3269-40)
fuel rod testing in-pile, Zircaloy-4 clad, 20: 5134(R) (WCAP-3269-12)
power disturbances in, local, (E/T), 20: 5134(R) (WCAP-3269-12)
Zircaloy-4 corrosion and hydriding in, under conditions of heat transfer, 20: 4331
SCANDIUM
determination in hydrochloric acid or methanol–nitric acid media, spectrophotometric, 20: 3888 (TID-22402)
determination of, titrimetric methods for, 20: 3863(R) (IS-1200(Sect. C))
electric conductivity at 1.5 to 300°K, 20: 4297(R) (IS-1200(Sect.M))
nuclear magnetic resonance in, (E), 20: 4476(R) (IS-1200(Sect.P))
SCANDIUM ALLOYS
nuclear magnetic resonance in, (E/T), 20: 4476(R) (IS-1200(Sect.P))
SCANDIUM ISOTOPES Sc-44
production in potassium-41 (α,n) reactions, isomeric cross section ratios for, 20: 4922
SCANDIUM ISOTOPES Sc-46
use in silt movement analysis, 20: 4166 (AERE-R-4980)
SCATTERING
amplitude in two-particle, S-matrix existence from probability, 20: 4687
amplitudes for potential, asymptotic behavior of, (T), 20: 4849(R) (UCRL-14360, pp 1-50)
amplitudes for two-body, threshold sheet structure of, (T), 20: 4668
angular momenta in relativistic, complex, (T), 20: 4636
angular momenta in, group theoretical properties of complex, (T), 20: 4700
angular momentum in, complex, (T), 20: 4697
Green function for, multiple poles in, 20: 4662
potential, theory for, 20: 4701
S-matrix for singular potentials of, properties of, (T), 20: 4640 (IC/65/75)
S-matrix in unified theories of, singularities of, (T), 20: 4639 (IC/65/73)
theory for high energy, 20: 4636
theory for system of identical particles, nonrelativistic time-dependent, 20: 4655
theory of high-energy, (T), 20: 4696
theory of, general and relativistic, 20: 4475(R) (ANL-7081, pp 95-119)
unitarity integral for three-body, (T), 20: 4647 (TID-22274)
SCINTILLATION DETECTORS
design for tritium-in-air monitoring, 20: 4235 (AECL-2283)
design of well-type, for annular counting of low γ activity in large liquid volumes, 20: 3817
development of cadmium-loaded, for neutrinos, 20: 4847 (UCRL-12085(Pt.1))
performance for neutrino detection, 20: 4848 (UCRL-12085(Pt.2))
performance of, for whole-body counting of man, 20: 3805
pulse-height distribution from neutron capture and inelastic scattering, 20: 4999(R) (ORNL-2599)
response functions of gamma, 20: 5181(R) (ORNL-3029)
use for low-level plutonium determination, comparison of autoradiography with, 20: 3877 (LA-DC-7483)
use in determining transmutation of carbon-14-labeled fructose in liver, 20: 3684
use of liquid, in neutron spectrometers, 20: 4249 (UCRL-16311)
SEA WATER
analysis for calcium, use of calcium-45 as tracer in, 20: 3902
desalination of, computer program for cost, heat, and material balance calculations for conversion plants for, 20: 3923 (ORNL-TM-1299)
desalination of, reactor fuel element fabrication cost estimates for, 20: 5173(R) (ORNL-3870, pp 191-3)
model of oceans in Northern Hemisphere, 20: 4153(R) (UCRL-14360, pp 73-85)
separation of iron-55 and -59 from, by precipitation, 20: 3891(T) (CEA-tr-A-1838)
SEALING MATERIALS
development for use in space vehicles, 20: 4312
SEALS AND GLANDS
design of metal-metal oxide, for refractory vessel containing radioactive wastes, 20: 5209(P)
design of thermally compensated, for autoclaves, 20: 4087 (ORNL-TM-1293)
radiation effects on, in rotary pumps, 20: 4299(R) (ORNL-2711)
testing of face-type shaft, for high-temperature pumps, 20: 4299(R) (ORNL-2711)
SEED
radiation effects on wheat, genetic, 20: 3762
radiosensitivity of *Crotalaria intermedia*, effects of nitric oxide on, 20: 3759
SEISMIC WAVES
production by nuclear explosions in cavities, 20: 4167 (RM-3727(RAND))
propagation in rock from surface nuclear explosions, 20: 4143 (AD-619969)
SEISMOMETERS
design and performance of, with leaf-spring suspension, 20: 4216 (AWRE-O-70/65)
SELENIUM
content in chondrites, 20: 4526
photoconductivity of, sensitivity to x radiation, 20: 4999(R) (ORNL-2599)
use as catalyst in destruction of radioactive celluloses using sulfuric acid, 20: 5208(P)
SELENIUM ISOTOPES Se-75
incorporation in cystine of, 20: 3661 (NP-15594)
incorporation in methionine of, 20: 3661 (NP-15594)
SEMICONDUCTOR DETECTORS
amplifier for, design of high-pulse-rate, 20: 4243 (LAL-1102)
design and performance of field-effect transistor, 20: 4250 (UCRL-16446)
efficiency of sandwich, as fission-neutron spectrometer, (E), 20: 4238 (EUR-2487.e)
performance for neutron spectrometry in shielding rigs, (E), 20: 4997(R) (EUR-2494.d)
performance of silicon, for neutron spectrometry in shielding rigs, (E), 20: 4997(R) (EUR-2494.d)
properties of high resistivity silicon, 20: 4259(P)
use in high-energy accelerator experiments, 20: 4243 (LAL-1102)
use of silicon surface-barrier, in fast-neutron spectrometers, 20: 5181(R) (ORNL-3029)
SEMICONDUCTORS
electric conductivity of magnesium-base, effects of pressure on, (E/T), 20: 4476(R) (IS-1200(Sect.P))
electron energy losses in, characteristic, (T), 20: 5015
properties of, effects of low-temperature on, 20: 4417
radiation effects on, review of, 20: 4464
radiation effects on electric properties of, role of doping in, 20: 4265
radiation- and stress-induced defects in germanium-diode, 20: 4264
superconductivity in, (T), 20: 4781
use as pressure transducers, (E), 20: 5216 (SC-TM-65-457)
SEPARATION PROCESSES
development for spent power reactor fuels, 20: 4069
development of reductive chlorination, for low-grade ores, 20: 4072(P)
SERVOMECHANISMS

development for radiological containment systems, 20: 4214
SHELLS
creep-buckling of thin metal, at 1500°F, 20: 4299(R) (ORNL-2711)
creep-buckling of hemispherical copper, 20: 4299(R) (ORNL-2711)
deformation, stability, and vibration of, bibliography on, 20: 4079 (UCRL-13187)
elastic properties, 20: 4299(R) (ORNL-2711)
stress analysis of, derivation of equations for, 20: 4100 (BW-67-2(a))
stress distributions in, 20: 4999(R) (ORNL-2599)
thermal stability of thin-metal, 20: 4999(R) (ORNL-2599)
SHIELDED CONTAINERS
materials transfer from, to hot cells, 20: 4208
SHIELDING
analysis for space vehicles, cross sections for, 20: 5181(R) (ORNL-3029)
analysis of accelerator, 20: 4514 (UCRL-16445)
calculations for SNAP-7, 20: 4278 (MND-P-2229)
design of LCBWR, 20: 5106 (ACNP-65544(Vol.II))
development for radiological containment systems, 20: 4214
development of cement-iron mixtures for accelerator, 20: 4998 (JINR-P-2359)
gamma heating in stratified lead and water slabs, 20: 4999(R) (ORNL-2599)
neutron transmission by, angular distributions in, 20: 5181(R) (ORNL-3029)
radiation heating in laminated, 20: 4299(R) (ORNL-2711)
research for SNAP, review of, 20: 5183 (ORNL-P-1736)
SHIELDING MATERIALS
research at Geesthacht Reactor Station, (E), 20: 4997(R) (EUR-2494.d)
temperature distribution in gamma-radiation, (T), 20: 5002
SHIPPING
regulations for, of radioactive materials, 20: 4181 (NP-15620)
SHIPPINGPORT PRESSURIZED WATER REACTOR
coolant flow distribution in core 1 seed 4, 20: 5133 (WAPD-PWR-TS-151)
coolant flow instrumentation for core 1 seed 4, calibration of, 20: 5133 (WAPD-PWR-TS-151)
development and engineering summary for April 24–July 23, 1965, 20: 5132(R) (WAPD-MRP-113)
fuel burnup in, 20: 5132(R) (WAPD-MRP-113)
reactivity lifetime in core 1 seed 4, 20: 5133 (WAPD-PWR-TS-151)
reactivity of core 2 seed 1, 20: 5132(R) (WAPD-MRP-113)
thermocouple elements for core 1 seed 4, periodic calibration of, 20: 5133 (WAPD-PWR-TS-151)
SHOCK TUBES
flow properties in explosive-driven, for blast simulation, 20: 4708(R) (UCRL-14360, pp 50-73)
uses of water-filled, for analyses of reactor coolant-loss accidents, (E), 20: 5023(R) (IITRI-578P21-15)
SHOCK WAVES
diagnostics of, use of microwave techniques for, 20: 4934 (AD-619093)
effect of solar-wind, on geomagnetic storms, (T), 20: 4745
effects of solar wind, on geomagnetic storms, (T), 20: 4744
effects on circular cylinders, (E/T), 20: 4132 (AWRE-O-93/65)
effects on crystal structure of bismuth and potassium bromide, 20: 4708(R) (UCRL-14360, pp 50-73)
effects on electric conductivity of aluminum oxide and carbon tetrachloride, 20: 4708(R) (UCRL-14360, pp 50-73)
effects on magnetic properties of nickel ferrite, 20: 4708(R) (UCRL-14360, pp 50-73)
effects on piezoelectricity of Z-cut tourmalines, (E), 20: 5011
effects on sugar-pine wood and reactor pressure vessels, (E), 20: 5023(R) (IITRI-578P21-15)
electron density ionization rate and thermal equilibrium behind, 20: 4934 (AD-619093)
motion of solar type II radio wave production from, (T), 20: 4524
propagation in fluids, (T), 20: 4707 (UCRL-14318)
structure of collisionless, in magnetized hydrogen plasma, (E), 20: 4977
SILANE
germyl-, mass spectra and preparation of, 20: 3863(R) (IS-1200(Sect. C))
SILANE, ETHYNYL-
microwave spectra and structure of, isotope effects on, 20: 3977
SILANES
chloropropyl-, radioinduced formation of, calculation of basic parameters for, 20: 3993
SILICIDES
properties as coating for refractory metals, 20: 4418
reactions with liquid titanium, 20: 3929
SILICON
bremsstrahlung reactions (γ,π^0) at 166 Mev, angular distributions from, (E), 20: 4898
determination in boron by activation methods, 20: 3879(R) (MLM-1266)
electric quadrupole and magnetic dipole transitions for isoelectronic sequence of, 20: 4553
performance of semiconductor detectors of, for neutron spectrometry, (E), 20: 4997(R) (EUR-2494.d)
properties of pressure transducers of, (E), 20: 5216 (SC-TM-65-457)
properties of single-crystal, as gamma or charged particle detector, 20: 4259(P)
radiation effects on transistors of, (E), 20: 4261 (AD-623078)
radiation effects on gain degradation in transistors of, effects of operating conditions on, 20: 4267
radioinduced defects in, electron, (E), 20: 4508(R) (RPI-328-40)
SILICON CARBIDES
properties as barrier shell for thermionic energy converters, (E), 20: 4359(R) (AD-618923)
SILICON CHLORIDES
radiation effects on aerosols of, x, 20: 4015
SILICON ISOTOPES
effects on microwave spectra and structure of ethynylsilane, 20: 3977
SILICON ISOTOPES Si-28
alpha elastic scattering at 28.5 Mev, optical potentials in, (E/T), 20: 4859
SILICON JUNCTIONS
radiation effects on diode, fast neutron, 20: 4999(R) (ORNL-2599)
SILICON OXIDES
radiation effects on aerosols of, x, 20: 4015
radiation effects on phase transformations in, neutron, 20: 4462
Gd_2O_3–SiO_2–Na_2O, glass forming temperature of, 20: 4077(R) (IS-1200 (Sect. E))
SILICON SYSTEMS
Al–Cr–Si–Ti–V, properties of aged, 20: 4360(R) (AD-619399)
B–Ni–Si, brazing alloy for tungsten carbide–cobalt cermet to TZM molybdenum alloy, 20: 4307(R) (ORNL-3870, pp 238-42)
Fe–Si, plastic deformation of, effects of atomic order on, 20: 4297(R) (IS-1200(Sect. M))
Fe–Si, properties of Cubex for use in space electric power systems, 20: 4379 (NASA-CR-54091)
SILICONE RUBBERS
properties of, effects of low temperature on, 20: 4417
SILICONES
radioinduced addition to textiles, for waterproofing, 20: 4033
SILICOÖRGANIC COMPOUNDS
radiation effects on, EPR study of, 20: 4012
SILTS
analysis for rare earths, thorium, and uranium by ion exchange, review on, 20: 3888 (TID-22402)
movement in Oxcars spoil ground, Firth of Forth, England, use of scandium-46 for, 20: 4166 (AERE-R-4980)
SILVER
determination in platinum by neutron activation, 20: 3863(R) (IS-1200 (Sect. C))
effects on copper oxidation, 20: 4320(R) (ORNL-3870, pp 70-4)
electron energy losses in, characteristic, (T), 20: 5015
electron scattering by films of, differential cross sections for multiple, (E), 20: 4485
electron scattering by, surface plasmon excitation radiation from, (E), 20: 5017
fission fragment ranges in, 20: 3982(R) (AGN-8156)
radiation effects on lead diffusion in, alpha, 20: 4385(R) (ORNL-3870, pp 15-19)
separation from other elements by partition chromatography, 20: 4054
thickness measurement by alpha energy degradation, 20: 3982(R) (AGN-8156)
Li–Ag, thermal conductivity, 20: 5181(R) (ORNL-3029)
Sm–Ag, crystal structure of intermetallic compounds AgSm and Ag_3Sm in, 20: 4447
SILVER ALLOYS
Ag–Tb–Y, crystallography, 20: 4391(R) (ORNL-3870, pp 75-82)
In–Ag–Tb, crystallography, 20: 4391(R) (ORNL-3870, pp 75-82)
La–Ag, vaporization of, mass spectrometric studies of, 20: 3957
La–Ag–Tb, crystallography, 20: 4391(R) (ORNL-3870, pp 75-82)
Pb–Ag, thermodynamic properties of, 20: 5223 (UCRL-16303)
Pd–Ag–Tb, crystallography, 20: 4391(R) (ORNL-3870, pp 75-82)
rare earth–Ag, magnetic properties and structure, 20: 4448
SILVER BROMIDES
thermodynamic properties in *N,N*-dimethylformamide and *N*-methylformamide solutions, 20: 3924 (TID-22366)
SILVER CHLORIDES
electric conductivity of crystalline, 20: 3863(R) (IS-1200(Sect. C))
SILVER HALIDES
space charge calculations, (E/T), 20: 4476(R) (IS-1200(Sect. P))
SILVER IODIDES
stability of, thermal, 20: 4185(R) (ORNL-3843, pp 169-234)
thermodynamic properties in *N,N*-dimethylformamide and *N*-methylformamide solutions, 20: 3924 (TID-22366)
SILVER ISOTOPES Ag-109

energy level transitions in, gamma spectra from, (E), 20: 4476(R) (IS-1200(Sect.P))
SINGLE CRYSTALS
growth by Verneuil method, 20: 3919(R) (ORNL-3870, pp 3-6)
preparation of bismuth and gadolinium, 20: 4077(R) (IS-1200(Sect. E))
preparation of high-melting, equipment for, 20: 4077(R) (IS-1200(Sect. E))
SIOUX FALLS POWER REACTOR
criticality studies, (E), 20: 5107(R) (ACNP-66589)
SKELETON
metabolism of, tracer studies in man during health and disease, 20: 3664(R) (TID-22324)
mineral changes in, use of iodine-125 in x-ray unit for measuring, 20: 3803 (ORNL-IIC-5, pp 257-76)
mineral content in, x-ray transmission measurement of, 20: 3886 (ORNL-IIC-5, pp 290-4)
SKIN
photosensitivity of, relation to uv sensitivity, 20: 3767
radiation effects of post-operative doses of gamma and x, used for breast carcinoma, 20: 3847
radiation effects on, cosmic, 20: 3731
radiation effects on herpes zoster inflammations in, x, 20: 3836
radiation effects on swine, effects of dose fractionation on fast neutrons and x, 20: 3735
radiosensitivity of, effects of oxygen pressure on, β, 20: 3727
SKIN GRAFTING
use for repair of radiation injuries, 20: 3724
SKIN LESIONS
pathology of radioinduced, 20: 3724
radiotherapy of benign, x, 20: 3812
SLUG ELEMENTS
canning apparatus for, design of, 20: 5029(P)
SMOKES
effects of chronic exposure to cigarette, on pulmonary clearance in dogs, 20: 3655 (BNWL-SA-224)
radiation effects on pyrolytic products of, from irradiated cigarettes, 20: 3984 (ORO-633)
SODIUM
analysis for impurities, evaluation of methods for, 20: 3880(R) (MSAR-65-150)
analysis for oxygen, operating manual for gas analyzer for, 20: 3889 (UNC-5113)
content in atmosphere and on beaches, effects of weather on, 20: 4148 (AD-623515)
corrosive effects on stainless steel and other structural materials, review on, 20: 4318 (CNLM-5359)
determination by flame photometry, 20: 4053
determination in tungsten bronze, spectrographic, 20: 3863(R) (IS-1200 (Sect. C))
flowmeters for, calibration of magnetic, 20: 4077(R) (IS-1200(Sect. E))
handling of liquid, 20: 4330(T) (ORNL-tr-854)
properties of, effects of low temperature on, 20: 4417
pump for, design of induction, 20: 4077(R) (IS-1200(Sect. E))
reactions with water, effects on design of steam generators, 20: 4100 (BW-67-2(a))
reactor criticality effects on plutonium–thorium and plutonium–uranium fueled fast reactors, 20: 5068
sampling of atmospheric, device for, 20: 4148 (AD-623515)
separation from other metal chlorides by ion exchange, 20: 4053
surface tension of, effects of oxygen on, 20: 3880(R) (MSAR-65-150)
technology of liquid, review on, 20: 4330(T) (ORNL-tr-854)
SODIUM ACETATES
polyethylene–sodium acetate, determination of fractional composition by x-ray beam attenuation measurements, 20: 3885 (ORNL-IIC-5, pp 277-89)
SODIUM ALLOYS
K–Na, corrosive effects on niobium and niobium–zirconium alloy, 20: 5181(R) (ORNL-3029)
K–Na, corrosive effects on stainless steel and other structural materials, review on, 20: 4318 (CNLM-5359)
K–Na, corrosive effects on niobium–1 zirconium and type 316 stainless steel, 20: 4323(R) (ORNL-3870, pp 308-11)
K–Na, corrosive effects on Croloy 9M, INOR-8, and type 347 stainless steel, 20: 4322(R) (ORNL-3870, pp 305-7)
SODIUM BROMIDES
thermodynamic properties in *N*-methylformamide solutions, 20: 3924 (TID-22366)
thermodynamic properties in anhydrous *N*-methylformamide solutions, 20: 3925 (TID-22366, App. B)
thermodynamics of, in anhydrous *N,N*-dimethylformamide and *N*-methylformamide at 25°C, 20: 3926 (TID-22374)
SODIUM CHLORIDES
effects on radiation stability of thiamine hydrochloride, 20: 4018
thermodynamic properties in *N,N*-dimethylformamide and *N*-methylformamide solutions, 20: 3924 (TID-22366)
thermodynamic properties in anhydrous *N*-methylformamide solutions, 20: 3925 (TID-22366, App. B)
thermodynamics of, in anhydrous *N*-methylformamide at 25°C, 20: 3926 (TID-22374)
$AlCl_3$–Bi–NaCl, spectra of reaction products of, absorption, 20: 3921(R) (ORNL-3870, pp 56-60)
$AlCl_3$–NaCl, density equations for molten, 20: 3921(R) (ORNL-3870, pp 56-60)
Bi–NaCl–$ZnCl_2$, spectra of reaction products of, absorption, 20: 3921(R) (ORNL-3870, pp 56-60)
$MgCl_2$–KCl–NaCl, separation from rare earth fission products by solvent extraction using magnesium alloys, 20: 3865 (ANL-7064)
$NiCl_2$–NaCl, spectra of nickel(II) in melts of, absorption, 20: 3921(R) (ORNL-3870, pp 56-60)
SODIUM FLUORIDES
properties of molten, for use as reactor fuel, 20: 4376 (JUL-268-RG)
thermodynamic properties in *N,N*-dimethylformamide and *N*-methylformamide solutions, 20: 3924 (TID-22366)
SODIUM HYDRIDES
Na–NaH–NaOH, corrosive effects on Croloy 2¼, 20: 4317 (BAW-1280-30)
SODIUM HYDROXIDES
corrosive effects of aqueous solutions of, on Croloy 2¼, 20: 4317 (BAW-1280-30)
corrosive effects on Croloy, 20: 4100 (BW-67-2(a))
solvent properties for aluminum, 20: 4048(R) (NP-15406)
Na–NaH–NaOH, corrosive effects on Croloy 2¼, 20: 4317 (BAW-1280-30)
Na–NaOH, corrosive effects on Croloy 2¼, 20: 4317 (BAW-1280-30)
SODIUM IODIDES
response of crystals of, to gamma radiation, 20: 5181(R) (ORNL-3029)
response of crystals of, to photons, 20: 4299(R) (ORNL-2711)
response of thallium-activated, to electrons, 20: 5181(R) (ORNL-3029)
thermodynamics of, in anhydrous *N,N*-dimethylformamide and *N*-methylformamide at 25°C, 20: 3926 (TID-22374)
SODIUM ISOTOPES Na-22
beta transitions in, comparative half lives of $\Delta I = 3$, (T), 20: 4874
content in Canadian biota, 20: 4161
use as tracer, for skeletal metabolism studies, 20: 3664(R) (TID-22324)
SODIUM MOLYBDATES
$H_4Fe(CN)_6$–Na_2MoO_4, ion exchange properties for cesium-137 and strontium-90, 20: 3871 (EUR-2497.e)
SODIUM NITRATES
radioinduced paramagnetic centers in, 20: 3988
SODIUM OXIDES
Gd_2O_3–SiO_2–Na_2O, glass forming temperature of, 20: 4077(R) (IS-1200 (Sect. E))
SODIUM SYSTEMS
Na–NaH–NaOH, corrosive effects on Croloy 2¼, 20: 4317 (BAW-1280-30)
Na–NaOH, corrosive effects on Croloy 2¼, 20: 4317 (BAW-1280-30)
SODIUM THIOSULFATES
effects on permeation of rubidium-86, in x-irradiated isolated frog heart, 20: 3794
SODIUM TUNGSTATES
electron spin resonance in, (E/T), 20: 4476(R) (IS-1200(Sect.P))
enthalpies at 80 to 300°C, 20: 4297(R) (IS-1200(Sect.M))
properties of, electronic, (E/T), 20: 4476(R) (IS-1200(Sect.P))
thermal capacity, (E), 20: 4476(R) (IS-1200(Sect.P))
$H_4Fe(CN)_6$–Na_2WO_4, ion exchange properties for cesium-137 and strontium-90, 20: 3871 (EUR-2497.e)
$Na_6(H_2W_{12}O_{40})$–Na_2WO_4, isotopic exchange in, 20: 3863(R) (IS-1200 (Sect. C))
SOILS
effects on strontium-90 uptake by agricultural plants, 20: 3679
nutrient distribution in, tracer studies, 20: 3710(R) (EUR-2493.e)
properties of, effects on enrichment of forage vegetation by cesium-137 and strontium-90, 20: 3665(T) (CEA-tr-X-619)
radiation effects on moisture content of, in forests, 20: 3653 (BNL-8466)
radiation monitoring in German, 1965, 20: 4164
radioactivity of, effects on incidence of stomach cancer in population of region, 20: 4197
SOLAR FLARES
effects on interplanetary magnetic fields, (E), 20: 4527
effects on materials in space vehicles, 20: 4312
SOLAR RADIATION
effects on lower ionospheric ionization, (E), 20: 4737
frequency harmonic structure and band splitting of type II r-f, (T), 20: 4524
interactions with interplanetary magnetic fields, 20: 4529
shock wave production in wind, effects on geomagnetic storms, (T), 20: 4744
structure of fast streams of, correlation with geomagnetic storm, (T), 20: 4745
SOLENOIDS

design for strong fields for adiabatic demagnetization, 20: 4489
design of superconducting, for operation at 1°K, 20: 4775 (UCRL-16376)
SOLID PROPELLANTS
radiation effects on, bibliography on, 20: 4461 (REIC-Memo-28)
SOLIDS
charged-particle tracks in, ion-explosion spike mechanism for, 20: 4548
diffusion of gases in, least-square determination of coefficient of, 20: 4377 (NAA-SR-Memo-10741)
diffusion of gases in, computer program for graphic display of coefficients of, 20: 4377 (NAA-SR-Memo-10741)
electron reactions with vacuum-contained, transition radiation from, (E/T), 20: 5008(T) (ORNL-tr-872)
equation of state of simple, 20: 4476(R) (IS-1200(Sect.P))
neutron scattering in, spectra from, (E), 20: 4476(R) (IS-1200(Sect.P))
phase transitions of repulsive lattice gas models, 20: 4708(R) (UCRL-14360, pp 50-73)
radioinduced defects in, scattering law for, 20: 4473
tensile properties of, review on, 20: 4399 (UCRL-16301)
thermal diffusion in, using flash-diffusivity technique, 20: 4310(R) (ORNL-P-1699)
SOLVENT EXTRACTION PROCESSES
development for plutonium and uranium recovery from spent fuels, 20: 4048(R) (NP-15406)
solvents for, properties of tertiary phosphine oxides as, 20: 3863(R) (IS-1200(Sect. C))
SOLVENTS
properties and structure of organophosphorus, 20: 3863(R) (IS-1200 (Sect. C))
SOUND
propagation, 20: 4153(R) (UCRL-14360, pp 73-85)
SOUTHWEST EXPERIMENTAL FAST OXIDE REACTOR
development, 20: 5120(R) (GEAP-4799)
SOVIET UNION
health physics programs in, instrumentation for, 20: 4198
SPACE
cosmic ray variations in interplanetary, (E/T), 20: 4522 (CNIE-PE-5)
properties of interplanetary, (E/T), 20: 4522 (CNIE-PE-5)
SPACE FLIGHT
development of manned exploratory, 20: 4525
SPACE VEHICLES
book: *Space Materials Handbook*, 20: 4312
instrumentation for cosmic ray intensity measurements, 20: 4252(T) (FTD-TT-64-1228)
power plants for, design studies of, 20: 4299(R) (ORNL-2711)
power supplies for, liquid metal MHD cell, 20: 4573
power systems for, design problems of, 20: 4999(R) (ORNL-2599)
SPAIN
electric power production and distribution in, 20: 4081
SPANISH REACTORS (JEN-1)
fuel elements for, design of pilot plant for reprocessing, 20: 4066
SPARK CHAMBERS
electrodes of, electrostatic field around, (T), 20: 4241 (JINR-P-2364)
SPECIFIC HEAT
measurement by pulse heating, circuit diagram for, 20: 4388(R) (ORNL-3870, pp 44-9)
SPECTROMETERS
operation of magnetic, sensitive to weak transverse static fields, (E/T), 20: 4255
SPECTROPHOTOMETERS
design for glove boxes, 20: 4048(R) (NP-15406)
SPECTROSCOPY
development for monitoring fissiochemical reactions, 20: 3982(R) (AGN-8156)
development of emission, for analytical uses, 20: 3863(R) (IS-1200 (Sect. C))
light sources for atomic absorption, performance of spectral continua as, 20: 3863(R) (IS-1200(Sect. C))
research on nuclear, (T), 20: 4475(R) (ANL-7081, pp 95-119)
SPERM
radiosensitivity of mouse, effects of genotype on, 20: 3711(R) (NYO-3314-2)
SPHERES
radiation dosimetry in, electrons, 20: 4204
SPINAL CORD
radioinduced myelitis in human, x, 20: 3771
SPLEEN
growth of bone marrow transplants in dog, 20: 3652
metabolism of colloids of gold-198 in, 20: 3822
radiation effects on exteriorized rat, x, 20: 3775
radiation effects on exteriorized rabbit, x, 20: 3775
SPONTANEOUS FISSION
half life of, from superfluid model, (T), 20: 4876
SPORES
radiation effects on germination of *Funaria hygrometrica*, 20: 3781
SPRAYS
powder feeder for ultrafine particles, development of arc, 20: 4298 (LA-DC-7275)
SPUTTERING
research using mass spectrometry, 20: 4215(R) (ANL-7081, pp 134-49)
SQUIRRELS
sodium-22 content in muscles of Canadian, 20: 4161
STABLE ISOTOPES
separation of economics of cascade, 20: 4284(T) (CEA-tr-X-617)
STACK DISPOSAL
iodine-131 monitoring of, for efficiency of activated charcoal, 20: 4179 (LA-3363)
STAINLESS STEEL
brazing stainless-steel-clad copper fins to tubes of, technique for, 20: 4307(R) (ORNL-3870, pp 238-42)
corrosion by acidic solutions, effects of molybdenum and uranium on, 20: 4325 (TB-58)
corrosion by boiling potassium, effects on mechanical properties, 20: 5181(R) (ORNL-3029)
corrosion by cesium at 400°C, 20: 4337
corrosion by potassium–sodium alloys and sodium, review on, 20: 4318 (CNLM-5359)
corrosion by water at 515°F, 20: 5134(R) (WCAP-3269-12)
corrosion failure in calcium, lithium, and magnesium chlorides, stress, 20: 4328 (WCAP-3269-50)
corrosion of chrome-plated, by water at 515°F, 20: 5134(R) (WCAP-3269-12)
corrosion of type 318, by lithium fluoride in cyclic high-temperature environment, 20: 4326 (TRW-ER-6561)
corrosion of type 316, by potassium at 870°C, 20: 4307(R) (ORNL-3870, pp 238-42)
corrosion of type 304, by fused fluoride salts, 20: 4308(R) (ORNL-3870, pp 243-60)
corrosion of type 410, by lead at 1215°F, 20: 4308(R) (ORNL-3870, pp 243-60)
corrosion of type 347, by potassium–sodium, effects of hydrogen and oxygen on, 20: 4322(R) (ORNL-3870, pp 305-7)
corrosion of type 316, by potassium–sodium eutectic, 20: 4323(R) (ORNL-3870, pp 308-11)
emissivity of type 316, commercial coating for improving, 20: 4307(R) (ORNL-3870, pp 238-42)
fabrication and properties of Types 304 and 347, for stress corrosion cracking tests, 20: 4370 (CEND-3256-250)
mechanical properties of 316, effects of lithium on, 20: 4299(R) (ORNL-2711)
neutron cross sections for 304, 20: 4829 (GEMP-173(Suppl.1))
properties of, effects of low temperature on, 20: 4417
radiation effects on stress-rupture properties of 304, 20: 5181(R) (ORNL-3029)
radioinduced embrittlement of type 304, effects of boron on neutron, 20: 4460(R) (ORNL-3870, pp 140-5)
radioinduced embrittlement of, effects of grain size on neutron, 20: 4460(R) (ORNL-3870, pp 140-5)
radioinduced embrittlement of types 304 and 304L, at 650 to 842°C, neutron, 20: 4460(R) (ORNL-3870, pp 140-5)
radioinduced embrittlement of type 304, effects of grain boundary carbides on neutron, 20: 4460(R) (ORNL-3870, pp 140-5)
radioinduced embrittlement of type 304, effects of titanium additions on neutron, 20: 4460(R) (ORNL-3870, pp 140-5)
reactions with europium molybdate, 20: 4305(R) (ORNL-3870, pp 187-90)
reactions with steam and water at high temperatures, 20: 4183(R) (ORNL-3843, pp 2-70)
removal from fuel elements by sulfex process, 20: 4048(R) (NP-15406)
rupture properties of niobium-stabilized austenitic, effects of heat treatments on, 20: 4306(R) (ORNL-3870, pp 194-213)
sorptive properties for cesium, 20: 4185(R) (ORNL-3843, pp 169-234)
wetting by bismuth–lead eutectics, 20: 4077(R) (IS-1200(Sect. E))
PuO_2–stainless steel, performance as fast-reactor driver fuel, (E), 20: 5192 (BNWL-SA-251)
PuO_2–stainless steel–UO_2, radiation effects on, in-pile, (E), 20: 5192 (BNWL-SA-251)
PuO_2–stainless steel, radiation effects on, in-pile, (E), 20: 5192 (BNWL-SA-251)
stainless steel–UO_2, radiation effects on, in-pile, (E), 20: 5192 (BNWL-SA-251)
STARK EFFECT
use in measuring molecular dipole moments, 20: 3958
STARS
energy spectra of neutron, at absolute zero temperature, (T), 20: 4531
neutrino and nuclear processes in, (T), 20: 4534
neutrino-cooling and observability of neutron, (T), 20: 4532
nuclear beta decay in interiors of, photon-induced, (T), 20: 4530

properties of, review of, (T), 20: 4533
STATISTICS
central force problems in, 20: 4488
STEAM
reactions in plutonium and uranium tetrafluorides, 20: 4046(R) (EURAEC-1340)
reactions with liquid urania in TREAT, 20: 4183(R) (ORNL-3843, pp 2-70)
air–steam, iodine sorption from, by charcoal, 20: 4086(R) (ORNL-3843, pp 137-67)
steam-water, heat flux dryout in internally heated annuli, (E), 20: 4099 (AECL-2332)
STEAM GENERATING HEAVY WATER MODERATED REACTOR
description, 20: 5163
design, 20: 5142
STEEL
analysis by x-ray fluorescence using promethium-147/aluminum source, 20: 3883 (ORNL-IIC-5, pp 154-81)
analysis for carbon by gamma spectroscopy, 20: 3894
analysis for impurities, spectrographic, 20: 3863(R) (IS-1200(Sect. C))
corrosion by cesium at 400°C, 20: 4337
creep rupture properties of welded HT70, in pressure vessels at 500 to 1350°C, 20: 4446
properties of, effects of substructure on mechanical and tensile, 20: 4372(R) (GA-6724)
radiation effects on nil ductility temperature and stress wave attenuation of, methods for determining, 20: 4457(R) (EURAEC-1474)
radiation effects on austenitic and ferritic, fission-fragment, 20: 4469
tensile strength of soft, 20: 4365 (AES-3)
STELLARATORS (C)
ion cyclotron wave production in deuterium-hydrogen plasma in, optimum, (E/T), 20: 4984
plasma losses from heating in, (E), 20: 4942 (MATT-372)
STERILITY
radioinduced in Mexican fruit flies, effects of dose on gamma, 20: 3745
STEROIDS
use for therapy of bone marrow failure induced by anemia or leukemia, 20: 3793
STILBENE, 4,4'-DIPHENYL-
radioinduced fluorescence of, in naphthalene, 20: 3994
STOMACH
cancer etiology in, 20: 4197
radiation effects on absorption of fatty acids in, tracer study, x, 20: 3754
STRAIN GAGES
design for studying strain anisotropy in Zircaloy-2 tubing, 20: 4304(R) (ORNL-3870, pp 171-83)
design of semiconductor, analysis for, (E), 20: 5216 (SC-TM-65-457)
STRANGE PARTICLES
interactions of, weak, (T), 20: 4634
STRATOSPHERE
eddy fluxes and biennial oscillations in, 20: 4150 (MIT-2241-7)
isobaric height conditions and wind temperature in, during IGY, 20: 4151 (MIT-2241-14)
STRESS ANALYSIS
computer program for, of composite bodies of revolution, 20: 5033 (GA-6588)
formulas for, of thick-wall cylinders, 20: 4076 (HIC-1-1564-3(Vol.2))
of conical, cylindrical, and spherical shells, 20: 4999(R) (ORNL-2599)
of heat exchangers for sodium-cooled reactors, 20: 5131(R) (UNC-5135)
STRONTIUM
content and ratio of strontium-87 to strontium-86 in oceanic theoleitic basalt, 20: 4145
determination by flame photometry, 20: 4053
diffusion from liquid urania in containment mockup experiments, 20: 4184(R) (ORNL-3843, pp 71-135)
intestinal absorption of, tracer study in rats, 20: 3669
separation from other metal chlorides by ion exchange, 20: 4053
separation from sulfate-containing waste solutions, 20: 5210(P)
STRONTIUM ALLOYS
Ni–Sr, phase studies, 20: 4442
STRONTIUM ISOTOPES Sr-85
binding of, by blood serum proteins, 20: 3697
use as tracer, for diagnosis of bone tumors, 20: 3805
STRONTIUM ISOTOPES Sr-89
content in sintered uranium dioxide pellet, radial distribution of, 20: 4472
distribution in food chain of, effects of transfer from food to milk of cattle, 20: 4162
metabolism by cattle of, effects of diet on, 20: 4162
metabolism by rat bones, effects of sodium alginates on, 20: 3671
separation from reservoir water by phosphate precipitation, 20: 4068
STRONTIUM ISOTOPES Sr-90
bremsstrahlung excitation by, in thin absorbers, 20: 5000 (ORNL-IIC-5, pp 91-8)
content in deciduous teeth, United States, 20: 4160
content in sintered uranium dioxide pellet, radial distribution of, 20: 4472
determination in drinking water, method for, 20: 3867 (CEA-R-2844)
distribution in food chain of, effects of transfer from food to milk of cattle, 20: 4162
metabolism by cattle of, effects of diet on, 20: 4162
metabolism by forage plants of, effects of soil type and fertilizers on, 20: 3665(T) (CEA-tr-X-619)
metabolism by *Nerita forskali*, 20: 3659(R) (NP-15156)
separation from other fission products by ion exchange, 20: 3871 (EUR-2497.e)
separation from reservoir water by coagulation with aluminum and iron and fast filtration, 20: 4068
separation from waste solutions using manganese dioxide, 20: 5206
uptake by agricultural plants of, effects of species, soil type, and agronomy practices on, 20: 3679
uptake by maize, effects of soil temperature on, 20: 3668
STRONTIUM SULFIDES
vaporization of, mass spectrometric studies of, 20: 3957
STRONTIUM TITANATES
superconductivity in, (T), 20: 4781
STRUCTURAL BEAMS
vibrations in, effects of water on natural frequency of, 20: 4080 (WAPD-TM-535)
STRUCTURES
blast effects from Salmon event on residential-type, 20: 4189 (VUF-1030)
blast effects from Salmon event on tall industrial and residential, 20: 4190 (VUF-1031)
STYRENE
radioinduced luminescence of, effects of methylmethacrylate on, 20: 4001
radioinduced polymerization with methylmethacrylate, 20: 4001
acrylonitrile–styrene, radioinduced graft copolymerization with chloroethylene, 20: 4038
STYRENE POLYMERS
radiation effects on EPR spectra of, 20: 4479(R) (TID-22179, pp 1-83)
SUCROSE
radiation effects on crystal structure and melting point, 20: 4020
SULFATE IONS
effects on determination of uranium(VI) in presence of uranium(IV), 20: 3903
SULFATES
effects on spectrophotometric determination of zirconium, 20: 3895
SULFEX PROCESS
development, 20: 4048(R) (NP-15496)
SULFIDES
reactions with liquid titanium, 20: 3929
sulfur-35 exchange with thiopene, 20: 3976
SULFONATES
radioinduced degradation of detergent, 20: 4025
SULFUR
bremsstrahlung reactions (γ,π^0) at 166 Mev, angular distributions from, (E), 20: 4898
determination in terphenyl by activation methods, 20: 3873 (EUR-2523.i)
diffusion in CGB graphite at 150°C, 20: 4308(R) (ORNL-3870, pp 243-60)
electric quadrupole and magnetic dipole transitions for isoelectronic sequence of, (T), 20: 4553
reactions with rhodium and zirconium, 20: 3863(R) (IS-1200(Sect. C))
sulfur-35 exchange with thiopene, 20: 3976
yields from radiolysis of hydrogen sulfides, 20: 4017
yields from radiolysis of carbon disulfide, 20: 4028
SULFUR DIOXIDES
reactions with uranium hexafluoride, kinetics of, 20: 3935
SULFUR ISOTOPES S-35
determination in radioisotope mixtures, microcalorimetric, 20: 3866 (CEA-R-2630)
exchange between elementary sulfur or sulfides and thiopene, 20: 3976
exchange between sulfuryl and thionyl chlorides, 20: 3965
SULFURIC ACID
corrosive effects on stainless steel, effects of molybdenum and uranium on, 20: 4325 (TB-58)
separation of titanium and zirconium from, by solvent extraction using organic solvents, 20: 4061
solvent properties for magnesium alloys and stainless steel, 20: 4048(R) (NP-15406)
use in destruction of radioactively contaminated celluloses, 20: 5208(P)
$HF–H_2SO_4$, solvent properties for zirconium, 20: 4055
SULFURYL CHLORIDE
chlorine-36 exchange with antimony pentachloride, 20: 3965

sulfur-35 exchange with thionyl chloride, 20: 3965
SUN
activity data for June 1965, 20: 4750
activity of, distribution of burst, 20: 4521 (AD-618222)
chromosphere of, structure of, 20: 4528
effects on cosmic ray anisotropy, upper limiting primary rigidity for, 20: 4563
magnetic field strength above photosphere, (T), 20: 4524
shock structure in M region disturbances of, correlation with geomagnetic impulse pairs, 20: 4758
SUPERCONDUCTIVITY
destruction in tin, magnetic induction distribution in, (E), 20: 4794
theory for alloys, review of, (T), 20: 4791
theory for, in nonmetallic systems, (T), 20: 4781
theory of, review of, 20: 4789
SUPERCONDUCTORS
critical current measurement in, method for, 20: 4390(R) (ORNL-3870, pp 65-9)
critical currents in, (T), 20: 4791
critical currents of alloy, method for increasing, 20: 4799(P)
domain structure instabilities in intermediate state of, 20: 4783
electron pairing and flux quantization in cylindrical, (T), 20: 4784
energy gap in lead, 20: 4782
fluxoid structure in films of, (T), 20: 4777
magnetic flux jumps and trapping in Nb_2Sn, (E), 20: 4793
magnetic induction distribution with temperature in superconductivity destruction in tin, (E), 20: 4794
magnetic transitions of thin-film, 20: 4785
ordering magnetic ions in, (E/T), 20: 4476(R) (IS-1200(Sect.P))
performance in solenoids for strong magnetic fields, 20: 4486
properties of high-purity niobium, 20: 4774 (IS-T-22)
properties of indium and tin whiskers, 20: 4795
properties of magnetic-impurity containing, (E/T), 20: 4476(R) (IS-1200(Sect.P))
properties of niobium–zirconium alloys, (E), 20: 4792
specific heat of gapless, (E), 20: 4476(R) (IS-1200(Sect.P))
structure of intermediate state and surface energy of indium, 20: 4778
theory for alloy, review of, (T), 20: 4791
thermal capacity of type II, in magnetic fields, 20: 4786
thermal equilibrium for, (T), 20: 4789
use in bolometer design, 20: 4229
SUPERFLUIDITY
properties of helium-3, 20: 4773 (COO-1198-306)
theory, 20: 4772
theory, 20: 4789
SUPERHEATERS (NUCLEAR)
fuel elements for, testing in E-SADE loop of VBWR, 20: 5104 (ACNP-65006)
SUPERSONIC FLOW
around blunt bodies, 20: 4153(R) (UCRL-14360, pp 73-85)
SURFACE PROPERTIES
research on, at Ames laboratory, 20: 3863(R) (IS-1200(Sect. C))
SURFACE WATERS
silt movement in Oxcars spoil ground, Firth of Forth, England, use of scandium-46 for, 20: 4166 (AERE-R-4980)
wave production by travelling pressure in shallow, 20: 4153(R) (UCRL-14360, pp 73-85)
SURFACES
reactions on metal, equipment for study of, 20: 3863(R) (IS-1200(Sect. C))
SURGERY
effects of preirradiation on results of, for breast tumor, 20: 3861
SUSPENSIONS
radioactivity measurements in, scintillation method for, 20: 3870 (EUR-2459.f)
SWEDEN
survey of oral radiography practices in, 20: 3846
SWEDISH REACTORS (R-3)
materials procurement aspects of, review, 20: 5110 (AES-4)
SWIMMING POOL REACTORS
coolant analysis for fission products in, design of monitor for, 20: 3909
research progress at NORA, 20: 5060(R) (TID-22357)
ventilation systems of IRT-2000, efficiency of, 20: 5201
SWINE
radiation effects on skin of, effects of dose fractionation on fast neutron and x, 20: 3735
radiation effects on behavior traits in, genetic analysis of, 20: 3784
radiography of knuckle of, for estimation of ham composition in slaughtered animals, 20: 5224
SWITZERLAND
radioactivity of rocks in, petrographic–microscopic study of, 20: 4157(T) (ORNL-tr-702)
SYENITES
radioactivity of Swiss, petrographic–microscopic study of, 20: 4157(T) (ORNL-tr-702)
SYNCHROCYCLOTRONS
beam separation in JINR, proton-antiproton, 20: 4496 (JINR-P-2375)
research using 460-Mev, 20: 4577 (AD-618067)
SYNCHROTRONS
beam orbit straight section for, design of, 20: 4512 (UCRL-16243)
operation of Cal. Tech. 1.5-Bev electron, developments for, 20: 4495 (CONF-650923-16)
personnel monitoring in environs of, performance of photographic film detectors for, 20: 4237 (BNL-9665)
radiation hazards to Brookhaven personnel from stray areas around proton, LET and quality factors in, 20: 4176 (BNL-9684)
SYSTEMS FOR NUCLEAR AUXILIARY POWER
pump for MPRE, fabrication of turbine-driven potassium boiler-feed, 20: 5184 (ORNL-P-1740)
radiation tolerance of electronic equipment for, 20: 4262 (NP-15610)
radiator development tests for MPRE, 20: 5182 (ORNL-P-1721)
shielding program on, review of, 20: 5183 (ORNL-P-1736)
SYSTEMS FOR NUCLEAR AUXILIARY POWER (SNAP-7)
heat transfer analysis of, 20: 4278 (MND-P-2229)
shielding calculations for, 20: 4278 (MND-P-2229)
SYSTEMS FOR NUCLEAR AUXILIARY POWER (SNAP-8)
cooling system of SNAP-8 Experimental Reactor, argon-41 production in, (E), 20: 5178 (NAA-SR-11303)
reactivity of beryllium oxide reflected, 20: 5180 (NAA-SR-Memo-11604)
SYSTEMS FOR NUCLEAR AUXILIARY POWER (SNAP-10)
thermoelectric converter of 10A, effect of dimensional tolerances on power output of, 20: 5179 (NAA-SR-Memo-6484)
SYSTEMS FOR NUCLEAR AUXILIARY POWER (SNAP-19)
re-entry heating of, flight test analysis of, 20: 4280 (SC-DC-65-1601)

T

TANTALUM
bonding to beryllium oxide, method for, 20: 4354(P)
bremsstrahlung yields from, with incorporated strontium-90–yttrium-90, 20: 5000 (ORNL-IIC-5, pp 91-8)
compatibility with uranium carbide–zirconium carbide system at 2000°C, 20: 4335
corrosion by cesium at 400°C, 20: 4337
corrosion by liquid chromium–uranium and manganese–uranium alloys, 20: 4077(R) (IS-1200(Sect. E))
corrosion by lithium, effects of oxygen content on, 20: 5181(R) (ORNL-3029)
deformation of, mechanism of thermally activated, 20: 4384(R) (ORNL-3870, pp 7-14)
deposition on finely dispersed particles, method for, 20: 4314(P)
determination in metals by neutron activation, 20: 3863(R) (IS-1200 (Sect. C))
determination in rare earths, spectrophotometric, 20: 3863(R) (IS-1200 (Sect. C))
determination of, hydrogen peroxide method for spectrophotometric, 20: 3904
diffusion of niobium-95 and tantalum-182 in, 20: 4385(R) (ORNL-3870, pp 15-19)
diffusion of niobium in, at 900 to 2500°C, 20: 4320(R) (ORNL-3870, pp 70-4)
electron work functions for thermionic cathodes of, effects of cesium fluorides on, 20: 4572 (EUR-2283.d)
fatigue of, effect of crystal structure on, 20: 4443
gamma elastic scattering at 1.12 Mev, cross sections for, (T), 20: 4864
grain growth and recrystallization of, effects of yttrium on, 20: 4424
neutron cross sections for, 9- and 16-group, 20: 4829 (GEMP-173(Suppl.1))
neutron cross sections for, 20: 4830 (GEMP-384)
oxidation at 600 to 925°C, effects of nitrogen on, 20: 4333
oxidation of, field-ion microscopic study of initial, 20: 4332
oxidation of, stress generation in surface layers during, 20: 4320(R) (ORNL-3870, pp 70-4)
preparation by reduction of pentachloride in hydrogen plasma jet, 20: 4314(P)
purification by electron-beam melting, 20: 5181(R) (ORNL-3029)
separation from low grade ores, reductive chlorination process for, 20: 4072(P)
solubility in rare earths at high temperatures, 20: 4297(R) (IS-1200 (Sect.M))
sorptive properties for carbon monoxide, kinetics of, 20: 4444
work hardening in, effects of alloying on, 20: 4384(R) (ORNL-3870, pp 7-14)
TANTALUM ALLOYS
deformation of, mechanism of thermally activated, 20: 4384(R) (ORNL-3870, pp 7-14)
fabrication of tube shells by flow turning, process development for,

20: 4301(R) (ORNL-3870, pp 102-35)
Al–Ta, mechanical properties of dispersions of, 20: 5174(R) (ORNL-3870, pp 241-29)
Al–Ta, properties as coating for refractory metals, 20: 4418
Hf–Ta, internal friction spectrum of, annealed at 2300°C, 20: 4301(R) (ORNL-3870, pp 102-35)
Hf–Ta–W, corrosion of T-111, by potassium, 20: 4301(R) (ORNL-3870, pp 102-35)
Hf–Ta–W, corrosion of T-111, by lithium, effects of oxygen on, 20: 4301(R) (ORNL-3870, pp 102-35)
Hf–Ta–W, evaporation losses in high vacuum of T-111, 20: 4301(R) (ORNL-3870, pp 102-35)
Hf–Ta–W, preparation and specifications for corrosion loop testing, 20: 4380 (NASA-CR-54761)
Hf–Ta–W, recovery and recrystallization of T-111, 20: 4301(R) (ORNL-3870, pp 102-35)
Hf–Ta–W, tensile properties of welded plates of T-111, 20: 4301(R) (ORNL-3870, pp 102-35)
Hf–Ta–W, thermal conductivity of T-111, at 30 to 120°C, 20: 4301(R) (ORNL-3870, pp 102-35)
Nb–Ta, thermal capacity of superconducting, in magnetic fields, 20: 4786
Nb–Ta, work hardening in tantalum-base, mechanisms of, 20: 4384(R) (ORNL-3870, pp 7-14)
Nb–Ta–V, development as brazing alloy for refractory metals, 20: 4301(R) (ORNL-3870, pp 102-35)
Nb–Ta–W–Zr, corrosion of FS-85, by lithium, effects of oxygen on, 20: 4301(R) (ORNL-3870, pp 102-35)
Nb–Ta–W–Zr, creep properties of FS-85, 20: 4301(R) (ORNL-3870, pp 102-35)
Nb–Ta–W–Zr, ductility of FS-85, effects of aging on bend, 20: 4301(R) (ORNL-3870, pp 102-35)
Nb–Ta–W–Zr, evaporation losses in high vacuum of FS-85, 20: 4301(R) (ORNL-3870, pp 102-35)
Nb–Ta–W–Zr, preparation and specifications for corrosion loop testing, 20: 4380 (NASA-CR-54761)
Ni–Ta, atomic structure of, short-range order and size-effect coefficients for, (E), 20: 4421
Re–Ta–W, tensile strength at 3500°F, 20: 4455(P)
Ta–Ti–V, development as brazing alloy for refractory metals, 20: 4301(R) (ORNL-3870, pp 102-35)
Ta–W, creep properties of, 20: 4301(R) (ORNL-3870, pp 102-35)

TANTALUM BROMIDES
phase studies, 20: 3863(R) (IS-1200(Sect. C))
preparation of polynuclear, 20: 3863(R) (IS-1200(Sect. C))

TANTALUM CARBIDES
electric conductivity of beta and gamma phases of, at 80 to 1500°K, 20: 4415
TaC–ZrC, properties at high temperatures, methods of determining, 20: 4297(R) (IS-1200(Sect.M))

TANTALUM CHLORIDES
reduction to metal in hydrogen plasma jet, 20: 4314(P)
separation from niobium chloride, methods for, 20: 4077(R) (IS-1200 (Sect. E))

TANTALUM IODIDES
phase studies, 20: 3863(R) (IS-1200(Sect. C))
preparation of polynuclear, 20: 3863(R) (IS-1200(Sect. C))

TANTALUM ISOTOPES Ta-175
gamma decay, 20: 4924

TANTALUM ISOTOPES Ta-176
gamma decay, 20: 4924

TANTALUM ISOTOPES Ta-182
beta decay of, conversion coefficients for, (E), 20: 4877
beta decay of, gamma directional correlations from, (E), 20: 4865
diffusion in beta-titanium, effects of atmosphere on, 20: 4385(R) (ORNL-3870, pp 15-19)
diffusion in niobium and tantalum, 20: 4385(R) (ORNL-3870, pp 15-19)

TANTALUM ORES
processing by reductive chlorination, 20: 4072(P)

TANTALUM SYSTEMS
C–Hf–Ta–W, preparation and specifications for corrosion loop testing, 20: 4380 (NASA-CR-54761)
C–Mo–Nb–Ta–W–Zr, preparation and specifications for corrosion loop testing, 20: 4380 (NASA-CR-54761)

TARTRATES
effects on spectrophotometric determination of zirconium, 20: 3895

TECHNETIUM
metabolism in man, tracer study, 20: 3663 (TID-22318)
Tc–W, compositions of second-phase regions of arc-melted, 20: 4367(R) (BNWL-162)

TECHNETIUM ALLOYS
Tc–Th, crystal structure of intermetallic compounds in, 20: 4428
Tc–U, crystal structure of intermetallic compounds in, 20: 4428

TECHNETIUM CHLORIDES
crystal structure, 20: 3932

TECHNETIUM ISOTOPES Tc-99
content in eluate from BNL molybdenum-99 cow, method for bulk calibration of, 20: 4269
use as tracer of, for brain tumor localization, 20: 3824
use in cardiac scanning of pertechnetate-incorporated, 20: 3831
use with nuclear image amplifier for blood flow and respiration measurements, 20: 3802 (ORNL-IIC-5, pp 239-42)

TECHNETIUM ISOTOPES Tc-102
beta decay of, gamma coincidences and spectra from, (E), 20: 4883

TECHNETIUM ISOTOPES Tc-104
beta decay of, gamma coincidences and spectra from, (E), 20: 4883

TECHNICAL REPORTS
publication by Argonne National Lab., July 1964 to June 1965, 20: 5211 (ANL-7087)

TEETH
radiation effects on development of, in monkeys, x, 20: 3743
radiography of, radiation dose of population of Japan from, 20: 4195
radiography of, radiation dose to gonads from, 20: 4206
radium content in deciduous, United States, 20: 4160
strontium-90 content in deciduous, United States, 20: 4160

TELEMETERING SYSTEMS
design of range indicating system for aircraft, 20: 5225(P)
tracking antenna positioning for, 20: 5215 (SC-TM-65-448)

TELEVISION EQUIPMENT
use in nondestructive testing of radioactive materials, 20: 4122

TELLURIUM
content in chondrites, 20: 4526
diffusion from liquid urania in containment mockup experiments, 20: 4184(R) (ORNL-3843, pp 71-135)

TELLURIUM SYSTEMS
Sb–Cr–Te, magnetic structure of CrSb–CrTe in, 20: 4358(R) (AD-438516)

TEMPERATURE
distribution in flat-plate fuel elements with fuel-clad bonding defects, model for, (T), 20: 4102 (HW-SA-3640)
distribution in thick-wall cylinders, analysis of, 20: 4076 (HIC-1-1564-3(Vol.2))
effects on fission-product behavior in reactor loss-of-coolant accidents, 20: 4183(R) (ORNL-3843, pp 2-70)
effects on human embryos, teratogenic, 20: 3747
effects on radionuclide uptake by maize, 20: 3668
measurement by electromagnetic induction, device for, 20: 5045(P)
measurement in sheathed reactor fuel plates, process of assembling device for, 20: 5098(P)
measurements in nuclear explosion cavities, 20: 4084 (VUF-3017)
relativistic transformation of, (T), 20: 4712

TEMPERATURE CONTROL
equipment for reactor coolant, 20: 5170(P)

TERBIUM
determination in hydrochloric acid or methanol–nitric acid media, spectrophotometric, 20: 3888 (TID-22402)
determination in potassium carbonate, fluorometric, 20: 3863(R) (IS-1200(Sect. C))
thermal conductivity, (E/T), 20: 4419

TERBIUM ALLOYS
Ag–Tb–Y, crystallography, 20: 4391(R) (ORNL-3870, pp 75-82)
Cu–Tb–Zn, crystallography, 20: 4391(R) (ORNL-3870, pp 75-82)
In–Ag–Tb, crystallography, 20: 4391(R) (ORNL-3870, pp 75-82)
La–Ag–Tb, crystallography, 20: 4391(R) (ORNL-3870, pp 75-82)
Pd–Ag–Tb, crystallography, 20: 4391(R) (ORNL-3870, pp 75-82)
Rh–Tb, crystallography of intermetallic compound $TbRh_2$, 20: 4391(R)

TERBIUM CHLORIDES
heat of dilution of aqueous, at 25°C, 20: 3956
heat of solution at 25°C, aqueous, 20: 3956

TERBIUM ISOTOPES Tb-159
nuclear quadrupole moment from ground-level hyperfine structures, (E), 20: 4857

TERBIUM OXIDES
magnetic properties and preparation, 20: 3863(R) (IS-1200(Sect. C))

TERBIUM SULFIDES
homogeneity regions in, 20: 3938

TERPHENYL
analysis for sulfur by activation methods, 20: 3873 (EUR-2523.i)
hexahydro-, preparation and properties of isomers of, 20: 3972 (EUR-2528.f)
neutron scattering by meta-, ortho-, and para-, angular distribution and diffusion constants from, (E), 20: 4817

TEXTILES
production of, radiation chemistry in, 20: 4031
production of, uses of radiation in, 20: 4032
production of, uses of radiation in, 20: 4034

radioinduced addition of vinyl silicone tc, for waterproofing, 20: 4033
radioisotope uses in production of, conference on, 20: 4274
THALLIUM
electric conductivity of single-crystal, effects of magnetic fields on, (E/T), 20: 4476(R) (IS-1200(Sect.P))
THALLIUM ALLOYS
In–Tl, elastic properties, 20: 4297(R) (IS-1200(Sect.M))
Pb–Tl, elastic properties, 20: 4297(R) (IS-1200(Sect.M))
THALLIUM CHLORIDES
spectra of, microwave rotational, 20: 3947
THALLIUM COMPOUNDS
thallium-204 exchange between inorganic and organic, 20: 3960
THALLIUM IONS
spectra in lithium chloride–potassium chloride eutectic, absorption, 20: 3921(R) (ORNL-3870, pp 56-60)
THALLIUM ISOTOPES Tl-197
isomeric transitions in, conversion coefficients, half life, and multipolarity of, (E), 20: 4921
production of isomers of, in alpha reactions (α,4n) with gold-197 at 49 Mev, 20: 4921
THALLIUM ISOTOPES Tl-202
decay energies of, coincidence methods for determining, (E), 20: 4843 (NP-15456)
decay of, K, L, M, and N electron capture for, (E), 20: 4875
THALLIUM ISOTOPES Tl-203
mass relative to thallium-205, from thallium monochloride rotational spectra, 20: 3947
THALLIUM ISOTOPES Tl-204
exchange between inorganic and organic thallium compounds, 20: 3960
THALLIUM ISOTOPES Tl-205
mass relative to thallium-203, from thallium monochloride rotational spectra, 20: 3947
THERMAL CONDUCTIVITY
measurement for molten fluoride salts and solids, 20: 4310(R) (ORNL-P-1699)
measurement in cylindrically symmetrical solids, method for, (E/T), 20: 4476(R) (IS-1200(Sect.P))
THERMAL DIFFUSION
columns for isotope enrichment by, 20: 3879(R) (MLM-1266)
THERMAL INSULATION
development for gas-cooled high-temperature reactor pressure vessel, 20: 5117(R) (GA-5866)
THERMAL RADIATION
effects on infectious activity of *Mycobacterium lepraemurium*, 20: 3752
THERMAL REACTORS
fuel development for, review of, 20: 4313
fuel for, development and properties of plutonium dioxide–uranium dioxide–zirconium dioxide, 20: 4382(R) (NUMEC-3505-8)
fuels for, economics of thorium and uranium, 20: 5114 (CRRP-1221)
THERMAL STRESSES
effects on structural materials, cycling, 20: 4299(R) (ORNL-2711)
THERMIONIC CELLS
barrier shell for, corrosion resistance and permeability of ceramics for, (E), 20: 4359(R) (AD-618923)
collector materials for, research on niobium and rhenium, 20: 4570(R) (AD-614592)
design for use in reactors, 20: 4576(P)
electrode design for, use of extended surfaces in, 20: 4574
electron work functions for cesium and cesium fluoride filled, (T), 20: 4572 (EUR-2283.d)
isotope heat sources for, gamma doses from 1-w promethium-147, 20: 4279 (ORNL-TM-1177)
THERMOCOUPLES
aging and thermoelectric power of Alumel–Chromel, 20: 4398 (TRG-Report-1021)
calibration for PWR core 1 seed 4, correction factors for, 20: 5133 (WAPD-PWR-TS-151)
errors from, evaluation of thermal loading, 20: 5026
performance in 300-watt portable thermoelectric generator, (E), 20: 4571(R) (AD-618037)
radiation effects on performance of stainless steel-clad Alumel–Chromel, in-pile, 20: 4263 (ORNL-TM-1320)
testing for use at high temperatures, 20: 4999(R) (ORNL-2599)
testing for use at high temperatures, 20: 4299(R) (ORNL-2711)
testing of Alumel–Chromel, 20: 4299(R) (ORNL-2711)
THERMODYNAMIC PROPERTIES
for repulsive lattice gas models, 20: 4708(R) (UCRL-14360, pp 50-73)
of molecular systems, cell theory for, 20: 4708(R) (UCRL-14360, pp 50-73)
THERMODYNAMICS
entropy density in three dimensions, continuum, (T), 20: 4706(R) (RPI-3036-1)
entropy in solid phase, 20: 4708(R) (UCRL-14360, pp 50-73)
irreversibility in, formulation and solution for, (T), 20: 4706(R) (RPI-3036-1)
series expansions in, approximation method for, 20: 4708(R) (UCRL-14360, pp 50-73)
solidification of systems of particles with repulsive forces, 20: 4708(R) (UCRL-14360, pp 50-73)
THERMOELECTRIC CELLS
performance of 300-watt portable, (E), 20: 4571(R) (AD-618037)
THERMOLUMINESCENT DETECTORS
development of lithium fluoride, for gamma and neutron dosimetry, 20: 4236 (BNL-9605)
THERMONUCLEAR EXPLOSIONS
population response to, behavioral factors, 20: 4200
THERMONUCLEAR REACTIONS
control of, for power production, (E/T), 20: 4992
THERMONUCLEAR REACTORS
development, 20: 4992
THERMONUCLEAR WEAPONS
radiation protection measures against fallout from, 20: 3797
radiation protection measures against fallout from, 20: 3799
THICKNESS GAGES
development of gamma radiometric, 20: 4114(T) (AD-621784)
self-compensation system for, 20: 4273
use of radiometric, for coatings, 20: 4219 (ORNL-IIC-5, pp 182-205)
THIONYL CHLORIDE
chlorine-36 exchange with antimony pentachloride, 20: 3965
sulfur-35 exchange with sulfuryl chloride, 20: 3965
THIOPHENE
labeling with sulfur-35 by isotopic exchange with nickel sulfide, 20: 3976
THIOPHOSPHORIC ACID, ALKYL ESTERS
solvent properties for silver, 20: 4054
THORIUM
content in oceanic theoleitic basalts, 20: 4145
content in porphyries in Saar-Nahe basin, Germany, 20: 4165
creep of high-purity, at room temperature, 20: 4297(R) (IS-1200(Sect.M))
determination in hydrochloric acid or methanol–nitric acid media, spectrophotometric, 20: 3888 (TID-22402)
determination in monazites by titration using fluoride ion, 20: 3905
diffusion in pyrolytic graphite, effects of structure on, 20: 4306(R) (ORNL-3870, pp 194-213)
effects on crystal structure and physical properties of cerium phosphate, 20: 4174
neutron scattering by, p-wave phase shifts in small-angle, (T), 20: 4909
oxygen surface potential on, 20: 4410
preparation by dioxide reduction, 20: 4316(P)
purification by electrotransport, 20: 4297(R) (IS-1200(Sect.M))
separation from aluminum nitrate–nitric acid systems by solvent extraction using TBP, 20: 4060
separation from aluminum nitrate–nitric acid systems by solvent extraction using TBP, 20: 4060
separation from aqueous nitrates by solvent extraction using tributyl phosphate, 20: 3863(R) (IS-1200(Sect. C))
separation from cerium and thorium ore by solvent extraction using tributyl phosphate, 20: 4059
separation from minerals, other metals, rocks, and sediments in mixed and nonaqueous solvents by ion exchange, 20: 3888 (TID-22402)
separation from rare earths, 20: 3905
separation from rare earths by extraction using fused chlorides 20: 4297(R) (IS-1200(Sect.M))
separation from thorium ore by solvent extraction using tributyl phosphate–n-hexane, solvent properties for thorium, 20: 4060
THORIUM ALLOYS
Fe–Th, crystal structure, 20: 4297(R) (IS-1200(Sect.M))
Gd–Th, electric conductivity in, (E), 20: 4476(R) (IS-1200(Sect.P))
Hg–Th, preparation and properties of intermetallic compounds in, 20: 4441
Hg–Th, vapor pressure of mercury over, 20: 4441
Tc–Th, crystal structure of intermetallic compounds in, 20: 4428
Th–U, fabrication as fuel cycle material, design and construction of facility for, 20: 4343(R) (ORNL-3870, pp 266-89)
THORIUM CARBIDES
electric conductivity of, effects of temperature on, 20: 4297(R) (IS-1200(Sect.M))
etching technique for, 20: 4309(R) (ORNL-3870, pp 300-4)
hydrolysis at 100°C, mechanism of, 20: 3937
phase studies, 20: 4297(R) (IS-1200(Sect.M))
ThC–UC, fabrication of graphite-coated, equipment and flowsheet for, 20: 4343(R) (ORNL-3870, pp 266-89)
ThC_2–UC_2, phase studies, 20: 4306 (ORNL-3870, pp 194-213)
ThC–UC, production from sol-gel microspheres, process for, 20: 4343(R) (ORNL-3970, pp 266-89)
ThC_2–UC_2, radiation effects on coated fuel particles of, 20: 4458

(GA-6485)
THORIUM CHLORIDES
oxidation by fused metal chlorides at high temperatures, 20: 4297(R) (IS-1200(Sect.M))
phase diagrams, 20: 4297(R) (IS-1200(Sect.M))
THORIUM(IV) CHLORIDES
preparation and reduction of, 20: 4297(R) (IS-1200(Sect.M))
reactions with o-phenanthroline and triphenylphosphine, effects of ethanol, ethyl acetate, and hydrochloric acid on, 20: 3933
$CaCl_2$–$ThCl_4$, phase studies, 20: 4297(R) (IS-1200(Sect.M))
THORIUM(IV) FLUORIDES
properties of molten, for use as reactor fuel, 20: 4376 (JUL-268-RG)
THORIUM ISOTOPES Th-228
diffusion in pyrolytic carbon deposits, rates of, 20: 5089(R) (GA-6181)
THORIUM ISOTOPES Th-230
spectra of, alpha, 20: 3879(R) (MLM-1266)
THORIUM ISOTOPES Th-232
content in breath, feces, urine, and whole-body of Thorotrast patients, 20: 3683
economics for use in thermal reactors, 20: 5114 (CRRP-1221)
meson (μ^-) capture by, x-ray spectra of, 20: 4825(R) (ANL-7081, pp 81-93)
THORIUM ORES
separation of thorium from, by solvent extraction using tributyl phosphate, 20: 4059
separation of thorium from, by solvent extraction using, 20: 4060
THORIUM OXIDES
formation in oxygen sorption on thorium films, 20: 4410
THORIUM(IV) OXIDES
compressive strength, 20: 4387(R) (ORNL-3870, pp 38-43)
creep rate at 1400 to 1800°C, 20: 4387(R) (ORNL-3870, pp 38-43)
creep rate, effects of alumina and calcia additions on, 20: 4387(R) (ORNL-3870, pp 38-43)
diffusion of rare gases in, 20: 3944
effects on bile duct, carcinogenic, 20: 3722
effects on man, late pathologic, 20: 3753
fabrication of fuel particles of, for gas-cooled high-temperature reactor, 20: 5117(R) (GA-5866)
preparation and properties of microspheres of, 20: 3922 (ORNL-TM-1281)
preparation and properties of carbon-coated sol-gel microspheres of, 20: 4344 (ORNL-P-1725)
preparation of hydrophilic or organophilic sols of, 20: 3969(P)
radiation effects on carbon-coated sol-gel microspheres of, 20: 4344 (ORNL-P-1725)
reduction to metal, 20: 4316(P)
sintering and grain growth of sol-gel, 20: 4343(R) (ORNL-3870, pp 266-89)
thorium-232 content in, 20: 3683
CaO–ThO_2, sintering of, material transport during, 20: 4387(R) (ORNL-3870, pp 38-43)
Ni–ThO_2, corrosion by lithium fluoride in cyclic high-temperature environment, 20: 4326 (TRW-ER-6561)
Ni–ThO_2, properties at high temperatures, 20: 4418
PuO_2–ThO_2, preparation and properties of carbon-coated sol-gel microspheres of, 20: 4344 (ORNL-P-1725)
PuO_2–ThO_2, radiation effects on carbon-coated sol-gel microspheres of, 20: 4344 (ORNL-P-1725)
ThO_2–UO_2, diffusion of rare gases in, 20: 3944
ThO_2–UO_2, fabrication of reactor fuel rods of, flowsheet for, 20: 4343(R) (ORNL-3870, pp 266-89)
ThO_2–UO_2, preparation and properties of carbon-coated sol-gel microspheres of, 20: 4344 (ORNL-P-1725)
ThO_2–UO_2, preparation and properties of microspheres of, 20: 3922 (ORNL-TM-1281)
ThO_2–UO_2, radiation effects on coated fuel particles of, 20: 4458 (GA-6485)
ThO_2–UO_2, radiation effects on properties of vibratory-compacted sol-gel fuel rods of, in reactor, 20: 4343(R) (ORNL-3870, pp 266-89)
ThO_2UO_2, reactivity sodium void effects on, in fast reactors, 20: 5068
ThO_2–UO_2, sintering and grain growth of sol-gel, 20: 4343(R) (ORNL-3870, pp 266-89)
Th_2–UO_2, radiation effects on carbon-coated sol-gel microspheres of, 20: 4344 (ORNL-P-1725)
THORIUM OXYIODIDES
preparation and reactions, 20: 3863(R) (IS-1200(Sect. C))
THORIUM PHOSPHIDES
crystal structure of, electrostatic and valence-bond theory of, 20: 4358(R) (AD-438516)
THRESHOLD DETECTORS
data from, calculation of differential fast-neutron spectra from, 20: 4256
THULIUM
determination in hydrochloric acid or methanol–nitric acid media, spectrophotometric, 20: 3888 (TID-22402)
THULIUM ISOTOPES Tm-165
gamma decay, 20: 4924
THULIUM ISOTOPES Tm-169
energy levels, (E), 20: 4476(R) (IS-1200(Sect.P))
THULIUM ISOTOPES Tm-170
beta decay of, conversion coefficients for, (E), 20: 4877
THULIUM OXIDES
phase studies at 1700 to 2400°C, 20: 3939
THULIUM SULFIDES
homogeneity regions in, 20: 3938
THYMIDINE
radiation effects on DNA metabolism of tritium-labeled, 20: 3702
radiation effects on metabolism in ascites sarcoma cells, tracer study, 20: 3702
THYMUS GLAND
radiation effects on immunological activity in cells of, in mice, 20: 3777
THYROID GLAND
iodine metabolism in mouse, effects of chlorpromazine on, tracer study, 20: 3677
iodine-131 metabolism in, effects of pathological conditions on, 20: 3660 (NP-15628)
radiodiagnosis of diseases of, 20: 3844
radiodiagnosis of diseases of, double-labeling method for, 20: 3658(R) (EUR-2414.f,i)
radioinduced carcinomas in, etiology of, 20: 3739
radiotherapy of diseases of, using iodine-131, 20: 3853
THYROXINE
effects on iodine transfer from plasma to milk, 20: 3674
synthesis in mice of, effects of chlorpromazine on, 20: 3677
TIME MEASUREMENT
variations in cesium-beam atomic clocks, effects of temperature on, 20: 4479(R) (TID-22179, pp 1-83)
TIMING CIRCUITS
development of transistorized, 20: 4048(R) (NP-15406)
TIN
bremsstrahlung yields from, with incorporated strontium-90–yttrium-90, 20: 5000 (ORNL-IIC-5, pp 91-8)
determination in mixtures by x-ray fluorescence using promethium-147/aluminum and tritium/zirconium sources, 20: 3883 (ORNL-IIC-5, pp 154-81)
electric conductivity of single-crystal, effects of magnetic fields on, (E/T), 20: 4476(R) (IS-1200(Sect.P))
magnetic resonance shifts at 4.2 to 450°K, (E), 20: 4476(R) (IS-1200 (Sect.P))
magnetic transitions of thin superconducting films of, 20: 4785
Mössbauer effect anisotropy of tin-120 enriched, (E), 20: 4932
phonon spectra of lattice of white, (T), 20: 5005 (IAE-926)
superconducting properties of whiskers of, (E), 20: 4795
superconductivity destruction in, magnetic induction distribution with temperature in, (E), 20: 4794
ultrasonic effects in, dependence on magnetic fields, (E), 20: 4476(R) (IS-1200(Sect.P))
TIN ALLOYS
Al–Sn, deposition on niobium for oxidation protection, 20: 4355(P)
Al–Sn, deposition on niobium and niobium alloys for oxidation protection, 20: 4357(P)
Bi–Sn, electric conductivity of liquid, 20: 4297(R) (IS-1200(Sect.M))
Bi–Sn, magnetic transitions of thin superconducting films of, 20: 4785
Ca–Sn, preparation and properties of single-crystal, (E), 20: 4476(R) (IS-1200(Sect.P))
Ce–Sn, magnetic properties of, at 2 to 300°K, 20: 4423
Cu–Sn, use in thin-film bolometers, 20: 4479(R) (TID-22179, pp 1-83)
Gd–Sn, magnetic properties of, at 2 to 300°K, 20: 4423
In–Sn, magnetic transitions of thin superconducting films of, 20: 4785
Mg–Sn, preparation and properties of single-crystal, (E), 20: 4476(R) (IS-1200(Sect.P))
Nb–Sn, crystal structure of intermetallic compounds in, 20: 4297(R) (IS-1200(Sect.M))
Nb–Sn, magnetic flux jumps and trapping in superconducting, (E), 20: 4793
Nd–Sn, magnetic properties of, at 2 to 300°K, 20: 4423
Pd–Sn, tin-119 Mössbauer spectra in, 20: 5014
Pr–Sn, magnetic properties of, at 2 to 300°K, 20: 4423
Pr–Sn, tin-119 magnetic hyperfine in, (E/T), 20: 4476(R) (IS-1200 (Sect.P))
Re–Sn, nuclear magnetic resonance in, (E), 20: 4476(R) (IS-1200 (Sect.P))
Sm–Sn, magnetic properties of, at 2 to 300°K, 20: 4423
TIN HYDRIDES
spectra of deuterium effects on infrared, 20: 3942
TIN ISOTOPES Sn-116
energy levels of, parity and spin of, 20: 4825(R) (ANL-7081, pp 81-93)
TIN ISOTOPES Sn-119

Mössbauer spectra of, in palladium-tin alloy, 20: 5014
reactions in praseodymium–tin intermetallics, (E/T), 20: 4476(R) (IS-1200(Sect.P))
TIN ISOTOPES Sn-120
Mössbauer effect anisotropy in, (E), 20: 4932
proton elastic scattering at 160 Mev, differential cross sections for, (E/T), 20: 4906
TIN MINERALS
analysis of, use of radioisotope methods for, 20: 3884 (ORNL-IIC-5, pp 206-21)
TISSUE CULTURES
alkaline phosphatase content of cancer cells in, effects of hydrocortisone on, 20: 5217 (TID-21169)
effects of radioprotective compounds on tumor cells in, morphological, 20: 3796
effects of water-d_2 on growth in, 20: 3651
radiation injuries of cells in, protective effects of inosine against, γ, 20: 3791
radioinduced chromosomal aberrations in mouse fibroblast, effects of culture density on x, 20: 3691
radiosensitivity of hamster cells in, tracer study, γ, 20: 3737
TISSUE TRANSPLANTS
growth of bone marrow, in dog spleen, 20: 3652
radiation effects on immune reactions of, in mice, 20: 3777
TISSUES
energy absorption in, as a function of neutron energy, 20: 3708 (CEA-R-2833)
neutron reactions in, effects of element composition on kerma, 20: 3708 (CEA-R-2833)
radiation effects on DNA synthesis in rat, tracer study, 20: 3702
TITANIUM
analysis for oxygen by neutron activation methods, 20: 3907
deposition on niobium and niobium alloys for oxidation protection, 20: 4356(P)
determination in molybdenum and molybdenum alloys by ion exchange, 20: 3896
determination in mixtures by x-ray fluorescence using promethium-147/aluminum and tritium/zirconium sources, 20: 3883 (ORNL-IIC-5, pp 154-81)
determination in yttrium, methods for, 20: 4299(R) (ORNL-2711)
diffusion of tantalum-182 in beta-phase, effects of atmosphere on, 20: 4385(R) (ORNL-3870, pp 15-19)
effects on neutron embrittlement of type 304 stainless steel, 20: 4460(R) (ORNL-3870, pp 140-5)
fabrication of fluted tubing of, evaluation of methods for, 20: 5173(R) (ORNL-3870, pp 191-3)
mechanical properties of, effects of hot plastic deformation on, 20: 4403(T) (JPRS-32317)
neutron cross sections for, 9- and 16-group, 20: 4829 (GEMP-173(Suppl.1))
reactions of liquid, with borides, carbides, silicides, and sulfides, 20: 3929
separation from low grade ores, reductive chlorination process for, 20: 4072(P)
separation from sulfuric acid solution by solvent extraction, evaluation of organic solvents for, 20: 4061
TITANIUM ALLOYS
preparation of stable-beta, 20: 4360(R) (AD-619399)
Al–Co–Fe–Ti–V, properties of aged, 20: 4360(R) (AD-619399)
Al–Cr–Co–Mo–Ni–Ti, corrosion of Udimet 500 by lithium fluoride in cyclic high-temperature environment, 20: 4326 (TRW-ER-6561)
Al–Cr–Ge–Ti–V, properties of aged, 20: 4360(R) (AD-619399)
Al–Cr–Ti–V, properties of aged, 20: 4360(R) (AD-619399)
Al–Fe–Mo–Ti–V, properties of aged, 20: 4360(R) (AD-619399)
Al–Fe–Ti–V, properties of aged, 20: 4360(R) (AD-619399)
Al–Mn–Ti–V, properties of aged, 20: 4360(R) (AD-619399)
Al–Nb–Ti–W–V–Zr, properties for use to 1200°F, 20: 4393 (PWAC-472)
Al–Ti–V, corrosion by cesium at 400°C, 20: 4337
Al–Ti–W–V–Zr, properties for use to 1200°F, 20: 4393 (PWAC-472)
Co–Ni–Ti–Zr, properties of Nivco in space electric power systems, 20: 4379 (NASA-CR-54091)
Mo–Ti, properties at high temperatures, 20: 4418
Mo–Ti–Zr, analysis for titanium and zirconium by ion exchange, 20: 3896
Mo–Ti–Zr, brazing tungsten carbide–cobalt cermet to TZM, use of boron–nickel–silicon for, 20: 4307(R) (ORNL-3870, pp 238-42)
Mo–Ti–Zr, corrosion of TZM, by potassium, 20: 4301(R) (ORNL-3870, pp 102-35)
Mo–Ti–Zr, creep properties of TZM, 20: 4301(R) (ORNL-3870, pp 102-35)
Nb–Ti, coating with aluminum alloy for oxidation protection, 20: 4315(P)
Ta–Ti–V, development as brazing alloy for refractory metals, 20: 4301(R) (ORNL-3870, pp 102-35)
Ti–V, diffusion of titanium-44 in, 20: 4385(R) (ORNL-3870, pp 15-19)
Ti–W, properties at high temperatures, 20: 4418
TITANIUM IONS
electron transfer between cobalt(III) and trivalent, oxyanions as bridging groups in, 20: 3967
TITANIUM ISOTOPES Ti-44
diffusion in vanadium–20 titanium alloy, 20: 4385(R) (ORNL-3870, pp 15-19)
TITANIUM ISOTOPES Ti-48
proton inelastic scattering by, gamma-proton angular correlations in, (E/T), 20: 4926
TITANIUM ORES
processing by reductive chlorination, 20: 4072(P)
TITANIUM(IV) OXIDES
solubility in borax at 760 to 900°C, 20: 3951
TITANIUM SYSTEMS
Al–Cr–Si–Ti–V, properties of aged, 20: 4360(R) (AD-619399)
Al–C–Ti, properties for use to 1200°F, 20: 4393 (PWAC-472)
Al–C–Ti–Zr, properties for use to 1200°F, 20: 4393 (PWAC-472)
C–Mo–Ti–Zr, preparation and specifications for corrosion loop testing, 20: 4380 (NASA-CR-54761)
TOBACCO
effects of chronic cigarette smoking, on pulmonary clearance in dogs, 20: 3655 (BNWL-SA-224)
radiation effects on pyrolytic products in smoke from irradiated cigarettes, 20: 3984 (ORO-633)
radiation effects on virus infections of plants of, γ, 20: 3768
TOLUENE
content in smoke from irradiated cigarettes, 20: 3984 (ORO-633)
hypersonic and ultrasonic velocities in, effects of relaxation on, 20: 4479(R) (TID-22179, pp 1-83)
radiolysis in 3-methyl pentane at 77°K, γ, (E), 20: 4013
TOURMALINES
shock effects on piezoelectricity of Z-cut, (E), 20: 5011
TOWER SHIELDING FACILITY
criticality studies for TSR-II, 20: 5181(R) (ORNL-3029)
criticality studies for TSR-II, 20: 4299(R) (ORNL-2711)
design of TSR-II, 20: 4999(R) (ORNL-2599)
dose rates in Pratt & Whitney divided shield experiment, (T), 20: 5181(R) (ORNL-3029)
gamma dose rates from, 20: 4999(R) (ORNL-2599)
gamma doses and spectra at, 2π measurements on, 20: 4299(R) (ORNL-2711)
neutron dose rates from, 20: 4999(R) (ORNL-2599)
neutron flux distributions in TSR-II, thermal, 20: 5181(R) (ORNL-3029)
neutron fluxes and dose rates at, 2π measurements on, 20: 4299(R) (ORNL-2711)
power distributions in TSR-II, 20: 5181(R) (ORNL-3029)
TRACER TECHNIQUES (AGRICULTURE)
development of, 20: 3710(R) (EUR-2493.e)
use in veterinary medicine, 20: 3859
TRACER TECHNIQUES (BIOLOGY)
for bacteria identification using labeled metabolites, 20: 3667
for metabolic studies, 20: 3685
use of carbon-14 for determining fructose metabolism in liver, 20: 3684
use of tritiated thymidine, determining DNA synthesis in irradiated rat tissues, 20: 3701
use of tritiated thymidine for determining synthesis in irradiated DNA, 20: 3702
TRACER TECHNIQUES (CHEMISTRY)
development for determining mercury solubility in organics, 20: 3863(R) (IS-1200(Sect. C))
development for determining isotopic exchange in polymeric tungstates, 20: 3863(R) (IS-1200(Sect. C))
iodine deposition and sorption, 20: 4086(R) (ORNL-3843, pp 137-67)
iodine retention by charcoal, 20: 4184(R) (ORNL-3843, pp 71-135)
TRACER TECHNIQUES (ENGINEERING)
particle residence times in fluidized beds, 20: 4106(T) (BNL-tr-43)
TRACER TECHNIQUES (MEDICINE)
evaluation of, for clinical cardiology, 20: 3818
for brain tumor localization, 20: 3824
for diagnosis of rickets, 20: 3672
for diagnosis of thyroid diseases, 20: 3844
for diagnosis of thyroid diseases, 20: 3844
for immuno assay of plasma thyrotropin, 20: 3829
for kidney function tests, 20: 3800(R) (NP-15150)
for liver function tests, 20: 3774
preparation of tritium-labeled digitoxin for use in, 20: 3810
reaction to subarachnoid injection of iodine-131-serum albumin used for, 20: 3843
review of, using whole-body counting, 20: 3805
TRANSDUCERS
testing of liquid-metal-level, 20: 4999(R) (ORNL-2599)

testing of liquid-metal-level, 20: 4299(R) (ORNL-2711)
TRANSFORMERS
design and testing of differential, 20: 5123(R) (HPR-61)
TRANSISTORS
design and performance of field-effect, for radiation detection, 20: 4250 (UCRL-16446)
radiation effects on germanium and silicon, (E), 20: 4261 (AD-623078)
radiation effects on electric properties of, role of doping in, 20: 4265
radiation effects on gain of silicon, effects of operating conditions on gamma, 20: 4267
research on thin-film field effect, (E), 20: 4220 (SC-TM-65-424)
TRANSPLUTONIC ELEMENTS
separation from irradiated targets, design of hot cells for, 20: 4065
TRAUMA
effects on human embryos, teratogenic, 20: 3747
TRIDODECYLAMINE
solvent properties for plutonium, 20: 3868 (CEA-R-2860)
TRINO POWER REACTOR
fuel pellet temperature for Doppler broadening of uranium-238 resonance, 20: 5135 (WCAP-3269-40)
TRITIUM
determination in samples, handling and preparation for, 20: 3876 (ISS-65/8)
effects on thermodynamic properties of hydrogen selenide and hydrogen sulfide, 20: 3950
exchange with hydrogen in methane, 20: 3980
incorporation in amino acids, 20: 3978
incorporation into digitoxin of, use of carriers for, 20: 3810
neutron reactions (n,3n) at 14 Mev, cross section for, (E), 20: 4849(R) (UCRL-14360, pp 1-50)
properties in x-ray source excitation, 20: 3883 (ORNL-IIC-5, pp 154-81)
radiation effects on DNA metabolism of thymidine-incorporated, 20: 3702
radiation effects on metabolism in ascites sarcoma cells of thymidine-incorporated, 20: 3702
reactions with alkanes, recoil, 20: 4024
reactions with chlorocarbons, recoil, 20: 4023
TRITONS
binding energy of, from deuteron-neutron interactions, (T), 20: 4614
energy distribution from neutron reactions (n,α) with lithium-6, 20: 5181(R) (ORNL-3029)
interactions with tritons, neutron spectra from, (E), 20: 4849(R) (UCRL-14360, pp 1-50)
reactions (t,α) with oxygen-16 at 1.4 to 3.4 Mev, excitation curves of, (E), 20: 4858
TRX REACTOR
criticality parameters for slightly enriched uranium dioxide, with H : U = 0.42, 20: 5071
TRYPSIN
radiation effects on albumin sensitivity to, γ, 20: 3687
TSURUGA POWER REACTOR (JAPAN)
fuel technology for, 20: 5147
TUBES
boiling burnout of annular forced-convection flows in, at 1000 psi, (E), 20: 4105 (TID-22321)
defects in, ultrasonic method for detecting, 20: 5227(P)
TUMORS
alkaline phosphatase content of cultured cells of, effects of hydrocortisone on, 20: 5217 (TID-21169)
chemotherapy of, computer calculation of treatment schedules, 20: 5222 (UCRL-14505)
effects of radioprotective compounds on tissue cultures of, morphological, 20: 3796
etiology of stomach, 20: 4197
etiology of, environmental factors, 20: 3779
incidence of, in population of areas underlain with uraniferous rock, 20: 4193
radiation dose calculations for gamma radiotherapy of, 20: 3855
radiation effects on isoenzymes of dehydrogenases and phosphatases in, during therapy, 20: 3845
radiation effects on growth of transplanted, in rats, 20: 3695
radiation effects on growth of transplanted, in mice, x, 20: 3751
radiation effects on enzyme activity in, 20: 3763
radiodiagnosis of brain, procedures at University of Mississippi for, 20: 3830
radioinduced bile duct, by deposited Thorotrast, 20: 3722
radioinduced in man, incidence of, 20: 3779
radioinduced pharynx, after radiotherapy of thyrotoxicosis, 20: 3806
radioinduced, after dermatologic radiotherapy, 20: 3812
radioinduced, by therapeutic doses of x, 20: 3841
radiosensitivity of mouse transplanted, effects of ploidy, on x, 20: 3751
radiosensitivity of transplanted mouse, effects of anoxia on, 20: 3750
radiotherapy of benign, hazards to children from, 20: 3850
radiotherapy of breast, prior to radical surgery, x, 20: 3861
radiotherapy of cervical, late pathological effects, 20: 3856
radiotherapy of hemangiomas in children, late effects on bone development, 20: 3808
radiotherapy of mouth, measures for preventing injuries from, 20: 3813
radiotherapy of oral, effects on mucosa, 20: 3744
radiotherapy of thyroid, using iodine-131, 20: 3853
radiotherapy of vaginal, doses and method for, 20: 3848
radiotherapy of Zollinger-Ellison syndrome induced by pancreatic tumor, 20: 3821
radiotherapy of, evaluation by content of isoenzymes in blood serum, 20: 3845
radiotherapy of, effects on enzyme activity, 20: 3763
radiotherapy of, method for, 20: 3842
radiotherapy of, protective effects of trihydroxyethylrutosidum against mucosal reactions during, 20: 3840
radiotherapy of, review of recent progress in, 20: 3849
radiotherapy of, use of cobalt-60 simulator for treatment planning, 20: 3827
radiotherapy of, using gold-198 colloids, 20: 3822
transplantation of mouse ascites lymphoma, 20: 3750
treatment of breast, by radioinduced pituitary ablation, 20: 3809
TUNGSTEN
ablation mechanism for copper-impregnated, 20: 4108
cesium ionization on porous, 20: 4135
compatibility with uranium carbide–zirconium carbide system at 2000°C, 20: 4335
corrosion by cesium at 400°C, 20: 4337
creep properties of thermochemically deposited and wrought, 20: 4302(R) (ORNL-3870, pp 155-63)
Debye temperature, 20: 4388(R) (ORNL-3870, pp 44-9)
deposition of, thermochemical, 20: 4342(R) (ORNL-3870, pp 85-101)
determination in metals by neutron activation, 20: 3863(R) (IS-1200 (Sect. C))
ductility of recrystallized, effects of hydrostatic prestrain on, 20: 4302(R) (ORNL-3870, pp 155-63)
effects on flow stress recovery of molybdenum, 20: 4409
electric conductivity of single crystals of, at 1.4 to 27°K, 20: 4453
electric conductivity and thermoelectric power, 20: 4301(R) (ORNL-3870, pp 102-35)
electron work functions for thermionic cathodes of, effects of cesium fluorides on, 20: 4572 (EUR-2283.d)
extrusion of, process development for, 20: 4301(R) (ORNL-3870, pp 102-35)
fatigue of, effect of crystal structure on, 20: 4443
Fermi surfaces calculations for, 20: 4476(R) (IS-1200(Sect.P))
heat of sublimation, 20: 4438
joining of, development of brazing, fusion welding, and thermochemical deposition methods for, 20: 4302(R) (ORNL-3870, pp 155-63)
magnetic susceptibility of, de Haas–Van Alphen effects in, (E), 20: 4476(R) (IS-1200(Sect.P))
neutron cross sections for, 9- and 16-group, 20: 4829 (GEMP-173 (Suppl.1))
neutron cross sections for, 20: 4830 (GEMP-384)
photoemission from, effects of radiation frequency and temperature on surface, 20: 4479(R) (TID-22179, pp 1-83)
production of sheets of, by thermochemical deposition, 20: 4302(R) (ORNL-3870, pp 155-63)
properties of thermochemically deposited, 20: 4302(R) (ORNL-3870, pp 155-63)
properties of, effects of grain boundaries on, 20: 4386(R) (ORNL-3870, pp 20-6)
purification by electron-beam melting, 20: 5181(R) (ORNL-3029)
separation from low grade ores, reductive chlorination process for, 20: 4072(P)
sputtering by argon ions at 1.5 to 30 kev, yields from, (E), 20: 4546
sputtering by xenon ions at 1.5 to 30 kev, yields from, (E), 20: 4546
structure of, electronic, (T), 20: 4476(R) (IS-1200(Sect.P))
tensile properties of, effects of carbon and heat treatments on, 20: 4408
thermal conductivity at 100 to 3400°C, 20: 4301(R) (ORNL-3870, pp 102-35)
thermal conductivity to 1000°C, 20: 4388(R) (ORNL-3870, pp 44-9)
thermionic emission in cesium vapor, dependence on crystallographic direction and temperature, 20: 4948(R) (TID-22179, pp 85-175)
vapor pressure at 2574 to 3183°K, 20: 4438
Tc–W, compositions of second-phase regions of arc-melted, 20: 4367(R) (BNWL-162)
TUNGSTEN ALLOYS
Al–Nb–Ti–W–V–Zr, properties for use to 1200°F, 20: 4393 (PWAC-472)
Al–Ti–W–V–Zr, properties for use to 1200°F, 20: 4393 (PWAC-472)
Cr–Fe–Mo–Ni–Nb–W, welding properties of Inco IN-102, 20: 4306(R) (ORNL-3870, pp 194-213)
Hf–Nb–W–Y, evaporation losses in high vacuum of C-129Y, 20: 4301(R)

(ORNL-3870, pp 102-35)
Hf–Ta–W, corrosion of T-111, by potassium, 20: 4301(R) (ORNL-3870, pp 102-35)
Hf–Ta–W, corrosion of T-111, by lithium, effects of oxygen on, 20: 4301(R) (ORNL-3870, pp 102-35)
Hf–Ta–W, evaporation losses in high vacuum of T-111, 20: 4301(R) (ORNL-3870, pp 102-35)
Hf–Ta–W, preparation and specifications for corrosion loop testing, 20: 4380 (NASA-CR-54761)
Hf–Ta–W, recovery and recrystallization of T-111, 20: 4301(R) (ORNL-3870, pp 102-35)
Hf–Ta–W, tensile properties of welded plates of T-111, 20: 4301(R) (ORNL-3870, pp 102-35)
Hf–Ta–W, thermal conductivity of T-111, at 30 to 120°C, 20: 4301(R) (ORNL-3870, pp 102-35)
Hf–W, emissivity properties of, 20: 4405(T) (K-Trans-9)
Hf–W, properties at high temperatures, 20: 4418
La–W, preparation and properties of single-crystal, (E), 20: 4476(R) (IS-1200(Sect.P))
Mo–W, stress recovery of, flow, 20: 4409
Nb–Ta–W–Zr, corrosion of FS-85, by lithium, effects of oxygen on, 20: 4301(R) (ORNL-3870, pp 102-35)
Nb–Ta–W–Zr, creep properties of FS-85, 20: 4301(R) (ORNL-3870, pp 102-35)
Nb–Ta–W–Zr, ductility of FS-85, effects of aging on bend, 20: 4301(R) (ORNL-3870, pp 102-35)
Nb–Ta–W–Zr, evaporation losses in high vacuum of FS-85, 20: 4301(R) (ORNL-3870, pp 102-35)
Nb–Ta–W–Zr, preparation and specifications for corrosion loop testing, 20: 4380 (NASA-CR-54761)
Nb–W–Zr, corrosion of Cb-752, by lithium, effects of oxygen on, 20: 4301(R) (ORNL-3870, pp 102-35)
Nb–W–Zr, creep properties of Cb-752, 20: 4301(R) (ORNL-3870, pp 102-35)
Ni–W, atomic structure of, short-range order and size-effect coefficients for, (E), 20: 4421
Re–Ta–W, tensile strength at 3500°F, 20: 4455(P)
Re–W, deposition of, thermochemical, 20: 4342(R) (ORNL-3870, pp 85-101)
Re–W, extrusion of, process development for, 20: 4301(R) (ORNL-3870, pp 102-35)
Re–W, fabrication and properties of tubes of, 20: 4340(R) (COO-1518-1)
Ta–W, creep properties of, 20: 4301(R) (ORNL-3870, pp 102-35)
Ti–W, properties at high temperatures, 20: 4418
W–Zr, properties at high temperatures, 20: 4418

TUNGSTEN BROMIDES
preparation of polynuclear, 20: 3863(R) (IS-1200(Sect. C))

TUNGSTEN BRONZE
analysis for lithium and sodium, spectrographic, 20: 3863(R) (IS-1200 (Sect. C))

TUNGSTEN CARBIDES
corrosion by cesium at 400°C, 20: 4337
Co–WC, brazing to TZM alloy, use of boron–nickel–silicon alloy for, 20: 4307(R) (ORNL-3870, pp 238-42)

TUNGSTEN ISOTOPES W-174
production, (E), 20: 4834 (JINR-E-2360)

TUNGSTEN ISOTOPES W-182
energy levels of, ground state rotational band in, (E), 20: 4865
energy levels of, half life of first excited, (E), 20: 4877

TUNGSTEN ORES
processing by reductive chlorination, 20: 4072(P)

TUNGSTEN OXIDES
solubility in borax at 760 to 900°C, 20: 3951

TUNGSTEN SYSTEMS
C–Hf–Ta–W, preparation and specifications for corrosion loop testing, 20: 4380 (NASA-CR-54761)
C–Mo–Nb–Ta–W–Zr, preparation and specifications for corrosion loop testing, 20: 4380 (NASA-CR-54761)
C–Nb–W–Zr, aging and recrystallization of D-43, 20: 4301(R) (ORNL-3870, pp 102-35)
C–Nb–W–Zr, corrosion of D-43, by potassium, 20: 4301(R) (ORNL-3870, pp 102-35)
C–Nb–W–Zr, corrosion of D-43, by lithium, effects of oxygen on, 20: 4301(R) (ORNL-3870, pp 102-35)
C–Nb–W–Zr, ductility of welds in D-43, effects of aging on bend, 20: 4301(R) (ORNL-3870, pp 102-33)
C–Nb–W–Zr, evaporation losses in high vacuum of D-43, 20: 4301(R) (ORNL-3870, pp 102-35)
C–Nb–W–Zr, preparation and specifications for corrosion loop testing, 20: 4380 (NASA-CR-54761)
C–Nb–W–Zr, tensile properties of welded plates of D-43, 20: 4301(R) (ORNL-3870, pp 102-35)
C–Nb–W–Zr, thermal conductivity of D-43, at 30 to 120°C, 20: 4301(R) (ORNL-3870, pp 102-35)

TURBINES
design for space power plants, 20: 4299(R) (ORNL-2711)
stress analysis of axisymmetric disks of, (T), 20: 4075 (GA-6267)

U

ULCERS
radiotherapy of duodenal, 20: 3821

ULTRASONICS
attenuation in normal and superconducting lead, 20: 4782
propagation in annealed and neutron-irradiated copper single crystals, (E), 20: 5012
use in inspection of duplex tubing, 20: 4999(R) (ORNL-2599)
use in size analysis of dust particles, 20: 4149 (AD-623639)
use of inspecting pipes and tubes, 20: 5227(P)

ULTRAVIOLET RADIATION
effects of wavelength of, on plant growth, 20: 3769
effects on amino acid changes in cattle insulin, 20: 4016
effects on Aspergillus, mutagenic, uv, 20: 3755(T)
effects on Aspergillus, genetic, 20: 3756(T)
effects on bacteriophage complexes with *Escherichia coli*, biological, 20: 3749
effects on β-galactosidase in bacterial cells, mechanism of inactivation, 20: 3686(R) (TID-22352)
effects on Chlorella, genetic, 20: 3716(T) (JPRS-31514, pp 65-76)
effects on *Corynebacterium fascians*, genetic, 20: 3723
effects on *Escherichia coli*, genetic, 20: 3757
effects on *Escherichia coli*, genetic, 20: 3758
effects on fluorescence of organic phosphors in naphthalene solutions, 20: 3994
effects on induction of β-galactosidase and galactoside permease, mechanism for, 20: 3688
effects on infectious activity of *Mycobacterium lepraemurium*, 20: 3752
effects on protein synthesis in *E. coli*, 20: 3726
effects on Saccharomyces, genetic, 20: 3717(T) (JPRS-31514, pp 77-91)
effects on *Serratia marcescens*, lethal, effects of humidity on, 20: 3740
effects on skin, photosensitivity test for, 20: 3767
effects on *Sordaria brevicollis*, genetic, 20: 3783

UNDERGROUND EXPLOSIONS
blast effects from Salmon event on residential-type structures, 20: 4189 (VUF-1030)
blast effects from Salmon event on tall industrial and residential structures, 20: 4190 (VUF-1031)
book: *The Peaceful Applications of Nuclear Explosions; A Report on the Plowshare Program*, 20: 4085
cavity pressure and temperature measurements for, 20: 4084 (VUF-3017)
crater formation by single-, double-, and triple-row, comparison of, 20: 4083 (SC-RR-65-478)
effects on shallow-buried model arches, 20: 4131 (AD-622552)
fission fragment beta decay in, detection of neutrino emission from, 20: 4848 (UCRL-12085(Pt.2))
fission fragment beta decay in, detection of neutrino emission in, (T), 20: 4847 (UCRL-12085(Pt.1))
seismic signals from nuclear, in cavities, 20: 4167 (RM-3727(RAND))
use in petroleum production stimulation, radioactive contamination from, 20: 4082 (BM-RI-6684)

UNDERGROUND STRUCTURES
blast load effects on shallow-buried model arches, Operation Snowball traveling-wave, 20: 4131 (AD-622552)

UNDERWATER EXPLOSIONS
base surge and column formation in, measurement of, (E/T), 20: 4141 (AD-618733)
waves from, feasibility of modeling run-up effects of dispersive, (T), 20: 4142 (AD-619053)

UNION OF SOUTH AFRICA
cosmic-ray energy spectra at high altitude over, in 1962, 20: 4569

UNITED STATES
fallout monitoring in, by analysis of deciduous teeth, 20: 4160
radiation monitoring systems for foods in, 20: 4201

URANIUM
analysis for trace amounts of niobium, 20: 3897
content in oceanic theoleitic basalts, 20: 4145
content in porphyries in Saar-Nahe basin, Germany, 20: 4165
determination by titration using EDTA, 20: 3863(R) (IS-1200(Sect. C))
determination in hydrochloric acid or methanol–nitric acid media, spectrophotometric, 20: 3888 (TID-22402)
determination in iron–nickel–uranium solutions, controlled-potential coulometric, 20: 3879(R) (MLM-1266)
determination in uranium alloys, review of methods for, 20: 3890(T) (AEC-tr-6617)
determination in waste from uranium tetrafluoride reduction with magnesium, 20: 3906

determination of hexavalent presence of tetravalent, by solvent extraction and titration, 20: 3903
diffusion of xenon-133 from low-dose, low-temperature irradiated, (E), 20: 4471
dissolution using nitric acid, flowsheet for, 20: 4048(RL (NP-15406)
distribution between γ-alumina and molten chlorides, 20: 3959
effects on corrosion resistance of stainless steel in acidic solutions, 20: 4325 (TB-58)
fracture stresses of alpha-, at −196 to 270°C, effects of grain size on, 20: 4430
gamma reactions at 0.01 to 10 Mev, cross sections for, 20: 4996 (AWRE-O-79/65)
neutron Doppler coefficient and resonance capture in graphite reactors, 20: 5092
neutron scattering by, p-wave phase shifts in small-angle, (T), 20: 4909
oxidation by air, carbon dioxide, and oxygen, kinetics of, 20: 4329(T) (CEA-tr-R-1868)
preparation by reduction of urania, 20: 4297(R) (IS-1200(Sect.M))
preparation from uranium tetrachloride by electrolysis, 20: 4346
preparation of single crystals, 20: 4350
production by fusion electrolysis in uranium fluoride–potassium chloride–lithium chloride system, 20: 4347
production in Portugal, 20: 4047
radiation effects on, facility for studying, 20: 4092
radioinduced expansion of, texture measurements for predicting, 20: 4470
separation from irradiated fuels, 20: 4073(P)
separation from minerals, other metals, rocks, and sediments in mixed and nonaqueous solvents by ion exchange, 20: 3888 (TID-22402)
separation from sintered graphite–uranium compact, 20: 4074(P)
separation from spent fuels by solvent extraction, flowsheets for, 20: 4048(R) (NP-15406)
use as tracer, for skeletal metabolism studies, 20: 3664(R) (TID-22324)

URANIUM ALLOYS
analysis for trace amounts of niobium, 20: 3897
analysis for uranium, review of methods for, 20: 3890(T) (AEC-tr-6617)
Al–U, preparation of intermetallic compound UAl_3, 20: 4342(R) (ORNL-3870, pp 85-101)
Al–U, thermal expansion of intermetallic compound UAl_3 at 20 to 750°C, 20: 4436
Al–U, uses as sintering aid for uranium mononitride, 20: 4342(R) (ORNL-3870, pp 85-101)
Cr–U, corrosive effects of liquid, on niobium, 20: 4077(R) (IS-1200 (Sect. E))
Cr–U, corrosive effects of liquid, on tantalum and yttrium, 20: 4077(R) (IS-1200(Sect. E))
Cr–U, melting point of, effects of impurities on eutectic, 20: 4077(R) (IS-1200(Sect. E))
Fe–Ni–U, analysis for iron and uranium by controlled-potential coulometry, 20: 3879(R) (MLM-1266)
Mn–U, corrosive effects of liquid, on tantalum and yttrium, 20: 4077(R) (IS-1200(Sect. E))
Mn–U, melting point of, effects of impurities on eutectic, 20: 4077(R) (IS-1200(Sect. E))
Mo–U, dissolution using nitric acid, equipment and procedures for, 20: 4048(R) (NP-15406)
Mo–U, processing reactor fuels of, 20: 4060(P)
Pd–U, preparation for standard foils, 20: 3982(R) (AGN-8156)
Re–U, phase studies, 20: 4297(R) (IS-1200(Sect.M))
Tc–U, crystal structure of intermetallic compounds in, 20: 4428
Th–U, fabrication as fuel cycle material, design and construction of facility for, 20: 4343(R) (ORNL-3870, pp 266-89)
U–Zr, superconducting properties, 20: 4390(R) (ORNL-3870, pp 65-9)

URANIUM CARBIDES
corrosion by moist air, mechanisms and morphology of, 20: 4336
creep tests on, out-of-pile compressive, 20: 4396 (PWAC-482(Pt.1))
diffusion of xenon-133 in, at 950 to 1830°C, 20: 4450
diffusion of xenon-133 from low-dose, low-temperature irradiated, (E), 20: 4471
effects on graphitization of pyrolytic carbon, 20: 4386(R) (ORNL-3870, pp 20-6)
reactions with metal chlorides at 540 to 800°C, 20: 4297(R) (IS-1200 (Sect.M))
sintering using uranium silicides as aid, 20: 4342(R) (ORNL-3870, pp 85-101)
thermal diffusion and thermal capacity of, heat pulse measurements of, 20: 3943
vaporization at 2190 to 2525°K, heats of formation and vaporization in, 20: 4395 (PWAC-478)
NbC–UC, diffusion of xenon-133 from low-dose, low-temperature irradiated fuels of, (E), 20: 4471
ThC–UC, fabrication of graphite-coated, equipment and flowsheet for, 20: 4343(R) (ORNL-3870, pp 266-89)
ThC–UC, production from sol-gel microspheres, process for, 20: 4343(R)
ThC_2–UC_2, phase studies, 20: 4306(R) (ORNL-3870, pp 194-213)
ThC_2–UC_2, radiation effects on coated fuel particles of, 20: 4458 (GA-6485)
UC–ZrC, compatibility with refractory metals at 2000°C, 20: 4335
UC–ZrC, diffusion of xenon-133 from low-dose, low-temperature irradiated fuels of, (E), 20: 4471

URANIUM(IV) CHLORIDES
electrolysis of, for preparation of uranium metal, 20: 4346

URANIUM COMPOUNDS
preparation of organic, methods for, 20: 3961

URANIUM(IV) FLUORIDES
properties of molten, for use as reactor fuel, 20: 4376 (JUL-268-RG)
reactions with oxygen and steam, pyrohydrolytic, 20: 4046(R) (EURAEC-1340)
reduction by magnesium, determination of uranium in waste from, 20: 3906
BeF_2–LiF–UF_4–ZrF_4, corrosive effects on type 304 stainless steel, 20: 4308(R) (ORNL-3870, pp 243-60)
UF_4–KCl–LiCl, electrolysis of fused, for production of high-purity uranium, 20: 4347

URANIUM(VI) FLUORIDES
properties of molten, for use as reactor fuel, 20: 4376 (JUL-268-RG)
reactions with lithium chloride–potassium chloride eutectics, 20: 4046(R) (EURAEC-1340)
reactions with sulfur dioxide, kinetics of, 20: 3935
sorption in fused salts, 20: 4046(R) (EURAEC-1340)

URANIUM GLASS
spectra of, absorption, 20: 4077(R) (IS-1200(Sect. E))

URANIUM IONS
reactions in pure and mixed solvents and in presence of inert salts, exchange, 20: 3964
separation of (VI) from other cations, chromatographic, 20: 3863(R) (IS-1200(Sect. C))

URANIUM ISOTOPES
neutron cross sections for Oralloy and Oralloy dioxide, 20: 4829 (GEMP-173(Suppl.1))

URANIUM ISOTOPES U-233
fabrication costs of fuels and fuel elements containing, economic study of, 20: 5024(R) (ORNL-3870, pp 261-5)

URANIUM ISOTOPES U-234
spectra of, alpha, 20: 3879(R) (MLM-1266)

URANIUM ISOTOPES U-235
fission fragment energy spectra of, 20: 3982(R) (AGN-8156)
fission of, gamma spectra from, (E), 20: 4849(R) (UCRL-14360, pp 1-50)
neutron cross sections for, 9- and 16-group, 20: 4829 (GEMP-173(Suppl.1))
neutron cross sections for, 20: 4830 (GEMP-384)
neutron Doppler coefficient in ZPR II 45A, 20: 5072
neutron fission of, prompt gamma spectra from thermal, 20: 5181(R) (ORNL-3029)
neutron fission of, prompt gamma spectra from thermal, 20: 4299(R) (ORNL-2711)

URANIUM ISOTOPES U-238
economics for use in thermal reactors, 20: 5114 (CRRP-1221)
meson (π^-) capture by, x-ray spectra of, 20: 4825(R) (ANL-7081, pp 81-93)
neutron cross sections for, 9- and 16-group, 20: 4829 (GEMP-173(Suppl.1))
neutron cross sections for, 20: 4830 (GEMP-384)
neutron resonances of, effective temperature for Doppler broadening of, 20: 5135 (WCAP-3269-40)

URANIUM LEACH RESIDUES (CARBONATE)
processing for vanadium removal, using column or bed of lead shot, 20: 4071(P)

URANIUM NITRATES
effects of injected in rats, pathological, 20: 3666

URANIUM NITRIDES
creep tests on, out-of-pile compressive, 20: 4396 (PWAC-482(Pt.1))
diffusion of fission gas from, 20: 4303(R) (ORNL-3870, pp 164-70)
diffusion of nitrogen in, activation energy and rate of self-, 20: 4394 (PWAC-477)
hardness of, effects of density on hot, 20: 4303(R) (ORNL-2870, pp 164-70)
lattice parameters of effects of carbon content on, 20: 4303(R) (ORNL-3870, pp 164-70)
separation of oxygen from, use of carbon for, 20: 4303(R) (ORNL-3870, pp 164-70)
sintering in pure argon at 1700°C, 20: 4349
sintering of cold-pressed, at 1700°C, 20: 4303(R) (ORNL-3870, pp 164-70)
sintering using UAl_3 as aid, 20: 4342(R) (ORNL-3870, pp 85-101)
solvent properties for nitrogen, 20: 4303(R) (ORNL-3870, pp 164-70)

URANIUM ORES
processing in Portugal, 20: 4047
radiation dose to population from, 20: 4193
URANIUM OXIDES
preparation of well-sintered, by thermal decomposition of ammonium uranyl nitrate, 20: 4052
URANIUM(IV) OXIDES
compatibility with niobium, 20: 5181(R) (ORNL-3029)
compatibility with niobium–zirconium alloy, 20: 5181(R) (ORNL-3029)
crystal growing technique, 20: 3919(R) (ORNL-3870, pp 3-6)
deposition of, thermochemical, 20: 4342(R) (ORNL-3870, pp 85-101)
destruction in-pile, fission product release during, 20: 4183(R) (ORNL-3843, pp 2-70)
diffusion in, alpha spectrometric studies of self-, 20: 4412
diffusion of fission-product krypton in, 20: 4435
diffusion of rare gases in, 20: 3944
diffusion of xenon-133 from low-dose, low-temperature irradiated, (E), 20: 4471
dimensional stability of fuels of, equipment for post-irradiation measurement of, 20: 5136 (WCAP-5564)
dissolution using nitric acid, flowsheet for, 20: 4048(R) (NP-15406)
electric properties of nonstoichiometric, 20: 4439
fission fragments from, ratio to ejected uranium atoms, 20: 3982(R) (AGN-8156)
fission product distributions in sintered, radial, (E), 20: 4472
oxidation studies, 20: 3952
preparation of hydrophilic or organophilic sols of, 20: 3969(P)
radiation effects on fuel rods of, produced by alternate fabrication processes, 20: 4459 (GEAP-4850)
radiation effects on fuel compacts and pellets of, produced by alternate fabrication processes, 20: 4459 (GEAP-4850)
radiation effects on properties of, at 1600 to 2400°C, 20: 4306(R) (ORNL-3870, pp 194-213)
reactions of clad, with 1000-psi steam in TREAT, 20: 4183(R) (ORNL-3843, pp 2-70)
reactions of stainless steel-clad, with high-temperature steam, 20: 4184(R) (ORNL-3843, pp 71-135)
reactions of Zircaloy-2-clad, in helium–steam mixtures at high temperatures, 20: 4184(R) (ORNL-3843, pp 71-135)
reactions with chlorine trifluoride and fluorine, 20: 4046(R) (EURAEC-1340)
separation from fused salts by electrodeposition, 20: 4046(R) (EURAEC-1340)
solvent properties for helium-4, 20: 3946
testing of irradiated, nondestructive methods for, 20: 4124
thermal conductivity of reactor fuel pellets of, 20: 5135 (WCAP-3269-40)
thermal stability of pyrolytic-carbon-coated fuel particles of, 20: 4306(R) (ORNL-3870, pp 194-213)
vapor pressure at 2200 to 2800°K, 20: 4369 (CEA-R-2871)
vaporization for reactor-accident simulation, methods for, 20: 4086(R) (ORNL-3843, pp 137-67)
Ni–UO_2, preparation of fibrous, for fissiochemical reactions, 20: 3982(R) (AGN-8156)
PuO_2–stainless steel–UO_2, radiation effects on, in-pile, (E), 20: 5192 (BNWL-SA-251)
PuO_2–UO_2, fabrication of fuel elements of, economics of, 20: 4339 (BNWL-131D)
PuO_2–UO_2, fluorination and hydrofluorination using chlorine trifluoride, 20: 4046(R) (EURAEC-1340)
PuO_2–UO_2, radiation effects on, in-pile, (E), 20: 5192 (BNWL-SA-251)
PuO_2–UO_2, reactivity sodium void effects on, in fast reactors, 20: 5068
PuO_2–UO_2–ZrO_2, properties for use in thermal reactors, 20: 4382(R) (NUMEC-3505-8)
stainless steel–UO_2, radiation effects on, in-pile, (E), 20: 5192 (BNWL-SA-251)
ThO_2–UO_2, diffusion of rare gases in, 20: 3944
ThO_2–UO_2, fabrication of reactor fuel rods of, flowsheet for, 20: 4343(R) (ORNL-3870, pp 266-89)
ThO_2–UO_2, preparation and properties of carbon-coated sol-gel microspheres of, 20: 4344 (ORNL-P-1725)
ThO_2–UO_2, preparation and properties of microspheres of, 20: 3922 (ORNL-TM-1281)
ThO_2–UO_2, radiation effects on coated fuel particles of, 20: 4458 (GA-6485)
ThO_2–UO_2, radiation effects on properties of vibratory-compacted sol-gel fuel rods of, in-reactor, 20: 4343(R) (ORNL-3870, pp 266-89)
ThO_2–UO_2, radiation effects on carbon-coated sol-gel microspheres of, 20: 4344 (ORNL-P-1725)
ThO_2–UO_2, reactivity sodium void effects on, in fast reactors, 20: 5068
ThO_2–UO_2, sintering and grain growth of sol-gel, 20: 4343(R) (ORNL-3870, pp 266-89)
UO_2–H_2O, neutron thermal disadvantage factors for, 20: 5073
UO_2–H_2O, reactivity temperature coefficient for, reflector effects on, (E), 20: 5067
UO_2–H_2O, volume ratio effects on reactor fuel cycle cost, 20: 5176 (EUR-2468.e)
URANIUM(IV-VI) OXIDES
phase transformation in, at 50 to 600°C, 20: 4429
properties of commercial powders of, 20: 4342(R) (ORNL-3870, pp 85-101)
URANIUM(VI) OXIDES
preparation from paste of uranyl nitrate or ammonium uranate and uranium oxide particles, 20: 3971(P)
URANIUM PHOSPHIDES
thermal diffusion and thermal capacity of, heat pulse measurements of, 20: 3943
URANIUM POISONING
effects on cholinesterase activity in mouse liver, 20: 3670
effects on cholinesterase activity in mouse kidney, 20: 3670
pathology of, in rats, 20: 3666
URANIUM SILICIDES
uses as sintering aid for uranium carbide, 20: 4342(R) (ORNL-3870, pp 85-101)
URANIUM SULFIDES
thermal diffusion and thermal capacity of, heat pulse measurements of, 20: 3943
URANIUM SYSTEMS
C–Ni–U, phase studies, 20: 4368 (CEA-R-2845)
C–N–O–Pu–U, corrosion by water at 550°F, 20: 4327(R) (UNC-5138)
C–N–O–Pu–U, preparation of single-phase compositions of, 20: 4327(R) (UNC-5138)
C–O–Pu–U, preparation of single-phase compositions of, 20: 4327(R) (UNC-5138)
graphite–U, separation of uranium from sintered, 20: 4074(P)
H–U, criticality studies of, 20: 5071
URANYL CHLORIDES
fluorescence spectra in rare earth chlorides, 20: 3948
preparation of anhydrous, 20: 3961
URANYL IONS
fluorescence spectra in rare earth chlorides, 20: 3948
URANYL NITRATES
solvent properties of aqueous solutions of, for tributyl phosphate, 20: 3955
toxic effects of, in mice, 20: 3670
use in preparation of uranium(VI) oxides, 20: 3971(P)
URIDINE, 5-BROMO-2'-DEOXY-
effects on DNA replication in animal cells, 20: 3737
URINARY TRACT
demonstration of vesicoureteral reflux by dye test, 20: 3834
morphology of, radiographic determination, 20: 3800(R) (NP-15150)
URINE
radiation effects on zinc content in human, x, 20: 3693
radioactivity in human, following injections of iodine-131-labeled polyvinylpyrrolidone, 20: 3675
thorium-232 content in, from Thorotrast patients, 20: 3683
UTERUS
radiotherapy of cancers of, late pathological effects, 20: 3856
radiotherapy of carcinomas in, method for, 20: 3807
radiotherapy of cervical carcinomas in human, rectal injuries following, 20: 3734

V

VAGINA
radiotherapy of, doses and methods for, 20: 3848
VALLECITOS BOILING WATER REACTOR
experimental facilities for testing superheater fuel elements, uses of E-SADE loop, 20: 5104 (ACNP-65006)
VALVES
design of gate, with obturating member to close off conduit, 20: 5042(P)
VAN ALLEN RADIATION BELTS
electron energy spectra and pitch angle distributions in, from high-altitude explosions, 20: 4732 (UCRL-14368-T(Rev.1))
electron spectra in, from Starfish detonation, 20: 4731 (UCRL-7659-T (Rev.1))
VAN DE GRAAFF ACCELERATORS
radiation dose distribution for electron, inhomogeneity of, 20: 4204
research at 12-Mev tandem, 20: 4823(R) (ANL-7081, pp 36-69)
research at 4.5-Mev, 20: 4822(R) (ANL-7081, pp 22-35)
VANADIUM
determination in hydrochloric acid or methanol–nitric acid media, spectrophotometric, 20: 3888 (TID-22402)
determination in mixtures by x-ray fluorescence using promethium-147/aluminum and tritium/zirconium sources, 20: 3883 (ORNL-IIC-5, pp 154-81)

ductility of, effects of nitrogen and oxygen on low-temperature, 20: 4297(R) (IS-1200(Sect.M))
meson (μ^-) transitions in mesic atoms of, energy of, 20: 4825(R) (ANL-7081, pp 81-93)
plasticity of, effects of hydrogen on, 20: 4297(R) (IS-1200(Sect.M))
preparation and purification, 20: 4297(R) (IS-1200(Sect. M))
purification by electron-beam melting, 20: 5181(R) (ORNL-3039)
separation from aqueous solutions using lead shot column or bed, 20: 4071(P)
separation from low grade ores, reductive chlorination process for, 20: 4072(P)
separation from silver by partition chromatography, 20: 4054

VANADIUM ALLOYS
Al–Co–Fe–Ti–V, properties of aged, 20: 4360(R) (AD-619399)
Al–Cr–Ge–Ti–V, properties of aged, 20: 4360(R) (AD-619399)
Al–Cr–Ti–V, properties of aged, 20: 4360(R) (AD-619399)
Al–Fe–Mo–Ti–V, properties of aged, 20: 4360(R) (AD-619399)
Al–Fe–Ti–V, properties of aged, 20: 4360(R) (AD-619399)
Al–Mn–Ti–V, properties of aged, 20: 4360(R) (AD-619399)
Al–Nb–Ti–W–V–Zr, properties for use to 1200°F, 20: 4393 (PWAC-472)
Al–Ti–V, corrosion by cesium at 400°C, 20: 4337
Al–Ti–W–V–Zr, properties for use to 1200°F, 20: 4393 (PWAC-472)
Co–Fe–V, properties of Hiperco 50 and Supermendur for use in space electric power systems, 20: 4379 (NASA-CR-54091)
Cr–Fe–Mo–V, properties of H-11 Steel for use in space electric power systems, 20: 4379 (NASA-CR-54091)
Cr–V, nuclear magnetic resonance of, (E), 20: 4476(R) (IS-1200(Sect.P))
Ga–V, superconductivity, 20: 4426
Mo–Nb–V–Zr, corrosion of B-66, by lithium, effects of oxygen on, 20: 4301(R) (ORNL-3870, pp 102-35)
Mo–Nb–V–Zr, evaporation losses in high vacuum of B-66, 20: 4301(R) (ORNL-3870, pp 102-35)
Mo–Nb–V–Zr, tensile properties of welded plates of B-66, 20: 4301(R) (ORNL-3870, pp 102-35)
Nb–Ta–V, development as brazing alloy for refractory metals, 20: 4301(R) (ORNL-3870, pp 102-35)
Nb–V, twinning in, relation of dislocation substructure to, 20: 4389(R) (ORNL-3870, pp 61-4)
Ta–Ti–V, development as brazing alloy for refractory metals, 20: 4301(R) (ORNL-3870, pp 102-35)
Ti–V, diffusion of titanium-44 in, 20: 4385(R) (ORNL-3870, pp 15-19)

VANADIUM IODIDES
phase studies, 20: 3863(R) (IS-1200(Sect. C))

VANADIUM IONS
effects on crystalline electric fields, method for calculating, 20: 5006(R) (ORNL-3870, pp 50-5)
electron transfer between cobalt(III) and divalent, oxyanions as bridging groups in, 20: 3967
oxidation by chromium(VI), 20: 3863(R) (IS-1200(Sect. C))

VANADIUM ISOTOPES V-50
energy levels of, from proton reactions (p,d) with vanadium-51 at 22 Mev, (E), 20: 4899

VANADIUM ISOTOPES V-51
proton reactions (p,d) at 22 Mev, energy levels from, (E), 20: 4899

VANADIUM NITRIDES
hardness of, effects of temperature on, 20: 4297(R) (IS-1200(Sect.M))

VANADIUM ORES
processing by reductive chlorination, 20: 4072(P)

VANADIUM SYSTEMS
Al–Cr–Si–Ti–V, properties of aged, 20: 4360(R) (AD-619399)

VAPOR PRESSURE
measurement by Knudsen effusion method, equipment for, 20: 4369 (CEA-R-2871)

VELA PROJECT
blast effects from Salmon event on residential-type structures, 20: 4189 (VUF-1030)
blast effects from Salmon event on tall industrial and residential structures, 20: 4190 (VUF-1031)
cavity pressure and temperature measurements in Dribble, 20: 4084 (VUF-3017)

VESPIDAE
radioinduced mutations of *Dahlbominus fuscipennis*, 20: 3733

VESSELS
pressurization in storage, effects on gas evolution from plutonium residues on, 20: 4364 (AERE-M-1644)

VIBRATIONS
effects of water on natural frequency of beam, 20: 4080 (WAPD-TM-535)

VIRUSES
effects on human embryos, teratogenic, 20: 3747
leukemia induced in mice by, immunological differences in, 20: 3694
radiation effects on inflammation induced by herpes zoster, x, 20: 3836
radiation effects on infections of plants caused by, y, 20: 3768

VISION
radiation effects on discriminatory, in monkeys, effects of age on, x, 20: 3721

VITAMIN B
radiation effects on, in presence of calcium carbonate, dibasic calcium phosphate, and sodium chloride, 20: 4018

VITAMIN B_{12}
radiation effects on intestinal absorption of, 20: 3851

VITAMIN D
effects on calcium-47 metabolism in normal and rachitic children, 20: 3672

VITAMIN D_2
content in irradiated yeast, chromatographic determination, 20: 3690

VOLCANOES
dust particles from ground surface of, method for size analysis of, 20: 4149 (AD-623639)

VOLTAGE REGULATORS
properties for electromagnetic isotope separators, 20: 4281 (IAE-926)

WASPALOY
corrosion by lithium fluoride in cyclic high-temperature environment, 20: 4326 (TRW-ER-6561)

W

WASTE DISPOSAL
at Hallam Nuclear Power Facility, 20: 5130(R) (TID-22355)
methods for, 20: 5207
methods for Eurochemic, 20: 4048(R) (NP-15406)
methods for LCBWR, 20: 5105 (ACNP-65544(Vol.I))
sealing in refractory vessels, method for, 20: 5209(P)

WASTE PROCESSING
facilities and methods for, design and engineering aspects of, 20: 5207
method of, using sulfuric acid dissolution, 20: 5208(P)

WASTE SOLUTIONS
analysis for polonium-210 by ion exchange and gamma counting, 20: 3879(R) (MLM-1266)
processing radioactive, using manganese dioxide, 20: 5206
processing sulfate-containing, for strontium recovery, 20: 5210(P)
separation of actinium-227 from, by ion exchange, 20: 3879(R) (MLM-1266)
treatment, 20: 5207

WATER
analysis for ethanol using beta-excited x-ray sources, absorptiometric, 20: 3882 (ORNL-IIC-5, pp 51-71)
analysis for fission products, design of monitor for, 20: 3909
boiling burnout heat flux in internally cooled tubes, effects of inlet flow conditions on, 20: 4101(R) (EURAEC-1354)
boiling burnout in annular flows at 1000 psi, (E), 20: 4105 (TID-22321)
corrosive effects on Zircaloy-4 under heat-transfer conditions, 20: 4331
corrosive effects on carbon- and nitrogen-stabilized plutonium–uranium monoxide at 550°F, 20: 4327(R) (UNC-5138)
corrosive effects on europium molybdate at 100 and 250°C, 20: 4305(R) (ORNL-3870, pp 187-90)
corrosive effects on aluminum–yttrium alloys, effects of yttrium content on, 20: 4320(R) (ORNL-3870, pp 70-4)
decontamination of, fast-filtration and ion-exchange methods for, 20: 4068
determination in sand, by neutron thermalization, 20: 3913(P)
determination in water-d_2, photometric, 20: 3970(P)
effects on natural frequency of beam vibration, 20: 4080 (WAPD-TM-535)
flow distribution in annular fuel elements for TSR-II, 20: 4299(R) (ORNL-2711)
gamma angular distributions and energy spectra in, calculation using Monte Carlo method, 20: 5181(R) (ORNL-3029)
gamma heating in slabs of, 20: 4999(R) (ORNL-2599)
heat of dilution and solution of rare earth chlorides in, 20: 3956
heat transfer in bulk boiling, nonuniform axial, 20: 4104 (NP-15622)
hypersonic and ultrasonic velocities in, effects of relaxation on, 20: 4479(R) (TID-22179, pp 1-83)
light scattering by, Cabannes factor and Rayleigh ratio for, 20: 3941
neutron flux measurements in, using gold activation, thermal, 20: 5181(R) (ORNL-3029)
neutron inelastic scattering by, cross sections for, (E), 20: 4807(R) (RPI-328-40, pp 56-66)
neutron scattering by, differential cross sections for thermal, (E/T), 20: 4801(R) (GA-6634)
neutron transmission by finite slabs of, 20: 4999(R) (ORNL-2599)
radiation effects on content of, in forest soils, 20: 3653 (BNL-8466)
radiation monitoring in German, 1965, 20: 4164
reactions with fission products, effects of chemical agents on, 20: 4185(R) (ORNL-3843, pp 169-234)
reactions with sodium, effects on design of steam generators, 20: 4100 (BW-67-2(a))
solvent properties for cerium(IV) nitrates, 20: 3954
thermal conductivity, 20: 4310(R) (ORNL-P-1699)

Fe–H_2O, neutron transport in, (E/T), 20: 4998 (JINR-P-2359)
Fe–H_2O, proton reactions at 170 to 660 Mev, neutron production in, (T), 20: 4998 (JINR-P-2359)
steam-water, heat flux dryout in internally heated annuli, (E), 20: 4099 (AECL-2332)
UO_2–H_2O, neutron thermal disadvantage factors for, 20: 5073
UO_2–H_2O, reactivity temperature coefficient for, reflector effects on, (E), 20: 5067
UO_2–H_2O, volume ratio effects on reactor fuel cycle cost, 20: 5176 (EUR-2468.e)

WATER-d_2
analysis for light water, photometric, 20: 3970(P)
effects on cells, review, 20: 3651
effects on growth in cell cultures and microorganisms, review, 20: 3651
light scattering by, Cabannes factor and Rayleigh ratio for, 20: 3941
loss from HBWR, Oct. 1964–Mar. 1965, 20: 5123(R) (HPR-61)
neutron scattering by, differential cross sections for thermal, (E/T), 20: 4801(R) (GA-6634)
piezo-optic coefficients, 20: 4484
use in reactors, problems in, 20: 5143
Fe–D_2O, neutron fluxes and leakage through perforated laminates of, (E/T), 20: 4800 (AE-198)

WATER-t_2
monitoring of vapors of, scintillation detector for, 20: 4235 (AECL-2283)

WATER COOLED REACTORS
development of direct-cycle steam-superheating, 20: 5113 (CONF-650602-59)
fuel element cans for, development of "nuclear vapotron," (E), 20: 5088(R) (EURAEC-1337)
physics methods development for large, 20: 5134(R) (WCAP-3269-12)

WATER MODERATED REACTORS
design, 20: 5086(P)
reactivity of homogeneous, 20: 5062

WATER SUPPLIES
analysis for strontium-90, method for, 20: 3867 (CEA-R-2844)
decontamination of, bacteriological, chemical, and radiological warfare agents, 20: 4192(T) (JPRS-32686)
radiation dose to population from, in regions with uranium ores, 20: 4193
radium content in, analysis of deciduous teeth for monitoring, 20: 4160

WATER VAPOR
convection in atmosphere, 20: 4153(R) (UCRL-14360, pp 73-85)
effects on atmospheric absorption at 1.35 cm wavelength, 20: 4479(R) (TID-22179, pp 1-83)
measurement in atmosphere and clouds using microwave radiometers, 20: 4479(R) (TID-22179, pp 1-83)
monitoring of tritiated, scintillation detector for, 20: 4235 (AECL-2283)
separation from barium, cadmium, molybdenum, and yttrium oxides for neutron transmission measurements, 20: 3914 (AERE-M-1654)

WATER WAVES
run-up effects of dispersive, feasibility of modeling, (T), 20: 4142 (AD-619053)

WELDED JOINTS
design of swaged, in aluminum-clad target rods, 20: 5175(R) (ORNL-3870, pp 230-7)

WELDS
effects on reactor accident containment, limiting, 20: 5034 (NOLTR-63-140)

WELL LOGGING
equipment and method for neutron–gamma, for detection of hydrocarbons, 20: 4170(P)
equipment for neutron–gamma, calibration of, 20: 4171(P)
radiometric, Monte Carlo fast convergence method in, 20: 4168

WHEAT
radioinduced mutations of *Triticum monococcum*, 20: 3762

WHISTLERS
interactions with electrons and protons in magnetosphere, gyroresonance radiation from, (T), 20: 4747

WIND
effects on cloud formation from chemical explosives, 20: 4152 (TID-22266)
effects on fallout transport and deposition, 20: 4154(R) (AD-620003)
properties of stratospheric, during IGY, 20: 4151 (MIT-2241-14)

WINDSCALE ADVANCED GAS COOLED REACTOR
operating experience, 20: 5164

WOOD
shock wave effects on sugar-pine, (E), 20: 5023(R) (IITRI-578P21-15)

X

X RADIATION
absorption by man of, during diagnostic radiography, 20: 3816
absorption in man and phantoms, measurements of, 20: 4207
diffraction by crystal dislocations, theory and uses of, 20: 5003 (CEA-R-2875)
dose measurements of, for gonads of children during diagnostic radiography, 20: 3854
dose measurements of, from diagnostic radiography during pregnancy, 20: 3823
dose of, from repeated diagnostic radiography, 20: 3834
dose to gonads during dental radiography, 20: 4206
dose to gonads from dental radiography in Japan, 20: 4196
dose to patient during urography, effects of contrast media dose in reducing, 20: 3857
dosimetry of, from chaoul-type tubes, 20: 3838
dosimetry of, phosphate glass element for, 20: 4258(P)
effects in mice, mechanism for leukemogenic, 20: 3696
effects of therapeutic doses of, carcinogenic, 20: 3841
effects of therapeutic doses of, on oral mucosa, 20: 3744
effects of therapeutic doses of, on enzyme activity of tumors, 20: 3763
effects of therapeutic doses of, on intestine, pathological, 20: 3820
effects on antigenic characteristics of virus-induced mouse leukemia, 20: 3694
effects on behavior of parabiotic rat partners, 20: 3706 (AD-623365)
effects on behavior traits in swine, genetic analysis of, 20: 3784
effects on blood picture in rabbits, 20: 3709 (CEA-R-2865)
effects on blood protein content in rabbits, 20: 3709 (CEA-R-2865)
effects on bone growth in rats, 20: 3707 (AD-623641)
effects on bones of therapeutic doses, pathological, 20: 3856
effects on breast tumors prior to radical surgery, 20: 3861
effects on cells of transplanted mouse tumors, 20: 3750
effects on Chlorella, genetic, 20: 3716(T) (JPRS-31514, pp 65-76)
effects on chlorophyll mutation rates in barley, 20: 3782
effects on chromosomes in mouse fibroblasts, effects of culture density on aberrant x, 20: 3691
effects on chromosomes in man, 20: 3705(R) (AD-617601)
effects on coercive magnetic field of rochelle salt, 20: 3995
effects on colloidal systems and suspensions, 20: 4015
effects on corneal graft material, 20: 3719
effects on crystalline sugars, 20: 4020
effects on development of myelitis, 20: 3771
effects on development of bones in children, pathological, 20: 3808
effects on development of teeth, in monkeys, 20: 3743
effects on Drosophila, genetic, 20: 3713(T) (JPRS-31514, pp 29-43)
effects on Drosophila, genetic, 20: 3714(T) (JPRS-31514, pp 44-58)
effects on Drosophila, genetic, 20: 3715(T) (JPRS-31514, pp 59-64)
effects on electrophysical properties of germanium, 20: 4465
effects on enzyme levels in monkey blood, 20: 3692
effects on exteriorized intestine and spleen of rabbits, 20: 3775
effects on exteriorized intestine and spleen of rats, 20: 3775
effects on fasting rats of, pathological, 20: 3766
effects on fatty acid absorption in rats, tracer study, 20: 3754
effects on *Funaria hygrometrica* plants, genetic, 20: 3781
effects on germ-free mice, lethal, 20: 3778
effects on glasses, ESR studies of, 20: 5019
effects on glucose metabolism in rats, tracer study, 20: 3678
effects on growth of transplanted tumors in rats, 20: 3695
effects on growth of tumor transplants in mice, 20: 3751
effects on hematopoietic system, leukemogenic, 20: 3730
effects on immune reactions to sheep erythrocytes in rabbits, 20: 3689
effects on immune reactions in rabbits, 20: 3738
effects on immune reactions in injected thymocytes and lymph node cells in mice, 20: 3777
effects on immune reactions in rabbits, 20: 3746
effects on inflammation associated with Mikulicz's disease, 20: 3826
effects on inflammation of herpes zoster, 20: 3836
effects on life span of mice, effects of genotype on, 20: 3711(R) (NYO-3314-2)
effects on life-span of x-ray technicians in, 20: 3760
effects on lungs of hamsters and rats, morphologic, 20: 3785
effects on lymph nodes and vessels in rats, 20: 3718
effects on lymph system of therapeutic doses of, 20: 3852
effects on man, low doses, biological, 20: 3779
effects on methyl methacrylate polymers, protective effects of organic additives against, 20: 4036
effects on mice, genetic, 20: 3711(R) (NYO-3314-2)
effects on mice, genetic and leukemogenic, 20: 3765
effects on mitosis in plant cells, 20: 3764
effects on mitosis in animal cells, 20: 3764
effects on monkey jaw bones, effects of dose fractionation on necrotic, 20: 3742
effects on mouse plasma lipids and serum lipoproteins, 20: 3704
effects on *Neurospora conida*, biological, 20: 3780
effects on Nitella cyclosis, recovery from, 20: 3698
effects on performance of learned response by rats, effects of nembutal on, 20: 3772
effects on permeability of isolated frog heart, 20: 3794

effects on pig skin, effects of dose fractionation on, 20: 3735
effects on rat lungs, effects of dose fractionation on histological, 20: 3700
effects on rats, pathological, 20: 3795
effects on rectum following bladder therapy, 20: 3734
effects on retinal development in embryos, 20: 3724
effects on Saccharomyces, genetic, 20: 3717(T) (JPRS-31514, pp 77-91)
effects on seeds, genetic, 20: 3759
effects on skin epitheliomas, late carcinogenic, 20: 3811
effects on skin of, post-operative therapeutic doses used for breast carcinoma, 20: 3847
effects on survival of transplanted tumors in mice, 20: 3751
effects on thyroid glands of therapeutic doses of, carcinogenic, 20: 3739
effects on T5 receptor, factors affecting inactivation, 20: 3787
effects on visual discrimination in monkeys, effects of ageing on, 20: 3721
effects on zinc content in urine, 20: 3693
effects on zinc in aqueous carbonic anhydrase, 20: 3693
effects on Zollinger-Ellison syndrome, 20: 3821
emission from fission products, (E), 20: 4849(R) (UCRL-14360, pp 1-50)
emission of monoenergetic, from alpha-emitting isotopes, (E/T), 20: 4268 (ORNL-IIC-5, pp 353-73)
flux in atmosphere at 40 to 190 kev, albedo, (E), 20: 4752
flux of auroral-zone, periodicity in, (E), 20: 4751
humoral mediation of radioinduced motivation of rats during, 20: 3706 (AD-623365)
scattering by aqueous sodium caprylate, intensity of, (E), 20: 4483
scattering by melt-crystallized polyethylene, 20: 5022
scattering from lattice structures, relative intensity in, (E), 20: 5010
transmission by bone, measurement of mineral content by, 20: 3886 (ORNL-IIC-5, pp 290-4)
tumors of pharynx induced by therapeutic doses of, use for treatment of of thyrotoxicosis, 20: 3806
use for therapy of benign skin lesions of, 20: 3812
use in materials testing, conference on, 20: 4116

X-RAY-ABSORPTION ANALYSIS
sources for, use of beta-excited copper, iron, and molybdenum, 20: 3882 (ORNL-IIC-5, pp 51-71)

X-RAY BEAMS
attenuation by body compositions, 20: 3885 (ORNL-IIC-5, pp 277-89)
protective effects of hardening, during radiography, 20: 3815

X-RAY-DIFFRACTION ANALYSIS
diffuse scattering due to static atomic displacement and thermal motion in method for correcting for, 20: 4391(R) (ORNL-3870, pp 75-82)

X-RAY DIFFRACTOMETERS
design modifications for examination of gamma emitters, engineering drawings for, 20: 3910

X-RAY EQUIPMENT
design for chest radiography using ytterbium-169, 20: 3804 (ORNL-IIC-5, pp 309-28)
design for radiotherapy, 20: 4517
design using iodine-125 for measuring mineral changes in bones, 20: 3803 (ORNL-IIC-5, pp 257-76)
development of portable fluorescent, using promethium-147/aluminum source, 20: 3883 (ORNL-IIC-5, pp 154-81)
nomenclature and properties of, 20: 4228
use in nondestructive testing of radioactive materials, 20: 4122
x-ray production in tubes, voltage wave form effects on, (T), 20: 4091

X-RAY SOURCES
calibration of chaoul-type tubes for therapeutic use, 20: 3838
developments and uses of low-energy, conference on, 20: 4111 (ORNL-IIC-5)
use of beta-excited, for absorptiometry, 20: 3882 (ORNL-IIC-5, pp 51-71)

X-RAY SPECTROMETERS
use in chemical analysis with electron microprobes, 20: 3912

X-RAY SPECTROSCOPY
development and use as analytical tool, 20: 3911

XENON
buildup in reactors after shutdown, 20: 5074
buildup in reactors, time optimal shutdown problem in, 20: 5075
determination using omegatron, 20: 3908
diffusion of fission-recoil, in ionic crystals and sinters, 20: 3944
reactions with mercury-199 and -201, hyperfine-level excitation in, (E), 20: 4544

XENON FLUORIDES
preparation and properties of, review on, 20: 3915 (CEA-Bib-61)

XENON HYDROXIDES
preparation and properties of, review on, 20: 3915 (CEA-Bib-61)

XENON IONS
sputtering on copper, molybdenum, and tungsten at 1.5 to 30 kev, (E), 20: 4546

XENON ISOTOPES Xe-131
concentration by thermal diffusion, 20: 3879(R) (MLM-1266)

XENON ISOTOPES Xe-133
diffusion from fuels during low-dose, low-temperature irradiation, (E), 20: 4471
diffusion in uranium carbide at 950 to 1830°C, 20: 4450
use with nuclear image amplifier for blood flow and respiration measurements, 20: 3802 (ORNL-IIC-5, pp 239-42)

XENON ISOTOPES Xe-138
diffusion from pyrolytic carbon deposits, 20: 5089(R) (GA-6181)

XENON ISOTOPES Xe-139
diffusion from pyrolytic carbon deposits, 20: 5089(R) (GA-6181)

XENON OXIDES
preparation and properties of, review on, 20: 3915 (CEA-Bib-61)

XENON OXYFLUORIDES
preparation and properties of, review on, 20: 3915 (CEA-Bib-61)

XYLENE
diffusion in CGB graphite, 20: 4308(R) (ORNL-3870, pp 243-60)

Y

YANKEE POWER REACTOR
fuel assemblies for, remote underwater devices for post-irradiation examination of, 20: 5136 (WCAP-5564)
fuel pellet temperature for Doppler broadening of uranium-238 resonance, 20: 5135 (WCAP-3269-40)
power disturbances in, local, (E/T), 20: 5134(R) (WCAP-3269-12)

YEASTS
metabolism of selenium-75 in *Saccharomyces cerevisiae*, 20: 3661 (NP-15594)
radiation effects on Saccharomyces, genetic, x, 20: 3717(T) (JPRS-31514, pp 77-91)
radiation effects on Saccharomyces, genetic, uv, 20: 3717(T) (JPRS-31514, pp 77-91)
vitamin D_2 content in irradiated, chromatographic determination, 20: 3690

YTTERBIUM
analysis for oxygen by neutron activation, 20: 3863(R) (IS-1200(Sect. C))
determination in hydrochloric acid or methanol–nitric acid media, spectrophotometric, 20: 3888 (TID-22402)
effects on grain growth and recrystallization of tantalum, 20: 4424

YTTERBIUM ALLOYS
Ca–Yb, phase diagrams, 20: 4297(R) (IS-1200(Sect.M))
Mg–Yb, phase studies, 20: 4297(R) (IS-1200(Sect.M))
Pb–Yb, phase diagrams, 20: 4297(R) (IS-1200(Sect.M))

YTTERBIUM CHLORIDES
heat of dilution of aqueous, at 25°C, 20: 3956

YTTERBIUM ISOTOPES Yb-169
properties in portable devices for chest radiography, 20: 3804 (ORNL-IIC-5, pp 309-28)

YTTERBIUM ISOTOPES Yb-170
energy levels of, half life of first excited, (E), 20: 4877

YTTRIUM
analysis of, methods for, 20: 4299(R) (ORNL-2711)
corrosion by hydrofluoric acid at high temperatures, 20: 4077(R) (IS-1200(Sect. E))
corrosion by liquid chromium–uranium and manganese–uranium alloys, 20: 4077(R) (IS-1200(Sect. E))
deformation mechanisms of, 20: 4299(R) (ORNL-2711)
determination in hydrochloric acid or methanol–nitric acid media, spectrophotometric, 20: 3888 (TID-22402)
determination in lithium fluoride–magnesium fluoride–yttrium fluoride, 20: 4999(R) (ORNL-2599)
effects on niobium, additive, 20: 4299(R) (ORNL-2711)
hardening of, effects of dispersion additives on, 20: 4297(R) (IS-1200(Sect.M))
nuclear magnetic resonance in, (E), 20: 4476(R) (IS-1200(Sect.P))
oxidation by air, impurity effects and mechanisms of, 20: 4297(R) (IS-1200(Sect.M))
oxidation in air at 1100°C, scale formation in, 20: 4334
oxidation protection of, coatings for, 20: 4077(R) (IS-1200(Sect. E))
plasticity of, effects of temperature on, 20: 4297(R) (IS-1200(Sect.M))
preparation and properties, 20: 4297(R) (IS-1200(Sect.M))
production, 20: 4299(R) (ORNL-2711)
production from yttrium fluoride, 20: 4999(R) (ORNL-2599)
purification by electron-beam melting, 20: 4999(R) (ORNL-2599)
purification by zone refining, 20: 4299(R) (ORNL-2711)
separation from aqueous solutions by solvent extraction using naphthenates, 20: 4051
solvent partition between magnesium alloys and magnesium–potassium–sodium chloride salt mixture, 20: 3865 (ANL-7064)
structure of, electronic, (T), 20: 4476(R) (IS-1200(Sect.P))

YTTRIUM ALLOYS
Ag–Tb–Y, crystallography, 20: 4391(R) (ORNL-3870, pp 75-82)
Al–Y, corrosion by water at 200°C, effects of yttrium content on, 20: 4320(R) (ORNL-3870, pp 70-4)

Al–Y, crystal structure of beta-phase, 20: 4297(R) (IS-1200(Sect.M))
Co–Y, crystal structure, 20: 4297(R) (IS-1200(Sect.M))
Hf–Nb–W–Y, evaporation losses in high vacuum of C-129Y, 20: 4301(R) (ORNL-3870, pp 102-35)
Mg–Y, enthalpies of formation and vapor pressures of, 20: 4297(R) (IS-1200(Sect.M))
Mg–Y, phase diagrams, 20: 4297(R) (IS-1200(Sect.M))
Nb–Y, corrosion by lithium at high temperatures, 20: 4299(R) (ORNL-2711)
Ni–Y, crystal structure, 20: 4297(R) (IS-1200(Sect.M))
Pb–Y, phase diagrams, 20: 4297(R) (IS-1200(Sect.M))

YTTRIUM CARBIDES
phase studies, 20: 4297(R) (IS-1200(Sect.M))

YTTRIUM ETHYL SULFATES
holmium spin-lattice relaxation in, 20: 5020

YTTRIUM FLUORIDES
production, 20: 4299(R) (ORNL-2711)
production by fluorination of yttrium oxide, 20: 4999(R) (ORNL-2599)
$LiF–MgF_2–YF_3$, analysis for magnesium and yttrium, 20: 4999(R) (ORNL-2599)
$LiF–MgF_2–YF_3$, analysis for oxygen, 20: 4299(R) (ORNL-2711)
$LiF–YF_2$, phase diagram, 20: 4999(R) (ORNL-2599)
$LiF–YF_3$, phase diagram, 20: 4299(R) (ORNL-2711)

YTTRIUM HYDRIDES
production, 20: 4299(R) (ORNL-2711)
radiation effects at high temperatures, 20: 4299(R) (ORNL-2711)

YTTRIUM ISOTOPES Y-88
decay scheme, 20: 3982(R) (AGN-8156)

YTTRIUM ISOTOPES Y-90
bremsstrahlung excitation by, in thin absorbers, 20: 5000 (ORNL-IIC-5, pp 91-8)
determination in radioisotope mixtures, microcalorimetric, 20: 3866 (CEA-R-2630)
separation from waste solutions using manganese dioxide, 20: 5206
use as beta source of, for pituitary ablation, 20: 3809

YTTRIUM NITRIDES
formation in scaling of high-purity yttrium metal, 20: 4334
phase studies, 20: 4297(R) (IS-1200(Sect.M))

YTTRIUM OXIDES
deformation characteristics, 20: 4297(R) (IS-1200(Sect.M))
dehydration to 600°C for neutron transmission measurements, 20: 3914 (AERE-M-1654)
effects on polymorphism of zirconium oxide, 20: 3953
elastic properties, 20: 4077(R) (IS-1200(Sect. E))
formation in scaling of high-purity yttrium metal, 20: 4334
phase studies at 1700 to 2400°C, 20: 3939
sintering mechanisms of, 20: 4077(R) (IS-1200(Sect. E))
$MgO–Y_2O_3–ZrO_2$, phase studies of, on annealing and cooling, 20: 3953

YTTRIUM SULFIDES
homogeneity regions in, 20: 3938

Z

ZINC
determination in plants by neutron activation methods, 20: 3901
distribution between γ-alumina and molten chlorides, 20: 3959
heat of fusion, 20: 4297(R) (IS-1200(Sect.M))
radiation effects on, in aqueous solutions of carbonic anhydrase, x, 20: 3693
radiation effects on content in human urine of, x, 20: 3693
vapor pressure over liquid and solid calcium–zinc alloys, 20: 4297(R) (IS-1200(Sect.M))

ZINC ALLOYS
Ca–Zn, zinc vapor pressure over liquid and solid, 20: 4297(R) (IS-1200 (Sect.M))
Cu–Tb–Zn, crystallography, 20: 4391(R) (ORNL-3870, pp 75-82)
Mg–Zn, solvent properties for rare earth elements in molten chloride salts, 20: 3865 (ANL-7064)
Sm–Zn, phase diagrams, 20: 4297(R) (IS-1200(Sect.M))

ZINC CHLORIDES
Bi–NaCl–$ZnCl_2$, spectra of reaction products of, absorption, 20: 3921(R) (ORNL-3870, pp 56-60)
LiCl–KCl–$ZnCl_2$, oxidizing effects of liquid, on thorium, 20: 4297(R) (IS-1200(Sect.M))
LiCl–KCl–$ZnCl_2$, reactions with uranium carbide at 540 to 800°C, 20: 4297(R) (IS-1200(Sect.M))

ZINC COMPOUNDS
with manganese nitrides, ferromagnetic properties of, 20: 4402(T) (ANL-Trans-230)

ZINC ISOTOPES Zn-64
neutron reactions (n,d) at 14 Mev, energy levels from, (E), 20: 4896

ZINC MINERALS
analysis of, use of radioisotope methods for, 20: 3884 (ORNL-IIC-5, pp 206-21)

ZINC OXIDES
analysis by x-ray fluorescence using promethium-147/aluminum source, 20: 3883 (ORNL-IIC-5, pp 154-81)

ZIRCALOY-2
analysis for oxygen by neutron activation methods, 20: 3907
anisotropy in, strain and yield, 20: 4304(R) (ORNL-3870, pp 171-83)
corrosion and oxidation of annealed and etched, by air and water, 20: 4319 (EURAEC-1457)
fabrication of tubing of, texture control during, 20: 4304(R) (ORNL-3870, pp 171-83)
hydride plates pole figure in, method for determining, 20: 4304(R) (ORNL-3870, pp 171-83)
hydride precipitation in, effects of preferred orientation and stress on, 20: 4304(R) (ORNL-3870, pp 171-83)
properties of, mechanical and physical, 20: 4400 (WCAP-3269-41)
reactions with steam and water at high temperatures, 20: 4183(R) (ORNL-3843, pp 2-70)
strain anisotropy in tubing of, apparatus for studying, 20: 4304(R) (ORNL-3870, pp 171-83)

ZIRCALOY-4
corrosion and hydriding of, under heat-transfer conditions, computer program for prediction of, 20: 4331
corrosion failure in aqueous iron chloride solutions, stress, 20: 4328 (WCAP-3269-50)
fatigue of fuel element cladding of, biaxial strain, 20: 5134(R) (WCAP-3269-12)
performance as fuel rod cladding, 20: 5134(R) (WCAP-3269-12)
properties of, mechanical and physical, 20: 4400 (WCAP-3269-41)

ZIRCONIUM
corrosion and oxidation of annealed and etched, by air and water, 20: 4319 (EURAEC-1457)
crystal structure of, effects of annealing on, 20: 4413
crystallization properties, 20: 4304(R) (ORNL-3870, pp 171-83)
determination by titration using EDTA, 20: 3893
determination in molybdenum and molybdenum alloys by ion exchange, 20: 3896
determination in mixtures by x-ray fluorescence using promethium-147/aluminum and tritium/zirconium sources, 20: 3883 (ORNL-IIC-5, pp 154-81)
determination in solutions using 8-quinolinol, spectrophotometric, 20: 3895
dissolution in hydrofluoric–sulfuric acid system, 20: 4055
ductility of polycrystalline alpha-, during tensile deformation, 20: 4374(R) (IITRI-578-P27-12)
effects on niobium, additive, 20: 4299(R) (ORNL-2711)
galvanomagnetic properties at 4.2°K, 20: 3920(R) (ORNL-3870, pp 27-37)
mechanical properties of, at 250 to 350°C, effects of oxygen on, 20: 4416
oxidation rate of single-crystal, effects of crystallographic orientation on, 20: 4304(R) (ORNL-3870, pp 171-83)
preparation of single crystals of, 20: 4304(R) (ORNL-3870, pp 171-83)
purification by zone fusion, 20: 4413
reactions with sulfur, 20: 3863(R) (IS-1200(Sect. C))
separation from hafnium, chromatographic, 20: 3863(R) (IS-1200(Sect. C))
separation from low grade ores, reductive chlorination process for, 20: 4072(P)
separation from solutions formed by dissolution of molybdenum–uranium fuel alloys, 20: 4070(P)
separation from sulfuric acid solution by solvent extraction, evaluation of organic solvents for, 20: 4061
thermal capacity of hexagonal, effects of niobium on low-temperature, 20: 3920(R) (ORNL-3870, pp 27-37)
use of tritium-excited, as source in x-ray fluorescence analysis, 20: 3883 (ORNL-IIC-5, pp 154-81)

ZIRCONIUM ALLOYS
preparation of, methods used in metallographic, 20: 4341 (NAA-SR-Memo-10927)
Al–Nb–Ti–W–V–Zr, properties for use to 1200°F, 20: 4393 (PWAC-472)
Al–Ti–W–V–Zr, properties for use to 1200°C, 20: 4393 (PWAC-472)
Co–Ni–Ti–Zr, properties of Nivco in space electric power systems, 20: 4379 (NASA-CR-54091)
Mg–Zr, dissolution using sulfuric acid, flowsheet for, 20: 4048(R) (NP-15406)
Mg–Zr, heat-treatment process for, 20: 4456(P)
Mo–Nb–V–Zr, corrosion of B-66, by lithium, effects of oxygen on, 20: 4301(R) (ORNL-3870, pp 102-35)
Mo–Nb–V–Zr, evaporation losses in high vacuum of B-66, 20: 4301(R) (ORNL-3870, pp 102-35)
Mo–Nb–V–Zr, tensile properties of welded plates of B-66, 20: 4301(R) (ORNL-3870, pp 102-35)
Mo–Ti–Zr, analysis for titanium and zirconium by ion exchange, 20: 3896
Mo–Ti–Zr, brazing tungsten carbide–cobalt cermet to TZM, use of boron–

nickel–silicon for, 20: 4307(R) (ORNL-3870, pp 238-42)
Mo–Ti–Zr, corrosion of TZM, by potassium, 20: 4301(R) (ORNL-3870, pp 102-35)
Mo–Ti–Zr, creep properties of TZM, 20: 4301(R) (ORNL-3870, pp 102-35)
Mo–Zr, properties at low temperatures, 20: 3920(R) (ORNL-3870, pp 27-37)
Mo–Zr, properties at high temperatures, 20: 4418
Nb–Ta–W–Zr, corrosion of FS-85, by lithium, effects of oxygen on, 20: 4301(R) (ORNL-3870, pp 102-35)
Nb–Ta–W–Zr, creep properties of FS-85, 20: 4301(R) (ORNL-3870, pp 102-35)
Nb–Ta–W–Zr, ductility of FS-85, effects of aging on bend, 20: 4301(R) (ORNL-3870, pp 102-35)
Nb–Ta–W–Zr, evaporation losses in high vacuum of FS-85, 20: 4301(R) (ORNL-3870, pp 102-35)
Nb–Ta–W–Zr, preparation and specifications for corrosion loop testing, 20: 4380 (NASA-CR-54761)
Nb–W–Zr, corrosion of Cb-752, by lithium, effects of oxygen on, 20: 4301(R) (ORNL-3870, pp 102-35)
Nb–W–Zr, creep properties of Cb-752, 20: 4301(R) (ORNL-3870, pp 102-35)
Nb–Zr, aging studies of, 20: 5181(R) (ORNL-3029)
Nb–Zr, aging studies on welds of, 20: 5181(R) (ORNL-3029)
Nb–Zr, brazing and welding of, 20: 5181(R) (ORNL-3029)
Nb–Zr, compatibility with uranium dioxide, 20: 5181(R) (ORNL-3029)
Nb–Zr, corrosion by potassium–sodium alloys, 20: 5181(R) (ORNL-3029)
Nb–Zr, corrosion by lead at 1400°F, 20: 4308(R) (ORNL-3870, pp 243-60)
Nb–Zr, corrosion by potassium–sodium eutectic, 20: 4323(R) (ORNL-3870, pp 308-11)
Nb–Zr, corrosion by lithium at high temperatures, 20: 4299(R) (ORNL-2711)
Nb–Zr, corrosion by potassium, 20: 4301(R) (ORNL-3870, pp 102-35)
Nb–Zr, corrosion by lithium, effects of oxygen on, 20: 4301(R) (ORNL-3870, pp 102-35)
Nb–Zr, effects of lithium and oxygen on tensile properties of, 20: 5181(R) (ORNL-3029)
Nb–Zr, emissivity, effects of surface treatments on, 20: 4301(R) (ORNL-3870, pp 102-35)
Nb–Zr, evaporation losses in high vacuum, 20: 4301(R) (ORNL-3870, pp 102-35)
Nb–Zr, mechanical properties of, effects of oxygen on, 20: 4297(R) (IS-1200(Sect.M))
Nb–Zr, performance of superconducting solenoids of, 20: 4775 (UCRL-16376)
Nb–Zr, phase transformation kinetics, 20: 4390(R) (ORNL-3870, pp 65-9)
Nb–Zr, properties at low temperatures, 20: 3920(R) (ORNL-3870, pp 27-37)
Nb–Zr, purification by electron-beam melting, 20: 5181(R) (ORNL-3029)
Nb–Zr, sorptive properties for nitrogen, kinetics of, 20: 4301(R) (ORNL-3870, pp 102-35)
Nb–Zr, stability of carbon-strengthened, at 2000°F, 20: 4397 (TIM-955)
Nb–Zr, superconducting properties, (E), 20: 4792
Nb–Zr, superconducting properties, 20: 4390(R) (ORNL-3870, pp 65-9)
Nb–Zr, tube-burst tests on, 20: 5181(R) (ORNL-3029)
Re–Zr, properties at low temperatures, 20: 3920(R) (ORNL-3870, pp 27-37)
Ru–Zr, properties at low temperatures, 20: 3920(R) (ORNL-3870, pp 27-37)
U–Zr, superconducting properties, 20: 4390(R) (ORNL-3870, pp 65-9)
W–Zr, properties at high temperatures, 20: 4418

ZIRCONIUM BORIDES
BeO–ZrB_2, fabrication of hot-pressed blocks of, 20: 4999(R) (ORNL-2599)

ZIRCONIUM CARBIDES
reactions with zirconium hydride, structure of ternary compound ZrC · ZrH_2 formed by, 20: 4378 (NAA-SR-Memo-11542)
C–ZrC, properties and structure of hot-pressed, 20: 5089(R) (GA-6181)
TaC–ZrC, properties at high temperatures, methods of determining, 20: 4297(R) (IS-1200(Sect.M))
UC–ZrC, compatibility with refractory metals at 2000°C, 20: 4335
UC–ZrC, diffusion of xenon-133 from low-dose, low-temperature irradiated fuels of, (E), 20: 4471

ZIRCONIUM FLUORIDES
properties of molten, for use as reactor fuels, 20: 4376 (JUL-268-RG)
BeF_2–LiF–UF_4–ZrF_4, corrosive effects on type 304 stainless steel, 20: 4308(R) (ORNL-3870, pp 243-60)

ZIRCONIUM HYDRIDES
neutron scattering by, differential cross sections for thermal, (E/T), 20: 4801(R) (GA-6634)
precipitation in Zircaloy-2, effects of preferred orientation and stress on, 20: 4304(R) (ORNL-3870, pp 171-83)
preparation of, methods used in metallographic, 20: 4341 (NAA-SR-Memo-10927)
reactions with zirconium carbide, structure of ternary compound ZrC · ZrH_2 formed by, 20: 4378 (NAA-SR-Memo-11542)

ZIRCONIUM ISOTOPES Zr-90
proton reactions (p,p), fine structure near isobaric analog resonances in, 20: 4923

ZIRCONIUM ISOTOPES Zr-91
gamma reactions (γ,n) with, cross sections for, (E), 20: 4849(R) (UCRL-14360, pp 1-50)

ZIRCONIUM ISOTOPES Zr-92
gamma reactions (γ,n) with, cross sections for, (E), 20: 4849(R) (UCRL-14360, pp 1-50)

ZIRCONIUM ISOTOPES Zr-93
gamma reactions (γ,n) with, cross sections for, (E), 20: 4849(R) (UCRL-14360, pp 1-50)

ZIRCONIUM ISOTOPES Zr-95
content in sintered uranium dioxide pellet, radial distribution of, 20: 4472
content of, in brown algae of Solway Firth, 20: 3662 (PG-Report-650)
determination in reactor cooling water, fission-product monitor based on, 20: 3909
uptake by maize, effects of soil temperature on, 20: 3668

ZIRCONIUM ORES
processing by reductive chlorination, 20: 4072(P)

ZIRCONIUM OXIDES
phase transformations of, effects of magnesium and yttrium oxides on, 20: 3953
radiation effects on optical properties of films of, fast neutrons, 20: 4304(R) (ORNL-3870, pp 171-83)
refractive indices of anodized films *in situ* and stripped, 20: 4304(R) 20: 4304(R) (ORNL-3870, pp 171-83)
solubility in borax at 760 to 900°C, 20: 3951
CaO–ZrO_2, internal friction, 20: 3945
MgO–Y_2O_3–ZrO_2, phase studies of, on annealing and cooling, 20: 3953
paraffin–ZrO_2, neutron spectra in, 20: 4806(R) (RPI-328-40, pp 1-42)
PuO_2–UO_2–ZrO_2, properties for use in thermal reactors, 20: 4382(R) (NUMEC-3505-8)

ZIRCONIUM PHOSPHATES
preparation of granular, for cation exchange use, 20: 3968(P)
separation from other fission products by ion exchange, 20: 3871 (EUR-2497.e)

ZIRCONIUM SYSTEMS
Al–C–Ti–Zr, properties for use to 1200°F, 20: 4393 (PWAC-472)
C–Mo–Nb–Ta–W–Zr, preparation and specifications for corrosion loop testing, 20: 4380 (NASA-CR-54761)
C–Mo–Ti–Zr, preparation and specifications for corrosion loop testing, 20: 4380 (NASA-CR-54761)
C–Nb–W–Zr, aging and recrystallization of D-43, 20: 4301(R) (ORNL-3870, pp 102-35)
C–Nb–W–Zr, corrosion of D-43, by potassium, 20: 4301(R) (ORNL-3870, pp 102-35)
C–Nb–W–Zr, corrosion of D-43, by lithium, effects of oxygen on, 20: 4301(R) (ORNL-3870, pp 102-35)
C–Nb–W–Zr, ductility of welds in D-43, effects of aging on bend, 20: 4301(R) (ORNL-3870, pp 102-35)
C–Nb–W–Zr, evaporation losses in high vacuum of D-43, 20: 4301(R) (ORNL-3870, pp 102-35)
C–Nb–W–Zr, preparation and specifications for corrosion loop testing, 20: 4380 (NASA-CR-54761)
C–Nb–W–Zr, tensile properties of welded plates of D-43, 20: 4301(R) (ORNL-3870, pp 102-35)
C–Nb–W–Zr, thermal conductivity of D-43, at 30 to 120°C, 20: 4301(R) (ORNL-3870, pp 102-35)
C–Nb–Zr, phase studies at 1092 and 1538°C, 20: 4392 (PWAC-461)
Nb–O–Zr, phase studies, 20: 4297(R) (IS-1200(Sect.M))

ZIRCONS
age of northeastern Minnesota, estimations of, 20: 4169

ZIRFLEX PROCESS
development, 20: 4048(R) (NP-15406)

REPORT NUMBER INDEX

Reports, conference papers and proceedings, numbered translations, and patents abstracted during the period are included in this index. Each item is listed by report number; this is followed by the abstract number and a brief notation regarding public availability. The index entries show which reports are on file in the depository libraries, which reports have been published in open-literature journals (journal citation given), and which reports can be purchased (source and price). Whenever a report is identified by more than one number, cross references from secondary to primary report numbers are cited.

The report number codes apply to AEC reports unless designated otherwise. Non-AEC reports are identified by parenthetical notes after the report codes; e.g., (non-AEC), (British), (Canadian), (French). The note (Misc.) identifies those codes used for both USAEC and non-AEC reports. Patents are listed under the heading "PATENTS"; the country of origin is included in parentheses.

A comprehensive listing of both AEC and non-AEC report codes is contained in TID-85(5th Rev.), *Report Number Series Used by the Division of Technical Information in Cataloging Reports*. This information is also included in the Cumulative Report Number Index (issued annually).

Public Availability of USAEC Reports

All USAEC reports abstracted in *NSA* are available to the public through one or more of the following sources:

(1) Depository libraries in the United States, in other countries, and in international agencies. A list of these depositories appears on the inside covers of each issue of *NSA*.

(2) Scientific and technical journals or other publications.

(3) Microcard Editions, Inc., in Microcard and micronegative form. Orders and inquiries should be sent to: Accounting and Shipping Department, West Salem, Wisconsin 54669.

(4) Clearinghouse for Federal Scientific and Technical Information, U. S. Department of Commerce, Springfield, Virginia 22151.

(5) Superintendent of Documents, U. S. Government Printing Office, Washington, D. C. 20402.

Public Availability of Non-AEC Reports

U. S. Reports. Many reports of U. S. Government agencies are available to the public from the Clearinghouse for Federal Scientific and Technical Information (CFSTI). This availability is given when known. Such reports should be ordered by AD number or NASA-N number. If availability is not shown, inquiries may be directed to CFSTI. In the case of NP numbers, inquiries should be by title and author.

Non-U. S. Reports. Many reports of atomic energy establishments of other countries are deposited in the libraries listed on the inside covers of each issue of *NSA*.

Additionally, the following have made their reports available as indicated.

AUSTRALIA

Australian Atomic Energy Commission Research Establishment. Available upon request from the Library, Australian Atomic Research Establishment, Private Mail Bag, Sutherland, New South Wales, Australia.

BELGIUM

Centre d'Étude de l'Énergie Nucléaire. Available upon request to individuals and organizations, from the Centre d'Étude de l'Énergie Nucléaire (CEN), 31, Rue Belliard, Bruxelles, Belgium.

CANADA

Atomic Energy of Canada Limited. For sale by the Technical Information Officer, Atomic Energy of Canada Limited, Chalk River, Ontario, Canada. Copies are also deposited in libraries in the United Kingdom.

National Research Council of Canada. Available from the National Research Council of Canada, Ottawa 2, Ontario, Canada.

DENMARK

Atomic Energy Commission Research Establishment, Risø. Available on exchange from the Library, Danish Atomic Energy Commission, Risø, Roskilde, Denmark. Also for sale by Jul. Gjellerup, Booksellers, 87 Sölvgade, København K., Denmark.

Danatom. Available on loan from Research Establishment, Risø, Roskilde, Denmark. Copies are available from Danatom, Aurehøjvej 2, Hellerup, Denmark.

EURATOM

Reports from the Commission of the European Atomic Energy Community are available from: Presses academiques europeennes, 98, chaussee de Charleroi, Brussels 6, Belgium; and Office central de vente des publications des Communautes eurodeennes 2, place de Metz, Luxemburg.

FRANCE

Commissariat à l'Énergie Atomique. Inquiries for reports numbered 1-2199 should be addressed to Commissariat à l'Énergie Atomique, Service Central de Documentation, Centre d'Études Nucléaires de Saclay, Boite Postale No. 2, Gif-sur-Yvette (S. et O.), France. Reports numbered 2200 and above are available from La Documentation Francaise, 16 Rue Lord-Byron, Paris VIII, France.

Service Central de Protection contre les Rayonnements Ionisants. Copies are available from Ministère de la Santé Publique, Service Central de Protection contre les Rayonnements Ionisants, B. P. n° 35—LE VESINET (S. et O.), France.

GERMANY

Deutsches Elektronen-Synchrotron DESY. Copies are available from Deutsches Elektronen-Synchrotron Desy, Dokumentation, 2000 Hamburg-Gr. Flottbek 1, Notkestieg 1, Germany.

Gesellschaft für Kernforschung mbH (KFK). Copies are available from Gesellschaft für Kernforschung mbH, 75 Karlsruhe, Postfach 947, Germany. Copies are also deposited in many national nuclear centers in the world.

Kernforschungsanlage. Copies may be ordered from Zentralbibliothek der Kernforschungsanlage Jülich, Jülich, Bundesrepublik Deutschland.

Hahn-Meitner-Institute für Kernforschung. Available without charge from Hahn-Meitner-Institute für Kernforschung Berlin, Bibliothek, Glienicker Strasse 100, 1 Berlin

39, Germany. Copies are deposited in many national nuclear centers in the world.

Johann-Wolfgang-Goethe Universität, Frankfurt Am Main, Institut für Kernphysik, (IKF). Copies are available from Gmelin Institut, 40-42 Varrentrappstrasse, Frankfurt (Main), West Germany.

ISRAEL

Israel Atomic Energy Commission. Available without charge from Ministry of Defence/Atomic Energy Commission, Soreq Research Establishment, Yavne, Israel. Copies are deposited in libraries in Israel and in other countries.

ITALY

Centro Informazioni Studi Esperienze (CISE). For sale at CISE Press Office, Casella Postale 3986, Milano, Italy. Copies are deposited in libraries in Italy.

Comitato Nazionale per l'Energia Nucleare. Copies are available from Comitato Nazionale per l'Energia Nucleare, Divisione Affari Internazionali e Studi Economici, Ufficio Pubblicazioni, Via Belisario, 15, Roma, Italy.

JAPAN

Japan Atomic Energy Research Institute (JAERI). Available from the Staff Supply Cooperative of Japan Atomic Energy Research Institute (JAERI), 1-1 Tamura-Cho, Shiba, Minato-Ku, Tokyo, Japan. Copies are deposited in depositories in Tokyo, Nagoya, and Osaka.

Nagoya University. Copies are available from Research Information Center, Institute of Plasma Physics, Nagoya University, Nagoya, Japan.

University of Tokyo. Available free of charge from Institute for Nuclear Study, University of Tokyo, Tanashi-Machi, Kitatama-gun, Tokyo, Japan.

NETHERLANDS

Reactor Centrum Nederland. For sale by Reactor Centrum Nederland, 112 Scheveningseweg, 's-Gravenhage, The Netherlands. Copies are deposited in university libraries in Holland and in many national nuclear centers in the world.

NEW ZEALAND

Institute of Nuclear Sciences. Copies are available from Librarian, Institute of Nuclear Sciences, D.S.I.R., Private Bag, Lower Hutt, New Zealand. Copies are deposited in other countries.

NORWAY

Forsvarets Forskningsinstitutt. Copies available from Norwegian Defence Research Establishment, Library, P. O. Box 25, Kjeller, Norway.

Institutt for Atomenergi. "KR" reports are available on an exchange basis from the Library, Institutt for Atomenergi, Box 40, Kjeller, Norway. Other series are not generally available to the public.

Norwegian Reactor School. Copies are available from The Library, Institutt for Atomenergi, P. O. Box 40, Kjeller, Norway.

PAKISTAN

Atomic Energy Center. Copies are available from Atomic Energy Center, P. O. Box 658, Lahore, (West Pakistan).

POLAND

Reports of the Polish nuclear institutes are published by the Nuclear Energy Information Center of the Government Commissioner for Use of Nuclear Energy. Copies are available from Ośrodek Informacji o Energii Jądrowej, Warszawa, PKiN, Poland.

SPAIN

Junta de Energia Nuclear. "JEN" reports are available without charge from Servicio de Documentation, Junta de Energia Nuclear, Ciudad Universitaria, Madrid (3), Spain.

SWEDEN

Aktiebolaget Atomenergi. "AE" reports are for sale from Aktiebolaget Atomenergi, Library Section, Box 43041, Stockholm 43, Sweden. Bibliographies and literature surveys of the VDDIT- series may be obtained from Aktiebolaget Atomenergi, Information Office, Scientific and Technical Information, Box 43041, Stockholm 43, Sweden. Other series are not generally available to the public. Organizations in the atomic energy field may obtain copies from Aktiebolaget Atomenergi. Microcopy of AE reports is available from the International Documentation Centre, Tumba, Sweden.

SWITZERLAND

CERN European Organization for Nuclear Research. Available without charge from CERN European Organization for Nuclear Research, Geneva 23, Switzerland. Copies are deposited in libraries in 13 countries.

Eidgenössisches Institut für Reaktorforschung. "EIR" reports are available from Eidgenössiches Institut für Reaktorforschung, c/o Bibliothek, Würenlingen/Ag, Switzerland.

TURKEY

Turkish Atomic Energy Commission. Copies are available free of charge from T.A.E.C., Çekmece Nuclear Research Center, P. O. Box 1, Airport, Istanbul, Turkey.

UNITED KINGDOM

United Kingdom Atomic Energy Authority. Some reports are for sale in the United States by the British Information Service (BIS), 845 Third Avenue, New York, N. Y. 10022, United Kingdom reports generally may be purchased from Her Majesty's Stationery Office, London. Copies not for sale by Her Majesty's Stationery Office may be purchased in microcopy form from Micro Methods Limited, East Ardsley, Wakefield, Yorks, England. Report copies are deposited in a large number of libraries in England.

Conferences

Published conference proceedings as well as individual unpublished papers from conferences are included in this index. A CONF number is assigned to the conference if published proceedings are received and also if only a single paper is received. The base number used is year-month-sequence. Thus, the number CONF-650101 would indicate that the conference was held in 1965, in January, and that this was the first January 1965 conference so received. This number would be assigned to complete published proceedings, or if individual papers are received, the base number would be extended to include a paper number, i.e., CONF-650101-1. As additional papers are received, they will be assigned consecutive numbers in the series, CONF-650101-1, 2, 3, 4, etc. This numbering system ensures that all papers received from a conference will be associated with that conference in this index.

If published proceedings are received after the receipt of individual papers, the complete proceedings will be abstracted and the abstract number will appear in this index with the base CONF number.

Abbreviations Used in Availability Column

AECL	For sale by Atomic Energy of Canada Ltd., Chalk River, Ontario, Canada.
BIS	For sale by British Information Service, 845 Third Avenue, New York, N. Y. 10022
CFSTI	For sale by the Clearinghouse for Federal Scientific and Technical Information, U. S. Department of Commerce, Spring-

field, Virginia 22151. The symbol "cy" indicates that the format of the item sold may be either a printed document or a photographic reproduction (two-thirds of original size) depending upon the availability of printed stock. The indicated price is for either format. The symbol "mn" is used to indicate that copy is also available in the form of micronegatives (microfiche).

Dep. — AEC reports: Full-size copy is on deposit in the depository libraries both inside and outside the United States. These reports are also for sale by Microcard Editions, Inc., Accounting and Shipping Department, West Salem, Wisconsin 54669.

Non-AEC reports: Full-size copy on deposit in the depository libraries in the United States only.

Dep.(mn) — Same as for Dep., except copy is in micronegative (microfiche) form.

DSIR — For sale by the National Lending Library for Science and Technology (D.S.I.R.), Boston Spa, Yorkshire, England.

DTI Extension — Available from the U. S. Atomic Energy Commission, Division of Technical Information Extension, P. O. Box 62, Oak Ridge, Tennessee 37830.

EM — Blueprints and microcopy of AEC engineering drawings are available from Clearinghouse for Federal Scientific and Technical Information, U. S. Department of Commerce, Springfield, Virginia 22151. Current prices of the CAPE- packages may be obtained from this address. TID-4100, available from the Division of Technical Information Extension, P. O. Box 62, Oak Ridge, Tennessee 37831, contains information on all the CAPE- packages for sale.

Gmelin — Available at a nominal charge and under the AED- number shown from Atomic Energy Documentation Center, Gmelin Institute, 40-42 Varrentrappstrasse Frankfurt (Main), West Germany.

GPO — For sale by the Superintendent of Documents, Government Printing Office, Washington, D. C. 20402.

HMSO — Her Majesty's Stationery Office, London.

IAEA — Available from the International Atomic Energy Agency, Vienna, Austria, and from its sales agencies in various countries throughout the world. A list of these agencies is found in each STI/DOC and STI/PUB publication.

JCL — For sale by the Special Libraries Association Translation Center, John Crerar Library, 35 West 33rd Street, Chicago, Illinois 60616.

NAS — National Academy of Sciences, National Research Council, Washington, D. C. 20418.

NRC — For sale by the National Research Council of Canada, Ottawa, Ontario, Canada.

ORAU — Available on interlibrary loan from the Library, Oak Ridge Associated Universities, Post Office Box 117, Oak Ridge, Tennessee 37830.

ORINS — See ORAU.

UKAEA, London — Available from United Kingdom Atomic Energy Authority, 11 Charles II Street, London, S. W. 1.

UN — United Nations Bookshop, United Nations Headquarters, New York, New York.

USGS — Available free of charge from the U. S. Geological Survey, Washington, D. C. 20242.

[The symbols "ph," "mf," and "fs" are used to designate that copy is available only in photostat, microfilm, or facsimile form. The symbol "mn" is used to designate that copy is available in micronegative (microfiche) form. The symbol "cy" is used to designate full size or photographically enlarged copy (two-thirds of original size).]

Report No.	Abstract No.	Availability
ACNP–	**(Misc.)**	
65006	20-5104	Dep. mn; CFSTI $4.00 cy, $0.75 mn
65544(Vol.I)	20-5105	Dep. mn; CFSTI $7.00 cy, $2.00 mn
65544(Vol.II)	20-5106	Dep. mn; CFSTI $7.76 cy, $2.25 mn
65589	20-5107	Dep. mn; CFSTI $2.00 cy, $0.50 mn
AD–	**(Misc.)**	
438516	20-4358	CFSTI $1.60 cy, $0.50 mn
614592	20-4570	CFSTI $3.00 cy, $0.75 mn
614633	20-4098	CFSTI $2.00 cy, $0.50 mn
617601	20-3705	CFSTI $2.00 cy, $0.50 mn
617965	20-4638	CFSTI $3.00 cy, $0.75 mn
618037	20-4571	CFSTI $1.00 cy, $0.50 mn
618054	20-4727	CFSTI $1.00 cy, $0.50 mn
618067	20-4577	CFSTI $1.00 cy, $0.50 mn
618118	20-4728	CFSTI $4.00 cy, $1.00 mn
618222	20-4521	CFSTI $1.00 cy, $0.50 mn
618376	20-5108	CFSTI $4.00 cy, $1.00 mn
618562	20-4560	CFSTI $1.00 cy, $0.50 mn
618660	20-4578	CFSTI $1.00 cy, $0.50 mn
618661	20-4579	CFSTI $1.00 cy, $0.50 mn
618662	20-4580	CFSTI $1.00 cy, $0.50 mn
618663	20-4581	CFSTI $1.00 cy, $0.50 mn
618676	20-4233	CFSTI $3.00 cy, $0.75 mn
618733	20-4141	CFSTI $6.00 cy, $1.50 mn
618923	20-4359	CFSTI $4.00 cy, $1.00 mn
619053	20-4142	CFSTI $3.00 cy, $0.75 mn
619093	20-4934	CFSTI $2.00 cy, $0.50 mn
619094	20-4702	CFSTI $2.00 cy, $0.50 mn
619101	20-4703	CFSTI $3.00 cy, $0.75 mn
619177	20-4234	CFSTI $2.00 cy, $0.50 mn
619399	20-4360	CFSTI $2.00 cy, $0.50 mn
619719	20-4361	CFSTI $2.00 cy, $0.50 mn
619969	20-4143	CFSTI $5.00 cy, $1.00 mn
620003	20-4154	CFSTI $3.00 cy, $0.75 mn
620033	20-4362	CFSTI $2.00 cy, $0.50 mn
620055	20-4338	CFSTI $3.00 cy, $0.75 mn
621784	20-4114	CFSTI $1.00 cy, $0.50 mn
622552	20-4131	CFSTI $4.00 cy, $1.00 mn
623078	20-4261	
623365	20-3706	
623515	20-4148	CFSTI $2.00 cy, $0.50 mn
623639	20-4149	CFSTI $1.00 cy, $0.50 mn
623641	20-3707	CFSTI $1.00 cy, $0.50 mn
AE–	**(Non-AEC)**	
198	20-4800	Dep. mn
AEC-tr–	**(For complete listing see TID-4025)**	
6486/2	20-4311	Dep.; CFSTI $3.00 cy, $0.75 mn
6617	20-3890	Dep. mn; JCL $5.60 fs, $1.94 mf
AECL–	**(Canadian)**	
2283	20-4235	Dep.; AECL $0.20
2290	20-5114	See CRRP-1221
2333	20-4099	Dep.; AECL $1.50
2360	20-5109	Dep.; AECL $1.00
AEET-CD–	**(Indian)**	
31	20-4363	Dep. mn
AERE-L–	**(British)**	
166	20-3864	Dep.; BIS $1.10; HMSO 5s. 6d.
AERE-M–	**(British)**	
1644	20-4364	Dep.; BIS $0.70; HMSO 3s. 6d.
1654	20-3914	Dep.; BIS $0.30; HMSO 1s. 9d.
AERE-R–	**(British)**	
4546	20-4469	J. Nucl. Mater., 17: 167-71(1965)
4662	20-4349	J. Nucl. Mater., 17: 142-8(1965)
4764	20-4335	J. Nucl. Mater., 17: 97-110(1965)
4908	20-4473	Phil. Mag. (8), 12: 741-65(1965)
4932	20-5188	Dep.; BIS $1.80; HMSO 9s. 0d.
4951	20-4410	Brit. J. Appl. Phys., 16: 1507-11(1965)
4980	20-4166	Dep.; BIS $0.90; HMSO 4s. 6d.
5051	20-3981	Dep.; BIS $0.50; HMSO 2s. 6d.
AERE-Trans–	**(British)**	
1026	20-3927	Dep.
AES–	**(Swedish)**	
3	20-4365	Dep. mn
4	20-5110	Dep. mn
AFCRL–	**(Non-AEC)**	
65-363	20-4521	See AD-618222
65-418	20-4560	See AD-618562
65-482	20-4727	See AD-618054
65-556	20-4935	CFSTI $1.00 cy, $0.50 mn
AFOSR–	**(Misc.)**	
65-1138	20-4934	See AD-619093
65-1312	20-4703	See AD-619101
AGN–	**(Misc.)**	
8128	20-4276	Dep. mn; CFSTI $3.00 cy, $0.50 mn
8156	20-3982	Dep. mn; CFSTI $5.00 cy, $1.00 mn
AHSB(S)–	**(British)**	
R-86	20-5030	Dep.; BIS $0.80; HMSO 4s. 0d.
Al-PC–		
710	20-5111	Dep. mn; CFSTI $4.00 cy, $0.75 mn
Al-Trans–		
201	20-4733	Dep. mn; CFSTI $1.00 cy, $0.50 mn; JCL $1.10 fs, $0.80 mf
ANL–		
6929	20-5189	Dep. mn; CFSTI $3.00 cy, $0.75 mn
7054	20-4286	Dep. mn; CFSTI $5.00 cy, $1.00 mn
7064	20-3865	Dep. mn; CFSTI $1.00 cy, $0.50 mn
7081	20-4474	Dep. mn; CFSTI $6.00 cy, $1.00 mn
7087	20-5211	Dep. mn; CFSTI $7.00 cy, $1.50 mn
7106	20-5190	Dep. mn; CFSTI $2.00 cy, $0.50 mn
ANL-Trans–		
218	20-4401	Dep. mn; JCL $2.60 fs, $0.92 mf
230	20-4402	Dep. mn; JCL $2.60 fs, $0.92 mf
AWRE-O–	**(British)**	
70/65	20-4216	Dep. mn; BIS $1.60; HMSO 8s. 0d.
79/65	20-4996	Dep.; BIS $1.10; HMSO 5s. 6d.
90/65	20-4366	Dep.; BIS $0.60; HMSO 3s.
93/65	20-4132	Dep. mn; BIS $1.00; HMSO 5s. 0d.
AWRE-R–	**(British)**	
4/65	20-5191	Dep.; BIS $0.30; HMSO 1s. 9d.
BAW–	**(Misc.)**	
1280-30	20-4317	Dep. mn; CFSTI $2.00 cy, $0.50 mn
1280-32	20-5031	Dep. mn; CFSTI $2.00 cy, $0.50 mn
BC-RLD–		
2801(Vol.1)	20-5185	Dep. mn; CFSTI $6.00 cy, $1.50 mn
2801(Vol.2)	20-5186	See UCRL-13095(Vol.2)
BM-RI–	**(Misc.)**	
6684	20-4082	Dep. mn; CFSTI $1.00 cy, $0.50 mn
BNL–		
930	20-5212	Dep. mn; CFSTI $1.00 cy, $0.50 mn
8466	20-3653	Dep. mn; CFSTI $1.00 cy, $0.50 mn
8820	20-3986	Ann. Rev. Phys. Chem., 16: 347-74(1965)
9233	20-4672	Phys. Rev., 140: B1099-1109(1965)
9276	20-4608	Phys. Rev., 140: B1027-38(1965)
9294	20-4662	Phys. Rev., 140: B947-56(1965)
9295	20-4605	Phys. Rev., 140: B1008-12(1965)
9360	20-4905	Phys. Rev., 140: B1202-25(1965)
9589	20-3983	Dep. mn; CFSTI $1.00 cy, $0.50 mn
9605	20-4236	Dep. mn; CFSTI $1.00 cy, $0.50 mn
9640	20-4492	Dep. mn; CFSTI $1.00 cy, $0.50 mn
9642	20-4493	Dep. mn; CFSTI $2.00 cy, $0.50 mn
9650	20-4175	Dep. mn; CFSTI $1.00 cy, $0.50 mn
9665	20-4237	Dep. mn; CFSTI $1.00 cy, $0.50 mn
9684	20-4176	Dep. mn; CFSTI $1.00 cy, $0.50 mn
BNL-tr–		
43	20-4106	Dep. mn; JCL $1.10 fs, $0.80 mf
BNWL–		
131D	20-4339	Dep. mn; CFSTI $1.00 cy, $0.50 mn
146	20-5055	Dep. mn; CFSTI $3.00 cy, $0.75 mn

Report No.	Abstract No.	Availability
162	20-4367	Dep. mn; CFSTI $1.00 cy, $0.50 mn
BNWL-SA–		
224	20-3655	Dep. mn; CFSTI $1.00 cy, $0.50 mn
225	20-3656	Dep. mn; CFSTI $1.00 cy, $0.50 mn
251	20-5192	Dep. mn; CFSTI $2.00 cy, $0.50 mn
319	20-3663	See TID-22318
BW–	(Misc.)	
67-2(a)	20-4100	Dep. mn; CFSTI $5.00 cy, $1.50 mn
CALT–		
68-45	20-4598	Phys. Rev., 140: B908-10(1965)
CAPE–		
1260	20-3910	EM
CEA-Bib–	(French)	
60	20-4827	Dep. mn
61	20-3915	Dep. mn
CEA-R–	(French)	
2630	20-3866	Dep. mn
2818	20-3657	Dep. mn
2833	20-3708	Dep. mn
2843	20-4494	Dep. mn
2844	20-3867	Dep. mn
2845	20-4368	Dep. mn
2860	20-3868	Dep. mn
2865	20-3709	Dep. mn
2869	20-3869	Dep. mn
2871	20-4369	Dep. mn
2875	20-5003	Dep. mn
CEA-tr–	(French)	
A-1838	20-3891	Dep. mn; JCL $1.60 fs, $0.80 mf
R-1868	20-4329	Dep. mn; JCL $1.60 fs, $0.80 mf
X-617	20-4284	Dep. mn; JCL $1.60 fs, $0.80 mf
X-619	20-3665	Dep. mn; JCL $5.60 fs, $1.91 mf
CEND–	(Misc.)	
507	20-5112	Dep. mn; CFSTI $3.00 cy, $0.75 mn
3256-250	20-4370	Dep. mn; CFSTI $2.00 cy, $0.50 mn
CNIE-PE–	(Argentinian)	
4	20-4729	Dep. mn
5	20-4522	Dep. mn
CNLM–	(Misc.)	
5359	20-4318	Dep. mn; CFSTI $1.00 cy, $0.50 mn
CONF-639–	(24th Annual Meeting of the Institute of Food Technologists, Washington, D. C., May 1964)	
4	20-4271	See WASH-1063
CONF-654–	19-2907 19-6030	(American Nuclear Society Meeting San Francisco, Nov. 30–Dec. 3, 1964) Proceedings
22	20-5056	Dep. mn; CFSTI $1.00 cy, $0.50 mn
98	20-4102	See HW-SA-3640
CONF-611102–	(World Conference on Energy, Lisbon, Nov. 27–Dec. 11, 1961)	
1	20-4047	See LFEN-32
CONF-621005–	20-3685	(Symposium on Uses of Radioisotopes in Nutritional Sciences and of Ionizing Radiation in Food Technology, Strasbourg, Oct. 1–7, 1962)
CONF-630913–	20-4790	(3rd Regional Conference on Physics and Techniques of Low Temperatures, Prague, Sept. 1963)
CONF-631109–	20-5166	(Symposium on Atomic Power, Sydney, Nov. 7, 1963)
CONF-640207–	20-4116	(American Society for Testing Materials Conference, Philadelphia, Feb. 3–6, 1964)
CONF-640510–	20-4296	(Regional Technical Conference on Heat Transfer, Kingston, Canada, May 9, 1964)
CONF-640707–	20-4274	(Symposium on Uses of Radioactive Isotope in Textile Research and Industry, Lindau/Bodensee, July 8–10, 1964)
CONF-641009–	20-4266	(Joint American Nuclear Society and American Society for Testing Materials Conference on Radiation Effects on Electronics, Syracuse, N. Y., Oct. 5–7, 1964)
CONF-641014–	20-4575	(2nd Annual Conference on Energy Conversion and Storage, Stillwater, Okla., Oct. 12–13, 1964)
CONF-641017–	20-4111	(Symposium on Low Energy X and Gamma Sources and Applications, Chicago, Oct. 20–21, 1964) See also ORNL-IIC-5
CONF-641118–	(Pittsburgh Diffraction Conference, Pittsburgh, Nov. 4–6, 1964)	
2	20-5022	Gmelin, AED-CONF-64-229-12
CONF-641125	20-5154 20-5161	(Symposium on Anglo-Spanish Nuclear Power, Madrid, Dec. 23–25, 1964)
CONF-650111–	(CERN Informal Neutrino Conference, Geneva, Jan. 1965)	
6	20-4523	See COO-818-63
7	20-4561	See COO-818-64
CONF-650320–	(IEEE International Convention, New York, Mar. 1965)	
2	20-3912	Gmelin, AED-CONF-65-114-1
CONF-650325–	(National Assn. of Corrosion Engineers, 21st Annual Meeting, St. Louis, Mar. 15–19, 1965)	
1	20-4337	Gmelin, AED-CONF-65-037-2 Corrosion, 21: 341-9(1965)
CONF-650410–	(American Physical Society, Washington, D. C., Apr. 26–29, 1965)	
45	20-4684	Phys. Rev., 140: B1407-14(1965)
CONF-650437–	(Cyclotron Colloquium, Eindhoven, Netherlands, Apr. 1965)	
2	20-4497	See KFK-310
CONF-650502–	(Electrochemical Society, San Francisco, May 9–14, 1965)	
6	20-4454	Gmelin, AED-CONF-65-169-7
CONF-650521–	(Conference on Purification of Materials, New York, May 6–8, 1965)	
3	20-3911	Gmelin, AED-CONF-65-113-2
CONF-650549–	(International Atomic Energy Agency, Symposium on Exchange Reactions, Upton, N. Y., May 31–June 4, 1965)	
9	20-3962	ORINS
11	20-3963	ORINS
12	20-3980	ORINS
14	20-3967	ORINS
16	20-3966	ORINS
17	20-3964	ORINS
19	20-3965	ORINS
CONF-650560–	(13th Annual Meeting of the Radiation Research Society, Philadelphia, May 23–26, 1965)	
7	20-3788	Gmelin, AED-CONF-65-157-10
CONF-650601–	20-4040	(Symposium on Working Methods in High-Activity Hot Labs, Paris, June 1965)
CONF-650602–	(American Nuclear Society 11th Annual Meeting, Gatlinburg, Tenn., June 20–24, 1965)	
59	20-5113	Dep. mn; CFSTI $1.00 cy, $0.50 mn
78	20-4841	See NAA-SR-Memo-11511
CONF-650637–	(International Conference on Luminescent Dosimetry, Palo Alto, Calif., June 21–23, 1965)	
5	20-3983	See BNL-9589
CONF-650652–	(International ^{14}C and ^{3}H Dating Conference, Pullman, Wash., June 7–11, 1965)	
9	20-4147	Gmelin, AED-CONF-65-158-14

Report No.	Abstract No.	Availability
CONF-650717–	**(Conference on Unified Field Theories, Feldafing, Germany, July 1965)**	
1	20-4639	See IC/65/73
2	20-4646	See NYO-3399-40
CONF-650806–	**(7th International Conference on Phenomena in Ionized Gases, Belgrade, Aug. 22–27, 1965)**	
17	20-4943	See MATT-379
CONF-650816–	**(Conference on Radiation Trapped in the Earth's Magnetic Field, Bergen, Norway, Aug. 16–Sept. 3, 1965)**	
3	20-4731	See UCRL-7659-T(Rev.1)
4	20-4732	See UCRL-14368-T(Rev.1)
CONF-650830–	**(Sagamore Conference, New York, Aug. 25–27, 1965)**	
1	20-4399	See UCRL-16301
CONF-650902–	**(American Chemical Society, 150th National Meeting, Atlantic City, Sept. 12–17, 1965)**	
20	20-3916	Dep. mn; CFSTI $1.00 cy, $0.50 mn
CONF-650906–	**(2nd International Symposium on Inhaled Particles and Vapours, Cambridge, England, Sept. 27–30, 1965)**	
1	20-3656	See BNWL-SA-225
2	20-3655	See BNWL-SA-224
CONF-650917–	**(International Conference on Industrial Electronics and Instrumentation, Philadelphia, Sept. 8–10, 1965)**	
3	20-5025	See WAPD-T-1832
CONF-650922–	**(1st International Symposium on Magnet Technology, Stanford, Calif., Sept. 8–10, 1965)**	
20	20-4775	See UCRL-16376
CONF-650923–	**(5th International Conference on High Energy Accelerators, Frascati, Italy, Sept. 9–16, 1965)**	
16	20-4495	Dep. mn; CFSTI $1.00 cy, $0.50 mn
17	20-4499	See LNF-65/26
18	20-4512	See UCRL-16243
21	20-4511	See UCRL-16242
22	20-4513	See UCRL-16440
CONF-650924–	**(Workshop Conference on Space Radiation Biology, Berkeley, Calif., Sept. 7–10, 1965)**	
6	20-4541	See UCRL-16405
CONF-650930–	**(International Conference on the Microwave Behavior of Ferrimagnetics and Plasmas, London, Sept. 1965)**	
1	20-4947	See SU-IPR-13
CONF-650935–	**(2nd IAEA Conference on Plasma Physics and Controlled Nuclear Fusion Research, Culham, England, Sept. 6–10, 1965)**	
39	20-4942	See MATT-372
CONF-650937–	**(Conference on Megagauss Magnetic Field Generation by Explosives and Related Experiments, Frascati, Italy, Sept. 21–23, 1965)**	
2	20-4477	See LA-DC-7289
3	20-4941	See LA-DC-7290
CONF-650945–	**(International Conference on Elementary Particles, Oxford, Sept. 19–25, 1965)**	
2	20-4641	See IC/65/76
CONF-650948–	**(9th International Conference on Cosmic Rays, London, Sept. 6–17, 1965)**	
1	20-4562	See MIT-2098-174
CONF-651001–	**(IEEE Nuclear Science Symposium, San Francisco, Oct. 1965)**	
8	20-4245	See ORNL-P-1723
9	20-4221	See UCRL-12394-T
CONF-651003–	**(4th Symposium on Detonation, Silver Spring, Md., Oct. 13–15, 1965)**	
7	20-3918	See LA-DC-7276
CONF-651008–	**(Annual Bio-Assay Meeting, Albuquerque, N. Mex., Oct. 7–8, 1965)**	
4	20-3877	See LA-DC-7483
CONF-651009–	**(Conference on Safety, Fuels and Core Design in Large Fast Power Reactors, Argonne, Oct. 11–14, 1965)**	
4	20-5127	See ORNL-P-1698
5	20-5119	See GA-6732
CONF-651010–	**(Electrochemical Society, 6th Regional AIChE Meeting, Union, Wash., Oct. 8, 1965)**	
2	20-4049	See RL-SA-52
CONF-651018–	**(Joint Electronics Fall and 8th Pacific Coast Regional Meeting, Los Angeles, Oct. 27–29, 1965)**	
3	20-4298	See LA-DC-7275
CONF-651020–	**(5th Thermal Conductivity Conference, Denver, Oct. 20–22, 1965)**	
5	20-4310	See ORNL-P-1699
CONF-651026–	**(1st AIAA Rankine Circle Space Power System Specialists Conference, Cleveland, Oct. 26, 1965)**	
2	20-5183	See ORNL-P-1736
3	20-5182	See ORNL-P-1721
4	20-5184	See ORNL-P-1740
CONF-651030–	**(German Physical Society, Annual Meeting, Frankfurt, Oct. 4–9, 1965)**	
1	20-4840	See LAL-1140
2	20-4773	See COO-1198-306
CONF-651041–	**(Nuclear and Engineering Ceramics Conference, Harwell, England, Oct. 25–27, 1965)**	
2	20-4344	See ORNL-P-1725
CONF-651101–	**20-3647**	**(American Nuclear Society, Winter Meeting, Washington, D. C., Nov. 15–18, 1965) (Revised 11-8-65)**
1	20-5136	See WCAP-5554
34	20-5036	See RL-SA-47
37	20-4280	See SC-DC-65-1601
CONF-651109–	**(1st Symposium on Accelerator Radiation Dosimetry and Experience, Upton, N. Y., Nov. 3–5, 1965)**	
2	20-4514	See UCRL-16445
3	20-4506	See PPAD-569E
4	20-4505	See ORNL-P-1738
5	20-4175	See BNL-9650
6	20-4250	See UCRL-16446
7	20-4237	See BNL-9665
8	20-4249	See UCRL-16311
12	20-4176	See BNL-9684
COO–		
30-101(Rev.)	20-4679	Phys. Rev., 140: B1366-7(1965)
264-238	20-4777	Ann. Phys., (N.Y.), 34: 363-76(1965)
264-265	20-4599	Phys. Rev., 140: B927-8(1965)
818-60	20-4828	Dep. mn; CFSTI $3.00 cy, $0.75 mn
818-61	20-4536	Dep. mn; CFSTI $3.00 cy, $0.75 mn
818-63	20-4523	Dep. mn; CFSTI $1.00 cy, $0.50 mn
818-64	20-4561	Dep. mn; CFSTI $1.00 cy, $0.50 mn
1198-252	20-4780	Physics, 1: 337-87(1965)
1198-306	20-4773	Dep. mn; CFSTI $3.00 cy, $0.75 mn
1420-116	20-4900	Phys. Rev., 140: B1177-81(1965)
1518-1	20-4340	Dep. mn; CFSTI $1.00 cy, $0.50 mn
CRRP–	**(Canadian)**	
1221	20-5114	Dep.; AECL $1.00
CU–	**(Misc.)**	
12-65-AF-2461-EE	20-4935	See AFCRL-65-556
DP–		
967	20-5193	Dep. mn; CFSTI $2.00 cy, $0.50 mn
971	20-5194	Dep. mn; CFSTI $2.00 cy, $0.50 mn
1012	20-4277	Dep. mn; CFSTI $2.00 cy, $0.50 mn
DUBNA REPORTS	**(Russian)**	
See JINR (Russian)		
ECOM–	**(Non-AEC)**	
00392-1	20-4154	See AD-620003
EUR–	**(European Atomic Energy Community)**	

Report No.	Abstract No.	Availability
2283.d	20-4572	Dep. mn
2313	20-5088	See EURAEC-1337
2386	20-4319	See EURAEC-1457
2395	20-4457	See EURAEC-1474
2398	20-5032	See EURAEC-1477
2414.f,i	20-3658	Dep. mn
2459.f	20-3870	Dep. mn
2468.e	20-5176	Dep. mn
2487.e	20-4238	Dep. mn
2493.e	20-3710	Dep. mn
2494.d	20-4997	Dep. mn
2497.e	20-3871	Dep. mn
2507.d	20-3872	Dep. mn
2514.e	20-4371	Dep. mn
2516.d,f,i,n	20-4155	Dep. mn
2519.e	20-4287	Dep. mn
2523.i	20-3873	Dep. mn
2528.f	20-3972	Dep. mn
2535.f	20-3874	Dep. mn
EURAEC–		
1337	20-5088	Dep. mn; CFSTI $5.00 cy, $1.00 mn
1340	20-4046	Dep. mn; CFSTI $2.00 cy, $0.50 mn
1354	20-4101	Dep. mn; CFSTI $3.00 cy, $0.50 mn
1457	20-4319	Dep. mn; CFSTI $1.00 cy, $0.50 mn
1474	20-4457	Dep. mn; CFSTI $2.00 cy, $0.50 mn
1477	20-5032	Dep. mn; CFSTI $1.00 cy, $0.50 mn
1494	20-4327	See UNC-5138
1507	20-4374	See IITRI-578-P27-12
1508	20-4370	See CEND-3256-250
1509	20-4382	See NUMEC-3505-8
1513	20-4372	See GA-6724
FTD-MT–	**(Non-AEC)**	
65-33	20-4114	For translation see AD-621784
FTD-TT–	**(Non-AEC)**	
64-1228	20-4252	CFSTI
GA–	**(Misc.)**	
4967	20-5115	Dep. mn; CFSTI $2.00 cy, $0.75 mn
5618	20-5116	Dep. mn; CFSTI $4.00 cy, $1.00 mn
5866	20-5117	Dep. mn; CFSTI $4.00 cy, $1.00 mn
6075	20-4818	Nukleonik, 7: 295-300(1965)
6131	20-5089	Dep. mn; CFSTI $3.00 cy, $0.75 mn
6267	20-4075	Dep. mn; CFSTI $5.00 cy, $1.00 mn
6485	20-4458	Dep. mn; CFSTI $2.00 cy, $0.50 mn
6540	20-5057	Dep. mn; CFSTI $2.00 cy, $0.50 mn
6588	20-5033	Dep. mn; CFSTI $2.00 cy, $0.50 mn
6634	20-4801	Dep. mn; CFSTI $3.00 cy, $0.75 mn
6647	20-5118	Dep. mn; CFSTI $2.00 cy, $0.50 mn
6724	20-4372	Dep. mn; CFSTI $1.00 cy, $0.50 mn
6732	20-5119	Dep. mn; CFSTI $3.00 cy, $0.75 mn
GAMD–	**(Misc.)**	
6676	20-5078	Dep. mn; CFSTI $2.00 cy, $0.50 mn
GEAP–	**(Misc.)**	
4794	20-4373	Dep. mn; CFSTI $2.00 cy, $0.50 mn
4799	20-5120	Dep. mn; CFSTI $4.00 cy, $1.00 mn
4850	20-4459	Dep. mn; CFSTI $3.00 cy, $0.75 mn
GEMP–	**(Misc.)**	
173(Suppl.1)	20-4829	Dep. mn; CFSTI $1.00 cy, $0.50 mn
384	20-4830	Dep. mn; CFSTI $4.00 cy, $0.75 mn
HEPL–	**(Misc.)**	
272	20-4831	
384	20-4578	See AD-618660
385	20-4579	See AD-618661
386	20-4580	See AD-618662
387	20-4581	See AD-618663
HIC–	**(Non-AEC)**	
1-1564-3(Vol.2)	20-4076	
HIT–		
161(Vol.1)	20-5121	See HIT-3459-11(Vol.1)
161(Vol.2)	20-5122	See HIT-3459-11(Vol.2)
3459-11(Vol.1)	20-5121	Dep. mn; CFSTI $3.00 cy, $0.75 mn
3459-11(Vol.2)	20-5122	Dep. mn; CFSTI $4.00 cy, $0.75 mn
HPR–	**(Norwegian)**	
61	20-5123	Dep. mn
HW–		
68082	20-5195	Dep. mn; CFSTI $1.00 cy, $0.50 mn
HW-SA–		
3640	20-4102	Dep. mn; CFSTI $1.00 cy, $0.50 mn
IA–	**(Non-AEC)**	
1040	20-4613	Phys. Rev., 140: B1151-6(1965)
IAE–	**(Non-AEC)**	
900	20-4239	Dep. mn
901	20-4832	Dep. mn
907	20-4937	Dep. mn
909	20-4938	Dep. mn
911	20-4939	Dep. mn
926	20-4281	Dep. mn
927	20-5004	Dep. mn
928	20-5005	Dep. mn
932	20-4940	Dep. mn
IC–	**(Misc.)**	
65/73	20-4639	Dep. mn
65/75	20-4640	Dep. mn
65/76	20-4641	Dep. mn
65/78	20-4642	Dep. mn
IDO–		
17115	20-4802	Dep. mn; CFSTI $3.00 cy, $0.75 mn
IITRI–	**(Misc.)**	
578P21-15	20-5023	Dep. mn; CFSTI $3.00 cy, $0.75 mn
578-P27-12	20-4374	Dep. mn; CFSTI $2.00 cy, $0.50 mn
B6035-12	20-4374	See IITRI-578-P27-12
INR–	**(Non-AEC)**	
607/VI/PH	20-4643	Dep.
630/IX-A/PR	20-4803	Dep.
IS–		
1158	20-4659	Phys. Rev., 140: B921-5(1965)
1200	20-5213	Dep. mn; CFSTI $7.87 cy, $2.25 mn
1222	20-3973	Dep. mn; CFSTI $4.00 cy, $0.75 mn
1241	20-4375	Dep. mn; CFSTI $2.00 cy, $0.50 mn
IS-T–		
22	20-4774	Dep. mn; CFSTI $4.00 cy, $0.75 mn
33	20-5214	Dep. mn; CFSTI $3.00 cy, $0.75 mn
37	20-3875	Dep. mn; CFSTI $2.00 cy, $0.50 mn
43	20-4833	Dep. mn; CFSTI $2.00 cy, $0.50 mn
ISS–	**(Italian)**	
65/8	20-3876	Dep. mn
JAERI–	**(Japanese)**	
1083	20-4177	Dep. mn
JINR–	**(Russian)**	
E-2360	20-4834	Dep. mn
P-2277	20-4240	Dep. mn
P-2287	20-4835	Dep. mn
P-2298	20-4836	Dep. mn
P-2299	20-4644	Dep. mn
P-2310	20-4837	Dep. mn
P-2314	20-4838	Dep. mn
P-2333	20-4839	Dep. mn
P-2335	20-5058	Dep. mn
P-2359	20-4998	Dep. mn
P-2361	20-4582	Dep. mn
P-2364	20-4241	Dep. mn
P-2371	20-4583	Dep. mn
P-2375	20-4496	Dep. mn
P-2376	20-4242	Dep. mn
P-2380	20-4584	Dep. mn
JPRS–	**(Non-AEC)**	
31193	20-5137	CFSTI $2.00 cy, $0.50 mn
31514	20-3712	CFSTI $4.00 cy, $0.75 mn
31814	20-4191	CFSTI $5.00 cy, $1.00 mn

Report No.	Abstract No.	Availability
32317	20-4403	CFSTI $1.00 cy, $0.50 mn
32686	20-4192	CFSTI $1.00 cy, $0.50 mn
32773	20-4404	CFSTI $1.00 cy, $0.50 mn
32813	20-4272	CFSTI $1.00 cy, $0.50 mn
32842	20-4090	CFSTI $1.00 cy, $0.50 mn
JüL–	**(German)**	
239-RE	20-5197	Dep. mn
268-RG	20-4376	Dep. mn
284-ST	20-4178	Dep. mn
K-Trans–		
9	20-4405	Dep. mn; CFSTI $1.00 cy, $0.50 mn; JCL $1.10 fs, $0.80 mf
KAPL–		
3098	20-4804	Dep. mn; CFSTI $2.00 cy, $0.50 mn
KFK–	**(German)**	
310	20-4497	Dep. mn
KRB–	**(German)**	
1965/1	20-5129	See TID-22328
LA–		
3363	20-4179	Dep. mn; CFSTI $1.00 cy, $0.50 mn
3381	20-5177	Dep. mn; CFSTI $2.00 cy, $0.50 mn
3405	20-3917	Dep. mn; CFSTI $2.00 cy, $0.50 mn
3419	20-4498	Dep. mn; CFSTI $3.00 cy, $0.50 mn
LA-DC–		
6742	20-4814	Nucl. Sci. Eng., 23: 380-91(1965)
7021	20-4139	AIAA (Amer. Inst. Aeron. Astronaut. J., 3: 1961-3(1965)
7123	20-4424	J. Less-Common Metals, 9: 393-408(1965)
7275	20-4298	Dep. mn; CFSTI $1.00 cy, $0.50 mn
7276	20-3918	Dep. mn; CFSTI $2.00 cy, $0.50 mn
7289	20-4477	Dep. mn; CFSTI $1.00 cy, $0.50 mn
7290	20-4941	Dep. mn; CFSTI $3.00 cy, $0.50 mn
7483	20-3877	Dep. mn; CFSTI $1.00 cy, $0.50 mn
LAL–	**(French)**	
1102	20-4243	Dep. mn
1140	20-4840	Dep. mn
LFEN–	**(Portuguese)**	
32	20-4047	Dep. mn
LNF–	**(Italian)**	
65/26	20-4499	Dep. mn
65/27	20-4500	Dep. mn
65/34	20-4501	Dep. mn
LYCEN–	**(French)**	
6524	20-3878	Dep. mn
M–	**(Misc.)**	
63-20-1	20-4098	See AD-614633
MATT–		
343	20-4984	Phys. Fluids, 8: 1886-9(1965)
372	20-4942	Dep. mn; CFSTI $1.00 cy, $0.50 mn
378	20-4217	Dep. mn; CFSTI $1.00 cy, $0.50 mn
379	20-4943	Dep. mn; CFSTI $1.00 cy, $0.50 mn
MD–	**(Misc.)**	
65-6	20-5220	See UCRL-13185
65-7	20-4222	See UCRL-13186
MIT–	**(Misc.)**	
2098-174	20-4562	Dep. mn; CFSTI $3.00 cy, $0.50 mn
2241-7	20-4150	Dep. mn; CFSTI $3.00 cy, $0.50 mn
2241-14	20-4151	Dep. mn; CFSTI $6.00 cy, $1.25 mn
ML-TR–	**(Non-AEC)**	
120	20-4362	See AD-620033
MLM–		
1266	20-3879	Dep. mn; CFSTI $2.00 cy, $0.50 mn
MND-P–		
2229	20-4278	Dep. mn; CFSTI $2.00 cy, $0.50 mn
MSAR–	**(Misc.)**	
65-150	20-3880	Dep. mn; CFSTI $2.00 cy, $0.50 mn
N–	**(Misc.)**	
64-25007	20-4133	CFSTI
64-30079	20-4734	CFSTI $1.10 cy
NAA-SR–		
11303	20-5178	Dep. mn; CFSTI $1.00 cy, $0.50 mn
NAA-SR-Memo–		
6484	20-5179	Dep. mn; CFSTI $1.00 cy, $0.50 mn
10741	20-4377	Dep. mn; CFSTI $3.00 cy, $0.75 mn
10927	20-4341	Dep. mn; CFSTI $1.00 cy, $0.50 mn
11099	20-4103	Dep. mn; CFSTI $2.00 cy, $0.50 mn
11511	20-4841	Dep. mn; CFSTI $1.00 cy, $0.50 mn
11542	20-4378	Dep. mn; CFSTI $1.00 cy, $0.50 mn
11604	20-5180	Dep. mn; CFSTI $1.00 cy, $0.50 mn
NASA-CR–	**(Misc.)**	
54049	20-4133	See N64-25007
54091	20-4379	
54761	20-4380	
54781	20-4326	See TRW-ER-6561
NASA-TN–	**(Misc.)**	
D-3058	20-4704	CFSTI $1.00 cy, $0.50 mn
D-3116	20-4842	CFSTI $2.00 cy, $0.50 mn
NASA-TT–	**(Non-AEC)**	
F-262	20-4107	CFSTI $5.00 cy, $1.00 mn
F-8700	20-4734	See N64-30079
NBL–		
228	20-3881	Dep. mn; CFSTI $1.00 cy, $0.50 mn
NC–	**(Norwegian)**	
72	20-5060	See TID-22357
NIRL-R–	**(British)**	
92	20-4502	Dep. mn
NMI–	**(Misc.)**	
8001.4	20-4381	
NOL-TR–	**(Non-AEC)**	
65-72	20-4233	See AD-618676
NOLTR–	**(Misc.)**	
63-140	20-5034	Dep. mn; CFSTI $5.00 cy, $1.00 mn
NP–	**(AEC File No. for Non-AEC Reports)**	
15150	20-3800	Dep. mn
15156	20-3659	Dep. mn
15340	20-4503	Dep. mn
15406	20-4048	Dep. mn
15416	20-4244	Dep. mn
15420	20-4504	Dep. mn
15456	20-4843	Dep. mn
15528	20-3660	Dep. mn
15571	20-4180	Dep. mn
15572	20-5079	Dep. mn
15576	20-4537	Dep. mn
15577	20-4538	Dep. mn
15594	20-3661	Dep. mn
15599	20-4645	Dep. mn
15610	20-4262	CFSTI $2.00 cy, $0.50 mn
15620	20-4181	Dep. mn
15622	20-4104	
NUMEC–		
3505-8	20-4382	Dep. mn; CFSTI $2.00 cy, $0.50 mn
NYO–		
1480-33	20-4705	Dep. mn; CFSTI $2.00 cy, $0.50 mn
3250-4	20-5124	Dep. mn; CFSTI $3.00 cy, $0.75 mn
3314-2	20-3711	Dep. mn; CFSTI $1.00 cy, $0.50 mn
3399-24	20-4667	Phys. Rev., 140: B1045-53(1965)
3399-25	20-4671	Phys. Rev., 140: B1091-9(1965)
3399-40	20-4646	Dep. mn; CFSTI $1.00 cy, $0.50 mn
3421-4	20-4218	Dep. mn; CFSTI $1.00 cy, $0.50 mn

Report No.	Abstract No.	Availability
10732	20-5125	Dep. mn; CFSTI $6.00 cy, $1.25 mn
ORNL–		
2599	20-4999	Dep. mn; CFSTI $6.00 cy, $1.25 mn
2711	20-4299	Dep. mn; CFSTI $5.00 cy, $1.00 mn
3029	20-5181	Dep. mn; CFSTI $4.00 cy, $0.75 mn
3795(Pt.2)	20-4383	Dep. mn; CFSTI $2.00 cy, $0.50 mn
3843	20-4182	Dep. mn; CFSTI $6.00 cy, $1.00 mn
3861	20-4282	Dep. mn; CFSTI $3.00 cy, $0.50 mn
3870	20-4300	Dep. mn; CFSTI $7.00 cy, $1.75 mn
3871	20-4944	Dep. mn; CFSTI $2.00 cy, $0.50 mn
ORNL-IIC–		
5	20-4111	Dep. mn; CFSTI $4.00 cy, $1.75 mn
ORNL-P–	**(Misc.)**	
1196	20-4055	J. Electrochem. Soc., 112: 1092-6(1965)
1197	20-4054	J. Chromatog., 20: 378-83(1965)
1257	20-4981	Phys. Fluids, 8: 1853-9(1965)
1292	20-5012	J. Appl. Phys., 36: 3486-90(1965)
1433	20-4899	Phys. Rev., 140: B904-7(1965)
1698	20-5127	Dep. mn; CFSTI $1.00 cy, $0.50 mn
1699	20-4310	Dep. mn; CFSTI $1.00 cy, $0.50 mn
1721	20-5182	Dep. mn; CFSTI $2.00 cy, $0.50 mn
1723	20-4245	Dep. mn; CFSTI $1.00 cy, $0.50 mn
1725	20-4344	Dep. mn; CFSTI $2.00 cy, $0.50 mn
1735	20-5183	Dep. mn; CFSTI $1.00 cy, $0.50 mn
1738	20-4505	Dep. mn; CFSTI $2.00 cy, $0.50 mn
1740	20-5184	Dep. mn; CFSTI $2.00 cy, $0.50 mn
ORNL-RSIC–		
9	20-5001	Dep. mn; ORNL Free
ORNL-TM–		
1177	20-4279	Dep. mn; CFSTI $1.00 cy, $0.50 mn
1234	20-4844	Dep. mn; CFSTI $2.00 cy, $0.50 mn
1245	20-4805	Dep. mn; CFSTI $1.00 cy, $0.50 mn
1278	20-5035	Dep. mn; CFSTI $1.00 cy, $0.50 mn
1281	20-3922	Dep. mn; CFSTI $2.00 cy, $0.50 mn
1290	20-5198	Dep. mn; CFSTI $2.00 cy, $0.50 mn
1293	20-4087	Dep. mn; CFSTI $1.00 cy, $0.50 mn
1299	20-3923	Dep. mn; CFSTI $3.00 cy, $0.75 mn
1306	20-4945	Dep. mn; CFSTI $1.00 cy, $0.50 mn
1307	20-4946	Dep. mn; CFSTI $1.00 cy, $0.50 mn
1314	20-3974	Dep. mn; CFSTI $1.00 cy, $0.50 mn
1318	20-4845	Dep. mn; CFSTI $1.00 cy, $0.50 mn
1320	20-4263	Dep. mn; CFSTI $1.00 cy, $0.50 mn
1328	20-5199	Dep. mn; CFSTI $1.00 cy, $0.50 mn
ORNL-tr–		
702	20-4157	Dep. mn; JCL $4.60 fs, $1.52 mf
854	20-4330	Dep. mn; JCL $8.60 fs, $3.08 mf
872	20-5008	Dep. mn; CFSTI $2.00 cy, $0.50 mn; JCL $3.60 fs, $1.37 mf
873	20-4406	Dep. mn; JCL $1.60 fs, $0.80 mf
ORO–		
633	20-3984	Dep. mn; CFSTI $2.00 cy, $0.50 mn
PATENTS	**(British)**	**4s. 6d. each, U. K. Patent Office**
1,007,091	20-4455	
1,007,139	20-4456	
1,007,173	20-4352	
1,007,206	20-5080	
1,007,207	20-5038	
1,007,208	20-5039	
1,007,212	20-5208	
1,007,371	20-4258	
1,007,871	20-3968	
1,007,884	20-4038	
1,007,974	20-5040	
1,007,975	20-5041	
1,007,997	20-4109	
1,008,000	20-5042	
1,008,066	20-4070	
1,008,506	20-5043	
1,008,517	20-4230	
1,008,541	20-4576	
1,008,590	20-4094	
1,008,712	20-5169	
1,008,713	20-5170	
1,008,804	20-4353	
1,008,865	20-4095	
1,008,945	20-4259	
1,008,956	20-5095	
1,008,966	20-4260	
1,009,000	20-4096	
PATENTS	**(U. S.)**	**$0.25 each, U. S. Patent Office**
3,184,915	20-4140	
3,198,709	20-5044	
3,202,582	20-5081	
3,205,141	20-5028	
3,210,943	20-5171	
3,211,002	20-5045	
3,211,518	20-3969	
3,211,548	20-4314	
3,211,621	20-5082	
3,211,622	20-5046	
3,211,623	20-5083	
3,211,624	20-5084	
3,211,625	20-5085	
3,211,626	20-5096	
3,211,627	20-5097	
3,211,909	20-4170	
3,211,961	20-3970	
3,212,178	20-5098	
3,212,845	20-4071	
3,212,846	20-3971	
3,212,847	20-4072	
3,212,974	20-4993	
3,212,976	20-5047	
3,212,977	20-5048	
3,212,978	20-5049	
3,212,979	20-5050	
3,212,980	20-5051	
3,212,981	20-5052	
3,212,983	20-5086	
3,212,984	20-5053	
3,212,985	20-5172	
3,212,988	20-5099	
3,212,990	20-5100	
3,212,992	20-5101	
3,213,031	20-5209	
3,213,279	20-4171	
3,213,280	20-3913	
3,214,833	20-4354	
3,215,569	20-4799	
3,215,606	20-5087	
3,215,607	20-5102	
3,215,608	20-5103	
3,216,010	20-5225	
3,216,174	20-5029	
3,216,806	20-4315	
3,216,851	20-4355	
3,216,903	20-5054	
3,217,199	20-4231	
3,217,322	20-5226	
3,217,471	20-4097	
3,217,591	20-4232	
3,218,123	20-5210	
3,218,160	20-4073	
3,218,235	20-4994	
3,218,781	20-4726	
3,218,845	20-5227	
3,219,408	20-4074	
3,219,441	20-4316	
3,219,474	20-4356	
3,219,477	20-4357	
3,219,534	20-4995	
PG-Report–	**(British)**	
650	20-3662	Dep.; BIS $0.60; HMSO 2s. 2d.
677	20-3887	Dep.; BIS $0.30; HMSO 1s. 9d.
PNE–		
810F	20-4144	Dep. mn; CFSTI $2.00 cy, $0.50 mn
PPAD–		
569E	20-4506	Dep. mn; CFSTI $2.00 cy, $0.50 mn
2137-544	20-4910	Phys. Rev., 140: B1272-6(1965)
2137-554	20-4616	Phys. Rev., 140: B1358-64(1965)
2137-560	20-4507	Dep. mn; CFSTI $3.00 cy, $0.75 mn

Report No.	Abstract No.	Availability
PWAC–	**(Misc.)**	
460	20-4324	Dep. mn; CFSTI $2.00 cy, $0.50 mn
461	20-4392	Dep. mn; CFSTI $3.00 cy, $0.50 mn
472	20-4393	Dep. mn; CFSTI $2.00 cy, $0.50 mn
477	20-4394	Dep. mn; CFSTI $1.00 cy, $0.50 mn
478	20-4395	Dep. mn; CFSTI $1.00 cy, $0.50 mn
482(Pt.1)	20-4396	Dep. mn; CFSTI $1.00 cy, $0.50 mn
R–	**(Misc.)**	
375	20-4131	See AD-622552
2355	20-4319	See EURAEC-1457
REIC-Memo–	**(Misc.)**	
28	20-4461	Dep. mn; CFSTI $2.00 cy, $0.50 mn
RFP–		
624	20-3985	Dep. mn; CFSTI $2.00 cy, $0.50 mn
RL-SA–		
47	20-5036	Dep. mn; CFSTI $1.00 cy, $0.50 mn
52	20-4049	Dep. mn; CFSTI $1.00 cy, $0.50 mn
RM–	**(Misc.)**	
3727(RAND)	20-4167	
RPI–	**(Misc.)**	
328-40	20-4508	Dep. mn; CFSTI $3.00 cy, $0.50 mn
3036-1	20-4706	Dep. mn; CFSTI $2.00 cy, $0.50 mn
RT/FIMA–	**(Italian)**	
(65)-1	20-5059	Dep. mn
S–	**(Misc.)**	
227-R	20-4262	See NP-15610
SC-DC–		
65-1601	20-4280	Dep. mn; CFSTI $1.00 cy, $0.50 mn
65-1797	20-4730	Dep. mn; CFSTI $2.00 cy, $0.50 mn
SC-DR–		
65-312	20-4288	Dep. mn; CFSTI $2.00 cy, $0.50 mn
65-318	20-4289	Dep. mn; CFSTI $1.00 cy, $0.50 mn
SC-RR–		
65-333	20-4187	Dep. mn; CFSTI $3.00 cy, $0.50 mn
65-478	20-4083	Dep. mn; CFSTI $2.00 cy, $0.50 mn
SC-TM–		
65-424	20-4220	Dep. mn; CFSTI $2.00 cy, $0.50 mn
65-443	20-4112	Dep. mn; CFSTI $2.00 cy, $0.50 mn
65-448	20-5215	Dep. mn; CFSTI $2.00 cy, $0.50 mn
65-457	20-5216	Dep. mn; CFSTI $3.00 cy, $0.75 mn
SEL–	**(Misc.)**	
63-120	20-4134	Dep. mn; CFSTI $1.00 cy, $0.50 mn
SGAE-PH–	**(Austrian)**	
27/1965	20-4283	Dep. mn
SLAC–		
43	20-4585	Dep. mn; CFSTI $2.00 cy, $0.50 mn
SR–	**(Misc.)**	
1	20-4521	See AD-618222
SU-IPR–		
13	20-4947	Dep. mn; CFSTI $1.00 cy, $0.50 mn
SWRI–		
1228-67	20-4078	Dep. mn; CFSTI $3.00 cy, $0.75 mn
TB–	**(Non-AEC)**	
58	20-4325	Dept. of Mines and Technical Surveys, Ottawa, $0.50
TE–	**(Non-AEC)**	
74-65	20-4570	See AD-614592
TID–		
3571(Suppl.1)	20-5200	Dep. mn; CFSTI $3.00 cy, $0.50 mn
21169	20-5217	Dep. mn; CFSTI $1.00 cy, $0.50 mn
21362	20-4247	Dep. mn; CFSTI $1.00 cy, $0.50 mn
21911	20-4420	J. Appl. Phys., 36: 3628-31(1965)
21991	20-5218	Dep. mn; CFSTI $3.00 cy, $0.75 mn
22042	20-5014	J. Chem. Phys., 43: 4057-9(1965)
22048	20-4600	Phys. Rev., 140: B959-66(1965)
22049	20-4601	Phys. Rev., 140: B967-76(1965)
22093	20-4682	Phys. Rev., 140: B1402-4(1965)
22142	20-4678	Phys. Rev., 140: B1365-6(1965)
22179	20-4478	Dep. mn; CFSTI $6.00 cy, $1.50 mn
22225	20-5128	Dep. mn; CFSTI $7.00 cy, $1.50 mn
22266	20-4152	Dep. mn; CFSTI $2.00 cy, $0.50 mn
22268	20-4188	Dep. mn; GPO $0.40
22274	20-4647	Dep. mn; CFSTI $3.00 cy, $0.75 mn
22285	20-4551	Phys. Rev., 140: B992-8(1965)
22315	20-4586	Dep. mn; CFSTI $4.00 cy, $0.75 mn
22318	20-3663	Dep. mn; CFSTI $1.00 cy, $0.50 mn
22321	20-4105	Dep. mn; CFSTI $2.00 cy, $0.50 mn
22324	20-3664	Dep. mn; CFSTI $2.00 cy, $0.50 mn
22328	20-5129	Dep. mn; CFSTI $4.00 cy, $1.00 mn
22333	20-4248	Dep. mn; CFSTI $2.00 cy, $0.50 mn
22352	20-3686	Dep. mn; CFSTI $1.00 cy, $0.50 mn
22355	20-5130	Dep. mn; CFSTI $2.00 cy, $0.50 mn
22357	20-5060	Dep. mn; CFSTI $2.00 cy, $0.50 mn
22358	20-4113	Dep. mn; CFSTI $1.00 cy, $0.50 mn
22366	20-3924	Dep. mn; CFSTI $3.00 cy, $0.50 mn
22366, App. B	20-3925	
22372	20-5219	Dep. mn; CFSTI $1.00 cy, $0.50 mn
22374	20-3926	Dep. mn; CFSTI $5.00 cy, $1.00 mn
22402	20-3888	Dep. mn; CFSTI $4.00 cy, $1.00 mn
TIM–	**(Misc.)**	
949	20-4088	Dep. mn; CFSTI $3.00 cy, $0.75 mn
955	20-4397	Dep. mn; CFSTI $1.00 cy, $0.50 mn
TLW–	**(Misc.)**	
1055A	20-4089	
TN-N–	**(Non-AEC)**	
691	20-4142	See AD-619053
TR–	**(Misc.)**	
16	20-4361	See AD-619719
TRG-Report–	**(British)**	
1021	20-4398	Dep.; BIS $0.60; HMSO 3s. 0d.
TRW-ER–	**(Misc.)**	
6561	20-4326	
TT–	**(Canadian)**	
65-31512	20-4191	See JPRS-31814
65-31690	20-5137	See JPRS-31193
65-32010	20-3712	See JPRS-31514
65-32807	20-4403	See JPRS-32317
65-33165	20-4192	See JPRS-32686
65-33351	20-4404	See JPRS-32773
65-33391	20-4272	See JPRS-32813
65-33420	20-4090	See JPRS-32842
UCRL–		
7659-T(Rev.1)	20-4731	Dep. mn; CFSTI $1.00 cy, $0.50 mn
11444	20-4539	Dep. mn; CFSTI $1.00 cy, $0.50 mn
11475	20-3649	Dep. mn; CFSTI $1.00 cy, $0.50 mn
11495	20-4587	Dep. mn; CFSTI $1.00 cy, $0.50 mn
11565	20-4588	Dep. mn; CFSTI $3.00 cy, $0.75 mn
11619(Rev.1)	20-4983	Phys. Fluids, 8: 1876-85(1965)
11634	20-4979	Phys. Fluids, 8: 1840-5(1965)
11754	20-4589	Dep. mn; CFSTI $1.00 cy, $0.50 mn
11802	20-4480	Dep. mn; CFSTI $4.00 cy, $0.75 mn
11922	20-4888	Phys. Rev., 140: B811-15(1965)
11926	20-4590	Dep. mn; CFSTI $4.00 cy, $0.75 mn
12085(Pt.1)	20-4847	Dep. mn; CFSTI $1.00 cy, $0.50 mn
12085(Pt.2)	20-4848	Dep. mn; CFSTI $1.00 cy, $0.50 mn
12162	20-4610	Phys. Rev., 140: B1123-31(1965)
12394-T	20-4221	Dep. mn; CFSTI $2.00 cy, $0.50 mn
13095(Vol.1)	20-5185	Dep. mn; CFSTI $6.00 cy, $1.50 mn
13095(Vol.2)	20-5186	Dep. mn; CFSTI $5.00 cy, $1.00 mn
13185	20-5220	Dep. mn; CFSTI $4.00 cy, $0.75 mn
13186	20-4222	Dep. mn; CFSTI $4.00 cy, $0.75 mn
13187	20-4079	Dep. mn; CFSTI $3.00 cy, $0.75 mn
14169	20-5011	J. Appl. Phys., 36: 3440-4(1965)
14170	20-4481	Dep. mn; CFSTI $2.00 cy, $0.50 mn
14228	20-5221	Dep. mn; CFSTI $4.00 cy, $0.75 mn

Report No.	Abstract No.	Availability
14318	20-4707	Dep. mn; CFSTI $1.00 cy, $0.50 mn
14343	20-4509	Dep. mn; CFSTI $1.00 cy, $0.50 mn
14345	20-4223	Dep. mn; CFSTI $1.00 cy, $0.50 mn
14360	20-4482	Dep. mn; CFSTI $4.00 cy, $0.75 mn
14364	20-4540	Dep. mn; CFSTI $3.00 cy, $0.75 mn
14368-T(Rev.1)	20-4732	Dep. mn; CFSTI $2.00 cy, $0.50 mn
14398	20-5007	Dep. mn; CFSTI $1.00 cy, $0.50 mn
14425	20-4291	Dep. mn; CFSTI $2.00 cy, $0.50 mn
14427-T	20-4292	CFSTI $4.00 cy, $0.75 mn
14432-T	20-4808	Dep. mn; CFSTI $3.00 cy, $0.75 mn
14448	20-4224	Dep. mn; CFSTI $1.00 cy, $0.50 mn
14496-T	20-4670	Phys. Rev., 140: B1079-87(1965)
14505	20-5222	Dep. mn; CFSTI $1.00 cy, $0.50 mn
16016	20-4510	Dep. mn; CFSTI $3.00 cy, $0.75 mn
16193	20-4668	Phys. Rev., 140: B1054-67(1965)
16202	20-4765	Phys. Rev., 140: B1110-22(1965)
16208	20-4914	Phys. Rev., 140: B1310-17(1965)
16224	20-4663	Phys. Rev., 140: B957-8(1965)
16234	20-4617	Phys. Rev., 140: B1421-6(1965)
16242	20-4511	Dep. mn; CFSTI $1.00 cy, $0.50 mn
16243	20-4512	Dep. mn; CFSTI $1.00 cy, $0.50 mn
16245	20-4686	Phys. Rev., 140: B1427-30(1965)
16301	20-4399	Dep. mn; CFSTI $3.00 cy, $0.75 mn
16303	20-5223	Dep. mn; CFSTI $2.00 cy, $0.50 mn
16311	20-4249	Dep. mn; CFSTI $1.00 cy, $0.50 mn
16376	20-4775	Dep. mn; CFSTI $1.00 cy, $0.50 mn
16405	20-4541	Dep. mn; CFSTI $1.00 cy, $0.50 mn
16440	20-4513	Dep. mn; CFSTI $2.00 cy, $0.50 mn
16445	20-4514	Dep. mn; CFSTI $1.00 cy, $0.50 mn
16446	20-4250	Dep. mn; CFSTI $2.00 cy, $0.50 mn
UCRL-Trans-		
1227	20-5009	Dep. mn; JCL $3.60 fs, $1.28 mf
1254(L)	20-3928	Dep. mn; JCL $8.60 fs, $2.93 mf
1261(L)	20-4950	Dep. mn; CFSTI $1.00 cy, $0.50 mn; JCL $2.60 fs, $0.86 mf
UNC-	**(Misc.)**	
5113	20-3889	Dep. mn; CFSTI $3.00 cy, $0.50 mn
5135	20-5131	Dep. mn; CFSTI $2.00 cy, $0.50 mn
5138	20-4327	Dep. mn; CFSTI $2.00 cy, $0.50 mn
UR-		
875-108	20-4591	Dep. mn; CFSTI $4.00 cy, $1.00 mn
USNRDL-TR-	**(Misc.)**	
885	20-4261	See AD-623078
891	20-3706	See AD-623365
898	20-3707	See AD-623641
899	20-4156	Dep. mn; $1.00 cy, $0.50 mn
902	20-4148	See AD-62315
907	20-4149	See AD-623639
917	20-4251	
VUF-		
1030	20-4189	Dep. mn; CFSTI $2.00 cy, $0.50 mn
1031	20-4190	Dep. mn; CFSTI $2.00 cy, $0.50 mn
3017	20-4084	Dep. mn; CFSTI $3.00 cy, $0.50 mn
WAL-TR-	**(Non-AEC)**	
405/2-8	20-4360	See AD-619399
WAPD-MRP-		
113	20-5132	Dep. mn; CFSTI $2.50 cy, $0.75 mn
WAPD-PWR-		
TE-151	20-5133	Dep. mn; CFSTI $4.00 cy, $0.75 mn
WAPD-T-		
1631	20-5071	Nucl. Sci. Eng., 23: 361-7(1965)
1832	20-5025	Dep. mn; CFSTI $2.00 cy, $0.50 mn
WAPD-TM-	**(Misc.)**	
535	20-4080	Dep. mn; CFSTI $1.00 cy, $0.50 mn
WASH-		
1063	20-4271	Dep. mn; CFSTI $1.00 cy, $0.50 mn
WCAP-	**(Misc.)**	
3269-12	20-5134	Dep. mn; CFSTI $3.00 cy, $0.75 mn
3269-40	20-5135	Dep. mn; CFSTI $2.00 cy, $0.50 mn
3269-41	20-4400	Dep. mn; CFSTI $3.00 cy, $0.75 mn
3269-50	20-4328	Dep. mn; CFSTI $4.00 cy, $1.00 mn
5554	20-5136	Dep. mn; CFSTI $1.00 cy, $0.50 mn
WL-TR-	**(Non-AEC)**	
64-113	20-4143	See AD-619969
64-179	20-4638	See AD-617965
65-91	20-5108	See AD-613376
WW-	**(Dutch)**	
016-R83	20-5032	See EURAEC-1477
YALE-		
1807-25	20-4850	Ann. Phys., (N.Y.), 34: 377-99(1965)
1807-26	20-4851	Ann. Phys., (N.Y.), 34: 400-14(1965)
1807-29	20-4901	Phys. Rev., 140: B1182-90(1965)
ZFK-RN-	**(German)**	
22	20-5061	Dep. mn

DEPOSITORIES OF USAEC REPORTS

In Countries Other than the U.S.

ARGENTINA
Buenos Aires, Comisión Nacional de Energía Atómica
AUSTRALIA
Canberra, Australian National Library
Sutherland, New South Wales, Australian Atomic Energy Commission
AUSTRIA
Vienna, Zentral Bibliothek der Physikalischen Institute der Universität
BELGIUM
Mol-Donk, Centre d'Etude de l'Energie Nucleaire
BOLIVIA
La Paz, Comisión Nacional de Energia Nuclear
BRAZIL
Rio de Janeiro, Instituto Brasileiro de Bibliografia e Documentacao
São Paulo, Instituto de Energia Atomica, Cidade Universitaria São Paulo
BURMA
Rangoon, Union of Burma Applied Research Institute, Atomic Energy Center Library
CANADA
Hamilton, McMaster University
Ottawa, National Research Council Library
Vancouver, University of British Columbia
CHILE
Santiago, Instituto de Fisica y Matematicas, Universidad de Chile
CHINA
Hsinchu, Taiwan, Free China, National Tsing Hua University
COLOMBIA
Bogota, Instituto De Asuntos Nucleares
COSTA RICA
San Pedro, University of Costa Rica Library
DENMARK
Risö, Danish Atomic Energy Commission
ECUADOR
Quito, Escuela Politécnica Nacional
EL SALVADOR
San Salvador, Universidad de El Salvador, Biblioteca de Energia Nuclear
FINLAND
Helsinki, Teknillisen Korkeakoulun Kirjasto
FRANCE
Gif-sur-Yvette, Centre d'Etudes Nucléaires de Saclay
Paris, Académie des Sciences
GERMANY
Berlin, Hahn-Meitner-Institut für Kernforschung Berlin
Frankfurt/Main, Gmelin-Institut
Munich, Technische Hochschule, Bibliothek
GHANA
Accra, University College of Ghana
GREECE
Athens, Nuclear Research Center "Democritus"
GUATEMALA
Guatemala, Comisión Nacional de Energía Nuclear
INDIA
Bombay, Department of Atomic Energy
INDONESIA
Djogjakarta, Java, Science Faculty, Gadjah Mada University
IRAN
Tehran, Tehran University Nuclear Centre
IRAQ
Baghdad, Iraqi Atomic Energy Commission
IRELAND
Dublin, University College
ISRAEL
Rehovoth, Israel Atomic Energy Commission
ITALY
Rome, Centro di Studi Nucleari della Casaccia
Rome, Comitato Nazionale per l'Energia Nucleare
JAPAN
Tokyo, National Diet Library
KOREA
Seoul, Office of Atomic Energy
LEBANON
Beirut, Lebanese National Council for Scientific Research
LUXEMBOURG
Luxembourg, Ministry of Transport and Electricity
MALAYSIA
Kuala Lumpur, University of Malaysia
MEXICO
Mexico, D.F., Comisión Nacional de Energía Nuclear
NETHERLANDS
The Hague, Reactor Centrum Nederland
NEW ZEALAND
Lower Hutt, Institute of Nuclear Sciences
NIGERIA
Ibadan, University of Ibadan
NORWAY
Lillestrøm, Institutt for Atomenergi
PAKISTAN
Lahore, West Pakistan, Atomic Energy Centre
PERU
Lima, Junta de Control de Energia Atomica
PHILIPPINE REPUBLIC
Manila, Philippine Atomic Energy Commission
POLAND
Warsaw, Biura Pelnomocnika Rzadu do Spraw Wykorzystania Energii Jadrowej
PORTUGAL
Sacavem, Junta de Energía Nuclear
REPUBLIC OF SOUTH AFRICA
Pretoria, Atomic Energy Board Library
REPUBLIC OF THE CONGO
Leopoldville, Université Lovanium
SPAIN
Madrid, Junta de Energía Nuclear, Biblioteca Documentación y Publicaciones, Ciudad Universitaria
SWEDEN
Nyköping, Aktiebolaget Atomenergi
SWITZERLAND
Zürich, Eidgenössische Technische Hochschule, Bibliothek
THAILAND
Bangkok, Office of the Thai Atomic Energy Commission, Department of Science
TURKEY
Ankara, Turkish Atomic Energy Commission, Atomic Energy Library
UNITED ARAB REPUBLIC
Cairo, Atomic Energy Commission
UNITED KINGDOM
Belfast, City Library
Birmingham, Central Library
Boston Spa, National Lending Library for Science and Technology
Bristol, Central Library
Glasgow, Mitchell Library
Kingston upon Hull, Central Library
Leeds, Central Library
Liverpool, Central Library
London, Central Library, Acton
London, Science Museum Library, South Kensington
Manchester, Central Library
Newcastle upon Tyne, Central Library
Nottingham, Central Library
Sheffield, Central Library
URUGUAY
Montevideo, Comision Nacional de Energia Atomica
VENEZUELA
Caracas, Instituto Venezolano de Investigaciones Científicas
VIET-NAM
Saigon, Atomic Energy Office
YUGOSLAVIA
Belgrade, Federal Commission for Nuclear Energy

In International Agencies

AUSTRIA
Vienna, International Atomic Energy Agency
BELGIUM
Brussels, La Bibliotheque EURATOM
FRANCE
Paris, European Nuclear Energy Agency, O.E.C.D.
ITALY
Ispra, EURATOM Research Center
SWITZERLAND
Geneva, United Nations Library

UNITED STATES
GOVERNMENT PRINTING OFFICE
DIVISION OF PUBLIC DOCUMENTS
WASHINGTON, D.C. 20402

OFFICIAL BUSINESS

POSTAGE AND FEES PAID
U.S. GOVERNMENT PRINTING OFFICE

TECHNICAL PROGRESS REVIEWS

The Division of Technical Information, U. S. Atomic Energy Commission, also publishes the Technical Progress Reviews, a series of five quarterly journals on nuclear technology. These journals, compiled by specialists and recognized authorities, summarize, evaluate, and reference the progress of development in five important fields.

Isotopes and Radiation Technology P. S. Baker, A. F. Rupp, and associates, Oak Ridge National Laboratory. Reviews AEC-sponsored projects and related significant worldwide developments in radioisotopes and radiation technology.

Nuclear Safety Wm. B. Cottrell, W. H. Jordan, and associates, Oak Ridge National Laboratory. Covers topics relevant to the analysis and control of hazards associated with nuclear reactors and with operations involving fissionable materials and the products of nuclear fission.

Power Reactor Technology Argonne National Laboratory. Reviews research, development, design practices, and operating experiences associated with power reactors, including aerospace applications.

Reactor Fuel Processing Stephen Lawroski and associates, Argonne National Laboratory. Reviews all aspects of the fuel-processing field, including aqueous and nonaqueous processing and waste disposal.

Reactor Materials R. W. Dayton, E. M. Simons, and associates, Battelle Memorial Institute. Covers the properties, behavior, and fabrication processes of materials used in nuclear reactors and associated equipment.

Availability

SUBSCRIPTION RATE: The Technical Progress Reviews may be purchased from the Superintendent of Documents, U. S. Government Printing Office, Washington, D. C. 20402, at $2.50 per year for each subscription or $0.70 per issue.

POSTAGE: Postpaid within the United States, Canada, Mexico, and all Central and South American countries except Argentina, Brazil, British and French Guiana, Surinam, and British Honduras. For these Central and South American countries and all other countries, add $0.75 per year or $0.20 per single issue.

REMITTANCE: Payment should be by check, money order, or document coupons and MUST accompany order. Remittances from foreign countries should be made by international money order or draft on an American bank payable to the Superintendent of Documents or by UNESCO book coupons.